Advances in Experimental Medicine and Biology 1074

John D. Ash · Robert E. Anderson
Matthew M. LaVail
Catherine Bowes Rickman
Joe G. Hollyfield · Christian Grimm
*Editors*

# Retinal Degenerative Diseases

## Mechanisms and Experimental Therapy

EXTRAS ONLINE

Springer

# Advances in Experimental Medicine and Biology



More information about this series at http://www.springer.com/series/5584

John D. Ash • Robert E. Anderson
Matthew M. LaVail • Catherine Bowes Rickman
Joe G. Hollyfield • Christian Grimm
Editors

# Retinal Degenerative Diseases

## Mechanisms and Experimental Therapy

Springer

*Editors*
John D. Ash
Department of Ophthalmology
University of Florida
Gainesville, FL, USA

Matthew M. LaVail
School of Medicine Beckman Vision Center
University of California San Francisco
San Francisco, CA, USA

Joe G. Hollyfield
Division of Ophthalmology
Case Western Reserve University
Cleveland, OH, USA

Robert E. Anderson
Ophthalmology and Cell Biology
University of Oklahoma Health
Sciences Center
Oklahoma City, OK, USA

Catherine Bowes Rickman
Departments of Ophthalmology
and Cell Biology
Duke Eye Center, Duke University
Medical Center
Durham, NC, USA

Christian Grimm
Department of Ophthalmology
University Hospital Zurich
Zurich, Switzerland

ISSN 0065-2598 ISSN 2214-8019 (electronic)
Advances in Experimental Medicine and Biology
ISBN 978-3-319-75401-7 ISBN 978-3-319-75402-4 (eBook)
https://doi.org/10.1007/978-3-319-75402-4

Library of Congress Control Number: 2018936145



Printed on acid-free paper

This Springer imprint is published by the registered company Springer International Publishing AG part of Springer Nature.
The registered company address is: Gewerbestrasse 11, 6330 Cham, Switzerland

# Dedication

*By all standards, the XVII International Symposium on Retinal Degeneration that was held in Kyoto, Japan, was a tremendous success. It is fitting that we dedicate this book of proceedings from the meeting to two pioneering scientists and ophthalmologists from Japan who have led and advocated for this field for many years. This book is dedicated to the careers of Professor Nagahisa Yoshimura, MD, PhD, and Professor Yozo Miyake MD, PhD.*

**Nagahisa Yoshimura**

*Yoshimura has extensive experience in clinical retina and retinal research and is known as an advocate for the field. Research interests of Dr. Yoshimura cover a wide range of retinal diseases. Among them, Dr. Yoshimura's group performed an extensive study on polypoidal choroidal vasculopathy (PCV) using new imaging devices in combination with genetic analyses of known age-related macular degeneration (AMD) risk mutations. Dr. Yoshimura's work demonstrated that PCV shares many common risk alleles with AMD, suggesting that PCV is a novel subtype of exudative AMD and not a distinct clinical entity. This important finding overturned a long-standing consensus that PCV was a distinct disease from AMD. Dr. Yoshimura also works to develop patient-derived iPS cells from patients with AMD and other retinal*

*degenerations to establish induced-RPE cells. This has led to the development of a novel assay system to evaluate iPS-derived RPE cell function.*

**Yozo Miyake**

*Miyake has had a long and productive career in ophthalmology. He served as Professor and Chairman of the Department of Ophthalmology, Nagoya University, until 2005. After retiring from Nagoya University, he served as the Director of National Institute of Sensory Organs in Tokyo, before becoming the President of Aichi Medical University in 2010. In addition, he served as the President of the International Society of Clinical Electrophysiology for Vision (ISCEV) from 2000 to 2004.*

*Dr. Miyake's major contributions to retinal degeneration include the development of ERG for clinical diagnostics. This includes pioneering use of systems for focal macular ERG (Arch Ophthalmol 1986, IOVS 1984, 1989). This allowed precision measurements of oscillatory potentials (Ops) of human macular ERGs for the first time in the history (IOVS 1989). Miyake's focal macular ERG system was in the forefront of the multifocal ERG developed by Sutter in 1994. The development of the focal macular ERG led to Dr. Miyake's most important work, which includes the discovery of "occult macular dystrophy" (OMD) (AJO 198v9, 1996). OMD is not a rare disease, and the focal macular ERG was key for its diagnosis. Dr. Miyake's group succeeded in identifying the gene mutation (RP1L1) causing OMD (Am J Hum Genet, 2010). Because of the substantial contribution of Dr. Miyake and his group, OMD diseases with the RP1L1 gene mutations are now referred to as "Miyake disease" (IOVS 2016). In 2015, the Japanese Ministry of Health, Labor and Welfare for medical care declared Miyake disease as one of the limited diseases for priority financial support.*

*Another highlight of Miyake's work using ERGs was the establishment of new clinical definitions of congenital stationary night blindness (Arch Ophthalmol 1986). Using a combination patient data and animal experiments, Dr. Miyake concluded that*

*complete CSNB has the complete defect of ON bipolar cell function, while incomplete CSNB has the incomplete defect of both ON and OFF bipolar cell function. Miyake's hypothesis has been well supported by data from other groups and still stands as the prevailing hypothesis (Nature Genet 1998, 2000).*

# Preface

The International Symposia on Retinal Degeneration have been held in conjunction with the biennial meeting of the International Society of Eye Research (ISER) since 1984. These RD Symposia have allowed basic and clinician scientists from around the world to convene and present their new research findings. They have been organized to allow substantial time for discussions and one-on-one interactions in a relaxed atmosphere, where international friendships and collaborations can be fostered. The XVII International Symposium on Retinal Degeneration (also known as RD2016) was held from September 19 to 24, 2016, at the Kyoto International Conference Center, in the beautiful and historic city of Kyoto, Japan. The meeting brought together 294 basic and clinician scientists, retinal specialists in ophthalmology, and trainees in the field from all parts of the world.

Abstract submissions to the RD2016 meeting exceeded all expectations, both in quantity and quality. The scientific program covered many aspects of retinal degeneration. The presentations included 42 platform talks and 151 posters. The program consisted of 3 full days of platform talks and 2 evening poster sessions. The RD2016 meeting was highlighted by five special keynote lectures. The first was given by **Robert Marc**, PhD, of the University of Utah, Salt Lake City, Utah. Dr. Marc discussed "Retinal Connectomes and Pathoconnectomes." The second keynote lecture was given by **José-Alain Sahel, MD, PhD**, Institut de la Vision, Paris, France. Dr. Sahel discussed "Maintaining and Restoring Cone-Mediated Vision in Rod-Cone Degenerations." The third keynote lecture was given by **Takeshi Iwata, PhD**, National Institute of Sensory Organs Tokyo, Japan. Dr. Iwata discussed "Genetic Factors and Molecular Mechanisms of Early Stage AMD: CNV Mouse and Drusen Primate Models." The fourth keynote lecture was given by **Yozo Miyake, MD, PhD**, Aichi Medical University, Nagoya, Japan. Dr. Miyake discussed "Establishment of New Concepts in Three Hereditary Retinal Diseases from Japan." The fifth and final keynote lecture was given by the 2012 Nobel Laureate **Shinya Yamanaka, MD, PhD**, Kyoto University, Kyoto, Japan. Dr. Yamanaka discussed "Recent Progress in iPS Cell Research and Application." The scientific meeting ended with a "Welcome to RD2018" by local organizer Dr. Peter Humphries, along with the organizers primarily responsible for the meeting, Drs. Cathy Bowes Rickman and Christian Grimm.

We thank the Local Organizing Committee Chair, **Nagahisa Yoshimura,** Kyoto University, and his local organizing committee Drs. **Shuichi Yamamoto**, Chiba University Hospital; **Akira Murakami**, Juntendo University Hospital; **Yoshiro Hotta**, Hamamatsu University School of Medicine; **Mineo Kondo**, Mie University Graduate School of Medicine; **Akihiro Ohira**, Shimane University Faculty of Medicine; and **Masaki Tanito**, Matsue Red Cross Hospital. In addition, we thank the outstanding management and staff of the meeting planning company, JTB Communication Design, for their assistance in making this an exceptionally smooth-running conference and a truly memorable experience for all of the attendees. These included, in particular, **Chika Okuhashi**, **Toshikazu Mogi**, and **Noriko Kataoka**.

The Symposium was able to fund 49 full-ride travel awards given to graduate students, postdocs, and junior faculty. The Travel Awardees were selected on the basis of 9 independent scores of their submitted abstracts, 6 from each of the organizers and 3 from the other members of the Travel Awards Committee for RD2016, Drs. Jacque Duncan, Michelle Pardue, and XianJie Yang. Travel awards were made possible in part by funding from the National Eye Institute of the National Institutes of Health. We are pleased to report this is the eight consecutive symposium in which the NEI has contributed travel awards to support young investigators. Additional awards were provided by generous international financial support from a number of organizations, including The Foundation Fighting Blindness; the BrightFocus Foundation; Pro Retina, Germany; the Fritz Tobler Foundation, Switzerland; and The Harrington Discovery Institute. Many of the contributing foundations sent members of their organizations to attend the meeting. Their participation and comments in the scientific sessions were instructive to many, offering new perspectives to some of the problems being discussed. For the first time, the Symposium held a Funders Lunch Forum where representatives from the Foundation Fighting Blindness, the Harrington Foundation, Fighting Blindness Ireland, BrightFocus Foundation, and the ProRetina Foundation held a panel discussion to discuss funding opportunities from their organizations. This was well received and will likely be repeated in future meetings.

We also acknowledge the diligent and outstanding efforts of Ms. **Holly Whiteside.** Holly is the Administrative Manager of Dr. Anderson's laboratory at the University of Oklahoma Health Sciences Center. Holly has been the RD Symposium Coordinator since 2000, and continues to serve the RD Symposia by providing administrate assistance with financial aspects of the meeting.

| | |
|---|---|
| Gainesville, FL, USA | John D. Ash |
| Oklahoma City, OK, USA | Robert E. Anderson |
| San Francisco, CA, USA | Matthew M. LaVail |
| Durham, NC, USA | Catherine Bowes Rickman |
| Cleveland, OH, USA | Joe G. Hollyfield |
| Zurich, Switzerland | Christian Grimm |

# Travel Awards

We gratefully acknowledge the support from the National Eye Institute, NIH, USA; the Foundation Fighting Blindness, USA; BrightFocus Foundation, USA; Pro Retina, Germany; and the Fritz Tobler Foundation, Switzerland, in their support of 49 travel awards. Eligibility for an award was restricted to graduate students, post-doctoral fellows, instructors, and assistant professors who were actively involved in retinal degeneration research. These awards were based on the quality of the abstract submitted by each applicant. The Travel Awards Committee consisted of nine senior retinal degeneration investigators and was chaired by Catherine Bowes Rickman.

**Kenkichi Baba**
Morehouse School of Medicine, Atlanta, GA, USA

**Petr Baranov**
Schepens Eye Research Institute, Massachusetts Eye and Ear, Boston, MA, USA

**Maya Barben**
University of Zurich, Zurich, Switzerland

**Pooja Biswas**
Shiley eye institute, University of California San Diego, La Jolla, CA, USA

**Vera Bonilha**
Cleveland Clinic Foundation, Cleveland, OH, USA

**Emily Brown**
University of Florida, Gainesville, FL, USA

**Soon Cheong**
University of Rochester, Rochester, NY, USA

**Conor Daly**
University College Dublin, Dublin, Ireland

**Astra Dinculescu**
University of Florida, Gainesville, FL, USA

**Sarah Doyle**
Trinity College Dublin, Dublin, Ireland

**Jianhai Du**
University of Washington, Seattle, WA, USA

**Jens Duebel**
Vision Institute Paris, Paris, France

**Cécile Fortuny**
University of California, Berkeley, CA, USA

**Ayako Furukawa**
Suzuka University of Medical Science, Suzuka, Japan

**Alejandro Garanto**
Radboud University Medical Center, Nijmegen, Netherlands

**Rosario Fernandez Godino**
Massachusetts Eye and Ear, Boston, MA, USA

**Anna Graca**
University College London, London, UK

**Felix Grassmann**
Institute of Human Genetics, University of Regensburg, Regensburg, Germany

**Karina Guziewicz**
University of Pennsylvania, PA, USA

**Christin Hanke-Gogokhia**
University of Utah, Salt Lake City, UT, USA

**Marcus Hooper**
University of Florida, Gainesville, FL, USA

**Cristhian Ildefonso**
University of Florida College of Medicine, Gainesville, FL, USA

**Helen Jiao**
John Curtin School of Medical Research, Australian National University (JCSMR, ANU), Australia

**Amir Kashani**
University of Southern California, Los Angeles, CA, USA

**Vladimir Khristov**
National Eye Institute, Washington, USA

**Byung-Jin Kim**
Johns Hopkins University, Baltimore, MD, USA

**Sophia-Martha kleine Holthaus**
UCL Institute of Ophthalmology, London, UK

**Mikael Klingeborn**
Duke University, Durham, NC, USA

**Susanne Koch**
Columbia University, New York, NY, USA

**Yang Kong**
The Jackson Laboratory, Bar Harbor, ME, USA

**Jonathan Lin**
Washington University School of Medicine, Saint Louis, MO, USA

**Martial Mbefo**
University of Lausanne, Jules-Gonin Eye Hospital, Lausanne, Switzerland

**Trevor McGill**
Oregon Health and Science University, Beaverton, OR, USA

**Keiko Miyadera**
University of Pennsylvania, Philadelphia, PA, USA

**Riccardo Natoli**
Australian National University, Canberra, Australia

**Rebecca Pfeiffer**
University of Utah Moran Eye Center, Salt Lake City, UT, USA

**Sheldon Rowan**
Tufts University, Boston, MS, USA

**Almudena Sacristan-Reviriego**
Institute of Ophthalmology, University College London, London, UK

**Nicole Schaefer**
University Hospital Regensburg, Regensburg, Germany

**Abdoulaye Sene**
Washington University in St Louis, Saint Louis, MO, USA

**Mandeep Singh**
Johns Hopkins University School of Medicine, Baltimore, MD, USA

**Raghavi Sudharsan**
University of Pennsylvania, Philadelphia, PA, USA

**Dragana Trifunovic**
University-Eye-Clinic Tuebingen, Tuebingen, Germany

**Keiko Ueda**
Columbia University, New York, NY, USA

**Stefanie Volland**
University of California Los Angeles, Los Angeles, CA, USA

**Sarah Walters**
University of Rochester, Rochester, NY, USA

**Yuhong Wang**
University of Oklahoma, Oklahoma City, OK, USA

**Joseph Wilkerson**
University of Oklahoma Health Sciences Center, Oklahoma City, OK, USA

# Contents

**Part I Age-Related Macular Degeneration (AMD)**

**1 Oxidative Stress Regulation and DJ-1 Function in the Retinal Pigment Epithelium: Implications for AMD** . . . . . 3
Vera L. Bonilha

**2 Mitochondria: Potential Targets for Protection in Age-Related Macular Degeneration** . . . . . 11
Emily E. Brown, Alfred S. Lewin, and John D. Ash

**3 Toll-Like Receptors and Age-Related Macular Degeneration** . . . . . 19
Kelly Mulfaul, Maedbh Rhatigan, and Sarah Doyle

**4 Alterations in Extracellular Matrix/Bruch's Membrane Can Cause the Activation of the Alternative Complement Pathway via Tick-Over** . . . . . 29
Rosario Fernandez-Godino

**5 MicroRNA as Therapeutics for Age-Related Macular Degeneration** . . . . . 37
Riccardo Natoli and Nilisha Fernando

**6 Anaphylatoxin Signaling in Retinal Pigment and Choroidal Endothelial Cells: Characteristics and Relevance to Age-Related Macular Degeneration** . . . . . 45
Bärbel Rohrer

**7 Estimations of Retinal Blue-Light Irradiance Values and Melatonin Suppression Indices Through Clear and Yellow-Tinted Intraocular Lenses** . . . . . 53
Masaki Tanito, Ichiya Sano, Tsutomu Okuno, Yoshihisa Ishiba, and Akihiro Ohira

**8 Co-Expression of Wild-Type and Mutant S163R C1QTNF5 in Retinal Pigment Epithelium** . . . . . 61
Astra Dinculescu, Frank M. Dyka, Seok-Hong Min, Rachel M. Stupay, Marcus J. Hooper, W. Clay Smith, and William W. Hauswirth

**Part II Gene Therapies**

**9 Mini-Review: Cell Type-Specific Optogenetic Vision Restoration Approaches** . . . . . 69
Antoine Chaffiol and Jens Duebel

**10 Mutation-Independent Gene Therapies for Rod-Cone Dystrophies** . . . . . 75
Cécile Fortuny and John G. Flannery

**11 Antisense Oligonucleotide-Based Splice Correction of a Deep-Intronic Mutation in *CHM* Underlying Choroideremia** . . . . . 83
Alejandro Garanto, Saskia D. van der Velde-Visser, Frans P. M. Cremers, and Rob W. J. Collin

**12 Gene Therapy Approaches to Treat the Neurodegeneration and Visual Failure in Neuronal Ceroid Lipofuscinoses** . . . . . 91
Sophia-Martha kleine Holthaus, Alexander J. Smith, Sara E. Mole, and Robin R. Ali

**13 Success of Gene Therapy in Late-Stage Treatment** . . . . . 101
Susanne F. Koch and Stephen H. Tsang

**14 Optimizing Non-viral Gene Therapy Vectors for Delivery to Photoreceptors and Retinal Pigment Epithelial Cells** . . . . . 109
Rahel Zulliger, Jamie N. Watson, Muayyad R. Al-Ubaidi, Linas Padegimas, Ozge Sesenoglu-Laird, Mark J. Cooper, and Muna I. Naash

**15 Nanoparticles as Delivery Vehicles for the Treatment of Retinal Degenerative Diseases** . . . . . 117
Yuhong Wang, Ammaji Rajala, and Raju V. S. Rajala

**16 Overexpression of Type 3 Iodothyronine Deiodinase Reduces Cone Death in the Leber Congenital Amaurosis Model Mice** . . . . . 125
Fan Yang, Hongwei Ma, Sanford L. Boye, William W. Hauswirth, and Xi-Qin Ding

**Part III In-Vivo Diagnostics for Structure and Function**

**17 In Vivo Functional Imaging of Retinal Neurons Using Red and Green Fluorescent Calcium Indicators** . . . . . 135
Soon K. Cheong, Wenjun Xiong, Jennifer M. Strazzeri, Constance L. Cepko, David R. Williams, and William H. Merigan

**18 Optimizing ERG Measures of Scotopic and Photopic Critical Flicker Frequency** . . . . . 145
Marci L. DeRamus and Timothy W. Kraft

**19 Repeatability and Reproducibility of In Vivo Cone Density Measurements in the Adult Zebrafish Retina** . . . . . 151
Alison Huckenpahler, Melissa Wilk, Brian Link, Joseph Carroll, and Ross F. Collery

**20 Normative Retinal Thicknesses in Common Animal Models of Eye Disease Using Spectral Domain Optical Coherence Tomography** . . . . . 157
Christy L. Carpenter, Alice Y. Kim, and Amir H. Kashani

**21 A Novel Approach for Integrating AF-SLO and SDOCT Imaging Data Demonstrates the Ability to Identify Early Retinal Abnormalities in Mutant Mice and Evaluate the Effects of Genetic and Pharmacological Manipulation** . . . . . 167
Brent A. Bell, Vera L. Bonilha, and Ivy S. Samuels

**Part IV Inflammation and Angiogenesis**

**22 The Role of Hypoxia, Hypoxia-Inducible Factor (HIF), and VEGF in Retinal Angiomatous Proliferation** . . . . . 177
Maya Barben, Marijana Samardzija, and Christian Grimm

**23 Neuroinflammation in Retinitis Pigmentosa, Diabetic Retinopathy, and Age-Related Macular Degeneration: A Minireview** . . . . . 185
Michael T. Massengill, Chulbul M. Ahmed, Alfred S. Lewin, and Cristhian J. Ildefonso

**24 Autoimmune Retinopathy: An Immunologic Cellular-Driven Disorder** . . . . . 193
John R. Heckenlively and Steven K. Lundy

**25 Inflammation-Induced Photoreceptor Cell Death** . . . . . 203
Abdoulaye Sene and Rajendra S. Apte

**26 Sall1 Regulates Microglial Morphology Cell Autonomously in the Developing Retina** . . . . . 209
Hideto Koso, Ryuichi Nishinakamura, and Sumiko Watanabe

**Part V Inherited Retinal Degenerations**

**27 Whole-Exome Sequencing Identifies Novel Variants that Co-segregates with Autosomal Recessive Retinal Degeneration in a Pakistani Pedigree** . . . . . 219
Pooja Biswas, Muhammad Asif Naeem, Muhammad Hassaan Ali, Muhammad Zaman Assir, Shaheen N. Khan, Sheikh Riazuddin, J. Fielding Hejtmancik, S. Amer Riazuddin, and Radha Ayyagari

**28 Identification of Novel Deletions as the Underlying Cause of Retinal Degeneration in Two Pedigrees** . . . . . 229
Kari Branham, Aditya A. Guru, Igor Kozak, Pooja Biswas, Mohammad Othman, Kameron Kishaba, Hassan Mansoor, Sheikh Riazuddin, John R. Heckenlively, S. Amer Riazuddin, J. Fielding Hejtmancik, Paul A. Sieving, and Radha Ayyagari

**29 Molecular Findings in Families with an Initial Diagnose of Autosomal Dominant Retinitis Pigmentosa (adRP)** . . . . . 237
Stephen P. Daiger, Sara J. Bowne, Lori S. Sullivan, Kari Branham, Dianna K. Wheaton, Kaylie D. Jones, Cheryl E. Avery, Elizabeth D. Cadena, John R. Heckenlively, and David G. Birch

**30 Pleiotropic Effects of Risk Factors in Age-Related Macular Degeneration and Seemingly Unrelated Complex Diseases** . . . . . 247
Christina Kiel, Bernhard H. F. Weber, and Felix Grassmann

**31 Mapping of Canine Models of Inherited Retinal Diseases** . . . . . 257
Keiko Miyadera

**32 A Mini-Review: Leber Congenital Amaurosis: Identification of Disease-Causing Variants and Personalised Therapies** . . . . . 265
J. A. Thompson, J. N. De Roach, T. L. McLaren, and T. M. Lamey

**Part VI Mechanisms of Degeneration**

**33 Role of Fibulins 2 and 5 in Retinal Development and Maintenance** . . . . . 275
Larissa Ikelle, Muna I. Naash, and Muayyad R. Al-Ubaidi

**34 Identifying Key Networks Linked to Light-Independent Photoreceptor Degeneration in Visual Arrestin 1 Knockout Mice** . . . 281
Hwa Sun Kim, Shun-Ping Huang, Eun-Jin Lee, and Cheryl Mae Craft

**35 How Excessive cGMP Impacts Metabolic Proteins in Retinas at the Onset of Degeneration** . . . . . 289
Jianhai Du, Jie An, Jonathan D. Linton, Yekai Wang, and James B. Hurley

**36 Protein Carbonylation-Dependent Photoreceptor Cell Death Induced by N-Methyl-N-nitrosourea in Mice** . . . . . 297
Ayako Furukawa, Kayo Sugitani, and Yoshiki Koriyama

**37 Müller Glia Reactivity and Development of Gliosis in Response to Pathological Conditions** . . . . . 303
Anna B. Graca, Claire Hippert, and Rachael A. Pearson

**38 Underdeveloped RPE Apical Domain Underlies Lesion Formation in Canine Bestrophinopathies** . . . . . 309
Karina E. Guziewicz, Emily McTish, Valerie L. Dufour, Kathryn Zorych, Anuradha Dhingra, Kathleen Boesze-Battaglia, and Gustavo D. Aguirre

**39 Binary Function of ARL3-GTP Revealed by Gene Knockouts** . . . . . 317
Christin Hanke-Gogokhia, Jeanne M. Frederick, Houbin Zhang, and Wolfgang Baehr

**40 Do cGMP Levels Drive the Speed of Photoreceptor Degeneration?** . . . . . 327
Maria Iribarne and Ichiro Masai

**41 Early Endosome Morphology in Health and Disease** . . . . . 335
Gulpreet Kaur and Aparna Lakkaraju

**42 The Retinal Circadian Clock and Photoreceptor Viability** . . . . . 345
Kenkichi Baba, Christophe P. Ribelayga, P. Michael Iuvone, and Gianluca Tosini

**43 The Role of c-Jun N-Terminal Kinase (JNK) in Retinal Degeneration and Vision Loss** . . . . . 351
Byung-Jin Kim and Donald J. Zack

**44 The Evaluation of BMI1 Posttranslational Modifications During Retinal Degeneration to Understand BMI1 Action on Photoreceptor Death Execution** . . . . . 359
Martial K. Mbefo and Yvan Arsenijevic

**45 Primary Rod and Cone Degeneration Is Prevented by HDAC Inhibition** . . . . . 367
Dragana Trifunović, Eleni Petridou, Antonella Comitato, Valeria Marigo, Marius Ueffing, and François Paquet-Durand

**46 Impact of MCT1 Haploinsufficiency on the Mouse Retina** . . . . . 375
Neal S. Peachey, Minzhong Yu, John Y. S. Han, Sylvain Lengacher, Pierre J. Magistretti, Luc Pellerin, and Nancy J. Philp

**47 The Leber Congenital Amaurosis-Linked Protein AIPL1 and Its Critical Role in Photoreceptors** . . . . . 381
Almudena Sacristan-Reviriego and Jacqueline van der Spuy

**48 Alternative Splicing for Activation of Coagulation Factor XIII-A in the Fish Retina After Optic Nerve Injury** . . . . . 387
Kayo Sugitani, Yoshiki Koriyama, Kazuhiro Ogai, Ayako Furukawa, and Satoru Kato

**49 Bisretinoid Photodegradation Is Likely Not a Good Thing** . . . . . 395
Keiko Ueda, Hye Jin Kim, Jin Zhao, and Janet R. Sparrow

**50 Further Characterization of the Predominant Inner Retinal Degeneration of Aging *Cln3*$^{\Delta ex7/8}$ Knock-In Mice** . . . . . 403
Cornelia Volz, Myriam Mirza, Thomas Langmann, and Herbert Jägle

**51 Differential Exon Expression in a Large Family of Retinal Genes Is Regulated by a Single Trans Locus** . . . . . 413
Jiaxing Wang, Felix L. Struebing, Salma Ferdous, Kevin Donaldson, Jeffrey H. Boatright, Eldon E. Geisert, and John M. Nickerson

**52 Molecular Chaperone ERp29: A Potential Target for Cellular Protection in Retinal and Neurodegenerative Diseases** . . . . . 421
Todd McLaughlin, Marek Falkowski, Joshua J. Wang, and Sarah X. Zhang

**53 The Role of Microbiota in Retinal Disease** . . . . . 429
Sheldon Rowan and Allen Taylor

**Part VII Neuroprotection**

**54 Current Pharmacological Concepts in the Treatment of the Retinitis Pigmentosa** . . . . . 439
Xiu-Feng Huang

**55 Valproic Acid Inhibits Human Retinal Pigment Epithelial (hRPE) Cell Proliferation Via a P38 MAPK Signaling Mechanism** . . . . . 447
Rohit Anand, Piyush C. Kothary, and Monte A. Del Monte

**56 Pigment Epithelium-derived Factor Protects Retinal Pigment Epithelial Cells Against Cytotoxicity "In Vitro"** . . . . . 457
Francisco M. Nadal-Nicolas and S. Patricia Becerra

**57 Brain-Derived Neurotrophic Factor as a Treatment Option for Retinal Degeneration** . . . . . 465
Conor Daly, Rebecca Ward, Alison L. Reynolds, Orla Galvin, Ross F. Collery, and Breandán N. Kennedy

**58 VEGF as a Trophic Factor for Müller Glia in Hypoxic Retinal Diseases** . . . . . 473
Shuhua Fu, Shuqian Dong, Meili Zhu, and Yun-Zheng Le

**59 Müller Cell Biological Processes Associated with Leukemia Inhibitory Factor Expression** . . . . . 479
Marcus J. Hooper and John D. Ash

**60 Retbindin Is Capable of Protecting Photoreceptors from Flavin-Sensitized Light-Mediated Cell Death In Vitro** . . . . . 485
Ryan A. Kelley, Muayyad R. Al-Ubaidi, and Muna I. Naash

**61 Constitutive Activation Mutant mTOR Promote Cone Survival in Retinitis Pigmentosa Mice** . . . . . 491
Ammaji Rajala, Yuhong Wang, and Raju V. S. Rajala

**62 Maintaining Cone Function in Rod-Cone Dystrophies** . . . . . 499
José-Alain Sahel and Thierry Léveillard

**63 PKG-Dependent Cell Death in 661W Cone Photoreceptor-like Cell Cultures (Experimental Study)** . . . . . 511
Stine Mencl, Dragana Trifunović, Eberhart Zrenner, and François Paquet-Durand

**Part VIII Retinal Cell Biology**

**64 More Than Meets the Eye: Current Understanding of RPGR Function** . . . . . 521
Hemant Khanna

**65 Polarized Exosome Release from the Retinal Pigmented Epithelium** . . . . . 539
Mikael Klingeborn, W. Daniel Stamer, and Catherine Bowes Rickman

**66 The Impact of Adherens and Tight Junctions on Physiological Function and Pathological Changes in the Retina** . . . . . 545
Yang Kong, Jürgen K. Naggert, and Patsy M. Nishina

**67 TRPV4 Does Not Regulate the Distal Retinal Light Response** . . . . . 553
Oleg Yarishkin, Tam T. T. Phuong, Monika Lakk, and David Križaj

**68 Role of Sirtuins in Retinal Function Under Basal Conditions** . . . . . 561
Jonathan B. Lin, Shunsuke Kubota, Raul Mostoslavsky, and Rajendra S. Apte

**69 The Retinol-Binding Protein Receptor 2 (Rbpr2) Is Required for Photoreceptor Survival and Visual Function in the Zebrafish** . . . . . 569
Glenn P. Lobo, Gayle Pauer, Joshua H. Lipschutz, and Stephanie A. Hagstrom

**70 Opposite Roles of MerTK Ligands Gas6 and Protein S During Retinal Phagocytosis** . . . . . 577
Emeline F. Nandrot

**71 Redundant and Nonredundant Functions of Akt Isoforms in the Retina** . . . . . 585
Raju V. S. Rajala and Ammaji Rajala

**72 Photoreceptor Outer Segment Isolation from a Single Canine Retina for RPE Phagocytosis Assay** . . . . . 593
Raghavi Sudharsan, Michael H. Elliott, Natalia Dolgova, Gustavo D. Aguirre, and William A. Beltran

**73 Preservation of Photoreceptor Nanostructure for Electron Tomography Using Transcardiac Perfusion Followed by High-Pressure Freezing and Freeze-Substitution** . . . . . 603
Stefanie Volland and David S. Williams

**74 Microtubule-Associated Protein 1 Light Chain 3 (LC3) Isoforms in RPE and Retina** . . . . . 609
Anuradha Dhingra, Desiree Alexander, Juan Reyes-Reveles, Rachel Sharp, and Kathleen Boesze-Battaglia

**Part IX Stem Cells**

**75 The iPSc-Derived Retinal Tissue as a Tool to Study Growth Factor Production in the Eye** . . . . . 619
Maryam Alavi and Petr Baranov

**76 Stem Cell-Based RPE Therapy for Retinal Diseases: Engineering 3D Tissues Amenable for Regenerative Medicine** . . . . . 625
Karim Ben M'Barek, Walter Habeler, and Christelle Monville

**77 Validation of iPS Cell-Derived RPE Tissue in Animal Models** . . . . . 633
Vladimir Khristov, Arvydas Maminishkis, Juan Amaral, Aaron Rising, Kapil Bharti, and Sheldon Miller

**78 Cell Transplantation for Retinal Degeneration: Transition from Rodent to Nonhuman Primate Models** . . . . . 641
Trevor J. McGill, David J. Wilson, Jonathan Stoddard, Lauren M. Renner, and Martha Neuringer

**79 Talaumidin Promotes Neurite Outgrowth of Staurosporine-Differentiated RGC-5 Cells Through PI3K/Akt-Dependent Pathways** . . . . . 649
Yoshiki Koriyama, Ayako Furukawa, Kayo Sugitani, Miwa Kubo, Kenichi Harada, and Yoshiyasu Fukuyama

**Index** . . . . . 655

# Contributors

**Gustavo D. Aguirre** Department of Clinical Studies-Philadelphia, School of Veterinary Medicine, University of Pennsylvania, Philadelphia, PA, USA

Division of Experimental Retinal Therapies, Department of Clinical Sciences and Advanced Medicine, School of Veterinary Medicine, University of Pennsylvania, Philadelphia, PA, USA

**Chulbul M. Ahmed** Department of Molecular Genetics & Microbiology, University of Florida College of Medicine, Gainesville, FL, USA

**Maryam Alavi** The Schepens Eye Research Institute, Massachusetts Eye and Ear, an affiliate of Harvard Medical School, Boston, MA, USA

**Desiree Alexander** Department of Biochemistry, SDM, University of Pennsylvania, Philadelphia, PA, USA

**Muhammad Hassaan Ali** Allama Iqbal Medical College, University of Health Sciences, Lahore, Pakistan

**Robin R. Ali** UCL Institute of Ophthalmology, Department of Genetics & NIHR BRC at Moorfields Eye Hospital, London, UK

**Muayyad R. Al-Ubaidi** Department of Biomedical Engineering, University of Houston, Houston, TX, USA

**Juan Amaral** Laboratory of Retinal Cell and Molecular Biology, National Eye Institute, Bethesda, MD, USA

**S. Amer Riazuddin** Department of Ophthalmology, The Wilmer Eye Institute, Johns Hopkins University School of Medicine, Baltimore, MD, USA

**Rohit Anand** Department of Ophthalmology and Visual Sciences, Kellogg Eye Center, University Michigan Medical School, Ann Arbor, MI, USA

**Jie An** Department of Medicine, University of Washington, Seattle, WA, USA

**Rajendra S. Apte** Department of Ophthalmology and Visual Sciences, Washington University School of Medicine, St. Louis, MO, USA

Department of Developmental Biology and Medicine, Washington University School of Medicine, St. Louis, MO, USA

Department of Biology, Allergan, Inc., Irvine, CA, USA

**Yvan Arsenijevic** Unit of Gene Therapy and Stem Cell Biology, Department of Ophtalmology, Jules-Gonin Eye Hospital, University of Lausanne, Lausanne, Switzerland

**John D. Ash** Department of Ophthalmology College of Medicine, University of Florida, Gainesville, FL, USA

Department of Molecular Genetics and Biology College of Medicine, University of Florida, Gainesville, FL, USA

**Muhammad Zaman Assir** Allama Iqbal Medical College, University of Health Sciences, Lahore, Pakistan

**Cheryl E. Avery** Human Genetics Center, School of Public Health, The University of Texas Health Science Center (UTHealth), Houston, TX, USA

**Radha Ayyagari** Shiley Eye Institute, University of California San Diego, La Jolla, CA, USA

**Kenkichi Baba** Neuroscience Institute, Department of Pharmacology and Toxicology Morehouse School of Medicine, Atlanta, GA, USA

**Wolfgang Baehr** Department of Ophthalmology and Visual Sciences, John A. Moran Eye Center, University of Utah School of Medicine, Salt Lake City, UT, USA

Department of Neurobiology and Anatomy, University of Utah School of Medicine, Salt Lake City, UT, USA

Department of Biology, University of Utah, Salt Lake City, UT, USA

**Petr Baranov** The Schepens Eye Research Institute, Massachusetts Eye and Ear, an affiliate of Harvard Medical School, Boston, MA, USA

**Maya Barben** Lab for Retinal Cell Biology, Department of Ophthalmology, University Hospital Zurich, University of Zurich, Schlieren, Switzerland

Neuroscience Center Zurich (ZNZ), University of Zurich, Zurich, Switzerland

**S. Patricia Becerra** Section of Protein Structure and Function, Laboratory of Retinal Cell and Molecular Biology, NEI, National Institutes of Health, Bethesda, MD, USA

**Brent A. Bell** Cole Eye Institute, Cleveland Clinic, Cleveland, OH, USA

Cole Eye Institute/Ophthalmic Research, Cleveland Clinic, Cleveland, OH, USA

**William A. Beltran** Division of Experimental Retinal Therapies, Department of Clinical Sciences and Advanced Medicine, School of Veterinary Medicine, University of Pennsylvania, Philadelphia, PA, USA

**Kapil Bharti** Unit on Ocular Stem Cell and Translational Research, National Eye Institute, Bethesda, MD, USA

**David G. Birch** The Retina Foundation of the Southwest, Dallas, TX, USA

**Pooja Biswas** Shiley Eye Institute, University of California San Diego, La Jolla, CA, USA

**Jeffrey H. Boatright** Department of Ophthalmology, Emory University, Atlanta, GA, USA

Center for Visual and Neurocognitive Rehabilitation, Atlanta VA Medical Center, Decatur, GA, USA

**Kathleen Boesze-Battaglia** Department of Biochemistry, School of Dental Medicine, University of Pennsylvania, Philadelphia, PA, USA

**Vera L. Bonilha** Cole Eye Institute (i31), Department of Ophthalmology, Cleveland Clinic Lerner College of Medicine, Cleveland, OH, USA

Cole Eye Institute, Cleveland Clinic, Cleveland, OH, USA

Cleveland Clinic Lerner College of Medicine of Case Western Reserve University, Cleveland, OH, USA

**Sara J. Bowne** Human Genetics Center, School of Public Health, The University of Texas Health Science Center (UTHealth), Houston, TX, USA

**Sanford L. Boye** Departments of Ophthalmology and Molecular Genetics and Microbiology, University of Florida, Gainesville, FL, USA

**Kari Branham** University of Michigan, Department of Ophthalmology and Visual Sciences, Ann Arbor, MI, USA

Kellogg Eye Center, University of Michigan, Ann Arbor, MI, USA

**Emily E. Brown** Department of Ophthalmology College of Medicine, University of Florida, Gainesville, FL, USA

Department of Molecular Genetics and Biology College of Medicine, University of Florida, Gainesville, FL, USA

**Elizabeth D. Cadena** Human Genetics Center, School of Public Health, The University of Texas Health Science Center (UTHealth), Houston, TX, USA

**Christy L. Carpenter** Department of Ophthalmology, USC Eye Institute, Keck School of Medicine of the University of Southern California, Los Angeles, CA, USA

**Joseph Carroll** Department of Cell Biology, Neurobiology, & Anatomy, Medical College of Wisconsin, Milwaukee, WI, USA

Departments of Ophthalmology, Medical College of Wisconsin, Milwaukee, WI, USA

**Constance L. Cepko** Departments of Genetics and Ophthalmology, Howard Hughes Medical Institute, Harvard Medical School, Boston, MA, USA

**Antoine Chaffiol** Sorbonne Université, INSERM, CNRS, Institut de la Vision, Paris, France

**Soon K. Cheong** Center for Visual Science, University of Rochester, Rochester, NY, USA

Flaum Eye Institute, University of Rochester, Rochester, NY, USA

**Ross F. Collery** Department of Cell Biology, Neurobiology, & Anatomy, Medical College of Wisconsin, Milwaukee, WI, USA

Department of Ophthalmology and Visual Sciences, Eye Institute, Medical College of Wisconsin, Milwaukee, WI, USA

**Rob W. J. Collin** Department of Human Genetics, Radboud University Medical Center, Nijmegen, The Netherlands

Donders Institute for Brain, Cognition and Behaviour, Radboud University Medical Center, Nijmegen, The Netherlands

**Antonella Comitato** Department of Life Sciences, University of Modena and Reggio Emilia, Modena, Italy

**Mark J. Cooper** Copernicus Therapeutics, Inc., Cleveland, OH, USA

**Cheryl Mae Craft** Laboratory for Vision Research, USC ROSKI Eye Institute, Department of Ophthalmology, Los Angeles, CA, USA

Department of Cell & Neurobiology, Keck School of Medicine, University of Southern California, Los Angeles, CA, USA

**Frans P. M. Cremers** Department of Human Genetics, Radboud University Medical Center, Nijmegen, The Netherlands

Donders Institute for Brain, Cognition and Behaviour, Radboud University Medical Center, Nijmegen, The Netherlands

**Stephen P. Daiger** Human Genetics Center, School of Public Health, The University of Texas Health Science Center (UTHealth), Houston, TX, USA

Ruiz Department of Ophthalmology and Visual Science, UTHealth, Houston, TX, USA

**Conor Daly** School of Biomolecular and Biomedical Science, University College Dublin, Belfield, Ireland

**Marci L. DeRamus** Department of Optometry and Vision Science, University of Alabama at Birmingham, Birmingham, AL, USA

**Anuradha Dhingra** Department of Biochemistry, School of Dental Medicine, University of Pennsylvania, Philadelphia, PA, USA

**Astra Dinculescu** Department of Ophthalmology, College of Medicine, University of Florida, Gainesville, FL, USA

**Xi-Qin Ding** Department of Cell Biology, University of Oklahoma Health Sciences Center, Oklahoma City, OK, USA

**Natalia Dolgova** Division of Experimental Retinal Therapies, Department of Clinical Sciences and Advanced Medicine, School of Veterinary Medicine, University of Pennsylvania, Philadelphia, PA, USA

**Kevin Donaldson** Department of Ophthalmology, Emory University, Atlanta, GA, USA

**Shuqian Dong** Department of Medicine Endocrinology, University of Oklahoma Health Sciences Center, Oklahoma City, OK, USA

**Sarah Doyle** Department of Clinical Medicine, School of Medicine, Trinity College Dublin, Dublin 2, Ireland

National Children's Research Centre, Our Lady's Children's Hospital Crumlin, Dublin 12, Ireland

**Jens Duebel** Sorbonne Université, INSERM, CNRS, Institut de la Vision, Paris, France

**Valerie L. Dufour** Department of Clinical Studies-Philadelphia, School of Veterinary Medicine, University of Pennsylvania, Philadelphia, PA, USA

**Jianhai Du** Department of Ophthalmology, University of Washington, Seattle, WA, USA

Departments of Ophthalmology, and Biochemistry, West Virginia University, Morgantown, WV, USA

**Frank M. Dyka** Department of Ophthalmology, College of Medicine, University of Florida, Gainesville, FL, USA

**Michael H. Elliott** Department of Ophthalmology, University of Oklahoma Health Science Centre, Oklahoma City, OK, USA

**Marek Falkowski** Departments of Ophthalmology and Biochemistry, Ross Eye Institute, University at Buffalo, State University of New York, Buffalo, NY, USA

**Salma Ferdous** Department of Ophthalmology, Emory University, Atlanta, GA, USA

**Rosario Fernandez-Godino** Ocular Genomics Institute, Massachusetts Eye and Ear Infirmary, Harvard Medical School, Boston, MA, USA

**Nilisha Fernando** John Curtin School of Medical Research, The Australian National University, Canberra, ACT, Australia

**J. Fielding Hejtmancik** Ophthalmic Genetics and Visual Function Branch, National Eye Institute, NIH, Bethesda, MD, USA

**John G. Flannery** Helen Wills Neuroscience Institute, Vision Science Graduate Group, University of California Berkeley, Berkeley, CA, USA

**Cécile Fortuny** Vision Science Graduate Group, Optometry School, University of California Berkeley, Berkeley, CA, USA

**Jeanne M. Frederick** Department of Ophthalmology and Visual Sciences, John A. Moran Eye Center, University of Utah School of Medicine, Salt Lake City, UT, USA

**Yoshiyasu Fukuyama** Faculty of Pharmaceutical Sciences, Tokushima Bunri University, Tokushima, Japan

**Ayako Furukawa** Graduate School and Faculty of Pharmaceutical Sciences, Suzuka University of Medical Science, Suzuka, Japan

**Shuhua Fu** Department of Ophthalmology, the Second Affiliated Hospital of Nanchang University, Nanchang, China

Department of Medicine Endocrinology, University of Oklahoma Health Sciences Center, Oklahoma City, OK, USA

**Orla Galvin** School of Biomolecular and Biomedical Science, University College Dublin, Belfield, Ireland

RenaSci Limited, BioCity, Nottingham, UK

**Alejandro Garanto** Department of Human Genetics, Radboud University Medical Center, Nijmegen, The Netherlands

Donders Institute for Brain, Cognition and Behaviour, Radboud University Medical Center, Nijmegen, The Netherlands

**Eldon E. Geisert** Department of Ophthalmology, Emory University, Atlanta, GA, USA

**Anna B. Graca** Department of Genetics, University College London Institute of Ophthalmology, London, UK

**Felix Grassmann** Institute of Human Genetics, University of Regensburg, Regensburg, Germany

**Christian Grimm** Lab for Retinal Cell Biology, Department of Ophthalmology, University Hospital Zurich, University of Zurich, Schlieren, Switzerland

Neuroscience Center Zurich (ZNZ), University of Zurich, Zurich, Switzerland

Zurich Center for Integrative Human Physiology (ZIHP), University of Zurich, Zurich, Switzerland

**Aditya A. Guru** Shiley Eye Institute, University of California San Diego, La Jolla, CA, USA

**Karina E. Guziewicz** Department of Clinical Studies-Philadelphia, School of Veterinary Medicine, University of Pennsylvania, Philadelphia, PA, USA

University of Pennsylvania, Ryan Veterinary Hospital, Philadelphia, PA, USA

**Walter Habeler** INSERM UMR861, I-Stem, AFM, Corbeil-Essonnes, France

UEVE UMR861, I-Stem, AFM, Corbeil-Essonnes, France

CECS-I-Stem, AFM, Corbeil-Essonnes, France

**Stephanie A. Hagstrom** Department of Ophthalmic Research, Cole Eye Institute, Cleveland Clinic, Cleveland, OH, USA

Department of Ophthalmology, Cleveland Clinic Lerner College of Medicine of Case Western Reserve University, Cleveland, OH, USA

**John Y. S. Han** Department of Pathology, Anatomy and Cell Biology, Thomas Jefferson University, Philadelphia, PA, USA

**Christin Hanke-Gogokhia** Department of Ophthalmology and Visual Sciences, John A. Moran Eye Center, University of Utah School of Medicine, Salt Lake City, UT, USA

Department of Biochemistry and Biology, University of Potsdam, Potsdam, Germany

**Kenichi Harada** Tokushima Bunri University, Tokushima, Japan

**William W. Hauswirth** Department of Ophthalmology, College of Medicine, University of Florida, Gainesville, FL, USA

Departments of Ophthalmology and Molecular Genetics and Microbiology, University of Florida, Gainesville, FL, USA

**John R. Heckenlively** Department of Ophthalmology and Visual Sciences, Kellogg Eye Center, University of Michigan Medical School, Ann Arbor, MI, USA

**Claire Hippert** Roche, Stem Cell Platform, Chemical Biology Roche Pharma Research and Early Development, Basel, Switzerland

**Marcus J. Hooper** Department of Ophthalmology, College of Medicine, University of Florida Health Science Center, Gainesville, FL, USA

**Shun-Ping Huang** Department of Ophthalmology, Taichung Tzu Chi Hospital, Taichung, Taiwan

Department of Molecular Biology and Human Genetics, Tzu Chi University, Hualien, Taiwan

Laboratory for Vision Research, USC ROSKI Eye Institute, Department of Ophthalmology, Los Angeles, CA, USA

**Xiu-Feng Huang** The Eye Hospital of Wenzhou Medical University, The State Key Laboratory Cultivation Base and Key Laboratory of Vision Science, Ministry of Health, Wenzhou, China

**Alison Huckenpahler** Department of Cell Biology, Neurobiology, & Anatomy, Medical College of Wisconsin, Milwaukee, WI, USA

**James B. Hurley** Department of Ophthalmology, University of Washington, Seattle, WA, USA

Department of Biochemistry, University of Washington, Seattle, WA, USA

**Larissa Ikelle** Department of Biomedical Engineering, University of Houston, Houston, TX, USA

**Cristhian J. Ildefonso** Department of Ophthalmology, University of Florida College of Medicine, Gainesville, FL, USA

**Maria Iribarne** Okinawa Institute of Science and Technology Graduate University, Okinawa, Japan

**Yoshihisa Ishiba** Technology Development Department, Yamamoto Kogaku Co. Ltd., Higashi-Osaka, Japan

**Herbert Jägle** Department of Ophthalmology, University Eye Clinic Regensburg, Regensburg, Germany

**Kaylie D. Jones** The Retina Foundation of the Southwest, Dallas, TX, USA

**Amir H. Kashani** Department of Ophthalmology, USC Eye Institute, Keck School of Medicine of the University of Southern California, Los Angeles, CA, USA

USC Roski Eye Institute, Los Angeles, CA, USA

**Satoru Kato** Wellness Promotion Science Center, Institute of Medical, Pharmaceutical and Health Science, Kanazawa University, Kanazawa, Japan

Department of Molecular Neurobiology, Graduate School of Medicine, Kanazawa University, Kanazawa, Japan

**Gulpreet Kaur** Cellular and Molecular Biology Graduate Training Program, University of Wisconsin-Madison, Madison, WI, USA

Department of Ophthalmology and Visual Sciences, School of Medicine and Public Health, University of Wisconsin-Madison, Madison, WI, USA

**Ryan A. Kelley** Department of Cell Biology, University of Oklahoma Health Sciences Center, Oklahoma City, OK, USA

Skaggs School of Pharmacy and Pharmaceutical Sciences, University of Colorado, Anschutz Medical Center, Aurora, CO, USA

**Breandán N. Kennedy** School of Biomolecular and Biomedical Science, University College Dublin, Belfield, Ireland

**Hemant Khanna** Department of Ophthalmology and Neurobiology, UMASS Medical School, Worcester, MA, USA

**Shaheen N. Khan** National Centre of Excellence in Molecular Biology, University of the Punjab, Lahore, Pakistan

**Vladimir Khristov** Section on Epithelial and Retinal Physiology and Disease, National Eye Institute, Bethesda, MD, USA

**Christina Kiel** Institute of Human Genetics, University of Regensburg, Regensburg, Germany

**Alice Y. Kim** Department of Ophthalmology, USC Eye Institute, Keck School of Medicine of the University of Southern California, Los Angeles, CA, USA

**Byung-Jin Kim** The Wilmer Eye Institute, Johns Hopkins University, School of Medicine, Baltimore, MD, USA

**Hwa Sun Kim** Laboratory for Vision Research, USC ROSKI Eye Institute, Department of Ophthalmology, Los Angeles, CA, USA

**Hye Jin Kim** Departments of Ophthalmology, Columbia University Medical Center, New York, NY, USA

**Kameron Kishaba** Shiley Eye Institute, University of California San Diego, La Jolla, CA, USA

**Sophia-Martha Kleine Holthaus** UCL Institute of Ophthalmology, Department of Genetics & NIHR BRC at Moorfields Eye Hospital, London, UK

MRC Laboratory for Molecular Cell Biology, UCL Institute of Child Health, Department of Genetics, Evolution and Environment, University College London, London, UK

**Mikael Klingeborn** Department of Ophthalmology, Duke University, Durham, NC, USA

**Susanne F. Koch** Physiological Genomics, Biomedical Center, Ludwig-Maximilians University Munich, Planegg/Munich, Germany

**Yang Kong** The Jackson Laboratory, Bar Harbor, ME, USA

The Graduate School of Biomedical Science and Engineering, University of Maine, Orono, ME, USA

**Yoshiki Koriyama** Graduate School and Faculty of Pharmaceutical Sciences, Suzuka University of Medical Science, Suzuka, Japan

**Hideto Koso** Division of Molecular and Developmental Biology, Institute of Medical Science, The University of Tokyo, Tokyo, Japan

**Piyush C. Kothary** Department of Ophthalmology and Visual Sciences, Kellogg Eye Center, University Michigan Medical School, Ann Arbor, MI, USA

**Igor Kozak** Shiley Eye Institute, University of California San Diego, La Jolla, CA, USA

Moorfields Eye Hospital Centre, Abu Dhabi, United Arab Emirates

**Timothy W. Kraft** Department of Optometry and Vision Science, University of Alabama at Birmingham, Birmingham, AL, USA

**David Križaj** Department of Ophthalmology & Visual Sciences, Moran Eye Institute, Salt Lake City, UT, USA

Department of Bioengineering, University of Utah, Salt Lake City, UT, USA

Department of Neurobiology & Anatomy, University of Utah, Salt Lake City, UT, USA

**Miwa Kubo** Tokushima Bunri University, Tokushima, Japan

**Shunsuke Kubota** Department of Ophthalmology & Visual Sciences, Washington University School of Medicine, St. Louis, MO, USA

**Aparna Lakkaraju** Department of Ophthalmology and Visual Sciences, School of Medicine and Public Health, University of Wisconsin-Madison, Madison, WI, USA

McPherson Eye Research Institute, University of Wisconsin-Madison, Madison, WI, USA

**Monika Lakk** Department of Ophthalmology & Visual Sciences, Moran Eye Institute, Salt Lake City, UT, USA

**T. M. Lamey** Australian Inherited Retinal Disease Registry & DNA Bank, Department of Medical Technology and Physics, Sir Charles Gairdner Hospital, Perth, WA, Australia

Centre for Ophthalmology and Visual Science, The University of Western Australia, Crawley, WA, Australia

**Thomas Langmann** Department of Experimental Immunology of the Eye, University of Cologne, Cologne, Germany

**Eun-Jin Lee** Department of Biomedical Engineering, Viterbi School of Engineering, University of Southern California, Los Angeles, CA, USA

Laboratory for Vision Research, USC ROSKI Eye Institute, Department of Ophthalmology, Los Angeles, CA, USA

**Sylvain Lengacher** Brain Mind Institute, Ecole Polytechnique Fédérale de Lausanne (EPFL), Lausanne, Switzerland

**Thierry Léveillard** Sorbonne Universités, UPMC Univ Paris 06, INSERM U968, CNRS UMR 7210, Institut de la Vision, Paris, France

**Alfred S. Lewin** Department of Molecular Genetics and Biology College of Medicine, University of Florida, Gainesville, FL, USA

**Yun-Zheng Le** Department of Medicine Endocrinology, University of Oklahoma Health Sciences Center, Oklahoma City, OK, USA

Department of Cell Biology, University of Oklahoma Health Sciences Center, Oklahoma City, OK, USA

Department of Ophthalmology, University of Oklahoma Health Sciences Center, Oklahoma City, OK, USA

Harold Hamm Diabetes Center, University of Oklahoma Health Sciences Center, Oklahoma City, OK, USA

**Jonathan B. Lin** Department of Ophthalmology & Visual Sciences, Washington University School of Medicine, St. Louis, MO, USA

Neuroscience Graduate Program, Division of Biology and Biomedical Sciences, Washington University School of Medicine, St. Louis, MO, USA

**Brian Link** Department of Cell Biology, Neurobiology, & Anatomy, Medical College of Wisconsin, Milwaukee, WI, USA

**Jonathan D. Linton** Department of Ophthalmology, University of Washington, Seattle, WA, USA

**Joshua H. Lipschutz** Division of Nephrology, Medical University of South Carolina, Charleston, SC, USA

**Glenn P. Lobo** Division of Nephrology, Medical University of South Carolina, Charleston, SC, USA

Department of Ophthalmology, Medical University of South Carolina, Charleston, SC, USA

**Steven K. Lundy** Department of Internal Medicine-Rheumatology, University of Michigan Medical School, Ann Arbor, MI, USA

Graduate Program in Immunology, University of Michigan Medical School, Ann Arbor, MI, USA

**Karim Ben M'Barek** INSERM UMR861, I-Stem, AFM, Corbeil-Essonnes, France

UEVE UMR861, I-Stem, AFM, Corbeil-Essonnes, France

CECS-I-Stem, AFM, Corbeil-Essonnes, France

**Pierre J. Magistretti** Brain Mind Institute, Ecole Polytechnique Fédérale de Lausanne (EPFL), Lausanne, Switzerland

Division of Biological and Environmental Sciences and Engineering, King Abdullah University of Science and Technology (KAUST), Thuwal, KSA, Saudi Arabia

**Hongwei Ma** Department of Cell Biology, University of Oklahoma Health Sciences Center, Oklahoma City, OK, USA

**Arvydas Maminishkis** Section on Epithelial and Retinal Physiology and Disease, National Eye Institute, Bethesda, MD, USA

**Hassan Mansoor** Al-Shifa Trust Eye Hospital, Rawalpindi, Pakistan

**Valeria Marigo** Department of Life Sciences, University of Modena and Reggio Emilia, Modena, Italy

**Ichiro Masai** Okinawa Institute of Science and Technology Graduate University, Okinawa, Japan

**Michael T. Massengill** Department of Molecular Genetics & Microbiology, University of Florida College of Medicine, Gainesville, FL, USA

**Martial K. Mbefo** Unit of Gene Therapy and Stem Cell Biology, Department of Ophtalmology, Jules-Gonin Eye Hospital, University of Lausanne, Lausanne, Switzerland

**Trevor J. McGill** Department of Ophthalmology, Casey Eye Institute, Oregon Health & Science University, Portland, OR, USA

Division of Neuroscience, Oregon National Primate Research Center, Oregon Health & Science University, Portland, OR, USA

**T. L. McLaren** Australian Inherited Retinal Disease Registry & DNA Bank, Department of Medical Technology and Physics, Sir Charles Gairdner Hospital, Perth, WA, Australia

**Todd McLaughlin** Departments of Ophthalmology and Biochemistry, Ross Eye Institute, University at Buffalo, State University of New York, Buffalo, NY, USA

SUNY Eye Institute, State University of New York, Buffalo, NY, USA

**Emily McTish** Department of Clinical Studies-Philadelphia, School of Veterinary Medicine, University of Pennsylvania, Philadelphia, PA, USA

**Stine Mencl** Department für Augenheilkunde, Forschungsinstitut für Augenheilkunde, Eberhard Karls Universität Tübingen, Tübingen, Germany

University Hospital Essen, Department of Neurology, Essen, Germany

**William H. Merigan** Center for Visual Science, University of Rochester, Rochester, NY, USA

**P. Michael Iuvone** Departments of Ophthalmology and Pharmacology, Emory University School of Medicine, Atlanta, GA, USA

**Sheldon Miller** Section on Epithelial and Retinal Physiology and Disease, National Eye Institute, Bethesda, MD, USA

**Seok-Hong Min** Department of Ophthalmology, College of Medicine, University of Florida, Gainesville, FL, USA

**Myriam Mirza** Institute of Human Genetics, University of Regensburg, Regensburg, Germany

Department of Experimental Immunology of the Eye, University of Cologne, Cologne, Germany

**Keiko Miyadera** School of Veterinary Medicine, University of Pennsylvania, Philadelphia, PA, USA

**Sara E. Mole** MRC Laboratory for Molecular Cell Biology, UCL Institute of Child Health, Department of Genetics, Evolution and Environment, University College London, London, UK

**Monte A. Del Monte** Department of Ophthalmology and Visual Sciences, Kellogg Eye Center, University Michigan Medical School, Ann Arbor, MI, USA

**Christelle Monville** INSERM UMR861, I-Stem, AFM, Corbeil-Essonnes, France

UEVE UMR861, I-Stem, AFM, Corbeil-Essonnes, France

**Raul Mostoslavsky** Massachusetts General Hospital Cancer Center, Harvard Medical School, Boston, MA, USA

**Kelly Mulfaul** Department of Clinical Medicine, School of Medicine, Trinity College Dublin, Dublin 2, Ireland

**Muna I. Naash** Department of Biomedical Engineering, University of Houston, Houston, TX, USA

**Francisco M. Nadal-Nicolas** Section of Protein Structure and Function, Laboratory of Retinal Cell and Molecular Biology, NEI, National Institutes of Health, Bethesda, MD, USA

**Muhammad Asif Naeem** National Centre of Excellence in Molecular Biology, University of the Punjab, Lahore, Pakistan

**Jürgen K. Naggert** The Jackson Laboratory, Bar Harbor, ME, USA

**Emeline F. Nandrot** Sorbonne Université, INSERM, CNRS, Institut de la Vision, Paris, France

**Riccardo Natoli** John Curtin School of Medical Research, The Australian National University, Canberra, ACT, Australia

ANU Medical School, The Australian National University, Canberra, ACT, Australia

**Martha Neuringer** Department of Ophthalmology, Casey Eye Institute, Oregon Health & Science University, Portland, OR, USA

Division of Neuroscience, Oregon National Primate Research Center, Oregon Health & Science University, Portland, OR, USA

**John M. Nickerson** Department of Ophthalmology, Emory University, Atlanta, GA, USA

**Ryuichi Nishinakamura** Department of Kidney Development, Institute of Molecular Embryology and Genetics, Kumamoto University, Kumamoto, Japan

**Patsy M. Nishina** The Jackson Laboratory, Bar Harbor, ME, USA

**Kazuhiro Ogai** Wellness Promotion Science Center, Institute of Medical, Pharmaceutical and Health Science, Kanazawa University, Kanazawa, Japan

**Akihiro Ohira** Department of Ophthalmology, Shimane University Faculty of Medicine, Izumo, Shimane, Japan

**Tsutomu Okuno** Graduate School of Science and Engineering, Tokyo Metropolitan University, Hachioji/Tokyo, Japan

**Mohammad Othman** University of Michigan, Department of Ophthalmology and Visual Sciences, Ann Arbor, MI, USA

**Linas Padegimas** Abeona Therapeutics Inc., Cleveland, OH, USA

**François Paquet-Durand** Institute for Ophthalmic Research, University of Tuebingen, Tuebingen, Germany

**François Paquet-Durand** Department für Augenheilkunde, Forschungsinstitut für Augenheilkunde, Eberhard Karls Universität Tübingen, Tübingen, Germany

**Gayle Pauer** Department of Ophthalmic Research, Cole Eye Institute, Cleveland Clinic, Cleveland, OH, USA

**Neal S. Peachey** Louis Stokes Cleveland VA Medical Center, Cleveland, OH, USA

Cole Eye Institute, Cleveland Clinic, Cleveland, OH, USA

Department of Ophthalmology, Cleveland Clinic Lerner College of Medicine of Case Western Reserve University, Cleveland, OH, USA

**Rachael A. Pearson** Department of Genetics, University College London Institute of Ophthalmology, London, UK

**Luc Pellerin** Department of Physiology, University of Lausanne, Lausanne, Switzerland

**Eleni Petridou** Institute for Ophthalmic Research, University of Tuebingen, Tuebingen, Germany

**Nancy J. Philp** Department of Pathology, Anatomy and Cell Biology, Thomas Jefferson University, Philadelphia, PA, USA

**Tam T. T. Phuong** Department of Ophthalmology & Visual Sciences, Moran Eye Institute, Salt Lake City, UT, USA

**Ammaji Rajala** Department of Ophthalmology, University of Oklahoma Health Sciences Center, Oklahoma City, OK, USA

Dean McGee Eye Institute, Oklahoma City, OK, USA

**Raju V. S. Rajala** Department of Ophthalmology, University of Oklahoma Health Sciences Center, Oklahoma City, OK, USA

Department of Physiology, University of Oklahoma Health Sciences Center, Oklahoma City, OK, USA

Department of Cell Biology, University of Oklahoma Health Sciences Center, Oklahoma City, OK, USA

Dean McGee Eye Institute, Oklahoma City, OK, USA

**Lauren M. Renner** Division of Neuroscience, Oregon National Primate Research Center, Oregon Health & Science University, Portland, OR, USA

**Juan Reyes-Reveles** Department of Biochemistry, SDM, University of Pennsylvania, Philadelphia, PA, USA

**Alison L. Reynolds** School of Veterinary Medicine, University College Dublin, Belfield, Ireland

**Maedbh Rhatigan** Department of Clinical Medicine, School of Medicine, Trinity College Dublin, Dublin 2, Ireland

Royal Victoria Eye and Ear Hospital, Dublin 2, Ireland

**Sheikh Riazuddin** National Centre of Excellence in Molecular Biology, University of the Punjab, Lahore, Pakistan

Allama Iqbal Medical College, University of Health Sciences, Lahore, Pakistan

National Centre for Genetic Diseases, Shaheed Zulfiqar Ali Bhutto Medical University, Islamabad, Pakistan

**Christophe P. Ribelayga** Ruiz Department of Ophthalmology and Visual Science, McGovern Medical School, The University of Texas Health Science Center at Houston, Houston, TX, USA

**Catherine Bowes Rickman** Department of Ophthalmology, Duke University, Durham, NC, USA

Department of Cell Biology, Duke University, Durham, NC, USA

**Aaron Rising** Section on Epithelial and Retinal Physiology and Disease, National Eye Institute, Bethesda, MD, USA

**J. N. De Roach** Australian Inherited Retinal Disease Registry & DNA Bank, Department of Medical Technology and Physics, Sir Charles Gairdner Hospital, Perth, WA, Australia

**Bärbel Rohrer** Departments of Ophthalmology, and Neurosciences, Medical University of South Carolina, Charleston, SC, USA

Research Service, Ralph H. Johnson VA Medical Center, Charleston, SC, USA

**Sheldon Rowan** USDA-JM Human Nutrition Research Center on Aging (HNRCA), Tufts University, Boston, MA, USA

Department of Ophthalmology, Tufts University School of Medicine, Boston, MA, USA

**Almudena Sacristan-Reviriego** UCL Institute of Ophthalmology, London, UK

**José-Alain Sahel** Sorbonne Universités, UPMC Univ Paris 06, INSERM U968, CNRS UMR 7210, Institut de la Vision, Paris, France

CHNO des Quinze-Vingts, DHU Sight Restore, INSERM-DGOS CIC 1423, Paris, France

Department of Ophthalmology, The University of Pittsburgh School of Medicine, Pittsburgh, PA, USA

**Marijana Samardzija** Lab for Retinal Cell Biology, Department of Ophthalmology, University Hospital Zurich, University of Zurich, Schlieren, Switzerland

**Ivy S. Samuels** Cole Eye Institute, Cleveland Clinic, Cleveland, OH, USA

Louis Stokes Cleveland VA Medical Center, Cleveland, OH, USA

**Ichiya Sano** Division of Ophthalmology, Matsue Red Cross Hospital, Matsue, Shimane, Japan

**Abdoulaye Sene** Department of Ophthalmology and Visual Sciences, Washington University School of Medicine, St. Louis, MO, USA

**Ozge Sesenoglu-Laird** Copernicus Therapeutics, Inc., Cleveland, OH, USA

**Rachel Sharp** Department of Biochemistry, SDM, University of Pennsylvania, Philadelphia, PA, USA

**Paul A. Sieving** Ophthalmic Genetics and Visual Function Branch, National Eye Institute, NIH, Bethesda, MD, USA

**Alexander J. Smith** UCL Institute of Ophthalmology, Department of Genetics & NIHR BRC at Moorfields Eye Hospital, London, UK

**W. Clay Smith** Department of Ophthalmology, College of Medicine, University of Florida, Gainesville, FL, USA

**Janet R. Sparrow** Departments of Ophthalmology, Columbia University Medical Center, New York, NY, USA

Departments of Pathology and Cell Biology, Columbia University Medical Center, New York, NY, USA

**Jacqueline van der Spuy** UCL Institute of Ophthalmology, London, UK

**W. Daniel Stamer** Department of Ophthalmology, Duke University, Durham, NC, USA

Department of Biomedical Engineering, Duke University, Durham, NC, USA

**Jonathan Stoddard** Division of Neuroscience, Oregon National Primate Research Center, Oregon Health & Science University, Portland, OR, USA

**Jennifer M. Strazzeri** Center for Visual Science, University of Rochester, Rochester, NY, USA

Flaum Eye Institute, University of Rochester, Rochester, NY, USA

**Felix L. Struebing** Department of Ophthalmology, Emory University, Atlanta, GA, USA

**Rachel M. Stupay** Department of Ophthalmology, College of Medicine, University of Florida, Gainesville, FL, USA

**Raghavi Sudharsan** Division of Experimental Retinal Therapies, Department of Clinical Sciences and Advanced Medicine, School of Veterinary Medicine, University of Pennsylvania, Philadelphia, PA, USA

**Kayo Sugitani** Division of Health Sciences, Graduate School of Medicine, Kanazawa University, Kanazawa, Japan

Department of Clinical Laboratory Science, Graduate School of Medical Science, Kanazawa University, Kanazawa, Japan

**Lori S. Sullivan** Human Genetics Center, School of Public Health, The University of Texas Health Science Center (UTHealth), Houston, TX, USA

**Masaki Tanito** Division of Ophthalmology, Matsue Red Cross Hospital, Shimane, Matsue, Japan

Department of Ophthalmology, Shimane University Faculty of Medicine, Izumo, Shimane, Japan

**Allen Taylor** USDA-JM Human Nutrition Research Center on Aging (HNRCA), Tufts University, Boston, MA, USA

Department of Ophthalmology, Tufts University School of Medicine, Boston, MA, USA

Friedman School of Nutrition Science and Policy, Tufts University, Boston, MA, USA

**J. A. Thompson** Australian Inherited Retinal Disease Registry & DNA Bank, Department of Medical Technology and Physics, Sir Charles Gairdner Hospital, Perth, WA, Australia

**Gianluca Tosini** Neuroscience Institute, Department of Pharmacology and Toxicology Morehouse School of Medicine, Atlanta, GA, USA

**Dragana Trifunović** Institute for Ophthalmic Research, University of Tuebingen, Tuebingen, Germany

Department für Augenheilkunde, Forschungsinstitut für Augenheilkunde, Eberhard Karls Universität Tübingen, Tübingen, Germany

**Stephen H. Tsang** Barbara & Donald Jonas Laboratory of Stem Cells & Regenerative Medicine and Bernard & Shirlee Brown Glaucoma Laboratory,

Departments of Pathology and Cell Biology, Columbia University, New York, NY, USA

Edward S. Harkness Eye Institute, New York Presbyterian Hospital, New York, NY, USA

Institute of Human Nutrition, College of Physicians and Surgeons, Columbia University, New York, NY, USA

Herbert Irving Comprehensive Cancer Center, Columbia University Medical Center, New York, NY, USA

**Keiko Ueda** Departments of Ophthalmology, Columbia University Medical Center, New York, NY, USA

**Marius Ueffing** Institute for Ophthalmic Research, University of Tuebingen, Tuebingen, Germany

**Saskia D. van der Velde-Visser** Department of Human Genetics, Radboud University Medical Center, Nijmegen, The Netherlands

**Stefanie Volland** Department of Ophthalmology, Stein Eye Institute, UCLA School of Medicine, Los Angeles, CA, USA

**Cornelia Volz** Department of Ophthalmology, University Eye Clinic Regensburg, Regensburg, Germany

**Jiaxing Wang** Department of Ophthalmology, Tianjin Medical University General Hospital, Tianjin, China

Department of Ophthalmology, Emory University, Atlanta, GA, USA

**Joshua J. Wang** Departments of Ophthalmology and Biochemistry, Ross Eye Institute, University at Buffalo, SUNY Eye Institute, State University of New York, Buffalo, NY, USA

SUNY Eye Institute, State University of New York, Buffalo, NY, USA

**Yekai Wang** Departments of Ophthalmology, and Biochemistry, West Virginia University, Morgantown, WV, USA

**Yuhong Wang** Department of Ophthalmology, University of Oklahoma Health Sciences Center, Oklahoma City, OK, USA

Dean McGee Eye Institute, Oklahoma City, OK, USA

**Rebecca Ward** School of Biomolecular and Biomedical Science, University College Dublin, Belfield, Ireland

**Sumiko Watanabe** Division of Molecular and Developmental Biology, Institute of Medical Science, The University of Tokyo, Tokyo, Japan

**Jamie N. Watson** Department of Cell Biology, University of Oklahoma Health Sciences Center, Oklahoma City, OK, USA

**Bernhard H. F. Weber** Institute of Human Genetics, University of Regensburg, Regensburg, Germany

**Dianna K. Wheaton** The Retina Foundation of the Southwest, Dallas, TX, USA

**Melissa Wilk** Department of Cell Biology, Neurobiology, & Anatomy, Medical College of Wisconsin, Milwaukee, WI, USA

**David R. Williams** Institute of Optics, University of Rochester, Rochester, NY, USA

Center for Visual Science, University of Rochester, Rochester, NY, USA

**David S. Williams** Department of Ophthalmology, Stein Eye Institute, UCLA School of Medicine, Los Angeles, CA, USA

Department of Neurobiology, UCLA School of Medicine, Los Angeles, CA, USA

Molecular Biology Institute, UCLA School of Medicine, Los Angeles, CA, USA

Brain Research Institute, UCLA School of Medicine, Los Angeles, CA, USA

**David J. Wilson** Department of Ophthalmology, Casey Eye Institute, Oregon Health & Science University, Portland, OR, USA

**Wenjun Xiong** Department of Biomedical Sciences, City University of Hong Kong, Kowloon, Hong Kong, SAR, China

**Fan Yang** Department of Cell Biology, University of Oklahoma Health Sciences Center, Oklahoma City, OK, USA

**Oleg Yarishkin** Department of Ophthalmology & Visual Sciences, Moran Eye Institute, Salt Lake City, UT, USA

**Minzhong Yu** Cole Eye Institute, Cleveland Clinic, Cleveland, OH, USA

Department of Ophthalmology, Cleveland Clinic Lerner College of Medicine of Case Western Reserve University, Cleveland, OH, USA

**Donald J. Zack** The Wilmer Eye Institute, Johns Hopkins University, School of Medicine, Baltimore, MD, USA

**Houbin Zhang** The Sichuan Provincial Key Laboratory for Human Disease Gene Study, The Institute of Laboratory Medicine, Hospital of University of Electronic Science and Technology of China and Sichuan Provincial People's Hospital, Chengdu, Sichuan, China

School of Medicine, University of Electronic Science and Technology of China, Chengdu, Sichuan, China

**Sarah X. Zhang** Departments of Ophthalmology and Biochemistry, Ross Eye Institute, University at Buffalo, State University of New York, Buffalo, NY, USA

SUNY Eye Institute, State University of New York, Buffalo, NY, USA

**Jin Zhao** Departments of Ophthalmology, Columbia University Medical Center, New York, NY, USA

**Meili Zhu** Department of Medicine Endocrinology, University of Oklahoma Health Sciences Center, Oklahoma City, OK, USA

**Kathryn Zorych** Department of Clinical Studies-Philadelphia, School of Veterinary Medicine, University of Pennsylvania, Philadelphia, PA, USA

**Eberhart Zrenner** Department für Augenheilkunde, Forschungsinstitut für Augenheilkunde, Eberhard Karls Universität Tübingen, Tübingen, Germany

Centre for Integrative Neuroscience (CIN), Eberhard Karls Universität Tübingen, Tübingen, Germany

**Rahel Zulliger** Department of Biomedical Engineering, University of Houston, Houston, TX, USA

# Part I
# Age-Related Macular Degeneration (AMD)

# Chapter 1
# Oxidative Stress Regulation and DJ-1 Function in the Retinal Pigment Epithelium: Implications for AMD

**Vera L. Bonilha**

**Abstract** In the retina, oxidative stress can initiate a cascade of events that ultimately leads to a focal loss of RPE cells and photoreceptors, a major contributing factor in geographic atrophy. Despite these implications, the molecular regulation of RPE oxidative metabolism under physiological and pathological conditions remains largely unknown. DJ-1 functions as an antioxidant, redox-sensitive molecular chaperone, and transcription regulator, which protected cells from oxidative stress. Here we discuss our progress toward characterization of the DJ-1 function in the protection of RPE to oxidative stress.

**Keywords** Oxidative stress · DJ-1 · Retinal pigment epithelium · Age-related macular degeneration · Neurodegenerative diseases · Posttranslational modifications

## 1.1 Introduction

DJ-1 is a multifunctional protein located in the cytosol, nucleus, and mitochondria of the cells, but it can also be secreted from the cells or tissues in cancer and PD patients (Kahle et al. 2009; Saito 2014). The protein robustly protects cells from oxidative stress by functioning primarily as an antioxidant protein, through a broad group of distinct cellular mechanisms (Raninga et al. 2014). More importantly, DJ-1 plays a protective role in cancer, neurodegenerative (e.g., Parkinson's disease, Alzheimer, Huntington's disease), and cardiovascular diseases (e.g., heart failure) as an endogenous antioxidant (Chan and Chan 2015). Here we further discuss DJ-1 function in the regulation of oxidative stress regulation of RPE cells.

V. L. Bonilha (✉)
Cole Eye Institute (i31), Department of Ophthalmology, Cleveland Clinic Lerner College of Medicine, Cleveland, OH, USA
e-mail: bonilhav@ccf.org



J. D. Ash et al. (eds.), *Retinal Degenerative Diseases*, Advances in Experimental Medicine and Biology 891, https://doi.org/10.1007/978-3-319-75402-4_1

## 1.2 Oxidative Stress and DJ-1 Function

In baseline conditions there exists a balance between the free radical generation as by-products of a metabolism based on reduction–oxidation reactions and the antioxidant defense in the cell (Babusikova et al. 2013). Conversely, in oxidative stress antioxidant mechanisms cannot properly metabolize the cellular content of free radicals generated. Oxidative stress accumulation in postmitotic cells damages nucleic acids, lipids, and proteins, ultimately resulting in cell death and impacting the pathogenesis of various chronic diseases. The cellular defensive mechanisms available to counteract generated reactive oxygen species (ROS) comprise antioxidant enzymes (e.g., superoxide dismutase, catalase, glutathione peroxidase) and low molecular weight antioxidants (e.g., vitamin C, vitamin E, glutathione, carotenoids, natural flavonoids, melatonin) (Halliwell and Gutteridge 1999; McCall and Frei 1999; Pham and Plakogiannis 2005; Atukeren 2011). A crucial mechanism in the cellular defense against oxidative stress is activation of the nuclear factor E2-related factor 2 (Nrf2) transcription factor that is responsible for the expression of antioxidant response element (ARE)-regulated genes that enable a coordinated protective response to stress (Nguyen et al. 2009).

DJ-1 participates in mitochondrial homeostasis through regulation of mitochondrial complex I (Hayashi et al. 2009; Mullett and Hinkle 2011). It can be found mostly diffused in the cytoplasm (Nagakubo et al. 1997; Bonifati et al. 2003) and to a lesser extent in the mitochondria (Zhang et al. 2005) and nucleus (Nagakubo et al. 1997; Hod et al. 1999) of cells under baseline conditions. Upon oxidative stress, more DJ-1 redistributes to either the mitochondria (Canet-Aviles et al. 2004) or the nucleus, and this cellular redistribution correlates with the ability of DJ-1 to foster neuroprotection (Canet-Aviles et al. 2004; Ashley et al. 2009; Junn et al. 2009; Kim et al. 2012).

Oxidation of DJ-1 at one of the three cysteines (C) at amino acid numbers 46, 53, and 106 regulates its function (Mitsumoto and Nakagawa 2001; Kinumi et al. 2004; Choi et al. 2006). However, evidence suggests that C106 is critical for DJ-1-mediated protection against oxidative stress (Waak et al. 2009; Wilson 2011). Upon oxidative stress, oxidation at C106 by sulfinic acid ($C\text{-}SO_2H$) regulates transcription factors and achieves optimal protective functions of DJ-1. On the other hand, oxidation by sulfonic acid ($C\text{-}SO_3H$) results in the destabilization of DJ-1 structure (Wilson 2011; Saito 2014). This hypothesis is supported by the identification of sulfonic form (over-oxidized) as the main oxidized form in PD and AD brains (Bandopadhyay et al. 2004; Choi et al. 2006).

Some of the protective actions of DJ-1 occur through its RNA-binding activity to regulate the translation of multiple protective transcripts. DJ-1 stabilizes Nrf2 by interfering with its ubiquitination and facilitates Nrf2 translocation to the nucleus by preventing the binding with Keap1 (Gan et al. 2010). Thus, DJ-1 may play a crucial role both sensing and conferring protection against a range of oxidative stressors, using different mechanisms.

## 1.3 DJ-1 Function in the RPE Cells

The RPE is highly predisposed to free radical formation and oxidative injury because these cells live under chronic oxidative stress due to the lifelong exposure to light, high oxygen consumption, and high oxygen partial pressure from the underlying choriocapillaris. Another factor increasing RPE oxidative stress is the daily phagocytosis of the shed photoreceptor outer segments, enriched in polyunsaturated fatty acids such as docosahexaenoic and retinoids, which have the detrimental property of being oxidized and damaged by light (Leveillard and Sahel 2016). Finally, phagocytosis is itself an oxidative stressor and results in the generation of endogenous ROS (Miceli et al. 1994; Tate et al. 1995). This hostile oxidative environment is thought to contribute to retinal disease. However, it remains to be determined why the initial retinal degeneration occurs and how degeneration processes progress as a result of continued oxidative insults.

In adult rodent retinas, DJ-1 is highly expressed in the RPE and photoreceptor cells (inner segments and cell body), while DJ-1 also displays lesser expression in the outer plexiform layer. Loss of DJ-1 resulted in mild structural and physiological changes in the retinas of the aged DJ-1 knockout (DJ-1 KO) mice in association with increased oxidative stress. These included an increase in the amplitude of the scotopic ERG b-wave and cone ERG, decreased amplitude of a subset of the dc-ERG components, RPE thinning, decreased tyrosine hydroxylase in dopaminergic neurons, and increased 7,8- dihydro-8-oxoguanine-labeled DNA oxidation (Bonilha et al. 2015).

In RPE cell lines under baseline conditions, different pools of DJ-1 are present in the cytoplasm and, in some cells, in the nuclei. Oxidative stress leads to a noticeable increase in immunocytochemical staining for DJ-1. Also, under these conditions, DJ-1 is redistributed to the mitochondria in RPE cultures (Shadrach et al. 2013).

Previously, we reported that DJ-1 was detected and highly expressed in the RPE lysates from age-related macular (AMD) donors when compared to the RPE lysates from non-AMD donors (Shadrach et al. 2013). To further understand how the AMD pathology relates to DJ-1 oxidation, we analyzed lysates of isolated human RPE probed with a new and specific C106-$SO_3$H DJ-1 antibody. Lysates from AMD donors displayed increased presence of C106-$SO_3$H DJ-1 when compared to non-AMD RPE (data not shown). This data suggest a loss of biological function of DJ-1 in AMD RPE. We also observed DJ-1 presence in Bruch's membrane and drusen isolated from different AMD donors, as previously reported for many of the proteins found in drusen, which are typically found intracellularly in the RPE (Shadrach et al. 2013). Recently, DJ-1 has emerged as a significant biomarker due to its presence in the extracellular fluids of patients affected by different types of cancer (Kahle et al. 2009) and in PD patients (Saito 2014). Future studies will be needed to investigate how RPE cells release DJ-1 and to determine if it can be detected in the serum of AMD patients.

In vitro experiments carried out in RPE cultures tested the role of DJ-1 oxidation at its C residues in protection against oxidative stress. ARPE-19 cells and ARPE-19 cells transduced with adenoviruses carrying both DJ-1 full length (hDJ-1) and DJ-1 with the three Cs at residues 46, 53, and 106 mutated to serine (CtoS) were subjected to oxidative stress, and the generation of ROS was monitored. Significant ROS production was observed when ARPE-19 cultures were exposed to oxidative stress and when ARPE-19 cultures overexpressing the CtoS DJ-1 were exposed to oxidative stress. In contrast, no significant ROS production was detected in ARPE-19 overexpressing exogenous full-length DJ-1 (Shadrach et al. 2013). This data suggested that high levels of full-length DJ-1 expression resulted in significant decrease in ROS generation in RPE cells exposed to oxidative stress.

These constructs were also used to analyze the effects of DJ-1 expression in the mitochondrial structure of primary human fetal RPE cells in culture (Bonilha et al. 2014). Overexpression of both exogenous full-length DJ-1 and CtoS DJ-1 resulted in significant increase in immunolabeling with an antibody specific to mitochondria (COX IV) and a mean increase in the diameter of mitochondria tubules. In contrast, mitochondria in the RPE from DJ-1 KO mice displayed loss of cristae associated with increases in matrix density and, in some cells, interruption of the mitochondrial internal and external membranes. This data suggested that mitochondrial morphology is altered with the loss and increased expression of DJ-1.

## 1.4 Conclusions

Knowledge about the DJ-1 function in RPE has greatly increased in the last few years. Research has shown that DJ-1 levels of expression modulate RPE response to oxidative stress. Based on our data, we surmised of a possible mechanistic pathway via which RPE degeneration results from overall low levels of native DJ-1 or post-translational modifications (PTMs) that impair its function. Our central hypothesis is that oxidative stress-induced RPE degeneration observed in diseases such as AMD is mediated by loss of the antioxidant functions of DJ-1 (Fig. 1.1).

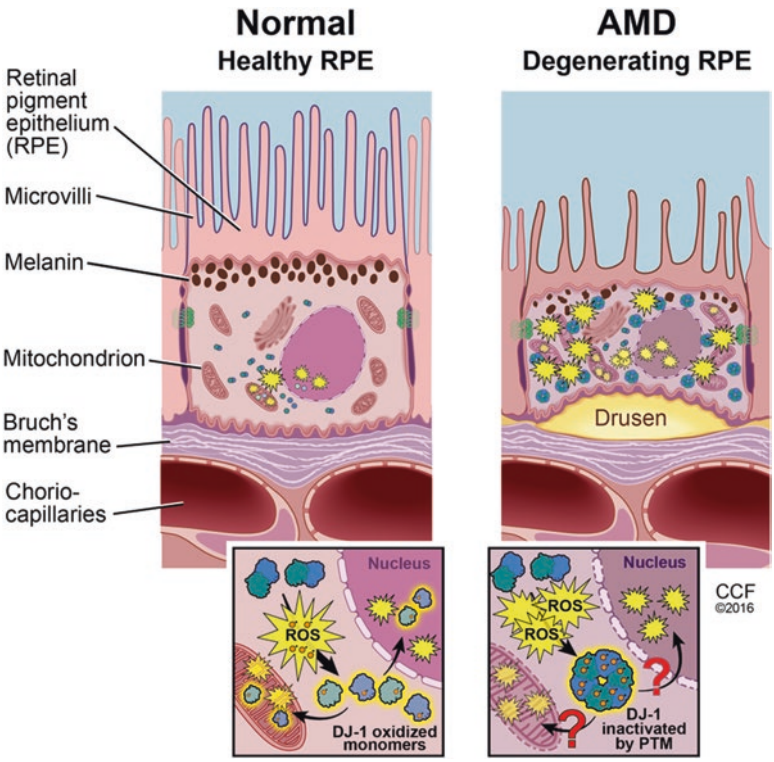


**Fig. 1.1** Schematic model of DJ-1 function in oxidative stress regulation of RPE. The healthy RPE cells metabolize generated ROS. Mitochondrial and nuclear DJ-1 translocation and functions as an antioxidant protein are enhanced by oxidation. The degenerating RPE cannot properly metabolize generated ROS. DJ-1 function is impaired by PTM due to over-oxidation of the protein (Reprinted with the permission of the Cleveland Clinic Center for Medical Art & Photography © 2016. All Rights Reserved)

**Acknowledgments** The author thanks David Schumick, BS, CMI for the preparation of the illustration on the role of DJ-1 in RPE oxidative stress. This work was supported by the NIH grant EY027750.

## References

Ashley AK, Hanneman WH, Katoh T et al (2009) Analysis of targeted mutation in DJ-1 on cellular function in primary astrocytes. Toxicol Lett 184:186–191

Atukeren P (2011) The impact of redox balance in brain tumors. In: Garami M (ed) Molecular targets of CNS tumors. InTech, Rijeka, Croatia

Babusikova E, Evinova A, Hatok J et al (2013) Oxidative changes and possible effects of polymorphism of antioxidant enzymes in neurodegenerative disease. In: Kishore U (ed) Neurodegenerative diseases. InTech, Rijeka, Croatia

Bandopadhyay R, Kingsbury AE, Cookson MR et al (2004) The expression of DJ-1 (PARK7) in normal human CNS and idiopathic Parkinson's disease. Brain (A Journal of Neurology) 127:420–430

Bonifati V, Rizzu P, van Baren MJ et al (2003) Mutations in the DJ-1 gene associated with autosomal recessive early-onset parkinsonism. Science 299:256–259

Bonilha VL, Shadrach KG, Rayborn ME (2014) Levels of DJ-1 perturb mitochondrial structure in the Retinal Pigment Epithelium (RPE). ARVO Meeting Abstract 55:4562

Bonilha VL, Bell BA, Rayborn ME et al (2015) Loss of DJ-1 elicits retinal abnormalities, visual dysfunction, and increased oxidative stress in mice. Exp Eye Res 139:22–36

Canet-Aviles RM, Wilson MA, Miller DW et al (2004) The Parkinson's disease protein DJ-1 is neuroprotective due to cysteine-sulfinic acid-driven mitochondrial localization. Proc Natl Acad Sci U S A 101:9103–9108

Chan JY, Chan SH (2015) Activation of endogenous antioxidants as a common therapeutic strategy against cancer, neurodegeneration and cardiovascular diseases: a lesson learnt from DJ-1. Pharmacol Ther 156:69–74

Choi J, Sullards MC, Olzmann JA et al (2006) Oxidative damage of DJ-1 is linked to sporadic Parkinson and Alzheimer diseases. J Biol Chem 281:10816–10824

Gan L, Johnson DA, Johnson JA (2010) Keap1-Nrf2 activation in the presence and absence of DJ-1. Eur J Neurosci 31:967–977

Halliwell B, Gutteridge JMC (1999) Free radicals in biology and medicine, 3rd edn. Oxford University Press, New York

Hayashi T, Ishimori C, Takahashi-Niki K et al (2009) DJ-1 binds to mitochondrial complex I and maintains its activity. Biochem Biophys Res Commun 390:667–672

Hod Y, Pentyala SN, Whyard TC et al (1999) Identification and characterization of a novel protein that regulates RNA-protein interaction. J Cell Biochem 72:435–444

Junn E, Jang WH, Zhao X et al (2009) Mitochondrial localization of DJ-1 leads to enhanced neuroprotection. J Neurosci Res 87:123–129

Kahle PJ, Waak J, Gasser T (2009) DJ-1 and prevention of oxidative stress in Parkinson's disease and other age-related disorders. Free Radic Biol Med 47:1354–1361

Kim SJ, Park YJ, Hwang IY et al (2012) Nuclear translocation of DJ-1 during oxidative stress-induced neuronal cell death. Free Radic Biol Med 53:936–950

Kinumi T, Kimata J, Taira T et al (2004) Cysteine-106 of DJ-1 is the most sensitive cysteine residue to hydrogen peroxide-mediated oxidation in vivo in human umbilical vein endothelial cells. Biochem Biophys Res Commun 317:722–728

Leveillard T, Sahel JA (2016) Metabolic and redox signaling in the retina. Cell Mol Life Sci 74(20):3649–3665

McCall MR, Frei B (1999) Can antioxidant vitamins materially reduce oxidative damage in humans? Free Radic Biol Med 26:1034–1053

Miceli MV, Liles MR, Newsome DA (1994) Evaluation of oxidative processes in human pigment epithelial cells associated with retinal outer segment phagocytosis. Exp Cell Res 214:242–249

Mitsumoto A, Nakagawa Y (2001) DJ-1 is an indicator for endogenous reactive oxygen species elicited by endotoxin. Free Radic Res 35:885–893

Mullett SJ, Hinkle DA (2011) DJ-1 deficiency in astrocytes selectively enhances mitochondrial Complex I inhibitor-induced neurotoxicity. J Neurochem 117:375–387

Nagakubo D, Taira T, Kitaura H et al (1997) DJ-1, a novel oncogene which transforms mouse NIH3T3 cells in cooperation with ras. Biochem Biophys Res Commun 231:509–513

Nguyen T, Nioi P, Pickett CB (2009) The Nrf2-antioxidant response element signaling pathway and its activation by oxidative stress. J Biol Chem 284:13291–13295

Pham DQ, Plakogiannis R (2005) Vitamin E supplementation in cardiovascular disease and cancer prevention: Part 1. Ann Pharmacother 39:1870–1878

Raninga PV, Trapani GD, Tonissen KF (2014) Cross talk between two antioxidant systems, Thioredoxin and DJ-1: consequences for cancer. Oncoscience 1:95–110

Saito Y (2014) Oxidized DJ-1 as a possible biomarker of Parkinson's disease. J Clin Biochem Nutr 54:138–144

Shadrach KG, Rayborn ME, Hollyfield JG et al (2013) DJ-1-dependent regulation of oxidative stress in the retinal pigment epithelium (RPE). PLoS One 8:e67983

Tate DJ Jr, Miceli MV, Newsome DA (1995) Phagocytosis and H2O2 induce catalase and metallothionein gene expression in human retinal pigment epithelial cells. Invest Ophthalmol Vis Sci 36:1271–1279

Waak J, Weber SS, Gorner K et al (2009) Oxidizable residues mediating protein stability and cytoprotective interaction of DJ-1 with apoptosis signal-regulating kinase 1. J Biol Chem 284:14245–14257

Wilson MA (2011) The role of cysteine oxidation in DJ-1 function and dysfunction. Antioxid Redox Signal 15:111–122

Zhang L, Shimoji M, Thomas B et al (2005) Mitochondrial localization of the Parkinson's disease related protein DJ-1: implications for pathogenesis. Hum Mol Genet 14:2063–2073

# Chapter 2
# Mitochondria: Potential Targets for Protection in Age-Related Macular Degeneration


**Emily E. Brown, Alfred S. Lewin, and John D. Ash**

**Abstract** Age-related macular degeneration (AMD) is the leading cause of blindness in older adults in developed countries. The molecular mechanisms of disease pathogenesis remain poorly understood; however, evidence suggests that mitochondrial dysfunction may contribute to the progression of the disease. Studies have shown that mitochondrial DNA lesions are increased in the retinal pigment epithelium (RPE) of human patients with the disease and that the number of these lesions increases with disease severity. Additionally, microscopy of human RPE from patients with dry AMD shows severe disruptions in mitochondrial inner and outer membrane structure, mitochondrial size, and mitochondrial cellular organization. Thus, improving our understanding of mitochondrial dysfunction in dry AMD pathogenesis may lead to the development of targeted therapies. We propose that mitochondrial dysfunction in the RPE can lead to the chronic oxidative stress associated with the disease. Therefore, one protective strategy may involve the use of small molecule therapies that target the regulation of mitochondrial biogenesis and mitochondrial fission and mitophagy.

**Keywords** Mitochondria · Age-related macular degeneration · Oxidative stress · Mitochondrial DNA · Fission · Fusion · Retinal pigment epithelium

E. E. Brown · J. D. Ash (✉)
Department of Ophthalmology College of Medicine, University of Florida, Gainesville, FL, USA

Department of Molecular Genetics and Biology College of Medicine, University of Florida, Gainesville, FL, USA
e-mail: jash@ufl.edu

A. S. Lewin
Department of Molecular Genetics and Biology College of Medicine, University of Florida, Gainesville, FL, USA



J. D. Ash et al. (eds.), *Retinal Degenerative Diseases*, Advances in Experimental Medicine and Biology 891, https://doi.org/10.1007/978-3-319-75402-4_2

## 2.1 Introduction

The cost of age-related macular degeneration (AMD) in the USA reaches 25 billion dollars annually (Brown et al. 2006), a large economic burden that demonstrates the critical need for effective therapies. Patients suffering from AMD lose high acuity central vision, resulting in a loss of independence and severe decrease in quality of life (Husler and Schmid 2013; Sorensen et al. 2015). Patients with dry AMD exhibit increased oxidative stress and inflammation in the RPE; however the molecular mechanisms of disease pathogenesis are poorly understood. Current treatments for dry AMD involve reducing the levels of reactive oxygen species (ROS) via treatment with an antioxidant formulation that slows the progression of AMD in a small subset of patients and potentially worsens disease in others (Awh et al. 2013, 2015).

Studies, which will be discussed in more detail in this review, suggest that mitochondrial dysfunction in the RPE could be a contributing factor to disease progression. Mitochondrial dysfunction can arise from mitochondrial DNA mutations, mutations in a gene in the nuclear DNA that encodes a component of the mitochondria, or due to oxidative damage. Mitochondria are a major source of reactive oxygen species (ROS), suggesting that they may contribute to the increase in oxidative stress observed in AMD. Studies focused on the role of mitochondrial dysfunction in AMD pathogenesis are necessary to further our understanding of disease progression and for the identification of small molecules that may prevent mitochondrial dysfunction in AMD.

## 2.2 Oxidative Stress Is Implicated in AMD

An increase in oxidative stress in the RPE is associated with AMD. A major risk factor for development of AMD is cigarette smoke, which is known to be a major producer of ROS, such as the oxidant hydroquinone (HQ), which is present in high concentrations in cigarette smoke-related tar (Pryor et al. 1983). Population-based studies examining almost 5,000 patients from throughout Europe have shown that current cigarette smokers have increased odds of developing neo-vascular AMD or geographic atrophy (odds ratios of 2.6 and 4.8, respectively), while previous smokers also had increase likelihood of developing the disease (odds ratio of 1.7) (Chakravarthy et al. 2007). This study found that about 27% of cases of AMD were attributed to smoking, highlighting the importance of this habit to development of disease. When mice are exposed to cigarette smoke or HQ, they develop an AMD-like phenotype, demonstrating that ROS exposure does lead to AMD-like disease (Espinosa-Heidmann et al. 2006).

The Age-Related Eye Disease Study (AREDS) formula, which is an antioxidant formulation that contains vitamin C, vitamin E, beta-carotene, zinc, and copper, has shown some efficacy in treating AMD, giving further support for the involvement of oxidative stress in this disease. This formula does not prevent the development of

geographic atrophy, but simply reduces the rate of onset of late AMD (Age-Related Eye Disease Study Research Group 2001). Therefore, it is necessary to develop a better understanding of the role that oxidative stress and mitochondrial dysfunction play in AMD pathogenesis, in order to develop effective targeted therapies.

## 2.3 Mitochondria Are a Major Source of Reactive Oxygen Species

Mitochondria are key regulators of inflammatory and oxidative signaling pathways (Medkour and Titorenko 2016), thus mitochondrial dysfunction has been proposed as a mechanism of cell death in AMD. Mitochondria are the major intracellular source of ROS, with superoxide anion produced mostly at complex I and III of the electron transport chain, due to premature electron leakage to oxygen. Increased intracellular oxidative stress poses a risk for oxidative damage to DNA, proteins, and lipids. Elevated oxidative stress can lead to decreased mitochondrial integrity, and prolonged oxidative stress has the potential to damage mitochondrial structure and decrease mitochondrial function.

Mitochondria are highly dynamic organelles, constantly undergoing fusion, biogenesis, fission, and mitophagy, processes that are important for maintaining mitochondrial function. Importantly, dysfunction in these processes is associated with neurodegeneration, which is extensively reviewed elsewhere (Itoh et al. 2013). Mitochondrial fusion is the process by which the outer membrane GTPase proteins mitofusin (Mfn) 1 and 2 on two separate mitochondria fuse the outer mitochondrial membranes to form one mitochondrion, while optic atrophy 1 (Opa1), the inner membrane GTPase, fuses the inner membranes. Mitochondrial fusion is thought to be a potential mitochondrial repair mechanism through the diffusion of mitochondrial DNA and proteins. Mitochondrial biogenesis involves the expression of mitochondrial DNA-encoded genes, as well as one to two thousand nuclear-encoded genes. Mitochondria can increase in number through the process of fission, during which the mitochondrial outer membrane proteins, mitochondrial fission factor (MFF), along with other proteins, recruit dynamin-related protein 1 (Drp1). Drp1 forms a ring around the mitochondrion, cinching it to eventually form two separate mitochondria. If the mitochondrion is no longer able to maintain its membrane potential, PTEN-induced putative kinase 1 (PINK1) becomes lodged in the translocase of the outer membrane (TOM). This results in recruitment of Parkin, an E3 ubiquitin ligase, which polyubiquitinates proteins on the outer mitochondrial membrane, marking the mitochondrion for degradation through mitochondrial-specific autophagy, known as mitophagy. These processes that regulate mitochondrial dynamics are important for maintaining mitochondrial integrity and function. Dysregulation of these processes can lead to mitochondrial dysfunction and disease.

## 2.4 Mitochondrial Dysfunction in AMD

We hypothesize that mitochondrial dysfunction is a major contributing factor to disease pathogenesis in AMD. Electron micrograph studies demonstrate that aged individuals have fewer and smaller mitochondria in the RPE. The depletion of mitochondria is even more severe in patients with AMD, who also have pronounced damage to mitochondrial structure and displaced localization (Bianchi et al. 2013). It remains unclear whether the observed alterations in mitochondrial structure are a contributing factor to disease progression or simply a result of disease.

Enhanced levels of mitochondrial DNA lesions have been observed in the RPE of human patients with AMD (Terluk et al. 2015). Genomic DNA from RPE and retina was extracted from aged patients with various grades of RPE health, and the mitochondrial genome was amplified using long-extension PCR. This group found that with increasing AMD disease severity, there was an increase in mitochondrial DNA lesions in the RPE. The increase in mitochondrial DNA lesions was specific to the RPE and was not found in the neuroretina. These results suggest that there are alterations to the mitochondrial DNA integrity in AMD that could lead to increased oxidative stress, through hindrance of transcription and replication of mitochondrial DNA required for mitochondrial biogenesis. However, it again remains unclear whether these lesions are a major contributing factor to disease pathogenesis or simply a result of other disease mechanisms.

Several research groups have demonstrated a link between mitochondrial haplogroups and AMD susceptibility. Studies have found that the H haplogroup is protective from AMD, while the J, T, S, and U haplogroups are associated with a higher risk for developing the disease (Mueller et al. 2012). Studies utilizing cybrid ARPE-19 cell lines, with the same nuclear genome, but either J or H haplotype mitochondria, have found that there are different metabolic profiles with different mitochondrial haplogroups. The J haplotype has a decreased ratio of oxygen consumption rate to extracellular acidification rate when compared to the H haplotype, suggesting that mitochondria from the J haplogroup have decreased bioenergetics (Kenney et al. 2014). This group found that the J haplotype has less expression of mitochondrial DNA-encoded respiratory complex components, as well as decreased expression of nuclear genes associated with the complement pathway, apoptosis, and inflammation. Alteration in expression of components of nuclear-encoded pathways suggests that mitochondrial DNA mediates regulation of not only mitochondrial-related genes but also plays a role in regulating these key cellular pathways. These studies suggest that the mitochondria may play a major role in AMD pathogenesis.

## 2.5 Targeting the Mitochondria to Provide Protection in AMD

Our group has found that treatment with metformin, an activator of adenosine monophosphate-activated protein kinase (AMPK), is protective to photoreceptors in mouse models with elevated ocular oxidative stress and in models of inherited

retinal degeneration (unpublished data). Our lab has shown that systemic treatment with metformin results in increases in mitochondrial DNA copy number, as well as nuclear- and mitochondrial-encoded proteins associated with mitochondrial biogenesis, in the neuroretina (unpublished data). Therefore, we hypothesize that the neuroprotection that we observe is, at least in part, due to an increase in mitochondrial biogenesis and overall mitochondrial health.

AMPK plays a major role in regulation of energy homeostasis through direct phosphorylation of substrates that stimulate ATP-producing processes and inhibit ATP-utilizing processes, reviewed extensively elsewhere (Burkewitz et al. 2014). AMPK has been shown to act as an important regulator of mitochondrial biogenesis through activation of peroxisome proliferator-activated receptor gamma coactivator 1 (PGC-1) (Ojuka 2004). The PGC-1 proteins (comprised of PGC-1α, PGC-1β, and PGC-1-related coactivator) are transcriptional coactivators responsible for regulation of energy metabolism, including promoting mitochondrial biogenesis. We hypothesize that activation of PGC-1 by AMPK is protective by increasing mitochondrial biogenesis. Therefore, targeting PGC-1 may be protective in AMD by increasing biogenesis of new healthy mitochondria in a system that may be overburdened with dysfunctional mitochondria.

Other groups have shown that activation of AMPK also leads to mitochondrial fission. Toyama et al. used small molecules that directly bind and activate AMPK (A769662, MT63–78, and 991) and found that AMPK activation leads to increased mitochondrial fission (Toyama et al. 2016). They hypothesize that AMPK is a master regulator of mitochondrial homeostasis not only through promotion of mitochondrial biogenesis through activation of PGC-1 but also by promoting fission through direct phosphorylation of mitochondrial fission factor (MFF). They also note that AMPK is involved in autophagy through phosphorylation and activation of ULK1 (the initial component of the autophagy cascade) (Egan et al. 2011; Lee et al. 2010). These results suggest that targeting AMPK may be protective under conditions of stress, not only by increasing mitochondrial biogenesis but also through promoting the removal of damaged mitochondria.

Our group has found that treatment with metformin protects the RPE from sodium iodate-induced damage, an acute model of RPE injury (unpublished data). Metformin treatment is able to protect from sodium iodate-induced injury resulting in preserved RPE integrity, preserved retinal function, as measured by electroretinography (ERG), and preserved retinal morphology, as measured by spectral-domain optical coherence tomography (SD-OCT). We hypothesize that this protection to the RPE is due to activation of AMPK, which results in increased mitochondrial biogenesis and enhanced fission and mitophagy of damaged mitochondria. We aim to extend this knowledge to disease models of AMD to determine whether metformin can protect the RPE in a mouse model of chronic mitochondrial oxidative stress. We aim to further investigate the mechanisms of protection and determine whether protection is due to an increase in mitochondrial biogenesis, fission, and mitophagy.

## 2.6 Conclusions

Damage to mitochondrial morphology, increases in mitochondrial DNA lesions, and altered bioenergetics in mitochondrial haplogroups associated with AMD have been observed. It is now important to clarify whether these changes lead to disease pathogenesis or whether these changes are simply a "bystander effect" of other disease processes. Preliminary work from our group suggests that activation of AMPK is protective to the photoreceptors and to the RPE under stress conditions. It has been shown that AMPK is involved in regulation of energy homeostasis and importantly is involved in mitochondrial biogenesis, as well as fission and mitophagy. We hypothesize that mitochondrial dysfunction is a contributing factor to disease progression in AMD and that treatment with activators of AMPK will be protective to the RPE in AMD by increasing mitochondrial health through activation of these processes.

**Acknowledgements** Funding provided by NIH R01EY016459-11, Foundation Fighting Blindness, Clinical and Translational Science TL1 Scholar Award (CTSA), and an unrestricted departmental grant from Research to Prevent Blindness, Inc.

## References

Age-Related Eye Disease Study Research Group (2001) A randomized, placebo-controlled, clinical trial of high-dose supplementation with vitamins C and E, beta carotene, and zinc for age-related macular degeneration and vision loss: AREDS report no. 8. Arch Ophthalmol (United States) 119:1417–1436

Awh CC, Lane AM, Hawken S, Zanke B, Kim IK (2013) CFH and ARMS2 genetic polymorphisms predict response to antioxidants and zinc in patients with age-related macular degeneration. Ophthalmology (United States) 120:2317–2323

Awh CC, Hawken S, Zanke BW (2015) Treatment response to antioxidants and zinc based on CFH and ARMS2 genetic risk allele number in the age-related eye disease study. Ophthalmology (United States) 122:162–169

Bianchi E, Scarinci F, Ripandelli G, Feher J, Pacella E, Magliulo G, Gabrieli CB, Plateroti R, Plateroti P, Mignini F, Artico M (2013) Retinal pigment epithelium, age-related macular degeneration and neurotrophic keratouveitis. Int J Mol Med (Greece) 31:232–242

Brown MM, Brown GC, Sharma S, Stein JD, Roth Z, Campanella J, Beauchamp GR (2006) The burden of age-related macular degeneration: a value-based analysis. Curr Opin Ophthalmol (United States) 17:257–266

Burkewitz K, Zhang Y, Mair WB (2014) AMPK at the nexus of energetics and aging. Cell Metab (United States) 20:10–25

Chakravarthy U, Augood C, Bentham GC, de Jong PT, Rahu M, Seland J, Soubrane G, Tomazzoli L, Topouzis F, Vingerling JR, Vioque J, Young IS, Fletcher AE (2007) Cigarette smoking and age-related macular degeneration in the EUREYE study. Ophthalmology (United States) 114:1157–1163

Egan DF, Shackelford DB, Mihaylova MM, Gelino S, Kohnz RA, Mair W, Vasquez DS, Joshi A, Gwinn DM, Taylor R, Asara JM, Fitzpatrick J, Dillin A, Viollet B, Kundu M, Hansen M, Shaw RJ (2011) Phosphorylation of ULK1 (hATG1) by AMP-activated protein kinase connects energy sensing to mitophagy. Science (United States) 331:456–461

Espinosa-Heidmann DG, Suner IJ, Catanuto P, Hernandez EP, Marin-Castano ME, Cousins SW (2006) Cigarette smoke-related oxidants and the development of sub-RPE deposits in an experimental animal model of dry AMD. Invest Ophthalmol Vis Sci (United States) 47:729–737

Husler S, Schmid H (2013) Coping with wet age-related macular degeneration–a study from Switzerland. Klin Monbl Augenheilkd (Germany) 230:1251–1256

Itoh K, Nakamura K, Iijima M, Sesaki H (2013) Mitochondrial dynamics in neurodegeneration. Trends Cell Biol (England) 23(2):64–71

Kenney MC, Chwa M, Atilano SR, Falatoonzadeh P, Ramirez C, Malik D, Tarek M, Caceres-del-Carpio J, Nesburn AB, Boyer DS, Kuppermann BD, Vawter M, Jazwinski SM, Miceli M, Wallace DC, Udar N (2014) Inherited mitochondrial DNA variants can affect complement, inflammation and apoptosis pathways: insights into mitochondrial-nuclear interactions. Hum Mol Genet (England) 23:3537–3551

Lee JW, Park S, Takahashi Y, Wang HG (2010) The association of AMPK with ULK1 regulates autophagy. PLoS One (United States) 5:e15394

Medkour Y, Titorenko VI (2016) Mitochondria operate as signaling platforms in yeast aging. Aging (Albany NY) (United States) 8:212–213

Mueller EE, Schaier E, Brunner SM, Eder W, Mayr JA, Egger SF, Nischler C, Oberkofler H, Reitsamer HA, Patsch W, Sperl W, Kofler B (2012) Mitochondrial haplogroups and control region polymorphisms in age-related macular degeneration: a case-control study. PLoS One (United States) 7:e30874

Ojuka EO (2004) Role of calcium and AMP kinase in the regulation of mitochondrial biogenesis and GLUT4 levels in muscle. Proc Nutr Soc (England) 63:275–278

Pryor WA, Hales BJ, Premovic PI, Church DF (1983) The radicals in cigarette tar: their nature and suggested physiological implications. Science (United States) 220(4595):425–427

Sorensen S, White K, Mak W, Zanibbi K, Tang W, O'Hearn A, Hegel MT (2015) The macular degeneration and aging study: design and research protocol of a randomized trial for a psychosocial intervention with macular degeneration patients. Contemp Clin Trials (United States) 42:68–77

Terluk MR, Kapphahn RJ, Soukup LM, Gong H, Gallardo C, Montezuma SR, Ferrington DA (2015) Investigating mitochondria as a target for treating age-related macular degeneration. J Neurosci (United States) 35:7304–7311

Toyama EQ, Herzig S, Courchet J, Lewis TL Jr, Loson OC, Hellberg K, Young NP, Chen H, Polleux F, Chan DC, Shaw RJ (2016) Metabolism. AMP-activated protein kinase mediates mitochondrial fission in response to energy stress. Science (United States) 351:275–281

# Chapter 3
# Toll-Like Receptors and Age-Related Macular Degeneration


**Kelly Mulfaul, Maedbh Rhatigan, and Sarah Doyle**

**Abstract** Age-related macular degeneration (AMD) is the leading cause of central vision loss in the over 50s worldwide. Activation of the immune system has been implicated in disease progression, but while polymorphisms in genes associated with the immune system have been identified as risk factors for disease, the underlying pathways and mechanisms involved in disease progression remain incompletely characterised. Typically inflammatory responses are mediated by microbial infection; however, in chronic conditions, a form of 'sterile' inflammation exists whereby immune responses occur in areas of the body, in the absence of microbes; 'sterile' inflammation is likely to be central to AMD. In this case the innate immune response is triggered when alarm signals released by stressed cells or damaged tissue are identified by pattern recognition receptors (PRRs). Toll-like receptors (TLRs) are a family of membrane-spanning PRRs for which host-derived ligands have been identified; these include heat shock proteins, extracellular matrix breakdown products, mRNA from necrotic cells and modified lipids. Here we review the evidence for TLR involvement in the pathogenesis of AMD.

**Keywords** Age-related macular degeneration (AMD) · Inflammation · Immunity · Pattern recognition receptors (PRR) · Toll-like receptors (TLRs) · TLR2

K. Mulfaul
Department of Clinical Medicine, School of Medicine, Trinity College Dublin, Dublin 2, Ireland

M. Rhatigan
Department of Clinical Medicine, School of Medicine, Trinity College Dublin, Dublin 2, Ireland

Royal Victoria Eye and Ear Hospital, Dublin 2, Ireland

S. Doyle (✉)
Department of Clinical Medicine, School of Medicine, Trinity College Dublin, Dublin 2, Ireland

National Children's Research Centre, Our Lady's Children's Hospital Crumlin, Dublin 12, Ireland
e-mail: sarah.doyle@tcd.ie



J. D. Ash et al. (eds.), *Retinal Degenerative Diseases*, Advances in Experimental Medicine and Biology 891, https://doi.org/10.1007/978-3-319-75402-4_3

## 3.1 Introduction

Age-related macular degeneration (AMD) is the leading cause of central retinal blindness in people aged 55 years and older in the world. The prevalence of AMD is 8.7% worldwide, and due to exponential population ageing, the projected number of people with AMD is estimated at 196 million in 2020, increasing to 288 million in 2040 (Wong et al. 2014). AMD is a heterogeneous and multifactorial disease; environmental factors, age and genetic susceptibility all play a role in the development of the disease. Strong and consistent risk factors for late AMD are increasing age, current cigarette smoking and positive family history (Chakravarthy et al. 2010). AMD is characterised by the accumulation of extracellular deposits termed drusen between Bruch's membrane and the retinal pigment epithelium (RPE). Early disease is often asymptomatic and may be an incidental finding on dilated fundus examination showing macular drusen and/or pigmentary changes. There are two forms of late AMD; the most common is termed geographic atrophy (GA) or dry AMD where focal degeneration of photoreceptors, RPE and choriocapillaris in the macula impairs visual acuity in a progressive manner. Wet AMD, termed a priority eye disease by the WHO, occurs due to penetration of choroidal vasculature into the subretinal space; this is known as choroidal neovascularisation. In contrast to GA, patients who develop neovascular AMD present with rapid onset of blurred central vision and distortion often occurring over several days or weeks. Current gold standard care for wet AMD involves use of intra-vitreal injections of anti-vascular endothelial growth factor (VEGF) agents every 4–6 weeks. There are no pharmacological treatments for dry AMD. The innate immune system is believed to play an important role in the pathogenesis of AMD; however the pathways involved remain unclear.

## 3.2 Sterile Inflammation and Pattern Recognition Receptors

Inflammation is a homeostatic biological response to defend the host from both infectious and non-infectious agents, to clear the body of the noxious stimuli and to restore status quo. The acute inflammatory response is characterised by the recruitment and activation of inflammatory cells, cytokine and chemokine production, increased vasodilation and subsequent vascular permeability. The five cardinal signs of acute inflammation are redness, swelling, heat, pain and loss of function. The inflammatory response that occurs in AMD occurs in the absence of infection, a so-called sterile inflammation, and does not show these signs of acute inflammation; rather it appears to be low-grade and chronic. Sterile inflammation occurs in response to a growing list of modified host-derived elements ranging from oxidised lipids or lipoproteins to deposits of protein/lipid aggregates or particulate matter (Rock et al. 2010). These stimuli trigger activation of pattern recognition receptors (PRRs) of the innate immune system, and, as they are not easily cleared, they

persist, causing over-activation of the immune system and contributing to the pathogenesis of disease.

PRRs are ancient evolutionarily conserved receptors that recognise sets of molecules on foreign organisms termed pathogen-associated molecular patterns (PAMPs) and endogenous molecules termed damage-associated molecular patterns (DAMPs). PAMPs are usually essential to the life cycle or existence of a pathogen but are not found in mammalian cells, such as bacterial lipopolysaccharides (Liew et al. 2005). DAMPs tend to be endogenous molecules either modified or released in times of cellular stress or injury. Necrotic cell death results in the rapid loss of membrane integrity and the release of intracellular DAMPs. NLRP3 is one PRR that has recently come under intense scrutiny in the context of AMD (its potential role in AMD is reviewed in Celkova et al. (2015)). This chapter will focus on reviewing what is known about Toll-like receptors (TLRs) in AMD.

## 3.3 Toll-Like Receptors

TLRs are a family of membrane-bound PRRs located either on the cell surface or in endosomal compartments. Ten human TLRs have been identified, five of which are broadly antibacterial (TLR1, TLR2, TLR4, TLR5, TLR6) and four of which are antiviral (TLR3, TLR7, TLR8, TLR9). Originally known for recognising pathogens, it is now accepted that TLRs also recognise and respond to disturbances in homeostasis through endogenous ligands. TLRs have a cytosolic Toll/IL-1 receptor (TIR) domain which is necessary for signal transduction and a horseshoe-shaped extracellular or intraluminal leucine-rich repeat (LRR) domain, required for ligand binding. The activation of TLRs initiates signal transduction pathways that determine the type and duration of the inflammatory response (Akira et al. 2001; Underhill and Ozinsky 2002; Kawai and Akira 2010). Upon encountering their cognate PAMP/DAMP, TLR homo- or heterodimers become active and recruit downstream signalling proteins to orchestrate a pro-inflammatory response. TLR4 is the most complex of all the TLRs engaging all four of the TIR adaptor proteins: MyD88, MyD88 adaptor-like protein (Mal), TIR domain-containing adaptor-inducing IFN-β (TRIF) and TRIF-related adaptor molecule (TRAM). Binding of LPS to the TLR4 complex causes recruitment of the bridging adaptor proteins Mal and TRAM. Mal and TRAM are sorting adaptors that recruit and control the localisation of the signalling adaptors MyD88 and TRIF, respectively, to TLR4 (Kagan and Medzhitov 2006; O'Neill and Bowie 2007; Kagan et al. 2008; Jenkins and Mansell 2010; Gay et al. 2011). A TLR4/Mal/MyD88 complex is formed at the plasma membrane (Kagan and Medzhitov 2006). This complex mediates MyD88-dependent signalling from the plasma membrane via IL-1R-associated kinases (IRAKs) and TNFR-associated factor 6 (TRAF6), leading to activation of mitogen-activated protein kinases (MAPKs) and transcription factors AP-1 and NFκB. A TLR4/TRAM/TRIF complex is formed at the membrane of endosomal compartments, and this signals via TRAF3 to activate the transcription factor IFN regulatory factor 3 (IRF3) (Kagan

et al. 2008). For TLR4 signalling, Mal-dependent NFκB activation upregulates inflammatory genes such as TNF-α, while TRAM-dependent IRF3 activation causes induction of IFNβ. TLR2 heterodimerises with either TLR1 or TLR6 and recognises diacylated and triacylated lipopeptides (Takeuchi et al. 2001, 2002). Similar to TLR4 signalling, Mal acts as a bridging adaptor between the TLR2 receptor complex and MyD88, although high TLR2 ligand concentrations can overcome the requirement for Mal in the signalling pathway, while some downstream TLR2 signals are entirely Mal-independent (Kenny et al. 2009; Santos-Sierra et al. 2009). TLR3 recognises and responds to dsRNA or its mimic Poly(I:C). TLR3 is the only TLR that does not utilise the MyD88 adaptor protein, instead binding TRIF directly and signalling mainly to activate IRF3 to induce IFNα/β (Doyle et al. 2002). TLR7, TLR8 and TLR9 similarly respond to nucleic acids and are found in endosomes, TLR7 and TLR8 recognise ssRNA and imiquimods, while TLR9 recognises unmethylated CpG-rich dsDNA. Each of these TLRs recruits MyD88 to engage its signalling pathways, preferentially activating the IRFs to induce an antiviral-type response (Kawai and Akira 2007).

## 3.4 Genetic Associations of TLR Family and AMD

TLRs, and in particular TLR2 and TLR4, have been found to play active roles in protection against infection in the anterior region of the eye (Kindzelskii et al. 2004; Kumar and Yu 2006). Investigations into roles for TLRs in AMD, however, are sparse and are mainly confined to genetic investigations. Genetic variation in TLRs and their signalling proteins have been described, and there has been a growing interest in the role these genetic variations play in both infectious and inflammatory disease susceptibility. As TLRs function to initiate a potent inflammatory signalling cascade, genetic variation resulting in either an overtly exuberant or inefficient inflammatory response would therefore be expected to influence the pathogenesis of disease. Polymorphisms in TLR2, TLR3, TLR4 and TLR7 have been investigated for associations with AMD (see Table 3.1). The earliest report assessed two variants of TLR4 and found an association between rs4986790 and increased risk of AMD (Zareparsi et al. 2005); however subsequent studies do not observe this association in either a Turkish or Indian population (Kaur et al. 2006; Güven et al. 2015). A single study has similarly failed to show an association between TLR7 and AMD (Edwards et al. 2008). Several contradictory reports have investigated TLR3 rs3775291 with AMD. Initially it was reported to be protective in GA in a Caucasian population (Yang et al. 2008); however, this association was not observed in multiple other populations (Caucasian, Chinese, Indian) (Edwards et al. 2008; Cho et al. 2009; Sng et al. 2010; Cheng et al. 2014; Sharma et al. 2014). Subsequently a meta-analysis of a large cohort of patients of different descent has suggested that rs3775291 is associated with AMD in the Caucasian and not Asian populations (Ma et al. 2016). Most recently rs5743708 in TLR2 has been associated with increased risk of AMD in a Turkish population; this remains to be confirmed in further population studies (Güven et al. 2015).

**Table 3.1** A list of reported genetic variants of TLR family receptors and their association status with risk for AMD

| Gene | SNP | Population | Association | Reference |
|---|---|---|---|---|
| TLR2 | rs5743708 | Turkey | Yes | Güven et al. (2015) |
| TLR3 | rs3775291 | American European descent | Protective T(GA) | Yang et al. (2008) |
| | rs3775291 | American Caucasian | X | Edwards et al. (2008) |
| | rs3775291<br>rs4986790 | National Eye Institute Clinical Center, the Age-Related Eye Disease Study (ARDES), the Blue Mountains Eye Study | X | Cho et al. (2009) |
| | rs3775291 | Chinese | X | Sng et al. (2011) |
| | rs3775291 | Chinese | X | Cheng et al. (2014) |
| | rs3775291 | North Indian | X | Sharma et al. (2014) |
| | rs3775291 | Caucasian<br>Asian | Yes<br>X | Ma et al. (2016) |
| TLR4 | rs4986790 | Caucasian | Yes | Zareparsi et al. (2005) |
| | rs4986791 | | X | |
| | rs4986790 | Indian | X | Kaur et al. (2006) |
| | rs4986791 | | X | |
| | rs4986790 | Turkey | X | Güven et al. (2015) |
| | rs498791 | | X | |
| TLR7 | rs179008 | American Caucasian | X | Edwards et al. (2008) |

## 3.5 TLR Activation of the Retinal Pigment Epithelium

TLR1–7, TLR9 and TLR10 are expressed by RPE cells. TLR3 activation of RPE results in an increase in the production of IL-6, IL-8, MCP-1 and sICAM-1 cytokines (Kumar et al. 2004). Whereas TLR9 activation only increased production of IL-8 and has been shown to enhance phagocytosis by RPE cells, suggesting dsRNA (TLR3) not dsDNA (TLR9) induces inflammatory changes in the RPE (Ebihara et al. 2007). Brosig et al. reported changes in the expression of TLRs, transcription factors, angiogenic growth factors, pro-inflammatory cytokines and complement factors in response to poly (I:C), while only moderate changes were observed in response to CpG-ODN (Brosig et al. 2015). In addition TLR3 activation on RPE

cells has been shown to induce activation of IL-6, IL-1beta and Cox2 in microglia (Klettner et al. 2014). A further study attributed another important function to plasma membrane-bound TLR4 in RPE cells. RPE mediates the recognition and clearance of effective photoreceptor outer segments (POS), a process central to the maintenance of normal vision. Exposure of human RPE cells to human, but not bovine POS, elicited transmembrane metabolic and calcium signals within RPE cells in a TLR4-dependent manner (Kindzelskii et al. 2004).

## 3.6 TLR Activation and AMD

In a sterile environment, TLRs recognise host products that are mis-localised or have acquired the appearance of 'non-self'. In the context of AMD, it has been suggested that a change in lipid constitution of the plasma membrane can force TLRs into lipid rafts allowing for proximity-enabled activation (Levy et al. 2015). Alternatively, carboxyethyl-pyrrole (CEP), an oxidative-stress modification found in the retina in AMD, is a TLR1/TLR2 ligand conceivably activating TLR2 in AMD (West et al. 2010). TLR3 is purported to be activated by RNA released from degenerating photoreceptors in genetic models of retinal degeneration (Shiose et al. 2011), a response that is also likely to occur during the neurodegeneration observed in AMD. While breakdown products of the extracellular matrix generated during tissue malfunction (Jiang et al. 2005) and oxidised plasma membrane (oxPAPC) present at sites of tissue injury (Imai et al. 2008) are recognised by the CD14/TLR4 complex, again these products are most likely available in the environment of the AMD eye.

Oxidative stress is thought to be a key trigger involved in the pathogenesis of AMD. The retina is an optimal environment for the generation of oxidative protein modifications due to incoming light and a high oxygen environment. Oxidative stress is the damage that occurs to cells by reactive oxygen species (ROS). With age, the digestion of photoreceptor outer segments becomes less efficient resulting in the accumulation of lipofuscin. When lipofuscin is exposed to visible light, ROS are generated, resulting in an accumulation of ROS in RPE cells (Khandhadia and Lotery 2010). Incoming light and a high oxygen supply provide an optimal environment for the generation of ROS. ROS damage lipids by a mechanism called lipid peroxidation. A number of proteins found in drusen contain such modifications (Crabb et al. 2002). Of note, carboxyethyl-pyrrole (CEP)-adducted proteins are abundant in the eyes and serum of patients with AMD compared with controls. CEP modifications are generated by the oxidation of docosahexaenoate (DHA)-containing lipids. DHA is found at high levels in the outer segments of photoreceptor cells. CEP has been reported to act as a TLR2 ligand on endothelial cells inducing angiogenesis in a VEGF-dependent manner (West et al. 2010; Doyle et al. 2012) and on macrophages priming cells for inflammasome activation. Given CEP's localisation and abundance in AMD patients and these downstream effects of CEP

activation of TLR2, it has been proposed as an endogenous DAMP for TLR2 activation in AMD (West et al. 2010, Doyle et al. 2012). TLRs can regulate autophagy (Delgado et al. 2008), and in parallel with the broad NFκB-dependent pro-inflammatory gene expression upregulated by TLR2, and its ability to induce endothelial cell angiogenesis (West et al. 2010), there is evidence that increased TLR2 activation specifically may in some cases block autophagy (Delgado et al. 2008), the method by which cells recycle old and damaged organelles (Levine and Klionsky 2004). This selection of TLR2-mediated effects is particularly interesting for the pathogenesis of AMD as aberrant angiogenesis causes choroidal neovascularisation and the onset of 'wet' AMD; and inefficient autophagy is purported to be involved in the deposition of drusen (Wang et al. 2009) and suggests there may be utility in blocking TLR2 activation in AMD. Furthermore, *Chlamydia pneumoniae* has been detected in human CNV samples but not in control eyes without AMD (Kalayoglu et al. 2005), and TLR2 activation by *Chlamydia pneumoniae* has been shown to enhance the development of laser-induced CNV (Fujimoto et al. 2010) lending support to the concept that TLR2 may involve disease pathogenesis.

## 3.7 Concluding Remarks

The field of Toll-like receptor research in the pathology of AMD is in its infancy. Despite this, the small amount of direct evidence of TLR activation in AMD taken together with the broad range of purported TLR 'self'-ligands most likely present in the environment of the AMD eye provides a tantalising foundation to hypothesise that TLRs play an important role in the progression of this blinding disease. Whether this is true will only be discovered through further research in this exciting area of immunobiology of AMD.

## References

Akira S, Takeda K, Kaisho T (2001) Toll-like receptors: critical proteins linking innate and acquired immunity. Nat Immunol 2:675–680

Brosig A, Kuhrt H, Wiedemann P, Kohen L, Bringmann A, Hollborn M (2015) Gene expression regulation in retinal pigment epithelial cells induced by viral RNA and viral/bacterial DNA. Mol Vis 21:1000

Celkova L, Doyle SL, Campbell M (2015) NLRP3 inflammasome and pathobiology in AMD. J Clin Med 4:172–192

Chakravarthy U, Wong TY, Fletcher A, Piault E, Evans C, Zlateva G, Buggage R, Pleil A, Mitchell P (2010) Clinical risk factors for age-related macular degeneration: a systematic review and meta-analysis. BMC Ophthalmol 10:31

Cheng Y, Li M, Li H, Zeng W, Zhou P, Huang L, Li X, Sun Y (2014) Toll-like receptor 3 polymorphism is not associated with neovascular age-related macular degeneration and polypoidal choroidal vasculopathy in the Chinese. Genet Mol Res 13:302–309

Cho Y, Wang JJ, Chew EY, Ferris FL, Mitchell P, Chan C-C, Tuo J (2009) Toll-like receptor polymorphisms and age-related macular degeneration: replication in three case–control samples. Invest Ophthalmol Vis Sci 50:5614–5618

Crabb JW, Miyagi M, Gu X, Shadrach K, West KA, Sakaguchi H, Kamei M, Hasan A, Yan L, Rayborn ME, Salomon RG, Hollyfield JG (2002) Drusen proteome analysis: an approach to the etiology of age-related macular degeneration. Proc Natl Acad Sci U S A 99:14682–14687

Delgado MA, Elmaoued RA, Davis AS, Kyei G, Deretic V (2008) Toll-like receptors control autophagy. EMBO J 27:1110–1121

Doyle SE, Vaidya SA, O'Connell R, Dadgostar H, Dempsey PW, Wu T-T, Rao G, Sun R, Haberland ME, Modlin RL (2002) IRF3 mediates a TLR3/TLR4-specific antiviral gene program. Immunity 17:251–263

Doyle SL, Campbell M, Ozaki E, Salomon RG, Mori A, Kenna PF, Farrar GJ, Kiang AS, Humphries MM, Lavelle EC, O'Neill LA, Hollyfield JG, Humphries P (2012) NLRP3 has a protective role in age-related macular degeneration through the induction of IL-18 by drusen components. Nat Med 18:791–798

Ebihara N, Chen L, Tokura T, Ushio H, Iwatsu M, Murakami A (2007) Distinct functions between Toll-like receptors 3 and 9 in retinal pigment epithelial cells. Ophthalmic Res 39:155–163

Edwards AO, Chen D, Fridley BL, James KM, Wu Y, Abecasis G, Swaroop A, Othman M, Branham K, Iyengar SK, Sivakumaran TA, Klein R, Klein BE, Tosakulwong N (2008) Toll-like receptor polymorphisms and age-related macular degeneration. Invest Ophthalmol Vis Sci 49:1652–1659

Fujimoto T, Sonoda K-H, Hijioka K, Sato K, Takeda A, Hasegawa E, Oshima Y, Ishibashi T (2010) Choroidal neovascularization enhanced by Chlamydia pneumoniae via Toll-like receptor 2 in the retinal pigment epithelium. Invest Ophthalmol Vis Sci 51:4694–4702

Gay NJ, Gangloff M, O'Neill LA (2011) What the Myddosome structure tells us about the initiation of innate immunity. Trends Immunol 32:104–109

Güven M, Batar B, Mutlu T, Bostancı M, Mete M, Aras C, Ünal M (2015) Toll-like receptors 2 and 4 polymorphisms in age-related macular degeneration. Curr Eye Res:1–6

Imai Y, Kuba K, Neely GG, Yaghubian-Malhami R, Perkmann T, van Loo G, Ermolaeva M, Veldhuizen R, Leung YC, Wang H (2008) Identification of oxidative stress and Toll-like receptor 4 signaling as a key pathway of acute lung injury. Cell 133:235–249

Jenkins KA, Mansell A (2010) TIR-containing adaptors in Toll-like receptor signalling. Cytokine 49:237–244

Jiang D, Liang J, Fan J, Yu S, Chen S, Luo Y, Prestwich GD, Mascarenhas MM, Garg HG, Quinn DA (2005) Regulation of lung injury and repair by Toll-like receptors and hyaluronan. Nat Med 11:1173–1179

Kagan JC, Medzhitov R (2006) Phosphoinositide-mediated adaptor recruitment controls Toll-like receptor signaling. Cell 125:943–955

Kagan JC, Su T, Horng T, Chow A, Akira S, Medzhitov R (2008) TRAM couples endocytosis of Toll-like receptor 4 to the induction of interferon-β. Nat Immunol 9:361–368

Kalayoglu MV, Bula D, Arroyo J, Gragoudas ES, D'Amico D, Miller JW (2005) Identification of Chlamydia pneumoniae within human choroidal neovascular membranes secondary to age-related macular degeneration. Graefes Arch Clin Exp Ophthalmol 243:1080–1090

Kaur I, Hussain A, Hussain N, Das T, Pathangay A, Mathai A, Hussain A, Nutheti R, Nirmalan PK, Chakrabarti S (2006) Analysis of CFH, TLR4, and APOE polymorphism in India suggests the Tyr402His variant of CFH to be a global marker for age-related macular degeneration. Invest Ophthalmol Vis Sci 47:3729–3735

Kawai T, Akira S (2007) Antiviral signaling through pattern recognition receptors. J Biochem 141:137–145

Kawai T, Akira S (2010) The role of pattern-recognition receptors in innate immunity: update on Toll-like receptors. Nat Immunol 11:373–384

Kenny EF, Talbot S, Gong M, Golenbock DT, Bryant CE, O'Neill LA (2009) MyD88 adaptor-like is not essential for TLR2 signaling and inhibits signaling by TLR3. J Immunol 183:3642–3651

Khandhadia S, Lotery A (2010) Oxidation and age-related macular degeneration: insights from molecular biology. Expert Rev Mol Med 12:e34

Kindzelskii AL, Elner VM, Elner SG, Yang D, Hughes BA, Petty HR (2004) Toll-like receptor 4 (TLR4) of retinal pigment epithelial cells participates in transmembrane signaling in response to photoreceptor outer segments. J Gen Physiol 124:139–149

Klettner A, Hamann T, Schlüter K, Lucius R, Roider J (2014) Retinal pigment epithelium cells alter the pro-inflammatory response of retinal microglia to TLR-3 stimulation. Acta Ophthalmol 92:e621-e629

Kumar A, Yu F-SX (2006) Toll-like receptors and corneal innate immunity. Curr Mol Med 6:327–337

Kumar MV, Nagineni CN, Chin MS, Hooks JJ, Detrick B (2004) Innate immunity in the retina: Toll-like receptor (TLR) signaling in human retinal pigment epithelial cells. J Neuroimmunol 153:7–15

Levine B, Klionsky DJ (2004) Development by self-digestion: molecular mechanisms and biological functions of autophagy. Dev Cell 6:463–477

Levy O, Calippe B, Lavalette S, Hu SJ, Raoul W, Dominguez E, Housset M, Paques M, Sahel JA, Bemelmans AP (2015) Apolipoprotein E promotes subretinal mononuclear phagocyte survival and chronic inflammation in age-related macular degeneration. EMBO Mol Med 7:211–226

Liew FY, Xu D, Brint EK, O'Neill LA (2005) Negative regulation of Toll-like receptor-mediated immune responses. Nat Rev Immunol 5:446–458

Ma L, Tang FY, Chu WK, Young AL, Brelen ME, Pang CP, Chen LJ (2016) Association of Toll-like receptor 3 polymorphism rs3775291 with age-related macular degeneration: a systematic review and meta-analysis. Sci Rep 6:19718

O'Neill LA, Bowie AG (2007) The family of five: TIR-domain-containing adaptors in Toll-like receptor signalling. Nat Rev Immunol 7:353–364

Rock KL, Latz E, Ontiveros F, Kono H (2010) The sterile inflammatory response. Annu Rev Immunol 28:321

Santos-Sierra S, Deshmukh SD, Kalnitski J, Küenzi P, Wymann MP, Golenbock DT, Henneke P (2009) Mal connects TLR2 to PI3Kinase activation and phagocyte polarization. EMBO J 28:2018–2027

Sharma NK, Sharma K, Gupta A, Prabhakar S, Singh R, Gupta PK, Anand A (2014) Does Toll-like receptor-3 (TLR-3) have any role in Indian AMD phenotype? Mol Cell Biochem 393:1

Shiose S, Chen Y, Okano K, Roy S, Kohno H, Tang J, Pearlman E, Maeda T, Palczewski K, Maeda A (2011) Toll-like receptor 3 is required for development of retinopathy caused by impaired all-trans-retinal clearance in mice. J Biol Chem 286:15543–15555

Sng CC, Cackett PD, Yeo IY, Thalamuthu A, Venkatraman A, Venkataraman D, Koh AH, Tai E-S, Wong TY, Aung T (2010) Toll-like receptor 3 polymorphism rs3775291 is not associated with choroidal neovascularization or polypoidal choroidal vasculopathy in Chinese subjects. Ophthalmic Res 45:191–196

Sng CC1, Cackett PD, Yeo IY, Thalamuthu A, Venkatraman A, Venkataraman D, Koh AH, Tai ES, Wong TY, Aung T, Vithana EN (2011). Toll-like receptor 3 polymorphism rs3775291 is not associated with choroidal neovascularization or polypoidal choroidal vasculopathy in Chinese subjects. Ophthalmic Res 45:191–196. https://doi.org/10.1159/000321387. Epub 2010 Nov 16

Takeuchi O, Kawai T, Mühlradt PF, Morr M, Radolf JD, Zychlinsky A, Takeda K, Akira S (2001) Discrimination of bacterial lipoproteins by Toll-like receptor 6. Int Immunol 13:933–940

Takeuchi O, Sato S, Horiuchi T, Hoshino K, Takeda K, Dong Z, Modlin RL, Akira S (2002) Cutting edge: role of Toll-like receptor 1 in mediating immune response to microbial lipoproteins. J Immunol 169:10–14

Underhill DM, Ozinsky A (2002) Toll-like receptors: key mediators of microbe detection. Curr Opin Immunol 14:103–110

Wang AL, Lukas TJ, Yuan M, Du N, Tso MO, Neufeld AH (2009) Autophagy, exosomes and drusen formation in age-related macular degeneration. Autophagy 5:563–564

West XZ, Malinin NL, Merkulova AA, Tischenko M, Kerr BA, Borden EC, Podrez EA, Salomon RG, Byzova TV (2010) Oxidative stress induces angiogenesis by activating TLR2 with novel endogenous ligands. Nature 467:972–976

Wong WL, Su X, Li X, Cheung CMG, Klein R, Cheng C-Y, Wong TY (2014) Global prevalence of age-related macular degeneration and disease burden projection for 2020 and 2040: a systematic review and meta-analysis. Lancet Glob Health 2:e106–16

Yang Z, Stratton C, Francis PJ, Kleinman ME, Tan PL, Gibbs D, Tong Z, Chen H, Constantine R, Yang X (2008) Toll-like receptor 3 and geographic atrophy in age-related macular degeneration. N Engl J Med 359:1456–1463

Zareparsi S, Buraczynska M, Branham KE, Shah S, Eng D, Li M, Pawar H, Yashar BM, Moroi SE, Lichter PR (2005) Toll-like receptor 4 variant D299G is associated with susceptibility to age-related macular degeneration. Hum Mol Genet 14:1449–1455

# Chapter 4
# Alterations in Extracellular Matrix/Bruch's Membrane Can Cause the Activation of the Alternative Complement Pathway via Tick-Over

**Rosario Fernandez-Godino**

**Abstract** Given the complex etiology of age-related macular degeneration (AMD), treatments are developed to target intermediate/late stages of the disease. Unfortunately, the design of therapies for early stages of the disease is limited by our understanding of the mechanisms involved in the formation of basal deposits and drusen, the first clinical signs of AMD. During the last decade, the identification of common and rare alleles in complement genes as risk AMD variants in addition to the presence of active complement components in basal deposits and drusen has provided compelling evidence that the complement system plays a key role in the pathobiology of AMD. However, the mechanisms for complement activation in AMD are unknown. Here we propose that the activation of the complement system is a consequence of alterations in the aged extracellular matrix (ECM) of the retinal pigment epithelium (RPE)/Bruch's membrane (BrM), which favors the anchoring of complement C3b generated by convertase-independent cleavage of C3 via tick-over and produces a chronic activation of the alternative complement pathway.

**Keywords** AMD · Complement · Tick-over · C3 · RPE · Bruch's membrane · Drusen · Basal deposits · C3(H2O) · C3(H2O)Bb-convertase · Anticomplement drugs

R. Fernandez-Godino (✉)
Ocular Genomics Institute, Massachusetts Eye and Ear Infirmary, Harvard Medical School, Boston, MA, USA
e-mail: rosario_godino@meei.harvard.edu



J. D. Ash et al. (eds.), *Retinal Degenerative Diseases*, Advances in Experimental Medicine and Biology 891, https://doi.org/10.1007/978-3-319-75402-4_4

## 4.1 Introduction

AMD is the most common cause of vision loss in elderly people in developed countries. Given the diverse etiology of AMD, treatments are developed to target intermediate and late stages of the disease, and there is no effective therapy for early AMD (Miller 2013a). The development of anti-VEGF therapies for choroidal neovascularization has been a major advance, and the AREDS trial showed some benefit of antioxidant supplementation for slowing AMD progression in patients with intermediate disease, but therapies for the more common atrophic form of AMD are necessary to prevent vision loss (Evans and Lawrenson 2012; Miller 2013b).

The first clinical sign of AMD is the formation of deposits and drusen between the basal lamina of the RPE and the BrM (Sarks et al. 1999). Although the mechanisms of deposit formation are not fully understood, some authors support the hypothesis that drusen is an inflammatory process (Mullins et al. 2000; Hageman et al. 2001; Anderson et al. 2002). Indeed, genetic variants in complement genes, such as *CFH*, *C3*, *CFB*, *CFI*, *C9*, and *C2*, have been associated with AMD (Hageman et al. 2005; Seddon et al. 2013). Further, active complement components have been identified in basal deposits and drusen, but their functional role in drusen formation remains to be defined (Mullins et al. 2000; Crabb et al. 2002; Wang et al. 2010; Garland et al. 2014).

Studies in mouse models also demonstrate a key role for the complement in the formation of basal laminar deposits (Fu et al. 2007; Ding et al. 2014, Fernandez-Godino 2015 #389; Garland et al. 2014). Thus, understanding the role of the complement system in early stages of AMD may help to design complement-modulating therapies that prevent the progression of drusen to geographic atrophy or neovascular AMD.

## 4.2 Activation of the Alternative Complement Pathway via Tick-Over Process

The complement system is a part of the innate immune system usually activated by external insults via three pathways: classical, lectin, and alternative (Ricklin et al. 2010). However, the complement system has the potential to be damaging to host tissues; hence, it is tightly regulated by complement-regulating proteins, such as CFH, CFI, DAF, etc. (Fig. 4.1) (Ricklin et al. 2010).

Under normal conditions, the alternative complement pathway can be activated by the tick-over process; C3 can be cleaved by convertase-independent proteolysis or physiological hydrolysis of its internal thioester, generating free C3b or C3(H2O) respectively, and C3a (Lachmann and Halbwachs 1975; Pangburn et al. 1981; Nilsson and Nilsson Ekdahl 2012) (Fig. 4.1). C3(H2O) is functionally similar to C3b and presents high affinity to adsorb surfaces, such as lipids or biomaterials (Pangburn et al. 1981; Andersson et al. 2005; Bexborn et al. 2008), and it has been

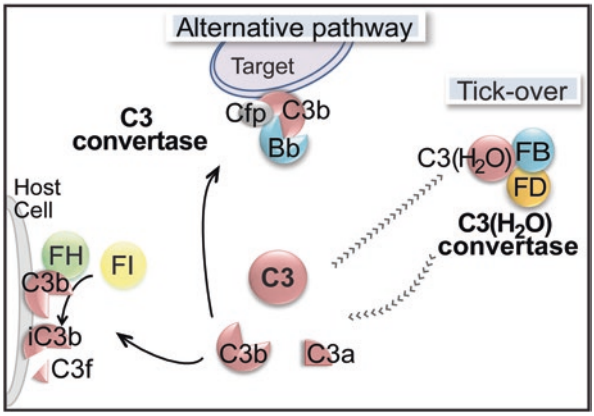


**Fig. 4.1** Schematic representation of the alternative complement pathway and tick-over process. C3 is cleaved to C3a and C3b, which forms C3-convertase unless it is inactivated by CFH and CFI. C3 is spontaneously hydrolyzed to C3(H2O) via tick-over process. C3(H2O) is functionally similar to C3b and binds CFB to form the C3(H2O)Bb-convertase, which is not recognized by CFH for inactivation

demonstrated to bind ECM proteins, such as collagen IV, fibronectin, and especially laminin (Leivo and Engvall 1986). C3(H2O) deposited on surfaces binds CFB, which is cleaved to Bb and Ba by CFD, creating a C3(H2O)Bb-convertase capable of binding complement receptors and activating the alternative pathway (Fig. 4.1) (Nilsson and Nilsson Ekdahl 2012), but that cannot be regulated by CFH and CFI (Andersson et al. 2005; Bexborn et al. 2008). Indeed, it has been postulated that CFB preferentially binds C3b/C3(H2O) bound to foreign surfaces, while CFH has major affinity for C3b bound to host surfaces to prevent C3b deposition in autologous tissue (Atkinson and Farries 1987). It is possible that changes in the BrM due to aging favor the anchoring of C3b/C3(H2O) to its ECM, which would enhance the local activation of the alternative complement pathway.

## 4.3 The Role of the Tick-Over Pathway in Basal Deposit Formation in AMD

With age, the BrM undergoes changes in structure and composition, and there is an accumulation of membranous debris, proteins, and lipids (Sarks et al. 1999; Curcio and Johnson. 2013). In AMD, material secreted by the RPE, especially collagen, is accumulated in the region of the macula and causes the thickening of the BrM and the formation of basal laminar deposits under the RPE (Hogan and Alvarado 1967; Reale et al. 2009). Given the affinity of C3(H2O) to adsorb biosurfaces, the tick-over process may play an important role in the formation of basal deposits in dry AMD. We think that the abnormal structure/composition of the aged BrM, as well

as the accumulation of proteins and lipids, may favor the anchoring of C3(H2O) generated by the physiological hydrolysis of C3. C3(H2O) would be recognized by CFB to form a C3(H2O)Bb-convertase that is deposited to the BrM in a stable manner and triggers the chronic activation of complement through the alternative pathway. Changes in extracellular matrix cause RPE cells to make basal deposits and activate the alternative complement pathway (Fernandez-Godino et al. 2018). This process generates more C3b and creates a positive feedback loop that results in increased release of the anaphylatoxin C3a, which initiates a local inflammatory process (Hindmarsh and Marks 1998; Harboe and Mollnes 2008). To support this hypothesis, C3a has been detected in basal deposits and drusen and has been reported to cause deposit formation by RPE cells in vitro (Nozaki et al. 2006; Fernandez-Godino et al. 2015). Moreover, we have shown that C3a produced locally by RPE cells stimulates deposit formation, suggesting that C3a is a potential target for therapeutic intervention (Fernandez-Godino et al. 2015).

## 4.4 Complement-Modulating Drugs to Treat AMD

The role of the complement system in deposit formation has led to the development of several anticomplement drugs, mostly directed to block complement activation through the alternative pathway, which are being tested in clinical trials but have not had significant success to date (Ricklin and Lambris 2013; Garcia Filho et al. 2014; Yehoshua et al. 2014). For example, drugs that block the terminal complement component C5 administered systemically have not shown any benefit in dry AMD patients (Garcia Filho et al. 2014; Yehoshua et al. 2014). Phase II trials using lampalizumab showed that inhibition of CFD reduced geographic atrophy only in some patients, although Phase III trials have been initiated (NCT02247531, NCT02247479).

There is controversy about which complement pathway is first initiated in AMD. Because C3 plays a central role in the activation of complement system through any of the three pathways, it is an attractive target for complement-modulating therapy administered locally. Compstatin is a peptide that inhibits complement activation by binding C3 and interfering with the formation of C3-convertase and C3 cleavage (Mastellos et al. 2015). The clinical efficacy of compstatin for AMD has been demonstrated in Phase I studies in patients (Mastellos et al. 2015). Further, POT-4, a compstatin analog with improved activity, was developed, but did not show efficacy in Phase II clinical trials (Clin Trial NCT01603043) (Qu et al. 2013).

In conclusion, complement-modulating therapies have shown some promising results; however, the design of novel drugs is limited by our understanding of the process of complement activation in AMD. Also, it remains unclear if regulation of the complement system locally or systemically is needed for the most effective treatment of AMD or at what stage of disease these treatments can be most usefully applied.

## 4.5 C3(H2O)Bb-Convertase and Response to Complement-Modulating Therapies

As previously mentioned, C3(H2O) generated by the hydrolysis of C3 is functionally similar to C3b because it can bind complement receptors and form C3(H2O)Bb- convertase (Nilsson and Nilsson Ekdahl 2012). However, the epitope recognized by CFH in C3b is not exposed in C3(H2O); thus, the formation of C3(H2O)Bb-convertase cannot be inhibited via CFH (Andersson et al. 2005; Bexborn et al. 2008). Alternatively, C3(H2O) can be inactivated by CFI and another cofactor, but the inactivation rate is much slower than the normal inactivation of C3b (Pangburn et al. 1981).

Differential activation of C3 via the alternative pathway or tick-over in AMD also has important consequences in response to complement-modulating drugs. Compstatin does not block or prevent the convertase-independent cleavage of C3 (Mastellos et al. 2015), which would explain the low efficiency of this drug in AMD patients. Thus, regarding therapies to treat AMD, an alternative approach may be needed to block local complement activation in basal deposits. Our hypothesis for the activation of complement system via tick-over caused by degeneration of ECM/BrM opens new avenues for the development of pharmaceutical compounds never considered for AMD to date, for example, regulators of the ECM synthesis and turnover, which have shown to be key for other human diseases like cancer, fibrosis, or cardiovascular disease (Tziakas et al. 2005; Overall and Kleifeld 2006; Sivakumar and Das 2008). Further, the local administration of complement-modulating drugs in combination with ECM-modulating drugs could avoid or at least delay the progression of the disease to legal blindness in dry AMD patients without compromising the whole immune system or vital biological processes.

## References

Anderson DH, Mullins RF, Hageman GS et al (2002) A role for local inflammation in the formation of drusen in the aging eye. Am J Ophthalmol 134:411–431

Andersson J, Ekdahl KN, Lambris JD et al (2005) Binding of C3 fragments on top of adsorbed plasma proteins during complement activation on a model biomaterial surface. Biomaterials 26:1477–1485

Atkinson JP, Farries T (1987) Separation of self from non-self in the complement system. Immunol Today 8:212–215

Bexborn F, Andersson PO, Chen H et al (2008) The tick-over theory revisited: formation and regulation of the soluble alternative complement C3 convertase (C3(H2O)Bb). Mol Immunol 45:2370–2379

Crabb JW, Miyagi M, Gu X et al (2002) Drusen proteome analysis: an approach to the etiology of age-related macular degeneration. Proc Natl Acad Sci U S A 99:14682–14687

Curcio CA, Johnson M (2013) Structure, function, and pathology of Bruch's membrane. Retina 1:465–481

Ding JD, Kelly U, Groelle M et al (2014) The role of complement dysregulation in AMD mouse models. Adv Exp Med Biol 801:213–219

Evans JR, Lawrenson JG (2012) Antioxidant vitamin and mineral supplements for slowing the progression of age-related macular degeneration. Cochrane Database Syst Rev 11:CD000254
Fernandez-Godino R, Garland DL, Pierce EA (2015) A local complement response by RPE causes early-stage macular degeneration. Hum Mol Genet 24:5555–5569
Fernandez-Godino R, Bujakowska KM, Pierce EA (2018) Hum Mol Genet 27(1):147–159
Fu L, Garland D, Yang Z et al (2007) The R345W mutation in EFEMP1 is pathogenic and causes AMD-like deposits in mice. Hum Mol Genet 16:2411–2422
Garcia Filho CA, Yehoshua Z, Gregori G et al (2014) Change in drusen volume as a novel clinical trial endpoint for the study of complement inhibition in age-related macular degeneration. Ophthalmic Surg Lasers Imaging Retina 45:18–31
Garland DL, Fernandez-Godino R, Kaur I et al (2014) Mouse genetics and proteomic analyses demonstrate a critical role for complement in a model of DHRD/ML, an inherited macular degeneration. Hum Mol Genet 23:52–68
Hageman GS, Luthert PJ, Victor Chong NH et al (2001) An integrated hypothesis that considers drusen as biomarkers of immune-mediated processes at the RPE-Bruch's membrane interface in aging and age-related macular degeneration. Prog Retin Eye Res 20:705–732
Hageman GS, Anderson DH, Johnson LV et al (2005) A common haplotype in the complement regulatory gene factor H (HF1/CFH) predisposes individuals to age-related macular degeneration. Proc Natl Acad Sci U S A 102:7227–7232
Harboe M, Mollnes TE (2008) The alternative complement pathway revisited. J Cell Mol Med 12:1074–1084
Hindmarsh EJ, Marks RM (1998) Complement activation occurs on subendothelial extracellular matrix in vitro and is initiated by retraction or removal of overlying endothelial cells. J Immunol 160:6128–6136
Hogan MJ, Alvarado J (1967) Studies on the human macula. IV. Aging changes in Bruch's membrane. Arch Ophthalmol 77:410–420
Lachmann PJ, Halbwachs L (1975) The influence of C3b inactivator (KAF) concentration on the ability of serum to support complement activation. Clin Exp Immunol 21:109–114
Leivo I, Engvall E (1986) C3d fragment of complement interacts with laminin and binds to basement membranes of glomerulus and trophoblast. J Cell Biol 103:1091–1100
Mastellos DC, Yancopoulou D, Kokkinos P et al (2015) Compstatin: a C3-targeted complement inhibitor reaching its prime for bedside intervention. Eur J Clin Investig 45:423–440
Miller JW (2013a) Age-related macular degeneration revisited–piecing the puzzle: the LXIX Edward Jackson memorial lecture. Am J Ophthalmol 155(1–35):e13
Miller JW (2013b) Age-related macular degeneration revisited–piecing the puzzle: the LXIX Edward Jackson memorial lecture. Am J Ophthalmol 155(1–35):e13
Mullins RF, Russell SR, Anderson DH et al (2000) Drusen associated with aging and age-related macular degeneration contain proteins common to extracellular deposits associated with atherosclerosis, elastosis, amyloidosis, and dense deposit disease. FASEB J (Official Publication of the Federation of American Societies for Experimental Biology) 14:835–846
Nilsson B, Nilsson Ekdahl K (2012) The tick-over theory revisited: is C3 a contact-activated protein? Immunobiology 217:1106–1110
Nozaki M, Raisler BJ, Sakurai E et al (2006) Drusen complement components C3a and C5a promote choroidal neovascularization. Proc Natl Acad Sci U S A 103:2328–2333
Overall CM, Kleifeld O (2006) Tumour microenvironment – opinion: validating matrix metalloproteinases as drug targets and anti-targets for cancer therapy. Nat Rev Cancer 6:227–239
Pangburn MK, Schreiber RD, Muller-Eberhard HJ (1981) Formation of the initial C3 convertase of the alternative complement pathway. Acquisition of C3b-like activities by spontaneous hydrolysis of the putative thioester in native C3. J Exp Med 154:856–867
Qu H, Ricklin D, Bai H et al (2013) New analogs of the clinical complement inhibitor compstatin with subnanomolar affinity and enhanced pharmacokinetic properties. Immunobiology 218:496–505

Reale E, Groos S, Eckardt U et al (2009) New components of 'basal laminar deposits' in age-related macular degeneration. Cells Tissues Organs 190:170–181

Ricklin D, Lambris JD (2013) Complement in immune and inflammatory disorders: pathophysiological mechanisms. J Immunol 190:3831–3838

Ricklin D, Hajishengallis G, Yang K et al (2010) Complement: a key system for immune surveillance and homeostasis. Nat Immunol 11:785–797

Sarks SH, Arnold JJ, Killingsworth MC et al (1999) Early drusen formation in the normal and aging eye and their relation to age related maculopathy: a clinicopathological study. Br J Ophthalmol 83:358–368

Seddon JM, Yu Y, Miller EC et al (2013) Rare variants in CFI, C3 and C9 are associated with high risk of advanced age-related macular degeneration. Nat Genet 45:1366–1370

Sivakumar P, Das AM (2008) Fibrosis, chronic inflammation and new pathways for drug discovery. Inflamm Res 57:410–418

Tziakas DN, Chalikias GK, Hatzinikolaou HI et al (2005) Levosimendan use reduces MMP-2 in patients with decompensated heart failure. Cardiovasc Drugs Ther 19:399–402

Wang L, Clark ME, Crossman DK et al (2010) Abundant lipid and protein components of drusen. PLoS One 5:e10329

Yehoshua Z, de Amorim Garcia Filho CA, Nunes RP et al (2014) Systemic complement inhibition with eculizumab for geographic atrophy in age-related macular degeneration: the COMPLETE study. Ophthalmology 121:693–701

# Chapter 5
# MicroRNA as Therapeutics for Age-Related Macular Degeneration

**Riccardo Natoli and Nilisha Fernando**

**Abstract** MicroRNA (miRNA) are a class of endogenously expressed small non-coding RNA molecules that function by repressing or silencing post-transcriptional gene expression. While miRNAs were only identified in humans as recently as the turn of this century, some miRNA-based agents are already in Phase 2 clinical trials (Christopher et al. 2016). This rapid progress from initial discovery to drug development reflects the effectiveness of miRNAs as therapeutic targets. Further, their use as therapeutic agents in the treatment of diseases such as Alzheimer's disease (Wang et al. 2014) supports their use in other neurodegenerative diseases, such as Age-Related Macular Degeneration (AMD). However, despite ~300 miRNAs reportedly expressed in the human retina (Xu 2009), relatively little research has been conducted into the therapeutic potential of miRNAs for the treatment of AMD. This review will investigate the use of miRNAs as therapeutic and diagnostic molecules for AMD.

**Keywords** miRNA · AMD · Complement · Neovascularisation · Inflammation · miR-146 · miR-155 · miR-9 · miR-125b

## 5.1 miRNA Biogenesis and AMD

miRNAs are approximately 19–24 nucleotides in length, are found in all Metazoa, are highly conserved across species and play a key role in post-transcriptional gene expression. A number of miRNA biogenesis pathways exist, with the main

R. Natoli (✉)
John Curtin School of Medical Research, The Australian National University, Canberra, ACT, Australia

ANU Medical School, The Australian National University, Canberra, ACT, Australia
e-mail: riccardo.natoli@anu.edu.au

N. Fernando
John Curtin School of Medical Research, The Australian National University, Canberra, ACT, Australia



J. D. Ash et al. (eds.), *Retinal Degenerative Diseases*, Advances in Experimental Medicine and Biology 891, https://doi.org/10.1007/978-3-319-75402-4_5

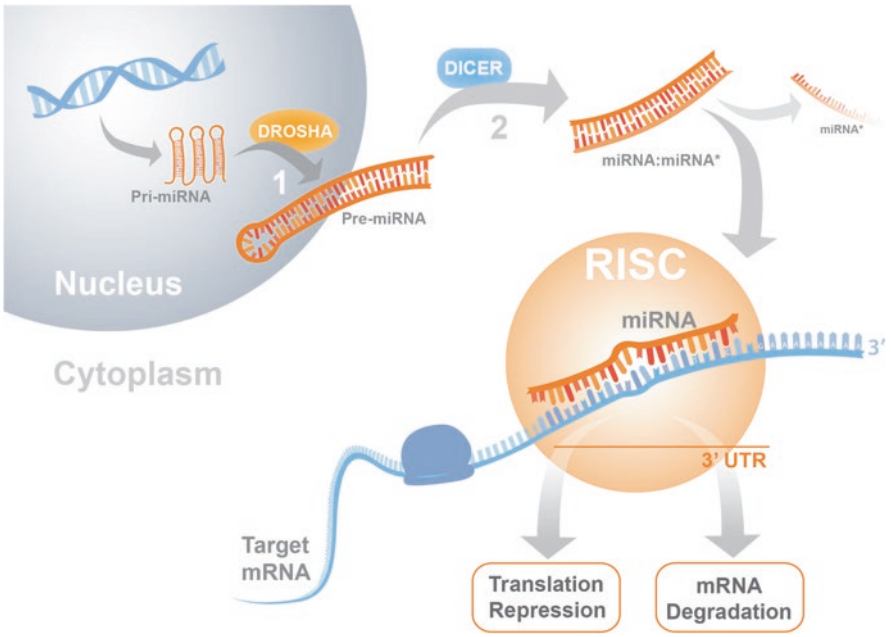


**Fig. 5.1** Schematic diagram showing the biogenesis and mode of action of mature microRNA (miRNA) sequences inside the cell. This canonical maturation of miRNAs includes two cleavage events, catalysed by *drosha* and *dicer*, respectively, resulting in the conversion of the long primary transcripts (Pri-miRNA) in the nucleus to small mature miRNA duplexes in the cytoplasm. Each strand of the mature duplex can then independently incorporate into the RNA-induced silencing complex (RISC) and lead to gene regulation by either translational repression or degradation through disruption or cleavage of the 3′ untranslated region (3′UTR) of the target mRNA

involving the production of mature miRNAs from the stepwise cleavage of a precursor hairpin transcript by enzymes Drosha and Dicer (Fig. 5.1, reviewed in Ha and Kim 2014). A single miRNA can regulate multiple genes and even pathways due to miRNA/mRNA interactions in the conserved 3′UTR regions of mRNA. Herein lies the power of miRNAs as therapeutic targets, as instead of acting on a single molecule, one miRNA can act on multiple genes, having the potential to shut down entire pathways. For multi-faceted diseases such as Age-Related Macular Degeneration (AMD), the diagnostic and therapeutic potentials of these molecules are only now starting to be explored.

## 5.2 miRNA as Potential Therapeutic Targets for Age-Related Macular Degeneration

Several miRNAs involved with angiogenesis and inflammation have already been shown to directly contribute to AMD progression (Berber et al. 2016). Specifically, miR-146a, miR-125b, miR-155 and miR-9 have all been identified in the literature as possible therapeutic targets for AMD.

miR-146a has been linked to the progression of a number of inflammatory disorders, including AMD (Wang et al. 2012). This miRNA has been found in the plasma (Ertekin et al. 2014; Menard et al. 2016) and retinas (Bhattacharjee et al. 2016; Staff 2016) of AMD patients and was modulated in human monocytes stimulated with lipopolysaccharide (LPS) (Taganov et al. 2006). Signalling of Toll-like receptors (TLR) induced a rapid upregulation of miR-146a, which acts as a negative feedback regulator of the signalling cascade, resulting in suppression of the immune response (Taganov et al. 2006). This miRNA is under the transcriptional control of nuclear factor-kappa B (NF-κB), and in microglial studies, miR-146a downregulated the expression of complement factor H (CFH), a key repressor of the innate immune response and a key player in AMD pathogenesis (Lukiw et al. 2012). Targeting miR-146a has been suggested as a potential therapeutic strategy (Lukiw et al. 2012) for slowing the progression of AMD. However, others have shown that miR-146a can directly modulate IL-6 (Bhaumik et al. 2009), a powerful pro-inflammatory cytokine associated with disease progression (Iyer et al. 2012), indicating a possible biphasic role of this miRNA in retinal inflammation (Berber et al. 2016).

miR-125b has been heavily associated with angiogenesis with downregulation observed in ovarian cancer (He et al. 2013) and deep burn patients (Zhou et al. 2015), two conditions which exhibit high levels of angiogenesis. This miRNA has been shown to be highly expressed in normal human retina (Karali et al. 2016). This high expression of miR-125b along with decreased expression in RPE cells under oxidative stress, in both mouse retinas exposed to oxidative-induced retinopathy and in AMD patients (Howell et al. 2013; Yan et al. 2015; Bhattacharjee et al. 2016), suggests a role for miR-125b in maintaining retinal vascular stability. As the wet form of AMD is heavily associated with neovascularisation, therapies which maintain the stability of miR-125b during ageing and potential overexpression of miR-125b could result in normal maintenance of retinal vessel architecture.

miR-155 has a role in both angiogenesis and inflammation and makes it a prime candidate for therapeutic interventions for AMD. Known to be involved in inflammation through TLR4 signalling with LPS (Taganov et al. 2006), it was later found that both viral and bacterial sensing TLRs induced miR-155 expression (reviewed in Sonkoly et al. 2008). The expression of miR-155 is also induced by a suite of inflammatory cytokines which have been associated with AMD, including IFN-β and IFN-γ signalling through TNF-α (O'Connell et al. 2007). LPS-stimulation of macrophages resulted in an increase of miR-155, and identified several genes involved in LPS signalling to be targeted by miR-155 (Tili et al. 2007), suggesting that similar to miR-146a, miR-155 is involved in the negative regulation of immune responses to LPS. Interestingly, miR-146a and miR-155 recognise an overlapping 3′ UTR in complement factor H (inhibitor of complement activation which is heavily associated with AMD), to which either or both of these miRNAs may interact (Lukiw et al. 2012). Work conducted in hindlimb ischaemic mice showed that miR-155 exerts both anti-angiogenic and pro-arteriogenic functions (Pankratz et al. 2015). In miR-155$^{-/-}$ mice, macrophages showed reduced expression of pro-arteriogenic cytokines, as well as decreased macrophage migration and chemokine expression upon LPS stimulation (Pankratz et al. 2015). These miR-155$^{-/-}$ mice

exhibited a specific alteration in the pro-arteriogenic cytokine profile, which was partly mediated by the anti-inflammatory regulator gene suppressor of cytokine signalling 1 (SOCS-1), another target of miR-155 expression. In animal studies modelling facets of AMD, miR-155 has been shown to be upregulated in correlation with increased cell death and inflammation (Saxena et al. 2015), while in a choroidal neovascularisation (CNV) model for wet AMD, miR-155 downregulation reduced retinal neovascularisation (Zhuang et al. 2015). Further exploration of the role of miR-155 in the development and progression of retinal degenerations is required, as well as investigation into the therapeutic properties of miR-155, as it is centrally involved in inflammation, complement activation and neovascularisation, which are major facets of AMD.

miR-9 has been shown to be vital in the development of the central nervous system; it is expressed in high levels in the developing forebrain, midbrain, hindbrain and spinal cord (reviewed in (Radhakrishnan and Alwin Prem Anand 2016)), and is further expressed in high levels in the human retina (Karali et al. 2016). miR-9 negatively regulates NF-κB-dependent inflammatory responses by suppressing expression of NF-κB1 transcripts in LPS-stimulated neutrophils and monocytes (Bazzoni et al. 2009), and has been shown to be downregulated in Alzheimer's disease patients (Cogswell et al. 2008). Further, it has been shown that TLR-4-activated NF-κB rapidly increased expression of miR-9, which operated as a feedback control to fine-tune the expression of key members of the NF-κB signalling pathway. Although little is known about its role in retinal function and its contribution to retinal degenerations, a recent study by Lukiw and colleagues (Lukiw et al. 2012) showed a direct link between upregulation of four miRNAs (miR-9, miR-125b, miR-146a and miR-155) and downregulation of complement factor H in human retinal tissue. Further, it has been demonstrated that miR-124, miR-9, and miR-9* in combination can promote Müller glia reprogramming into retinal progenitor cells and neurons (Wohl and Reh, 2016), indicating a novel role for miR-9 in retinal degenerations.

## 5.3 miRNA as Biomarkers of Retinal Disease

miRNAs are not just limited to the nucleus and cytoplasm of cells, but are present in the blood where they are found in plasma, platelets, erythrocytes and nucleated blood cells (Chen et al. 2008). Circulating miRNAs have been found to be associated with retinal diseases, including AMD (Berber et al. 2016). Circulating miRNAs are remarkably stable, even under degrading conditions, largely due to protection in lipid microparticles (Kosaka et al. 2010). The stability of miRNAs in the plasma, their ease of detection and measurable changes in disease have ignited interest in the use of circulating miRNAs as biomarkers for disease (Creemers et al. 2012).

The use of miRNAs as biomarkers for retinal degenerations has been investigated in a number of human studies and animal models. In a rat model of retinal toxicity, animals exposed to pan-CDK inhibitors showed increased levels of miR-96, miR-124 and miR-183 in the blood, and found that increases in levels of these

miRNAs correlated to decreased retinal function and retinal damage (Peng et al. 2014). Further these researchers showed that in two other models of retinal degeneration, the sodium iodate model and laser-induced choroidal neovascularisation (CNV), there were increases in the retinal enriched miR-183/96/182 cluster and miR-124 (anti-inflammatory miRNA) in the blood.

The serum profiles of patients with both wet and dry AMD have shown differences in several miRNAs (Szemraj et al. 2015; Berber et al. 2016). One study identified changes in a number of novel miRNAs and also showed there was little overlap in the types of miRNA expressed in serum in both forms of AMD; miR-661 and miR-3132 changed in the serum of patients with dry AMD, and miR-4258, miR-889 and Let-7 changed in patients with wet AMD (Szemraj et al. 2015). The differences in miRNA profile between wet and dry AMD, as well as reported variability across studies (Berber et al. 2016), reflects the difficulty of reducing biomarkers for AMD to one common group of molecules.

## 5.4 Future Experimental Approaches

miRNAs are involved in processes such as inflammation, complement activation and neovascularisation, which are central facets of AMD, making them ideal therapeutic and diagnostic candidates. However, before meaningful attempts can be made to develop miRNAs into diagnostic or therapeutic tools for AMD, a number of facets of miRNA biology must be further understood, including the establishment of a complete retinal miRNA target profile. A deeper understanding of all the target mRNA/miRNA interactions using both experimental and computational analysis is required before miRNAs can be considered as therapeutics for the treatment of AMD.

## References

Bazzoni F, Rossato M, Fabbri M et al (2009) Induction and regulatory function of miR-9 in human monocytes and neutrophils exposed to proinflammatory signals. Proc Natl Acad Sci U S A 106:5282–5287

Berber P, Grassmann F, Kiel C et al (2016) An eye on age-related macular degeneration: the role of MicroRNAs in disease pathology. Mol Diagn Ther 21:31–43

Bhattacharjee S, Zhao Y, Dua P et al (2016) microRNA-34a-mediated down-regulation of the microglial-enriched triggering receptor and phagocytosis-sensor TREM2 in age-related macular degeneration. PLoS One 11:e0150211

Bhaumik D, Scott GK, Schokrpur S et al (2009) MicroRNAs miR-146a/b negatively modulate the senescence-associated inflammatory mediators IL-6 and IL-8. Aging 1:402–411

Chen X, Ba Y, Ma L et al (2008) Characterization of microRNAs in serum: a novel class of biomarkers for diagnosis of cancer and other diseases. Cell Res 18:997–1006

Christopher AF, Kaur RP, Kaur G et al (2016) MicroRNA therapeutics: discovering novel targets and developing specific therapy. Perspect Clin Res 7:68–74

Cogswell JP, Ward J, Taylor IA et al (2008) Identification of miRNA changes in Alzheimer's disease brain and CSF yields putative biomarkers and insights into disease pathways. J Alzheimers Dis (JAD) 14:27–41

Creemers EE, Tijsen AJ, Pinto YM (2012) Circulating microRNAs: novel biomarkers and extracellular communicators in cardiovascular disease? Circ Res 110:483–495

Ertekin S, Yildirim O, Dinc E et al (2014) Evaluation of circulating miRNAs in wet age-related macular degeneration. Mol Vis 20:1057–1066

Ha M, Kim VN (2014) Regulation of microRNA biogenesis. Nat Rev Mol Cell Biol 15:509–524

He J, Jing Y, Li W et al (2013) Roles and mechanism of miR-199a and miR-125b in tumor angiogenesis. PLoS One 8:e56647

Howell JC, Chun E, Farrell AN et al (2013) Global microRNA expression profiling: curcumin (diferuloylmethane) alters oxidative stress-responsive microRNAs in human ARPE-19 cells. Mol Vis 19:544–560

Iyer A, Zurolo E, Prabowo A et al (2012) MicroRNA-146a: a key regulator of astrocyte-mediated inflammatory response. PLoS One 7:e44789

Karali M, Persico M, Mutarelli M et al (2016) High-resolution analysis of the human retina miRNome reveals isomiR variations and novel microRNAs. Nucleic Acids Res 44:1525–1540

Kosaka N, Iguchi H, Yoshioka Y et al (2010) Secretory mechanisms and intercellular transfer of microRNAs in living cells. J Biol Chem 285:17442–17452

Lukiw WJ, Surjyadipta B, Dua P et al (2012) Common micro RNAs (miRNAs) target complement factor H (CFH) regulation in Alzheimer's disease (AD) and in age-related macular degeneration (AMD). Int J Biochem Mol Biol 3:105–116

Menard C, Rezende FA, Miloudi K et al (2016) MicroRNA signatures in vitreous humour and plasma of patients with exudative AMD. Oncotarget 7:19171–19184

O'Connell RM, Taganov KD, Boldin MP et al (2007) MicroRNA-155 is induced during the macrophage inflammatory response. Proc Natl Acad Sci U S A 104:1604–1609

Pankratz F, Bemtgen X, Zeiser R et al (2015) MicroRNA-155 exerts cell-specific antiangiogenic but Proarteriogenic effects during adaptive neovascularization. Circulation 131:1575–1589

Peng Q, Huang W, John-Baptiste A (2014) Circulating microRNAs as biomarkers of retinal toxicity. J Appl Toxicol (JAT) 34:695–702

Radhakrishnan B, Alwin Prem Anand A (2016) Role of miRNA-9 in brain development. J Exp Neurosci 10:101–120

Saxena K, Rutar MV, Provis JM et al (2015) Identification of miRNAs in a model of retinal degenerations. Invest Ophthalmol Vis Sci 56:1820–1829

Sonkoly E, Stahle M, Pivarcsi A (2008) MicroRNAs and immunity: novel players in the regulation of normal immune function and inflammation. Semin Cancer Biol 18:131–140

Staff PO (2016) Correction: microRNA-34a-mediated down-regulation of the microglial-enriched triggering receptor and phagocytosis-sensor TREM2 in age-related macular degeneration. PLoS One 11:e0153292

Szemraj M, Bielecka-Kowalska A, Oszajca K et al (2015) Serum MicroRNAs as potential biomarkers of AMD. Med Sci Monit (International Medical Journal of Experimental and Clinical Research) 21:2734–2742

Taganov KD, Boldin MP, Chang KJ et al (2006) NF-kappaB-dependent induction of microRNA miR-146, an inhibitor targeted to signaling proteins of innate immune responses. Proc Natl Acad Sci U S A 103:12481–12486

Tili E, Michaille JJ, Cimino A et al (2007) Modulation of miR-155 and miR-125b levels following lipopolysaccharide/TNF-alpha stimulation and their possible roles in regulating the response to endotoxin shock. J Immunol 179:5082–5089

Wang S, Koster KM, He Y et al (2012) miRNAs as potential therapeutic targets for age-related macular degeneration. Future Med Chem 4:277–287

Wang C, Ji B, Cheng B et al (2014) Neuroprotection of microRNA in neurological disorders (review). Biomed Rep 2:611–619

Wohl S, Reh T (2016) miR-124-9-9* potentiates Ascl1-induced reprogramming of cultured Muller glia. Glia 64 5:743–762

Xu S (2009) microRNA expression in the eyes and their significance in relation to functions. Prog Retin Eye Res 28:87–116

Yan L, Lee S, Lazzaro DR et al (2015) Single and compound knock-outs of microRNA (miRNA)-155 and its angiogenic gene target CCN1 in mice alter vascular and neovascular growth in the retina via resident microglia. J Biol Chem 290:23264–23281

Zhou S, Zhang P, Liang P et al (2015) The expression of miR-125b regulates angiogenesis during the recovery of heat-denatured HUVECs. Burns (Journal of the International Society for Burn Injuries) 41:803–811

Zhuang Z, Xiao Q, Hu H et al (2015) Down-regulation of microRNA-155 attenuates retinal neovascularization via the PI3K/Akt pathway. Mol Vis 21:1173–1184

# Chapter 6
# Anaphylatoxin Signaling in Retinal Pigment and Choroidal Endothelial Cells: Characteristics and Relevance to Age-Related Macular Degeneration

**Bärbel Rohrer**

**Abstract** Age-related macular degeneration (AMD) is the leading cause of blindness in the USA. Polymorphisms in various complement components are associated with an increased risk for AMD, and it has been hypothesized that an overactive complement system is partially responsible for the pathology of AMD. AMD is classified as early, intermediate, or late AMD, depending on the degree of the associated pathologies. Late AMD can be characterized as either lesions associated with neovascular AMD or geographic atrophy. Both sets of lesions are associated with pathology at the RPE/choroid interface, which include a thickening of Bruch's membrane, presence of drusen, and pigmentary alterations, and deterioration of the blood-retina barrier has been reported. These changes can lead to the slow degeneration and atrophy of the photoreceptors in the macula in dry AMD, or progress to choroidal neovascularization (CNV) and leakage of these new vessels in wet AMD. It has been shown previously that complement anaphylatoxins C3a and C5a, signaling via their respective G-protein-coupled receptors, can alter RPE cell function and promote choroidal neovascularization. However, it is important to note these components also play a role in tissue repair. Here we discuss anaphylatoxin signaling in AMD-related target cells and the potential implications for the design of anti-complement therapeutics.

**Keywords** Anaphylatoxin · G-protein-coupled receptors · Complement activation · Retinal pigment epithelium · Choroidal endothelial cells · Age-related macular degeneration

B. Rohrer (✉)
Departments of Ophthalmology, and Neurosciences, Medical University of South Carolina, Charleston, SC, USA

Research Service, Ralph H. Johnson VA Medical Center, Charleston, SC, USA
e-mail: rohrer@musc.edu



J. D. Ash et al. (eds.), *Retinal Degenerative Diseases*, Advances in Experimental Medicine and Biology 891, https://doi.org/10.1007/978-3-319-75402-4_6

## 6.1 Introduction

Age-related macular degeneration (AMD) is a complex multifactorial disease. The primary risk factor for AMD is aging (Chakravarthy et al. 2010); other risk factors include genetics (see Retnet.org) as well as environmental risk factors that cause oxidative stress such as smoking (Chakravarthy et al. 2010), or even light exposure (Taylor et al. 1990). Finally, based on histological (Anderson et al. 2002) and genetic findings (Anderson et al. 2010), complement activation has been proposed as a contributing factor to AMD pathology, resulting in an inflammatory phenotype.

## 6.2 The Complement System

The complement system is an essential part of the evolutionarily ancient innate immune system, whose main role is to eliminate foreign antigens and pathogens as part of the normal host response. The complement system can be activated by three distinct pathways: the classical (CP), lectin (LP), and alternative (AP) pathways (Muller-Eberhard 1988). Its activators are specific for the individual pathways; the CP and LP activators are related to injury, immunity, infection, or even aging, whereas the AP tends to be spontaneously and continuously activated. All arms trigger the common terminal pathway, which results in the generation of three sets of effector molecules. The anaphylatoxins, C3a and C5a, are soluble signaling molecules that lead to inflammation and chemotaxis of invading cells such as leukocytes and macrophages. Cleavage fragments of C3, C3b, iC3b, and C3d are covalently bound to surfaces that have undergone complement activation and act as ligands for receptors on immune effector cells. This opsonization step is involved in B-cell response, apoptotic cell/debris clearance, and immune complex clearance. Finally, the membrane attack complex (MAC), which forms a nonspecific pore in the cell membrane, triggers lysis of non-self cells or mediates sublytic activation under limiting activation conditions. Self cells have available to them both cell-bound and soluble complement inhibitors to prevent or limit complement activation.

## 6.3 Anaphylatoxins

The anaphylatoxins C3a and C5a are generated by cleavage of C3 and C5, respectively. C3a is an unglycosylated polypeptide; C5a is naturally glycosylated. The anaphylatoxin levels are regulated by three processes, generation, inactivation, and clearance. Generation is controlled by enzyme kinetics, with C3a being generated ~300x faster than C5a (Pangburn and Muller-Eberhard 1986; Rawal and Pangburn 2001). Both are rapidly inactivated by removal of the C-terminal arginine, resulting in the production of C3a- and C5a-desArg (Mueller-Ortiz et al. 2009). While

C3a-desArg no longer binds to its receptor, C5a-desArg is still stimulatory, but its activity is reduced 10x (reviewed by Klos et al. 2009). Finally, removal from circulation is thought to be controlled by binding to their respective receptors (C3aR, C5aR) followed by receptor internalization and digestion of C3a and C5a. The anaphylatoxins act through their respective G-protein-coupled receptors, C3aR and C5aR, which are widely distributed, including in lymphoid cells and the CNS. The anaphylatoxin receptors specifically bind their ligands with a $K_d$ of ~1 nM and, upon ligand binding, trigger heterotrimeric G-protein-mediated signaling. The most common intracellular response triggered by the engagement of C3aR or C5aR is the mobilization of calcium, generating many downstream responses depending on the cellular context (reviewed in Klos et al. 2009).

Based on the original discovery of the complement system as a mechanism to enhance/complement the immune system, much of the research efforts were focused on these aspects. However, observations stemming from diseases due to complement deficiencies, deficiencies in complement regulators, or the use of knockout mouse technologies suggest that the anaphylatoxins and their receptors may also play a role in CNS development and disease (Horstman et al. 2011) as well as tissue regeneration (Alawieh et al. 2015).

## 6.4 Anaphylatoxin Signaling in RPE

The RPE is thought to play a central role in AMD, since RPE cells are affected early and in all forms of AMD. Its single layer of hexagonal highly pigmented cells is part of the blood-retina barrier, separating the light-sensitive photoreceptors from the choroidal blood supply. The RPE serves many functions (Strauss 2005); relevant for this discussion, those functions include secretion of proteins that mediate health and disease of photoreceptors, Bruch's membrane, and the choroid such as growth factors and proteases, and modulation of the immune response by secreting both immunosuppressive factors and inflammatory proteins, such as complement components and cytokines.

Anaphylatoxins have been shown to be present in pathological structures of the RPE (Nozaki et al. 2006), yet receptors could not be identified by immunohistochemistry (Vogt et al. 2006). Nevertheless, gene expression studies in ARPE-19 cells (Brandstetter et al. 2015) and our unpublished microarray analyses on RPE/choroid from C57BL/6 J mice (U74Av2, Affymetrix; C3aR, $P = 0.001$; C5aR, $P = 0.05$) suggest that both receptors are expressed.

Anaphylatoxin signaling in RPE cells has, however, been analyzed with respect to readouts relevant for AMD. Cytokine production and secretion can be stimulated by anaphylatoxins; C3a increases gene expression of the pro-angiogenic growth factor VEGF and decreases that of the antiangiogenic factor PEDF in human RPE cells (Long et al. 2016), and C5a was found to increase VEGF secretion from ARPE-19 cells (Cortright et al. 2009). The ubiquitin proteasome pathway, a protein-degradation mechanism, is reduced with aging; and a role for C3a, but not C5a, was

identified for decreasing proteasome activity in primary human RPE cells (Ramos de Carvalho et al. 2013). Intracellular and extracellular lipid and protein aggregation are contributing to AMD pathology. A role for C3a signaling was identified in ARPE-19 cells exposed to smoke, in which smoke-mediated production of C3a was found to cause endoplasmic reticulum stress and lipid accumulation (Kunchithapautham et al. 2014); and C3a was found to contribute to the formation of sub-RPE basal deposits in mouse RPE (Fernandez-Godino et al. 2015). The NLRP3 inflammasome, another part of the innate immune system and thought to contribute to AMD, requires a priming followed by an activation signal. C5a was found to act as a primer for inflammasome activation by lipofuscin-mediated photooxidative damage (Brandstetter et al. 2015). Finally, we tested whether anaphylatoxin signaling can contribute to ion channel activity in RPE cells. Interestingly, aging-associated changes in L-type voltage-sensitive $Ca^{2+}$ channels have been shown in neurons (Thibault and Landfield 1996) and other cell types. We reported a combined effect of C3a, C5a, and non-pore-forming MAC on increased activation of L-type $Ca^{2+}$ as well as maxi-K channels (Genewsky et al. 2015).

## 6.5 Anaphylatoxin Signaling in Choroid

Another tissue thought to play a critical role in the development of AMD is the choroid. The choroid is the vascular layer of the eye, located between the RPE and the sclera, and is responsible for providing blood supply to the RPE and outer retina. Many structural and molecular changes occur in the aging choroid (Chirco et al. 2017), including a reduction in the number of choroidal endothelial cells (CECs) and in vascular density within the choriocapillaris, changes in Bruch's membrane, and an overall thinning of the choroid.

Similar to the RPE, neither of the two receptors could originally be identified by immunohistochemistry (Vogt et al. 2006), although, with the use of a different antibody, the presence of C5aR was later confirmed (Skeie et al. 2010). Again, functional assays appear to be more conclusive. In mice, C3aR and C5aR were shown to contribute to laser-induced choroidal neovascularization (CNV) (Nozaki et al. 2006); however these results did not identify target cells. The CNV results would suggest that the anaphylatoxins should promote choroidal endothelial cell (CEC) migration, an effect that could not, however, be demonstrated (Skeie et al. 2010). Nevertheless, C5a did increase ICAM-1 mRNA and protein production in CECs. In HUVEC and immortalized human dermal microvascular endothelial cells on the other hand, both C3aR and C5aR were detected; however only C5a caused a loss of barrier function, whereas C3a was ineffective (Schraufstatter et al. 2015). Recently, numbers and degranulation state of mast cells have been found to be associated with AMD (Bhutto et al. 2016). Interestingly, mast cells degranulate in response to C3a and increase chemokine production (Venkatesha et al. 2005). Finally, since

choroidal fibroblasts contribute to fibrovascular subretinal scarring, it is of relevance to note that activation of C3aR and C5aR is involved in the pathogenesis of pulmonary fibrosis (Gu et al. 2016).

## 6.6 Future Experimental Approaches

Taken together, there is evidence that anaphylatoxin signaling alters the cellular behavior of RPE and cells within the choroid, overall generating a pro-inflammatory microenvironment.

To date, the majority of studies were designed to identify pro-inflammatory effects of anaphylatoxins in individual cell types. However, complement activation in vivo occurs in the context of an environment consisting of many different cell types, and typically, both anaphylatoxins are generated in concert. Also, complement activation has typically been considered a pathological signal, however, experiments to understand complement signaling as a homeostatic signal, or even one involved in repair, have not been tackled in the eye. Hence, co-culture experiments such as those used by Benedicto to understand the cross talk between RPE and choroid endothelium (Benedicto et al. 2015) should be further investigated. The two anaphylatoxins could have additive, synergistic or even antagonistic effects. Synergistic effects of C3aR and C5aR signaling have been shown to promote edema formation and intracerebral hemorrhage (Garrett et al. 2009), and both anaphylatoxins together are required for liver regeneration (Strey et al. 2003). Also, recently it has been reported that C3a is not just confined to the extracellular space, but can also signal intracellularly (Liszewski et al. 2013). Current efforts in my lab are aimed at examining the types of C3a/C5a (inter)actions in RPE cells. Finally, since complement is also being increasingly implicated in repair and regeneration (Strey et al. 2003; Alawieh et al. 2015), we have collected preliminary data that indicates that repair of CNV lesions in the mouse can be impaired by administration of a C3a-receptor antagonist (Rohrer et al. 2016). However, future work is required to identify the cells that specifically respond to anaphylatoxin stimulation and that are required for this type of wound healing reaction.

Overall, what these observations suggest is that when designing complement inhibitory strategies for AMD, one needs to (i) consider differential effects on different types of target cells and (ii) provide sufficient complement inhibition during the acute injury phase while (iii) allowing adequate generation of anaphylatoxins to promote recovery during the repair phase.

**Acknowledgments** This work was supported in part by the National Institutes of Health (R01EY019320), Veterans Affairs (I01 RX000444), and the South Carolina SmartState Endowment.

## References

Alawieh A, Elvington A, Zhu H et al (2015) Modulation of post-stroke degenerative and regenerative processes and subacute protection by site-targeted inhibition of the alternative pathway of complement. J Neuroinflammation 12:247

Anderson DH, Mullins RF, Hageman GS et al (2002) A role for local inflammation in the formation of drusen in the aging eye. Am J Ophthalmol 134:411–431

Anderson DH, Radeke MJ, Gallo NB et al (2010) The pivotal role of the complement system in aging and age-related macular degeneration: hypothesis re-visited. Prog Retin Eye Res 29:95–112

Benedicto I, Lehmann-Mantaras G, Ginsberg M et al (2015) Crosstalk between RPE and choroid endothelium regulates RPE tight junctions. Invest Ophthalmol Vis Sci 56:41–41

Bhutto IA, McLeod DS, Jing T et al (2016) Increased choroidal mast cells and their degranulation in age-related macular degeneration. Br J Ophthalmol 100:720–726

Brandstetter C, Holz FG, Krohne TU (2015) Complement component C5a primes retinal pigment epithelial cells for Inflammasome activation by Lipofuscin-mediated photooxidative damage. J Biol Chem 290:31189–31198

Chakravarthy U, Wong TY, Fletcher A et al (2010) Clinical risk factors for age-related macular degeneration: a systematic review and meta-analysis. BMC Ophthalmol 10:31

Chirco KR, Sohn EH, Stone EM et al (2017) Structural and molecular changes in the aging choroid: implications for age-related macular degeneration. Eye (Lond) 31(1):10–25. https://doi.org/10.1038/eye.2016.216. Epub 2016 Oct 7

Cortright DN, Meade R, Waters SM et al (2009) C5a, but not C3a, increases VEGF secretion in ARPE-19 human retinal pigment epithelial cells. Curr Eye Res 34:57–61

Fernandez-Godino R, Garland DL, Pierce EA (2015) A local complement response by RPE causes early-stage macular degeneration. Hum Mol Genet 24:5555–5569

Garrett MC, Otten ML, Starke RM et al (2009) Synergistic neuroprotective effects of C3a and C5a receptor blockade following intracerebral hemorrhage. Brain Res 1298C:171–177

Genewsky A, Jost I, Busch C et al (2015) Activation of endogenously expressed ion channels by active complement in the retinal pigment epithelium. Pflugers Arch 467:2179–2191

Gu H, Fisher AJ, Mickler EA et al (2016) Contribution of the anaphylatoxin receptors, C3aR and C5aR, to the pathogenesis of pulmonary fibrosis. FASEB J 30:2336–2350

Horstman LL, Jy W, Ahn YS et al (2011) Complement in neurobiology. Front Biosci (Landmark Ed) 16:2921–2960

Klos A, Tenner AJ, Johswich KO et al (2009) The role of the anaphylatoxins in health and disease. Mol Immunol 46:2753–2766

Kunchithapautham K, Atkinson C, Rohrer B (2014) Smoke exposure causes endoplasmic reticulum stress and lipid accumulation in retinal pigment epithelium through oxidative stress and complement activation. J Biol Chem 289:14534–14546

Liszewski MK, Kolev M, Le Friec G et al (2013) Intracellular complement activation sustains T cell homeostasis and mediates effector differentiation. Immunity 39:1143–1157

Long Q, Cao X, Bian A et al (2016) C3a Increases VEGF and decreases PEDF mRNA levels in human retinal pigment epithelial cells. Biomed Res Int 2016:6958752

Mueller-Ortiz SL, Wang D, Morales JE et al (2009) Targeted disruption of the gene encoding the murine small subunit of carboxypeptidase N (CPN1) causes susceptibility to C5a anaphylatoxin-mediated shock. J Immunol 182:6533–6539

Muller-Eberhard HJ (1988) Molecular organization and function of the complement system. Annu Rev Biochem 57:321–347

Nozaki M, Raisler BJ, Sakurai E et al (2006) Drusen complement components C3a and C5a promote choroidal neovascularization. Proc Natl Acad Sci U S A 103:2328–2333

Pangburn MK, Muller-Eberhard HJ (1986) The C3 convertase of the alternative pathway of human complement. Enzymic properties of the bimolecular proteinase. Biochem J 235:723–730

Ramos de Carvalho JE, Klaassen I, Vogels IM et al (2013) Complement factor C3a alters proteasome function in human RPE cells and in an animal model of age-related RPE degeneration. Invest Ophthalmol Vis Sci 54(10):6489–6501

Rawal N, Pangburn M (2001) Formation of high-affinity C5 convertases of the alternative pathway of complement. J Immunol 166:2635–2642

Rohrer B, Parsons N, Schnabolk G et al (2016) The complement system is dual-hatted, acting in both damage and repair processes in the murine model of choroidal neovascularization. Invest Ophthalmol Vis Sci 57:2123–2123

Schraufstatter IU, Khaldoyanidi SK, DiScipio RG (2015) Complement activation in the context of stem cells and tissue repair. World J Stem Cells 7:1090–1108

Skeie JM, Fingert JH, Russell SR et al (2010) Complement component C5a activates ICAM-1 expression on human choroidal endothelial cells. Invest Ophthalmol Vis Sci 51:5336–5342

Strauss O (2005) The retinal pigment epithelium in visual function. Physiol Rev 85:845–881

Strey CW, Markiewski M, Mastellos D et al (2003) The proinflammatory mediators C3a and C5a are essential for liver regeneration. J Exp Med 198:913

Taylor HR, Munoz B, West S et al (1990) Visible light and risk of age-related macular degeneration. Trans Am Ophthalmol Soc 88:163–173. discussion 173-168

Thibault O, Landfield PW (1996) Increase in single L-type calcium channels in hippocampal neurons during aging. Science 272:1017–1020

Venkatesha RT, Berla Thangam E, Zaidi AK et al (2005) Distinct regulation of C3a-induced MCP-1/CCL2 and RANTES/CCL5 production in human mast cells by extracellular signal regulated kinase and PI3 kinase. Mol Immunol 42:581–587

Vogt SD, Barnum SR, Curcio CA et al (2006) Distribution of complement anaphylatoxin receptors and membrane-bound regulators in normal human retina. Exp Eye Res 83:834–840

# Chapter 7
# Estimations of Retinal Blue-Light Irradiance Values and Melatonin Suppression Indices Through Clear and Yellow-Tinted Intraocular Lenses


**Masaki Tanito, Ichiya Sano, Tsutomu Okuno, Yoshihisa Ishiba, and Akihiro Ohira**

**Abstract** Spectral transmittance values in the wavelength range of 300 to 800 nanometers were measured using a spectrophotometer for 18 intraocular lenses (IOLs) including clear (ZCB00) and yellow-tinted (ZCB00V, both from AMO Japan) IOLs with three different lens powers. Also measured were the blue-light irradiance (BLI) values, which might reflect retinal damage caused by sunlight, and the melatonin suppression indices (MSIs), which might reflect the nonvisual photoreception function, through these IOLs. The BLIs (in $mWcm^{-2}$) calculated were 7.62, 7.50, and 7.46 for the +10-diopter (D), +20-D, and +30-D ZCB00 IOLs, respectively; 4.10, 3.92, and 4.00 for the +10-D, +20-D, and +30-D ZCB00V IOLs, respectively; 5.76 for phakic eyes; and 15.00 for aphakic eyes. The MSIs (in mWcm-2sr-1) calculated were 1.18, 1.19, and 1.18 for the +10-D, +20-D, and +30-D ZCB00 IOLs, respectively; 0.98, 0.94, and 0.95 for the +10-D, +20-D, and +30-D ZCB00V IOLs, respectively; 1.03 for phakic eyes; and 1.21 for aphakic eyes. The data from the six clear IOLs (SA60AT, Alcon Japan; VA-60BBR, Hoya; AU6 K, Kowa,

M. Tanito (✉)
Division of Ophthalmology, Matsue Red Cross Hospital, Shimane, Matsue, Japan

Department of Ophthalmology, Shimane University Faculty of Medicine, Izumo, Shimane, Japan
e-mail: tanito-oph@umin.ac.jp

I. Sano
Division of Ophthalmology, Matsue Red Cross Hospital, Shimane, Matsue, Japan

T. Okuno
Graduate School of Science and Engineering, Tokyo Metropolitan University, Hachioji, Tokyo, Japan

Y. Ishiba
Technology Development Department, Yamamoto Kogaku Co. Ltd., Higashi-Osaka, Japan

A. Ohira
Department of Ophthalmology, Shimane University Faculty of Medicine, Izumo, Shimane, Japan



J. D. Ash et al. (eds.), *Retinal Degenerative Diseases*, Advances in Experimental Medicine and Biology 891, https://doi.org/10.1007/978-3-319-75402-4_7

N4-18B, Nidek; X-60, Santen; KS-3Ai, Staar Japan) and seven yellow-tinted IOLs (SN60AT; YA-60BBR, Hoya; AU6N, Kowa; N4-18YG, Nidek; NX-60, Santen; KS-AiN, Staar Japan; XY-1, Hoya) reported previously also were discussed. Compared to aphakic eyes, ZCB00 and ZCB00V IOLs reduce the BLI values by 49–50% and 73–74%, respectively; and currently available ultraviolet-blocking clear and yellow-tinted IOLs reduce the BLI values by 43–82%, respectively. Yellow-tinted IOLs absorb more circadian rhythm-associated light than clear IOLs. Although the data presented in this study cannot be applied directly to IOL implanted in patients, the balance between photoprotection and photoreception must be considered when using IOLs in a clinical setting.

**Keywords** Yellow-tinted intraocular lenses · Spectral transmittance · Blue-light irradiance · Retinal light damage · Melatonin suppression index · Circadian rhythm

## 7.1 Introduction

Cataract surgery, aphakia, and pseudophakia are substantial risk factors for development of late-stage age-related macular degeneration (AMD), and increased amounts of blue light reaching the retina postoperatively might be a major cause (Tanito 2014). In the early 1980s (Mainster and Sparrow 2003), intraocular lenses (IOLs) with ultraviolet radiation (UVR)-blocking chromophores bonded to optic polymers were introduced. The transmission properties of the colorless UVR-blocking IOLs might not absorb blue light as efficiently compared to aging crystalline lenses and cause Ham-type retinal phototoxicity (Ham et al. 1976). To compensate for the reduced filtration of blue light by the colorless UVR-blocking IOLs, blue light- and UVR-absorbing yellow-tinted polymethyl methacrylate IOLs were introduced in the 1990s. These IOLs are now made of either foldable silicone or soft acrylic material, and there is great interest in using IOLs designed to block blue light (Braunstein and Sparrow 2005).

Environmental light information orchestrates critical daily circadian rhythms involving metabolic homeostasis and sleep-wake cycles by transmission of light information through rod and cone photoreceptor cells and blue light-sensitive photoreceptive retinal ganglion cells to nonvisual brain centers including the suprachiasmatic nucleus (SCN) of the hypothalamus (Turner and Mainster 2008). SCN closely controls the hormone melatonin, and because of this, the phase of the daily melatonin rhythm is an accepted indicator of the phase of the circadian clock. Several studies have shown that the human circadian system is particularly sensitive to the short wavelength portion of the light spectrum, as melatonin suppression is greatest during exposure to a narrow band of light stimulus between 460 and 480 nanometers (Brainard et al. 2001; Thapan et al. 2001).

We previously measured the spectral transmittance of various IOLs, used blue-light irradiance (BLI) values to quantify the ability of the IOLs to prevent retinal

damage caused by sun-gazing (Tanito et al. 2010, 2012) and used the melatonin suppression indices (MSI) to evaluate a possible effect on nonvisual photoreception (Sano et al. 2014). In the current study, we also measured the spectral transmittance values of IOLs that we had not measured previously and estimated the BLIs and MSIs.

## 7.2 Materials and Methods

### *7.2.1 IOLs*

We tested six soft acrylic IOL models including clear UV-blocking (ZCB00) and yellow-tinted (ZCV00V, both from AMO Japan, Tokyo, Japan) IOLs with +10-, +20-, and +30-D IOL powers (Fig. 7.1). Three IOL models were tested to ensure reproducibility, for a total of 18 IOLs.

### *7.2.2 Measurement of Spectral Transmittance of IOLs*

The spectral transmittance values of the IOLs placed in quartz cells filled with saline solution were measured in wavelengths ranging from 300 to 800 nanometers (1563 data points/scan) using a spectrophotometer (U-3410, Hitachi High-Technologies, Tokyo, Japan) as described previously (Tanito et al. 2010).

### *7.2.3 Calculation of the BLI*

The BLI values in pseudophakic eyes when viewing targets in sunlight were calculated by integrating the aphakic retinal hazard function by light (International Commission on Non-Ionizing Radiation Protection 2013; American Conference of

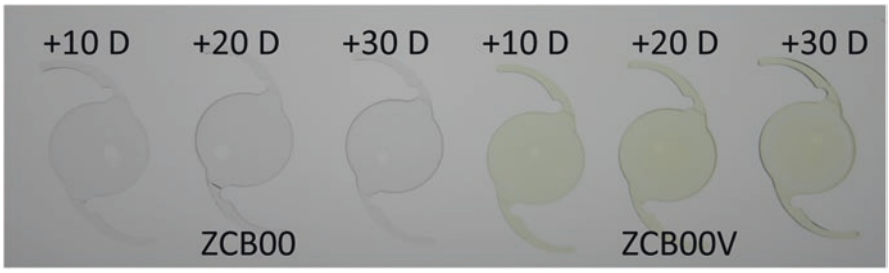


**Fig. 7.1** Intraocular lenses (IOLs) analyzed in this study. D = diopters

Governmental Industrial Hygienists 2015), the direct normal solar spectral irradiance (American Society for Testing and Materials 1998), and the measured spectral transmittance values of the IOLs, as we described previously (Tanito et al. 2010). The maximal permissible daily exposure duration ($t_{max}$) values were obtained for each ocular condition by dividing 10 mJcm$^{-2}$ by the obtained BLI value (Tanito et al. 2010).

### *7.2.4 Calculation of the MSI*

The MSI values obtained in pseudophakic eyes under fluorescent light were calculated by integrating the action spectrum for melatonin suppression (Brainard et al. 2001), the spectral intensity of a 20-watt white fluorescent lamp (Okuno 1999), and the measured spectral transmittance values of the IOLs, as we described previously (Sano et al. 2014).

## 7.3 Results

### *7.3.1 Transmittance of IOLs*

To obtain spectral transmittance information, 18 scans of the 18 IOLs were performed. The transmittance curves obtained from the +20-D IOLs are shown in Fig. 7.2. The clear IOLs (ZCB00) completely absorbed the light in the UV-B range (−320 nanometers), transmitted substantial light at the longer wavelength end of the UV-A light range (320–400 nanometers) (0.8% transmittance at 370 nanometers, 17% at 380 nanometers, and 55% at 390 nanometers), and almost completely transmitted (≥98%) the light in the visible light spectrum at 435 nanometers and longer wavelengths. The yellow-tinted IOL (ZCB00V) completely absorbed the UV-B, UV-A, and shorter wavelength end of the visible light ranges (0.6% transmittance at 415 nanometers, 25% at 430 nanometers, and 68% at 440 nanometers), and almost completely transmitted (≥95%) the light at 455 nanometer and longer wavelengths.

### *7.3.2 BLIs*

The BLIs (mWcm$^{-2}$) calculated were 7.62 ± 0.04, 7.50 ± 0.03, and 7.46 ± 0.04 for the +10-, +20-, and +30-D ZCB00 lens, respectively; 4.10 ± 0.02, 3.92 ± 0.03, and 4.00 ± 0.03 for the+10-, +20-, and +30-D ZCB00V lens, respectively; 5.76 for phakic eyes; and 15.00 for aphakic eyes. The $t_{max}$ values (seconds) were 1.31 ± 0.01,

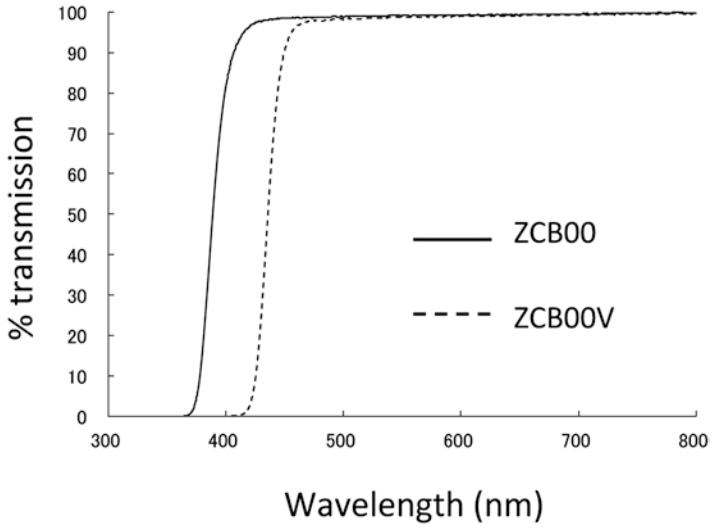


**Fig. 7.2** Transmission curves from the +20-diopter intraocular lenses (IOLs). The mean values derived from three independent measurements of three IOLs in each model are used to generate the curves

1.33 ± 0.01, and 1.34 ± 0.01 for the +10-, +20-, and +30-D ZCB00 lens, respectively; 2.44 ± 0.01, 2.55 ± 0.02, and 2.50 ± 0.02 for the +10-, +20-, and +30-D ZCB00V lens, respectively; 1.73 for the phakic eyes; and 0.67 for the aphakic eyes.

### *7.3.3 MSIs*

The MSIs ($mWcm^{-2}sr^{-1}$) calculated were 1.18 ± 0.00, 1.19 ± 0.00, and 1.18 ± 0.00 for the +10-, +20-, and +30-D ZCB00 IOLs, respectively; 0.98 ± 0.00, 0.94 ± 0.0.1, and 0.95 ± 0.00 for the +10-, +20-, and +30-D ZCB00V lens, respectively; 1.03 for the phakic eyes; and 1.21 for the aphakic eyes.

## 7.4 Discussion

We measured the spectral transmittance capabilities of 18 IOL samples in this study and of 117 IOL samples in our previous studies and estimated the BLI and MSI values (Tanito et al. 2010, 2012; Sano et al. 2014). Figures 7.3 and 7.4, respectively, show the percent cutoff values of the BLI and MSI values with various IOLs compared to aphakic eyes.

Compared to the clear IOLs, the corresponding yellow-tinted IOLs had greater reductions in their BLI values (Fig. 7.3). All the clear and yellow-tinted IOL showed

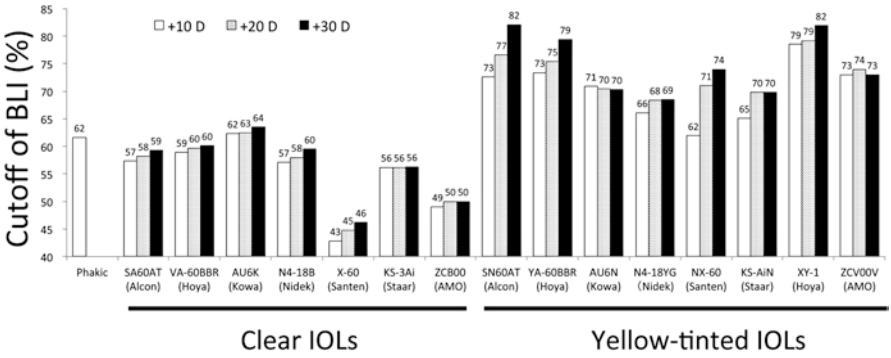


**Fig. 7.3** Percent cutoff values of the blue-light irradiance indices (BLIs) by various intraocular lenses (IOLs) compared with aphakic eyes. The percent cutoff value of the BLI by IOL is calculated as (BLI for aphakic eye – BLI for IOL)/BLI for aphakic eye × 100, where the BLI for aphakic eyes = 15.0 mWcm$^{-2}$. Instead of a+10-diopter (D) lens, a+12.5-D lens is analyzed for the KS-3Ai and KS-AiN IOLs, and a+12.0-D lens is analyzed for the XY-1 IOL; and instead of a+30-D lens, a+27.0-D lens is analyzed for the X-60 and NX-60 IOLs, a+28.5-D lens is analyzed for the KS-3Ai and KS-AiN IOLs, and a+26.0-D lens is analyzed for the XY-1 IOL. To generate this figure, the BLI values of IOLs other than ZCB00 and ZCB00V were adopted from our previous publications (Tanito et al. 2010, 2012)

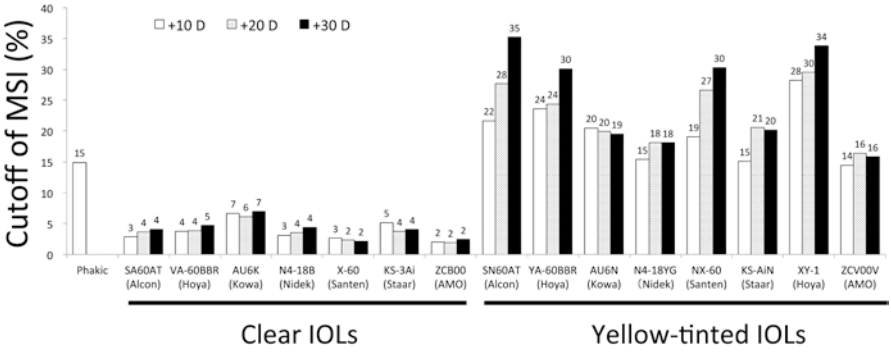


**Fig. 7.4** Percent cutoff values of melatonin suppression indices (MSIs) by various intraocular lenses (IOLs) compared with aphakic eyes. The percent cutoff values of the MSIs by IOL are calculated as (MSI for aphakic eye – BLI for IOL)/MSI for aphakic eye × 100, where the BLI for aphakic eyes = 1.21 mWcm$^{-2}$sr$^{-1}$. Instead of a+10-diopter (D) lens, a+12.5-D lens is analyzed for the KS-3Ai and KS-AiN IOLs, and a+12.0-D lens is analyzed for the XY-1 IOL; and instead of a+30-D lens, a+27.0-D lens is analyzed for the X-60 and NX-60 IOLs, a+28.5-D lens is analyzed for the KS-3Ai and KS-AiN IOLs, and a+26.0-D lens is analyzed for the XY-1 IOL. To generate this figure, the MSI values of IOLs other than ZCB00 and ZCB00V were adopted from our previous publication (Sano et al. 2014)

greater BLI reductions than aphakic eyes, and all the yellow-tinted IOLs except for the +10-D NX-60 lens showed greater BLI reductions than the phakic eyes. Although previous studies have suggested but do not confirm that blue light is a risk factor for development of AMD (Margrain et al. 2004; Mainster 2006; Sui et al.

2013), the yellow-tinted IOLs can protect the retina from phototoxicity if the blue-light theory is valid in the pathogenesis of retinal degeneration. Among the clear IOLs, the cutoff values of the BLIs was relatively small with the X-60 and ZCB00 IOLs due to the higher transmittance of UV-A light with these lenses; thus, the retinal protection provided by these IOLs would increase if the efficacy of longer UV-A light absorption was at the same level as the other IOL models.

Compared to the clear IOLs, the corresponding yellow-tinted IOLs had higher cutoff values of their MSI values (Fig. 7.4). All the clear and yellow-tinted IOL showed greater MSI cutoff values than the aphakic eyes. Compared to the phakic eyes, all the clear IOLs had lower MSI cutoff values and all the yellow-tinted IOLs had higher MSI cutoff values. In the current study, the transmittance data from young monkey eyes (Maher 1978) were used to calculate the phakic and aphakic MSIs. Turner and Mainster (2008) estimated that after 35 years of age, even the +30-D yellow-tinted IOL provided a "gain" in circadian photoreception compared with the crystalline lens. Brondsted et al. suggested that, even though the violet-blocking and/or blue-blocking IOLs potentially impair photoentrainment of the circadian rhythm, the effects were small compared to that of the natural lens and did not exceed the effect of a 22.2-year-old natural lens (Brondsted et al. 2011). Accordingly, the current data showed that the "loss" of the MSI by yellow-tinted IOLs compared with phakic eyes is likely to become a "gain" if the transmittance data from aged human eyes are used instead of that from monkey eyes.

In summary, compared to aphakic eye, the ZCB00 and ZCB00V IOLs reduced the BLI values by 49–50% and 73–74%, respectively; currently available UV-blocking clear and yellow-tinted IOLs reduced the BLI values by 43–82%. Yellow-tinted IOLs absorbed more circadian rhythm-associated light than clear IOLs. Although the current data cannot be directly applicable to humans implanted with IOLs, the balance between photoprotection and photoreception must be considered when IOLs are used in a clinical situation.

This chapter includes text extracts from our previous publications (Tanito et al. 2012; Sano et al. 2014) that were used with permission from Japanese Ophthalmological Society.

## References

American_Conference_of_Governmental_Industrial_Hygienists (2015) Light and near-infrared radiation. TLVs and BEIs Cincinnati, USA:CD-ROM

American_Society_for_Testing_and_Materials (1998) ASTM G159-98 standard tables for references Solar Spectral Irradiance at Air Mass 1.5: direct normal and iemispherical for a 37° tilted surface. http://www.astm.org/

Brainard GC, Hanifin JP, Greeson JM et al (2001) Action spectrum for melatonin regulation in humans: evidence for a novel circadian photoreceptor. J Neurosci 21:6405–6412

Braunstein RE, Sparrow JR (2005) A blue-blocking intraocular lens should be used in cataract surgery. Arch Ophthalmol 123:547–549

Brondsted AE, Lundeman JH, Kessel L (2011) Short wavelength light filtering by the natural human lens and IOLs – implications for entrainment of circadian rhythm. Acta Ophthalmol 91:52–57

Ham WT Jr, Mueller HA, Sliney DH (1976) Retinal sensitivity to damage from short wavelength light. Nature 260:153–155

ICNIRP_Guidelines (2013) ICNIRP guidelines on limits of exposure to incoherent visible and infrared radiation. International Commission on Non-Ionizing Radiation Protection. Health Phys 105:74–96

Maher EF (1978) Transmission and absorption coefficients for ocular media of the rhesus monkey. Report SAM-TR-78-32. Brooks Air Force Base (TX): USAF School of Aerospace Medicine:1–104

Mainster MA (2006) Violet and blue light blocking intraocular lenses: photoprotection versus photoreception. Br J Ophthalmol 90:784–792

Mainster MA, Sparrow JR (2003) How much blue light should an IOL transmit? Br J Ophthalmol 87:1523–1529

Margrain TH, Boulton M, Marshall J et al (2004) Do blue light filters confer protection against age-related macular degeneration? Prog Retin Eye Res 23:523–531

Okuno T (1999) Various light sources and blue-light hazards. Saf Health Dig 45:24–33

Sano I, Tanito M, Okuno T et al (2014) Estimation of the melatonin suppression index through clear and yellow-tinted intraocular lenses. Jpn J Ophthalmol 58:320–326

Sui GY, Liu GC, Liu GY et al (2013) Is sunlight exposure a risk factor for age-related macular degeneration? A systematic review and meta-analysis. Br J Ophthalmol 97:389–394

Tanito M (2014) Chapter 15 Retinal photooxidative stress and its modifiers. In: Neuroprotection and Neurodegeneration for Retinal Diseases. Springer Japan, Tokyo, pp 205–226

Tanito M, Okuno T, Ishiba Y et al (2010) Transmission spectrums and retinal blue-light irradiance values of untinted and yellow-tinted intraocular lenses. J Cataract Refract Surg 36:299–307

Tanito M, Okuno T, Ishiba Y et al (2012) Measurements of transmission spectrums and estimation of retinal blue-light irradiance values of currently available clear and yellow-tinted intraocular lenses. Jpn J Ophthalmol 56:82–90

Thapan K, Arendt J, Skene DJ (2001) An action spectrum for melatonin suppression: evidence for a novel non-rod, non-cone photoreceptor system in humans. J Physiol 535:261–267

Turner PL, Mainster MA (2008) Circadian photoreception: ageing and the eye's important role in systemic health. Br J Ophthalmol 92:1439–1444

# Chapter 8
# Co-Expression of Wild-Type and Mutant S163R C1QTNF5 in Retinal Pigment Epithelium


**Astra Dinculescu, Frank M. Dyka, Seok-Hong Min, Rachel M. Stupay, Marcus J. Hooper, W. Clay Smith, and William W. Hauswirth**

**Abstract** The pathogenic mutation S163R in C1QTNF5 causes a disorder known as autosomal dominant late-onset retinal degeneration (L-ORD), characterized by the presence of thick extracellular sub-RPE deposits, similar histopathologically to those found in AMD patients. We have previously shown that the S163R C1QTNF5 mutant forms globular aggregates within the RPE in vivo following its AAV-mediated expression in the RPE and exhibits a reversely polarized distribution, being routed toward the basal rather than apical RPE. We show here that when both wild-type and mutant S163R C1QTNF5 are simultaneously delivered subretinally to mouse RPE cells, the mutant impairs the wild-type protein secretion from the RPE, and both proteins are dispersed toward the basal and lateral RPE membrane. This result has mechanistic and therapeutic implications for L-ORD disorder.

**Keywords** RPE · Basal laminar deposit · AMD · Late-onset retinal degeneration · C1QTNF5 · AAV · Protein aggregation

## 8.1 Introduction

C1QTNF5 belongs to a large family of secreted multimeric proteins, the C1q and tumor necrosis factor-related superfamily (C1q/TNF), whose members are thought to play numerous roles in immunity, inflammation, and glucose and lipid metabolism (Schaffler and Buechler 2012). Every C1q/TNF family member, including

A. Dinculescu (✉) · F. M. Dyka · S. -H. Min · R. M. Stupay · M. J. Hooper
W. C. Smith · W. W. Hauswirth
Department of Ophthalmology, College of Medicine, University of Florida, Gainesville, FL, USA
e-mail: astra@ufl.edu



J. D. Ash et al. (eds.), *Retinal Degenerative Diseases*, Advances in Experimental Medicine and Biology 891, https://doi.org/10.1007/978-3-319-75402-4_8

C1QTNF5, contains a signal peptide to direct protein secretion, a collagen-like domain with variable numbers of Gly-X-Y repeats, and a C-terminal globular C1q domain with sequence homology to the immune complement protein C1q. Several of these members, including C1QTNF5, are secreted by the adipose tissue and circulate abundantly in human serum (Seldin et al. 2014). In addition, C1QTNF5 is also secreted apically from the RPE toward the outer limiting membrane and has been shown to interact with its dicistronic partner, the frizzled-related protein MFRP located at the RPE apical membrane and its microvilli (Mandal et al. 2006a; b).

The S163R mutation in the globular C1q domain of C1QTNF5 causes an autosomal dominant late-onset retinal degeneration (L-ORD) disorder, leading to severe loss of both central and peripheral vision (Hayward et al. 2003; Ayyagari et al. 2005). A characteristic feature of the disorder is the presence of abnormal extracellular thick deposits between the RPE and Bruch's membrane that have a widespread distribution, extending outside the macular region into the peripheral retina (Kuntz et al. 1996). We have previously shown that in contrast to wild-type C1QTNF5, which is apically secreted from RPE, the S163R mutant forms large globular aggregates within the RPE and exhibits a reversely polarized distribution, being routed toward the basal rather than apical RPE, where it forms thick, continuous extracellular basal deposits that lead to regional loss of photoreceptors and RPE atrophy (Dinculescu et al. 2015). In this study, our goal was to test the effects of co-expressing wild-type and mutant S163R C1QTNF5 proteins in vivo in RPE cells by using a similar AAV-mediated RPE targeted approach. Our results show that mutant S163R protein prevents the normal apical directional secretion of wild-type C1QTNF5, and both proteins are distributed toward the lateral and basal regions of RPE cells.

## 8.2 Materials and Methods

### *8.2.1 AAV Vector Production and Delivery*

AAV viral vectors were packaged, purified, and titered according to the previously published methods (Jacobson et al. 2006). Approximately 1 μL of balanced salt solution (BSS) containing AAV vectors ($10^{12}$ vector genomes/mL) was delivered subretinally into one eye of adult C57BL/6 mice (Jackson Laboratory, Bar Harbor, ME, USA), while the contralateral eyes remained uninjected and served as controls. All experiments were approved by University of Florida Institutional Animal Care and Use Committees and conducted in accordance with the ARVO Statement for the Use of Animals in Ophthalmic and Vision Research.

### 8.2.2 *Immunostaining of Retinal Sections*

Eyes were harvested, processed for paraffin embedding, and sectioned at a thickness of 4 μm. The tissue sections were dewaxed in xylene and rehydrated in a graded series of ethanol, then incubated with 0.3% Triton X-100 for 10 min, followed by blocking with a solution of 2% albumin for 1 h. The expression of the hemagglutinin-tagged S163R C1QTNF5 mutant protein (S163R C1QTNF5-HA) in the AAV-treated eyes was detected by immunostaining with a high-affinity anti-HA-fluorescein antibody (3F10; Roche Diagnostics, Indianapolis, IN, USA). The C1QTNF5-myc-tagged wild-type protein was detected with the mouse monoclonal anti-Myc antibody produced and purified from the hybridoma cell line 9E10.

### 8.2.3 *Electroretinographic Analysis*

Subretinally injected C57BL/6 mice were dark-adapted (>12 h) and anesthetized by intraperitoneal injection. Full-field ERGs were recorded as previously described (Dinculescu et al. 2015), using a UTAS Visual Diagnostic System (LKC Technologies, Gaithersburg, MD, USA). Differences in b-wave maximum amplitudes between AAV-injected and uninjected contralateral control eyes were analyzed by Student's t-test for paired samples (GraphPad Prism 6.0; GraphPad Software) and considered statistically significant if $P < 0.05$.

## 8.3 Results

We generated scAAV vectors with the AAV2 quad YF capsid containing either wild-type C1QTNF5-myc-tagged cDNA or mutant S163R C1QTNF5-HA-tagged cDNA, driven by an RPE-specific BEST1 promoter. These vectors were either delivered individually or as a mixture containing equal amounts of wild-type and mutant S163R AAV.

We have previously shown that the AAV-expressed wild-type C1QTNF5 is secreted apically from the RPE, in a similar pattern to that of the endogenous protein (Dinculescu et al. 2015). We have also shown that the AAV-expressed S163R mutant forms large globular aggregates in the RPE and is routed toward the basal side, where it forms thick deposits over time (Dinculescu et al. 2015), a result confirmed in these experiments (Fig. 8.1). This AAV-based model is very robust, with every AAV-S163R injected eye showing the presence of characteristic spherical aggregates by 4 months postinjection, followed by the gradual accumulation of thick S163R basal deposits by 9 months postinjection, as detected by immunofluorescence (Fig. 8.1). In order to determine if the mutant S163R aggregate formation could be prevented by increasing the amount of wild-type C1QTNF5 protein in the RPE relative to its endogenous levels, we delivered a mixture containing equal

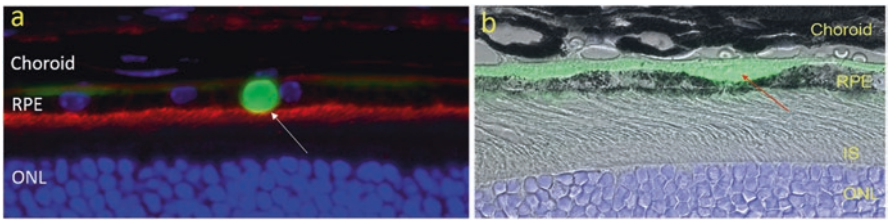


**Fig. 8.1** Detection of AAV-expressed mutant S163R C1QTNF5 mutant (green) by immunofluorescence microscopy. (**a**) Note the large S163R globular aggregate (arrow) present in the RPE cytoplasm (4 months postinjection). The apical RPE microvilli are labelled with an anti-MFRP antibody (*red*). (**b**) Retinal section showing the presence of a dome-shaped basal RPE deposit containing the S163R mutant protein (9 months postinjection). *IS* inner segment, *ONL* outer nuclear layer

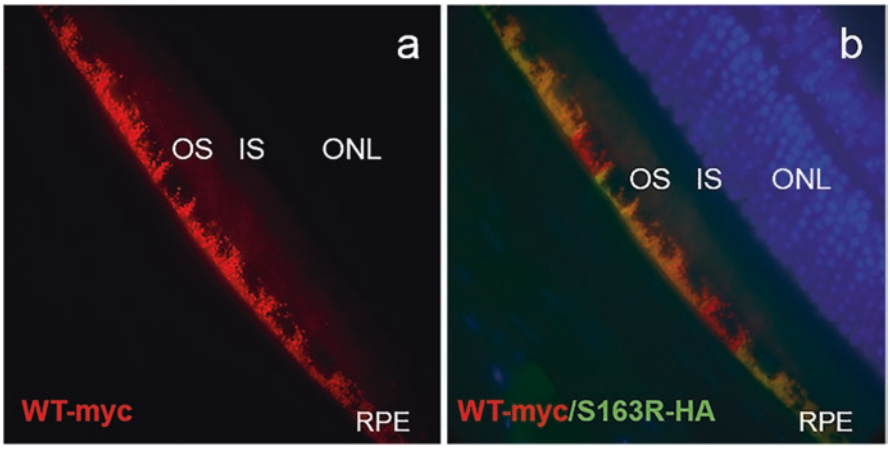


**Fig. 8.2** Evaluation of retinal sections by immunostaining following co-delivery of epitope-tagged wild-type and mutant S163R C1QTNF5. (**a**) Detection of wild-type C1QTNF5 (myc-tagged) by immunofluorescence microscopy. (**b**) Merged image showing the detection of AAV-expressed wild-type C1QTNF5 (red) and HA-tagged mutant S163R (green) at 4 months postinjection

amounts of AAV vectors expressing the epitope-tagged wild-type and mutant S163R C1QTNF5. Surprisingly, under these conditions, the S163R mutant no longer forms the characteristic large globular aggregates in the RPE, and instead it is found dispersed toward the RPE lateral and basal membrane, where it co-localizes with the AAV-expressed wild-type protein (Fig. 8.2). Full-field ERG analysis was performed under scotopic dark-adapted and photopic light-adapted cone-mediated conditions to evaluate the effects of co-expressing the wild-type and mutant S163R in RPE on retinal function (Fig. 8.3). Although treated eyes displayed low ERG amplitudes, the difference between the maximum b-wave amplitude average in injected and

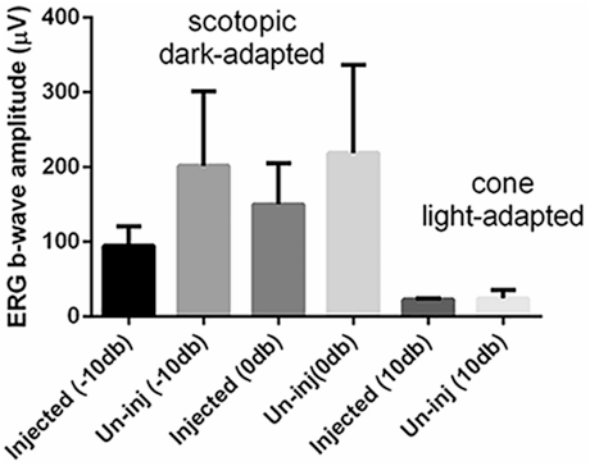


**Fig. 8.3** Evaluation of retinal function by ERG analysis at 4 months following co-delivery of wild-type and mutant S163R C1QTNF5 vectors. Bar graph shows the maximum ERG b-wave amplitudes in the injected eyes compared with untreated contralateral controls under dark-adapted (−10 and 0 dB scotopic) or light-adapted (10 dB photopic) conditions. The differences between injected and uninjected eyes were not statistically significant at all light intensities examined ($n = 4$ mice)

untreated control eyes at various light intensities was not significant, perhaps due to the large variability in ERG responses among different animals and the small sample size.

## 8.4 Discussion

C1QTNF5 is a membrane-bound and secreted protein of unknown function, highly expressed in the RPE and ciliary epithelium (Mandal et al. 2006b). Previous studies have shown that wild-type C1QTNF5 can assemble into trimers, hexamers, and bouquet-like octadecameric species, similar to other C1q/TNF family members (Tu and Palczewski 2012). The function of this multimerization process and the disease mechanism caused by the S163R mutation in C1QTNF5 are not currently understood.

Wild-type and S163R mutant gC1q domains have been previously shown to interact by in vitro studies (Shu et al. 2006), and it has also been suggested that they may coexist in the globular heads of the C1QTNF5 octadecameric structure (Tu and Palczewski 2014). Our previous studies, confirmed by experiments described here, have determined that mutant S163R forms large intracellular globular aggregates following its overexpression in murine RPE, leading to its accumulation as thick, continuous, basal deposits between the choroid and RPE, visible by light microscopy (Dinculescu et al. 2015). Moreover, our results show that the presence of the S163R mutant significantly impairs the wild-type C1QTNF5 apical secretion from

the RPE when both tagged proteins are co-delivered using AAV vectors of similar titers, leading to their aggregation in distinct ring-shaped structures and their abnormal distribution toward the lateral and basal RPE membranes. Consequently, these results suggest that wild-type and mutant C1QTNF5 are able to interact in vivo and have implications for understanding the disease pathology.

**Acknowledgments** This study was supported in part by an unrestricted grant from Research to Prevent Blindness, NIH grants EY021721 and EY018331, FFB, and MVRF.

## References

Ayyagari R, Mandal MN, Karoukis AJ et al (2005) Late-onset macular degeneration and long anterior lens zonules result from a CTRP5 gene mutation. Invest Ophthalmol Vis Sci 46:3363–3371

Dinculescu A, Min SH, Dyka FM et al (2015) Pathological effects of mutant C1QTNF5 (S163R) expression in murine retinal pigment epithelium. Invest Ophthalmol Vis Sci 56:6971–6980

Hayward C, Shu X, Cideciyan AV et al (2003) Mutation in a short-chain collagen gene, CTRP5, results in extracellular deposit formation in late-onset retinal degeneration: a genetic model for age-related macular degeneration. Hum Mol Genet 12:2657–2667

Jacobson SG, Acland GM, Aguirre GD et al (2006) Safety of recombinant adeno-associated virus type 2-RPE65 vector delivered by ocular subretinal injection. Mol Ther J Am Soc Gene Ther 13:1074–1084

Kuntz CA, Jacobson SG, Cideciyan AV et al (1996) Sub-retinal pigment epithelial deposits in a dominant late-onset retinal degeneration. Invest Ophthalmol Vis Sci 37:1772–1782

Mandal MN, Vasireddy V, Jablonski MM et al (2006a) Spatial and temporal expression of MFRP and its interaction with CTRP5. Invest Ophthalmol Vis Sci 47:5514–5521

Mandal MN, Vasireddy V, Reddy GB et al (2006b) CTRP5 is a membrane-associated and secretory protein in the RPE and ciliary body and the S163R mutation of CTRP5 impairs its secretion. Invest Ophthalmol Vis Sci 47:5505–5513

Schaffler A, Buechler C (2012) CTRP family: linking immunity to metabolism. Trends Endocrinol Metab 23:194–204

Seldin MM, Tan SY, Wong GW (2014) Metabolic function of the CTRP family of hormones. Rev Endocr Metab Disord 15:111–123

Shu X, Tulloch B, Lennon A et al (2006) Disease mechanisms in late-onset retinal macular degeneration associated with mutation in C1QTNF5. Hum Mol Genet 15:1680–1689

Tu X, Palczewski K (2012) Crystal structure of the globular domain of C1QTNF5: implications for late-onset retinal macular degeneration. J Struct Biol 180:439–446

Tu X, Palczewski K (2014) The macular degeneration-linked C1QTNF5 (S163) mutation causes higher-order structural rearrangements. J Struct Biol 186:86–94

# Part II
# Gene Therapies

# Chapter 9
# Mini-Review: Cell Type-Specific Optogenetic Vision Restoration Approaches


**Antoine Chaffiol and Jens Duebel**

**Abstract** The expression of light-sensitive microbial opsins is a promising mutation-independent approach to restore vision in retinal degenerative diseases. Using viral vectors, optogenetic tools can be genetically expressed in various subpopulations of retinal neurons. The choice of cell type depends on the availability of surviving retinal cells. If cones are still alive but they lack outer segments, they can be targeted with optogenetic inhibitors, such as halorhodopsin. Alternatively, it is possible to bypass the photoreceptors and to target bipolar cells. In late-stage degeneration, when bipolar cells degenerate, "artificial photoreceptors" can be made from retinal ganglion cells, but with this approach, upstream retinal processing cannot be utilized. However, when ganglion cells are stimulated directly, higher brain regions might be able to compensate for some loss of retinal processing, which is indicated by clinical studies with epiretinal implants, where patients can perform simple visual tasks. Finally, optogenetics in combination with neuroprotective approaches could serve as a valuable strategy to restore the function of remaining cells, as well as to rescue retinal neurons from progressive degeneration.

**Keywords** Retina · Optogenetics · Vision restoration · Channelrhodopsin · Opsins · Retinal disease

Optogenetics is a technique that allows for the optical control of neural activity (Boyden et al. 2005; Deisseroth et al. 2006; Häusser 2014) by using light-sensitive ion channels or pumps derived from algae or bacteria (e.g., channelrhodopsin or halorhodopsin) (Nagel et al. 2003; Oesterhelt and Stoeckenius 1971; Sugiyama and Mukohata 1984), as well as other optogenetic tools, such as vertebrate opsins (Herlitze and Landmesser 2007). In a degenerated blind retina, the specific

A. Chaffiol · J. Duebel (✉)
Sorbonne Université, INSERM, CNRS, Institut de la Vision, 17 rue Moreau, Paris, France
e-mail: jens.duebel@inserm.fr



J. D. Ash et al. (eds.), *Retinal Degenerative Diseases*, Advances in Experimental Medicine and Biology 891, https://doi.org/10.1007/978-3-319-75402-4_9

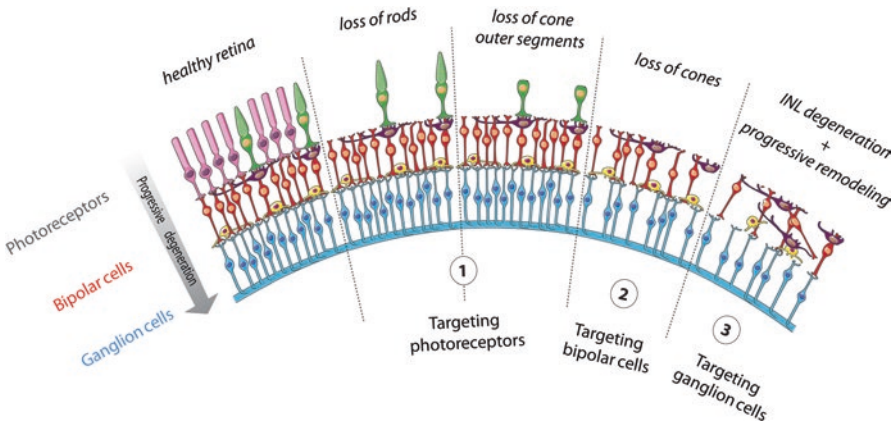


**Fig. 9.1** Schematic diagram of a healthy retina compared to retinae with progressive degeneration and circuit remodeling. The choice of the therapeutic strategy is determined by the availability of persisting cell types, ranging from targeting "dormant" cones (1), bipolar cells (2), to retinal ganglion cells (3). Horizontal cells and amacrine cells are shown in dark purple and yellow, respectively. *INL* inner nuclear layer

expression of optogenetic tools enables to convert specific retinal cells types into "artificial photoreceptors" (Sahel and Roska 2013).

Depending on the degenerative state of the retina, different optogenetic strategies can be used (Fig. 9.1). Targeting of retinal photoreceptors could be an option for RP patients with remaining cone cell bodies lacking their light-sensitive outer segments. Anatomical studies, using postmortem retinal tissue (Lin et al. 2009) or in vivo imaging (optical coherence tomography) from RP patients (Jacobson et al. 2013), have shown that some patients with late-stage RP had residual cone cell bodies. These observations suggest that there are candidates who could be eligible for photoreceptor-based strategies. In the mouse model, the reactivation of nonfunctional but surviving "dormant" cones, using the light-sensitive chloride pump halorhodopsin, has been shown by Botond Roska's group (Busskamp et al. 2010). Halorhodopsin was able to substitute for the impaired phototransduction cascade in treated blind mice. These reactivated cones could drive retinal circuit functions, including lateral inhibition and directional selectivity, and they mediated cortical processing as well as visually guided behavior. Moreover, human retinal explants were used to reactivate light-insensitive photoreceptors with halorhodopsin, demonstrating the functionality of the microbial opsin in the human retina.

However, it is unknown how long synaptic connection from photoreceptors to bipolar cells will remain under degenerative conditions. Therefore, cell type-specific targeting of optogenetic tools to retinal bipolar cells would be another attractive option. In a pioneering study, Lagali et al. used electroporation to express channelrhodopsin (ChR2) under control of the ON bipolar cell promoter in ON bipolar cells of blind mice (*rd1*), leading to the recovery of visually evoked potentials in the cortex and visually guided behavior (Lagali et al. 2008). Electroporation, however,

had to be replaced by viral gene delivery suitable for potential clinical applications. Meanwhile, AAV-based vectors with improved retinal diffusion properties have been developed (Dalkara et al. 2013), and it has been shown that these engineered AAVs can efficiently deliver ChR2 variants to ON bipolar cells (Cronin et al. 2014; Macé et al. 2015) of blind mice. Importantly, ChR2 targeted to ON bipolar cells restored both ON and OFF component of the visual responses, which is mediated by inner retinal processing. The restoration of the ON/OFF pathway was also observed in the retina and in the visual cortex. In addition, light-induced behavior was observed in these treated blind mice (Cehajic-Kapetanovic et al. 2015; Gaub et al. 2014, 2015; Macé et al. 2015; van Wyk et al. 2015), but targeting of bipolar cells has not yet been accomplished in non-human primates.

Finally, optogenetic targeting of ganglion cells could be a therapeutic strategy for patients with late-stage degeneration and advanced remodeling of inner retinal circuits (Jacobson et al. 2013; Jones et al. 2016). Bi and Pan were the first to show that light sensitivity can be restored through expression of ChR2 in retinal ganglion cells after complete photoreceptor degeneration (Bi et al. 2006), which was followed by other studies (Caporale et al. 2011; Greenberg et al. 2011; Ivanova and Pan 2009; Lin et al. 2008; Sengupta et al. 2016; Tomita et al. 2010; Tomita et al. 2007; Wu et al. 2013; Zhang et al. 2009). A disadvantage of this approach is that neural circuits upstream of ganglion cells cannot be utilized. On the other hand, clinical studies using direct electrical stimulation of ganglion cells with epiretinal implants have shown that patients are able to perform visual tasks, such as object localization or motion discrimination (Humayun et al. 2012; Shepherd et al. 2013). This indicates that the plasticity of higher brain regions can compensate for some loss of retinal image processing and that the human cortex has the capability to adapt to a visual code that is different from the natural activity pattern conveyed by a healthy retina.

In summary, optogenetics enables to confer light sensitivity to distinct retinal cell types, thus offering new therapeutic approaches to restore vision in a wide range of retinal degenerative diseases. In a future perspective, combined approaches of optogenetics with neuroprotection could be a therapeutic option, not only to restore the function of remaining cells but also to rescue retinal structures from progressive degeneration (Sahel and Roska 2013). Although the therapeutic benefits of optogenetic approaches remain to be determined, first steps toward clinical application (ClinicalTrials.gov Identifiers: NCT02556736, NCT03326336) have been taken.

## References

Bi A, Cui J, Ma YP et al (2006) Ectopic expression of a microbial-type rhodopsin restores visual responses in mice with photoreceptor degeneration. Neuron 50:23–33

Boyden ES, Zhang F, Bamberg E et al (2005) Millisecond-timescale, genetically targeted optical control of neural activity. Nat Neurosci 8:1263–1268

Busskamp V, Duebel J, Balya D et al (2010) Genetic reactivation of cone photoreceptors restores visual responses in retinitis pigmentosa. Science 329:413–417

Caporale N, Kolstad KD, Lee T et al (2011) LiGluR restores visual responses in rodent models of inherited blindness. Mol Ther 19:1212–1219. article

Cehajic-Kapetanovic J, Eleftheriou C, Allen AEE et al (2015) Restoration of vision with ectopic expression of human rod opsin. Curr Biol 25:2111–2122. article

Cronin T, Vandenberghe LHH, Hantz P et al (2014) Efficient transduction and optogenetic stimulation of retinal bipolar cells by a synthetic adeno-associated virus capsid and promoter. EMBO Mol Med 6:1175–1190. article

Dalkara D, Byrne LC, Klimczak RR et al (2013) In vivo-directed evolution of a new adeno-associated virus for therapeutic outer retinal gene delivery from the vitreous. Sci Transl Med 5:189ra76

Deisseroth K, Feng G, Majewska AK et al (2006) Next-generation optical technologies for illuminating genetically targeted brain circuits. J Neurosci 26:10380–10386

Gaub BMM, Berry MHH, Holt AEE et al (2014) Restoration of visual function by expression of a light-gated mammalian ion channel in retinal ganglion cells or ON-bipolar cells. Proc Natl Acad Sci U S A 111:E5574–E5583. article

Gaub BM, Berry MH, Holt AE et al (2015) Optogenetic vision restoration using rhodopsin for enhanced sensitivity. Mol Ther 23(10):1562–1571. article

Greenberg KP, Pham A, Werblin FS (2011) Differential targeting of optical neuromodulators to ganglion cell soma and dendrites allows dynamic control of center-surround antagonism. Neuron 69:713–720. article

Häusser M (2014) Optogenetics: the age of light. Nat Methods 11:1012–1014

Herlitze S, Landmesser LT (2007) New optical tools for controlling neuronal activity. Curr Opin Neurobiol 16(1):87–94

Humayun MS, Dorn JD, da Cruz L et al (2012) Interim results from the international trial of second Sight's visual prosthesis. Ophthalmology 119:779–788

Ivanova E, Pan Z-H (2009) Evaluation of the adeno-associated virus mediated long-term expression of channelrhodopsin-2 in the mouse retina. Mol Vis 15:1680–1689

Jacobson SG, Sumaroka A, Luo X et al (2013) Retinal optogenetic therapies: clinical criteria for candidacy. Clin Genet 84:175–182. article

Jones BW, Pfeiffer RL, Ferrell WD et al (2016) Retinal remodeling in human retinitis pigmentosa. Exp Eye Res 150:149–165

Lagali PS, Balya D, Awatramani GB et al (2008) Light-activated channels targeted to ON bipolar cells restore visual function in retinal degeneration. Nat Neurosci 11:667–675. article

Lin B, Koizumi A, Tanaka N et al (2008) Restoration of visual function in retinal degeneration mice by ectopic expression of melanopsin. Proc Natl Acad Sci U S A 105:16009–16014. article

Lin B, Masland RH, Strettoi E (2009) Remodeling of cone photoreceptor cells after rod degeneration in rd mice. Exp Eye Res 88:589–599

Macé E, Caplette R, Marre O et al (2015) Targeting channelrhodopsin-2 to ON-bipolar cells with vitreally administered AAV restores ON and OFF visual responses in blind mice. Mol Ther 23:7–16. article

Nagel G, Szellas T, Huhn W et al (2003) Channelrhodopsin-2, a directly light-gated cation-selective membrane channel. Proc Natl Acad Sci U S A 100:13940–13945. article

Oesterhelt D, Stoeckenius W (1971) Rhodopsin-like protein from the purple membrane of Halobacterium halobium. Nat New Biol 233:149–152

Sahel J-AA, Roska B (2013) Gene therapy for blindness. Annu Rev Neurosci 36:467–488

Sengupta A, Chaffiol A, Macé E et al (2016) Red-shifted channelrhodopsin stimulation restores light responses in blind mice, macaque retina, and human retina. EMBO Mol Med 8:1248–1264

Shepherd RK, Shivdasani MN, Nayagam DAX et al (2013) Visual prostheses for the blind. Trends Biotechnol 31:562–571. article

Sugiyama Y, Mukohata Y (1984) Isolation and characterization of halorhodopsin from Halobacterium halobium. J Biochem 96:413–420

Tomita H, Sugano E, Yawo H et al (2007) Restoration of visual response in aged dystrophic RCS rats using AAV-mediated channelopsin-2 gene transfer. Invest Ophthalmol Vis Sci 48:3821–3826. article

Tomita H, Sugano E, Isago H et al (2010) Channelrhodopsin-2 gene transduced into retinal ganglion cells restores functional vision in genetically blind rats. Exp Eye Res 90:429–436

Wu C, Ivanova E, Zhang Y et al (2013) rAAV-mediated subcellular targeting of optogenetic tools in retinal ganglion cells in vivo. PLoS One 8:e66332. article

van Wyk M, Pielecka-Fortuna J, Löwel S et al (2015) Restoring the ON switch in blind retinas: opto-mGluR6, a next-generation, cell-tailored optogenetic tool. PLoS Biol 13:e1002143. article

Zhang Y, Ivanova E, Bi A et al (2009) Ectopic expression of multiple microbial rhodopsins restores ON and OFF light responses in retinas with photoreceptor degeneration. J Neurosci 29:9186–9196

# Chapter 10
# Mutation-Independent Gene Therapies for Rod-Cone Dystrophies


**Cécile Fortuny and John G. Flannery**

**Abstract** The clinical success of gene replacement therapies in recent years has served as a proof of concept for the treatment of inherited retinal degenerations using adeno-associated virus (AAV) as viral vector. However, inherited retinal degenerative diseases showcase a broad genetic and mechanistic heterogeneity, challenging the development of mutation-specific therapies for each specific mutation. Mutation-independent approaches must be developed to slow down retinal degeneration regardless of the underlying genetic mutation and onset of the disease. New understanding of cell death mechanisms in rod-cone dystrophies have led to promising rescue of photoreceptor cell death by virally mediating expression of anti-apoptotic factors and secretion of retinal neurotrophic factors. Optogenetic therapies are also able to restore light sensitivities in blind retinas.

**Keywords** Adeno-associated virus · Retinitis pigmentosa · Mutation-independent · Cell death · Gene therapy · Müller glia · Photoreceptor · Apoptosis · Neuroprotection · Optogenetics

## 10.1 Introduction

Rods and cones are the two main photoreceptor cells contributing to the first steps in sensing light in the retina and translating it to an electric signal to the other neuronal cells downstream to finally be processed in the primary visual cortex. Many hundreds of proteins are involved in the light response and keeping the cells of the retina nourished and healthy. This high degree of metabolic activity makes the

C. Fortuny
Vision Science Graduate Group, Optometry School, University of California Berkeley, Berkeley, CA, USA
e-mail: cecile.fortuny@berkeley.edu

J. G. Flannery (✉)
Helen Wills Neuroscience Institute, Vision Science Graduate Group, University of California Berkeley, Berkeley, CA, USA
e-mail: flannery@berkeley.edu



J. D. Ash et al. (eds.), *Retinal Degenerative Diseases*, Advances in Experimental Medicine and Biology 891, https://doi.org/10.1007/978-3-319-75402-4_10

retina more sensitive to mutations and degeneration: when a gene mutation occurs, the protein may be incorrectly synthetized and act abnormally or may not be expressed, triggering a loss of function and vision. The majority of inherited retinopathies (IR) are caused by mutations found in photoreceptors and to a lesser extent in the retinal pigment epithelium (RPE). Most of the mutations identified in IR affect genes involved in either the photoreceptor structural integrity (*CEP290*, *USH2A*, etc.) or in the phototransduction cascade (*RHO*, *PD6EB*, *CNGA3*, etc.) leading to blindness as a result of loss of photoreceptors. Among them, retinitis pigmentosa (RP) is the most common inherited cause of blindness in the world (Hartong et al. 2006). Currently, no effective treatment exists to treat those diseases, but gene therapy approaches have been developed and have begun to show success at delaying retinal degeneration. This review will focus on current mutation-independent gene therapy approaches for treating RP.

## 10.2 Gene Therapy for the Retina

Different therapies have attempted to reduce retinal degeneration in RP. Before recent progress in gene-based therapeutics, surgery and vitaminotherapy were the most common treatments employed to treat RP. Gene therapy has been a growing field in the past decade for treating ocular disease and has proven to be an efficient and safe way of treating single-gene mutations leading to blindness by providing therapeutic DNA to targeted cells in the retina by the use of viral or non-viral vectors. A determining element in gene therapy studies is the vector used to administer the payload. In vivo, viral vectors are the most successful in long-term expression and delivery of genetic material to cells within tissues. Different viruses have been used in clinical trials although adeno- associated virus (AAV) is currently the gold standard for viral vectors for gene delivery in the retina due to its excellent safety profile as well as its efficiency in transducing a large spectrum of cells. AAV is a small non-enveloped icosahedral parvovirus with a genome (4.9 kb) that consists of three open reading frames (rep, cap, and the assembly-activating protein) flanked by two inverted terminal repeats (ITRs) that form hairpin structures and are essential for viral packaging. The rep gene encodes for proteins involved in viral replication and packaging, and the cap gene encodes for the capsid proteins (VP1, VP2, VP3) of the virus. The assembly-activating protein participates in the process of capsid assembly (Mitchell et al. 2010; Sonntag et al. 2011). AAV-mediated gene therapy has shown many advantages over other viruses as viral vectors for the retina. As a *Dependovirus*, AAV is unable to replicate in the absence of a helper virus with no risk of genetic integration in the genome. The virus infects quiescent and dividing cells, leading to long-term expression of the transgene in the cells without any known pathogenicity for the host. Different serotypes of AAV have been discovered and used to infect retinal cells, highlighting that the AAV capsid sequence and the route of delivery (intravitreal or subretinal) are two major components affecting the cell tropism (Watanabe et al. 2013). The clinical trials for Leber's congenital

amaurosis (LCA) type 2 were the first to validate the proof of concept for safe AAV-mediated therapies after successfully rescuing vision in patients after delivery of a healthy copy of the affected RPE65 gene to the RPE. However, most of the successful clinical trials for retinal degeneration have been gene replacement. It requires the disease to be monogenic and the genetic cause to be known as well as its retinal phenotype characterized. It also only holds promise if implemented early on in the disease progression of the patient. However, more than 40–50% of genes involved in degeneration remain unknown in RP. For those patients, a gene replacement strategy is not possible and requires other approaches such as mutation-independent gene therapies.

## 10.3 Cell Death Mechanisms in RP

Despite the genetic heterogeneity of RP, these diseases share a similar phenotype in which rod photoreceptors die first followed by cone cell death. One treatment approach is to delay rod photoreceptor cell death, in order to preserve cone health and function as long as possible considering these cells are responsible for central, color, and day vision. Cell death mechanisms governing retinal degenerations were poorly understood at the time. Animals of RP mimicking human diseases have been used to study these mechanisms. The classical pathway for rod photoreceptor cell death was believed to be caspase-mediated apoptosis. A number of anti-apoptotic genes have been identified and used in therapeutic approaches including the BCL-2 family (Chen et al. 1996) and the anti-apoptotic protein family (IAP) (Liston et al. 2003). X-linked inhibitor of apoptosis protein (XIAP) is one of the most potent proteins from IAP family and has been shown to efficiently delay cell death in models of retinal degeneration (Leonard et al. 2007; Shan et al. 2011). However, recent work demonstrated that caspase-independent pathways are activated as a result of secondary cell messenger increase (e.g., cGMP, calcium). Research performed in rd1 and rd10 mice by Paquet-Durant et al. (2007) showed that PDE6B deficiency leads to an increase in extracellular levels of calcium by 190% compared to a healthy retina (Zhivotovsky and Orrenius 2011; Sahaboglu et al. 2013). Calpains, calcium-activated cysteines, are known to contribute to this secondary neurodegenerative cascade in the same pattern as caspases, by cleaving cellular substrates, and are also involved in the cell's autophagy pathway (Nguyen et al. 2011). Calpastatin is the only known endogenous inhibitor of calpains and has been studied as a potential gene candidate for delaying cell death in rod photoreceptors. Other caspase-independent pathways involving poly (ADP-ribose) polymerase or histone deacetylase (Kaur et al. 2011) are activated in dying rods in several models of RP and will lead to the development of new therapeutics to treat rod photoreceptor cell death. In contrast, the mode of cone cell death is less characterized. Multiple studies have shown that these cells undergo necrosis after the loss of rods. Previous studies have suggested that this could be due to environmental alterations such as the release of toxins from rod apoptosis, loss of rod-cone gap junctions, microglia activation, and

oxidative stress. The later and slower onset of cone death suggested that rod cell death is not the primary reason for cone cell death, but a long-term change of photoreceptor environment (e.g., cell density). The insulin/signaling pathway is key in sensing trophic factors and nutrients and assessing the energy status of the cell. In RP, mTOR levels in cones after rod loss are downregulated. Punzo et al. found that degenerative cones expressed higher levels of HIF-1, a transcription factor that improves glycolysis in stressed conditions, proving that cones are dying as a result of starvation and nutritional losses (Bovolenta and Cisneros 2009; Wojno et al. 2013; Ma et al. 2015).

## 10.4 Neuroprotection

Studies have highlighted the importance of neurotrophic factor signaling in the healthy and diseased retina. Trophic or growth factors are endogenously secreted molecules that stimulate cellular growth, proliferation, cellular differentiation, and regeneration. In the eye, the major layers secreting these factors are the RPE and Müller cells. The Müller glial cells represent an excellent target for neurotrophin secretions. Being very numerous, they span the entire retina and are directly involved in maintaining photoreceptors. Also, their close contact with neuronal cells makes them ideal candidates for the secretion of neurotrophic factors. Dalkara et al. (2011) showed how a novel AAV vector, ShH10, was able to transduce efficiently and selectively glia cells through intravitreal injection, generating high levels of glial cell-derived neurotrophic factor (GDNF) expression, which promotes neuronal survival and leads to rescue in S334-4ter rat model lasting up to 6 months postinjection. José-Alain Sahel and Thierry Léveillard's group discovered and characterized the rod-derived cone viability factor (RdCVF), a survival factor secreted by rod photoreceptors that signal to the cone photoreceptors (Aït-Ali et al. 2015). During degeneration, the loss of neurotrophic support due to rod cell death has been hypothesized as the main cause of secondary cone degeneration. AAV-RdCVF has been shown to delay cone cell death in models of RP (Byrne et al. 2015). Other trophic factors such as the ciliary neurotrophic factor (CNTF), brain-derived neurotropic factor (BDNF), and basic fibroblast growth factor (bFGF) have also been extensively studied as potential neuroprotective candidates (Buch et al. 2006).

## 10.5 Optogenetics for the Blind Retina

At the final stages of RP, the photoreceptor layer is completely lost. There is currently no treatment available for patients at that point. Optogenetic tools have emerged as promising therapies, converting the surviving retinal interneurons into light-sensitive cells by using genetic-encoded light gated proteins. The main actuators are channelrhodopsin 2 (ChR2), which mediates an excitatory cation current

when activated with blue light, and halorhodopsin (NpHR), which mediates an inhibitory current via yellow light. Bi et al. (2006) delivered AAV-ChR2 to ganglion cells in the rd1 mouse and restored visually evoked responses in the retina and visual cortex. Novel ChR variants with improved kinetics have been engineered to increase light sensitivity of the system. Alternative approaches have been developed with engineering endogenous mammalian channels sensitized to light by chemical modifications. The light-gated ionotropic glutamate receptor (LiGluR) consists of iGluR6 with an introduced cysteine in position 439 (L439C) for the covalent attachment of a photoisomerable molecule ("photoswitch") that reversibly activates the receptor. The LiGluR photoswitch has a maleimide linked to a glutamate by a photoisomerizable azobenzene linker (maleimide-azobenzene-glutamate (MAG)). When excited at 380 nm (near UV-range), MAG triggers the opening of the ion channel, which could be closed when excited at a different wavelength, enabling the channel to be turned on and off with light stimulation. This system was later on optimized by engineering a second-generation photoswitch, MAG(460), that is activated by white light and turns off naturally in the dark (Caporale et al. 2011; Gaub et al. 2014). Research has shifted away from targeting only ganglion cells since they bypass other inner retinal cells resulting in a loss of spatial and temporal information. Targeting ON-bipolar cells is a challenging approach as natural AAVs have shown very low efficiency in those cells. New viral variants and promoters have been engineered to overcome these delivery barriers and showed promising results in restoring light sensitivity in blind mice (Lagali et al. 2008; Cronin et al. 2014; Gaub et al. 2015).

## 10.6 Conclusion

The rare nature of most retinal dystrophies, associated with genotypic and phenotypic heterogeneity observed in patients, means that only a relatively small number might benefit from treatments targeting specific gene mutations. Alternatives such as mutation-independent therapies must be developed and adapted to the patient's particular stage of degeneration. Single-treatment therapies marked the beginning of vector gene therapy, but emerging studies show a synergistic effect by combining two treatments. AAV vector gene replacement therapy can be complemented with anti-apoptotic proteins to prolong the efficacy of the treatment or the combination of trophic factors, demonstrating that these approaches can promote photoreceptor survival through a synergistic combination and be adapted to orphan diseases. Targeting two different pathways/cell types in a combination therapy is also promising, increasing the protection of photoreceptors (Fortuny et al. 2013). However, advances in gene therapy for retinal disease need to improve the vector capacity (4.7 kb cargo capacity) as well as increase the number of transduced cells while remaining safe, noninvasive, and cell-specific.

## References

Aït-Ali N, Fridlich R, Millet-Puel G, Clérin E et al (2015) Rod-derived cone viability factor promotes cone survival by stimulating aerobic glycolysis. Cell 161:817–832

AMA M, Nicolson SC et al (2010) AAV's anatomy: roadmap for optimizing vectors for translational success. Curr Gene Ther 10:319–340

Bi A, Cui J, Ma YP, Olshevskaya E et al (2006) Ectopic expression of a microbial-type rhodopsin restores visual responses in mice with photoreceptor degeneration. Neuron 50:23–33. https://doi.org/10.1016/j.neuron.2006.02.026

Bovolenta P, Cisneros E (2009) Retinitis pigmentosa: cone photoreceptors starving to death. Nat Neurosci 12(1):5–6

Buch PK, MacLaren RE, Durán Y et al (2006) In contrast to AAV-mediated Cntf expression, AAV-mediated Gdnf expression enhances gene replacement therapy in rodent models of retinal degeneration. Mol Ther 14:10–10

Byrne LC, Dalkara D, Luna G et al (2015) Viral-mediated RdCVF and RdCVFL expression protects cone and rod photoreceptors in retinal degeneration. J Clin Invest 125:105–116

Caporale N, Kolstad KD, Lee T et al (2011) LiGluR restores visual responses in rodent models of inherited blindness. Mol Ther 19(7):1212–1219

Chen J, Flannery JG, LaVail MM et al (1996) bcl-2 overexpression reduces apoptotic photoreceptor cell death in three different retinal degenerations. PNAS 93:7042–7047

Cronin T, Vandenberghe LH, Hantz P et al (2014) Efficient transduction and optogenetic stimulation of retinal bipolar cells by a synthetic adeno-associated virus capsid and promoter. EMBO Mol Med 6:1175–1190

Dalkara D, Kolstad KD, Guerin KI et al (2011) AAV mediated GDNF secretion from retinal glia slows down retinal degeneration in a rat model of retinitis pigmentosa. Mol Ther 19:1602–1608

Fortuny C, Byrne L, Dalkara D et al (2013) AAV-mediated combination therapy of neurotrophic and anti-apoptotic factors in a mouse model of inherited retinal degeneration. Invest Ophthalmol Vis Sci 54:2746–2746

Gaub BM, Berry MH, Holt AE et al (2014) Restoration of visual function by expression of a light-gated mammalian ion channel in retinal ganglion cells or ON-bipolar cells. Proc Natl Acad Sci 111:E5574–E5583

Gaub BM, Berry MH, Holt AE et al (2015) Optogenetic vision restoration using rhodopsin for enhanced sensitivity. Mol Ther 23:1562–1571

Hartong DT, Berson EL, Dryja TP (2006) Retinitis pigmentosa. Lancet 368:1795–1809

Kaur J, Mencl S, Sahaboglu A et al (2011) Calpain and PARP activation during photoreceptor cell death in P23H and S334ter rhodopsin mutant rats. PLoS One 6:e22181

Lagali PS, Balya D, Awatramani GB et al (2008) Light-activated channels targeted to ON bipolar cells restore visual function in retinal degeneration. Nat Neurosci 11:667–675

Leonard KC, Petrin D, Coupland SG et al (2007) XIAP protection of photoreceptors in animal models of retinitis pigmentosa. PLoS One 2:e314

Liston P, Fong WG, Korneluk RG (2003) The inhibitors of apoptosis: there is more to life than Bcl2. Oncogene 22:8568–8580

Ma S, Venkatesh A, Langellotto F, Le YZ et al (2015) Loss of mTOR signaling affects cone function, cone structure and expression of cone specific proteins without affecting cone survival. Exp Eye Res 135:1–13

Nguyen ATH, Campbell M, Kenna PF et al (2011) Calpain and photoreceptor apoptosis. In: Retinal degenerative diseases, Advances in experimental medicine and biology. Springer US, Boston, MA, pp 547–552

Paquet-Durand F, Johnson L, Ekström P (2007) Calpain activity in retinal degeneration. J Neurosci Res 85:693–702

Sahaboglu A, Paquet-Durand O, Dietter J et al (2013) Retinitis pigmentosa: rapid neurodegeneration is governed by slow cell death mechanisms. Cell Death Dis 4:e488

Shan H, Ji D, Barnard AR et al (2011) AAV-mediated gene transfer of human X-Linked inhibitor of apoptosis protects against oxidative cell death in human RPE cells. Invest Ophthalmol Vis Sci 52(13):9591–9597

Sonntag F, Köther K, Schmidt K, Weghofer M et al (2011) The assembly-activating protein promotes capsid assembly of different adeno-associated virus serotypes. J Virol 85:12686–12697

Watanabe S, Sanuki R, Ueno S et al (2013) Tropisms of AAV for subretinal delivery to the neonatal mouse retina and its application for in vivo rescue of developmental photoreceptor disorders. PLoS One 8:e54146

Wojno AP, Pierce EA, Bennett J (2013) Seeing the light. Sci Transl Med 5:175fs8

Zhivotovsky B, Orrenius S (2011) Calcium and cell death mechanisms: a perspective from the cell death community. Cell Calcium 50:211–221

# Chapter 11
# Antisense Oligonucleotide-Based Splice Correction of a Deep-Intronic Mutation in *CHM* Underlying Choroideremia


**Alejandro Garanto, Saskia D. van der Velde-Visser, Frans P. M. Cremers, and Rob W. J. Collin**

**Abstract** Choroideremia is a progressive genetic eye disorder caused by mutations in the *CHM* gene that encodes the Rab escort protein-1 (REP-1). One of the many *CHM* mutations described so far is a deep-intronic variant, c.315-4587T>A, that creates a novel splice acceptor site resulting in the insertion of a 98-bp pseudoexon in the *CHM* transcript. Antisense oligonucleotides (AONs) are a potential therapeutic tool for correcting splice defects, as they have the properties to bind to the pre-mRNA and redirect the splicing process. Previously, we used AONs to correct aberrant splicing events caused by a recurrent intronic mutation in *CEP290* underlying Leber congenital amaurosis. Here, we expand the use of these therapeutic molecules for the c.315-4587T>A deep-intronic mutation in *CHM* by demonstrating splice correction in patient-derived lymphoblast cells.

**Keywords** *CHM* · Antisense oligonucleotide · Genetic therapy · Splice modulation · Choroideremia · AON · Intronic mutation

A. Garanto (✉) · F. P. M. Cremers · R. W. J. Collin
Department of Human Genetics, Radboud University Medical Center, Nijmegen, The Netherlands

Donders Institute for Brain, Cognition and Behaviour, Radboud University Medical Center, Nijmegen, The Netherlands
e-mail: alex.garanto@radboudumc.nl

S. D. van der Velde-Visser
Department of Human Genetics, Radboud University Medical Center, Nijmegen, The Netherlands



J. D. Ash et al. (eds.), *Retinal Degenerative Diseases*, Advances in Experimental Medicine and Biology 891, https://doi.org/10.1007/978-3-319-75402-4_11

## 11.1 Introduction

Choroideremia (CHM, OMIM #303100) is an X-linked inherited retinal disease affecting 1 every 50,000 males worldwide (Kalatzis et al. 2013; MacLaren et al. 2014). Mutations in the *CHM* gene are the only known genetic cause of this disease (Cremers et al. 1990). Choroideremia, also known as X-linked chorioretinal dystrophy, is characterized by progressive degeneration of the choroid, photoreceptors, and retinal pigment epithelium (RPE) with an onset in the first decade of life (Kalatzis et al. 2013).

*CHM* is a widely expressed 15-exon gene located on chromosome Xq21.2 and encodes the Rab escort protein-1 (REP-1) (Cremers et al. 1990; Seabra et al. 1992; van Bokhoven et al. 1994). The physiological function of REP-1 consists of presenting newly generated Rab proteins to the enzymes that will add geranylgeranyl moieties (i.e., prenylation) in order to allow membrane association and interaction with other proteins. The prenylation defect caused by the absence of REP-1 has been discovered to be the main cause of the chorioretinal degeneration associated with *CHM* mutations (Seabra et al. 1993).

Recently, a phase I/II clinical trial delivering the complete cDNA of *CHM* cloned into an adeno-associated virus (AAV) showed promising results in choroideremia patients suffering from this disease (MacLaren et al. 2014; Barnard et al. 2015). In the retina, gene augmentation was first applied in retinal dystrophy patients harboring *RPE65* mutations, with acceptable safety profiles and moderate efficacy in some patients (summarized by Jacobson et al. (2012)). In these studies, the complete *RPE65* cDNA was delivered to the retina under the control of specific promoters and packaged into AAVs. However, gene augmentation therapies still entail some challenges such as controlling the expression levels of transgene and finding safe vectors and strategies that allow the delivery of genes whose cDNA does not fit in the commonly used AAV-based vectors. In order to circumvent these problems, alternative therapeutic strategies can be considered, such as splice modulation therapy (Gerard et al. 2016). We and others have investigated an antisense oligonucleotide (AON)-based approach to correct splice defects associated with the most recurrent Leber congenital amaurosis mutation, i.e., a deep-intronic mutation in *CEP290* (Collin et al. 2012; Gerard et al. 2012; Garanto et al. 2016; Parfitt et al. 2016). AONs are small RNA molecules that bind complementary to the pre-mRNA and can redirect splicing events (Hammond and Wood 2011). These molecules have shown to be safe and effective when delivered to the retina (Gerard et al. 2015; Murray et al. 2015; Garanto et al. 2016).

To assess the suitability of splice modulation for other intronic mutations causing inherited retinal dystrophy, we here designed an AON-based approach to target the 98-bp pseudoexon insertion caused by a deep-intronic mutation (c.315-4587T>A) in *CHM*.

## 11.2 Materials and Methods

### *11.2.1 AON Design*

AON sequences were designed as described previously (Aartsma-Rus 2012; Garanto and Collin 2018). Briefly, the exon of interest (in this case the 98-bp pseudoexon) and the 50-bp flanking intronic regions were used to detect splicing enhancers. Once identified, the strongest SC35 motif was selected, and AONs targeting this region were designed. Subsequently, RNA structure and free energy predictions were performed using freely available database tools. This resulted in the design of an antisense oligonucleotide (AON; 5′-GCUGGGGGCCCUUGUUG-3′) and its sense counterpart (SON; 5′-CAACAAGGGCCCCCAGC-3′) (Eurogentec).

### *11.2.2 Cell Culture*

Lymphoblast cell lines were established from blood samples of two male patients carrying the same deep-intronic mutation in *CHM* (c.315-4587T>A), coined PAT1 and PAT2, and of a healthy male individual that was used as a control (CON). Cells were immortalized using Epstein-Barr virus and cultured in suspension in RPMI medium supplemented with 15% fetal calf serum (v/v), 2% HEPES 1 M (v/v), 100 U penicillin, and 100 μg streptomycin. All cell lines grew at similar speed and did not show any abnormalities in cell growth or morphology.

### *11.2.3 Transfection and RT-PCR Analysis*

Prior to transfection, ~$1.9 \times 10^6$ cells (in 2 ml) per well were grown in suspension in a 6-well plate for each cell line. Next morning, cells were transfected with 1 μM of AON or SON using FuGene (Promega) according to the provider's instruction. Forty-eight hours post-transfection, cells were harvested, rinsed in PBS, and subjected to RNA isolation using NucleoSpin RNAII (Macherey-Nagel) according to manufacturer's instructions. Subsequently, 1 μg of RNA was used for cDNA synthesis using iScript cDNA synthesis kit (Bio-Rad). The cDNA was diluted by adding 50 μl of MQ. *CHM* and actin expression was assessed by PCR. All PCR reaction mixtures (25 μl) contained 10 μM of each primer pair, 2 μM of dNTPs, 1.5 mM $MgCl_2$, 10% Q-solution (Qiagen), 1 U of Taq polymerase (Roche), and 4 μl of diluted cDNA. PCR conditions were 94 °C for 2 min, followed by 35 cycles of 20 s at 94 °C, 30 s at 58 °C, and 30 s at 72 °C, with a final extension step of 2 min at 72 °C. Amplicons were analyzed by agarose electrophoresis. For *CHM* amplification we used the following forward (5′-AGCCATTGCTCTTAGCAGGA-3′)

and reverse (5′-TGCAGCTTCTGTGGAGTTTG-3′) primers; for actin, 5′-ACTGGGACGACATGGAGAAG-3′ (forward) and 5′-CTCAGCTGTGGTGG TGAAG-3′ (reverse) were used.

## 11.3 Results

### *11.3.1 AONs Redirect Aberrant Splicing*

Previous studies have revealed that patients carrying the deep-intronic c.315-4587T>A mutation in *CHM* have a 98-bp pseudoexon insertion into the mRNA (van den Hurk et al. 2003) (Fig. 11.1a). AONs are small molecules able to redirect pre-mRNA splicing and thus good candidates to restore the splice defects associated with this *CHM* mutation. In this study, a 2′ O-Methyl RNA oligonucleotide with a phosphorothioate backbone was designed to target the 98-bp pseudoexon. By

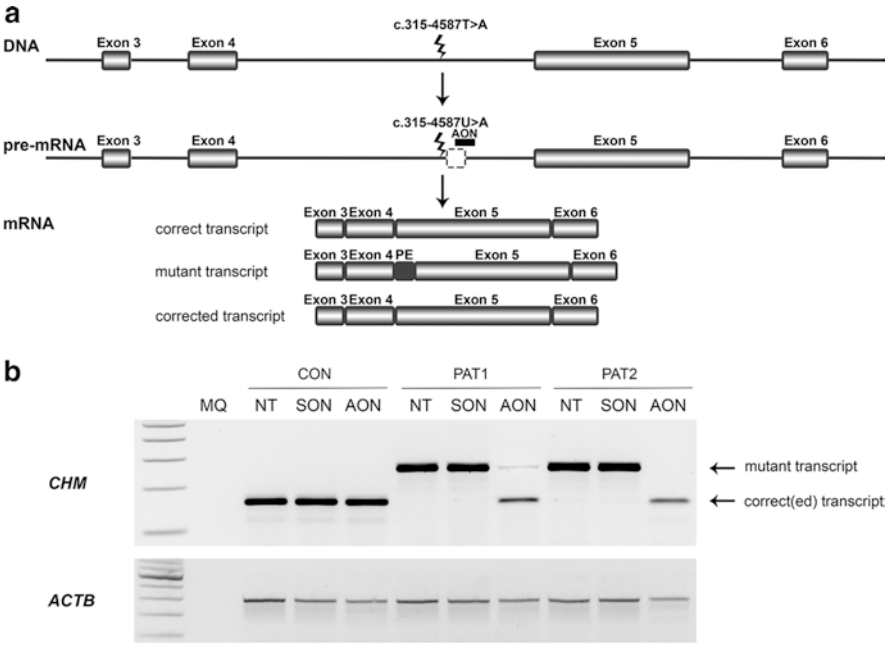


**Fig. 11.1** AON delivery corrected *CHM* mRNA aberrant transcript. (**a**) Schematic representation of the molecular mechanism related to the c.315-4587T>A mutation in *CHM* and the predicted effect of the AON delivery. (**b**) RT-PCR of one control (CON) and two patient-derived lymphoblast cell lines (PAT1 and PAT2). Amplification from exon 4 to exon 5 showed the insertion of a 98-bp pseudoexon (PE) in the mRNA (upper panel). This aberrantly spliced transcript was corrected in the presence of AON, whereas the non-treated (NT) and SON-treated cells did not show any splicing redirection. Actin was used to normalize samples (lower panel). MQ was the negative control of the PCR reaction

delivering AON molecules to the patient-derived cells, we expect that the mRNA transcript will be corrected (Fig. 11.1a). In order to test this hypothesis, 1 μM (final concentration) of the AON molecule was administered to patient-derived lymphoblast cells. Forty-eight hours after treatment, cells were harvested, and RT-PCR revealed that AONs can indeed redirect splicing in both patient cell lines (PAT1 and PAT2), while no effect was observed in the control (CON) cell line (Fig. 11.1b). The amplification from exon 4 to exon 5 revealed a single band of 151 bp in the control, while in untreated patient-derived cells, a band of 249 bp was observed. After AON delivery, in both patients the splicing was restored to different extents. In the case of PAT1, only little amounts of aberrant transcript were still detected, while in the PAT2 cells, the redirection was complete. However, the *CHM* levels in the patient cells treated with AON appeared to be lower compared to all other conditions. In addition, a sense oligonucleotide (SON) consisting of the reverse complement sequence of the AON was used as a control. When the SON molecule was transfected into the lymphoblast cells, only the mutant transcript was detected, indicating that the restoration of the splicing was specific for the AON. In all cases, actin was used to normalize samples.

## 11.4 Discussion

In this manuscript, we described an AON-based splice modulation approach where AON molecules specifically bind to their target sequence in the pre-mRNA, restricting their function to the cells where the gene is expressed. In addition, gene expression levels remain unaltered, minimizing possible toxicity due to overexpression. In animal studies, AONs have shown to be effective and safe when delivered to the eye (Gerard et al. 2015; Murray et al. 2015; Garanto et al. 2016). Importantly, an AON treatment has recently been approved for the treatment of CMV-induced retinitis in humans (Tawse and Baumal 2014). Thus, the therapeutic potential of these molecules is increasing, although it remains a mutation-specific approach thereby limiting its application.

One inconvenience of working with genes involved in inherited retinal disorders is that the expression of these genes is often restricted to the retina. This fact complicates functional studies to elucidate for instance the molecular mechanisms underlying the disease. However, some genes are expressed in almost all cell types of the body. This is the case for *CEP290* and *CHM* and therefore extremely useful since blood or skin cells can be easily obtained from patients and used for in vitro experiments. Using lymphoblast cells, the c.315-4587T>A mutation was identified and immediately led to the discovery of the disease mechanism, i.e., the insertion of a pseudoexon that contains a premature stop codon. As a result, choroideremia patients with this mutation are predicted to have no functional REP-1 protein (van den Hurk et al. 2003). Although lymphoblast cells are notoriously difficult to transfect, the small size of AONs allows them to easily penetrate into cells, in some cases even without any transfection reagent. By delivering these molecules to the

three different cell lines (two patients and one control), we observed that the splicing was redirected and the corrected transcript appeared in the patient samples treated with AONs (Fig. 11.1b). Nevertheless, PAT1 cells showed traces of remaining mutant *CHM* transcript. This could be explained by the fact that lymphoblast cells grow in suspension and tend to make clumps. At the moment of transfection, cells from the control and PAT2 were a bit more disperse, and clumps were smaller compared to the PAT1 cells. Therefore, the most logical explanation for this observation is that the AONs did not reach all the cells. Furthermore, we observed that in both patient cell lines, the expression levels of *CHM* in the AON-treated samples were lower compared to untreated or SON-treated cells. Here, several hypotheses could explain this fact. One option could be that the binding of the AON, besides pseudoexon skipping, also induces other types of splicing events that were not detected under the PCR conditions used. Also, the binding of the AON molecules may result somehow in some degradation of the aberrant transcript, although we have never observed this phenomenon in our previous studies with other AONs (Collin et al., 2012; Garanto et al., 2016). Further work to elucidate the mechanism of action of the AONs in this particular case needs to be performed.

Taken together, the data presented here show that AON can redirect aberrant *CHM* pre-mRNA splicing and highlights the therapeutic potential of these molecules to treat other subtypes of IRDs.

**Acknowledgments** We would like to acknowledge the patients that participated in this study. This work was supported by the following foundations: Algemene Nederlandse Vereniging ter Voorkoming van Blindheid, Stichting Blinden-Penning, Landelijke Stichting voor Blinden en Slechtzienden, Stichting Oogfonds Nederland, Stichting MD Fonds, and Stichting Retinal Nederland Fonds that contributed through UitZicht 2015-31, together with the Rotterdamse Stichting Blindenbelangen, Stichting Blindenhulp, Stichting tot Verbetering van het Lot der Blinden, Stichting voor Ooglijders, and Stichting Dowilvo, granted to AG and RWJC. This work was also supported by the Foundation Fighting Blindness USA, grant no. PPA-0517-0717-RAD (to AG, FPMC and RWJC). The funding organizations had no role in the design or conduct of this research. They provided unrestricted grants.

## References

Aartsma-Rus A (2012) Overview on AON design. Methods Mol Biol 867:117–129

Barnard AR, Groppe M, MacLaren RE (2015) Gene therapy for choroideremia using an adeno-associated viral (AAV) vector. Cold Spring Harb Perspect Med 5:a017293

Collin RWJ, den Hollander AI, van der Velde-Visser SD et al (2012) Antisense oligonucleotide (AON)-based therapy for Leber congenital amaurosis caused by a frequent mutation in *CEP290*. Mol Ther Nucleic Acids 1:e14

Cremers FPM, van de Pol DJ, van Kerkhoff LP et al (1990) Cloning of a gene that is rearranged in patients with choroideraemia. Nature 347:674–677

Garanto A, Chung DC, Duijkers L et al (2016) In vitro and in vivo rescue of aberrant splicing in *CEP290*-associated LCA by antisense oligonucleotide delivery. Hum Mol Genet 25(12):2552–2563

Garanto A, Collin RWJ (2018) Design and in vitro use of antisense oligonucleotides to correct pre-mRNA splicing defects in inherited retinal dystrophies. Methods Mol Biol 1715:61–78. https://doi.org/10.1007/978-1-4939-7522-8_5. PMID: 29188506

Gerard X, Perrault I, Hanein S et al (2012) AON-mediated exon skipping restores ciliation in fibroblasts harboring the common Leber congenital amaurosis *CEP290* mutation. Mol Ther Nucleic Acids 1:e29

Gerard X, Perrault I, Munnich A et al (2015) Intravitreal injection of splice-switching oligonucleotides to manipulate splicing in retinal cells. Mol Ther Nucleic Acids 4:e250

Gerard X, Garanto A, Rozet JM et al (2016) Antisense oligonucleotide therapy for inherited retinal dystrophies. Adv Exp Med Biol 854:517–524

Hammond SM, Wood MJ (2011) Genetic therapies for RNA mis-splicing diseases. Trends Genet TIG 27:196–205

Jacobson SG, Cideciyan AV, Ratnakaram R et al (2012) Gene therapy for leber congenital amaurosis caused by RPE65 mutations: safety and efficacy in 15 children and adults followed up to 3 years. Arch Ophthalmol 130:9–24

Kalatzis V, Hamel CP, MacDonald IM et al (2013) Choroideremia: towards a therapy. Am J Ophthalmol 156(433–437):e433

MacLaren RE, Groppe M, Barnard AR et al (2014) Retinal gene therapy in patients with choroideremia: initial findings from a phase 1/2 clinical trial. Lancet 383:1129–1137

Murray SF, Jazayeri A, Matthes MT et al (2015) Allele-specific inhibition of rhodopsin with an antisense oligonucleotide slows photoreceptor cell degeneration. Invest Ophthalmol Vis Sci 56:6362–6375

Parfitt DA, Lane A, Ramsden CM et al (2016) Identification and correction of mechanisms underlying inherited blindness in human iPSC-derived optic cups. Cell Stem Cell 18:769–781

Seabra MC, Brown MS, Slaughter CA et al (1992) Purification of component A of Rab geranylgeranyl transferase: possible identity with the choroideremia gene product. Cell 70:1049–1057

Seabra MC, Brown MS, Goldstein JL (1993) Retinal degeneration in choroideremia: deficiency of rab geranylgeranyl transferase. Science 259:377–381

Tawse KL, Baumal CR (2014) Intravitreal foscarnet for recurring CMV retinitis in a congenitally infected premature infant. J AAPOS Off Publ Am Assoc Pediatr Ophthalmol Strabismus/Am Assoc Pediatr Ophthalmol Strabismus 18:78–80

van Bokhoven H, van den Hurk JA, Bogerd L et al (1994) Cloning and characterization of the human choroideremia gene. Hum Mol Genet 3:1041–1046

van den Hurk JA, van de Pol DJ, Wissinger B et al (2003) Novel types of mutation in the choroideremia (*CHM*) gene: a full-length L1 insertion and an intronic mutation activating a cryptic exon. Hum Genet 113:268–275

# Chapter 12
# Gene Therapy Approaches to Treat the Neurodegeneration and Visual Failure in Neuronal Ceroid Lipofuscinoses

**Sophia-Martha kleine Holthaus, Alexander J. Smith, Sara E. Mole, and Robin R. Ali**

**Abstract** Neuronal ceroid lipofuscinoses (NCLs) are a group of fatal, inherited lysosomal storage disorders mostly affecting the central nervous system of children. Symptoms include vision loss, seizures, motor deterioration and cognitive decline ultimately resulting in premature death. Studies in animal models showed that the diseases are amenable to gene supplementation therapies, and over the last decade, major advances have been made in the (pre)clinical development of these therapies. This mini-review summarises and discusses current gene therapy approaches for NCL targeting the brain and the eye.

**Keywords** Neuronal ceroid lipofuscinoses · NCL · Batten disease · AAV · Gene therapy · Neurodegeneration · Retinal degeneration

S.-M. kleine Holthaus (✉)
UCL Institute of Ophthalmology, Department of Genetics & NIHR BRC at Moorfields Eye Hospital, London, UK

MRC Laboratory for Molecular Cell Biology, UCL Institute of Child Health, Department of Genetics, Evolution and Environment, University College London, London, UK
e-mail: s.kleine.holthaus.11@ucl.ac.uk

A. J. Smith · R. R. Ali
UCL Institute of Ophthalmology, Department of Genetics & NIHR BRC at Moorfields Eye Hospital, London, UK

S. E. Mole
MRC Laboratory for Molecular Cell Biology, UCL Institute of Child Health, Department of Genetics, Evolution and Environment, University College London, London, UK



J. D. Ash et al. (eds.), *Retinal Degenerative Diseases*, Advances in Experimental Medicine and Biology 891, https://doi.org/10.1007/978-3-319-75402-4_12

## 12.1 Introduction

Neuronal ceroid lipofuscinoses (NCLs), more commonly referred to as Batten disease, are a group of rare, fatal, autosomal recessively inherited diseases that predominantly affect the central nervous system (CNS) with onset typically during childhood. Patients manifest with visual impairment, seizures, mental retardation, motor deterioration and premature death due to widespread loss of cells in the CNS including the retina. The disease is characterised by the progressive accumulation of autofluorescent storage material in the lysosome of neuronal and non-neuronal cells, which classifies this condition as a lysosomal storage disorder (Jalanko and Braulke 2009; Mole et al. 2005). The NCLs encompass a genetically heterogeneous group of diseases linked with 14 genes and over 400 mutations (www.ucl.ac.uk/ncl/mutation) (Kousi et al. 2011; Warrier et al. 2013). Five NCL genes encode soluble lysosomal enzymes and proteins (PPT1, TPP1, CLN5, CTSD, CTSF), and five encode transmembrane proteins localised in the lysosome and pre-lysosomal processing (CLN3, CLN7, CLN12), in the endoplasmic reticulum (ER) (CLN6, CLN8) and ER-Golgi intermediate compartment (CLN8). The genes CLN4, CLN11 and CLN14 express the soluble proteins DNAJC5, GRN and KCTD7 with less well-defined subcellular localisation. Whilst the function of many NCL genes coding for a soluble enzyme is known, the role of the genes coding for membrane-bound proteins is not fully resolved (Kollmann et al. 2013). Nomenclature of NCLs takes into account the gene afflicted and the age of disease onset (Williams and Mole 2012). For example, juvenile-onset NCL, the form of the disease with the highest prevalence in the USA, is referred to as CLN3 disease, classic juvenile. NCLs are rare with a combined incidence of 1 in 100,000 worldwide and up to 1 in 12,500 in some regions of Northern Europe and the USA. (Jalanko and Braulke 2009).

Several genetically engineered and naturally occurring animal models (Bond et al. 2013) have been used to investigate various therapeutic strategies for NCLs including gene supplementation therapy, enzyme replacement, stem cell transplantation and small compound delivery (Neverman et al. 2015; Geraets et al. 2016). This mini-review focuses on current gene therapy approaches for NCLs and highlights challenges for the development of gene supplementation therapies across different forms of NCL.

## 12.2 Progress Towards NCL Gene Therapy Targeting the Brain

An important consideration for the design of therapies for NCLs is whether the affected gene encodes a soluble lysosomal enzyme or a transmembrane protein. The supplementation of soluble enzymes is aided by the phenomenon of lysosomal cross-correction, which allows lysosomal enzymes to be taken up by cells from the circulation and other cells via the mannose-6-phosphate pathway (Kornfeld 1992;

Neufeld and Fratantoni 1970). Cross-correction does not occur with membrane-bound proteins, and therapies are required to target a greater number of cells to achieve meaningful therapeutic outcomes.

### *12.2.1 Gene Therapies for Soluble Enzyme Deficiencies*

A large proportion of studies have focused on the development of AAV-mediated gene therapies targeting the brain in CLN2 disease, late infantile, caused by the deficiency in the soluble lysosomal enzyme tripeptidyl peptidase 1 (TPP1). Patients present with seizures, language delay, decline in cognition and motor function from 2 to 4 years. Classic disease progression is rapid, resulting in death at around 10 years of age (Fietz et al. 2016; Jadav et al. 2014). Various studies have used AAV vectors to deliver recombinant TPP1 to $Tpp1^{-/-}$ mice. Intracranial administration of AAV2/1 and AAVrh.10 carrying human *TPP1* driven by an ubiquitous promoter showed widespread TPP1 enzyme activity outside the injection site (Cabrera-Salazar et al. 2007; Passini et al. 2006; Sondhi et al. 2007). Delivery of AAVrh.10.hTPP1 and AAV2/1.hTPP1 led to better performances in motor and behavioural tasks as well as an increased lifespan with a mean of 162 days in AAVrh.10-treated and a mean of 216 days in AAV2/1-treated animals compared with a mean of 138 days in untreated mice. Administration of the vectors reduced reactive gliosis, autofluorescent inclusions and axonal degeneration (Cabrera-Salazar et al. 2007). In 2004, the first gene therapy safety trial was conducted in patients suffering from CLN2 disease, late infantile. Ten affected children between 3 and 10 years of age received injections through 6 burr holes in 12 cortical locations with an AAV2/2.hCLN2 vector harbouring a CAG promoter and the human *CLN2* transgene at an average dose of $2.5 \times 10^{12}$ particles (Crystal et al. 2004). Shortly after vector administration, an 8-year-old subject died without signs of CNS inflammation. Another patient died in the follow-up period. The other eight subjects did not show adverse effects towards the treatment and initially a slight but non-significant slowing of the disease progression was reported (Worgall et al. 2008). Long-term follow-up results have not been published yet. Based on the higher transduction efficiency of AAVrh.10 in rodents and non-human primates (Cearley and Wolfe 2006; Jui-Yun Lua et al. 2010; Sondhi et al. 2007, 2012), a new phase I/II clinical trial has been initiated to deliver AAVrh.10.hCLN2 in 12 cortical locations in CLN2 disease patients (NCT01161576).

To avoid multiple brain injections, the therapeutic effect of transducing ependymal cells through intracerebroventricular (ICV) AAV injections was investigated in *Tpp1*-deficient dogs, resulting in recombinant Tpp1 release to the CNS. Dogs treated with AAV2/2 carrying canine *Tpp1* maintained high levels of the recombinant enzyme in the ependyma and various brain regions (thalamus, medulla, caudate, cerebellum and occipital cortex), leading to long-term relief of motor and cognitive symptoms as well as an increased average life span of 17.5 months compared with 10.5 months in untreated dogs. Notably, inadequate immunosuppression

in these animals resulted in the presence of neutralising antibodies and reduction of recombinant Tpp1 activity back to baseline levels after 2 months (Katz et al. 2015). It remains to be seen whether this gene therapy approach is sufficient to deliver therapeutic levels of Tpp1 in larger brains and whether the production of neutralising antibodies can be prevented in a clinical setting.

Support for CNS-directed, AAV-mediated therapies in humans is provided by an unpublished large animal study involving sheep deficient in the soluble lysosomal protein Cln5. After ICV injections of AAV2/9, the mutant sheep presented with reduced neurological symptoms, preservation of intracranial volumes and decreases in neuronal atrophy, lysosomal storage material and gliosis. Their survival was significantly prolonged, and one treated sheep was kept up to 37 months, 13 months longer than the average lifespan for this model. Further characterisation of treated animals is currently ongoing (Mitchell et al. 2016).

In more severe and faster progressing animal models of NCL, brain-directed AAV treatments alone did not have clear beneficial effects. A combined treatment of ICV and intraperitoneal injections with AAVrh8.Ctsd was required to extend lifespan from a mean of 29 days in untreated to 35 days in treated mice lacking *Cathepsin D* (Ctsd), a model for CLN10 disease, congenital (Pike et al. 2011). Similarly, administration of AAV1/2.Ctsd into the striatum extended survival to 63 days, but in combination with injections into the liver and stomach, the survival of the mice ranged from 63 to 198 days (Shevtsova et al. 2010). In *Ppt1*-deficient mice that model CLN1 disease, infantile, and that have a considerably slower disease progression than *CtsD*-deficient mice, CNS-directed gene therapy approaches only partially rescued the disease phenotype. Multiple intracranial injections with AAV2/2.hPPT1 or AAV2/5.hPPT1 in neonates slowed built-up of autofluorescent material, rescued brain histology and behavioural abnormalities, yet only moderately increased longevity (Griffey et al. 2004, 2006; Macauley et al. 2012). This treatment combined with bone marrow transplants, however, enhanced rotarod performance and survival for almost 10 months compared with an average lifespan of 9 months in untreated animals (Macauley et al. 2012). Collectively, these studies demonstrate that although neurodegeneration is the predominant feature in all NCLs, gene therapies directly targeting the brain alone may prove an incomplete strategy.

### *12.2.2 Gene Therapy for Transmembrane Protein Deficiencies*

Fewer gene therapy approaches have been published for transmembrane protein deficiencies in NCL due to the challenge to deliver transgenes efficiently throughout the brain. The most common form of these NCLs is CLN3 disease, classic juvenile, which manifests with vision loss followed by cognitive and motor deteriorations, behavioural abnormalities and seizures leading to death in the late 20s or early 30s (Schulz et al. 2013; Williams et al. 2006). The *CLN3* gene encodes a lowly expressed, lysosomal membrane-bound protein of unknown function (The International Batten

Disease Consortium 1995; Mao et al. 2003). When newborn *Cln3*-deficient mice received six intracranial injections of AAVrh.10.CAG.hCLN3, a reduction in storage material and astrocytosis, but not gliosis and neuronal loss, was observed 18 months post vector administration. Behavioural and motor performances were not assessed due to the lack of obvious motor defects between untreated mutant animals and wild type controls at 18 months (Sondhi et al. 2014). Recently, another group has reported that intravenous (IV) delivery of a self-complementary (sc) AAV2/9.hCLN3 vector can have beneficial effects in *Cln3*-deficient mice (Bosch et al. 2016). This work followed studies demonstrating that scAAV2/9 can cross the blood-brain barrier (BBB) and reduces neurological symptoms and extends the lifespan of mouse models of spinal muscular atrophy and Rett syndrome (Foust et al. 2010; Garg et al. 2013). In the study by Bosch et al., *Cln3*-deficient mice received IV injections at 4 weeks of age with vectors carrying *CLN3* under the control of a ubiquitous β-actin promoter or a weak neuron-specific MeCP2 (methyl-CpG-binding protein 2) promoter. The animals were examined up to 5 months later (Bosch et al. 2016). It is not clear why the treatment with the weak MeCP2 promoter, but not with the stronger ubiquitous promoter, led to rescue of a nonprogressive rotarod defect and to less lysosomal storage material, gliosis and astrocytosis. Long-term effects of treatment on motor function and disease pathology were not investigated. scAAV2/9 vectors have also been used to treat *Cln6*$^{nclf}$ mice, a model for CLN6 disease, variant late infantile, that has a deficiency in the membrane-bound protein Cln6. In a pilot study, *Cln6*-deficient mice received ICV injections with scAAV2/9.CB.hCLN6, which resulted in an improved rotarod motor performance and less lysosomal storage material up to 3 months of age (Cain et al. 2016). In view of the widespread transduction of cells in the CNS following intrathecal injections in rodents and non-human primates (Meyer et al. 2014), a phase I/II trial has started for CLN6 patients to receive intrathecal administration of scAAV2/9.CB.hCLN6 (NCT02725580).

## 12.3 Ocular Gene Therapy Approaches for NCL

The majority of gene therapy studies on NCL have focused on the delivery of transgenes to the brain. However, visual failure is a key feature in NCL. In classic CLN3 disease, visual decline starts between 4 and 7 years of age and leads to total blindness within a couple of years. Once vision is lost, it can take up to 5 years before more severe neurological symptoms manifest, creating a time window for ocular treatments. The development of ocular therapies has been hampered by the lack of animal models for CLN3 disease with an early, pronounced visual failure. Focusing on the ocular phenotype of *Cln6*-deficient mice, we have demonstrated that although *Cln6*$^{nclf}$ animals presented with severe photoreceptor degeneration, transduction of photoreceptors with AAV2/8.hCLN6 did not restore retinal function or morphology. Since endogenous CLN6 was not only expressed in photoreceptors but also in bipolar cells, mutant mice were treated intravitreally with the novel AAV serotype, 7m8,

to target the inner retina resulting in a significantly slowed loss of retinal function and photoreceptors (Holthaus et al. 2018). This indicates that NCL transmembrane protein defects are amenable to ocular gene therapies and that the transduction of the inner retina may be vital to achieve a therapeutic effect, in line with the reported expression of *Cln3* in the bipolar cells and inner retinal abnormalities in patients (Collins et al. 2006; Ding et al. 2011). In *Ppt1*-deficient mice, a model characterised by mild photoreceptor degeneration, intravitreal administration of AAV2/2.hPTT1 provided a significant increase in retinal function and reduced loss of photoreceptors (Griffey et al. 2005), further supporting the notion that AAV-based gene therapies are a valid strategy to combat vision loss in NCL.

## 12.4 Summary

Promising progress has been made in the development of gene therapies for the NCLs (for an overview, see Table 12.1). Whilst the development of brain-directed gene supplementation strategies for membrane-bound protein defects is more challenging than for soluble enzyme deficiencies, the advent of more potent AAV serotypes that are able to cross the BBB may result in major clinical advances in the near future. Gene therapy studies on soluble enzyme defects established that therapies

**Table 12.1** Summary of preclinical gene therapy approaches in NCL

| Gene/protein defect | Protein solubility | Common mammalian NCL model | Preclinical gene therapies | | |
|---|---|---|---|---|---|
| | | | Delivery route | AAV serotype | Organ/tissue targeted |
| CLN1/PPT1 | Soluble | Murine | ICRN and IV<br>IVT | AAV2/5 and BMT<br>AAV2/2 | Brain and systemic<br>Retina |
| CLN2/TPP1 | Soluble | Murine | ICRN<br>ICRN | AAV2/1<br>AAVrh.10 | Brain<br>Brain |
| | | Canine | ICV | AAV2/2 | Ependyma |
| CLN3 | TM | Murine | ICRN<br>IV | AAVrh.10<br>scAAV2/9 | Brain<br>Systemic |
| CLN4/ DNAJC5 | Soluble | – | – | – | – |
| CLN5 | Soluble | Murine | – | – | – |
| | | Ovine | ICV | ssAAV2/9 | Brain |
| CLN6 | TM | Murine | IVT<br>IT | 7m8<br>scAAV2/9 | Retina<br>Brain and spinal cord |
| | | Ovine | – | – | – |
| CLN7 | TM | Murine | – | – | – |
| CLN8 | TM | Murine | – | – | – |
| | | Canine | – | – | – |

(continued)

**Table 12.1** (continued)

| Gene/protein defect | Protein solubility | Common mammalian NCL model | Preclinical gene therapies | | |
|---|---|---|---|---|---|
| | | | Delivery route | AAV serotype | Organ/tissue targeted |
| CLN10/ CTSD | Soluble | Murine | IVC and IP<br>ICRN, IH, IL | AAVrh.8<br>AAV1/2 | Brain and systemic<br>Brain, liver and stomach |
| CLN11/GRN | Soluble | – | – | – | – |
| CLN12 | TM | – | – | – | – |
| CLN13/ CTSF | Soluble | – | – | – | – |
| CLN14/ KCTD7 | Soluble | – | – | – | – |

*TM* transmembrane, *ICRN* intracranial, *IV* intravenous, *IVT* intravitreal, *IVC* intracerebroventricular, *IT* intrathecal, *IP* intraperitoneal, *IH* intrahepatic, *IL* intraluminal, *ss* single stranded, *sc* self-complementary

targeting the brain alone are not always sufficient. A combination of treatments targeting the brain and other affected organs may be essential for some forms of NCL such as CLN1 disease. Furthermore, it can be anticipated that combination therapies, for example, targeting the brain and eye, will significantly increase quality of life of patients.

## References

Bond M, Holthaus SM, Tammen I et al (2013) Use of model organisms for the study of neuronal ceroid lipofuscinosis. Biochim Biophys Acta 1832:1842–1865

Bosch ME, Aldrich A, Fallet R et al (2016) Self-complementary AAV9 gene delivery partially corrects pathology associated with juvenile neuronal ceroid lipofuscinosis (CLN3). J Neurosci 36:9669–9682

Cabrera-Salazar MA, Roskelley EM, Bu J et al (2007) Timing of therapeutic intervention determines functional and survival outcomes in a mouse model of late infantile batten disease. Mol Ther 15:1782–1788

Cain J, Likhite S, Whitel K et al (2016) Testing saftey and efficacy of AAV9-CLN6 gene therapy in a mouse model of CLN6-Batten disease. Presented at the 15th International Conference on Neuronal Ceroid Lipofuscinoses, 5th-8th October 2016, Boston, Massachusetts, USA

Cearley CN, Wolfe JH (2006) Transduction characteristics of adeno-associated virus vectors expressing cap serotypes 7, 8, 9, and Rh10 in the mouse brain. Mol Ther 13:528–537

Collins J, Holder GE, Herbert H et al (2006) Batten disease: features to facilitate early diagnosis. Br J Ophthalmol 90:1119–1124

Crystal RG, Sondhi D, Hackett NR et al (2004) Administration of a replication-deficient adeno-associated virus gene transfer vector expressing the human CLN2 cDNA to the brain of children with late infantile neuronal ceroid lipofuscinosis. Hum Gene Ther 15:1331–1354

Ding SL, Tecedor L, Stein CS et al (2011) A knock-in reporter mouse model for Batten disease reveals predominant expression of Cln3 in visual, limbic and subcortical motor structures. Neurobiol Dis 41:237–248

Fietz M, AlSayed M, Burke D et al (2016) Diagnosis of neuronal ceroid lipofuscinosis type 2 (CLN2 disease): Expert recommendations for early detection and laboratory diagnosis. Molecular Genetics and Metabolism 119(1-2):160–167

Foust KD, Xueyong Wang, McGovern VL et al (2010) Rescue of the spinal muscular atrophy phenotype in a mouse model by early postnatal delivery of SMN. Nature Biotechnology 28(3):271–274

Garg SK, Lioy DT, Cheval H et al (2013) Systemic delivery of MeCP2 rescues behavioral and cellular deficits in female mouse models of rett syndrome. Journal of Neuroscience 33(34):13612–13620

Geraets RD, Seung yon Koh, Hastings ML et al (2016) Moving towards effective therapeutic strategies for neuronal ceroid lipofuscinosis. Orphanet Journal of Rare Diseases 11(1)

Griffey MA, Bible E, Vogler C et al (2004) Adeno-associated virus 2-mediated gene therapy decreases autofluorescent storage material and increases brain mass in a murine model of infantile neuronal ceroid lipofuscinosis. Neurobiol Dis 16:360–369

Griffey MA, Macauley S, Ogilvie J et al (2005) AAV2-mediated ocular gene therapy for infantile neuronal ceroid lipofuscinosis. Mol Ther 12:413–421

Griffey MA, Wozniak D, Wong M et al (2006) CNS-directed AAV2-mediated gene therapy ameliorates functional deficits in a murine model of infantile neuronal ceroid lipofuscinosis. Mol Ther 13:538–547

Holthaus SM, Ribeiro J, Abelleira-Hervas L et al (2018) Prevention of photoreceptor cell loss in a Cln6nclf mouse model of Batten disease requires CLN6 gene transfer to bipolar cells. Molecular Therapy, in press

Jadav RH, Sinha S, Yasha TC et al (2014) Clinical,electrophysiological, imaging, and ultrastructural description in 68 patients with neuronal ceroid lipofuscinoses and its subtypes. Pediatric Neurology 50(1):85–95

Jalanko A, Braulke T (2009) Neuronal ceroid lipofuscinoses. Biochim Biophys Acta 1793:697–709

Jui-Yun Lua B, Hub J, Hofmann SL (2010) Human recombinant palmitoyl protein thioesterase-1 (PPT1) for preclinical evaluation of enzyme replacement therapy for infantile neuronal ceroid lipofuscinosis. Mol Genet Meta 99:374–378

Katz ML, Tecedor L, Yonghong Chen et al (2015) AAV gene transfer delays disease onset in a TPP1-deficient canine model of the late infantile form of Batten disease. Science Translational Medicine 7(313):313ra180–313ra180

Kollmann K, Uusi-Rauva K, Scifo E et al (2013) Cell biology and function of neuronal ceroid lipofuscinosis-related proteins. Biochim Biophys Acta 1832:1866–1881

Kornfeld S (1992) Structure and function of the mannose 6-phosphate/insulinlike growth factor II receptors. Annu Rev Biochem 61:307–330

Kousi M, Lehesjoki AE, Mole SE (2011) Update of the mutation spectrum and clinical correlations of over 360 mutations in eight genes that underlie the neuronal ceroid lipofuscinoses. Hum Mutat 33:42–63

Macauley SL, Roberts MS, Wong AM et al (2012) Synergistic effects of central nervous system-directed gene therapy and bone marrow transplantation in the murine model of infantile neuronal ceroid lipofuscinosis. An Neurol 71:797–804

Mao Q, Xia H, Davidson BL (2003) Intracellular trafficking of CLN3, the protein underlying the childhood neurodegenerative disease, Batten disease. FEBS Lett 555:351–357

Meyer K, Ferraiuolo L, Schmelzer L et al (2014) Improving single injection CSF delivery of AAV9-mediated gene therapy for SMA: A dose–response study in mice and nonhuman primates. Molecular Therapy 23(3): 477–487

Mitchell NL, Barrell GK, Russell KN al (2016) Gene transfer can prevent stereotypical disease development in ovine CLN5 and CLN6 models of NCL. Presented at the 15th International Conference on Neuronal Ceroid Lipofuscinoses, 5th-8th October 2016, Boston, Massachusetts, USA

Mole SE, Williams RE, Goebel HH (2005) Correlations between genotype, ultrastructural morphology and clinical phenotype in the neuronal ceroid lipofuscinoses. Neurogenetics 6:107–126

Neufeld EF, Fratantoni JC (1970) Inborn errors of mucopolysaccharide metabolism: faulty degradative mechanisms are implicated in this group of human diseases. Science 169:141–146

Neverman NJ, Best HL, Hofmann SL et al (2015) Experimental therapies in the neuronal ceroid lipofuscinoses. Biochimica et Biophysica Acta (BBA) - Molecular Basis of Disease 1852(10):2292–2300

Passini MA, Dodge JC, Bu J et al (2006) Intracranial delivery of CLN2 reduces brain pathology in a mouse model of classical late infantile neuronal ceroid lipofuscinosis. J Neurosci 26:1334–1342

Pike LS, Tannous BA, Deliolanis NC et al (2011) Imaging gene delivery in a mouse model of congenital neuronal ceroid lipofuscinosis. Gene Ther 18:1173–1178

Schulz A, Kohlschütter A, Mink J et al (2013) NCL diseases - clinical perspectives. Biochim Biophys Acta 1832:1801–1806

Shevtsova Z, Garrido M, Weishaupt J et al (2010) CNS-expressed cathepsin D prevents lymphopenia in a murine model of congenital neuronal ceroid lipofuscinosis. Am J Pathol 177:271–279

Sondhi D, Hackett NR, Peterson DA et al (2007) Molecular therapy – enhanced survival of the LINCL mouse following CLN2 gene transfer using the rh.10 rhesus macaque-derived adeno-associated virus vector. Mol Ther 15:481–491

Sondhi D, Johnson L, Purpura K et al (2012) Long-term expression and safety of administration of AAVrh.10hCLN2 to the brain of rats and nonhuman primates for the treatment of late infantile neuronal ceroid lipofuscinosis. Hum Gene Ther Meth 23:324–335

Sondhi D, Scott EC, Chen A et al (2014) Partial correction of the CNS lysosomal storage defect in a mouse model of juvenile neuronal ceroid lipofuscinosis by neonatal CNS administration of an adeno-associated virus serotype rh.10 vector expressing the human CLN3Gene. Hum Gene Ther 25:223–239

The International Batten Disease Consortium (1995) Isolation of a novel gene underlying Batten disease, CLN3. Cell 82:949–957

Warrier V, Vieira M, Mole SE (2013) Genetic basis and phenotypic correlations of the neuronal ceroid lipofusinoses. Biochim Biophys Acta 1832:1827–1830

Williams RE, Mole SE (2012) New nomenclature and classification scheme for the neuronal ceroid lipofuscinoses. Neurology 79:183–191

Williams RE, Aberg L, Autti T et al (2006) Diagnosis of the neuronal ceroid lipofuscinoses: an update. Biochim Biophys Acta 1762:865–872

Worgall S, Sondhi D, Hackett NR et al (2008) Treatment of late infantile neuronal ceroid lipofuscinosis by CNS administration of a serotype 2 adeno-associated virus expressing CLN2 cDNA. Hum Gene Ther 19:463–474

# Chapter 13
# Success of Gene Therapy in Late-Stage Treatment


**Susanne F. Koch and Stephen H. Tsang**

**Abstract** Retinal gene therapy has yet to achieve sustained rescue after disease onset – perhaps because transduction efficiency is insufficient ("too little") and/or the disease is too advanced ("too late") in humans. To test the latter hypothesis, we used a mouse model for retinitis pigmentosa (RP) that allowed us to restore the mutant gene in all diseased rod photoreceptor cells, thereby generating optimally treated retinas. We then treated mice at an advanced disease stage and analyzed the rescue. We showed stable, sustained rescue of photoreceptor structure and function for at least 1 year, demonstrating gene therapy efficacy after onset of degeneration. The results suggest that RP patients are treatable, even when the therapy is administered at late disease stages.

**Keywords** Retinitis pigmentosa · Gene therapy · Late-stage treatment · Photoreceptor degeneration · Rescue · PDE6b · Inducible rod-specific Cre driver

S. F. Koch
Physiological Genomics, Biomedical Center, Ludwig-Maximilians University Munich, 82152 Planegg/Munich, Germany

S. H. Tsang (✉)
Barbara & Donald Jonas Laboratory of Stem Cells & Regenerative Medicine and Bernard & Shirlee Brown Glaucoma Laboratory, Departments of Pathology and Cell Biology, Columbia University, New York, NY, USA

Edward S. Harkness Eye Institute, New York Presbyterian Hospital, New York, NY, USA

Institute of Human Nutrition, College of Physicians and Surgeons, Columbia University, New York, NY, USA

Herbert Irving Comprehensive Cancer Center, Columbia University Medical Center, New York, NY, USA
e-mail: sht2@columbia.edu



J. D. Ash et al. (eds.), *Retinal Degenerative Diseases*, Advances in Experimental Medicine and Biology 891, https://doi.org/10.1007/978-3-319-75402-4_13

## 13.1 Introduction

RP is a progressive neurodegenerative disorder and one of the leading causes of hereditary blindness (Hartong et al. 2006). In the early stage of the disease, peripheral rod photoreceptor degeneration is underway and patients experience night blindness. Rod degeneration continues in mid and late stages, causing tunnel vision. In the late stage, macular cone loss becomes significant enough that patients lose daylight vision (Sahel et al. 2010).

Gene therapy is currently the most promising treatment for RP and other inherited retinal degenerative diseases. In preclinical studies, gene therapeutics are almost always delivered before the onset of cell degeneration. However, patients are typically diagnosed after onset of degeneration – with the majority already exhibiting significant loss of rods and cones (Mitamura et al. 2012). Therefore, a therapeutic must be able to demonstrate efficacy *after* disease onset – even at late-stage disease. However, it has been suggested that treatment at later stages might be hindered by a "point of no return" – beyond which, photoreceptor cell death is unpreventable (Cepko and Vandenberghe 2013). An important research priority, therefore, is to understand whether late-stage treatment is even feasible.

In the present study, we used an RP mouse model in which mutant rod-specific cGMP phosphodiesterase 6b (PDE6b) can be restored to wild type in all rod photoreceptors. Mutations in gene encoding *PDE6B* have been linked to RP (Cheng et al. 2016). Using this novel tool to achieve optimal gene delivery, we then determined whether photoreceptor degeneration can be halted after disease onset. We demonstrate significant sustained rescue, even when the therapy was administered at late disease stage.

## 13.2 Material and Methods

### *13.2.1 Animals*

All experiments were approved by the Institutional Animal Care and Use Committee (IACUC) at Columbia University in New York. Mice were used in accordance with the Statement for the Use of Animals in Ophthalmic and Vision Research of the Association for Research in Vision and Ophthalmology and the Policy for the Use of Animals in Neuroscience Research of the Society for Neuroscience. *Pde6b*$^{H620Q}$ mice were rederived via oviduct transfer from morulae provided by the European Mouse Mutant Archive (Hart et al. 2005; Davis et al. 2008). *Pde6b*$^{Stop}$ and *Pde6g*$^{CreERT2}$ mice were generated in the Tsang laboratory, as previously described (Davis et al. 2013; Koch et al. 2015; Koch et al. 2017). All mice were maintained in the Columbia University Pathogen-free Eye Institute Annex Animal Care Services Facility under a 12-h light-dark cycle.

### 13.2.2 Tamoxifen Injection

Tamoxifen (100 mg/ml in ethanol; Sigma-Aldrich T5648) was thoroughly mixed at 42 °C, diluted with corn oil to a final concentration of 10 mg/ml, and then injected at a concentration of 100 μg/g body weight on three consecutive days (1 injection/day), at the age of 2 months.

### 13.2.3 Immunohistochemistry and Morphometry

Mice were euthanized according to established IACUC guidelines and previously described procedures (Koch et al. 2012). Antibodies were mouse anti-PDE6b (1:1000, PA1-7222, Thermo Scientific) and 488-coupled anti-PNA (1:800, L21409, Invitrogen). Quantitative analyses of outer nuclear layer (ONL) thickness were performed on sections containing the optic nerve (at least three sections per eye) (Koch et al. 2017).

### 13.2.4 Electroretinography (ERG)

ERG analysis was performed at 1 year of age according to procedures described previously (Koch et al. 2015).

## 13.3 Results

### 13.3.1 Photoreceptor Degeneration in 2-Month-Old *Pde6b*$^{Stop}$/*Pde6b*$^{H620Q}$, *PDE6g*$^{CreERT2}$ Mice

To investigate whether RP can be treated well after the onset of photoreceptor degeneration, we administered treatment to our RP mouse model *Pde6b*$^{STOP}$/*Pde6b*$^{H620Q}$, *Pde6g::CreERT2* at an advanced disease stage. In the *Pde6b*$^{STOP}$/*Pde6b*$^{H620Q}$, *Pde6g::CreERT2* mice, one allele of *Pde6b* carries a point mutation (*Pde6b*$^{H620Q}$) that dramatically reduces function of PDE6b (Hart et al. 2005; Davis et al. 2008). The second allele carries a floxed Stop cassette (*Pde6b*$^{Stop}$) that prevents gene expression in the absence of Cre recombinase activity. After IP injection of tamoxifen, *Pde6g*$^{CreERT2}$ is activated, the Stop cassette is removed, and PDE6b is expressed in all rods (Koch et al. 2015). We administered treatment (i.e., tamoxifen) to 2-month-old *Pde6b*$^{STOP}$/*Pde6b*$^{H620Q}$, *Pde6g::CreERT2* mice. At 2 months of age, the photoreceptors dramatically degenerated (Fig. 13.1a), and this was reflected by a significant decrease in ONL thickness compared to wild-type mice ($P < 0.001$)

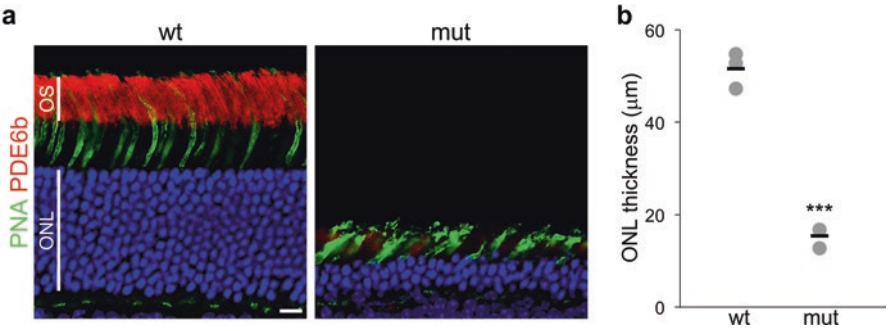


**Fig. 13.1** Photoreceptor degeneration in untreated mutant *Pde6b*$^{Stop}$/*Pde6b*$^{H620Q}$, *PDE6g*$^{CreERT2}$ retinas. Wild-type (wt) and mutant (mut) retinas were analyzed at 2 months of age, using immunostaining and quantitative analyses of sections. (**a**) Anti-PDE6b antibody (red) labels rod OSs. Anti-PNA antibody (green) labels cones. Nuclei were stained with Hoechst dye (blue). (**b**) Quantification of ONL thickness. Each gray dot represents an individual mouse ($n = 3$, for every group). Horizontal black lines represent the group means. An unpaired Student's t-test was used to compare groups. Significant differences between wt and untreated mutant groups are labeled as follows: $P < 0.001$. *OS* outer segment, *ONL* outer nuclear layer. Scale bar, 10 μm

(Fig. 13.1b). In addition, the PNA-labeled cone outer segment (OS) length was dramatically decreased (Fig. 13.1a). Based on this decrease in ONL thickness, by about 70%, compared to wild-type retina, we defined the 2-month-old *Pde6b*$^{STOP}$/*Pde6b*$^{H620Q}$, *Pde6g::CreERT2* mice as being in late stage of RP disease.

### *13.3.2 Structural and Functional Rescue Despite Late-Stage Treatment*

After tamoxifen treatment in 2-month-old *Pde6b*$^{STOP}$/*Pde6b*$^{H620Q}$, *Pde6g::CreERT2* mice (i.e., late-stage treatment), we tested whether the remaining photoreceptors were rescued. To assess structural rescue, retinal sections from 1-year-old mice were immune labeled with PDE6b and PNA antibodies (Fig. 13.2a), which label rod and cone OSs, respectively. In untreated mutant *Pde6b*$^{STOP}$/*Pde6b*$^{H620Q}$, *Pde6g::CreERT2* retinas, the ONL was gone due to photoreceptor cell loss, and rod and cone OSs were complete degenerated. However, late-stage treatment preserved the remaining photoreceptors, as well as the rod and cone OSs. We next quantified the observed changes in ONL thickness. ONL thickness was significantly greater in retinas of mice treated at 2 months, compared to untreated mutants ($P < 0.001$) (Fig. 13.2b).

We next tested whether retinal function was rescued after treatment at 2 months of age (i.e., late-stage disease). To do so, we performed ERG analysis in 1-year-old mice. Under light-adapted conditions with very bright flashes, to derive cone responses, wild-type retinas exhibited a cone-specific b-wave, which was strongly reduced in mutant *Pde6b*$^{STOP}$/*Pde6b*$^{H620Q}$, *Pde6g::CreERT2* mice; treatment rescued

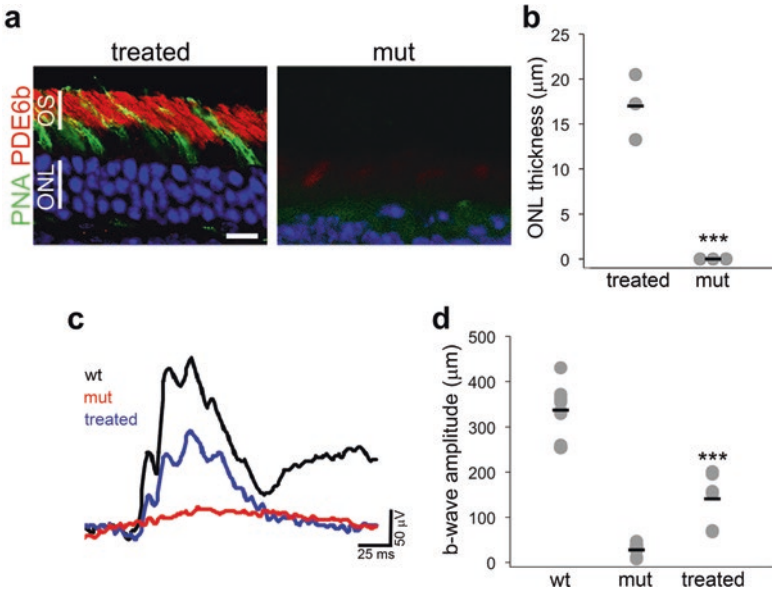


**Fig. 13.2** Preservation of retinal structure and function after gene therapy administered at late disease stage. Treated and mutant (mut) retinas were analyzed at 1 year of age, using immunostaining and ERG. Mutant mice were treated with tamoxifen at 2 months of age. (**a**) Anti-PDE6b antibody (red) labels rod OSs. Anti-PNA antibody (green) labels cones. Nuclei were stained with Hoechst dye (blue). (**b**) Quantification of ONL thickness. Each gray dot represents an individual mouse ($n = 3$, for every group). (**c**) Representative ERG responses for cones from wild-type (black, wt), mutant (red, mut), and treated (blue) mice. (**d**) Statistical analysis of ERG amplitudes for the photopic cone-specific b-wave. Gray dots represent individual eyes ($n = 8$ for wt and mut, $n = 6$ for treated eyes). An unpaired Student's t-test was used to compare treated and untreated mutant groups. Significant differences between treated and untreated mutant groups are labeled as follows: *** $P < 0.001$. Horizontal black lines represent the group means. *OS* outer segment, *ONL* outer nuclear layer. Scale bar, 10 µm

the cone responses (Fig. 13.2c). The amplitudes of the b-wave were quantified, comparing treated and untreated mutants (Fig. 13.2d). Treatment at 2 months significantly increased the cone b-wave amplitude ($P < 0.001$); this indicates that treatment prevented the progressive degeneration of cones. Thus, we are able to demonstrate structural and functional rescue of photoreceptors – even when the therapy was administered at late disease stage.

## 13.4 Discussion

In the present study, we used an RP mouse model $Pde6b^{Stop}/Pde6b^{H620Q}$, $PDE6g^{CreERT2}$, which allowed us to deliver the gene *Pde6b* uniformly to all rods in the retina, while also eliminating the problems associated with subretinal injections.

By administering tamoxifen at late disease stage, we mimicked the clinical scenario, in which patients are typically diagnosed after onset of degeneration – with the majority already exhibiting significant loss of rods and cones (Mitamura et al. 2012). In contrast, most previous animal studies administered the gene therapy before the onset of degeneration (Dejneka et al. 2004; Bennicelli et al. 2008). Our data clearly show long-term stability of both functional and structural rescue.

In recent retinal gene therapy clinical trials, some of the research subjects showed functional improvement (Bainbridge et al. 2008; Cideciyan et al. 2009; Maguire et al. 2009). However, it was also noted that photoreceptor loss had not been halted or even slowed (Cideciyan et al. 2013; Bainbridge et al. 2015; Jacobson et al. 2015; Wright 2015). It was suggested that there is a threshold of accumulated changes as a result of the mutation, after which photoreceptor death is inevitable (Cideciyan et al. 2013) – which has been called the "point of no return" (Cepko and Vandenberghe 2013). If such a threshold (i.e., "point of no return") exists, our mouse data demonstrate that it would have to occur at very terminal disease stages – after our "late stage." Instead, our study points to nonoptimal delivery of the gene therapeutic and clearly suggests that the way forward for developing RP therapeutics is to focus on optimizing delivery.

**Acknowledgments** The Barbara & Donald Jonas Laboratory of Regenerative Medicine and Bernard & Shirlee Brown Glaucoma Laboratory are supported by the National Institutes of Health [5P30EY019007, R01EY018213, R01EY024698, 1R01EY026682, R21AG050437], National Cancer Institute Core (5P30CA013696), the Research to Prevent Blindness (RPB) Physician-Scientist Award, unrestricted funds from RPB, New York, NY, USA. S.H.T. is a member of the RD-CURE Consortium and is supported by the Tistou and Charlotte Kerstan Foundation, the Schneeweiss Stem Cell Fund, New York State (C029572), the Foundation Fighting Blindness New York Regional Research Center Grant (C-NY05-0705-0312), and the Gebroe Family Foundation. The authors declare no conflicts of interest.

## References

Bainbridge JW, Smith AJ, Barker SS et al (2008) Effect of gene therapy on visual function in Leber's congenital amaurosis. N Engl J Med 358:2231–2239

Bainbridge JW, Mehat MS, Sundaram V et al (2015) Long-term effect of gene therapy on Leber's congenital amaurosis. N Engl J Med 372:1887–1897

Bennicelli J, Wright JF, Komaromy A et al (2008) Reversal of blindness in animal models of leber congenital amaurosis using optimized AAV2-mediated gene transfer. Mol Ther J Am Soc Gene Ther 16:458–465

Cepko CL, Vandenberghe LH (2013) Retinal gene therapy coming of age. Hum Gene Ther 24:242–244

Cheng LL, Han RY, Yang FY et al (2016) Novel mutations in PDE6B causing human retinitis pigmentosa. Int J Ophthalmol 9:1094–1099

Cideciyan AV, Hauswirth WW, Aleman TS et al (2009) Human RPE65 gene therapy for Leber congenital amaurosis: persistence of early visual improvements and safety at 1 year. Hum Gene Ther 20:999–1004

Cideciyan AV, Jacobson SG, Beltran WA et al (2013) Human retinal gene therapy for Leber congenital amaurosis shows advancing retinal degeneration despite enduring visual improvement. Proc Natl Acad Sci U S A 110:E517–E525

Davis RJ, Tosi J, Janisch KM et al (2008) Functional rescue of degenerating photoreceptors in mice homozygous for a hypomorphic cGMP phosphodiesterase 6 b allele (Pde6bH620Q). Invest Ophthalmol Vis Sci 49:5067–5076

Davis RJ, Hsu CW, Tsai YT et al (2013) Therapeutic margins in a novel preclinical model of retinitis pigmentosa. J Neurosci Off J Soc Neurosci 33:13475–13483

Dejneka NS, Surace EM, Aleman TS et al (2004) In utero gene therapy rescues vision in a murine model of congenital blindness. Mol Ther J Am Soc Gene Ther 9:182–188

Hart AW, McKie L, Morgan JE et al (2005) Genotype-phenotype correlation of mouse pde6b mutations. Invest Ophthalmol Vis Sci 46:3443–3450

Hartong DT, Berson EL, Dryja TP (2006) Retinitis pigmentosa. Lancet 368:1795–1809

Jacobson SG, Cideciyan AV, Roman AJ et al (2015) Improvement and decline in vision with gene therapy in childhood blindness. N Engl J Med 372:1920–1926

Koch S, Sothilingam V, Garcia Garrido M et al (2012) Gene therapy restores vision and delays degeneration in the CNGB1(-/-) mouse model of retinitis pigmentosa. Hum Mol Genet 21:4486–4496

Koch SF, Tsai YT, Duong JK et al (2015) Halting progressive neurodegeneration in advanced retinitis pigmentosa. J Clin Invest 125:3704–3713

Koch SF, Duong JK, Hsu C-W et al (2017) Genetic rescue models refute nonautonomous rod cell death in retinitis pigmentosa. Proc Natl Acad Sci 114(20):5259–5264

Maguire AM, High KA, Auricchio A et al (2009) Age-dependent effects of RPE65 gene therapy for Leber's congenital amaurosis: a phase 1 dose-escalation trial. Lancet 374:1597–1605

Mitamura Y, Mitamura-Aizawa S, Nagasawa T et al (2012) Diagnostic imaging in patients with retinitis pigmentosa. J Med Invest JMI 59:1–11

Sahel J, Bonnel S, Mrejen S et al (2010) Retinitis pigmentosa and other dystrophies. Dev Ophthalmol 47:160–167

Wright AF (2015) Long-term effects of retinal gene therapy in childhood blindness. N Engl J Med 372:1954–1955

# Chapter 14
# Optimizing Non-viral Gene Therapy Vectors for Delivery to Photoreceptors and Retinal Pigment Epithelial Cells


**Rahel Zulliger, Jamie N. Watson, Muayyad R. Al-Ubaidi, Linas Padegimas, Ozge Sesenoglu-Laird, Mark J. Cooper, and Muna I. Naash**

**Abstract** Considerable progress has been made in the design and delivery of non-viral gene therapy vectors, but, like their viral counterparts, therapeutic levels of transgenes have not met the requirements for successful clinical applications so far. The biggest advantage of polymer-based nanoparticle vectors is the ease with which they can be modified to increase their ability to penetrate the cell membrane and target specific cells by simply changing the formulation of the nanoparticle compaction. We took advantage of this characteristic to improve transfection rates of our particles to meet the transgene levels which will be needed for future treatment of patients. For this study, we successfully investigated the possibility of our established pegylated polylysine particles to be administered via intravitreal rather than subretinal route to ease the damage during injection. We also demonstrated that our particles are flexible enough to sustain changes in the formulation to accommodate additional targeting sequences without losing their efficiency in transfecting neuronal cells in the retina. Together, these results give us the opportunity to even further improve our particles.

**Keywords** Non-viral · Gene therapy · Nanoparticles · Inherited retinal degeneration · Photoreceptor · Retinal pigment epithelium

R. Zulliger · M. R. Al-Ubaidi · M. I. Naash (✉)
Department of Biomedical Engineering, University of Houston, Houston, TX, USA
e-mail: mnaash@central.uh.edu

J. N. Watson
Department of Cell Biology, University of Oklahoma Health Sciences Center, Oklahoma City, OK, USA

L. Padegimas
Abeona Therapeutics Inc., Cleveland, OH, USA

O. Sesenoglu-Laird · M. J. Cooper
Copernicus Therapeutics, Inc., Cleveland, OH, USA



J. D. Ash et al. (eds.), *Retinal Degenerative Diseases*, Advances in Experimental Medicine and Biology 891, https://doi.org/10.1007/978-3-319-75402-4_14

## 14.1 Introduction

Following major advances in molecular biology, the goal of gene therapy for the treatment of inherited diseases is about to become a reality. The eye is an ideal organ for gene therapy due to its relative isolation from the rest of the body via the blood-retina barrier (Shakib and Cunha-Vaz 1966) and the availability of noninvasive methods to measure visual performance. Inherited retinal degeneration is currently among the leading causes of blindness in developed countries, which only underlines the need for adequate gene therapy approaches. Major adverse events in patients treated with viral gene therapy vectors promoted the search for non-viral alternatives (Marshall 1999; 2002; Hacein-Bey-Abina et al. 2003) involving polymers which have the ability to compact the negatively charged DNA into nano-sized particles with almost neutral charge capable of penetrating the cell membrane. Our lab has successfully delivered many different transgenic DNA vectors via compaction with polylysine modified with polyethylene glycol (CK30PEG) (Farjo et al. 2006; Cai et al. 2010; Koirala et al. 2013b; Han et al. 2015). The CK30PEG particles are non-immunogenic and completely biodegradable and can carry vectors over 20 kb in size, which by far exceeds the payload of commonly used viral vectors (Vitiello et al. 1996; Ziady et al. 2003). Our experiments have shown that the CK30PEG particles easily transfect the cells in the retinal pigment epithelium (RPE) cells with high efficiency (Koirala et al. 2011, 2013b) and also lead to appreciable transgene expression in photoreceptors which are notoriously difficult to transfect (Farjo et al. 2006; Han et al. 2015). However, to reach wild-type levels of therapeutic proteins and to make the particles suitable for clinical trials, the transfection efficiency needs to be improved further. The present study shows how this goal can be reached by modifying the particle size and shape by variations in the compaction formulation. We also investigated a possible alternative administration via intravitreal injection which is much less invasive as well as the possibility of altering the peptide sequence for compaction. For this purpose, the transfection efficiency of our particles was tested via a quantitative reporter assay using the luciferase gene with our well-characterized plasmid vectors.

## 14.2 Material and Methods

### *14.2.1 Animals*

All experiments were performed according to protocols approved by the University's Institutional Animal Care and Use Committee (IACUC) and followed the guidelines introduced by the Association for Research in Vision and Ophthalmology (ARVO). For this study, newborn wild-type (WT) agouti or 30-day-old Balb/C mice were injected subretinally or intravitreally under anesthesia induced with a mixture of ketamine and xylazine (Henry Schein Animal Health) or via hypothermia (for

pups). The eyes were dilated with 1% cyclopentolate and the cornea kept moist with Gonak™ 2.5% (Akorn Inc., Lake Forest, IL). The cornea was penetrated with a 33G insulin needle, and nanoparticles, naked DNA, or saline were delivered. Intraocular injections are described in detail in (Cai et al. 2010).

### *14.2.2 Vectors and Compaction*

Vectors were constructed by the addition of the luciferase gene (described in Padegimas et al. (2012)) into different vector backbones described in earlier publications (Koirala et al. 2011, 2013a). Vector constructs were compacted into nanoparticles with CK30PEG and other peptides with different lysine lengths (described in detail in Ziady et al. (2003)). The resulting nanoparticles were concentrated to ~4 mg/ml. Quality control of the nanoparticles was determined by a panel of studies as described in Liu et al. and Ziady et al. (Liu et al. 2003; Ziady et al. 2003).

### *14.2.3 Luciferase Assays*

Whole eyes were extracted at the indicated postinjection (PI) time points. Luciferase activity was measured by addition of luciferase reagent (Promega, Madison WI) to extracted protein and read on a luminometer (Turner BioSystems, Sunnyvale, CA) as described in Yurek et al. (2009a). Statistical analyses were performed with the GraphPad Prism 5 (GraphPad Software Inc., La Jolla, CA) using Kruskal-Wallis for nonparametric distribution with a Dunn's posttest.

## 14.3 Results

### *14.3.1 Enhanced Transgene Expression in the RPE*

Size and shape can have great influence on the capacity of CK30PEG particles to penetrate the tissue and mediate cellular uptake, and these parameters can be changed with variations in the compaction process. The counterion during compaction can have a significant impact on these parameters as shown before with acetate, which forms rod-shaped particles (diameter <11 nm), and with trifluoroacetate (TFA), which leads to ellipsoidal particles (diameter <22 nm for a 5 kbp plasmid) (Fink et al. 2006). The tissue penetration depth of these particles is of particular interest, as the subretinal injection pathway is traumatic and generally leads to retinal detachment and significant functional loss (Farjo et al. 2006), while

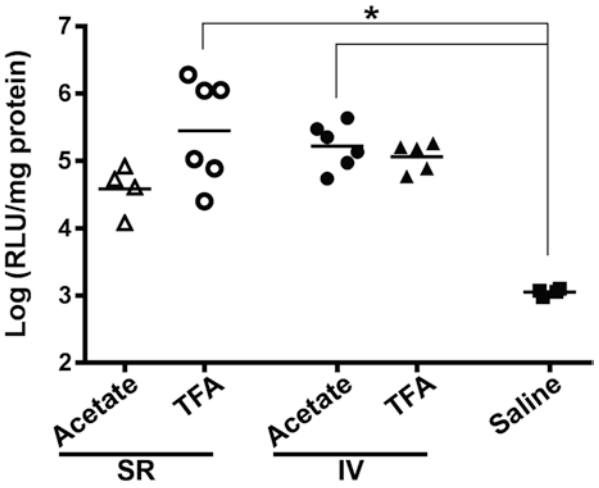


**Fig. 14.1** pVMD_Luc vectors were compacted with CK30P10K and two different counterions (acetate (Ac) or TFA) and subretinally or intravitreally injected into adult BALB/c mice. Analysis of luciferase activity in the eye was performed at PI-3. Averages were compared to saline-injected eyes (statistically significant means are highlighted with an asterisk)

the intravitreal route only causes minor tissue irritation and does not affect the retina. To test these different variables, we used our well-described pEPI delivery vector with the RPE-cell-specific promoter VMD2 in our CK30PEG particles. Encouragingly, the intravitreal injection route led to transgenic expression levels in the RPE equal if not better than the subretinal approach, even though the particles had to penetrate the whole retina to reach the RPE. In addition, intravitreal injection may lead to a more reliable outcome as the distribution of the particles is more even in the vitreous than in the subretinal space where efficient distribution is dependent on the degree of retinal detachment. The use of TFA as a counterion yielded an increase in transgene levels after subretinal injection but is comparable to acetate after intravitreal administration (Fig. 14.1).

### *14.3.2 Enhanced Transfection Efficiency in Photoreceptors*

Due to their phagocytic activity, RPE cells have always been easier to target by gene delivery, while the neuronal photoreceptors have proven to be more challenging. However, we have previously shown that our CK30PEG particles are capable of transfecting the photoreceptors, especially when the particles were administered early in the life of the animal (Cai et al. 2010; Han et al. 2015). Our standard pEPI plasmid was equipped with the luciferase reporter gene as well as the well-characterized rhodopsin kinase (RK) promoter to ensure photoreceptor-specific expression. Three different sizes of polylysine were tested after injection of mice at postnatal day 5 (P5), CK14, CK21, and CK42 and compared to the established CK30 via the luciferase reporter assay (Fig. 14.2). The results showed that, indeed, the polylysine chain can be shortened to 21 repeats without negatively impacting

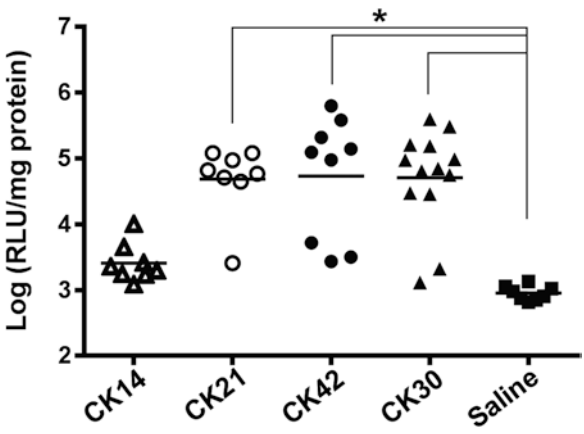


**Fig. 14.2** WT agoutis at postnatal day 1 (P1) were injected subretinally with pEPI-RK_Luc compacted with different lengths of polylysine and assessed at PI-30. Statistical analysis was performed comparing nanoparticle-injected to saline-injected eyes (significantly different means are highlighted with an asterisk)

the efficiency of transfection and increasing the chain length to 42 does not improve the effectiveness any further.

## 14.4 Discussion

In this report, we share some of the results from our recent studies in formulation engineering of nanoparticles. The goal of these experiments is to take our successful non-viral vectors for gene therapy and apply some structural changes to the compaction peptide to potentially make them suitable for clinical trials. The CK30PEG particles previously used have been well characterized and are among the most successful versions of polymeric compaction agents for neurons in the retina and the brain as well as lung epithelial cells (Yurek et al. 2009b; Ziady et al. 2010; Harmon et al. 2014; Han et al. 2015). Our first experiment was aimed at testing if our particles can be administered by the less invasive intravitreal approach without losing any transgene expression in the RPE in comparison to the subretinal injection. Our nanoparticles are not only performing at an equal rate when injected into the vitreous but also appear to show better reproducibility across the samples. This is very important for the applicability of the particles for future clinical trials. In the same experiment, we tested the influence of the size and shape of the particles on tissue penetration by changing the counterion during compaction. Interestingly, the difference between the two different particles was not significant in the mouse retina after intravitreal injection, but it might prove to be important in the larger retinas of patients. Also, this highlights one of the biggest advantages of our CK30PEG particles, as it shows the ease with which important particle characteristics can be modified.

An emerging topic in research for non-viral gene therapy vectors is the use of targeting sequences, which may either enhance the uptake rate or increase the cell specificity by docking the particles to specific cell-surface receptors (Wagner et al.

2010). In some systems, the addition of intracellular targeting signals can increase the availability of vectors for gene expression, and short nuclear targeting peptides have been shown to increase nuclear localization (Kalderon et al. 1984). The CK30PEG nanoparticles, however, already have the advantage of interacting with the nucleolin receptor which mediates their fast cellular uptake and transcellular transport to the nucleus (Chen et al. 2008). To possibly improve gene transfection further, we are working on including other peptide sequences as mentioned above. The goal of our second experiment was to determine if structural changes in the compaction peptide can improve transgene activity. The results showed very clearly that a particle made with a polylysine chain shorter than CK21 is no longer mediating transfection of photoreceptor cells. Increasing the chain length to CK42 on the other hand did not increase transfection rates. Therefore, we can conclude that we have a solid 20 amino acid window to add targeting sequences in our future experiments without significantly impacting the overall size of the particles. This again emphasizes the great versatility of our particles and suggests that they will be a good addition to the current viral delivery vectors.

**Acknowledgments** This work was supported by the NIH (EY18656 and EY022778), the Foundation Fighting Blindness (MIN, MRA), and the Knights Templar Eye Foundation (RZ).

## References

(2002) Assessment of adenoviral vector safety and toxicity: report of the National Institutes of Health Recombinant DNA Advisory Committee. Hum Gene Ther 13:3–13

Cai X, Conley SM, Nash Z et al (2010) Gene delivery to mitotic and postmitotic photoreceptors via compacted DNA nanoparticles results in improved phenotype in a mouse model of retinitis pigmentosa. FASEB J 24:1178–1191

Chen X, Kube DM, Cooper MJ et al (2008) Cell surface nucleolin serves as receptor for DNA nanoparticles composed of pegylated polylysine and DNA. Mol Ther 16:333–342

Farjo R, Skaggs J, Quiambao AB et al (2006) Efficient non-viral ocular gene transfer with compacted DNA nanoparticles. PLoS One 1:e38

Fink TL, Klepcyk PJ, Oette SM et al (2006) Plasmid size up to 20 kbp does not limit effective in vivo lung gene transfer using compacted DNA nanoparticles. Gene Ther 13:1048–1051

Hacein-Bey-Abina S, von Kalle C, Schmidt M et al (2003) A serious adverse event after successful gene therapy for X-linked severe combined immunodeficiency. N Engl J Med 348:255–256

Han Z, Banworth MJ, Makkia R et al (2015) Genomic DNA nanoparticles rescue rhodopsin-associated retinitis pigmentosa phenotype. FASEB J 29:2535–2544

Harmon BT, Aly AE, Padegimas L et al (2014) Intranasal administration of plasmid DNA nanoparticles yields successful transfection and expression of a reporter protein in rat brain. Gene Ther 21:514–521

Kalderon D, Roberts BL, Richardson WD et al (1984) A short amino acid sequence able to specify nuclear location. Cell 39:499–509

Koirala A, Makkia RS, Cooper MJ et al (2011) Nanoparticle-mediated gene transfer specific to retinal pigment epithelial cells. Biomaterials 32:9483–9493

Koirala A, Makkia RS, Conley SM et al (2013a) S/MAR-containing DNA nanoparticles promote persistent RPE gene expression and improvement in RPE65-associated LCA. Hum Mol Genet 22:1632–1642

Koirala A, Conley SM, Makkia R et al (2013b) Persistence of non-viral vector mediated RPE65 expression: case for viability as a gene transfer therapy for RPE-based diseases. J Control Release 172:745–752

Liu G, Li D, Pasumarthy MK et al (2003) Nanoparticles of compacted DNA transfect postmitotic cells. J Biol Chem 278:32578–32586

Marshall E (1999) Gene therapy death prompts review of adenovirus vector. Science 286:2244–2245

Padegimas L, Kowalczyk TH, Adams S et al (2012) Optimization of hCFTR lung expression in mice using DNA nanoparticles. Mol Ther 20:63–72

Shakib M, Cunha-Vaz JG (1966) Studies on the permeability of the blood-retinal barrier. IV. Junctional complexes of the retinal vessels and their role in the permeability of the blood-retinal barrier. Exp Eye Res 5:229–234

Vitiello L, Chonn A, Wasserman JD et al (1996) Condensation of plasmid DNA with polylysine improves liposome-mediated gene transfer into established and primary muscle cells. Gene Ther 3:396–404

Wagner S, Rothweiler F, Anhorn MG et al (2010) Enhanced drug targeting by attachment of an anti alphav integrin antibody to doxorubicin loaded human serum albumin nanoparticles. Biomaterials 31:2388–2398

Yurek DM, Flectcher AM, Kowalczyk TH et al (2009a) Compacted DNA nanoparticle gene transfer of GDNF to the rat striatum enhances the survival of grafted fetal dopamine neurons. Cell Transplant 18:1183–1196

Yurek DM, Fletcher AM, Smith GM et al (2009b) Long-term transgene expression in the central nervous system using DNA nanoparticles. Mol Ther 17:641–650

Ziady AG, Gedeon CR, Muhammad O et al (2003) Minimal toxicity of stabilized compacted DNA nanoparticles in the murine lung. Mol Ther 8:948–956

Ziady AG, Kotlarchyk M, Bryant L et al (2010) Bioluminescent imaging of reporter gene expression in the lungs of wildtype and model mice following the administration of PEG-stabilized DNA nanoparticles. Microsc Res Tech 73:918–928

# Chapter 15
# Nanoparticles as Delivery Vehicles for the Treatment of Retinal Degenerative Diseases


**Yuhong Wang, Ammaji Rajala, and Raju V. S. Rajala**

**Abstract** Over the last few years, huge progress has been made in the understanding of molecular mechanisms underlying the pathogenesis of retinal degenerative diseases. Such knowledge has led to the development of gene therapy approaches to treat these devastating disorders. Non-viral gene delivery has been recognized as a prospective treatment for retinal degenerative diseases. In this review, we will summarize the constituent characteristics and recent applications of three representative nanoparticles (NPs) in ocular therapy.

**Keywords** Nanoparticles · Retinal degeneration · Metal-based nanoparticles · Polymer-based nanoparticles · Lipid nanoparticles · Ocular diseases · Non-viral vectors · Blindness

Y. Wang · A. Rajala
Department of Ophthalmology, University of Oklahoma Health Sciences Center, Oklahoma City, OK, USA

Dean McGee Eye Institute, Oklahoma City, OK, USA

R. V. S. Rajala (✉)
Department of Ophthalmology, University of Oklahoma Health Sciences Center, Oklahoma City, OK, USA

Department of Physiology, University of Oklahoma Health Sciences Center, Oklahoma City, OK, USA

Department of Cell Biology, University of Oklahoma Health Sciences Center, Oklahoma City, OK, USA

Dean McGee Eye Institute, Oklahoma City, OK, USA
e-mail: raju-rajala@ouhsc.edu



J. D. Ash et al. (eds.), *Retinal Degenerative Diseases*, Advances in Experimental Medicine and Biology 891, https://doi.org/10.1007/978-3-319-75402-4_15

## 15.1 Introduction

Ocular diseases currently still lack effective treatments; thus, the development of effective therapeutics is a primary research goal. So far, many delivery strategies have been explored, with gene delivery systems emerging as the most promising approach in this field (Han et al. 2011; Walkey et al. 2015; Wang et al. 2015). Gene delivery systems can be broadly classified into two groups, viral and non-viral delivery approaches. Each system comes with its own advantages and disadvantages. Although adeno-associated viral (AAV) vectors have high gene transduction efficiency, they face a major biosafety issue for clinical applications. Therefore, development of effective non-viral approaches for ocular disease is of very high importance.

The advantages of non-viral nanoparticles include biodegradability, biocompatibility, minimal toxicity, relatively large capacity, and simplicity of use (Adijanto and Naash 2015; Silva et al. 2015). Functionally, nanoparticles can serve as intrinsic antioxidants or as carriers to deliver drugs and biological macromolecules to target regions.

Nanoparticles for molecular therapy could be classified into three groups: (1) metal-based nanoparticles (metal NPs), (2) polymer-based nanoparticles (polymer NPs), and (3) lipid-based nanoparticles (lipid-protamine-DNA, LPD). The characteristic features of these particles are described in Table 15.1. They differ in size, charge, shape, and structure, but all possess a mechanism to enter the cell, avoid or escape from endosomes, and finally enter the nucleus in order to deliver therapeutic agents (Adijanto and Naash 2015; Wang et al. 2015). The eye has unique advantages for the study of therapeutic agents due to the immune privilege, the ability to directly visualize the expression and locally treat the target tissue, and the benefit of a simultaneous control provided by the other eye.

**Table 15.1** Three non-viral nanoparticles' comparison in the eye

| Nanoparticle | Type | Size | Shape | Charge | Carrier | Target cell |
|---|---|---|---|---|---|---|
| Nanoceria | Metal NPs | 3–5 nm | Octahedral | Positive | Intrinsic | Photoreceptors RPE |
| | | | | Negative | | |
| | | | | Neutral | | |
| CK30 | Polymer NPs | <25 nm | Rod | Positive | cDNA | Photoreceptors RPE Ganglion cells |
| | | | | | MicroRNA | |
| | | | | | Genomic DNA | |
| LPD | Lipid NPs | 50–250 nm | Sphere | Positive | cDNA | Photoreceptors RPE Ganglion cells |
| | | | | | MicroRNA | |
| | | | | | Lipid | |

## 15.2 Metal-Based Nanoparticles

Over the past decade, several different types of metal nanoparticles have been characterized. For example, cerium oxide (CeO2) nanoparticles and yttrium oxide ($Y_2O_3$) nanoparticles have been shown to have a high redox scavenging capability with little or no toxicity after delivery to the eye (Cai and McGinnis 2016b; Mitra et al. 2014; Wong and McGinnis 2014). Cerium oxide (CeO2) nanoparticles also have intrinsic antioxidant properties (Chen et al. 2006). Cerium is a rare earth element, and cerium oxide (CeO2) is an inorganic compound that possesses catalytic antioxidant activity (Kong et al. 2011; Walkey et al. 2015; Zhou et al. 2011). These nanoceria particles can act as antioxidants similar to vitamins C and E. In addition, these particles also possess the catalytic antioxidant enzymatic activities of superoxide dismutase (SOD) and catalase (Kong et al. 2011; Walkey et al. 2015; Zhou et al. 2011).

## 15.3 Metal-Based Nanoparticle Application in Ocular Disease

The retina is exposed to chronic oxidative stress through several mechanisms, including constant exposure to light leading to reactive oxygen species generation by visual signal transduction pathways due to high oxygen consumption, oxidization of polyunsaturated fatty acids, and phagocytosis of photoreceptor cells. In the healthy state, all cell types in the retina are able to maintain homeostasis under conditions of oxidative stress. However, when the balance between pro- and antioxidative signaling is compromised, excessive oxidative stress induces dysregulation of functional networks and deleterious changes that result in visual impairment. Nanoceria particles have been used as therapeutics to destroy reactive oxygen species (ROS) and prevent retinal degenerative disease phenotypes in animal models of diabetic retinopathy, dry age-related macular degeneration, neovascularization, and retinitis pigmentosa including inhibition of tumor growth of retinoblastoma (Cai et al. 2014a, b; Cai and McGinnis 2016a, b; Kong et al. 2011; Wong and McGinnis 2014). These studies suggest that nanoceria have the potential to provide effective protection in retinal diseases and open a promising avenue for the treatment of ocular diseases due to their antioxidative properties.

## 15.4 Polymer-Based Nanoparticles

Researchers have used multiple polymer nanoparticles to deliver genes to ocular tissues; however, the most extensively characterized particle is CK30-PEG (Conley and Naash 2010). The CK30-PEG polymer nanoparticle contains a single molecule

of plasmid DNA compacted into nanoparticles (NPs) by a 10 kDa PEG-substituted lysine 30-mers (CK30-PEG). As a nanoparticle therapy, CK30-PEG NPs can directly transport molecules to the nucleus, where gene expression occurs. CK30-NPs have advantages in driving long-term, safe gene expression and improving ocular disease based on several key characteristics (Conley and Naash 2010). CK30-NPs have no theoretical limitation on plasmid size, and they do not provoke an immune response, and the compacted particle is efficiently taken up into both dividing and nondividing cells (Conley and Naash 2010; Han et al. 2011).

## 15.5 Polymer Nanoparticle Application in Ocular Disease

CK30-PEG NPs have been successfully used for the delivery of retinal pigment epithelium 65 (*Rpe65*) gene to rescue cone degeneration associated with *Rpe65*$^{-/-}$mice (Koirala et al. 2013a, b). This approach has been shown to improve retinal morphology and function (Cai et al. 2010; Han et al. 2012a, b) (Koirala et al. 2013a, b, 2014). CK30-PEG nanoparticles have also been used in packaging genomic DNA to rescue a rhodopsin-associated retinitis pigmentosa phenotype (Han et al. 2015). MicroRNAs (miRNAs) are a class of naturally occurring small, noncoding RNA molecules. miRNAs have been recognized as a key component in regulating cell biological development and may be involved in the pathogenesis of diabetic retinopathy (DR); therefore, CK30-PEG nanoparticle-mediated miR200-b have been delivered for the treatment of DR and lead to an effective anti-angiogenic therapy for DR (Mitra et al. 2016). Polymer NPs have a tolerable safety profile with a lack of immunogenicity in the retina. As such, CK30-PEG nanoparticles become a promising non-viral gene delivery vehicle for ocular diseases.

## 15.6 Lipid-Based Nanoparticles

Lipids, with their amphipathic properties, provide a potent tool for nanotechnology (Mashaghi et al. 2013). They can be self-assembled into nano-films and other nanostructures, including micelles, reverse micelles, and liposomes (Mashaghi et al. 2013). The use of lipid nanoparticles as part of a gene or drug delivery system to provide treatment to the retina has been suggested (del Pozo-Rodriguez et al. 2013). Lipid-protamine-DNA (LPD) complexes have been characterized for in vivo gene delivery with reporter plasmid constructs (Li et al. 1998; Li and Huang 1997). Liposome nanoparticles have been widely studied in molecular therapy due to their ease of use, commercial availability, efficient delivery, and biocompatibility advantages (Honda et al. 2013; Wang et al. 2015; Zhu et al. 1993). Although multiple different types of liposome nanoparticles have been used in molecular therapy, peptide-modified LPD nanoparticles have been among the most successful in improving disease progression. LPD nanoparticles are electrostatically assembled from cationic liposomes and an anionic protamine-DNA complex with two peptides

NLS (nuclear localization peptides) and TAT (transactivator of transcription), and thereby peptide-modified LPD reach optimal transfer efficiency (Ma et al. 2013; Rajala et al. 2014; Wang et al. 2015). These peptide-modified LPD have many advantages for future clinical applications. First, liposome nanoparticles are able to deliver large molecular cargo. Second, the optimization of peptide-modified LPD nanoparticles allows multiple genes to be delivered simultaneously. Third, peptide-modified LPD formulations are more biocompatible and safe than viral vectors.

## 15.7 Lipid Nanoparticle Application for Ocular Diseases

In the eye, Rpe65 is a key enzyme, gene deficiency of which results in cone photoreceptor degeneration in murine models (Znoiko et al. 2005). Our laboratory tested LPD nanoparticle delivery of Rpe65 gene in Rpe65-knockout mice, leading to correction of blindness. The efficacy of this method in restoring vision is comparable to AAV and lentiviral gene transfer (Rajala et al. 2014). LPD nanoparticles can also deliver microRNA-184 to the retina and successfully repress Wnt-mediated ischemia-induced neovascularization (Takahashi et al. 2015). One of the disadvantages of lipid nanoparticles is that they cannot achieve cell specificity. The retina is composed of seven different kinds of neural cell layers, and improper delivery can lead to potentially harmful ectopic expression. We recently overcome this limitation using cell-specific promoters to delivery to specific cell types of retina, such as RPE, rod cell, cone cell, and ganglion cell (Wang et al. 2016). These studies suggest that peptide-modified LPD nanoparticles are attractive vehicles for ocular gene therapy in retinal disease treatment.

## 15.8 Conclusions

A successful molecular therapy strategy should encapsulate and protect the molecular materials, escape endosomal degradation, and reach the specific target site. The most challenging aspect of molecular therapy is delivering precisely the right quantity of therapy molecule to stimulate optimal levels of expression in a specific cell type, without stimulating an immunity response from the host. Despite rapid advances in molecular therapy during the last two decades, major obstacles to clinical applications for human diseases still exist. These impediments include managing the immune response, vector toxicity, and the lack of sustained therapeutic gene expression. The nanoparticles described above will overcome these barriers, allowing us to achieve safe and effective molecular therapy.

**Acknowledgments** Dr. Yuhong Wang is a Foundation Fighting Blindness Travel Awardee. This study was supported by grants from the National Institutes of Health (EY00871 and NEI core grant EY021725) and an unrestricted grant from Research to Prevent Blindness, Inc., to the Department of Ophthalmology. The authors thank Mr. Christopher Kooker for reading the manuscript.

## References

Adijanto J, Naash MI (2015) Nanoparticle-based technologies for retinal gene therapy. Eur J Pharm Biopharm 95(Pt B):353–367

Cai X, McGinnis JF (2016a) Diabetic retinopathy: animal models, therapies, and perspectives. J Diabetes Res 2016:3789217

Cai X, McGinnis JF (2016b) Nanoceria: a potential therapeutic for dry AMD. Adv Exp Med Biol 854:111–118

Cai X, Conley SM, Nash Z et al (2010) Gene delivery to mitotic and postmitotic photoreceptors via compacted DNA nanoparticles results in improved phenotype in a mouse model of retinitis pigmentosa. FASEB J 24:1178–1191

Cai X, Seal S, McGinnis JF (2014a) Sustained inhibition of neovascularization in vldlr−/− mice following intravitreal injection of cerium oxide nanoparticles and the role of the ASK1-P38/JNK-NF-kappaB pathway. Biomaterials 35:249–258

Cai X, Yodoi J, Seal S et al (2014b) Nanoceria and thioredoxin regulate a common antioxidative gene network in tubby mice. Adv Exp Med Biol 801:829–836

Chen J, Patil S, Seal S et al (2006) Rare earth nanoparticles prevent retinal degeneration induced by intracellular peroxides. Nat Nanotechnol 1:142–150

Conley SM, Naash MI (2010) Nanoparticles for retinal gene therapy. Prog Retin Eye Res 29:376–397

del Pozo-Rodriguez A, Delgado D, Gascon AR et al (2013) Lipid nanoparticles as drug/gene delivery systems to the retina. J Ocul Pharmacol Ther 29:173–188

Han Z, Conley SM, Naash MI (2011) AAV and compacted DNA nanoparticles for the treatment of retinal disorders: challenges and future prospects. Invest Ophthalmol Vis Sci 52:3051–3059

Han Z, Conley SM, Makkia R et al (2012a) Comparative analysis of DNA nanoparticles and AAVs for ocular gene delivery. PLoS One 7:e52189

Han Z, Conley SM, Makkia RS et al (2012b) DNA nanoparticle-mediated ABCA4 delivery rescues Stargardt dystrophy in mice. J Clin Invest 122:3221–3226

Han Z, Banworth MJ, Makkia R et al (2015) Genomic DNA nanoparticles rescue rhodopsin-associated retinitis pigmentosa phenotype. FASEB J 29:2535–2544

Honda M, Asai T, Oku N et al (2013) Liposomes and nanotechnology in drug development: focus on ocular targets. Int J Nanomedicine 8:495–503

Koirala A, Conley SM, Makkia R et al (2013a) Persistence of non-viral vector mediated RPE65 expression: case for viability as a gene transfer therapy for RPE-based diseases. J Control Release 172:745–752

Koirala A, Makkia RS, Conley SM et al (2013b) S/MAR-containing DNA nanoparticles promote persistent RPE gene expression and improvement in RPE65-associated LCA. Hum Mol Genet 22:1632–1642

Koirala A, Conley SM, Naash MI (2014) Episomal maintenance of S/MAR-containing non-viral vectors for RPE-based diseases. Adv Exp Med Biol 801:703–709

Kong L, Cai X, Zhou X et al (2011) Nanoceria extend photoreceptor cell lifespan in tubby mice by modulation of apoptosis/survival signaling pathways. Neurobiol Dis 42:514–523

Li S, Huang L (1997) In vivo gene transfer via intravenous administration of cationic lipid-protamine-DNA (LPD) complexes. Gene Ther 4:891–900

Li S, Rizzo MA, Bhattacharya S et al (1998) Characterization of cationic lipid-protamine-DNA (LPD) complexes for intravenous gene delivery. Gene Ther 5:930–937

Ma K, Wang DD, Lin Y et al (2013) Synergetic targeted delivery of sleeping-beauty transposon system to mesenchymal stem cells using LPD nanoparticles modified with a phage-displayed targeting peptide. Adv Funct Mater 23:1172–1181

Mashaghi S, Jadidi T, Koenderink G et al (2013) Lipid nanotechnology. Int J Mol Sci 14:4242–4282

Mitra RN, Merwin MJ, Han Z et al (2014) Yttrium oxide nanoparticles prevent photoreceptor death in a light-damage model of retinal degeneration. Free Radic Biol Med 75:140–148

Mitra RN, Nichols CA, Guo J et al (2016) Nanoparticle-mediated miR200-b delivery for the treatment of diabetic retinopathy. J Control Release 236:31–37

Rajala A, Wang Y, Zhu Y et al (2014) Nanoparticle-assisted targeted delivery of eye-specific genes to eyes significantly improves the vision of blind mice in vivo. Nano Lett 14:5257–5263

Silva AC, Amaral MH, Lobo JM et al (2015) Lipid nanoparticles for the delivery of biopharmaceuticals. Curr Pharm Biotechnol 16:291–302

Takahashi Y, Chen Q, Rajala RV et al (2015) Micro RNA-184 modulates cannocial Wnt signaling through regulation of frizzled-7 expression in the retina with ischemia-induced neovascularization. FEBS Lett 589:1143–1149

Walkey C, Das S, Seal S et al (2015) Catalytic properties and biomedical applications of cerium oxide nanoparticles. Environ Sci Nano 2:33–53

Wang Y, Rajala A, Rajala RV (2015) Lipid nanoparticles for ocular gene delivery. J Funct Biomater 6:379–394

Wang Y, Rajala A, Cao B et al (2016) Cell-specific promoters enable lipid-based nanoparticles to deliver genes to specific cells of the retina in vivo. Theranostics 6:1514–1527

Wong LL, McGinnis JF (2014) Nanoceria as bona fide catalytic antioxidants in medicine: what we know and what we want to know…. Adv Exp Med Biol 801:821–828

Zhou X, Wong LL, Karakoti AS et al (2011) Nanoceria inhibit the development and promote the regression of pathologic retinal neovascularization in the Vldlr knockout mouse. PLoS One 6:e16733

Zhu N, Liggitt D, Liu Y et al (1993) Systemic gene expression after intravenous DNA delivery into adult mice. Science 261:209–211

Znoiko SL, Rohrer B, Lu K et al (2005) Downregulation of cone-specific gene expression and degeneration of cone photoreceptors in the Rpe65−/− mouse at early ages. Invest Ophthalmol Vis Sci 46:1473–1479

# Chapter 16
# Overexpression of Type 3 Iodothyronine Deiodinase Reduces Cone Death in the Leber Congenital Amaurosis Model Mice

**Fan Yang, Hongwei Ma, Sanford L. Boye, William W. Hauswirth, and Xi-Qin Ding**

**Abstract** Leber congenital amaurosis (LCA) is a devastating pediatric retinal degenerative disease, accounting for 20% of blindness in children attending schools for the blind. Mutations in the *RPE65* gene, which encodes the retinal pigment epithelium-specific isomerohydrolase RPE65, account for 16% of all LCA cases. Recent findings have linked cone photoreceptor viability to thyroid hormone (TH) signaling. TH signaling regulates cell proliferation, differentiation, and metabolism. At the cellular level, TH action is regulated by the two iodothyronine deiodinases, DIO2 and DIO3. DIO2 converts the prohormone thyroxine (T4) to the bioactive hormone triiodothyronine (T3), and DIO3 inactivates T3 and T4. The present work investigates the effects of overexpression of DIO3 to suppress TH signaling and thereby modulate cone death/survival. Subretinal delivery of AAV5-IRBP/GNAT2-*hDIO3* induced robust expression of DIO3 in the mouse retina and significantly reduced the number of TUNEL-positive cells in the cone-dominant LCA model *Rpe65*$^{-/-}$/*Nrl*$^{-/-}$ mice. Our work shows that suppressing TH signaling by overexpression of DIO3 preserves cones, supporting that suppressing TH signaling locally in the retina may represent a treatment strategy for LCA management.

**Keywords** Thyroid hormone · Leber congenital amaurosis · Retina degeneration · Cone photoreceptors · Type 3 iodothyronine deiodinase

F. Yang · H. Ma · X. -Q. Ding (✉)
Department of Cell Biology, University of Oklahoma Health Sciences Center, Oklahoma City, OK, USA
e-mail: xi-qin-ding@ouhsc.edu

S. L. Boye · W. W. Hauswirth
Departments of Ophthalmology and Molecular Genetics and Microbiology, University of Florida, Gainesville, FL, USA



J. D. Ash et al. (eds.), *Retinal Degenerative Diseases*, Advances in Experimental Medicine and Biology 891, https://doi.org/10.1007/978-3-319-75402-4_16

## 16.1 Introduction

Rod and cone photoreceptors degenerate in a wide array of hereditary retinal diseases, including the pediatric blinding disease Leber congenital amaurosis (LCA). LCA is a severe autosomal recessive retinal disease that appears at birth and early childhood, accounting for blindness in over 20% of children attending schools for the blind. Genetic studies have shown that mutations in at least 24 genes are associated with LCA (https://sph.uth.edu/retnet/). Among these, mutations in the *RPE65* gene, which encodes the retinal pigment epithelium-specific isomerohydrolase RPE65, account for about 16% of all LCA cases. Though there are multiple pathological determinants, it is the death of cone photoreceptors that eventually leads to the loss of vision/blindness.

Thyroid hormone (TH) signaling regulates cell growth, differentiation, and metabolism. In the retina, TH signaling is well known for its regulation of cone opsin expression (Ng et al. 2001). TH signaling has also been linked to cone viability. Treatment with the TH triiodothyronine (T3) leads to cone death (Ng et al. 2010). Recent studies have implicated a role of TH signaling in retinal degeneration, including LCA cone degeneration. Treatment with an antithyroid drug and targeting the cellular TH components significantly increased cone density in the LCA model *Rpe65*$^{-/-}$ mice (Ma et al. 2014; Yang et al. 2016). The intracellular TH signaling is primarily regulated by the two iodothyronine deiodinases: type 2 iodothyronine deiodinase (DIO2) and type 3 iodothyronine deiodinase (DIO3). DIO2 converts the prohormone thyroxine (T4) to T3, which then binds to the TH receptors in the nucleus to initiate downstream gene expression alterations, whereas DIO3 deactivates both T4 and T3 (Fig. 16.1). We have shown that overexpression of DIO3 specifically in cones significantly increased cone density in *Rpe65*$^{-/-}$ mice and the achromatopsia model *Cpfl1* mice with *Pde6c* defect (Yang et al. 2016). Here we report that subretinal delivery of AAV5-IRBP/GNAT2-*hDIO3* significantly reduced cone death in the cone-dominant LCA model *Rpe65*$^{-/-}$/*Nrl*$^{-/-}$ mice.

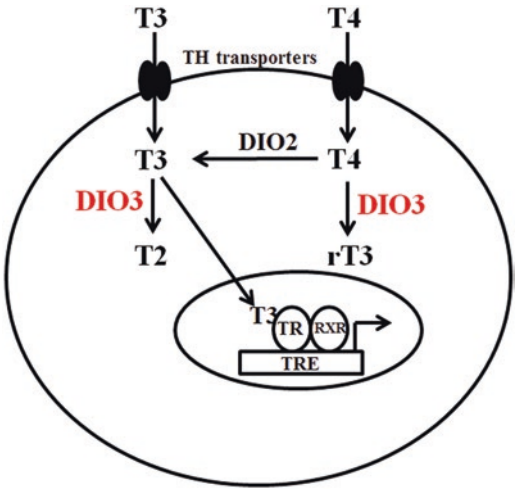


**Fig. 16.1** The TH signaling. Circulating T4 and T3 are transported into cells where T4 is converted to T3 by DIO2. T3 is then transferred to the nucleus and binds to TRs to initiate the downstream gene expression alterations. T4 and T3 are degraded to T2 and reverse T3 (rT3) by DIO3

## 16.2 Materials and Methods

### *16.2.1 Experimental Mice*

The *Rpe65*$^{-/-}$ mouse line was provided by Dr. T. Michael Redmond (NEI/NIH) (Redmond et al. 1998). The *Nrl*$^{-/-}$ mouse line was provided by Dr. Anand Swaroop (NEI/NIH) (Mears et al. 2001). As a unique cone-dominant mouse model, the *Nrl*$^{-/-}$ mouse line has been commonly used to study cone biology *and disease* (Farjo et al. 2006; Ma et al. 2013). The *Rpe65*$^{-/-}$/*Nrl*$^{-/-}$ mouse line was generated by cross-mating. All mice were maintained under cyclic light (12-hour light-dark) conditions. All animal maintenance and experiments were approved by the local Institutional Animal Care and Use Committee (OUHSC, Oklahoma City, OK) and conformed to the guidelines on the care and use of animals adopted by the Society for Neuroscience and the Association for Research in Vision and Ophthalmology (Rockville, MD).

### *16.2.2 Construction of AAV5-IRBP/GNAT2-hDIO3 Vectors*

The pCDM8 vector containing the *DIO3*-WT was provided by Dr. P. Reed Larsen at the Brigham and Women's Hospital (Boston, MA). The pCDM8-*hDIO3*-Cys was generated by replacing codons TGA for selenocysteine (Sec) residue at positon 144 with codons TGC for cysteine (Cys) by mutagenesis. The AAV5-IRBP/GNAT2-*hDIO3*-WT and AAV5-IRBP/GNAT2-*hDIO3*-Cys vectors were constructed and produced as we described previously (Yang et al. 2016).

### *16.2.3 Subretinal Injection of AAV5-IRBP/GNAT2-hDIO3 Vectors*

The subretinal injection was performed as described previously (Yang et al. 2016). One microliter of AAV5-IRBP/GNAT2-*hDIO3* ($1 \times 10^{10}$ vector genomes) vector in PBS was injected subretinally into one eye of each mouse, and the contralateral eye was injected with 1 μl of vehicle (PBS). Only eyes with no apparent surgical complications were retained for further evaluation.

### *16.2.4 qRT-PCR*

Total RNA preparation and reverse transcription were performed as described previously (Ma et al. 2013). The primers used to detect *hDIO3* and the mouse hypoxanthine guanine phosphoribosyl transferase 1 (*Hprt1*) were described previously (Yang et al. 2016).

### 16.2.5 TUNEL Assay

The TUNEL assays were performed to evaluate photoreceptor apoptotic death using the In Situ Cell Death Fluorescein Detection Kit (Roche Diagnostics, Indianapolis, IN), as described previously (Ma et al. 2015).

## 16.3 Results

### 16.3.1 Expression of DIO3 in Retinas of $Nrl^{-/-}$ Mice After Subretinal Delivery of AAV5-IRBP/GNAT2-hDIO3

We examined the expression of the transgenes in vivo using $Nrl^{-/-}$ mice, a cone-dominant mouse line. $Nrl^{-/-}$ mice at postnatal day 5 (P5) received subretinal injections of the two AAV5-IRBP/GNAT2-*hDIO3* viral vectors or vehicle and were analyzed for retinal expression of *hDIO3* by qRT-PCR at P30. The mRNA expression levels of *DIO3*-WT and *DIO3*-Cys were increased by about 70-fold and 3500-fold, respectively, compared to vehicle-treated controls (data not shown). These results showed that both the wild-type and the cysteine mutant transgenes induced robust expression of DIO3 in the mouse retina, and the expression of cysteine mutant transgene was much higher than the wild-type transgene.

### 16.3.2 Subretinal Delivery of AAV5-IRBP/GNAT2-hDIO3 Reduced Cone Death in $Rpe65^{-/-}/Nrl^{-/-}$ Mice

The effects of overexpression of DIO3 on the cone death/survival were then investigated in $Rpe65^{-/-}/Nrl^{-/-}$ mice. $Rpe65^{-/-}/Nrl^{-/-}$ mice exhibit a cone defect phenotype similar to that in $Rpe65^{-/-}$ mice and have been used to study LCA cone defects (Kunchithapautham et al. 2009). Animals were subretinally injected with virus or vehicle at P5 and were evaluated for cone death by TUNEL labeling at P30. The number of TUNEL-positive cells in $Rpe65^{-/-}/Nrl^{-/-}$ mice treated with AAV5-IRBP/GNAT2-*hDIO3* virus was reduced by 20–30%, compared to vehicle-treated controls (Fig. 16.2), suggesting that overexpression of DIO3 reduced cone death. Although the expression level of the Cys mutant was much higher than that of the wild-type, the wild-type and the Cys mutant induced similar functional effects, which is consistent with the previous structure-function relationship studies showing that replacing Sec with Cys increases the protein expression but reduces the activity (Kuiper et al. 2003).

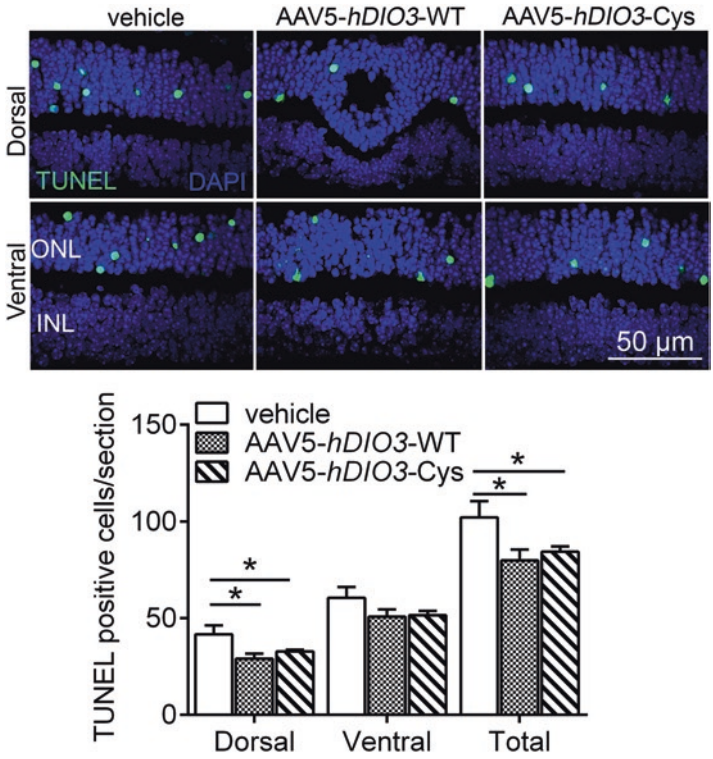


**Fig. 16.2** Subretinal injection of AAV5-IRBP/GNAT2-*hDIO3* reduced cone death in *Rpe65*$^{-/-}$/*Nrl*$^{-/-}$ mice. *Rpe65*$^{-/-}$/*Nrl*$^{-/-}$ mice at P5 received subretinal injections of AAV5-IRBP/Gnat2-*hDIO3*-WT and AAV5-IRBP/Gnat2-*hDIO3*-Cys ($1 \times 10^{10}$ vector genomes, 1.0 μl) or vehicle (PBS) and were analyzed for cone death by TUNEL labeling at P30. Shown are representative confocal images showing TUNEL-positive cells on retinal sections and the corresponding quantitative analysis. Data are represented as mean ± *SEM* of 4–5 mice in each group. Unpaired two-sample Student's *t*-test was used to determine significance between the viral-treated and vehicle-treated groups (* $p < 0.05$). ONL Outer nuclear layer, INL inner nuclear layer

## 16.4 Discussion

Based on our previous findings that antithyroid drug treatment and overexpression of DIO3 preserved cones in retinal degeneration model mice, including *Rpe65*$^{-/-}$ mice (Ma et al. 2014; Yang et al. 2016), this work investigated the effects of overexpression of DIO3 on cone death, using the cone-dominant *Rpe65*$^{-/-}$/*Nrl*$^{-/-}$ model. We found that subretinal injection of AAV5-IRBP/GNAT2-*hDIO3* induced robust expression of *hDIO3* and significantly decreased cone death in *Rpe65*$^{-/-}$/*Nrl*$^{-/-}$ mice. Our findings support the protective role of TH signaling suppression in degenerating cones and that the increased cone density observed in *Rpe65*$^{-/-}$ (and *Cpfl1*) after TH signaling suppression is attributed to reduced cell death.

The importance of DIO3 in cellular TH signaling regulation has been well documented in retinal and other neuronal tissues using *Dio3*$^{-/-}$ mice. These mice displayed auditory defects (Ng et al. 2009), premature cochlear differentiation (Ng et al. 2009), and loss of cones (Ng et al. 2010), which were rescued or partially rescued by deletion of the TH receptors. The importance of DIO3 in local TH signaling regulation and cell survival has also been supported by its induction/upregulation under a variety of pathological conditions, critical illnesses, and regeneration processes. The significance of such induction regulation has been attributed to decreased expenditure and reduced cell metabolism in the face of hypoxic and stress conditions (Dentice et al. 2014).

The mechanism(s) by which TH signaling suppression preserves cones remains to be determined. One of the potential mechanisms is overexpression of the TH components under pathological conditions. We have shown that the expression levels of the TH components, including DIO2 (Yang et al. 2016), the TH transporter MCT8 (Yang et al. 2016), and TH receptors (Ma et al. 2017), were significantly increased in the cone degeneration retinas. Upregulation of the TH components has also been reported in other pathological conditions (Curcio et al. 2001). This upregulation could be a result of the pathological conditions, which could in turn further contribute to the disease progression. Nevertheless, the findings that the expressions of TH components are upregulated in degenerating cones explain, at least in part, how suppressing TH signaling preserves cones.

In summary, we demonstrate that ocular inhibition of TH signaling by overexpression of DIO3 reduces cone death in LCA mouse model. Our findings suggest that targeting TH signaling locally in the retina represents a novel strategy for cone protection in LCA management. Indeed, the effective cone preservation is essential for a useful vision and maintenance of life quality.

**Acknowledgments** We thank Dr. T. Michael Redmond (NEI/NIH) for the *Rpe65*$^{-/-}$ mouse line and Dr. Anand Swaroop (NEI/NIH) for the *Nrl*$^{-/-}$ mouse line. We thank Dr. P. Reed Larsen (the Brigham and Women's Hospital) for human DIO3 cDNA. We thank the Imaging Core Facility of the Department of Cell Biology at OUHSC for technical assistance.

This work was supported by grants from the National Eye Institute (P30EY021725, P30EY021721, R01EY019490, and R21EY024583); the Research to Prevent Blindness for an unrestricted grant to the University of Florida, Department of Ophthalmology; the Foundation Fighting Blindness; and the Knights Templar Eye Foundation.

## References

Curcio C, Baqui MM, Salvatore D, Rihn BH, Mohr S, Harney JW, Larsen PR, Bianco AC (2001) The human type 2 iodothyronine deiodinase is a selenoprotein highly expressed in a mesothelioma cell line. J Biol Chem 276:30183–30187

Dentice M, Ambrosio R, Damiano V, Sibilio A, Luongo C, Guardiola O, Yennek S, Zordan P, Minchiotti G, Colao A, Marsili A, Brunelli S, Del Vecchio L, Larsen PR, Tajbakhsh S, Salvatore D (2014) Intracellular inactivation of thyroid hormone is a survival mechanism for muscle stem cell proliferation and lineage progression. Cell Metab 20:1038–1048

Farjo R, Skaggs JS, Nagel BA, Quiambao AB, Nash ZA, Fliesler SJ, Naash MI (2006) Retention of function without normal disc morphogenesis occurs in cone but not rod photoreceptors. J Cell Biol 173:59–68

Kuiper GG, Klootwijk W, Visser TJ (2003) Substitution of cysteine for selenocysteine in the catalytic center of type III iodothyronine deiodinase reduces catalytic efficiency and alters substrate preference. Endocrinology 144:2505–2513

Kunchithapautham K, Coughlin B, Crouch RK, Rohrer B (2009) Cone outer segment morphology and cone function in the Rpe65−/− Nrl−/− mouse retina are amenable to retinoid replacement. Invest Ophthalmol Vis Sci 50:4858–4864

Ma H, Thapa A, Morris LM, Michalakis S, Biel M, Frank MB, Bebak M, Ding XQ (2013) Loss of cone cyclic nucleotide-gated channel leads to alterations in light response modulating system and cellular stress response pathways: a gene expression profiling study. Hum Mol Genet 22:3906–3919

Ma H, Thapa A, Morris L, Redmond TM, Baehr W, Ding XQ (2014) Suppressing thyroid hormone signaling preserves cone photoreceptors in mouse models of retinal degeneration. Proc Natl Acad Sci U S A 111:3602–3607

Ma H, Butler MR, Thapa A, Belcher J, Yang F, Baehr W, Biel M, Michalakis S, Ding XQ (2015) cGMP/protein kinase G signaling suppresses inositol 1,4,5-trisphosphate receptor phosphorylation and promotes endoplasmic reticulum stress in photoreceptors of cyclic nucleotide-gated channel-deficient mice. J Biol Chem 290:20880–20892

Ma H, Yang F, Butler MR, Belcher J, Redmond TM, Placzek AT, Scanlan TS, Ding XQ (2017) Inhibition of thyroid hormone receptor locally in the retina is a therapeutic strategy for retinal degeneration. FASEB J 31(8):3425–3438

Mears AJ, Kondo M, Swain PK, Takada Y, Bush RA, Saunders TL, Sieving PA, Swaroop A (2001) Nrl is required for rod photoreceptor development. Nat Genet 29:447–452

Ng L, Hurley JB, Dierks B, Srinivas M, Salto C, Vennstrom B, Reh TA, Forrest D (2001) A thyroid hormone receptor that is required for the development of green cone photoreceptors. Nat Genet 27:94–98

Ng L, Hernandez A, He W, Ren T, Srinivas M, Ma M, Galton VA, St Germain DL, Forrest D (2009) A protective role for type 3 deiodinase, a thyroid hormone-inactivating enzyme, in cochlear development and auditory function. Endocrinology 150:1952–1960

Ng L, Lyubarsky A, Nikonov SS, Ma M, Srinivas M, Kefas B, St Germain DL, Hernandez A, Pugh EN Jr, Forrest D (2010) Type 3 deiodinase, a thyroid-hormone-inactivating enzyme, controls survival and maturation of cone photoreceptors. J Neurosci 30:3347–3357

Redmond TM, Yu S, Lee E, Bok D, Hamasaki D, Chen N, Goletz P, Ma JX, Crouch RK, Pfeifer K (1998) Rpe65 is necessary for production of 11-cis-vitamin A in the retinal visual cycle. Nat Genet 20:344–351

Yang F, Ma H, Butler M, Redmond TM, Boye SL, Hauswirth WW, Ding XQ (2016) Targeting iodothyronine deiodinases locally in the retina is a therapeutic strategy for retinal degeneration. FASEB J 30(12):4313–4325

# Part III
# In-Vivo Diagnostics for Structure and Function

# Chapter 17
# In Vivo Functional Imaging of Retinal Neurons Using Red and Green Fluorescent Calcium Indicators

**Soon K. Cheong, Wenjun Xiong, Jennifer M. Strazzeri, Constance L. Cepko, David R. Williams, and William H. Merigan**

**Abstract** Adaptive optics retinal imaging of fluorescent calcium indicators is a minimally invasive method used to study retinal physiology over extended periods of time. It has potential for discovering novel retinal circuits, tracking retinal function in animal models of retinal disease, and assessing vision restoration therapy. We previously demonstrated functional adaptive optics imaging of retinal neurons in the living eye using green fluorescent calcium indicators; however, the use of green fluorescent indicators presents challenges that stem from the fact that they are excited by short-wavelength light. Using red fluorescent calcium indicators such as jRGECO1a, which is excited with longer-wavelength light (~560 nm), makes imaging approximately five times safer than using short-wavelength light (~500 nm) used to excite green fluorescent calcium indicators such as GCaMP6s. Red fluorescent indicators also provide alternative wavelength imaging regimes to overcome cross talk with the sensitivities of intrinsic photoreceptors and blue light-activated channelrhodopsins. Here we evaluate jRGECO1a for in vivo functional adaptive

S. K. Cheong · J. M. Strazzeri
Center for Visual Science, University of Rochester, Rochester, NY, USA

Flaum Eye Institute, University of Rochester, Rochester, NY, USA
e-mail: kcheong@mail.cvs.rochester.edu

W. Xiong
Department of Biomedical Sciences, City University of Hong Kong, Kowloon, Hong Kong SAR, China

C. L. Cepko
Departments of Genetics and Ophthalmology, Howard Hughes Medical Institute, Harvard Medical School, Boston, MA, USA

D. R. Williams
Institute of Optics, University of Rochester, Rochester, NY, USA

Center for Visual Science, University of Rochester, Rochester, NY, USA

W. H. Merigan (✉)
Center for Visual Science, University of Rochester, Rochester, NY, USA
e-mail: billm@cvs.rochester.edu



J. D. Ash et al. (eds.), *Retinal Degenerative Diseases*, Advances in Experimental Medicine and Biology 891, https://doi.org/10.1007/978-3-319-75402-4_17

optics imaging of retinal neurons using single-photon excitation in mice. We find that jRGECO1a provides similar fidelity as the established green indicator GCaMP6s.

**Keywords** Adaptive optics · jRGECO1a · Calcium indicator · Retinal imaging · Ganglion cells

## 17.1 Introduction

We previously demonstrated functional imaging of retinal neurons in the living eye by combining adaptive optics (AO) and green fluorescent genetically encoded calcium indicators (Yin et al. 2013, 2014). In vivo functional imaging enables long-term study of the same retinal neurons over weeks to months making it ideal for the study of the time course of retinal function at a cellular scale during retinal disease and after vision restoration therapy. Because in vivo retinal imaging uses light to probe retinal function, the challenges of using green fluorescent indicators such as those of the GCaMP family are particularly relevant and stem from the fact that they are excited by short-wavelength light around 500 nm. Short-wavelength light is more phototoxic than long-wavelength light (Ham et al. 1976); the maximum permissible exposure of the longer 561 nm wavelength light used to excite the red fluorescent genetically encoded calcium indicator jRGECO1a (Dana et al. 2016) is approximately five times greater compared to 488 nm light used to excite GCaMP6s (Zhang et al. 2016). The excitation spectra of GCaMP indicators overlap with the spectral sensitivities of mouse medium-wavelength-sensitive (M)opsin, rhodopsin, and melanopsin (Fig. 17.1a, Lyubarsky et al. 1999; Walker et al. 2008; Wang et al. 2011). The excitation spectra of GCaMP indicators also overlap with blue light-sensitive ion channels such as channelrhodopsin-2 (Nagel et al. 2003) making it challenging to use with optogenetics. To advance the utility of functional AO retinal imaging, we imaged jRGECO1a with single-photon excitation in mice. We found that jRGECO1a provides similar fidelity as GCaMP6s (Chen et al. 2013), which provides an alternative wavelength regime for functional AO retinal imaging along with improved light safety.

## 17.2 Materials and Methods

All animal procedures were conducted according to the ARVO Statement for the Use of Animals in Ophthalmic and Visual Research and the Guidelines of the Office of Laboratory Animal Care at the University of Rochester. All protocols were approved by the University Committee on Animal Resources at the University of Rochester.

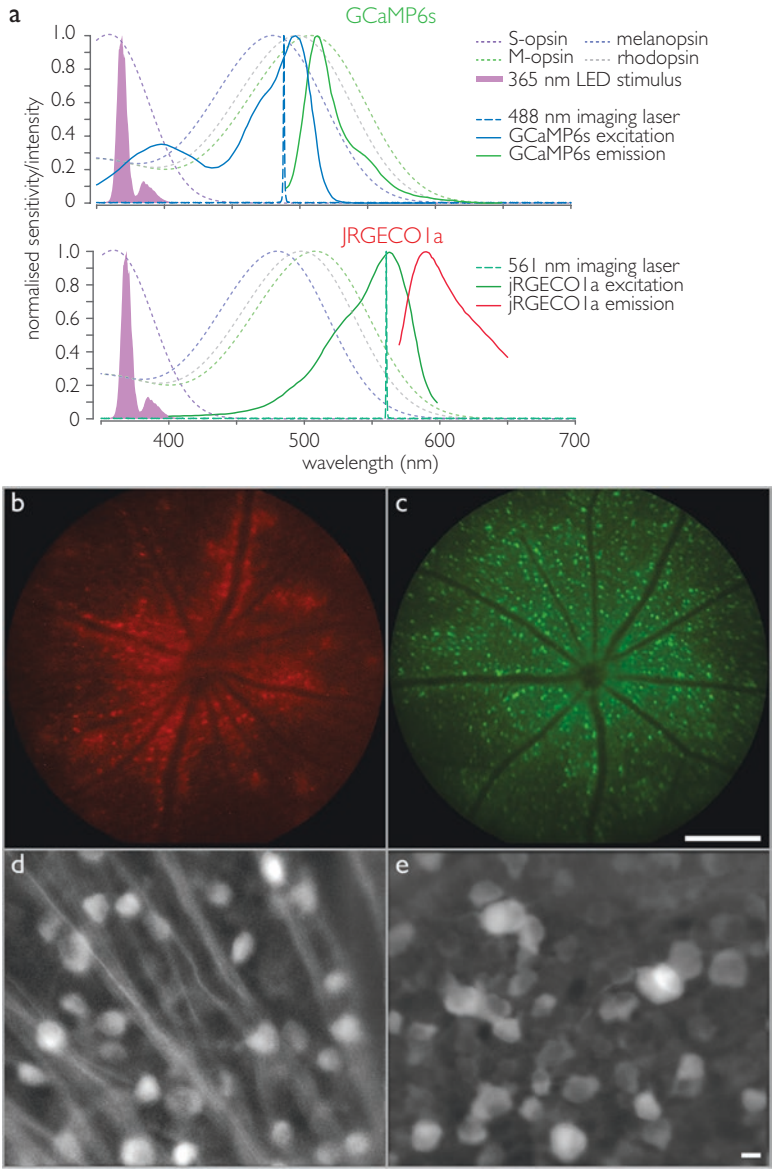


**Fig. 17.1** (**a**) Action spectra of mouse opsins, 365 nm LED stimulus, excitation and emission spectra of GCaMP6s and jRGECO1a, and fluorescence excitation imaging lasers. (**b**, **c**) Fluorescent fundus images of jRGECO1a (**b**) and GCaMP6s (**c**) expression. Scale bar: 500 μm. (**d**, **e**) In vivo adaptive optics images of jRGECO1a (**d**) and GCaMP6s (**e**) fluorescent neurons. Scale bar: 10 μm

### 17.2.1 Animal Preparation

Adult C57BL/6 J mice (The Jackson Laboratory, USA) were used in this study. For short (<30 min) procedures including intravitreal injections and fundus imaging, mice were anaesthetised using ketamine (0.1 mg $g^{-1}$, JHP Pharmaceuticals, USA) and xylazine (0.01 mg $g^{-1}$, Akorn Inc., USA). For AO imaging (~ 2 h), mice were anaesthetised using a cocktail containing fentanyl (0.05 μg $g^{-1}$, West-Ward Pharmaceuticals Corp., USA), dexmedetomidine (Dexdomitor, 0.5 μg $g^{-1}$, Orion Corp., Finland), and midazolam (5 μg $g^{-1}$, West-Ward Pharmaceuticals Corp., USA). At the conclusion of the AO imaging session, mice were given a reversal cocktail containing naloxone (1.2 μg $g^{-1}$, Hospira Inc., USA), atipamezole (Antisedan, 2.5 μg $g^{-1}$, Orion Corp., Finland), and flumazenil (0.5 μg $g^{-1}$, Hikma Pharmaceuticals, UK). Drugs were administered intraperitoneally. Adequate anaesthesia was evaluated by checking the toe-pinch and corneal reflexes. During AO imaging, additional heating was provided to maintain the internal body temperature at 37 °C, and animals were ventilated on 100% oxygen.

### 17.2.2 AAV-Mediated Gene Transfection of Mouse Retinal Neurons

Adeno-associated viral (AAV) vectors were used to transfect mouse retinal neurons with genes of interest. Constructs used were AAV2.CAG.jRGECO1a.WPRE.SV40, titre $5 \times 10^{12}$ GC $mL^{-1}$, produced in the laboratory of Dr. Cepko, Harvard Medical School; AAV9.Syn.GCaMP6s.WPRE.SV40, titre $4.04 \times 10^{13}$ GC $mL^{-1}$; and AAV2.Syn.GCaMP6s.WPRE.SV40, titre $2.38 \times 10^{13}$ GC $mL^{-1}$ purchased from the University of Pennsylvania Vector Core. Intravitreal injections of 2 μl per eye were made in 3-week-old animals. One male and one female mouse received AAV2.jRGECO1a, two males received AAV9.GCaMP6s, and four females received AAV2.GCaMP6s. A fundus camera (Micron III, Phoenix Research Laboratories, USA) with custom filters (GCaMP6s, excitation FF01–498 SP [Semrock Inc., USA], emission ET525/50 [Chroma Technology Corporation, USA]; jRGECO1a, excitation FF02–525/40 [Semrock Inc., USA], emission band-pass 590/47) was used to assess and map gene expression.

### 17.2.3 In Vivo Functional AO Calcium Imaging

In vivo retinal imaging was done with a custom-built mouse adaptive optics scanning light ophthalmoscope (see Geng et al. 2012 for system details). Reflectance imaging of blood vessels was performed using an infrared 790 nm laser diode (S790-G-I-15, Superlum Diodes Ltd., Ireland), and simultaneous fluorescence

imaging of either GCaMP6s or jRGECO1a was performed using a multichannel laser diode (iChrome MLE-L, Toptica Photonics Inc., USA); GCaMP6s (excitation, 488 nm; emission band-pass filter, FF01–520/35) (Semrock Inc., USA); and jRGECO1a (excitation, 561 nm; emission band-pass filter, FF01–630/92) (Semrock Inc., USA). Wavefront sensing was performed using a 905 nm laser diode (QFLD-905-10S, QPhotonics LLC, USA). All imaging lights were scanned over a 5 × 6.7° field on the retina. Light intensity at the pupil was 185 μW for 796 nm, 100 μW for both 488 and 561 nm, and 7 μW for 904 nm. A 50 μm confocal pinhole was used for infrared reflectance and 75 μm pinhole for fluorescence.

Mice were positioned in a custom-built holder with bite bar, and contact lenses were placed on the eyes to prevent the corneas from drying. A 365 nm LED (M365 L2-UV; Thorlabs, USA) was presented in Maxwellian view over an 8° diameter patch of the retina to drive short-wavelength-sensitive (S-)opsin. Stimuli were temporally modulated, uniform field, square waves. Figure 17.1a shows the measured spectra of the stimulus and imaging lights, spectral sensitivities of mouse opsins, and action spectra of GCaMP6s and jRGECO1a.

Eye motion was computed using the reflectance images of retinal vasculature (Dubra and Harvey 2010), and motion correction was applied to both reflectance and fluorescence data. Cell segmentation was performed manually. Response time course was obtained by calculating the mean pixel intensity of each region of interest as a function of time. A fast Fourier transform algorithm was used to compute the signal amplitude and phase at the stimulus frequency (F1) and the DC component (F0). Normalised response was quantified as the ratio F1/F0. All data analysis used MATLAB (MathWorks, USA).

## 17.3 Results

Widespread expression of jRGECO1a and GCaMP6s was achieved in C57BL/6 J mice retina. Figure 17.1b, c shows fluorescent fundus images of jRGECO1a and GCaMP6s expression, respectively. Both AAV9.Syn.GCaMP6s and AAV2.Syn.GCaMP6s resulted in expression of GCaMP6s; however, AAV2.Syn.GCaMP6s produced more consistent expression across eyes injected as well as more widespread retinal coverage in each eye (data not shown). Figure 17.1d, e shows fluorescent neurons expressing jRGECO1a and GCaMP6s imaged in vivo with AO. Note the visibility of axon bundles in Fig. 17.1d indicating expression in ganglion cells. Axon bundles were also observed in retina expressing GCaMP6s but are not visible in Fig. 17.1e.

Robust measurements of neuronal responses to a flashing 365 nm LED stimulus were made using jRGECO1a. Figure 17.2a–f shows response time courses for six example neurons; ON cells are shown in a, c, and e and OFF cells in b, d, and f. Response amplitude was quantified (see methods), and histograms of responses to a 365 nm stimulus and “no stimulus” are shown in Fig. 17.2g, h, respectively. No response amplitudes above 0.04 were observed in the “no stimulus” condition so we

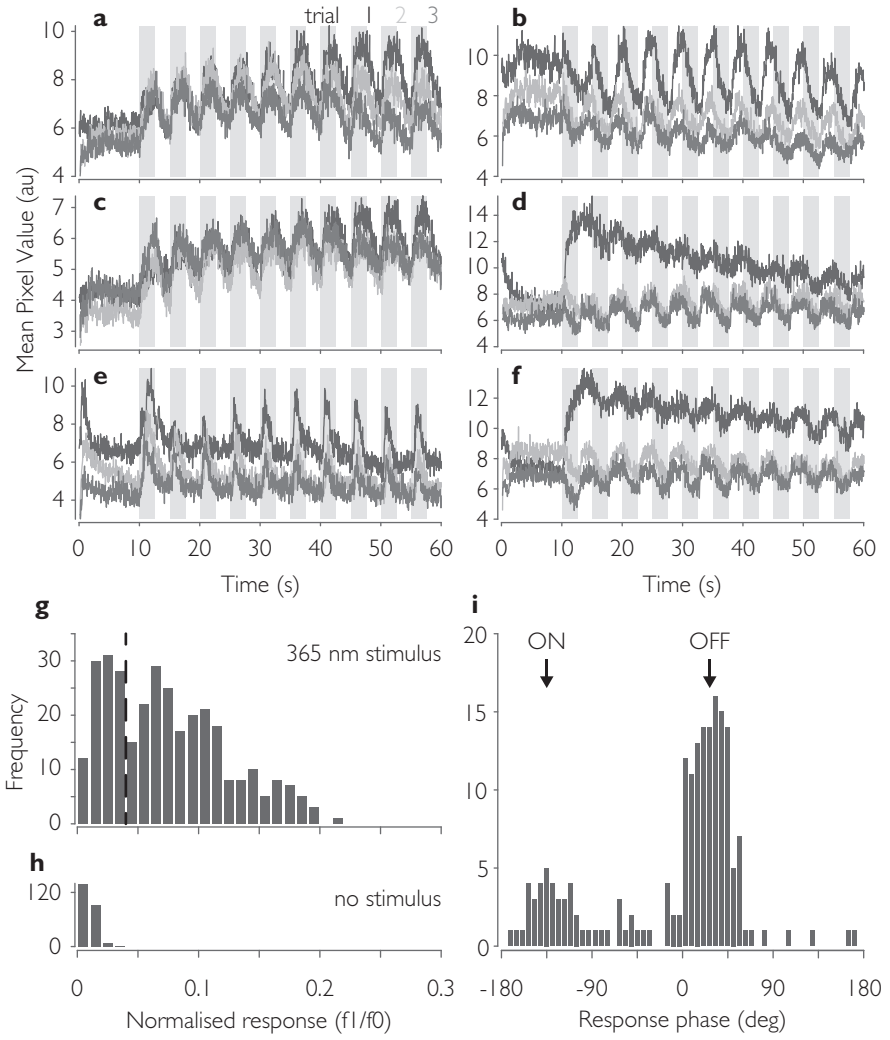


**Fig. 17.2** Responses measured with jREGECO1a. (**a–f**) Response time courses of cells to a 365 nm LED stimulus. Shaded bars indicate stimulus presentation. Three trials for each cell are shown. ON responses are shown in **a**, **c**, and **e** and OFF responses in **b**, **d**, and **f**. (**g**) Frequency histogram of cell responses to 365 nm stimulus ($n = 323$). Dashed vertical line indicates a response threshold of 0.04. (**h**) Frequency histogram of cell responses to "no stimulus" ($n = 238$). (**i**) Frequency histogram of response phase for cells with response greater than 0.04 in the 365 nm stimulus condition ($n = 185$). ON and OFF labels indicate cells with respective responses

considered cells with response amplitudes above 0.04 in the 365 nm stimulus condition as "responsive" and further analysed their response phase. Figure 17.2i shows a frequency response phase histogram of "responsive" cells. Note that the histogram appears bimodal; the two separate distributions correspond to ON and OFF cells.

Robust measurements of neuronal responses were also made using GCaMP6s. No differences in function between AAV9.GCaMP6s and AAV2.GCaMP6s were observed so data were pooled. Figure 17.3 shows responses to 365 nm LED stimuli measured with GCaMP6s. Data are presented as in Fig. 17.2; example response time courses of ON and OFF cells are shown in Fig. 17.2a–f, histogram of response amplitudes to 365 nm LED stimulus in Fig. 17.2g, histogram of response amplitudes to "no stimulus" in Fig. 17.2h, and response phase histogram for all cells with response amplitude greater than 0.04 in Fig. 17.2i.

## 17.4 Discussion

The purpose of this study was to explore the use of a red-shifted genetically encoded calcium indicator for in vivo functional AO imaging of the retina. We show that AO ophthalmoscopy of both red-shifted and green fluorescent calcium indicators, jRGECO1a and GCaMP6s, provide robust measurements of neuronal activity in the retina. Our virus constructs resulted in widespread and bright expression of jRGECO1a and GCaMP6s; however, the mean intensity and signal-to-noise ratio of jRGECO1a were lower than GCaMP6s (Figs. 17.2a–f and 17.3a–f). Response amplitudes measured with GCaMP6s also tended to be larger than with jRGECO1a (Figs. 17.2g and 17.3g); however, these differences do not permit a precise comparison of the two because many factors affect measured intensity. For example, measured resting fluorescence and signal-to-noise ratio are dependent on the ocular optics as well as level of expression, which often differs from eye to eye despite consistent injection parameters. In the original report on jRGECO1a, the authors show that jRGECO1a exhibits similar performance to the GCaMP6 indicators; however, jRGECO1a responses in vivo were still smaller than GCaMP6s likely because of signal saturation at high firing rates (Dana et al. 2016).

One of the benefits of using red fluorescent calcium indicators for functional AO retinal imaging is improved light safety from imaging with longer-wavelength light. It is well established that high-intensity blue light induces photochemical damage in the retina and retinal pigment epithelium (Ham et al. 1976; Wu et al. 2006; Hunter et al. 2012). The longer-wavelength 561 nm light used in this study to excite jRGECO1a provides approximately a fivefold improvement in light safety compared to the 488 nm light used to excite GCaMP6s (Zhang et al. 2016). The greater safety of red fluorescent calcium indicators is particularly important for in vivo imaging of the retina because a major benefit of this technique is the ability to perform repeated imaging of the retina over weeks to months, which carries the risk of phototoxicity.

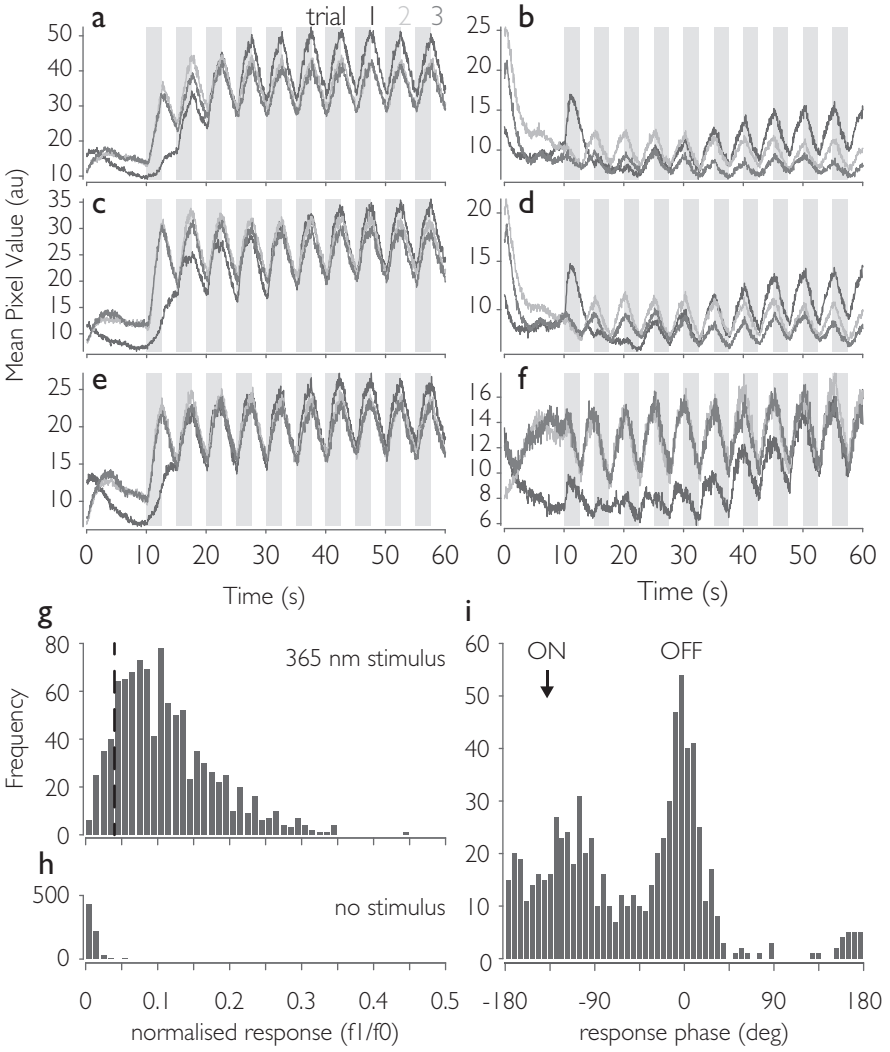


**Fig. 17.3** Responses measured with GCaMP6s. (**a–f**) Response time courses of cells to a 365 nm LED stimulus. Shaded bars indicate stimulus presentation. Three trials for each cell are shown. ON responses are shown in **a**, **c**, and **e** and OFF responses in **b**, **d**, and **f**. (**g**) Frequency histogram of cell responses to 365 nm stimulus ($n = 987$). Dashed vertical line indicates a response threshold of 0.04. (**h**) Frequency histogram of cell responses to "no stimulus" ($n = 681$). (**i**) Frequency histogram of response phase for cells with response greater than 0.04 in the 365 nm stimulus condition ($n = 752$). ON and OFF labels indicate cells with respective responses

Recently discovered red-shifted channelrhodopsins (Lin et al. 2013; Klapoetke et al. 2014; Tomita et al. 2014) may be used with green fluorescent calcium indicators to enable all optical recording and activation of neuronal responses. However, the most sensitive channelrhodopsin found to date is activated by blue light (Klapoetke et al. 2014). Thus, a red fluorescent calcium indicator would be necessary in a combined preparation.

Red calcium indicators derived from mRuby such as jRCaMP1a and jRCaMP1b may be more ideal for combined use with optogenetics because they do not exhibit photoswitching in response to blue light, unlike jRGECO1a (Dana et al. 2014).

A remaining serious challenge for optical recording of neuronal responses in the eye is the activation and bleaching of photoreceptors with the intense light needed to excite the fluorescent calcium indicator. Shifting the excitation spectra to longer wavelengths reduces photoreceptor activation with single-photon excitation. Future implementation of two-photon imaging of red fluorescent calcium indicator will greatly reduce photoreceptor activation and bleaching.

**Acknowledgements** We thank Sophia Zhao for making the jRGECO1a virus, Jie Zhang for designing and constructing the visual stimulus apparatus, and Keith Parkins for programing data acquisition software. This work was supported by grants from the National Eye Institute of the National Institutes of Health, EY001319 and EY021166; an Unrestricted Grant to the University of Rochester Department of Ophthalmology from Research to Prevent Blindness, New York, New York; as well as a Beckman-Argyros Award from the Arnold and Mabel Beckman Foundation. The content is solely the responsibility of the authors and does not necessarily represent the official views of the National Institutes of Health. The Genetically-Encoded Neuronal Indicator and Effector (GENIE) Project and the Janelia Farm Research Campus of the Howard Hughes Medical Institute have generously allowed these GECI materials to be distributed with the understanding that requesting investigators need to acknowledge the GENIE Program and the Janelia Farm Research Campus in any publication in which the material was used, specifically Vivek Jayaraman, PhD; Rex A. Kerr, PhD; Douglas S. Kim, PhD; Loren L. Looger, PhD; and Karel Svoboda, PhD from the GENIE Project, Janelia Farm Research Campus, Howard Hughes Medical Institute.

## References

Chen TW, Wardill TJ, Sun Y et al (2013) Ultrasensitive fluorescent proteins for imaging neuronal activity. Nature 499:295–300

Dana H, Sun Y, Hasseman JP et al (2014) Improved red protein indicators for in vivo calcium imaging. In: Proceedings of the Society for Neuroscience, Washington DC

Dana H, Mohar B, Sun Y et al (2016) Sensitive red protein calcium indicators for imaging neural activity. eLife 5:e12727

Dubra A, Harvey Z (2010) Registration of 2D images from fast scanning ophthalmic instruments. In: Biomedical image registration lecture notes in computer science. Springer, Berlin

Geng Y, Dubra A, Yin L et al (2012) Adaptive optics retinal imaging in the living mouse eye. Biomed Opt Express 3:715–734

Ham WT Jr, Mueller HA, Sliney DH (1976) Retinal sensitivity to damage from short wavelength light. Nature 260:153–155

Hunter JJ, Morgan JI, Merigan WH et al (2012) The susceptibility of the retina to photochemical damage from visible light. Prog Retin Eye Res 31:28–42

Klapoetke NC, Murata Y, Kim SS et al (2014) Independent optical excitation of distinct neural populations. Nat Methods 11:338–346

Lin JY, Knutsen PM, Muller A et al (2013) ReaChR: a red-shifted variant of channelrhodopsin enables deep transcranial optogenetic excitation. Nat Neurosci 16:1499–1508

Lyubarsky AL, Falsini B, Pennesi ME et al (1999) UV- and midwave-sensitive cone-driven retinal responses of the mouse: a possible phenotype for coexpression of cone photopigments. J Neurosci 19:442–455

Nagel G, Szellas T, Huhn W et al (2003) Channelrhodopsin-2, a directly light-gated cation-selective membrane channel. Proc Natl Acad Sci U S A 100:13940–13945

Tomita H, Sugano E, Murayama N et al (2014) Restoration of the majority of the visual spectrum by using modified Volvox channelrhodopsin-1. Mol Ther J Am Soc Gene Ther 22:1434–1440

Walker MT, Brown RL, Cronin TW et al (2008) Photochemistry of retinal chromophore in mouse melanopsin. Proc Natl Acad Sci U S A 105:8861–8865

Wang YV, Weick M, Demb JB (2011) Spectral and temporal sensitivity of cone-mediated responses in mouse retinal ganglion cells. J Neurosci 31:7670–7681

Wu J, Seregard S, Algvere PV (2006) Photochemical damage of the retina. Surv Ophthalmol 51:461–481

Yin L, Geng Y, Osakada F et al (2013) Imaging light responses of retinal ganglion cells in the living mouse eye. J Neurophysiol 109:2415–2421

Yin L, Masella B, Dalkara D et al (2014) Imaging light responses of foveal ganglion cells in the living macaque eye. J Neurosci 34:6596–6605

Zhang J, Sabarinathan R, Bubel T et al (2016) Spectral dependence of light exposure on retinal pigment epithelium (RPE) disruption in living primate retina. Invest Ophthalmol Vis Sci 57:2220–2220

# Chapter 18
# Optimizing ERG Measures of Scotopic and Photopic Critical Flicker Frequency


**Marci L. DeRamus and Timothy W. Kraft**

**Abstract** A visual response to flickering light requires complex retinal computation, and thus ERG measures are an excellent test of retinal circuit fidelity. Critical flicker frequency (CFF) is the frequency at which the retinal response is no longer modulated. Traditionally, CFF is obtained with a series of steady flicker stimuli with increasing frequencies. However, this method is slow and susceptible to experimental drift and/or adaptational effects. The current study compares the steady flicker method to CFF measurements obtained using a frequency sweep protocol. We introduce a light source programmed to produce a linear sweep of frequencies in a single trial. Using the traditional steady flicker method and a criterion response of 3 μV, we obtained a scotopic CFF of 18.4 ± 0.66 Hz and a photopic CFF of 44.4 ± 1.67 Hz. Our sweep flicker method, used on the same animals, produces a waveform best analyzed by Fourier transform; wherein a 6.18 log $\mu V^2$ threshold was found to yield CFF values equal to those of the steady flicker method. Thus, the two flicker ERG techniques give comparable results, under both dark- and light-adapted conditions, and the flicker sweep method is faster to administer and analyze and may be less susceptible to blinking, breathing, and eye movement artifacts.

**Keywords** Electroretinography · Critical flicker frequency · Sweep flicker · Photoreceptors · Murine retina

## 18.1 Introduction

Electroretinogram (ERG) is an in vivo method used to assess electrophysiological health of the retina by measuring the massed electrical responses of retinal cells to light. Changing the intensity, length, and characteristics of the light stimuli used can

M. L. DeRamus · T. W. Kraft (✉)
Department of Optometry and Vision Science, University of Alabama at Birmingham, Birmingham, AL, USA
e-mail: twkraft@uab.edu



J. D. Ash et al. (eds.), *Retinal Degenerative Diseases*, Advances in Experimental Medicine and Biology 891, https://doi.org/10.1007/978-3-319-75402-4_18

parse out the roles of different retinal cell types (Fishman et al. 2001; Frishman and Wang 2011; Tanimoto et al. 2009; Pardue and Peachey 2014). Assessment of the different waves produced provides insights about the health of the different retinal cell types. Sinusoidal flickering stimuli will produce a modulated ERG response, following the stimulus, with decreasing ERG amplitude to higher frequencies of flicker (Nowak and Green 1983; Rubin and Kraft 2007; Bowles and Kraft 2012). Flicker ERG can be used to isolate rod and cone function independently of each other using the proper light intensities and frequencies (Rubin and Kraft 2007; Zhang et al. 2012). Critical flicker frequency (CFF), the frequency at which the response to a flickering light appears steady, can be obtained by measuring flicker ERG responses to many frequencies of sinusoidal flicker. However, this method is tedious and time consuming; it allows possible drift or adaptation over time as well as possible interruptions in experimentation, confounding the results. In order to provide a more efficient and stable measurement of CFF, the current study used a high-luminance LED light source programmed to produce a linear sweep of flicker frequency in a single trial. Steps of steady equiluminant light before and after the frequency sweep ensure a stable baseline from which to measure response to flicker.

## 18.2 Materials and Methods

### *18.2.1 Experiment with Animals*

All mice procedures were approved by the Institutional Animal Care and Use Committee at the University of Alabama at Birmingham. Wild-type (WT) animals on a C57BL/6 J background were maintained in animal care facilities on a standard 12/12-h light/dark cycle. Mice of either sex, between 1 and 5 months of age, were used for all experiments.

### *18.2.2 Scotopic and Photopic Critical Flicker Frequency*

The LED light source was a high efficient luminance green LED (LZ1-00G102, LED Engin, San Jose, CA) with a center wavelength of 525 nm and a bandwidth of 36 nm. For the flicker stimulus, the photopic mean power was 7.42 W/s delivered uniformly across a 2 mm diameter contact lens. The maximum and minimum intensity values measured were 14.56 and 0.468 W/s, respectively, resulting in a Michaelis contrast of 94%. The scotopic intensity was produced by attenuating with calibrated Wratten neutral density filters, reducing intensities by 3.49 log units to a mean level of 2.40 mW/s. Using pulse width modulation, the LED was programmed to produce a linear sweep of flicker frequency in a single trial, with the starting frequency, ending frequency, and duration set by the operator. Percent contrast obtained with this

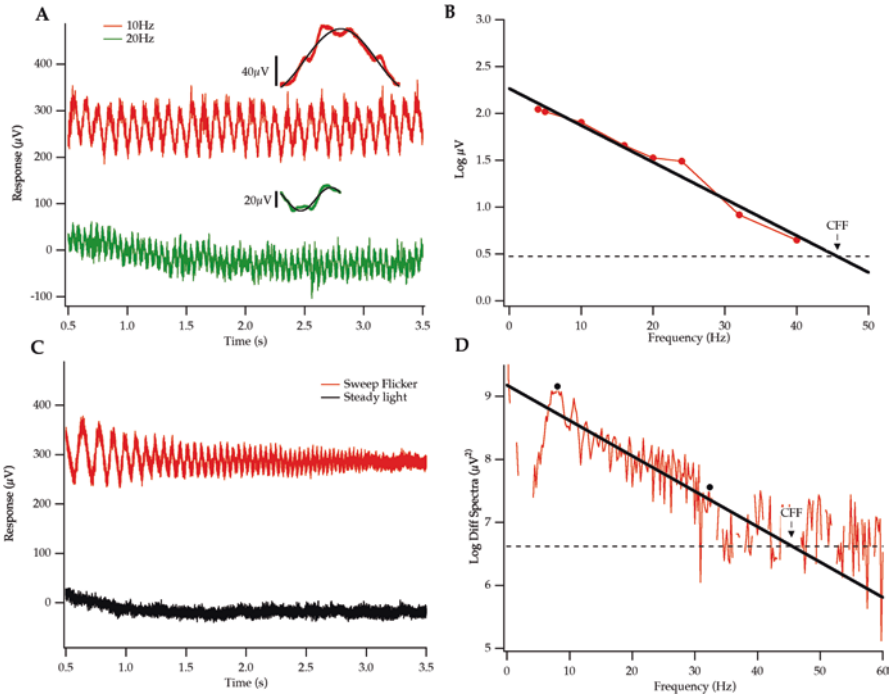


**Fig. 18.1** Scotopic and photopic CFF determined by ERG: two methods. (**a**) The central 3 s of the responses to 5 s steps of flickering stimuli, 10 Hz (red) and 20 Hz (green), are shown (average waveform inset). The on (b-wave) and off (d-wave) transient responses are at $t = 0$ s and $t = 5$ s, respectively. (**b**) A linear regression fitted to a plot of the log of the response amplitudes (from panel (**a**)) vs frequency defines CFF at 3 μV. (**c**) The central 3 s of the ERG responses to a linear frequency sweep stimulus (red) or equiluminant step of steady light (black). (**d**) The difference spectra between the Fourier transforms of the baseline and flickering responses. The CFF determined in panel (**b**) was used to identify an FFT criterion response. The average criterion CFF log response for dark- and light-adapted conditions combined was 6.18 ± 0.11 log $\mu V^2$

LED light source was calculated as 94%, but this depth of modulation was also programmable. The aim of this new sweep flicker approach is to provide a more efficient measurement of critical flicker frequency (CFF). Verification of this modified flicker protocol was completed by comparison with standard flicker protocol. Steady flickering stimuli at 4, 5, 10, 16, and 20 Hz were used for scotopic testing (Fig. 18.1a). For photopic testing, these same frequencies with the addition of 24, 32, and 40 Hz were tested. Analysis was restricted to the central portion of the response to avoid *on* and *off* transients. A computer algorithm (Igor Pro; WaveMetrics Inc., Lake Oswego, OR) was used to compute the average response for a single cycle within the 5-s trace created at each frequency. A best-fit sine wave was used to quantify the response amplitude for the averaged cycle. The log of the response amplitudes vs frequency was plotted (Fig. 18.1b), and a linear fit was used to determine the CFF response at 3 μV (0.477log μV; Pinilla et al. 2005; Rubin and Kraft

2007). The second method of CFF determination was with flicker sweep ERG. A linear frequency sweep of the stimulus from 0.1 to 35 Hz (scotopic) or 0.1–55 Hz (photopic) was presented over 5 s (Fig. 18.1c). ERG responses evoked by steady light steps of equal luminance were measured before and after the flickering light as a baseline and to protect from drift or adaptation. The difference spectra were obtained from the Fourier transform of the flickering and steady light responses (Fig. 18.1d). A linear best fit was plotted to determine the log $\mu V^2$ response at the CFF value calculated from the steady flickering stimuli. This verification procedure was repeated for 11 wild-type animals, under both dark-adapted and light-adapted conditions.

## 18.3 Results

The average CFF calculated using steady flickering stimuli and a 0.477 log μV threshold criterion was 18.4 ± 0.66 Hz under dark-adapted conditions and 44.4 ± 1.67 Hz under light-adapted conditions. The CFF determined for each animal was then applied to the sweep flickering responses to determine a threshold criterion for the sweep flicker method. The average CFF threshold criterion determined was 6.33 ± 0.2 log $\mu V^2$ under dark-adapted conditions and 6.04 ± 0.16 log $\mu V^2$ under light-adapted conditions ($n$ = 11). A Student's t-test was performed to determine whether the dark- and light-adapted log $\mu V^2$ thresholds were significantly different from one another. The t-test showed no statistically significant difference between dark- and light-adapted log $\mu V^2$ cutoffs ($p$ = 0.18). The average dark- and light-adapted log $\mu V^2$ threshold was 6.18 ± 0.11 log $\mu V^2$. Therefore, further experiments using the sweep flicker technique will use the 6.18 log $\mu V^2$ threshold to determine CFF.

A correlation analysis of scotopic b-wave amplitude vs CFF showed no correlation ($r$ = 0.23, $p$ = 0.25) (Fig. 18.2, black triangles). The photopic CFF was more distributed, but again there was no correlation of CFF with b-wave amplitude ($r$ = −0.11, $p$ = 0.62) (Fig. 18.2, red circles). Thus, the CFF, as calculated here, is independent of b-wave amplitude and therefore resistant to minor differences in the quality of the recording setup.

## 18.4 Discussion

Flicker ERG and determination of CFF are powerful tools to examine underlying health of the retinal cell types; it is particularly useful as a method to separate rod and cone function. However, standard flicker protocols using a steady flickering light are tedious and lengthy, introducing possible artifacts due to drift of electrical resistance in circuit or light adaptation. By interleaving trials with and without modulation of the light, the concern over experimental drift is eliminated and capture of

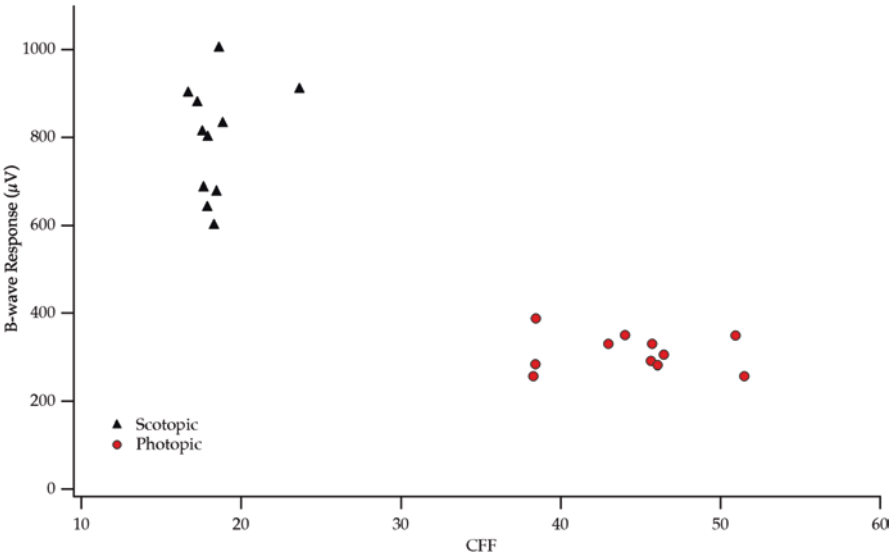


**Fig. 18.2** Scotopic (black triangles) and photopic (red circles) b-wave maximum amplitudes vs CFF showed no correlation, indicating that CFF is not dependent on b-wave amplitude

the entire frequency response function in a single trial is feasible; repeated tests are only used to increase the signal to noise ratio. The results of the current study show that standard steadily flickering stimuli and the modified linear sweep flickering stimuli are comparable, regardless of dark- or light-adapted conditions. The flicker sweep technique is likely to be less sensitive to eye movement artifacts as these produce such high-frequency electrical signals they would not interfere with the signals in the range typically used for the CFF estimates (0.1–55 Hz). In addition to providing a more efficient method of CFF determination, use of this new flicker technique, because of its speed, allows easier concurrent examination of other ERG responses, such as c-wave and photopic negative responses in the same testing period.

**Acknowledgments** We thank Alex Zotov for computational programming, Eric Wellington for fabrication of light bench components, and Wes Moore for fabrication of electrical components. This study was supported by an NIH grant EY023603 (TWK) and a core grant P30EY003039.

## References

Bowles KE, Kraft TW (2012) ERG critical flicker frequency assessment in humans. In: Retinal degenerative diseases LaVail et al (eds) Adv Exp Med Biol 723:503–509

Fishman GA, Birch DG, Holder GE et al (2001) Electrophysiologic testing in disorders of the retina, optic nerve, and visual pathway. In: American Academy Ophthalmology, 2nd edn, San Francisco, Oxford University Press

Frishman LJ, Wang MH (2011) Electroretinogram of human, monkey and mouse. In: Levin LA, Nilsson SFE, Ver Hoeve J et al (eds) Adler's physiology of the eye, 11th edn. Saunders Elsevier, New York

Nowak LM, Green DG (1983) Flicker fusion characteristics of rod photoreceptors in the toad. Vis Res 23:845–849

Panilla I, Lund RD, Suavé Y (2005) Cone function studied with flicker electroretinogram during progressive retinal degeneration in RCS rats. Exp Eye Res 80:51–59

Pardue MT, Peachey NS (2014) Mouse b-wave mutants. Doc Ophthalmol 128:77–89

Rubin GR, Kraft TW (2007) Flicker assessment of rod and cone function in a model of retinal degeneration. Doc Ophthalmol 115:165–172

Tanimoto N, Muehlfriedel RL, Fischer MD et al (2009) Vision tests in the mouse: functional phenotyping with electroretinography. Front Biosci 14:2730–2737

Zhang Y, Rubin GR, Fineberg N et al (2012) Age-related changes in Cngb1-X1 knockout mice: prolonged cone survival. Doc Ophthalmol 124:163–175

# Chapter 19
# Repeatability and Reproducibility of In Vivo Cone Density Measurements in the Adult Zebrafish Retina

**Alison Huckenpahler, Melissa Wilk, Brian Link, Joseph Carroll, and Ross F. Collery**

**Abstract** Zebrafish (*Danio rerio*) are widely used as an experimental model for a wide range of retinal diseases. Previously, optical coherence tomography (OCT) was introduced for quantitative analysis of the zebrafish cone photoreceptor cell mosaic; however no data exists on the intersession reproducibility or intrasession repeatability of such measurements. We imaged 14 wild-type (WT) fish three times each, with 48 h between each time point. En face images of the UV cone mosaic were generated from the OCT volume scans at each time point. These images were then aligned and the overlapping area cropped for analysis. Using a semiautomated cone-counting algorithm, a single observer identified each cone to calculate the cone density for every image, counting each image twice (84 total counts). The OCT cone density measurements were found to have an intersession reproducibility of 0.9988 (95% CI = 0.9978–0.9999) and an intrasession repeatability of 136.0 ± 10.5 cones/mm$^2$ (about 0.7%). Factors affecting image quality include gill movement during acquisition of the OCT volume and variable inclusion of non-UV cone mosaics in the contours used to generate the en face images.

**Keywords** Repeatability · Reproducibility · Optical Coherence Tomography (OCT) · Zebrafish · Cone Mosaic · Photoreceptor · Cone Density

A. Huckenpahler · M. Wilk · B. Link · R. F. Collery (✉)
Department of Cell Biology, Neurobiology, & Anatomy, Medical College of Wisconsin, Milwaukee, WI, USA
e-mail: rcollery@mcw.edu

J. Carroll
Department of Cell Biology, Neurobiology, & Anatomy, Medical College of Wisconsin, Milwaukee, WI, USA

Departments of Ophthalmology, Medical College of Wisconsin, Milwaukee, WI, USA



J. D. Ash et al. (eds.), *Retinal Degenerative Diseases*, Advances in Experimental Medicine and Biology 891, https://doi.org/10.1007/978-3-319-75402-4_19

## 19.1 Introduction

Zebrafish (*Danio rerio*) are widely used to model human development and disease. Zebrafish have orthologs to many disease-causing proteins, whose functional domains are often similar to those found in human proteins (Langheinrich 2003; Howe et al. 2013). Zebrafish are especially valuable as an ocular model system since their cone-rich retinas mimic the human retina (Allison et al. 2004) and multiple zebrafish models exist for ocular diseases (Link and Collery 2015). In addition, zebrafish are a cost-effective model for drug development and have been used to accurately predict mammalian teratogenicity (Van Leeuwen et al. 1990) as well as drug oculotoxicity (Deeti et al. 2014), which is especially important given the number of drugs with ocular side effects (Santaella and Fraunfelder 2007). Finally, zebrafish mature quickly and breed prolifically, making them well-suited for high-throughput screening (Schutera et al. 2016; Truong et al. 2016).

Optical coherence tomography (OCT) is a noninvasive, high-resolution imaging modality that has previously been used to examine zebrafish retina, lens, and anterior segment (Rao et al. 2006; Bailey et al. 2012; Collery et al. 2014). Recently, an OCT-based method for deriving in vivo estimates of cone density in the adult zebrafish retina was introduced (Huckenpahler et al. 2016). This method could allow researchers to quantify photoreceptor changes in response to disease or drug treatment, though the repeatability of these measurements has not been studied. Here we assess the intrasession repeatability and intersession reproducibility of OCT-based measurements of UV cone density in the adult zebrafish.

## 19.2 Methods

Volumetric images (1000 A-scans/B-scan, 1000 B-scans, nominal scan width of $1.2 \times 1.2$ mm) of the zebrafish retina were obtained using a Bioptigen Envisu R2200 SD-OCT (Research Triangle Park, NC) equipped with a 186.3 nm bandwidth SLD (center wavelength = 878.4 nm). Fourteen WT zebrafish were imaged three times each, with 48 h between imaging sessions. En face images of the UV cone mosaic were generated from the OCT volumes as previously described (Huckenpahler et al. 2016). The en face images for each fish were manually aligned using Photoshop (Adobe Photosystems, San Jose, CA), and a common region of interest (ROI) was cropped (ROI size varied from 12.18 to $102*10^{-3}$ $mm^2$). A low-pass filter was applied to each ROI, and cones were identified using semiautomated cone-counting software (Garrioch et al. 2012; Cooper et al. 2016a). Axial length values were obtained as previously described (Collery et al. 2014) and used to calculate the lateral scale of each en face image (Huckenpahler et al. 2016), thus enabling measurements of cone density. Cone density was taken as the number of cones with bound Voronoi cells divided by the total area of the Voronoi cells (Cooper et al. 2013).

To assess the intrasession repeatability, the cropped ROI from each imaging session was counted twice. The within-subject standard deviation ($S_w$) was taken as the square root of the average variance across all fish (Bland and Altman 1996). The repeatability is calculated by multiplying $S_w$ by 2.77 and the 95% confidence interval calculated with the formula:

$$\mathrm{CI}_{95\%} = 1.96 \times \frac{S_w}{\sqrt{2n(m-1)}} \tag{19.1}$$

where $n$ is the number of zebrafish imaging sessions (42), and $m$ is the number of counts for each image (2). The measurement error can also be estimated as $S_w \times 1.96$ (Bland and Altman 1996).

To calculate the intersession reproducibility of the cone density measurements, both cone density estimates at each time point were averaged and used to calculate the intraclass correlation coefficient (ICC) using R statistical package (the R Foundation for Statistical Computing, Vienna, Austria).

## 19.3 Results

Qualitatively, we observed variability in image quality across fish and imaging sessions. Factors such as shadowing from the overlying blood vessels and movement of the fish during scan acquisition can result in distortions or missing data in the resultant en face images of the cone mosaic (Fig. 19.1), though this rarely affected the ability to identify whether a cone was present or not. Across the 14 fish, the average cone density was found to be 20,588 cones/mm$^2$, with densities ranging from 12,326 to 39,254 cones/mm$^2$ (Table 19.1). Differences between repeated measures of cone density ranged from 0 to 246 cones/mm$^2$ with an average within-fish standard deviation ($S_w$) of 49.1 cones/mm$^2$. Intrasession repeatability was 136.0 ± 10.5 cones/mm$^2$ (about 0.7%). This means that the difference between two measurements for the same fish would be expected to be less than this value for 95% of pairs of measurements. The measurement error for this same data was determined to be 96.2 cones/mm$^2$ (about 0.5%), meaning that the difference between a given measurement of cone density and the true value would be expected to be less than this value for 95% of observations. Examining the cone density measurements over time, we found the ICC to be 0.9988 (95% CI = 0.9978–0.9999), indicating that 99.88% of the total variance is due to real differences in cone density across fish.

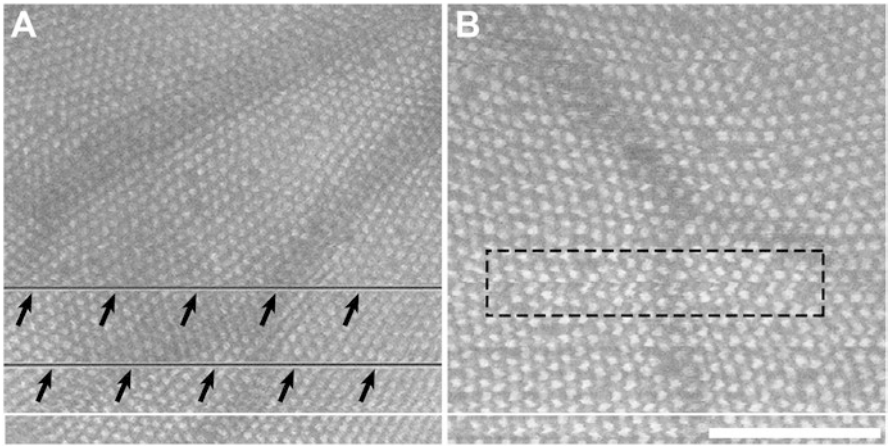


**Fig. 19.1** Disruptions in en face images of the cone mosaic derived from OCT volume scans. (**a**) Significant gill movements during the process of scanning result in missing data in the en face image (arrows). (**b**) Subtler gill movements and/or errors in contour placement can result in localized distortions (dashed rectangle). While these distortions may not affect the ability to identify the cones in the images, they would affect measurements of mosaic geometry (Cooper et al. 2016b). In addition, shadowing from overlying retinal vasculature was seen in many images. Scale bar = 100 μm

**Table 19.1** Zebrafish scaling information and density measurements

| Fish | Axial length (mm) | Region of interest (μm$^2$) | Time point 1 (cones/mm$^2$) | | Time point 2 (cones/mm$^2$) | | Time point 3 (cones/mm$^2$) | |
|---|---|---|---|---|---|---|---|---|
| 1 | 1.41 | 49,644 | 20,527 | 20,482 | 20,632 | 20,683 | 19,496 | 19,401 |
| 2 | 1.60 | 12,185 | 19,980 | 19,986 | 20,614 | 20,734 | 20,684 | 20,893 |
| 3 | 1.91 | 42,025 | 12,453 | 12,479 | 12,578 | 12,593 | 12,563 | 12,526 |
| 4 | 1.88 | 29,649 | 18,589 | 18,557 | 19,047 | 19,170 | 18,711 | 18,664 |
| 5 | 1.39 | 50,392 | 26,185 | 26,231 | 25,810 | 25,756 | 26,400 | 26,439 |
| 6 | 1.56 | 98,882 | 15,238 | 15,224 | 15,450 | 15,427 | 15,248 | 15,281 |
| 7 | 1.60 | 38,325 | 12,711 | 12,645 | 12,435 | 12,373 | 12,761 | 12,802 |
| 8 | 1.56 | 64,947 | 18,939 | 18,926 | 18,669 | 18,687 | 18,792 | 18,756 |
| 9 | 1.75 | 102,133 | 12,339 | 12,394 | 12,472 | 12,447 | 12,368 | 12,326 |
| 10 | 1.69 | 75,105 | 13,038 | 13,031 | 13,477 | 13,495 | 13,260 | 13,260 |
| 11 | 1.66 | 50,265 | 15,067 | 15,089 | 15,071 | 15,068 | 14,875 | 14,817 |
| 12 | 1.26 | 24,073 | 28,636 | 28,513 | 28,113 | 28,095 | 28,016 | 27,993 |
| 13 | 1.11 | 20,022 | 35,651 | 35,405 | 35,508 | 35,531 | 35,828 | 35,836 |
| 14 | 1.22 | 35,429 | 38,598 | 38,587 | 39,229 | 39,254 | 38,717 | 38,666 |

## 19.4 Discussion

Our data demonstrate excellent repeatability and reproducibility of in vivo measurements of cone density, using en face images of the UV cone mosaic derived from volumetric OCT scans. However, this study has some limitations. Firstly, the repeatability of the OCT density measurements will depend on the quality of the en face images. A low-quality OCT scan with multiple breathing artifacts or low signal will produce a low-quality en face image of the cone mosaic and subsequently impact the repeatability of the cone density measurements. Secondly, the repeatability and reproducibility measurements were performed by an expert who was proficient in both acquiring OCT images and generating en face images. For other observers, the repeatability and reliability of this technique may be worse (Bartlett and Frost 2008; Liu et al. 2014). Finally, our analysis was limited to the UV cone submosaic—as other submosaics are more difficult to visualize (Huckenpahler et al. 2016); thus our results should not be assumed to apply to the R/G or S cone submosaic.

Adaptive optics scanning light ophthalmoscopy (AOSLO) is another technique capable of providing high-resolution in vivo images of the cone mosaic (Williams 2011) and has been used for examining cone density in a wide range of retinal diseases (Carroll et al. 2013; Roorda and Duncan 2015). Semiautomated techniques have shown an intrasession repeatability of 2.7% for measures of parafoveal cone density (Garrioch et al. 2012). Fully automated methods have been shown to have excellent reproducibility, with one study reporting an ICC of 0.989 (Chui et al. 2013). Thus, the repeatability of our OCT-derived cone density measurements in the zebrafish retina are at least as good (if not slightly better) than AOSLO-derived measurements from the human retina. This may be due to the increased regularity of the zebrafish mosaic compared to humans, making it easier for the observer to see when the automated algorithm has missed a cone. In conclusion, with the noninvasive nature of the technique and availability of quantitative tools for analyzing images, the OCT-based method described here could be used to quantitatively study ocular disease, monitor retinal development, and facilitate drug discovery in zebrafish with high reproducibility and repeatability.

**Acknowledgments** The authors would like to thank Christine Skumatz and Alexis Visotcky for their assistance with this study and Robert Cooper for providing the cone-counting software. Research reported in this publication was supported by the National Eye Institute and the National Institute of General Medical Sciences of the NIH under award numbers R01EY016060, T32EY014537, P30EY001931, and T32GM080202. The content is solely the responsibility of the authors and does not necessarily represent the official views of the NIH.

## References

Allison WT, Haimberger TJ, Hawryshyn CW et al (2004) Visual pigment composition in zebrafish: evidence for a rhodopsin-porphyropsin interchange system. Vis Neurosci 21:945–952

Bailey TJ, Davis DH, Vance JE et al (2012) Spectral-domain optical coherence tomography as a noninvasive method to assess damaged and regenerating adult zebrafish retinas. Invest Ophthalmol Vis Sci 53:3126–3138

Bartlett JW, Frost C (2008) Reliability, repeatability and reproducibility: analysis of measurement errors in continuous variables. Ultrasound Obstet Gynecol 31:466–475

Bland JM, Altman DG (1996) Statistics notes: measurement error. Br Med J 313:744

Carroll J, Kay DB, Scoles D et al (2013) Adaptive optics retinal imaging-clinical opportunities and challenges. Curr Eye Res 38:709–721

Chui TYP, Gast TJ, Burns SA (2013) Imaging of vascular wall fine structure in human retina using adaptive optics scanning laser ophthalmoscopy. Invest Ophthalmol Vis Sci 54:7115–7124

Collery RF, Veth KN, Dubis AM et al (2014) Rapid, accurate, and non-invasive measurement of zebrafish axial length and other eye dimensions using SD-OCT allows longitudinal analysis of myopia and emmetropization. PLoS One 9:e110699

Cooper RF, Harvey Z, Dubow M et al (2013) The effect of AOSLO image distortion on metrics of mosaic geometry. Invest Ophthalmol Vis Sci 54:5546

Cooper RF, Wilk MA, Tarima S et al (2016a) Evaluating descriptive metrics of the human cone mosaic. Invest Ophthalmol Vis Sci 57:2992–3001

Cooper RF, Sulai YN, Dubis AM et al (2016b) Effects of intraframe distortion on measures of cone mosaic geometry from adaptive optics scanning light ophthalmoscopy. Transl Vis Sci Technol 5:e10

Deeti S, O'Farrell S, Kennedy BN (2014) Early safety assessment of human oculotoxic drugs using the zebrafish visualmotor response. J Pharmacol Toxicol Methods 69:1. Epub

Garrioch R, Langlo C, Dubis AM et al (2012) Repeatability of in vivo parafoveal cone density and spacing measurements. Optom Vis Sci 89:632–643

Howe K, Clark MD, Torroja CF et al (2013) The zebrafish reference genome sequence and its relationship to the human genome. Nature 496:498–503

Huckenpahler AL, Wilk MA, Cooper RF et al (2016) Imaging the adult zebrafish cone mosaic using optical coherence tomography. Vis Neurosci. (in press)

Langheinrich U (2003) Zebrafish: anew model on the pharmaceutical catwalk. BioEssays 25:904–912

Link BA, Collery RF (2015) Zebrafish models of retinal disease. Annu Rev Vis Sci 1:125–153

Liu B, Tarima S, Visotcky A et al (2014) The reliability of parafoveal cone density measurements. Br J Ophthalmol 98:1126–1131

Rao KD, Verma Y, Patel HS et al (2006) Non-invasive ophthalmic imaging of adult zebrafish eye using optical coherence tomography. Curr Sci 90:1506–1510

Roorda A, Duncan JL (2015) Adaptive optics ophthalmoscopy. Annu Rev Vis Sci 1:19–50

Santaella RM, Fraunfelder FW (2007) Ocular adverse effects associated with systemic medications: recognition and management. Drugs 67:75–93

Schutera M, Dickmeis T, Mione M et al (2016) Automated phenotype pattern recognition of zebrafish for high-throughput screening. Bioengineered 7:261–265

Truong L, Bugel SM, Chlebowski A et al (2016) Optimizing multi-dimensional high-throughput screening using zebrafish. Reprod Toxicol 65:139–147

Van Leeuwen CJ, Grootelaar EM, Niebeek G (1990) Fish embryos as teratogenicity screens: a comparison of embryotoxicity between fish and birds. Ecotoxicol Environ Saf 20:42–52

Williams DR (2011) Imaging single cells in the living retina. Vis Res 51:1379–1396

# Chapter 20
# Normative Retinal Thicknesses in Common Animal Models of Eye Disease Using Spectral Domain Optical Coherence Tomography


**Christy L. Carpenter, Alice Y. Kim, and Amir H. Kashani**

## Abstract

### Purpose
This study demonstrates a standardized approach to measuring retinal thickness (RT) using spectral domain optical coherence tomography (SD-OCT) in commonly used animal models of disease and reports a normative data set for future use.

### Materials and Methods
Twenty normal eyes of 4 adult animal models (5 rats, 5 rabbits, 5 canines, and 5 mini-pigs) were used. Manual measurements were made on the commercially available Heidelberg Spectralis™ SD-OCT to determine the total, inner, and outer retinal thickness (RT) at fixed distances from the optic nerve head (ONH) (1, 2, 3, 4, 5, and 6 mm away) in order to control for normal variation in retinal thickness. Analysis of variance (ANOVA) with $P$ value <0.05 indicated statistical significance.

### Results
Total RT significantly decreased with increasing distance from the ONH for the canine, mini-pig, and rabbit vascular models. Inner RT significantly decreased for the canine, mini-pig, rabbit vascular, and rabbit avascular models; and outer RT significantly decreased for only the canine model. Among the animal models, RT at similar distances from the ONH were significantly different for total, inner, and outer RT.

### Conclusion
There are significant differences in the total, inner, and outer RT of normal canine, mini-pig, rabbit, and rat retinas with SD-OCT using a standardized approach.

C. L. Carpenter · A. Y. Kim
Department of Ophthalmology, USC Eye Institute, Keck School of Medicine of the University of Southern California, Los Angeles, California, USA

A. H. Kashani (✉)
Department of Ophthalmology, USC Eye Institute, Keck School of Medicine of the University of Southern California, Los Angeles, California, USA

USC Roski Eye Institute, Los Angeles, CA, USA
e-mail: ahkashan@usc.edu



J. D. Ash et al. (eds.), *Retinal Degenerative Diseases*, Advances in Experimental Medicine and Biology 891, https://doi.org/10.1007/978-3-319-75402-4_20

These measurements provide a normative reference for future studies and illustrate a standardized method of assessing RT.

**Keywords** Animal Model · Retina · Optical coherence tomography · SD-OCT · Retinal thickness

## 20.1 Introduction

Spectral domain optical coherence tomography (SD-OCT) is a noninvasive imaging modality that uses the unique light-scattering properties of biological tissue to capture the structural characteristics of the retina (Drexler and Fujimoto 2008). SD-OCT findings correlate very well with histological sections of the same animal model (Costa et al. 2006; Remtulla and Hallett 1985; Kim et al. 2008; Nagata et al. 2009). In addition, morphological dimensions such as RT can be measured with high reproducibility, as found in previous studies with humans and animal models (Costa et al. 2006; Remtulla and Hallett 1985; Kim et al. 2008; Nagata et al. 2009; Hernandez-Merino et al. 2011; Rosolen et al. 2012; Ferguson et al. 2013; Ruggeri et al. 2007; Alkin et al. 2013; Ducros et al. 1999; Gilger 2014; Srinivasan et al. 2006; Ferguson et al. 2014; Sadda et al. 2007; Garcia Garrido et al. 2014). However, comparisons of RT between various animal models as well as normative data for commonly used animal models using SD-OCT are lacking in the current literature. The purpose of this study is to establish a standardized protocol and normative data set for measuring total, inner, and outer RT for common animal models. Rats, rabbits, mini-pigs, and canines were chosen for this study based on their common use in studies on ophthalmic disease (Remtulla and Hallett 1985; Kim et al. 2008; Nagata et al. 2009; Hernandez-Merino et al. 2011; Rosolen et al. 2012; Ferguson et al. 2013; Ruggeri et al. 2007; Alkin et al. 2013; Ducros et al. 1999; Gilger 2014; Srinivasan et al. 2006). Using SD-OCT to quantify RT among multiple animal models is integral to the reliability and reproducibility of future studies using these animal models.

## 20.2 Materials and Methods

### *20.2.1 Experiments with Animals*

The OCT database of the USC vivarium was reviewed for the records of animals that had undergone OCT imaging as part of previously approved protocols. Institutional Animal Care and Use Committee (IACUC) approved studies at USC only allow invasive procedures and studies of a single eyes. The contralateral eye is commonly used as a control. The OCT database was reviewed to identify OCT images from the control eye of such animals at baseline for this study. Therefore,

this was a retrospective, secondary analysis of OCT data from the control eyes of animals that were used for various studies of the retina under previously approved IACUC protocols. The health, safety, and comfort of all the animals were ensured under appropriate IACUC practices of the University of Southern California. Twenty eyes of 20 animals were identified as follows: 5 eyes of 5 pigmented Copenhagen rats, 5 eyes of 5 pigmented New Zealand rabbits, 5 eyes of 5 pigmented Göttingen mini-pigs, and 5 eyes of 5 pigmented beagle canines. All animals were imaged under standard imaging protocols and appropriate anesthesia. Pupils were dilated with phenylephrine hydrochloride 2.5% and tropicamide 0.5% eye drops.

### *20.2.2 Imaging Methods*

A commercially available Spectralis™ HRA + OCT device (Heidelberg Engineering, Heidelberg, Germany) was used for imaging. A dense raster scan of 48 B-scans, each separated by 120 μm acquired over a field of 20 × 15 degrees (horizontal × vertical), was used in each animal. At least three raster scans for the specified areas of each eye were taken. Twenty SD-OCT images with good or excellent signal-to-noise ratio were selected for analysis. Images were assessed as "good" or "excellent" based on the readers ability to clearly distinguish a distinctive border between the vitreous humor and the inner limiting membrane (ILM), a distinctive border between the outer plexiform layer (OPL) and outer nuclear layer (ONL), and a distinctive border of the hyperreflective retinal pigment epithelium (RPE) band and interdigitation zone (IDZ).

Total RT was defined as the linear distance between the ILM and the RPE as measured by the manual caliper tool. The inner RT was defined as the distance between the ILM and the anterior edge of the ONL. The outer RT was defined as the distance between the anterior border of the ONL and the RPE. This segmentation scheme is depicted in Fig. 20.1. The total, inner, and outer RT were manu-

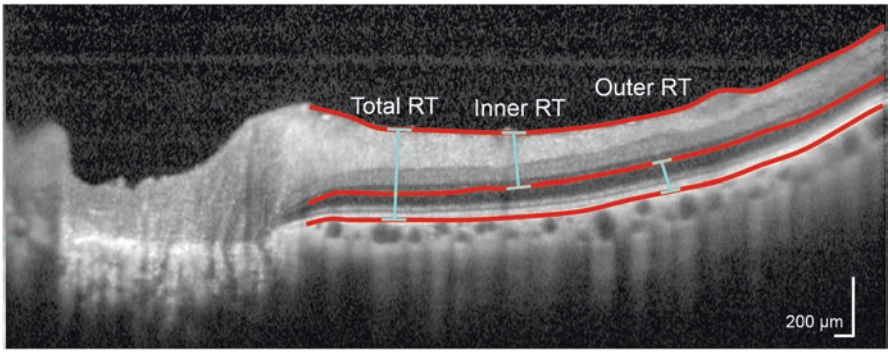


**Fig. 20.1** Normal porcine retinal layer definitions. Red lines denote the boundaries between layers. Layer measurements used in this study include inner, outer, and total RT

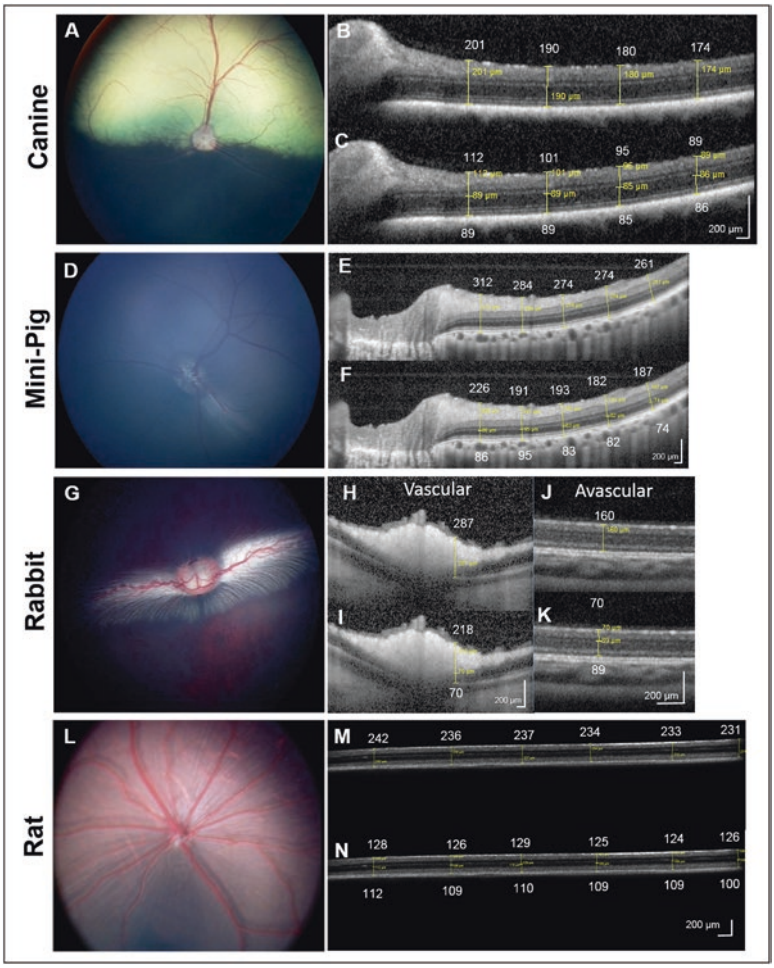


**Fig. 20.2** Color fundus images and retinal thickness measurements of healthy (**a**–**c**) canine, (**d**–**f**) mini-pig, (**g**–**k**) rabbit, and (**l**–**n**) rat retinas. For each animal model, representative color fundus images are shown on the left and SD-OCT scans are to the right. The top SD-OCT scan shows the total RT, and the bottom SD-OCT scan shows the inner and outer RT. The rabbit retina was measured in two regions: the (**h**, **i**) vascular area and the (**j**, **k**) avascular area. Measurements are recorded in white along with the original caliper measures in yellow for clarity (all measurements in microns)

ally measured at 1, 2, 3, 4, 5, and 6 mm from the ONH. Distances from the ONH were measured as a line starting from the edge of the ONH and extending radially (Fig. 20.2).

### *20.2.3 Statistics*

The mean and standard deviations of RT measurements were calculated at each distance from the ONH and recorded in microns (μm). RT values were compared at each distance from the ONH within each animal model and between the different animal models at each distance. Analysis of variance (ANOVA) values were calculated using Soper's analysis of variance calculator (Wiley, New York, NY) with $p < 0.05$ for significance.

## 20.3 Results

Table 20.1 shows the mean RT at 1, 2, 3, 4, 5, and 6 mm from the ONH as well as the results of ANOVA analysis. Table 20.2 shows the results of ANOVA analysis when comparing values among the animal models at each distance from the ONH. There were several instances in which the image of the peripheral retina was too unclear to measure the farthest distances. Among canines, there was poor visualization past the 3 mm or 4 mm mark in 4 subjects. Among mini-pigs, there was poor visualization past the 5 mm mark in 4 subjects. Among rabbits, there was poor visualization past the 4 mm or 5 mm mark in 4 subjects. Among rats, there was poor visualization past the 3 mm, 4 mm, or 5 mm mark in 3 subjects. In these cases, the RT measurements were not included in the subsequent analysis to maintain integrity of the analysis.

In the canine, the mean total RT decreased significantly with increasing distance from the ONH from 207 to 164 μm (Fig. 20.2a–c). The inner RT also decreased from 111.6 to 79 μm, and the outer RT decreased from 95.4 to 86 μm ($p < 0.001$ for all). This animal model showed the only statistically significant difference found for outer RT ($p = 0.016$).

In the mini-pig animal model (Fig. 20.2d–f), there was a relatively steady decrease in mean total RT. Both the total and inner RT decreased significantly from 327 to 245 μm and 221 to 149 μm, respectively ($p < 0.001$ for both). The outer RT decreased from 105 to 96 μm but was not statistically significant ($p = 0.559$).

In the rabbit model (Fig. 20.2g–k), the mean RT for the vascular area of the retina decreased most dramatically compared to all of the animal models observed. The total vascular RT decreased significantly from 341 to 163 μm, and the vascular inner RT decreased from 252 to 121 μm at increasing distance from the ONH ($p < 0.001$ for all). However, there were no statistically significant differences in the outer RT of the vascular section of the eye ($p = 0.456$). For the avascular regions of the rabbit eyes, only the mean inner RT showed statistically significant changes as it decreased from 75 to 55 μm ($p < 0.001$). The avascular total RT, which decreased from 168 to 142 μm, and the avascular outer RT, which decreased from 98 to 87 μm, were not statistically different ($p = 0.069$ and 0.402, respectively).

**Table 20.1** Total, inner, and outer retinal thicknesses for each animal model

| Distance from ONH (mm) | 1 | 2 | 3 | 4 | 5 | 6 | *P* value |
|---|---|---|---|---|---|---|---|
| Mean total RT (μm) | | | | | | | Total RT |
| Canine | 207.00 ± 7.58 | 198.00 ± 7.97 | 191.00 ± 6.16 | 184.00 ± 11.02 | 178.00 ± 0.00 | 164.00 ± 0.00 | <0.001* |
| Mini-pig | 327.40 ± 10.21 | 311.60 ± 15.01 | 293.80 ± 11.50 | 281.00 ± 16.55 | 264.60 ± 13.81 | 245.00 ± 0.00 | <0.001* |
| Rabbit V | 340.80 ± 5.17 | 294.80 ± 9.73 | 246.60 ± 9.21 | 214.80 ± 20.29 | 189.00 ± 19.70 | 163.00 ± 0.00 | <0.001* |
| Rabbit AV | 168.40 ± 13.30 | 162.80 ± 14.29 | 162.00 ± 16.55 | 156.60 ± 18.40 | 153.50 ± 14.01 | 142.00 ± 0.00 | 0.07 |
| Rat | 235.80 ± 16.63 | 230.40 ± 18.39 | 226.00 ± 18.95 | 223.75 ± 20.43 | 229.00 ± 17.35 | 219.50 ± 0.00 | 0.73 |
| Mean inner RT (μm) | | | | | | | Inner RT |
| Canine | 111.60 ± 5.94 | 105.00 ± 4.64 | 99.80 ± 4.15 | 94.30 ± 6.11 | 89.00 ± 0.00 | 79.00 ± 0.00 | <0.001* |
| Mini-pig | 221.60 ± 8.11 | 208.40 ± 10.88 | 193.00 ± 8.09 | 183.20 ± 9.98 | 168.80 ± 11.39 | 149.00 ± 0.00 | <0.001* |
| Rabbit V | 252.25 ± 14.31 | 207.50 ± 12.56 | 168.00 ± 19.58 | 144.25 ± 28.36 | 121.00 ± 39.60 | – | <0.001* |
| Rabbit AV | 75.00 ± 8.25 | 70.00 ± 7.48 | 68.50 ± 5.00 | 65.25 ± 4.27 | 58.25 ± 3.30 | 55.00 ± 0.00 | <0.001* |
| Rat | 125.40 ± 6.69 | 122.60 ± 9.73 | 119.80 ± 10.11 | 118.75 ± 11.18 | 120.00 ± 8.72 | 118.50 ± 0.00 | 0.77 |
| Mean outer RT (μm) | | | | | | | Outer RT |
| Canine | 95.40 ± 4.77 | 93.00 ± 4.24 | 89.60 ± 5.08 | 90.33 ± 5.03 | 89.00 ± 0.00 | 86.00 ± 0.00 | 0.016* |
| Mini-pig | 105.80 ± 12.95 | 103.20 ± 12.64 | 100.80 ± 11.08 | 97.80 ± 9.88 | 95.80 ± 8.53 | 96.00 ± 0.00 | 0.56 |
| Rabbit V | 89.00 ± 9.13 | 84.00 ± 10.55 | 79.75 ± 10.97 | 75.25 ± 12.82 | 76.00 ± 19.80 | – | 0.46 |
| Rabbit AV | 97.75 ± 11.87 | 97.75 ± 9.71 | 100.00 ± 11.02 | 98.00 ± 10.13 | 97.75 ± 12.42 | 87.00 ± 0.00 | 0.40 |
| Rat | 110.40 ± 11.04 | 107.80 ± 10.16 | 106.20 ± 9.04 | 105.00 ± 9.56 | 109.00 ± 9.00 | 101.00 ± 0.00 | 0.63 |

Abbreviations: *ONH* optic nerve head, *RT* retinal thickness, *V* vascular area of rabbit retina, *AV* avascular area of rabbit retina. The mean RT for each animal model at increasing distances from the ONH are provided. *P* values comparing RT at all distances within each animal model are shown in the right column. Asterisks indicate significant differences in RT at varying distances from the ONH for that particular animal model.

**Table 20.2** Comparison of mean RT between each of the five animal models with increasing eccentricity from the ONH

| Distance from ONH (mm) | 1 | 2 | 3 | 4 | 5 | 6 |
|---|---|---|---|---|---|---|
| Total RT | <0.001 | <0.001 | <0.001 | <0.001 | <0.001 | <0.001 |
| Inner RT | <0.001 | <0.001 | <0.001 | <0.001 | <0.001 | <0.001 |
| Outer RT | 0.029 | 0.011 | 0.003 | 0.001 | 0.025 | <0.001 |

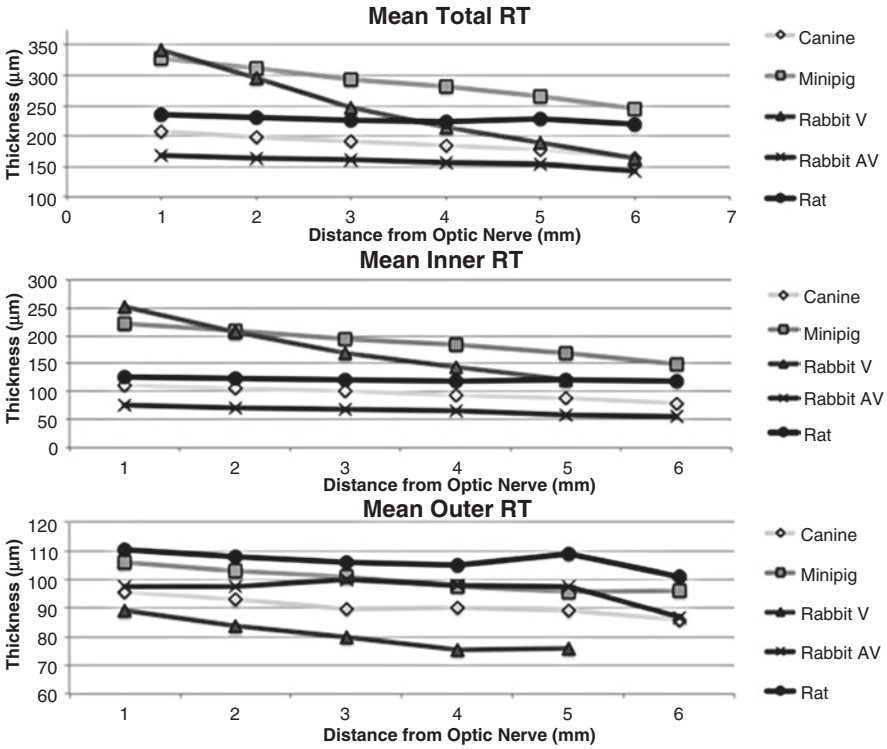


**Fig. 20.3** Correlation of the mean RT with increasing eccentricity from the ONH for each animal model

In the rat animal model (Fig. 20.2l–n), there was no statistically significant change in RT with increasing distance from ONH. The mean total RT decreased from 236 to 220 µm ($p = 0.725$); the mean inner RT decreased from 125 to 119 µm ($p = 0.771$); and the mean outer RT decreased from 110 to 101 µm ($p = 0.630$).

Among all animal models, there were statistically significant differences in total RT at similar distances from the ONH ($p < 0.001$; Table 20.2). The same held true for all inner RT and outer RT measurements among the animal models ($p < 0.001$ and $p < 0.029$, respectively; Fig. 20.3).

## 20.4 Discussion

We demonstrate a standardized approach to reporting retinal thickness measurements in multiple commonly used animal models using SD-OCT. Specifically we quantify the total, inner, and outer RT of healthy canine, mini-pig, rabbit, and rat retina at specific distances from the ONH. In general, total RT and inner RT decreased with increasing distance from the optic nerve head in all the animal models, although with differing magnitudes. The outer RT did not have a similar pattern, and we only detected a change in outer retinal thickness with distance from the ONH in the canine. The greater magnitude and consistency of decrease in inner RT measurements compared to outer RT measurements with increasing distance from the ONH may be attributed to the retinal nerve fiber layer (RNFL).

Among the animal models, there were significant differences in RT at similar distances from the ONH for total, inner, and outer RT. This shows that the healthy canine, mini-pig, rabbit, and rat models each serve as a unique models with significant differences in retinal anatomy. Thus, it is important to establish normative RT for each of these models as in this study, so that they may be used in future studies involving any of the same animals.

Non-OCT-based measurements of normative RT have previously been reported in canine (Hernandez-Merino et al. 2011; Rosolen et al. 2012; Gilger 2014), mini-pig (Rosolen et al. 2012; Gilger 2014), mouse/rat (Remtulla and Hallett 1985; Kim et al. 2008; Nagata et al. 2009; Ferguson et al. 2013; Ruggeri et al. 2007; Gilger 2014; Srinivasan et al. 2006), and rabbit models (Alkin et al. 2013; Ducros et al. 1999; Gilger 2014). These studies are not OCT based but produced results similar to those obtained in this study at equivalent distances from the ONH. Therefore, the validity of SD-OCT-based measurements for in vivo assessment of retinal thickness is demonstrated in this study. Our study also investigates these retinal thickness measurements at 6 points from the ONH (approximately 1 mm apart), offering a more standardized and reproducible approach to measuring RT in various parts of the retina. In addition, we measure specific sections of the cross-sectional retina to include the inner and outer segments, not just the total RT. In this manner, we account for inherent anatomical variations such as the presence of the RNFL in the inner retinal segment.

This study is limited by the reliance on manual measurements of retinal thicknesses, which are subjectively biased. This error was minimized, but not alleviated, with strict criteria for layer boundaries, as defined in our measurement protocol. We also observed that the rabbit vascular streak had lower image quality in the deeper retinal sections compared to the other animal models. This may be attributed to the effect of the thicker RNFL. However, all SD-OCT images obtained were of sufficient quality to measure all layers of interest, with results showing similar findings to histology from previous studies (Alkin et al. 2013).

In most research practice, establishing histological measurements of normal RT provides the main methodology by which to distinguish between diseased and normal animal retinas. However, this method is invasive and time-consuming, making

it difficult to conduct a longitudinal study. SD-OCT is a useful imaging modality that is commonly used in studies involving animal models given its ability to quickly and noninvasively obtain high-resolution, cross-sectional images of the retina. This could reduce the number of animals needed for future quantitative and descriptive studies of the retina while offering more reliable and accurate analysis of the retina over a longer follow-up period.

## References

Alkin Z, Kashani AH, Lopez-Jaime GR, Ruiz Garcia H, Humayun MS, Sadda SR (2013) Quantitative analysis of retinal structures using spectral domain optical coherence tomography in normal rabbits. Curr Eye Res 38(2):299–304. https://doi.org/10.3109/02713683.2012.757625. PubMed PMID: 23373715

Costa RA, Skaf M, Melo LA Jr, Calucci D, Cardillo JA, Castro JC et al (2006) Retinal assessment using optical coherence tomography. Prog Retin Eye Res 25(3):325–353. https://doi.org/10.1016/j.preteyeres.2006.03.001. PubMed PMID: 16716639

Drexler W, Fujimoto JG (2008) State-of-the-art retinal optical coherence tomography. Prog Retin Eye Res 27(1):45–88. https://doi.org/10.1016/j.preteyeres.2007.07.005. PubMed PMID: 18036865

Ducros MG, Huang H, Chao LC, Chen Z, Nelson JS, Rylander HG et al (1999) Polarization sensitive optical tomography of the rabbit eye. IEEE J Sel Top Quantum Electron 5(4):1159–1167

Ferguson LR, Dominguez JM, Balaiya S, Grover S, Chalam KV (2013) Retinal thickness normative data in wild-type mice using customized miniature SD-OCT. PLoS One 8(6):e67265. https://doi.org/10.1371/journal.pone.0067265. PubMed PMID: 23826252; PubMed Central PMCID: PMCPMC3695045

Ferguson LR, Grover S, Dominguez JM 2nd, Balaiya S, Chalam KV (2014) Retinal thickness measurement obtained with spectral domain optical coherence tomography assisted optical biopsy accurately correlates with ex vivo histology. PLoS One 9(10):e111203. https://doi.org/10.1371/journal.pone.0111203. PubMed PMID: 25360629; PubMed Central PMCID: PMCPMC4216007

Garcia Garrido M, Beck SC, Muhlfriedel R, Julien S, Schraermeyer U, Seeliger MW (2014) Towards a quantitative OCT image analysis. PLoS One 9(6):e100080. https://doi.org/10.1371/journal.pone.0100080. PubMed PMID: 24927180; PubMed Central PMCID: PMCPMC4057353

Gilger BC (2014) Ocular pharmacology and toxicology. Humana Press/Springer, New York. x, 323 p

Hernandez-Merino E, Kecova H, Jacobson SJ, Hamouche KN, Nzokwe RN, Grozdanic SD (2011) Spectral domain optical coherence tomography (SD-OCT) assessment of the healthy female canine retina and optic nerve. Vet Ophthalmol 14(6):400–405. https://doi.org/10.1111/j.1463-5224.2011.00887.x. PubMed PMID: 22050777

Kim KH, Puoris'haag M, Maguluri GN, Umino Y, Cusato K, Barlow RB et al (2008) Monitoring mouse retinal degeneration with high-resolution spectral-domain optical coherence tomography. J Vis 8(1):17.1–1711. https://doi.org/10.1167/8.1.17. PubMed PMID: 18318620

Nagata A, Higashide T, Ohkubo S, Takeda H, Sugiyama K (2009) In vivo quantitative evaluation of the rat retinal nerve fiber layer with optical coherence tomography. Invest Ophthalmol Vis Sci 50(6):2809–2815. https://doi.org/10.1167/iovs.08-2764. PubMed PMID: 19182247

Remtulla S, Hallett PE (1985) A schematic eye for the mouse, and comparisons with the rat. Vis Res 25(1):21–31. PubMed PMID: 3984214

Rosolen SG, Riviere ML, Lavillegrand S, Gautier B, Picaud S, LeGargasson JF (2012) Use of a combined slit-lamp SD-OCT to obtain anterior and posterior segment images in selected

animal species. Vet Ophthalmol 15(Suppl 2):105–115. https://doi.org/10.1111/j.1463-5224.2012.01037.x. PubMed PMID: 22616780

Ruggeri M, Wehbe H, Jiao S, Gregori G, Jockovich ME, Hackam A et al (2007) In vivo three-dimensional high-resolution imaging of rodent retina with spectral-domain optical coherence tomography. Invest Ophthalmol Vis Sci 48(4):1808–1814. https://doi.org/10.1167/iovs.06-0815. PubMed PMID: 17389515

Sadda SR, Joeres S, Wu Z, Updike P, Romano P, Collins AT et al (2007) Error correction and quantitative subanalysis of optical coherence tomography data using computer-assisted grading. Invest Ophthalmol Vis Sci 48(2):839–848. https://doi.org/10.1167/iovs.06-0554. PubMed PMID: 17251486

Srinivasan VJ, Ko TH, Wojtkowski M, Carvalho M, Clermont A, Bursell SE et al (2006) Noninvasive volumetric imaging and morphometry of the rodent retina with high-speed, ultrahigh-resolution optical coherence tomography. Invest Ophthalmol Vis Sci 47(12):5522–5528. https://doi.org/10.1167/iovs.06-0195. PubMed PMID: 17122144; PubMed Central PMCID: PMCPMC1941766

# Chapter 21
# A Novel Approach for Integrating AF-SLO and SDOCT Imaging Data Demonstrates the Ability to Identify Early Retinal Abnormalities in Mutant Mice and Evaluate the Effects of Genetic and Pharmacological Manipulation


**Brent A. Bell, Vera L. Bonilha, and Ivy S. Samuels**

**Abstract** Noninvasive ocular imaging platforms are undeniably useful in identifying retinal abnormalities. The purpose of this study was to investigate a novel method for integrating information acquired from two independent imaging platforms, AF-SLO and SDOCT, in order to demonstrate retinal perturbations as a result of genetic or pharmacological manipulation. Two cohorts of mice were investigated, *Nyx*$^{nob}$ and C57BL/6 J. In *Nyx*$^{nob}$ mice, SLO revealed an atypical but variable amount of autofluorescent foci (AFF); SDOCT showed altered photoreceptor outer segment architecture. Naïve *Nyx*$^{nob}$ had significantly more AFF than C57BL/6 J, suggesting that *Nyx*$^{nob}$ have some predisposition for developing AFF. Interestingly, both findings were significantly ameliorated in diabetic *Nyx*$^{nob}$ mice as compared to the controls. These data were incorporated into a novel analysis plot comparing AF-SLO and SDOCT results. The integration of the qualitative changes and

**Electronic supplementary material:** The online version of this chapter (https://doi.org/10.1007/978-3-319-75402-4_21) contains supplementary material, which is available to authorized users.

B. A. Bell (✉)
Cole Eye Institute/Ophthalmic Research, Cleveland Clinic, Cleveland, OH, USA

Cole Eye Institute, Cleveland Clinic, Cleveland, OH, USA
e-mail: bellb3@ccf.org

V. L. Bonilha
Cleveland Clinic Lerner College of Medicine of Case Western Reserve University, Cleveland, OH, USA

Cole Eye Institute, Cleveland Clinic, Cleveland, OH, USA

I. S. Samuels (✉)
Cole Eye Institute, Cleveland Clinic, Cleveland, OH, USA

Louis Stokes Cleveland VA Medical Center, Cleveland, OH, USA
e-mail: Ivy.Samuels@va.gov



J. D. Ash et al. (eds.), *Retinal Degenerative Diseases*, Advances in Experimental Medicine and Biology 891, https://doi.org/10.1007/978-3-319-75402-4_21

accompanying quantitative analysis approach described herein provide a sensitive means for detecting whether a mouse model is susceptible to degeneration before other hallmark indicators are observed.

**Keywords** AF-SLO · SDOCT · Fundus · Retina · Autofluorescent foci · Longitudinal reflectance profile · Outer segments · Nyctalopin · Streptozotocin

## 21.1 Introduction

Noninvasive imaging with autofluorescence confocal scanning laser ophthalmoscopy (AF-SLO) and spectral-domain optical coherence tomography (SDOCT) is now common practice in vision research. We have previously shown that altered outer retina morphology can be visualized and quantified by AF-SLO and SDOCT (Bell et al. 2015; Bonilha et al. 2015). In these studies, changes occurred many weeks prior to photoreceptor degeneration and RPE changes. In this current work, we demonstrate a useful manner in which one can quantify and integrate observational findings collected independently via AF-SLO and SDOCT imaging modalities.

## 21.2 Materials and Methods

### *21.2.1 Ethical Approval*

All experiments were conducted in compliance with the ARVO Resolution on Treatment of Animals in Research and the Institutional Animal Care and Use Committees at the Louis Stokes Cleveland VA Medical Center and the Cleveland Clinic.

### *21.2.2 Mouse Models*

*Nyx*$^{nob}$ mice (backcrossed to C57BL/6 J for 10 generations) were obtained from a local breeding colony (Pardue et al. 1998). Cohort 1 included *Nyx*$^{nob}$ mice 9–20 weeks of age randomly assigned to diabetic (STZ, $n = 8$) or nondiabetic (CNTL, $n = 12$) groups. Diabetes induction of *Nyx*$^{nob}$ mice via streptozotocin (STZ) and maintenance for 4 weeks of hyperglycemia were previously described (Tarchick et al. 2016). Cohort 2 included naïve, 3-month-old *Nyx*$^{nob}$ mice ($n = 6$) and C57BL/6 J mice ($n = 6$) used to establish baseline levels and for comparison to a common wild-type strain.

### *21.2.3 In Vivo Ocular Imaging*

AF-SLO and SDOCT imaging and animal preparation were previously described (Bell et al. 2015).

### *21.2.4 AF-SLO and SDOCT Image Analysis*

AF-SLO images were analyzed as previously described (Bell et al. 2015). Briefly, the number of AFF was manually counted from each AF-SLO image. Longitudinal reflectance profiles (LRP) from SDOCT images were created and analyzed in a similar manner as previously described (Bonilha et al. 2015); however, rather than use an area-under-the-curve analysis, we measured changes to the reflectance signal slope over a range of 10 pixels (~10 μm) exclusive to the photoreceptor outer segments (Suppl. Fig. 21.1). GraphPad Prism 6 was used for all statistical analyses.

## 21.3 Results

In cohort 1, AF-SLO showed the presence of AFF to varying degrees in all mice. Figure 21.1a$^{1–3}$, b$^{1–3}$ are representative AF-SLO images illustrating the range of AFF in CNTL vs. STZ. Elevated AFF counts are an atypical occurrence in young wild-type mice (Xu et al. 2008), and these observations indicate inflammatory monocytes localized to the subretinal space (Ng and Streilein 2001). We next performed imaging in 3-month-old *Nyx$^{nob}$* and C57BL/6 J mice (cohort 2, Fig. 21.1c$^{1–3}$, d$^{1–3}$) to establish baseline AFF levels for these two strains of mice that could also be compared to animals from cohort 1. The mean AFF count was significantly larger in 3-month-old *Nyx$^{nob}$* (19.8 ± 16.4) than C57BL/6 J (1.083 ± 1.084, mean ± SD) mice (Suppl. Fig. 21.2a, Mann-Whitney test, $^{****}p < 0.0001$).

When we compared AFF counts from naïve 3-month-old *Nyx$^{nob}$* mice with the CNTL- and STZ-treated *Nyx$^{nob}$* mice (13 and 24 weeks of age at testing), we found that the CNTL group displayed significantly more AFF than the other two groups (Suppl. Fig. 21.2b, one-way ANOVA with Tukey's posttest $^{*}p = 0.0299$, $^{***}p = 0.0004$). However, the STZ group was not significantly different from the 3-month naïve *Nyx$^{nob}$* group. Importantly, we observed a general trend for an increase in AFF with age in the *Nyx$^{nob}$* mice regardless of treatment, essentially tripling between 13 and 24 weeks (data not shown); and the amount of AFF per mouse did not correlate with glucose levels.

SDOCT imaging of these animals showed qualitative differences in the alternating bright-dark banding observed in the photoreceptor layer of the outer retina (Fig. 21.2a–d). Representative SDOCT B-scans from each cohort are presented in Supplemental Fig. 21.3. The region of interest (ROI) from the B-scan of a

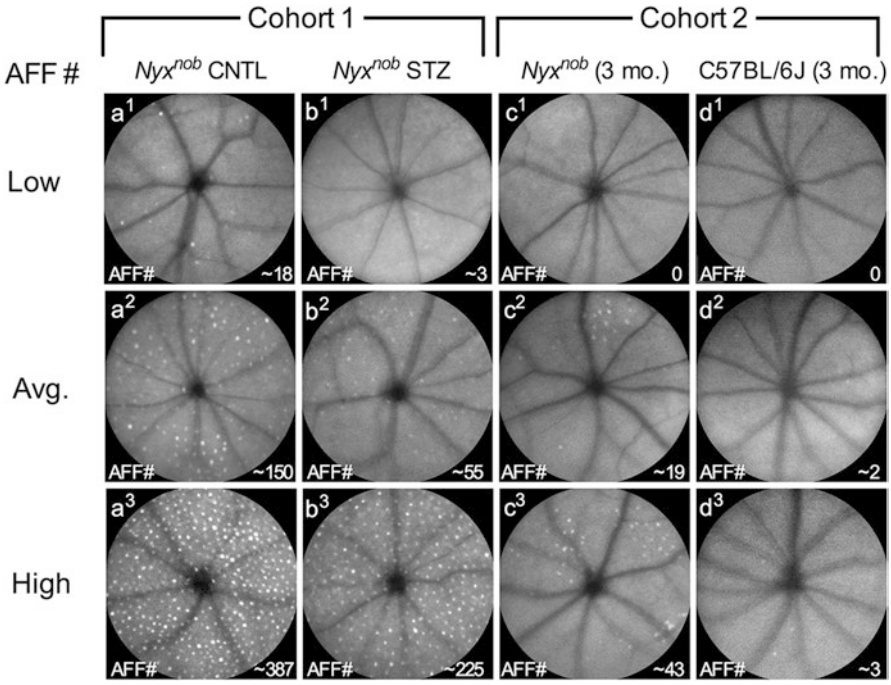


**Fig. 21.1** Autofluorescent foci observed in *Nyx*$^{nob}$ mice by AF-SLO. AF-SLO images demonstrating the presence and variability [low ($a^1$–$d^1$); average ($a^2$–$d^2$); high ($a^3$–$d^3$)] in AFF count among CNTL, STZ, and naïve *Nyx*$^{nob}$ and C57BL/6 J mice

representative mouse from each group, spanning the retina from choroid to the outer nuclear layer, is presented in Fig. 21.2a–d. The OS region analyzed is denoted by white brackets (see bracketed spaces in Fig. 21.2a–d). In normal C57BL/6 J and *Nyx*$^{nob}$ mice, the proximal OS region (p) appears dark in relation to the bright reflective band that originates from the distal OS (d) (Fig. 21.2$a^1$, $d^2$). We observed a definitive brightening (hyper-reflectivity) of the proximal OS in CNTL *Nyx*$^{nob}$ mice with average-high AFF counts, leading to the apparent loss of banding. This loss of banding is visualized by comparing Fig. 21.2$a^1$ (low AFF) with Fig. 21.2$a^2$ (average AFF) or Fig. 21.2$a^3$ (high AFF). OS reflectivity in some STZ mice was also altered, but this change was opposite; the proximal OSs appeared hyporeflective (Fig. 21.2$b^2$), making the bands appear more distinct.

To quantify the degree of change in OS reflectivity, we obtained the reflectance signal slope derived from the LRP of each averaged SDOCT B-scan (see Suppl. Fig. 21.3). *Nyx*$^{nob}$ mice exhibited a significant increase in signal slope compared to C57BL/6 J (Suppl. Fig. 21.2c, Mann-Whitney test, $***p = 0.0001$) indicating that *Nyx*$^{nob}$ mice have more definitive banding as compared to WTs. Analysis of the OS signal slope between naïve, CNTL, and STZ *Nyx*$^{nob}$ groups also revealed significant differences for each comparison (Suppl. Fig. 21.2d, one-way ANOVA with Tukey's posttest, $**p = 0.0091$, $***p = 0.0004$, $****p < 0.0001$).

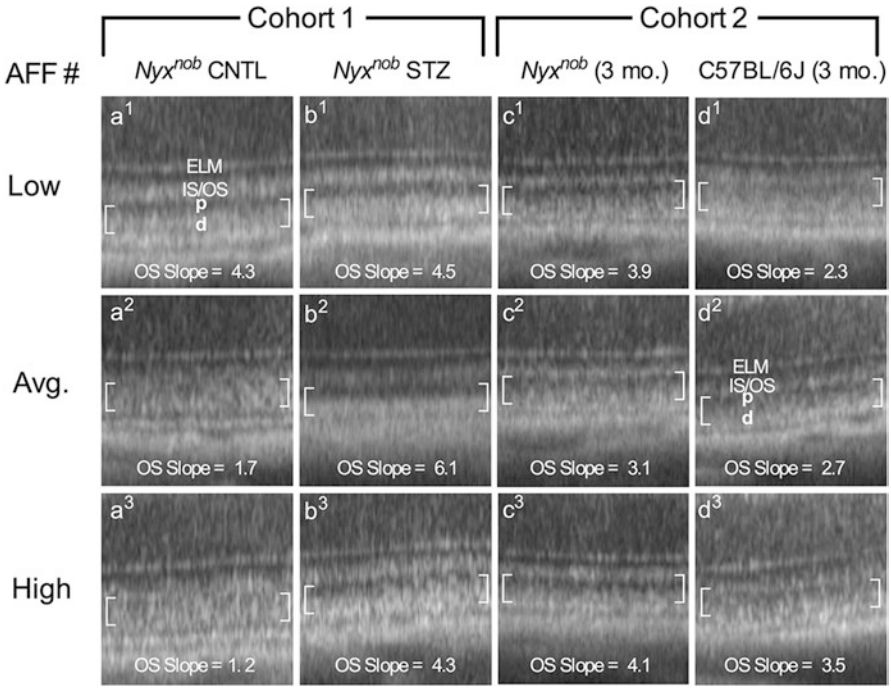


**Fig. 21.2** SDOCT of *Nyx*$^{nob}$ mice display changes to photoreceptor OS reflectivity depending on AFF count and diabetic status. SDOCT images from CNTL (**a**) and STZ *Nyx*$^{nob}$ (**b**) and naïve *Nyx*$^{nob}$ (**c**) and C57BL/6 J (**d**) mice binned by the number of AFF visualized by AF-SLO. Regions of interest from SDOCT B-scans through the horizontal meridian of SLO images illustrate the OS reflective changes [white brackets = photoreceptor outer segments (**a**–**d**), ELM external limiting membrane, IS/OS inner segment-outer segment transition, p proximal outer segments, d distal outer segments ($a^1$ & $d^2$)]

The integration of the data in Figs. 21.1 and 21.2 is presented using the scatterplot shown in Fig. 21.3. By generating a semilog plot of the signal slope on the abscissa and AFF on the ordinate, one can interrogate the relationship between these two findings across different groups. Notably, the OS signal slope changes dramatically with increasing AFF in CNTL *Nyx*$^{nob}$ mice. Analysis of the slope relative to AFF number revealed an inversely proportional trend (Pearson correlation = −0.6610) observed within the CNTL group (the more AFF, the more hyperreflective and smaller the signal slope) as depicted by a linear regression curve (R-squared = 0.437). STZ *Nyx*$^{nob}$ mice did not follow the same trend as the OS signal slope as values go in the completely opposite direction (from being hyperreflective to hyporeflective). These findings suggest that the increase in AFF number accounts for the change in the LRP and the OS signal slope. For comparison to naïve controls, data obtained from cohort 2 was overlaid in the scatterplot and compared to STZ and CNTL *Nyx*$^{nob}$ animals. From this graph, clear differences due to genotype and pharmacological manipulation are readily observed.

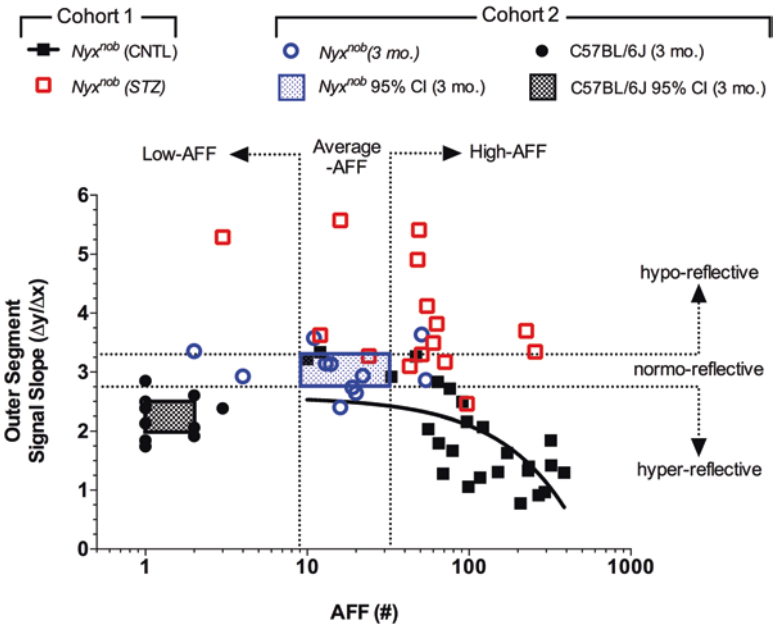


**Fig. 21.3** Scatterplot showing the relationship between AFF count and OS signal slope. Each eye evaluated is represented by an individual data point. A negative correlation (solid line) was observed between AFF and slope for *Nyx*$^{nob}$ CNTLS. Horizontal-dotted lines represent normo-reflective ranges and deviations to hypo- and hyper-reflectivity from naïve 3-month-old *Nyx*$^{nob}$ mice. Vertical-dotted lines represent Average-AFF and deviations to Low- and High-AFF counts from naive 3-month-old *Nyx*$^{nob}$ mice

## 21.4 Discussion

This study documents unexpected retinal findings in a bipolar cell mutant mouse model by in vivo retinal imaging. Although *Nyx*$^{nob}$ mice do not exhibit an ERG b-wave, we do not believe the mutation is responsible for these findings, as other bipolar cell mutants (nob3, nob5, lrit3) (Pardue and Peachey 2014) imaged did not exhibit a similar pattern of AFF (data not shown). This supports the notion that AFF in *Nyx*$^{nob}$ mice is likely due to a yet undetermined background effect.

Importantly, the quantitative nature of the novel analysis paradigm presented here allowed for the comparison of AFF counts in CNTL and STZ mice and showed that STZ mice had significantly fewer AFF per eye than CNTLs. This suggests that the STZ injection or elevated blood glucose levels moderated the accumulation of AFF (i.e., inflammatory monocytes) in the outer retina of diabetic animals. Moreover, the quantitative analysis of the SDOCT in the form of the signal slope also revealed that subsets of *Nyx*$^{nob}$ mice from both groups, regardless of treatment, were observed to have abnormal photoreceptor OS morphology. The direct comparison of signal slopes between *Nyx*$^{nob}$ treatment groups (Fig. 21.3) demonstrated that the diabetic mice swing the hyper-reflective changes observed in OS of CNTLs

in a completely opposite direction by making them hyporeflective instead. Thus, as with the AFF data, the manipulation by STZ seems to moderate OS reflectivity in the outer retina of *Nyx*$^{nob}$ mice. It is important to note, however, that we did not identify a correlation between either AFF or signal slope and blood glucose level in CNTL or STZ groups, and, therefore, the changes do not necessarily reflect a result of the diabetes.

Herein we have identified novel changes to the outer retina of a mutant mouse with and without pharmacological intervention by in vivo imaging and presented a sensitive means by which one can analyze the qualitative data obtained using AF-SLO and SDOCT. Monitoring the outer retina can be a very sensitive technique capable of indicating problems at an early onset. Inflammatory cells that are actively phagocytizing outer segments and/or RPE cells form the bright AFF that can be visualized with AF-SLO. Furthermore, the SDOCT can demonstrate that OSs are altered by stress. Therefore, this novel approach for integrating findings from both the AF-SLO and SDOCT is applicable to the analysis of many mutant mouse models and can be useful in differentiating phenotypes due to both genetic and pharmacological manipulation.

**Acknowledgments** This work was supported by a CDA to ISS from the US Dept. of Veterans Affairs Biomedical Laboratory Research and Development Service, VA Merit Award I01BX002754 (ISS) and an unrestricted grant from the Research to Prevent Blindness to the Cleveland Clinic Lerner College of Medicine of Case Western Reserve University.

**Disclaimer** The contents of this work do not represent the views of the United States Department of Veterans Affairs or the United States Government.

## References

Bell BA, Kaul C, Bonilha VL et al (2015) The BALB/c mouse: effect of standard vivarium lighting on retinal pathology during aging. Exp Eye Res 135:192–205

Bonilha VL, Bell BA, Rayborn ME et al (2015) Loss of DJ-1 elicits retinal abnormalities, visual dysfunction, and increased oxidative stress in mice. Exp Eye Res 139:22–36

Ng TF, Streilein JW (2001) Light-induced migration of retinal microglia into the subretinal space. Invest Ophthalmol Vis Sci 42:3301–3310

Pardue MT, Peachey NS (2014) Mouse b-wave mutants. Doc Ophthalmol 128:77–89

Pardue MT, McCall MA, LaVail MM et al (1998) A naturally occurring mouse model of X-linked congenital stationary night blindness. Invest Ophthalmol Vis Sci 39:2443–2449

Tarchick MJ, Bassiri P, Rohwer RM et al (2016) Early functional and morphologic abnormalities in the diabetic Nyxnob mouse retina. Invest Ophthalmol Vis Sci 57:3496–3508

Xu H, Chen M, Manivannan A et al (2008) Age-dependent accumulation of lipofuscin in perivascular and subretinal microglia in experimental mice. Aging Cell 7:58–68

# Part IV
# Inflammation and Angiogenesis

# Chapter 22
# The Role of Hypoxia, Hypoxia-Inducible Factor (HIF), and VEGF in Retinal Angiomatous Proliferation


**Maya Barben, Marijana Samardzija, and Christian Grimm**

**Abstract** In industrialized countries, age-related macular degeneration (AMD) is the leading cause of blindness in elderly people. Hallmarks of the non-neovascular (dry) form of AMD are the formation of drusen and geographic atrophy, whereas the exudative (wet) form of the disease is characterized by invading blood vessels. In retinal angiomatous proliferation (RAP), a special form of wet AMD, intraretinal vessels grow from the deep plexus into the subretinal space. Little is known about the mechanisms leading to intraretinal neovascularization, but age-related changes such as reduction of choroidal blood flow, accumulation of drusen, and thickening of the Bruch's membrane may lead to reduced oxygen availability in photoreceptors. Such a chronic hypoxic situation may induce several cellular response pathways including the stabilization of hypoxia-inducible factors (HIFs) and the production of angiogenic factors, such as vascular endothelial growth factor (VEGF). Here, we discuss the potential contribution of hypoxia and HIFs in RAP disease pathology and in some mouse models for subretinal neovascularization.

M. Barben
Lab for Retinal Cell Biology, Department of Ophthalmology, University Hospital Zurich, University of Zurich, Wagistr. 14, 8952 Schlieren, Switzerland

Neuroscience Center Zurich (ZNZ), University of Zurich, Zurich, Switzerland
e-mail: maya.barben@uzh.ch

M. Samardzija
Lab for Retinal Cell Biology, Department of Ophthalmology, University Hospital Zurich, University of Zurich, Wagistr. 14, 8952 Schlieren, Switzerland
e-mail: marijana.samardzija@usz.uzh.ch

C. Grimm (✉)
Lab for Retinal Cell Biology, Department of Ophthalmology, University Hospital Zurich, University of Zurich, Wagistr. 14, 8952 Schlieren, Switzerland

Neuroscience Center Zurich (ZNZ), University of Zurich, Zurich, Switzerland

Zurich Center for Integrative Human Physiology (ZIHP), University of Zurich, Zurich, Switzerland
e-mail: cgrimm@opht.uzh.ch



J. D. Ash et al. (eds.), *Retinal Degenerative Diseases*, Advances in Experimental Medicine and Biology 891, https://doi.org/10.1007/978-3-319-75402-4_22

**Keywords** Retinal angiomatous proliferation (RAP) · Age-related macular degeneration (AMD) · Hypoxia · HIF1A · Neovascularization · Vascular endothelial growth factor (VEGF) · Mouse model

## Abbreviations

| | |
|---|---|
| AMD | Age-related macular degeneration |
| CNV | Choroidal neovascularization |
| HIF | Hypoxia-inducible factors |
| PND | Postnatal day |
| RAP | Retinal angiomatous proliferation |
| RPE | Retinal pigment epithelium |
| VEGF | Vascular endothelial growth factor |
| VLDLR | Very low-density lipoprotein receptor |

## 22.1 Introduction

Retinal function can be affected by three variants of neovascularization (Grossniklaus et al. 2010). In retinal neovascular diseases such as diabetic retinopathy, central retinal vein occlusion, and retinopathy of prematurity, retinal vessels grow along the inner retinal surface and/or extend into the vitreous (Grossniklaus et al. 2010) due to retinal ischemia and increased concentrations of vascular endothelial growth factor (VEGF) (Aiello et al. 1994; Lashkari et al. 2000). In choroidal neovascularization (CNV) new vessels originate in the choroid and grow toward the retina, characteristic for wet age-related macular degeneration (AMD) (Bressler et al. 1988; Spaide 2013). Additionally, retinal angiomatous proliferation (RAP), also known as deep retinal vascular anomalous complexes, has been described (Yannuzzi et al. 2001). RAP is a distinct form of neovascular AMD, characterized by the growth of vessels that invade the subretinal space not from the choroid but from the retina. In RAP, vessels originate from the deep retinal plexus and cause intraretinal neovascularization mainly in the photoreceptor layer resulting in an abnormal communication between retinal and choroidal vasculatures (Hartnett et al. 1996; Yannuzzi et al. 2008; Atmani et al. 2010). However, since vessels originating from the choroid in CNV of late stage neovascular AMD can form connections with the retinal vasculature known as retinal-choroidal anastomosis, the distinction between a retinal or choroidal origin of vessel growth is sometimes difficult (Slakter et al. 2000; Scott and Bressler 2010). Therefore, the more general term “type 3 neovascularization” has been suggested (Freund et al. 2008), but RAP

is still the most frequently used designation. RAP has a poor clinical prognosis, and treatment of RAP remains difficult (Bottoni et al. 2005; Gross et al. 2005). The prevalence of RAP is estimated at 15–20% of neovascular AMD (Cohen et al. 2007; Massacesi et al. 2008).

## 22.2 Hypoxia and Hypoxia-Inducible Factors

The exact cause for neovascular AMD and particularly RAP is still unclear. Although VEGF plays a critical role in neovascularization, the triggering factor is still largely unknown. Hypoxia activates regulatory systems in the body with hypoxia-inducible factor 1 (HIF1) playing a central role. HIF1 heterodimers are composed of an oxygen-labile $\alpha$-subunit and a constitutively expressed $\beta$-subunit. Under normal oxygen levels, the HIF1A protein is rapidly degraded, which is mediated by hydroxylation of HIF1A by prolyl hydroxylases promoting its interaction with the von Hippel-Lindau ubiquitin E3 ligase complex. As a result, the HIF1A protein is degraded via the proteasomal pathway. Under hypoxia, hydroxylation does not occur, and hence, HIF1A gets stabilized, translocates into the nucleus, and enables transcription of target genes such as *VEGF* (Jaakkola et al. 2001; Grimm et al. 2002; Caprara and Grimm 2012). This can trigger neovascularization in an attempt to resolve the long-term tissue hypoxia. Besides hypoxia, other factors such as oxidative stress, inflammation, and disturbance in energy metabolism may also be involved in HIF1A stabilization (Cash et al. 2007; Dehne and Brune 2009; Joyal et al. 2016). Since a chronic hypoxic situation has been suggested to play an important role in RAP and AMD pathology (Arjamaa et al. 2009; Kent 2014), we discuss the potential contribution of tissue hypoxia and HIF1A stabilization for disease development.

## 22.3 Hypoxia and HIF in Neovascular AMD and RAP Pathology

In AMD patients, abnormalities in choroidal perfusion and vascular defects were described (reviewed in (Harris et al. 1999)), suggesting tissue hypoxia. In effect, strong VEGF protein immunoreactivity has been shown in surgically excised CNV membranes and transdifferentiated retinal pigment epithelial (RPE) cells of AMD patients (Kvanta et al. 1996; Lopez et al. 1996). Additionally, stabilized HIF1A and HIF2A were detected in the endothelium and macrophages of human choroidal neovascular membranes associated with AMD (Inoue et al. 2007).

In human patients with RAP, vitreous VEGF levels determined by ELISA are higher compared to control subjects (Joyal et al. 2016). Intravitreally injected anti-VEGF agents have been shown to be effective in blocking vessel growth and

improving vision in neovascular AMD (Solomon et al. 2014) and in RAP (Engelbert et al. 2009; Atmani et al. 2010). Evidence indicates that hypoxia and HIF transcription factors are important driving forces in RAP disease development. For example, Hartnett and colleagues hypothesized that large drusen and Bruch's membrane deposits observed in RAP could decrease retinal oxygenation and create a hypoxic microenvironment in the outer retina which may stimulate angiogenic growth factor release, vessel growth, and retinal degeneration (Hartnett et al. 1996). A thinner choroid and greater density of drusen have been observed in RAP patients compared to typical neovascular AMD patients, two factors that may cause ischemia and/or restrict oxygen availability for photoreceptors (Kim et al. 2013). Additionally, RPE detachment could intensify the hypoxic challenge by increasing the distance between the photoreceptors and the choroid (Hartnett et al. 1996). Shimada et al. reported HIF1A and HIF2A expression in the surroundings of VEGF-positive retinal neovascular areas in RAP specimens (Shimada et al. 2007). This suggests a hypoxia-mediated mechanism leading to VEGF expression in RAP.

In summary, hypoxic factors such as VEGF and HIF1 may be involved in both typical neovascular AMD and RAP disease pathology. However, RAP does not require perturbation of Bruch's membrane and/or RPE, unlike CNV (Campochiaro 2013).

## 22.4 *Rho/VEGF* and *Vldlr*$^{-/-}$ Mice: Two Animal Models for RAP

Transgenic mice expressing VEGF driven by the rhodopsin promoter (*rho/VEGF*) develop vessels that originate in the deep capillary bed of the retina and extend through the outer nuclear layer into the subretinal space (Okamoto et al. 1997). CNV has not been observed in these mice (Tobe et al. 1998). In addition, VEGF overexpression caused retinal neovascularization even in adult mice with a completely developed retinal vasculature (Ohno-Matsui et al. 2002). Less neovascularization has been observed in mice with ischemic retinopathy lacking the hypoxia response element in the *Vegf* promoter compared to control mice (Vinores et al. 2006), suggesting an important role for HIF1 in the regulation of VEGF-mediated neovascularization.

Mice with a partial deletion of exon 5 of the very low-density lipoprotein receptor gene lack functional VLDLR (*Vldlr*$^{-/-}$) (Frykman et al. 1995) and show a retinal phenotype resembling RAP lesions (Heckenlively et al. 2003). Due to increased VEGF levels (see below), *Vldlr*$^{-/-}$ mice exhibit retinal neovascularization with vessels originating within the outer plexiform layer. Vessels start to grow at postnatal day (PND) 15 and reach the subretinal space by PND20, and anastomoses with the choriocapillaris are observed at 3 months of age. This is accompanied by photoreceptor degeneration affecting predominantly cone cells (Hu et al. 2008; Dorrell et al. 2009). The increased VEGF levels observed in *Vldlr*$^{-/-}$ mice were initially

suggested to be linked to the negative regulatory role of VLDLR on Wnt signaling, which targets VEGF (Dorrell et al. 2009). However, since VLDLR has important functions in cholesterol homeostasis, lipid metabolism, and transport (Tiebel et al. 1999), Joyal and colleagues demonstrated that impaired fatty acid uptake in *Vldlr*$^{-/-}$ mice results in a reduction of $\alpha$-ketoglutarate, which decreases prolyl hydroxylase dehydrogenase activity and promotes the stabilization of HIF1A. Subsequently, VEGF levels are increased, leading to a RAP-like neovascular phenotype (Joyal et al. 2016). Thus, dysregulated energy metabolism might drive pathological neovascularization by stabilizing HIF1A.

## 22.5 Concluding Remarks and Future Therapeutic Perspectives

Pathological vessel growth in wet AMD and RAP are both associated with increased VEGF levels and are currently treated by frequent intraocular injections of anti-VEGF agents. However, such treatment should not downregulate VEGF below basal concentrations since physiological levels of VEGF are needed for proper visual function. It has been shown for example that an RPE-specific *Vegf* deletion leads to atrophy of the choriocapillaris and cone degeneration (Kurihara et al. 2012; Kurihara et al. 2016). Its hypoxia-specific regulator *Hif1a*, however, can be safely inactivated in RPE (Kurihara et al. 2012), adult rods (Thiersch et al. 2009), and cones (author's unpublished data). Therefore, tissue-specific targeting HIF1A may provide a valid and safe therapeutical approach to treat RAP and potentially AMD. Animal models such as *rho/VEGF* and *Vldlr*$^{-/-}$ mice are clearly important to test and improve such treatment strategies. However, considering that these mice lack a cone-rich region resembling the human macular region, more research is needed to determine the influence of hypoxia, HIF1A, and VEGF on cone survival and function.

## References

Aiello LP, Avery RL, Arrigg PG et al (1994) Vascular endothelial growth factor in ocular fluid of patients with diabetic retinopathy and other retinal disorders. N Engl J Med 331:1480–1487

Arjamaa O, Nikinmaa M, Salminen A et al (2009) Regulatory role of HIF-1 a in the pathogenesis of age-related macular. Ageing Res Rev 8:349–358

Atmani K, Voigt M, Le Tien V et al (2010) Ranibizumab for retinal angiomatous proliferation in age-related macular degeneration. Eye (Lond) 24:1193–1198

Bottoni F, Massacesi A, Cigada M et al (2005) Treatment of retinal angiomatous proliferation in age-related macular degeneration: a series of 104 cases of retinal angiomatous proliferation. Arch Ophthalmol 123:1644–1650

Bressler NM, Bressler SB, Fine SL (1988) Age-related macular degeneration. Surv Ophthalmol 32:375–413

Campochiaro PA (2013) Ocular neovascularization. J Mol Med (Berl) 91:311–321
Caprara C, Grimm C (2012) From oxygen to erythropoietin: relevance of hypoxia for retinal development, health and disease. Prog Retin Eye Res 31:89–119
Cash TP, Pan Y, Simon MC (2007) Reactive oxygen species and cellular oxygen sensing. Free Radic Biol Med 43:1219–1225
Cohen SY, Creuzot-Garcher C, Darmon J et al (2007) Types of choroidal neovascularisation in newly diagnosed exudative age-related macular degeneration. Br J Ophthalmol 91:1173–1176
Dehne N, Brune B (2009) HIF-1 in the inflammatory microenvironment. Exp Cell Res 315:1791–1797
Dorrell MI, Aguilar E, Jacobson R et al (2009) Antioxidant or neurotrophic factor treatment preserves function in a mouse model of neovascularization-associated oxidative stress. J Clin Invest 119:611–623
Engelbert M, Zweifel SA, Freund KB (2009) "Treat and extend" dosing of intravitreal antivascular endothelial growth factor therapy for type 3 neovascularization/retinal angiomatous proliferation. Retina 29:1424–1431
Freund KB, Ho IV, Barbazetto IA et al (2008) Type 3 neovascularization: the expanded spectrum of retinal angiomatous proliferation. Retina 28:201–211
Frykman PK, Brown MS, Yamamoto T et al (1995) Normal plasma lipoproteins and fertility in gene-targeted mice homozygous for a disruption in the gene encoding very low density lipoprotein receptor. Proc Natl Acad Sci U S A 92:8453–8457
Grimm C, Wenzel A, Groszer M et al (2002) HIF-1-induced erythropoietin in the hypoxic retina protects against light-induced retinal degeneration. Nat Med 8:718–724
Gross NE, Aizman A, Brucker A et al (2005) Nature and risk of neovascularization in the fellow eye of patients with unilateral retinal angiomatous proliferation. Retina 25:713–718
Grossniklaus HE, Kang SJ, Berglin L (2010) Animal models of choroidal and retinal neovascularization. Prog Retin Eye Res 29:500–519
Harris A, Chung HS, Ciulla TA et al (1999) Progress in measurement of ocular blood flow and relevance to our understanding of glaucoma and age-related macular degeneration. Prog Retin Eye Res 18:669–687
Hartnett ME, Weiter JJ, Staurenghi G et al (1996) Deep retinal vascular anomalous complexes in advanced age-related macular degeneration. Ophthalmology 103:2042–2053
Heckenlively JR, Hawes NL, Friedlander M et al (2003) Mouse model of subretinal neovascularization with choroidal anastomosis. Retina 23:518–522
Hu W, Jiang A, Liang J et al (2008) Expression of VLDLR in the retina and evolution of subretinal neovascularization in the knockout mouse model's retinal angiomatous proliferation. Invest Ophthalmol Vis Sci 49:407–415
Inoue Y, Yanagi Y, Matsuura K et al (2007) Expression of hypoxia-inducible factor 1alpha and 2alpha in choroidal neovascular membranes associated with age-related macular degeneration. Br J Ophthalmol 91:1720–1721
Jaakkola P, Mole DR, Tian YM et al (2001) Targeting of HIF-alpha to the von Hippel-Lindau ubiquitylation complex by O2-regulated prolyl hydroxylation. Science 292:468–472
Joyal JS, Sun Y, Gantner ML et al (2016) Retinal lipid and glucose metabolism dictates angiogenesis through the lipid sensor Ffar1. Nat Med 22:439–445
Kent DL (2014) Age-related macular degeneration: beyond anti-angiogenesis. Mol Vis 20:46–55
Kim JH, Kim JR, Kang SW et al (2013) Thinner choroid and greater drusen extent in retinal angiomatous proliferation than in typical exudative age-related macular degeneration. Am J Ophthalmol 155:743–749. 749 e741–742
Kurihara T, Westenskow PD, Bravo S et al (2012) Targeted deletion of Vegfa in adult mice induces vision loss. J Clin Invest 122:4213–4217
Kurihara T, Westenskow PD, Gantner ML et al (2016) Hypoxia-induced metabolic stress in retinal pigment epithelial cells is sufficient to induce photoreceptor degeneration. elife 5:pii:e14319

Kvanta A, Algvere PV, Berglin L et al (1996) Subfoveal fibrovascular membranes in age-related macular degeneration express vascular endothelial growth factor. Invest Ophthalmol Vis Sci 37:1929–1934

Lashkari K, Hirose T, Yazdany J et al (2000) Vascular endothelial growth factor and hepatocyte growth factor levels are differentially elevated in patients with advanced retinopathy of prematurity. Am J Pathol 156:1337–1344

Lopez PF, Sippy BD, Lambert HM et al (1996) Transdifferentiated retinal pigment epithelial cells are immunoreactive for vascular endothelial growth factor in surgically excised age-related macular degeneration-related choroidal neovascular membranes. Invest Ophthalmol Vis Sci 37:855–868

Massacesi AL, Sacchi L, Bergamini F et al (2008) The prevalence of retinal angiomatous proliferation in age-related macular degeneration with occult choroidal neovascularization. Graefes Arch Clin Exp Ophthalmol 246:89–92

Ohno-Matsui K, Hirose A, Yamamoto S et al (2002) Inducible expression of vascular endothelial growth factor in adult mice causes severe proliferative retinopathy and retinal detachment. Am J Pathol 160:711–719

Okamoto N, Tobe T, Hackett SF et al (1997) Transgenic mice with increased expression of vascular endothelial growth factor in the retina: a new model of intraretinal and subretinal neovascularization. Am J Pathol 151:281–291

Scott AW, Bressler SB (2010) Retinal angiomatous proliferation or retinal anastomosis to the lesion. Eye (Lond) 24:491–496

Shimada H, Kawamura A, Mori R et al (2007) Clinicopathological findings of retinal angiomatous proliferation. Graefes Arch Clin Exp Ophthalmol 245:295–300

Slakter JS, Yannuzzi LA, Schneider U et al (2000) Retinal choroidal anastomoses and occult choroidal neovascularization in age-related macular degeneration. Ophthalmology 107:742–753. discussion 753–744

Solomon SD, Lindsley K, Vedula SS et al (2014) Anti-vascular endothelial growth factor for neovascular age-related macular degeneration. Cochrane Database Syst Rev: CD005139

Spaide RF (2013) Clinical manifestations of choroidal neovascularization in AMD. In: Holz FG, Pauleikhoff D, Spaide RF, Bird AC (eds) Age-related macular degeneration. Springer, Berlin, Heidelberg

Thiersch M, Lange C, Joly S et al (2009) Retinal neuroprotection by hypoxic preconditioning is independent of hypoxia-inducible factor-1 alpha expression in photoreceptors. Eur J Neurosci 29:2291–2302

Tiebel O, Oka K, Robinson K et al (1999) Mouse very low-density lipoprotein receptor (VLDLR): gene structure, tissue-specific expression and dietary and developmental regulation. Atherosclerosis 145:239–251

Tobe T, Okamoto N, Vinores MA et al (1998) Evolution of neovascularization in mice with overexpression of vascular endothelial growth factor in photoreceptors. Invest Ophthalmol Vis Sci 39:180–188

Vinores SA, Xiao WH, Aslam S et al (2006) Implication of the hypoxia response element of the Vegf promoter in mouse models of retinal and choroidal neovascularization, but not retinal vascular development. J Cell Physiol 206:749–758

Yannuzzi LA, Negrao S, Iida T et al (2001) Retinal angiomatous proliferation in age-related macular degeneration. Retina 21:416–434

Yannuzzi LA, Freund KB, Takahashi BS (2008) Review of retinal angiomatous proliferation or type 3 neovascularization. Retina 28:375–384

# Chapter 23
# Neuroinflammation in Retinitis Pigmentosa, Diabetic Retinopathy, and Age-Related Macular Degeneration: A Minireview

**Michael T. Massengill, Chulbul M. Ahmed, Alfred S. Lewin, and Cristhian J. Ildefonso**

**Abstract** The eye is an immuno-privileged organ. However, certain diseases such as uveitis are intrinsically linked to inflammation. In several retinal degenerative diseases, there is a unique damage at the onset of the disease, but evidence suggests that chronic and low-grade inflammatory processes play an important role in their progression. Studies have identified similar signaling pathways and changes in resident immune cells within the retina among these diseases. Herein, we will discuss some of these studies and propose how understanding this inflammatory response could aid in the development of therapies.

**Keywords** Inflammation · Microglia · Müller glia · Diabetic retinopathy · Retinitis pigmentosa · Age-related macular degeneration

## 23.1 Introduction

Retinal degenerative diseases are characterized by the progressive loss of retinal function. The cause of degeneration can vary significantly from genetic mutations as in retinitis pigmentosa (RP) to metabolic changes in diabetic retinopathy (DR). In age-related macular degeneration (AMD), both genetic predisposition and environmental cues (i.e., such as smoking) are the main causes of the disease. Studies indicate that these diseases share a common chronic inflammatory process that are mediated by Müller glial and microglial cells.

M. T. Massengill · C. M. Ahmed · A. S. Lewin
Department of Molecular Genetics & Microbiology, University of Florida College of Medicine, Gainesville, FL, USA

C. J. Ildefonso (✉)
Department of Ophthalmology, University of Florida College of Medicine, Gainesville, FL, USA
e-mail: ildefons@ufl.edu



J. D. Ash et al. (eds.), *Retinal Degenerative Diseases*, Advances in Experimental Medicine and Biology 891, https://doi.org/10.1007/978-3-319-75402-4_23

The functions of glial cells are to support and maintain tissue homeostasis within the retina. Müller glia are known for their elongated body spanning the entire retinal thickness. These cells have multiple roles within the retina including buffering ion concentrations, secreting neuroactive molecules (e.g., GABA), and responding to alterations to the retinal damage by secreting cytokines, a process known as "gliosis." Another group of resident glial cells are the microglia. These cells are derived from erythro-myeloid progenitor cells from the yolk sac (Gomez Perdiguero et al. 2015). Microglia are important in the maintenance of the synaptic function of the photoreceptors (Wang et al. 2016). When responding to damage, microglia change their morphology from "branched" to an "amoeboid" morphology. These activated microglia upregulate the expression of pro-inflammatory cytokines (i.e., IL-1β and TNF-α) and cellular markers such as Iba-1 and TSPO (Karlstetter et al. 2014). This activation starts a complex inflammatory process that, when unresolved, leads to the recruitment of peripheral macrophages and significant retinal damage.

## 23.2 Neuroinflammation in Retinitis Pigmentosa

A current perspective in the field of RP proposes that photoreceptor degeneration is potentiated by molecular mechanisms that occur outside of rods and in a manner that is independent of the inciting mutation. Thus, a shared death pathway that exacerbates photoreceptor damage may exist (Hicks and Sahel 1999).

A number of studies in humans suggest that inflammatory processes occur during RP. An elevation in several pro-inflammatory cytokines, including IL-1β and IL-6, was reported in vitreal samples belonging to humans affected by RP (Yoshida et al. 2013). Also, Gupta et al. observed that microglia engulf rods during RP pathogenesis in human samples (Gupta et al. 2003).

Several animal models of RP corroborate the existence of inflammation during RP pathogenesis. For example, cytokines that are intimately associated with the pro-inflammatory transcription factor NF-κB, including IL-1β, were elevated in the T17 M rhodopsin mouse model of RP (Rana et al. 2014). Data suggest that the inflammatory processes detected during retinal degeneration in RP provoke further damage to photoreceptors. RP mice containing a knockout of inflammatory signaling proteins, including MyD88 (Syeda et al. 2015) or caspase-1 (Samardzija et al. 2006), exhibited slower retinal degeneration. Furthermore, pharmacologic blockade of key pro-inflammatory cytokines, such as IL-1β (Zhao et al. 2015), also decreased photoreceptor loss in animal models of RP.

Growing evidence suggests that dysregulated activation of microglia propagates photoreceptor injury in RP through phagocytosis of photoreceptors, generation of ROS (Zeng et al. 2014), and secretion of IL-1β (Zabel et al. 2016). Therefore, an effort has been made to elucidate the specific roles of microglia during retinal degeneration in order to target microglial activity as a treatment (Peng et al. 2014). The activation of microglia likely involves a complex interplay with other cells types in the retina and multiple signaling pathways, such as CCL2 (Guo et al. 2012).

Kohno et al. suggested that photoreceptor proteins can activate microglia via TLR4 (Kohno et al. 2013), perhaps after their phagocytosis of rods (Zhao et al. 2015). Additionally, the CX3CR1-CX3CL1 axis, which represents cross talk between degenerating neurons and microglia, has received attention, whose overexpression may prove effective in abrogating noxious microglial activity in RP (Zabel et al. 2016). Furthermore, Müller cell gliosis likely boasts protective properties early in disease course, with the release of molecules like glial-derived neurotrophic factor (Sanftner et al. 2001). However, Müller cells may promote microglia activation via decreasing their expression of anti-inflammatory molecules, like TGF-β, as well as engaging in a positive feedback loop of pro-inflammatory cytokine signaling with microglia (Wang et al. 2011).

## 23.3 Neuroinflammation in Diabetic Retinopathy

DR is a visual comorbidity of both type 1 and type 2 diabetes. Increases in glucose are known to lead to both increases in oxidative stress and inflammation (El-Remessy et al. 2015). The generation of advanced glycated end products (AGEs) and their engagement of the receptor for AGEs (RAGEs) are known to play an important role in the pathophysiology of DR. In their article, McVicar et al. observed that compared to wild-type diabetic mice, the $RAGE^{-/-}$ mice had less microvascular alterations as well as decreased microglia activation as determined by immunofluorescence (McVicar et al. 2015). Studies have also demonstrated that the effects of RAGE activation in microglia are mediated by NF-κB and PPARγ (Wang et al. 2015), leading to the production of TNF-α.

The changes in glucose metabolism are linked to increase in pro-inflammatory cytokines, chemokines, growth factors, and cellular changes. Arroba et al. showed that db/db mice have an increase in TNF-α and IL-1β with an increase in the number of M2 microglia (Arroba et al. 2016). Using a bone marrow transplant model, Chakravarthy et al. reported similar results (Chakravarthy et al. 2016). In mice transplanted with $GFP^+$ monocytes/macrophages, the induction of diabetes caused an increase in the recruitment of $GFP^+$/Iba-$1^+$ cells within their retinas suggesting the recruitment and activation of peripheral monocytes. Further characterization identified a reduction in circulating bone marrow-derived angiogenic cells with an increase of these cells in the bone marrow. This indicates a recruitment of inflammatory macrophage/microglia concomitant with a sequestration of protective cells within the bone marrow.

## 23.4 Neuroinflammation in Age-Related Macular Degeneration

AMD is the leading cause of loss of vision and affects nearly 50 million elderly people worldwide. It affects the macula which is required for central vision. Accumulation of oxidized lipoproteins as well as free radicals in the retina, RPE, and choroidal tissue activates the innate immune response, termed as para-inflammation. Drusen deposits between the RPE and choroid are seen as a compartmentalized accumulation of cellular debris consisting of oxidized lipids and proteins originating from RPE, complement factor proteins, Alzheimer's amyloid-β (Aβ) peptide, serum amyloid P component, immunoglobulin light chains, and the glycoprotein vitronectin. In a seminal discovery, Doyle et al. demonstrated that human drusen was capable of activating the NLRP3 inflammasome and inducing the secretion of active IL-1β and IL-18 (Doyle et al. 2012). Since oxidative stress is the main initiator of AMD, products of lipid oxidation (carboxyethyl pyrrole, CEP-protein adducts) and oxidative protein modifications and advanced glycation products are present in AMD drusen. Activation of the inflammasome NLRP3 takes place when the components of drusen gain entry into RPE. The inflammatory cytokines (IL-1β, IL-6, TNFα), the ligands of TLRs, or PRRs, acting through their cognate receptors activate the transcription factor, NF-kB, which results in the transcription of NLRP3, pre-IL-1β, and pre-IL-18. Stimulus for the formation of the NLRP3 inflammasome comes from the complement factor(s), reactive oxygen species (ROS), or oxidized proteins and DNA, arising from damaged mitochondria, cathepsin B from lysosomal degradation, or the Alu RNA generated from a deficiency of DICER1 (Ildefonso et al. 2016). Formation of the NLRP3 inflammasome requires NLRP3 oligomerization, recruitment of an adaptor protein ASC and procaspase-1. This leads to autocatalytic cleavage of inactive procaspase-1 to mature and active caspase-1. Caspase-1 cleaves pre-IL-1β and pre-IL-18 to generate the mature and secreted forms of IL-1β and IL-18. Generation of caspase-1 can lead to cell death by pyroptosis, which is characterized by rupture of plasma membrane and release of cellular contents. The oxidized proteins, lipids, and DNA thus released form neoantigens due to desequestration and after they are taken up by the neighboring dendritic cells and macrophages. Thus, AMD has been regarded as an autoimmune response due to the high titers of anti-carboxyethyl pyrrole (CEP) adducts in AMD patients (Perez and Caspi 2015).

Release of IL-1β induces expression and secretion of the chemokines IL-8 and MCP-1 in RPE cells, together with the loss of tight junction proteins. This leads to a breakage of blood-brain barrier (BBB) and the recruitment of leukocytes and macrophages, thus amplifying the inflammatory response. IL-18 expression enhances the production of IFNγ, leading to generation of Th1 cells causing greater inflammation. In addition, enhanced production of IL-17 has been reported in patients with advanced AMD (Ardeljan et al. 2014). The simultaneous enhancement of Th1 and Th17 responses in AMD is reminiscent of the situation in uveitis.

## 23.5 Conclusions

Studies on inflammation in retinal degenerative diseases suggest common pathways that could be potentially targeted. Anti-inflammatory biological agents used in other conditions such as arthritis (i.e., adalimumab, etanercept, and infliximab) could hold great promise when tested in retinal degenerative diseases (Wu et al. 2011). Alternatively, viral vectors in the retina have been very well studied and clinical trials suggest their safety (Boye et al. 2013). Our group is currently exploring this venue by developing anti-inflammatory gene therapy approaches with both eukaryotic and viral genes (Ildefonso et al. 2015a, b).

Future studies should address how inflammatory cells are recruited into the retina during retinal degeneration. A better understanding of the resolution phase in these diseases could provide novel targets for therapeutic interventions. Although inflammation seems to be secondary in retinal degeneration, it is perhaps an important disease modifier. Thus, anti-inflammatory therapies could hold potential as they could slow retinal degeneration significantly, having a great impact in the quality of life of affected individuals.

**Acknowledgments** This work was supported by a grant from the National Eye Institute (EY026268), a BrightFocus Foundation travel award, and a grant from the Research to Prevent Blindness Foundation.

## References

Ardeljan D, Wang Y, Park S, Shen D, Chu XK, Yu C-R, Abu-Asab M, Tuo J, Eberhart CG, Olsen TW, Mullins RF, White G, Wadsworth S, Scaria A, Chan C-C (2014) Interleukin-17 retinotoxicity is prevented by gene transfer of a soluble Interleukin-17 receptor acting as a cytokine blocker: implications for age-related macular degeneration. PLoS One 9:e95900

Arroba AI, Alcalde-Estevez E, García-Ramírez M, Cazzoni D, de la Villa P, Sánchez-Fernández EM, Mellet CO, García Fernández JM, Hernández C, Simó R, Valverde ÁM (2016) Modulation of microglia polarization dynamics during diabetic retinopathy in db/db mice. Biochim Biophys Acta (BBA) Mol Basis Dis 1862:1663–1674

Boye SE, Boye SL, Lewin AS, Hauswirth WW (2013) A comprehensive review of retinal gene therapy. Mol Ther 21:509–519

Chakravarthy H, Beli E, Navitskaya S, O'Reilly S, Wang Q, Kady N, Huang C, Grant MB, Busik JV (2016) Imbalances in mobilization and activation of pro-inflammatory and vascular reparative bone marrow-derived cells in diabetic retinopathy. PLoS One 11:e0146829

Doyle SL, Campbell M, Ozaki E, Salomon RG, Mori A, Kenna PF, Farrar GJ, Kiang A-S, Humphries MM, Lavelle EC, O'Neill LAJ, Hollyfield JG, Humphries P (2012) NLRP3 has a protective role in age-related macular degeneration through the induction of IL-18 by drusen components. Nat Med 18:791–798

El-Remessy A, Coucha M, Elshaer S, Eldahshan W, Mysona B (2015) Molecular mechanisms of diabetic retinopathy: potential therapeutic targets. Middle East Afr J Ophthalmol 22:135

Gomez Perdiguero E, Klapproth K, Schulz C, Busch K, Azzoni E, Crozet L, Garner H, Trouillet C, de Bruijn MF, Geissmann F, Rodewald H-R (2015) Tissue-resident macrophages originate from yolk-sac-derived erythro-myeloid progenitors. Nature 518:547–551

Guo C, Otani A, Oishi A, Kojima H, Makiyama Y, Nakagawa S, Yoshimura N (2012) Knockout of ccr2 alleviates photoreceptor cell death in a model of retinitis pigmentosa. Exp Eye Res 104:39–47

Gupta N, Brown KE, Milam AH (2003) Activated microglia in human retinitis pigmentosa, late-onset retinal degeneration, and age-related macular degeneration. Exp Eye Res 76:463–471

Hicks D, Sahel J (1999) The implications of rod-dependent cone survival for basic and clinical research. Invest Ophthalmol Vis Sci 40:3071–3074

Ildefonso CJ, Jaime H, Biswal MR, Boye SE, Li Q, Hauswirth WW, Lewin AS (2015a) Gene therapy with the caspase activation and recruitment domain reduces the ocular inflammatory response. Mol Ther J Am Soc Gene Ther 23:875–884

Ildefonso CJ, Jaime H, Rahman MM, Li Q, Boye SE, Hauswirth WW, Lucas AR, McFadden G, Lewin AS (2015b) Gene delivery of a viral anti-inflammatory protein to combat ocular inflammation. Hum Gene Ther 26:59–68

Ildefonso CJ, Biswal MR, Ahmed CM, Lewin AS (2016) The NLRP3 inflammasome and its role in age-related macular degeneration. Adv Exp Med Biol 854:59–65

Karlstetter M, Nothdurfter C, Aslanidis A, Moeller K, Horn F, Scholz R, Neumann H, Weber BHF, Rupprecht R, Langmann T (2014) Translocator protein (18 kDa) (TSPO) is expressed in reactive retinal microglia and modulates microglial inflammation and phagocytosis. J Neuroinflammation 11:3

Kohno H, Chen Y, Kevany BM, Pearlman E, Miyagi M, Maeda T, Palczewski K, Maeda A (2013) Photoreceptor proteins initiate microglial activation via toll-like receptor 4 in retinal degeneration mediated by all-trans-retinal. J Biol Chem 288:15326–15341

McVicar CM, Ward M, Colhoun LM, Guduric-Fuchs J, Bierhaus A, Fleming T, Schlotterer A, Kolibabka M, Hammes H-P, Chen M, Stitt AW (2015) Role of the receptor for advanced glycation endproducts (RAGE) in retinal vasodegenerative pathology during diabetes in mice. Diabetologia 58:1129–1137

Peng B, Xiao J, Wang K, So K-F, Tipoe GL, Lin B (2014) Suppression of microglial activation is neuroprotective in a mouse model of human retinitis pigmentosa. J Neurosci 34:8139–8150

Perez VL, Caspi RR (2015) Immune mechanisms in inflammatory and degenerative eye disease. Trends Immunol 36:354–363

Rana T, Shinde VM, Starr CR, Kruglov AA, Boitet ER, Kotla P, Zolotukhin S, Gross AK, Gorbatyuk MS (2014) An activated unfolded protein response promotes retinal degeneration and triggers an inflammatory response in the mouse retina. Cell Death Dis 5:e1578

Samardzija M, Wenzel A, Thiersch M, Frigg R, Remé C, Grimm C (2006) Caspase-1 ablation protects photoreceptors in a model of autosomal dominant retinitis pigmentosa. Invest Ophthalmol Vis Sci 47:5181–5190

Sanftner LHM, Abel H, Hauswirth WW, Flannery JG (2001) Glial cell line derived neurotrophic factor delays photoreceptor degeneration in a transgenic rat model of retinitis pigmentosa. Mol Ther 4:622–629

Syeda S, Patel AK, Lee T, Hackam AS (2015) Reduced photoreceptor death and improved retinal function during retinal degeneration in mice lacking innate immunity adaptor protein MyD88. Exp Neurol 267:1–12

Wang M, Ma W, Zhao L, Fariss RN, Wong WT (2011) Adaptive Müller cell responses to microglial activation mediate neuroprotection and coordinate inflammation in the retina. J Neuroinflammation 8:173

Wang L, Chen K, Liu K, Zhou Y, Zhang T, Wang B, Mi M (2015) DHA inhibited AGEs-induced retinal microglia activation via suppression of the PPARγ/NFκB pathway and reduction of signal transducers in the AGEs/RAGE axis recruitment into lipid rafts. Neurochem Res 40:713–722

Wang X, Zhao L, Zhang J, Fariss RN, Ma W, Kretschmer F, Wang M, hua QH, Badea TC, Diamond JS, Gan W-B, Roger JE, Wong WT (2016) Requirement for microglia for the maintenance of synaptic function and integrity in the mature retina. J Neurosci 36:2827–2842

Wu L, Hernandez-Bogantes E, Roca JA, Arevalo JF, Barraza K, Lasave AF (2011) Intravitreal tumor necrosis factor inhibitors in the treatment of refractory diabetic macular edema: a pilot study from the Pan-American Collaborative Retina Study Group. Retina Phila Pa 31:298–303

Yoshida N, Ikeda Y, Notomi S, Ishikawa K, Murakami Y, Hisatomi T, Enaida H, Ishibashi T (2013) Clinical evidence of sustained chronic inflammatory reaction in retinitis pigmentosa. Ophthalmology 120:100–105

Zabel MK, Zhao L, Zhang Y, Gonzalez SR, Ma W, Wang X, Fariss RN, Wong WT (2016) Microglial phagocytosis and activation underlying photoreceptor degeneration is regulated by CX3CL1-CX3CR1 signaling in a mouse model of retinitis pigmentosa. Glia 64:1479–1491

Zeng H, Ding M, Chen X-X, Lu Q (2014) Microglial NADPH oxidase activation mediates rod cell death in the retinal degeneration in rd mice. Neuroscience 275:54–61

Zhao L, Zabel MK, Wang X, Ma W, Shah P, Fariss RN, Qian H, Parkhurst CN, Gan W-B, Wong WT (2015) Microglial phagocytosis of living photoreceptors contributes to inherited retinal degeneration. EMBO Mol Med 7(9): 1087–1243

# Chapter 24
# Autoimmune Retinopathy: An Immunologic Cellular-Driven Disorder


**John R. Heckenlively and Steven K. Lundy**

**Abstract** Autoimmune retinopathy (AIR) was often mistaken for retinitis pigmentosa (RP), due to an overlap of clinical findings, but increasingly has been recognized as a unique entity in the last decade. AIR has distinctive features: sudden onset of photopsias and scotomata in patients with no family history of RP, followed by visual field and central vision loss. Initially, retina exams are normal with no sign of pigment deposits or retinal degeneration. A family history of autoimmune diseases (all types) occurs in 60% of patients. One hallmark of AIR has been the presence of anti-retinal autoimmune antibodies (ARAs) in patients' sera, but patients can continue to have ARAs even when the disease has been quiescent for years. The accumulation of ARAs represents a breakdown of retinal immune tolerance with many different immunoreactive bands found at different reference weights in AIR patients. We began investigating cellular immunity using flow cytometry and found abnormal distributions (>2 StDev) of increased memory lymphocytes and NK cells and decreased regulatory B cell subsets in many AIR patients compared to normal controls. Culture of patient lymphocytes with small amounts (25 μg) of recoverin protein for 6 days led to significant elevations of interferon gamma (IFNγ) and in some cases tumor necrosis factor alpha (TNFα) production. We found the IFNγ/IL-10 ratio in response to recoverin was elevated in patients with more active disease (defined by visual field contraction between visits), but in some patients, there also appeared to be independent factors influencing severity, suggesting other autoimmune mechanisms were at play. These cellular immune parameters may provide improved markers for active AIR.

J. R. Heckenlively (✉)
Department of Ophthalmology and Visual Sciences, Kellogg Eye Center, University of Michigan Medical School, Ann Arbor, MI, USA
e-mail: jrheck@umich.edu

S. K. Lundy
Department of Internal Medicine-Rheumatology, University of Michigan Medical School, Ann Arbor, MI, USA

Graduate Program in Immunology, University of Michigan Medical School, Ann Arbor, MI, USA



J. D. Ash et al. (eds.), *Retinal Degenerative Diseases*, Advances in Experimental Medicine and Biology 891, https://doi.org/10.1007/978-3-319-75402-4_24

**Keywords** Autoimmune retinopathy · Immune tolerance · Cellular immunity · Anti-retinal antibodies · Cytokines · Retinitis pigmentosa · Recoverin

## 24.1 Introduction

While autoimmune retinopathy (AIR) in the form of cancer-associated retinopathy was demonstrated in 1987 to be a paraneoplastic event (Thirkill et al. 1989), it was reported in 2009 that most cases of AIR are not associated with cancer (Ferreyra et al. 2009); these cases were termed nonneoplastic AIR. In a recent consensus paper, the term np-AIR was switched to AIR since most cases do not have cancer (Fox et al. 2016). The diagnosis of autoimmune retinopathy (AIR) is usually challenging, since a constellation of findings and symptoms have to be recognized to fulfill the diagnosis. The initial symptoms are vague and the lack of fundus changes in particular is confounding (Fig. 24.1a). Patients report that the initial symptom is abrupt onset of photopsia followed by scotomata. An abnormal electroretinogram (Fig. 24.1b) and

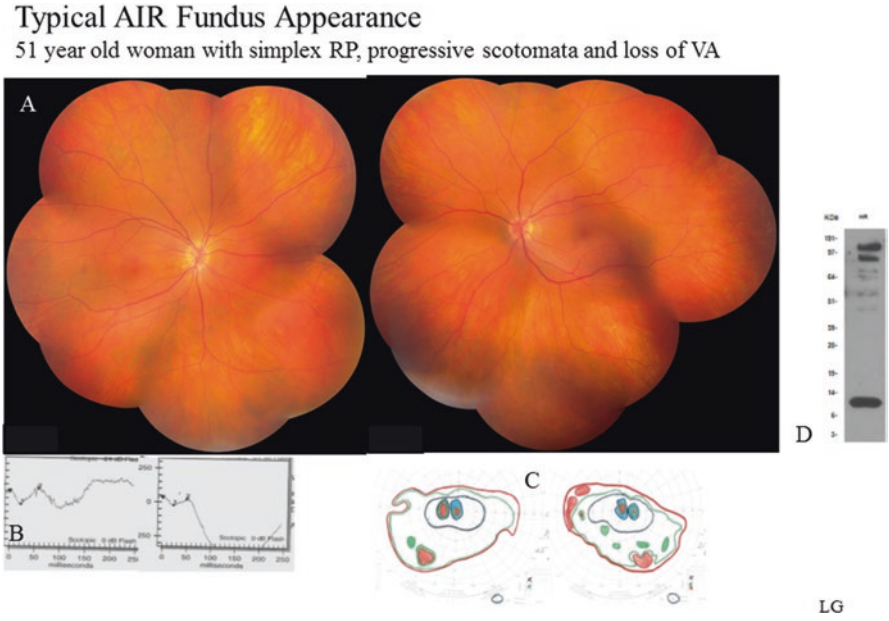


**Fig. 24.1** Composite, typical case autoimmune retinopathy of a 51-year-old female with 2-year history of sudden onset of vision loss, photopsias, blind spots, and decreased visual acuity. There was no history of retinitis pigmentosa, but her sister had lupus and her mother rheumatoid arthritis. (**a**) Relatively normal-looking fundus. (**b**) Bright-flash dark-adapted electroretinograms showing negative waveforms in both eyes. (**c**) Goldmann visual fields with central and scattered scotomata, contraction of I-4e isopter. (**d**) Western blot demonstrating three strong and four weak anti-retinal immunoreactive bands

**Table 24.1** Summary and additional points

| |
|---|
| 1. Active AIR is associated with high ratio of IFNγ/IL-10 (60%) or >2 SD elevated IFNγ. Rituxan-treated patients lose these markers temporarily |
| 2. About 25% of AIR patients develop elevations of NK cells, and those who have >2 SD values above controls have faster visual field loss |
| 3. About 10% of patients have elevated TNFα suggesting they may respond to infliximab. About 60% of AIR patients show stabilization on mycophenolate mofetil and other immunosuppressants |
| 4. Collaboration with rheumatology in managing the immunosuppression and in detecting other AI disorders is recommended |
| 5. Tapering medications in AIR has to be done cautiously, and patients should be followed closely as they can show regression |
| 6. The tests described in this talk are still in the research arena and are not commercially available |
| 7. Testing for anti-retinal antibodies as a marker of the disease plus documenting disease progression (activity) currently should be sufficient evidence to initiate treatment |
| 8.When available, the IFNγ/IL-10 ratio may aid in tracking disease activity |

visual field changes (Fig. 24.1c) confirm the clinical diagnosis of AIR in the face of a normal-appearing symptomatic patient (Fox et al. 2016). Detection of serum anti-retinal antibodies helps diagnostically (Fig. 24.1d), but does not tell specifically if the disease is active or in a quiescent stage. Serial visual field testing and interviewing the patient for active vision loss will often clarify if the disease is active. Another source of confusion is that a minority of cases that has yet to be exactly quantified have concurrent autoimmune optic neuropathy and thus have contracted visual fields from the neuropathy. Many of these cases can be identified because they have better electroretinogram amplitudes than would be expected from the small field size. Some of these patients have anti-optic nerve antibodies on Western blot (with homogenized optic nerve tissue), but this is a variable finding in our experience (Thirkill et al. 1989; Oyama et al. 2009; Adamus et al. 2011) (Table 24.1).

## 24.2 Materials and Methods

### *24.2.1 Patients and Blood Samples*

Patients with AIR are often referred to the retinal dystrophy clinic for evaluation because of overlapping features to retinitis pigmentosa (RP). From April 2014 to October 2015, after informed consent, 150 patients with AIR had blood drawn for flow cytometry and other tests as shown diagrammatically in Fig. 24.2. Within this group, 13 patients were newly diagnosed and had not been on any previous immunosuppressive therapies, and comparisons were made between these untreated AIR patients and 8 individuals with RP and no signs of autoimmunity and 6 age-matched healthy controls.

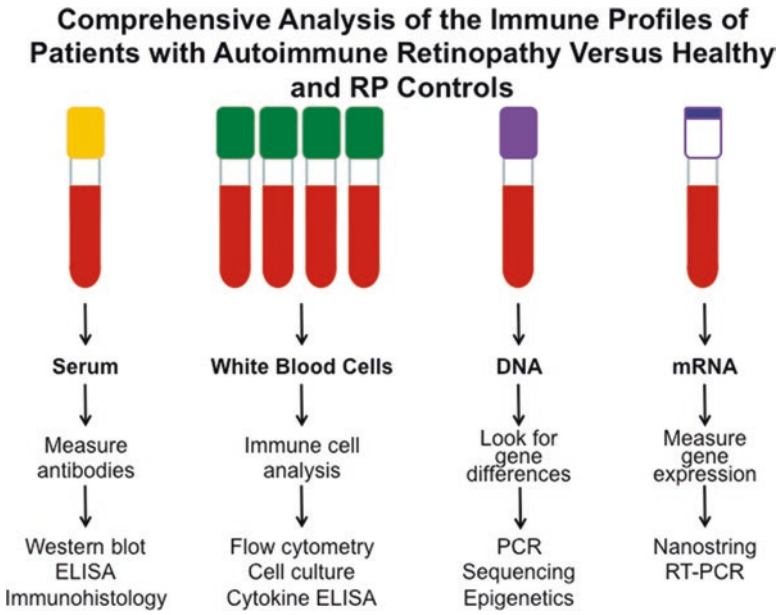


**Fig. 24.2** Protocol for testing autoimmune profiles in AIR patients. Blood is drawn after informed consent and tested by Western blot for human anti-retinal antibodies and flow cytometry to identify the lymphocyte markers and cell types, after which the lymphocytes are cultured for 6 days and cytokines induced by 25 μg recoverin. Cytokines levels are determined by ELISA. DNA is used to check autoimmune genes for mutations or genetic differences or probe epigenetics. Purified whole blood mRNA is used to measure gene expression employing NanoString™ technology

### *24.2.2 Immunologic Assays*

Serum samples were analyzed for anti-retinal antibodies using Western blots. Plasma was analyzed for recoverin-specific IgG and IgM antibodies by ELISA. Peripheral blood mononuclear cells (PBMC) were isolated using Ficoll-Histopaque and analyzed to detect T and B lymphocyte subsets and lymphocyte activation markers by ten-color flow cytometry. Lymphocyte cultures were exposed to 25 μg recombinant human recoverin for 6 days, and ELISA was used to quantify levels of interferon gamma (IFNγ), tumor necrosis factor alpha (TNFα), and interleukin 10 (IL-10) produced by the lymphocytes. An "AIR inflammatory index" was determined as the ratio of recoverin-induced IFNγ to IL-10 concentration in the culture medium. RNA was purified from whole blood that was collected in PAXgene tubes, and copy numbers of mRNA were quantified using NanoString™ technology.

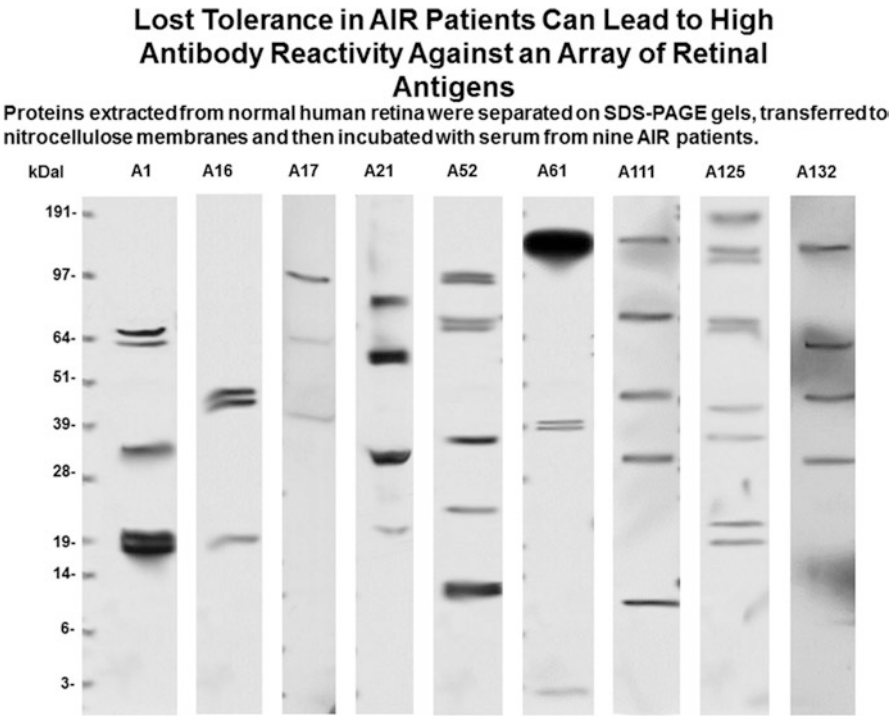


**Fig. 24.3** Western blot of AIR patients' serum for anti-retinal antibodies. Normal retinal proteins from donor eyes (Michigan Eye Bank) were separated on SDS-PAGE gels, transferred to nitrocellulose membranes, and incubated with serum from the AIR patients

## 24.3 Results

### *24.3.1 Anti-Retinal Antibodies in Patients Diagnosed with AIR*

Patients had serial blood testing every 4–6 months. Western blots showed immunoreactive anti-retinal antibody bands for all AIR patients. Typical results for nine newly diagnosed AIR patients are shown in Fig. 24.3. In our experience, the average AIR patient has five bands, while non-autoimmune RP patients or healthy controls may have up to two bands and average less than one band on the anti-retinal Western blot. There was no pattern or correlation of clinical findings to the molecular weight distribution on Western blot to antibody antigens (Fig. 24.3), and clinically inactive cases of AIR also showed positive Western blots. As an example, there was one AIR case with a 15-year history of disease inactivity, yet the patient still had ARAs on Western blot.

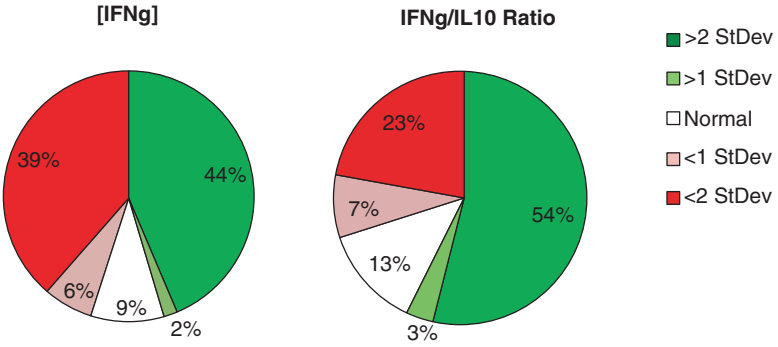


**Fig. 24.4** Interferon-γ and IL-10 were induced in AIR patient lymphocytes in culture with human recoverin for 6 days, and levels were measured by ELISA. Forty-four percent of AIR patients presenting in clinic had elevations of interferon-γ, and 54% had interferon to IL-10 ratios more than 2 SD above healthy controls

### *24.3.2 Peripheral Blood Cell Profiles in Newly Diagnosed AIR Patients*

Blood samples from the untreated AIR patients, RP control patients, and healthy donors were compared by cell counting and flow cytometry. No significant differences were found in total peripheral blood mononuclear cells (PBMC) or in percentages of lymphocytes or granulocytes (data not shown). Nine of the thirteen untreated AIR patients had CD4+ T cell percentages below 38%, which was the average for RP patients, while the healthy controls averaged 54% CD4+ T cells and were statistically different than the AIR patients but not the RP patients (data not shown). None of the other major lymphocyte subsets ($CD8^+$ T cells, NK cells, or B cells) were significantly different between the three groups.

### *24.3.3 Cytokine Responses Toward Recoverin*

In a survey lasting over 1.5 years of 150 AIR patients, 46% showed significant elevations of IFNγ cytokine produced by their lymphocytes in culture when exposed to 25 μg of recoverin for 6 days compared to normal controls (Fig. 24.4). Many patients also had lower IL-10 production than controls resulting in 57% of AIR patients having elevations of the IFNγ/IL-10 ratio that were significantly higher than controls. Elevated IFNγ/IL-10 ratios tended to correlate with clinically active disease (Fig. 24.4). These cytokine results were from a mixture of AIR patients at various points in the disease process. Most of the patients were receiving systemic immunosuppression treatment with prednisone, mycophenolate mofetil, and/or cyclosporine A, and a minority were treated with other medications or some had no active treatment at the time of blood draw.

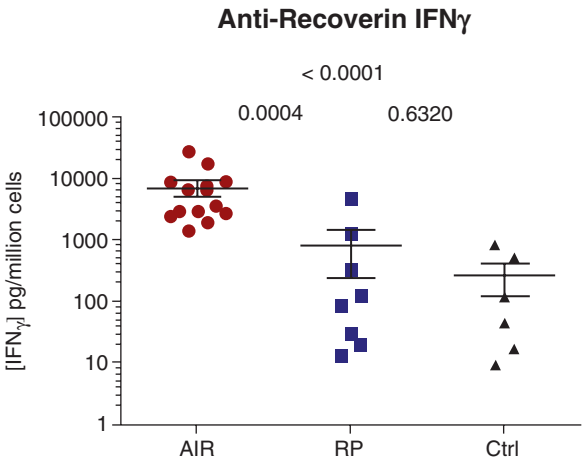


**Fig. 24.5** Untreated AIR patients ($n = 13$), non-autoimmune RP patients ($n = 8$), and healthy controls ($n = 6$) were compared for production of IFNγ after 6 days of culture stimulation with human recoverin. Exact $P$ values from Mann-Whitney nonparametric t tests were calculated using GraphPad Prism software and appear below the figure title

To obtain a clearer picture of the effect of patients' disease status prior to treatment, new cases were selected prospectively who had never had immunosuppressive treatment at time of blood draw. Thirteen new AIR cases, eight RP cases with typical slow visual field loss that had been followed for years, and six normal controls were analyzed. The ELISA data for these cell culture recoverin-induced IFNγ values are shown in Fig. 24.5. There was a significant difference ($P > 0.0001$) in anti-recoverin IFNγ cytokine levels by cells from untreated AIR patients compared to non-autoimmune RP patients and normal control lymphocytes.

### *24.3.4 Gene Expression Abnormalities*

We have been screening AIR patients for differences in gene expression using an array produced by NanoString Technologies. The array uses a barcoding strategy to fluorescently tag cDNA specific to 580 genes associated with inflammation. The method allows for direct quantification of copy numbers of mRNA in whole blood samples without amplification. Remarkably, there were only four genes that were twofold or more differentially expressed between the RP patients and healthy controls, and all of these were at copy numbers averaging less than 100 per sample. In contrast, this analysis showed that AIR patients had twofold or greater increases in gene expression for 33 genes compared to RP controls (all less than 100 copy numbers) and decreased blood mRNA levels of 19 genes of which 17 were at copy numbers greater than 100 per sample. One of the most striking differences was that all the newly diagnosed AIR patients we tested ($n = 10$) had relatively low expression of TGF-beta receptor 1 (TGFβ R1) mRNA (Fig. 24.6). Another notable difference was in expression of the chemokine receptor CCR7 (Fig. 24.6).

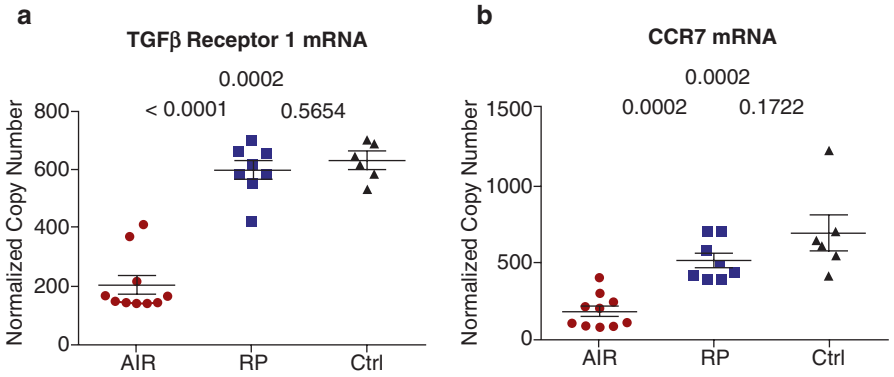


**Fig. 24.6** NanoString™ analysis of mRNA identified TGFβR1 and CCR7 as significantly down-regulated genes in the same set of AIR patients as in Fig. 24.5 when compared to controls or RP patients. These genes regulate inflammation and lymphocyte trafficking to sites of inflammation, respectively

## 24.4 Discussion

The diagnostic features and pathophysiology of AIR have slowly been emerging, and we are finding many distinctive changes in the immune system in AIR patients. While the presence of anti-retinal antibodies is found in all untreated AIR patients, their presence does not validate if the disease is active or quiescent. Working under the hypothesis that AIR patients have a loss of tolerance to retinal proteins, we were able to stimulate lymphocytes in culture with recoverin to produce inflammatory cytokines indicative of cellular immunity found in other autoimmune diseases. We found that interferon gamma was frequently elevated and that IL-10 was often at or below levels occurring in normal controls. The ratio of IFNγ/IL-10 was 2 standard deviations above normal in roughly half of all patients identified in clinic with AIR despite many patients being on general immunosuppressive therapy. This AIR inflammatory index is likely to give a more direct assessment of disease activity and responsiveness to therapy. Since IFNγ drives type 1 cellular immunity mediated by cytotoxic cells of the immune system, these data suggest that the pathogenesis of AIR may be more similar to other IFNγ-mediated autoimmune diseases than previously thought. These findings put AIR in the same category as multiple sclerosis and type 1 diabetes, rather than other autoimmune diseases that are more dependent on the involvement of antibodies in disease pathogenesis. Thus, more specific therapies aimed at type 1 cellular immune responses may prove to be more effective at controlling AIR.

Elevated production of another type 1 cytokine, TNF alpha (TNFα), was less common, occurring in about 15% of patients. These patients tended to have elevations of NK cells, which have direct cytotoxic potential. Control of NK cells is highly dependent on the interaction of signals from interleukin 15 and is antagonized by the immunosuppressive cytokine transforming growth factor beta (TGFβ). The importance of TNFα in some types of autoimmunity can be best exemplified by

the effectiveness of TNF blockers in the treatment of rheumatoid arthritis and other rheumatologic diseases.

We found that newly diagnosed AIR patients who had not been on treatment were deficient in mRNA for the TGFβ receptor 1 molecule. TGFβ plays an important role in immune regulation and is known to control susceptibility to autoimmune disease. Mice deficient in TGFβ receptor expression have defects in regulatory T cell development and have hyper-responsive NK cells due to dysregulation of IL-15 expression (Zhang and Bevan 2012; Gorelik and Flavell 2000). We also found that mRNA for CCR7, a chemokine receptor responsible for lymphocyte homing to secondary lymphoid organs, was significantly reduced in AIR patients compared to the other groups. Low expression of CCR7 is associated with transition of lymphocytes from naïve and central memory phenotypes toward cells that can leave lymphoid organs and home to sites of inflammation where they can carry out effector functions.

Taken together, the data suggest that loss of tolerance toward recoverin and potentially other retinal antigens may result in type 1 cellular immunity that may be the basis for retinal degeneration in patients with AIR. This represents a major shift in what was previously thought to be the pathogenic mechanisms involved and, therefore, should be considered when developing strategies to identify and get approval for more specific autoimmune therapies that may better treat patients with AIR. In the meantime, we are recommending the more generalized approaches of immunosuppression as clinically appropriate to prevent vision loss in these patients.

**Acknowledgments** Supported by an unrestricted grant from Research to Prevent Blindness to Department of Ophthalmology and Paul R. Lichter Chair of Ophthalmic Genetics and the Opler fund.

## References

Adamus G, Brown L, Schiffman J, Iannaccone A (2011) Diversity in autoimmunity against retinal, neuronal, and axonal antigens in acquired neuro-retinopathy. J Ophthalmic Inflam Infect 1:111–121

Ferreyra HA, Jayasundera T, Khan NW, He S, Lu Y, Heckenlively JR (2009) Management of autoimmune retinopathies with immunosuppression. Arch Ophthalmol 127:390–397

Fox AR, Gordon LK, Heckenlively JR, Davis JL, Goldstein DA, Lowder CY, Nussenblatt RB, Butler NJ, Dalal M, Jayasundera T, Smith WM, Lee RW, Adamus G, Chan CC, Hooks JJ, Morgans CW, Detrick B, Sen HN (2016) Consensus on the diagnosis and management of non-paraneoplastic autoimmune retinopathy using a modified Delphi approach. Am J Ophthalmol 168:183–190

Gorelik L, Flavell RA (2000) Abrogation of TGFbeta signaling in T cells leads to spontaneous T cell differentiation and autoimmune disease. Immunity 12:171–181

Oyama Y, Burt RK, Thirkill C, Hanna E, Merrill K, Keltner J (2009) A case of autoimmune-related retinopathy and optic neuropathy syndrome treated by autologous nonmyeloablative hematopoietic stem cell transplantation. J Neuroophthal Off J N Am NeuroOphthalmol Soc 29:43–49

Thirkill CE, FitzGerald P, Sergott RC, Roth AM, Tyler NK, Keltner JL (1989) Cancer-associated retinopathy (CAR syndrome) with antibodies reacting with retinal, optic-nerve, and cancer cells. N Engl J Med 321:1589–1594

Zhang N, Bevan MJ (2012) TGF-beta signaling to T cells inhibits autoimmunity during lymphopenia-driven proliferation. Nat Immunol 13:667–673

# Chapter 25
# Inflammation-Induced Photoreceptor Cell Death


**Abdoulaye Sene and Rajendra S. Apte**

**Abstract** Neuroinflammation is an important aspect of many diseases of the eye, and experimental animal models have been widely used to determine its impact on retinal homeostasis and neuron survival. Physical separation of the neurosensory retina from the underlying retinal pigment epithelium (RPE) results in activation and infiltration of macrophages. Numerous studies have shown the critical role of macrophages in retinal disease processes. In retinal detachment, accumulation of macrophages in the subretinal space is associated with changes in cytokine and chemokine profile which lead to photoreceptor cell death. Targeted disruption of macrophage chemotaxis significantly reduces retinal detachment-induced photoreceptor degeneration. Apoptosis is the predominant mechanism of cell death; however regulated necrosis is also a contributor of photoreceptor loss. Therefore, effective neuroprotective approaches could integrate combined inhibition of both apoptotic and regulated necrosis pathways.

**Keywords** Neuroinflammation · Macrophages · Photoreceptor degeneration · Retinal detachment

A. Sene (✉)
Department of Ophthalmology and Visual Sciences, Washington University School of Medicine, St. Louis, MO, USA
e-mail: abdoulaye.sene@allergan.com

R. S. Apte
Department of Ophthalmology and Visual Sciences, Washington University School of Medicine, St. Louis, MO, USA

Department of Developmental Biology and Medicine, Washington University School of Medicine, St. Louis, MO, USA

Department of Biology, Allergan, Inc., Irvine, CA, USA
e-mail: apte@wustl.edu



J. D. Ash et al. (eds.), *Retinal Degenerative Diseases*, Advances in Experimental Medicine and Biology 891, https://doi.org/10.1007/978-3-319-75402-4_25

## 25.1 Introduction

Photoreceptor degeneration is a common feature in many retinal disorders including retinitis pigmentosa, age-related macular degeneration (AMD), and retinal detachment (Stone et al. 1999; Wright et al. 2010). Numerous efforts are directed toward identifying a neuroprotective strategy that prevents or slows photoreceptor loss. Although the etiologies may be unrelated, photoreceptor cell death that leads to blindness is often triggered by similar mechanisms in diverse eye diseases. Therefore, inhibition of these cell death pathways is a very attractive therapeutic approach to prevent blindness (Bird 2007). It is well established that photoreceptor loss leads to remodeling of retinal structure that is often associated with immune activation (Noailles et al. 2016; Xi et al. 2016). Although recruitment of immune cells in the retina of patients with retinal detachment or AMD has been well documented, the contribution of resident and recruited macrophages in disease pathogenesis is unclear (Friedlander 2007; Karlstetter et al. 2015).

For instance, in animal models and patients with retinal detachment, macrophages are present in the subretinal space during the course of photoreceptor degeneration (Kunikata et al. 2013; Matsumoto et al. 2014). Given the role of macrophages in phagocytosis, antigen presentation, and cell clearance in response to danger signals such as damaged or injured tissue, an important question is whether macrophages cause the cell death or are merely associated with disease-related injury (Karlstetter et al. 2015). Similar concerns were also reported regarding the role of macrophages in AMD (Sene and Apte 2014). Although resident macrophages are present in healthy eyes, their number and activation signature change during the course of the disease (Cherepanoff et al. 2010). In experimental animal models of non-neovascular AMD, inhibition of macrophage recruitment significantly reduced the photoreceptor cell death, further confirming the key role of macrophages in mediating photoreceptor loss as seen in advanced stages of the disease (Cruz-Guilloty et al. 2013; Kohno et al. 2013; Sennlaub et al. 2013). In the neovascular form of the disease, it has been shown that macrophages can either inhibit or promote pathological angiogenesis (Sene et al. 2015; Grunin et al. 2016). This elasticity of function is dictated by their activation state, which in turn can be regulated by many factors including aging, photooxidative stress, and lipid metabolism (Kelly et al. 2007; Sene et al. 2013). Recent evidence shows that tissue macrophages can exhibit a distinct activation profile to modulate photoreceptor survival (Lewis et al. 2005). Macrophage infiltration in the subretinal space and the outer nuclear layer has also been shown in experimental models of light-induced retinal degeneration (Santos et al. 2010). In addition, several studies have demonstrated that preventing macrophage accumulation and activation is sufficient to significantly reduce light-induced retinal degeneration (Kohno et al. 2013). The use of experimental models of diseases along with genetic engineering approaches has unraveled a mechanistic link between macrophage recruitment and photoreceptor cell death (Rutar et al. 2012). Furthermore, coculture studies of photoreceptors with either retina-derived

microglial cells or conditioned media from these cells demonstrated that these cells or cell-derived factors can lead to photoreceptor death (Yang et al. 2007).

## 25.2 Modeling Macrophage-Mediated Retinal Cell Death

The physical separation of the neurosensory retina from the underlying retinal pigment epithelium (RPE) can occur due to (a) retinal breaks which allow vitreous fluid access to the subretinal space called rhegmatogenous detachments, (b) tractional preretinal membranes as seen in diabetic retinopathy, or (c) defective fluid transport/exudation seen in inflammatory or neoplastic conditions (Kang and Luff 2008). Retinal cell death correlates with the size and the duration of the detachment (Lewis et al. 2002). In response to the detachment, there is a profound remodeling of the retinal tissue. These changes are associated with reactive gliosis of Muller glial cells which is characterized by an upregulation of a specific cytoskeletal protein, glial fibrillary acidic protein (GFAP) (Erickson et al. 1987). In the detached retina, there is also an increased expression of vimentin in astroglial cells (Lewis and Fisher 2003). In addition, ion and water transport through Muller cells are dysregulated leading to defective fluid absorption (Wurm et al. 2006). The reactive astroglial response plays a determinant role in photoreceptor cell death. It has been demonstrated that in mice lacking both GFAP and vimentin, there was reduced photoreceptor degeneration after retinal detachment as compared to wild-type mice. Depletion of GFAP and vimentin prevented retinal detachment-induced macrophage infiltration in the subretinal space (Nakazawa et al. 2007a). In response to retinal detachment, there is an induction of inflammatory mediators such as MCP-1. In contrast, its levels were unchanged in double knockout (KO) mice further confirming the predominant role of the reactive gliosis in macrophage recruitment under the detached retina.

## 25.3 Macrophage Recruitment and Activation

The loss-of-function studies targeting GFAP and vimentin suggest that astroglial cells are one of first responders in the detached retina. In addition to the reactive gliosis, these cells exhibit rapid changes in retinal cytokine and chemokine profile that modulates immune and inflammatory responses (Bringmann and Wiedemann 2012). Injury-induced glial response and the sequential events that lead to macrophage recruitment and activation have also been observed in ischemia-reperfusion and light-induced degeneration. In experimental rodent models, it has been shown that retinal levels of TNF-α, IL-1β, and MCP-1 were about tenfold higher as early as 1 h following the retinal detachment (Nakazawa et al. 2006). Interestingly, MCP-1 is mostly produced by Muller cells in the early stages of the injury therefore initiating the activation of resident microglial cells and the infiltration of

macrophages in the subretinal space. Many studies have demonstrated the central role of MCP-1 in injury-induced neuroinflammation and photoreceptor cell death (Nakazawa et al. 2007b; Rutar et al. 2012). Indeed, defective chemotaxis of macrophages mediated by MCP-1 prevents retinal degeneration. In the detached retina, in addition to Muller cells, high MCP-1 levels are maintained by activated and infiltrating macrophages along with injured photoreceptors. A sustained pro-inflammatory status can also be amplified through a positive feedback loop resulting from the interaction of microglia and Muller cells. Activated microglia can modulate Muller cells morphology and inflammatory status. The expression of MCP-1 and inflammatory cytokines such as IL-1β and IL6 is significantly increased in Muller cells when exposed to activated microglia (Wang et al. 2011). These data further confirm the interplay between retinal glial cells and resident and infiltrating macrophages in order to maintain neuroinflammation. Detachment-induced macrophage activation and recruitment have been reported in patients as well as in various experimental animal models (Lewis et al. 2005).

## 25.4 Cell Death Mechanisms

In experimental models of retinal detachment, photoreceptor loss peaks at day 3 post induction and correlates with the thickness of the outer nuclear layer (Yang et al. 2004). Electroretinograms recorded 3 days after retinal detachment confirmed functional changes of photoreceptors (Hisatomi et al. 2002). Numerous studies have shown that apoptosis is the predominant mechanism of photoreceptor cell degeneration in humans with retinal detachment and experimental animal models (Chang et al. 1995; Cook et al. 1995; Arroyo et al. 2005; Lo et al. 2011). Indeed, inhibition of apoptotic pathways as a treatment strategy has been explored in order to prevent photoreceptor degeneration in detached retinas (Yang et al. 2004; Zacks et al. 2007). In many studies, interfering with apoptotic pathways resulted in a significant reduction of photoreceptor cell death. However, pan-caspase inhibition did not prevent retinal detachment-induced photoreceptor loss therefore confirming the activation of other cell death mechanisms (Trichonas et al. 2010). These studies demonstrated that necrosis is also a key mechanism of detachment-induced photoreceptor cell death. Using genetic and specific pharmacological tools, the authors demonstrated that disruption of receptor-interacting protein (RIP) kinase-mediated necrosis reduced photoreceptor loss after retinal detachment. Interestingly, inhibition of caspase-dependent apoptotic pathways in detached retinas is associated with a significant increase in necrosis-mediated photoreceptor cell death. These data suggest that this programmed necrosis is a redundant death mechanism in retinal detachment-induced photoreceptor loss. Therefore an effective therapeutic strategy would integrate a combined inhibition of apoptotic and regulated necrosis pathways.

**Acknowledgements** This work was supported by the Foundation Fighting Blindness Travel Fellowship, The Starr Foundation, The Jeffrey Fort Innovation Fund, a Research to Prevent

Blindness Physician Scientist Award (RSA) and a Research to Prevent Blindness Nelson Trust Award for Retinitis Pigmentosa. The Department of Ophthalmology, Washington University School of Medicine, is supported by an unrestricted grant from the Research to Prevent Blindness, New York City, NY.

## References

Arroyo JG, Yang L, Bula D et al (2005) Photoreceptor apoptosis in human retinal detachment. Am J Ophthalmol 139:605–610

Bird A (2007) How to keep photoreceptors alive. Proc Natl Acad Sci U S A 104:2033–2034

Bringmann A, Wiedemann P (2012) Muller glial cells in retinal disease. Ophthalmologica 227:1–19

Chang CJ, Lai WW, Edward DP et al (1995) Apoptotic photoreceptor cell death after traumatic retinal detachment in humans. Arch Ophthalmol 113:880–886

Cherepanoff S, McMenamin P, Gillies MC et al (2010) Bruch's membrane and choroidal macrophages in early and advanced age-related macular degeneration. Br J Ophthalmol 94:918–925

Cook B, Lewis GP, Fisher SK et al (1995) Apoptotic photoreceptor degeneration in experimental retinal detachment. Invest Ophthalmol Vis Sci 36:990–996

Cruz-Guilloty F, Saeed AM, Echegaray JJ et al (2013) Infiltration of proinflammatory m1 macrophages into the outer retina precedes damage in a mouse model of age-related macular degeneration. Int J Inflamm 2013:503725

Erickson PA, Fisher SK, Guerin CJ et al (1987) Glial fibrillary acidic protein increases in Muller cells after retinal detachment. Exp Eye Res 44:37–48

Friedlander M (2007) Fibrosis and diseases of the eye. J Clin Invest 117:576–586

Grunin M, Hagbi-Levi S, Rinsky B et al (2016) Transcriptome analysis on monocytes from patients with neovascular age-related macular degeneration. Sci Rep 6:29046

Hisatomi T, Sakamoto T, Goto Y et al (2002) Critical role of photoreceptor apoptosis in functional damage after retinal detachment. Curr Eye Res 24:161–172

Kang HK, Luff AJ (2008) Management of retinal detachment: a guide for non-ophthalmologists. BMJ 336:1235–1240

Karlstetter M, Scholz R, Rutar M et al (2015) Retinal microglia: just bystander or target for therapy? Prog Retin Eye Res 45:30–57

Kelly J, Ali Khan A, Yin J et al (2007) Senescence regulates macrophage activation and angiogenic fate at sites of tissue injury in mice. J Clin Invest 117:3421–3426

Kohno H, Chen Y, Kevany BM et al (2013) Photoreceptor proteins initiate microglial activation via Toll-like receptor 4 in retinal degeneration mediated by all-trans-retinal. J Biol Chem 288:15326–15341

Kunikata H, Yasuda M, Aizawa N et al (2013) Intraocular concentrations of cytokines and chemokines in rhegmatogenous retinal detachment and the effect of intravitreal triamcinolone acetonide. Am J Ophthalmol 155:1028–1037. e1021

Lewis GP, Fisher SK (2003) Up-regulation of glial fibrillary acidic protein in response to retinal injury: its potential role in glial remodeling and a comparison to vimentin expression. Int Rev Cytol 230:263–290

Lewis GP, Charteris DG, Sethi CS et al (2002) Animal models of retinal detachment and reattachment: identifying cellular events that may affect visual recovery. Eye (Lond) 16:375–387

Lewis GP, Sethi CS, Carter KM et al (2005) Microglial cell activation following retinal detachment: a comparison between species. Mol Vis 11:491–500

Lo AC, Woo TT, Wong RL et al (2011) Apoptosis and other cell death mechanisms after retinal detachment: implications for photoreceptor rescue. Ophthalmologica 226(Suppl 1):10–17

Matsumoto H, Kataoka K, Tsoka P et al (2014) Strain difference in photoreceptor cell death after retinal detachment in mice. Invest Ophthalmol Vis Sci 55:4165–4174

Nakazawa T, Matsubara A, Noda K et al (2006) Characterization of cytokine responses to retinal detachment in rats. Mol Vis 12:867–878

Nakazawa T, Takeda M, Lewis GP et al (2007a) Attenuated glial reactions and photoreceptor degeneration after retinal detachment in mice deficient in glial fibrillary acidic protein and vimentin. Invest Ophthalmol Vis Sci 48:2760–2768

Nakazawa T, Hisatomi T, Nakazawa C et al (2007b) Monocyte chemoattractant protein 1 mediates retinal detachment-induced photoreceptor apoptosis. Proc Natl Acad Sci U S A 104:2425–2430

Noailles A, Maneu V, Campello L et al (2016) Persistent inflammatory state after photoreceptor loss in an animal model of retinal degeneration. Sci Rep 6:33356

Rutar M, Natoli R, Provis JM (2012) Small interfering RNA-mediated suppression of Ccl2 in Muller cells attenuates microglial recruitment and photoreceptor death following retinal degeneration. J Neuroinflammation 9:221

Santos AM, Martin-Oliva D, Ferrer-Martin RM et al (2010) Microglial response to light-induced photoreceptor degeneration in the mouse retina. J Comp Neurol 518:477–492

Sene A, Apte RS (2014) Eyeballing cholesterol efflux and macrophage function in disease pathogenesis. Trends Endocrinol Metab 25:107–114

Sene A, Khan AA, Cox D et al (2013) Impaired cholesterol efflux in senescent macrophages promotes age-related macular degeneration. Cell Metab 17:549–561

Sene A, Chin-Yee D, Apte RS (2015) Seeing through VEGF: innate and adaptive immunity in pathological angiogenesis in the eye. Trends Mol Med 21:43–51

Sennlaub F, Auvynet C, Calippe B et al (2013) CCR2(+) monocytes infiltrate atrophic lesions in age-related macular disease and mediate photoreceptor degeneration in experimental subretinal inflammation in Cx3cr1 deficient mice. EMBO Mol Med 5:1775–1793

Stone J, Maslim J, Valter-Kocsi K et al (1999) Mechanisms of photoreceptor death and survival in mammalian retina. Prog Retin Eye Res 18:689–735

Trichonas G, Murakami Y, Thanos A et al (2010) Receptor interacting protein kinases mediate retinal detachment-induced photoreceptor necrosis and compensate for inhibition of apoptosis. Proc Natl Acad Sci U S A 107:21695–21700

Wang M, Ma W, Zhao L et al (2011) Adaptive Muller cell responses to microglial activation mediate neuroprotection and coordinate inflammation in the retina. J Neuroinflammation 8:173

Wright AF, Chakarova CF, Abd El-Aziz MM et al (2010) Photoreceptor degeneration: genetic and mechanistic dissection of a complex trait. Nat Rev Genet 11:273–284

Wurm A, Pannicke T, Iandiev I et al (2006) Changes in membrane conductance play a pathogenic role in osmotic glial cell swelling in detached retinas. Am J Pathol 169:1990–1998

Xi H, Katschke KJ Jr, Li Y et al (2016) IL-33 amplifies an innate immune response in the degenerating retina. J Exp Med 213:189–207

Yang L, Bula D, Arroyo JG et al (2004) Preventing retinal detachment-associated photoreceptor cell loss in Bax-deficient mice. Invest Ophthalmol Vis Sci 45:648–654

Yang LP, Zhu XA, Tso MO (2007) A possible mechanism of microglia-photoreceptor crosstalk. Mol Vis 13:2048–2057

Zacks DN, Boehlke C, Richards AL et al (2007) Role of the Fas-signaling pathway in photoreceptor neuroprotection. Arch Ophthalmol 125:1389–1395

# Chapter 26
# Sall1 Regulates Microglial Morphology Cell Autonomously in the Developing Retina

**Hideto Koso, Ryuichi Nishinakamura, and Sumiko Watanabe**

**Abstract** Retinal degeneration often accompanies microglial activation and infiltration of monocyte-derived macrophages into the retina, resulting in the coexistence of microglia and monocyte-derived macrophages in the retina. We previously showed that the Sall1 zinc-finger transcriptional factor is expressed specifically in microglia within the retinal phagocyte pool, and analyses of *Sall1* knockout mice revealed that microglial morphology changed from a ramified to a more amoeboid appearance in the developing retina. To investigate further whether Sall1 functions autonomously in microglia, we generated *Sall1* conditional knockout mice, in which *Sall1* was depleted specifically in the Cx3cr1+ microglial compartment of the developing retina. Sall1-deficient microglia exhibited morphological abnormalities on embryonic day 18 that strikingly resembled the phenotype observed in *Sall1* knockout mice, demonstrating that Sall1 regulates microglial morphology cell autonomously. Analysis of the postnatal retina revealed that *Sall1*-deficient microglia extended their processes and their morphology became comparable to that of wild-type microglia on postnatal day 21, indicating that Sall1 is essential for microglial ramification in the developing retina, but not in the postnatal retina.

**Keywords** Sall1 · Microglia · Microglial development · Microglial morphology · Retinal development · Transcriptional factor · Retinal degeneration · Conditional knockout mice

H. Koso · S. Watanabe (✉)
Division of Molecular and Developmental Biology, Institute of Medical Science, The University of Tokyo, Tokyo, Japan
e-mail: sumiko@ims.u-tokyo.ac.jp

R. Nishinakamura
Department of Kidney Development, Institute of Molecular Embryology and Genetics, Kumamoto University, Kumamoto, Japan



J. D. Ash et al. (eds.), *Retinal Degenerative Diseases*, Advances in Experimental Medicine and Biology 891, https://doi.org/10.1007/978-3-319-75402-4_26

## 26.1 Introduction

Recent studies have suggested pathogenic roles for microglia and infiltrating macrophages in mouse models of retinal degeneration (Sennlaub et al. 2013; Zhao et al. 2015); however, the distinct roles of these two phagocytic populations remain unclear. We recently developed a new genetic mouse model of retinal degeneration, in which rods were induced to degenerate in a temporally regulated manner by expressing diphtheria toxin fragment A in rod photoreceptor cells (Koso et al. 2016). By combining bone marrow transplantation with this model, we revealed the coexistence of microglia and monocyte-derived macrophages in the retina. Comparisons of the microglia and monocyte-derived macrophage gene expression profiles identified *Sall1* as a gene specifically expressed in microglia. To investigate Sall1 functions in microglia, we analyzed *Sall1* knockout mice. Microglial colonization of the developing retina occurred normally in *Sall1* knockout mice; however, microglial ramification was significantly reduced in the retina of *Sall1* knockout mice (Koso et al. 2016). The morphological defect was not rescued by the presence of wild-type non-microglial cells in vitro, suggesting a cell-autonomous role of Sall1 in microglial morphology. To investigate further whether Sall1 functions in cell autonomously in vivo, we generated *Sall1* conditional knockout (CKO) mice, in which Sall1 was specifically depleted in microglia. *Salll1* CKO mice also allowed us to investigate Sall1 functions in microglia during postnatal stages.

## 26.2 Materials and Methods

### *26.2.1 Mouse Strains*

*B6.129P2(C)-Cx3cr1*$^{tm2.1(cre/ERT2)Jung}$*/J* (*Cx3cr1*$^{CreER}$) transgenic mice (Yona et al. 2013) (Jackson Laboratory, Bar Harbor, ME, USA) were bred with *B6;129-Sall1*$^{tm1(flox)Imeg}$ (*Sall1*$^{flox}$) (Yuri et al. 2009; Kanda et al. 2014) to obtain double transgenic animals. The genetic background of these animals was C57BL/6 x129 mixed. Animals of either sex were used in the study. All animal procedures were performed according to the guidelines of the ARVO statement for the "Use of Animals in Ophthalmic and Vision Research" and were approved by the Institutional Animal Care and Use Committees.

### *26.2.2 Tamoxifen Treatment*

Tamoxifen (Sigma-Aldrich, St. Louis, MO, USA) was prepared as a 20 mg/ml stock solution in corn oil. At E12, 6 mg of tamoxifen was administered by oral gavage to a pregnant mouse. Mouse embryos were analyzed at embryonic day (E)18. Caesarian section was performed on E19, and the retinas were analyzed on postnatal day 8 or 21.

### *26.2.3 Immunohistochemical Analysis*

The entire embryonic head was fixed, incubated in 25% sucrose/PBS, and embedded in FSC22 compound (Leica Microsystems, Buffalo Grove, IL, USA). Postnatal retinas were embedded as flattened whole mounts and sectioned along the apicobasal axis. Frozen sections (10 μm) were prepared using a CM1950 cryostat (Leica). The following antibodies were used: rabbit polyclonal anti-Iba1 (Wako Pure Chemical, Osaka, Japan), mouse monoclonal anti-Sall1 (Perseus Proteomics, Tokyo, Japan), and Alexa488 or 594-conjugated appropriate secondary antibodies (Thermo Fisher Scientific, Rockford, IL, USA). Samples were counterstained with DAPI and analyzed with an Axioplan 2 imaging microscope (Carl Zeiss, Jena, Germany). Embryonic microglial morphology was analyzed as described previously (Koso et al. 2016) and that in postnatal retinas was analyzed using microglia located in the inner plexiform layer.

## 26.3 Results

### *26.3.1 Sall1 Regulates Microglial Morphology Cell Autonomously in the Developing Retina*

The Cx3cr1 chemokine receptor is expressed in mature monocytes and in a subset of peripheral mononuclear phagocytes (Geissmann et al. 2003). Only microglia in the brain parenchyma express this marker (Prinz et al. 2011; Goldmann et al. 2013); thus, we used *Cx3cr1*$^{CreER}$ knock-in mice to deplete Sall1 specifically in microglia (Yuri et al. 2009; Kanda et al. 2014). The *Sall1*$^{floxed}$ allele contains two loxP sites flanking exon 1 of the *Sall1* gene, resulting in complete absence of the Sall1 protein after Cre-mediated recombination (Yuri et al. 2009). Yolk sac-derived Cx3cr1-expressing microglial precursors start to colonize the neural tube in the developing central nervous system (CNS) on E9.5 (Kierdorf et al. 2013); thus, we administered tamoxifen to pregnant mice on E12 and induced recombination in control (*Sall1*$^{flox/flox}$) or *Sall1* CKO embryos (*Cx3cr1*$^{CreER}$*; Sall1*$^{flox/flox}$) (Fig. 26.1a). Analysis of the retina on E18 revealed that microglia had extended their processes toward the basal side of the retina in control mice; however, this was rarely observed in the retina of *Sall1* CKO mice (Fig. 26.1b). The number of microglial branches and maximum length of the branches were both reduced in microglia of *Sall1* CKO mice (Fig. 26.1c, d). These phenotypes strikingly resembled the microglial abnormalities observed in *Sall1* KO mice (Koso et al. 2016), indicating that Sall1 regulates microglial morphology cell autonomously in the developing retina.

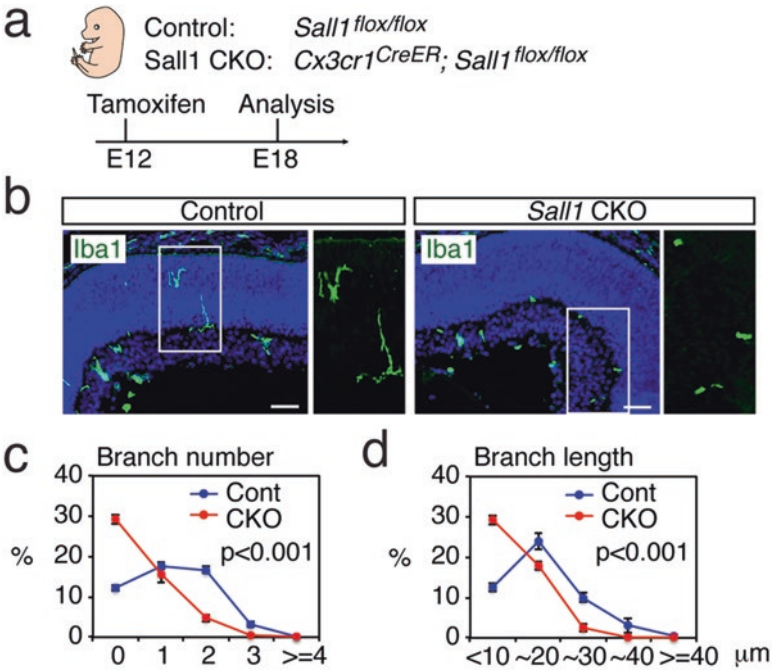


**Fig. 26.1 Microglial morphology in the *Sall1* CKO retina during development**. (**a**) A schematic diagram showing tamoxifen treatment. Tamoxifen was administered to a pregnant mother to induce recombination in control (*Sall1*$^{flox/flox}$) or *Sall1* CKO mice (*Cx3cr1*$^{CreER}$; *Sall1*$^{flox/flox}$) at E12. The retina was analyzed at E18. (**b**) Representative expression patterns of Iba1 in the retina of control and *Sall1* CKO mice at E18.5. White squares represent the regions magnified. (**c, d**) Distributions of the number of microglial branches (**c**) and the maximum length of microglial processes (**d**) in the retina of control and *Sall1* CKO mice at E18 ($n = 4$ per group). At least one hundred microglia were measured for each animal. Mann-Whitney U test $^{***}p < 0.001$. Data represent Mean ± SEM. Scale bars, 50 μm

### *26.3.2 Sall1-Deficient Microglia Extend Their Processes During the Postnatal Stage*

Sall1 is essential for kidney development, and *Sall1* knockout mice exhibit neonatal lethality (Nishinakamura et al. 2001). *Sall1* CKO mice allowed us to circumvent this problem and analyze microglial morphology in the postnatal retina. We used the same protocol for tamoxifen treatment as described above and analyzed the retina of control and *Sall1* CKO mice during postnatal stages (Fig. 26.2a). Sall1 expression was absent in microglia of *Sall1* CKO mice on postnatal day (P)8, as expected (Fig. 26.2b). Unlike embryonic microglia, Sall1-deficient microglia normally extended their processes on P8, although arborization appeared to have decreased slightly (Fig. 26.2b), which was reminiscent of the morphological abnormalities observed in embryonic microglia. Sall1-deficient microglia acquired a branched,

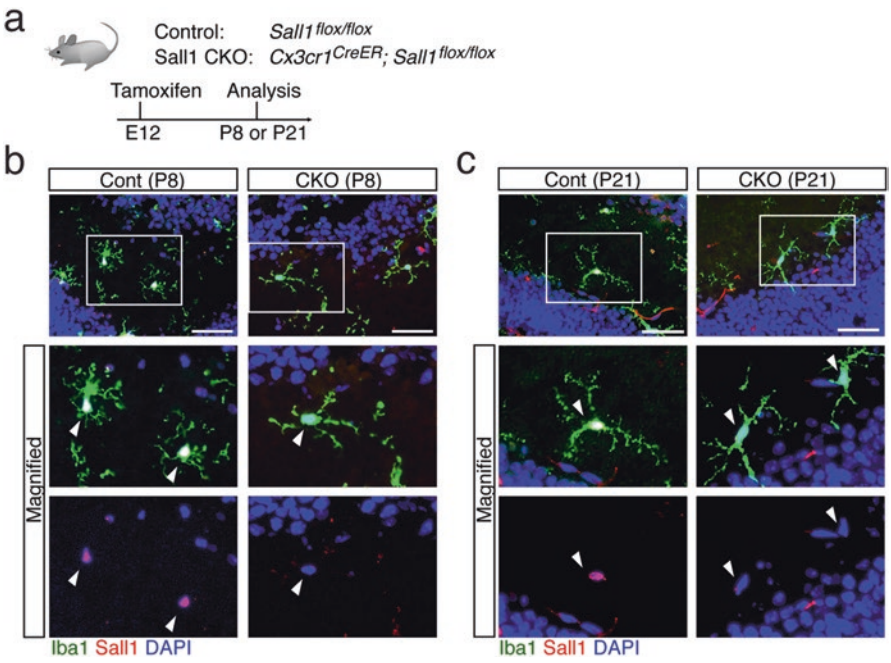


**Fig. 26.2 Microglial morphology in the *Sall1* CKO retina at postnatal stages**. (**a**) A schematic diagram showing tamoxifen treatment. Tamoxifen was administered to a pregnant mother at E12, and the retina was analyzed at P8 or P21. (**b, c**) Representative expression patterns of Iba1 and *Sall1* in the retina of control and *Sall1* CKO mice at P8 (**b**) and P21 (**c**). White squares in upper panels represent the regions magnified. Arrows point to microglial nuclei. Scale bars, 50 μm

ramified morphology on P21, which was comparable between control and Sall1-deficient microglia (Fig. 26.2c). These data suggest that Sall1 is not essential for microglia to become fully ramified cells in the postnatal retina.

## 26.4 Discussion

In this study, we used *Cx3cr1*$^{CreER}$ transgenic mice for the specific depletion of Sall1 in microglia of the developing retina. Embryonic microglia in the *Sall1* CKO retina showed morphological abnormalities that strikingly resembled the phenotype observed in *Sall1* KO retinas. The microglial abnormalities were observed not only in the retina but also in the cortex of *Sall1* CKO mice (data not shown), indicating that Sall1 regulates microglial morphology cell autonomously in at least two regions of the developing CNS. *Sall1* acts as a strong transcriptional repressor in mammalian cells; however, its direct target genes remain unknown (Netzer et al. 2001). Microglia emerge from erythromyeloid progenitors in the yolk sac during embryonic development (Kierdorf et al. 2013). A recent single-cell transcriptome analysis

revealed that *Sall1* is not expressed in erythromyeloid progenitors in the yolk sac, but begins to be expressed in microglial progenitors in the brain as early as E10.5 (Matcovitch-Natan et al. 2016), suggesting that Sall1 expression is initiated in microglia after colonization of the brain. These findings support the notion that locally derived signals in the developing brain induce *Sall1* expression in microglial progenitors, which, in turn, facilitates morphological specification into ramified microglia.

Sall1-deficient microglia showed morphological abnormalities in the developing retina, but they eventually underwent a morphological transition to branched and ramified mature microglia. The most likely explanation for this phenotype is that other SALL family proteins may have redundant functions and rescued the morphological defects induced by the Sall1 deficiency. Sall3 is such a candidate because Sall1 and Sall3 share a similar domain structure and have redundant roles during limb morphogenesis (Kawakami et al. 2009). In fact, *Sall3* is relatively strongly expressed in microglia (Koso et al. 2016). As Sall3 knockout mice exhibit perinatal lethality (Parrish et al. 2004), microglia-specific depletion of both Sall1 and Sall3 remains a task for future studies. Resting microglia dynamically extend and retract their processes to monitor neuronal synapses in their microenvironment (Wake et al. 2009). Although we could not detect any morphological abnormalities in Sall1-deficient microglia on P21 from static microscopic images, our study does not rule out the possibility that dynamic movement of microglial processes may be altered by Sall1 deficiency. A detailed analysis of the dynamic behavior of microglial processes in Sall1-deficient microglia remains an important target for future investigation.

**Acknowledgments** We thank A. Tsuhako for technical assistance. This study was supported by the Japan Society for Promotion of Science.

## References

Geissmann F, Jung S, Littman DR (2003) Blood monocytes consist of two principal subsets with distinct migratory properties. Immunity 19:71–82

Goldmann T, Wieghofer P, Muller PF et al (2013) A new type of microglia gene targeting shows TAK1 to be pivotal in CNS autoimmune inflammation. Nat Neurosci 16:1618–1626

Kanda S, Tanigawa S, Ohmori T et al (2014) Sall1 maintains nephron progenitors and nascent nephrons by acting as both an activator and a repressor. J Am Soc Nephrol 25:2584–2595

Kawakami Y, Uchiyama Y, Rodriguez Esteban C et al (2009) Sall genes regulate region-specific morphogenesis in the mouse limb by modulating Hox activities. Development 136:585–594

Kierdorf K, Erny D, Goldmann T et al (2013) Microglia emerge from erythromyeloid precursors via Pu.1- and Irf8-dependent pathways. Nat Neurosci 16:273–280

Koso H, Tsuhako A, Lai CY et al (2016) Conditional rod photoreceptor ablation reveals Sall1 as a microglial marker and regulator of microglial morphology in the retina. Glia 64:2005–2024

Matcovitch-Natan O, Winter DR, Giladi A et al (2016) Microglia development follows a stepwise program to regulate brain homeostasis. Science 353:aad8670

Netzer C, Rieger L, Brero A et al (2001) SALL1, the gene mutated in Townes-Brocks syndrome, encodes a transcriptional repressor which interacts with TRF1/PIN2 and localizes to pericentromeric heterochromatin. Hum Mol Genet 10:3017–3024

Nishinakamura R, Matsumoto Y, Nakao K et al (2001) Murine homolog of SALL1 is essential for ureteric bud invasion in kidney development. Development 128:3105–3015

Parrish M, Ott T, Lance-Jones C et al (2004) Loss of the Sall3 gene leads to palate deficiency, abnormalities in cranial nerves, and perinatal lethality. Mol Cell Biol 24:7102–7012

Prinz M, Priller J, Sisodia SS et al (2011) Heterogeneity of CNS myeloid cells and their roles in neurodegeneration. Nat Neurosci 14:1227–1235

Sennlaub F, Auvynet C, Calippe B et al (2013) CCR2(+) monocytes infiltrate atrophic lesions in age-related macular disease and mediate photoreceptor degeneration in experimental subretinal inflammation in Cx3cr1 deficient mice. EMBO Mol Med 5:1775–1793

Wake H, Moorhouse AJ, Jinno S et al (2009) Resting microglia directly monitor the functional state of synapses in vivo and determine the fate of ischemic terminals. J Neurosci 29:3974–3980

Yona S, Kim KW, Wolf Y et al (2013) Fate mapping reveals origins and dynamics of monocytes and tissue macrophages under homeostasis. Immunity 38:79–91

Yuri S, Fujimura S, Nimura K et al (2009) Sall4 is essential for stabilization, but not for pluripotency, of embryonic stem cells by repressing aberrant trophectoderm gene expression. Stem Cells 27:796–805

Zhao L, Zabel MK, Wang X et al (2015) Microglial phagocytosis of living photoreceptors contributes to inherited retinal degeneration. EMBO Mol Med 7:1179–1197

# Part V
# Inherited Retinal Degenerations

# Chapter 27
# Whole-Exome Sequencing Identifies Novel Variants that Co-segregates with Autosomal Recessive Retinal Degeneration in a Pakistani Pedigree

**Pooja Biswas, Muhammad Asif Naeem, Muhammad Hassaan Ali, Muhammad Zaman Assir, Shaheen N. Khan, Sheikh Riazuddin, J. Fielding Hejtmancik, S. Amer Riazuddin, and Radha Ayyagari**

## Abstract

### Purpose

To identify the molecular basis of inherited retinal degeneration (IRD) in a familial case of Pakistani origin using whole-exome sequencing.

This work was supported by NIH-EY021237, NIH- EY002162, NIH-EY0020846, NIH-P30EY022589, Foundation Fighting Blindness (RA), and Research to Prevent Blindness (RA).

P. Biswas · R. Ayyagari (✉)
Shiley Eye Institute, University of California San Diego, La Jolla, CA, USA
e-mail: rayyagari@ucsd.edu

M. A. Naeem · S. N. Khan
National Centre of Excellence in Molecular Biology, University of the Punjab, Lahore, Pakistan

M. H. Ali · M. Z. Assir
Allama Iqbal Medical College, University of Health Sciences, Lahore, Pakistan

S. Riazuddin
National Centre for Genetic Diseases, Shaheed Zulfiqar Ali Bhutto Medical University, Islamabad, Pakistan

National Centre of Excellence in Molecular Biology, University of the Punjab, Lahore, Pakistan

Allama Iqbal Medical College, University of Health Sciences, Lahore, Pakistan

J. F. Hejtmancik
Ophthalmic Genetics and Visual Function Branch, National Eye Institute, NIH, Bethesda, MD, USA

S. A. Riazuddin (✉)
Department of Ophthalmology, The Wilmer Eye Institute, Johns Hopkins University School of Medicine, Baltimore, MD, USA
e-mail: riazuddin@ncemb.org



J. D. Ash et al. (eds.), *Retinal Degenerative Diseases*, Advances in Experimental Medicine and Biology 891, https://doi.org/10.1007/978-3-319-75402-4_27

**Methods**
A thorough ophthalmic examination was completed, and genomic DNA was extracted using standard protocols. Whole exome(s) were captured with Agilent V5 + UTRs probes and sequenced on Illumina HiSeq genome analyzer. The exome-Suite software was used to filter variants, and the candidate causal variants were prioritized, examining their allele frequency and PolyPhen2, SIFT, and MutationTaster predictions. Sanger dideoxy sequencing was performed to confirm the segregation with disease phenotype and absence in ethnicity-matched control chromosomes.

**Results**
Ophthalmic examination confirmed retinal degeneration in all affected individuals that segregated as an autosomal recessive trait in the family. Whole-exome sequencing identified two homozygous missense variants: c.1304G > A; p.Arg435Gln in *ZNF408* (NM_024741) and c.902G > A; p.Gly301Asp in *C1QTNF4* (NM_031909). Both variants segregated with the retinal phenotype in the PKRD320 and were absent in ethnically matched control chromosomes.

**Conclusion**
Whole-exome sequencing coupled with bioinformatics analysis identified potential novel variants that might be responsible for IRD.

**Keywords** Retinal degeneration · Whole-exome sequencing · Novel variants · *ZNF408* · *C1QTNF4*

## 27.1 Introduction

Retinal degenerations (RD) are the most common form of retinal dystrophy that affects 1 in 3000 individuals (Boughman et al. 1980). The disease is characterized by the progressive degeneration of photoreceptors, ultimately leading to blindness (Heckenlively 1988; Inglehearn 1998; Daiger et al. 2013). In the Retinal Information Network, currently, there are approximately 256 retinal disease-causing genes (RetNet; Hartong et al. 2006).

Mutations in these genes have been associated with a wide range of retinal phenotypes including cone or cone-rod dystrophy, leber congenital amaurosis, optic atrophy, retinitis pigmentosa, Usher syndrome, x-linked, and mitochondrial (Carr et al. 1978; Boughman and Fishman 1983; Boughman et al. 1983; Cremers et al. 1998; Morimura et al. 1998; Ayyagari et al. 2000; Nochez et al. 2009; Kenney et al. 2013). More than 187 genes have been reported that are involved with arRD (RetNet). Patients with arRD have a wide variation in the age of onset, the rate of progression, the severity of disease, and clinical symptoms (Heckenlively 1988; Zheng et al. 2015).

Here we describe the identification of the pathogenic candidate variants in a pedigree originating in Pakistan by linkage analysis and whole-exome sequencing.

## 27.2 Methods

### *27.2.1 Ethics*

All research procedures were approved by the Institutional Review Boards (IRB) of National Centre of Excellence in Molecular Biology in Lahore, Pakistan; National Eye Institute in Bethesda, MD; University of California San Diego, in La Jolla, CA; and Johns Hopkins University in Baltimore, MD. Each participant in this study was informed and provided written consent in accordance with the Declaration of Helsinki.

### *27.2.2 Subjects and Clinical Examination*

A three-generation pedigree with multiple affected family members was recruited from the Punjab province of Pakistan. The ophthalmic evaluation was performed as described previously (Duncan et al. 2007).

### *27.2.3 Exclusion Analysis*

The genomic DNA used in all experiments was extracted from the white blood cells of whole-blood samples using QIAamp DNA blood mini kit (QIAGEN, Valencia, CA 91355). Short tandem repeat (STR) markers spanning known and/or reported IRD loci were selected for exclusion analysis. PCR products were mixed with a loading cocktail containing HD-400 size standards (Applied Biosystems) and resolved in an Applied Biosystems 3100 DNA Analyzer. Genotypes were assigned using the GeneMapper software from Applied Biosystems. Linkage analysis was performed with alleles of PKRD320 obtained through the genome-wide scan using the FASTLINK version of MLINK from the LINKAGE Program Package (Lathrop and Lalouel 1984; Schaffer et al. 1994; Naeem et al. 2015).

### *27.2.4 Whole-Exome Sequencing and Variant Calling*

Genomic DNA from two affected and one unaffected individual was used for whole-exome sequencing. Whole-exome sequencing was performed using Agilent V5 + UTRs probes on the Illumina HiSeq (Illumina, San Diego, CA). The paired end (2 × 100 bases) reads were aligned to human genome hg19 after quality control check (Li and Durbin 2009; Genomes Project et al. 2015). The aligned reads were sorted by using SAMtools and stored in BAM format files. The GATK guidelines

**Table 27.1** The list of databases we used for variant annotation

| Category | Database | References |
|---|---|---|
| Mutation frequency | dbSNP 138 | Sherry et al. (2001) |
| | ExAC | Lek et al. (2016) |
| | HGMD | Stenson et al. (2014) |
| Gene | GENCODE (gene, exon, and transcript) | Harrow et al. (2012) |
| microRNA | mirBase | Kozomara and Griffiths-Jones (2011) |
| Expression | UniGene | – |
| Impact prediction | PolyPhen2 | – |
| | SIFT | – |
| | MutationTaster | – |
| Retina | RetNet | RetNet |

were followed to call the variants (DePristo et al. 2011; Tarasov et al. 2015). Variants were filtered using exomeSuite, a software (Maranhao et al. 2014) for a homozygous recessive inheritance pattern. Subsequently, we examined the allele frequency, impact of mutation, and expression profile of promising candidate variants (Table 27.1). Finally, all variants were confirmed by segregation analysis through dideoxy sequencing (MacDonald et al. 2012).

## 27.3 Results

### *27.3.1 Linkage Analysis*

The linkage analysis localized the disease interval to chromosome 11q. The haplotype constructed from alleles of additional short tandem repeat (STR) markers in that region further supported localization to chromosome 11q (Fig. 27.1).

### *27.3.2 Identification of Rare and Potentially Damaging Variants*

59,064–63,286 SNPs were identified from two affected individuals (III:4 and III:7), whereas 63,996 SNPs were identified in the unaffected individual (III:1). On average, 5900 indels were found in each sample (the range 5295–6490). Analysis based on the pattern of inheritance identified 34,972 homozygous common variants in two affected individuals, which were absent or heterozygous in the unaffected. Among the identified variants, only 18 variants were rare (below 0.5%) and also present in

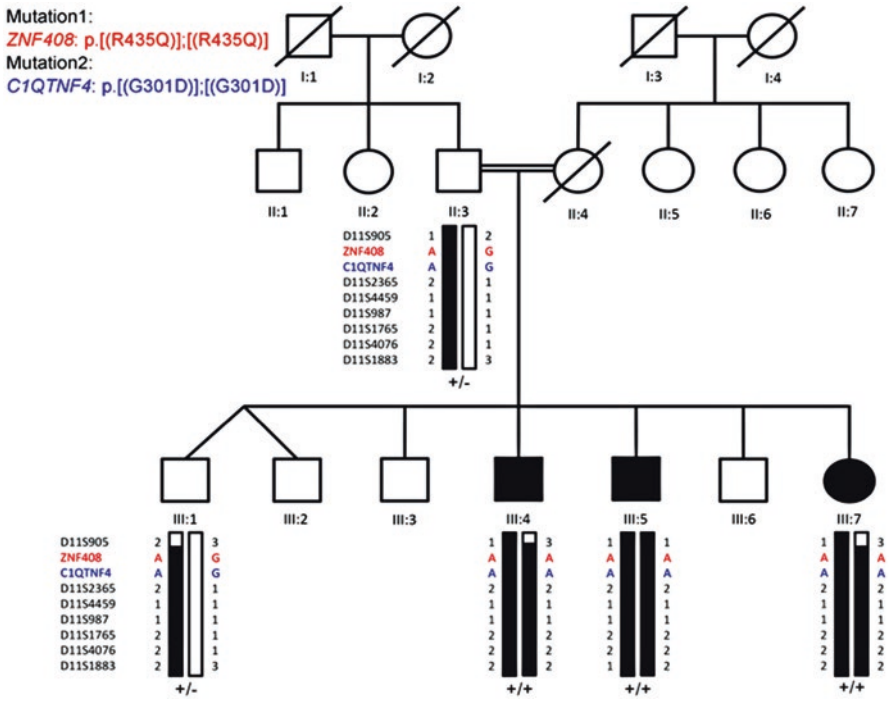


**Fig. 27.1** Pedigree drawing of family PKRD320 illustrates segregation of variants identified in *ZNF408* and *C1QTNF4* with the retinal phenotype. Asterisk indicates the individuals that were chosen for whole-exome sequencing

the exonic sequence. Further analysis based on expression profile identified seven candidate variants (Table 27.2). Among these, PolyPhen2 predicted three missense variants to be damaging. Sanger sequencing revealed the novel, homozygous missense variant, c.1304G > A; p.Arg435Gln in the *ZNF408* gene (NM_024741) segregating with disease in PKRD320 (Fig. 27.1). This variant was predicted to be probably damaging (PolyPhen2 = 0.983). Likewise, another homozygous missense variant c.902G > A; p.Gly301Asp in *C1QTNF4* (NM_031909), a gene that is not yet associated with RD, co-segregated with IRD in PKRD320 (Fig. 27.1). This missense variant was predicted to be damaging (PolyPhen2 = 1.000). The arginine 435 in *ZNF408* and glycine 301 in *C1QTNF4* are highly conserved through evolution (Fig. 27.2). *ZNF408* and *C1QTNF4* genes are located on chromosome 11 and only 884,907 base-pair distance apart (Table 27.2). Both these variants are rare (0.0001 for the *ZNF408* variant and the *C1QTNF4* variant is novel) and located in the disease interval identified by the haplotype (Fig. 27.1).

**Table 27.2** Candidate variants observed in PKRD320

| CHR | POS | rsID | ExAC | REF | ALT | GENE | cDNA Change | AA Change | PolyPhen2 |
|---|---|---|---|---|---|---|---|---|---|
| chr11 | 46,726,554 | rs185413257 | 0.0001 | G | A | *ZNF408* | c.1304G > A | p.R435Q | Probably damaging (0.983) |
| chr11 | 47,380,364 | rs201791759 | 0.0034 | C | T | *SPI1* | c.524G > A | p.R175Q | Benign |
| chr11 | 47,611,461 | – | | C | T | *C1QTNF4* | c.902G > A | p.G301D | Probably damaging (1) |
| chr11 | 61,730,439 | – | | C | A | *BEST1* | c.1633C > A | p.P545T | Benign |
| chr11 | 63,525,727 | – | | A | ACGTCGAC | *RTN3* | c.509_510insCGTCGAC | p.(N171 fs) | Did not segregate |
| chr11 | 71,948,779 | rs200679872 | 0.0016 | G | A | *INPPL1* | c.2765G > A | p.R922Q | Benign |
| chr13 | 111,294,837 | – | | A | C | *CARS2* | c.1448 T > G | p.L483 W | Probably damaging did not segregate |

Conserved region of p.Arg435 *ZNF408*

| Human | V430 | H431 | S432 | G433 | A434 | R435 | P436 | F437 | A438 | C439 | D440 |
|---|---|---|---|---|---|---|---|---|---|---|---|
| Chimp | V | H | S | G | A | R | P | F | A | C | D |
| Gorila | V | H | S | G | A | R | P | F | A | C | D |
| Orangutan | V | H | S | G | A | R | P | F | A | C | D |
| Baboon | I | H | S | G | A | R | P | F | A | C | D |
| Marmoset | V | H | S | G | A | R | P | F | A | C | D |
| Squirrel | V | H | S | G | A | R | P | F | A | C | D |
| Hamstar | V | H | S | G | A | R | P | F | A | C | D |
| Mouse | V | H | S | G | A | R | P | F | V | C | E |
| Rat | V | H | S | G | A | R | P | F | V | C | E |
| Rabbit | V | H | S | G | A | R | P | F | A | C | D |
| Pig | V | H | S | G | A | R | P | F | A | C | D |
| Cow | V | H | S | G | A | R | P | F | T | C | E |
| Horse | V | H | S | G | A | R | P | F | A | C | D |
| Dog | V | H | S | G | A | R | P | F | A | C | D |
| Microbat | V | H | S | G | A | R | P | F | A | C | D |
| Eleplant | V | H | S | G | A | R | P | F | A | C | D |
| X_Tropicalis | L | H | T | G | Q | R | P | Y | R | C | E |

Conserved region of p.Gly301 *C1QTNF4*

| Human | F296 | T297 | I298 | Y299 | K300 | G301 | H302 | N303 | S304 | Y305 | A306 |
|---|---|---|---|---|---|---|---|---|---|---|---|
| Chimp | F | T | I | Y | K | G | H | N | S | Y | A |
| Gorila | F | T | I | Y | K | G | H | N | S | Y | A |
| Orangutan | F | T | I | Y | K | G | H | N | S | Y | A |
| Baboon | F | T | I | Y | K | G | H | N | S | Y | A |
| Marmoset | F | T | I | Y | K | G | H | N | S | Y | A |
| Squirrel | F | T | I | Y | K | G | H | N | S | Y | A |
| Hamstar | F | T | I | Y | K | G | H | N | S | Y | A |
| Mouse | F | T | I | Y | K | G | H | N | S | Y | A |
| Rat | F | T | I | Y | K | G | H | N | S | Y | A |
| Rabbit | F | T | I | Y | K | G | H | N | S | Y | A |
| Pig | F | T | I | Y | K | G | H | N | S | Y | A |
| Cow | F | T | A | R | A | G | L | Y | R | P | A |
| Horse | F | T | I | Y | K | G | H | N | S | Y | A |
| Dog | F | T | I | Y | K | G | H | N | S | Y | A |
| Microbat | F | T | A | R | A | G | R | K | S | R | A |
| Eleplant | F | T | I | Y | K | G | H | N | S | Y | A |
| X_Tropicalis | F | T | I | Y | K | G | H | N | S | Y | A |

**Fig. 27.2** Illustration of amino acid conservation of Arg435 in *ZNF408* and Gly301 in *C1QTNF4* in their respective orthologs

### *27.3.3 Control Analysis*

Analysis of 100 ethnicity-matched appropriate controls did not detect the novel causative variants identified in this study, indicating that these variants are rare in the Pakistani population.

## 27.4 Discussion

We report the use of whole-exome sequencing coupled with bioinformatic analysis to identify potential novel variants segregating with IRD in a large inbred family of Pakistani origin. Our analysis identified two homozygous potentially pathogenic variants segregating with disease. These variants reside in a previously reported Zinc Finger Protein 408 (*ZNF408*) gene and Tumor Necrosis Factor-Related Protein 4 (*C1QTNF4*) gene, which has not been associated with IRD.

*ZNF408* encodes a transcription factor, and mutations in this gene have been associated with vitreoretinopathy and retinitis pigmentosa (Collin et al. 2013; Avila-Fernandez et al. 2015). *ZNF408* is expressed in both cone and rod photoreceptor retinal layer. The *znf408* knockdown transgenic zebrafish showed abnormal ventral retinal fusion and absence of blood vessels, leading to severe necrosis for the early stage of eye development (Collin et al. 2013).

*C1QTNF4* is a member of the CTRPs family and has an important function on cytokine activity. Interestingly, another member of this family, *C1QTNF5*, has been associated with autosomal dominant late-onset retinal degeneration (Hayward et al. 2003; Ayyagari et al. 2005). This suggests that the homozygous variant identified in *C1QTNF4* might play an important role in development of retinal pathology.

In conclusion, this study identified two homozygous variants in two different genes, i.e., *ZNF408* and *C1QTNF4*, segregating with IRD in a Pakistani family. It is rather challenging to delineate the contribution of each of these variants toward the development of the retinal phenotype and establish the causative role of the *C1QTNF4* variant in this pedigree. We speculate that the variant identified in *ZNF408*, a known IRD gene, is the primary cause of the phenotype in PKDR320. If the *C1QTNF4* variant has any effect on the retinal tissue, it may exasperate the phenotype due to the *ZNF408* variant. Future studies on the role of these mutant proteins and generation of animal models may reveal the potential role of the *C1QTNF4* gene in the pathophysiology of retinal degeneration.

**Acknowledgments** Dr. Ayyagari, the principal investigator and corresponding author had full access to all the data in the study and takes responsibility for the integrity of the data and the accuracy of the data analysis. Support: This work was supported by NEI-NIH grants EY014375, NIH-R01EY021237, NIH-R01EY013198, Foundation Fighting Blindness, and Research to Prevent Blindness.

## References

Avila-Fernandez A, Perez-Carro R, Corton M et al (2015) Whole-exome sequencing reveals ZNF408 as a new gene associated with autosomal recessive retinitis pigmentosa with vitreal alterations. Hum Mol Genet 24:4037–4048

Ayyagari R, Kakuk LE, Bingham EL et al (2000) Spectrum of color gene deletions and phenotype in patients with blue cone monochromacy. Hum Genet 107:75–82

Ayyagari R, Mandal MN, Karoukis AJ et al (2005) Late-onset macular degeneration and long anterior lens zonules result from a CTRP5 gene mutation. Invest Ophthalmol Vis Sci 46:3363–3371
Boughman JA, Fishman GA (1983) A genetic analysis of retinitis pigmentosa. Br J Ophthalmol 67:449–454
Boughman JA, Conneally PM, Nance WE (1980) Population genetic studies of retinitis pigmentosa. Am J Hum Genet 32:223–235
Boughman JA, Vernon M, Shaver KA (1983) Usher syndrome: definition and estimate of prevalence from two high-risk populations. J Chronic Dis 36:595–603
Carr RE, Noble KG, Nasaduke I (1978) Hereditary hemorrhagic macular dystrophy. Am J Ophthalmol 85:318–328
Collin RW, Nikopoulos K, Dona M et al (2013) ZNF408 is mutated in familial exudative vitreoretinopathy and is crucial for the development of zebrafish retinal vasculature. Proc Natl Acad Sci U S A 110:9856–9861
Cremers FP, van de Pol DJ, van Driel M et al (1998) Autosomal recessive retinitis pigmentosa and cone-rod dystrophy caused by splice site mutations in the Stargardt's disease gene ABCR. Hum Mol Genet 7:355–362
Daiger SP, Sullivan LS, Bowne SJ (2013) Genes and mutations causing retinitis pigmentosa. Clin Genet 84:132–141
DePristo MA, Banks E, Poplin R et al (2011) A framework for variation discovery and genotyping using next-generation DNA sequencing data. Nat Genet 43:491–498
Duncan JL, Zhang Y, Gandhi J et al (2007) High-resolution imaging with adaptive optics in patients with inherited retinal degeneration. Invest Ophthalmol Vis Sci 48:3283–3291
Genomes Project C, Auton A, Brooks LD et al (2015) A global reference for human genetic variation. Nature 526:68–74
Harrow J, Frankish A, Gonzalez JM et al (2012) GENCODE: the reference human genome annotation for the ENCODE project. Genome Res 22:1760–1774
Hartong DT, Berson EL, Dryja TP (2006) Retinitis pigmentosa. Lancet 368:1795–1809
Hayward C, Shu X, Cideciyan AV et al (2003) Mutation in a short-chain collagen gene, CTRP5, results in extracellular deposit formation in late-onset retinal degeneration: a genetic model for age-related macular degeneration. Hum Mol Genet 12:2657–2667
Heckenlively JR (1988) Retinitis Pigmentosa, 1st edn. J.B. Lippincott Company, Philadelphia
Inglehearn CF (1998) Molecular genetics of human retinal dystrophies. Eye (Lond) 12(Pt 3b):571–579
Kenney MC, Chwa M, Atilano SR et al (2013) Mitochondrial DNA variants mediate energy production and expression levels for CFH, C3 and EFEMP1 genes: implications for age-related macular degeneration. PLoS One 8:e54339
Kozomara A, Griffiths-Jones S (2011) miRBase: integrating microRNA annotation and deep-sequencing data. Nucleic Acids Res 39:D152–D157
Lathrop GM, Lalouel JM (1984) Easy calculations of lod scores and genetic risks on small computers. Am J Hum Genet 36:460–465
Lek M, Karczewski KJ, Minikel EV et al (2016) Analysis of protein-coding genetic variation in 60,706 humans. Nature 536:285–291
Li H, Durbin R (2009) Fast and accurate short read alignment with Burrows-Wheeler transform. Bioinformatics 25:1754–1760
MacDonald IM, Gudiseva HV, Villanueva A et al (2012) Phenotype and genotype of patients with autosomal recessive bestrophinopathy. Ophthalmic Genet 33:123–129
Maranhao B, Biswas P, Duncan JL et al (2014) exomeSuite: whole exome sequence variant filtering tool for rapid identification of putative disease causing SNVs/indels. Genomics 103:169–176
Morimura H, Fishman GA, Grover SA et al (1998) Mutations in the RPE65 gene in patients with autosomal recessive retinitis pigmentosa or leber congenital amaurosis. Proc Natl Acad Sci U S A 95:3088–3093
Naeem MA, Gottsch AD, Ullah I et al (2015) Mutations in GRM6 identified in consanguineous Pakistani families with congenital stationary night blindness. Mol Vis 21:1261–1271

Nochez Y, Arsene S, Gueguen N et al (2009) Acute and late-onset optic atrophy due to a novel OPA1 mutation leading to a mitochondrial coupling defect. Mol Vis 15:598–608

RetNet In: http://www.sph.uth.tmc.edu/Retnet/

Schaffer AA, Gupta SK, Shriram K et al (1994) Avoiding recomputation in linkage analysis. Hum Hered 44:225–237

Sherry ST, Ward MH, Kholodov M et al (2001) dbSNP: the NCBI database of genetic variation. Nucleic Acids Res 29:308–311

Stenson PD, Mort M, Ball EV et al (2014) The human gene mutation database: building a comprehensive mutation repository for clinical and molecular genetics, diagnostic testing and personalized genomic medicine. Hum Genet 133:1–9

Tarasov A, Vilella AJ, Cuppen E et al (2015) Sambamba: fast processing of NGS alignment formats. Bioinformatics 31:2032–2034

Zheng A, Li Y, Tsang SH (2015) Personalized therapeutic strategies for patients with retinitis pigmentosa. Expert Opin Biol Ther 15:391–402

# Chapter 28
# Identification of Novel Deletions as the Underlying Cause of Retinal Degeneration in Two Pedigrees

**Kari Branham, Aditya A. Guru, Igor Kozak, Pooja Biswas, Mohammad Othman, Kameron Kishaba, Hassan Mansoor, Sheikh Riazuddin, John R. Heckenlively, S. Amer Riazuddin, J. Fielding Hejtmancik, Paul A. Sieving, and Radha Ayyagari**

**Abstract** Retinal dystrophies are a phenotypically and genetically complex group of conditions. Because of this complexity, it can be challenging in many families to determine the inheritance based on pedigree analysis alone. Clinical examinations were performed and blood samples were collected from a North American (M1186) and a consanguineous Pakistani (PKRD168) pedigree affected with two different retinal dystrophies (RD). Based on the structure of the pedigrees, inheritance patterns in the families were difficult to determine. In one family, linkage analysis was performed with markers on X-chromosome. In the second family, whole-exome sequencing (WES) was performed. Subsequent Sanger sequencing of genes of interest was performed. Linkage and haplotype analysis localized the disease interval to a 70 Mb region on the X chromosome that encompassed *RP2* and *RPGR* in M1186. The disease haplotype segregated with RD in all individuals except for an unaffected man (IV:3) and his affected son (V:1) in this pedigree. Subsequent analysis identified a novel *RPGR* mutation (p. Lys857Glu fs221X) in all affected members of M1186 except V:1. This information suggests that there is an unidentified second cause of retinitis pigmentosa (RP) within the family. A

Kari Branham and Aditya A. Guru are contributed equally to this work.

This work was supported by NIH-EY021237; NIH- EY002162, NIH-EY0020846, NIH-P30EY022589, Foundation Fighting Blindness (RA), Research to Prevent Blindness (RA).

K. Branham · M. Othman · J. R. Heckenlively
University of Michigan, Department of Ophthalmology and Visual Sciences, Ann Arbor, MI, USA

A. A. Guru · P. Biswas · K. Kishaba · R. Ayyagari (✉)
Shiley Eye Institute, University of California San Diego, La Jolla, CA, USA
e-mail: rayyagari@ucsd.edu

I. Kozak
Shiley Eye Institute, University of California San Diego, La Jolla, CA, USA

Moorfields Eye Hospital Centre, Abu Dhabi, United Arab Emirates



J. D. Ash et al. (eds.), *Retinal Degenerative Diseases*, Advances in Experimental Medicine and Biology 891, https://doi.org/10.1007/978-3-319-75402-4_28

novel two-base-pair deletion (p. Tyr565Ter fsX) in *CHM* (choroideremia) was found to segregate with RD in PKRD168. This paper highlights the challenges of interpreting family history in families with RD and reports on the identification of novel mutations in two RD families.

**Keywords** XLRP · Choroideremia · RPGR · Deletions · Exome sequencing · Linkage analysis

## 28.1 Introduction

Retinal dystrophies (RD) encompass a clinically and phenotypically diverse group of retinal diseases which cause a significant impact on visual functioning and often the quality of life (Berger et al. 2010). Mutations in more than 260 genes have been identified which are known to cause syndrome and non-syndromic forms of autosomal dominant (AD), autosomal recessive (AR) and X-linked (XL) forms of the disease. Due to the extreme genetic heterogeneity and diverse inheritance patterns, genetic testing and genetic counseling for patients affected with RD can prove to be challenging. Complexities such as de novo mutations, expressive variability, reduced penetrance, and manifesting female carriers of the XL disease can make determining the inheritance very complicated. Similarly, pseudo dominant inheritance in which a high degree of consanguinity or high carrier frequencies of common mutations in a population may also complicate determination of inheritance patterns of pedigrees mimicking AD inheritance (Churchill et al. 2013; Huckfeldt et al. 2016).

Depending on the specific diagnosis, female carriers of X-linked RD (XLRD), such as XL retinitis pigmentosa (XLRP) and choroideremia may manifest disease symptoms and/or have fundus findings consistent with being a carrier (Vajaranant

H. Mansoor
Al-Shifa Trust Eye Hospital, Rawalpindi, Pakistan

S. Riazuddin
National Centre of Excellence in Molecular Biology, University of the Punjab, Lahore, Pakistan

Allama Iqbal Medical College, University of Health Sciences, Lahore, Pakistan

National Centre for Genetic Diseases, Shaheed Zulfiqar Ali Bhutto Medical University, Islamabad, Pakistan

S. A. Riazuddin (✉)
Department of Ophthalmology, The Wilmer Eye Institute, Johns Hopkins University School of Medicine, Baltimore, MD, USA
e-mail: riazuddin@ncemb.org

J. F. Hejtmancik · P. A. Sieving
Ophthalmic Genetics and Visual Function Branch, National Eye Institute, NIH, Bethesda, MD, USA

et al. 2008; Comander et al. 2015). In addition, XL dominant forms of RP with severely affected females (Wu et al. 2010) and ADRP with reduced penetrance have also been reported (Sullivan et al. 2006; Bowne et al. 2013). In fact, 8.5% of families, which were originally thought to be AD, were determined to be XL families (Churchill et al. 2013). Because of these complexities, it can be particularly difficult to distinguish between AD and XL families.

We examined a North American family and a Pakistani family affected with an RD. In both families, it was challenging to determine the inheritance of the condition based on pedigree analysis alone, but this was resolved through genetic analysis.

## 28.2 Materials and Methods

### *28.2.1 Ethics*

All research procedures were approved by the Institutional Review Boards (IRB) of all participating institutions. Each participant in this study provided written consent in accordance with the Declaration of Helsinki.

### *28.2.2 Subjects and Clinical Examination*

Two large pedigrees with multiple affected family members were recruited from the Punjab province of Pakistan and from North America. The ophthalmic evaluation was performed as described previously (Ayyagari et al. 2005; Duncan et al. 2007).

### *28.2.3 Genetic Analysis in M1186*

Two-point linkage analysis was carried out using the MLINK program of the LINKAGE package (Lathrop and Lalouel 1984). Following the identification of disease interval that encompassed *RP2* and *RPGR*, sequencing of the *RP2*, *RPGR*, and ORF15 region of *RPGR* was performed in 14 available family members as described earlier (Branham et al. 2012).

### *28.2.4 Whole-Exome Sequencing (WES) and Variant Calling in PKRD168*

Genomic DNA from two affected males (R2821 and R2827) was used for WES using Agilent V5 + UTRs probes on the Illumina HiSeq (Illumina, San Diego, CA). Read mapping and variant calling were done as described before

(Maranhao et al. 2014). Variants were filtered using exomeSuite (Maranhao et al. 2014) for low-frequency, deleterious mutations in genes expressed in the retina. Finally, candidate variants were confirmed by segregation analysis through Sanger dideoxy sequencing.

## 28.3 Results

### *28.3.1 Clinical and Pedigree Characterization*

In Family M1186 (Fig. 28.1), the pedigree analysis was performed to determine the possible genetic inheritance of RP. Males in the family showed severe retinal degeneration with typical bone spicule changes, non-recordable electroretinogram (ERG) by the age of 20, and childhood onset of night vision abnormalities. Most females in the family demonstrated a reduction in ERG parameters, mild vision loss, and fundus changes consistent with being a carrier (Fig. 28.2). However, one female (M1186-IV:1) had a non-recordable rod and cone electroretinogram (ERG) at the age of 29. Therefore, the phenotype within the family was most suggestive of XLRP, but the pedigree with the instance of an unaffected man (IV:3) having an affected

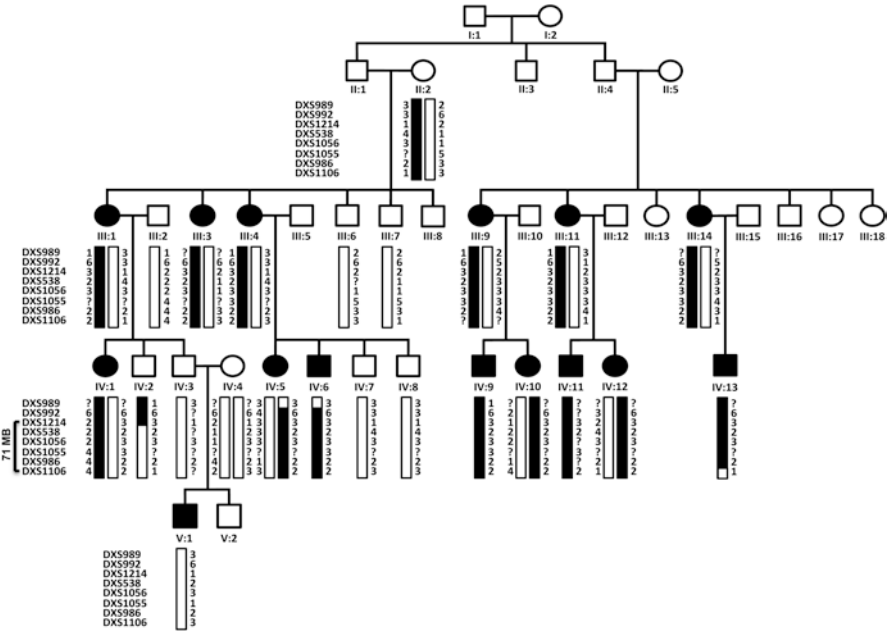


**Fig. 28.1** Pedigree drawing and haplotype analysis of Family M1186. Haplotype was constructed using microsatellite markers on the X chromosome and identified DXS1214 and DXS1106 as the boundaries of the disease interval


**Fig. 28.2** Fundus image of a female M1186-III-3 showing patchy bone spicule-like changes and loss of RPE in the inferior retina consistent with being an XLRP carrier

son (V:1) was more suggestive of ADRP with incomplete penetrance. In this case, both IV:3 and his wife were unaffected with disease, and their son V:1 was affected from the age of 8.

In parallel, a five-generation family, PKRD168 with two consanguineous marriages was investigated to delineate the genetic determinants that are responsible for RD (Fig. 28.3). Fundus photographs demonstrated loss of RPE and attenuated vessels in affected males and milder changes in females (Fig. 28.4). Abnormal ERGs were observed in affected males. The pedigree structure, especially the consanguinity within the family, was suggestive of AR inheritance. However, we could not rule out XL inheritance due to the fact that only males in the family manifested the retinal phenotype. Furthermore, we could not rule out AD inheritance with reduced penetrance as individuals in two generations of this family are affected.

### *28.3.2 Genetic Analysis*

In Family M1186, linkage analysis localized the RP gene in this family between markers DXS1214 and DXS1106. Analysis with markers linked to *RP2*, DXS8080 ($Z$ = 2.65 at theta = 0.0), DXS1055 ($Z$ = 2.58 at theta = 0), DXS6619 ($Z$ = 2.0 at theta = 0), and DXS1003 ($Z$ = 1.16 at theta = 0), and markers linked to *RP3*, DXS1056 ($Z$ = 2.48 at theta = 0), DXS538 ($Z$ = 2.5 at theta = 0), and DXS6616 ($Z$ = 1.9 at theta = 0), gave significant positive LOD scores. Haplotype analysis further confirmed the localization of disease interval between DXS1214 and DXS1106 (Fig. 28.1). Sequencing of the *ORF15* region of *RPGR* (reference sequence NM_001034853.1) identified a novel frameshift mutation c. 2568_2569 ins G (p. Lys857Glu fs) which

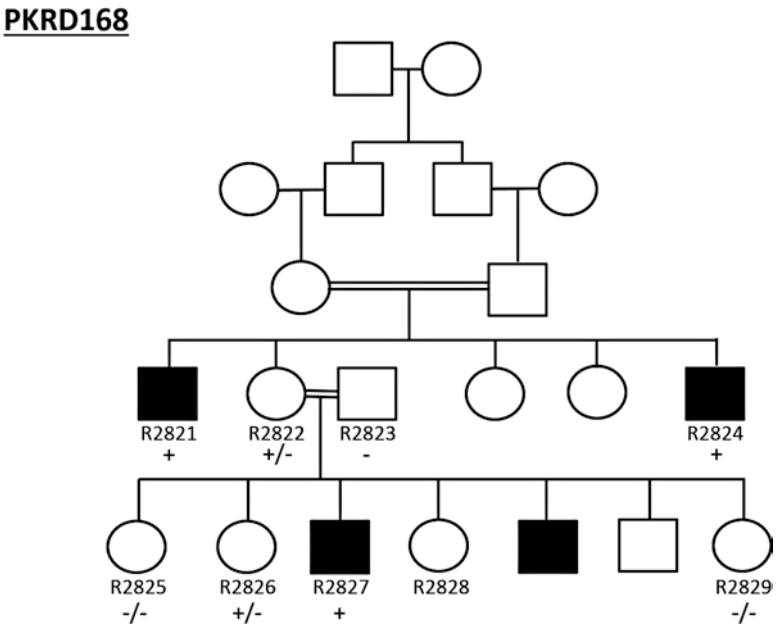


**Fig. 28.3** Pedigree drawing of Family PKRD168 showing segregation of mutations and individuals who are positive (+) and negative (−) for the *CHM* mutation

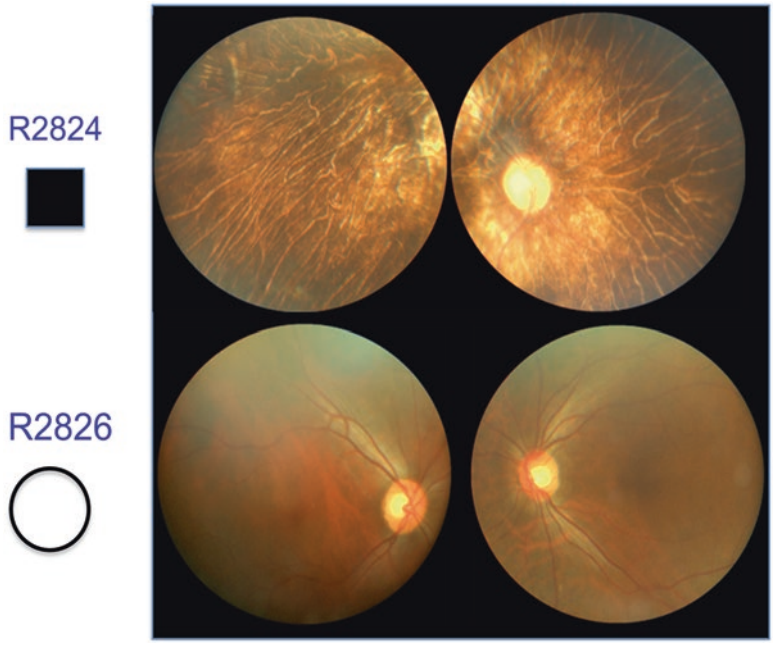


**Fig. 28.4** Fundus photographs of affected male R2824 and carrier female R2826 from Family PKRD168. Affected males in this family showed loss of RPE and attenuated vessels, and the carrier female showed optic nerve pallor in the right eye and widespread loss of RPE and attenuated retinal vessels

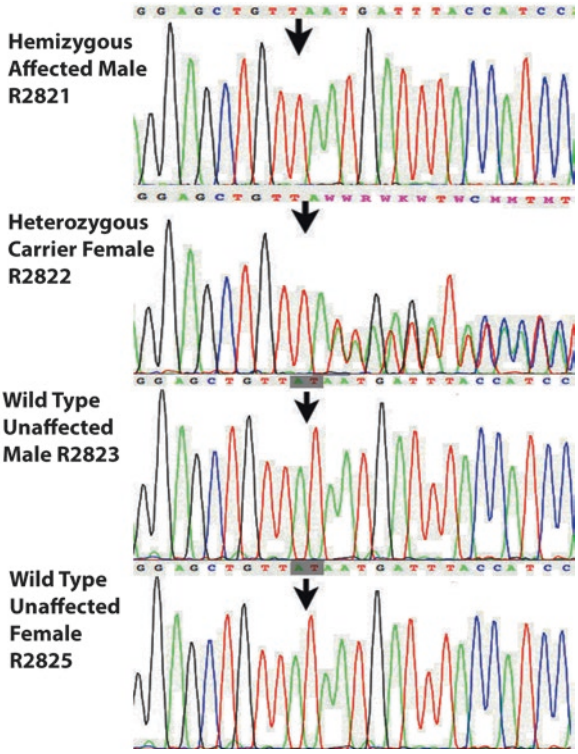


**Fig. 28.5** Electropherograms of sequence encompassing the *CHM* mutation in members of PKRD168. Arrows are pointing the location of the mutation

was found in all affected males except M1186-V:1. A similar mutation was reported affecting the same amino acid but with a deletion of c.2571_2572delAG (Sharon et al. 2003). A missense change c.2565 A > G was also present but is unlikely to be disease causing as it is a synonymous change (Glu855Glu). The frameshift change was also detected in the heterozygous state in six female carriers with disease manifestations and was not found in three males reported to be unaffected. Interestingly, the affected male V:1 and his unaffected parents IV:3 and IV:4 did not carry the disease haplotype or the p. Lys857Glufs mutation observed in this family, indicating that the affected male V:1 has a different and unidentified cause for his RP.

In PKRD168, the exomes of two affected males were sequenced that identified a total of 61,717 single nucleotide variants (SNV) along with 4344 indels (insertion/deletions). Subsequent filtering of these variants with exomeSuite identified a novel two-base pair (AT) deletion (c.1694_1695del) in exon 14 of the *CHM* (choroideremia) on the X chromosome. The deletion variant was confirmed by Sanger sequencing (Fig. 28.5), which segregated with the RD phenotype in PKRD168 (Fig. 28.1). This mutation was not observed in 100 ethnically matched controls, ExAc, and 1000 genome databases. The mutation is predicted to cause premature termination of the CHM protein at amino acid 564, resulting in the loss of 89 amino acids at the C-terminal end of the protein. The phenotype of RD in this family is consistent with choroideremia.

## 28.4 Conclusion and Discussion

Patterns of inheritance can often be challenging to determine when working with patients affected with inherited retinal disease. These two cases demonstrate pedigree complications, such as more than one genetic cause of RP within a single family and multiple levels of consanguinity which can make it challenging to determine the most likely inheritance within a family. Moreover, they highlight the importance of genetic testing for these families to allow for accurate genetic counseling.

## References

Ayyagari R, Mandal MN, Karoukis AJ et al (2005) Late-onset macular degeneration and long anterior lens zonules result from a CTRP5 gene mutation. Invest Ophthalmol Vis Sci 46:3363–3371

Berger W, Kloeckener-Gruissem B, Neidhardt J (2010) The molecular basis of human retinal and vitreoretinal diseases. Prog Retin Eye Res 29:335–375

Bowne SJ, Sullivan LS, Avery CE et al (2013) Mutations in the small nuclear riboprotein 200 kDa gene (SNRNP200) cause 1.6% of autosomal dominant retinitis pigmentosa. Mol Vis 19:2407–2417

Branham K, Othman M, Brumm M et al (2012) Mutations in RPGR and RP2 account for 15% of males with simplex retinal degenerative disease. Invest Ophthalmol Vis Sci 53:8232–8237

Churchill JD, Bowne SJ, Sullivan LS et al (2013) Mutations in the X-linked retinitis pigmentosa genes RPGR and RP2 found in 8.5% of families with a provisional diagnosis of autosomal dominant retinitis pigmentosa. Invest Ophthalmol Vis Sci 54:1411–1416

Comander J, Weigel-DiFranco C, Sandberg MA et al (2015) Visual function in carriers of X-linked retinitis pigmentosa. Ophthalmology 122:1899–1906

Duncan JL, Zhang Y, Gandhi J et al (2007) High-resolution imaging with adaptive optics in patients with inherited retinal degeneration. Invest Ophthalmol Vis Sci 48:3283–3291

Huckfeldt RM, East JS, Stone EM et al (2016) Phenotypic variation in a family with pseudodominant stargardt disease. JAMA Ophthalmol 134:580–583

Lathrop GM, Lalouel JM (1984) Easy calculations of lod scores and genetic risks on small computers. Am J Hum Genet 36:460–465

Maranhao B, Biswas P, Duncan JL et al (2014) exomeSuite: whole exome sequence variant filtering tool for rapid identification of putative disease causing SNVs/indels. Genomics 103:169–176

Sharon D, Sandberg MA, Rabe VW et al (2003) RP2 and RPGR mutations and clinical correlations in patients with X-linked retinitis pigmentosa. Am J Hum Genet 73:1131–1146

Sullivan LS, Bowne SJ, Seaman CR et al (2006) Genomic rearrangements of the PRPF31 gene account for 2.5% of autosomal dominant retinitis pigmentosa. Invest Ophthalmol Vis Sci 47:4579–4588

Vajaranant TS, Fishman GA, Szlyk JP et al (2008) Detection of mosaic retinal dysfunction in choroideremia carriers electroretinographic and psychophysical testing. Ophthalmology 115:723–729

Wu DM, Khanna H, Atmaca-Sonmez P et al (2010) Long-term follow-up of a family with dominant X-linked retinitis pigmentosa. Eye (Lond) 24:764–774

# Chapter 29
# Molecular Findings in Families with an Initial Diagnose of Autosomal Dominant Retinitis Pigmentosa (adRP)

**Stephen P. Daiger, Sara J. Bowne, Lori S. Sullivan, Kari Branham, Dianna K. Wheaton, Kaylie D. Jones, Cheryl E. Avery, Elizabeth D. Cadena, John R. Heckenlively, and David G. Birch**

**Abstract** Genetic testing of probands in families with an initial diagnosis of autosomal dominant retinitis pigmentosa (adRP) usually confirms the diagnosis, but there are exceptions. We report results of genetic testing in a large cohort of adRP families with an emphasis on exceptional cases including X-linked RP with affected females; homozygous affected individuals in families with heterozygous, dominant disease; and independently segregating mutations in the same family. Genetic testing was conducted in more than 700 families with a provisional or probable diagnosis of adRP. Exceptions to the proposed mode of inheritance were extracted from our comprehensive patient and family database. In a subset of 300 well-characterized families with a probable diagnosis of adRP, 195 (70%) have dominant mutations in known adRP genes but 25 (8%) have X-linked mutations, 3 (1%) have multiple segregating mutations, and 3 (1%) have dominant-acting mutations in genes previously associated with recessive disease. It is currently possible to determine the underlying disease-causing gene and mutation in approximately 80% of families with an initial diagnosis of adRP, but 10% of "adRP" families have a variant mode of inheritance. Informed genetic diagnosis requires close collaboration between clinicians, genetic counselors, and laboratory scientists.

S. P. Daiger (✉)
Human Genetics Center, School of Public Health, The University of Texas Health Science Center (UTHealth), Houston, TX, USA

Ruiz Department of Ophthalmology and Visual Science, UTHealth, Houston, TX, USA
e-mail: stephen.p.daiger@uth.tmc.edu

S. J. Bowne · L. S. Sullivan · C. E. Avery · E. D. Cadena
Human Genetics Center, School of Public Health, The University of Texas Health Science Center (UTHealth), Houston, TX, USA

K. Branham · J. R. Heckenlively
Kellogg Eye Center, University of Michigan, Ann Arbor, MI, USA

D. K. Wheaton · K. D. Jones · D. G. Birch
The Retina Foundation of the Southwest, Dallas, TX, USA



J. D. Ash et al. (eds.), *Retinal Degenerative Diseases*, Advances in Experimental Medicine and Biology 891, https://doi.org/10.1007/978-3-319-75402-4_29

**Keywords** Retinitis pigmentosa (RP) · Autosomal dominant retinitis pigmentosa · Next-generation sequencing · Linkage mapping · X-linked retinitis pigmentosa · Semidominant inheritance · Prevalence of mutations

## 29.1 Introduction

Retinitis pigmentosa (RP) has a prevalence of approximately 1 in 3,100 and affects more than 1.5 million individuals worldwide (Haim 2002; Daiger et al. 2013). RP is extremely heterogeneous: mutations in more than 80 genes cause syndromic and non-syndromic forms of RP, more than 3,500 mutations have been described in these genes, and disease symptoms and progression are highly variable (Berger et al. 2010; Wright et al. 2010; Daiger et al. 2013; RetNet 2018). To date, mutations in 29 genes are known to cause autosomal dominant RP (adRP), and these genes are themselves highly heterogeneous (Daiger et al. 2014; RetNet 2018).

Our research focuses on genes and mutations causing adRP. Over the past 30 years, we have assembled a cohort of adRP families and applied a wide range of methods to detect the disease-causing mutation in each family, including linkage mapping and next-generation sequencing (NGS) (Sohocki et al. 2001; Sullivan et al. 2006; Bowne et al. 2011a; Koboldt et al. 2013; Wang et al. 2013). As more and more RP genes have been identified, the fraction of adRP families in which we can identify the underlying disease-causing gene and mutation has increased from a few percent to the majority of patients. However, a substantial fraction of families with a provisional diagnosis of adRP (5–10%) have an alternative or more complicated molecular diagnosis. To illustrate this problem, we provide several examples of "complicated" families selected from the larger set of adRP families.

## 29.2 Materials and Methods

### *29.2.1 Family Ascertainment and Clinical Characterization*

Families in our studies are ascertained by clinical collaborators in Houston, the Retina Foundation of the Southwest, the Kellogg Eye Center, and other retinal genetics centers. Genetic testing is done in the Laboratory for Molecular Diagnosis of Inherited Eye Diseases, CLIA ID 45D0935007, Human Genetics Center, School of Public Health, the Univ. of Texas Health Science Center (UTHealth), Houston. Families are included in the AdRP Cohort if they have an initial diagnosis of adRP and three or more affected generations with affected females or two or more generations with male-to-male transmission.

The research adheres to tenets of the Declaration of Helsinki, and the studies were approved by the Committee for the Protection of Human Subjects at UTHealth and by human subjects review boards at participating institutions.

### *29.2.2 Next-Generation Sequencing (NGS)*

Whole-exome and whole-genome NGS was done at The Genome Institute, Washington Univ., St. Louis (Bowne et al. 2011a). Retinal targeted-capture NGS was done in the DNA Diagnostic Laboratory, UTHealth, and in collaboration with Dr. Rui Chen, Dept. of Molecular and Human Genetics, Baylor College of Medicine, Houston (Wang et al. 2013; Bowne et al. 2015).

### *29.2.3 Linkage Mapping and Haplotype Analysis*

Genotyping for linkage mapping was done at the Hussman Institute for Human Genomics, Univ. of Miami, using Affymetrix Genome-Wide Human SNP 6.0 array data, and at the UCLA Sequencing and Genotyping Center using an ABI High Density 5 cM STR marker set (Bowne et al. 2011b, 2016; Sullivan et al. 2014). Analysis was conducted using PLINK and Merlin. Haplotypes were determined by inspection and confirmed by segregation analysis.

## 29.3 Results

### *29.3.1 Background*

The Laboratory for Molecular Diagnosis of Inherited Eye Diseases (LMDIED) in Houston is focused on finding genes and mutations causing autosomal dominant retinitis pigmentosa (adRP) and related diseases. Patients are enrolled and examined by clinical collaborators. Support is provided through several projects including FFB Research Centers, the NEI-NIH eyeGENE Network® (Sullivan et al. 2013), and the Texas 1000 Project (Daiger et al. 2016).

Currently, 2,300 families with inherited retinal disease are enrolled; of these, approximately 50% have a diagnosis of adRP. Samples are available from 4,600 members of these families; approximately 75% are affected, the rest are at-risk or unaffected family members for linkage testing. Among the families, a subset of 300 is designated as the AdRP Cohort and a further 400 are an adRP confirmation panel. The AdRP Cohort consists of families with a likely diagnosis of dominant disease

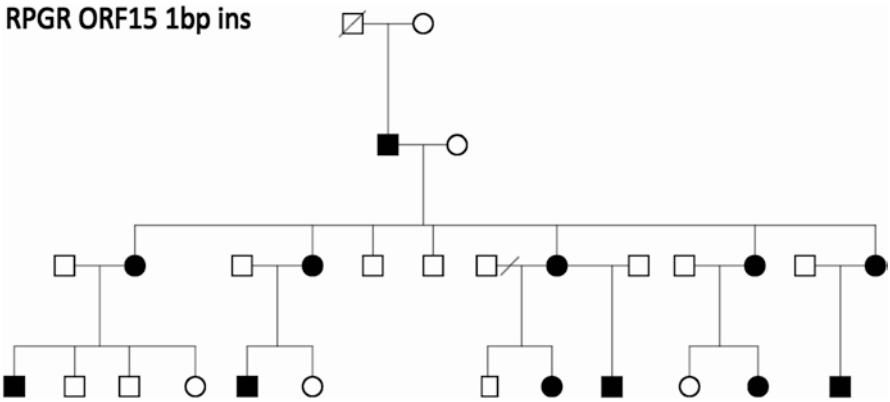


**Fig. 29.1** Pedigree of a family with a clinical diagnosis of RP and apparent autosomal dominant inheritance. The disease-causing mutation in the family is a 1 bp deletion in ORF15 of the X-linked *RPGR* gene (Mears et al. 2000)

based on clinical examination and pedigree. The confirmation panel has less stringent criteria. The following exceptional families are drawn from the AdRP Cohort.

### *29.3.2 X-Linked RP in Apparent adRP Families*

Figure 29.1 is the pedigree of a family with a diagnosis of RP and apparent autosomal dominant inheritance (Mears et al. 2000). There are at least three generations of inheritance, and males and females are equally likely to be affected. However, there is no male-to-male transmission, which would exclude X-linked inheritance, and in retrospect, the affected females are less severely affected on average than the males. In fact, the family has X-linked RP with a mutation in *RPGR*. It is now clear that carrier females with X-linked RP mutations may be affected (Comander et al. 2015); however, the extent to which X-linked families may be misdiagnosed is striking. In the AdRP Cohort, at least 8% of families with a provisional diagnosis of adRP have X-linked RP (Churchill et al. 2013). Further, up to 15% of males with isolated (simplex) RP have *RPGR* or *RP2* mutations (Branham et al. 2012). This may be the single most common diagnostic complication with RP.

### *29.3.3 Semidominant Inheritance*

The expectation is that an autosomal mutation in a single family is either dominant acting or recessive acting, but not both. However, two families in the Cohort, Figs. 29.2 and 29.3, display both modes. Figure 29.2 is the pedigree of an adRP family with a Glu847Lys mutation in *HK1* (Sullivan et al. 2014). Although

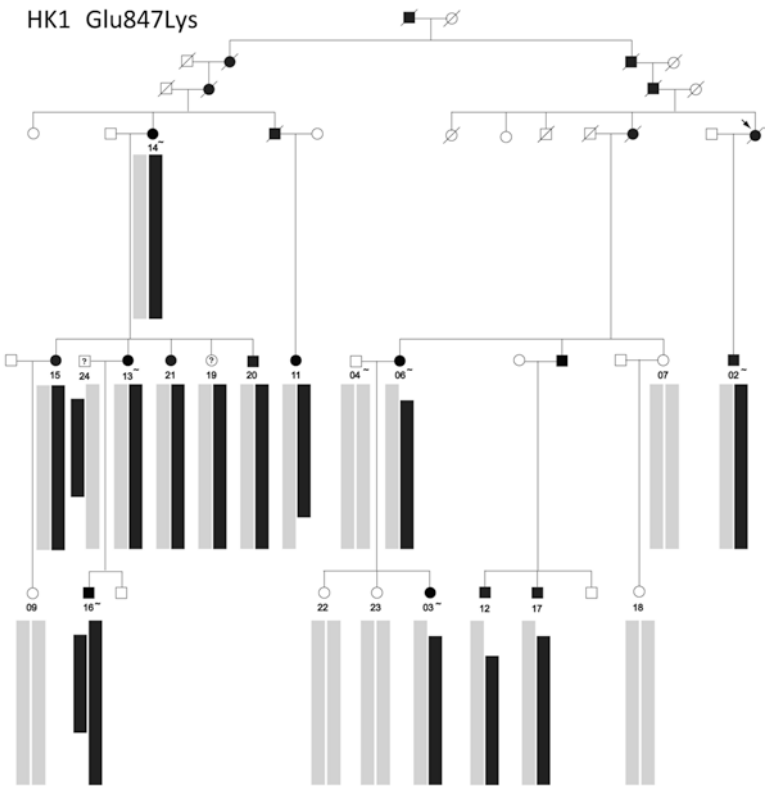


**Fig. 29.2** Pedigree and segregating haplotypes in a family with adRP caused by a Glu847Lys missense mutation in *HK1* (Sullivan et al. 2014). Black bars show the shared haplotype segregating with the *HK1* mutation on chromosome 10q22.1, and gray bars represent the unrelated haplotypes in *trans*. Individual 16 carries two copies of the mutation-associated haplotype but with different recombinant end points

consanguinity is not reported in the family, one individual, number 16, has two copies of the mutation and severe RP. Although he is homozygous for the mutation, the two associated haplotypes differ in flanking sequences, suggesting they descend from a distant ancestor. He has no other apparent clinical findings.

Figure 29.3 is the pedigree of a nuclear family within a larger family with adRP caused by an RP1 Arg677X mutation (Sullivan et al. 1999). The parents, 04 and 05, are distantly related. Of the six children in the pedigree, three, 07–09, inherited one copy of the *RP1* mutation; two, 06 and 07, inherited two copies; and 10 has wild-type *RP1* only. Family members with one copy of the mutation have classical RP with onset in late adolescence, whereas individuals homozygous for the mutation have early-onset, rapidly progressing RP, consistent with Leber congenital amaurosis. Like the HK1 homozygote, the RP1 homozygotes did not show apparent non-ocular disease at the last examination.

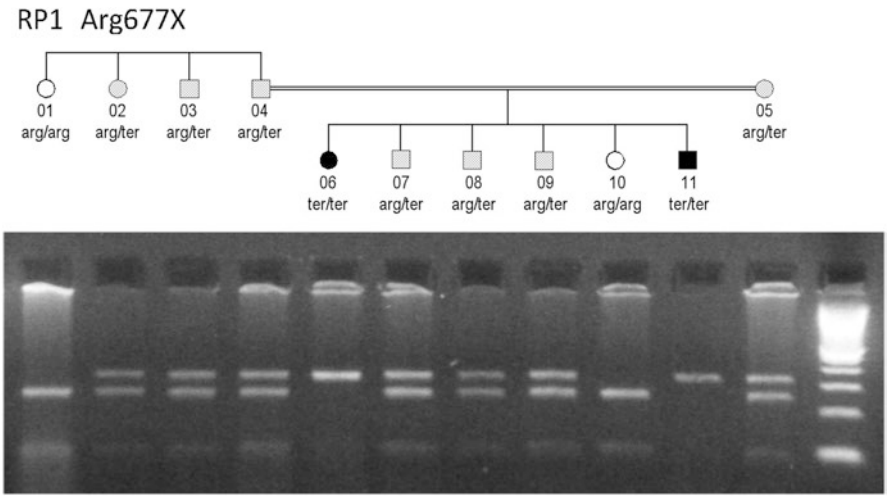


**Fig. 29.3** Pedigree of a nuclear family within a larger family with adRP caused by an *RP1* Arg677X mutation (Sullivan et al. 1999). Parents 04 and 05 are related and both are heterozygous for the *RP1* mutation. Individuals 07–09 inherited one copy of the mutation, and individuals 06 and 11 inherited two copies. Photograph below is a restriction digest showing segregation of the wild-type (lower band) and mutant (upper band) *RP1* alleles of the individuals in the pedigree

This type of inheritance is semidominant, that is, a single allele causing both dominant and recessive disease but with more severe disease in the homozygote – in this case apparently limited to a single tissue.

### *29.3.4 Independently Segregating Mutations*

Figure 29.4 is the pedigree of a family with apparent adRP but a possible non-penetrant individual (Wheaton et al. 2016). Targeted capture NGS, though, revealed mutations in two disease-causing genes, a dominant-acting RP1 Arg677X mutation, and compound heterozygous, recessive mutations in *USH2A*, Cys419Phe, and Glu767Serfs*21. This is notable for several reasons. First, if just the *RP1* mutation had been reported, individual 3.3 would have been misdiagnosed. For this reason, it is wrong to assume that all affected individuals in a family share the same cause. Second, this is one example of many in which *USH2A* mutations are associated with RP alone, not Usher syndrome (Seyedahmadi et al. 2004). Finally, at least three families in our AdRP Cohort have multiple, independently segregating mutations, with additional families in the extended cohort: this is not a rare phenomenon.

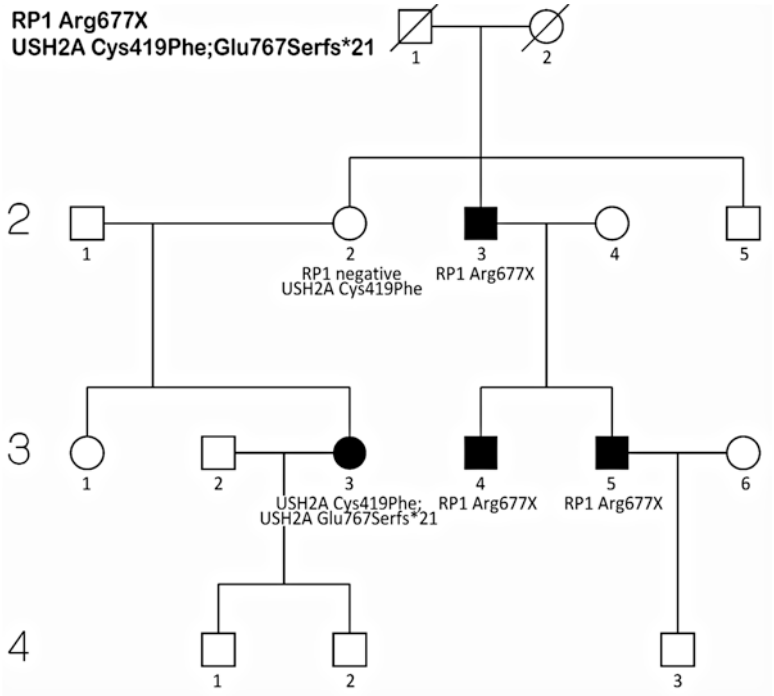


**Fig. 29.4** Pedigree of a family with a provisional diagnosis of adRP but an apparent non-penetrant individual, 2.2 (Wheaton et al. 2016). Molecular testing showed an autosomal dominant *RP1* Arg677X mutation segregating in individuals 2.3, 3.4, and 3.5, whereas individual 3.3 is a compound heterozygote for *USH2A* [Cys419Phe];[Glu767Serfs*21] mutations. Individual 2.2 is a carrier of the *USH2A* Cys419Phe mutation but does not carry the *RP1* mutation

## 29.4 Discussion and Conclusion

William Batson said "treasure your exceptions" (Bateson 1908). In genetics, and the biological sciences in general, exceptions provide insight into processes that would otherwise be inaccessible. For inherited retinal diseases, and RP in particular, families with exceptional modes of inheritance reveal new information about underlying mechanisms of disease. For example, the fact that specific mutations in *RP1* and *HK1* can be both dominant and recessive, with different degrees of retinal disease but no other obvious clinical consequences, shows that these mutations are not lethal and have dose-dependent effects but do not affect other tissues (Sullivan et al. 1999, 2014). From another perspective, though, the "treasure" is the affected families who participate in our research and expect reliable genetic information. From this perspective, the many exceptions to textbook models of inheritance for RP and related diseases mandate particular caution in diagnosis and interpretation of genetic findings.

In practice, evaluation of a patient or family with an inherited retinal disease can be divided into three overlapping stages: clinical characterization of the patient and available family members, family history including pedigree, and molecular testing. Because of the complexity of inherited retinal diseases, it is often necessary to *reconcile clinical diagnosis*, *family diagnosis*, *and molecular diagnosis*. This can best be done in centers that include retinal specialists, genetic counselors, molecular biologists, and other experts. Until we have a much better understanding of the complexity of RP and related diseases, diagnosis and treatment must be approached with caution and an open mind.

**Acknowledgments** This work was supported by NIH grants EY007142 and EY09076, a Wynn-Gund TRAP Award, and grants from the Foundation Fighting Blindness, the William Stamps Farish Fund, and the Hermann Eye Fund.

## References

Bateson W (1908) The methods and scope of genetics: an inaugural lecture delivered 23 October 1908. Cambridge University Press, Fetter Lane, E.C, London, UK

Berger W, Kloeckener-Gruissem B, Neidhardt J (2010) The molecular basis of human retinal and vitreoretinal diseases. Prog Retin Eye Res 29:335–375

Bowne SJ, Sullivan LS, Koboldt DC et al (2011a) Identification of disease-causing mutations in autosomal dominant retinitis pigmentosa (adRP) using next-generation DNA sequencing. Invest Ophthalmol Vis Sci 52:494–503

Bowne SJ, Humphries MM, Sullivan LS et al (2011b) A dominant mutation in RPE65 identified by whole-exome sequencing causes retinitis pigmentosa with choroidal involvement. Euro. J Hum Genet 19:1074–1081

Bowne SJ, Sullivan LS, Wheaton DK et al (2015) Retinal targeted-capture next generation sequencing and CLIA confirmation in a representative range of patients with inherited retinal degeneration. Invest Ophthalmol Vis Sci E-Abstr 56:1241

Bowne SJ, Sullivan LS, Wheaton DK et al (2016) North Carolina macular dystrophy (MCDR1) caused by a novel tandem duplication of the PRDM13 gene. Mol Vis 22:1239–1247

Branham K, Othman M, Brumm M et al (2012) Mutations in RPGR and RP2 account for 15% of males with simplex retinal degenerative disease. Invest Ophthalmol Vis Sci 53:8232–8237

Churchill JD, Bowne SJ, Sullivan LS et al (2013) Mutations in the X-linked retinitis pigmentosa genes RPGR and RP2 found in 8.5% of families with a provisional diagnosis of autosomal dominant retinitis pigmentosa. Invest Ophthalmol Vis Sci 54:1411–1416

Comander J, Weigel-DiFranco C, Sandberg MA et al (2015) Visual function in carriers of X-linked retinitis pigmentosa. Ophthalmology 122:1899–1906

Daiger SP, Sullivan LS, Bowne SJ (2013) Genes and mutations causing retinitis pigmentosa. Clin Genet 84:132–141

Daiger SP, Bowne SJ, Sullivan LS (2014) Genes and mutations causing autosomal dominant retinitis pigmentosa. Cold Spring Harb Perspect Med October 2015;5:a017129. https://doi.org/10.1101/cshperspect.a017129

Daiger SP, Bowne SJ, Sullivan LS et al (2016) Retinal targeted-capture next generation sequencing and CLIA confirmation in patients with a range of inherited retinal degeneration. Invest Ophthalmol Vis Sci 57:e1417

Haim M (2002) Epidemiology of retinitis pigmentosa in Denmark. Acta Ophthalmol Scand Suppl 233:1–34

Koboldt DC, Larson DE, Sullivan LS et al (2013) Linkage mapping using whole-exome next-generation sequencing in families with autosomal dominant retinitis pigmentosa. Invest Ophthalmol Vis Sci E-Abstract, ARVO Annual Meeting

Mears AJ, Hiriyanna S, Vervoort R et al (2000) Remapping of the RP15 locus for X-linked cone-rod degeneration to Xp11.4-p21.1, and identification of a de novo insertion in the RPGR exon ORF15. Am J Hum Genet 67:1000–1003

RetNet (2016) The Retinal Information Network, http://www.sph.uth.tmc.edu/RetNet/. In: Stephen P. Daiger, PhD, Administrator, The Univ. of Texas Health Science Center at Houston

Seyedahmadi BJ, Rivolta C, Keene JA et al (2004) Comprehensive screening of the *USH2A* gene in Usher syndrome type II and non-syndromic recessive retinitis pigmentosa. Exp Eye Res 79:167–173

Sohocki MM, Daiger SP, Bowne SJ et al (2001) Prevalence of mutations causing retinitis pigmentosa and other inherited retinopathies. Hum Mutat 17:42–51

Sullivan LS, Heckenlively JR, Bowne SJ et al (1999) Mutations in a novel retina-specific gene cause autosomal dominant retinitis pigmentosa. Nat Genet 22:255–259

Sullivan LS, Bowne SJ, Birch DG et al (2006) Prevalence of disease-causing mutations in families with autosomal dominant retinitis pigmentosa: a screen of known genes in 200 families. Invest Ophthalmol Vis Sci 47:3052–3064

Sullivan LS, Bowne SJ, Reeves MJ et al (2013) Prevalence of mutations in eyeGENE probands with a diagnosis of autosomal dominant retinitis pigmentosa. Invest Ophthalmol Vis Sci 54:6255–6261

Sullivan LS, Koboldt DC, Bowne SJ et al (2014) A dominant mutation in hexokinase 1 (HK1) causes retinitis pigmentosa. Invest Ophthalmol Vis Sci 55:7147–7158

Wang F, Wang H, Tuan HF et al (2013) Next generation sequencing-based molecular diagnosis of retinitis pigmentosa: identification of a novel genotype-phenotype correlation and clinical refinements. Hum Genet 133:331–345

Wheaton DK, Webb-Jones KD, Bowne SJ et al (2016) Complex multi-allelic inherited retinal dystrophy: multiple genes contributing independently and concurrently in extended families. Invest Ophthalmol Vis Sci E-Abstr 57:3135

Wright AF, Chakarova CF, Abd El-Aziz MM et al (2010) Photoreceptor degeneration: genetic and mechanistic dissection of a complex trait. Nat Rev Genet 11:273–284

# Chapter 30
# Pleiotropic Effects of Risk Factors in Age-Related Macular Degeneration and Seemingly Unrelated Complex Diseases


**Christina Kiel, Bernhard H. F. Weber, and Felix Grassmann**

**Abstract** Age-related macular degeneration (AMD) is a complex disease with both environmental and genetic factors influencing disease risk. Genome-wide case-control association studies, candidate gene analyses, and epidemiological studies reinforced the notion that AMD is predominantly a disease of an impaired complement system and an altered high-density lipoprotein (HDL) metabolism. Recent reports demonstrated the pleiotropic role of the complement system and HDL in complex diseases such as cardiovascular disease, autoimmune disorders, cancer, and Alzheimer's disease. In light of these findings, we explore current evidence for a shared genetic and environmental risk of AMD and unrelated complex diseases based on epidemiological studies. Shared risk factors may indicate common pathways in disease pathology and thus may have implications for novel treatment options of AMD pathology.

**Keywords** Age-related macular degeneration · Pleiotropy · Cardiovascular disease · Autoimmune disease · Cancer · Cholesterol metabolism

## 30.1 Introduction

Age-related macular degeneration (AMD) is a common, sight-threatening condition affecting the elderly. The prevalence of the disease is estimated to reach 30 million worldwide in the next few decades and as such poises a massive burden on affected individuals but also the national health care systems (Wong et al. 2014). Initially, the disease manifests as yellowish deposits between Bruch's membrane and the retinal pigment epithelium (RPE). The presence of these deposits appear not to influence visual acuity but may delay dark adaptation (Jackson et al. 2014). Advanced stages of the disease are presenting as either widespread RPE cell death in well-defined

C. Kiel · B. H. F. Weber · F. Grassmann (✉)
Institute of Human Genetics, University of Regensburg, Regensburg, Germany
e-mail: felix.grassmann@klinik.uni-regensburg.de



J. D. Ash et al. (eds.), *Retinal Degenerative Diseases*, Advances in Experimental Medicine and Biology 891, https://doi.org/10.1007/978-3-319-75402-4_30

areas (geographic atrophy, GA-AMD) or by disruptive growth of new vessels from the choriocapillaris into the neural retina (neovascular complications, NV-AMD). Both late-stage forms can occur in the same eye or in different eyes and eventually lead to irreversible vision loss in affected individuals.

A strong risk factor for AMD is increasing age, and thus, the prevalence of the disease is growing with age (Jonasson et al. 2011). Among the modifiable environmental risk factors, smoking has been recognized to increase the risk for AMD by about two-fold. In addition, diet and other lifestyle factors may have an effect on disease risk, although this observation remains controversial (Broadhead et al. 2015). Twin studies as well as familial aggregation and case-control association studies have emphasized a critical role of genetic factors in disease risk, possibly responsible for up to 70% of observed cases (Grassmann et al. 2015). A recent genome-wide case-control association study implicated 34 genetic loci in AMD disease risk, explaining almost 50% of the heritability (Fritsche et al. 2016; Grassmann et al. 2016b). The association signals in six of these loci were attributed to common and rare genetic variations affecting genes implicated in the complement system (Weber et al. 2014). A recent candidate gene study further strengthened the notion that dysregulation of the complement system plays a crucial role in AMD etiology by demonstrating that copy number variations in the complement component 4 gene (C4) are associated with AMD risk (Grassmann et al. 2016a). Furthermore, 4 out of the 34 disease loci harbor genes implicated in high-density lipoprotein (HDL) metabolism. These findings are in line with recent studies that reinforced the notion that elevated serum HDL levels are involved in AMD risk (Chakravarthy et al. 2010; Cougnard-Grégoire et al. 2014; Klein et al. 2014a, b; Cezario et al. 2015; Paun et al. 2015; Grassmann et al. 2017, Fritsche et al. 2016).

Genetic and molecular studies in recent years have implicated dysregulation of the complement system in a number of complex human diseases such as cardiovascular diseases (Lappegård et al. 2014; Vlaicu et al. 2016), autoimmune conditions (Bene et al. 2003; Wu et al. 2008), and cancer (Pio et al. 2013; Woo et al. 2015). Similarly, a potential pleiotropic role for HDL in various diseases and traits was recently described (summarized in Parra et al. 2015). These findings in turn raise the question whether dysregulation of the complement system and altered HDL metabolism found in seemingly unrelated complex diseases might influence the risk for AMD.

In this review, we explore the overlap of genetic and environmental risk factors of AMD and other diseases and traits. In addition, we highlight epidemiological evidence demonstrating that the occurrence of certain diseases also increases the risk for AMD. Such information could provide novel insight into the risk architecture of AMD and could reveal unexpected new pathways in disease pathology that may be addressed for prevention or treatment.

## 30.2 AMD, Cardiovascular Diseases, and Related Traits

There is an ongoing debate about a possible connection between cardiovascular disease risk and AMD pathology with conflicting results (Duan et al. 2007; Tan et al. 2008; Hu et al. 2010; Keilhauer et al. 2013; Fernandez et al. 2015). For both cardiovascular risk and risk for AMD, multiple shared risk factors are known such as increasing age (Jonasson et al. 2011), diet (Broadhead et al. 2015), smoking (Seddon et al. 2010), an elevated body mass index (BMI) (Zhang et al. 2016), type 2 diabetes (Vassilev et al. 2015; Das 2016), or high blood pressure (Hyman et al. 2000; Klein et al. 2003; Erke et al. 2014). In addition, the complement system as well as HDL metabolism had been implicated in the risk for both diseases.

High levels of serum HDL are linked to a healthy cardiovascular system due to its association with longevity (Barzilai et al. 2003) and its protective effect against atherosclerosis (Rader 2006). Current findings indicate that AMD patients have elevated levels of serum HDL (Chakravarthy et al. 2010; Cougnard-Grégoire et al. 2014; Klein et al. 2014a, b; Cezario et al. 2015; Paun et al. 2015, Grassmann et al. 2017), which should be protective against cardiovascular disease. In contrast, genetic variants associated with AMD in the Apolipoprotein E (*APOE*) gene which raise HDL serum levels also increase C-reactive protein concentration in serum (Dehghan et al. 2011; Paun et al. 2015) and thus promote complement activation (Sjöberg et al. 2009). These observations are in line with recent reports indicating that HDL may have a pleiotropic effect in different diseases, although in a not fully understood functional context (Parra et al. 2015).

In conclusion, although one would expect to identify less cases with cardiovascular complications in a group of AMD patients, this is not entirely reflected in current epidemiological studies, probably due to confounding environmental factors. Thus, further studies are required to establish a link between cardiovascular disease and related factors in AMD risk, preferably in large population-based cohorts accounting for various environmental and lifestyle factors.

## 30.3 Are AMD Patients More Likely to Have Autoimmune Diseases?

Autoimmune diseases are defined by an abnormal immune system which attacks healthy cells and tissue. Since AMD is predominantly a disease of an overactive innate immune system (Zipfel et al. 2010; Weber et al. 2014), one can argue that AMD is in fact an autoimmune disease. The discovery that autoantibodies against oxidized lipoproteins and normal proteins are elevated in AMD patients adds further weight to this notion (Gu et al. 2003; Morohoshi et al. 2012; Iannaccone et al. 2015; Pujol-Lereis et al. 2016). Autoimmune diseases partially share a common genetic basis (Cotsapas et al. 2011), and individuals affected by one type of autoimmune disease are prone to complications in other autoimmune diseases as well (Criswell

et al. 2005; Eaton et al. 2007). Indeed, there are several studies demonstrating that the presence of an autoimmune-related disease, such as systemic lupus erythematosus, rheumatoid arthritis, or osteoarthritis, results in a higher risk to develop AMD pathology (Nitsch et al. 2008; Kao et al. 2015; Keenan et al. 2015). In contrast, the presence of any type of allergy was protective for AMD (Ristau et al. 2014). It remains to be determined if this latter association is due to anti-allergy treatment or other factors. Taken together, these findings suggest that AMD is sharing risk factors with other systemic autoimmune diseases, although it is not clear at present whether this is due to genetic or environmental factors. Importantly, it remains to be seen whether patients at risk for AMD might profit from anti-inflammatory or immunosuppressive medication (Morohoshi et al. 2009; Iannaccone et al. 2012; Camelo 2014).

## 30.4 Are AMD Patients at Increased Risk for Cancer?

As AMD is a disease related to an overactive innate immune response, this may also increase the risk for AMD patients to diseases where long-term inflammation is a risk factor. A class of such diseases are malignant conditions of various tissues (Fernandes et al. 2015; Raposo et al. 2015), a notion strengthened by recent work that implicated complement system inflammation in various steps of cancer formation and progression (Rutkowski et al. 2010; Mamidi et al. 2017). In addition, smoking, age, diet, and potentially sunlight exposure (Sun et al. 2014) are risk factors for both AMD and cancer. Several epidemiological studies provided evidence that AMD patients are at increased risk for liver cancer (Pukkala et al. 1999; Cho et al. 2014) and lung cancer (Pukkala et al. 1999; Cheung et al. 2007). The latter malignancy can probably be attributed to the shared risk factor of smoking habit, which increases the risk for both diseases. There is no sufficient epidemiological evidence for an increased risk for skin cancer in AMD patients (Clemons et al. 2005), although both conditions share several risk factors such as light skin pigmentation (Langholz et al. 2000). Taken together, there is evidence for an increased risk for cancer in AMD patients either due to shared environmental/lifestyle factors or due to a shared genetic basis. Treating individuals at high risk for AMD with immunosuppressive drugs may therefore be problematic and should be considered with caution (Vajdic and van Leeuwen 2009).

## 30.5 AMD and Alzheimer's Disease

Alzheimer's disease (AD), a neurodegenerative disease of the brain, has frequently been linked to AMD pathology (Wostyn et al. 2016; Yu et al. 2016). Both diseases are related to increased age, the occurrence of protein deposits like amyloid-β in drusenoid bodies, and the upregulation of the complement system (Yasojima et al.

1999; Harvey and Durant 2014). In contrast to cardiovascular diseases, few epidemiological studies focused on the association between AMD and AD. Some studies reported a positive association between AMD and AD (Seden et al. 2015; Frost et al. 2016), while others did not find any association (Keenan et al. 2014; Williams et al. 2014). In the largest study to date which included medical records from around 65,000 AMD cases and 168,000 dementia or AD cases, the authors could not find a significant association between these two diseases (Keenan et al. 2014). This latter finding may, however, be influenced by the study design as patients with a diagnosis of AD were not readily screened for AMD and vice versa, eventually attributing the patient's deteriorating vision to AD and the deteriorating mind to the decline of vision. Nevertheless, this lack of epidemiological association between AMD and AD is in accordance with the results of others which investigated the association of variations in different complement genes with AMD and AD: Proitsi and colleagues concluded that, although AMD and AD are both associated with the complement system, these associations might be linked to different genetic models (Proitsi et al. 2012). Still, due to the striking similarities between AMD and AD, further epidemiological research is needed, potentially supplemented by genetic studies of AD risk variations in AMD.

## 30.6 Conclusions and Perspective

The complement system has been recognized as a major risk factor for AMD. Also, the role of HDL serum levels as an AMD risk factor was recently reinforced by both genetic and epidemiological data. Due to the pleiotropic roles of the complement system and HDL metabolism, one would expect that patients affected with AMD may also share an increased risk for other diseases.

So far, there is limited epidemiological evidence for a strong effect of risk sharing between AMD and such other diseases. This is mainly due to the lack of large population-based studies in the elderly, while at the same time potential confounding lifestyle and environmental risk factors need to be accounted for. Although AMD patients are at increased risk for lung cancer, liver cancer, and various systemic autoimmune diseases, there is no consensus so far as to whether this is also true for cardiovascular diseases, Alzheimer's disease, and other types of cancer.

To shed light onto potential connections, we propose to analyze the aggregate genetic risk of other diseases in AMD patients and compare it to controls while adjusting for potential confounders like smoking and age. This could provide insight into a potentially shared genetic basis between these complex disorders. Such efforts are currently underway in the International AMD Genomics Consortium (IAMDGC) (Grassmann et al. 2016b, Grassmann et al. 2017), and the results are expected to reveal novel pathways and genes involved in AMD pathogenesis.

## References

Barzilai N, Atzmon G, Schechter C et al (2003) Unique lipoprotein phenotype and genotype associated with exceptional longevity. JAMA 290:2030–2040

Bene L, Füst G, Fekete B et al (2003) High normal serum levels of C3 and C1 inhibitor, two acute-phase proteins belonging to the complement system, occur more frequently in patients with Crohn's disease than ulcerative colitis. Dig Dis Sci 48:1186–1192

Broadhead GK, Grigg JR, Chang AA et al (2015) Dietary modification and supplementation for the treatment of age-related macular degeneration. Nutr Rev 73:448–462

Camelo S (2014) Potential sources and roles of adaptive immunity in age-related macular degeneration: shall we rename AMD into autoimmune macular disease? Autoimmun Dis 2014:1–11

Cezario SM, Calastri MCJ, Oliveira CIF et al (2015) Association of high-density lipoprotein and apolipoprotein E genetic variants with age-related macular degeneration. Arq Bras Oftalmol 78:85–88

Chakravarthy U, Wong TY, Fletcher A et al (2010) Clinical risk factors for age-related macular degeneration: a systematic review and meta-analysis. BMC Ophthalmol 10:31

Cheung N, Shankar A, Klein R et al (2007) Age-related macular degeneration and cancer mortality in the atherosclerosis risk in communities study. Arch Ophthalmol (Chicago, Ill 1960) 125:1241–1247

Cho B-J, Heo JW, Shin JP et al (2014) Epidemiological association between systemic diseases and age-related macular degeneration: the Korea National Health and Nutrition Examination Survey 2008–2011. Invest Ophthalmol Vis Sci 55:4430–4437

Clemons TE, Milton RC, Klein R et al (2005) Risk factors for the incidence of advanced age-related macular degeneration in the Age-Related Eye Disease Study (AREDS) AREDS report no. 19. Ophthalmology 112:533–539

Cotsapas C, Voight BF, Rossin E et al (2011) Pervasive sharing of genetic effects in autoimmune disease. Dermitzakis ET (ed). PLoS Genet 7:e1002254

Cougnard-Grégoire A, Delyfer M-N, Korobelnik J-F et al (2014) Elevated high-density lipoprotein cholesterol and age-related macular degeneration: the Alienor study. PLoS One 9:e90973

Criswell LA, Pfeiffer KA, Lum RF et al (2005) Analysis of families in the multiple autoimmune disease genetics consortium (MADGC) collection: the PTPN22 620W allele associates with multiple autoimmune phenotypes. Am J Hum Genet 76:561–571

Das UN (2016) Diabetic macular edema, retinopathy and age-related macular degeneration as inflammatory conditions. Arch Med Sci 5:1142–1157

Dehghan A, Dupuis J, Barbalic M et al (2011) Meta-analysis of genome-wide association studies in >80 000 subjects identifies multiple loci for C-reactive protein levels. Circulation 123:731–738

Duan Y, Mo J, Klein R et al (2007) Age-related macular degeneration is associated with incident myocardial infarction among elderly Americans. Ophthalmology 114:732–737

Eaton WW, Rose NR, Kalaydjian A et al (2007) Epidemiology of autoimmune diseases in Denmark. J Autoimmun 29:1–9

Erke MG, Bertelsen G, Peto T et al (2014) Cardiovascular risk factors associated with age-related macular degeneration: the Tromsø Study. Acta Ophthalmol 92:662–669

Fernandes JV, Cobucci RNO, Jatobá CAN et al (2015) The role of the mediators of inflammation in cancer development. Pathol Oncol Res 21:527–534

Fernandez AB, Panza GA, Cramer B et al (2015) Age-related macular degeneration and incident stroke: a systematic review and meta-analysis. Chiu C-J (ed). PLoS One 10:e0142968

Fritsche LG, Igl W, Bailey JNC et al (2016) A large genome-wide association study of age-related macular degeneration highlights contributions of rare and common variants. Nat Genet 48:134–143

Frost S, Guymer R, Aung KZ et al (2016) Alzheimer's disease and the early signs of age-related macular degeneration. Curr Alzheimer Res 13(11):1259–1266

Grassmann F, Ach T, Brandl C et al (2015) What does genetics tell us about age-related macular degeneration? Annu Rev Vis Sci 1:73–96

Grassmann F, Cantsilieris S, Schulz-Kuhnt A-S et al (2016a) Multiallelic copy number variation in the complement component 4A (C4A) gene is associated with late-stage age-related macular degeneration (AMD). J Neuroinflammation 13:81

Grassmann F, Heid IM, Weber BHF (2016b) Recombinant haplotypes narrow the ARMS2/HTRA1 association signal for age-related macular degeneration. Genetics 205(2):919–924

Grassmann F, Kiel C, Zimmermann ME et al (2017) Genetic pleiotropy between age-related macular degeneration and 16 complex diseases and traits. Genom Med 9: 29

Gu X, Meer SG, Miyagi M et al (2003) Carboxyethylpyrrole protein adducts and autoantibodies, biomarkers for age-related macular degeneration. J Biol Chem 278:42027–42035

Harvey H, Durant S (2014) The role of glial cells and the complement system in retinal diseases and Alzheimer's disease: common neural degeneration mechanisms. Exp Brain Res 232:3363–3377

Hu C-C, Ho J-D, Lin H-C (2010) Neovascular age-related macular degeneration and the risk of stroke: a 5-year population-based follow-up study. Stroke 41:613–617

Hyman L, Schachat AP, He Q et al (2000) Hypertension, cardiovascular disease, and age-related macular degeneration. Age-Related Macular Degeneration Risk Factors Study Group. Arch Ophthalmol (Chicago, Ill 1960) 118:351–358

Iannaccone A, Neeli I, Krishnamurthy P et al (2012) Autoimmune biomarkers in age-related macular degeneration: a possible role player in disease development and progression. Adv Exp Med Biol 723:11–16

Iannaccone A, Giorgianni F, New DD et al (2015) Circulating autoantibodies in age-related macular degeneration recognize human macular tissue antigens implicated in autophagy, immunomodulation, and protection from oxidative stress and apoptosis. Lewin AS (ed). PLoS One 10:e0145323

Jackson GR, Clark ME, Scott IU et al (2014) Twelve-month natural history of dark adaptation in patients with AMD. Optom Vis Sci 91:925–931

Jonasson F, Arnarsson A, Eiríksdottir G et al (2011) Prevalence of age-related macular degeneration in old persons: Age, Gene/environment Susceptibility Reykjavik Study. Ophthalmology 118:825–830

Kao L-T, Wang K-H, Lin H-C et al (2015) Association between psoriasis and neovascular age-related macular degeneration: a population-based study. J Am Acad Dermatol 72:1090–1092

Keenan TDL, Goldacre R, Goldacre MJ (2014) Associations between age-related macular degeneration, Alzheimer disease, and dementia: record linkage study of hospital admissions. JAMA Ophthalmol 132:63–68

Keenan TDL, Goldacre R, Goldacre MJ (2015) Associations between age-related macular degeneration, osteoarthritis and rheumatoid arthritis: record linkage study. Retina 35:2613–2618

Keilhauer CN, Fritsche LG, Guthoff R et al (2013) Age-related macular degeneration and coronary heart disease: evaluation of genetic and environmental associations. Eur J Med Genet 56:72–79

Klein R, Klein BEK, Marino EK et al (2003) Early age-related maculopathy in the cardiovascular health study. Ophthalmology 6420:25–33

Klein R, Myers CE, Buitendijk GHS et al (2014a) Lipids, lipid genes, and incident age-related macular degeneration: the three continent age-related macular degeneration consortium. Am J Ophthalmol 158:513–524. e3

Klein R, Myers CE, Cruickshanks KJ et al (2014b) Markers of inflammation, oxidative stress, and endothelial dysfunction and the 20-year cumulative incidence of early age-related macular degeneration: the Beaver Dam Eye Study. JAMA Ophthalmol 132:446–455

Langholz B, Richardson J, Rappaport E et al (2000) Skin characteristics and risk of superficial spreading and nodular melanoma (United States). Cancer Causes Control 11:741–750

Lappegård KT, Garred P, Jonasson L et al (2014) A vital role for complement in heart disease. Mol Immunol 61:126–134

Mamidi S, Höne S, Kirschfink M (2017) The complement system in cancer: ambivalence between tumour destruction and promotion. Immunobiology 222:45–54

Morohoshi K, Goodwin AM, Ohbayashi M et al (2009) Autoimmunity in retinal degeneration: autoimmune retinopathy and age-related macular degeneration. J Autoimmun 33:247–254

Morohoshi K, Patel N, Ohbayashi M et al (2012) Serum autoantibody biomarkers for age-related macular degeneration and possible regulators of neovascularization. Exp Mol Pathol 92:64–73
Nitsch D, Douglas I, Smeeth L et al (2008) Age-related macular degeneration and complement activation-related diseases: a population-based case-control study. Ophthalmology 115:1904–1910
Parra S, Castro A, Masana L (2015) The pleiotropic role of HDL in autoimmune diseases. Clínica e Investig en Arterioscler 27:97–106
Paun CC, Ersoy L, Schick T et al (2015) Genetic variants and systemic complement activation levels are associated with serum lipoprotein levels in age-related macular degeneration. Invest Ophthalmol Vis Sci 56:7766
Pio R, Ajona D, Lambris JD (2013) Complement inhibition in cancer therapy. Semin Immunol 25:54–64
Proitsi P, Lupton MK, Dudbridge F et al (2012) Alzheimer's disease and age-related macular degeneration have different genetic models for complement gene variation. Neurobiol Aging 33:1843.e9-17
Pujol-Lereis LM, Schäfer N, Kuhn LB et al (2016) Interrelation between oxidative stress and complement activation in models of age-related macular degeneration. Adv Exp Med Biol 854:87–93
Pukkala E, Verkasalo PK, Ojamo M et al (1999) Visual impairment and cancer: a population-based cohort study in Finland. Cancer Causes Control 10:13–20
Rader DJ (2006) Molecular regulation of HDL metabolism and function: implications for novel therapies. J Clin Invest 116:3090–3100
Raposo TP, Beirão BCB, Pang LY et al (2015) Inflammation and cancer: till death tears them apart. Vet J 205:161–174
Ristau T, Ersoy L, Lechanteur Y et al (2014) Allergy is a protective factor against age-related macular degeneration. Invest Ophthalmol Vis Sci 55:210–214
Rutkowski MJ, Sughrue ME, Kane AJ et al (2010) Cancer and the complement cascade. Mol Cancer Res 8:1453–1465
Seddon JM, Reynolds R, Rosner B (2010) Associations of smoking, body mass index, dietary lutein, and the LIPC gene variant rs10468017 with advanced age-related macular degeneration. Mol Vis 16:2412–2424
Seden D, Alime G, Kadir D et al (2015) Is Alzheimer disease related to age-related macular degeneration? Turk J Med Sci 45:1115–1121
Sjöberg AP, Trouw LA, Blom AM (2009) Complement activation and inhibition: a delicate balance. Trends Immunol 30:83–90
Sun H-P, Lin Y, Pan C-W (2014) Iris color and associated pathological ocular complications: a review of epidemiologic studies. Int J Ophthalmol 7:872–878
Tan JSL, Wang JJ, Liew G et al (2008) Age-related macular degeneration and mortality from cardiovascular disease or stroke. Br J Ophthalmol 92:509–512
Vajdic CM, van Leeuwen MT (2009) Cancer incidence and risk factors after solid organ transplantation. Int J Cancer 125:1747–1754
Vassilev ZP, Ruigomez A, Soriano-Gabarro M et al (2015) Diabetes, cardiovascular morbidity, and risk of age-related macular degeneration in a primary care population. Invest Ophthalmol Vis Sci 56:1585–1592
Vlaicu SI, Tatomir A, Rus V et al (2016) The role of complement activation in atherogenesis: the first 40 years. Immunol Res 64:1–13
Weber BHF, Charbel Issa P, Pauly D et al (2014) The role of the complement system in age-related macular degeneration. Dtsch Arztebl Int 111:133–138
Williams MA, Silvestri V, Craig D et al (2014) The prevalence of age-related macular degeneration in Alzheimer's disease. J Alzheimers Dis 42:909–914
Wong WL, Su X, Li X et al (2014) Global prevalence of age-related macular degeneration and disease burden projection for 2020 and 2040: a systematic review and meta-analysis. Lancet Glob Health 2:e106–e116

Woo S-R, Corrales L, Gajewski TF (2015) Innate immune recognition of cancer. Annu Rev Immunol 33:445–474

Wostyn P, De Groot V, Van Dam D et al (2016) Age-related macular degeneration, glaucoma and Alzheimer's disease: amyloidogenic diseases with the same glymphatic background? Cell Mol Life Sci 73:4299–4301

Wu YL, Yang Y, Chung EK et al (2008) Phenotypes, genotypes and disease susceptibility associated with gene copy number variations: complement C4 CNVs in European American healthy subjects and those with systemic lupus erythematosus. Cytogenet Genome Res 123:131–141

Yasojima K, Schwab C, McGeer EG et al (1999) Up-regulated production and activation of the complement system in Alzheimer's disease brain. Am J Pathol 154:927–936

Yu SS, Tang X, Ho Y-S et al (2016) Links between the brain and retina: the effects of cigarette smoking-induced age-related changes in Alzheimer's disease and macular degeneration. Front Neurol 7:119

Zhang Q-Y, Tie L-J, Wu S-S et al (2016) Overweight, obesity, and risk of age-related macular degeneration. Invest Opthalmol Vis Sci 57:1276

Zipfel PF, Lauer N, Skerka C (2010) The role of complement in AMD. Adv Exp Med Biol 703:9–24

# Chapter 31
# Mapping of Canine Models of Inherited Retinal Diseases


**Keiko Miyadera**

**Abstract** The gene/mutation discovery approaches for inherited retinal diseases (RDs) in the dog model have seen considerable development over the past 25 years. Initial attempts were focused on candidate genes, followed by genome-wide approaches including linkage analysis and DNA-chip-based genome-wide association study. Combined, there are as many as 32 mutations in 27 genes that have been associated with canine retinal diseases to date. More recently, next-generation sequencing has become one of the key methods of choice. With increasing knowledge of the molecular basis of RDs and follow-up surveys in different subpopulations, the conventional understanding of RDs as simple Mendelian traits is being challenged. Modifiers and involvement of multiple genes that alter the disease expression are complicating the prediction of the disease course. In this chapter, advances in the gene/mutation discovery approaches for canine RDs are reviewed, and a multigenic form of canine RD is discussed using a form of canine cone-rod dystrophy as an example.

**Keywords** Animal model · Canine · Genome-wide association study · Mapping · Next-generation sequencing · Cone-rod dystrophy · Multigenic · Modifier

## 31.1 Introduction

The domestic dog has achieved considerable recognition as excellent models for understanding inherited retinal diseases (RDs) in human patients and for developing new therapies. Naturally-occurring inherited RDs in a variety of canine breeds have been shown to be true clinical and genetic homologues of retinitis pigmentosa, cone-rod dystrophy, Leber congenital amaurosis, Best macular dystrophy, and achromatopsia in human patients. To date, up to 32 forms of canine retinal diseases

K. Miyadera (✉)
School of Veterinary Medicine, University of Pennsylvania, Philadelphia, PA, USA
e-mail: kmiya@upenn.edu



J. D. Ash et al. (eds.), *Retinal Degenerative Diseases*, Advances in Experimental Medicine and Biology 891, https://doi.org/10.1007/978-3-319-75402-4_31

have been characterized at the molecular level (Miyadera et al. 2012a; Miyadera 2014). Due to the unique histories of early domestication and the more recent breed establishment, the dog genomic architecture has been found to be highly homogeneous across a given dog breed. Therefore, each pathogenic mutation emerging in the uniform genomic background gives rise to a predictable disease course across affected dogs of the same breed.

## 31.2 Gene/Mutation Discovery in Canine Retinal Disease

The strategies to search for the genes and mutations underlying inherited RDs of domestic dogs have evolved over the past 25 years, as canine genetic markers, the reference genome, and known sequence variants became available (Lindblad-Toh et al. 2005). As shown in Fig. 31.1, candidate gene analysis was initially the only method. However, whole-genome scans that allow a more comprehensive search have largely taken over as the primary approach.

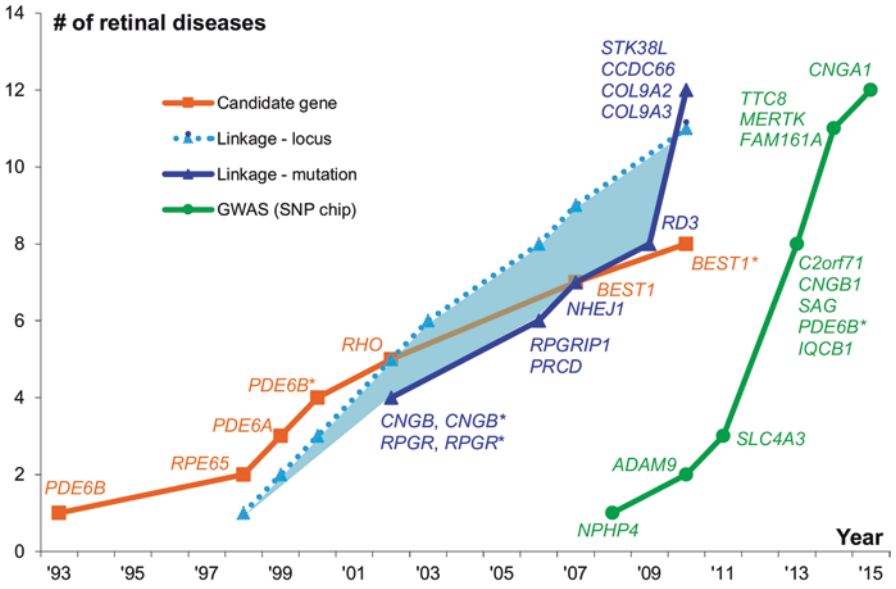


**Fig. 31.1** Trends in the method of choice to search for loci, genes, and mutations underlying canine RD. The cumulative numbers of genes/loci associated with canine RD are shown for each discovery approach used. For those RDs that were mapped initially as chromosomal loci by linkage analysis (shown in dotted light blue line), the time until identification of the actual gene mutation (shown in blue line) ranged from 0 (e.g., *CNGB*, *RPGRIP1*) to 11 (e.g., *STK38L*) years. * indicates a new mutation identified in a gene that was previously associated with another form of canine RD

### *31.2.1 Candidate Genes*

Early studies relied on a candidate gene approach where genes were selected for evaluation based on a priori knowledge of the biochemical pathway or defect involved or on information from other species. An array of candidate genes has been examined over time but with limited success. Nonetheless, the "classic" candidate gene approach has remained to be successful in certain examples where the clinical, pathologic, and molecular course of the canine disease closely resembles those of the human counterpart (Guziewicz et al. 2007).

### *31.2.2 Linkage Analysis*

There was then a shift to linkage mapping and positional cloning strategies. Unlike candidate gene approaches where only selected genes are inspected, a whole-genome scan via linkage analysis screens the entire genome including unknown genes. For linkage analysis mapping, large and complete multigenerational canine pedigrees that are "informative" and includes affected and unaffected animals are utilized. Co-segregation of genetic markers with the phenotype is analyzed to identify recombination, or lack thereof, between the disease phenotype and marker alleles. Once a chromosomal locus is mapped, the region of interest is fine-mapped using additional markers to increase the resolution, and positional candidate genes are analyzed. In many cases, there is a time lag of up to 10 years between mapping of the chromosomal location and the eventual identification of the actual gene/mutation, as shown in Fig. 31.1. This is largely due to the long linkage disequilibrium (LD) blocks which facilitated the mapping process, but then in turn hindered narrowing of the critical interval.

### *31.2.3 Genome-Wide Association Studies (GWAS)*

More recently, GWAS that utilize SNP chips have become widely applied in order to rapidly map disease loci in the form of case-control association studies. While the original canine SNP chip successfully mapped the first few canine RDs with only 22k SNPs (Illumina), the platform that is commonly used currently is the 230k SNP chip (Illumina), with 460k and 670k SNP chips (Applied Biosystems) recently arriving on the market.

The major advantages of utilizing dogs of the same breed in GWAS is that the number of samples required for mapping is significantly less compared to that required for studies in human populations. This is due to the recent history of breed establishment involving tight bottlenecks, strict gene flow regulation, and often extensive close breeding practices resulting in long chromosomal blocks of LD. In

**Table 31.1** Canine-inherited retinal diseases mapped by GWAS leading to gene/mutation discovery

| Gene | Breed | Mode of inheritance | # of cases | # of controls | Mapped locus size (Mb) | References |
|---|---|---|---|---|---|---|
| *NPHP4* | Standard wire-haired dachshund | AR | 13 | 13 | 6.5 | Wiik et al. (2008) |
| *ADAM9* | Glen of Imaal terrier | AR | 20 | 22 | 2.7 | Goldstein et al. (2010) |
| *SLC4A3* | Golden retriever | AR | 27 | 19 | 0.6 | Downs et al. (2011) |
| *C2orf71* | Gordon/Irish setter | AR | 16 | 22 | 3.2 | Downs et al. (2013) |
| *CNGB1* | Papillon | AR | 6 | 14 | 1.9 | Ahonen et al. (2013) |
| *SAG* | Basenji | AR | 6 | 3 | 2.1 | Goldstein et al. (2013a) |
| *PDE6B* | American Staffordshire terrier | AR | 17 | 18 | 1.1 | Goldstein et al. (2013b) |
| *IQCB1* | Pit bull terrier | AR | 14 | 13 | 2.3 | Goldstein et al. (2013b) |
| *TTC8* | Golden retriever | AR | 10 | 16 | 0.7 | Downs et al. (2014) |
| *MERTK*[a] | Swedish Vallhund | AR | 18 | 10 | 6.1 | Ahonen et al. (2014) |
| *FAM161A* | Tibetan spaniels/ terriers | AR | 22 | 10 | 3.8 | Downs and Mellersh (2014) |
| *CNGA1* | Shetland sheepdog | AR | 15 | 14 | 7.4 | Wiik et al. (2015) |

*AR* autosomal recessive
[a]Gene upregulation identified in the affected but no coding mutation found

turn, once the chromosomal locus is mapped, the extensive LD block complicates focusing into the causal gene. Table 31.1 enlists canine RDs successfully mapped by GWAS and shows that mapping of autosomal recessive RDs can be done using 5–20 cases and controls of the same breed but that the interval mapped would be relatively broad.

### *31.2.4 Next-Generation Sequencing*

In recent years, next-generation sequencing (NGS) has been increasingly utilized in mapping of canine traits. Of the different forms of NGS, targeted capture sequencing, exome sequencing, whole-genome sequencing (WGS), or whole-transcriptome sequencing (RNA-seq) may be utilized for gene/mutation discovery.

Targeted capture sequencing allows enrichment of a specific genomic region of interest for NGS. This method may be implemented where a disease locus has already been mapped by linkage analysis or GWAS, but the interval is too large, making positional candidate gene analysis inefficient both in time and cost. In exome sequencing, the known or predicted exons of canine genes are enriched from the original genomic DNA material, and subjected to NGS (Evans et al. 2016). It is indeed reasonable to focus on the exons for mutation discovery as much of the pathogenic RD mutations have so far been found in the exons and that it is more straightforward to establish the mutation-disease association based on changes in the amino acid sequence and therefore conformational and functional changes to the protein product.

Still, as the cost of NGS continues to come down, rather than going through the trouble to enrich certain genomic region of interest, sequencing the entire genomic DNA material by WGS is becoming a reasonable choice (Sayyab et al. 2016). Again, due to extensive within-breed genetic uniformity, WGS of even a few cases and controls can map the disease locus by analyzing blocks of sequence variants or "haplotypes" and, at the same time, survey for pathogenic mutations using the sequences already available.

RNA-seq allows capturing of the transcribed sequences of the genes that are expressed in the tissue of interest at a given time point. This approach has great advantage in that the genes that are more likely to be functionally relevant in the tissue of interest and in the disease are examined for changes in sequence as well as expression. In the case of RDs, the retina may be examined but availability of tissues may often be limited. It is important to note that the disease stage when the tissue was harvested as well as secondary changes from the primary disease process can affect the data. RNA-seq approaches have been successfully implemented as the primary and only approach used to survey the whole genome to identify a canine disease mutation (Forman et al. 2012) and also in combination with other DNA-based mapping and other NGS approaches to provide functional evidence (Fenn et al. 2016; Waluk et al. 2016).

## 31.3 Multigenic Form of Canine RD

While the classic gene mutation discovery approaches have been effective in dissecting simple monogenic RDs, phenotypic variabilities among family members as well as genotype-phenotype discordance have increasingly been recognized, suggesting involvement of genetic modifiers. We have been investigating a form of canine cone-rod dystrophy (cord1) that is considered the first canine RD model in which the involvement of a genetic modifier has been demonstrated.

### 31.3.1 Linkage Mapping Using Research Colony Identifies RPGRIP1

Cord1 was originally reported in the miniature longhaired dachshunds (MLHDs) as autosomal recessive (Curtis and Barnett 1993). As in other known canine RDs that are typically monogenic, the cord1 phenotype followed a uniform disease course in a research colony, early cone-led ERG dysfunction at 6 weeks of age, leading to total blindness by 1–2 years. Subsequently, a whole-genome scan using dogs of the same research colony identified a homozygous mutation in *RPGRIP1* (*RPGRIP1*$^{ins/ins}$) (Mellersh et al. 2006). While cord1 was found to segregate completely with *RPGRIP1*$^{ins/ins}$, at least within the research colony, screening of client-owned MLHDs in Japan showed that the age of onset ranged significantly, extending up to 15 years of age (Miyadera et al. 2009).

### 31.3.2 GWAS Using Client-Owned Animals Identifies MAP9 as Modifier

To account for this disparity, GWAS were carried out using *RPGRIP1*$^{ins/ins}$ dogs differing by the ages of disease onset. This led to the identification of an independently segregating homozygous modifier locus on chromosome 15 (Miyadera et al. 2012b). The gene mutation corresponding to the mapped modifier was subsequently identified as a ~22 kb deletion in *MAP9* (Forman et al. 2016).

As described, two genes (*RPGRIP1*, *MAP9*) that are involved in cord1 were each mapped successively using different subpopulations of the same canine breed. The modifier *MAP9* was fixed in the affected state in the original research colony which was used to map *RPGRIP1*. In turn, *MAP9* emerged as a modifier in the subsequent mapping once study animals from a different subpopulation of MLHDs were fixed in the *RPGRIP1*$^{ins/ins}$ state in the GWAS to investigate the molecular basis of the varying age of onset.

## 31.4 Conclusion and Prospects

While RDs have largely been considered as simple monogenic traits, there is increasing evidence to suggest that more than one gene mutation could affect the phenotype. This is not surprising considering the large number of genes – 256 and counting (RetNet; www.sph.uth.tmc.edu/RetNet/) – associated with RDs to date. Genetic polymorphisms in any of these genes, albeit nonpathogenic on their own, could potentially function as modifiers altering the effect of the primary mutation. Modifier genes may be ubiquitous ones that lead to a pathology only with the presence of the primary mutation, and possibly in a tissue-speciffic manner. While as

many as 32 gene mutations underlying canine RDs have been identified to date, the role of the gene mutation in RD pathogenesis remains largely unexplored. Our current focus is to study the interaction between the associated gene products RPGRIP1, MAP9 and other molecules, and determine the complex molecular mechanism underlying cord1.

**Acknowledgments** The author was supported by Foundation Fighting Blindness Career Development Award for Veterinary Residents, University Research Foundation (University of Pennsylvania), and NEI/NIH R01EY-06855 (PI: Gustavo Aguirre).

## References

Ahonen SJ, Arumilli M, Lohi H (2013) A CNGB1 frameshift mutation in Papillon and Phalène dogs with progressive retinal atrophy. PLoS One 8:1–8

Ahonen SJ, Arumilli M, Seppälä E et al (2014) Increased expression of MERTK is associated with a unique form of canine retinopathy. PLoS One 9:1–19

Curtis R, Barnett KC (1993) Progressive retinal atrophy in miniature longhaired dachshund dogs. Br Vet J 149:71–85

Downs LM, Mellersh CS (2014) An Intronic SINE insertion in FAM161A that causes exon-skipping is associated with progressive retinal atrophy in Tibetan Spaniels and Tibetan Terriers. PLoS One 9:e93990

Downs LM, Wallin-Håkansson B, Boursnell M et al (2011) A frameshift mutation in Golden Retriever dogs with progressive retinal atrophy endorses SLC4A3 as a candidate gene for human retinal degenerations. PLoS One 6:e21452

Downs LM, Bell JS, Freeman J et al (2013) Late-onset progressive retinal atrophy in the Gordon and Irish Setter breeds is associated with a frameshift mutation in C2orf71. Anim Genet 44:169–177

Downs LM, Wallin-Håkansson B, Bergström T et al (2014) A novel mutation in TTC8 is associated with progressive retinal atrophy in the golden retriever. Canine Genet Epidemiol 1:4

Evans JM, Cox ML, Huska J et al (2016) Exome sequencing reveals a nebulin nonsense mutation in a dog model of nemaline myopathy. Mamm Genome 27:495–502

Fenn J, Boursnell M, Hitti RJ et al (2016) Genome sequencing reveals a splice donor site mutation in the SNX14 gene associated with a novel cerebellar cortical degeneration in the Hungarian Vizsla dog breed. BMC Genet 17:123

Forman OP, De Risio L, Stewart J et al (2012) Genome-wide mRNA sequencing of a single canine cerebellar cortical degeneration case leads to the identification of a disease associated SPTBN2 mutation. BMC Genet 13:55

Forman OP, Hitti RJ, Boursnell M et al (2016) Canine genome assembly correction facilitates identification of a MAP9 deletion as a potential age of onset modifier for RPGRIP1-associated canine retinal degeneration. Mamm Genome 27:1–9

Goldstein O, Mezey JG, Boyko AR et al (2010) An ADAM9 mutation in canine cone-rod dystrophy 3 establishes homology with human cone-rod dystrophy 9. Mol Vis 16:1549–1569

Goldstein O, Jordan JA, Aguirre GD et al (2013a) A non-stop S-antigen gene mutation is associated with late onset hereditary retinal degeneration in dogs. Mol Vis 19:1871–1884

Goldstein O, Mezey JG, Schweitzer PA et al (2013b) IQCB1 and PDE6B mutations cause similar early onset retinal degenerations in two closely related terrier dog breeds. Invest Ophthalmol Vis Sci 54:7005–7019

Guziewicz KE, Zangerl B, Lindauer SJ et al (2007) Bestrophin gene mutations cause canine multifocal retinopathy: a novel animal model for best disease. Investig Ophthalmol Vis Sci 48:1959–1967

Lindblad-Toh K, Wade CM, Mikkelsen TS et al (2005) Genome sequence, comparative analysis and haplotype structure of the domestic dog. Nature 438:803–819

Mellersh CS, Boursnell MEG, Pettitt L et al (2006) Canine RPGRIP1 mutation establishes cone-rod dystrophy in miniature longhaired dachshunds as a homologue of human Leber congenital amaurosis. Genomics 88:293–301

Miyadera K (2014) Inherited retinal diseases in dogs: advances in gene/mutation discovery. Dobutsu Iden Ikushu Kenkyu 42:79–89

Miyadera K, Kato K, Aguirre-Hernández J et al (2009) Phenotypic variation and genotype-phenotype discordance in canine cone-rod dystrophy with an RPGRIP1 mutation. Mol Vis 15:2287–2305

Miyadera K, Acland GM, Aguirre GD (2012a) Genetic and phenotypic variations of inherited retinal diseases in dogs: the power of within- and across-breed studies. Mamm Genome 23:40–61

Miyadera K, Kato K, Boursnell M et al (2012b) Genome-wide association study in RPGRIP1 −/− dogs identifies a modifier locus that determines the onset of retinal degeneration. Mamm Genome 23:212–223

Sayyab S, Viluma A, Bergvall K et al (2016) Whole-genome sequencing of a canine family trio reveals a FAM83G variant associated with hereditary footpad hyperkeratosis. G3 Genes|Genomes|Genetics 6:521–527

Waluk DP, Zur G, Kaufmann R et al (2016) A splice defect in the EDA gene in dogs with an X-linked hypohidrotic ectodermal dysplasia (XLHED) phenotype. G3 Genes|Genomes|Genetics 6:2949–2954

Wiik AC, Wade C, Biagi T et al (2008) A deletion in nephronophthisis 4 (NPHP4) is associated with recessive cone-rod dystrophy in standard wire-haired dachshund. Genome Res 18:1415–1421

Wiik AC, Ropstad EO, Ekesten B et al (2015) Progressive retinal atrophy in Shetland sheepdog is associated with a mutation in the CNGA1 gene. Anim Genet 46:515–521

# Chapter 32
# A Mini-Review: Leber Congenital Amaurosis: Identification of Disease-Causing Variants and Personalised Therapies


**J. A. Thompson, J. N. De Roach, T. L. McLaren, and T. M. Lamey**

**Abstract** Leber congenital amaurosis (LCA) encompasses a group of severe inherited retinal dystrophies (IRDs) responsible for early childhood blindness. There are currently 25 genes implicated in the pathogenesis of these diseases, and identification of disease-causing variants will be required for personalised therapies. Whole exome and whole genome sequencing is informative for detecting novel disease-causing genes, whilst next-generation sequencing has excelled at detecting novel variants in known disease-causing genes.

A global effort will be required to identify patient populations for early intervention. At the Australian Inherited Retinal Disease Registry and DNA Bank, we seek to identify genetic variants in individuals with IRDs in the Australian population to identify potential candidates for clinical trials, to inform clinical management of patients including reproductive options and to expand existing knowledge of IRDs.

Due to the diversity of genes implicated, personalised strategies are likely to be the benchmark for treating these diseases, and a combined approach of different therapies may be optimal in treating some of these diseases.

**Keywords** Leber congenital amaurosis · Inherited retinal dystrophies · Retinal disease · Genetic variants · Next-generation sequencing · Personalised therapies · Registry

J. A. Thompson (✉) · T. L. McLaren
Australian Inherited Retinal Disease Registry & DNA Bank, Department of Medical Technology and Physics, Sir Charles Gairdner Hospital, Perth, WA, Australia
e-mail: jennifer.thompson3@health.wa.gov.au

J. N. De Roach · T. M. Lamey
Australian Inherited Retinal Disease Registry & DNA Bank, Department of Medical Technology and Physics, Sir Charles Gairdner Hospital, Perth, WA, Australia

Centre for Ophthalmology and Visual Science, The University of Western Australia, Crawley, WA, Australia



J. D. Ash et al. (eds.), *Retinal Degenerative Diseases*, Advances in Experimental Medicine and Biology 891, https://doi.org/10.1007/978-3-319-75402-4_32

**Table 32.1** Genes implicated in the pathogenesis of LCA and their mode of inheritance

| Mode of inheritance | Genes |
|---|---|
| Autosomal dominant LCA | *CRX*, *IMPDH1*, *OTX2* |
| Autosomal recessive LCA | *AIPL1*, *CABP4*, *CCT2, CEP290*, *CLUAP1*, *CRB1*, *CRX*, *DTHD1*, *GDF6*, *GUCY2D*, *IFT140*, *IQCB1*, *KCNJ13*, *LCA5*, *LRAT*, *NMNAT1*, *PRPH2*, *RD3*, *RDH12*, *RPE65*, *RPGRIP1*, *SPATA7*, *TULP1* |

## 32.1 Introduction

Leber congenital amaurosis (LCA) encompasses a group of severe inherited retinal dystrophies (IRDs) responsible for early childhood blindness. These diseases affect 2–3/100,000 newborns with a suspected prevalence of around 180,000 individuals worldwide (Koenekoop 2004). There are currently 25 genes implicated in the pathogenesis of these diseases (see Table 32.1; RetNet 2018), which is characterised by severe and early visual impairment, nystagmus, amaurotic pupils and a severely subnormal or non-detectable ERG, the latter two being indicative of altered visual circuitry. Associated clinical findings may include nyctalopia, photophobia, Franceschetti's oculodigital sign, keratoconus, enophthalmos, cataracts and refractive errors (Koenekoop 2004).

Due to the diversity of genes implicated in these diseases, it is likely that personalised therapeutic strategies will be required to impact on the severity and progression of disease. This approach will require identification of disease-causing variants, and larger populations will be required to attract industry funding for gene therapies (Estrada-Cuzcano et al. 2012; den Hollander 2016) and to maximise therapeutic potential. As the general consensus is that early intervention is likely to maximise the outcome of therapy, identification of causative genes in IRD populations such as LCA is an important endeavour for current research.

## 32.2 Identification of Disease-Causing Genes and Variants

### *32.2.1 Introduction*

Precision medicine, in the form of personalised therapeutic strategies, appears to hold great promise for ameliorating the symptoms of LCA. To subserve this purpose, identification of causative genes and genetic variants in individuals will be paramount for advancing this field, with the added benefit of informing clinicians and families for the benefit of patient management, including reproductive options, and to discriminate possible syndromic forms of disease.

### 32.2.2 Identification of Novel Disease-Causing Genes

Numerous techniques have been employed to reveal the genes considered causative for LCA, ranging from analysis of candidate genes (those expressed specifically in the retina) to homozygosity mapping (for regions of common ancestry) and exome sequencing (targeting coding regions) (a historic assessment of methodology is outside the scope of this review: for excellent timeline/reviews, see Koenekoop 2004; den Hollander 2016). Genes currently implicated in the pathogenesis of LCA (RetNet 2018) are listed in Table 32.1.

Whole exome and whole genome sequencing is informative for detecting novel disease-causing genes, as illustrated by the recent discovery of new candidate genes for LCA in the Chinese population (Wang et al. 2016). Costs associated with these broader testing methodologies will likely limit their use to the detection of novel genes, rather than the detection of variants in known genes (Chiang et al. 2015).

### 32.2.3 Identification of Disease-Causing Variants in Known Genes

Whilst microarray-based tests have proved beneficial for the detection of known variants in LCA genes historically (Henderson et al. 2007; Simonelli et al. 2007; Vallespin et al. 2007), next-generation sequencing (NGS) has excelled at improving the resolution of causative genes in LCA and other IRDs due to its ability to detect novel variants in known disease-associated genes. Disease-specific panels (e.g. LCA or macular dystrophy) may be utilised as a form of hypothesis testing, but due to the phenotypic heterogeneity of IRDs, non-hypothesis testing is proving beneficial for resolving cases of IRDs (Chiang et al. 2015).

This improvement in technology, however, has resulted in an increased detection of variants of unknown significance, and a current challenge is to discriminate pathogenic variants from those which are benign, often producing a large amount of data that must be interpreted in the context of the individual, their family and the disease. The recent publication of guidelines for assessment of variant pathogenicity (Richards et al. 2015; Jarvik and Browning 2016) will hopefully provide some uniformity for the challenging task of ascribing pathogenic potential to variants from information gleaned from in silico prediction programmes, allele frequency and variation databases and the scientific literature.

### 32.2.4 Global Efforts to Identify Patient Populations

International pooling of data to produce large patient populations will be needed to establish large databases to inform research groups, facilitate identification of the remaining genetic causes and attract industry funding for therapeutic research (Estrada-Cuzcano et al. 2012; den Hollander 2016). Subtle differences do exist in the genetic profile of LCA geographically (Simonelli et al. 2007; Vallespin et al. 2007; Astuti et al. 2016; Xu et al. 2016), and this is likely to have an effect at the variant level.

### 32.2.5 The Australian Inherited Retinal Disease Registry and DNA Bank

The Australian Inherited Retinal Disease Registry (AIRDR) and DNA Bank is a national registry for IRDs, operating under the auspices of Sir Charles Gairdner Hospital, Perth, Australia. We seek to identify genetic variants in individuals with IRDs in the Australian population. This research is conducted with a view to expediting clinical trials by identifying potential candidates, to inform clinical management of patients including reproductive options and to expand existing genetic knowledge of IRDs. At the AIRDR, we employ predominantly non-hypothesis NGS testing to resolve cases of IRDs, and our Australian cohort of LCA currently involves 36 pedigrees.

## 32.3 Gene-Specific, Pharmacologic and Pharmacogenetic Therapies

Due to the severity of these diseases, fervent research is underway to identify therapeutic strategies that may impact on their severity or progression. This is challenged by the diversity of causative genes and subsequent molecular aetiology, and it would thus appear intuitive that personalised strategies are likely to be the benchmark for treating these diseases. As an example, *LRAT* and *RPE65* encode proteins essential for the retinoid cycle, and mutations in either gene result in deficiency of the visual chromophore, 11-*cis* retinal (Redmond et al. 1998; Batten et al. 2004), with photoreceptor degeneration as a sequela (Maeda et al. 2008). A number of clinical trials are currently investigating the ability of gene-specific therapies to impact on these diseases, with the most studied to date being *RPE65* gene augmentation therapy. Three independent, concurrent trials have shown some improvements in visual parameters after AAV2/2-*RPE65* gene therapy in LCA individuals (Bainbridge et al. 2008; Hauswirth et al. 2008; Maguire et al. 2008), but this treatment has failed to rescue photoreceptor cell loss (Cideciyan et al. 2013; Bainbridge et al. 2015;

Jacobson et al. 2015), suggesting that earlier intervention may be a key factor for success (Weleber et al. 2016). A clinical trial using an optimised AAV2/5-OPTIRPE65 vector platform (Georgiadis et al. 2016) is currently recruiting for *RPE65* gene therapy, as is a phase 1 clinical trial for *MERTK* therapy (clinicaltrials.gov).

In a pharmacological approach to replace 11-*cis* retinal, Koenekoop et al. (2014) treated 14 LCA patients with mutations in *LRAT* and *RPE65* for 7 days with oral QLT091001, which becomes converted to 9-*cis* retinoid and combines with opsin to participate in the phototransduction cascade. This phase 1b clinical trial produced meaningful improvements in visual function in most patients. Similarly, systemic administration of sodium 4-phenylbutyrate (PBA) in a *RPE65* mouse model of LCA resulted in increased synthesis of visual chromophores and amelioration of cone survival and vision (Li et al. 2016), suggesting that a combined approach of gene therapy and pharmacological intervention may be beneficial in treating this disease (Cideciyan et al. 2013; Li et al. 2016).

A more tailored molecular approach may target a specific variant. A prime example is the use of antisense oligonucleotides (AONs) as a treatment strategy for the hypomorphic *CEP290* c.2991 + 1655A > G variant, the most frequently detected variant in LCA (den Hollander et al. 2008), which incorporates an aberrant exon in the *CEP290* mRNA, resulting in a premature termination codon (den Hollander et al. 2006). AONs targeting this variant induce skipping of the aberrant exon and almost fully restore normal splicing and protein synthesis in cultured cells (Collin et al. 2012; Gerard et al. 2012; Garanto et al. 2016) and induced pluripotent stem cell (iPSC)-derived optic cups (Parfitt et al. 2016) of LCA-affected individuals. Other pharmacogenetic approaches may target nonsense mutations by utilising translation-inducing drugs to promote partial read-through of premature termination codons to increase protein synthesis (Nagel-Wolfrum et al. 2016), as has occurred experimentally for nonsense mutations in *USH1C* (HEK293T cells and retinal explants) and *RP2* (iPSC-derived RPE) (Goldmann et al. 2010; Schwarz et al. 2015).

## 32.4 Conclusion

Due to the diversity of genes implicated in LCA, personalised strategies are likely to be the benchmark for treating these diseases, and a combined approach of different therapies may be optimal. In order to facilitate such personalised strategies, identification of disease-causing genetic variants in LCA individuals will be crucial to successful outcomes.

**Acknowledgements** The Australian Inherited Retinal Disease Registry and DNA Bank is financially supported by Retina Australia. The support of the Department of Medical Technology and Physics, Sir Charles Gairdner Hospital, is gratefully acknowledged.

## References

Astuti GD, Bertelsen M, Preising MN et al (2016) Comprehensive genotyping reveals RPE65 as the most frequently mutated gene in Leber congenital amaurosis in Denmark. Eur J Hum Genet 24:1071–1079

Bainbridge JWB, Smith AJ, Barker SS et al (2008) Effect of gene therapy on visual function in Leber's congenital amaurosis. N Engl J Med 358:2231–2239

Bainbridge JW, Mehat MS, Sundaram V et al (2015) Long-term effect of gene therapy on Leber's congenital amaurosis. N Engl J Med 372:1887–1897

Batten ML, Imanishi Y, Maeda T et al (2004) Lecithin-retinol acyltransferase is essential for accumulation of all-trans-retinyl esters in the eye and in the liver. J Biol Chem 279:10422–10432

Chiang JP, Lamey T, McLaren T et al (2015) Progress and prospects of next-generation sequencing testing for inherited retinal dystrophy. Expert Rev Mol Diagn 15:1269–1275

Cideciyan AV, Jacobson SG, Beltran WA et al (2013) Human retinal gene therapy for Leber congenital amaurosis shows advancing retinal degeneration despite enduring visual improvement. Proc Natl Acad Sci U S A 110:E517–E525

Collin RW, den Hollander AI, van der Velde-Visser SD et al (2012) Antisense oligonucleotide (AON)-based therapy for Leber congenital amaurosis caused by a frequent mutation in CEP290. Mol Ther Nucleic Acids 1:e14

den Hollander AI (2016) Omics in ophthalmology: advances in genomics and precision medicine for Leber congenital amaurosis and age-related macular degeneration. Invest Ophthalmol Vis Sci 57:1378–1387

den Hollander AI, Koenekoop RK, Yzer S et al (2006) Mutations in the CEP290 (NPHP6) gene are a frequent cause of Leber congenital amaurosis. Am J Hum Genet 79:556–561

den Hollander AI, Roepman R, Koenekoop RK et al (2008) Leber congenital amaurosis: genes, proteins and disease mechanisms. Prog Retin Eye Res 27:391–419

Estrada-Cuzcano A, Roepman R, Cremers FP et al (2012) Non-syndromic retinal ciliopathies: translating gene discovery into therapy. Hum Mol Genet 21:R111–R124

Garanto A, Chung DC, Duijkers L et al (2016) In vitro and in vivo rescue of aberrant splicing in CEP290-associated LCA by antisense oligonucleotide delivery. Hum Mol Genet 25(12):2552–2563

Georgiadis A, Duran Y, Ribeiro J et al (2016) Development of an optimized AAV2/5 gene therapy vector for Leber congenital amaurosis owing to defects in RPE65. Gene Ther 23(12):857–862

Gerard X, Perrault I, Hanein S et al (2012) AON-mediated exon skipping restores ciliation in fibroblasts harboring the common Leber congenital amaurosis CEP290 mutation. Mol Ther Nucleic Acids 1:e29

Goldmann T, Rebibo-Sabbah A, Overlack N et al (2010) Beneficial read-through of a USH1C nonsense mutation by designed aminoglycoside NB30 in the retina. Invest Ophthalmol Vis Sci 51:6671–6680

Hauswirth WW, Aleman TS, Kaushal S et al (2008) Treatment of Leber congenital amaurosis due to RPE65 mutations by ocular subretinal injection of adeno-associated virus gene vector: short-term results of a phase I trial. Hum Gene Ther 19:979–990

Henderson RH, Waseem N, Searle R et al (2007) An assessment of the apex microarray technology in genotyping patients with Leber congenital amaurosis and early-onset severe retinal dystrophy. Invest Ophthalmol Vis Sci 48:5684–5689

Jacobson SG, Cideciyan AV, Roman AJ et al (2015) Improvement and decline in vision with gene therapy in childhood blindness. N Engl J Med 372:1920–1926

Jarvik GP, Browning BL (2016) Consideration of cosegregation in the pathogenicity classification of genomic variants. Am J Hum Genet 98:1077–1081

Koenekoop RK (2004) An overview of Leber congenital amaurosis: a model to understand human retinal development. Surv Ophthalmol 49:379–398

Koenekoop RK, Sui R, Sallum J et al (2014) Oral 9-cis retinoid for childhood blindness due to Leber congenital amaurosis caused by RPE65 or LRAT mutations: an open-label phase 1b trial. Lancet 384:1513–1520

Li S, Samardzija M, Yang Z et al (2016) Pharmacological amelioration of cone survival and vision in a mouse model for Leber congenital amaurosis. J Neurosci 36:5808–5819

Maeda A, Maeda T, Golczak M et al (2008) Retinopathy in mice induced by disrupted all-trans-retinal clearance. J Biol Chem 283:26684–26693

Maguire AM, Simonelli F, Pierce EA et al (2008) Safety and efficacy of gene transfer for Leber's congenital amaurosis. N Engl J Med 358:2240–2248

Nagel-Wolfrum K, Moller F, Penner I et al (2016) Targeting nonsense mutations in diseases with translational read-through-inducing drugs (TRIDs). BioDrugs 30:49–74

Parfitt DA, Lane A, Ramsden CM et al (2016) Identification and correction of mechanisms underlying inherited blindness in human iPSC-derived optic cups. Cell Stem Cell 18:769–781

Redmond TM, Yu S, Lee E et al (1998) Rpe65 is necessary for production of 11-cis-vitamin A in the retinal visual cycle. Nat Genet 20:344–351

RetNet (2018) RetNet – Retinal Information Network. In: University of Texas-Houston Health Science Center. Laboratory for the Molecular Diagnosis of Inherited Eye Diseases, Houston

Richards S, Aziz N, Bale S et al (2015) Standards and guidelines for the interpretation of sequence variants: a joint consensus recommendation of the American College of Medical Genetics and Genomics and the Association for Molecular Pathology. Genet Med 17:405–424

Schwarz N, Carr AJ, Lane A et al (2015) Translational read-through of the RP2 Arg120stop mutation in patient iPSC-derived retinal pigment epithelium cells. Hum Mol Genet 24:972–986

Simonelli F, Ziviello C, Testa F et al (2007) Clinical and molecular genetics of Leber's congenital amaurosis: a multicenter study of Italian patients. Invest Ophthalmol Vis Sci 48:4284–4290

Vallespin E, Cantalapiedra D, Riveiro-Alvarez R et al (2007) Mutation screening of 299 Spanish families with retinal dystrophies by Leber congenital amaurosis genotyping microarray. Invest Ophthalmol Vis Sci 48:5653–5661

Wang SY, Zhang Q, Zhang X et al (2016) Comprehensive analysis of genetic variations in strictly-defined Leber congenital amaurosis with whole-exome sequencing in Chinese. Int J Ophthal 9:1260–1264

Weleber RG, Pennesi ME, Wilson DJ et al (2016) Results at 2 years after gene therapy for RPE65-deficient Leber congenital amaurosis and severe early-childhood-onset retinal dystrophy. Ophthalmology 123:1606–1620

Xu Y, Xiao X, Li S et al (2016) Molecular genetics of Leber congenital amaurosis in Chinese: new data from 66 probands and mutation overview of 159 probands. Exp Eye Res 149:93–99

# Part VI
# Mechanisms of Degeneration

# Chapter 33
# Role of Fibulins 2 and 5 in Retinal Development and Maintenance


**Larissa Ikelle, Muna I. Naash, and Muayyad R. Al-Ubaidi**

**Abstract** Fibulins 2 and 5 are part of a seven-member family of proteins integral to the retinal extracellular matrix. Our study aimed to further explore the roles of both fibulins in retinal function. We obtained knockout mouse models of both fibulins and performed immunohistochemistry, electroretinography, and histology to investigate the outcome of eliminating these proteins. Immunohistochemical analysis showed that both fibulins are localized to the RPE, choroid, and Bruch's membrane. Functional testing showed a significantly reduced scotopic A response at 1 month of age, when compared to their wild-type counterpart. This functional reduction remained constant throughout the age of the animal and only declined as a result of normal aging. The functional decline was associated with reduced number of photoreceptor cells. The results presented clearly demonstrate that fibulins 2 and 5, as extracellular proteins, are necessary for normal retinal development.

**Keywords** Fibulin 2 · Fibulin 5 · Retinal development · Age-related macular degeneration · Knockout mice · Extracellular matrix

## 33.1 Introduction

As studies delve deeper into the pathologies of retinal diseases, it becomes increasingly evident that the extracellular matrix (ECM) has a profound influence on the development, overall health, and proper functionality of the retina (Varshney et al. 2015). The molecular components of the ECM consist of proteoglycans and fibrous proteins such as collagens, fibronectins, elastins, lamins, and fibulins (Hubmacher and Apte 2013). These proteins are integral to cellular structure, adhesion, and migration (Hubmacher and Apte 2013). Fibulins are expressed primarily in elastic fibers and basement membranes (Scott Argraves et al. 2003). In ocular tissue, fibulin

L. Ikelle · M. I. Naash · M. R. Al-Ubaidi (✉)
Department of Biomedical Engineering, University of Houston, Houston, TX, USA
e-mail: malubaid@central.uh.edu



J. D. Ash et al. (eds.), *Retinal Degenerative Diseases*, Advances in Experimental Medicine and Biology 891, https://doi.org/10.1007/978-3-319-75402-4_34

2 has been localized to the retinal pigment epithelium (RPE), Bruch's membrane, and choriocapillaris and in the retina (Kanan et al. 2014).

Fibulins belong to a seven-member family of ECM proteins, characterized by an array of calcium-binding epidermal growth factors (EGF) like modules (Scott Argraves et al. 2003) hypothesized to be crucial for protein-protein interactions (Scott Argraves et al. 2003). They are divided into two classes based upon size (Yanagisawa et al. 2009). Fibulin 1 and fibulin 2 have three anaphylatoxin domains that precede the calcium binding EGF repeats, making these fibulins larger than fibulins 3, 4, 5, and 7 (Yanagisawa et al. 2009).

Most members of the fibulin family interface with other major basement membrane proteins such as tropoelastin, fibrillin, fibronectin, and proteoglycan to greater or lesser degrees (Timpl et al. 2003). Consequently, mutations in many fibulins can cause problems in connective tissue formation, organogenesis, and even osteogenesis (Scott Argraves et al. 2003; Cooley et al. 2014). Mutations in fibulins 4 and 5 cause a rare connective tissue disorder, known as cutis laxa, resulting in inelastic skin that tends to hang off the body (Hucthagowder et al. 2006). A mutation in fibulin 1D has also been traced to synpolydactyly, a congenital malformation of the hand (Scott Argraves et al. 2003). In eye diseases, fibulins 1 and 4 have been traced to inherited retinopathies (Scott Argraves et al. 2003). For example, a mutation in the fibulin 4 gene has been linked to neovascular inflammatory vitreoretinopathy, an autoimmune disease characterized by vascularization of the retina and iris, cystoid macular edema, inflammation and opacity of the vitreous, and ultimately blindness (Stone et al. 1992). An Arg345Trp mutation in fibulin 3 is associated with Malattia Leventinese, a form of macular degeneration (Scott Argraves et al. 2003). Additionally, age-related macular degeneration (AMD) has been linked to variations in fibulin 5 (Stone et al. 2004). In comparison to control patients, the fibulin 5 amino acid variants showed a phenotype of small round drusen in the basal laminal of Bruch's membrane, contributing to detachment in that region (Stone et al. 2004).

Here, our primary focus was to analyze the role of fibulins 2 and 5 in retinal function and structure using knockout mice. Fibulin 2 null mice (*Fbln2*$^{-/-}$) are fertile and have no obvious abnormalities (Scott Argraves et al. 2003). On the contrary, fibulin 5 null mice (*Fbln5*$^{-/-}$) show no outward abnormalities, but show a propensity for organ prolapse. Furthermore, *Fbln5*$^{-/-}$ mice have proven to have severe disruptions in connectivity of elastic fibers (Nakamura et al. 2002). We have previously demonstrated that fibulin 2 is present in the RPE, choroid, and Bruch's membrane and that it is upregulated after retinal detachment (Kanan et al. 2014). We determined that fibulins 2 and 5 are critical for proper development of the choroid and Bruch's membrane and ultimately cause reduced retinal function.

## 33.2 Experimental Procedures

### *33.2.1 Fibulins 2 and 5 Knockout Mice*

*Fbln2&5*$^{-/-}$ mice were described elsewhere and were kindly provided by Dr. Hiromi Yanagisawa (University of Texas Southwestern Medical Center, Dallas, Texas, USA). All experiments, described herein, were performed after receiving approval from local IACUC and adhered to guidelines by the Association of Research in Vision and Ophthalmology (ARVO) and NIH.

### *33.2.2 Electroretinography for Functional Testing*

Functional testing by electroretinography, histological analysis, and immunohistochemical analysis were all performed as previously described (Murray et al. 2015).

## 33.3 Results

### *33.3.1 Immunohistochemistry*

Immunohistochemical analysis (IHC) was performed on retinal sections of wild-type mice that showed (Fig. 33.1) that both fibulins 2 and 5 are present in the retinal pigment epithelium (RPE), Bruch's membrane, and the choroid, similar to previously shown localization for fibulin 2 (Kanan et al. 2014). However, unlike fibulin 2 which is also present around the photoreceptor inner segments, fibulin 5 was absent from around inner segments.

### *33.3.2 Electroretinography*

To determine whether fibulins 2 and 5 play any role in retinal function, wild-type (WT), *Fbln2*$^{-/-}$, and *Fbln5*$^{-/-}$ mice were tested for their retinal functional competence by electroretinography (ERG). Developmental ERG testing showed that, compared to WT, both knockout mice showed reduced scotopic response as early as 1 month of age (Fig. 33.2). However, *Fbln5*$^{-/-}$ mice initially showed more severe phenotype compared to *Fbln2*$^{-/-}$. But at 3 months of age, the responses of both knockout mice were equivalent with loss of ~45% of responses compared to WT. Interestingly, this deficit in ERG responses did not get any worse as the animal got older; rather it followed an age-dependent decline similarly presented in WT.

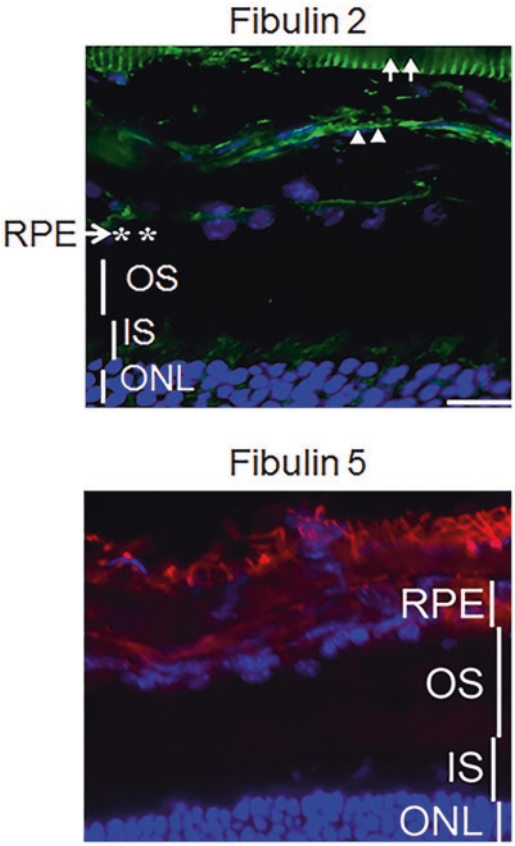


**Fig. 33.1** Immunohistochemistry of fibulins 2 and 5. Immunohistochemistry was performed on frozen retinal sections of WT mouse retina. Fibulin 2 (green) and fibulin 5 (red) are seen in the choroid, Bruch's membrane, and RPE. Fibulin 2 can be found around the inner segment as well. DAPI (blue) marked nuclei. Arrows indicate the sclera, and the arrowheads denote the choroid

### *33.3.3 Histological Analysis*

To determine whether the decline in ERG responses is solely the result of changes in the extracellular matrix resulting from the elimination of fibulin 2 or 5, or caused by loss of photoreceptor cell, we performed histologic examinations. As shown in Fig. 33.2b, the lack of both fibulins led to loss of photoreceptor cells and structural abnormalities of the outer segments. However, *Fbln5*$^{-/-}$ retinas seem to have lost more photoreceptors than *Fbln2*$^{-/-}$ (compare 11–12 rows in *Fbln2*$^{-/-}$ versus 10–11 rows in *Fbln5*$^{-/-}$; Fig. 33.2b). Similar to ERG responses, histologic changes followed those in WT retina as animals aged (data not shown).

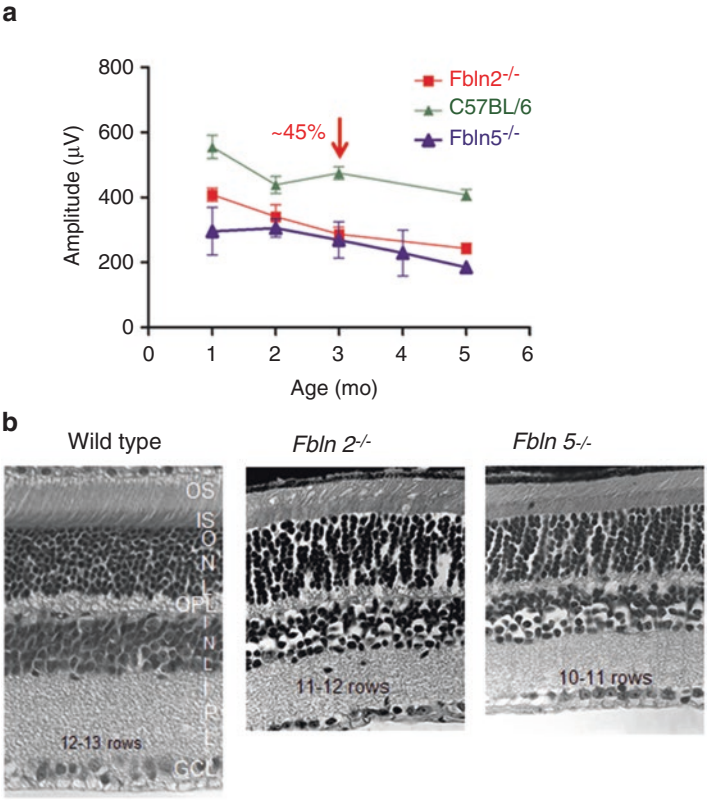


**Fig. 33.2** Electroretinography and histological analyses. (**a**) Electroretinography was performed on *Fbln* $2^{-/-}$, *Fbln* $5^{-/-}$, and WT mice. $N \geq 3$ for each data point. All show the same decline in response due to aging. However, both knockout lines have significantly reduced scotopic response at 1 month of age. (**b**) Histology was performed on WT, *Fbln* $2^{-/-}$, and *Fbln* $5^{-/-}$ mice, presented respectively. There is reduction in the number of photoreceptors in the knockout animals compared to the wild type

## 33.4 Discussion

Fibulins 2 and fibulin 5, to a greater degree, have both been implicated in the pathology of age-related macular degeneration (Stone et al. 2004). To start to understand the role an ECM protein like fibulin 2 or 5 plays in retinal diseases, we determined the functional and the structural consequences of eliminating both. We show that eliminating either of those two proteins led to a functional and structural changes that did not progress further with age. This implicates both proteins in a developmental role in the retina. Interestingly, that elimination of fibulin 5 leads to a more severe phenotype than lack of fibulin 2 despite the fact that fibulin 5 is not present anywhere around photoreceptors. Due to the potential role of fibulin 5 in the development of AMD, our future studies will focus on the role of these fibulins in cone function and structure.

## References

Cooley MA, Harikrishnan K et al. (2014) Fibulin-1 is required for bone formation and Bmp-2-mediated induction of Osterix. HHS Public Access 30–38

Hubmacher D, Apte SS (2013) The biology of the extracellular matrix: novel insights. Curr Opin Rheumatol 65–70

Hucthagowder V, Sausgruber N et al (2006) Fibulin-4: a novel gene for an autosomal recessive cutis laxa syndrome. Am J Hum Genet 76:1075–1080

Kanan Y, Brobst D et al (2014) Fibulin 2, a tyrosine O-sulfated protein, is up-regulated following retinal detachment. J Biol Chem 289:15. https://doi.org/10.1074/jbc.M114.562157

Murray AR, Vuong L et al (2015) Glycosylation of rhodopsin is necessary for its stability and incorporation into photoreceptor outer segment discs. Hum Mol Genet 24:2709–2723

Nakamura T et al (2002) Fibulin 5/DANCE is essential for elastogeneisis in vivo. Nature 415:171–175

Scott Argraves W, Greene LM et al (2003) Fibulins: physiological and disease perspectives. EMBO Rep 5:1127–1131

Stone EM, Kimura AE et al (1992) Genetic linkage of autosomal dominant neovascular inflammatory vitreoretinopathy to chromosome 11q13. Hum Mol Genet 1(9):685

Stone EM et al (2004) Missense variations in the Fibulin 5 gene and age related macular degeneration. N Engl J Med 351:346–353

Timpl R et al (2003) Fibulins: a versatile family of extracellular matrix proteins. Nat Rev Mol Cell Biol 4:479–489

Varshney S, Hunter DD, Brunken WJ (2015) Extracellular matrix components regulate cellular polarity and tissue structure in the developing and mature retina. J Ophthalmic Vis Res 10:329–339

Yanagisawa H, Schluterman MK et al (2009) Fibulin-5, an integrin-binding matricellular protein: its function in development and disease. J Cell Commun Signal 3:337–347

# Chapter 34
# Identifying Key Networks Linked to Light-Independent Photoreceptor Degeneration in Visual Arrestin 1 Knockout Mice

**Hwa Sun Kim, Shun-Ping Huang, Eun-Jin Lee, and Cheryl Mae Craft**

**Abstract** When visual arrestin 1 (ARR1, S-antigen, 48 KDa protein) was genetically knocked out in mice (original *Arr1*$^{-/-}$, designated *Arr1*$^{-/-A}$), rod photoreceptors degenerated in a light-dependent manner. Subsequently, a light-independent cone dystrophy was identified with minimal rod death in ARR1 knockout mice (*Arr1*$^{-/-A}$*Arr4*$^{+/+}$, designated *Arr1*$^{-/-B}$), which were F2 littermates from

**Electronic supplementary material:** The online version of this chapter (https://doi.org/10.1007/978-3-319-75402-4_34) contains supplementary material, which is available to authorized users.

Hwa Sun Kim and Shun-Ping Huang contributed equally to this work.

H. S. Kim
Laboratory for Vision Research, USC ROSKI Eye Institute,
Department of Ophthalmology, Los Angeles, CA, USA

S.-P. Huang
Department of Ophthalmology, Taichung Tzu Chi Hospital,
Taichung, Taiwan

Department of Molecular Biology and Human Genetics, Tzu Chi University, Hualien, Taiwan

Laboratory for Vision Research, USC ROSKI Eye Institute,
Department of Ophthalmology, Los Angeles, CA, USA

E.-J. Lee
Department of Biomedical Engineering, Viterbi School of Engineering,
University of Southern California, Los Angeles, CA, USA

Laboratory for Vision Research, USC ROSKI Eye Institute,
Department of Ophthalmology, Los Angeles, CA, USA

C. M. Craft (✉)
Laboratory for Vision Research, USC ROSKI Eye Institute,
Department of Ophthalmology, Los Angeles, CA, USA

Department of Cell & Neurobiology, Keck School of Medicine,
University of Southern California, Los Angeles, CA, USA
e-mail: cherylmae.craft@med.usc.edu



J. D. Ash et al. (eds.), *Retinal Degenerative Diseases*, Advances in Experimental Medicine and Biology 891, https://doi.org/10.1007/978-3-319-75402-4_34

breeding the original *Arr1*$^{-/-A}$ and cone arrestin knockout 4 (*Arr4*$^{-/-}$) mice. To resolve the genetic and phenotypic differences between the two ARR1 knockouts, we performed Affymetrix™ exon array analysis to focus on the potential differential gene expression profile and to explore the molecular and cellular pathways leading to this observed susceptibility to cone dystrophy in A*rr1*$^{-/-B}$ compared to *Arr1*$^{-/-A}$ or control *Arr1*$^{+/+}$*Arr4*$^{+/+}$ (wild type [WT]). Only in the A*rr1*$^{-/-B}$ retina did we observe an up-regulation of retinal transcripts involved in the immune response, inflammatory response and JAK-STAT signaling molecules, OSMRβ and phosphorylation of STAT3. Of these responses, the complement system was significantly higher, and a variety of inflammatory responses by complement regulation and anti-inflammatory cytokine or factors were identified in *Arr1*$^{-/-B}$ retinal transcripts. This discovery supports that *Arr1*$^{-/-B}$ has a distinct genetic background from *Arr1*$^{-/-A}$ that results in alterations in its retinal phenotype leading to susceptibility to cone degeneration induced by inappropriate inflammatory and immune responses.

**Keywords** Cone dystrophy · Visual arrestin 1 · Genetic susceptibility · Retinitis pigmentosa

## 34.1 Introduction

Visual arrestin 1 (ARR1, S-antigen [SAG], 48 KDa protein) and cone ARR4 (Craft et al. 1994) were discovered to be critical regulators to shut off the light-activated phototransduction cascade. Previous studies clearly demonstrated distinct functional roles of visual arrestins and their contribution to the visual system, especially rod and cone photoreceptors in mouse models in which these two genes, *Arr1* and *Arr4,* were individually or simultaneously knocked out (Chen et al. 1999; Nikonov et al. 2008; Brown et al. 2010; Huang et al. 2010). Published work from the original *Arr1*$^{-/-}$ (designated *Arr1*$^{-/-A}$) mice retina compared to wild-type (WT) mice revealed nearly identical gene expression profiles and no retinal degeneration when dark-reared (Roca et al. 2004). In a later study (Nikonov et al. 2008), we observed an unexpected cone dystrophy of dark-reared *Arr1*$^{-/-A}$*Arr4*$^{+/+}$ (designated *Arr1*$^{-/-B}$) mice through cone loss by apoptosis even when the rods are maintained, suggesting alternatively *light-independent* retinal degeneration in our colony of F2 littermates (*Arr1*$^{-/-A}$*Arr4*$^{+/+}$) from backcrossing the original *Arr1*$^{-/-A}$ and *Arr4*$^{-/-}$ mice (Brown et al. 2010). These studies suggested that a constitutive light activation of the phototransduction cascade may not be the only mechanism of retinal degeneration in ARR1 knockout mice (*Arr1*$^{-/-B}$). The microarray data revealed that dark-reared

*Arr1*$^{-/-B}$ mice have a variable genetic background compared to the original *Arr1*$^{-/-A}$ colony, which may contribute to susceptibility to the observed *light-independent* retinal degeneration.

## 34.2 Materials and Methods

### *34.2.1 Animals*

Mice were dark-reared in the USC vivarium following the appropriate established guidelines of the ARVO Statement for the Use of Animals in Ophthalmic and Vision Research and approved by the Institutional Animal Care and Use Committee of the University of Southern California. Our *Arr1*$^{-/-B}$ colony (*Arr1*$^{-/-A}$*Arr4*$^{+/+}$) was derived from the crossing of the original *Arr1*$^{-/-}$ and *Arr4*$^{-/-}$ (cone arrestin, *Arr4*, NP_573468) mice (Nikonov et al. 2008). All WT *(Arr1*$^{+/+}$*Arr4*$^{+/+}$, designated WT colony) and visual arrestin knockout mice (*Arr1*$^{-/-A}$, *Arr1*$^{-/-B}$) used in this study were on a mixed C57/Bl6J:129SVJ background and resulted from breeding homozygous F2 littermates. All offspring were verified by PCR genotype analysis for *Arr1*$^{-/-A}$, *Arr1*$^{-/-B}$, and WT and used as breeders (Nikonov et al. 2008; Brown et al. 2010).

### *34.2.2 Affymetrix™ GeneChip Microarray Hybridization and Ingenuity Pathway Analysis*

According to previously published protocols (Yetemian et al. 2010), total RNA was purified and then measured using spectrophotometry $A_{260}/A_{280}$ ratios. Affymetrix™ GeneChip Mouse Exon 1.0 ST Arrays (Affymetrix Inc., Santa Clara, CA) were used for hybridization. The exon arrays were scanned according to established Affymetrix™ protocols. Experiments were performed in triplicate for statistical and biological relevance. The original Affymetrix™ raw intensity files were imported into Partek Genomics Suite (Partek Inc.) and processed with GC-RMA (Robust Multi-array Average) background correction and quantile normalization algorithms. The log2 transformed data was then subjected to a two-way mixed-model factorial ANOVA analysis, and the list of differentially expressed genes between the two strains (WT vs *Arr1*$^{-/-A}$, *WT* vs *Arr1*$^{-/-B}$, and *Arr1*$^{-/-A}$ vs *Arr1*$^{-/-B}$) was subsequently generated. Transcripts of *Arr1*$^{-/-B}$ with statistically significant differences compared to WT and annotated function were categorized using Ingenuity Pathway Analysis (IPA; QIAGEN, Redwood City, CA). Scores for top networks were based on the hypergeometric distribution and calculated with the right-tailed Fisher's Exact Test by IPA.

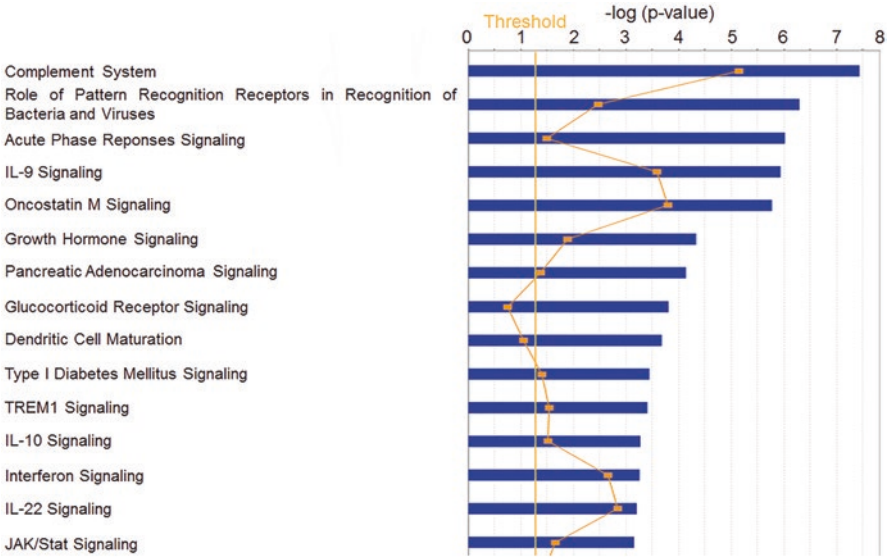


**Fig. 34.1** Transcripts categorized by Ingenuity Pathway Analysis (IPA) between *Arr1*$^{-/-B}$ retina and WT. Canonical pathways are presented on the x axis, and the statistical significance of each pathway with a threshold of 0.05 is presented on the y axis, −log (*p* value, blue bar). Top canonical pathways above the threshold value are presented. The orange line displays the ratio of upregulated transcripts in the dataset to the number of genes in each pathway, revealing that complement system has the largest ratio, while others such as acute phase response signaling, IL-10 signaling, and JAK/STAT signaling are above threshold for statistical significance

## 34.3 Results

### *34.3.1 Affymetrix™ Exon Array Data in* Arr1$^{-/-B}$ *Mice Retina*

To identify potential genetic modifiers and cellular pathways involved in cell death in *Arr1*$^{-/-B}$ mice retina at postnatal 30 (P30), when apoptosis was documented and prior to severe morphological changes in dark-reared environment, compared with WT colony and *Arr1*$^{-/-A}$ retina, we performed exon array analysis in triplicate and analyzed the data using statistical analysis software (Partek Genomics Suite; Partek Inc., St. Louis, MO, Supplemental Table 34.1). Gene expression profiles in dark-reared *Arr1*$^{-/-A}$ mice are nearly similar to those in WT (Roca et al. 2004) and that dark-reared *Arr1*$^{-/-B}$ has a variety of functional alterations in genomic or proteomic level due to their distinct genetic background. Individual transcripts in *Arr1*$^{-/-B}$ mice retina were categorized using IPA with respect to diseases and disorders, molecular and cellular functions, and physiological system development and function (Fig. 34.1). Of these systems, complement system, IL-9 signaling, oncostatin M signaling, and interferon signaling were each ranked as the top categories according to *p* value and the number of molecules categorized. The complement system was the top recognized pathway identified, which was previously implicated in the

pathogenesis of age-related macular degeneration (Haines et al. 2005; McGeer et al. 2005; Souied et al. 2005; McKay et al. 2010), while others such as acute phase response, triggering receptor expressed on myeloid cells 1 (TREM1), IL-10 as an anti-inflammatory factor, growth hormone, and JAK/STAT signaling transcripts are above threshold for statistical significance. These pathways implicate a variety of inflammatory responses by complement regulation, acute phase reactants, and anti-inflammatory cytokine or factors and a potential unique involvement in $Arr1^{-/-B}$ retina not observed in either the WT or $Arr1^{-/-A}$ retina, implicating that these pathways are ultimately associated with the observed cone cell death phenotype.

## 34.4 Discussion

In this study, we investigated the distinct differences in a gene expression profile associated with cone dystrophy in our mice colony $Arr1^{-/-B}$ (Brown et al. 2010) with an exon array analysis. Additionally, we focused on determining the initial potential interacting networks that trigger the retinal cone degenerative processes in the genetic mouse model of dark-reared $Arr1^{-/-B}$ versus colony controls. The gene array results show shared pathways involving complement cascade, gliosis, immune response, autophagy, and apoptosis that may contribute to the cone degeneration in the $Arr1^{-/-B}$. These data suggest that the retinal gene expression profile in $Arr1^{-/-B}$ represents a distinct and separate susceptibility response to retinal degeneration in the light-independent environment that may enhance the development and progression of disease, depending on their genetic background (Haider et al. 2008). Additionally, we observed that the OSM signaling pathway was ranked as the second top candidate following complement system by IPA analysis from the microarray data in $Arr1^{-/-B}$ retina. OSM, a member of the interleukin 6 (IL-6) family cytokines, signals through two types of receptor complexes that have been identified in human for OSM signal transduction. It has been also reported that OSM has the protective effect on photoreceptors, inducing STAT3 phosphorylation in the retinal degeneration of several models (Mechoulam and Pierce 2005; Samardzija et al. 2006; Ueki et al. 2008). As shown in the schematic representation of the hypothetical network for photoreceptor degeneration (Fig. 34.2), we hypothesize that OSM signaling via pSTAT3 is simultaneously upregulated to protect photoreceptors against inflammatory or immune response in the susceptible $Arr1^{-/-B}$; however, these defense mechanisms are not resistant to overcoming the harmful responses that occur in this mutated retina.

In summary, the microarray analysis of retinas in $Arr1^{-/-B}$ undergoing retinal degeneration with cone dystrophy identified a unique subset of activated gene expression profiles including inflammatory cytokines and complement components. This novel discovery leads us to further genetic studies that will determine the genetic link between susceptibility and resistance to retinal degeneration induced by inappropriate inflammatory and immune responses. We propose that by defining the molecular mechanisms of susceptibility triggering cone photoreceptor cell death,

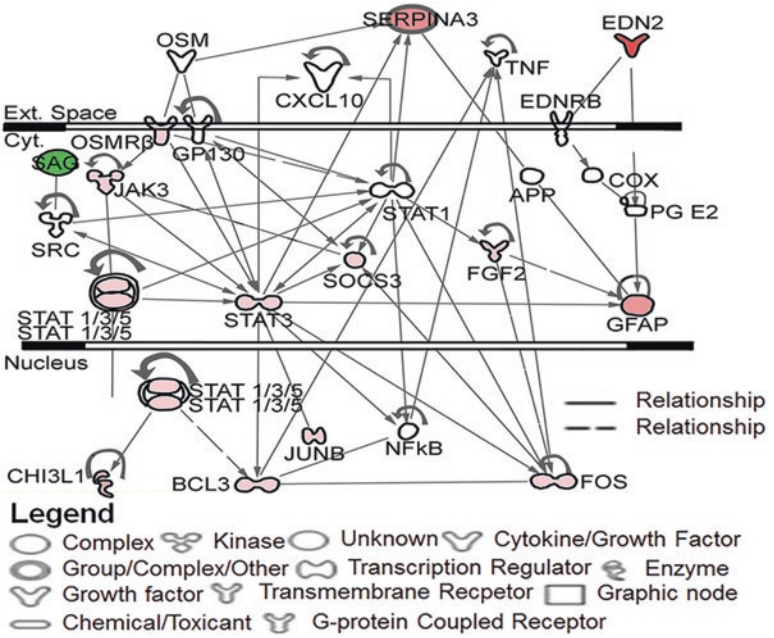


**Fig. 34.2** Schematic representation of the hypothetical network for the *light-independent* cone photoreceptor degeneration in $Arr1^{-/-B}$ retina. Exon array dataset analysis was used to generate a hypothetical network based on upregulated transcripts. Dotted lines represent indirect protein relationships, whereas solid lines represent direct relationship, including protein-protein interactions, activation, phosphorylation, and ligand-receptor binding. Molecules in red represent significantly upregulated transcripts, green represent significantly downregulated transcripts, and uncolored molecules were not differentially expressed but are included because they are important components of the total network (SAG; arrestin 1)

it may lead to resolving the etiology of retinal degeneration with genetic heterogeneity such as Oguchi's disease, retinitis pigmentosa (RP), and age-related macular degeneration. In the future, these studies will contribute to the design of modifier gene therapeutics to slow and prevent visual loss.

**Acknowledgments** We thank Andrew Vargus and other members in the USC Rocki Eye Institute Laboratory in Vision Research for technical support with data analysis, Neena Haider (Schepens Eye Research Institute, Harvard) for scientific discussions, Jeannie Chen for providing $Arr1^{-/-A}$ mice, and the Children's Hospital Los Angeles Microarray Core Facility and USC NML Bioinformatics Service for technical support. Grant support, in part, from NEI EY015851 and core grants: EY03040, Research to Prevent Blindness (USC Ophthalmology), and the M. D. Allen Foundation.

## References

Brown BM, Ramirez T, Rife L, Craft CM (2010) Visual Arrestin 1 contributes to cone photoreceptor survival and light adaptation. Invest Ophthalmol Vis Sci 51:2372–2380

Chen J, Simon MI, Matthes MT, Yasumura D, LaVail MM (1999) Increased susceptibility to light damage in an arrestin knockout mouse model of Oguchi disease (stationary night blindness). Invest Ophthalmol Vis Sci 40:2978–2982

Craft CM, Whitmore DH, Wiechmann AF (1994) Cone arrestin identified by targeting expression of a functional family. J Biol Chem 269:4613–4619

Haider NB, Zhang W, Hurd R, Ikeda A, Nystuen AM, Naggert JK, Nishina PM (2008) Mapping of genetic modifiers of Nr2e3 rd7/rd7 that suppress retinal degeneration and restore blue cone cells to normal quantity. Mamm Genome 19:145–154

Haines JL, Hauser MA, Schmidt S, Scott WK, Olson LM, Gallins P, Spencer KL, Kwan SY, Noureddine M, Gilbert JR, Schnetz-Boutaud N, Agarwal A, Postel EA, Pericak-Vance MA (2005) Complement factor H variant increases the risk of age-related macular degeneration. Science 308:419–421

Huang SP, Brown BM, Craft CM (2010) Visual Arrestin 1 acts as a modulator for N-ethylmaleimide-sensitive factor in the photoreceptor synapse. J Neurosci 30:9381–9391

McGeer EG, Klegeris A, McGeer PL (2005) Inflammation, the complement system and the diseases of aging. Neurobiol Aging 26(Suppl 1):94–97

McKay GJ, Dasari S, Patterson CC, Chakravarthy U, Silvestri G (2010) Complement component 3: an assessment of association with AMD and analysis of gene-gene and gene-environment interactions in a Northern Irish cohort. Mol Vis 16:194–199

Mechoulam H, Pierce EA (2005) Expression and activation of STAT3 in ischemia-induced retinopathy. Invest Ophthalmol Vis Sci 46:4409–4416

Nikonov SS, Brown BM, Davis JA, Zuniga FI, Bragin A, Pugh EN Jr, Craft CM (2008) Mouse cones require an arrestin for normal inactivation of phototransduction. Neuron 59:462–474

Roca A, Shin KJ, Liu X, Simon MI, Chen J (2004) Comparative analysis of transcriptional profiles between two apoptotic pathways of light-induced retinal degeneration. Neuroscience 129:779–790

Samardzija M, Wenzel A, Aufenberg S, Thiersch M, Reme C, Grimm C (2006) Differential role of Jak-STAT signaling in retinal degenerations. FASEB J 20:2411–2413

Souied EH, Leveziel N, Richard F, Dragon-Durey MA, Coscas G, Soubrane G, Benlian P, Fremeaux-Bacchi V (2005) Y402H complement factor H polymorphism associated with exudative age-related macular degeneration in the French population. Mol Vis 11:1135–1140

Ueki Y, Wang J, Chollangi S, Ash JD (2008) STAT3 activation in photoreceptors by leukemia inhibitory factor is associated with protection from light damage. J Neurochem 105:784–796

Yetemian RM, Brown BM, Craft CM (2010) Neovascularization, enhanced inflammatory response, and age-related cone dystrophy in the Nrl−/−Grk1−/− mouse retina. Invest Ophthalmol Vis Sci 51:6196–6206

# Chapter 35
# How Excessive cGMP Impacts Metabolic Proteins in Retinas at the Onset of Degeneration

**Jianhai Du, Jie An, Jonathan D. Linton, Yekai Wang, and James B. Hurley**

**Abstract** Aryl-hydrocarbon receptor interacting protein-like 1 (AIPL1) is essential to stabilize cGMP phosphodiesterase 6 (PDE6) in rod photoreceptors. Mutation of AIPL1 leads to loss of PDE6, accumulation of intracellular cGMP, and rapid degeneration of rods. To understand the metabolic basis for the photoreceptor degeneration caused by excessive cGMP, we performed proteomics and phosphoproteomics analyses on retinas from AIPL1−/− mice at the onset of rod cell death. AIPL1−/− retinas have about 18 times less than normal PDE6a and no detectable PDE6b. We identified twelve other proteins and thirty-nine phosphorylated proteins related to cell metabolism that are significantly altered preceding the massive degeneration of rods. They include transporters, kinases, phosphatases, transferases, and proteins involved in mitochondrial bioenergetics and metabolism of glucose, lipids, amino acids, nucleotides, and RNA. In AIPLI−/− retinas mTOR and proteins involved in mitochondrial energy production and lipid synthesis are more dephosphorylated, but glycolysis proteins and proteins involved in leucine catabolism are more phosphorylated than in normal retinas. Our findings indicate that elevating cGMP rewires

J. Du
Departments of Ophthalmology, and Biochemistry, West Virginia University, Morgantown, WV, USA

Department of Ophthalmology, University of Washington, Seattle, WA, USA

J. An
Department of Medicine, University of Washington, Seattle, WA, USA

J. D. Linton
Department of Ophthalmology, University of Washington, Seattle, WA, USA

Y. Wang
Departments of Ophthalmology, and Biochemistry, West Virginia University, Morgantown, WV, USA

J. B. Hurley (✉)
Department of Ophthalmology, University of Washington, Seattle, WA, USA

Department of Biochemistry, University of Washington, Seattle, WA, USA
e-mail: jbhhh@u.washington.edu



J. D. Ash et al. (eds.), *Retinal Degenerative Diseases*, Advances in Experimental Medicine and Biology 891, https://doi.org/10.1007/978-3-319-75402-4_35

cellular metabolism prior to photoreceptor degeneration and that targeting metabolism may be a productive strategy to prevent or slow retinal degeneration.

**Keywords** cGMP · Metabolism · Retinal degeneration · Proteomics · Phosphoproteomics · AIPL1

## 35.1 Introduction

Inherited retinal diseases cause blindness or severe visual loss in humans. Excessive accumulation of cGMP in photoreceptors is likely to be a major factor in retinal degenerations caused by mutations in the genes encoding PDE6a, PDE6b (Rd1 and Rd10), PDE6c (Cpfl1), aryl-hydrocarbon receptor interacting protein-like 1 (AIPL1), Cngb1, and Cngb3 (Huang et al. 1995; Ramamurthy et al. 2004; Huttl et al. 2005; Chang et al. 2007; Arango-Gonzalez et al. 2014). Mutations in AIPL1 cause severe retinal degeneration. AIPL1 deficiency in mice causes rod and cone photoreceptors (PRs) to degenerate within 4 weeks after birth (Dyer et al. 2004; Ramamurthy et al. 2004). Intracellular cGMP levels increase 5–10 times higher than normal just before the onset of degeneration. We are investigating the idea that accumulation of cGMP causes metabolic failure in several retinal degeneration models (Trifunovic et al. 2012; Arango-Gonzalez et al. 2014). To understand the link between cGMP accumulation and photoreceptor degeneration, we used mass spectrometry to quantify changes in protein and protein phosphorylation caused by AIPL1 deficiency. We found that loss of AIPL1 causes depletion of PDE6a/b, dephosphorylation of mTOR and proteins involved in lipid synthesis and mitochondrial energy production, increases in glycolysis proteins, and altered phosphorylation of proteins involved in solute transport and in nucleotide and RNA metabolism.

## 35.2 Materials and Methods

### *35.2.1 Animals*

AIPL1 +/− mice were crossed to produce AIPL1−/− and AIPL1+/+ control littermates in C57BL6 background. Experiments were performed in accordance with the Institutional Animal Care and Use Committee (IACUC) recommendations at the University of Washington guidelines after IACUC approval.

### *35.2.2 Retinal Proteomics and Phosphoproteomics*

Four retinas were isolated from P10 pups (Du et al. 2016) and pooled into one tube to be homogenized with 6 M urea in 50 mM ammonium bicarbonate. Proteins were extracted and prepared for proteomics analysis as reported (An et al. 2016). Briefly, the protein samples were reduced by TCEP and alkylated with iodoacetamide for 1 h at room temperature. After digestion by trypsin at 1:50 (enzyme:protein) ratio overnight, the peptides were then washed three times and desalted by C18 columns. Phosphopeptides were enriched by $TiO_2$ column and desalted by graphite columns according to the manufacturer's instructions. Protein peptides and phosphopeptides were analyzed by UPLC (Waters, USA) coupled with Orbitrap Fusion mass spectrometer (Thermal Scientific, USA). Acquired data were converted to the mzXML format and searched against a mouse proteome database using Comet. The search results were further processed by PeptideProphet and ProteinProphet.

## 35.3 Results

### *35.3.1 AIPL1 Deficiency Changes the Profile of Metabolic Proteins in the Retina*

To understand how accumulation of cGMP influences retinal metabolism prior to retinal degeneration, we isolated retinas from AIPL1−/− mice at postnatal 10 days (P10). At P10, cGMP accumulates in AIPL1−/− retinas, but there are no obvious morphological changes. We used mass spectrometry in 7 separate experiments to identify 7304 unique proteins in AIPL1−/− retinas and in retinas from their homozygous wild-type littermate. A stringent criterion (the fold change >2 or < −2 in at least 5 hits of 7 samples with spectral count more than 2) was applied, and 30 proteins were identified with significantly different expressions. Twelve of them were metabolism-related proteins (Table 35.1). As expected, AIPL1 was not detected, and we found that PDE6a/PDE6b is substantially decreased in the AIPL1−/− retinas. Most of the differentially expressed proteins were related to nucleotide metabolism such as proteins involved in nucleotide binding, nucleotide exchange, and mRNA modification and processing (Table 35.1). AIPL1 deficiency also increases levels of proteins involved in catabolism, including collagen degradation and leucine degradation. Zinc homeostasis is essential for photoreceptor survival (Grahn et al. 2001). The zinc transporter SLC39A7 is upregulated in AIPL1−/− retinas.

**Table 35.1** Changes in the amounts of metabolism proteins in AIPL−/− retinas. P10 retinas from AIPL1−/− and littermates were analyzed by proteomics. Significant changes in levels of proteins related to metabolism are listed. Green highlights downregulated and red highlights upregulated proteins compared to control. $N = 7$. Spectral count was shown as mean ± SD

| Gene | Protein | WT | AIPL1 | Metabolic pathway |
|---|---|---|---|---|
| AIPL1 | Aryl-hydrocarbon-interacting protein-like 1 | 11±1.5 | 0 | cGMP degradation |
| PDE6b | Phosphodiesterase 6B | 40±1.6 | 0 | cGMP degradation |
| PDE6a | Phosphodiesterase 6A | 53±1.6 | 3±1.4 | cGMP degradation |
| Cmtr1 | S-adenosyl-L-methionine-dependent methyltransferase | 7±2.5 | 3±0.4 | RNA methyl transferase |
| Sar1b | GTP-binding protein SAR1b | 4±1.5 | 1±0.4 | Nucleotide binding |
| Ehd4 | EH domain-containing protein 4 | 3±1.0 | 1±0.4 | Nucleotide binding |
| Gng11 | Guanine nucleotide-binding protein G(I)/G(S)/G(O) subunit gamma-11 | 3±1 | 1±0.4 | Nucleotide binding |
| **Pepd** | Xaa-Pro dipeptidase | 2±0 | 4±1.5 | Collagen metabolism |
| **Rab3ip** | Rab-3A-interacting protein | 2±0.5 | 4±1.5 | Nucleotide exchange |
| **Mbnl2** | Isoform 2 of muscleblind-like protein 2 | 1±0.4 | 5±1.5 | RNA metabolism |
| **Slc39a7** | Zinc transporter SLC39A7 | 0 | 3±1.0 | Metal transport |
| **Mccc2** | Methylcrotonoyl-CoA carboxylase beta chain, mitochondria | 0 | 3±0.6 | Leucine degradation |

### *35.3.2 AIPL1 Deficiency Influences the Phosphorylation State of Metabolic Enzymes*

Phosphorylation is an important regulator of protein function. To evaluate phosphorylation of proteins in P10 retinas, we enriched phosphorylated peptides with $TiO_2$ chromatography and analyzed them by mass spectrometry. From a total of 2550 detected phosphoproteins, we identified 128 proteins that were phosphorylated differently in AIPL1−/− than in control retinas. One third of these phosphoproteins are involved in cellular metabolism. These include transporters, kinases, phosphatases, transferases, and proteins in glucose, lipid, and nucleotide metabolism (Fig. 35.1). At the onset of retinal degeneration, AIPL1 deficiency changes the phosphorylation of transporters for sodium, calcium, and potassium. Surprisingly, the proteins in mitochondrial energy production and phospholipid synthesis are less phosphorylated, while the glycolysis enzyme 6-phosphofructokinase (Pfkl) is more phosphorylated in AIPL−/− retinas. Mammalian target of rapamycin (mTOR) is a key regulator of cellular energy metabolism. We found that Mapka1, a component of the mTOR2 complex, is less phosphorylated in AIPL1-deficient retinas than in

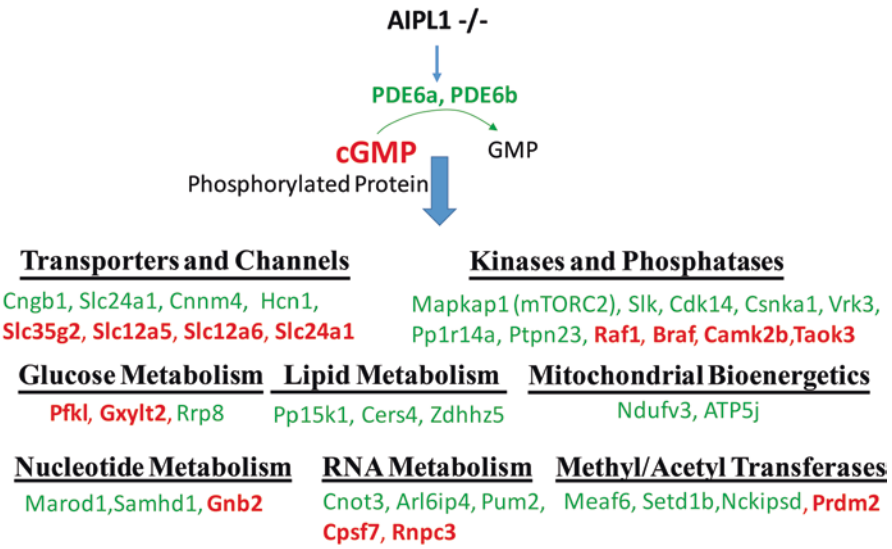


**Fig. 35.1** Changes in phosphorylation state of metabolic proteins in AIPL−/− retinas. P10 retinas from AIPL1−/− and littermates were enriched for phosphorylated peptides and analyzed by phosphoproteomics. Significantly changed proteins related to metabolism are listed. The proteins in green represent downregulation and in red represent upregulation of phosphorylation compared to control. $N = 5$

controls. We also identified changes in the phosphorylation state of enzymes involved in nucleotide and RNA metabolism. Enzymes that transfer methyl or acetyl groups to DNA and histones also were substantially altered.

## 35.4 Discussion

Our study surveys proteins and phosphoproteins in AIPL1 −/− retinas at the onset of degeneration and provides evidence that cellular metabolism may be fundamentally rewired prior to massive and rapid photoreceptor degeneration. AIPL1 is essential to maintain the stability of PDE6a and PDE6b (Ramamurthy et al. 2004; Kolandaivelu et al. 2009; Kolandaivelu et al. 2014). As predicted, our proteomics analysis detected no PDE6b. PDE6a was about 18 times lower than normal in all AIPL1−/− retinas. PDE6a or PDE6b deficiencies cause accumulation of cGMP. In other studies we have found that the 5′GMP level decreases in these retinas (not shown here). 5′GMP is a key feedback regulator of purine synthesis. Normally the cellular purine and pyrimidine nucleotide levels are tightly regulated and balanced. They are the basic building blocks for RNA and DNA biosynthesis. Our findings are consistent with an imbalance of nucleotide levels in AIPL1−/− retinas altering expression and phosphorylation of proteins involved in nucleotide and RNA metabolism.

Recent studies have shown that disruption of mitochondrial energy metabolism can cause an imbalance of ribonucleotides, which then contributes to neurodegeneration (Fasullo and Endres 2015; Nikkanen et al. 2016). Deficient mitochondrial energy production makes *Drosophila* photoreceptors more vulnerable to light-induced degeneration and produces a visual defect in zebrafish (Taylor et al. 2004; Jaiswal et al. 2015). We found that mitochondrial complex I subunit (ndufv3) and ATP synthase subunit (ATP5j) are dephosphorylated in AIPL1-deficient mouse retinas. The inhibition of mitochondrial bioenergetics may activate glycolysis to generate more energy, increase utilization of amino acids, and decrease other anabolic activities such as lipid synthesis. However, retina has an extremely high demand for energy and for lipid turnover for outer segment synthesis. The significant upregulation of the leucine catabolism protein, Mccc2, in the AIPL1−/− retina may decrease cellular leucine, which then could lead to dephosphorylation of mTOR. That also may contribute to dysregulation of cellular metabolism and deactivation of other downstream cell survival signaling pathways.

Taken altogether these findings suggest that metabolic rewiring is likely to be both a cause and a consequence of photoreceptor degeneration. Therapeutic approaches that make photoreceptor metabolism more robust may be an effective strategy to prevent or slow retinal degeneration.

**Acknowledgments** This study was supported by EY06641 (JBH), EY017863 (JBH), and Knights Templar Career Starter grant (JD).

## References

An J, Briggs TA, Dumax-Vorzet A et al (2017) Tartrate-resistant acid phosphatase deficiency in the predisposition to systemic lupus erythematosus. Arthritis Rheumatol 69(1):131–142

Arango-Gonzalez B, Trifunovic D, Sahaboglu A et al (2014) Identification of a common non-apoptotic cell death mechanism in hereditary retinal degeneration. PLoS One 9:e112142

Chang B, Hawes NL, Pardue MT et al (2007) Two mouse retinal degenerations caused by missense mutations in the beta-subunit of rod cGMP phosphodiesterase gene. Vis Res 47:624–633

Du J, Rountree A, Cleghorn WM et al (2016) Phototransduction influences metabolic flux and nucleotide metabolism in mouse retina. J Biol Chem 291:4698–4710

Dyer MA, Donovan SL, Zhang J et al (2004) Retinal degeneration in Aipl1-deficient mice: a new genetic model of Leber congenital amaurosis. Brain Res Mol Brain Res 132:208–220

Fasullo M, Endres L (2015) Nucleotide salvage deficiencies, DNA damage and neurodegeneration. Int J Mol Sci 16:9431–9449

Grahn BH, Paterson PG, Gottschall-Pass KT et al (2001) Zinc and the eye. J Am Coll Nutr 20:106–118

Huang SH, Pittler SJ, Huang X et al (1995) Autosomal recessive retinitis pigmentosa caused by mutations in the alpha subunit of rod cGMP phosphodiesterase. Nat Genet 11:468–471

Huttl S, Michalakis S, Seeliger M et al (2005) Impaired channel targeting and retinal degeneration in mice lacking the cyclic nucleotide-gated channel subunit CNGB1. J Neurosci Off J Soc Neurosci 25:130–138

Jaiswal M, Haelterman NA, Sandoval H et al (2015) Impaired mitochondrial energy production causes light-induced photoreceptor degeneration independent of oxidative stress. PLoS Biol 13:e1002197

Kolandaivelu S, Huang J, Hurley JB et al (2009) AIPL1, a protein associated with childhood blindness, interacts with alpha-subunit of rod phosphodiesterase (PDE6) and is essential for its proper assembly. J Biol Chem 284:30853–30861

Kolandaivelu S, Singh RK, Ramamurthy V (2014) AIPL1, A protein linked to blindness, is essential for the stability of enzymes mediating cGMP metabolism in cone photoreceptor cells. Hum Mol Genet 23:1002–1012

Nikkanen J, Forsstrom S, Euro L et al (2016) Mitochondrial DNA replication defects disturb cellular dNTP pools and remodel one-carbon metabolism. Cell Metab 23:635–648

Ramamurthy V, Niemi GA, Reh TA et al (2004) Leber congenital amaurosis linked to AIPL1: a mouse model reveals destabilization of cGMP phosphodiesterase. Proc Natl Acad Sci U S A 101:13897–13902

Taylor MR, Hurley JB, Van Epps HA et al (2004) A zebrafish model for pyruvate dehydrogenase deficiency: rescue of neurological dysfunction and embryonic lethality using a ketogenic diet. Proc Natl Acad Sci U S A 101:4584–4589

Trifunovic D, Sahaboglu A, Kaur J et al (2012) Neuroprotective strategies for the treatment of inherited photoreceptor degeneration. Curr Mol Med 12:598–612

# Chapter 36
# Protein Carbonylation-Dependent Photoreceptor Cell Death Induced by N-Methyl-N-nitrosourea in Mice


**Ayako Furukawa, Kayo Sugitani, and Yoshiki Koriyama**

**Abstract** Retinal degenerative diseases, such as retinitis pigmentosa, are characterized by night blindness and peripheral vision loss caused by the slowly progressive loss of photoreceptor cells. A comprehensive molecular mechanism of the photoreceptor cell death remains unclear. We previously reported that heat shock protein 70 (HSP70), which has a protective effect on neuronal cells, was cleaved by a calcium-dependent protease, calpain, in N-methyl-N-nitrosourea (MNU)-treated mice retina. Carbonylated HSP70 is much more vulnerable than noncarbonylated HSP70 to calpain cleavage. However, it was not known whether protein carbonylation occurs in MNU-treated mice retina. In this study, we clearly show protein carbonylation-dependent photoreceptor cell death induced by MNU in mice. Therefore, protein carbonylation and subsequent calpain-dependent cleavage of HSP70 are key events in MNU-mediated photoreceptor cell death. Our data provide a comprehensive molecular mechanism of the photoreceptor cell death.

**Keywords** Oxidative stress · Protein carbonylation · HSP70 · N-Methyl-N-nitrosourea · Photoreceptor cell death · Retinitis pigmentosa · 4HNE · Calpain

## 36.1 Introduction

Retinitis pigmentosa is a disease characterized by a loss of photoreceptor cells. Although many causative gene mutations have been reported, the final common end stage is photoreceptor cell death. Herrold et al. originally reported that

A. Furukawa · Y. Koriyama (✉)
Graduate School and Faculty of Pharmaceutical Sciences, Suzuka University of Medical Science, Suzuka, Japan
e-mail: koriyama@suzuka-u.ac.jp

K. Sugitani
Division of Health Sciences, Graduate School of Medicine, Kanazawa University, Kanazawa, Japan



J. D. Ash et al. (eds.), *Retinal Degenerative Diseases*, Advances in Experimental Medicine and Biology 891, https://doi.org/10.1007/978-3-319-75402-4_36

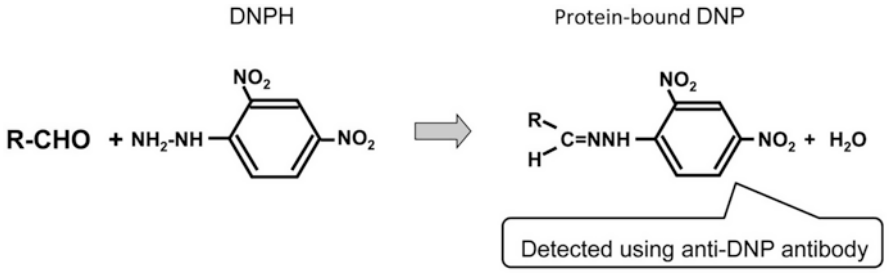


**Fig. 36.1** Pretreatment with 2,4-dinitrophenylhydrazine (DNPH) to detect protein carbonyls by immunohistochemistry. DNPH reacts with protein carbonyls to form protein-bound 2,4-dinitrophenyl hydrazone (DNP). By using anti-DNP antibody, protein carbonyls were detected

N-methyl-N-nitrosourea (MNU) causes photoreceptor cell loss in golden hamsters (Herrold 1967). We have tried to clarify the mechanisms of photoreceptor cell death by using the MNU-injected mice model. Intraperitoneal injection of MNU causes selective photoreceptor cell loss and significantly decreases the outer nuclear layer (ONL) thickness. Intraperitoneal injection of MNU induces the accumulation of intracellular $Ca^{2+}$ in the retina and increases calpain activation, which leads to photoreceptor cell death (Oka et al. 2007). We have revealed that the calpain-dependent cleavage of HSP70 occurs in MNU-treated mice retina (Koriyama et al. 2014). HSP70 is highly conserved and functions as a chaperone molecule to protect cells against various stresses. Under pathological conditions of neuronal tissues, such as glaucoma and ischemic/reperfusion of the hippocampus, HSP70 is a common substrate of calpain (Nakajima et al. 2006). In addition, carbonylated HSP70 caused by oxidative stresses such as 4-hydroxy-2-nonenal (4HNE) is much more vulnerable than noncarbonylated HSP70 to calpain cleavage (Sahara and Yamashima 2010). We have found that MNU induced the generation of 4HNE, an oxidative stress marker on lipids, in retinal photoreceptor cells. However, it is not known whether protein carbonylation occurs in MNU-treated mice retina.

Oxidative stress, which attacks lipids, proteins, and DNA, is one of the causative factors of photoreceptor cell death. Oxidative stresses give rise to a variety of modifications in amino acid residues. Protein carbonyls formed by oxidation of arginine, lysine, threonine, or proline residues are often used as a marker of major forms of oxidatively damaged proteins. In contrast to methionine sulfoxide and cysteine disulfide bond formation, carbonylation is an irreversible oxidative process (Dalle-Donne et al. 2006). These features make protein carbonyls a useful marker for oxidative damage to proteins. 2,4-Dinitrophenylhydrazine (DNPH) reacts with protein carbonyls to form protein-bound 2,4-dinitrophenyl hydrazone (DNP) (Nakamura and Goto 1996). We can detect carbonylated proteins by using anti-DNP antibody (Fig. 36.1). In this study, we examined whether protein carbonylation occurs in MNU-treated mice retina.

## 36.2 Materials and Methods

### *36.2.1 Animal Experiments*

Male C57BL/6 mice (8–9 weeks old) were purchased from Japan SLC (Hamamatsu, Japan). All animals were maintained and handled in accordance with the ARVO Statement for the Use of Animals in Ophthalmic and Vision Research, the guidelines of the Declaration of Helsinki, the Guiding Principles for the Care and Use of Animals, and Suzuka University of Medical Science's guidelines for animal experiments. MNU was dissolved in saline and administered by intraperitoneal injection at a dose of 60 mg/kg body weight.

### *36.2.2 Retinal Sections and Immunohistochemistry*

Immunohistochemistry was performed by using cryoprotected retinal sections. MNU-treated mice were anesthetized by intraperitoneal injection of sodium pentobarbital (30–40 mg/kg body weight). Mouse eyes were enucleated and fixed overnight in 0.1 M phosphate buffer (pH 7.4) containing 4% paraformaldehyde and 5% sucrose. Fixed eyes were cryoprotected in 30% sucrose and frozen in OCT medium. Retinal sections in central areas (within 300 μm of the optic disc) were cut at 12 μm thickness. For immunological detection of carbonylated proteins, the carbonyl group was derivatized by DNPH (Fig. 36.1). Sections were incubated with Blocking One (Nacalai Tesque, Kyoto, Japan), followed by incubation with primary antibody against DNP (1:500; Cell Signaling Technology, Tokyo, Japan). Sections were then incubated with biotin-conjugated secondary antibody and avidin-horseradish peroxidase substrate. Carbonylation signals were detected by 3-amino-9-ethylcarbazole (DAKO, Kyoto, Japan).

## 36.3 Results

One day after MNU infection, the generation of 4HNE was detected in the ONL (Koriyama et al. 2014). To elucidate the protein carbonylation, retinal immunohistochemistry for DNP was performed. Compared to the control sections, ONL thickness became significantly thinner by 3 days after MNU injection (Fig. 36.2a, b). Immunohistochemistry with anti-DNP revealed many DNP-immunopositive cells in the ONL 3 days after MNU injection (Fig. 36.2b). DNP-positive cells were almost undetectable in control mice retina (Fig. 36.2a).

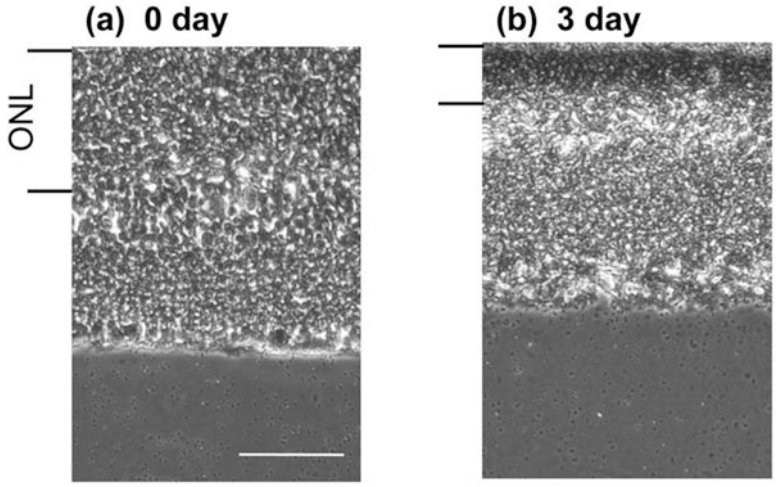


**Fig. 36.2** Oxidative damage to protein in the retina following MNU injection. Mice received an intraperitoneal injection of 60 mg/kg of MNU and were subjected to histological analysis at 3 days after MNU administration. Control mice were treated with saline. Compared to control mice (**a**), MNU-treated mice retina showed thinning of ONL and strong immunoreactivity for carbonylated proteins (**b**). Scale = 100 μm

## 36.4 Discussion

Retinitis pigmentosa (RP) is one of the major retinal degenerative diseases. Unfortunately, no effective treatments or therapeutic agents have been discovered. Reactive oxygen species, calcium-calpain activation, and lipid peroxidation are involved in the initiation of photoreceptor cell death, but the total process of cell death signaling remains obscure. Oxidative stress is one of the main causative factors contributing to photoreceptor cell death in the progression of a number of retinal diseases, such as RP. RP patients showed a significant decrease in the ratio of reduced glutathione to oxidized glutathione and a significant increase in protein carbonyl content in aqueous humor (Campochiaro et al. 2015). In some RP models, accumulation of 4HNE, an oxidative stress marker, was detected in photoreceptor cells (Tanito et al. 2006). We detected 4HNE accumulation in the ONL of MNU-treated mice retina (Koriyama et al. 2014). 4HNE is a highly reactive aldehyde that forms as a result of nonenzymatic lipid peroxidation of long-chain polyunsaturated fatty acids and may be considered as a secondary toxic messenger that disseminates and augments initial free radical events (Esterbauer et al. 1991, Uchida 2003). Lipid peroxidation-modified proteins, such as 4HNE or malondialdehyde, may participate in the pathogenesis of complex and monogenetic retinal degenerative diseases (Schutt et al. 2003). Despite well-known involvement of lipid peroxidation in retinal degenerative diseases, the role of protein carbonylation during photoreceptor cell death remains unknown. In this study, we clarify that protein carbonylation occurs in MNU-treated mice retina (Fig. 36.2).

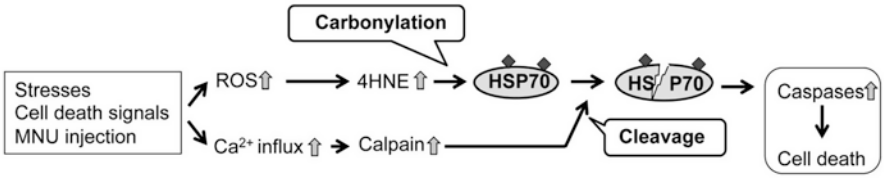


**Fig. 36.3** Protein carbonylation-dependent photoreceptor cell death by MNU

Intraperitoneal injection of MNU induces the accumulation of intracellular $Ca^{2+}$ in the retina and increases calpain activation, which leads to photoreceptor cell death (Oka et al. 2007). Carbonylated HSP70 is much more vulnerable than noncarbonylated HSP70 to calpain cleavage; calpain-mediated cleavage of HSP70 results in cell death through cathepsin-dependent proteostasis disruption (Sahara and Yamashima 2010; Yamashima 2012). We previously reported that HSP70 was rapidly and calpain-dependently cleaved after MNU treatment. Therefore, protein carbonylation by 4HNE is a very important event to induce calpain-dependent HSP70 cleavage in photoreceptor cell death (Fig. 36.3). Some antioxidants protect retina-derived cells from oxidative stress (Rezaie et al. 2012). In some RP model mice, antioxidants can inhibit photoreceptor cell death (Komeima et al. 2006; Lee et al. 2011). These data support our conclusion that photoreceptor cell death is due to oxidative damage and suggest that the inhibition of oxidative stress by antioxidants may provide therapeutic benefit via the suppression of protein carbonylation.

**Acknowledgments** This study was supported by Grants-in-Aid for Scientific Research from the Japan Society for the Promotion of Science (KAKENHI:16K11335 to YK).

## References

Campochiaro PA, Strauss RW, Lu L et al (2015) Is there excess oxidative stress and damage in eyes of patients with retinitis pigmentosa? Antioxid Redox Signal 23:643–648

Dalle-Donne I, Aldini G, Carini M et al (2006) Protein carbonylation, cellular dysfunction, and disease progression. J Cell Mol Med 10:389–406

Esterbauer H, Schaur RJ, Zollner H (1991) Chemistry and biochemistry of 4-hydroxynonenal, malonaldehyde and related aldehydes. Free Radic Biol Med 11:81–128

Herrold KM (1967) Pigmentary degeneration of the retina induced by N-methyl-N-nitrosourea. An experimental study in syrian hamsters. Arch Ophthalmol 78:650–653

Komeima K, Rogers BS, Lu L, Campochiaro PA (2006) Antioxidants reduce cone cell death in a model of retinitis pigmentosa. Proc Natl Acad Sci U S A 103:11300–11305

Koriyama Y, Sugitani K, Ogai K et al (2014) Heat shock protein 70 induction by valproic acid delays photoreceptor cell death by N-methyl-N-nitrosourea in mice. J Neurochem 130:707–719

Lee SY, Usui S, Zafar AB et al (2011) N-acetylcysteine promotes long-term survival of cones in a model of retinitis pigmentosa. J Cell Physiol 226:1843–1849

Nakajima E, David LL, Bystrom C et al (2006) Calpain-specific proteolysis in primate retina: contribution of calpains in cell death. Invest Ophthalmol Vis Sci 47:5469–5475

Nakamura A, Goto S (1996) Analysis of protein carbonyls with 2,4-dinitrophenyl hydrazine and its antibodies by immunoblot in two-dimensional gel electrophoresis. J Biochem 119:768–774
Oka T, Nakajima T, Tamada Y et al (2007) Contribution of calpains to photoreceptor cell death in N-methyl-N-nitrosourea-treated rats. Exp Neurol 204:39–48
Rezaie T, McKercher SR, Kosaka K et al (2012) Protective effect of carnosic acid, a pro-electrophilic compound, in models of oxidative stress and light-induced retinal degeneration. Invest Ophthalmol Vis Sci 53:7847–7854
Sahara S, Yamashima T (2010) Calpain-mediated Hsp70.1 cleavage in hippocampal CA1 neuronal death. Biochem Biophys Res Commun 393:806–811
Schutt F, Bergmann M, Holz FG et al (2003) Proteins modified by malondialdehyde, 4-hydroxynonenal, or advanced glycation end products in lipofuscin of human retinal pigment epithelium. Invest Ophthalmol Vis Sci 44:3663–3668
Tanito M, Haniu H, Elliott MH et al (2006) Identification of 4-hydroxynonenal-modified retinal proteins induced by photooxidative stress prior to retinal degeneration. Free Radic Biol Med 41:1847–1859
Uchida K (2003) 4-Hydroxy-2-nonenal: a product and mediator of oxidative stress. Prog Lipid Res 42:318–343
Yamashima T (2012) Hsp70.1 and related lysosomal factors for necrotic neuronal death. J Neurochem 120:477–494

# Chapter 37
# Müller Glia Reactivity and Development of Gliosis in Response to Pathological Conditions


**Anna B. Graca, Claire Hippert, and Rachael A. Pearson**

**Abstract** Within the mammalian retina, both Müller glia and astrocytes display reactivity in response to many forms of retinal injury and disease in a process termed gliosis. Reactive gliosis is a complex process that is considered to represent a cellular response to protect the retina from further damage and to promote its repair following pathological insult. It includes morphological, biochemical and physiological changes, which may vary depending on the type and degree of the initial injury. Not only does gliosis have numerous triggers, but also there is a great degree of heterogeneity in the glial response, creating multiple levels of complexity. For these reasons, understanding the process of glial scar formation and how this process differs in different pathological conditions and finding strategies to circumvent these barriers represent major challenges to the advancement of many ocular therapies.

**Keywords** Glial hypertrophy · Gliosis · Intermediate filament proteins · Müller glia · Retinal diseases · Retinal remodelling

## 37.1 Introduction

In the vertebrate retina, Müller cells account for approximately 90% of the glial population and exhibit a complex structural architecture spanning its entire thickness, allowing them to interact with all retinal cell types. Together with astrocytes, these cells perform a variety of physiological roles, including supplying metabolic support by means of glutamine and taurine in the normal retina; maintaining $K^+$, $H^+$

A. B. Graca (✉) · R. A. Pearson (✉)
Department of Genetics, University College London Institute of Ophthalmology, London, UK
e-mail: anna.graca.11@ucl.ac.uk; rachael.pearson@ucl.ac.uk

C. Hippert
Roche, Stem Cell Platform, Chemical Biology Roche Pharma Research and Early Development, Basel, Switzerland



J. D. Ash et al. (eds.), *Retinal Degenerative Diseases*, Advances in Experimental Medicine and Biology 891, https://doi.org/10.1007/978-3-319-75402-4_37

and water balance; protecting against oxidative stress; recycling cone photopigments; releasing neuro- and vasoactive substances; and serving as scaffolds for neurovascular guidance (Bringmann et al. 2006). Following any insult to the retina, these cells are one of the first to respond, by becoming rapidly activated in order to safeguard the retinal structure and the immune privilege of the nervous tissue. Physically, they become more rigid (Lundkvist et al. 2004), most likely due to an increase in the density of intermediate filaments (IFs) (Lu et al. 2013). This increase in stiffness is a major factor that contributes to the viscoelastic properties of the glial cells. It is coupled with a remodelling of the glial network and sprouting of the glial processes throughout the retina (Fisher and Lewis 2003) and is associated with changes in the retinal architecture, such as folding and shrinkage (Lu et al. 2011). In some of the more severe forms of reactive gliosis, Müller cells lose their functionality and form glial scars that are inhibitory to neuronal regeneration and survival, with some glial cells undergoing proliferation. Although the precise role of gliosis is still to be determined, its extent is driven by the size and nature of the neuronal damage (Ridet et al. 1997; Bringmann et al. 2006; Bringmann and Wiedemann 2012). This brief review will discuss typical changes that accompany activation of the Müller cells in a state of injury or disease and their potential impact on the outcome of therapeutic interventions.

## 37.2 Characteristics of Reactive Müller Glia

An increase in IF expression and glial hypertrophy are, perhaps, the most prominent features of reactive gliosis. The upregulation of IFs (typically GFAP, Vimentin and Nestin) seems to be a crucial step for the gliotic response; however, to date, the exact purpose of IF upregulation in the process of gliosis remains a matter of considerable debate. In particular, the role of GFAP in the retina has been the subject of many apparently contradictory findings. Under normal conditions, Müller glial cells maintain high levels of filamentous Vimentin, but GFAP is expressed only minimally. In the uninjured retina, GFAP is normally found in astrocytes and the inner half of the retinal Müller cells and their end feet terminals (Hippert et al. 2015). Following trauma to the retina, such as retinal detachment, GFAP undergoes rapid upregulation in the Müller glia (Lewis and Fisher 2003). Elevated levels of GFAP have also been found after the introduction of retinal ischemia (Kim et al. 1998) or hypoxia (Kaur et al. 2007). In studies of experimental glaucoma, increases in the expression of *Gfap* and *Nestin* were reported as early as 2 h after induction of elevated intraocular pressure (Xue et al. 2006). Although, the *Gfap* mRNA levels rapidly increase in Müller cells following the initial retinal insult, they do revert to normal levels a few days later (Sarthy and Egal 1995); however the newly formed filaments may remain in the glial cells for many months after injury (Seoane et al. 1999). Interestingly, it has been suggested that the magnitude of the GFAP response to mechanical insult is age-dependent, meaning that the older the retina, the more marked the response (Cao et al. 2001). In animal models of inherited retinopathies,

the increase in GFAP levels is highly varied between models and may take weeks or months after the start of photoreceptor death depending on the type of retinal condition (Ekström et al. 1988; Hippert et al. 2015). In chronic pathological conditions, the hypertrophied filamentous glial processes help to fill the 'holes' left by dying photoreceptors and participate in the formation of 'rings', which appear to prolong the survival of remaining cone photoreceptors (Lee et al. 2011). Moreover, these hypertrophied processes help to reseal the neuroretina by building a glial barrier at the outer edges of the neuroretina, which is thought to prevent neurovascularisation and reduce monocyte infiltration (Nakazawa et al. 2007). In mice lacking GFAP and Vimentin, mechanical challenge revealed an exaggerated fragility of Müller cells, accelerated monocyte infiltration and faster degeneration of photoreceptors following retinal trauma (Lundkvist et al. 2004; Nakazawa et al. 2007).

Apart from providing structural support, reactive glia also may bolster neuroprotection by releasing angiogenic and neurotrophic factors such as GDNF, CNTF, VEGF or bFGF, as well as antioxidants that favour the survival of retinal neurons and limit the extent of tissue damage (Eichler et al. 2004; Yafai et al. 2004; Pease et al. 2009; Fu et al. 2015). However, if Müller glial cell reactivity is prolonged, these same cells may become detrimental to neuronal tissue and accelerate neuronal death through interactions with microglial and monocyte cells. For example, studies on retina showed that Müller cells secrete TNF-$\alpha$, which increases the expression of interleukin chemokinases, promoting microglia infiltration into the neuroretina (Lebrun-Julien et al. 2009; Eastlake et al. 2015). Apart from releasing chemokinases, the reactive glia are also reported to provide an adhesive cellular scaffold that guides the movement of the resident microglia across various retinal layers in the injured retina (Wang et al. 2011).

## 37.3 Heterogeneity of the Glial Responses

It is well documented that Muller glia do not represent a homogenous group of cells and that their responses to pathological responses may differ among individual cells and between Müller cells in different species. A number of studies have reported significant differences in the distribution of proteins, including IFs even in the non-reactive Müller glial cells of different species. For example, in mouse, squirrel and rabbit, Vimentin is found in high levels across the entire Müller cell, whereas in feline and human retina, Vimentin is only expressed in their outer terminals (Lewis and Fisher 2003). In most mammalian species, retinal detachment results in Müller cell proliferation, hypertrophy, and an increase in the expression of GFAP (Bringmann et al. 2006). However, these alterations are not observed after detachment of the cone-dominant ground squirrel retina (Linberg et al. 2002; Merriman et al. 2016). In our study, we observed striking differences in the presentation and magnitude of the Müller glia response between models of inherited retinal degenerations (Hippert et al. 2015). Interestingly, disease severity was not a predictor of the strength of the glial response. Together, these studies indicate that the

pathological stimulus plays a key role in dictating the retinal and glial responses. Interestingly, Müller cells have been shown to initiate IF upregulation on an individual cell-by-cell basis rather than across all the cells in a uniform manner following retinal injury (Luna et al. 2010). This is in keeping with our own observations of murine Müller glia in culture, where IF expression can vary markedly between individual glial cells in the same culture (A.B.G. and C.H., unpublished observations). Such observations raise some fundamental questions about the heterogeneity of signalling pathways that activate glia cells and the diversity of glia participating in the cellular response and the signalling mechanisms that are activated in response to different types of injury.

## 37.4 Reactive Gliosis and Its Impact on Ocular Therapies

Following retinal detachment, the resulting glial reactivity and subsequent glial scar formation at the outer edge of the neuroretina were reported to impede tissue regeneration, including the regrowth of photoreceptor outer segments (OS) (Lewis and Fisher 2003). Strikingly, it has been suggested that a single Müller cell process lying between the reattached neuroretina and the RPE is sufficient to completely inhibit OS regeneration in that region (Anderson et al. 1986). The increase in Müller glial rigidity may also be one of the reasons for a failed axonal regeneration as growing neurites seem to favour softer substrates (Bringmann and Wiedemann 2012). In more severe forms of reactive gliosis, glial processes may also start to extend into the vitreous side where they start to form fibrotic scar tissue characteristic of proliferative vitreoretinopathy (Lewis and Fisher 2006). This scar can become contractile and lead to folds and/or deformations in the retina causing visual distortions and, in the worst cases, can cause retinal detachments (Jünemann et al. 2015). As such, glial membranes or scars are a significant issue in the treatment of visual disorders in humans, occurring in approximately 15% of retinal detachments (Fisher et al. 2005). Finding ways to reduce this increase in Müller glial rigidity could prove a valuable strategy in reducing scar-induced retinal detachments. The formation of glial scars has also been implicated as one of the reasons for a failure in visual recovery after subretinal implantation of microphotodiode arrays and foetal sheet tissue grafts. The presence of a glial scar impedes the contact between the implants/grafts and the host neuroretina by creating a physical barrier between the two (Radtke et al. 1999; Pardue et al. 2001; Peng et al. 2008). Improvements in visual function following the transplantation of healthy photoreceptors into models of retinal degeneration were also reported to depend on the extent of the reactive gliosis (Hippert et al. 2016). Recently, we (Pearson et al. 2016) and others (Santos-Ferreira et al. 2016) have reported that, alongside donor cell integration, a previously undescribed mechanism of cytoplasmic material transfer between donor and host cells plays a major role in rescue after photoreceptor transplantation into the non- or slowly degenerating retina. It will be of significant interest to determine the relative influences of reactive gliosis on donor cell integration and/or cytoplasmic material transfer.

There is no doubt that gliosis is a complicated process worthy of future research and determining which particular aspects of this process are key to disease progression, as well as therapeutic outcome, will be major future objectives.

## References

Anderson DH, Guérin CJ, Erickson PA et al (1986) Morphological recovery in the reattached retina. Invest Ophthalmol Vis Sci 27:168–183

Bringmann A, Wiedemann P (2012) Müller glial cells in retinal disease. Ophthalmologica 227:1–19

Bringmann A, Pannicke T, Grosche J et al (2006) Müller cells in the healthy and diseased retina. Prog Retin Eye Res 25:397–424

Cao W, Li F, Steinberg RH et al (2001) Development of normal and injury-induced gene expression of aFGF, bFGF, CNTF, BDNF, GFAP and IGF-I in the rat retina. Exp Eye Res 72:591–604

Eastlake K, Banerjee PJ, Angbohang A et al (2016) Müller glia as an important source of cytokines and inflammatory factors present in the gliotic retina during proliferative vitreoretinopathy. Glia 64(4):495–506

Eichler W, Yafai Y, Wiedemann P et al (2004) Angiogenesis-related factors derived from retinal glial (Müller) cells in hypoxia. Neuroreport 15:1633–1637

Ekström P, Sanyal S, Narfström K et al (1988) Accumulation of glial fibrillary acidic protein in Muller radial glia during retinal degeneration. Invest Ophthalmol Vis Sci 29:1363–1371

Fisher SK, Lewis GP (2003) Müller cell and neuronal remodeling in retinal detachment and reattachment and their potential consequences for visual recovery: a review and reconsideration of recent data. Vis Res 43:887–897

Fisher SK, Lewis GP, Linberg KA et al (2005) Cellular effects of detachment and reattachment on the neural retina and the retinal pigment epithelium. Prog Retin Eye Res 24:1991–2012

Fu S, Dong S, Zhu M et al (2015) Müller glia are a major cellular source of survival signals for retinal neurons in diabetes. Diabetes 64:3554–3563

Hippert C, Graca AB, Barber AC et al (2015) Müller glia activation in response to inherited retinal degeneration is highly varied and disease-specific. PLoS One 10:e0120415

Hippert C, Graca AB, Pearson RA (2016) Gliosis can impede integration following photoreceptor transplantation into the diseased retina. Adv Exp Med Biol 854:579–585

Jünemann AGM, Rejdak R, Huchzermeyer C et al (2015) Elevated vitreous body glial fibrillary acidic protein in retinal diseases. Graefes Arch Clin Exp Ophthalmol 253:2181–2186

Kaur C, Sivakumar V, Yong Z et al (2007) Blood-retinal barrier disruption and ultrastructural changes in the hypoxic retina in adult rats: the beneficial effect of melatonin administration. J Pathol 212:429–439

Kim IB, Kim KY, Joo CK et al (1998) Reaction of Müller cells after increased intraocular pressure in the rat retina. Exp Brain Res 121:419–424

Lebrun-Julien F, Duplan L, Pernet V et al (2009) Excitotoxic death of retinal neurons in vivo occurs via a non-cell-autonomous mechanism. J Neurosci 29:5536–5545

Lee E-J, Ji Y, Zhu CL et al (2011) Role of Müller cells in cone mosaic rearrangement in a rat model of retinitis pigmentosa. Glia 59:1107–1117

Lewis GP, Fisher SK (2003) Up-regulation of glial fibrillary acidic protein in response to retinal injury: its potential role in glial remodeling and a comparison to vimentin expression. Int Rev Cytol 230:263–290

Lewis GP, Fisher SK (2006) Retinal plasticity and interactive cellular remodeling in retinal detachment and reattachment. Plast Vis Syst 55–78

Linberg KA, Sakai T, Lewis GP et al (2002) Experimental retinal detachment in the cone-dominant ground squirrel retina: morphology and basic immunocytochemistry. Vis Neurosci 19:603–619

Lu Y-B, Iandiev I, Hollborn M et al (2011) Reactive glial cells: increased stiffness correlates with increased intermediate filament expression. FASEB J 25:624–631
Lu Y-B, Pannicke T, Wei E-Q et al (2013) Biomechanical properties of retinal glial cells: comparative and developmental data. Exp Eye Res 113:60–65
Luna G, Lewis GP, Banna CD et al (2010) Expression profiles of nestin and synemin in reactive astrocytes and Müller cells following retinal injury: a comparison with glial fibrillar acidic protein and vimentin. Mol Vis 16:2511–2523
Lundkvist A, Reichenbach A, Betsholtz C et al (2004) Under stress, the absence of intermediate filaments from Müller cells in the retina has structural and functional consequences. J Cell Sci 117:3481–3488
Merriman DK, Sajdak BS, Li W et al (2016) Seasonal and post-trauma remodeling in cone-dominant ground squirrel retina. Exp Eye Res 150:90–105
Nakazawa T, Takeda M, Lewis GP et al (2007) Attenuated glial reactions and photoreceptor degeneration after retinal detachment in mice deficient in glial fibrillary acidic protein and vimentin. Invest Ophthalmol Vis Sci 48:2760–2768
Pardue MT, Stubbs EB, Perlman JI et al (2001) Immunohistochemical studies of the retina following long-term implantation with subretinal microphotodiode arrays. Exp Eye Res 73:333–343
Pearson RA, Gonzalez-Cordero A, West EL et al (2016) Donor and host photoreceptors engage in material transfer following transplantation of post-mitotic photoreceptor precursors. Nat Commun 7:13029
Pease ME, Zack DJ, Berlinicke C et al (2009) Effect of CNTF on retinal ganglion cell survival in experimental glaucoma. Invest Ophthalmol Vis Sci 50:2194–2200
Peng YW, Zallocchi M, Meehan DT et al (2008) Progressive morphological and functional defects in retinas from alpha1 integrin-null mice. Invest Ophthalmol Vis Sci 49:4647–4654
Radtke ND, Aramant RB, Seiler M et al (1999) Preliminary report: indications of improved visual function after retinal sheet transplantation in retinitis pigmentosa patients. Am J Ophthalmol 128:384–387
Ridet JL, Malhotra SK, Privat A et al (1997) Reactive astrocytes: cellular and molecular cues to biological function. Trends Neurosci 20:570–577
Santos-Ferreira T, Llonch S, Borsch O et al (2016) Retinal transplantation of photoreceptors results in donor-host cytoplasmic exchange. Nat Commun 7:13028
Sarthy V, Egal H (1995) Transient induction of the glial intermediate filament protein gene in Müller cells in the mouse retina. DNA Cell Biol 14:313–320
Seoane A, Espejo M, Pallàs M et al (1999) Degeneration and gliosis in rat retina and central nervous system following 3,3′-iminodipropionitrile exposure. Brain Res 833:258–271
Wang M, Ma W, Zhao L et al (2011) Adaptive Müller cell responses to microglial activation mediate neuroprotection and coordinate inflammation in the retina. J Neuroinflammation 8:173
Xue LP, Lu J, Cao Q et al (2006) Müller glial cells express nestin coupled with glial fibrillary acidic protein in experimentally induced glaucoma in the rat retina. Neuroscience 139:723–732
Yafai Y, Iandiev I, Wiedemann P et al (2004) Retinal endothelial angiogenic activity: effects of hypoxia and glial (Müller) cells. Microcirculation 11:577–586

# Chapter 38
# Underdeveloped RPE Apical Domain Underlies Lesion Formation in Canine Bestrophinopathies


**Karina E. Guziewicz, Emily McTish, Valerie L. Dufour, Kathryn Zorych, Anuradha Dhingra, Kathleen Boesze-Battaglia, and Gustavo D. Aguirre**

**Abstract** Canine bestrophinopathy (cBest) is an important translational model for *BEST1*-associated maculopathies in man that recapitulates the broad spectrum of clinical and molecular disease aspects observed in patients. Both human and canine bestrophinopathies are characterized by focal to multifocal separations of the retina from the RPE. The lesions can be macular or extramacular, and the specific pathomechanism leading to formation of these lesions remains unclear. We used the naturally occurring canine *BEST1* model to examine factors that underlie formation of vitelliform lesions and addressed the susceptibility of the macula to its primary detachment in *BEST1*-linked maculopathies.

**Keywords** *BEST1* · Bestrophinopathies · Canine model · Macula · Vitelliform lesion formation · RPE-photoreceptor interface · RPE microvilli · Cone photoreceptors · RPE apical domain · Insoluble interphotoreceptor matrix

K. E. Guziewicz (✉)
Department of Clinical Studies-Philadelphia, School of Veterinary Medicine, University of Pennsylvania, Philadelphia, PA, USA

University of Pennsylvania, Ryan Veterinary Hospital, Philadelphia, PA, USA
e-mail: karinag@vet.upenn.edu

E. McTish · V. L. Dufour · K. Zorych · G. D. Aguirre
Department of Clinical Studies-Philadelphia, School of Veterinary Medicine, University of Pennsylvania, Philadelphia, PA, USA

A. Dhingra · K. Boesze-Battaglia
Department of Biochemistry, School of Dental Medicine, University of Pennsylvania, Philadelphia, PA, USA



J. D. Ash et al. (eds.), *Retinal Degenerative Diseases*, Advances in Experimental Medicine and Biology 891, https://doi.org/10.1007/978-3-319-75402-4_39

## 38.1 Introduction

Bestrophinopathies are caused by mutations in the *BEST1* gene expressed in the retinal pigment epithelium (RPE) (Petrukhin et al. 1998; Marmorstein et al. 2000). Among this group of disorders, Best vitelliform macular dystrophy (BVMD) and autosomal recessive bestrophinopathy (ARB) are the most common and best studied juvenile macular dystrophies, characterized by an excessive accumulation of lipofuscin within RPE, reduction in the electrooculogram (EOG) light peak, and formation of bilateral macular to multifocal subretinal lesions (Boon et al. 2009). Despite extensive research, the pathological mechanism of *BEST1* still remains elusive, and factors leading to formation of macular lesions are largely unexplored. We used the spontaneous dog Best disease model, canine bestrophinopathy (cBest) (a.k.a. canine multifocal retinopathy, *cmr*) (Guziewicz et al. 2007; Zangerl et al. 2010), to study the architecture of the RPE-photoreceptor interface and define factors that promote development of vitelliform lesions.

## 38.2 Materials and Methods

### *38.2.1 Study Animals and Ethics Statement*

cBest-affected and control dogs were genotyped and ophthalmoscopically examined, and ocular tissue was collected and processed as previously described (Guziewicz et al. 2007; Beltran et al. 2014). The studies were carried out in strict accordance with the recommendations in the Guide for the Care and Use of Laboratory Animals of the NIH and in compliance with the ARVO Statement for the Use of Animals in Ophthalmic and Vision Research. The protocols were approved by the Institutional Animal Care and Use Committee of the University of Pennsylvania (IACUC Protocol #s 801870, 803422). Adult dogs (age 1–3 years) after disease onset and young (aged 6wks) before development of clinical phenotype were selected for histological and immunohistochemical (IHC) analyses.

### *38.2.2 Histological and IHC Assessments*

Retinal structure was examined in 10-μm-thick cryosections by H&E staining and IHC using a set of RPE- and photoreceptor-specific markers: 1/400 mouse anti-Best1 (ab2182), 1/400 mouse anti-EZR (ab4069), 1/500 rabbit anti-MCT1 (courtesy of N. Philp, Thomas Jefferson University), 1/500 rabbit anti-E2F1 (sc-193) or 1/10,000 rabbit anti-hCAR (courtesy of C. Craft, USC), and PNA (L-32458). Slides were evaluated with transmitted light microscopy, epifluorescence, and confocal

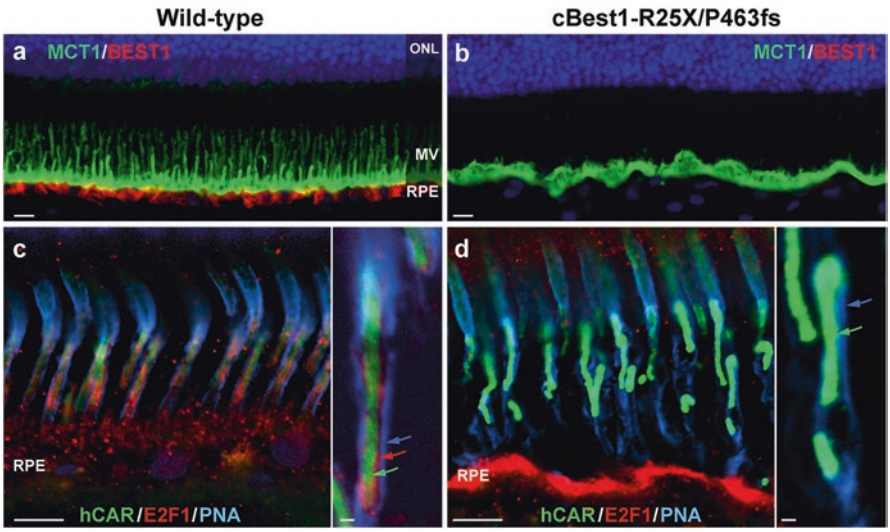


**Fig. 38.1** Abnormal RPE-photoreceptor interface in canine bestrophinopathies (**a**, **b**) Representative images of anti-MCT1 (monocarboxylate transporter 1) and anti-Best1 double-labeling in 2-yr-old cBest1-R25X/P463fs-affected retina (**b**) vs age-matched wild-type control (**a**). Note the absence of Best1 basolateral labeling and lack of MCT1-positive apical RPE microvillous (MV) extensions in the mutant retina (**b**). (**c**, **d**) Direct comparison of multilabeled (hCAR human cone arrestin, E2F1 transcription factor 1, PNA peanut agglutinin lectin) confocal photomicrographs showing the absence of E2F1-positive cone-associated RPE microvilli (**d**) when compared to the wild-type control (**c**, inset, red arrow) and compromised insoluble interphotoreceptor matrix domain (insets, blue arrow) in the mutant retina (**d**). Cone outer segments (insets, green arrows) appeared disordered (**d**) in comparison to the control tissue (**c**). Scale bars: 10 μm (**a**–**d**) and 1 μm (insets)

laser scanning microscopy. All ex vivo analyses were carried out in comparison to the age-matched control eyes.

## 38.3 Results

### *38.3.1 Molecular Pathology of the RPE-Photoreceptor Interface in cBest*

IHC evaluation of cBest retinae (age 1–3 years) revealed an abnormal RPE-photoreceptor interface with an apparent loss of cone-ensheathing RPE apical processes and compromised cone-associated insoluble interphotoreceptor matrix (IPM) (Fig. 38.1). Specific immunostaining against MCT1 (UniProt#P53985) was present in both the normal control and mutant retinae, but in the latter the labeling was limited to the RPE apical surface, but not along apical extensions (Fig. 38.1b). Further

analysis with an alternative marker, E2F1 (UniProt#Q01094), confirmed these results in cBest (Fig. 38.1d) and exposed a bilayered extracellular compartmentalization of the cone-specific escheatment responsible for a normal apposition of RPE-cone OS (Fig. 38.1c, inset). This well-defined extracellular structure was lost in the affected retinae, revealing a dearth of the intrinsic RPE-associated apical microvillus layer accompanied by a fragmented external insoluble cone-specific matrix domain (Fig. 38.1d, inset). As a result cone OS stripped of their protective sheaths appeared undermined with no direct contact with the underlying RPE (Fig. 38.1d).

### *38.3.2 Underdeveloped RPE Apical Domain Promotes Retinal Detachment in cBest*

Comparable studies on the RPE-photoreceptor interface were performed in 6-week-old retinae, at the time when the canine retina completes its development (Acland and Aguirre 1987) (Fig. 38.2). Immunolabeling with MCT1 and Ezrin (UniProt#P15311) exposed underdeveloped RPE apical domain in the young cBest retina, with only a few longer RPE microvilli and a highly disorganized distribution of Ezrin (Fig. 38.2a–d). In comparison to the age-matched controls, the 6-wk-old cBest retina showed diminished expression of Ezrin at the RPE apical surface, accompanied by an increase of Ezrin-positive signals associated with microvilli of Müller cells (Fig. 38.2d). Although the young cBest retinae appeared histologically intact, cone photoreceptor outer segments (hCAR) appeared compromised, further suggesting perturbations in the homeostatic mechanism of subretinal space in bestrophinopathies.

## 38.4 Discussion

We have previously shown that canine bestrophinopathy (cBest or *cmr*) serves as an important translational model for *BEST1*-associated maculopathies in man, as it recapitulates all fundamental aspects of human disease, including the salient predilection of subretinal lesions to the canine macular region (Guziewicz et al. 2007; Beltran et al. 2014; Singh et al. 2015). In this study, cBest model proved instrumental for defining the early structural alterations at the RPE-photoreceptor interface, which may explain the susceptibility of the macula to its primary detachment in *BEST1*-associated maculopathies.

Apical microvilli, an integral structure of RPE cells, are essential for mediating basic RPE functions, including daily phagocytosis of OS and transport of nutrients into and removal of byproducts from the photoreceptor cells (Bonilha et al. 2004, 2006). It is important to note that these RPE projections greatly increase the apical

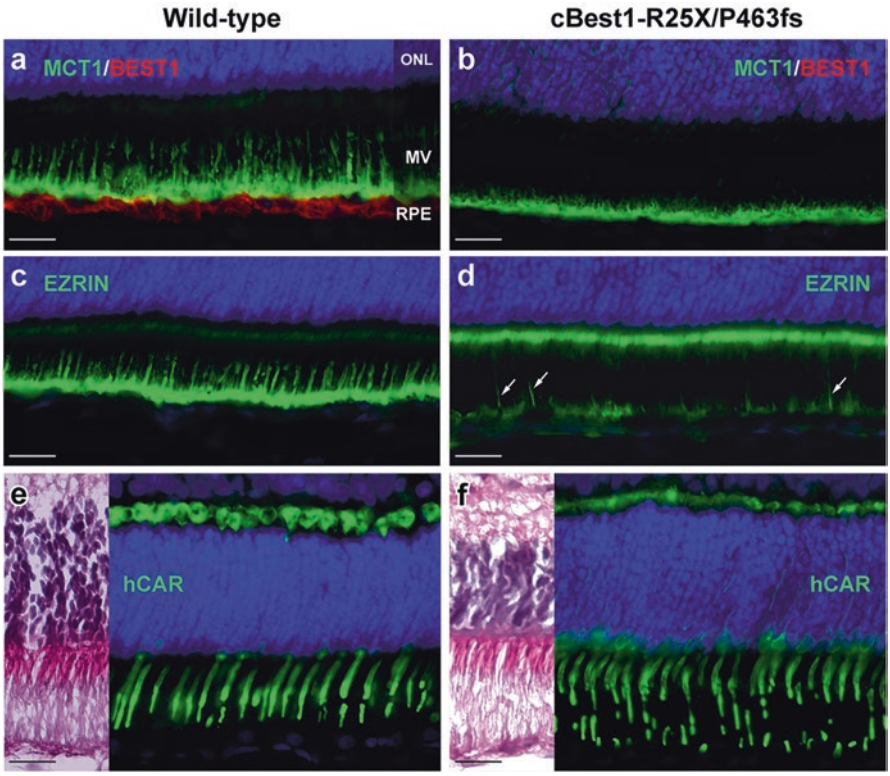


**Fig. 38.2** Underdeveloped RPE apical domain promotes formation of subretinal lesions in bestrophinopathies**.** Immunohistochemical evaluation of 6-week-old wild-type (**a**, **c**, **e**) and cBest1-R25X/P463fs-affected (**b**, **d**, **f**) retinae revealed underdevelopment of RPE apical domain of cBest-mutant retina, demonstrated by anti-MCT1 (**a**, **b**), and anti-Ezrin (**c**, **d**) labeling. Note the absence of Best1 basolateral labeling (**b**), reduced Ezrin immunostaining at the RPE apical surface with only a few Ezrin-positive RPE processes (**d**, arrows), and a increase of Ezrin labeling associated with microvilli of Müller cells (**d**). Cone outer segments (green) appear compromised (**f**, hCAR) when compared to the wild-type retina (**e**). Scale bar: 20 μm applies to all panels

surface area and, consequently, the transport of signaling molecules it contains, thereby enhancing the epithelial functional capacity (Bonilha et al. 2004). Thus, it is very likely that most of the major hallmarks of bestrophinopathies, e.g., disrupted ion transport, impaired phagocytosis, abnormal accumulation of autofluorescent debris in the subretinal space, and finally RPE-neuroretinal detachment and formation of serous lesions (Boon et al. 2009; Singh et al. 2015), arise directly from the dearth of properly formed microvilli and impaired interaction/adhesiveness with OS. The report by Bonilha et al. provided strong evidence that Ezrin is a major determinant in the maturation of surface differentiations of RPE, promoting morphogenesis of apical microvilli (Bonilha et al. 1999). Our findings in the canine *BEST1* model support these results and strongly suggest that underdevelopment of

cone-associated apical projections constitutes a key factor that underlies formation of macular lesions in bestrophinopathies. The fact that these prominent structural alterations associated with cone ensheathment are observed in cBest dogs as early as 6 weeks of age would also explain the early onset of ARB and BVMD along with the predilection of the cone-packed macular region to its primary detachment in affected dogs and patients.

As evinced by numerous studies, IPM is critical for maintaining the homeostatic milieu of the subretinal space, serving a range of biochemical and physical functions; these include the regulation of oxygen, nutrients, and retinoid transport, preservation of retinal adhesion by providing electrostatic support for photoreceptors, and participating in cytoskeletal organization in the surrounding cells (Ishikawa et al. 2015). Thus, together with the impaired microvillar ensheathment, the compromised IPM accounts for the two major pathological culprits responsible for weakening of the RPE-neuroretina interactions in bestrophinopathies. We posit that these salient interface defects may also be responsible for the difference in photoreceptor equivalent thickness found in BVMD patients (Kay et al. 2012) and the abnormal EOG and Arden ratio in bestrophinopathy patients. As such, this study provides new critical insights into the molecular basis of bestrophinopathies that would assist in the development of outcome measures for assessing therapeutic strategies in ARB and BVMD patients.

**Acknowledgments** This study was supported by FFB-TRAP and FFB-Facility grants, MVRF, NEI/NIH EY06855, EY10420, and Hope for Vision.

## References

Acland GM, Aguirre GD (1987) Retinal degenerations in the dog: IV. Early retinal degeneration (erd) in Norwegian elkhounds. Exp Eye Res 44:491–521

Beltran WA, Cideciyan AV, Guziewicz KE et al (2014) Canine retina has a primate fovea-like bouquet of cone photoreceptors which is affected by inherited macular degenerations. PLoS One 3:e90390

Bonilha VL, Finnemann SC, Rodriguez-Boulan E (1999) Ezrin promotes morphogenesis of apical microvilli and basal infoldings in retinal pigment epithelium. J Cell Biol 147:1533–1548

Bonilha VL, Bhattacharya SK, West KA et al (2004) Support for a proposed retinoid-processing protein complex in apical retinal pigment epithelium. Exp Eye Res 79:419–422

Bonilha VL, Rayborn ME, Bhattacharya SK et al (2006) The retinal pigment epithelium apical microvilli and retinal function. Adv Exp Med Biol 572:519–524

Boon CJ, Klevering BJ, Leroy BP et al (2009) The spectrum of ocular phenotypes caused by mutations in the BEST1 gene. Prog Retin Eye Res 28:187–205

Guziewicz KE, Zangerl B, Lindauer SJ et al (2007) Bestrophin gene mutations cause canine multifocal retinopathy: a novel animal model for best disease. Invest Ophthalmol Vis Sci 48:1959–1967

Ishikawa M, Sawada Y, Yoshitomi T (2015) Structure and function of the interphotoreceptor matrix surrounding retinal photoreceptor cells. Exp Eye Res 133:3–18

Kay CN, Abramoff MD, Mullins RF et al (2012) Three-dimensional distribution of the vitelliform lesion, photoreceptors and retinal pigment epithelium in the macula of patients with best vitelliform macular dystrophy. Arch Ophthalmol 130:357–364

Marmorstein AD, Marmorstein LY, Rayborn M et al (2000) Bestrophin the product of the best vitelliform macular dystrophy gene (VMD2) localizes to the basolateral plasma membrane of the retinal pigment epithelium. Proc Natl Acad Sci U S A 97:12758–12763

Petrukhin K, Koisti MJ, Bakall B et al (1998) Identification of the gene responsible for best macular dystrophy. Nat Genet 19:241–247

Singh R, Kuai D, Guziewicz KE et al (2015) Pharmacological modulation of photoreceptor outer segment degradation in a human iPS cell model of inherited macular degeneration. Mol Ther 23:1700–1711

Zangerl B, Wickström K, Slavik J et al (2010) Assessment of canine BEST1 variations identifies new mutations and establishes an independent bestrophinopathy model (cmr3). Mol Vis 16:2791–2804

# Chapter 39
# Binary Function of ARL3-GTP Revealed by Gene Knockouts


**Christin Hanke-Gogokhia, Jeanne M. Frederick, Houbin Zhang, and Wolfgang Baehr**

**Abstract** UNC119 and PDEδ are lipid-binding proteins and are thought to form diffusible complexes with transducin-α and prenylated OS proteins, respectively, to mediate their trafficking to photoreceptor outer segments. Here, we investigate mechanisms of trafficking which are controlled by Arf-like protein 3 (Arl3), a small GTPase. The activity of ARL3 is regulated by a GEF (ARL13b) and a GAP (RP2). In a mouse germline knockout of RP2, ARL3-GTP is abundant as its intrinsic GTPase activity is extremely low. High levels of ARL3-GTP impair binding and trafficking of cargo to the outer segment. Germline knockout of

C. Hanke-Gogokhia (✉)
Department of Ophthalmology and Visual Sciences, John A. Moran Eye Center, University of Utah School of Medicine, Salt Lake City, UT, USA

Department of Biochemistry and Biology, University of Potsdam, Potsdam, Germany
e-mail: Christin.Hanke@hsc.utah.edu

J. M. Frederick
Department of Ophthalmology and Visual Sciences, John A. Moran Eye Center, University of Utah School of Medicine, Salt Lake City, UT, USA

H. Zhang
The Sichuan Provincial Key Laboratory for Human Disease Gene Study, The Institute of Laboratory Medicine, Hospital of University of Electronic Science and Technology of China and Sichuan Provincial People's Hospital, Chengdu, Sichuan, China

School of Medicine, University of Electronic Science and Technology of China, Chengdu, Sichuan, China

W. Baehr (✉)
Department of Ophthalmology and Visual Sciences, John A. Moran Eye Center, University of Utah School of Medicine, Salt Lake City, UT, USA

Department of Neurobiology and Anatomy, University of Utah School of Medicine, Salt Lake City, UT, USA

Department of Biology, University of Utah, Salt Lake City, UT, USA
e-mail: wbaehr@hsc.utah.edu



J. D. Ash et al. (eds.), *Retinal Degenerative Diseases*, Advances in Experimental Medicine and Biology 891, https://doi.org/10.1007/978-3-319-75402-4_39

ARL3 is embryonically lethal generating a syndromic ciliopathy-like phenotype. Retina- and rod-specific knockout of ARL3 allow to determine the precise mechanisms leading to photoreceptor degeneration. The knockouts reveal binary functions of ARL3-GTP as a key molecule in late-stage photoreceptor ciliogenesis and cargo displacement factor.

**Keywords** ARL3 · ARL13b · PDEδ · UNC119 · RP2 · Photoreceptor · Germline knockout · Retina disease

## 39.1 Introduction

Photoreceptor outer segments (OS) are modified primary cilia specializing in phototransduction (Wright et al. 2010; Gilliam et al. 2012). Replacement of entire outer segments every 10 days in mouse necessitates efficient trafficking of membrane-associated proteins (Young, 1976). We are interested to learn how peripherally membrane-associated proteins traffic to the outer segment. These proteins are lipidated (prenylated or acylated) for membrane attachment but can be solubilized by interaction with lipid binding proteins ("solubilization factors"), forming diffusible complexes (for detailed references, see (Hanke-Gogokhia et al. 2016)). Well-characterized lipid-binding proteins are PDEδ (alias PrBP/δ or PDE6D) (Zhang et al. 2012) and UNC119 paralogs (UNC119a and UNC119b) (Zhang et al. 2011; Constantine et al. 2012). A main player in regulating trafficking of lipidated proteins is Arf-like protein 3 (ARL3), a small ubiquitously expressed GTPase (Hanke-Gogokhia et al. 2016). Its activity is regulated by a GEF (ARL13b) (turning on) and a GAP (RP2) (turning off).

## 39.2 PDEδ and UNC119

PDEδ (Hanzal-Bayer et al. 2002) and UNC119 (Zhang et al. 2011) share an immunoglobulin-like beta-sandwich fold consisting of a hydrophobic cavity that can accommodate lipid side chains. PDEδ accepts C-terminal prenyl side chains, whereas UNC119 binds N-terminal acyl chains of transducin-α. The correct functioning of the proteins is important for photoreceptor survival. *PDE6D* null mutations are associated with Joubert syndrome in humans, a severe syndromic ciliopathy affecting many tissues (Thomas et al. 2014; Duldulao et al. 2009); by contrast, *Pde6d*$^{-/-}$ mice develop recessive cone-rod dystrophy (Zhang et al. 2007). A heterozygous stop codon (K57ter) in human *UNC119* gene causes dominant cone-rod dystrophy (Kobayashi et al. 2000).

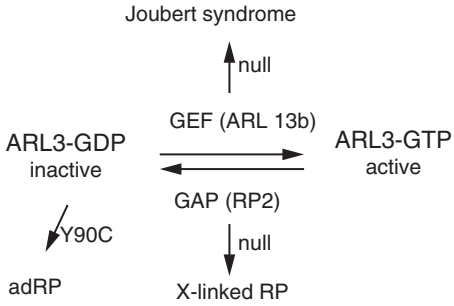


**Fig. 39.1** Posttranslational prenylation and acylation. Farnesyl and geranylgeranyl chains are attached to a C-terminal Cys of a CAAX box motif. Acyl chains (lauroyl and myristoyl) are attached to the N-terminal Gly

## 39.3 Lipidated Cargo

Peripheral membrane proteins participating in phototransduction are rhodopsin kinase (GRK1, G protein receptor kinase 1), GRK7 (not present in mouse) (Palczewski and Benovic 1991; Maeda et al. 2003), the heterotrimeric G protein transducin (Tαβγ) (Arshavsky et al. 2002), and heterotetrameric cGMP phosphodiesterase (PDE6αβγγ) (Baehr et al. 1979; Fung et al. 1990). These proteins or one of their subunits carries a CAAX box motif at the C-terminus signaling prenylation (Manolaridis et al. 2013). Prenyl side chains consist either of C15 (farnesyl) or C20 moieties (geranylgeranyl) (Fig. 39.1). GRK1, Tγ, and PDE6α are farnesylated, while GRK7 and PDE6β are geranylgeranylated. PDEδ accommodates both C15 and C20 side chains. During biogenesis, the proteins are prenylated and dock to the ER where CAAX box processing occurs. Tα is heterogeneously acylated at the N-terminus (C12 and C14) and combines with Tβγ to dock to the ER as a heterotrimer. Transducin is the only acylated protein in rods and cones that depends on UNC119 and ARL3 for trafficking, especially after light-induced translocation (Zhang et al. 2011).

## 39.4 ARL3, RP2, and ARL13b

Arf-like protein 3 (ARL3) is a small GTPase existing in an inactive GDP-bound and active GTP-bound conformation (Fig. 39.2). GDP/GTP exchange is catalyzed by a guanine nucleotide exchange factor (GEF), recently identified as ARL13b (Gotthardt et al. 2015). The lifetime of ARL3-GTP is controlled by its GTPase-activating protein (GAP), retinitis pigmentosa protein 2 (RP2) (Veltel et al. 2008; Kuhnel et al. 2006). The intrinsic GTPase activity of ARL3 is slow, but accelerates over 6000-fold with catalytic amounts of RP2 and 90,000-fold at saturating conditions of RP2 (Veltel et al. 2008). Mutations in the human *RP2* gene are associated with X-linked retinitis pigmentosa (RP) (Jayasundera et al. 2010), and null mutations in the human

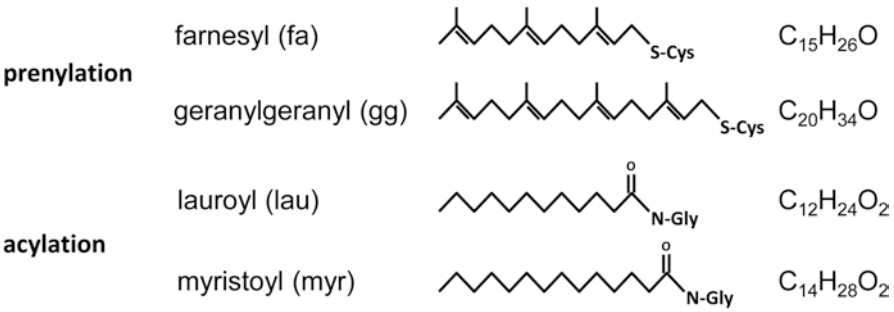


**Fig. 39.2** Regulation of ARL3 activity by its GEF and GAP. Human diseases associated with mutations in ARL13b, RP2, and ARL3 are shown

*ARL13b* gene cause Joubert syndrome (Cantagrel et al. 2008). A Y90C mutation in *ARL3* was associated with autosomal dominant retinitis pigmentosa (adRP) (Strom et al. 2016). In mice, germline deletions of *Arl3* (Schrick et al. 2006) and *Arl13b* (Caspary et al. 2007) are embryonically lethal due to ciliary dysfunction affecting several organs, including the eyes.

## 39.5 WT Transport of Lipidated Proteins in Photoreceptors

ARL3-GTP, its GAP, and GEF play a key role in trafficking of lipidated proteins in photoreceptors (Hanke-Gogokhia et al. 2016; Zhang et al. 2015; Gotthardt et al. 2015). To briefly summarize previous results, PDEδ solubilizes prenylated OS proteins and UNC119 acylated Tα bound to the ER (Fig. 39.3). The soluble complexes form a transient ternary complex with ARL3-GTP and dock to the destination membrane, presumably using RPGR as a docking station. ARL3-GTP forces PDEδ to assume a "closed pocket" conformation evicting prenylated cargo. By contrast, interaction of ARL3-GTP with UNC119 widens the hydrophobic pocket releasing acylated cargo. By forcing cargo release, ARL3-GTP functions as a GDI-displacement factor (GDF), or for simplicity in this context as a cargo displacement factor (CDF). Membrane association of ARL3-GTP/PDEδ/cargo (ternary complex) is essential for RP2 to execute its GAP activity; RP2 is acylated (G2-myritoyl, C3-palmitoyl) and targets to the inner plasma membrane in photoreceptors. The GEF activity of ARL13b will catalyze GDP/GTP exchange on ARL3-GDP to form ARL3-GTP, and the trafficking cycle starts all over again, pumping lipidated proteins into the outer segment. ARL13b locates to the OS and transition zone and is membrane-associated by palmitoylation.

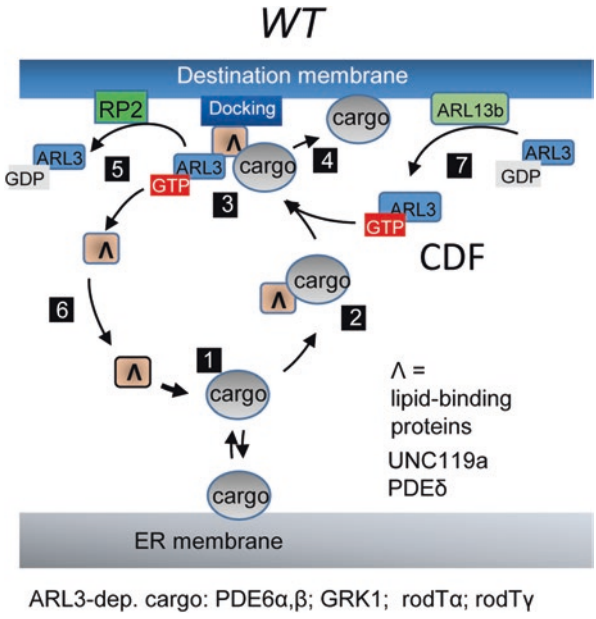


**Fig. 39.3** Model of **Λ**/ARL3/RP2 (**Λ** = lipid binding protein) dependent trafficking in WT photoreceptors. After biosynthesis and lipidation, cargo docks to the ER membrane (1). Cargo and **Λ** form a soluble complex (2), and binding of ARL3-GTP (3) evicts cargo to bind to the destination membranes (4). ARL3-GTP acts as cargo displacement factor (CDF) for cargo delivery. GTP hydrolysis at ARL3-GTP by RP2 (5) releases **Λ** to begin another round of transport (6). GDP/GTP exchange catalyzed by ARL13b regenerates ARL3-GTP (**7**)

## 39.6 The Consequence of RP2 Deletion in Mouse

The *Rp2h*$^{-/-}$ mice exhibited a slowly progressing rod-cone dystrophy, and surprisingly, photoreceptor outer segments were maintained up to 24 months of age. Prenylated rhodopsin kinase GRK1 and cGMP phosphodiesterase PDE6 subunits were unable to traffic effectively to the *Rp2h*$^{-/-}$ outer segments and mislocalized to the photoreceptor inner segment and outer nuclear layer, whereas rhodopsin and other integral membrane proteins are not affected (Zhang et al. 2015) (Fig. 39.4). Mechanistically, absence of RP2 GAP activity increases ARL3-GTP levels, forcing PDEδ to assume a predominantly "closed" conformation that impedes binding of lipids and impairs trafficking of PDE6 and GRK1 to their destination. We propose that hyperactivity of ARL3-GTP in *Rp2h* knockout mice and human patients with *RP2* null alleles leads to X-linked retinitis pigmentosa. The slow degeneration in *Rp2h*$^{-/-}$ mice may be the result of nonspecific GAP activities in mouse, reducing the levels of ARL3-GTP. Accumulated lipidated cargo in the ER, where prenylated proteins are posttranslationally modified, most likely results in UPR (unfolded protein response), ERAD (ER-associated degradation), and photoreceptor degeneration.

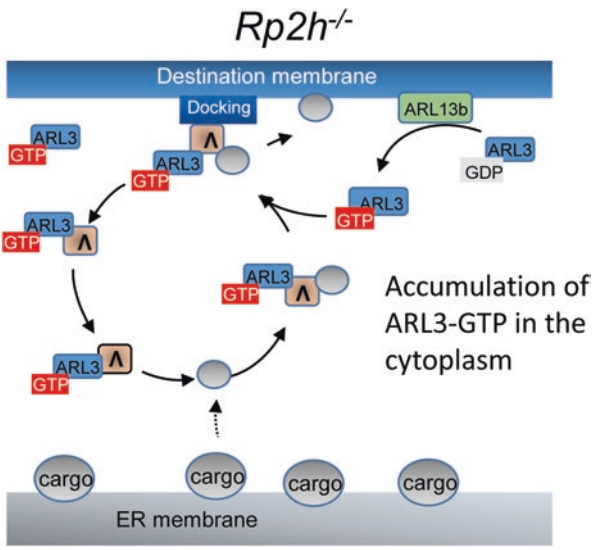


**Fig. 39.4** Cargo mistrafficking in *Rp2h*$^{-/-}$ photoreceptors. Absence of RP2 shuts down hydrolysis of GTP bound to ARL3. As a result, ARL3-GTP accumulates in the IS, the ARL3-GTP/PDEδ complex inefficiently binds GRK1, and trafficking of GRK1 is impaired

## 39.7 Retina-Specific Deletion of ARL3 ($^{ret}$*Arl3*$^{-/-}$)

$^{ret}$*Arl3*$^{-/-}$ knockouts were generated by mating *Arl3*$^{flox/flox}$ with Six3-Cre mice which deletes ARL3 during embryonic development (Hanke-Gogokhia et al. 2016). In the mutant mice, rod and cone photoreceptors do not form outer segments, and consequently, all outer segment proteins accumulate in the inner segment and outer nuclear layer. At a time when ciliogenesis should be completed (P10 and P15), only mother and daughter centrioles were present in mutant retina, and functional basal bodies, transition zones, and axonemes were not formed. At P15, rod and cone photoreceptors degenerated massively, and degeneration is complete at P30. ARL13b, an outer segment protein and palmitoylated, was restricted in the mutant retina to the apical IS. Absence of outer segments as early as P10 in central $^{ret}$*Arl3*$^{-/-}$ photoreceptors suggests that ARL3, a known microtubule-interacting protein, may regulate a late stage of ciliogenesis or intraflagellar transport. The $^{ret}$*Arl3*$^{-/-}$ phenotype is strikingly similar to retina-specific knockouts of KIF3A (obligatory subunit of the heterotrimeric kinesin-2, KIF3) and IFT88 (particle of the IFT-B complex). KIF3 and IFT88 are responsible for IFT of tubulin and axoneme building blocks.

## 39.8 Rod-Specific Deletion of ARL3 ($^{rod}$*Arl3*$^{-/-}$)

We initiated rod deletion of ARL3 by crossing *Arl3*$^{flox/flox}$ mice with iCre75 transgenic mice expressing Cre at postnatal day 7 (P7) and later (3). Presence of rod ERG responses at P15 demonstrated that postnatal development, including

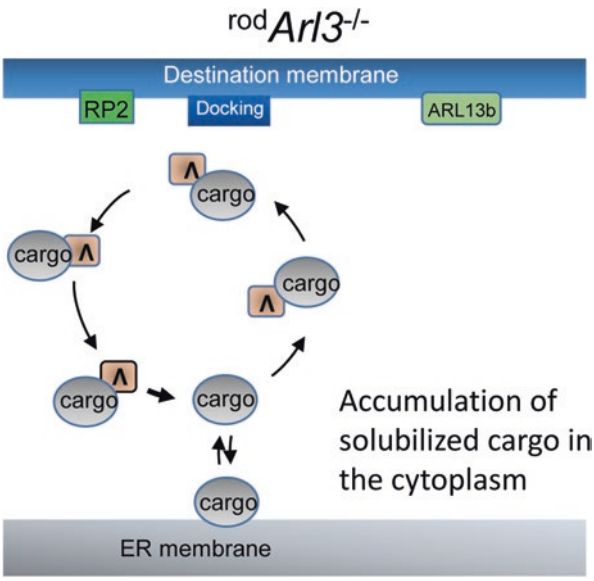


**Fig. 39.5** Absence of ARL3 in photoreceptors prevents delivery of cargo to the destination membrane, and cargo accumulates in the inner segments bound to their lipid binding protein (**Λ**). As a result, photoreceptors degenerate

ciliogenesis and OS formation, occurred normally. Axoneme, including transition zone, and mother centriole (basal body) and daughter centriole developed normally. Transmembrane proteins such as rhodopsin trafficked to the OS and were unaffected by absence of ARL3. Farnesylated GRK1, prenylated rod PDE6, acylated rod Tα, and farnesylated Tβγ mistrafficked to the inner segments, the outer nuclear layer, and synaptic terminals (Fig. 39.5). That is, lipidated proteins accumulated in the outer nuclear layer and inner segments of $^{rod}Arl3^{-/-}$ photoreceptors as inactivation of the *Arl3* gene by Cre-mediated recombination increased and ARL3 loses its ability to function as CDF. The degeneration is fast, most likely due to a combination of its binary function as regulator in IFT and as CDF in OS protein trafficking, and is completed at 2 M of age/P50.

## 39.9 Outlook: Generation of ARL13b Retina-Specific Knockout

As germline deletion of ARL13b is embryonically lethal, our next step will be to generate ARL13b retina-specific and tamoxifen-induced knockouts. ARL13b will be deleted pre-ciliogenesis during embryonic development and post-ciliogenesis in the adult mouse, respectively. We expect rapid photoreceptor degeneration, including mistrafficking of prenylated and acylated OS cargo and defect in ciliogenesis, most likely caused by the absence of active ARL3-GTP.

**Acknowledgments** This research was supported by a National Eye Institute grants EY08123, EY019298 (WB), EY014800-039003 (NEI core grant), unrestricted grants to the Departments of Ophthalmology at the University of Utah from Research to Prevent Blindness (RPB; New York), the Retina Research Foundation, Houston (Alice McPherson, MD), and the Foundation for Retina Research (David Brint, MD). WB is a recipient of a Research to Prevent Blindness Senior Investigator and Nelson Trust Award.

## References

Arshavsky VY, Lamb TD, Pugh EN Jr (2002) G proteins and phototransduction. Annu Rev Physiol 64:153–187

Baehr W, Devlin MJ, Applebury ML (1979) Isolation and characterization of cGMP phosphodiesterase from bovine rod outer segments. J Biol Chem 254:11669–11677

Cantagrel V, Silhavy JL, Bielas SL et al (2008) Mutations in the cilia gene ARL13B lead to the classical form of Joubert syndrome. Am J Hum Genet 83:170–179

Caspary T, Larkins CE, Anderson KV (2007) The graded response to Sonic Hedgehog depends on cilia architecture. Dev Cell 12:767–778

Constantine R, Zhang H, Gerstner CD et al (2012) Uncoordinated (UNC)119: coordinating the trafficking of myristoylated proteins. Vis Res 75:26–32

Duldulao NA, Lee S, Sun Z (2009) Cilia localization is essential for in vivo functions of the Joubert syndrome protein Arl13b/Scorpion. Development 136:4033–4042

Fung BKK, Young JH, Yamane HK et al (1990) Subunit stoichiometry of retinal rod cGMP phosphodiesterase. Biochemistry 29:2657–2664

Gilliam JC, Chang JT, Sandoval IM et al (2012) Three-dimensional architecture of the rod sensory cilium and its disruption in retinal neurodegeneration. Cell 151:1029–1041

Gotthardt K, Lokaj M, Koerner C et al (2015) A G-protein activation cascade from Arl13b to Arl3 and implications for ciliary targeting of lipidated proteins. elife 4:e11859

Hanke-Gogokhia C, Wu Z, Gerstner CD et al (2016) Arf-like protein 3 (ARL3) regulates protein trafficking and ciliogenesis in mouse photoreceptors. J Biol Chem 291:7142–7155

Hanzal-Bayer M, Renault L, Roversi P et al (2002) The complex of Arl2-GTP and PDE delta: from structure to function. EMBO J 21:2095–2106

Jayasundera T, Branham KE, Othman M et al (2010) RP2 phenotype and pathogenetic correlations in X-linked retinitis pigmentosa. Arch Ophthalmol 128:915–923

Kobayashi A, Higashide T, Hamasaki D et al (2000) HRG4 (UNC119) mutation found in cone-rod dystrophy causes retinal degeneration in a transgenic model. Invest Ophthalmol Vis Sci 41:3268–3277

Kuhnel K, Veltel S, Schlichting I et al (2006) Crystal structure of the human retinitis pigmentosa 2 protein and its interaction with Arl3. Structure 14:367–378

Maeda T, Imanishi Y, Palczewski K (2003) Rhodopsin phosphorylation: 30 years later. Prog Retin Eye Res 22:417–434

Manolaridis I, Kulkarni K, Dodd RB et al (2013) Mechanism of farnesylated CAAX protein processing by the intramembrane protease Rce1. Nature 504:301–305

Palczewski K, Benovic JL (1991) G-protein-coupled receptor kinases. TIBS 16:387–391

Schrick JJ, Vogel P, Abuin A et al (2006) ADP-ribosylation factor-like 3 is involved in kidney and photoreceptor development. Am J Pathol 168:1288–1298

Strom SP, Clark MJ, Martinez A et al (2016) De novo occurrence of a variant in ARL3 and apparent autosomal dominant transmission of retinitis pigmentosa. PLoS One 11:e0150944

Thomas S, Wright KJ, Le CS et al (2014) A homozygous PDE6D mutation in Joubert syndrome impairs targeting of farnesylated INPP5E protein to the primary cilium. Hum Mutat 35:137–146

Veltel S, Gasper R, Eisenacher E et al (2008) The retinitis pigmentosa 2 gene product is a GTPase-activating protein for Arf-like 3. Nat Struct Mol Biol 15:373–380
Wright AF, Chakarova CF, Abd El-Aziz MM et al (2010) Photoreceptor degeneration: genetic and mechanistic dissection of a complex trait. Nat Rev Genet 11:273–284
Young RW (1976) Visual cells and the concept of renewal. Invest Ophthalmol Vis Sci 15:700–725
Zhang H, Li S, Doan T et al (2007) Deletion of PrBP/{delta} impedes transport of GRK1 and PDE6 catalytic subunits to photoreceptor outer segments. Proc Natl Acad Sci U S A 104:8857–8862
Zhang H, Constantine R, Vorobiev S et al (2011) UNC119 is required for G protein trafficking in sensory neurons. Nat Neurosci 14:874–880
Zhang H, Constantine R, Frederick JM et al (2012) The prenyl-binding protein PrBP/delta: a chaperone participating in intracellular trafficking. Vis Res 75:19–25
Zhang H, Hanke-Gogokhia C, Jiang L et al (2015) Mistrafficking of prenylated proteins causes retinitis pigmentosa 2. FASEB J 29:932–942

# Chapter 40
# Do cGMP Levels Drive the Speed of Photoreceptor Degeneration?


**Maria Iribarne and Ichiro Masai**

**Abstract** Humans with mutations in the phototransduction pathway develop forms of retinal degeneration, such as retinitis pigmentosa, cone dystrophy, or Leber congenital amaurosis. Similarly, numerous phototransduction mutant animal models resemble retinal degeneration. In our lab, using a zebrafish model, we study cone-specific phototransduction mutants. cGMP is the second messenger in the phototransduction pathway, and abnormal cGMP levels are associated with photoreceptor death. *Rd1*, a rod-specific phosphodiesterase 6 (Pde6) subunit mutant in mice, is one of the most widely used animal models for retinal degeneration. *Rd1* mutant mice accumulate cGMP, causing rapid photoreceptor degeneration. However, much less is known about photoreceptor mutants producing abnormally low levels of cGMP. Here, focusing on *Pde6* mutants in zebrafish and mice, we propose a correlation between cGMP levels and speed of photoreceptor degeneration.

**Keywords** Photoreceptor degeneration · cGMP · Pde6 · Zebrafish · Mouse · Rapid degeneration · Slow degeneration

## 40.1 Introduction

Loss or dysfunction of any component of the phototransduction cascade results in photoreceptor degeneration and blindness in humans. More than 40 years ago, Farber and Lolley established that in the *rd1* mouse mutant, which carries a mutation in rod-specific Pde6b, cGMP accumulates before the photoreceptor degenerates (Farber and Lolley 1974). cGMP accumulation is not always expected to occur in phototransduction mutants, but rather in mutations of certain phototransduction components. For example, mutants of guanylyl cyclase are believed to result in low cGMP levels. Thus, cGMP level is critical for photoreceptor survival and is tightly regulated under normal physiological conditions. Here we will

M. Iribarne (✉) · I. Masai
Okinawa Institute of Science and Technology Graduate University, Okinawa, Japan
e-mail: miribarn@nd.edu



J. D. Ash et al. (eds.), *Retinal Degenerative Diseases*, Advances in Experimental Medicine and Biology 891, https://doi.org/10.1007/978-3-319-75402-4_40

discuss cGMP levels in cone photoreceptor degeneration in different alleles of a zebrafish cone-specific cGMP phosphodiesterase type 6 (PDE6) mutant, and we will compare their phenotypes with those of cone- or rod photoreceptor-specific mouse mutants, and human patients.

## 40.2 Phototransduction Pathway in Photoreceptors

In the dark, a high level of cGMP maintains cyclic nucleotide-gated (CNG) channels in an open state, maintaining a steady influx of $Na^+$ and $Ca^{2+}$ ions. Once the phototransduction cascade is activated by light stimuli, PDE6 hydrolyses cGMP. In this state, the CNG channel is dissociated from cGMP and closed, leading to reduced ion influx and hyperpolarization of photoreceptors. PDE6 and guanylyl cyclase (GC) regulate cGMP metabolism. GC is activated in response to calcium binding to guanylyl cyclase-activating proteins (GCAPs). Thus, after light stimuli close the CNG channel and intracellular $Ca^{2+}$ decreases, GCAPs activate GC to recover cGMP levels.

## 40.3 PDE6: The Primary Effector Enzyme in the Phototransduction Cascade

Through their opposing actions, PDE6 and GC are the central enzymes governing cGMP levels in the retina, hydrolyzing or synthesizing cGMP, respectively. PDE6 is a membrane-associated protein, composed of four subunits. α (PDE6a) and β (PDE6b) catalytic subunits and two inhibitory γ subunits (designated PDE6g) are expressed in rods, whereas two α' subunits (designated PDE6c) and two inhibitory γ subunits (designated PDE6h) are expressed in cones. Here, we will focus on cone- or rod-specific PDE6 mutants from zebrafish and mice and summarize existing results concerning cGMP levels and photoreceptor degeneration.

### *40.3.1 The Zebrafish Mutant,* pde6c $^{rw76a}$*, Shows Slow Cone Degeneration*

A nonsense mutation allele of *pde6c*, called *pde6c*$^{w59}$, was isolated in zebrafish by Brockerhoff's lab (Stearns et al. 2007). With this allele, loss of pde6c activity induces rapid cone degeneration. Some rods also undergo degeneration, but degeneration is limited to areas with a low rod density. Concurrently in our lab, we isolated and characterized a hypomorphic mutant allele of *pde6c,* called *pde6c*$^{rw76a}$ (Nishiwaki et al. 2008). *pde6c*$^{rw76a}$ had a missense mutation in the pde6c gene

causing a substitution at a conserved position, which probably compromises pde6 activity. This allele showed cell death in both cones and rods at an early embryonic stage. In later stages of development, cones undergo a slow but progressive degeneration and are completely eliminated by 6 months post-fertilization, but rods are retained to form the outer nuclear layer, suggesting that cones specifically degenerate in this allele. Interestingly, human patients carrying mutations in PDE6c show autosomal recessive achromatopsia and autosomal recessive cone dystrophy (Chang et al. 2009; Thiadens et al. 2009). Achromatopsia is a congenital disorder with loss of cone functions, low visual acuity, photophobia, a lack of cone electroretinogram (ERG) responses, and loss of color discrimination. However, PDE6c mutant patients have normal or slightly decreased rod function. These data suggest conservation of PDE6c function from fish to humans.

### *40.3.2 The Zebrafish* pde6c$^{rw76a}$ *Mutant Shows No cGMP Accumulation*

It is likely that cGMP concentration is increased in *pde6c*$^{rw76a}$ cone photoreceptor mutants because of a severe reduction of pde6c. We evaluated cGMP levels by immunofluorescence, using the most popular antibody against formaldehyde-fixed cGMP (de Vente et al. 1987). Surprisingly, when we examined cGMP concentration in *pde6c*$^{rw76a}$ mutant retinas at an early stage of photoreceptor maturation (4 days post-fertilization) in light-adapted conditions, no antibody signal was observed. However, sometimes we observed an accumulation of cGMP in only a few cone photoreceptors near the ciliary marginal zone where photoreceptors are newly produced from retinal stem cells. In contrast to the retina, we observed very strong signals in *pde6c*$^{rw76a}$ mutant pineal glands, while no cGMP signal was observed in wild-type pineal glands. These data suggest that cGMP accumulation does not occur early in photoreceptor differentiation in the *pde6c*$^{rw76a}$ mutant (Iribarne et al. 2017). Further experiments revealed the downregulation of cone-specific GC, gc3 in the *pde6c*$^{rw76a}$ mutant, which explains the low level of cGMP (Iribarne et al. 2017; Iribarne and Masai 2017).

In contrast to our results, it was reported that cGMP levels are elevated in the zebrafish nonsense mutant allele, *pde6c*$^{w59}$, at 4 dpf (Viringipurampeer et al. 2014). They also evaluated cGMP levels by immunolabeling using a different cGMP antibody, which may have different affinity than ours. They found strong signals that did not overlap with rods and assumed that the cGMP accumulation occurred in cones.

It is possible that two zebrafish pde6c mutant alleles, the null *pde6c*$^{w59}$ and the hypomorphic *pde6c*$^{rw76a}$ allele, trigger different cell death mechanisms. *pde6c*$^{w59}$ shows rapid photoreceptor degeneration associated with cGMP accumulation, while *pde6c*$^{rw76a}$ presents a slow degeneration associated low cGMP levels. cGMP levels may correlate with the speed of photoreceptor degeneration, but probably through different cell death mechanisms.

### 40.3.3 *Evidence from Mice with Cone* Pde6c *Mutations*

Results in zebrafish *pde6c* mutants led us to compare evidence from mouse *Pde6* mutants. Results from mouse mutants supported our hypothesis about the connection between the speed of photoreceptor degeneration and the level of cGMP. A spontaneous mouse mutant, *cone photoreceptor function loss-1* (*cpfl1*), was identified in The Jackson Laboratories (Chang et al. 2002). *cpfl1* was the first spontaneous mutation known to cause loss of cone functions in mice. In this mutant, cones suffer rapid degeneration, while rods are maintained. Cones begin to be eliminated at an early stage of development (P14), and the peak of cell death occurred at P24 (Trifunovic et al. 2010). A mapping study revealed that *cpfl1* has mutations in the *Pde6c* gene. An insertion of 116-pb between exons 4 and 5 and a deletion of 1-bp in exon 7 produced a premature stop codon (Chang et al. 2009). cGMP accumulation was evaluated by immunohistochemistry at P11, P18, P30, and P60. cGMP accumulated specifically in cone cells and peaked at P18 (Trifunovic et al. 2010).

Later, another cone-specific mutant, *cpfl3*, was reported (Chang et al. 2006). *cpfl3* shows a reduced response of cone ERG and a slow degeneration of cones, which survived 14 weeks after birth. Sequencing analysis revealed a missense mutation in exon 6 (G to A) in the *Gnat2* gene, which encodes the α-subunit of cone-specific transducin. A second missense mutation in the *Gnat2* gene was reported (Jobling et al. 2013), and mutant mice showed cone-specific degeneration that progressed slowly. No measurable cone response was observed at 3 months of age. At 12 months, the number of cones was reduced 27% versus controls. Even though these *cpfl3* mutants are not *Pde6c* mutants, since they show slow cone degeneration, it will be interesting to determine whether they exhibit low cGMP levels.

### 40.3.4 *Evidence from Mice with Rod* Pde6b *Mutations*

The original rodless mice, which are genetically the same as *rd1*, were first described more than 90 years ago (Keeler 1924; Pittler et al. 1993). These seminal works demonstrated the specific elimination of photoreceptors. Since then, many groups have detailed the progression of retinal degeneration in *rd1* mice. Briefly, *rd1* mice were characterized as exhibiting rapid rod degeneration. Degeneration begins at P8, and no rod photoreceptors survive beyond 4 weeks (Farber et al. 1994). Calpain activity analysis and TUNEL revealed that the peak of photoreceptor cell death occurs at P13 (Trifunovic et al. 2010). *Pde6b* was identified as the gene responsible for the *rd1* mutation, which contains both an MLV virus insertion in intron 1 and a nonsense point mutation in exon 7 (Pittler and Baehr 1991; Bowes et al. 1993). As mentioned before, cGMP level was measured using homogenates of *rd1* mutant retinas. cGMP level was normal until P6 in *rd1*, and then cGMP accumulation commenced, peaking at P14-P16 (Farber and Lolley 1974). cGMP was also evaluated by immunolabeling with anti-cGMP antibody. cGMP antibody signals were not detected in wild-type retinas at P11, whereas *rd1* retinas showed very strong positive signals in the outer nuclear layer (Paquet-Durand et al. 2009).

In contrast to *rd1*, *rd10* mice have a later onset of milder photoreceptor degeneration. Histological studies showed that retinal degeneration started in the central retina at P16 and spread to the peripheral retina by P20. ERG response was maximal at 3 weeks, but undetectable at 2 months of age (Han et al. 2013). The *rd10* mouse carries a missense mutation in exon 13 of *Pde6b* (R560C) and is a hypomorphic mutant (Chang et al. 2007). In another missense *Pde6b* mutant, $Pde6b^{H620Q}$, cGMP level was measured in retinal homogenates at P14, P18, and P21. At all time points, mutant cGMP levels were similar to those of controls (Davis et al. 2008). Taken together, these two *Pde6b* mouse mutations suggest the correlation of cGMP level with the severity of rod photoreceptor degeneration.

Mutations in PDE6b have been implicated in human photoreceptor degeneration as causing one of the most aggressive types of retinitis pigmentosa with the earliest onset (Han et al. 2013). Initial symptoms of retinitis pigmentosa involve night blindness and "tunnel vision" caused by rod photoreceptor loss. Secondary loss of cones leads to impaired central vision and ultimately legal blindness. It is important to evaluate whether cGMP levels are correlated with severity of rod degeneration in humans, as in mice and zebrafish.

## 40.4 Conclusions and Future Directions

Pde6 plays a central role in regulation of intracellular cGMP levels. Mutations in Pde6 are expected to lead to an increase in photoreceptor cGMP concentration. Here we show that cGMP level is not necessarily elevated in Pde6 mutants. We hypothesize that cGMP level determines the speed of photoreceptor degeneration. Figure 40.1 summarizes mutant data discussed above. In the case of low cGMP

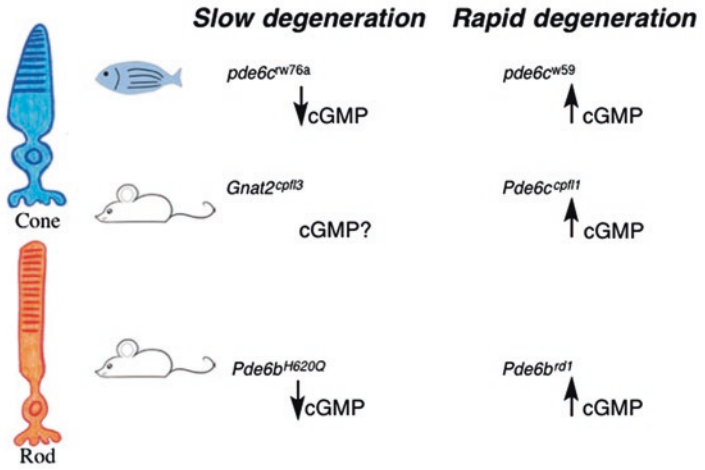


**Fig. 40.1** In zebrafish and mouse cone- or rod-*Pde6* mutants, the speed and severity of retinal degeneration are correlated with cGMP levels

levels, photoreceptor degeneration proceeds slowly and mildly, as in *rd10* mutant mice and zebrafish *pde6c*$^{rw76a}$ mutants. If cGMP levels are higher than those of wild type, photoreceptor degeneration becomes severe, as in *rd1* mutant mice and zebrafish *pde6c*$^{w59}$ mutants. In the future, it is important to determine how intracellular cGMP levels differentially influence photoreceptor cell survival. Understanding these mechanisms will contribute to development of therapies for patients suffering from photoreceptor degeneration in response to PDE6 genetic mutations.

**Acknowledgments** We thank Steven D. Aird for editing this review.

## References

Bowes C, Li T, Frankel WN et al (1993) Localization of a retroviral element within the rd gene coding for the beta subunit of cGMP phosphodiesterase. Proc Natl Acad Sci U S A 90:2955–2959

Chang B, Hawes NL, Hurd RE et al (2002) Retinal degeneration mutants in the mouse. Vis Res 42:517–525

Chang B, Dacey MS, Hawes NL et al (2006) Cone photoreceptor function loss-3, a novel mouse model of achromatopsia due to a mutation in Gnat2. Invest Ophthalmol Vis Sci 47:5017–5021

Chang B, Hawes NL, Pardue MT et al (2007) Two mouse retinal degenerations caused by missense mutations in the beta-subunit of rod cGMP phosphodiesterase gene. Vis Res 47:624–633

Chang B, Grau T, Dangel S et al (2009) A homologous genetic basis of the murine cpfl1 mutant and human achromatopsia linked to mutations in the PDE6C gene. Proc Natl Acad Sci U S A 106:19581–19586

Davis RJ, Tosi J, Janisch KM et al (2008) Functional rescue of degenerating photoreceptors in mice homozygous for a hypomorphic cGMP phosphodiesterase 6 b allele (Pde6bH620Q). Invest Ophthalmol Vis Sci 49:5067–5076

de Vente J, Steinbusch HW, Schipper J (1987) A new approach to immunocytochemistry of 3′,5′-cyclic guanosine monophosphate: preparation, specificity, and initial application of a new antiserum against formaldehyde-fixed 3′,5′-cyclic guanosine monophosphate. Neuroscience 22:361–373

Farber DB, Lolley RN (1974) Cyclic guanosine monophosphate: elevation in degenerating photoreceptor cells of the C3H mouse retina. Science 186:449–451

Farber DB, Flannery JG, Bowes-Rickman. C (1994) The rd mouse story: seventy years of research on an animal model of inherited retinal degeneration. Prog Reti Eye Res 13:32–64

Han J, Dinculescu A, Dai X et al (2013) Review: the history and role of naturally occurring mouse models with Pde6b mutations. Mol Vis 19:2579–2589

Iribarne M, Masai I (2017) Neurotoxicity of cGMP in the vertebrate retina: from the initial research on rd mutant mice to zebrafish genetic approaches. J Neurogenet 31(3):88–101. https://doi.org/10.1080/01677063.2017.1358268. Epub 2017 Aug 16

Iribarne M, Nishiwaki Y, Nakamura S, Araragi M, Oguri E, Masai I (2017) Aipl1 is required for cone photoreceptor function and survival through the stability of Pde6c and Gc3 in zebrafish. Sci Rep 7:45962. https://doi.org/10.1038/srep45962

Jobling AI, Vessey KA, Waugh M et al (2013) A naturally occurring mouse model of achromatopsia: characterization of the mutation in cone transducin and subsequent retinal phenotype. Invest Ophthalmol Vis Sci 54:3350–3359

Keeler CE (1924) The inheritance of a retinal abnormality in white mice. Proc Natl Acad Sci U S A 10:329–333

Nishiwaki Y, Komori A, Sagara H et al (2008) Mutation of cGMP phosphodiesterase 6alpha'-subunit gene causes progressive degeneration of cone photoreceptors in zebrafish. Mech Dev 125:932–946

Paquet-Durand F, Hauck SM, van Veen T et al (2009) PKG activity causes photoreceptor cell death in two retinitis pigmentosa models. J Neurochem 108:796–810

Pittler SJ, Baehr W (1991) Identification of a nonsense mutation in the rod photoreceptor cGMP phosphodiesterase beta-subunit gene of the rd mouse. Proc Natl Acad Sci U S A 88:8322–8326

Pittler SJ, Keeler CE, Sidman RL et al (1993) PCR analysis of DNA from 70-year-old sections of rodless retina demonstrates identity with the mouse rd defect. Proc Natl Acad Sci U S A 90:9616–9619

Stearns G, Evangelista M, Fadool JM et al (2007) A mutation in the cone-specific pde6 gene causes rapid cone photoreceptor degeneration in zebrafish. J Neurosci : Off J Soci Neurosci 27:13866–13874

Thiadens AA, den Hollander AI, Roosing S et al (2009) Homozygosity mapping reveals PDE6C mutations in patients with early-onset cone photoreceptor disorders. Am J Hum Genet 85:240–247

Trifunovic D, Dengler K, Michalakis S et al (2010) cGMP-dependent cone photoreceptor degeneration in the cpfl1 mouse retina. J Comp Neurol 518:3604–3617

Viringipurampeer IA, Shan X, Gregory-Evans K et al (2014) Rip3 knockdown rescues photoreceptor cell death in blind pde6c zebrafish. Cell Death Differ 21:665–675

# Chapter 41
# Early Endosome Morphology in Health and Disease


**Gulpreet Kaur and Aparna Lakkaraju**

**Abstract** Early endosomes are organelles that receive macromolecules and solutes from the extracellular environment. The major function of early endosomes is to sort these cargos into recycling and degradative compartments of the cell. Degradation of the cargo involves maturation of early endosomes into late endosomes, which, after acquisition of hydrolytic enzymes, form lysosomes. Endosome maturation involves recruitment of specific proteins and lipids to the early endosomal membrane, which drives changes in endosome morphology. Defects in early endosome maturation are generally accompanied by alterations in morphology, such as increase in volume and/or number. Enlarged early endosomes have been observed in Alzheimer's disease and Niemann Pick Disease type C, which also exhibit defects in endocytic sorting. This article discusses the mechanisms that regulate early endosome morphology and highlights the potential importance of endosome maturation in the retinal pigment epithelium.

**Keywords** Early endosome · Enlarged endosome · Endosome morphology · Endosome maturation · Age-related macular degeneration

G. Kaur
Cellular and Molecular Biology Graduate Training Program, University of Wisconsin-Madison, Madison, WI, USA

Department of Ophthalmology and Visual Sciences, School of Medicine and Public Health, University of Wisconsin-Madison, Madison, WI, USA

A. Lakkaraju (✉)
McPherson Eye Research Institute, University of Wisconsin-Madison, Madison, WI, USA

Department of Ophthalmology and Visual Sciences, School of Medicine and Public Health, University of Wisconsin-Madison, Madison, WI, USA
e-mail: lakkaraju@wisc.edu



J. D. Ash et al. (eds.), *Retinal Degenerative Diseases*, Advances in Experimental Medicine and Biology 891, https://doi.org/10.1007/978-3-319-75402-4_41

## 41.1 Introduction

Animal cells transfer various macromolecules (nutrients, receptors, ligands) and solutes from the surrounding medium to the interior of the cell by endocytosis. These macromolecules and solutes are then transported to various compartments in the cell by a system of endocytic vesicles (Mellman 1996; Jovic et al. 2010). These vesicles, especially the early endosomes that are the first endocytic vesicles to receive this cargo, play important roles in the proper functioning of the cell (Gruenberg et al. 1989). Early endosomes are responsible for nutrient uptake, degradation of metabolic by-products, transport of materials to specific compartments in the cell, and regulating the cell-surface expression of receptors and transporters. Defects in early endosomes have been implicated in neurological disorders such as Alzheimer's disease and Niemann Pick Disease type C (Nixon 2005; Maxfield 2014).

Early endosomes have specific proteins and lipids on their membranes that confer organelle identity and regulate association with other effector proteins (Huotari and Helenius 2011; Jovic et al. 2010). Defective association of proteins with early endosomes interferes with endosome maturation and early endosome function. In this review, we focus on mechanisms that regulate endosome maturation, which in turn impact the morphology of early endosomes.

## 41.2 Early Endosomes: Morphology and Maturation

Early endosomes are very heterogeneous in terms of morphology and have a high capacity for homotypic and heterotypic fusion (Gruenberg et al. 1989). During endocytosis, primary vesicles carrying cargo bud off from the plasma membrane and fuse with early endosomes to deliver their contents (Mellman 1996; Jovic et al. 2010) (see Fig. 41.1). Early endosomes continue to receive cargo by fusion, which leads to an increase in size (Dunn et al. 1989; Maxfield and McGraw 2004). As a result, these endosomes can display a network of tubular, cisternal, and tubulovesicular morphologies (Gruenberg et al. 1989). A major role of early endosomes is to sort various proteins into recycling and degradative compartments (Huotari and Helenius 2011). Plasma membrane proteins, lipids, and ligands, such as transferrin, are recycled back to the cell membrane by the fission of smaller, recycling endosomes from the early sorting endosomes (Dunn et al. 1989; Ciechanover et al. 1983). The proteins marked for degradation, such as the EGF receptor, are sorted to cisternal parts of early endosomes, which mature into late endosomes. These late endosomes either mature into lysosomes or fuse with pre-existing lysosomes to degrade the cargo (Carpenter and Cohen 1979, Dunn and Maxfield 1992). During maturation of early endosomes to late, some proteins also get shuttled to the trans-Golgi network via the retromer complex (Progida and Bakke 2016). On the other hand, early endosomes undergoing

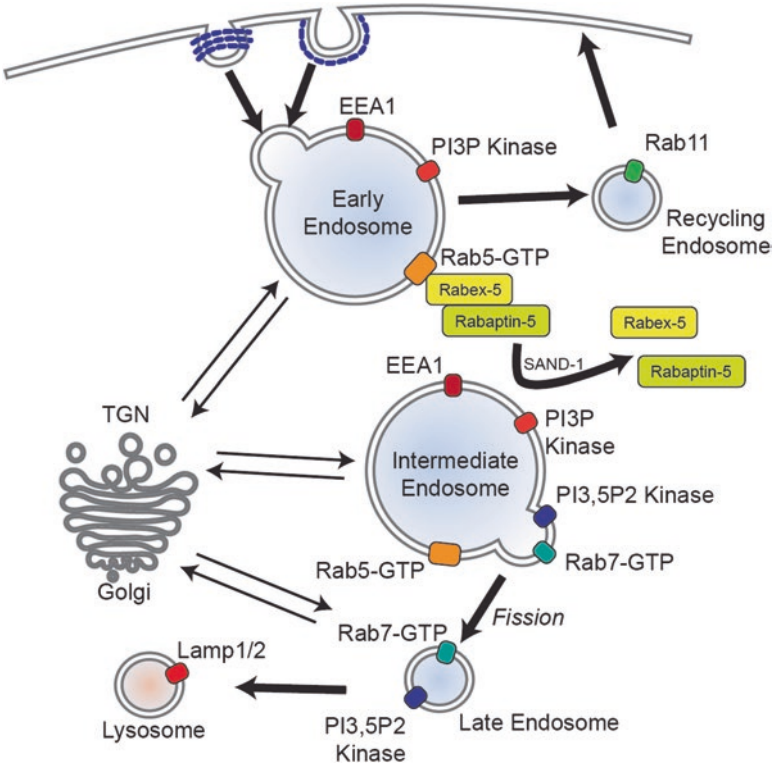


**Fig. 41.1** Primary vesicles carrying endocytosed cargo fuse with the early endosome, which is marked by EEA1, PI3P kinase, and Rab5-GTP. Some cargo is recycled back to the plasma membrane by the recycling endosomes. On the early endosomes, Rabex-5 and Rabaptin-5 binding maintains Rab5 in its GTP state. SAND-1/Mon1 can dissociate Rabex-5 and Rabaptin-5 from the endosome membrane and allow association with Rab7. Early endosomes also undergo bidirectional transport with the trans-Golgi network. Rab7 is added onto domains of the endosome as Rab5 is removed. Endocytic carrier vesicles bud off from the endosomal membrane and mature into late endosomes. Alternatively, early endosomes may gradually mature into late endosomes also. Ultimately, late endosomes fuse with, or mature into, lysosomes and degrade their materials

maturation receive membrane proteins and hydrolytic enzymes by fusion of secretory vesicles from the trans-Golgi network, which is essential for the maturation process.

Early endosomes have specific protein and lipid compositions that confer organelle identity. One such protein is Rab5, which regulates both early endosome morphology and function (Gorvel et al. 1991; Bucci et al. 1992). Rabs are small GTP-binding membrane proteins that switch between a GTP-bound active state and a GDP-bound inactive state. Rab5 regulates fusion of endocytic vesicles with early endosomes, motility of early endosomes, and generation of phosphotidylinositol-3-phosphate (PtdIns-3-P) and activates signaling pathways from early endosomes (Gorvel et al. 1991, Christoforidis et al. 1999;

Murray et al. 2002; Nielsen et al. 1999; Benmerah et al. 2004). Rab5 localizes to the early endosome membrane upon activation by Rabex5, which is a guanine exchange factor (GEF) specific for Rab5 (Horiuchi et al. 1997; Barr and Lambright 2010). The GEF activity of Rabex-5 is promoted by a Rab5 effector, Rabaptin-5, which provides a positive feedback loop for Rab5 activation (Lippe et al. 2001). This allows the recruitment of several Rab effectors on to early endosomes. Key Rab5 effectors are PtdIns-3-P kinases, Vps34 and p150, which are responsible for generating PtdIns-3-P. PtdIns-3-P is the most abundant phosphoinositide on the early endosome membrane and acts as a signal to recruit other effector proteins such as early endosome autoantigen 1 (EEA1), which is essential for homotypic early endosome fusions. EEA1, Rab5, and PtdIns-3-P are three essential components that specify the identity of early endosomes (Mills et al. 1998, 1999).

A switch in GTPases – from Rab5 to Rab7 – on the endosomal membrane marks maturation of early endosomes to late endosomes (Huotari and Helenius 2011). A Rab7 domain forms on early endosomes before maturation to late endosomes leading to a transient, hybrid Rab5/Rab7 endosome (Fig. 41.1). The Rab7 domains then are removed from the early endosome by fission of endosomal carrier vesicles (Gruenberg and Stenmark 2004). Another possible mechanism is that existing early endosomes gradually mature into late endosomes (Rink et al. 2005). In yeast, the Rab5-to-Rab7 switch has been shown to be regulated by SAND-1/Mon1 that disrupts the Rab5/Rabex-5/Rabaptin-5 complex and actively drives the recruitment of Rab7 onto endosomes (Poteryaev et al. 2010). During endosomal maturation, there is also a switch in the phosphoinositides on the membrane, from PtdIns-3-P to PtdIns-3,5-P by recruitment on PIKfyve. Maturation of endosomes also involves formation of intraluminal vesicles, acidification, and a switch in fusion specificity (Huotari and Helenius 2011).

## 41.3 Defects in Endosome Maturation Cause Enlarged Early Endosomes

As described above, endosome maturation is a complex process that requires the concerted action of a series of factors at specific steps. Defects in the recruitment of these factors or the completion of any of these steps of endosome maturation can result in a block in the endocytic pathway. Several studies have identified that defects in the endocytic pathway, particularly those of endosome maturation, are accompanied by an enlargement of early endosomes. Thus, endosome morphology could be used as a marker for early endocytic pathway defects in disease conditions.

Several studies show that interfering with the Rab5-to-Rab7 switch has marked effects on endosome maturation. Hyperactivation of Rab5 by overexpression of wild-type Rab5 leads to giant early endosomes (Bucci et al. 1992;

Stenmark et al. 1994). The same effect is seen upon expression of a constitutively active, GTPase-deficient Rab5 mutant, Rab5Q79L. These Enlarged endosomes show both early and late endosome markers indicating that late endosomal markers are being acquired without the loss of early endosomal markers (Hirota et al. 2007; Wegener et al. 2010). Maturing endosomes retained early endosome markers and the ability to fuse with other such endosomes, leading to increased fusion and size of the endosomes (Wegener et al. 2010). Cells expressing constitutively active Rab5 mutant, Rab5Q79L, showed disrupted sorting of transferrin and non-activated EGF receptors in the internal vesicles of enlarged early endosomes, pointing to a functional defect in the endocytic pathway (Ceresa et al. 2001; Wegener et al. 2010). Thus, overactivation of Rab5 leads to defects in both endosome maturation and function.

Overexpression of Rabex-5 and Rabaptin-5, which are required to activate Rab5, is sufficient to cause enlargement of early endosomes (Stenmark et al. 1995; Kälin et al. 2015; Mattera and Bonifacino 2008). Besides, loss of SAND-1 also results in enlarged early endosomes that also express late endosomal markers (Poteryaev et al. 2010). These endosomes have Rabex-5 trapped in them, indicating that SAND-1-mediated removal of Rabex-5 cannot occur anymore. Thus, disruption of the Rab5-to-Rab7 switch during endosome maturation is a possible mechanism that results in enlarged endosomes.

Other mechanisms could also alter endosomal morphology. PIKFyve is a PtdIns-3,5-P2 kinase that converts PtdIns-3-P to PtdIns-3,5-P2 during maturation of endosomes. Although PIKFyve has been traditionally found on late endosomes, a study by Rutherford et al. found that PIKFyve is also enriched on early endosomes (Shisheva 2008; Rutherford et al. 2006). Overexpression of a kinase-dead mutant of PIKFyve or its suppression by siRNA leads to enlarged early and late endosomes (Rutherford et al. 2006). This indicates that lack of PtdIns-3,5-P2 synthesis leads to an increase in the cellular pool of PtdIns-3-P, which promotes homotypic early endosome fusion. Suppression of PIKFyve also results in reduced rate of transport from early endosomes to trans-Golgi network, although receptor sorting to lysosomes or recycling back to plasma membrane remains unaffected (Ikonomov et al. 2003; Rutherford et al. 2006). Thus, PIKFyve can regulate the morphology of early endosomes by regulating PtdIns-3-P levels and the exit of cargo from early endosomes to late endosomes.

Studies by Skjeldal et al. have indicated that disruption of the microtubule network by nocodazole treatment can lead to an increase in the size of early endosomes (Skjeldal et al. 2012). This has been attributed to an increased fusion rate and disruption of fission after microtubule depolymerization. Fusion of early endosomes can result in destabilization of the membrane, which results in fission of smaller endosomal carrier vesicles (Stenmark et al. 1994; Roux et al. 2002). This fission process is dependent on molecular motors such as the kinesin Kif16b and the dynein-dynactin motor (Skjeldal et al. 2012). Thus, conditions that alter the microtubule network also impact endosome maturation and size. It remains to be determined whether this causes a functional defect in the endocytic pathway.

## 41.4 Enlarged Endosomes in Disease

Studies of human donor tissue by Cataldo et al. have shown that at the earliest stages of Alzheimer's disease, many neurons have increased levels of Aβ peptide and also exhibit enlarged Rab5-positive early endosomes (Cataldo et al. 2000, 2004). Early endosomes are the site where amyloidogenic processing of amyloid precursor protein (APP) occurs to form toxic beta-amyloid (Aβ) peptides. These enlarged early endosomes showed immunoreactivity for other early endosome markers such as EEA1, Rab4, and also Aβ, implying that accumulation of Aβ in early Alzheimer's disease neurons is correlated with enlarged early endosomes. Studies by Grbovic et al. have shown that enlargement of early endosomes by overexpression of Rab5 in a murine cell line leads to increased accumulation of Aβ peptides in the extracellular medium (Grbovic et al. 2003). Thus, early endosome morphology in neurons appears to be critical for regulating Aβ levels in neurons.

Similar endocytic defects are seen in a mouse model of Down's syndrome (TS65Dn) (Cataldo et al. 2003), which replicates neurological symptoms seen in Down's syndrome patients (Galdzicki and Siarey 2003). Most patients with Down's syndrome develop Alzheimer's disease pathology by the age of 45. The early onset of Alzheimer's disease is thought to be a result of three copies of *App* gene in Down's syndrome patients. Since it appears that endosomal abnormalities contribute to Alzheimer's disease pathology, it is likely that the same pathological mechanisms could play a role in Down's syndrome (Nixon 2005).

Early endosomes in Purkinje neurons of Niemann-Pick Disease type C (NPC) patients are also enlarged (Jin et al. 2004). These cells also have cholesterol accumulation in late endosomes, indicating other defects in the endocytic pathway (Kobayashi et al. 1999). NPC is a lysosomal storage disease caused by mutations in the NPC1 and NPC2 cholesterol transporters. Defective functioning of these proteins causes massive accumulation of cholesterol and sphingolipids resulting in neurological problems and metabolic defects.

We have observed cholesterol accumulation in late endosomes and lysosomes in the retinal pigment epithelium (RPE) of the *Abca4*$^{-/-}$ mouse model of Stargardt macular degeneration (Lakkaraju et al. 2007; Toops et al. 2015; Tan et al. 2016). It remains to be determined if enlarged early endosomes and other early endocytic defects are also seen in the RPE of these mice. Early endosome function in the RPE is especially important because this compartment takes in macromolecules and solutes from the choroidal circulation at the basal side and the subretinal space at the apical side. Disruption of early endosome maturation or function can have deleterious consequences for the health of the RPE and the retina because it can interfere with several support functions of the RPE (Toops et al. 2014) and, in a manner analogous to Alzheimer's disease, contribute to the pathogenesis of macular degeneration.

## 41.5 Concluding Remarks

Enlargement of early endosomes has been observed in several disease conditions that have underlying defects in the endocytic pathway, particularly in endosome maturation. However, the exact mechanism leading to this phenotype remains unexplored. Yet, given that endosome enlargement is observed in the early stages of neurodegenerative disease, for example, in early Alzheimer's patients, it is possible that in age-related, progressive neuropathies, endocytic defects precede other pathologies. Endosome morphology could thus be a useful marker for early endocytic pathway defects in Alzheimer's disease and other age-related pathologies such as age-related macular degeneration.

Owing to advances in fluorescence microscopy, we are now easily able to observe the dynamics of subcellular organelles using high-speed live-cell imaging. This allows us the unique opportunity to observe the changing morphologies of organelles under different conditions and quantify various parameters such as volume, number, transport, etc. Carefully analyzing the morphology of these organelles might lead us to identify early signs of a disease or discover an unknown defect in the endosomal sorting pathway.

**Acknowledgments** Supported by NIH R01EY023299, Research to Prevent Blindness, and the Retina Research Foundation Rebecca Meyer Brown Professorship

## References

Barr F, Lambright DG (2010) Rab GEFs and GAPs. Curr Opin Cell Biol 22:461–470

Benmerah A (2004) Endocytosis: signaling from endocytic membranes to the nucleus. Curr Biol 14:R314–R316

Bucci C, Parton RG, Mather IH et al (1992) The small GTPase rab5 functions as a regulatory factor in the early endocytic pathway. Cell 70:715–728

Carpenter G, Cohen S (1979) Epidermal growth factor. Annu Rev Biochem 48:193–216

Cataldo AM, Peterhoff CM, Troncoso JC et al (2000) Endocytic pathway abnormalities precede amyloid beta deposition in sporadic Alzheimer's disease and Down syndrome: differential effects of APOE genotype and presenilin mutations. Am J Pathol 157:277–286

Cataldo AM, Petanceska S, Peterhoff CM et al (2003) App gene dosage modulates endosomal abnormalities of Alzheimer's disease in a segmental trisomy 16 mouse model of down syndrome. J Neurosci Off J Soc Neurosc 23:6788–6792

Cataldo AM, Petanceska S, Terio NB et al (2004) Abeta localization in abnormal endosomes: association with earliest Abeta elevations in AD and Down syndrome. Neurobiol Aging 25:1263–1272

Ceresa BP, Lotscher M, Schmid SL (2001) Receptor and membrane recycling can occur with unaltered efficiency despite dramatic Rab5(q79l)-induced changes in endosome geometry. J Biol Chem 276:9649–9654

Christoforidis S, McBride HM, Burgoyne RD et al (1999) The Rab5 effector EEA1 is a core component of endosome docking. Nature 397:621–625

Ciechanover A, Schwartz AL, Lodish HF (1983) Sorting and recycling of cell surface receptors and endocytosed ligands: the asialoglycoprotein and transferrin receptors. J Cell Biochem 23:107–130

Dunn KW, Maxfield FR (1992) Delivery of ligands from sorting endosomes to late endosomes occurs by maturation of sorting endosomes. J Cell Biol 117:301–310

Dunn KW, McGraw TE, Maxfield FR (1989) Iterative fractionation of recycling receptors from lysosomally destined ligands in an early sorting endosome. J Cell Biol 109:3303–3314

Galdzicki Z, Siarey RJ (2003) Understanding mental retardation in Down's syndrome using trisomy 16 mouse models. Genes Brain Behav 2:167–178

Gorvel JP, Chavrier P, Zerial M et al (1991) Rab5 controls early endosome fusion in vitro. Cell 64:915–925

Grbovic OM, Mathews PM, Jiang Y et al (2003) Rab5-stimulated up-regulation of the endocytic pathway increases intracellular beta-cleaved amyloid precursor protein carboxyl-terminal fragment levels and Abeta production. J Biol Chem 278:31261–31268

Gruenberg J, Stenmark H (2004) The biogenesis of multivesicular endosomes. Nat Rev Mol Cell Biol 5:317–323

Gruenberg J, Griffiths G, Howell KE (1989) Characterization of the early endosome and putative endocytic carrier vesicles in vivo and with an assay of vesicle fusion in vitro. J Cell Biol 108:1301–1316

Hirota Y, Kuronita T, Fujita H et al (2007) A role for Rab5 activity in the biogenesis of endosomal and lysosomal compartments. Biochem Biophys Res Commun 364:40–47

Horiuchi H, Lippe R, McBride HM et al (1997) A novel Rab5 GDP/GTP exchange factor complexed to Rabaptin-5 links nucleotide exchange to effector recruitment and function. Cell 90:1149–1159

Huotari J, Helenius A (2011) Endosome maturation. EMBO J 30:3481–3500

Ikonomov OC, Sbrissa D, Mlak K et al (2003) Active PIKfyve associates with and promotes the membrane attachment of the late endosome-to-trans-Golgi network transport factor Rab9 effector p40. J Biol Chem 278:50863–50871

Jin LW, Shie FS, Maezawa I et al (2004) Intracellular accumulation of amyloidogenic fragments of amyloid-beta precursor protein in neurons with Niemann-Pick type C defects is associated with endosomal abnormalities. Am J Pathol 164:975–985

Jovic M, Sharma M, Rahajeng J et al (2010) The early endosome: a busy sorting station for proteins at the crossroads. Histol Histopathol 25:99–112

Kalin S, Hirschmann DT, Buser DP et al (2015) Rabaptin5 is recruited to endosomes by Rab4 and Rabex5 to regulate endosome maturation. J Cell Sci 128:4126–4137

Kobayashi T, Beuchat MH, Lindsay M et al (1999) Late endosomal membranes rich in lysobisphosphatidic acid regulate cholesterol transport. Nat Cell Biol 1:113–118

Lakkaraju A, Finnemann SC, Rodriguez-Boulan E (2007) The lipofuscin fluorophore A2E perturbs cholesterol metabolism in retinal pigment epithelial cells. Proc Natl Acad Sci U S A 104:11026–11031

Lippe R, Miaczynska M, Rybin V et al (2001) Functional synergy between Rab5 effector Rabaptin-5 and exchange factor Rabex-5 when physically associated in a complex. Mol Biol Cell 12:2219–2228

Mattera R, Bonifacino JS (2008) Ubiquitin binding and conjugation regulate the recruitment of Rabex-5 to early endosomes. EMBO J 27:2484–2494

Maxfield FR (2014) Role of endosomes and lysosomes in human disease. Cold Spring Harb Perspect Biol 6:a016931

Maxfield FR, McGraw TE (2004) Endocytic recycling. Nat Rev Mol Cell Biol 5:121–132

Mellman I (1996) Endocytosis and molecular sorting. Annu Rev Cell Dev Biol 12:575–625

Mills IG, Jones AT, Clague MJ (1998) Involvement of the endosomal autoantigen EEA1 in homotypic fusion of early endosomes. Curr Biol 8:881–884

Mills IG, Jones AT, Clague MJ (1999) Regulation of endosome fusion. Mol Membr Biol 16:73–79

Murray JT, Panaretou C, Stenmark H et al (2002) Role of Rab5 in the recruitment of hVps34/p150 to the early endosome. Traffic (Copenhagen, Denmark) 3:416–427
Nielsen E, Severin F, Backer JM et al (1999) Rab5 regulates motility of early endosomes on microtubules. Nat Cell Biol 1:376–382
Nixon RA (2005) Endosome function and dysfunction in Alzheimer's disease and other neurodegenerative diseases. Neurobiol Aging 26:373–382
Poteryaev D, Datta S, Ackema K et al (2010) Identification of the switch in early-to-late endosome transition. Cell 141:497–508
Progida C, Bakke O (2016) Bidirectional traffic between the Golgi and the endosomes – machineries and regulation. J Cell Sci 129:3971–3982
Rink J, Ghigo E, Kalaidzidis Y et al (2005) Rab conversion as a mechanism of progression from early to late endosomes. Cell 122:735–749
Roux A, Cappello G, Cartaud J et al (2002) A minimal system allowing tubulation with molecular motors pulling on giant liposomes. Proc Natl Acad Sci U S A 99:5394–5399
Rutherford AC, Traer C, Wassmer T et al (2006) The mammalian phosphatidylinositol 3-phosphate 5-kinase (PIKfyve) regulates endosome-to-TGN retrograde transport. J Cell Sci 119:3944–3957
Shisheva A (2008) PIKfyve: partners, significance, debates and paradoxes. Cell Biol Int 32:591–604
Skjeldal FM, Strunze S, Bergeland T et al (2012) The fusion of early endosomes induces molecular-motor-driven tubule formation and fission. J Cell Sci 125:1910–1919
Stenmark H, Vitale G, Ullrich O et al (1995) Rabaptin-5 is a direct effector of the small GTPase Rab5 in endocytic membrane fusion. Cell 83:423–432
Stenmark H, Parton RG, Steele-Mortimer O et al (1994) Inhibition of rab5 GTPase activity stimulates membrane fusion in endocytosis. EMBO J 13:1287–1296
Tan LX, Toops KA, Lakkaraju A (2016) Protective responses to sublytic complement in the retinal pigment epithelium. Proc Natl Acad Sci U S A 113:8789–8794
Toops KA, Tan LX, Lakkaraju A (2014) A detailed three-step protocol for live imaging of intracellular traffic in polarized primary porcine RPE monolayers. Exp Eye Res 124:74–85
Toops KA, Tan LX, Jiang Z et al (2015) Cholesterol-mediated activation of acid sphingomyelinase disrupts autophagy in the retinal pigment epithelium. Mol Biol Cell 26:1–14
Wegener CS, Malerod L, Pedersen NM et al (2010) Ultrastructural characterization of giant endosomes induced by GTPase-deficient Rab5. Histochem Cell Biol 133:41–55

# Chapter 42
# The Retinal Circadian Clock and Photoreceptor Viability


**Kenkichi Baba, Christophe P. Ribelayga, P. Michael Iuvone, and Gianluca Tosini**

**Abstract** Circadian rhythms are present in most living organisms, and these rhythms are not just a consequence of the day/night fluctuation, but rather they are generated by endogenous biological clocks with a periodicity of about 24 h. In mammals, the master pacemaker of circadian rhythms is localized in the suprachiasmatic nuclei (SCN) of the hypothalamus. The SCN controls circadian rhythms in peripheral organs. The retina also contains circadian clocks which regulate many aspects of retinal physiology, independently of the SCN. Emerging experimental evidence indicates that the retinal circadian clocks also affect ocular health, and a few studies have now demonstrated that disruption of retinal clocks may contribute to the development of retinal diseases. Our study indicates that in mice lacking the clock gene *Bmal1*, photoreceptor viability during aging is significantly reduced. *Bmal1* knockout mice at 8–9 months of age have 20–30% less nuclei in the outer nuclear layer. No differences were observed in the other retinal layers. Our study suggests that the retinal circadian clock is an important modulator of photoreceptor health.

**Keywords** Circadian rhythm · Clock genes · Retinal degeneration · Photoreceptors · Cell viability · Cone · Aging · Oscillation · Knockout mice

K. Baba (✉) · G. Tosini
Neuroscience Institute, Department of Pharmacology and Toxicology Morehouse School of Medicine, Atlanta, GA, USA
e-mail: bkenkichi@msm.edu

C. P. Ribelayga
Ruiz Department of Ophthalmology and Visual Science, McGovern Medical School, The University of Texas Health Science Center at Houston, Houston, TX, USA

P. Michael Iuvone
Departments of Ophthalmology and Pharmacology, Emory University School of Medicine, Atlanta, GA, USA



J. D. Ash et al. (eds.), *Retinal Degenerative Diseases*, Advances in Experimental Medicine and Biology 891, https://doi.org/10.1007/978-3-319-75402-4_42

## 42.1 Introduction

Circadian rhythms have been observed in animals, plants, fungi, and even *Cyanobacteria*. In mammals, including humans, the master pacemaker controlling 24-h rhythms is localized in the suprachiasmatic nuclei (SCN) of the hypothalamus. The SCN is responsible for orchestrating circadian clocks in peripheral organs to regulate physiological functions such as behavior, sleep, body temperature, blood pressure, and hormone release (Herzog and Tosini 2001). Accumulating evidence indicates that dysfunction of the circadian rhythms due to genetic mutations or environmental factors (i.e., jet lag or shift work) may contribute to the development of many serious diseases, including cancer and type 2 diabetes (Evans and Davidson 2013).

The retinal circadian clock was the first extra-SCN circadian oscillator to be discovered in mammals (Tosini and Menaker 1996). The molecular clockwork mechanism of the retinal clock is similar to what has been reported for the SCN (Tosini et al. 2008), albeit it appears that the retinal clock is less robust (Ruan et al. 2012; Jaeger et al. 2015). Several studies have also established that many aspects of retinal physiology and function are under the control of retinal circadian clocks (see McMahon et al. 2014 for a review), and new experimental evidence suggests that other ocular structures (e.g., cornea, retinal pigment epithelium) also possess circadian clocks that control important physiological functions (Yoo et al. 2005; Baba et al. 2010, 2015; Buhr et al. 2015). Interestingly, as seen in the SCN, it appears that the neural retina communicates the photic information to the other ocular structures via humoral signals (e.g., melatonin and dopamine; Ruan et al. 2008; Baba et al. 2015) since most of these ocular structures are not capable of direct light transduction (Baba et al. 2010).

## 42.2 The Retinal Circadian Clock and Ocular Health

Similar to molecular circadian clock in SCN, the retinal clock also consists of autoregulatory transcriptional/translational negative feedback loops involving several clock genes and their protein products which generate approximately 24 h cycle. The primary core loop involves two basic helix-loop-helix-PAS domain transcription factors, BMAL1 and CLOCK, which heterodimerize and bind to E-box elements in promoter region to enhance transcription of *Period 1* and *2* and *Cryptochrome 1*and *2*. The protein products, PERIOD and CRYPTOCHROME, together then inhibit their own transcription by blocking CLOCK-/BMAL1-mediated transactivation (see Tosini et al. 2008, Fig. 1, for a schematic illustration). The second feedback loop involves the negative and positive transactivation of five other genes, *Rev-erb α* and *Rev-erb β* and *Ror α*, *Ror β*, and *Ror c* via REV-ERB/ROR response element (RRE) promoter elements in promoter regions. REV-ERB as a negative element inhibits *Clock* and *Bmal1* transcription, whereas ROR as a positive element promotes *Clock* and *Bmal1* transcription. The transcriptions of *Rev-erb*s and *Ror*s are regulated via E-box elements in their promoter regions. REV-ERBs and RORs

compete for binding to RRE in the *Bmal1* promoter regions to regulate rhythmic expression of *Bmal1*. These intertwining oscillation signals also regulate transcription of other clock-controlled genes via E-box or RRE elements, and the products of these genes serve as circadian clock outputs (Takahashi et al. 2008). In the mouse, clock genes are rhythmically expressed in the different retinal layers (Hiragaki et al. 2014). In the photoreceptor layer, only the cones appear to express all the circadian clock proteins (Lui et al. 2012).

Emerging evidence suggests that retinal circadian clocks and their output signals contribute to retinal disease and pathology, as well as normal retinal function. For example, diabetic retinopathy is associated with reduced clock gene expression in the retina (Busik et al. 2009), circadian disruption recapitulates diabetic retinopathy in mice (Bhatwadekar et al. 2013), and removal of *Period2* induces dysfunction in the retinal microvasculature (Jadhav et al. 2016).

Trophic signaling by the retinal clock and its outputs seems to play a role in the regulation of eye growth and refractive errors (reviewed in Stone et al. 2013). A recent study has also reported that mice lacking *Period1* and *Period2* show significant alteration in the distribution of cone photoreceptors (Ait-Hmyed et al. 2013) and mice lacking *Rev-erb α* show a significant alteration in photoreceptor response to light (Ait-Hmyed et al. 2016).

Finally, it is worth mentioning that the retinal clock influences the susceptibility of photoreceptors to light-induced damage (Organisciak et al. 2000), and recent genomic studies have also implicated the clock genes *Rev-erb* α and *Rora* in retinal functioning (Mollema et al. 2011) and age-related macular degeneration (Jun et al. 2011).

## 42.3 Bmal1 and Retinal Cell Viability

As previously mentioned, *Bmal1* gene (also known as *Arntl*) is a key component of the mammalian circadian clock. *Bmal1* knockout mice (*Bmal1*$^{-/-}$) do not show any circadian rhythmicity (Bunger et al. 2000) and develop several pathologies (Kondratov et al. 2006). *Bmal1*$^{-/-}$ mice show premature aging and their lifespan is significantly reduced (about 9 months) (Kondratov et al. 2006). In the mouse retina, *Bmal1* is expressed in many cell types (Ruan et al. 2008), but within the photoreceptor layer, BMAL1 was only detected in the cones (Liu et al. 2012). Storch et al. (2007) reported that many genes (more than a thousand) show a daily rhythm in mouse retina, but a large fraction of these genes are no longer rhythmically expressed or have reduced amplitude in *Bmal1*$^{-/-}$ mice. In *Bmal1*$^{-/-}$ mice, the day/night (circadian) changes in the amplitude of the photopic b-wave are no longer present (Storch et al. 2007). The same result has been also obtained from the mice lacking *Bmal1* only in the retina (*Chx10-Cre-Arntl*$^{loxP/loxP}$ mice; Storch et al. 2007), thus indicating that retinal *Bmal1* is required for the circadian rhythm in visual processing. Interestingly, the photoreceptors of these mice (2–3 months) appear to be normal and unaffected by the lack of *Bmal1* (Storch et al. 2007). Additional studies have reported that in mice lacking the *Bmal1* gene, there is a significant increase in the rate of cataract development and corneal inflammation during aging (Kondratov et al. 2006).

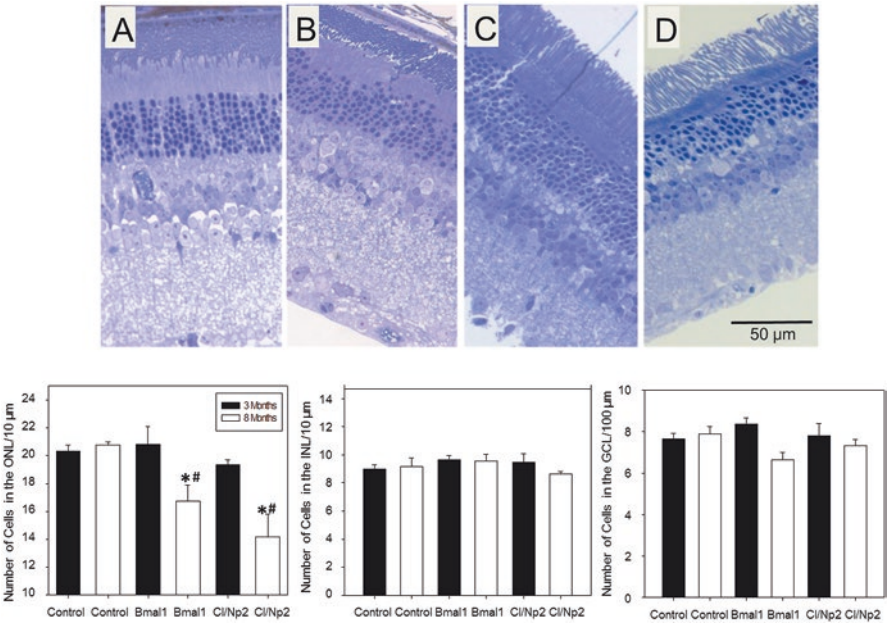


**Fig. 42.1** The microphotographs in **a**, **b**, **c**, and **d** represent a typical example of a section obtained from 3-month-old *Bmal1* KO (**a**), 8-month-old *Bmal1* KO (**b**), 3-month-old *Clock/Npas2* KO (**c**), and 8-month-old *Clock/Npas2* KO (**d**) Morphometric analysis of retinas obtained from young (3 months old, black bars) and old (8 months old, white bars) of control, *Bmal1*$^{-/-}$, and *Clock*$^{-/-}$/*Npas2*$^{-/-}$ (*Cl/Np2*) mice. The number of cells in the ONL of 8-month-old *Bmal1* (**b**) and *Clock/Npas2* KOs (**d**) was significantly lower than the number of cells in 3-month-old mice (**a**, **c**) of the same genotype (one-way ANOVA following post hoc test $^{*}p < 0.05$) and age-matched control group ($^{\#}p < 0.05$). No differences in the number of cells were observed in the INL and/or GCL ($n = 3$–4). The number of cells in the ONL of young *Bmal1* and *Clock/Npas2* KO mice was not different from the number of cells in control mice of the same genotype (C57BL/6).

Previous studies have shown that the effects of circadian disruption become evident during the aging process (Baba et al. 2009; Musiek et al. 2013). Hence we decided to investigate whether removal of the *Bmal1* gene affects retinal cell viability during aging. Eyes from *Bmal1*$^{-/-}$ and control mice at two different ages (3 months and 7–8 months) were obtained, and then the morphometric analysis of the retina was performed according to a well-established method in our laboratory (see Baba et al. 2009 for details). As expected, and previously reported by Storch et al. (2007), young *Bmal1*$^{-/-}$ did not show any significant variation in the number of cells in the outer nuclear layer or in any other retinal layers (Fig. 42.1), whereas in older *Bmal1*$^{-/-}$ mice, we observed a significant reduction in the number of photoreceptor cell nuclei (about 20–30%) with respect to control. No changes were detected in the other retinal layers (Fig. 42.1). Previous studies have shown that *Bmal1* can interact with a large number of genes (more than 1000), and therefore the phenotypes observed in *Bmal1* KOs may or may not be the consequence of a dysfunctional circadian clock (Rey et al. 2011). Thus we decided to investigate the retinal morphometry in another mouse model in which the circadian clock has been

disabled. A previous investigation reported that *Clock/Npas2* KO mice do not have a functional circadian clock (DeBruyne et al. 2007; Musiek et al. 2013). Eyes from young (3 months) and old (9 months) *Clock/Npas2* KO mice were obtained from Dr. David Weaver's laboratory (University of Massachusetts Medical School), and the retinal morphometry was investigated using the same method mentioned for *Bmal1*$^{-/-}$ mice retinas. As shown in Fig. 42.1, *Clock/Npas2* KO mice showed an almost identical phenotype as *Bmal1*$^{-/-}$ animals. The fact that almost identical results were obtained in *Bmal1* and *Clock/Npas2* KOs indicates that the reduced photoreceptor viability observed in *Bmal1*$^{-/-}$ is likely due to lack of a functional circadian clock in these cells and not to a possible pleiotropic effect of *Bmal1*. Our preliminary data indicate that dysfunctions of circadian clock genes may affect the photoreceptor cell viability during aging.

## 42.4 Conclusions

The circadian clock is responsible for a wide variety of physiological functions, and a large number of studies have now demonstrated that retinal circadian clocks regulate many functions in the eye. Experimental evidence also suggests that dysfunction of the retinal clocks may promote ocular diseases. In addition, our preliminary data indicate that genetic removal of clock genes affects photoreceptor viability during aging. Further studies are required to fully understand the role of circadian clock and its associated gene product in the regulation of retinal function and health.

**Acknowledgments** Research in the author's laboratories is supported by NIH grants GM116760 to KB, EY018640 to CR, R01EY004864 and P30EY006360 to PMI, EY022216, EY026291 to GT, and an unrestricted departmental grant from Research to Prevent Blindness (Emory Department of Ophthalmology).

## References

Ait-Hmyed HO, Felder-Schmittbuhl MP, Garcia-Garrido M et al (2013) Mice lacking Period 1 and Period 2 circadian clock genes exhibit blue cone photoreceptor defects. Eur J Neurosci 37:1048–1060

Ait-Hmyed HO, Acar N, Savier E et al (2016) Rev-Erbα modulates retinal visual processing and behavioral responses to light. FASEB J pii:fj.201600414R

Baba K, Pozdeyev N, Mazzoni F et al (2009) Melatonin modulates visual function and cell viability in the mouse retina via the MT1 melatonin receptor. Proc Natl Acad Sci U S A 106:15043–15048

Baba K, Sengupta A, Tosini M et al (2010) Circadian regulation of the PERIOD 2::LUCIFERASE bioluminescence rhythm in the mouse retinal pigment epithelium-choroid. Mol Vis 16:2605–2611

Baba K, Davidson AJ, Tosini G (2015) Melatonin entrains PER2::LUC bioluminescence circadian rhythm in the mouse cornea. Invest Ophthalmol Vis Sci 56:4753–4758

Bhatwadekar AD, Yan Y, Qi X et al (2013) Per2 mutation recapitulates the vascular phenotype of diabetes in the retina and bone marrow. Diabetes 62:273–282

Buhr ED, Yue WW, Ren X et al (2015) Neuropsin (OPN5)-mediated photoentrainment of local circadian oscillators in mammalian retina and cornea. Proc Natl Acad Sci U S A 112:13093–13098
Bunger MK, Wilsbacher LD, Moran SM et al (2000) Mop3 is an essential component of the master circadian pacemaker in mammals. Cell 103:1009–1017
Busik JV, Tikhonenko M, Bhatwadekar A et al (2009) Diabetic retinopathy is associated with bone marrow neuropathy and a depressed peripheral clock. J Exp Med 206:2897–2906
DeBruyne JP, Weaver DR, Reppert SM (2007) CLOCK and NPAS2 have overlapping roles in the suprachiasmatic circadian clock. Nat Neurosci 10(5):543
Evans JA, Davidson AJ (2013) Health consequences of circadian disruption in humans and animal models. Prog Mol Biol Transl Sci 119:283–323
Herzog ED, Tosini G (2001) The mammalian circadian clock shop. Semin Cell Dev Biol 4:295–303
Hiragaki S, Baba K, Coulson E et al (2014) Melatonin signaling modulates clock genes expression in the mouse retina. PLoS One 9:e106819
Jadhav V, Luo Q, Dominguez JM 2nd et al (2016) Per2-mediated vascular dysfunction is caused by the upregulation of the connective tissue growth factor (CTGF). PLoS One 9:e0163367
Jaeger C, Sandu C, Malan A et al (2015) Circadian organization of the rodent retina involves strongly coupled, layer-specific oscillators. FASEB J 4:1493–1504
Jun G, Nicolaou M, Morriso MA et al (2011) Influence of ROBO1 and RORA on risk of age-related macular degeneration reveals genetically distinct phenotypes in disease pathophysiology. PLoS One 6:e25775
Kondratov RV, Kondratova AA, Gorbacheva VY et al (2006) Early aging and age-related pathologies in mice deficient in BMAL1, the core component of the circadian clock. Genes Dev 20:1868–1873
Liu X, Zhang Z, Ribelayga CP (2012) Heterogeneous expression of the core circadian clock proteins among neuronal cell types in mouse retina. PLoS One 11:e50602
McMahon DG, Iuvone PM, Tosini G (2014) Circadian organization of the mammalian retina: from gene regulation to physiology and diseases. Prog Retin Eye Res 39C:58–76
Mollema NJ, Yuan Y, Jelcick AS et al (2011) Nuclear receptor Rev-erb alpha (Nr1d1) functions in concert with Nr2e3 to regulate transcriptional networks in the retina. PLoS One 6:e17494
Musiek ES, Lim MM, Yang G et al (2013) Circadian clock proteins regulate neuronal redox homeostasis and neurodegeneration. J Clin Invest 123:5389–5400
Organisciak DT, Darrow RM, Barsalou L et al (2000) Circadian-dependent retinal light damage in rats. Invest Ophthalmol Vis Sci 41:3694–3701
Rey G, Cesbron F, Rougemont J et al (2011) Genome-wide and phase-specific DNA-binding rhythms of BMAL1 control circadian output functions in mouse liver. PLoS Biol 9:e1000595
Ruan GX, Allen GC, Yamazaki S et al (2008) An autonomous circadian clock in the inner mouse retina regulated by dopamine and GABA. PLoS Biol 6:e249. Ken this is not the right paper. The right one is the 2006 PNAS
Ruan GX, Gamble KL, Risner ML et al (2012) Divergent roles of clock genes in retinal and suprachiasmatic nucleus circadian oscillators. PLoS One 6:e3898
Stone RA, Pardue MT, Iuvone PM et al (2013) Pharmacology of myopia and potential role for intrinsic retinal circadian rhythms. Exp Eye Res 114:35–47
Storch KF, Paz C, Signorovitch J et al (2007) Intrinsic circadian clock of the mammalian retina: importance for retinal processing of visual information. Cell 130:730–741
Takahashi JS, Hong HK, Ko CH et al (2008) The genetics of mammalian circadian order and disorder: implications for physiology and disease. Nat Rev Genet 10:764–775
Tosini G, Menaker M (1996) Circadian rhythms in cultured mammalian retina. Science 272:419–421
Tosini G, Pozdeyev N, Sakamoto K et al (2008) The circadian clock system in the mammalian retina. BioEssays 30:624–633
Yoo SH, Ko CH, Lowrey PL (2005) A noncanonical E-box enhancer drives mouse Period2 circadian oscillations in vivo. Proc Natl Acad Sci U S A 102:2608–2613

# Chapter 43
# The Role of c-Jun N-Terminal Kinase (JNK) in Retinal Degeneration and Vision Loss


**Byung-Jin Kim and Donald J. Zack**

**Abstract** c-Jun N-terminal kinase (JNK), a member of stress-induced mitogen-activated protein (MAP) kinase family, has been shown to modulate a variety of biological processes associated with neurodegenerative pathology of the retina. In particular, various retinal cell culture and animal models related to glaucoma, age-related macular degeneration (AMD), and retinitis pigmentosa indicate that JNK signaling may contribute to disease pathogenesis. This mini-review discusses the impact of JNK signaling in retinal disease, with a focus on retinal ganglion cells (RGCs), photoreceptor cells, retinal pigment epithelial (RPE) cells, and animal studies, with particular attention to modulation of JNK signaling as a potential therapeutic target for the treatment of retinal disease.

**Keywords** c-Jun N-terminal Kinase (JNK) · Retinal degeneration · Retinal ganglion cell (RGC) · Optic neuropathy · Retinal pigmented epithelial (RPE) cell · Age-related macular degeneration (AMD) · Photoreceptor cells · Retinitis pigmentosa · Therapeutic target

## 43.1 Introduction

The activation of mitogen-activated protein (MAP) kinase family, including extracellular signal-regulated kinase (ERK), p38, and c-Jun N-terminal kinase (JNK), is often observed, playing a critical role in fate-determining process of neuronal cells (Kyosseva 2004). Together with p38, JNK is known as a stress-induced MAP kinase, which is involved in neuronal development as well as degenerative diseases such as Alzheimer's disease and Parkinson's disease (Ries et al. 2008; Sclip et al. 2014). The intracellular signaling cascade of JNK is initiated by many stressors followed by subsequent activation of downstream

B. -J. Kim · D. J. Zack (✉)
The Wilmer Eye Institute, Johns Hopkins University, School of Medicine, Baltimore, MD, USA
e-mail: dzack@jhmi.edu



J. D. Ash et al. (eds.), *Retinal Degenerative Diseases*, Advances in Experimental Medicine and Biology 891, https://doi.org/10.1007/978-3-319-75402-4_43

signaling molecules (Barr and Bogoyevitch 2001; Weston and Davis 2002). These molecular events result in various gene transcription and following diverse biological outcomes, which promote the next step of disease progression (Mizuno et al. 2005; Morishima et al. 2001; Podkowa et al. 2010). The retina is comprised of several types of neurons, glial, and other supporting cells. The retina receives visual information, converts it into a neurochemical signal by phototransduction, initiates signal processing, and transmits the signal information to the brain via the optic nerve (Heavner and Pevny 2012). Dysfunction and/or death of many of the cells involved in this complex process, whether due to abnormalities in development or due to later disease processes, can result in vision loss and even blindness. To both better understand and develop improved methods to prevent and treat visual loss, numerous studies have been directed at understanding the molecular mechanisms of injury in the visual system. In this review, we will summarize current knowledge on the role of the c-JNK signaling pathway on retinal degeneration.

## 43.2 JNK Signaling and Axonal Degeneration of RGC Related to Glaucoma and Other Diseases

Retinal ganglion cells (RGCs) transmit visual information from bipolar cells to vision relay centers in the brain, such as the lateral geniculate nucleus (LGN) and superior colliculus (SC), and ultimately to the visual cortex (Yu et al. 2013). Injury and death of RGCs, which together constitute the so-called optic neuropathies, are a major cause of vision loss and blindness worldwide (Quigley 1999). The impact of JNK and its upstream/downstream pathways in RGC death has been actively investigated using various in vivo models of optic nerve disease, such as neuronal excitotoxicity by NMDA (Bessero et al. 2010), experimental optic nerve crush (ONC) (Fernandes et al. 2012; Welsbie et al. 2013), and retinal ischemic injury (Kim et al. 2016; Roth et al. 2003). In particular, Fernandez and colleagues demonstrated that combined deletion of JNK2 and JNK3 inhibited RGC death with long-term protection after ONC injury, and a similar effect was shown by conditional deletion of JUN, a downstream signaling molecule of JNK (Fernandes et al. 2012). In addition, blocking upstream signaling of JNK led to significantly decreased JNK activation that was associated with enhanced RGC survival following ONC (Welsbie et al. 2013). Similar results have been reported with cell death caused by ischemic injury (Biousse and Newman 2014), a disorder of the inner retinal blood supply which results in a temporary or persistent ischemic environment for RGCs, resulting in cell death.(Havens and Gulati 2016; Sugawara et al. 2004). As with the other conditions described above, ischemic injury also upregulates JNK activation in inner retinal layer cells, including RGCs (Roth et al. 2003), and results in RGC death accompanied with progressive inner retinal remodeling (Kim et al. 2013). Importantly, several studies

suggest that pharmacological inhibition of JNK activation can significantly increase RGC viability and prevented inner retinal degeneration (Kim et al. 2016). In particular, Kim et al. demonstrated that ischemia/reperfusion (I/R) triggered JNK activation in various cells in the inner retinal layers and RGC axonal loss were significantly inhibited by administration of SP600125. This finding suggested that activation of JNK plays a pivotal role in RGC death (Kim et al. 2016). In this study, Kim and colleagues also showed that ischemic injury initiated early JNK activation in RGC as well as non-RGC cells in the NFL/RGC layer at later post-injury time, which suggests that RGCs may be the most susceptible cell type for ischemic injury. In addition, this finding also suggested that ischemic injury possibly triggers JNK activation in non-RGCs in the NFL/RGC layer such as displaced amacrine cells and astrocytes. One interesting observation related to this finding is that the role of JNK may be different in different retinal cell types treated with the same pathological impact. For example, Dvoriantchikova and Ivanov showed that RGCs treated with the proinflammatory cytokine tumor necrosis factor (TNF) did not demonstrate NF-kB activation but showed sustained JNK activation (Dvoriantchikova and Ivanov 2014). In contrast, TNF-treated astrocytes showed induced NF-kB activation with transient JNK activation, which was associated with prolonged astrocyte survival. Taken together, these findings indicate that JNK inhibitors may be an interesting class of pharmacological molecules for promoting RGC survival through inhibiting JNK activation to prevent RGC death and simultaneously inhibiting proinflammatory responses in glial cells.

## 43.3 JNK Signaling and Retinal Pigment Epithelium Cells: Possible Relationship with Age-Related Macular Degeneration

Retinal pigment epithelial (RPE) cells are a retinal cell type underlying and supporting photoreceptor cells through various functions to maintain functional and structural integrity (Boulton and Dayhaw-Barker 2001; Strauss 2005). The biological aspects RPE cells in human diseases have been actively investigated, particularly in age-related macular degeneration (AMD) (Young 1987). AMD is a leading cause of vision loss in the elderly in the United States and other developed Western countries (Gehrs et al. 2006), associated with multiple mechanisms and risk factors of AMD (Gehrs et al. 2006; Tan et al. 2016). AMD can be categorized into two broad types in late stage, a non-neovascular (dry) form and a neovascular (wet) form (Gehrs et al. 2006). The non-neovascular form is more common, but the neovascular form is generally associated with more severe vision loss. Neovascular AMD is characterized by aberrant choroidal neovascularization mediated, at least in part, by the angiogenic growth factor vascular endothelial growth factor (VEGF). In the retina, VEGF both

stimulates neovascularization and increases vascular permeability, resulting in abnormalities in the macular region that are associated with central vision loss (Gehrs et al. 2006). Among other important roles that the RPE plays in AMD pathogenesis, RPE cells constitutively produce VEGF, and they show increased production in response to pathologic conditions (Blaauwgeers et al. 1999; Holtkamp et al. 2001). Importantly, JNK has been suggested as a key signaling molecule promoting VEGF expression through phosphorylation of c-Jun and binding to the VEGF promotor mediating neovascularization (Du et al. 2013; Guma et al. 2009). Dry AMD, characterized by regional loss of RPE cells followed by photoreceptor cell dysfunction and cell loss, is currently untreatable (Ambati and Fowler 2012; Gehrs et al. 2006). To better understand RPE cell death mechanisms, in vitro studies of primary human RPE cells and cell lines have been widely used to define JNK-associated RPE cell death under various pathologic conditions (Cao et al. 2012; Roduit and Schorderet 2008; Westlund et al. 2009). Despite these many studies, the role of JNK in RPE viability remains controversial. Cao and colleagues showed that ultraviolet B radiation induced apoptotic cell death of the ARPE-19 RPE cell line. Surprisingly, inhibition of JNK exacerbated apoptosis, whereas activation of JNK attenuated ARPE-19 cell death, suggesting an anti-apoptotic role of JNK (Cao et al. 2012). In contrast, Roduit et al. reported enhanced RPE cell survival upon JNK inhibition under UV irradiation (Roduit and Schorderet 2008). However, this issue is not resolved and warrants further research.

## 43.4 JNK Signaling and Photoreceptor Degeneration

Many vision diseases associated with photoreceptor loss have been reported, which are briefly categorized into inherited degeneration, such as retinitis pigmentosa, and adaptive degenerations caused by age and other multiple factors, such as AMD (Wright et al. 2010). Notably, nonsyndromic retinitis pigmentosa is highly polygenic, associated with mutation of more than 50 genes (Bowne et al. 2011; Nishiguchi et al. 2013; https://sph.uth.edu/Retnet/). The association of JNK with photoreceptor cell death is relatively less known compared to other retinal cell types. Nonetheless, several in vitro and animal models have suggested a role of JNK as a mediator of photoreceptor cell death, initiated by various genetic and environmental factors. Using the photoreceptor cell line 661 W, Choudhury showed that reprogramming of the unfolded protein response (UPR) by genetic deletion of caspase 7 resulted in a decrease of JNK-induced apoptosis (Choudhury et al. 2013). This finding suggested that JNK is an important apoptotic mediator of UPR, which is known as a major causative process of photoreceptor cell death in some forms of retinitis pigmentosa (Galy et al. 2005; Kang et al. 2012). These findings indicate that JNK may play an important role in photoreceptor cell death.

## 43.5 Conclusions: JNK Signaling Pathway as a Potential Therapeutic Target in Retinal Degenerative Disease?

In summary, as described above, apoptosis of a variety of retinal cells is associated with activation of the JNK pathway. In addition, in a number of different retinal degeneration models, genetic and pharmacological inhibition of JNK signaling results in protection from cell death and reduced pathologic progression. As a common mediator of retinal cell death, pharmacological inhibition of JNK, or associated family members, may provide a pathway for a "generic" treatment strategy that is relatively independent of the specific genetic mutation causing the disease. Additionally, JNK inhibition strategies may provide a complementary treatment approach to gene-specific therapies. For these reasons, it seems reasonable to pursue the JNK pathway as a promising target for the development of novel therapeutic strategies for treatment of the photoreceptor degenerative diseases.

## References

Ambati J, Fowler BJ (2012) Mechanisms of age-related macular degeneration. Neuron 75(1):26–39

Barr RK, Bogoyevitch MA (2001) The c-Jun N-terminal protein kinase family of mitogen-activated protein kinases (JNK MAPKs). Int J Biochem Cell Biol 33(11):1047–1063

Bessero AC, Chiodini F, Rungger-Brandle E et al (2010) Role of the c-Jun N-terminal kinase pathway in retinal excitotoxicity, and neuroprotection by its inhibition. J Neurochem 113(5):1307–1318

Biousse V, Newman N (2014) Retinal and optic nerve ischemia. Continuum (Minneap Minn) 20 (4 Neuro-ophthalmology):838–856

Blaauwgeers HG, Holtkamp GM, Rutten H et al (1999) Polarized vascular endothelial growth factor secretion by human retinal pigment epithelium and localization of vascular endothelial growth factor receptors on the inner choriocapillaris. Evidence for a trophic paracrine relation. Am J Pathol 155(2):421–428

Boulton M, Dayhaw-Barker P (2001) The role of the retinal pigment epithelium: topographical variation and ageing changes. Eye (Lond) 15(Pt 3):384–389

Bowne SJ, Sullivan LS, Koboldt DC et al (2011) Identification of disease-causing mutations in autosomal dominant retinitis pigmentosa (adRP) using next-generation DNA sequencing. Invest Ophthalmol Vis Sci 52(1):494–503

Cao G, Chen M, Song Q et al (2012) EGCG protects against UVB-induced apoptosis via oxidative stress and the JNK1/c-Jun pathway in ARPE19 cells. Mol Med Rep 5(1):54–59

Choudhury S, Bhootada Y, Gorbatyuk O et al (2013) Caspase-7 ablation modulates UPR, reprograms TRAF2-JNK apoptosis and protects T17M rhodopsin mice from severe retinal degeneration. Cell Death Dis 4:e528

Du H, Sun X, Guma M et al (2013) JNK inhibition reduces apoptosis and neovascularization in a murine model of age-related macular degeneration. Proc Natl Acad Sci U S A 110(6):2377–2382

Dvoriantchikova G, Ivanov D (2014) Tumor necrosis factor-alpha mediates activation of NF-κB and JNK signaling cascades in retinal ganglion cells and astrocytes in opposite ways. Eur J Neurosci 40(8):3171–3178

Fernandes KA, Harder JM, Fornarola LB et al (2012) JNK2 and JNK3 are major regulators of axonal injury-induced retinal ganglion cell death. Neurobiol Dis 46(2):393–401

Galy A, Roux MJ, Sahel JA et al (2005) Rhodopsin maturation defects induce photoreceptor death by apoptosis: a fly model for RhodopsinPro23His human retinitis pigmentosa. Hum Mol Genet 14(17):2547–2557

Gehrs KM, Anderson DH, Johnson LV et al (2006) Age-related macular degeneration--emerging pathogenetic and therapeutic concepts. Ann Med 38(7):450–471

Guma M, Rius J, Duong-Polk KX et al (2009) Genetic and pharmacological inhibition of JNK ameliorates hypoxia-induced retinopathy through interference with VEGF expression. Proc Natl Acad Sci U S A 106(21):8760–8765

Havens SJ, Gulati V (2016) Neovascular Glaucoma. Dev Ophthalmol 55:196–204

Heavner W, Pevny L (2012) Eye development and retinogenesis. Cold Spring Harb Perspect Biol 4(12):a008391

Holtkamp GM, Kijlstra A, Peek R et al (2001) Retinal pigment epithelium-immune system interactions: cytokine production and cytokine-induced changes. Prog Retin Eye Res 20:29–48

Kang MJ, Chung J, Ryoo HD (2012) CDK5 and MEKK1 mediate pro-apoptotic signalling following endoplasmic reticulum stress in an autosomal dominant retinitis pigmentosa model. Nat Cell Biol 14(4):409–415

Kim BJ, Braun TA, Wordinger RJ et al (2013) Progressive morphological changes and impaired retinal function associated with temporal regulation of gene expression after retinal ischemia/reperfusion injury in mice. Mol Neurodegener 8:21

Kim BJ, Silverman SM, Liu Y et al (2016) In vitro and in vivo neuroprotective effects of cJun N-terminal kinase inhibitors on retinal ganglion cells. Mol Neurodegener 11:30

Kyosseva SV (2004) Mitogen-activated protein kinase signaling. Int Rev Neurobiol 59:201–220

Mizuno N, Kokubu H, Sato M et al (2005) G protein-coupled receptor signaling through Gq and JNK negatively regulates neural progenitor cell migration. Proc Natl Acad Sci U S A 102(35):12365–12370

Morishima Y, Gotoh Y, Zieg J et al (2001) Beta-amyloid induces neuronal apoptosis via a mechanism that involves the c-Jun N-terminal kinase pathway and the induction of Fas ligand. J Neurosci 21(19):7551–7560

Nishiguchi KM, Tearle RG, Liu YP et al (2013) Whole genome sequencing in patients with retinitis pigmentosa reveals pathogenic DNA structural changes and NEK2 as a new disease gene. Proc Natl Acad Sci U S A 110(40):16139–16144

Podkowa M, Zhao X, Chow CW et al (2010) Microtubule stabilization by bone morphogenetic protein receptor-mediated scaffolding of c-Jun N-terminal kinase promotes dendrite formation. Mol Cell Biol 30(9):2241–2250

Quigley HA (1999) Neuronal death in glaucoma. Prog Retin Eye Res 18(1):39–57

Ries V, Silva RM, Oo TF et al (2008) JNK2 and JNK3 combined are essential for apoptosis in dopamine neurons of the substantia nigra, but are not required for axon degeneration. J Neurochem 107(6):1578–1588

Roduit R, Schorderet DF (2008) MAP kinase pathways in UV-induced apoptosis of retinal pigment epithelium ARPE19 cells. Apoptosis 13(3):343–353

Roth S, Shaikh AR, Hennelly MM et al (2003) Mitogen activated protein kinases and retinal ischemia. Invest Ophthalmol Vis Sci 44(12):5383–5395

Sclip A, Tozzi A, Abaza A et al (2014) c-Jun N-terminal kinase has a key role in Alzheimer disease synaptic dysfunction in vivo. Cell Death Dis 5:e1019

Strauss O (2005) The retinal pigment epithelium in visual function. Physiol Rev 85(3):845–881

Sugawara T, Fujimura M, Noshita N et al (2004) Neuronal death/survival signaling pathways in cerebral ischemia. NeuroRx 1(1):17–25

Tan PL, Bowes Rickman C, Katsanis N (2016) AMD and the alternative complement pathway: genetics and functional implications. Hum Genomics 10(1):23

Welsbie DS, Yang Z, Ge Y et al (2013) Functional genomic screening identifies dual leucine zipper kinase as a key mediator of retinal ganglion cell death. Proc Natl Acad Sci U S A 110(10):4045–4050

Westlund BS, Cai B, Zhou J et al (2009) Involvement of c-Abl, p53 and the MAP kinase JNK in the cell death program initiated in A2E-laden ARPE-19 cells by exposure to blue light. Apoptosis 14(1):31–41

Weston CR, Davis RJ (2002) The JNK signal transduction pathway. Curr Opin Genet 12(1):14–21

Wright AF, Chakarova CF, Abd El-Aziz MM et al (2010) Photoreceptor degeneration: genetic and mechanistic dissection of a complex trait. Nat Rev Genet 11(4):273–284

Young RW (1987) Pathophysiology of age-related macular degeneration. Surv Ophthalmol 31(5):291–306

Yu DY, Cringle SJ, Balaratnasingam C et al (2013) Retinal ganglion cells: energetics, compartmentation, axonal transport, cytoskeletons and vulnerability. Prog Retin Eye Res 36:217–246

# Chapter 44
# The Evaluation of BMI1 Posttranslational Modifications During Retinal Degeneration to Understand BMI1 Action on Photoreceptor Death Execution


**Martial K. Mbefo and Yvan Arsenijevic**

**Abstract** Retinitis Pigmentosa (RP) is a class of hereditary retinal dystrophy associated with gradual visual failure and a subsequent loss of light-sensitive cells in the retina, leading to blindness. Many mutated genes were found to be causative of this disease. Despite a number of compiling efforts, the process of cell death in photoreceptors remains to be clearly elucidated. We recently reported an abnormal cell cycle reentry in photoreceptors undergoing degeneration in *Rd1* mice, a model of RP, and identified the polycomb repressive complex 1 (PRC1) core component BMI1 as a critical molecular factor orchestrating the cell death mechanism. As the cell death rescue in *Rd1;Bmi-1* KO mice was independent on the conventional *Ink4a/Arf* pathways, we now explored the structural properties of BMI1 in order to examine the differential expression of its posttranslational modifications in *Rd1* retina. Our results suggest that BMI1 cell death induction in *Rd1* is not related to its phosphorylation status. We therefore propose the epigenetic activity of BMI1 as an alternative route for BMI1-mediated toxicity in *Rd1*.

**Keywords** *Rd1* · BMI1 · Posttranslational modifications · Phosphorylation · Polycomb repressive complexes · Retinal degeneration · Epigenetic

## 44.1 Introduction

Cell death process in highly specialized cells such as neurons and photoreceptors has so far been at the center of constructive debates to understand the successive molecular event steps and to define those occurring in parallel, but the complexity

M. K. Mbefo · Y. Arsenijevic (✉)
Unit of Gene Therapy and Stem Cell Biology, Department of Ophtalmology, Jules-Gonin Eye Hospital, University of Lausanne, Lausanne, Switzerland
e-mail: yvan.arsenijevic@fa2.ch



J. D. Ash et al. (eds.), *Retinal Degenerative Diseases*, Advances in Experimental Medicine and Biology 891, https://doi.org/10.1007/978-3-319-75402-4_44

of the process raises many questions to solve. Although the initiating hits are different in neurodegenerative disease such as Alzheimer's and Parkinson's disease or in amyotrophic lateral sclerosis, some common mechanisms are activated during the cell death process (Soto and Estrada 2008). Similarly, investigating the mechanistic events orchestrating photoreceptor cell death in retinal dystrophies (RD) has gained increasing attention in revealing certain common pathways that participate to the cell death process after some steps of cell regulation alterations.

As DNA fragmentation and pro-inflammatory responses occur in absence of certain classical actors of apoptosis, it is clear that the degenerative process in photoreceptors is not common and different denominations of cell death process were proposed such as necroptosis (Barabino et al. 2016; Murakami et al. 2012). In 2014, Erkström and his group have developed mathematical models for the better understanding of the temporal process that underlies cell death in *Rd1* model. Analysis of the results, obtained from organotypic retinal explant culture that mimics the *Rd1* degeneration using the zaprinast drug to block the PDE6β to mimic the *Rd1* model, provided strong evidence that at least 80 h was required for the completion of cell death in *Rd1* mice (Sahaboglu et al. 2013). Therefore, the data rule out the normal process described until now for necrosis or apoptosis in which DNA fragmentation occurs within 1 h or the next 24 h respectively (Zong and Thompson 2006; Oppenheim et al. 2001).

We and other research groups (Gardiner et al. 2016) have recently demonstrated an accumulation of the cyclin-dependent kinases (CDKs) and many other components of the cell cycle throughout the outer nuclear layer (ONL), where the photoreceptors reside, during the temporal manifestation of cell death. The interests behind this observation are inherent on the fact that many RD rodent models exhibited enhanced expression of such markers (Zencak et al. 2013). Genetic deletion of *Bmi1*, regulating the cell cycle signaling pathway, significantly delays cell death and generated the most potent photoreceptor rescue that was never achieved in vitro and in vivo for the *Rd1* model (Zencak et al. 2013). Unfortunately, the drawback behind *Bmi1* is that the KO mouse is viable but not healthy, displaying severe neuronal disorders associated with impaired cerebellar formation (ataxia), loss of synapsis connections, axon demyelination, as well as deficit of glutamate transporters with subsequent neurodegenerative processes (Cao et al. 2012). This suggests a meaningless benefit in targeting the *Bmi1* gene for long-term therapeutic approaches against RP. To this end, studies have been carried out in order to screen for BMI1 downstream targets to potentially identify more promising pathway for gene therapy or drug delivery applications. Preliminary results from these studies have shown that BMI1 toxicity is independent to the classical *Ink4a/Arf* pathways, highlighting the complexity surrounding the *Bmi1* biology in vivo.

Accordingly, BMI1 posttranslational modification and its potential effect during retinal degeneration in *Rd1* are yet to be investigated. Importantly, phosphorylation of BMI1 at S316 has been reported to suppress its ability to transform the mouse embryonic fibroblast cells in vitro (Liu et al. 2012) suggesting that such modification may also occur in disease situations.

In this study, we explored the structural properties of BMI1 in *Rd1* at onset of photoreceptor maturation. We further examined the folding state of native

BMI1 by evaluating biochemically its posttranslational modifications, notably phosphorylation, in comparison to the WT retinal extracts. Our preliminary result indicated that BMI1 toxicity is initiated very early during the developmental stages and seems to be independent on its phosphorylation status.

## 44.2 Material and Method

*Mice and livestock* The generation of the FVB-WT, FVB-*Rd1*, mice was described previously (Zencak et al. 2013). All the mice were treated according to the institutional and national as well as the Association for Research in Vision and Ophthalmology (ARVO) guidelines. The experimental procedures were approved by national veterinary authorities.

*Preparation of Tissue homogenate* Freshly dissected retinas from WT and *Rd1* mice were homogenized in lysis buffer made of 50 mM Tris-HCl pH 7.6, 150 mM Nacl, 1 mM EDTA, 0.25% Triton X-100 and 0.25% Nonidet NP40, and proteases inhibitors cocktail (Sigma). Subsequent sonication step at 30% amplitude for 1 s at 4 °C was performed to release the components of the nuclei. Cytoskeleton and debris were pelleted at 14,000 g, 10 min, and stored at −80 °C until the day of analysis.

*Western blotting* Equal amount (twenty micrograms) of tissue homogenate was resolved on 12% polyacrylamide gel electrophoresis. The proteins were then transferred to polyvinylidene fluoride (PVDF) membrane and blocked 1 h with 5% non-fat dried milk in PBS 1X at RT. The primary antibody diluted in blocking buffer +0.1% Tween 20 (PBST) was added for ON at 4 °C. The membrane was incubated 1 h at RT with HRP-conjugated secondary antibody diluted in PBS 0.1% Tween 20. Finally, the highest sensitivity chemiluminescent HRP substrate (Witec AG) was added and the bands revealed with Fujifilm chemiluminescent cassette according to manufacturer's instructions.

## 44.3 Result

*Does* BMI1 *undergo phosphorylation in Rd1*?: In previous studies, we showed that cell death in *Rd1* photoreceptors was in part dependent on BMI1 polycomb ring finger oncogene and that the recruitment of BMI1 in degenerating photoreceptors was, however, independent of the conventional *Ink4a/Arf* pathways, downstream to the BMI1 signaling (Soto and Estrada 2008).

As a follow-up to this observation, we intended to explore the possibilities of BMI1 being structurally affected at some point during the development stage, in order to better understand the complexity behind the toxicity observed (i.e., cell death)

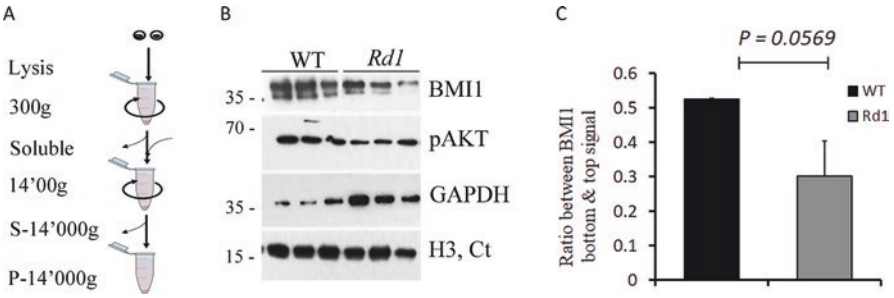


**Fig. 44.1** Conserved BMI1 phosphorylation status in *Rd1*. The left panel summarizes the processing of PN12 retinal extracts analyzed (**A**), whereas BMI1 and its isoforms analyzed by Western blot are shown in the right panel (**B**). (**C**), The degree of BMI1 phosphorylation is expressed as ratio of the integrated density of the bottom band over the top BMI1 band of WT and *Rd1* mice. Data are $n = 3$

with the *Rd1* model. We therefore opened a new avenue toward determining if any alteration at the level of BMI1 metabolism could be somehow critical for the establishment of toxicity.

Given the equal expression levels of *Bmi1* mRNA between age-matched *Rd1* and WT (Zencak et al. 2013), we asked if the toxic effects could be mediated by any differential expression at the protein level and thereby by its posttranslational regulation status. Western blot of total proteome extracted from WT and *Rd1* retinas was used to evaluate the expression levels of all BMI1 species (including truncations if applicable), whereas the migration profile and the visualization of individual bands was an asset for revealing the phosphorylation status, if any, in *Rd1* compared to WT. We focused on BMI1 phosphorylation because it has been shown previously that its activity can be in part mediated by its phosphorylation status (Liu et al. 2012). Using a panel of anti-BMI1-specific antibodies from commercial source, Western blot analysis reveals a band at ~ 36 kDa which is the expected molecular weight of BMI1 (Fig. 44.1A, B, bottom). Moreover, we detected an additional band right above the expected BMI1, which could correspond to the posttranslationally modified form of BMI1. The evaluation of the ratio between the non-phosphorylated and phosphorylated forms in the three animals analyzed barely reaches no significance (Fig. 44.1C), suggesting a potential higher level of non-active form of BMI1 in the *Rd1* retina. The phosphorylation of BMI1 at Ser(316) by AKT upon activation by PI3K has been reported to impair its function, notably its association with chromatin, thereby inhibiting its growth-promoting properties (Liu et al. 2012). In *Rd1* extract, however, the protein levels of pAKT in *Rd1* were slightly lower to that of the WT, and only mild changes of pAKT protein were seen in the three mice analyzed. Altogether, these data indicate that *Bmi1*-mediated toxicity in *Rd1* may be independent of its phosphorylation status as well and suggest additional molecular targets or partners involved in this retinal degeneration model. Interestingly,

however, we noticed enhanced metabolic process in *Rd1* mice as shown by increasing levels of endogenous GAPDH in mutant mice compared to WT.

## 44.4 Discussion

BMI1 *phosphorylation status might be identical in Rd1 and* WT *mice at PN12*. In this report, we attempted to explore the possibilities of BMI1 being posttranslationally modified during the course of *Rd1* pathophysiology. Posttranslational modifications account for biological processes that play a role in maintaining protein homeostasis in the cellular microenvironment. Alteration in proper metabolism of several proteins can affect their folding capacity, with deleterious consequences like in a number of neuronal disorders such as Parkinson's and Alzheimer's diseases (Soto and Estrada 2008). The exact mechanism by which *Bmi1* mediates toxicity in *Rd1* is still unsolved, although we already showed that the deletion of *Bmi1* in the *Rd1* mouse markedly reduces the CDK4 level in the ONL. In this study, we hypothesized a BMI1 gain of function consecutive to a post-processing modification of the protein in *Rd1* retina. The fact that we did not observe such changes in BMI1 between *Rd1* and WT at this stage does not necessarily fully refute our hypothesis. This is because the method that we used to identify BMI1 species in this study may not be enough sensitive to properly cover the BMI1 posttranslational modifications. Moreover, we may have to consider different time points during the temporal manifestation of the disease in order to investigate whether phosphorylated form of BMI1 is more abundant at a precise degenerative time frame as well. In parallel, other powerful and more sophisticated biophysical approaches will be employed to reveal other possible modifications. We thus still need to prospect whether a BMI1 modification may account to promote its interaction with DNA, thereby producing dramatic epigenetic changes that may be driven the cell death process encountered in this RP model.

*A possible mechanism of Bmi1 induced toxicity in Rd1 mice.* In view of our progress in elucidating the molecular mechanism of *Bmi1* dependent toxicity in *Rd1* (see also (Zencak et al. 2013)), the bona fide target remains to be identified. BMI1 is the core component of the polycomb repressive complex 1 (PRC1), one of the two well-defined PcG complexes that regulate gene activity via chromatin remodeling. The primary activity of the PRC1 is the mono-ubiquitination of H2A at Lys119, in which BMI1 plays an essential role as catalyst, stimulating the E3 ligase activity of RING1B (Cao et al. 2005). The core component of PRC2 is composed of embryonic ectoderm development (EED), suppressor of zeste 12 homolog (SUZ12), and enhancer of zeste 2 (EZH2) which is critical for the methyltransferase activity on H3K27 (Margueron and Reinberg 2011). There is strong evidence from the litera-

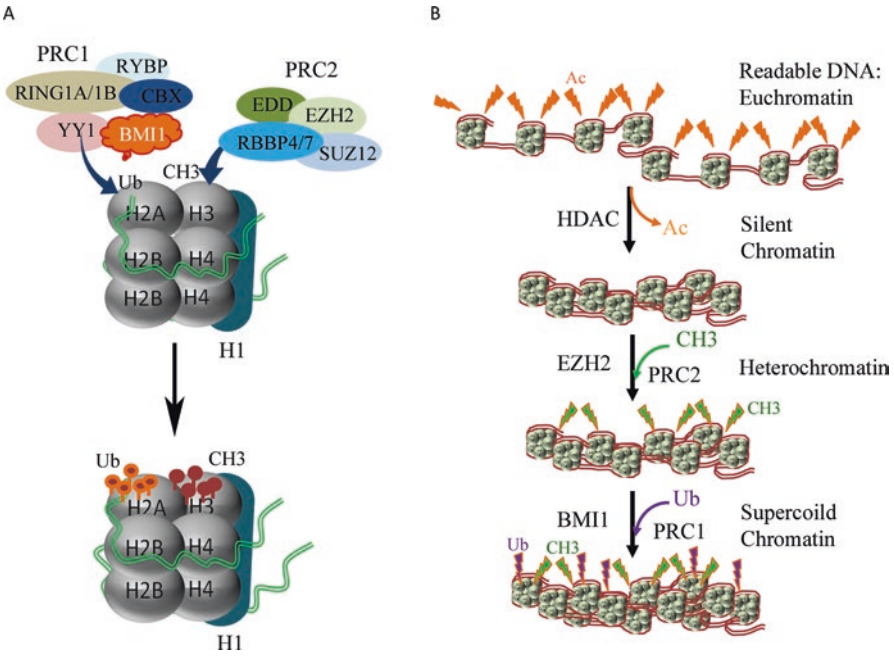


**Fig. 44.2** Prospected epigenetic changes occurring in *Rd1*. Schematic representation of PRC1- and PRC2-dependent posttranslational modifications of H2A and H3K27 (**A**). EZH2 and BMI1 activities are required for the formation of supercoiled chromatin and may be accelerated in *Rd1* mutants (**B**). This model however does not exclude the possibilities that the PRC1 complex can first bind the chromatin before recruitment of PRC2 for H3K27 tri-methylation

ture that gene repression upon PcG is achieved by a synergistic interaction between PRC1 and PRC2 (Kuzmichev et al. 2002). Given the central role of BMI1 in regulating the PcG activities, and considering the impact that alteration in chromatin signature can provoke in health and disease, it is perhaps worth it to consider a similar scenario in retinal dystrophies (Fig. 44.2A, B).

## References

Barabino A et al (2016) Loss of Bmi1 causes anomalies in retinal development and degeneration of cone photoreceptors. Development 143(9):1571–1584

Cao R, Tsukada Y, Zhang Y (2005) Role of Bmi-1 and Ring1A in H2A ubiquitylation and Hox gene silencing. Mol Cell 20(6):845–854

Cao G et al (2012) Bmi-1 absence causes premature brain degeneration. PLoS One 7(2):e32015

Gardiner KL et al (2016) Photoreceptor proliferation and dysregulation of cell cycle genes in early onset inherited retinal degenerations. BMC Genomics 17:221

Kuzmichev A et al (2002) Histone methyltransferase activity associated with a human multiprotein complex containing the enhancer of Zeste protein. Genes Dev 16(22):2893–2905
Liu Y et al (2012) Akt phosphorylates the transcriptional repressor bmi1 to block its effects on the tumor-suppressing ink4a-arf locus. Sci Signal 5(247):ra77
Margueron R, Reinberg D (2011) The Polycomb complex PRC2 and its mark in life. Nature 469(7330):343–349
Murakami Y et al (2012) Receptor interacting protein kinase mediates necrotic cone but not rod cell death in a mouse model of inherited degeneration. Proc Natl Acad Sci U S A 109(36):14598–14603
Oppenheim RW et al (2001) Programmed cell death of developing mammalian neurons after genetic deletion of caspases. J Neurosci 21(13):4752–4760
Sahaboglu A et al (2013) Retinitis pigmentosa: rapid neurodegeneration is governed by slow cell death mechanisms. Cell Death Dis 4:e488
Soto C, Estrada LD (2008) Protein misfolding and neurodegeneration. Arch Neurol 65(2):184–189
Zencak D et al (2013) Retinal degeneration depends on Bmi1 function and reactivation of cell cycle proteins. Proc Natl Acad Sci U S A 110(7):E593–E601
Zong WX, Thompson CB (2006) Necrotic death as a cell fate. Genes Dev 20(1):1–15

# Chapter 45
# Primary Rod and Cone Degeneration Is Prevented by HDAC Inhibition

**Dragana Trifunović, Eleni Petridou, Antonella Comitato, Valeria Marigo, Marius Ueffing, and François Paquet-Durand**

**Abstract** Photoreceptor cell death in inherited retinal degeneration is accompanied by over-activation of histone deacetylases (HDAC). Excessive HDAC activity is found both in primary rod degeneration (such as in the *rd10* mouse) and in primary cone death, including the cone photoreceptor function loss 1 (*cpfl1*) mouse. We evaluated the potential of pharmacological HDAC inhibition to prevent photoreceptor degeneration in primary rod and cone degeneration. We show that a single in vivo treatment of *cpfl1* mice with the HDAC inhibitor trichostatin A (TSA) resulted in a significant protection of *cpfl1* mutant cones. Similarly, HDAC inhibition with the clinically approved HDAC inhibitor vorinostat (SAHA) resulted in a significant improvement of rod survival in *rd10* retinal explant cultures. Altogether, these results highlight the feasibility of targeted neuroprotection in vivo and create hope to maintain vision in patients suffering from both rod and cone dystrophies.

**Keywords** Rod degeneration · Cone degeneration · HDAC · Trichostatin A (TSA) · Vorinostat (SAHA) · *cpfl1* · *rd10* · Inhibition · Neuroprotection

## 45.1 Introduction

Hereditary retinal degenerations are blinding diseases characterized by high genetic heterogeneity. Mutation-induced rod cell death will lead to night blindness and tunnel vision, while cone demise will cause loss of color perception and accurate vision. The development of treatment paradigms targeting common cell death promoting processes would enable targeting a broader population of patients suffering from a variety of different genetic causes (Trifunovic et al. 2012).

D. Trifunović (✉) · E. Petridou · M. Ueffing · F. Paquet-Durand
Institute for Ophthalmic Research, University of Tuebingen, Tuebingen, Germany
e-mail: dragana.trifunovic@uni-tuebingen.de

A. Comitato · V. Marigo
Department of Life Sciences, University of Modena and Reggio Emilia, Modena, Italy



J. D. Ash et al. (eds.), *Retinal Degenerative Diseases*, Advances in Experimental Medicine and Biology 891, https://doi.org/10.1007/978-3-319-75402-4_45

There are numerous animal models for hereditary retinal degenerations, including the retinal degeneration 10-(*rd10*) mouse, which shows an early-onset and fast progression of rod cell death caused by a mutation in the rod-specific *Pde6b* gene (Arango-Gonzalez et al. 2014). Similarly, the cone-photoreceptor-function-loss-1 (*cpfl1*) mouse shows an early-onset and fast loss of cones, due to a mutation in the cone-specific *Pde6c* gene (Trifunovic et al. 2010).

In many different retinal degeneration models, cell death is characterized by excessive activities of a number of enzymes, including histone deacetylases (HDAC) (Arango-Gonzalez et al. 2014). Beyond retinal degeneration, aberrant activity of HDAC is associated with a number of diseases with very different etiology, ranging from cancer to neurodegenerative diseases (Haberland et al. 2009).

We have previously shown that HDAC inhibition with trichostatin A (TSA) efficiently protects degenerating rods in *rd1* explant cultures (Sancho-Pelluz et al. 2010). More importantly, we have recently demonstrated that TSA also protects dying cones in *cpfl1* mice in vivo (Trifunovic et al. 2016). Here, we present an extended analysis of the cone protection observed in *cpfl1* retina, and, in addition, we show that vorinostat (SAHA), a clinically approved HDAC inhibitor, has similar protective effects in *rd10* rod photoreceptor degeneration. The significant improvement of cone and rod survival after treatment with both TSA and SAHA, respectively, suggests a central role of HDAC in inherited photoreceptor degeneration.

## 45.2 Materials and Methods

### *45.2.1 Animals*

C57BL/6, *rd10*, c*pfl1*, and congenic wild-type (wt) animals were housed under standard white cyclic lighting, had free access to food and water, and were used irrespective of gender. All procedures were performed in accordance with the ARVO statement for the use of animals in ophthalmic and visual research. Procedures performed at the polistab of the University of Modena and Reggio Emilia (in vivo treatment on *cpfl1* and wt animals) were reviewed and approved by the local ethical committee.

### *45.2.2 In Vitro Retinal Explant Cultures and In Vivo Injections*

Retinas from *rd10* P15 animals were used to generate retinal explants as described before (Trifunovic et al. 2016). Cultures were exposed to 1 μM SAHA in R16 culture medium (Gibco, Paisley, UK) or kept as untreated control. Cultures were stopped at PN29 by 4% PFA fixation, cryoprotected and embedded in a tissue freezing medium. For in vivo injections, *cpfl1* and wt animals were anesthetized with an intraperitoneal injection of 250 mg/kg body weight of Avertin

(1.25% (w/v) 2,2,2-tribromoethanol and 2.5% (v/v) 2-methyl-2-butanol), and single intravitreal injections were performed at PN14 in one eye, while the other eye was sham injected with 0.0001% DMSO as contralateral control. Injections were performed with 0.5 µl of 10 nM and 100 nM TSA in order to have a final concentration of 1 nM and 10 nM, respectively (Trifunovic et al. 2016).

### *45.2.3 TUNEL and Immunostaining*

Immunostaining was performed on retinal cryosections from SAHA treated and untreated *rd10* explanted retinas, as well as on TSA treated and untreated *cpfl1* and wt retinas. Cryosections were incubated with primary antibodies specific for glycogen phosphorylase (Glyphos (Pfeiffer-Guglielmi et al. 2005)) and rhodopsin at 4 °C overnight. Alexa Fluor 488- or 566-conjugated were used as secondary antibodies. Sections were mounted in Vectashield with DAPI. Terminal deoxynucleotidyl transferase dUTP nick end labeling (TUNEL) assay was performed using an in situ cell death detection kit.

The total number of photoreceptor cells was estimated by dividing the outer nuclear layer (ONL) area by the averaged cell size. The quantification of cones was performed by manually counting the number of positively labeled cones in the ONL. Values obtained are given as a fraction of the total ONL cell number (i.e., as percentage). TUNEL-positive cells were quantified in the same fashion.

## 45.3 Results

### *45.3.1 TSA Protects Degenerating cpfl1 Cones In Vivo*

In a previous study, *cpfl1* mice were treated with a single intravitreal TSA injection at the onset of cone cell death (PN14), and cone survival was assessed at the peak of degeneration (PN24) (Trifunovic et al. 2016). Here, we evaluated whether the treatment prevented photoreceptor cell death. Briefly, animals were injected with 1 nM or 10 nM TSA solution into one eye. The contralateral eyes were sham injected with vehicle to control for injection-specific effects. As an additional control, we used the same treatment on wild-type (wt) animals. The percentage of cones in sham-injected eyes was similar to non-treated *cpfl1* (Fig. 45.1b), suggesting that the injection itself had no effect on cone survival or death. On the other hand, both 1 nM and 10 nM TSA treatments led to a significant improvement of *cpfl1* cone survival, with ~ 5.4% of cones surviving up to PN24, compared to ~ 4.5% in sham-treated eyes, corresponding to 98% of wt cones (Fig. 45.1a, b, e). The number of cones in sham- or TSA-treated wt retinas was similar to non-treated wt retinas suggesting that TSA in the studied dosage had no deleterious effects on healthy cones (Fig. 45.1c–e). The effect of in vivo TSA treatment on *cpfl1* cell death was evaluated using the TUNEL assay.

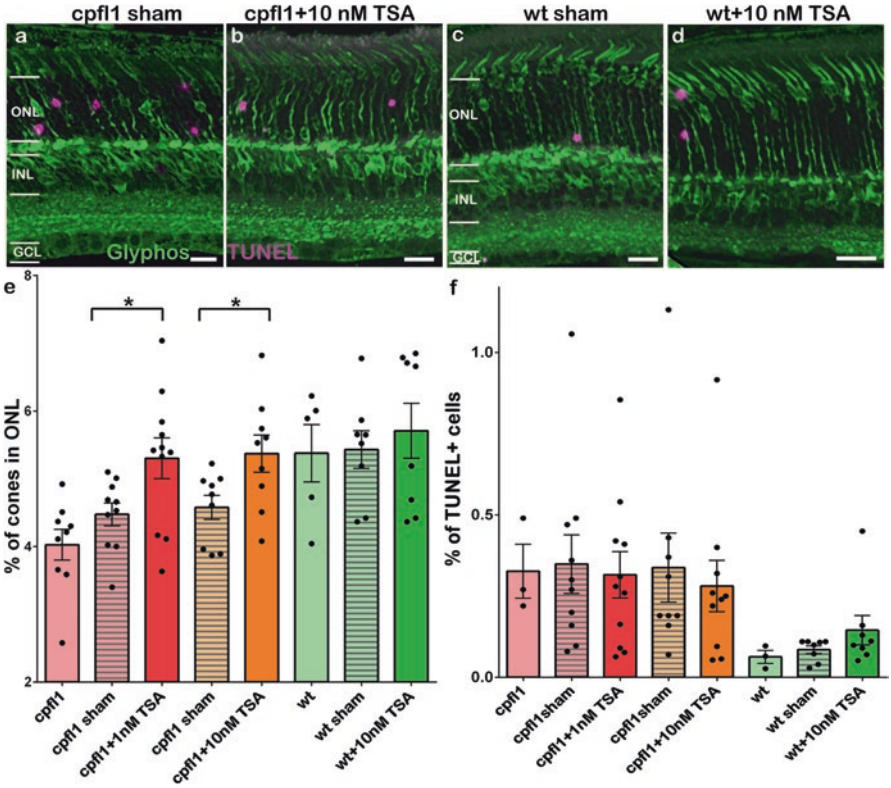


**Fig. 45.1** TSA protects degenerating cones in vivo. A single intravitreal injection of 1 nM or 10 nM TSA at PN14 was sufficient to significantly increase the number of *cpfl1* mutant cones (green) in treated compared to sham-injected retinas at PN24 (**a**, **b**, **e**), while the treatment of wt animals showed no effects on the cone number (**c**, **d**, **e**). Data presentation for cone survival (**e**) modified after Trifunovic et al. (2016) and shown for comparison only. TUNEL staining (magenta) indicated a lower number of ONL dying cells after the TSA treatment in *cpfl1* (**a**, **b**, **f**) and a slight increase in wt retina (**c**, **d**, **f**). Co-labeling with Glyphos (in green) failed to show co-localization with TUNEL, hampering the quantification of dying cones. Scale bars are 20 μm

Although there was a tendency toward a decrease in cell death after the treatment, statistical significance was not observed (Fig. 45.1a, b, f), possibly due to the very low numbers of cones degenerating at any single time point.

### *45.3.2 Vorinostat Protects Degenerating rd10 Rods In Vitro*

Long-term *rd10* cultures (PN15-PN29) were used to assess the potential of SAHA to protect degenerating *rd10* rod photoreceptors. *rd10* retinas were explanted at the onset of degeneration (PN15) and were either not treated or treated with 1 μM

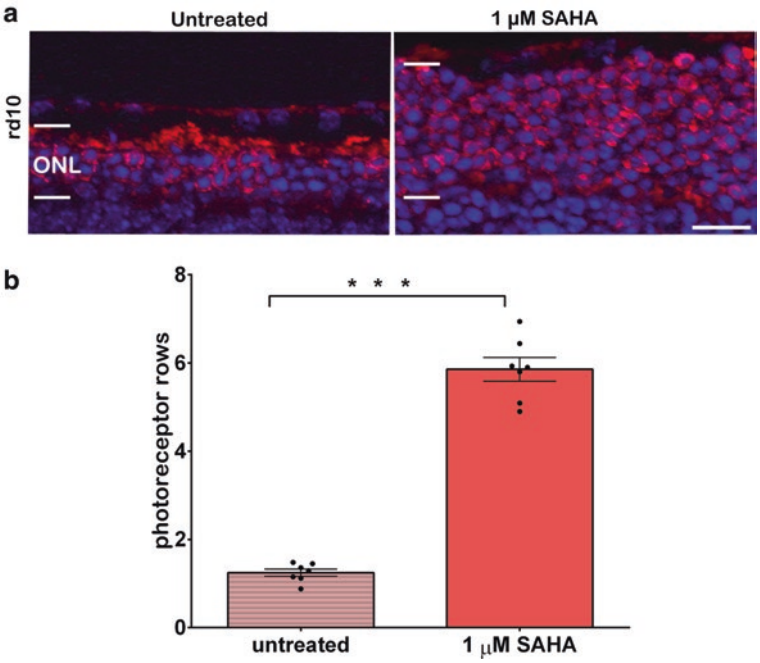


**Fig. 45.2** SAHA protects dying rods in vitro. Long-term retinal explant cultures from *rd10* animals were subjected to 1 μM SAHA or control condition from PN15 to PN29. (**a**) Nuclear staining with DAPI (blue) showed that very few photoreceptors survived at PN29 in untreated *rd10* explant cultures, while SAHA-treated retinas displayed remarkable increase in photoreceptor rows. Rhodopsin staining in red suggested that the increase in ONL thickness is due to rod survival. (**b**) The protective effect of SAHA on photoreceptor is summarized in the bar graph. Error bars represent SEM; scale bars are 20 μm

SAHA every other day. At PN29 untreated *rd10* retina had less than two rows of photoreceptors (1.15 ± 0.14 SEM), while SAHA treatment led to a fivefold increase in the number of surviving *rd10* photoreceptors (5.86 ± 0.27, $p = 0.0006$) (Fig. 45.2). Rhodopsin staining confirmed that most of the surviving ONL cells were indeed rod photoreceptors.

## 45.4 Discussion

The prevention of neuronal cell death by targeting processes common to different hereditary diseases of the photoreceptors could open new therapeutic perspectives for patients suffering from rod and cone dystrophies. Our studies in *rd10* and *cpfl1* mice demonstrate a long-lasting protection of both rods and cones after HDAC inhibition, in vitro and in vivo, confirming excessive HDAC activity as an important factor in hereditary photoreceptor degeneration. In the retina, HDAC inhibition was

shown to slow rod photoreceptor degeneration in the *rd1* mouse model for retinitis pigmentosa (Sancho-Pelluz et al. 2010), and importantly, beneficial effects of a treatment with a HDAC inhibitor were also reported in patients suffering from retinitis pigmentosa (Kumar et al. 2014).

Cones constitute only 3–5% of photoreceptors making them rather difficult to study. This is mirrored by a lack of studies on cone cell death prevention. Using HDAC inhibition, we recently demonstrated an almost complete protection of cone viability in the *cpfl1* mouse model for hereditary cone degeneration (Trifunovic et al. 2016). Remarkably, a single TSA injection in vivo was sufficient for a prolonged effect, maintaining cone numbers at wild-type levels. Although there was a clear tendency toward a decrease in photoreceptor cell death after the treatment, in the TUNEL assay, a statistical significance was not observed. This lack of significance may be due in part to the overlap between mutation-induced and developmental cell death in the ONL at this age (Young 1984). Moreover, the overall low absolute numbers of TUNEL-positive cells in the *cpfl1* retina restrict reliable statistical analysis. We were unable to colocalize the TUNEL assay with cone-specific markers (e.g., Glyphos), indicating that during the final stages of cell death, as labeled by the TUNEL assay, the dying cells have already lost their cell-type-specific markers. Unfortunately, this means that we cannot unambiguously distinguish the TUNEL signal of *cpfl1* mutation-induced cone cell death from developmental cell death.

Here, we also tested the clinically approved HDAC inhibitor, SAHA, (Olsen et al. 2007) for its protective effects on rod cell death in the *rd10* model. The pro-survival effect of SAHA treatment in the long-term *rd10* explants was remarkable, leading to a fivefold increase in ONL thickness. Surviving photoreceptors were positive for rhodopsin, suggesting a massive protection of *rd10* rods after HDAC inhibition. Further in vivo studies followed by functional evaluations of the retina will define the therapeutic potential of such treatment.

In summary, our studies provide a proof-of-principle for HDAC inhibition as a strategy for general photoreceptor protection, regardless whether the primary genetic mutation affects rods or cones.

**Acknowledgments** We thank K. Masarini and N. Rieger for skillful technical assistance. This work was supported by the Kerstan Foundation, DFG TR-1238/4-1, DFG PA1751/4-1, DRUGSFORD: HEALTH-F2-2012-304963.

## References

Arango-Gonzalez B, Trifunovic D, Sahaboglu A et al (2014) Identification of a common non-apoptotic cell death mechanism in hereditary retinal degeneration. PLoS One 9:e112142

Haberland M, Montgomery RL, Olson EN (2009) The many roles of histone deacetylases in development and physiology: implications for disease and therapy. Nat Rev Genet 10:32–42

Kumar A, Midha N, Gogia V et al (2014) Efficacy of oral valproic acid in patients with retinitis pigmentosa. J Ocul Pharmacol Ther 30:580–586

Olsen EA, Kim YH, Kuzel TM et al (2007) Phase IIb multicenter trial of vorinostat in patients with persistent, progressive, or treatment refractory cutaneous T-cell lymphoma. J Clin Oncol 25:3109–3115

Pfeiffer-Guglielmi B, Francke M, Reichenbach A et al (2005) Glycogen phosphorylase isozyme pattern in mammalian retinal Muller (glial) cells and in astrocytes of retina and optic nerve. Glia 49:84–95

Sancho-Pelluz J, Alavi M, Sahaboglu A et al (2010) Excessive HDAC activation is critical for neurodegeneration in the rd1 mouse. Cell Death Dis 1:1–9

Trifunovic D, Dengler K, Michalakis S et al (2010) cGMP-dependent cone photoreceptor degeneration in the cpfl1 mouse retina. J Comp Neurol 518:3604–3617

Trifunovic D, Sahaboglu A, Kaur J et al (2012) Neuroprotective strategies for the treatment of inherited photoreceptor degeneration. Curr Mol Med 12:598–612

Trifunovic D, Arango-Gonzalez B, Comitato A et al (2016) HDAC inhibition in the cpfl1 mouse protects degenerating cone photoreceptors in vivo. Hum Mol Genet 25:4462–4472

Young RW (1984) Cell death during differentiation of the retina in the mouse. J Comp Neurol 229:362–373

# Chapter 46
# Impact of MCT1 Haploinsufficiency on the Mouse Retina


**Neal S. Peachey, Minzhong Yu, John Y. S. Han, Sylvain Lengacher, Pierre J. Magistretti, Luc Pellerin, and Nancy J. Philp**

**Abstract** The monocarboxylate transporter 1 (MCT1) is highly expressed in the outer retina, suggesting that it plays a critical role in photoreceptors. We examined *MCT1*$^{+/-}$ heterozygotes, which express half of the normal complement of MCT1. The *MCT1*$^{+/-}$ retina developed normally and retained normal function, indicating that MCT1 is expressed at sufficient levels to support outer retinal metabolism.

**Keywords** MCT1 · Retina · Lactate · Transgenic mice · Electroretinogram

N. S. Peachey (✉)
Louis Stokes Cleveland VA Medical Center, Cleveland, OH, USA

Cole Eye Institute, Cleveland Clinic, Cleveland, OH, USA

Department of Ophthalmology, Cleveland Clinic Lerner College of Medicine of Case Western Reserve University, Cleveland, OH, USA
e-mail: neal.peachey@va.gov

M. Yu
Cole Eye Institute, Cleveland Clinic, Cleveland, OH, USA

Department of Ophthalmology, Cleveland Clinic Lerner College of Medicine of Case Western Reserve University, Cleveland, OH, USA

J. Y. S. Han · N. J. Philp
Department of Pathology, Anatomy and Cell Biology, Thomas Jefferson University, Philadelphia, PA, USA

S. Lengacher
Brain Mind Institute, Ecole Polytechnique Fédérale de Lausanne (EPFL), Lausanne, Switzerland

P. J. Magistretti
Brain Mind Institute, Ecole Polytechnique Fédérale de Lausanne (EPFL), Lausanne, Switzerland

Division of Biological and Environmental Sciences and Engineering, King Abdullah University of Science and Technology (KAUST), Thuwal, KSA, Saudi Arabia

L. Pellerin
Department of Physiology, University of Lausanne, Lausanne, Switzerland



J. D. Ash et al. (eds.), *Retinal Degenerative Diseases*, Advances in Experimental Medicine and Biology 891, https://doi.org/10.1007/978-3-319-75402-4_46

## 46.1 Introduction

The retina is among the most metabolically active tissues in the body and metabolizes glucose through both glycolytic and oxidative pathways to support the high-energy demands of visual transduction and outer segment renewal. Like cancer cells, the retina utilizes aerobic glycolysis (Weinhouse 1976). The majority of glucose transported into the outer retina is metabolized to lactate (Wang et al. 1997). This raises the question: what becomes of the lactate? In the brain there is considerable evidence to suggest glucose is metabolized by astrocytes through aerobic glycolysis to generate lactate that is shuttled to adjacent neurons for oxidation (Pellerin and Magistretti 2012). A lactate shuttle was also proposed to support metabolism in the outer retina (Poitry-Yamate and Tsacopoulos 1991; Poitry-Yamate et al. 1995). In vitro studies showed isolated Müller glial cells (MGCs) metabolized glucose and released lactate into the media. When photoreceptor cells were added, lactate levels in the media decreased, suggesting photoreceptor cells utilized the lactate (Poitry-Yamate and Tsacopoulos 1991; Poitry-Yamate et al. 1995).

The cloning of MCT1 (SCL16A1) paved the way for identification of other members of the MCT family and the development of antibodies, siRNA, and inhibitors for studying their tissue-specific expression and activity (Adijanto and Philp 2012). Several MCT isoforms are expressed in the retina, and their specific distribution provides insight into the production and utilization of lactate in the outer retina. MCT1 is found in many cells but is expressed at the highest levels in cells that oxidize lactate such as type l muscle fibers and cardiac muscle. In the retina, MCT1 is expressed in the inner segment of photoreceptor cells and endothelial cells and in the apical membrane of the retinal pigment epithelium (RPE).

MCT1 is a heteromeric transporter that requires the accessory protein CD147 (*Bsg*) for trafficking to the plasma membrane (Kirk et al. 2000). Like other heteromeric transporters, the absence of one subunit results in the targeting of the other subunit for degradation. Mice lacking CD147 ($Bsg^{-/-}$) have severely reduced electroretinograms (ERGs), progressive photoreceptor degeneration (Hori et al. 2000), and reduced levels of MCT1, MCT3, and MCT4 in the retina (Philp et al. 2003). These findings indicate that aerobic glycolysis and the lactate shuttle are essential for supporting photoreceptor cell activity and viability. To understand the specific contribution of MCT1 in supporting visual function, we examined the ocular phenotype of $MCT1^{+/-}$ mice, which have axonopathy due to disruption of the lactate shuttle between oligodendrocytes and motor neuron axons (Lee et al. 2012).

## 46.2 Materials and Methods

### *46.2.1 Mice*

The generation of *MCT1* mutant mice has been described (Lee et al. 2012). While MCT1 homozygous mutant mice do not survive, mice used in these studies were generated by crossing $MCT1^{+/-}$ and C57BL/6J (WT) mice.

### 46.2.2 Visual Electrophysiology

The methods used to record ERGs and visual evoked potentials (VEPs) have been described (Yu et al. 2012). In brief, after overnight dark adaptation, mice were anesthetized with ketamine (80 mg/kg) and xylazine (16 mg/kg) after which ERGs or VEPs were recorded to strobe flash stimuli presented in a ganzfeld bowl.

### 46.2.3 Western Blotting

RPE and retinas were microdissected from mouse eyes and homogenized in RIPA buffer (50 mM Tris-HCl pH 7.5, 150 mM NaCl, 1% NP-40, 0.5% Na deoxycholate, 0.1% SDS) containing protease inhibitors (Sigma) as described (Philp et al. 2003). Detergent soluble lysates (5 μg) were loaded onto a NuPAGE® 4–12% Tris-acetate gel (Invitrogen) for electrophoresis. Proteins were subsequently transferred onto PVDF membranes using XCell II™ Blot Module (Invitrogen). Nonspecific binding sites were blocked with TBS (+0.1% Tween 20) containing 5% w/v powdered milk. Antibodies used in this study were against cyclophilin A (Upstate Cell Signaling Solutions), Glut1 (Abcam), CD147 (G19; Santa Cruz), and MCT1 (Philp Lab) (Philp et al. 2003).

### 46.2.4 Immunofluorescence and Imaging

Mouse eyes were fixed using methanol/acetic acid at −80 °C as described (Sun et al. 2015). Cryosections (8 μm) were collected on glass slides and labeled with anti-MCT1 and CD147 antibodies as described (Philp et al. 2003).

## 46.3 Results

Figure 46.1a presents frozen sections of an *MCT1*$^{+/-}$ retina analyzed at 14 months of age. MCT1 antibody labels the apical membrane of the RPE, photoreceptor cell inner segments, and capillaries in the outer and inner plexiform layers. The overall appearance of the *MCT1*$^{+/-}$ retina showed no structural abnormalities, and there was no evidence of photoreceptor degeneration. Similar results were obtained by OCT imaging (not shown). Immunoblot analysis demonstrated that the *MCT1*$^{+/-}$ RPE and retina are both haploinsufficient for MCT1, as compared to WT littermates (Fig. 46.1b).

To examine if there was a functional impact of MCT1 haploinsufficiency, we examined visual electrophysiology. ERGs recorded from *MCT1*$^{+/-}$ mice under dark-adapted conditions had a waveform that was not different from WT littermates (Fig. 46.2a). The major ERG components did not differ in amplitude from those of

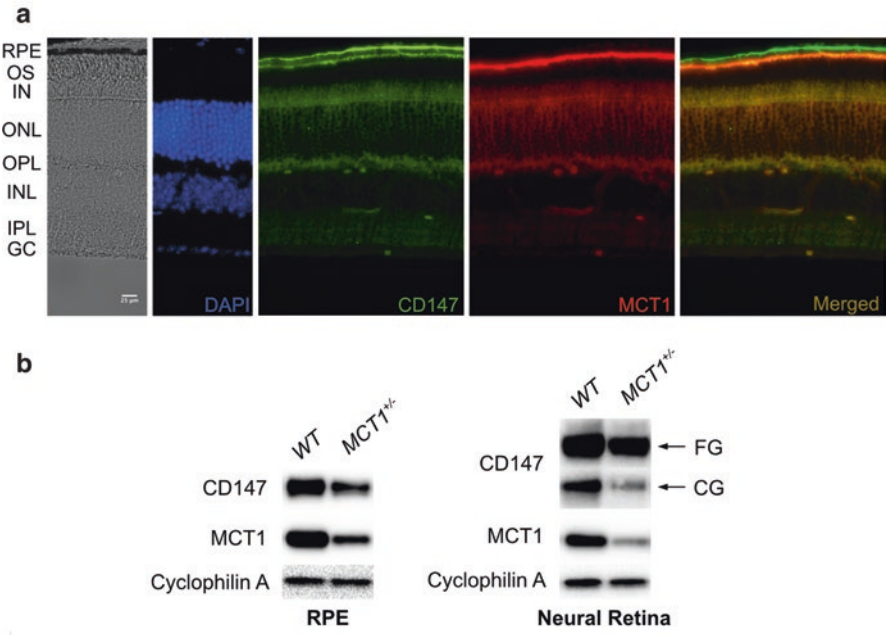


**Fig. 46.1** *MCT1*$^{+/-}$ retina has normal structure but reduced levels of MCT1. (**a**) Frozen section of 14-month-old *MCT1*$^{+/-}$ retina. Retinal structure is normal, and while the abundance of MCT1 is decreased relative to age-matched WT littermates, the distribution of MCT1 is not changed. (**b**) Immunoblot analysis of RPE and retinal lysates demonstrates greater than 50% reduction in MCT1 levels in *MCT1*$^{+/-}$ as compared to WT mice

WT littermates (Fig. 46.2b), indicating normal function of photoreceptors (a-wave) and rod bipolar cells (b-wave). Similar results were obtained for the light-adapted ERG (not shown). We also examined transmission through the visual pathway, by recording VEPs over the visual cortex. The VEP of *MCT1*$^{+/-}$ mice had a normal waveform (Fig. 46.2c), and implicit time measurements were not different from WT littermates (Fig. 46.2d).

## 46.4 Discussion

In the central nervous system, MCT1 is expressed in oligodendrocytes and facilitates lactate transport to the axon to support their energy demands. The *MCT1*$^{+/-}$ haploinsufficient adult mice exhibit widespread axonopathy in the central nervous system that does not result from demyelination or oligodendrocyte death (Lee et al. 2012). In the retina and RPE, we and others have shown MCT1 is primarily expressed in the RPE and photoreceptor cells suggesting that lactate provides a key energy substrate for these cells (Philp et al. 2003). Mice expressing a single *MCT1* allele had reduced levels of MCT1 in the retina, indicating the absence of a

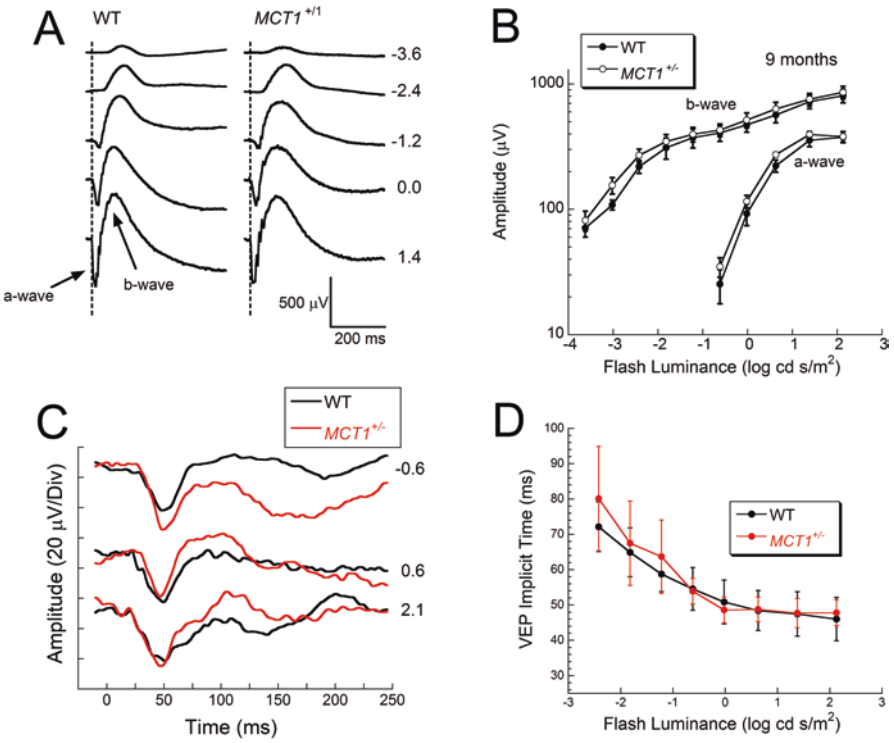


**Fig. 46.2** Normal visual electrophysiology in *MCT1*$^{+/-}$ mice. (**a**) Dark-adapted ERGs obtained from 9-month-old *MCT1*$^{+/-}$ and WT littermates. (**b**) Amplitude of the major components of the dark-adapted ERG. Data points indicate average ± sem from four mice per genotype. (**c**) VEPs obtained from 8-month-old *MCT1*$^{+/-}$ and WT littermates. (**d**) Implicit time of the major VEP component plotted as a function of flash luminance. Data points indicate average ± sem from 15 WT and 11 *MCT1*$^{+/-}$ mice

mechanism to upregulate expression of the single allele present in *MCT1*$^{+/-}$ mice or to stabilize the protein for a longer period of time. Despite this reduction, we detected no changes in retinal structure. Moreover, our visual electrophysiology data indicate that a single allele of *MCT1* generates sufficient protein to support normal function of photoreceptors and bipolar cells, as the ERG a- and b-waves of *MCT1*$^{+/-}$ mice were comparable to WT. Transmission through the *MCT1*$^{+/-}$ visual pathway was also comparable to WT. These results, coupled with the absence of visual abnormalities in patients with *GLUT1* haploinsufficiency (Levy et al. 2010), indicate that the retina enjoys high expression of transporters related to supplying this tissue with metabolic substrates.

**Acknowledgments** This work was supported by grants from NIH (R01EY12042) and Department of Veterans Affairs (I01BX2340) and by the Foundation Fighting Blindness and Research to Prevent Blindness.

## References

Adijanto J, Philp NJ (2012) The SLC16A family of monocarboxylate transporters (MCTs)--physiology and function in cellular metabolism, pH homeostasis, and fluid transport. Curr Top Membr 70:275–311

Hori K, Katayama N, Kachi S et al (2000) Retinal dysfunction in basigin deficiency. Invest Ophthal Vis Sci 41:3128–3133

Kirk P, Wilson MC, Heddle C et al (2000) CD147 is tightly associated with lactate transporters MCT1 and MCT4 and facilitates their cell surface expression. EMBO J 19:3896–3904

Lee Y, Morrison BM, Li Y et al (2012) Oligodendroglia metabolically support axons and contribute to neurodegeneration. Nature 487:443–448

Levy B, Wang D, Ullner PM et al (2010) Uncovering microdeletions in patients with severe Glut1 deficiency syndrome using SNP oligonucleotide microarray analysis. Mol Genet Metab 100:129–135

Pellerin L, Magistretti PJ (2012) Sweet sixteen for ANLS. Cereb Blood Flow Metab 32:1152–1166

Philp NJ, Ochrietor JD, Rudoy C et al (2003) Loss of MCT1, MCT3, and MCT4 expression in the retinal pigment epithelium and neural retina of the 5A11/basigin-null mouse. Invest Ophth Vis Sci 44:1305–1311

Poitry-Yamate C, Tsacopoulos M (1991) Glial (Müller) cells take up and phosphorylate [$^3$H]2-deoxy-D-glucose in mammalian retina. Neurosci Lett 122:241–244

Poitry-Yamate CL, Poitry S, Tsacopoulos M (1995) Lactate released by Müller glial cells is metabolized by photoreceptors from mammalian retina. J Neurosci 15:5179–5191

Sun N, Shibata B, Hess JF, FitzGerald PG (2015) An alternative means of retaining ocular structure and improving immunoreactivity for light microscopic studies. Mol Vis 21:428–442

Wang L, Tornquist P, Bill A (1997) Glucose metabolism in pig outer retina in light and darkness. Acta Physiol Scand 160:75–81

Weinhouse S (1976) The Warburg hypothesis fifty years later. Z Krebsforsch 87:115–126

Yu M, Sturgill-Short G, Ganapathy P et al (2012) Age-related changes in visual function in *cystathionine-beta-synthase* mutant mice, a model of hyperhomocysteinemia. Exp Eye Res 96:142–131

# Chapter 47
# The Leber Congenital Amaurosis-Linked Protein AIPL1 and Its Critical Role in Photoreceptors

**Almudena Sacristan-Reviriego and Jacqueline van der Spuy**

**Abstract** Mutations in the photoreceptor/pineal-expressed gene, *aryl hydrocarbon receptor-interacting protein-like 1* (*AIPL1*), are mainly associated with autosomal recessive Leber congenital amaurosis (LCA), the most severe form of inherited retinopathy that occurs in early childhood. AIPL1 functions as a photoreceptor-specific molecular co-chaperone that interacts specifically with the molecular chaperones HSP90 and HSP70 to facilitate the correct folding and assembly of the retinal cGMP phosphodiesterase (PDE6) holoenzyme. The absence of AIPL1 leads to a dramatic degeneration of rod and cone cells and a complete loss of any light-dependent electrical response. Here we review the important role of AIPL1 in photoreceptor functionality.

**Keywords** AIPL1 · LCA · HSP90 · Retinal degeneration · PDE6 · Photoreceptor · Rod · Cone · Prenylation

## 47.1 Introduction

LCA is the most rapid and severe inherited retinopathy and the most frequent cause of congenital blindness diagnosed in infancy. LCA is characterized by the presence of nystagmus, very poor vision, and a severely reduced or non-detectable electroretinogram (ERG) (Koenekoop 2004). There are currently 26 genes associated with LCA (RetNet https://sph.uth.edu/retnet), encoding a variety of proteins that have critical roles for normal retinal function (den Hollander et al. 2008). One of the causative LCA genes is *AIPL1* (Sohocki et al. 2000b), accounting for between 5 and 10% of cases resulting in one of the most clinically severe forms of the disease (LCA type 4) (Hanein et al. 2004). According to the Human Gene Mutation Database (HGMD), LCA4-causing mutations include small insertions or deletions

A. Sacristan-Reviriego · J. van der Spuy (✉)
UCL Institute of Ophthalmology, London, UK
e-mail: j.spuy@ucl.ac.uk



J. D. Ash et al. (eds.), *Retinal Degenerative Diseases*, Advances in Experimental Medicine and Biology 891, https://doi.org/10.1007/978-3-319-75402-4_47

and missense and nonsense changes distributed throughout the *AIPL1* gene. Variations located in the coding or noncoding regions of *AIPL1* have been shown to cause aberrant pre-mRNA splicing leading to alternative transcripts predicted to encode functionally deficient protein isoforms (Bellingham et al. 2015). Some mutations in *AIPL1* have been associated with less severe dominant cone-rod dystrophy and juvenile retinitis pigmentosa (Sohocki et al. 2000a).

*AIPL1* is a 11.5 kb gene of 6 exons, encoding a 384 amino acid protein expressed exclusively in retinal photoreceptors and the pineal gland (Sohocki et al. 2000b; van der Spuy et al. 2002). AIPL1 was originally described as the aryl hydrocarbon receptor (AhR)-interacting protein (AIP)-like 1 as it shares 49% identity with the ubiquitously expressed AIP (Sohocki et al. 2000b). Although AIPL1 and AIP share partial sequence homology with the well-studied immunophilins FKBP52 and FKBP51, the N-terminal FK506-binding protein (FKBP)-like domain of AIPL1 does not bind FK506 and lacks peptidylprolyl isomerase activity in vitro (Li et al. 2013). A tetratricopeptide repeat (TPR) domain, comprising three consecutive TPR motifs, is conserved both in AIPL1 and the co-chaperones AIP, FKBP51, and FKBP52. The TPR motif is a degenerate 34 amino acid repeat involved in tight electrostatic interactions with the main chain carboxylate of the ultimate aspartic acid residue in the conserved C-terminal EEVD motif of the chaperone HSP90 (Scheufler et al. 2000). The co-chaperones AIP and FKBP52 participate in the client protein functional maturation mediated by HSP70 and HSP90 to facilitate the targeted translocation and transcriptional activation of their respective client proteins (Pearl and Prodromou 2006). Yeast two-hybrid analysis and in vitro binding assays revealed that AIPL1 is also able to interact with HPS90 and HSP70 via its TPR domain suggesting that AIPL1 is a potential photoreceptor-specific molecular co-chaperone involved in the regulation of cognate clients in an analogous manner to AIP (Hidalgo-de-Quintana et al. 2008; Li et al. 2013). Interestingly, human AIPL1 harbors a very C-terminal polyproline-rich domain (PRD) of 56 amino acids, which is primate-specific and adopts an unordered extended conformation (Sohocki et al. 2001; Yadav et al. 2015). Deletion of the PRD has been reported to have no effect on the interaction of human AIPL1 with a C-terminal HSP90 peptide; however, the PRD was shown to influence the association with full-length human HSP90 in an inhibitory manner (Li et al. 2013). Hence, the role of the primate-specific PRD is unclear; however mutations in this domain lead to pathogenesis. Because *AIPL1* mutations are associated with LCA and this protein functions as a co-chaperone, it follows that phototransduction cascade effectors are candidate client proteins for AIPL1.

## 47.2 AIPL1 as a Specific Co-chaperone for PDE6

Cyclic nucleotide phosphodiesterase of the sixth family (PDE6) is a critical enzyme in the visual transduction cascade that hydrolyzes cyclic GMP in photoreceptor cells upon light stimulation. It is a heterotetrameric holoenzyme composed of two

catalytic and two inhibitory subunits (γ). In cones, PDE6 is a catalytic homodimer composed of two identical α′ subunits, while in rods, α and β subunits dimerize to form the catalytic core (Cote 2004). In the *rd1* mouse model lacking the PDE6β subunit, the accumulation of cGMP levels results in sustained increases of intracellular $Ca^{2+}$ that triggers rod cell degeneration and death (Arshavsky and Burns 2012). Cone photoreceptors lacking PDE6α′ also have elevated cGMP in their outer segments (Trifunovic et al. 2010).

Similarly, cGMP accumulates in *Aipl1*-deficient mice and triggers rapid degeneration of rod cells and lack of ERG response to light stimuli (Ramamurthy et al. 2004). All three subunits of the rod PDE6 holoenzyme are downregulated at the protein but not at the mRNA level both in *Aipl1* knockout and hypomorphic mice (Liu et al. 2004; Ramamurthy et al. 2004). Further studies demonstrated that rod PDE6 subunits are synthesized but rapidly degraded by the proteasome in the absence of AIPL1, suggesting that the drastic reduction of PDE6 protein is due to a posttranslational processing defect. Moreover, the PDE6 subunits were not assembled into a functional native PDE6 heterotetramer (Kolandaivelu et al. 2009). Altogether these data revealed that in the absence of AIPL1, the rod PDE6 subunits are misassembled and rapidly targeted to proteasomes for degradation. Interestingly AIPL1 has been reported to downregulate the proteasomal degradation of substrates targeted by NUB1, a protein that interacts directly with the proteasome to target ubiquitin-like proteins (Bett et al. 2012). However, whether this is involved in protecting the PDE6 subunits from proteasomal degradation is unknown.

The mechanism behind cone degeneration in cone-only ($Nrl^{-/-}$) mice lacking AIPL1 is slightly different because it is triggered by a reduction of cGMP levels. In this model, AIPL1 is needed for the stability, assembly, and localization not only of cone PDE6 (Kirschman et al. 2010) but also RetGC1 (retinal guanylate cyclase-1), an enzyme that mediates cGMP synthesis in response to changes in calcium. As a consequence of reduced levels of RetGC1, the cGMP levels are downregulated in the entire retina (Kolandaivelu et al. 2014).

The requirement of AIPL1 for the catalytic activity of the PDE6 holoenzyme has recently been confirmed in vitro through heterologous expression of cone PDE6 (Gopalakrishna et al. 2016). Moreover, AIPL1 has been shown to interact with the catalytic subunits PDE6α and PDE6α′ of rods and cones, respectively (Kolandaivelu et al. 2009; Kolandaivelu et al. 2014). In vitro binding assays revealed that AIPL1 also interacts with the inhibitory γ subunit (PDEγ) (Yadav et al. 2015). Since AIPL1 also binds HSP90 and HSP70 (Hidalgo-de-Quintana et al. 2008), the resulting chaperone heterocomplex is involved in the proper folding and assembly of PDE6 subunits in photoreceptors. Inhibition of HSP90 in the retina in vivo leads to a significant reduction in the posttranscriptional levels of PDE6 (Aguila et al. 2014), suggesting that PDE6 is a specific substrate for HSP90 and underlying the important role of AIPL1 in directing client specificity.

## 47.3 AIPL1 and Prenylation of PDE6

Many phototransduction signaling proteins in the retina depend on prenylation for their correct subcellular localization, stability, and function (Roosing et al. 2014). This posttranslational modification leads to the addition of a farnesyl or geranylgeranyl isoprenoid lipid at a C-terminal cysteine residue of proteins ending in a CAAX motif (C, cysteine; A, aliphatic amino acid residue; X, any amino acid residue) (Lane and Beese 2006). Prenylation enables proteins to anchor to cell membranes or intracellular structures and facilitates their interaction with protein partners (Wang and Casey 2016). Defects in prenylation trigger complete degeneration of photoreceptor inner and outer segments and are the cause of several inherited retinopathies (Roosing et al. 2014).

Interestingly, the rod PDE6 catalytic α subunit is farnesylated, while the β subunit is geranylgeranylated (Cote 2004). The identity of the prenyl group attached to the cone PDE6α′ subunit is still unknown but based on the last amino acid residue is thought to be geranylgeranyl. A yeast two-hybrid screen revealed that AIPL1 interacts specifically with farnesylated proteins (Ramamurthy et al. 2003). Further studies showed that the AIPL1 FKBP domain mediates the direct interaction with a mimetic of the processed C-terminal cysteine of farnesylated proteins in vitro and is therefore proposed to bind the C-terminal farnesyl moiety of PDE6α (Majumder et al. 2013). *Aipl1* knockout and hypomorphic mice did not show global defects in farnesylation (Liu et al. 2004; Ramamurthy et al. 2004) ruling out the possibility of a general role of AIPL1 in protein farnesylation. Although there is no evidence of a direct interaction between AIPL1 and geranylgeranylated proteins, a geranylgeranyl moiety could partially reverse the binding between AIPL1 and the farnesylated PDE6α mimetic in vitro (Yadav et al. 2015). Because AIPL1 has an obvious effect on cone PDE6α′ (Kirschman et al. 2010) which is thought to be geranylgeranylated, further studies are needed to clarify the mechanism behind the interaction of AIPL1 with cone PDE6α′.

Prenylated proteins are synthesized in the cytosol, dock to the endoplasmic reticulum (ER), are further processed by ER-associated proteins, and are transferred to vesicles for transport to and through the connecting cilium to reach the outer segments (OS) (Karan et al. 2008). We propose that AIPL1 binds farnesylated PDE6α and PDEγ in the cytosol thereby allowing the correct and stable assembly of the heterotetramer, which is then targeted to the ER membrane by the geranylgeranylated C-terminus of PDE6β, which is the main PDE6-membrane binding site (Cote 2004), for further processing. The transfer of prenylated proteins from the ER to transport vesicles is proposed to be mediated by cytosolic prenyl-binding proteins (Karan et al. 2008). AIPL1 localization is enriched at the tip of the inner segment, close to the connecting cilia in human rods and cones (Hendrickson et al. 2008; Hidalgo-de-Quintana et al. 2015). Hence, whether AIPL1 remains associated with the PDE6 holoenzyme during targeted translocation to the connecting cilium or indeed facilitates this process is an interesting question which requires further investigation.

## 47.4 Conclusion

Molecular chaperones have a role in protein folding of nascent chains, oligomeric assembly and disassembly of protein complexes, intracellular transport of proteins across membranes, and protein quality control and degradation (Ellis 2006). This review has focused on the essential function of AIPL1 as a photoreceptor-specific molecular co-chaperone for PDE6, acting in a heterocomplex with HSP90 to facilitate its folding and assembly in rods and cones. Important unresolved questions concern how this function of AIPL1 may differ in rods and cones.

## References

Aguila M, Bevilacqua D, McCulley C et al (2014) Hsp90 inhibition protects against inherited retinal degeneration. Hum Mol Genet 23:2164–2175

Arshavsky VY, Burns ME (2012) Photoreceptor signaling: supporting vision across a wide range of light intensities. J Biol Chem 287:1620–1626

Bellingham J, Davidson AE, Aboshiha J et al (2015) Investigation of aberrant splicing induced by AIPL1 variations as a cause of Leber congenital amaurosis. Invest Ophthalmol Vis Sci 56:7784–7793

Bett JS, Kanuga N, Richet E et al (2012) The inherited blindness protein AIPL1 regulates the ubiquitin-like FAT10 pathway. PLoS One 7:e30866

Cote RH (2004) Characteristics of photoreceptor PDE (PDE6): similarities and differences to PDE5. Int J Impot Res 16(Suppl 1):S28–S33

den Hollander AI, Roepman R, Koenekoop RK et al (2008) Leber congenital amaurosis: genes, proteins and disease mechanisms. Prog Retin Eye Res 27:391–419

Ellis RJ (2006) Molecular chaperones: assisting assembly in addition to folding. Trends Biochem Sci 31:395–401

Gopalakrishna KN, Boyd K, Yadav RP et al (2016) Aryl hydrocarbon receptor-interacting protein-like 1 is an obligate chaperone of phosphodiesterase 6 and is assisted by the gamma-subunit of its client. J Biol Chem 291:16282–16291

Hanein S, Perrault I, Gerber S et al (2004) Leber congenital amaurosis: comprehensive survey of the genetic heterogeneity, refinement of the clinical definition, and genotype-phenotype correlations as a strategy for molecular diagnosis. Hum Mutat 23:306–317

Hendrickson A, Bumsted-O'Brien K, Natoli R et al (2008) Rod photoreceptor differentiation in fetal and infant human retina. Exp Eye Res 87:415–426

Hidalgo-de-Quintana J, Evans RJ, Cheetham ME et al (2008) The Leber congenital amaurosis protein AIPL1 functions as part of a chaperone heterocomplex. Invest Ophthalmol Vis Sci 49:2878–2887

Hidalgo-de-Quintana J, Schwarz N, Meschede IP et al (2015) The Leber congenital amaurosis protein AIPL1 and EB proteins co-localize at the photoreceptor cilium. PLoS One 10:e0121440

Karan S, Zhang H, Li S et al (2008) A model for transport of membrane-associated phototransduction polypeptides in rod and cone photoreceptor inner segments. Vis Res 48:442–452

Kirschman LT, Kolandaivelu S, Frederick JM et al (2010) The Leber congenital amaurosis protein, AIPL1, is needed for the viability and functioning of cone photoreceptor cells. Hum Mol Genet 19:1076–1087

Koenekoop RK (2004) An overview of Leber congenital amaurosis: a model to understand human retinal development. Surv Ophthalmol 49:379–398

Kolandaivelu S, Huang J, Hurley JB et al (2009) AIPL1, a protein associated with childhood blindness, interacts with alpha-subunit of rod phosphodiesterase (PDE6) and is essential for its proper assembly. J Biol Chem 284:30853–30861

Kolandaivelu S, Singh RK, Ramamurthy V (2014) AIPL1, a protein linked to blindness, is essential for the stability of enzymes mediating cGMP metabolism in cone photoreceptor cells. Hum Mol Genet 23:1002–1012

Lane KT, Beese LS (2006) Thematic review series: lipid posttranslational modifications. Structural biology of protein farnesyltransferase and geranylgeranyltransferase type I. J Lipid Res 47:681–699

Li J, Zoldak G, Kriehuber T et al (2013) Unique proline-rich domain regulates the chaperone function of AIPL1. Biochemistry 52:2089–2096

Liu X, Bulgakov OV, Wen XH et al (2004) AIPL1, the protein that is defective in Leber congenital amaurosis, is essential for the biosynthesis of retinal rod cGMP phosphodiesterase. Proc Natl Acad Sci U S A 101:13903–13908

Majumder A, Gopalakrishna KN, Cheguru P et al (2013) Interaction of aryl hydrocarbon receptor-interacting protein-like 1 with the farnesyl moiety. J Biol Chem 288:21320–21328

Pearl LH, Prodromou C (2006) Structure and mechanism of the Hsp90 molecular chaperone machinery. Annu Rev Biochem 75:271–294

Ramamurthy V, Roberts M, van den Akker F et al (2003) AIPL1, a protein implicated in Leber's congenital amaurosis, interacts with and aids in processing of farnesylated proteins. Proc Natl Acad Sci U S A 100:12630–12635

Ramamurthy V, Niemi GA, Reh TA et al (2004) Leber congenital amaurosis linked to AIPL1: a mouse model reveals destabilization of cGMP phosphodiesterase. Proc Natl Acad Sci U S A 101:13897–13902

Roosing S, Collin RW, den Hollander AI et al (2014) Prenylation defects in inherited retinal diseases. J Med Genet 51:143–151

Scheufler C, Brinker A, Bourenkov G et al (2000) Structure of TPR domain–peptide complexes. Cell 101:199–210

Sohocki MM, Perrault I, Leroy BP et al (2000a) Prevalence of AIPL1 mutations in inherited retinal degenerative disease. Mol Genet Metab 70:142–150

Sohocki MM, Bowne SJ, Sullivan LS et al (2000b) Mutations in a new photoreceptor-pineal gene on 17p cause Leber congenital amaurosis. Nat Genet 24:79–83

Sohocki MM, Sullivan LS, Tirpak DL et al (2001) Comparative analysis of aryl-hydrocarbon receptor interacting protein-like 1 (Aipl1), a gene associated with inherited retinal disease in humans. Mamm Genome Off J Int Mamm Genome Soc 12:566–568

Trifunovic D, Dengler K, Michalakis S et al (2010) cGMP-dependent cone photoreceptor degeneration in the cpfl1 mouse retina. J Comp Neurol 518:3604–3617

van der Spuy J, Chapple JP, Clark BJ et al (2002) The Leber congenital amaurosis gene product AIPL1 is localized exclusively in rod photoreceptors of the adult human retina. Hum Mol Genet 11:823–831

Wang M, Casey PJ (2016) Protein prenylation: unique fats make their mark on biology. Nat Rev Mol Cell Biol 17:110–122

Yadav RP, Majumder A, Gakhar L et al (2015) Extended conformation of the proline-rich domain of human aryl hydrocarbon receptor-interacting protein-like 1: implications for retina disease. J Neurochem 135:165–175

# Chapter 48
# Alternative Splicing for Activation of Coagulation Factor XIII-A in the Fish Retina After Optic Nerve Injury

**Kayo Sugitani, Yoshiki Koriyama, Kazuhiro Ogai, Ayako Furukawa, and Satoru Kato**

**Abstract** Factor XIII-A (FXIII-A), which has become known as cellular transglutaminase, plays important roles in mediating cross-linking reactions in various tissues. FXIII-A acts as one of the regeneration molecules in the fish retina and optic nerve after optic nerve injury and becomes activated at the site of injury within a few hours. Previous research has shown that activated FXIII-A induces neurite outgrowth from injured retinal ganglion cells and supports elongation of the regenerating optic nerve. However, the activation mechanism of FXIII-A remains unknown. Furthermore, the injured tissues do not express thrombin, a known activator of plasma FXIII. Here, we investigated the mRNA expression of FXIII-A based on two different regions, one encoding the activation peptide and the other encoding the enzymatic active site. We found that expression of the region encoding the activation peptide was markedly suppressed compared with the region encoding the active site. An overexpression study with a short-type FXIII-A cDNA lacking the activation peptide revealed induction of long neurite outgrowth in fish retinal explant cultures compared with full-length FXIII-A cDNA. The present findings suggest

K. Sugitani (✉)
Department of Clinical Laboratory Science, Graduate School of Medical Science, Kanazawa University, Kanazawa, Japan
e-mail: sugitani@staff.kanazawa-u.ac.jp

Y. Koriyama · A. Furukawa
Graduate School and Faculty of Pharmaceutical Sciences, Suzuka University of Medical Science, Suzuka, Japan

K. Ogai
Wellness Promotion Science Center, Institute of Medical, Pharmaceutical and Health Science, Kanazawa University, Kanazawa, Japan

S. Kato
Wellness Promotion Science Center, Institute of Medical, Pharmaceutical and Health Science, Kanazawa University, Kanazawa, Japan

Department of Molecular Neurobiology, Graduate School of Medicine, Kanazawa University, Kanazawa, Japan



J. D. Ash et al. (eds.), *Retinal Degenerative Diseases*, Advances in Experimental Medicine and Biology 891, https://doi.org/10.1007/978-3-319-75402-4_48

that alternative splicing may occur in the FXIII-A gene, resulting in deletion of the region encoding the activation peptide and thus allowing direct production of activated FXIII-A protein in the fish retina and optic nerve after optic nerve injury.

**Keywords** Factor XIII-A · Optic nerve regeneration · Neurite outgrowth · Retina · Zebrafish · Explant culture · Thrombin · Alternative splicing · Transglutaminase · Wound healing

## 48.1 Introduction

Unlike mammalian retinal ganglion cells (RGCs), fish RGCs have the capacity to repair their axons, even after optic nerve transection. A large number of regeneration-associated genes (RAGs) are upregulated to restore the visual system after optic nerve injury (Kato et al. 2013). RAGs can be classified into cell survival-related genes (Koriyama et al. 2007, 2009), dedifferentiation-related genes (e.g., Yamanaka factors: Ogai et al. 2012, 2014), and axonal regeneration-related genes (Sugitani et al. 2006; Koriyama et al. 2009). Studies on the regeneration mechanism of the fish visual system can provide insights into the activation mechanisms for the expression of such RAGs. Factor XIII-A (FXIII-A) has been recognized as one of the RAG molecules belonging to the axonal regeneration-related genes in the damaged retina (Sugitani et al. 2012).

FXIII-A was originally identified as a plasma transglutaminase that promotes clot stabilization in polymerized fibrin as a blood coagulation factor. FXIII exists in plasma as $A_2B_2$ heterodimers composed of two catalytic A subunits ($A_2$) and two carrier B subunits ($B_2$) of the inactive form (Muszbek et al. 1996; Lorand 2001). It is well known that activation of plasma FXIII requires cleavage of an activation peptide by thrombin enzymatic activity. However, the activation mechanism for cellular FXIII-A remains unclear. In the present study, we focused on the activation mechanism of FXIII-A existing in various tissues as cellular FXIII-A (Derrick et al. 1993; Quatresooz et al. 2008). To investigate the mechanism for FXIII-A activation, we chose the fish retina as an experimental model, because activation of FXIII-A occurs spontaneously in both the retina and optic nerve after fish optic nerve injury (Sugitani et al. 2012). In this study, we compared the expression patterns of FXIII-A mRNA based on two distinct regions, one containing the exon 1–2 region cleaved by thrombin and the other containing the exon 7–8 active site region. To investigate the expression patterns of FXIII-A, real-time PCR amplifications were performed. In addition, we prepared retinal explant cultures to investigate the effects of overexpression of different constructs of the FXIII-A gene.

## 48.2 Methods

### *48.2.1 Animal Experiments*

Adult zebrafish (*Danio rerio*; 3–4 cm in length) were used for the nerve injury study. Briefly, the fish were anesthetized by immersion in 0.02% MS222 (Sigma-Aldrich, MO, USA) in 10-mM phosphate-buffered saline (pH 7.4). Under anesthesia, the optic nerve was carefully crushed at 1 mm posterior to the eyeball using microscissors. The fish were then reared in 28 °C water until appropriate time points. All animal care was performed according to the guidelines for animal experiments of Kanazawa University. We paid specific attention to minimizing the number of experimental animals required and their suffering.

### *48.2.2 Quantitative Real-Time PCR*

Total RNA was extracted, and single-stranded cDNAs were synthesized using a Transcriptor High Fidelity cDNA Synthesis Kit (Roche, Mannheim, Germany). Quantitative real-time PCR was performed with FastStart Essential DNA Probes Master (Roche) using a LightCycler 96 (Roche). Based on the zebrafish FXIII-A cDNA sequence (GenBank Accession No. BC124320), gene-specific primers were created. To investigate the mRNA expression of the two distinct regions of FXIII-A, we used two sets of gene-specific primers and probes (Table 48.1) selected from the Universal Probe Library (UPL; Roche). The expression levels were analyzed by the ΔΔCt method, using GAPDH as a reference gene.

**Table 48.1** Gene-specific primers and probes for quantitative real-time PCR

| Gene | Position | Primer name | Primer sequence | UPL probe |
|---|---|---|---|---|
| FXIII-A | 25–117 (93 nt) | *F13-1* | Forward, 5'-AGAAGCCGTCCTGATGTGAT-3′ Reverse, 5'-CAGCCATGATAGATAAGGGAAGA-3' | #109 |
| FXIII-A | 1115–1179 (65 nt) | *F13-2* | Forward, 5'-CTACGCCGCTGTCTTCAAC-3′ Reverse, 5'-AGTTGGTCACGACTCTGCTG-3' | #4 |
| GAPDH | 18–122 (105 nt) | *GAPDH* | Forward, 5'-TCAGTCCACTCACACCAAGTG-3′ Reverse, 5'-CGACCGAATCCGTTAATACC-3′ | #110 |

### *48.2.3 Overexpression of FXIII-A in Goldfish Retinal Cultures*

Goldfish retinal explants were prepared as previously described (Sugitani et al. 2006, 2012). Naïve retinas, without optic nerve crushing, were used for retinal explant cultures. Briefly, retinas were isolated under sterile conditions and cut into 0.5-mm squares using scissors. After washing, the retinal explants were resuspended in L-15 medium without fetal calf serum or antibiotics. For overexpression of goldfish FXIII-A (DNA Data Bank of Japan, Mishima, Japan; Accession No. AB622931), we prepared two types of FXIII-A cDNA, one designated F13-L containing the full-length FXIII-A cDNA in the pEGFP-C1 plasmid vector (Clontech, CA, USA) and the other designated F13-S containing a short-type cDNA partially lacking the 5′ region (1–277) of FXIII-A cDNA in the pEGFP-C1 vector. Both vectors were transfected using Lipofectamine 2000 (Invitrogen, CA, USA). Following each transfection procedure, the retinal pellets were resuspended in L-15 medium containing 10% fetal calf serum, 100 U/ml penicillin, and 100 μg/ml streptomycin. The retinal explants were then cultured with 0.5 ml of medium per dish in polyornithine-coated 35-mm dishes at 28 °C. Neurite outgrowth from the retinal explants was assayed by measuring the length and density of neurites in each explant for a total of 40–50 explants per 35-mm dish.

### *48.2.4 Statistical Analysis*

To evaluate the expression of the two distinct regions of FXIII-A, the expression levels of the mRNAs were expressed as mean ± SEM, and the differences were evaluated by one-way ANOVA. Neurite outgrowth from retinal explants under various culture conditions was expressed as a percentage of the number of neurite-bearing explants among 40–50 explants per 35-mm dish. Differences among conditions in the number of explants producing long neurite outgrowth (>250 μm) were analyzed by the chi-square test, followed by Bonferroni's multiple comparison. Statistical significance was set at $P < 0.05$.

## 48.3 Results

### *48.3.1 Real-Time PCR of Zebrafish FXIII-A Gene Expression Using Two Primer Sets*

To investigate FXIII-A gene expression in the retina after optic nerve injury, we compared the expression levels of distinct regions of the FXIII-A gene using two pairs of primer sets (Table 48.1). The first, designated F13-1, targeted the exon 1–2 region of the zebrafish FXIII cDNA. This region is translated to the noncoding region and part of the activation peptide, which is deleted by thrombin during

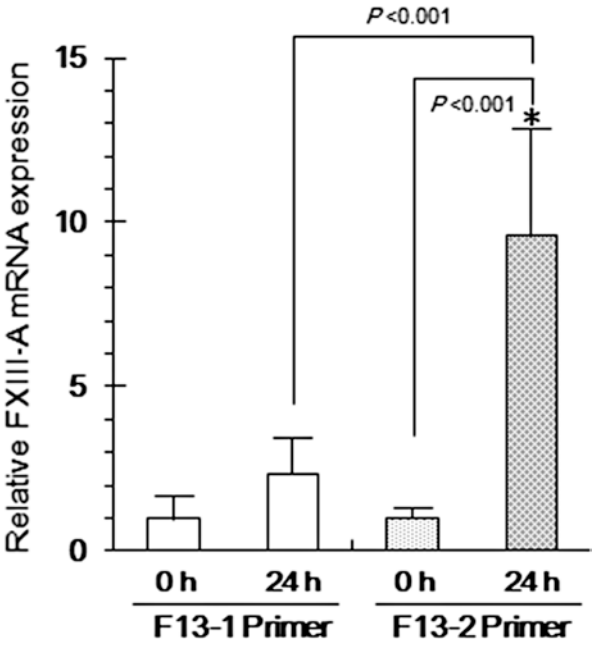


**Fig. 48.1** Upregulation of FXIII-A mRNA in zebrafish retina after optic nerve injury. Real-time PCR analysis showed that FXIII-A mRNA was significantly upregulated at 24 h after optic nerve injury using the F13-2 primer set (F13-2, 24 h). Analysis with the F13-1 primer showed that there was no significant change at 24 h after optic nerve injury (F13-1, 24 h) compared with the control (F13-1, 0 h). *$P < 0.001$ ($n = 3$)

enzymatic activation of plasma FXIII. The second, designated F13-2, amplified the exon 7–8 region, the essential coding region for activated FXIII-A enzyme protein. As shown in Fig. 48.1, the mRNA amplified by F13-2 was significantly upregulated at 24 h after optic nerve injury in the zebrafish retina (F13-2, 24 h) compared with the control retina (F13-2, 0 h). However, expression of the exon 1–2 region of FXIII-A mRNA was strikingly suppressed in the retina after optic nerve injury (F13-1, 24 h) compared with the exon 7–8 region (F13-2, 24 h).

### *48.3.2 Overexpression Study of the FXIII-A Gene in Goldfish Naïve Retinal Cultures*

Next, we analyzed the effects of overexpression of the two types of FXIII-A gene using goldfish naïve retinal explant cultures. One construct was full-length FXIII-A (F13-L), and the other was a modified short-type FXIII-A gene lacking the exon 1–2 region (F13-S). Successful transfection was confirmed by significant increases in the expression of enhanced green fluorescent protein (EGFP) levels in the retinal explants. Explants expressing EGFP only (mock) showed no significant neurite outgrowth. Meanwhile, both types of FXIII-A-overexpressing explants showed induction of neurite outgrowth compared with mock transfection (Fig. 48.2). Furthermore, F13-S transfection clearly promoted more long neurite outgrowth from retinal explant cultures than F13-L transfection (Fig. 48.2).

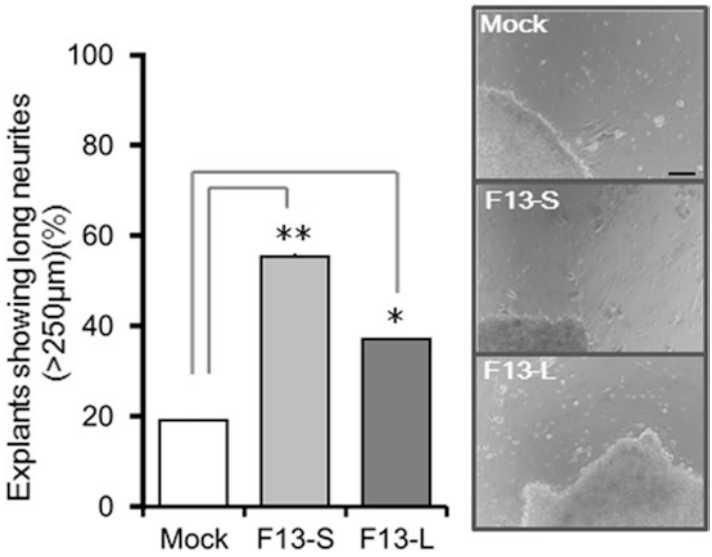


**Fig. 48.2** Overexpression study using two types of FXIII-A cDNA for neurite outgrowth in goldfish retinal explant cultures. Overexpression of FXIII-A cDNA increased the length of neurite outgrowth compared with mock-transfected cells. Overexpression of full-length FXIII-A (F13-L) induced about 40% explants to show >250-μm neurite outgrowth (*$P < 0.05$, significant increase relative to mock). Greater effects were observed for overexpression of short-type FXIII-A (**$P < 0.005$, significant increase relative to mock) after 5 days of culture. The differences among conditions in the number of explants producing neurite outgrowth were analyzed by the chi-square test, followed by Bonferroni's multiple comparison. F13-S, short-type FXIII-A gene construct (deletion of activation peptide); F13-L, full-length FXIII-A gene construct. The experiments were repeated four to five times. Scale bar = 100 μm

## 48.4 Discussion

For enzymatic activation, plasma FXIII requires $Ca^{2+}$ and thrombin to cleavage the residues between Arg37 and Gly38 in the N-terminus and release the activation peptide (Lorand 2001). Meanwhile, the activation mechanism for cellular FXIII, which exists as dimers of FXIII-A in various tissues or cells, is not fully understood. As a first step in this study, we used the zebrafish visual system to examine whether or not thrombin was activated in the retina after optic nerve injury. RT-PCR analysis showed that the levels of thrombin mRNA expression were undetectable in the retina both before and after optic nerve injury (data not shown). Therefore, we raised the hypothesis that there is another activation mechanism for conversion of FXIII-A to the activated form in the fish retina and optic nerve after optic nerve injury. Analysis of FXIII-A mRNA expression by real-time PCR indicated that expression of the 5′ region of FXIII-A was clearly suppressed after optic nerve injury (Fig. 48.1, F13-1). Specifically, there was no significant difference between 0 h and 24 h in the analysis using primer F13-1. In contrast, expression of the main

part of FXIII-A was significantly upregulated by about 9 times compared with the control (0 h) at 24 h after optic nerve injury (Fig. 48.1, F13-2). As the same samples were used in both analyses, this difference in the expression levels of FXIII-A suggested the occurrence of alternative splicing in the FXIII-A gene, resulting in deletion of the region encoding the activation peptide. Moreover, the overexpression study in goldfish retinal explant cultures showed that the short-type FXIII-A gene, which lacked the coding region for the activation peptide, was more effective for neurite outgrowth and elongation from injured RGCs. If an atypical translation mechanism for FXIII-A occurs in the fish retina after optic nerve injury, this would allow direct production of activated FXIII-A protein. In addition, the activated FXIII-A would act to induce neurite outgrowth from the damaged retina in the absence of thrombin.

**Acknowledgments** This work was supported by Grants-in-Aid for Scientific Research to K.S. (No. 26350958 and No. 17K01945) from the Ministry of Education, Culture, Sports, Science and Technology, Japan.

## References

Derrick EK, Barker JN, Khan A, Price ML, Macdonald DM (1993) The tissue distribution of factor XIIIa positive cells. Histopathology 22:157–162

Kato S, Matsukawa T, Koriyama Y, Sugitani K, Ogai K (2013) A molecular mechanism of optic nerve regeneration in fish: the retinoid signaling pathway. Prog Retin Eye Res 37:13–30

Koriyama Y, Homma K, Sugitani K, Higuchi Y, Matsukawa T, Murayama D, Kato S (2007) Upregulation of IGF-I in the goldfish retinal ganglion cells during the early stage of optic nerve regeneration. Neurochem Int 50:749–756

Koriyama Y, Yasuda R, Homma K, Mawatari K, Nagashima M, Sugitani K, Matsukawa T, Kato S (2009) Nitric oxide-cGMP signaling regulates axonal elongation during optic nerve regeneration in the goldfish in vitro and in vivo. J Neurochem 110:890–901

Lorand L (2001) Factor XIII: structure, activation and interactions with fibrinogen and fibrin. Ann N Y Acad Sci 936:291–311

Muszbek L, Ádány R, Mikkola H (1996) Novel aspects of blood coagulation factor XIII. I. Structure, distribution, activation, function. Crit Rev Clin Lab Sci 33:357–421

Ogai K, Hisano S, Mawatari K, Sugitani K, Koriyama Y, Nakashima H, Kato S (2012) Upregulation of anti-apoptotic factors in upper motor neurons after spinal cord injury in adult zebrafish. Neurochem Int 61:1202–1211

Ogai K, Nakatani K, Hisano S, Sugitani K, Koriyama Y, Kato S (2014) Function of Sox2 in ependymal cells of lesioned spinal cords in adult zebrafish. Neurosci Res 88:84–87

Quatresooz P, Paquet P, Hermanns-Lê T, Piérard GE (2008) Molecular mapping of factor XIIIa-enriched dendrocytes in the skin. Int J Mol Med 22:403–409

Sugitani K, Matsukawa T, Koriyama Y, Shintani T, Nakamura T, Noda M, Kato S (2006) Upregulation of retinal transglutaminase during the axonal elongation stage of goldfish optic nerve regeneration. Neuroscience 142:1081–1092

Sugitani K, Ogai K, Hitomi K, Nakamura-Yonehara K, Shintani T, Noda M, Koriyama Y, Tanii H, Matsukawa T, Kato S (2012) A distinct effect of transient and sustained upregulation of cellular factor XIII in the goldfish retina and optic nerve on optic nerve regeneration. Neurochem Int 61:423–432

# Chapter 49
# Bisretinoid Photodegradation Is Likely Not a Good Thing


**Keiko Ueda, Hye Jin Kim, Jin Zhao, and Janet R. Sparrow**

**Abstract** Retinaldehyde adducts (bisretinoids) accumulate in retinal pigment epithelial (RPE) cells as lipofuscin. Bisretinoids are implicated in some inherited and age-related forms of macular degeneration that lead to the death of RPE cells and diminished vision. By comparing albino and black-eyed mice and by rearing mice in darkness and in cyclic light, evidence indicates that bisretinoid fluorophores undergo photodegradation in the eye (Ueda et al. Proc Natl Acad Sci 113:6904–6909, 2016). Given that the photodegradation products modify and impair cellular and extracellular molecules, these processes likely impart cumulative damage to retina.

**Keywords** Retinal degeneration · Age-related macular degeneration · ABCA4-associated disease · Bisretinoid · Visual cycle · Lipofuscin · Retinaldehyde · Vitamin E

## 49.1 Introduction

Adducts of vitamin A aldehyde having bisretinoid structures form in photoreceptor cells by non-enzymatic reactions between retinaldehyde and amine moieties (Sparrow et al. 2010). These fluorophores are deposited in RPE cells as components of phagocytosed outer segments and constitute the lipofuscin of RPE. Various bisretinoids of RPE lipofuscin have been isolated and structurally characterized (Sparrow et al. 2012).

K. Ueda · H. J. Kim · J. Zhao
Departments of Ophthalmology, Columbia University Medical Center, New York, NY, USA

J. R. Sparrow (✉)
Departments of Ophthalmology, Columbia University Medical Center, New York, NY, USA

Departments of Pathology and Cell Biology, Columbia University Medical Center, New York, NY, USA
e-mail: jrs88@cumc.columbia.edu



J. D. Ash et al. (eds.), *Retinal Degenerative Diseases*, Advances in Experimental Medicine and Biology 891, https://doi.org/10.1007/978-3-319-75402-4_49

Bisretinoids form in particular abundance in recessive Stargardt disease (STGD1) caused by mutations in the gene encoding the ATP-binding cassette transporter (ABCA4). This accumulation culminates in the death of RPE. Marked bisretinoid accumulation is replicated in *Abca4* null mutant mice (Weng et al. 1999; Kim et al. 2004), and the relationship between RPE lipofuscin accumulation and retinal disease is evidenced in the *Abca4* mouse model by Bruch's membrane changes and by a progressive loss of photoreceptor cells (Radu et al. 2008; Wu et al. 2010a; Radu et al. 2011; Sparrow et al. 2013; Zhou et al. 2015). *Abca4*$^{-/-}$ mice burdened by elevated levels of bisretinoid lipofuscin are also more susceptible to light damage than are wild-type mice (Wu et al. 2014). Here we review recent work establishing that photodegradation of bisretinoid and its adverse consequences are ongoing in the eye.

## 49.2 Bisretinoid Photooxidation and Photodegradation in Vitro

Given the adverse consequences of bisretinoid accumulation, efforts have been made to elucidate mechanisms by which these fluorophores damage cells. For instance, bisretinoids photogenerate reactive oxygen species such as singlet oxygen and superoxide anion (Gaillard et al. 1995; Rozanowska et al. 1995; Ben-Shabat et al. 2002; Jang et al. 2005; Kim et al. 2007; Yamamoto et al. 2011). By quenching these reactive forms of oxygen, bisretinoids are subsequently photooxidized, and with photocleavage at these oxidation sites, aldehyde- and dicarbonyl-carrying fragments are released (Wu et al. 2010b). Proteins modified by these dicarbonyls are constituents of drusen (Farboud et al. 1999; Handa et al. 1999); they cross-link protein and promote resistance to the activity of matrix metalloproteinases (Zhou et al. 2015).

## 49.3 Bisretinoid Levels in Albino and Black Mice Housed in Cyclic Light or Darkness

The photodegradation of bisretinoid was also demonstrated in mice by comparing levels of bisretinoid in mice raised in cyclic light (12 h on/12 h off) as opposed to darkness and by comparing albino (C57BL/6J$^{c2j}$) and black (C57BL/6 J) mice. In the absence of melanin, light entering the eye is substantially increased (LaVail and Battelle 1975; van den Berg et al. 1991). The bisretinoid A2E was detected in eyes from both cyclic light- and dark-reared mice (Fig. 49.1) (Boyer et al. 2012). Whereas it might be expected that the added photon catch in the albino eye would drive the formation of these visual cycle adducts (bisretinoids), instead A2E levels were

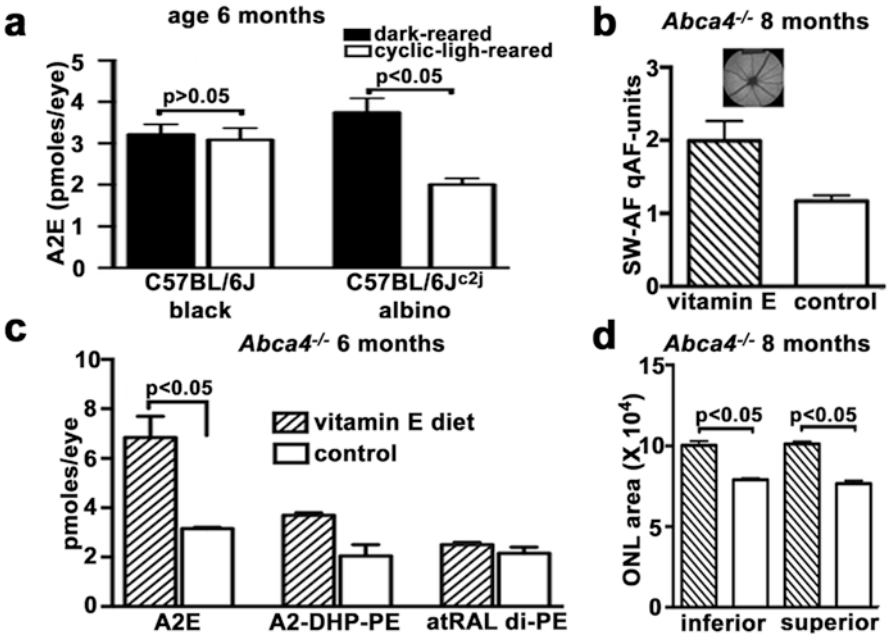


**Fig. 49.1** *The RPE bisretinoid A2E accumulates in both light- and dark-reared mice, levels are reduced in light-reared* versus *dark-reared albino mice*, and levels are modulated by antioxidant status. Analysis by reverse-phase HPLC. (**a**): Quantitation of the bisretinoid A2E in 6-month-old black C57BL/6J and albino C57BL/6J–$^{c2j}$ mice that were dark reared or cyclic light reared from birth. Means ± SEM of five or seven independent samples six to eight eyes/sample p-values determined by one-way ANOVA and Tukey's multiple comparison test and two-tailed *t*-test. (**b, c**): Reduction in bisretinoid photooxidation by vitamin E supplementation is detected as reduced bisretinoid loss and measured as increased quantitative fundus autofluorescence (qAF) (b) and increased HPLC-quantified A2E, A2-DHP-PE, and atRAL di-PE (c). Means ± SEM of eight mice, $p < 0.05$, two-tailed *t*-test. (a); Two samples (six eyes per sample), ANOVA and Sidak's multiple comparison test (b). (**d**): Reduced bisretinoid photooxidation/photodegradation also protects against outer nuclear layer (ONL) thinning. ONL area (microns$^2$) calculated as the sum of the ONL thicknesses in the superior and inferior retina (0.2–2.0 mm from optic nerve head) multiplied by the measurement interval of 200 microns; means ± SEM, two-tailed *t*-test

lower in albino C57BL/6J$^{c2j}$ mice maintained under cyclic light than in albino C57BL/6J$^{c2j}$ mice reared in darkness ($p < 0.05$) (Fig. 49.1).

Given in vitro evidence of photodegradation (Wu et al. 2010b) and the presence of oxidized bisretinoid in human and mouse retina (Jang et al. 2005; Kim et al. 2007), the most parsimonious explanation for the light-related differences is photooxidation-associated photodegradative loss of these light-sensitive fluorophores.

It is likely that bisretinoid formation under cyclic light is more pronounced than the levels observed here; for instance, photodegradative loss could mask even greater lipofuscin formation under cyclic light. The comparison of albino versus black-eyed mice presumably allowed photodegradative loss of A2E to be detected

over a relatively short period of time. These photobleaching processes have been replicated in cell-based and non-cellular assays (Yamamoto et al. 2012), and examples of photooxidation and photodegradation of RPE bisretinoids (photobleaching) in retinae of human and nonhuman primates are reported (Hunter et al. 2012; Sparrow and Duncker 2014).

## 49.4 Vitamin E-Treated Mice: Evidence Supporting Photooxidative Processes in Modulating Bisretinoid Levels

It has been shown previously that the lipid-soluble antioxidant vitamin E can suppress bisretinoid oxidation by quenching singlet oxygen (Sparrow et al. 2003b). In albino *Abca4*$^{-/-}$ mice given a vitamin E-supplemented diet (960 mg (IU)/kg vitamin E as dl-alpha-tocopheryl acetate) from 1 to 6 months of age, levels of the bisretinoids A2E ($p < 0.05$ one-way ANOVA and Sidak's multiple comparison test), A2-DHP-PE, and all-*trans*-retinal dimer-PE were greater than in control mice. Quantitation of short-wavelength fundus autofluorescence (quantitative fundus autofluorescence, qAF) (Sparrow et al. 2013; Flynn et al. 2014) that originates from bisretinoid lipofuscin also revealed higher levels of fundus autofluorescence in the vitamin E-treated mice ($p < 0.05$, two-tailed *t*-test) (Fig. 49.1). Importantly, the thinning of outer nuclear layer that is indicative of reduced photoreceptor cell viability and that has been observed in albino *Abca4*$^{-/-}$ mice (Wu et al. 2010a; Sparrow et al. 2013; Wu et al. 2014) was less pronounced in the vitamin E-treated mice ($p < 0.05$, two-tailed *t*-test) (Fig. 49.1). The greater levels of bisretinoid and qAF in the vitamin E-treated versus control mice are consistent with a mechanism involving a reduction in photooxidation-associated consumption of bisretinoid in the presence of the antioxidant vitamin E.

## 49.5 Implications

The findings discussed here indicate that although light deprivation does not prevent the formation of bisretinoids (Boyer et al. 2012; Ueda et al. 2016), limiting light exposure can protect against damaging bisretinoid photodegradation. Thus not surprisingly, a black contact lens that blocked >90% of light in one eye of STGD1 patients was found to reduce the progression of decreased fundus autofluorescence (four of five patients) as compared with the patients' unprotected eyes (Teussink et al. 2015). Sunglasses that attenuate light over a broad range of wavelengths or yellow lenses that reduce "blue" wavelengths might also be used to advantage.

Several studies, most notably the Age-Related Eye Disease Study (AREDS), have demonstrated that dietary antioxidants and intake of antioxidants by

supplementation reduces incidence or progression of AMD (Snodderly 1995; Age-Related Eye Disease Study Research 2001; SanGiovanni et al. 2007; Sobrin and Seddon 2014). Given that antioxidants can protect against AMD and that vitamins E and C have also been shown to reduce A2E photooxidation/photodegradation (Sparrow et al. 2003; Zhou et al. 2006), the beneficial effects of antioxidant intake could be mediated at least in part by intercepting bisretinoid photooxidation and degradation. Similarly, a contribution of lifetime light exposure to AMD risk (Cruickshanks et al. 2001; Tomany et al. 2004; Fletcher et al. 2008; Sui et al. 2013; Huang et al. 2014; Klein et al. 2014; Fritsche et al. 2016) could be mediated in part by the cellular damage imposed by bisretinoid photodegradation.

## References

Age-Related Eye Disease Study Research G (2001) A randomized, placebo-controlled, clinical trial of high-dose supplementation with vitamins C and E, beta carotene, and zinc for age-related macular degeneration and vision loss: AREDS report no. 8. Arch Ophthalmol 119:1417–1436

Ben-Shabat S, Itagaki Y, Jockusch S et al (2002) Formation of a nona-oxirane from A2E, a lipofuscin fluorophore related to macular degeneration, and evidence of singlet oxygen involvement. Angew Chem Int Ed 41:814–817

Boyer NP, Higbee D, Currin MB et al (2012) Lipofuscin and N-retinylidene-N-retinylethanolamine (A2E) accumulate in the retinal pigment epithelium in the absence of light exposure: their origin is 11-cis retinal. J Biol Chem 287:22276–22286

Cruickshanks KJ, Klein R, Klein BEK et al (2001) Sunlight and the 5-year incidence of early age-related maculopathy: the Beaver Dam Eye Study. Arch Ophthalmol 119:246–250

Farboud B, Aotaki-Keen A, Miyata T et al (1999) Development of a polyclonal antibody with broad epitope specificity for advanced glycation endproducts and localization of these epitopes in Bruch's membrane of the aging eye. Mol Vis 5:11

Fletcher AE, Bentham GC, Agnew M et al (2008) Sunlight exposure, antioxidants, and age-related macular degeneration. Arch Ophthalmol 126:1396–1403

Flynn E, Ueda K, Auran E et al (2014) Fundus autofluorescence and photoreceptor cell rosettes in mouse models. Invest Ophthalmol Vis Sci 55:5643–5652

Fritsche LG, Igl W, Bailey JN et al (2016) A large genome-wide association study of age-related macular degeneration highlights contributions of rare and common variants. Nat Genet 48(2):134–143

Gaillard ER, Atherton SJ, Eldred G et al (1995) Photophysical studies on human retinal lipofuscin. Photochem Photobiol 61:448–453

Handa JT, Verzijl N, Matsunaga H et al (1999) Increase in advanced glycation end product pentosidine in Bruch's membrane with age. Invest Ophthalmol Vis Sci 40:775–779

Huang EJ, Wu SH, Lai CH et al (2014) Prevalence and risk factors for age-related macular degeneration in the elderly Chinese population in south-western Taiwan: the Puzih eye study. Eye (Lond) 28:705–714

Hunter JJ, Morgan JI, Merigan WH et al (2012) The susceptibility of the retina to photochemical damage from visible light. Prog Retin Eye Res 31:28–42

Jang YP, Matsuda H, Itagaki Y et al (2005) Characterization of peroxy-A2E and furan-A2E photooxidation products and detection in human and mouse retinal pigment epithelial cells lipofuscin. J Biol Chem 280:39732–39739

Kim SR, Fishkin N, Kong J et al (2004) The Rpe65 Leu450Met variant is associated with reduced levels of the RPE lipofuscin fluorophores A2E and iso-A2E. Proc Natl Acad Sci U S A 101:11668–11672

Kim SR, Jang YP, Jockusch S et al (2007) The all-trans-retinal dimer series of lipofuscin pigments in retinal pigment epithelial cells in a recessive Stargardt disease model. Proc Natl Acad Sci U S A 104:19273–19278

Klein BE, Howard KP, Iyengar SK et al (2014) Sunlight exposure, pigmentation, and incident age-related macular degeneration. Invest Ophthalmol Vis Sci 55:5855–5861

LaVail MM, Battelle B-A (1975) Influence of eye pigmentation and light deprivation on inherited retinal dystrophy in the rat. Exp Eye Res 21:167

Radu RA, Yuan Q, Hu J et al (2008) Accelerated accumulation of lipofuscin pigments in the RPE of a mouse model for ABCA4-mediated retinal dystrophies following vitamin A supplementation. Invest Ophthalmol Vis Sci 49:3821–3829

Radu RA, Hu J, Yuan Q et al (2011) Complement system dysregulation and inflammation in the retinal pigment epithelium of a mouse model for Stargardt macular degeneration. J Biol Chem 286:18593–18601

Rozanowska M, Jarvis-Evans J, Korytowski W et al (1995) Blue light-induced reactivity of retinal age pigment. In vitro generation of oxygen-reactive species. J Biol Chem 270:18825–18830

SanGiovanni JP, Chew EY, Clemons TE et al (2007) The relationship of dietary lipid intake and age-related macular degeneration in a case-control study: AREDS report no. 20. Arch Ophthalmol 125:671–679

Snodderly DM (1995) Evidence for protection against age-related macular degeneration by carotenoids and antioxidant vitamins. Am J Clin Nutr 62(suppl):1448S–1461S

Sobrin L, Seddon JM (2014) Nature and nurture- genes and environment- predict onset and progression of macular degeneration. Prog Retin Eye Res 40:1–15

Sparrow JR, Duncker T (2014) Fundus autofluorescence and RPE lipofuscin in age-related macular degeneration. J Clin Med 3:1302–1321

Sparrow JR, Vollmer-Snarr HR, Zhou J et al (2003) A2E-epoxides damage DNA in retinal pigment epithelial cells. Vitamin E and other antioxidants inhibit A2E-epoxide formation. J Biol Chem 278:18207–18213

Sparrow JR, Yoon K, Wu Y et al (2010) Interpretations of fundus autofluorescence from studies of the bisretinoids of retina. Invest Ophthalmol Vis Sci 51:4351–4357

Sparrow JR, Gregory-Roberts E, Yamamoto K et al (2012) The bisretinoids of retinal pigment epithelium. Prog Retin Eye Res 31:121–135

Sparrow JR, Blonska A, Flynn E et al (2013) Quantitative fundus autofluorescence in mice: correlation with HPLC quantitation of RPE lipofuscin and measurement of retina outer nuclear layer thickness. Invest Ophthalmol Vis Sci 54:2812–2820

Sui GY, Liu GC, Liu GY et al (2013) Is sunlight exposure a risk factor for age-related macular degeneration? A systematic review and meta-analysis. Br J Ophthalmol 97:389–394

Teussink MM, Lee MD, Smith RT et al (2015) The effect of light deprivation in patients with Stargardt disease. Am J Ophthalmol 159(964–972):e962

Tomany SC, Cruickshanks KJ, Klein R et al (2004) Sunlight and the 10-year incidence of age-related maculopathy. The Beaver Dam Eye Study. Arch Ophthalmol 122:750–757

Ueda K, Zhao J, Kim HJ et al (2016) Photodegradation of retinal bisretinoids in mouse models and implications for macular degeneration. Proc Natl Acad Sci 113:6904–6909

van den Berg TJTP, IJspeert JK, deWaard PWT (1991) Dependence of intraocular straylight on pigmentation and light transmission through the ocular wall. Vis Res 31:1361–1367

Weng J, Mata NL, Azarian SM et al (1999) Insights into the function of Rim protein in photoreceptors and etiology of Stargardt's disease from the phenotype in abcr knockout mice. Cell 98:13–23

Wu L, Nagasaki T, Sparrow JR (2010a) Photoreceptor cell degeneration in *Abcr*$^{-/-}$ mice. Adv Exp Med Biol 664:533–539

Wu Y, Yanase E, Feng X et al (2010b) Structural characterization of bisretinoid A2E photocleavage products and implications for age-related macular degeneration. Proc Natl Acad Sci 107:7275–7280

Wu L, Ueda K, Nagasaki T et al (2014) Light damage in Abca4 and Rpe65rd12 mice. Invest Ophthalmol Vis Sci 55:1910–1918

Yamamoto K, Yoon KD, Ueda K et al (2011) A novel bisretinoid of retina is an adduct on glycerophosphoethanolamine. Invest Ophthalmol Vis Sci 52:9084–9090

Yamamoto K, Zhou J, Hunter JJ et al (2012) Toward an understanding of bisretinoid autofluorescence bleaching and recovery. Invest Ophthalmol Vis Sci 53:3536–3544

Zhou J, Gao X, Cai B et al (2006) Indirect antioxidant protection against photooxidative processes initiated in retinal pigment epithelial cells by a lipofuscin pigment. Rejuvenation Res 9:256–263

Zhou J, Ueda K, Zhao J et al (2015) Correlations between photodegradation of bisretinoid constituents of retina and dicarbonyl-adduct deposition. J Biol Chem 290:27215–27227

# Chapter 50
# Further Characterization of the Predominant Inner Retinal Degeneration of Aging *Cln3*$^{\Delta ex7/8}$ Knock-In Mice

**Cornelia Volz, Myriam Mirza, Thomas Langmann, and Herbert Jägle**

**Abstract** Neuronal ceroid lipofuscinosis (NCL) is the most common group of neurogenetic storage diseases typically beginning in childhood. The juvenile form (JNCL), also known as Batten disease, is the most common form. Vision-related problems are often an early sign, appearing prior to motor and mental deficits. We have previously investigated disease progression with age in the *Cln3*$^{\Delta ex7/8}$ KI mouse model for JNCL and showed a decline of visual acuity and a predominant decline of the inner retinal function in mice, similar to human disease. The aim of this study was to further characterize this degeneration by means of flicker ERGs. For the scotopic flicker ERG, we found a significantly lower magnitude for *Cln3*$^{\Delta ex7/8}$ KI mice already at 6 months of age for low stimulus frequencies, while the difference declines with increasing frequency. Under photopic conditions there was no magnitude difference at 6 months, but a cumulative magnitude reduction with further aging. For both conditions the phases were similar for both groups. There was a similar magnitude reduction for the responses of both the slow and fast rod pathway in the 15 Hz experiments, and there were no differences in response phase. Low-frequency flicker responses seem to be sensitive to very early disease manifestations, and while the degeneration is associated with a reduction of predominating inner retinal responses in the scotopic flash ERG, this predominance seems not to be related to a selective involvement of the slow and fast rod pathways.

**Keywords** Neuronal ceroid lipofuscinosis · *Cln3* · Retinal function · Electroretinography · Flicker ERG

C. Volz (✉) · H. Jägle
Department of Ophthalmology, University Eye Clinic Regensburg, Regensburg, Germany
e-mail: Cornelia.Volz@ukr.de

M. Mirza
Institute of Human Genetics, University of Regensburg, Regensburg, Germany

Department of Experimental Immunology of the Eye, University of Cologne, Cologne, Germany

T. Langmann
Department of Experimental Immunology of the Eye, University of Cologne, Cologne, Germany



J. D. Ash et al. (eds.), *Retinal Degenerative Diseases*, Advances in Experimental Medicine and Biology 891, https://doi.org/10.1007/978-3-319-75402-4_50

## 50.1 Introduction

Neurodegenerative diseases are rare in childhood. Neuronal ceroid lipofuscinosis (NCL) is the most common group of neurogenetic storage diseases and begins in childhood with an estimated frequency of 1 in 100,000 live births worldwide (Jalanko and Braulke 2009). The juvenile form (JNCL), also known as Batten disease, is the most common form. Decreased vision is often an early sign, leading parents to consult an ophthalmologist, who can diagnose the disease at an incipient stage. Later the disease progresses to blindness and other neurological symptoms occur.

Diverse animal models are available for different NCL forms (Ruther 2010). We have previously investigated disease progression with age in a mouse model for JNCL and showed a decline of visual acuity and amplitudes of scotopic and photopic flash electroretinography. In detail, our results showed a predominant decline of the inner retinal function in *Cln3*$^{\Delta ex7/8}$ KI mice, similar to human disease. In this study we use flicker ERG to extend our understanding of the retinal degeneration in this model.

## 50.2 Materials and Methods

### *50.2.1 Experiments with Animals*

Wild-type (*Cln3*$^{+/+}$) and homozygous *Cln3*$^{\Delta ex7/8}$ knock-in mice were all on a C57BL/6 background. All mice tested positive for the Crb1$^{rd8}$ mutation. Animals were maintained in an air-conditioned environment on a 12-h light-dark schedule at 22 °C and had free access to food and water. The health of the animals was regularly monitored, and all procedures were approved by the University of Regensburg animal rights committee and complied with the German Law on Animal Protection and the Institute for Laboratory Animal Research Guide for the Care and Use of Laboratory Animals, 2011.

### *50.2.2 Electroretinography*

ERGs were obtained according to the following protocol. Mice were dark adapted for at least 12 h before the experiments and subsequently anesthetized by subcutaneous injection of ketamine (65 mg/kg bw) and xylazine (13 mg/kg bw). Pupils were dilated with tropicamide eye drops (Mydriaticum Stulln; Pharma Stulln, Germany). Silver needle electrodes served as reference (forehead) and ground (tail)

and gold wire ring electrodes as active electrodes. Corneregel (Bausch & Lomb, Berlin, Germany) was applied to keep the eye hydrated and maintain good electrical contact. ERGs were recorded using a Ganzfeld bowl (Ganzfeld QC450 SCX, Roland Consult, Brandenburg, Germany) and an amplifier and recording unit (RETI-Port, Roland Consult, Brandenburg, Germany). ERGs were recorded from both eyes simultaneously, band-pass filtered (1–300 Hz) and averaged. ERG measurements were performed at 6, 12, and 18 months of age. After dark adaptation scotopic flicker ERGs were recorded to stimuli with an intensity of 0.5 log cds/m$^2$ and frequencies ranging from 4 to 25 Hz. Next dual rod pathways, comprising rod photoreceptors and rod and cone bipolar and amacrine cells, were investigated by means of 15 Hz flicker response recordings to increasing intensities ranging from −3.5 to 1.0 log cds/m$^2$. After 10 minutes of adaptation to a white background illumination (20 cd/m$^2$), responses to flickering stimuli (intensity 0.5 log cds/m$^2$) with frequencies ranging from 4 to 25 Hz were recorded. All flicker response waveforms were analyzed by means of a fast Fourier transform to calculate response magnitude and phase. All analysis and plotting was carried out with R version 3.2.1 (The R Foundation for Statistical Computing, Vienna, Austria) and ggplot2 version 2.1.0.

## 50.3 Results

### *50.3.1 Scotopic Flicker ERG*

For evaluation of the temporal characteristics of the rod system, responses to flickering stimuli with a fixed intensity (0.5 log cds/m$^2$) were recorded after dark adaptation. Compared to wild type, response waveforms of the *Cln3*$^{\Delta ex7/8}$ mice showed reduced magnitudes at 6 months of age already. Starting with magnitude reductions for low frequencies, with disease duration the magnitude diminishes for all frequencies (Fig. 50.1). Still the waveform is similar, and the response phase is not significantly different between *Cln3*$^{\Delta ex7/8}$ and wild-type mice.

### *50.3.2 Photopic Flicker ERG*

After adaptation to a white background illumination (20 cd/m$^2$), responses to flickering stimuli with a fixed intensity (0.5 log cds/m$^2$) represent responses of the cone system. While the response magnitude of the 18-month-old *Cln3*$^{\Delta ex7}$*/8* mice was significantly smaller for low-frequency stimuli compared to wild-type mice (Fig. 50.2), we found no group difference for 6-month-old mice, indicating a predominant rod degeneration. Again, there was no difference in response phase between groups at all ages.

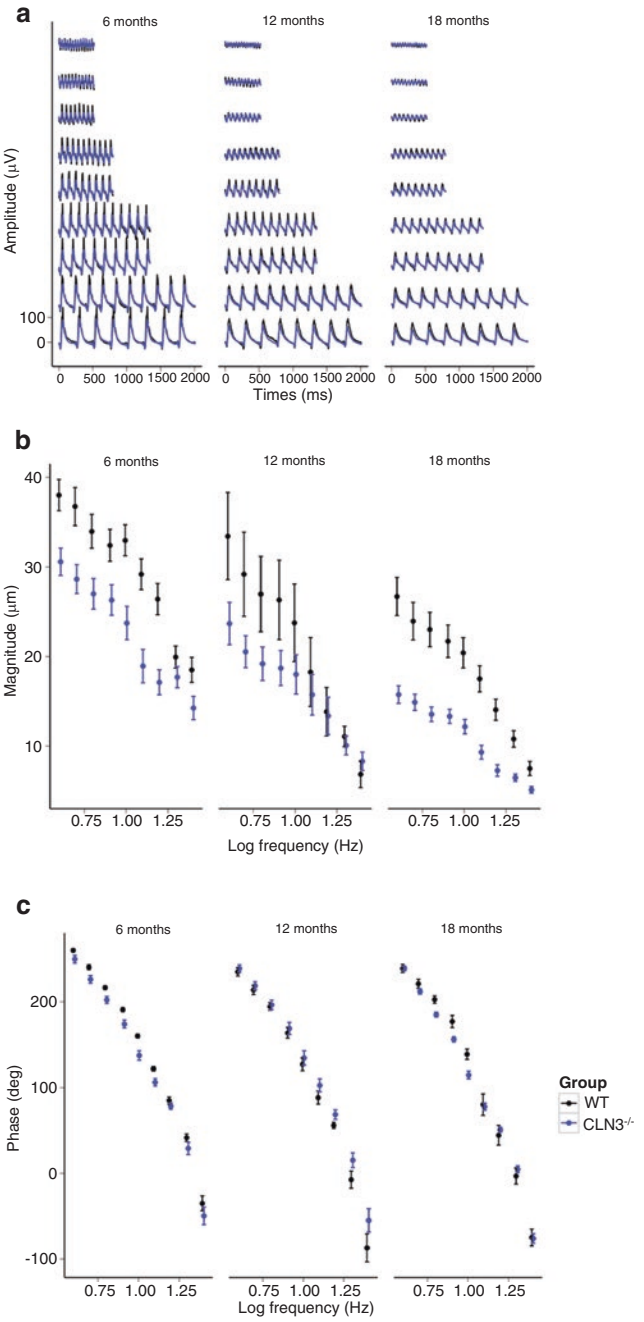


**Fig. 50.1** (**a**) Scotopic flicker ERG waveforms for 6-, 12-, and 18-month-old wild-type *Cln3*$^{+/+}$ (black trace) and homozygous *Cln3*$^{\Delta ex7/8}$ mice (blue trace). (**b**) Response magnitudes for the three age groups show significantly reduced magnitudes for the homozygous *Cln3*$^{\Delta ex7/8}$ mice starting at lower frequencies and affecting the full frequency range in advanced ages. (**c**) There is no significant difference in response phase

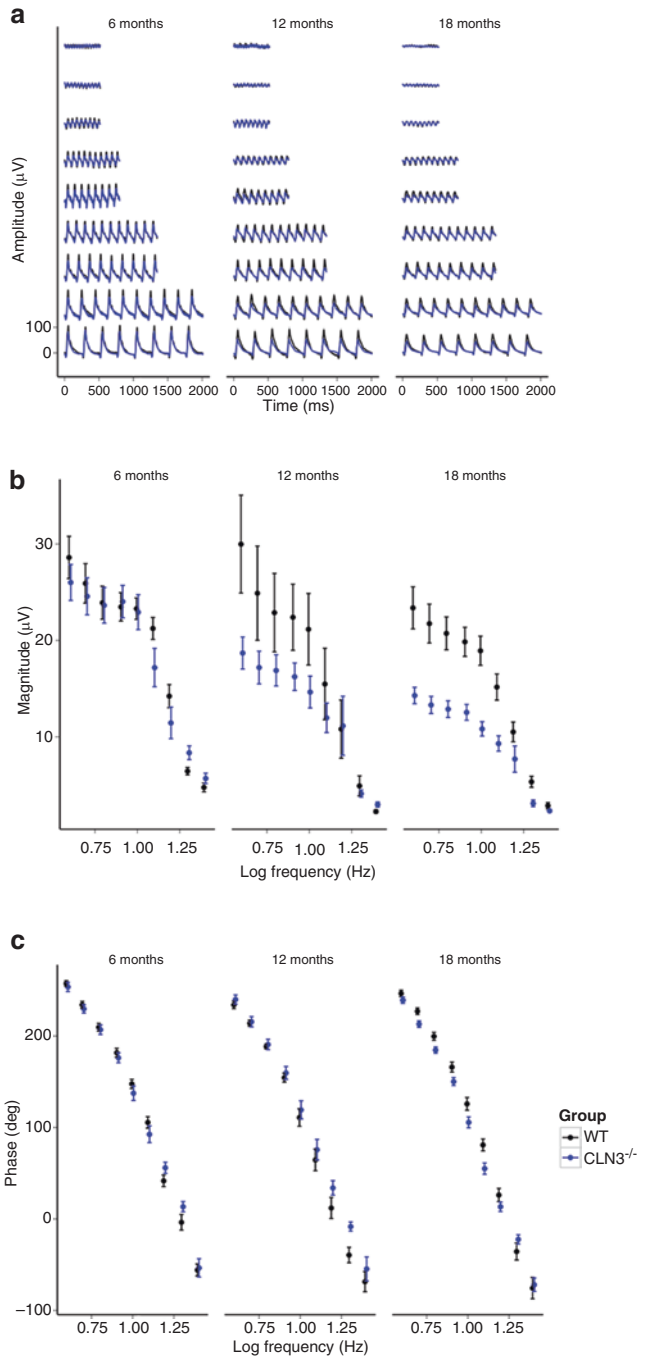


**Fig. 50.2** (**a**) Photopic flicker ERG waveforms for 6-, 12-, and 18-month-old wild-type *Cln3*$^{+/+}$(black trace) and homozygous *Cln3*$^{\Delta ex7/8}$ mice (blue trace). (**b**) Response magnitude of homozygous *Cln3*$^{\Delta ex7/8}$ mice was similar at 6 months of age but declining with age. At 18 months a significant reduction of response magnitude for low and middle frequencies, but not for the higher frequencies, was seen. (**c**) There is no significant difference in response phase between groups

### *50.3.3 15 Hz ERG*

A negative ERG waveform as described in the scotopic single-flash results shown in our previous paper may be associated with selective changes in the two rod pathways. Thus we recorded responses to a series of scotopic flicker intensities at a frequency of 15 Hz (Fig. 50.3). While for low stimulus intensities the response waveforms predominantly originate from the slow rod pathway, at a certain intensity a phase shift indicates the transition to predominance of the fast rod pathway (Sharpe and Stockman 1999). At 6 and 12 months of age, we found no significant difference of the response magnitude for both the slow and fast rod pathway, between the groups of homozygous *Cln3*$^{\Delta ex7/8}$ and wild-type mice. At 18 months of age, the magnitude was significantly lower for *Cln3*$^{\Delta ex7/8}$ mice compared to wild-type mice. However, there was no significant difference between the magnitude reduction of the responses from the slow and fast rod pathway. Again, there is no difference in response phase.

## 50.4 Discussion

In our previous work, we characterized the retinal degeneration in a *Cln3*$^{\Delta ex7/8}$ mouse model for JNCL. We showed a decline of retinal function noticeable in the photopic ERG as early as in the age of 6 months. In our study scotopic ERG responses to a series of single flashes showed similar response amplitudes at the age of 6 months with a decline of the response amplitudes with age. This amplitude reduction was consistent with a predominant degeneration of the inner retinal layers, indicated by the decline of the b-wave amplitudes with preservation of the a-wave amplitudes (Volz et al. 2014). While in general our data was consistent with the report of Staropoli et al., they did not find a differential degeneration between the rod and cone system (Staropoli et al. 2012). However, they also showed a predominance of the inner retinal degeneration in *Cln3*$^{\Delta ex7/8}$ mice. The flicker data we here present would suggest a somewhat earlier or more pronounced rod system degeneration. Taking the single flash data into account, it seems more likely that the rod and cone system is affected similarly.

While the single-flash ERGs allow distinguishing at least to some extent between the outer and inner retinal function, flicker ERGs reflect inner retinal responses only. Under scotopic conditions the responses to stimuli with a frequency below 5 Hz are thought to be dominated by the rod pathways, between 5 and 15 Hz by the cone ON-pathway and above 15 Hz by the cone OFF-pathway (Tanimoto et al. 2015). Krishna et al. studied the cellular origin of the temporal response function of the mouse cone ERG and found that at low temporal frequencies, the mouse cone ERG is dominated by depolarizing bipolar cells (DBC), but the relative DBC contribution decreases systematically with increasing temporal frequency (Krishna et al. 2002). Since the responses to stimuli with higher frequencies were largely

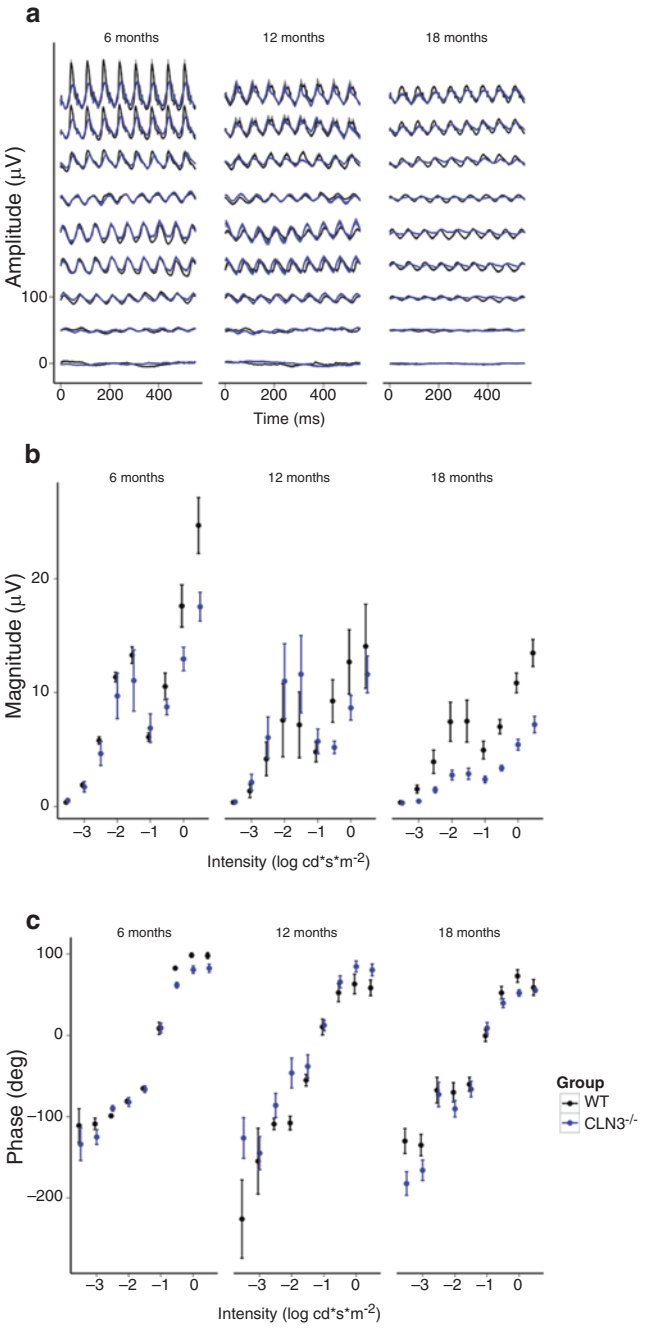


**Fig. 50.3** (**a**) 15 Hz ERG waveforms are shown for 6-, 12-, and 18-month-old wild-type (*Cln3*$^{+/+}$, black trace) and homozygous *Cln3*$^{\Delta ex7/8}$ mice (blue trace). (**b**) Response magnitude was reduced for both groups as mice age. At 18 months only, the homozygous *Cln3*$^{\Delta ex7/8}$ mice showed a significant reduction of response magnitude. However, both pathways were affected similarly. (**c**) The response phase did not differ between groups

preserved in our study under scotopic and photopic conditions, the retinal degeneration in *Cln3*$^{\Delta ex7/8}$ mice seems to predominantly affect the rod and cone ON-pathways and may preserve the function of the cone OFF-pathway.

In the mammalian retina, there are at least two rod pathways: The first is "slow" rod pathway that transmits signals from the rod photoreceptors to the rod ON bipolar cells, to AII amacrine cells, then to cone ON and OFF bipolar cells, and subsequently to ganglion cells. A second rod pathway, the "fast" pathway, transmits signals from rod to cone photoreceptors via gap junctions and then to cone ON and OFF bipolar cells and their ganglion cells (Park et al. 2015). The two pathways differ in response timing and in the luminance range over which they operate. Only older, 18-month-old *Cln3*$^{\Delta ex7/8}$ mice had smaller response magnitudes when compared to age-matched controls. The degeneration seems to affect the slow and the fast pathway to the same extent. Lei described two different contributions to the two peaks in the amplitude-intensity profile of the dark-adapted 10 Hz flicker ERG of wild-type mice (Lei 2012). Based on recordings from rod-only and cone-only mice, he concluded that the first part including the first peak gets input from the rod system, while the second part at higher intensities gets input from the cone system. We obtained 15 Hz flicker ERGs under scotopic conditions and observed a similar intensity dependency with two peaks likely corresponding to rod-driven and cone-driven responses in both *Cln3*$^{\Delta ex7/8}$ and wild-type mice at all tested ages.

Weleber et al. analyzed ERG response from three JNCL patients who had severely subnormal scotopic ERG responses with an electronegative configuration. He also described the deterioration of responses to 30 Hz flicker stimuli. However, the flicker responses were delayed and had subnormal amplitudes (Weleber 1998) but were still clearly present. In contrast, in our study the phase of the response waveform was not different from that of wild-type mice.

In summary, there was a similar magnitude reduction for the responses of both the slow and fast rod pathway in the 15 Hz experiments, and there were no differences in response phase. Low-frequency flicker responses seem to be sensitive to very early disease manifestations, and while the degeneration is associated with a reduction of predominating inner retinal responses in the scotopic flash ERG, this predominance seems not to be related to a selective involvement of the slow and fast rod pathways.

**Acknowledgments** We would like to thank Dr. Klaus Rüther for providing *Cln3*$^{\Delta ex7/8}$ mice. We thank Dr. Frank Stehr for his support. This work was funded by the NCL Foundation and the Auerbach Foundation.

## References

Jalanko A, Braulke T (2009) Neuronal ceroid lipofuscinoses. Biochim Biophys Acta 1793:697–709

Krishna VR, Alexander KR, Peachey NS (2002) Temporal properties of the mouse cone electroretinogram. J Neurophysiol 87:42–48

Lei B (2012) Rod-driven OFF pathway responses in the distal retina: dark-adapted flicker electroretinogram in mouse. PLoS One 7:e43856

Park JC, Cao D, Collison FT et al (2015) Rod and cone contributions to the dark-adapted 15-Hz flicker electroretinogram. Doc Ophthalmol 130:111–119

Ruther K (2010) NCL in animal models. Ophthalmologe 107:621–627

Sharpe LT, Stockman A (1999) Rod pathways: the importance of seeing nothing. Trends Neurosci 22:497–504

Staropoli JF, Haliw L, Biswas S et al (2012) Large-scale phenotyping of an accurate genetic mouse model of JNCL identifies novel early pathology outside the central nervous system. PLoS One 7:e38310

Tanimoto N, Sothilingam V, Kondo M et al (2015) Electroretinographic assessment of rod- and cone-mediated bipolar cell pathways using flicker stimuli in mice. Sci Rep 5:10731

Volz C, Mirza M, Langmann T et al (2014) Retinal function in aging homozygous Cln3 (Deltaex7/8) knock-in mice. Adv Exp Med Biol 801:495–501

Weleber RG (1998) The dystrophic retina in multisystem disorders: the electroretinogram in neuronal ceroid lipofuscinoses. Eye (Lond) 12(Pt 3b):580–590

# Chapter 51
# Differential Exon Expression in a Large Family of Retinal Genes Is Regulated by a Single Trans Locus

**Jiaxing Wang, Felix L. Struebing, Salma Ferdous, Kevin Donaldson, Jeffrey H. Boatright, Eldon E. Geisert, and John M. Nickerson**

**Abstract** Transcription and RNA processing can generate many variant mRNAs (isoforms) from a given genomic locus. The more we learn about RNA processing the more we realize how complex it can be. Examining the expression profiles of individual exons, we observed that specific exons were differentially expressed across a large number of genes in mice. We found that each isoform or exon is independently expressed compared to other exons from the same gene and regulated separately in *trans*. Each *trans* locus was identified by mapping using linkage analysis in a large mouse recombinant inbred strain set. We present evidence for a limited number of these master regulatory loci in the retina. One major locus controls about half the expression of the individual exons and resides on Chromosome 4, between 133 and 136 Mb.

**Keywords** Differential splicing · Genomic regulation · Transcriptome

Eldon E. Geisert and John M. Nickerson contributed equally to this work.

J. Wang
Department of Ophthalmology, Tianjin Medical University General Hospital, Tianjin, China

Department of Ophthalmology, Emory University, Atlanta, GA, USA

F. L. Struebing · S. Ferdous · K. Donaldson · E. E. Geisert · J. M. Nickerson (✉)
Department of Ophthalmology, Emory University, Atlanta, GA, USA
e-mail: litjn@emory.edu

J. H. Boatright
Department of Ophthalmology, Emory University, Atlanta, GA, USA

Center for Visual and Neurocognitive Rehabilitation, Atlanta VA Medical Center, Decatur, GA, USA



J. D. Ash et al. (eds.), *Retinal Degenerative Diseases*, Advances in Experimental Medicine and Biology 891, https://doi.org/10.1007/978-3-319-75402-4_51

## 51.1 Introduction

Genes in eukaryotes are interrupted by introns. Sophisticated RNA transcription and processing machinery exists, which provides for differential expression of genes and the generation of a great diversity in multiple mRNA isoforms from a single gene (Sharp 1994). Differential expression and multiple isoforms can generate widely varying levels of each exon of a gene, despite the equimolar amounts of given exons in a single mature mRNA as illustrated in Fig. 51.1.

This was obvious early in the study of gene expression in the retina. For example, there is only one rhodopsin gene (i.e., no copy number variants), yet many bands of RNA appear on northern blots, indicating multiple isoforms of mature opsin mRNA (Al-Ubaidi et al. 1990). Many genes have alternative promoters, terminators, and splicing patterns.

In this study, we sought to learn how differential expression is controlled in the mouse retina. Our central hypothesis is that many exons from different genes change their expression patterns in concert in a sweeping, coordinated, and consistent manner in the retina. Here, we established the existence of a small number of master regulatory loci responsible for the differential expression of exons, and we were able to map these controllers via genetic linkage analysis.

## 51.2 Materials and Methods

### *51.2.1 Measurement of Exon Expression Variability*

In the present study, we used a publically available microarray database (DoD Retina Normal Affy MoGene 2.0 ST (May15) RMA Exon Level) presented on GeneNetwork.org. This database is based on 55 BXD recombinant inbred (RI) strains and relies heavily on the bioinformatics tools presented on GeneNetwork.

**Fig. 51.1** (continued) Equimolar amounts of each of the other exons (1, 2, 4, and 5) make up the mature mRNA. (**c**) Normal promoter but an early terminator provides a short primary transcript containing only the first three exons. (**d**) An alternative promoter site at the beginning of Exon 3 and a normal terminator result in a short primary transcript. When spliced, the mature mRNA contains only Exons 3, 4, and 5. **(e)** An alternative promoter and early terminator produce a very short primary transcript. Once matured, the mRNA contains only Exon 3. (**f**) A normal promoter and an early terminator create a short transcript as in panel **c**, but an aberrant splice process generates a short mature mRNA containing only Exon 3. Several variants on this theme may be conjectured using nonstandard promoters, terminators, and polymerases or trans-splicing to generate other transcripts that contain solely Exon 3 from this gene; these include siRNAs and lncRNAs or transcripts from the other strand of DNA within this gene. In net, for Exon 3 to be detected at lower levels than its adjacent Exons, Exon 3 is spliced out during maturation. Critically, to observe higher expression of Exon 3 compared to the four other exons in B6 mice, isoforms from mechanisms **e** or **f** or a combination of two or more of the alternatives in panels **c–f** are proposed. *For example, if mechanisms in both **c** and **d** were to occur equally in a single retina, then Exon 3 would be detected at twice the level of the other four exons (1, 2, 4, and 5).* Symbols: Gray boxes represent exons. Blue V's represent splicing of a primary transcript. Green arrows indicate transcription start sites. Red T's indicate transcription termination

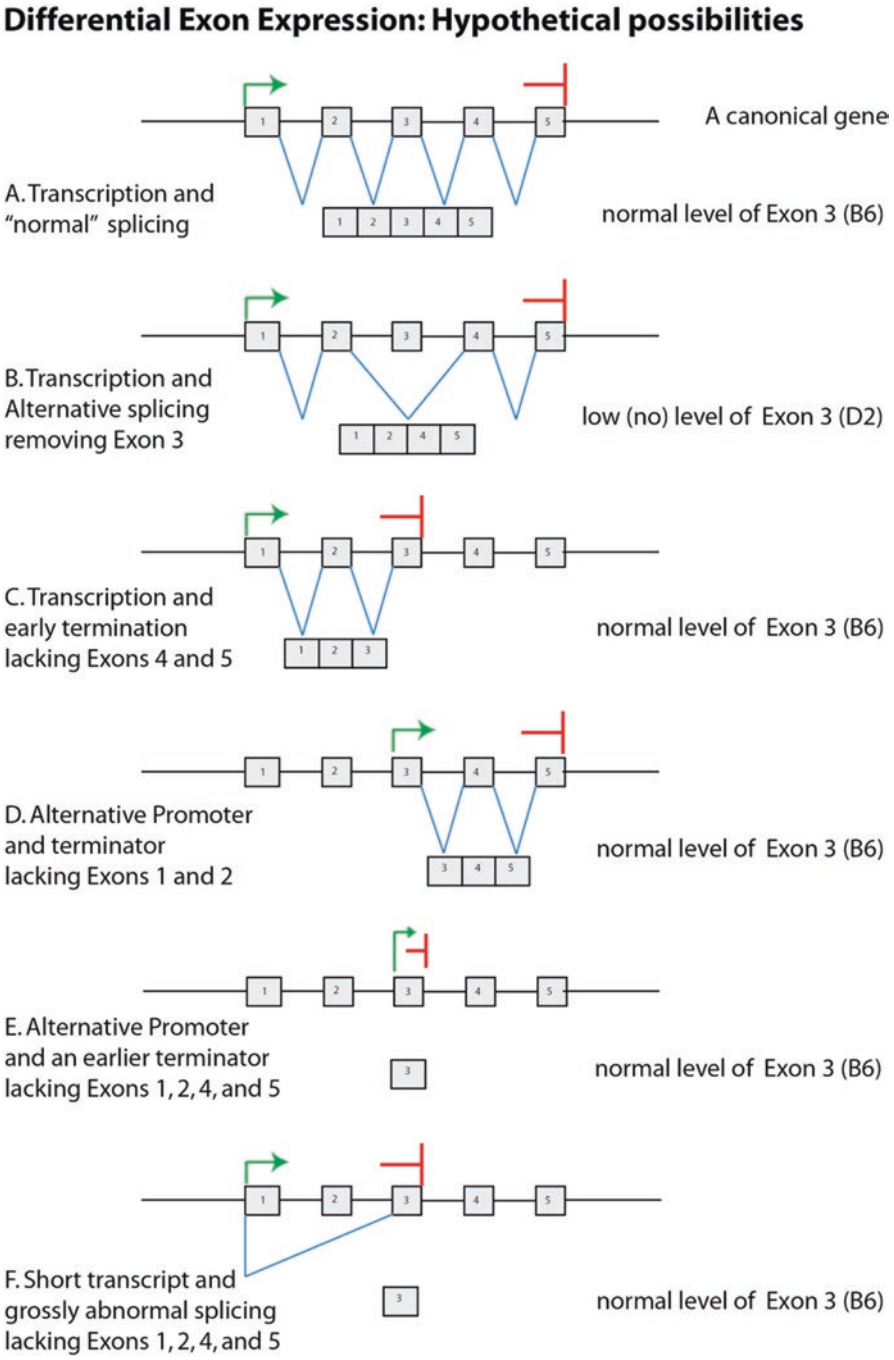


**Fig. 51.1** Hypothetical differential expression of one exon. Here variability in expression of Exon 3 is determined by the particular isoforms of mature mRNAs and abundance of each that are produced in the retina. Panels (**a**–**f**) each illustrate generation of a different isoform from a 5-exon gene. (**a**) Normal transcription and splicing of the gene illustrates a single mature mRNA with equimolar amounts of each exon. (**b**) Normal transcription and alternative splicing lacking Exon 3.

org. We previously observed that individual exons within a single gene were differentially expressed across the database (King et al. 2015). A single exon's bulk expression level by this array analysis is the sum of signals measured from numerous expressed isoforms of mature RNAs of a single gene.

### *51.2.2 Linkage Analysis of the Variability-In-Expression Phenotype*

When the expression of individual exons was examined across genes expressed in the normal retina of the BXD strains, specific exons were identified with expressed levels significantly greater than the other exons within the same gene. The expression levels of these exons across the BXD RI strains were biphasic, being high in some strains and low in others (high-low phenotype). We conducted linkage mapping across the BXD strains to identify potential *trans*-acting loci that drive differentially expressed exons. The variation in expression of an exon is a phenotypic trait that we used exactly like any other trait used in a linkage analysis, whether a disease gene trait (diseased or normal) or any other phenotypic characteristic such as eye color (blue or brown) or ability to taste phenylthiocarbamide. We selected 100 variably expressed exons (with the high-low expressed phenotype), each exon from a different gene. The 100 genes were spread throughout the mouse genome randomly. We used the *high-low* phenotype of each exon individually to map a *trans* locus that controlled the phenotype of the given exon. Each exon's phenotype (high or low) was inherited in a Mendelian pattern, and in most cases the high expression level was associated with the B6 strain and the low level with the D2 strain. In total we conducted 100 different linkage analyses. This traditional linkage analysis approach identified a *trans* locus (that is, a locus at least 10 Mb away from the variably expressed exon) that contains the regulatory genomic element. This was achieved using the bioinformatics tool in GeneNetwork on the "Select and Search" page in the "combined" text box by entering the text command "trans-LRS = (75,999 10)." "Heat maps" were built in GeneNetwork by first collecting the top 100 variable exons from the above page, selecting each one, and pressing the HeatMap button.

## 51.3 Results

### *51.3.1 Exon-Level Expression Patterns from a Single Gene*

We found the selective expression of many individual exons was relatively frequent across the retina, and the remaining exons were expressed at a lower level. As one example, across many strains of BXD RI mice, the expression levels of Exon 3 of

the *Kap* gene segregated into two categories with either high (31 BXD strains and B6) or low (22 BXD strains and D2) expression, while the other exons of *Kap* were expressed at approximately the same level.

### *51.3.2 Linkage Analysis*

The linkage analysis reveals that the variation in exon expression is a *trans*-acting element and can be mapped by genetic linkage analysis using the phenotype of expression level. A linkage map showing one concordant *trans* locus is illustrated in Fig. 51.2a. The genome-wide map of loci driving the expression phenotype of Exon 3 in *Kap* along with exons from a large population of genes is mapped to a single *trans* locus in the mouse genome on Chromosome 4 between roughly 133 and 136 Mb. The score for this locus was 122 by likelihood ratio statistic (LRS), which is equivalent to a logarithm of the odds (LOD) score of +26.5. This single locus was by far the largest signal on the interval map. It is important to note that this locus is in *trans* to Exon 3 of *Kap*, a gene found on Chromosome 6. An expanded view of this locus, illustrated in Fig. 51.2b, includes an arrangement of the BXD strain genotypes with alleles in red for B6 and in green for D2. The BXD strains are ordered from top to bottom with the upper half indicating the strains that expressed high levels of exon expression and the bottom half at low level. At one small location, there was a perfect concordance of high expression of Exon 3 of *Kap* and the B6 genotype. At the same point, all the strains that express a low level of Exon 3 of *Kap* had the D2 allele. This perfect concordance only occurred at 133–136 Mb, and in closer views, the breakpoints were only separated by 1 Mb. This mapped the controlling *trans-acting* locus quite accurately and established the location of a regulatory genomic element.

### *51.3.3 Heat Map Analyses*

Clustered heat maps allowed us to detect other *trans* loci that control the variability of phenotype for many single exons, each exon from a different gene. Each vertical lane in the heat map (Fig. 51.3) uses a color intensity gradient to indicate tight, loose, or no linkage along the genome. Most of the map is black indicating no linkage. Intense red or blue indicates tight linkage. The heat map has 100 lanes, one for each variable exon. The vertical lanes are ordered by similarity among a group of the exons. The results indicated a small number of groups or clusters, each cluster being driven by a different *trans* locus. The leftmost cluster included half the exons and contains Exon 3 of *Kap*. This group is the largest cluster and suggests that half the exons are controlled by the predominant locus on Chromosome 4 at 133–136 Mb. Other clusters were found. One cluster had a locus immediately adjacent to the first major controlling locus on Chromosome 4 but distal to the 133–136 Mb

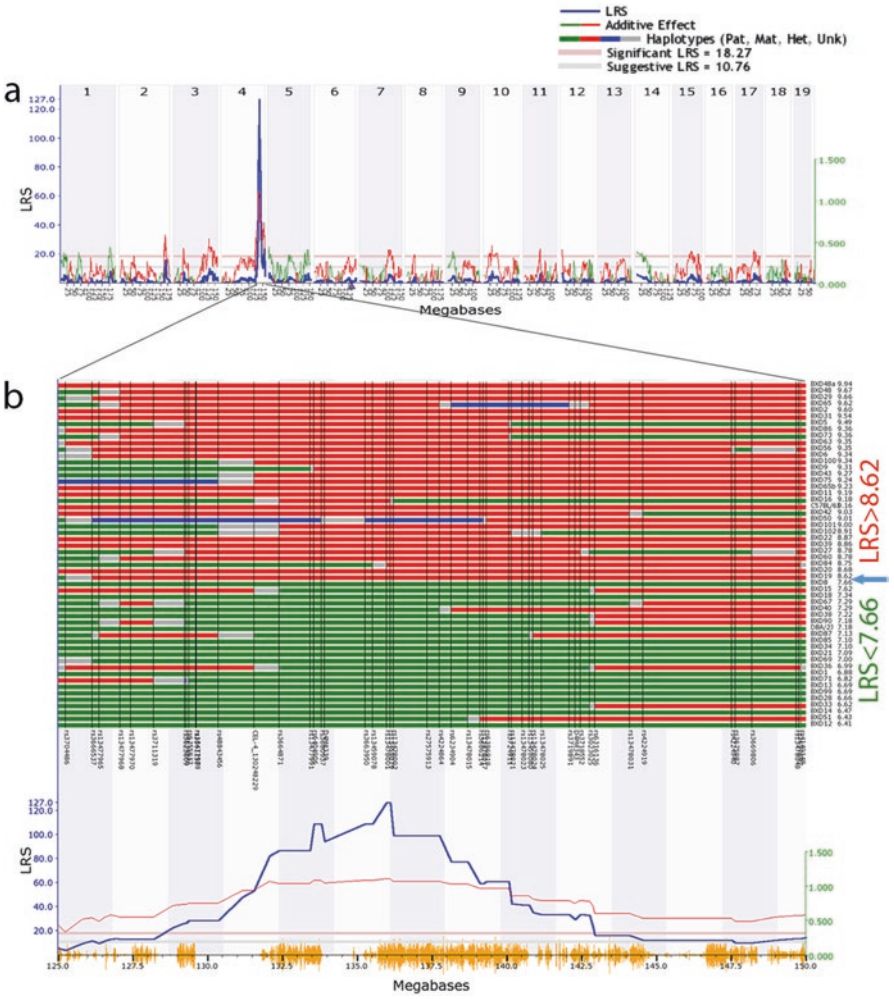


**Fig. 51.2** Genome-wide map showing tight linkage on Chromosome 4 (133–136 Mb) for variation in expression of *Kap* Exon 3. (**a**) The x-axis is a linear representation of all mouse chromosomes (Chr. 1–19 from left to right). The y-axis is a likelihood ratio statistic (LRS, defined as the natural logarithm of the odds ratio of linkage versus no linkage). (**b**) When one expands the peak region on Chromosome 4 (125 Mb~150 Mb), the haplotype map for Exon 3 of *Kap* reveals an allelic segregation across the BXD strains. Expression levels of each strain are indicated on the right of each line, ranked from highest (top) to lowest (bottom). Notice that the haplotype map at the peak region is divided into well-separated green (D2) and red (B6) genotypes. This illustrates a near perfect concordance of B6 with high expression and D2 with low expression of Exon 3 only. Blue haplotype, heterozygote; gray, unknown haplotype

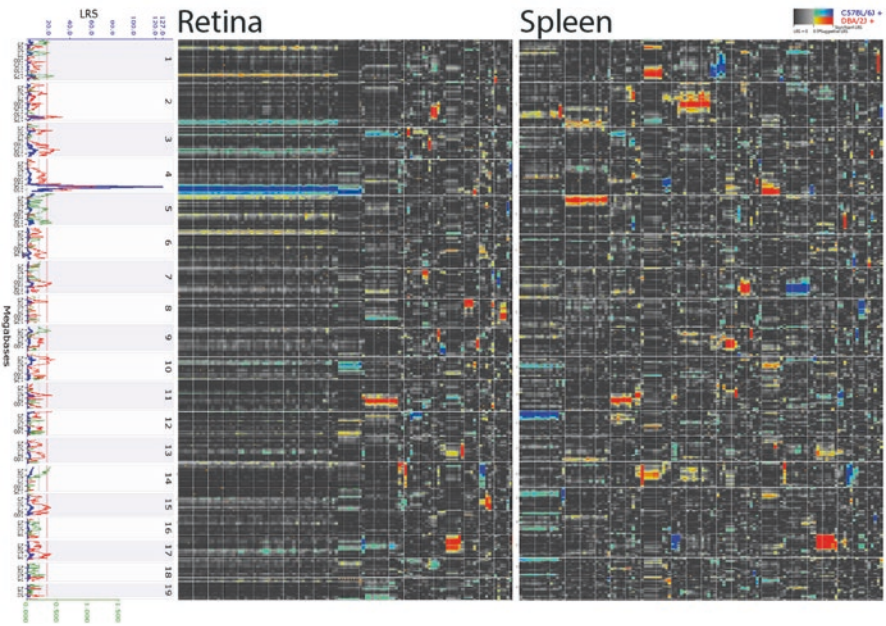


**Fig. 51.3** Genome-wide heat maps from the retina and spleen representing tight linkage at *trans*-acting loci driving a phenotype of variable expression in numerous exons. A linkage map is shown to the left of two heat maps (one from retina and one from spleen) for reference. Each intense blue or red band indicates a *trans-acting* locus with a high LRS

locus. This cluster included about 15% of the exons. Other trans-acting loci were found on Chromosomes 11, 17, and 2. The specificity of these trans-acting loci is demonstrated by examining the pattern observed in the spleen. In the spleen, the *trans* loci (Fig. 51.3) differ from that observed in the retina, with the Chromosome 4 band being retina-specific. This clear distinction may represent the basis of tissue-specific differential expression.

## 51.4 Discussion

A small number of loci that act *in trans* were mapped that account for the bulk of isoform pattern changes between B6 and D2 mice in the retina. Each of these loci controls a different cluster of isoforms from many different genes. This small number of master regulatory loci in terminally differentiated long-lived cells of the retina has implications for rapid responses to insults and environmental changes.

The general utility of differential gene expression is that it uses a minimum number of genes but reuses parts of these genes by transcription and RNA processing to generate diverse isoforms. One isoform of a gene may work better in one situation,

and a different isoform might work better in a different circumstance. One great advantage of differential gene expression is that it requires no changes in the genome, and different terminally differentiated cells can vary isoform patterns to accommodate changing needs. A second advantage is that this can occur immediately, allowing a cell to nimbly respond to rapidly changing circumstances. Switching these programs can quickly adapt phenotypes at the subcellular to organismal, behavioral levels to defend against threats, adapt to changes in environment, provide a competitive advantage, and hedge bets against unknowns by increasing diversity and change in expression during development. There are five master regulatory loci in the retina that may correspond to the regulation of differential expression of exons in the retina. The type of selective exon expression identified in this study may represent a novel form of tissue-specific genomic control.

**Acknowledgments** We are grateful for support provided by the DoD CDMRP W81XWH1210255 (EEG), R01EY017841 (EEG), The Owens Foundation (EEG), R01EY021592 (JMN), R01EY017470 (JMN), R01EY014625 (JHB), The Katz Foundation (JHB), VA RR&D C1924P I21RX001924 (JHB), VA RR&D C9246C (Atlanta VA Center of Excellence in Vision and Neurocognitive Rehabilitation), P30EY006360 (PMI), T32EY00792 (PMI), and Unrestricted Funds from Research to Prevent Blindness, Inc.

## References

Al-Ubaidi MR, Pittler SJ, Champagne MS et al (1990) Mouse opsin. Gene structure and molecular basis of multiple transcripts. J Biol Chem 265:20563–20569

King R, Lu L, Williams RW et al (2015) Transcriptome networks in the mouse retina: an exon level BXD RI database. Mol Vis 21:1235–1251

Sharp PA (1994) Split genes and RNA splicing (Nobel Lecture). Angew Chem Int Ed Engl 33:1229–1240

# Chapter 52
# Molecular Chaperone ERp29: A Potential Target for Cellular Protection in Retinal and Neurodegenerative Diseases


**Todd McLaughlin, Marek Falkowski, Joshua J. Wang, and Sarah X. Zhang**

**Abstract** The molecular chaperone endoplasmic reticulum protein 29 (ERp29) plays a critical role in protein folding, trafficking, and secretion. Though ubiquitously expressed, ERp29 is upregulated in response to ER stress and is found at higher levels in certain cell types such as secretory epithelial cells and neurons. As an ER resident protein, ERp29 shares many structural and functional similarities with protein disulfide isomerases, but is not regarded as part of this family due to several key differences. The broad expression and myriad roles of ERp29 coupled with its upregulation via the unfolded protein response (UPR) upon ER stress have implicated ERp29 in a range of cellular processes and diseases. We summarize the diverse activities of ERp29 in protein trafficking, cell survival and apoptosis, and ER homeostasis and highlight a potential role of ERp29 in neuroprotection in retinal and neurodegenerative diseases.

**Keywords** ERp29 · Retina · Neuroprotection · Neurodegeneration · Protein trafficking

## 52.1 Introduction

Endoplasmic reticulum protein 29 (ERp29) was molecularly described via a proteomic study of rat enamel cells in the late 1990s revealing a hydrophobic signal sequence and a variant of endoplasmic reticulum (ER) retention motif KDEL

T. McLaughlin · J. J. Wang · S. X. Zhang (✉)
Departments of Ophthalmology and Biochemistry, Ross Eye Institute, University at Buffalo, State University of New York, Buffalo, NY, USA

SUNY Eye Institute, State University of New York, Buffalo, NY, USA
e-mail: xzhang38@buffalo.edu

M. Falkowski
Departments of Ophthalmology and Biochemistry, Ross Eye Institute, University at Buffalo, State University of New York, Buffalo, NY, USA



J. D. Ash et al. (eds.), *Retinal Degenerative Diseases*, Advances in Experimental Medicine and Biology 891, https://doi.org/10.1007/978-3-319-75402-4_52

(Lys-Asp-Glu-Leu) (Demmer et al. 1997). Further studies demonstrate that ERp29 is a reticuloplasmin, i.e., a luminal component of the ER. Although expressed ubiquitously, ERp29 is highly expressed in secretory tissues, such as the pituitary, adrenal, and salivary glands, pancreas, liver, and kidney (Sargsyan et al. 2002a), and in neurons throughout the central nervous system (MacLeod et al. 2004). In addition, ERp29 was identified in the neural retina and retinal pigment epithelium (RPE), and the level of ERp29 is reduced in human retina with age-related macular degeneration (AMD) (Ethen et al. 2006).

Structurally, ERp29 contains an N-terminal domain that is homologous to thioredoxin-like domains in protein disulfide isomerase (PDI). However, unlike the PDI family members and some ER chaperones, such as glucose-regulated protein 78 (GRP78), GRP94, and calnexin, ERp29 lacks the conventional disulfide reductase/isomerase and calcium-binding activities (Demmer et al. 1997). Functionally, ERp29 acts as a putative chaperone that facilitates the processing and transport of secretory and membrane proteins from the ER to the Golgi apparatus. Apart from direct binding to its protein substrate, ERp29 interacts with other ER chaperones to promote the formation of a chaperone-substrate complex (Sargsyan et al. 2002b). In addition, ERp29 is believed to be a major chaperone in the trafficking of membrane proteins, such as Connexin43, to the plasma membrane (Das et al. 2009).

Like other PDI-like proteins, an important function of ERp29 is to prevent protein aggregation by keeping unfolded proteins in a folding-competent state and promote the protein-degrading apparatus to remove denatured proteins from the ER. This function is critical for minimizing the level of harmful proteins in ER and is vital for protein homeostasis. Additionally, recent studies have discovered some new and important roles of ERp29 in regulation of cellular stress response, gap junction formation, cell survival, and neuroprotection, though the molecular mechanisms underlying these diverse actions are not fully understood. We briefly summarize recent advances in ERp29 research in the areas related to cellular stress response, highlighting the evidence and perspective of this protein as a potential target for neuroprotection in retinal and neurodegenerative diseases.

## 52.2 ERp29 and Cellular Stress Response

The ability of a cell to respond and adapt to stress conditions is critical to maintaining its normal function and structure and ultimately determines its fate. The unfolded protein response (UPR) is a cellular stress response activated by ER stress, an accumulation of unfolded or misfolded proteins in the ER lumen, resulting from imbalances between protein synthesis, folding, trafficking, and degradation. The UPR consists of three sophisticated signaling pathways initiated by ER membrane proteins inositol-requiring enzyme 1 (IRE1), PKR-like ER kinase (PERK), and activating transcription factor 6 (ATF6). In most physiological conditions, activation of these pathways restores ER homeostasis through well-orchestrated programs, including promoting protein folding and accelerating

protein degradation while simultaneously slowing down protein synthesis (Zhang et al. 2014). However, in some extreme scenarios when the UPR fails to eliminate the accumulation of unfolded/misfolded protein in the ER, the UPR will switch from a cell-adaptive and cell-protective mode into a cell-destructive mode by induction of apoptotic pathways of C/EBP homologous protein (CHOP), JNK, NF-kB, and caspase-4, promoting apoptosis and inflammation and eventually leading to cell death (Zhang et al. 2014).

Although it is well established that ERp29 is critical in maintaining ER homeostasis, the promoter region of the ERp29 gene lacks an ER-stress response element, the DNA motif characteristic for the UPR target genes. On the contrary, it possesses characteristics (e.g., GC-rich sequence, lack of a TATA box, multiple transcription start sites) of a constitutively expressed housekeeping gene (Sargsyan et al. 2002a). Furthermore, recent evidence shows that ERp29 interacts with, and regulates, PERK (Farmaki et al. 2011) and ATF6 (Hirsch et al. 2014), two important branches of the UPR pathways. Overexpression of ERp29 increases total PERK protein level without altering PERK phosphorylation (Farmaki et al. 2011). Deletion of ERp29 selectively impairs the activation of ATF6 and CHOP, but has no effect on other UPR branches, such as the PERK downstream activating transcription factor 4 (ATF4) and eukaryotic initiation factor 2 alpha (eIF2α), and the X-box binding protein 1 (XBP1) pathways (Hirsch et al. 2014). Additional studies suggest that ERp29 upregulates the chaperones involved in stress response pathways, such as $p58^{IPK}$, p-eIF2α, p38, or Hsp27, promoting cell survival under stress conditions. For instance, ERp29 increases the level of ER chaperone $p58^{IPK}$ (Gao et al. 2012), which in turn inhibits ER stress-associated proapoptotic cascades (Huber et al. 2013) through downregulation of the CHOP pathway (Boriushkin et al. 2014). Additionally, ERp29 regulates MAPK activity by increasing P38 phosphorylation (Gao et al. 2012) but downregulating ERK activity by changing the ratio of p-ERK1 to p-ERK2 (Bambang et al. 2009).

## 52.3 ERp29, Connexin43 Trafficking, and Gap Junctions

Connexins (Cx) are a family of integral transmembrane proteins that form gap junctions between cells. Approximately 20 members (in higher vertebrates) of the connexin family are assembled in groups of six to form homo- and heteromeric connexons; connexons from adjacent cells form a gap junction (Laird 2006). Gap junctions are critical for the intercellular exchange of ions, small molecule metabolites, and electrical signals, though each combination has variable pore conductance, size selectivity, charge selectivity, voltage gating, and chemical gating. Gap junctions enable chemical and electrical coupling between cells throughout the organism and are found on dozens of cells types. In the retina alone, gap junctions are found between every major cell type (i.e., bipolar cells, horizontal cells, amacrine cells, RGCs, photoreceptors, and glia; Danesh-Meyer et al. 2016). Though the specific functional consequences of many of these distinct couplings are unknown,

the gap junctions enabling electrical coupling among bipolar cells have recently been discovered to affect the release of glutamate in the inner plexiform layer in a manner that laterally spreads bipolar cell signaling and specifically enhances RGC sensitivity to motion (Kuo et al. 2016).

Connexin43 (Cx43) is the most common gap junction protein in the organism and is present in multiple retinal cell types, including the RPE. The appropriate trafficking of Cx43 through the ER to the Golgi complex is dependent on ERp29 (Das et al. 2009). Cx43 must leave the ER as a monomer and oligomerize in the Golgi complex. To this end, ERp29 forms a complex with Cx43 in the ER which stabilizes Cx43 monomers, likely by stopping the formation of disulfide bonds through blocking cysteine oxidases in an extracellular loop domain (Das et al. 2009).

In addition, Cx43 is downregulated in Müller glia in high glucose conditions, which leads to decreased gap junctions with pericytes and increased apoptosis in Müller glia and retinal microvascular endothelial cells (Li and Roy 2009; Muto et al. 2014). Furthermore, retinas from diabetic or Cx43 heterozygous knockout mice develop retinal vascular lesions associated with diabetic retinopathies (Bobbie et al. 2010). Though neither ERp29 nor protein trafficking has been directly implicated in these results, it is straightforward to suggest that increased ER stress under disease conditions results in the compromised ability of ERp29 to appropriately chaperone Cx43 through the ER. The continual synthesis of connexins due to their remarkably short half-life of just a few hours only magnifies the potential consequences of impaired protein trafficking in the ER and the potential that this dysfunction underlies, in part, these retinal lesions (Laird 2006).

## 52.4 ERp29, Neuroprotection, and Neurodegenerative Disease

ERp29 is a probable neuroprotectant and can potentially facilitate axonal regeneration. ERp29, normally present at high levels in the brain, is downregulated in rat motor cortex following spinal cord injury (SCI; Liu et al. 2014). Intriguingly, lentiviral expression of ERp29 in the cortex increases motor neuron survival and decreases apoptosis after SCI, while virally mediated suppression of ERp29 increases cortical neuron death (Liu et al. 2014). Remarkably, viral-mediated overexpression of ERp29 after SCI also results in marked improvement in motor function within weeks, suggesting a potential role for ERp29 in axon regeneration as well, potentially via its regulation of ERK pathways (Liu et al. 2014).

ERp29 has been implicated in models of retinal disease where it may also act as a neuroprotectant. Proteomic and immunohistochemical analyses of human donor eyes with AMD and a mouse model of AMD reveal that ERp29 is significantly downregulated in the retina (Ethen et al. 2006; Tuo et al. 2007). The role of the ER chaperone ERp29 in AMD is intriguing given that drusen (accumulations of protein and lipid) are an early sign of AMD. Additionally, a primary risk factor for AMD is smoking, and cultured RPE cells exposed long-term (3 weeks) to cigarette smoke

extract (CSE) have a decrease in ERp29 level (Huang et al. 2015). Furthermore, overexpression of ERp29 protects RPE cells in vitro from CSE exposure by increasing chaperones such as GRP78 and p58IPK and decreasing levels of proapoptotic proteins such as CHOP (Huang et al. 2015).

In parallel with the role of ERp29 in gap junction formation described above, overexpression of ERp29 in CSE-treated RPE cells in vitro attenuated the decreases in ZO-1, a tight junction protein, and cadherin levels and the corresponding damage to tight junctions (Huang et al. 2015). Thus, ERp29 may generally be critical to cell-cell contact and barrier integrity. Indeed, ERp29 has been implicated in cancer progression, in part through an effect on epithelial-mesenchymal transition (Chen and Zhang 2015).

Collectively, these results indicate a role for ERp29 in attenuating ER stress in disease and promoting retinal cell survival and cell membrane integrity in vivo and suggest a potential path to a preventative therapeutic regimen in at-risk or diseased patients.

## 52.5 Conclusions/Summary

The ubiquitous ER chaperone, ERp29, is critical to protein trafficking through the ER in a variety of cells, notably secretory cells and neurons. Recent work has demonstrated a wide variety of functions for ERp29 in many different pathways (Fig. 52.1), including a protective role for ERp29 in various diseases and injury models. These results are intriguing and correlate well with the reduction in ERp29 in AMD in human. The idea of expression of ERp29 as protective against cell death pathways in some circumstances including retinal degeneration is

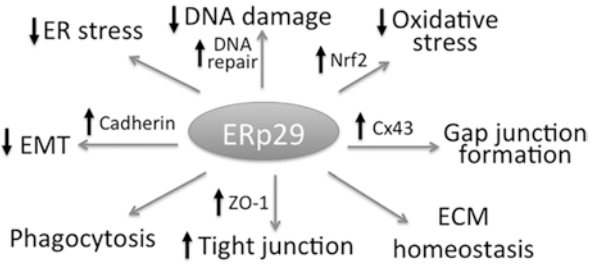


**Fig. 52.1** Schematic summary of potential roles of ERp29 in cell survival and homeostasis**.** The ubiquitous ER chaperone, ERp29, has myriad functions, some of which are illustrated here. ERp29 appears to play a prominent role in protein trafficking and participate in a wide range of pathways of cell survival pertinent to ER stress, oxidative stress, and DNA repair. In addition, ERp29 is implicated critically in maintaining the integrity of cell membrane and cell-cell contact through regulation of the epithelial-mesenchymal transition (EMT), tight junction formation, gap junction formation, and extracellular matrix (ECM) homeostasis. These functions suggest a potentially strong premise of ERp29 as a therapeutic target for human diseases including retinal degeneration

promising. In addition, the key role of ERp29 in coordinating the appropriate trafficking of membrane proteins such as Cx43 is intriguing but has not been investigated in the retina. Potential implications of ERp29 in maintaining protein homeostasis thus reducing or delaying the proteinopathy and its consequent catastrophic disruption of retinal neurons in various degenerative diseases are also worth pursuing.

## References

Bambang IF, Xu S, Zhou J et al (2009) Overexpression of endoplasmic reticulum protein 29 regulates mesenchymal-epithelial transition and suppresses xenograft tumor growth of invasive breast cancer cells. Lab Investig 89:1229–1242

Bobbie MW, Roy S, Trudeau K et al (2010) Reduced connexin 43 expression and its effect on the development of vascular lesions in retinas of diabetic mice. Invest Ophthalmol Vis Sci 51:3758–3763

Boriushkin E, Wang JJ, Zhang SX (2014) Role of p58IPK in endoplasmic reticulum stress-associated apoptosis and inflammation. J Ophthalmic Vis Res 9:134–143

Chen S, Zhang D (2015) Friend or foe: endoplasmic reticulum protein 29 (ERp29) in epithelial cancer. FEBS Open Bio 5:91–98

Danesh-Meyer HV, Zhang J, Acosta ML et al (2016) Connexin43 in retinal injury and disease. Prog Retin Eye Res 51:41–68

Das S, Smith TD, Das Sharma J et al (2009) ERp29 restricts Connexin43 oligomerization in the endoplasmic reticulum. Mol Biol Cell 20:2593–2604

Demmer J, Zhou C, Hubbard MJ (1997) Molecular cloning of ERp29, a novel and widely expressed resident of the endoplasmic reticulum. FEBS Lett 402:145–150

Ethen CM, Reilly C, Feng X et al (2006) The proteome of central and peripheral retina with progression of age-related macular degeneration. Invest Ophthalmol Vis Sci 47:2280–2290

Farmaki E, Mkrtchian S, Papazian I et al (2011) ERp29 regulates response to doxorubicin by a PERK-mediated mechanism. Biochim Biophys Acta 1813:1165–1171

Gao D, Bambang IF, Putti TC et al (2012) ERp29 induces breast cancer cell growth arrest and survival through modulation of activation of p38 and upregulation of ER stress protein p58IPK. Lab Investig 92:200–213

Hirsch I, Weiwad M, Prell E et al (2014) ERp29 deficiency affects sensitivity to apoptosis via impairment of the ATF6–CHOP pathway of stress response. Apoptosis 19:801–815

Huang C, Wang JJ, Jing G et al (2015) ERp29 attenuates cigarette smoke extract–induced endoplasmic reticulum stress and mitigates tight junction damage in retinal pigment epithelial cells. Invest Ophthalmol Vis Sci 56:6196–6207

Huber AL, Lebeau J, Guillaumot P et al (2013) p58(IPK)-mediated attenuation of the pro-apoptotic PERK-CHOP pathway allows malignant progression upon low glucose. Mol Cell 49:1049–1059

Kuo SP, Schwartz GW, Rieke F (2016) Nonlinear spatiotemporal integration by electrical and chemical synapses in the retina. Neuron 90:320–332

Laird DW (2006) Life cycle of connexins in health and disease. Biochem J 394:527–543

Li AF, Roy S (2009) High glucose-induced downregulation of connexin 43 expression promotes apoptosis in microvascular endothelial cells. Invest Ophthalmol Vis Sci 50:1400–1407

Liu R, Zhao W, Zhao Q et al (2014) Endoplasmic reticulum protein 29 protects cortical neurons from apoptosis and promoting corticospinal tract regeneration to improve neural behavior via caspase and Erk signal in rats with spinal cord transection. Mol Neurobiol 250:1035–1048

MacLeod JC, Sayer RJ, Lucocq JM et al (2004) ERp29, a general endoplasmic reticulum marker, is highly expressed throughout the brain. J Comp Neurol 477:29–42

Muto T, Tien T, Kim D et al (2014) High glucose alters Cx43 expression and gap junction intercellular communication in retinal Müller cells: promotes Müller cell and pericyte apoptosis. Invest Ophthalmol Vis Sci 55:4327–4337

Sargsyan E, Baryshev M, Backlund M et al (2002a) Genomic organization and promoter characterization of the gene encoding a putative endoplasmic reticulum chaperone, ERp29. Gene 285:127–139

Sargsyan E, Baryshev M, Szekely L et al (2002b) Identification of ERp29, an endoplasmic reticulum lumenal protein, as a new member of the thyroglobulin folding complex. J Biol Chem 277:17009–17015

Tuo J, Bojanowski CM, Zhou M et al (2007) Murine Ccl2/Cx3cr1 deficiency results in retinal lesions mimicking human age-related macular degeneration. Invest Ophthalmol Vis Sci 48:3827–3836

Zhang SX, Sanders E, Fliesler SJ et al (2014) Endoplasmic reticulum stress and the unfolded protein responses in retinal degeneration. Exp Eye Res 125:30–40

# Chapter 53
# The Role of Microbiota in Retinal Disease


**Sheldon Rowan and Allen Taylor**

**Abstract** The ten years since the first publications on the human microbiome project have brought enormous attention and insight into the role of the human microbiome in health and disease. Connections between populations of microbiota and ocular disease are now being established, and increased accessibility to microbiome research and insights into other diseases is expected to yield enormous information in the coming years. With the characterization of the ocular microbiome, important insights have already been made regarding corneal and conjunctival tissues. Roles for non-ocular microbiomes in complex retinal diseases are now being evaluated. For example, the gut microbiome has been implicated in the pathogenesis of uveitis. This short review will summarize the few studies linking gut or oral microbiota to diabetic retinopathy (DR), glaucoma, and age-related macular degeneration (AMD). We will also conjecture where the most significant findings still remain to be elucidated. Finally, we will propose the gut-retina axis, related but distinct from the gut-brain axis.

**Keywords** Gut microbiome · Oral microbiome · Microbiota · Gut dysbiosis · Age-related macular degeneration · Diabetic retinopathy · Glaucoma · Uveitis · Glycemic index · Gut-retina axis

S. Rowan (✉)
USDA-JM Human Nutrition Research Center on Aging (HNRCA), Tufts University, Boston, MA, USA

Department of Ophthalmology, Tufts University School of Medicine, Boston, MA, USA
e-mail: sheldon.rowan@tufts.edu

A. Taylor
USDA-JM Human Nutrition Research Center on Aging (HNRCA), Tufts University, Boston, MA, USA

Department of Ophthalmology, Tufts University School of Medicine, Boston, MA, USA

Friedman School of Nutrition Science and Policy, Tufts University, Boston, MA, USA
e-mail: Allen.taylor@tufts.edu



J. D. Ash et al. (eds.), *Retinal Degenerative Diseases*, Advances in Experimental Medicine and Biology 891, https://doi.org/10.1007/978-3-319-75402-4_53

## 53.1 Introduction

There are diverse and continually changing populations of microbiota throughout our bodies, and the composition and function of our microbiota have important roles in health and disease (Clemente et al. 2012). The ocular microbiome has now been carefully characterized and shown to have important functions in the cornea and conjunctiva, particularly for regulation of ocular immunity and prevention of proliferation of pathogens (Kugadas and Gadjeva 2016; Lu and Liu 2016). However, it is more likely that other microbiota populations, particularly those of the gut and the oral cavity, will impact on retinal disease. Gut dysbiosis has been linked to diverse diseases at proximal and distal sites in the human, and a theme of this review is that mechanisms of disease pathogenesis will be shared in common with the major human eye diseases. Such themes include compromised barrier function, alterations in the adaptive and innate immune system, vascular dysfunction, and metabolic reprogramming.

## 53.2 Uveitis and the Gut Microbiome

One of the most convincing demonstrations for the importance of the gut microbiome in ocular disease comes from studies of autoimmune uveitis, a major cause of human blindness. Using a transgenic mouse model of uveitis, it was demonstrated that gut microbiota are responsible for priming autoreactive IL-17 expressing T-cells that then directly trigger uveitis in the retina (Horai et al. 2015). This direct connection between the gut and the eye was confirmed by administration of antibiotics to the mice, which reduced both uveitis and retinal antigen-specific T-cells in the gut, or by evaluation in germ-free mice (Horai et al. 2015). A complementary study using a different mouse model of uveitis showed that broad-spectrum antibiotic administration led to increased numbers of regulatory T-cells in the lamina propria concomitant with decreased numbers of effector CD4+ T-cells (Nakamura et al. 2016). In humans, uveitis and associated autoimmune diseases are associated with the human leukocyte antigen-B27, which itself is associated with gut dysbiosis in humans and animal models, leading to increased gut permeability and associated innate and adaptive immune responses, locally and distally (Rosenbaum et al. 2016).

## 53.3 Diabetic Retinopathy and the Gut Microbiome

A large and growing literature informs us that type 2 diabetes is associated with an altered gut microbiota and some degree of gut dysbiosis (Qin et al. 2012; Karlsson et al. 2013). Mechanisms for this association include increased inflammation, increased oxidative stress, increased vascular permeability, increased obesity and insulin resistance, and altered glycemic control (Allin et al. 2015; Arora

and Backhed 2016). These factors influence development and progression of DR, and although alterations in the gut microbiome have not been directly linked to DR, each of the intermediary processes has. Diabetes itself impacts microbiota populations and has been shown to influence the conjunctival microbiome (Yang et al. 2015). Therefore, multiple tissues and microbiota populations need to be considered in DR.

A further connection between the gut microbiota and DR may exist in the interaction of antihyperglycemic drugs and the microbiome. Metformin is one of the most commonly prescribed medications for treatment of diabetes and is a frontline treatment for diabetic complications. Studies in mice and preliminary studies in humans indicate that metformin can partially reduce DR (Munie et al. 2014; Yi et al. 2016). However, the mechanisms of metformin action are unclear, as metformin appears to simultaneously target glycemic, lipid, and vascular pathways (McCreight et al. 2016). Recent work has shown that metformin exerts a strong effect on the gut microbiome, forming a treatment signature that is independent of the glycemic effect (Lee and Ko 2014; Forslund et al. 2015). We predict that some of the variation in treatment response to metformin and several of its protective effects in diabetic complications will be related to differential effects on the gut microbiome and that new treatment modalities for diabetic retinopathy will directly target the gut microbiome to ameliorate undesirable side effects while maximizing efficacy.

## 53.4 Glaucoma and the Oral Microbiome

In contrast to DR and AMD, where systemic inflammation clearly play a role in disease pathogenesis, glaucoma has been more associated with sources of local inflammation, and therefore distal microbiota, like those in the gut, are less likely to contribute. The oral microbiome has been queried for association with neurodegeneration in glaucoma. One study found that the number of oral microbiota was increased in patients with glaucoma relative to healthy controls (Astafurov et al. 2014). Using two different mouse models of glaucoma, they showed that administration of lipopolysaccharide, a bacterial toxin, could activate Toll-like receptor 4 (TLR4) and its target genes associated with local inflammation and complement activation in the retina, but not the brain. TLR4 activation was associated with worse glaucomatous degeneration, whereas oral administration of a TLR4 inhibitor, naloxone, protected retinal ganglion cells and optic nerve axons from degeneration. Administration of lipopolysaccharide did not affect the number of macrophage/microglial cells in the eye; however, CD11, a marker of microglial activation, was increased in lipopolysaccharide-treated mice, as were other morphological microglial characteristics.

The above study emphasized the total burden of oral microbiota on glaucoma, but other studies have pointed to one specific bacterial species, *Helicobacter pylori*, as being potentially pathogenic in glaucoma. Antibodies to *H. pylori* were assessed in the serum and aqueous humor of patients with primary open-angle glaucoma or exfoliation glaucoma and were more prevalent in glaucoma than control patients.

The association of *H. pylori* with glaucoma has been inconsistent between studies, and a causal relationship has not yet been demonstrated (Kountouras et al. 2003; Kim et al. 2011; Zullo et al. 2012). Nevertheless, a recent meta-analysis supported the associations between *H. pylori* infection and open-angle glaucoma (Zeng et al. 2015). Pertinent to the topic of this mini-review, *H. pylori* infection has also been associated with central serous chorioretinopathy, potentially via endothelial dysfunction and systemic and vascular inflammation, a common link between bacterial dysbiosis and multiple retinal diseases (Sacca et al. 2014).

## 53.5 AMD and the Gut Microbiome

At the time of writing, no studies linking the gut microbiome to AMD development or progression have been published, but there are several compelling reasons to think that such an association exists and can be exploited therapeutically: (i) Chronic inflammation plays an important role in AMD, and there is ample evidence that gut dysbiosis causes increased inflammation via alteration of pro-inflammatory and regulatory T-cell numbers. (ii) Gut microbiota have important roles in metabolic disease, including glycemic control and adiposity – factors important in AMD (Weikel et al. 2012a). (iii) Gut microbiota affect host- and bacterial-derived metabolites, which signal distally to the brain and the eye. (iv) Gut microbiota affect lipid metabolism systemically and have been shown to affect the lipid composition of the retina (Oresic et al. 2009), which has important roles in pathogenesis of AMD.

A recent National Eye Institute symposium on the role of immunity in AMD included a closed-panel discussion on the microbiome and AMD. In this discussion, it was agreed that the microbiome, particularly the gut microbiome, should be assessed in a case-control study comparing AMD patients to age-matched controls and should be assessed longitudinally during the course of disease. As a second step, it was suggested that preliminary investigations be performed examining the effect of the microbiome on mouse models of AMD, which could then be augmented with gnotobiotic mouse models or antibiotic modifications to the microbiome. A review of ongoing clinical trials indicates that a number of investigators are undertaking human observational studies, evaluating the composition of the gut microbiome in AMD versus non-AMD patients, and further stratifying by genetic risk factors. It is expected that specific bacterial taxa will be enriched or depleted in AMD patients and that different classes of genetic susceptibility factors (in particular those that may modify the innate immune system like *CFH* variants) will have distinct microbiota associations.

We have taken on this second step utilizing a mouse model of AMD based on modification of the diet. In this model, mice fed high glycemic index diets (HG) develop AMD features with aging, while mice fed matched low glycemic index diets (LG) do not (Uchiki et al. 2012; Weikel et al. 2012b). By querying the gut microbiota over the course of such diet/aging studies, we have identified microbiota that change with diet and microbiota that are significantly associated with AMD

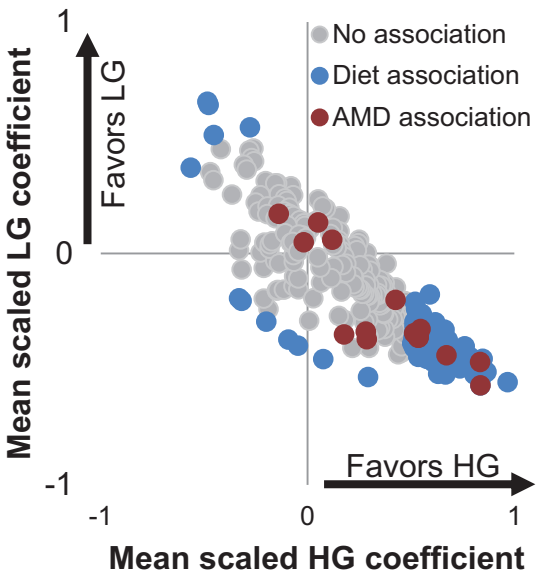


**Fig. 53.1** Microbiota can be identified that have diet association, AMD association, or both. Each point represents a bacterial OTU. Coefficients were calculated from ANOVA. Not shown are coefficients associated with dietary change of HG to LG diet

phenotypes (Fig. 53.1). We have further evaluated the importance of gut microbiota-associated metabolites in AMD development to determine the mechanism by which gut microbiota impact AMD.

## 53.6 The Gut-Retina Axis and Future Directions

Evidence from germ-free mice and antibiotic-treated mice indicate a range of cognitive and neurodevelopmental deficits in the absence of a gut microbiome (Mayer et al. 2015). It is now appreciated that neurodegenerative diseases like Alzheimer's disease and Parkinson's disease are linked to alterations in the gut microbiome as part of the gut-brain axis (Ghaisas et al. 2016). The pathological mechanisms implicated in Alzheimer's disease pathogenesis like impaired blood-brain barrier function, increased inflammation, metabolic disease, and vascular dysfunction are shared in common with AMD (Kaarniranta et al. 2011). Mechanistic studies of the communication between this two-way axis indicate that tryptophan metabolites such as serotonin and kynurenine have important functions in the brain and in the gut (O'Mahony et al. 2015). Based on the evidence presented here linking the gut microbiome to retinal diseases like diabetic retinopathy and AMD, we propose that a gut-retina axis also exists and that the modulation of the gut microbiome via diet, probiotics, or antibiotics will impact development of retinal disease. The gut-retina axis may yield insights into other retinal diseases like retinopathy of prematurity, which may be impacted by an immature gut microbiome and chronic antibiotic usage (Neu 2013). The interplay between the ocular, oral, and gut microbiomes and the eye will be a rich field for new discoveries and new treatments.

## References

Allin KH, Nielsen T, Pedersen O (2015) Mechanisms in endocrinology: gut microbiota in patients with type 2 diabetes mellitus. Eur J Endocrinol 172:R167–R177

Arora T, Backhed F (2016) The gut microbiota and metabolic disease: current understanding and future perspectives. J Intern Med 280:339–349

Astafurov K, Elhawy E, Ren L et al (2014) Oral microbiome link to neurodegeneration in glaucoma. PLoS One 9:e104416

Clemente JC, Ursell LK, Parfrey LW et al (2012) The impact of the gut microbiota on human health: an integrative view. Cell 148:1258–1270

Forslund K, Hildebrand F, Nielsen T et al (2015) Disentangling type 2 diabetes and metformin treatment signatures in the human gut microbiota. Nature 528:262–266

Ghaisas S, Maher J, Kanthasamy A (2016) Gut microbiome in health and disease: linking the microbiome-gut-brain axis and environmental factors in the pathogenesis of systemic and neurodegenerative diseases. Pharmacol Ther 158:52–62

Horai R, Zarate-Blades CR, Dillenburg-Pilla P et al (2015) Microbiota-dependent activation of an autoreactive T cell receptor provokes autoimmunity in an immunologically privileged site. Immunity 43:343–353

Kaarniranta K, Salminen A, Haapasalo A et al (2011) Age-related macular degeneration (AMD): Alzheimer's disease in the eye? J Alzheimers Dis 24:615–631

Karlsson FH, Tremaroli V, Nookaew I et al (2013) Gut metagenome in European women with normal, impaired and diabetic glucose control. Nature 498:99–103

Kim JM, Kim SH, Park KH et al (2011) Investigation of the association between Helicobacter pylori infection and normal tension glaucoma. Invest Ophthalmol Vis Sci 52:665–668

Kountouras J, Mylopoulos N, Konstas AG et al (2003) Increased levels of Helicobacter pylori IgG antibodies in aqueous humor of patients with primary open-angle and exfoliation glaucoma. Graefes Arch Clin Exp Ophthalmol 241:884–890

Kugadas A, Gadjeva M (2016) Impact of microbiome on ocular health. Ocul Surf 14:342–349

Lee H, Ko G (2014) Effect of metformin on metabolic improvement and gut microbiota. Appl Environ Microbiol 80:5935–5943

Lu LJ, Liu J (2016) Human microbiota and ophthalmic disease. Yale J Biol Med 89:325–330

Mayer EA, Tillisch K, Gupta A (2015) Gut/brain axis and the microbiota. J Clin Invest 125:926–938

McCreight LJ, Bailey CJ, Pearson ER (2016) Metformin and the gastrointestinal tract. Diabetologia 59:426–435

Munie M, Ryu C, Noorulla S et al (2014) Effect of metformin on the development and severity of diabetic retinopathy. Invest Ophthalmol Vis Sci 55:ARVO e-abstract 1069

Nakamura YK, Metea C, Karstens L et al (2016) Gut microbial alterations associated with protection from autoimmune uveitis. Invest Ophthalmol Vis Sci 57:3747–3758

Neu J (2013) The microbiome and its impact on disease in the preterm patient. Curr Pediatr Rep 1:215–221

O'Mahony SM, Clarke G, Borre YE et al (2015) Serotonin, tryptophan metabolism and the brain-gut-microbiome axis. Behav Brain Res 277:32–48

Oresic M, Seppanen-Laakso T, Yetukuri L et al (2009) Gut microbiota affects lens and retinal lipid composition. Exp Eye Res 89:604–607

Qin J, Li Y, Cai Z et al (2012) A metagenome-wide association study of gut microbiota in type 2 diabetes. Nature 490:55–60

Rosenbaum JT, Lin P, Asquith M (2016) The microbiome, HLA, and the pathogenesis of uveitis. Jpn J Ophthalmol 60:1–6

Sacca SC, Vagge A, Pulliero A et al (2014) Helicobacter pylori infection and eye diseases: a systematic review. Medicine (Baltimore) 93:e216

Uchiki T, Weikel KA, Jiao W et al (2012) Glycation-altered proteolysis as a pathobiologic mechanism that links dietary glycemic index, aging, and age-related disease (in non diabetics). Aging Cell 11:1–13

Weikel KA, Chiu CJ, Taylor A (2012a) Nutritional modulation of age-related macular degeneration. Mol Asp Med 33:318–375

Weikel KA, Fitzgerald P, Shang F et al (2012b) Natural history of age-related retinal lesions that precede AMD in mice fed high or low glycemic index diets. Invest Ophthalmol Vis Sci 53:622–632

Yang C, Fei Y, Qin Y et al (2015) Bacterial flora changes in conjunctiva of rats with streptozotocin-induced type I diabetes. PLoS One 10:e0133021

Yi QY, Deng G, Chen N et al (2016) Metformin inhibits development of diabetic retinopathy through inducing alternative splicing of VEGF-A. Am J Transl Res 8:3947–3954

Zeng J, Liu H, Liu X et al (2015) The relationship between Helicobacter pylori infection and open-angle glaucoma: a meta-analysis. Invest Ophthalmol Vis Sci 56:5238–5245

Zullo A, Ridola L, Hassan C et al (2012) Glaucoma and Helicobacter pylori: eyes wide shut? Dig Liver Dis 44:627–628

# Part VII
# Neuroprotection

# Chapter 54
# Current Pharmacological Concepts in the Treatment of the Retinitis Pigmentosa


**Xiu-Feng Huang**

**Abstract** Retinitis pigmentosa (RP) encompasses a heterogeneous group of inherited retinal disorders characterized by progressive photoreceptor and/or retinal pigment epithelial (RPE) degenerations with a prevalence approximately 1 in 4000 in the general population. Over 70 causative genes have been defined in RP families, and a number of animal models have been identified so far. However there have been no widely recognized treatments able to recover or reverse the degenerating retina, to prevent the disease deterioration, ultimately to restore the remaining vision. Therapeutics advancements have been achieved including gene therapy, pharmacotherapy, cell replacement, neurotrophic factors, and retinal prosthesis. In this review, we focus on the pharmaceutical drugs for RP with emphases on the context of drug discovery, development, and clinical translation.

**Keywords** Retinitis pigmentosa · Pharmacotherapy · Treatment · Vitamin A · Lutein · Docosahexaenoic acid · Valproic acid · Neurotrophic factor and growth factor

## 54.1 Introduction

Retinitis pigmentosa (RP) encompasses a heterogeneous group of inherited retinal disorders characterized by progressive photoreceptor and/or retinal pigment epithelial (RPE) degenerations with a prevalence approximately 1 in 4000 in the general population (Hartong et al. 2006). Great efforts have been paid to understand the disease etiology. Over 70 causative genes have been defined in RP families (Hamel 2006), and a number of animal models have been identified so far. However there have been no widely recognized treatments able to recover or reverse the degenerating retina, to prevent the disease deterioration, ultimately to restore the remaining

X. -F. Huang (✉)
The Eye Hospital of Wenzhou Medical University, The State Key Laboratory Cultivation Base and Key Laboratory of Vision Science, Ministry of Health, Wenzhou, China



J. D. Ash et al. (eds.), *Retinal Degenerative Diseases*, Advances in Experimental Medicine and Biology 891, https://doi.org/10.1007/978-3-319-75402-4_54

vision. Therapeutics advancements have been achieved including gene therapy, pharmacotherapy, cell replacement, neurotrophic factors, and retinal prosthesis (Shintani et al. 2009). In this review, we focus on the pharmaceutical drugs for RP with emphases on the context of drug discovery, development, and clinical translation.

To date, the pharmacological agents include food supplementation (vitamin A, lutein, and docosahexaenoic acid) and neuroprotective agents (valproic acid, ciliary neurotrophic factor, glial cell-derived neurotrophic factor, basic fibroblast growth factor). This review summarizes briefly the current clinical management of RP.

## 54.2 Vitamin A

Vitamin A has been found to be related to retinitis pigmentosa since the 1960s and has been indicated for almost 30 years as a possible way to slow down the retinal degeneration (Berson 1982). The first clinical trial with randomized, controlled, double-masked protocol by Berson et al. extensively demonstrated that vitamin A may protect the photoreceptors by trophic. Long-term vitamin A supplementation in doses of 15,000 IU per day slowed down the loss of ERG amplitudes, while vitamin E supplementation at 4000 IU per day had an adverse effect (Berson et al. 1993). A further investigation reported that prolonged daily consumption of <25,000 IU vitamin A/d can be considered safe in the aged 18–54 group (Sibulesky et al. 1999). However, vitamin A could be toxic and should be avoided in patients with RP caused by mutations in the ABCA4 gene and women planning to conceive or with severe osteoporosis (Radu et al. 2008; Sahni et al. 2011), while this study and its recommendation were controversial on the significance of this work on clinical practice. Recently, an oral treatment with 9-cis-retinal led to reversal of a human retinal dystrophy (Rotenstreich et al. 2010), based on the study of a mouse model of fundus albipunctatus treated with 9-cis-retinal, which demonstrated structural and electroretinographic evidence of significant improvement in visual function (Maeda et al. 2006).

There is no consensus about the utility of vitamin A treatment yet. Although no serious problems of safety in the recommended dose were encountered, the long-term safety of taking high-dose vitamin A supplements for many decades is uncertain. The view is adopted by ophthalmologists in many parts of the world that vitamin A may be of marginal benefit, at best, in patients with RP and this must be weighed against the somewhat uncertain risks associated with its use (Marmor 1993). One more issue is vitamin A slowed the rate of decline of retinal function (ERG or visual field) without toxic adverse effects, but no significant effects on decline in distance or visual acuity (VA) were reported. Therefore, other clinical trials have been conducted in combination with vitamin A and other synthetic vitamins.

## 54.3 Lutein

Lutein has also been presumed as a potential therapeutic modality in preserving the visual function of patients with RP (Semba and Dagnelie 2003). Bahrami et al. completed a randomized placebo-controlled double-masked clinical trial of lutein supplementation (10 mg/d for 12 weeks followed by 30 mg/d) and suggested lutein supplementation improves visual field and also might improve visual acuity slightly, although these results should be interpreted cautiously (Bahrami et al. 2006). Then, Berson et al. reported another clinical trial on patients taking vitamin A randomly assigned to either lutein supplementation (12 mg/day) or placebo over a 4-year interval. Lutein appeared to slow loss of midperipheral visual field on average among nonsmoking adults with retinitis pigmentosa taking vitamin A by the Humphrey Field Analyzer (HFA) 60–4 program (Berson et al. 2010), while Massof et al. argued the evidence is not very strong (Massof and Fishman 2010).

Lutein is proved as an antioxidant and a neuroprotective treatment, and no significant adverse effects were seen in participants while they were taking lutein supplementation. However, mechanistic evidence for their effects at the molecular level has been very limited. Lutein had a statistically significant effect on VF but without a significant effect on VA.

## 54.4 Docosahexaenoic Acid

Researches have investigated the role of docosahexaenoic acid (DHA) as a neuroprotective factor against oxidative stress in photoreceptors (German et al. 2006) and important in the retinal development (Rotstein et al. 1997). It has been demonstrated that DHA supplementation reduces the cell loss in the inner nuclear layer and ganglion cell layer induced in rats (Mizota et al. 2001), and increasing dietary ω-3 fatty acids has beneficial effects across the retina, improvement occurring in ganglion cell function (Nguyen et al. 2008).

A trial of oral supplementation with 400 mg/day DHA for 4 years in the patients with X-linked RP demonstrated a correlation of preservation of cone ERG with red blood cell DHA level suggesting that DHA may be of possible benefit for patients (Hoffman et al. 2004). Further studies from Berson et al. have shown that supplementation with 1200 mg/day of DHA in addition to vitamin A initially slowed down the progress of the disease; however, this beneficial effect did not go beyond over 2 years (Berson et al. 2004b). Moreover, results have shown the benefits to RP patients of a diet rich in omega-3 fatty acids (equivalent to eating salmon, tuna, mackerel, herring, or sardines, once to two times a week), with taking vitamin A, but not DHA capsules (Berson et al. 2004a). The most recent study made by Berson et al. reported that mean annual rates of decline in distance and retinal visual acuities in adults with retinitis pigmentosa receiving vitamin A (15 000 IU/d) are slower

over 4–6 years among those consuming a diet rich (≥0.20 g/d) in ω-3 fatty acids (Berson et al. 2012).

## 54.5 Valproic Acid

The study made by Gottlicher et al. suggested VPA has the ability to reverse photoreceptor damage by inducing cells to differentiate in culture (Gottlicher et al. 2001). And VPA has also been shown to stimulate glial cells to differentiate into photoreceptor-like cells (Kubota et al. 2006), provided neuroprotection and axonal regrowth after optic nerve crush (ONC) (Biermann et al. 2010). Recently, the research made by Clemson et al. showed a therapeutic benefit to patients with RP. In total 13 eyes examined, 9 had improved visual fields with treatment, 2 had decreased visual fields, and 2 eyes experienced no change, with an overall average increase of 11% (Clemson et al. 2011). However, there are three comments arguing the study with the scientific rationale, the design of experiments, and the side effects (Sandberg et al. 2011; van Schooneveld et al. 2011; Sisk 2012). Taken together, a placebo-controlled clinical trial should be necessary to assess the efficacy and safety rigorously.

## 54.6 Neurotrophic Factor and Growth Factor

Several neurotrophic factors or growth factors have been proved to protect photoreceptors from degeneration, including ciliary neurotrophic factor (CNTF), glial cell-derived neurotrophic factor (GDNF), and basic fibroblast growth factor (bFGF).

CNTF was shown to delay photoreceptor degeneration in several animal models of retinal degeneration (Liang et al. 2001; Sieving et al. 2006). The use of encapsulated cell therapy (ECT) secreting CNTF into the vitreous has shown preservation of retinal integrity in *PDE6B*-deficient rcd1 canine model (Tao et al. 2002). A phase 1 study of CNTF delivered by intravitreal implantation of a device (NT-501, Neurotech USA) containing encapsulated cells transfected with the human CNTF gene showed positive results in ten patients with inherited retinal degeneration (Sieving et al. 2006). Two phase 2 studies were initiated in patients with earlier-stage (NCT00447980) and later-stage (NCT00447993) inherited retinal degeneration. However, a longitudinal study of cone photoreceptor structure and function in three patients with inherited retinal degenerations treated with sustained-release CNTF showed no significant changes in visual acuity (VA), visual field sensitivity, or ERG responses, suggesting larger studies urgently needed (Talcott et al. 2011).

GDNF has also been shown to have a neuroprotective effect on degenerating photoreceptors by slowing down the degeneration of rods while preserving visual function (Frasson et al. 1999). Prior studies showed the increased expression of

GDNF in the retina slows the death of rod photoreceptors in retinal degeneration models (Del Rio et al. 2011).

Injection of bFGF in RP rat models showed to delay degeneration of photoreceptors for at least 2 months after a single injection (Faktorovich et al. 1990). Then the encapsulated cells producing bFGF have been transplanted to the vitreous cavity of rats, showing delay of photoreceptor cell degeneration (Uteza et al. 1999). However, further clinical researches are needed to show the safety of treatment with bFGF.

## 54.7 Conclusions

The future for treating retinitis pigmentosa is still a serious situation for both ophthalmologists and scientists. However, there is no satisfied effective treatment that can prevent or reverse the devastating vision loss in present. Although previous studies demonstrated stem cell transplantation and gene therapy with enormous potential in treating the patients with RP, there remain several hurdles. The biggest challenges are the safety and the limited patients because of the enormous genetic and clinical heterogeneous of RP, suggesting further researches and clinical studies needed which will take a long period. Therefore, the effective pharmacologic treatment will benefit a part of RP patients' vision, maybe also in the psychology. The current pharmacologic treatment of RP is not effective enough, as different mutations causing rod cell death by different mechanisms requiring mutation-specific treatments are needed. As the induced pluripotent stem cells (iPSC) are developing rapidly, drug screening models using iPSC derived from patients are showing the reliability, robustness, and rapidity leading a much brighter future for the patients with RP.

## References

Bahrami H, Melia M, Dagnelie G (2006) Lutein supplementation in retinitis pigmentosa: PC-based vision assessment in a randomized double-masked placebo-controlled clinical trial [NCT00029289]. BMC Ophthalmol 6:23

Berson EL (1982) Nutrition and retinal degenerations. Vitamin A, taurine, ornithine, and phytanic acid. Retina 2(4):236–255

Berson EL, Rosner B, Sandberg MA, Hayes KC, Nicholson BW, Weigel-DiFranco C, Willett W (1993) A randomized trial of vitamin A and vitamin E supplementation for retinitis pigmentosa. Arch Ophthalmol 111(6):761–772

Berson EL, Rosner B, Sandberg MA, Weigel-DiFranco C, Brockhurst RJ, Hayes KC, Johnson EJ, Anderson EJ, Johnson CA, Gaudio AR et al (2010) Clinical trial of lutein in patients with retinitis pigmentosa receiving vitamin A. Arch Ophthalmol 128(4):403–411

Berson EL, Rosner B, Sandberg MA, Weigel-DiFranco C, Moser A, Brockhurst RJ, Hayes KC, Johnson CA, Anderson EJ, Gaudio AR et al (2004a) Clinical trial of docosahexaenoic acid in patients with retinitis pigmentosa receiving vitamin A treatment. Arch Ophthalmol 122(9):1297–1305

Berson EL, Rosner B, Sandberg MA, Weigel-DiFranco C, Moser A, Brockhurst RJ, Hayes KC, Johnson CA, Anderson EJ, Gaudio AR et al (2004b) Further evaluation of docosahexaenoic acid in patients with retinitis pigmentosa receiving vitamin A treatment: subgroup analyses. Arch Ophthalmol 122(9):1306–1314

Berson EL, Rosner B, Sandberg MA, Weigel-DiFranco C, Willett WC (2012) Omega-3 intake and visual acuity in patients with retinitis pigmentosa receiving vitamin A. Arch Ophthalmol 130(6):707–711

Biermann J, Grieshaber P, Goebel U, Martin G, Thanos S, Di Giovanni S, Lagreze WA (2010) Valproic acid-mediated neuroprotection and regeneration in injured retinal ganglion cells. Invest Ophthalmol Vis Sci 51(1):526–534

Clemson CM, Tzekov R, Krebs M, Checchi JM, Bigelow C, Kaushal S (2011) Therapeutic potential of valproic acid for retinitis pigmentosa. Br J Ophthalmol 95(1):89–93

Del Rio P, Irmler M, Arango-Gonzalez B, Favor J, Bobe C, Bartsch U, Vecino E, Beckers J, Hauck SM, Ueffing M (2011) GDNF-induced osteopontin from Muller glial cells promotes photoreceptor survival in the Pde6brd1 mouse model of retinal degeneration. Glia 59(5):821–832

Faktorovich EG, Steinberg RH, Yasumura D, Matthes MT, LaVail MM (1990) Photoreceptor degeneration in inherited retinal dystrophy delayed by basic fibroblast growth factor. Nature 347(6288):83–86

Frasson M, Picaud S, Leveillard T, Simonutti M, Mohand-Said S, Dreyfus H, Hicks D, Sabel J (1999) Glial cell line-derived neurotrophic factor induces histologic and functional protection of rod photoreceptors in the rd/rd mouse. Invest Ophthalmol Vis Sci 40(11):2724–2734

German OL, Insua MF, Gentili C, Rotstein NP, Politi LE (2006) Docosahexaenoic acid prevents apoptosis of retina photoreceptors by activating the ERK/MAPK pathway. J Neurochem 98(5):1507–1520

Gottlicher M, Minucci S, Zhu P, Kramer OH, Schimpf A, Giavara S, Sleeman JP, Lo Coco F, Nervi C, Pelicci PG et al (2001) Valproic acid defines a novel class of HDAC inhibitors inducing differentiation of transformed cells. EMBO J 20(24):6969–6978

Hamel C (2006) Retinitis pigmentosa. Orphanet J Rare Dis 1:40

Hartong DT, Berson EL, Dryja TP (2006) Retinitis pigmentosa. Lancet 368:1795–1809

Hoffman DR, Locke KG, Wheaton DH, Fish GE, Spencer R, Birch DG (2004) A randomized, placebo-controlled clinical trial of docosahexaenoic acid supplementation for X-linked retinitis pigmentosa. Am J Ophthalmol 137(4):704–718

Kubota A, Nishida K, Nakashima K, Tano Y (2006) Conversion of mammalian Muller glial cells into a neuronal lineage by in vitro aggregate-culture. Biochem Biophys Res Commun 351(2):514–520

Liang FQ, Aleman TS, Dejneka NS, Dudus L, Fisher KJ, Maguire AM, Jacobson SG, Bennett J (2001) Long-term protection of retinal structure but not function using RAAV.CNTF in animal models of retinitis pigmentosa. Mol Ther 4(5):461–472

Maeda A, Maeda T, Palczewski K (2006) Improvement in rod and cone function in mouse model of fundus albipunctatus after pharmacologic treatment with 9-cis-retinal. Invest Ophthalmol Vis Sci 47(10):4540–4546

Marmor MF (1993) A randomized trial of vitamin A and vitamin E supplementation for retinitis pigmentosa. Arch Ophthalmol 111(11):1460–1461; author reply 1463–5

Massof RW, Fishman GA (2010) How strong is the evidence that nutritional supplements slow the progression of retinitis pigmentosa? Arch Ophthalmol 128(4):493–495

Mizota A, Sato E, Taniai M, Adachi-Usami E, Nishikawa M (2001) Protective effects of dietary docosahexaenoic acid against kainate-induced retinal degeneration in rats. Invest Ophthalmol Vis Sci 42(1):216–221

Nguyen CT, Vingrys AJ, Bui BV (2008) Dietary omega-3 fatty acids and ganglion cell function. Invest Ophthalmol Vis Sci 49(8):3586–3594

Radu RA, Yuan Q, Hu J, Peng JH, Lloyd M, Nusinowitz S, Bok D, Travis GH (2008) Accelerated accumulation of lipofuscin pigments in the RPE of a mouse model for ABCA4-mediated retinal dystrophies following Vitamin A supplementation. Invest Ophthalmol Vis Sci 49(9):3821–3829

Rotenstreich Y, Harats D, Shaish A, Pras E, Belkin M (2010) Treatment of a retinal dystrophy, fundus albipunctatus, with oral 9-cis-{beta}-carotene. Br J Ophthalmol 94(5):616–621

Rotstein NP, Aveldano MI, Barrantes FJ, Roccamo AM, Politi LE (1997) Apoptosis of retinal photoreceptors during development in vitro: protective effect of docosahexaenoic acid. J Neurochem 69(2):504–513

Sahni JN, Angi M, Irigoyen C, Semeraro F, Romano MR, Parmeggiani F (2011) Therapeutic challenges to retinitis pigmentosa, from neuroprotection to gene therapy. Curr Genomics 12(4):276–284

Sandberg MA, Rosner B, Weigel-DiFranco C, Berson EL (2011) Lack of scientific rationale for use of valproic acid for retinitis pigmentosa. Br J Ophthalmol 95(5):744

Semba RD, Dagnelie G (2003) Are lutein and zeaxanthin conditionally essential nutrients for eye health? Med Hypotheses 61(4):465–472

Shintani K, Shechtman DL, Gurwood AS (2009) Review and update: current treatment trends for patients with retinitis pigmentosa. Optometry 80(7):384–401

Sibulesky L, Hayes KC, Pronczuk A, Weigel-DiFranco C, Rosner B, Berson EL (1999) Safety of <7500 RE (<25000 IU) vitamin A daily in adults with retinitis pigmentosa. Am J Clin Nutr 69(4):656–663

Sieving PA, Caruso RC, Tao W, Coleman HR, Thompson DJ, Fullmer KR, Bush RA (2006) Ciliary neurotrophic factor (CNTF) for human retinal degeneration: phase I trial of CNTF delivered by encapsulated cell intraocular implants. Proc Natl Acad Sci U S A 103(10):3896–3901

Sisk RA (2012) Valproic acid treatment may be harmful in non-dominant forms of retinitis pigmentosa. Br J Ophthalmol 96(8):1154–1155

Talcott KE, Ratnam K, Sundquist SM, Lucero AS, Lujan BJ, Tao W, Porco TC, Roorda A, Duncan JL (2011) Longitudinal study of cone photoreceptors during retinal degeneration and in response to ciliary neurotrophic factor treatment. Invest Ophthalmol Vis Sci 52(5):2219–2226

Tao W, Wen R, Goddard MB, Sherman SD, O'Rourke PJ, Stabila PF, Bell WJ, Dean BJ, Kauper KA, Budz VA et al (2002) Encapsulated cell-based delivery of CNTF reduces photoreceptor degeneration in animal models of retinitis pigmentosa. Invest Ophthalmol Vis Sci 43(10):3292–3298

Uteza Y, Rouillot JS, Kobetz A, Marchant D, Pecqueur S, Arnaud E, Prats H, Honiger J, Dufier JL, Abitbol M et al (1999) Intravitreous transplantation of encapsulated fibroblasts secreting the human fibroblast growth factor 2 delays photoreceptor cell degeneration in Royal College of Surgeons rats. Proc Natl Acad Sci U S A 96(6):3126–3131

van Schooneveld MJ, van den Born LI, van Genderen M, Bollemeijer JG (2011) The conclusions of Clemson et al concerning valproic acid are premature. Br J Ophthalmol 95(1):153; author reply 153–4

# Chapter 55
# Valproic Acid Inhibits Human Retinal Pigment Epithelial (hRPE) Cell Proliferation Via a P38 MAPK Signaling Mechanism


**Rohit Anand, Piyush C. Kothary, and Monte A. Del Monte**

**Abstract** Valproic acid (VPA) has been reported to inhibit cancer cell growth and has therapeutic use in retinal diseases. However, the mechanism of this action remains unclear. In order to explore this mechanism, primary human retinal pigment epithelial (hRPE) cell cultures were established. Cell viability was assessed by the trypan blue exclusion method (T), and the cell proliferation was measured by $^{3}$H–thymidine incorporation (3H–thy). P38 synthesis was quantitated by using 14C-methionine-labeled P38 (14C-P38) by using P38-specific antibody. SB203580 (SB), a selective inhibitor of p38 MAPK, was also used to test the specificity of P38 stimulation. Antinuclear staining (NS) studies were performed by DAPI. Statistical significance was established by student's t-test. We observed that VPA (1 mM) inhibited 10% fetal bovine serum (FBS)-stimulated cell proliferation (1.75 ± 0.37 vs. 3.25 ± 0.68 cells per 1 μl ± SEM, $p < 0.05$, $n = 4$). VPA also stimulated 14C-P38 synthesis in a dose-dependent manner. SB (30 μM) inhibited VPA (4 mM)-stimulated 14C-P38 synthesis (197.74 ± 41.17 vs. 425.89 ± 59.17, CPM ± SEM, $p < 0.05$, $n = 4$) and increased hRPE cell proliferation (1.79 ± 0.45 vs. 4.93 ± 1.12 cells per 1 μl ± SEM, $p < 0.05$, $n = 4$); NS demonstrated VPA-induced cell damage. We conclude that VPA inhibits hRPE cell growth via P38 MAP mechanism and may be of therapeutic value in treating or preventing proliferative eye diseases.

**Keywords** VPA · Valproic acid · Retinal pigment epithelium · MAPK · P38

R. Anand · P. C. Kothary (✉) · M. A. Del Monte
Department of Ophthalmology and Visual Sciences, Kellogg Eye Center, University Michigan Medical School, Ann Arbor, MI, USA
e-mail: kotha@umich.edu



J. D. Ash et al. (eds.), *Retinal Degenerative Diseases*, Advances in Experimental Medicine and Biology 891, https://doi.org/10.1007/978-3-319-75402-4_55

## 55.1 Introduction

The human retinal pigment epithelium (hRPE) is a mitotically inactive monolayer of cells in the adult eye located under the sensory retina which plays a critical role in proper visual function (Boulton and Dayhaw-Barker 2001). Derangements in the hRPE cell morphology and function are involved in the pathogenesis of several eye conditions. Central among these impairments is pathological RPE cell proliferation and metaplasia, a phenomenon which is present in diseases such as proliferative vitreoretinopathy and in tumors of the choroid and inner retina (Stern and Temple 2015). Currently, the leading treatment strategy for pathological RPE proliferation in these settings includes surgery, anti-inflammatory agents, and anti-growth factor therapies (Sadaka and Giuliari 2012). However the prognosis for diseases involving RPE cell proliferation remains unsatisfactory. Therefore, it is necessary to identify novel molecular targets and therapies to improve outcomes for patients suffering from these sight-threatening conditions.

Valproic acid (VPA) is an epigenetic factor that can readily cross the blood-brain barrier and has been used clinically to treat epilepsy (Monti et al. 2009). Recently, VPA has been reported to inhibit cellular proliferation in cancer cells and has also shown potential for use in some retinal diseases. However, the mechanistic role of VPA in treating proliferative eye disorders in the hRPE is not yet well understood. This led us to examine the mechanism of VPA action on the proliferation of hRPE cells in vitro to improve our understanding of the possible role of VPA in treating vitreoretinal diseases.

## 55.2 Materials and Methods

### *55.2.1 Establishment and Maintenance of hRPE Cell Culture*

Primary hRPE cell cultures were established and maintained using techniques developed in our laboratory as previously described (Weng et al. 2009). Specimens were obtained from disease-free eyes that were obtained from Eversight Michigan within 24 h of patient death. Posterior segments of eyes were preserved and rinsed with Hank's balanced salt solution and plated with Ham's F-12 nutrient medium containing 16% FBS, 100 U/ml penicillin, 100 microgram/ml streptomycin, and 0.075% (wt/vol) sodium bicarbonate. HRPE cells were detached under direct observation with a dissecting microscope and then placed in 16 mm Primaria plates and incubated at 37C in a 95% humidified air/5% CO2 incubator. Medium was replaced every 72 h until confluent. Primary cultures were washed with Hank's balanced salt solution and then subcultured with 0.5 g/100 mL trypsin and 0.2 g/100 mL EDTA in Hank's solution (Sigma T-3924) at 37C for 10 min as previously described.

### 55.2.2 Cellular Proliferation Assays

Human RPE cells were trypsinized and plated at $2 \times 10^4$ cells/well in 16-mm wells of 24-well plates containing growth medium. In order to measure a dose-response effect of FBS, 0.1–10% FBS in serum-free Ham's F12 nutrient medium was added for 24 h. To examine the effect of FBS on cellular proliferation, cells were combined with either F-12 alone, FBS 0.1% in F12, FBS 1% in F-12, FBS 5% in F-12, or FBS 10% in F-12; cells were then pulsed with 1uCi/100ul of [H] thymidine and incubated at 37C for 48 h. Cells were washed with 0.5 mL ice-cold phosphate-buffered saline (PBS, pH 7.4) and 0.5 mL ice-cold 5% trichloroacetic acid, and 0.5 mL of 0.1 M NaOH was then added to each well. Cell lysate was added to 10 mL of scintillation fluid (EcoLite™) and counted in a Beckman scintillation counter. In a separate experiment, the effect of VPA on cellular proliferation was determined by adding VPA to 10% FBS-stimulated hRPE cell culture. This was compared to a hRPE cells in F-12 and with hRPE cell culture treated with 10% FBS in F-12 medium. The number of cells was determined as mentioned above. Last, 30 mM of SB203580, a known MAPK inhibitor, was added to cell culture with 1 mM VPA and 10% FBS to determine the mechanism of action of VPA.

### 55.2.3 14C Immunoprecipitation Assay

Human RPE cells were trypsinized and plated at 2 × 104 cells/well in 16-mm wells of 24-well plates containing growth medium and grown to confluence. To measure a dose-response effect of VPA, 0–4 mM VPA in serum-free Ham's F-12 nutrient medium was added for 2 days. To examine the effect of VPA on P38 synthesis, cells were incubated with either F-12 alone, VPA at 0.1 mM, VPA at 1 mM, VPA at 2 mM, or VPA at 4 mM or VPA (1 or 4 mM) + SB203580 (SB) (30 μM); cells were then pulsed with 1 microCi/100 micro L of [14C] methionine and incubated at 37C for 48 h. Cells were washed with 0.5 mL ice-cold phosphate-buffered saline (PBS, pH 7.4), and then 200 microL of Zwittergent in 0.2% bovine serum albumin (BSA) was added to each well for 5 min. Cell lysate was transferred to microfuge tubes and precipitated using 10 microL of anti-P38 antibody (diluted to 1:500 with PBS). Cells were then refrigerated for 24 h at 4C. 10ul of protein A was then added to each tube and allowed to incubate for 1 h at room temperature. Cell lysate in the microfuge tubes was then centrifuged and the supernatant was discarded, and 0.5 ml of NaOH was added to each tube to dissolve the invisible precipitate. Cell lysate was then transferred to 10 mL of scintillation fluid (EcoLite™) and counted in Beckman scintillation counter.

### *55.2.4 Nuclear Staining*

Human RPE cells were grown to confluence on glass coverslips placed in 6-well plates. Forty-eight hours later, F12, FBS 1% in F-12, or VPA 1–4 mM in F-12 was added to each well. Plates were incubated at 37C for another 24 h. Cells were washed twice with ice-cold phosphate-buffered saline (PBS, pH 7.4) and then fixed with formaldehyde in PBS for 20 min at room temperature. After two additional 10 min washes with ice-cold PBS to prevent nonspecific binding, 2 mL of Zwittergent in 0.2% BSA was added for 1 h. Coverslips were subsequently washed twice with Zwittergent in 0.2% BSA and twice with PBS before incubating with rhodamine-conjugated anti-rabbit IgG (diluted 1:100 in Zwittergent) for 1 h at room temperature. Cells were then treated 1:100 concentration of anti-P38 antibody (this data not shown). Coverslips were washed twice with Zwittergent and twice with PBS before being mounted and then viewed on a Nikon Eclipse E800 epifluorescence microscope in TRITC setting, captured with a Nikon DXM1200 digital camera, and digitized to jpg format using ACT-1 Version 2.62. All images were captured at 20× or 40× magnification with a 3-second shutter speed.

### *55.2.5 Statistical Analysis*

The results are expressed as mean +/− the standard error of the mean (SEM). A p-value was determined by student t-test. A p-value of less than or equal to 0.05 was considered significant. *, ** = significantly different from each other as determined by student t-test.

## 55.3 Results

### *55.3.1 Effect of FBS on hRPE Cell Proliferation*

To create a model of HRPE cell proliferation in vitro for study, we treated hRPE cell cultures with FBS in a dose-dependent manner as previously described (Weng et al. 2009). FBS stimulated hRPE cell proliferation in a dose-dependent manner which became statistically significant at 10% FBS. In separate experiments FBS also stimulated 3H–thymidine incorporation in hRPE cells (data not shown) (Fig. 55.1).

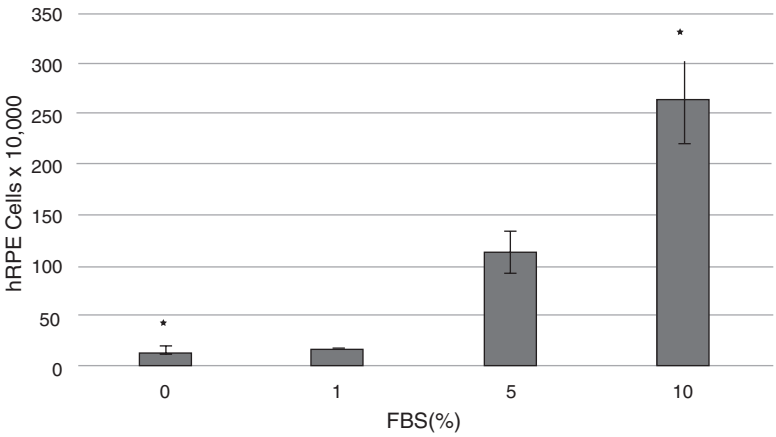


**Fig. 55.1** Effect of FBS on hRPE cell proliferation

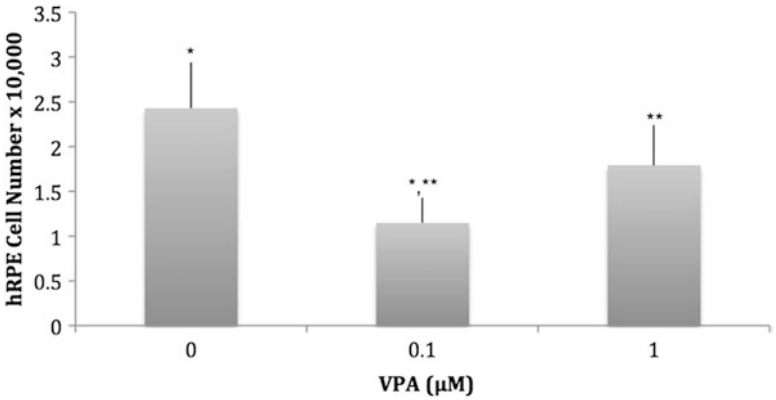


**Fig. 55.2** Effect of VPA on hRPE cell proliferation

### *55.3.2 Effect of VPA on hRPE Cell Proliferation*

We sought to determine the effect of valproic acid in this FBS-stimulated hRPE cellular proliferation model. HRPE cells treated with 10% FBS in F-12 medium were also exposed to 1 mM VPA. VPA statistically and significantly inhibited hRPE cell proliferation in this FBS-stimulated hRPE cell model (Fig. 55.2).

### 55.3.3 *Effect of VPA and SB on hRPE Cell Proliferation*

SB203580, a known inhibitor of MAPK, was added to FBS-stimulated hRPE cells treated with VPA. VPA-stimulated inhibition of hRPE cellular proliferation was significantly reversed in cells treated with 30 μM SB203580. This suggests that the mechanism by which VPA inhibits FBS-stimulated hRPE cell proliferation involves the MAPK signaling pathway (Fig. 55.3).

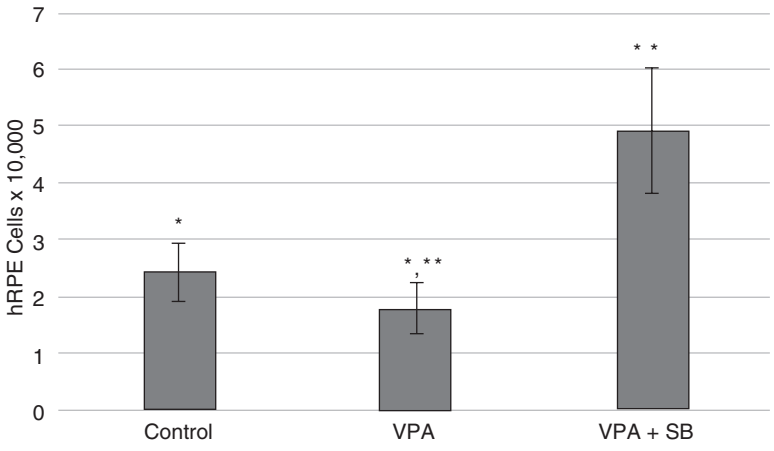


**Fig. 55.3** Effect of VPA and 30 μM SB on hRPE cell proliferation

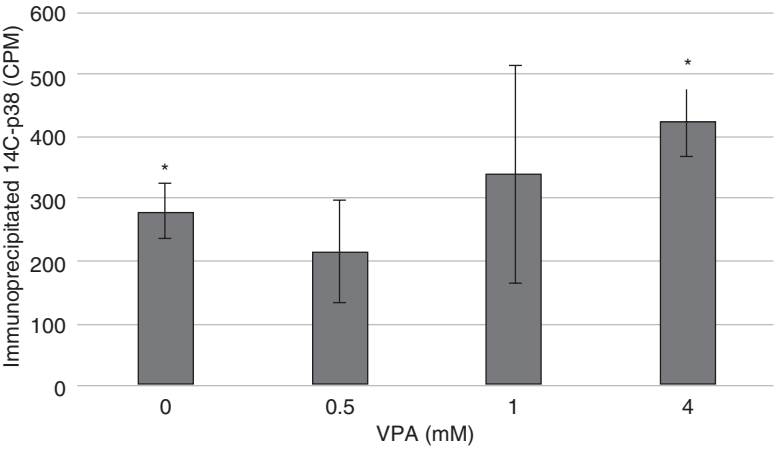


**Fig. 55.4** Effect of VPA on synthesis of $C^{14}$-p38 protein

### 55.3.4 *Effect of VPA on Synthesis of p38 Protein*

In order to ascertain the effect of VPA on p38 synthesis in hRPE cells, we treated hRPE cells with the increasing concentrations of VPA. Increasing concentrations of VPA increased immunoprecipitated p38 synthesis in hRPE cells in a dose-dependent manner (Fig. 55.4).

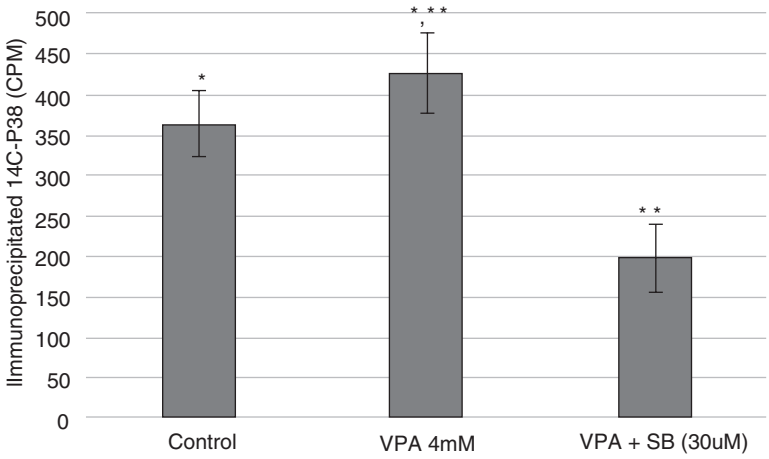


**Fig. 55.5** Effect of SB203580 + VPA on $C^{14}$-P38 protein synthesis in hRPE cells

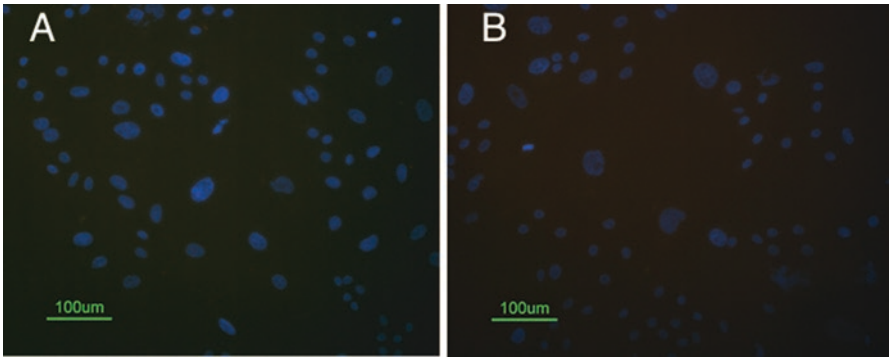


**Fig. 55.6** ab Effect of VPA on hRPE cell nuclear morphology (**b**) when compared with control (**a**) using DAPI (blue). Coverslips in Fig. **a** were incubated with serum-free F-12 medium and in Fig. **b** with F-12 medium and VPA

### *55.3.5 Effect of SB on Synthesis of Immunoprecipitated p38 Protein*

To determine if MAPK p38 signaling was involved in the VPA stimulation of hRPE proliferation, we evaluated the effect of exposure to 30 μM SB203580, an inhibitor of MAPK p38 synthesis. SB decreased p38 immunoprecipitation in a statistically significant manner in hRPE cells (Fig. 55.5).

### *55.3.6 VPA Effect on the hRPE Cell Nucleus*

To visualize the effect of VPA on hRPE cell morphology, nuclear staining studies were performed. In FBS-treated hRPE cells, hRPE cells remain intact, and there were very few damaged cells (Fig.55.6a). However, addition of VPA decreased the number of intact hRPE cells resulting in greater numbers of cells with damaged nuclei (Fig.55.6b).

## 55.4 Discussion

The therapeutic value of VPA in retinal disease is in a state of evolution. VPA has been shown to halt and reverse vision loss in patients with retinitis pigmentosa (Kumar et al. 2014; Iraha et al. 2016). The action and mechanism of VPA in treating atypical hRPE cellular proliferation however has not yet been fully understood.

Our experiments demonstrated that FBS-stimulated hRPE cell proliferation is significantly decreased with the addition of VPA, and fluorescence microscopy confirmed that cells treated with FBS alone proliferated in number and in viability in comparison to cells treated with VPA. In order to explore the mechanism of this action, we conducted several experiments using SB203580, a known inhibitor of MAPK. We demonstrate that the administration of SB203580 significantly reversed the antiproliferative effects of VPA in hRPE. Additionally, we observed that with VPA alone, hRPE cells produced increased p38 synthesis. These experiments suggest that the mechanism by which VPA acts to reduce proliferation and induce apoptosis in hRPE cells involves stimulation of the MAPK signaling pathway with synthesis of p38 protein. Our results are supported by Xie et al. (2010) who demonstrate that VPA promotes p38 MAPK-mediated apoptosis in microglia.

Previously, our research group and others identified that VPA stimulates caspase-3, another known marker of apoptosis, in hRPE cells (Berner and Kleinman 2016). Our current study adds further evidence to the theory that VPA induces programmed cell death in RPE via several different mechanisms.

Conversely, our research group also previously demonstrated that VPA has a protective effect by downregulating P38 in hRPE cells exposed to oxidative dam-

age, such as $H_2O_2$ (Kothary et al. 2016). These previous findings combined with our current study show that VPA may be acting by several different mechanisms to protect hRPE cell form and function, depending on the cellular environment.

These studies further support the possibility that VPA may be useful as a therapeutic agent to treat and/or even prevent the blinding complications in multiple vitreoretinal proliferative or neoplastic eye diseases. VPA has already been proven safe and useful as an anticonvulsant and in the treatment of cancer; however, studies like ours now highlight its potential future use in treating blinding retinal diseases as well.

**Acknowledgments** We thank Skillman Foundation for their support. This chapter is dedicated to late Dr. Sarla P. Kothary (wife of Dr. Piyush C Kothary). Sarla attended Retinal Degeneration (RD) meeting for two decades and forged friendship with many attendees and their spouses. PCK misses Sarla's spirit of adventure. The next RD meetings will not be the same.

## References

Berner AK, Kleinman ME (2016) Therapeutic approaches to histone reprogramming in retinal degeneration. Adv Exp Med Biol 854:39–44

Boulton M, Dayhaw-Barker P (2001) The role of the retinal pigment epithelium: topographical variation and ageing changes. Eye (Lond) 15:384–389

Iraha S, Hirami Y, Ota S, Sunagawa GA, Mandai M, Tanihara H, Takahashi M, Kurimoto Y (2016) Efficacy of valproic acid for retinitis pigmentosa patients: a pilot study. Clin Ophthalmol 10:1375–1384

Kothary PC, Rossi B, Del Monte MA (2016) Valproic acid induced human retinal pigment epithelial cell death as well as its survival after hydrogen peroxide damage is mediated by P38 Kinase. Adv Exp Med Biol 854:765–772

Kumar A, Midha N, Gogia V, Gupta S, Sehra S, Chohan A (2014) Efficacy of oral valproic acid in patients with retinitis pigmentosa. J Ocul Pharmacol Ther 30:580–586

Monti B, Polazzi E, Contestabile A (2009) Biochemical, molecular and epigenetic mechanisms of valproic acid neuroprotection. Curr Mol Pharmacol 2:95–109

Sadaka A, Giuliari GP (2012) Proliferative vitreoretinopathy: current and emerging treatments. Clin Ophthalmol 6:1325–1333

Stern J, Temple S (2015) Retinal pigment epithelial cell proliferation. Exp Biol Med (Maywood) 240:1079–1086

Weng CY, Kothary PC, Verkade AJ, Reed DM, Del Monte MA (2009) MAP kinase pathway is involved in IGF-1-stimulated proliferation of human retinal pigment epithelial cells (hRPE). Curr Eye Res 34:867–876

Xie N, Wang C, Lin Y, Li H, Chen L, Zhang T, Sun Y, Zhang Y, Yin D, Chi Z (2010) The role of p38 MAPK in valproic acid induced microglia apoptosis. Neurosci Lett 482:51–56

# Chapter 56
# Pigment Epithelium-derived Factor Protects Retinal Pigment Epithelial Cells Against Cytotoxicity "In Vitro"


**Francisco M. Nadal-Nicolas and S. Patricia Becerra**

**Abstract** Oxidative stress has been implicated in neurodegenerative diseases, such as age-related macular degeneration. Hydrogen peroxide and sodium iodate can mediate oxidative injury. Sodium iodate induces a selective retinal degeneration targeting the RPE. We describe a method of chronic sodium iodate-mediated injury on RPE cells that may serve to evaluate protective factors against oxidative stress. Cytotoxicity and cell viability curves of ARPE-19 cells with sodium iodate were generated. The antioxidant pigment epithelium-derived factor decreased sodium iodate-mediated cytotoxicity without affecting ARPE-19 cell viability. A cell culture system to evaluate protection against oxidative stress injury with PEDF is discussed.

**Keywords** Pigment epithelium-derived factor (PEDF) · Retinal pigment epithelium (RPE) · ARPE-19 cells · Toxicity · Oxidative stress · Sodium iodate ($NaIO_3$) · Viability · Age-related macular degeneration

## 56.1 Introduction

The retinal pigment epithelium (RPE), a monolayer located at the back of the eye, plays a critical role in the development and maintenance of photoreceptors in the vertebrate retina. The importance of the RPE resides in the nearby relationship with the light-sensitive photoreceptors, which allows transmission of information, transfer of nutrients to photoreceptors, and phagocytosis of metabolic waste (Bok 1993; Rizzolo 1997). Thus, structural or functional injury of RPE can trigger pathologic events in retinal diseases. In fact, age-related macular degeneration (AMD), the most common cause of vision loss in patients over 60 years old, is characterized by

F. M. Nadal-Nicolas · S. P. Becerra (✉)
Section of Protein Structure and Function, Laboratory of Retinal Cell and Molecular Biology, NEI, National Institutes of Health, Bethesda, MD, USA
e-mail: becerras@nei.nih.gov



J. D. Ash et al. (eds.), *Retinal Degenerative Diseases*, Advances in Experimental Medicine and Biology 891, https://doi.org/10.1007/978-3-319-75402-4_56

RPE degeneration that eventually leads to blindness (VanNewkirk et al. 2000; Friedman et al. 2004). Although the pathophysiology of AMD is not well understood, one of the risk factors associated with it is oxidative stress injury of the RPE (Cai and McGinnis 2012). Thereby, cumulative and prolonged oxidative damage of the RPE may contribute to development of AMD. Administration of sodium iodate ($NaIO_3$) in rabbit and mouse eyes causes specific and selective RPE cell damage resulting in a reproducible AMD model (Sorsby 1941; Wang et al. 2014; Obata et al. 2004; Hariri 2013; Bonilha et al. 2015). $NaIO_3$ retinal toxicity has also been studied in cultured RPE cells (Wang et al. 2014; Balmer et al. 2015; Hanus et al. 2016).

The RPE secretes PEDF into the interphotoreceptor matrix (Wu et al. 1995; Becerra et al. 2004) to act in neuronal differentiation, survival, inhibition of angiogenesis, tumorigenesis, and metastasis in retinal cells (Becerra 1997; Becerra and Notario 2013; Barnstable and Tombran-Tink 2004; Bouck 2002; Bullock and Becerra 2015; Polato and Becerra 2016). Of more interest to this study are the reported antioxidant effects of PEDF on retinal pericytes, granulosa cells, and cardiomyocytes (Amano et al. 2005; Bar-Joseph et al. 2014; Zhuang et al. 2016). Tsao et al. (2006) have reported that PEDF attenuates oxidative stress-induced cell death in ARPE-19 cells using hydrogen peroxide ($H_2O_2$) as an oxidative agent. However, it is not known whether PEDF can protect RPE cells against other oxidative agents.

The aim of this study is to investigate the effects of PEDF on ARPE-19 cells after exposure to prolonged nonlethal oxidative damage. Toxicity and viability of the RPE cells subjected to treatments with oxidative agents were determined.

## 56.2 Material and Methods

### *56.2.1 Materials*

Freshly prepared stock solutions of $NaIO_3$ (90 mg/ml, Sigma, St. Louis, MO) in deionized water were filter-sterilized and was diluted in media for the assays. Stock solution of $H_2O_2$ (30%; Sigma, St. Louis, MO) was diluted in media for assays.

### *56.2.2 Cell Culture*

Human ARPE-19 cells, obtained from the American Type Culture Collection (Manassas, VA, USA), were cultured in Dulbecco's modified eagle medium (F:12, cat.11330–032) supplemented with 10% fetal bovine serum (FBS, cat.26140–079) and 1% penicillin/streptomycin (cat.15070–063) at 37 °C with 5% $CO_2$. All reagents were purchased from Gibco, Grand Island, NY. Assays were performed with ARPE-19 cultures between passages 30 and 38.

### 56.2.3 Cell Toxicity Assay

Cells were seeded in 96-well plates ($1.3 \times 10^4$ cells/well) and incubated at 37 °C for 50 h to allow them to reach confluence. Culture media were replaced with serum-free media containing $NaIO_3$ or $H_2O_2$ at indicated concentrations and incubated at 37 °C for 16 h. Toxicity was determined by measuring the cytoplasmic lactate dehydrogenase enzyme (LDH cytotoxicity assay, Pierce™, Life Technologies, Carlsbad, CA) in conditioned media following the instructions of the manufacturer. The absorbance was measured using a microplate reader (SpectraMax5, Molecular Devices, Downingtown, PA).

### 56.2.4 Cell Viability Assay

Intracellular ATP levels, as an indicator of metabolically active cells, determined cell viability using CellTiter-Glo® Luminescent Cell Viability Assay (Promega, Madison, WI) following the instructions of the manufacturer. Medium was removed from cells plated in opaque 96-well plates, and 100 µl of each PBS and CellTiter-Glo® Reagent were added, mixed, and incubated at 25 °C for 10 min before measuring luminescence using an automated plate reader (Envision, Perkin Elmer, MA).

### 56.2.5 Recombinant PEDF

Full-length human PEDF purified from conditioned medium of baby hamster kidney cells stably transfected with pBK-PEDF vectors was as previously described (Stratikos et al. 1996).

### 56.2.6 Statistical Analysis

Data are expressed as the average ± SD. The one-way ANOVA and Tukey post hoc test were used to determine the statistically significant differences, and $p < 0.05$ was considered significant (*).

## 56.3 Results

### *56.3.1 Toxicity and Viability of ARPE-19 Cells Treated with $NaIO_3$ and $H_2O_2$*

ARPE-19 cells were exposed to toxic agents to examine concentration-response curves after chronic damage. Increasing concentrations of $NaIO_3$ or $H_2O_2$ in media without serum for 16 h were added before cell toxicity and viability were determined (Fig. 56.1a). Both toxicity and viability curves with $NaIO_3$ concentrations ranging between 0 and 15 mM were sigmoidal and inverse (Fig. 56.1b). The curves revealed a similar estimated concentration value for half-maximal effect (EC50 = 6.5 mM) at which both curves seemed to intersect. While detectable levels of toxicity were observed with >6 mM $NaIO_3$, cell viability decreased with ≥5 mM $NaIO_3$ (≤70%). Cytotoxicity reached 80% with >9 mM $NaIO_3$. We compared these results with those obtained with $H_2O_2$ treatments. Curves for toxicity and viability were also sigmoidal and inverse to each other (Fig. 56.1c). The estimated EC50 for toxicity and viability were ~450 μM $H_2O_2$ and ~600 μM $H_2O_2$, respectively. $H_2O_2$ at 200–600 μM increased toxicity and was maximum at ≥600 μM $H_2O_2$. The cell viability curve had a minimum decrease in values between 0 and 500 μM $H_2O_2$, which decreased drastically with ≥700 μM $H_2O_2$, *i.e.*, there were an estimated 85% viable ARPE-19 cells with 500 μM and only 8% with 700 μM $H_2O_2$. Similar results were obtained with at least two independent experiments.

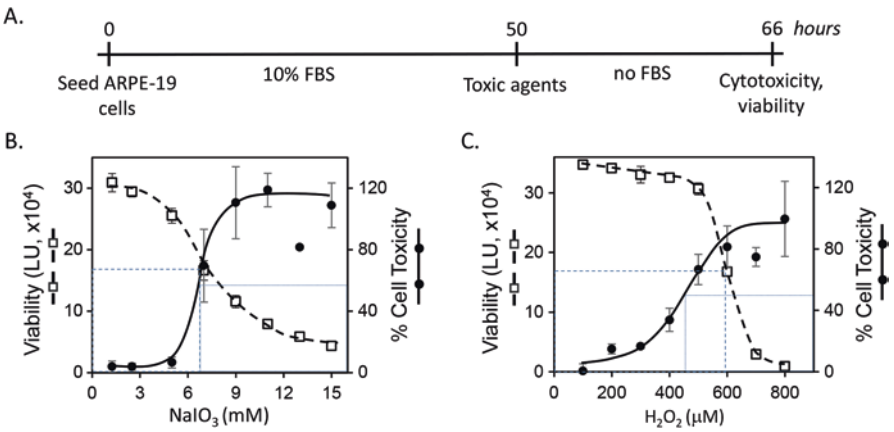


**Fig. 56.1** Cytotoxicity and viability of ARPE-19 cells with $NaIO_3$ and $H_2O_2$. (**a**) Timeline of experimental design on ARPE-19 cells. (**b–c**) The cells were incubated with $NaIO_3$ or $H_2O_2$ at indicated concentrations (*x-axis*) for 16 h. After treatment, the cytotoxicity and viability were determined by the LDH and CellTiter-Glo® assays, respectively. Plots show cytotoxicity values (right *y-axis*) and viability values (left *y-axis*) as a function of agent concentration. The dotted lines correspond to the estimated value for EC50 for each activity: viability $NaIO_3$, 6.5 mM; cytotoxicity $NaIO_3$, 6.5 mM; viability $H_2O_2$, 600 μM; and cytotoxicity $H_2O_2$, 450 μM. Each data point is the average of four replicate assays ± SD. LU luminescence units

### 56.3.2 *Protection of ARPE-19 Cells Against $NaIO_3$-induced Cytotoxicity*

PEDF protects ARPE-19 cells against acute $H_2O_2$ injury (Tsao et al. 2006). To evaluate its potential protective effect against chronic $NaIO_3$-induced cytotoxicity, we exposed ARPE-19 cells to PEDF (10 nM) during treatments with 6–8 mM $NaIO_3$ before determining cell toxicity and viability (Fig. 56.2a). PEDF decreased ARPE-19 cytotoxicity with 6 mM and 7 mM $NaIO_3$, while there was insignificant change with 8 mM $NaIO_3$ (Fig. 56.2b). PEDF protection efficacy against cytotoxicity decreased significantly with $NaIO_3$ concentration from 75% to 12% for 6 to 8 mM $NaIO_3$ (Fig. 56.2c). PEDF did not increase the cell viability in response to 6–8 mM $NaIO_3$ (Fig. 56.2d). Similar results were obtained with at least two independent experiments.

To determine the concentration curve of PEDF protection against $NaIO_3$-mediated injury, we treated ARPE-19 cells with 6 mM $NaIO_3$ in combination with PEDF ranging 0–10 nM, as above. The cytotoxicity curve shows a well-defined decrease in injury with increasing concentrations of PEDF (Fig. 56.3a). Additions of PEDF at 5 nM and 10 nM decreased 50% the levels of LDH cytotoxicity. PEDF had minor effects on viability at the concentrations tested. Similar results were obtained with at least two independent experiments.

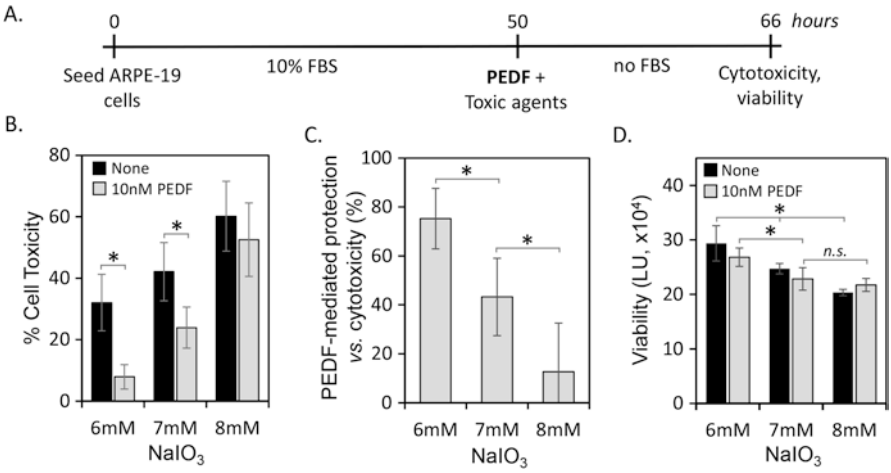


**Fig. 56.2** PEDF effects on $NaIO_3$-induced injury of ARPE-19 cell. (**a**) Timeline showing the experimental design. (**b**) Cytotoxicity of ARPE-19 cells treated with the indicated concentrations of $NaIO_3$ and PEDF (*x-axis*). Toxicity values (y-axis) are expressed as percentage being 100% the maximum LDH in lysed cells with Triton-X100. (**c**) Efficacy of PEDF protection is plotted as percentage of protection at each $NaIO_3$ concentration (*x-axis*), being 100% the toxicity value of cells not treated with PEDF. (**d**) Cell viability of ARPE-19 exposed to $NaIO_3$ (*x-axis*) with and without PEDF. Each bar is the average of four replicate assays ± SD. LU luminescence units, n.s. not significant

## 56.4 Discussion

The study establishes an in vitro model system to induce cytotoxicity injury to ARPE-19 cells with $NaIO_3$, an oxidative toxic agent that can be applied to evaluate protective effects of PEDF against RPE cell injury. We chose agents known to generate oxidative stress and found that cell toxicity and viability occurred in a concentration-dependent fashion for both $H_2O_2$ and $NaIO_3$. Moreover, PEDF can protect against cytotoxicity from $NaIO_3$ and $H_2O_2$ (Fig. 56.3; Tsao et al. 2006). This model system may be useful in studies to elucidate mechanisms that attenuate $NaIO_3$-mediated injury of RPE cells. The results are of interest given that oxidative stress is an important mediator of neuronal cell death that contributes to the pathogenesis of retinal degeneration (Cai et al. 2000; Cai and McGinnis 2012; Bonet-Ponce et al. 2016).

The addition of $H_2O_2$ to cultured RPE cells is a classic model to study oxidative stress (Geiger et al. 2005; Kaczara et al. 2010). $NaIO_3$ toxicity of retinal cells appears to be dependent on serum level, as serum-free media condition elicited a much higher and reliable LDH release (Wang et al. 2014). Our results indicate that ARPE-19 cells are vulnerable to chronic $NaIO_3$- and $H_2O_2$-mediated cell injury, in agreement with previous reports (Fig. 56.1; Wang et al. 2014; Balmer et al. 2015).

We chose PEDF for protection against $NaIO_3$-mediated injury because it is a naturally occurring protein of the interphotoreceptor matrix that has demonstrable antioxidant properties in ARPE-19, specifically against $H_2O_2$-mediated apoptosis (Wu et al. 1995; Becerra et al. 2004; Reinoso et al. 2008; Mukherjee et al. 2007; Tsao et al. 2006). The PEDF-mediated protection against cytotoxicity contrasts with its lack of cell viability increase, which may be due to differences in mechanisms of action of PEDF to protect against $NaIO_3$-mediated injury. In this regard, ARPE-19 cells exposed to $H_2O_2$ concentrations between 400 and 600 μM die by apoptosis, whereas necrosis is triggered at higher concentrations (Kim et al. 2003). Cell viability may require that the cells recover after the acute $H_2O_2$ damage (2 h), as Tsao et al. (2006) observed that PEDF decreases apoptotic nuclei numbers with an increase in cell viability after a recovery time of 16 h in media with 10% FBS. In contrast, our model system uses a chronic induction of injury in which the

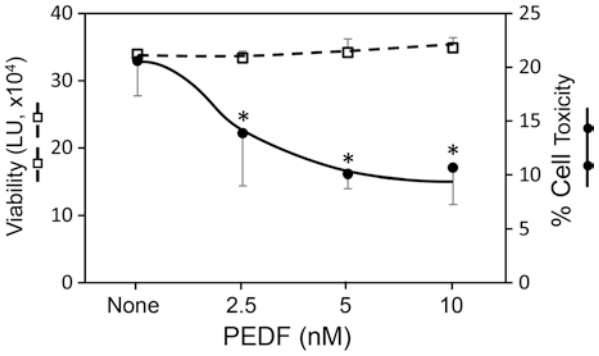


**Fig. 56.3** PEDF concentration curve. Plot showing concentration-response of PEDF (*x-axis*) on cytotoxicity (right *y-axis*) and viability (left *y-axis*) of ARPE-19 cells treated with 6 mM $NaIO_3$. Each bar is the average of four replicate assays ± SD. LU luminescence units

cells are exposed to $NaIO_3$ for more than 16 h with no serum. Although PEDF may not be protective when $NaIO_3$-mediated injury of ARPE-19 is devastating (*e.g.*, at 8 mM $NaIO_3$), PEDF protection efficacy with $NaIO_3$ at concentrations around the EC50 (*e.g.*, 6 mM) clearly suggests that cell toxicity or death can be overcome with this factor.

In summary, the $NaIO_3$-mediated injury of ARPE-19 cell model can serve to study RPE degeneration and protection by relevant survival and antioxidant factors.

**Acknowledgments** We thank Dr. Preeti Subramanian for cell culture assistance. This work was supported by the NEI, NIH Intramural Research Program.

## Bibliography

Amano S, Yamagishi S, Inagaki Y, Nakamura K, Takeuchi M, Inoue H, Imaizumi T (2005) Pigment epithelium-derived factor inhibits oxidative stress-induced apoptosis and dysfunction of cultured retinal pericytes. Microvasc Res 69(1–2):45–55

Balmer J, Zulliger R, Roberti S, Enzmann V (2015) Retinal cell death caused by Sodium Iodate involves multiple Caspase-dependent and Caspase-independent cell-death pathways. Int J Mol Sci 16(7):15086–15103

Bar-Joseph H, Ben-Ami I, Ron-El R, Shalgi R, Chuderland D (2014) Pigment epithelium-derived factor exerts antioxidative effects in granulosa cells. Fertil Steril 102(3):891–898.e3

Barnstable CJ, Tombran-Tink J (2004) Neuroprotective and antiangiogenic actions of PEDF in the eye: molecular targets and therapeutic potential. Prog Retin Eye Res 23(5):561–577

Becerra SP (1997) Structure–function studies on PEDF: a non-inhibitory serpin with neurotrophic activity. Adv Exp Med Biol 425:223–237

Becerra SP, Notario V (2013) The effects of PEDF on cancer biology: mechanisms of action and therapeutic potential. Nat Rev Cancer 13(4):258–271

Becerra SP, Fariss RN, Wu YQ, Montuenga LM, Wong P, Pfeffer BA (2004) Pigment epithelium-derived factor in the monkey retinal pigment epithelium and interphotoreceptor matrix: apical secretion and distribution. Exp Eye Res 78(2):223–234

Bok D (1993) The retinal pigment epithelium: a versatile partner in vision. J Cell Sci Suppl 17:189–195

Bonet-Ponce L, Saez-Atienzar S, da Casa C et al (2016) Rotenone induces the formation of 4-hydroxynonenal aggresomes. Role of ROS-mediated tubulin hyperacetylation and autophagic flux disruption. Mol Neurobiol 53(9):6194–6208

Bonilha VL, Bell BA, Rayborn ME et al (2015) Loss of DJ-1 elicits retinal abnormalities, visual dysfunction, and increased oxidative stress in mice. Exp Eye Res 139:22–36

Bouck N (2002) PEDF: antiangiogenic guardian of ocular function. Trends Mol Med 8:330–334

Bullock J, Becerra SP (2015) PEDF in the retina. In: Geiger M (ed) The Serpin Family. Proteins with multiple functions in health and disease. Springer, Cham, pp 197–212

Cai X, McGinnis JF (2012) Oxidative stress: the achilles' heel of neurodegenerative diseases of the retina. Front Biosci (Landmark Ed) 17(1):1976–1995

Cai J, Nelson KC, Wu M, Sternberg P Jr, Jones DP (2000) Oxidative damage and protection of the RPE. Prog Retin Eye Res 19:205–221

Friedman DS, O'Colmain BJ et al (2004) Prevalence of age-related macular degeneration in the United States. Arch Ophthalmol 122:564–572

Geiger RC, Waters CM, Kamp DW, Glucksberg MR (2005) KGF prevents oxygen-mediated damage in ARPE-19 cells. Invest Ophthalmol Vis Sci 46:3435–3442

Hanus J, Anderson C, Sarraf D, Ma J, Wang S (2016) Retinal pigment epithelial cell necroptosis in response to sodium iodate. Cell Death Discov 2:16054

Hariri S (2013) Noninvasive imaging of the early effect of sodium iodate toxicity in a rat model of outer retina degeneration with spectral domain optical coherence tomography. J Biomed Opt 18:026017

Kaczara P, Sarna T, Burke JM (2010) Dynamics of $H_2O_2$ availability to ARPE-19 cultures in models of oxidative stress. Free Radic Biol Med 48:1064–1070

Kim MH, Chung J, Yang JW, Chung SM, Kwag NH, Yoo JS (2003) Hydrogen peroxide-induced cell death in a human retinal pigment epithelial cell line, ARPE-19. Korean J Ophthalmol 17:19–28

Mukherjee PK, Marcheselli VL, Barreiro S, Hu J, Bok D, Bazan NG (2007) Neurotrophins enhance retinal pigment epithelial cell survival through neuroprotectin D1 signaling. Proc Natl Acad Sci U S A 104(32):13152–13157

Obata R, Yanagi Y, Tamaki Y, Hozumi K, Mutoh M, Tanaka Y (2004) Retinal degeneration is delayed by tissue factor pathway inhibitor-2 in RCS rats and a sodium-iodate-induced model in rabbits. Eye 19:464–468

Polato F, Becerra SP (2016) Pigment epithelium-derived factor, a protective factor for photoreceptors in vivo. Adv Exp Med Biol 854:699–706

Reinoso MA, Mukherjee P, Marcheselli V, Bergsma D, Hesse R, Bazan N (2008) PEDF promotes biosynthesis of a novel anti-inflammatory and anti-apoptotic mediator NPD1 in retinal pigment epithelial cells. Ochsner J 8(1):39–43

Rizzolo LJ (1997) Polarity and the development of the outer blood–retinal barrier. Histol Histopathol 12:1057–1067

Sorsby A (1941) Experimental pigmentary degeneration of the retina by sodium iodate. Br J Ophthalmol 25:58–62

Stratikos E, Alberdi E, Gettins PG, Becerra SP (1996) Recombinant human pigment epithelium-derived factor (PEDF): characterization of PEDF overexpressed and secreted by eukaryotic cells. Protein Sci 5(12):2575–2582

Tsao YP, Ho TC, Chen SL, Cheng HC (2006) Pigment epithelium-derived factor inhibits oxidative stress-induced cell death by activation of extracellular signal-regulated kinases in cultured retinal pigment epithelial cells. Life Sci 79(6):545–550

VanNewkirk MR, Nanjan MB et al (2000) The prevalence of age-related maculopathy: the visual impairment project. Ophthalmology 107:1593–1600

Wang J, Iacovelli J, Spencer C, Saint-Geniez M (2014) Direct effect of sodium iodate on neurosensory retina. Invest Ophthalmol Vis Sci 55(3):1941–1953

Wu YQ, Notario V, Chader GJ, Becerra SP (1995) Identification of pigment epithelium-derived factor in the interphotoreceptor matrix of bovine eyes. Protein Expr Purif 6(4):447–456

Zhuang W, Zhang H, Pan J et al (2016) PEDF and PEDF-derived peptide 44mer inhibit oxygen-glucose deprivation-induced oxidative stress through upregulating PPARγ via PEDF-R in H9c2 cells. Biochem Biophys Res Commun 472(3):482–488

# Chapter 57
# Brain-Derived Neurotrophic Factor as a Treatment Option for Retinal Degeneration


**Conor Daly, Rebecca Ward, Alison L. Reynolds, Orla Galvin, Ross F. Collery, and Breandán N. Kennedy**

**Abstract** This review discusses the therapeutic potential of brain-derived neurotrophic factor (BDNF) for retinal degeneration. BDNF, nerve growth factor (NGF), neurotrophin 3 (NT-3) and NT-4/NT-5 belong to the neurotrophin family. These neuronal modulators activate a common receptor and a specific tropomyosin-related kinase (Trk) receptor. BDNF was identified as a photoreceptor protectant in models of retinal degeneration as early as 1992. However, development of effective therapeutics that exploit this pathway has been difficult due to challenges in sustaining therapeutic levels in the retina.

**Keywords** Brain-Derived Neurotrophic Factor · BDNF · Neuroprotection · Retinal degeneration · Photoreceptor

## Abbreviations

| | |
|---|---|
| BCL-2 | B-cell lymphoma 2 |
| BDNF | Brain-derived neurotrophic factor |
| HDACi | Histone deacetylase inhibitor |
| LE | Light exposure |

C. Daly · R. Ward · B. N. Kennedy (✉)
School of Biomolecular and Biomedical Science, University College Dublin, Belfield, Ireland
e-mail: brendan.kennedy@ucd.ie

A. L. Reynolds
School of Veterinary Medicine, University College Dublin, Belfield, Ireland

O. Galvin
School of Biomolecular and Biomedical Science, University College Dublin, Belfield, Ireland

RenaSci Limited, BioCity, Nottingham, UK

R. F. Collery
Department of Ophthalmology and Visual Sciences, Eye Institute, Medical College of Wisconsin, Milwaukee, WI, USA



J. D. Ash et al. (eds.), *Retinal Degenerative Diseases*, Advances in Experimental Medicine and Biology 891, https://doi.org/10.1007/978-3-319-75402-4_57

| | |
|---|---|
| MAPK | Mitogen-activated protein kinase |
| NGF | Nerve growth factor |
| ONL | Outer nuclear layer |
| PI3K | Phosphoinositide 3-kinase |
| Trk | Tropomyosin-related kinase |

## 57.1 Localisation and Expression

In vertebrate retinae, BDNF protein localises to the inner and outer plexiform layers and outer nuclear layer (ONL) (Ghazi-Nouri et al. 2008; Germana et al. 2010). TrkB expression is reported in the inner plexiform layer (Vecino et al. 2002) and photoreceptor outer segments (Di Polo et al. 2000). Originally considered biologically inactive, neurotrophin pro-isoforms preferentially bind a p75 neurotrophin receptor and sortilin heterodimer to initiate apoptosis (Koshimizu et al. 2009). In contrast, mature neurotrophins bind cognate Trk receptors promoting neuronal differentiation, survival and synaptic plasticity (Lee et al. 2001). NGF is a ligand for TrkA, BDNF and NT-4/NT-5 ligands for TrkB and NT-3 for TrkC (Lu 2003). BDNF binding to TrkB requires proteolytic release of mature 14 kDa BDNF from a 32 kDa precursor (Numakawa et al. 2010).

## 57.2 BDNF/TrkB Signalling

BDNF can mediate retinal neuroprotection (Vecino et al. 2002; Okoye et al. 2003). Mechanistically, BDNF activation of TrkB receptors on Müller glia leads to increased expression of neurotrophic factors, including BDNF (Harada et al. 2002). Intracellularly, neuroprotection is mediated by pro-survival pathways. TrkB autophosphorylation leads to conjugation with Shc and phospholipase Cγ1 (PLCγ1). These adaptors activate phosphoinositide 3-kinase (PI3K), mitogen-activated protein kinase (MAPK) and PLCγ–$Ca^{2+}$ pathways (Kaplan and Miller 2000; Nakazawa et al. 2002). The PI3K and MAPK pathways downstream of Shc enhance transcription of pro-survival B-cell lymphoma 2 (*BCL-2*) family member genes (*BCL-XL* and *BCL-2*) (Almeida et al. 2005; Nguyen et al. 2009). Akt phosphorylation of mouse double minute 2 (MDM2) homolog inhibits p53 activity and phosphatase and tensin homolog (PTEN) expression (Abraham and O'Neill 2014); additional pro-apoptotic signals are inhibited by phosphorylation of BCL-2-associated agonist of cell death (BAD) (Wu et al. 2014). Inhibition of p53 activity blocks cytochrome C release and mitochondrial cell death.

## 57.3 Photoreceptor Protection

BDNF-mediated photoreceptor protection in vivo is variable. In light exposure (LE) models, BDNF provides photoreceptor protection (two to three additional nuclear rows), but in inherited models, partial rescue was observed only in one of seven models (LaVail et al. 1992; LaVail et al. 1998). Similarly, in cone-rod dystrophy, BDNF failed to prevent photoreceptor degeneration (Chong et al. 1999). Notably, BDNF was administered prior to neurodegeneration in LE models but typically administered after onset of degeneration in inherited models. Table 57.1 summarises studies evaluating BDNF neuroprotection. Retinal neuroprotection is generally reported as structural and functional, e.g. reduced apoptosis and increased ONL, photoreceptor outer segments and electroretinographic responses. Variability may reflect timing of BDNF delivery, duration of action, retinal concentration, differences in homology between mouse and human BDNF protein (3%; source UniProtKB) or the underlying neurodegenerative pathways.

## 57.4 Clinical Development

Collectively, recombinant BDNF is a promising neuroprotective agent. However, clinical development is impeded by challenges to effectively deliver BDNF to the posterior eye. For oral administration, absorption from the gastrointestinal tract is anticipated to be poor, and the blood-retinal barrier (BRB) limits BDNF bioavailability in the retina. The 9.7 min half-life (Sakane and Pardridge 1997) of recombinant BDNF requires repeat dosing which may attenuate efficacy due to feedback downregulation of TrkB (Frank et al. 1997; Chen and Weber 2004). Other concerns are enhanced neuronal excitability by BDNF leading to seizures (Scharfman et al. 2002) and increased free radical formation, promoting cell death (Klocker et al. 1998). Approaches to overcome these challenges exploit local eye administration. Direct intravitreal injection of recombinant BDNF can temporarily rescue retinal ganglion cells; however, continued delivery is required for long-term recovery (Mansour-Robaey et al. 1994). Unfortunately, multiple intravitreal injections are burdensome for patients and clinics and increase risk of cataracts, ischaemia and endophthalmitis (Marticorena et al. 2012). In a cell-based approach, Schwann cells expressing BDNF preserved photoreceptor structure and function for at least 4 months when transplanted into the subretinal space (Lawrence et al. 2004). Similarly, transplanted BDNF-expressing bone marrow stem cells protected light-damaged retinas for 14 days (Zhang and Wang 2010).

Alternatively, localised BDNF gene therapy with adeno-associated virus (AAV) was safe and sustained recombinant BDNF expression (Guy et al. 1999). Indeed, BDNF gene transfer to Müller cells protects photoreceptors from LE-induced retinal degeneration (Gauthier et al. 2005). Delayed onset of gene expression is a limitation of viral vectors (Ferrari et al. 1996), but this can be overcome by combination

**Table 57.1** Summary of BDNF efficacy in retinal degeneration models

| Drug | Type | Model | Effect | Reference |
|---|---|---|---|---|
| BDNF (intravitreal) | Human recombinant | LE (rat) | Photoreceptor survival | LaVail et al. (1992) |
| BDNF (intravitreal) | Human recombinant | rd mouse<br>rds mouse<br>nr mouse<br>pcd mouse<br>[a]P23H (mouse)<br>[a]Q344Ter (mouse)<br>[a]VPP (mouse)<br>LE (mouse)<br>LE (rat) | No protection<br>No protection<br>PR protection in 3/31 mice<br>No protection<br>No protection<br>No protection<br>No protection<br>PR protection<br>PR protection | LaVail et al. (1998) |
| BDNF (intravitreal) | Human recombinant | Cone-rod iRD (cat) | No rescue | Chong et al. (1999) |
| BDNF knock-in (tet) | DOX-induced expression | Rod iRD (mouse) | Photoreceptor survival, functional rescue (ERG) | Okoye et al. (2003) |
| AAV2-BDNF-IPE | Viral transduced cell transplantation | LE (rat) | Photoreceptor survival | Hojo et al. (2004) |
| Ad-BDNF-Müller glia | Viral | LE (rat) | Photoreceptor survival, functional rescue | Gauthier et al. (2005) |
| BDNF-transduced RPE cells | Cell transplantation | LE (rat) | Photoreceptor survival | Abe et al. (2005) |
| Knockdown | Transgenic BDNF+/− mouse | LE (mouse) | More PR survival in mice with reduced BDNF levels | Wilson et al. (2007) |
| BDNF-treated retinal progenitor sheets | BDNF cell transplantation | Rod iRD (rat) | Improved function RPC-BDNF microspheres, but not BDNF microspheres alone | Seiler et al. (2008) |
| BDNF-transduced RPE cells (tet) | Dox-induced BDNF cell transplantation | LE (rat) | Photoreceptor survival, functional rescue (ERG) | Abe et al. (2008) |
| BDNF-expressing plasmid | Subretinal injection, electroporation | RCS rat | Photoreceptor survival | Zhang et al. (2009) |
| BDNF (intravitreal) | Human recombinant | Blue LE (rat) | Cone survival | Ortín-Martínez et al. (2014) |
| BDNF (i/o or topical) | Human recombinant | LE (rat) | Photoreceptor survival, functional rescue (ERG) | Cerri et al. (2015) |

[a]Rhodopsin mutant mouse model
*iRD* inherited retinal degeneration, *LE* light exposure

with initial intravitreal injection of recombinant BDNF (Ren et al. 2012). However, viral vector and cell-based therapy via subretinal injection technique are not without complications including retinal folding and splitting, rejection, tumour growth, proliferative vitreoretinopathy and choroidal neovascularisation (Johnson et al. 2011). An alternative strategy for long-term ocular delivery applies sustained-release BDNF microparticles, as exemplified by a combination therapy where subretinal transplantation of retinal progenitor cells (RPC) with recombinant BDNF microspheres improved their functional efficacy in a rat model of retinal degeneration (Seiler et al. 2008). In terms of patient independence and compliance, topical administration is desirable. Encouraging results in a murine glaucoma model with eye drop BDNF increased retinal BDNF ~10-fold and rescued visual responses (Domenici et al. 2014; Cerri et al. 2015).

An alternative to recombinant BDNF is small-molecule BDNF mimetics (e.g. 7,8-dihydroxyflavone) proposed as therapies for Alzheimer's disease (Liu et al. 2016) and amyotrophic lateral sclerosis (Ochs et al. 2000). The histone deacetylase inhibitor (HDACi) valproic acid has efficacy in retinitis pigmentosa patients (Iraha et al. 2016), and BDNF is induced by HDACi treatment (Wu et al. 2008; Yasuda et al. 2009). BDNF agonists also increased ganglion cell survival in models of optic nerve injury and N-methyl-D-aspartate (NMDA)-induced cell death (Chen and Weber 2001; Kimura et al. 2014).

## 57.5 Conclusion

BDNF is of clinical interest in retinal degenerations. Challenges in clinical development may be overcome with improved delivery methods and identification of alternative BDNF/TrkB pathway modulators.

## References

Abe T, Saigo Y, Hojo M et al (2005) Protection of photoreceptor cells from Phototoxicity by transplanted retinal pigment epithelial cells expressing different neurotrophic factors. Cell Transplant 14:799–808

Abe T, Wakusawa R, Seto H et al (2008) Topical doxycycline can induce expression of BDNF in transduced retinal pigment epithelial cells transplanted into the subretinal space. Invest Ophthalmol Vis Sci 49:3631–3639

Abraham AG, O'Neill E (2014) PI3K/Akt-mediated regulation of p53 in cancer. Biochem Soc Trans 42:798–803

Almeida RD, Manadas BJ, Melo CV et al (2005) Neuroprotection by BDNF against glutamate-induced apoptotic cell death is mediated by ERK and PI3-kinase pathways. Cell Death Differ 12:1329–1343

Cerri E, Origlia N, Falsini B et al (2015) Conjunctivally applied BDNF protects photoreceptors from light-induced damage. Transl Vis Sci Technol 4:1

Chen H, Weber AJ (2001) BDNF enhances retinal ganglion cell survival in cats with optic nerve damage. Invest Ophthalmol Vis Sci 42:966–974

Chen H, Weber AJ (2004) Brain-derived neurotrophic factor reduces TrkB protein and mRNA in the normal retina and following optic nerve crush in adult rats. Brain Res 1011:99–106

Chong NH, Alexander RA, Waters L et al (1999) Repeated injections of a ciliary neurotrophic factor analogue leading to long-term photoreceptor survival in hereditary retinal degeneration. Invest Ophthalmol Vis Sci 40:1298–1305

Di Polo A, Cheng L, Bray GM et al (2000) Colocalization of TrkB and brain-derived neurotrophic factor proteins in green-red-sensitive cone outer segments. Invest Ophthalmol Vis Sci 41:4014–4021

Domenici L, Origlia N, Falsini B et al (2014) Rescue of retinal function by BDNF in a mouse model of glaucoma. PLoS One 9:e115579

Ferrari FK, Samulski T, Shenk T et al (1996) Second-strand synthesis is a rate-limiting step for efficient transduction by recombinant adeno-associated virus vectors. J Virol 70:3227–3234

Frank L, Wiegand SJ, Siuciak JA et al (1997) Effects of BDNF infusion on the regulation of TrkB protein and message in adult rat brain. Exp Neurol 145:62–70

Gauthier R, Joly S, Pernet V et al (2005) Brain-derived neurotrophic factor gene delivery to muller glia preserves structure and function of light-damaged photoreceptors. Invest Ophthalmol Vis Sci 46:3383–3392

Germana A, Sanchez-Ramos C, Guerrera MC et al (2010) Expression and cell localization of brain-derived neurotrophic factor and TrkB during zebrafish retinal development. J Anat 217:214–222

Ghazi-Nouri SM, Ellis JS, Moss S et al (2008) Expression and localisation of BDNF, NT4 and TrkB in proliferative vitreoretinopathy. Exp Eye Res 86:819–827

Guy J, Qi X, Muzyczka N et al (1999) Reporter expression persists 1 year after adeno-associated virus-mediated gene transfer to the optic nerve. Arch Ophthalmol 117:929–937

Harada T, Harada C, Kohsaka S et al (2002) Microglia-Muller glia cell interactions control neurotrophic factor production during light-induced retinal degeneration. J Neurosci 22:9228–9236

Hojo M, Abe T, Sugano E et al (2004) Photoreceptor protection by iris pigment epithelial transplantation transduced with AAV-mediated brain-derived neurotrophic factor gene. Invest Ophthalmol Vis Sci 45:3721–3726

Iraha S, Hirami Y, Ota S et al (2016) Efficacy of valproic acid for retinitis pigmentosa patients: a pilot study. Clin Ophthalmol 10:1375–1384

Johnson TV, Bull ND, Martin KR (2011) Neurotrophic factor delivery as a protective treatment for glaucoma. Exp Eye Res 93:196–203

Kaplan DR, Miller FD (2000) Neurotrophin signal transduction in the nervous system. Curr Opin Neurobiol 10:381–391

Kimura A, Namekata K, Guo X et al (2014) Valproic acid prevents NMDA-induced retinal ganglion cell death via stimulation of neuronal TrkB receptor signaling. Am J Pathol 185(3):756–764

Klocker N, Cellerino A, Bahr M (1998) Free radical scavenging and inhibition of nitric oxide synthase potentiates the neurotrophic effects of brain-derived neurotrophic factor on axotomized retinal ganglion cells in vivo. J Neurosci 18:1038–1046

Koshimizu H, Kiyosue K, Hara T et al (2009) Multiple functions of precursor BDNF to CNS neurons: negative regulation of neurite growth, spine formation and cell survival. Mol Brain 2:27–27

LaVail MM, Unoki K, Yasumura D et al (1992) Multiple growth factors, cytokines, and neurotrophins rescue photoreceptors from the damaging effects of constant light. Proc Natl Acad Sci U S A 89:11249–11253

LaVail MM, Yasumura D, Matthes MT et al (1998) Protection of mouse photoreceptors by survival factors in retinal degenerations. Invest Ophthalmol Vis Sci 39:592–602

Lawrence JM, Keegan DJ, Muir EM et al (2004) Transplantation of Schwann cell line clones secreting GDNF or BDNF into the retinas of dystrophic Royal College of surgeons rats. Invest Ophthalmol Vis Sci 45:267–274

Lee R, Kermani P, Teng KK et al (2001) Regulation of cell survival by secreted Proneurotrophins. Science 294:1945–1948

Liu C, Chan CB, Ye K (2016) 7,8-dihydroxyflavone, a small molecular TrkB agonist, is useful for treating various BDNF-implicated human disorders. Transl Neurodegener 5:2

Lu B (2003) BDNF and activity-dependent synaptic modulation. Learn Mem (Cold Spring Harbor, NY) 10:86–98

Mansour-Robaey S, Clarke DB, Wang Y et al (1994) Effects of ocular injury and administration of brain-derived neurotrophic factor on survival and regrowth of axotomized retinal ganglion cells. Proc Natl Acad Sci U S A 91(5):1632–1636

Marticorena J, Romano V, Gomez-Ulla F (2012) Sterile endophthalmitis after intravitreal injections. Mediat Inflamm 2012:928123

Nakazawa T, Tamai M, Mori N (2002) Brain-derived neurotrophic factor prevents axotomized retinal ganglion cell death through MAPK and PI3K signaling pathways. Invest Ophthalmol Vis Sci 43:3319–3326

Nguyen N, Lee SB, Lee YS et al (2009) Neuroprotection by NGF and BDNF against neurotoxin-exerted apoptotic death in neural stem cells are mediated through Trk receptors, activating PI3-kinase and MAPK pathways. Neurochem Res 34:942–951

Numakawa T, Suzuki S, Kumamaru E et al (2010) BDNF function and intracellular signaling in neurons. Histol Histopathol 25:237–258

Ochs G, Penn RD, York M et al (2000) A phase I/II trial of recombinant methionyl human brain derived neurotrophic factor administered by intrathecal infusion to patients with amyotrophic lateral sclerosis. Amyotroph Lateral Scler Other Motor Neuron Disord 1:201–206

Okoye G, Zimmer J, Sung J et al (2003) Increased expression of brain-derived neurotrophic factor preserves retinal function and slows cell death from rhodopsin mutation or oxidative damage. J Neurosci 23:4164–4172

Ortín-Martínez A, Valiente-Soriano FJ, García-Ayuso D et al (2014) A novel in vivo model of focal light emitting diode-induced cone-photoreceptor Phototoxicity: neuroprotection afforded by Brimonidine, BDNF, PEDF or bFGF. PLoS One 9:e113798

Ren R, Li Y, Liu Z et al (2012) Long-term rescue of rat retinal ganglion cells and visual function by AAV-mediated BDNF expression after acute elevation of intraocular pressure. Invest Ophthalmol Vis Sci 53:1003–1011

Sakane T, Pardridge WM (1997) Carboxyl-directed pegylation of brain-derived neurotrophic factor markedly reduces systemic clearance with minimal loss of biologic activity. Pharm Res 14:1085–1091

Scharfman HE, Goodman JH, Sollas AL et al (2002) Spontaneous limbic seizures after intrahippocampal infusion of brain-derived neurotrophic factor. Exp Neurol 174:201–214

Seiler MJ, Thomas BB, Chen Z et al (2008) BDNF-treated retinal progenitor sheets transplanted to degenerate rats: improved restoration of visual function. Exp Eye Res 86:92–104

Vecino E, Garćia-Grespo D, Garćia M et al (2002) Rat retinal ganglion cells co-express brain derived neurotrophic factor (BDNF) and its receptor TrkB. Vis Res 42:151–157

Wilson RB, Kunchithapautham K, Br R (2007) Paradoxical role of BDNF: BDNF+/− retinas are protected against light damage–mediated stress. Invest Ophthalmol Vis Sci 48:2877–2886

Wu X, Chen PS, Dallas S et al (2008) Histone deacetylase inhibitors up-regulate astrocyte GDNF and BDNF gene transcription and protect dopaminergic neurons. Int J Neuropsychopharmacol 11:1123–1134

Wu CH, Hung TH, Chen CC et al (2014) Post-injury treatment with 7,8-dihydroxyflavone, a TrkB receptor agonist, protects against experimental traumatic brain injury via PI3K/Akt signaling. PLoS One 9:e113397

Yasuda S, Liang MH, Marinova Z et al (2009) The mood stabilizers lithium and valproate selectively activate the promoter IV of brain-derived neurotrophic factor in neurons. Mol Psychiatry 14:51–59

Zhang Y, Wang W (2010) Effects of bone marrow mesenchymal stem cell transplantation on light-damaged retina. Invest Ophthalmol Vis Sci 51:3742–3748

Zhang M, Mo X, Fang Y et al (2009) Rescue of photoreceptors by BDNF gene transfer using in vivo electroporation in the RCS rat of retinitis pigmentosa. Curr Eye Res 34:791–799

# Chapter 58
# VEGF as a Trophic Factor for Müller Glia in Hypoxic Retinal Diseases


**Shuhua Fu, Shuqian Dong, Meili Zhu, and Yun-Zheng Le**

**Abstract** Age-related macular degeneration (AMD) and diabetic retinopathy (DR), leading causes of blindness, share a common retinal environment: hypoxia which is a major stimulator for the upregulation of vascular endothelial growth factor (VEGF), a cardinal pathogenic factor for the breakdown of blood-retina barrier (BRB). As a result of intensive studies on VEGF pathobiology, anti-VEGF strategy has become a major therapeutics for wet AMD and DR. To investigate the potential impact of anti-VEGF strategy on major retinal supporting cells, Müller glia (MG), we disrupted VEGF receptor-2 (VEGFR2) in MG with conditional knockout (CKO) and examined the effect of VEGFR2-null on MG viability and neuronal integrity in mice. VEGFR2 CKO mice demonstrated a significant loss of MG density in diabetes/hypoxia, which in turn resulted in accelerated retinal degeneration. These defects appear similar to the clinical characteristics in a significant portion of wet-AMD patients with long-term anti-VEGF therapies. In this article, we will discuss the

S. Fu
Department of Ophthalmology, the Second Affiliated Hospital of Nanchang University, Nanchang, China

Department of Medicine Endocrinology, University of Oklahoma Health Sciences Center, Oklahoma City, OK, USA

S. Dong · M. Zhu
Department of Medicine Endocrinology, University of Oklahoma Health Sciences Center, Oklahoma City, OK, USA

Y. -Z. Le (✉)
Department of Medicine Endocrinology, University of Oklahoma Health Sciences Center, Oklahoma City, OK, USA

Department of Cell Biology, University of Oklahoma Health Sciences Center, Oklahoma City, OK, USA

Department of Ophthalmology, University of Oklahoma Health Sciences Center, Oklahoma City, OK, USA

Harold Hamm Diabetes Center, University of Oklahoma Health Sciences Center, Oklahoma City, OK, USA
e-mail: Yun-Le@ouhsc.edu



J. D. Ash et al. (eds.), *Retinal Degenerative Diseases*, Advances in Experimental Medicine and Biology 891, https://doi.org/10.1007/978-3-319-75402-4_58

potential relevance of these clinical characteristics to the critical role of VEGF signaling in MG viability and neuronal integrity in hypoxia.

**Keywords** VEGF · AMD · DR · Hypoxia · Müller glia

## 58.1 Introduction

The discovery of hypoxia-induced upregulation of vascular endothelial growth factor (VEGF) during the breakdown of blood-retina barrier (BRB) in diabetic retinopathy (DR), wet age-related macular degeneration (AMD), retinopathy of prematurity (ROP), and other BRB diseases (Aiello et al. 1994; Miller et al. 1994; Alon et al. 1995; Kvanta et al. 1996; Lopez et al. 1996) has led to the intensive studies of VEGF pathobiology for the past two decades. As a result, FDA-approved and off-label anti-VEGF drugs are now widely used for the treatment of wet AMD, DR, diabetic macular edema (DME), and other hypoxic BRB diseases. To investigate the potential impact of anti-VEGF strategy on the retina and the effect of VEGFR2-null on major retinal supporting cells, Müller glia (MG), we disrupted VEGF receptor-2 (VEGFR2) in MG with conditional knockout (CKO) and characterized the VEGFR2 CKO mice. In this article, we will discuss the significance of VEGF signaling in MG viability and neuronal integrity and their relevance to potential adverse effects of anti-VEGF therapies and to neuroprotection in hypoxic BRB diseases.

## 58.2 Function of VEGF in Müller Glia

MG are present in close proximity to all retinal neurons, which is ideal for them to serve as major retinal supporting cells and to play many essential roles in retinal metabolism, function, maintenance, stress response, and protection. To determine the role of MG-derived VEGF in DR and retinopathy of prematurity (ROP), we generated MG-specific VEGF KO mice. Although VEGF CKO mice exhibited a significant reduction in retinal VEGF, inflammation, neovascularization, and vascular leakage and lesion in hypoxic/ischemic ROP model and streptozotocin (STZ)-induced diabetic model (Bai et al. 2009; Wang et al. 2010), we did not observe any detectable alteration in retinal morphology under diabetic/ischemic conditions. As VEGF is a secreted protein, a reduction of overall retinal VEGF could be compensated by other cell types; we therefore disrupted VEGFR2 in mouse MG using our MG Cre-drive line (Ueki et al. 2009). While VEGFR2 CKO mice did not have any detectable morphological and functional changes normally, there was a near 50% loss of MG viability in STZ-induced diabetic model when the retina became hypoxic (late stage of DR, Fig 58.1a), which in turn resulted in accelerated retinal neuronal degeneration (Fig 58.1b) and a substantial reduction of two neurotrophins: retinal brain-derived neurotrophic factor (BDNF) and glial cell line-derived neurotrophic factor (GDNF) (Fig 58.1d; for detail, see Fu et al. (2015)).

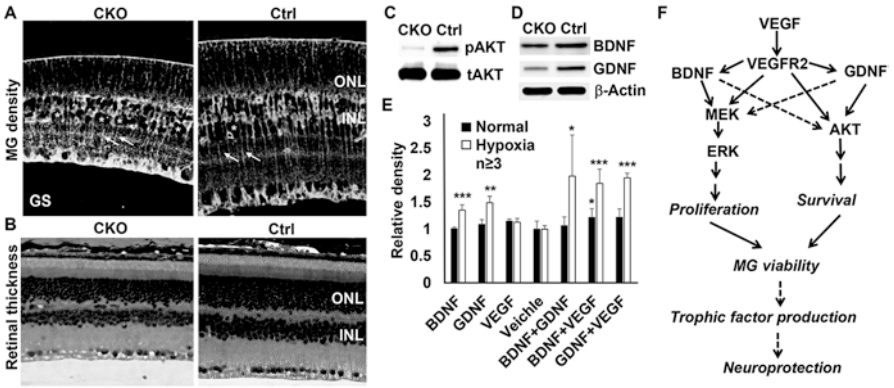


**Fig. 58.1** *Supporting data and working hypothesis*. (**a**–**b**) Representative images of immunohistochemical-stained retinal sections for MG marker glutamine synthetase (GS, (**a**)) and hematoxylin- and eosin-stained retinal sections (**b**) showing a significant loss of MG and neuronal densities and retinal thickness in 10-month-old diabetic/hypoxic VEGFR2 CKO mice. Ctrl control, ONL outer nuclear layer, INL inner nuclear layer. * loss of cells. Arrows, MG (GS-positive). (**c**–**d**) Representative Western blot images showing a significant loss of phosphorylated AKT (pAKT) in primary VEGFR2-null Müller cells cultured under diabetes-like conditions (**c**) and a significant loss of BDNF and GDNF in retinal extracts of 10-month-old diabetic/hypoxic VEGFR2 CKO mice (**d**), respectively. (**e**): Relative density of live rMC1 cells grown in normal and hypoxic ($CoCl_2$ (100 mM)) media supplemented with VEGF, BDNF, or/and GDNF for 22 h. Growth factor supplement, 0.24 ng/mL. ***$p < 0.001$; **$p < 0.01$; *$p < 0.05$. Error bar, SD. $p$-values, represent pairwise comparison with vehicle by $t$-test. (**f**): Putative mechanism of VEGF signaling-mediated MG viability and its role in neuroprotection in hypoxic retinal diseases. Solid arrows, with supporting data. Broken arrows, unproven

To ascertain if hypoxia was a major inducing factor for the loss of MG viability in VEGFR2 CKO mice, we used a chemical hypoxic model (Dong et al. 2014) and recapitulated the loss of MG viability and neurons in the animals (data not shown).

## 58.3 Potential Adverse Effect of Anti-VEGF Drugs on Retinal Integrity

Although the goal of using anti-VEGF drugs, namely, VEGF-neutralizing antibodies, is to reduce the level of VEGF below pathological thresholds, anti-VEGF drugs are antibodies by nature and may interfere with VEGFRs in physiological process. While there is a significant amount of literatures on the pathological role of VEGF, surprisingly little is known about the physiological function of VEGF in adult retinas, except a handful of studies suggesting that VEGF is a trophic factor for MG, ganglion layer neurons, and the retinal pigment epithelium (Kilic et al. 2006; Saint-Geniez et al. 2008; Saint-Geniez et al. 2009). However, the lessons learned from the brain suggest that VEGF could potentially serve as a modulator for neuronal function (McCloskey et al. 2005). Recent publications on anti-VEGF clinical trials have reached a consensus that, while the drugs

may be effective in reducing BRB breakdown and in improving visual acuity in some patients, average gain of visual acuities has not been maintained for wet-AMD patients after 5-year anti-VEGF treatment (Arevalo et al. 2016a; Comparison of Age-related Macular Degeneration Treatments Trials Research et al. 2016), which also occurred in a 5-year DME clinical trial (Arevalo et al. 2016b). Geographic atrophy-like pathology and retinal, choroidal, and scleral thinning, clinical characteristics that are most likely caused by altered VEGF signaling, occur frequently in anti-VEGF trial patients (Arevalo et al. 2016a; Grunwald et al. 2015). Moreover, a significant portion (36%) of wet-AMD patients appears to have very thin retinas, thinning in all retinal layers, after 5-year anti-VEGF treatment (Comparison of Age-related Macular Degeneration Treatments Trials Research et al. 2016), suggesting potential neuronal degeneration in the whole retina. This clinical characteristic bears striking resemblance to the accelerated degeneration of all retinal neurons in hypoxic/diabetic MG-specific VEGFR2 KO mice (Fig 58.1b left), which supports the notion that VEGF signaling in MG is critical in protecting themselves and neurons in hypoxic retinal diseases. While longer-term anti-VEGF clinical trial data for DR are not available, the observation that a VEGF-neutralizing antibody causes retinal degeneration in experimental diabetes (Hombrebueno et al. 2015) and short hairpin (sh)RNA targeting VEGF in MG results in retinal thinning in a ROP model (Jiang et al. 2014) strongly suggests a similar outcome.

## 58.4 Mechanism to Support MG Viability and Its Effect on Neuroprotection in Hypoxia

Primary VEGFR2-null Müller cells (MCs) grown under diabetes-like condition had a substantial elevation of apoptotic retinal cells (Fu et al. 2015) and a significant reduction of activated AKT survival signal (Fig 58.1c), suggesting that VEGFR2-AKT survival mechanism is at least partially responsible for MG viability in diabetes/hypoxia (Fig 58.1f). MG are considered as a source for BDNF, GDNF, and other trophic factors (Reichenbach and Bringmann 2013). Many translational studies have shown the efficacies of these trophic factors in rescuing retinal degeneration under various stress conditions (LaVail et al. 1992). Among a few trophic factors tested, only the levels of BDNF and GDNF were altered in diabetic/hypoxic VEGFR2 CKO mice (Fu et al. 2015). This observation suggests that MG may be the major cellular source for BDNF/GDNF in the retina and VEGF signaling in MG is important in maintaining a proper level of BDNF and GDNF in diabetic/hypoxic retinas, either by supporting MG viability, BDNF/GDNF production/secretion, or both. In rat MC line rMC1 (Sarthy et al. 1998), BDNF or GDNF did not appear to have an apparent effect on viability under normal conditions; however, BDNF and GDNF promoted MC viability under hypoxia (Fig 58.1e). Moreover, the effects of BDNF, GDNF, and VEGF on MC viability appeared to be synergistic in hypoxia. This observation suggests that, in addition to VEGFR2-AKT survival pathway-mediated MG viability, VEGF singling may interact with BDNF- or/and GDNF-specific pathways and promote MG survival and proliferation, as sketched in our working hypothesis (Fig 58.1f). This is not unprecedented as these trophic factors

can act synergistically on motor neurons in familial amyotrophic lateral sclerosis and Parkinson disease (Herran et al. 2013; Krakora et al. 2013).

In summary, VEGF signaling-mediated MG viability is likely through a number of alternative pathways that could work synergistically in hypoxia, which is likely a major stress response for MG to protect themselves and neurons in hypoxia. Therefore, VEGF signaling in MG is critical to MG viability and neuroprotection in wet AMD, DR, and other hypoxic BRB diseases. Identifying alternative mechanisms that bypass VEGF/VEGFR2 signaling but promote MG viability in hypoxia is an urgent task to the design of safer anti-VEGF therapies for patients with wet AMD, DR, and other hypoxic BRB diseases.

**Acknowledgment** We thank Dr. V. P. Sarthy for providing rMC1 cells. Our work was supported by NIH grants GM104934, EY020900, and EY26970 and grants from Research to Prevent Blindness, International Retinal Research Foundation, Presbyterian Health Foundation, Oklahoma Center for the Advancement of Science and Technology, and Oklahoma Center for Adult Stem Cell Research and an endowment from Choctaw Nation.

## References

Aiello LP, Avery RL, Arrigg PG, Keyt BA, Jampel HD, Shah ST, Pasquale LR, Thieme H, Iwamoto MA, Park JE et al (1994) Vascular endothelial growth factor in ocular fluid of patients with diabetic retinopathy and other retinal disorders. N Engl J Med 331:1480–1487

Alon T, Hemo I, Itin A, Pe'er J, Stone J, Keshet E (1995) Vascular endothelial growth factor acts as a survival factor for newly formed retinal vessels and has implications for retinopathy of prematurity. Nat Med 1:1024–1028

Arevalo JF, Lasave AF, Wu L, Acon D, Berrocal MH, Diaz-Llopis M, Gallego-Pinazo R, Serrano MA, Alezzandrini AA, Rojas S, Maia M, Lujan S, Pan-American Collaborative Retina Study G (2016a) Intravitreal bevacizumab for choroidal neovascularization in age-related macular degeneration: 5-Year Results of The Pan-American Collaborative Retina Study Group. Retina 36:859-867.

Arevalo JF, Lasave AF, Wu L, Acon D, Farah ME, Gallego-Pinazo R, Alezzandrini AA, Fortuna V, Quiroz-Mercado H, Salcedo-Villanueva G, Maia M, Serrano M, Rojas S, Pan-American Collaborative Retina Study G (2016b) Intravitreal bevacizumab for diabetic macular oedema: 5-year results of the Pan-American Collaborative Retina Study group. Br J Ophthalmol 100:1605–1610.

Bai Y, Ma JX, Guo J, Wang J, Zhu M, Chen Y, Le YZ (2009) Muller cell-derived VEGF is a significant contributor to retinal neovascularization. J Pathol 219:446–454

Comparison of Age-related Macular Degeneration Treatments Trials Research G, Maguire MG, Martin DF, Ying GS, Jaffe GJ, Daniel E, Grunwald JE, Toth CA, Ferris FL 3rd, Fine SL (2016) Five-year outcomes with anti-vascular endothelial growth factor treatment of Neovascular age-related macular degeneration: the comparison of age-related macular degeneration treatments trials. Ophthalmology 123(8):1751–1761

Dong S, Liu Y, Zhu M, Xu X, Le Y (2014) Simplified system to investigate alteration of retinal neurons in diabetes. Adv Exp Med Biol 801:139–143

Fu S, Dong S, Zhu M, Sherry DM, Wang C, You Z, Haigh JJ, Le YZ (2015) Müller glia are a major cellular source of survival signals for retinal neurons in diabetes. Diabetes 64:3554–3563

Grunwald JE, Pistilli M, Ying GS, Maguire MG, Daniel E, Martin DF, Comparison of Age-related Macular Degeneration Treatments Trials Research G (2015) Growth of geographic atrophy in the comparison of age-related macular degeneration treatments trials. Ophthalmology 122:809–816

Herran E, Ruiz-Ortega JA, Aristieta A, Igartua M, Requejo C, Lafuente JV, Ugedo L, Pedraz JL, Hernandez RM (2013) In vivo administration of VEGF- and GDNF-releasing biodegradable polymeric microspheres in a severe lesion model of Parkinson's disease. Eur J Pharm Biopharm 85:1183–1190

Hombrebueno JR, Ali IH, Xu H, Chen M (2015) Sustained intraocular VEGF neutralization results in retinal neurodegeneration in the Ins2(Akita) diabetic mouse. Sci Rep 5:18316

Jiang Y, Wang H, Culp D, Yang Z, Fotheringham L, Flannery J, Hammond S, Kafri T, Hartnett ME (2014) Targeting Muller cell-derived VEGF164 to reduce intravitreal neovascularization in the rat model of retinopathy of prematurity. Invest Ophthalmol Vis Sci 55:824–831

Kilic U, Kilic E, Jarve A, Guo Z, Spudich A, Bieber K, Barzena U, Bassetti CL, Marti HH, Hermann DM (2006) Human vascular endothelial growth factor protects axotomized retinal ganglion cells in vivo by activating ERK-1/2 and Akt pathways. J Neurosci 26:12439–12446

Krakora D, Mulcrone P, Meyer M, Lewis C, Bernau K, Gowing G, Zimprich C, Aebischer P, Svendsen CN, Suzuki M (2013) Synergistic effects of GDNF and VEGF on lifespan and disease progression in a familial ALS rat model. Mol Ther 21:1602–1610

Kvanta A, Algvere PV, Berglin L, Seregard S (1996) Subfoveal fibrovascular membranes in age-related macular degeneration express vascular endothelial growth factor. Invest Ophthalmol Vis Sci 37:1929–1934

LaVail MM, Unoki K, Yasumura D, Matthes MT, Yancopoulos GD, Steinberg RH (1992) Multiple growth factors, cytokines, and neurotrophins rescue photoreceptors from the damaging effects of constant light. Proc Natl Acad Sci U S A 89:11249–11253

Lopez PF, Sippy BD, Lambert HM, Thach AB, Hinton DR (1996) Transdifferentiated retinal pigment epithelial cells are immunoreactive for vascular endothelial growth factor in surgically excised age-related macular degeneration-related choroidal neovascular membranes. Invest Ophthalmol Vis Sci 37:855–868

McCloskey DP, Croll SD, Scharfman HE (2005) Depression of synaptic transmission by vascular endothelial growth factor in adult rat hippocampus and evidence for increased efficacy after chronic seizures. J Neurosci 25:8889–8897

Miller JW, Adamis AP, Shima DT, D'Amore PA, Moulton RS, O'Reilly MS, Folkman J, Dvorak HF, Brown LF, Berse B et al (1994) Vascular endothelial growth factor/vascular permeability factor is temporally and spatially correlated with ocular angiogenesis in a primate model. Am J Pathol 145:574–584

Reichenbach A, Bringmann A (2013) New functions of Muller cells. Glia 61:651–678

Saint-Geniez M, Kurihara T, Sekiyama E, Maldonado AE, D'Amore PA (2009) An essential role for RPE-derived soluble VEGF in the maintenance of the choriocapillaris. Proc Natl Acad Sci U S A 106:18751–18756

Saint-Geniez M, Maharaj AS, Walshe TE, Tucker BA, Sekiyama E, Kurihara T, Darland DC, Young MJ, D'Amore PA (2008) Endogenous VEGF is required for visual function: evidence for a survival role on muller cells and photoreceptors. PLoS One 3:e3554

Sarthy VP, Brodjian SJ, Dutt K, Kennedy BN, French RP, Crabb JW (1998) Establishment and characterization of a retinal Muller cell line. Invest Ophthalmol Vis Sci 39:212–216

Ueki Y, Ash JD, Zhu M, Zheng L, Le YZ (2009) Expression of Cre recombinase in retinal Muller cells. Vis Res 49:615–621

Wang J, Xu X, Elliott MH, Zhu M, Le YZ (2010) Muller cell-derived VEGF is essential for diabetes-induced retinal inflammation and vascular leakage. Diabetes 59:2297–2305

# Chapter 59
# Müller Cell Biological Processes Associated with Leukemia Inhibitory Factor Expression


**Marcus J. Hooper and John D. Ash**

**Abstract** Müller cells provide support to photoreceptors under many conditions of stress and degeneration. Leukemia inhibitory factor is known to be expressed in Müller cells, which is necessary to promote photoreceptor survival in stress. We hypothesize that Müller cells that express LIF are undergoing other biological processes or functions which may benefit photoreceptors in disease. In this study, we analyze an existing single Müller cell microarray dataset to determine which processes are upregulated in Müller cells that express LIF, by correlating LIF expression to the expression of other genes using a robust correlation method. Some enriched processes include divalent inorganic cation homeostasis, negative regulation of stem cell proliferation, and gamma-glutamyl transferase activity.

**Keywords** Leukemia inhibitory factor · Retinal degeneration · Neuroprotection · Müller cell · Glia · Stress · Gene expression · Photoreceptor degeneration

## 59.1 Introduction

Müller cells provide support, trophic factors and contribute to the survival of retinal neurons under conditions of stress (Joly et al. 2008; Burgi et al. 2009; Rhee et al. 2013). Additionally, Müller cells are known to express leukemia inhibitory factor (LIF), a cytokine that is required for protection of retinal photoreceptors under inducible and inherited models of degeneration (Joly et al. 2008; Ueki et al. 2009). Müller cells that express LIF have been suggested to be a subset of a heterogeneous population of Müller cells, a population which may be static or dynamic. Müller

**Electronic supplementary material:** The online version of this chapter (https://doi.org/10.1007/978-3-319-75402-4_59) contains supplementary material, which is available to authorized users.

M. J. Hooper · J. D. Ash (✉)
Department of Ophthalmology, College of Medicine, University of Florida Health Science Center, Gainesville, FL, USA
e-mail: jash@ufl.edu



J. D. Ash et al. (eds.), *Retinal Degenerative Diseases*, Advances in Experimental Medicine and Biology 891, https://doi.org/10.1007/978-3-319-75402-4_59

cells that express LIF may be displaying a phenotype that is generally protective for photoreceptors. Thus, it would be of interest to determine which other biological processes LIF-expressing Müller cells are undergoing.

As Müller cells make up a small fraction of the retina, gene expression in Müller cells may be hidden by the rest of the cells in the retina (Jeon et al. 1998). Thus, it is difficult to study Müller cell gene expression using whole retina. Roesch et al. have isolated single Müller cells from mice under multiple models of retinitis pigmentosa, at multiple time points. These included rhodopsin knockout (KO) mice at 8 weeks and 25 weeks of age, rd1 mice at 13 days and 5 weeks of age, as well as control mice. These time points were chosen according to the time course of degeneration in each model (Punzo et al. 2009). These single Müller cells were used to measure Müller cell-specific gene expression using microarrays (Roesch et al. 2012). This dataset may provide the means to ask and answer some important questions about the Müller cell biology in disease.

We accessed this dataset using the gene expression omnibus (GEO, accession number: GSE35386) (Edgar et al. 2002; Roesch et al. 2012; Barrett et al. 2013). Our strategy was to find genes and processes in Müller cells that correlate strongly with expression of LIF. This dataset is rather noisy, which should be expected of a dataset derived from individual cells in a complex environment such as the retina in disease (Roesch et al. 2012). Because of this, there are influential outliers in the data, which will affect the performance of a Pearson correlation. Hardin et al. published a manuscript describing the use of Tukey's biweight function for correlating genes in microarray data (Hardin et al. 2007). This is important, because Tukey's biweight function is robust and much less susceptible to outliers than Pearson's correlation, and thus should perform better when correlating expression between two genes. We sorted genes following correlation with LIF, with the goal of identifying additional, potentially protective processes that may be enriched for in LIF-expressing Müller cells.

## 59.2 Results

Using this strategy, we correlated LIF expression to the expression of all other genes across 28 single Müller cells using the BIWT function in R (Hardin et al. 2007). Often, but not always, genes that correlated well with LIF using the Pearson correlation coefficient also correlated well with LIF using the biweight function. We wanted to avoid filtering interesting genes from our analysis. As such, the expression patterns (fold changes) of all genes were correlated with the expression of LIF, prior to any other manipulation of the data. Only those genes with >0.8 correlation with LIF and >100 average raw expression intensity in the highest-expressing group were included in our analysis.

In this dataset, there are two probe sets for detection of LIF transcripts. One (1450160) binds mostly to the latter part of the protein-coding region and partly to the proximal part of the 3'UTR. The other (1421207) binds to the distal 3'UTR of LIF and LIF has a very large 3'UTR, which suggests additional regulatory mechanisms may apply to the

**Table 59.1** *Biological processes in Müller cells that correlate with LIF expression*. Genes that had a >0.8 correlation with LIF were set as the target genes, using GOrilla. Biological processes that were enriched are shown. The FDR *p*-value is the corrected value for multiple hypothesis testing (Benjamini)

| LIF gene body, proximal 3'UTR (1,450,160_at) | | | LIF, distal 3'UTR (1,421,207_at) | | |
|---|---|---|---|---|---|
| Process or function | Enrichment | *p*-value | Process or function | Enrichment | *p*-value |
| Regulation of stem cell proliferation | *6.68* | 3.49E-2 | Gamma-glutamyl transferase activity | 13.14 | 2.89E-2 |
| Upregulation of cytosolic [$Ca^{2+}$] | *1.98* | 5.83E-2 (n.s.) | Glutathione hydrolase activity | 13.14 | 3.61E-2 |
| Divalent inorganic cation homeostasis | *1.82* | 2.57E-2 | Transmembrane receptor activity | 1.54 | 1.35E-2 |
| Cell differentiation | *1.31* | 3.47E-2 | | | |

complete transcript. We used both regions for correlation with other genes. Table 59.1 shows some of the more enriched biological processes that were co-regulated with LIF expression. We plotted the genes that made up these processes in heatmaps. Shown in Fig. 59.1a is a legend that shows raw expression intensity for each gene. Figure 59.1b shows genes that are in the categories in Table 59.1 that also correlate strongly with LIF (1,450,160, gene body). Figure 59.1c, as in Fig. 59.1b, but for LIF (1,421,207, distal 3'UTR). The expression patterns of both regions of LIF were very similar, but not identical (top row in Fig. 59.1b, c). Both regions of LIF showed upregulation primarily in Müller cells of the rhodopsin KO mice at the 8-week time point, which is consistent with our understanding of LIF's role in the retina. LIF has been reported to be induced at time points just prior to the onset and during early stages of degeneration. All genes which correlated with either probe set for LIF showed a very similar expression pattern (Fig. 59.1b, c). However, enriched processes were not the same, which may be due to the threshold for correlation that we set (Tukey's biweight correlation of >0.8), or alternatively, regulation of LIF 3'UTR length.

Cell differentiation was another category that was correlated with LIF expression, shown in Table 59.1. Supplemental Fig. 59.1 shows the large group of genes in this process that co-regulate with LIF.

## 59.3 Discussion

The large 3'UTR of LIF implies that LIF may be highly regulated. The data in Fig. 59.1 suggest that expression patterns of the distal 3'UTR of LIF and the gene body are largely similar but may be slightly different. This could be a result of RNA splicing, polyadenylation, or simply due to error in detection. We used a robust correlation strategy to find processes that are enriched in Müller cells in inherited retinal degeneration, with the goal of identifying additional big picture processes that may impact photoreceptor survival.

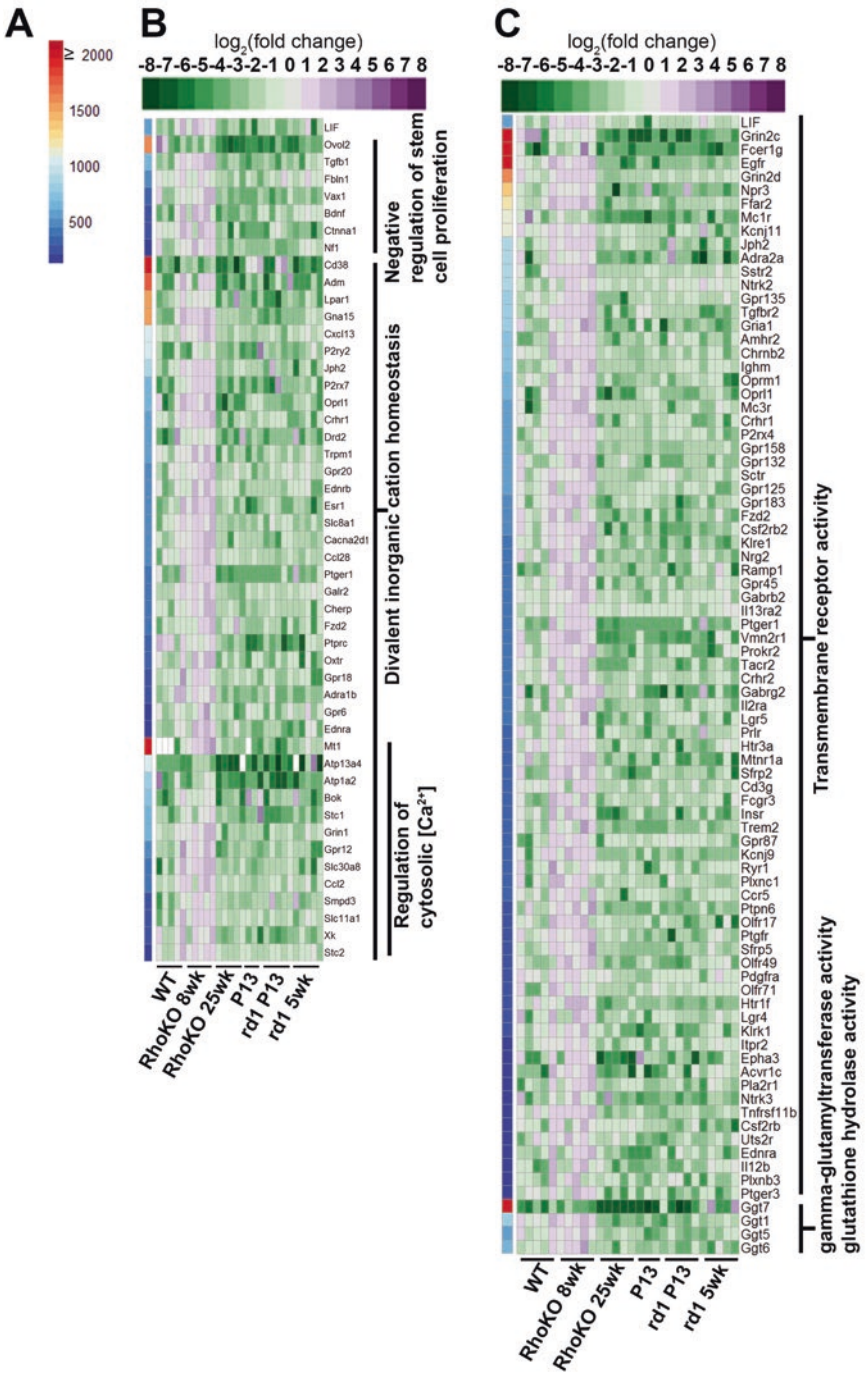


**Fig. 59.1** (**a**) Legend which maps expression intensity to each gene. To the left of each heatmap is an image showing for each gene, the average intensity of expression in the highest-expressing group. (**b**, **c**) Heatmaps showing genes that are in processes that were enriched for in Table 59.1, following correlation with LIF (**b**) is following correlation with 1,450,160, (**c**) as in **b**, but for 1,421,207

The strongest enrichment of gene function that we observed was of gamma-glutamyl transferase (GGT) activity, which was enriched for following correlation with the distal 3'UTR of LIF. All were relatively highly expressed. Muller cells are known to be important for maintaining glutathione (GSH) levels in the retina. Elevated GSH levels confer protection in oxidative stress. Gamma-glutamyl transferase (GGT) is known to be upregulated in stress and is involved in the biosynthesis of GSH. GGT is the only enzyme in production of glutathione on the outer surface of the plasma membrane. GGT functions to break down extracellular GSH, GSSG, and glutathione S-conjugates into components. These can then be taken up by adjacent cells to produce intracellular GSH (Zhang et al. 2005). It may be that as part of a protective response, Muller cells are upregulating GGT to produce the components needed for photoreceptors to synthesize GSH de novo. Interestingly, GGTs are known to be increased in oxidative stress and are targets of NRF2, a well-known factor in retinal neuroprotection.

Additionally, we observed an enrichment of transmembrane receptor activity. Within this group are many receptors and proteins involved in signaling. The highest expressing of which include ionotropic glutamate receptors, potassium voltage-gated channels, epidermal growth factor receptor (EGFR), and G protein-coupled receptors (GPCRs), including endothelin receptor A (EdnrA).

The processes associated with detection of the protein-coding region of LIF were negative regulation of stem cell proliferation, cell differentiation, and divalent inorganic cation homeostasis; a large subset of this category is involved in regulating calcium ion concentration, although not a statistically significant observation on its own. It is clear that glial cells play an important role in regulating ion homeostasis in the retina and brain, and this may be an activity that is upregulated in Müller cells that are protecting photoreceptors. Interestingly, ednrA is also part of this latter group, as is ednrB. Our work (currently unpublished) and the work of others have suggested that endothelin signaling may be part of the same pathway as LIF. This is additional validation for our current study and further may suggest calcium signaling as an important downstream pathway for endothelin receptors in the retina.

**Acknowledgments** We thank K. Roesch and the Cepko group for developing the dataset that made this study possible. This study was supported by NIH grant R01 EY016459-11, training grant EY007132, Foundation Fighting Blindness, and an unrestricted departmental grant from Research to Prevent Blindness.

## References

Barrett T, Wilhite SE, Ledoux P et al (2013) NCBI GEO: archive for functional genomics data sets–update. Nucleic Acids Res 41:D991–D995

Burgi S, Samardzija M, Grimm C (2009) Endogenous leukemia inhibitory factor protects photoreceptor cells against light-induced degeneration. Mol Vis 15:1631–1637

Edgar R, Domrachev M, Lash AE (2002) Gene expression omnibus: NCBI gene expression and hybridization array data repository. Nucleic Acids Res 30:207–210

Hardin J, Mitani A, Hicks L et al (2007) A robust measure of correlation between two genes on a microarray. BMC Bioinformatics 8:220

Jeon CJ, Strettoi E, Masland RH (1998) The major cell populations of the mouse retina. J Neurosci Off J Soc Neurosci 18:8936–8946

Joly S, Lange C, Thiersch M et al (2008) Leukemia inhibitory factor extends the lifespan of injured photoreceptors in vivo. J Neurosci Off J Soc Neurosci 28:13765–13774

Punzo C, Kornacker K, Cepko CL (2009) Stimulation of the insulin/mTOR pathway delays cone death in a mouse model of retinitis pigmentosa. Nat Neurosci 12:44–52

Rhee KD, Nusinowitz S, Chao K et al (2013) CNTF-mediated protection of photoreceptors requires initial activation of the cytokine receptor gp130 in Muller glial cells. Proc Natl Acad Sci U S A 110:E4520–E4529

Roesch K, Stadler MB, Cepko CL (2012) Gene expression changes within Muller glial cells in retinitis pigmentosa. Mol Vis 18:1197–1214

Ueki Y, Le YZ, Chollangi S et al (2009) Preconditioning-induced protection of photoreceptors requires activation of the signal-transducing receptor gp130 in photoreceptors. Proc Natl Acad Sci U S A 106:21389–21394

Zhang H, Forman HJ, Choi J (2005) Gamma-glutamyl transpeptidase in glutathione biosynthesis. Methods Enzymol 401:468–483

# Chapter 60
# Retbindin Is Capable of Protecting Photoreceptors from Flavin-Sensitized Light-Mediated Cell Death In Vitro


**Ryan A. Kelley, Muayyad R. Al-Ubaidi, and Muna I. Naash**

**Abstract** Retbindin (Rtbdn) is a novel protein of unknown function found exclusively in the retina. Recently, our group has suggested, from in silico analysis of the peptide sequence and in vitro binding data, that Rtbdn could function to bind riboflavin (RF) and its derivatives flavin adenine dinucleotide (FAD) and flavin mononucleotide (FMN), collectively known as flavins. Here we confirm that Rtbdn is capable of flavin binding and that this characteristic can protect photoreceptors from flavin-sensitized light damage.

**Keywords** Retbindin · Flavin · Flavoprotein · Retina · Photoreceptor

## 60.1 Introduction

Through in silico analysis, our group found that Rtbdn (NCBI Protein Database, accession number _659178.1) is a 744-nucleotide message translated into a 247-amino acid protein and that residues 1–31 constitute a potential secretory signal. The sequence contains no transmembrane domains, amphipathic loops, or membrane-anchoring domains. In a previous publication (Kelley et al. 2015), our group found that Rtbdn is a mammalian-specific homologue of the avian riboflavin-binding protein (RBP). Experimental analysis of the Rtbdn protein found that it was expressed as a ~27 kDa protein in the murine, bovine, and human retinas. While these immunoblots (IB) showed only one band in murine and bovine neural

R. A. Kelley
Department of Cell Biology, University of Oklahoma Health Sciences Center, Oklahoma City, OK, USA

Skaggs School of Pharmacy and Pharmaceutical Sciences, University of Colorado, Anschutz Medical Center, Aurora, CO, USA

M. R. Al-Ubaidi · M. I. Naash (✉)
Department of Biomedical Engineering, University of Houston, Houston, TX, USA
e-mail: mnaash@central.uh.edu



J. D. Ash et al. (eds.), *Retinal Degenerative Diseases*, Advances in Experimental Medicine and Biology 891, https://doi.org/10.1007/978-3-319-75402-4_60

retina samples, two bands were observed in human retinal extracts suggesting that alternative splicing, alternate promoter utilization, or different posttranslational modifications are at play. However, the band observed in murine retina was absent when P30 *Rd./Rd.* (no rod photoreceptors) (Carter-Dawson et al. 1978) neural retina samples were analyzed, suggesting that Rtbdn was a rod photoreceptor-specific protein. In contrast, IB of P21 $Rho^{-/-}$ neural retinas (without rod outer segments) (Lem et al. 1999) showed no change in protein levels compared to wild-type (WT), suggesting that photoreceptor expression of Rtbdn was not dependent on outer segment formation.

Immunohistochemistry (IHC) confirmed that Rtbdn was localized specifically to the photoreceptor cell layer. Interestingly, this specific localization was further confined to the tips of the rod outer segments and to a much lesser extent to the inner segments. IHC of P21 $Rho^{-/-}$ retinas showed Rtbdn signal above the photoreceptor cell bodies, suggesting that it is present in the inter-photoreceptor matrix (IPM). Fractionation of IPM to soluble and insoluble components showed that Rtbdn is not part of the soluble IPM, while sodium carbonate treatment revealed that it is part of the insoluble IPM as a peripheral membrane protein (Kelley et al. 2015). IHC co-localization studies with wheat germ agglutinin (rod IPM marker) and ezrin (basal RPE marker) revealed that Rtbdn is expressed specifically at the interface between the photoreceptor outer segments and the basal microvilli of the retinal pigment epithelium (Kelley et al. 2015). This places Rtbdn at the precise location where metabolite exchange occurs between the photoreceptors and RPE (Hollyfield 1999; Strauss 2005). Since in silico analysis showed that Rtbdn shares the highest degree of homology with chick oviduct RBP, we tested its capacity to bind flavins, in vitro. It was found that Rtbdn bound riboflavin as efficiently as RBP (Kelley et al. 2015). These findings support the hypothesis that Rtbdn functions as a mammalian riboflavin-binding protein in the retina and that it may potentially play a role in flavin acquisition, protection from light, and/or transport.

Flavin binding and transport are of great importance to the retina as photoreceptors are highly metabolically active (Alder et al. 1990; Braun et al. 1995) and FAD/FMN are heavily involved as redox molecules in the citric acid cycle and beta oxidation (Kim and Winge 2013). These metabolites are acquired from the choroidal blood supply by way of the RPE. Paradoxically, flavins can photosensitize cells to light via a process known as "photoreduction" by which light reduces the flavin molecules by addition of an electron from surrounding aqueous medium, generally oxygen (Treadwell et al. 1968; Song and Metzler 1967; McBride and Metzler 1967). In turn these oxygen molecules "steal" electrons from nearby membrane lipids and start a runaway process known as "lipid peroxidation," which can result in cell death (Huvaere et al. 2010). This is very pertinent to photoreceptor cells as their outer segments are particularly sensitive to this type of damage because they contain large amounts of polyunsaturated fatty acids, which are particularly susceptible to lipid peroxidation (Cardoso et al. 2013; Eckhert et al. 1993). However, protein binding to flavins protects the molecules from light and prevents "photoreduction." Given this information it is logical to hypothesize that photoreceptors

produce a flavin-binding molecule responsible for safeguarding themselves from flavin-sensitized light-mediated damage. In this short chapter, we present experimental data showing that Rtbdn is capable of protecting 661 W cells (derived from a cone cell lineage (Tan et al. 2004), from flavin-sensitized light damage, using cell death as the readout.

## 60.2 Materials and Methods

Ten million COS-7 cells were grown overnight in 150 $cm^2$ flasks in complete DMEM media supplemented with 10% fetal bovine serum. The following morning (~90% confluency), cells were transfected with 1.8 μg of either pK-Rtbdn, pK-*RBP*, or pK vector alone (mock) using Lipofectamine 2000 (Invitrogen, Carlsbad, CA, USA). Twenty-four hours later, cells were incubated with 1200 μl of 100 mM sodium carbonate for 30 minutes at room temperature to release peripheral membrane proteins from the cells (Kelley et al. 2015). The resulting solution was then collected and brought to pH 7.0 with HCl. Concomitantly, 1 million 661 W cells were grown overnight in 150 $cm^2$ flasks in complete DMEM media supplemented with 10% fetal bovine serum. The following morning, the complete media of the 661 W cells were exchanged with riboflavin-free DMEM media supplemented with 0.75 μM riboflavin. The 661 W flasks were then incubated on a light box at 12,000 lux for 1 h at room temperature. Individual 661 W flasks were supplemented with 100, 200, or 400 ml of Rtbdn solution, RBP solution, or pK alone solution. One hundred μl of 100 nM docosahexaenoic acid (DHA) was used as a positive control (protectant) and no supplementation as a negative control. Following 1 h incubation, cells were processed for viability measurements via the MTT assay as described in the manufacturer's protocol (ATCC, Manassas, Virginia, USA).

## 60.3 Retbindin Is Protective Against Light Damage

We found that 661 W cells exposed to riboflavin-supplemented media and high intensity light exhibited significant cell death: ~70% (Fig. 60.1, black bars). However, when Rtbdn or RBP (stripped from transfected COS-7 cells with sodium carbonate) was added to this media, an ~3 fold increase was observed in the number of viable 661 W cells (Fig.60.1, blue and red bars, respectively). This level of protection was comparable to 100 nM added DHA (Fig.60.1, green bar), which has been previously shown to protect cells from light damage (Kanan et al. 2007). To corroborate this observation, we increased the concentration of Rtbdn and RBP protein in the media and found an increase in the number of surviving cells; however, this increase was not significant compared to the original concentration. This data confirms that Rtbdn is capable of binding riboflavin and in doing so is capable of protecting 661 W cells from riboflavin-sensitized light damage.

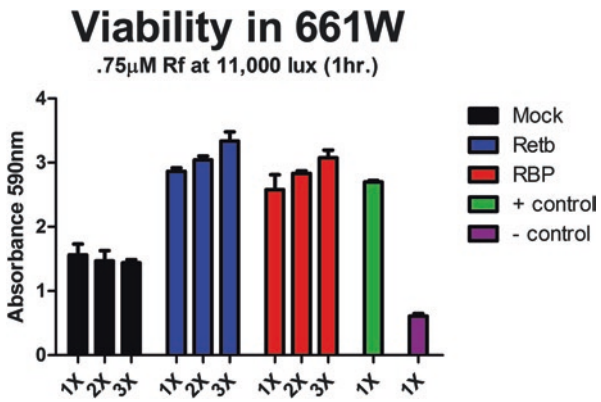


**Fig. 60.1** Retb protects 661 W cells from riboflavin photosensitization. Absorbance of cell lysates isolated from 661 W cells exposed to 0.75 μM riboflavin and 12,000 lux white light for 1 h. Experimental groups were treated with peripheral membrane proteins extracted from mock, Retb, and RBP transfected COS cells. DHA was used as a positive control and no added protein was used as a negative control. The higher viability in Retb- and RBP-treated cells shows that riboflavin is protected from photoreduction by protein binding

## 60.4 Discussion

As shown in Fig. 60.1, Rtbdn and RBP are capable of protecting 661 W cells from riboflavin-sensitized light-mediated cell death. This is of great importance as it further suggests that Rtbdn is a mammalian equivalent of RBP in the retina. Furthermore, this data suggests that Rtbdn is capable of protecting RF from light reduction, thereby guarding retinal cells from light-mediated cell damage. This data taken together with Rtbdn localization in the retina potentially carves out a role for Rtbdn in protecting photoreceptors from this type of determinantal insult. However, this claim still requires in vivo confirmation. It is also equally important to determine whether Rtbdn is simply a flavin-binding protein produced to protect flavins from photoreduction or if it is also involved in the transport of flavins to the photoreceptor cells. This is logical due to Rtbdn localization at the outer segment tips (likely where flavin acquisition occurs) and to a lesser extent at the inner segments (where flavins are metabolically needed in the mitochondria). Concentration of flavins is significantly high in the retina compared to other tissues (Batey and Eckhert 1990; Batey and Eckhert 1991; Batey et al. 1992); thus it is possible that Rtbdn serves as a sink blocking excess flavin from flooding the light-sensitive outer segments. As needed, Rtbdn could respond to flavin/energy levels (or another signal) and transport flavins to the inner segments. Experiments analyzing Rtbdn levels and localization in response to dietary riboflavin deficiency should help to clarify if Rtbdn is involved in transport or not.

Given its peripheral attachments to membranes (Kelley et al. 2015), Rtbdn may actually transport flavins into the cell. It is also likely that Rtbdn works with a yet unidentified membrane transporter to get the flavins into the cells. Identifying

potential Rtbdn interacting partners should aid in determining exactly how Rtbdn functions in flavin binding/transport. Given the rod photoreceptor specificity of Rtbdn, it is evident that the protein is important for photoreceptor health. However, it is evident from the gaps in literature that flavin involvement in photoreceptor homeostasis is grossly overlooked. Rtbdn localization and its capability for flavin binding make the protein a great target to investigate its role and that of flavins in photoreceptor health. Given the roles of flavins in cellular activities, it is not a stretch to hypothesize that modulation of flavins could play a major role in photoreceptor cell death, through lipid peroxidation and energy production in the cell.

**Acknowledgments** This work was supported by the NIH (EY010609-MIN, EY18656, and EY022778) and the Foundation Fighting Blindness (MIN, MRA).

## References

Alder VA, Ben-Nun J, Cringle SJ (1990) PO2 profiles and oxygen consumption in cat retina with an occluded retinal circulation. Invest Ophthalmol Vis Sci 31:1029–1034

Batey DW, Eckhert CD (1990) Identification of FAD, FMN, and riboflavin in the retina by microextraction and high-performance liquid chromatography. Anal Biochem 188:164–167

Batey DW, Eckhert CD (1991) Analysis of flavins in ocular tissues of the rabbit. Invest Ophthalmol Vis Sci 32:1981–1985

Batey DW, Daneshgar KK, Eckhert CD (1992) Flavin levels in the rat retina. Exp Eye Res 54:605–609

Braun RD, Linsenmeier RA, Goldstick TK (1995) Oxygen consumption in the inner and outer retina of the cat. Invest Ophthalmol Vis Sci 36:542–554

Cardoso DR, Scurachio RS, Santos WG, Homem-de-Mello P, Skibsted LH (2013) Riboflavin-photosensitized oxidation is enhanced by conjugation in unsaturated lipids. J Agric Food Chem 61:2268–2275

Carter-Dawson LD, LaVail MM, Sidman RL (1978) Differential effect of the rd mutation on rods and cones in the mouse retina. Invest Ophthalmol Vis Sci 17:489–498

Eckhert CD, Hsu MH, Pang N (1993) Photoreceptor damage following exposure to excess riboflavin. Experientia 49:1084–1087

Hollyfield JG (1999) Hyaluronan and the functional organization of the interphotoreceptor matrix. Invest Ophthalmol Vis Sci 40:2767–2769

Huvaere K, Cardoso DR, Homem-de-Mello P, Westermann S, Skibsted LH (2010) Light-induced oxidation of unsaturated lipids as sensitized by flavins. J Phys Chem B 114:5583–5593

Kanan Y, Moiseyev G, Agarwal N, Ma JX, Al-Ubaidi MR (2007) Light induces programmed cell death by activating multiple independent proteases in a cone photoreceptor cell line. Invest Ophthalmol Vis Sci 48:40–51

Kelley RA, Al-Ubaidi MR, Naash MI (2015) Retbindin is an extracellular riboflavin-binding protein found at the photoreceptor/retinal pigment epithelium interface. J Biol Chem 290:5041–5052

Kim HJ, Winge DR (2013) Emerging concepts in the flavinylation of succinate dehydrogenase. Biochim Biophys Acta 1827:627–636

Lem J, Krasnoperova NV, Calvert PD, Kosaras B, Cameron DA, Nicolò M, Makino CL, Sidman RL (1999) Morphological, physiological, and biochemical changes in rhodopsin knockout mice. Proc Natl Acad Sci U S A 96:736–741

McBride MM, Metzler DE (1967) Photochemical degradation of flavins. 3. Hydroxyethyl and formylmethyl analogs of riboflavin. Photochem Photobiol 6:113–123

Song PS, Metzler DE (1967) Photochemical degradation of flavins. IV. Studies of the anaerobic photolysis of riboflavin. Photochem Photobiol 6:691–709

Strauss O (2005) The retinal pigment epithelium in visual function. Physiol Rev 85:845–881

Tan E, Ding XQ, Saadi A, Agarwal N, Naash MI, Al-Ubaidi MR (2004) Expression of cone-photoreceptor-specific antigens in a cell line derived from retinal tumors in transgenic mice. Invest Ophthalmol Vis Sci 45:764–768

Treadwell GE, Cairns WL, Metzler DE (1968) Photochemical degradation of flavins. V. Chromatographic studies of the products of photolysis of riboflavin. J Chromatogr 35:376–388

# Chapter 61
# Constitutive Activation Mutant mTOR Promote Cone Survival in Retinitis Pigmentosa Mice

**Ammaji Rajala, Yuhong Wang, and Raju V. S. Rajala**

**Abstract** Studies form our laboratory and others show that the oncogenic tyrosine kinase and serine threonine kinase signaling pathways are essential for cone photoreceptor survival. These pathways are downregulated in mouse models of retinal degenerative diseases. In the present study, we found that activation mutants of mTOR delayed the death of cones in a mouse model of retinal degeneration. These studies suggest that oncogenic protein kinases may be useful as therapeutic agents to treat retinal degenerations that affect cones.

**Keywords** Oncogene · Cone photoreceptors · Survival · Retinal degeneration · mTOR · Insulin receptor · Retinitis pigmentosa · Protein kinases

A. Rajala · Y. Wang
Department of Ophthalmology, University of Oklahoma Health Sciences Center, Oklahoma City, OK, USA

Dean McGee Eye Institute, Oklahoma City, OK, USA

R. V. S. Rajala (✉)
Department of Ophthalmology, University of Oklahoma Health Sciences Center, Oklahoma City, OK, USA

Department of Physiology, University of Oklahoma Health Sciences Center, Oklahoma City, OK, USA

Department of Cell Biology, University of Oklahoma Health Sciences Center, Oklahoma City, OK, USA

Dean McGee Eye Institute, Oklahoma City, OK, USA
e-mail: raju-rajala@ouhsc.edu



J. D. Ash et al. (eds.), *Retinal Degenerative Diseases*, Advances in Experimental Medicine and Biology 891, https://doi.org/10.1007/978-3-319-75402-4_61

## 61.1 Introduction

Studies from our laboratory clearly suggest that insulin receptor (IR) is functionally important for cone photoreceptor survival. Deletion of IR from cones resulted in age-related cone degeneration. We found a ligand-independent IR activation in both rod and cone photoreceptor cells (Rajala et al. 2016, 2002). This activation occurs through inhibition of a protein tyrosine phosphatase by phosphorylated Grb14. Cone opsin bleaching promotes phosphorylation of a non-receptor tyrosine kinase, Src, which in turn phosphorylates Grb14 (Rajala et al. 2007, 2016). Thus, activated IR further activates the downstream signaling cascade, which includes mammalian target of rapamycin (mTOR) signaling. Our studies also suggest that mice deficient in photobleaching of opsins and with mutations in the rhodopsin gene fail to promote Src activation and subsequent Grb14 phosphorylation (Rajala et al. 2007, 2016). This failure results in increased PTP1B activity and thus dephosphorylates IR and inactivates its signaling. It has also been shown that stimulation of insulin/mTOR pathway promotes cone survival in animal models of *retinitis pigmentosa* (RP; (Punzo et al. 2009). Insulin receptor, Src, and mTOR are protein tyrosine or serine/threonine kinases; their overexpression in cancer cells indicates a poor prognosis. Interestingly, these oncogenic proteins promote cone survival. Photoreceptors are highly metabolic, and their energy demands are equivalent to those of cancer cells (Rajala and Gardner 2016; Warburg 1956).

mTOR is the downstream effector of IR/PI3K/Akt signaling (Schmelzle and Hall 2000), which was shown to be reduced in cones of *rd1* mice after the rods had died but could be rescued by insulin injections (Punzo et al. 2009). mTOR integrates the input, including insulin, growth factors, and amino acids, from upstream pathways and senses cellular nutrient, oxygen, and energy levels (Kim et al. 2013; Reiling and Sabatini 2006; Sabatini 2006; Sarbassov et al. 2005). mTOR exists in two distinct protein complexes: (1) mTORC1, which is rapamycin-sensitive and consists of mTOR, Raptor, and mLST8 (Sato et al. 2010; Urano et al. 2007), and (2) mTORC2, which is rapamycin-insensitive and consists of mTOR, Rictor, mLST8, and mSin (Urano et al. 2007). Complex 1 phosphorylates S6K and 4E–BP1 and thereby regulates protein synthesis (Urano et al. 2007). Complex 2 phosphorylates Akt and regulates the actin cytoskeleton (Sabatini 2006).

Cepko's lab proposed that cone cell death in RP mouse models is due to starvation that occurs through a downregulation of the insulin/mTOR signaling pathway in cones (Punzo et al. 2009). If so, nutrition-independent constitutive activation mutants of mTOR should rescue cone cell death due to starvation in *rd1* mice (Punzo et al. 2009). Two different point mutations in mTOR, S2215Y and R2505P, each of which confers constitutive activation of mTOR signaling even under nutrient starvation conditions, have been identified in the human cancer genome database (Sato et al. 2010). In the mammalian system, two additional point mutations in mTOR, L1460P and E2419K, have also been identified and are constitutively activated in nutrient-starved cells (Urano et al. 2007). These point mutants have been shown to form functional complexes with mTORC1 and mTORC2 in the activation

(phosphorylation) of their respective substrates, Akt, S6K, and 4E–BP1 (Sato et al. 2010). In the present study, we examined whether the mutant mTOR-E2419K is able to rescue the cone degeneration in *rd1* mice.

## 61.2 Materials and Methods

### *61.2.1 Plasmids and Vectors*

The pcDNA3-Au1-mTOR-wild-type (Addgene plasmid # 26036) and pcDNA3-AU1-mTOR-E2419K (Addgene plasmid # 19994) were gifts from Dr. Fuyuhiko Tamanoi (Urano et al. 2007). A breeding colony of Balb/C, *rd1*, *Nrl*$^{-/-}$, and LacZ mice under the control of human red/green cone opsin promoter (provided by Dr. Jeremy Nathans, Johns Hopkins School of Medicine) was maintained in our vivarium on cyclic light (5 lux; 12 h on/12 h off). Experiments were carried out with postnatal day 5 (P5) male and female pups.

### *61.2.2 Subretinal Injection*

The subretinal injections were performed via the transscleral route. Mice were anesthetized by intramuscular injection of a ketamine (80–100 mg/kg) and xylazine (5 mg/kg) mixture of approximately 0.1 ml, until mice did not display a blink reflex to a touch on the corneal surface. Eyes were dilated with 1% cyclopentolate hydrochloride ophthalmic solution applied to the cornea (Akron, Lake Forest, IL). The mice were kept on a 37 °C regulated heating pad under a surgical microscope (Carl Zeiss Surgical, NY). An insulin syringe with a beveled 30-gauge needle was used to puncture a hole in the cornea. Next, a 33-gauge blunt-end needle attached to a 10-μl Nanofil® syringe controlled by a UMP3 pump controller (World Precision Instruments, Sarasota, FL) was positioned toward the superior nasal portion of the retina. Then, 1 μl of LPD nanoparticles (~85 ng of DNA) were injected into the subretinal space. The needle was retracted 10–15 s after injection, when a bleb of retinal detachment was visible. Following complete removal of the injection needle, the eye was carefully observed for any indication of postsurgical complications, such as iris and subretinal bleeding, pronounced retinal detachment or damage, or excessive vitreous loss. Saline and GenTeal lubricant eye gel (Alcon, Fort Worth, TX) were applied topically to the eye 3–4 times daily for 3–4 days after injection, to keep the eye continually moist. The severity of acute postsurgical complications and subsequent long-term complications, including eye infection, loss of visual function, and atrophy, were carefully evaluated. In the absence of any severe complications, the procedure was deemed successful, and the animal remained in the study.

### 61.2.3 X-Gal Staining

Two months later, flat mounts were prepared and stained with X-gal to examine cone cell density, according to the method described earlier (Punzo and Cepko 2007). Retinal whole-mounts were imaged using a Nikon Eclipse E800 (Tokyo, Japan) microscope.

## 61.3 Results

### 61.3.1 Expression of mTOR Signaling Proteins in Wild-Type and Cone-Dominant Nrl Knockout Mouse Retinas

We examined the expression of mTOR signaling proteins on immunoblots in both wild-type Balb/c and cone-dominant Nrl knockout mouse retinas (Mears et al. 2001). Our results revealed the expression of mTOR, p70S6K, and 4E-BP. It is interesting to note that the levels of these proteins are much higher in cone-dominant retina than in rod-dominant retina (Fig. 61.1). We also found that these proteins undergo phosphorylation on specific residues. The rod and cone cell-specific markers show that rhodopsin is absent from Nrl knockout mice, whereas M-opsin was higher in Nrl knockout mice than in wild-type mice (Fig. 61.1).

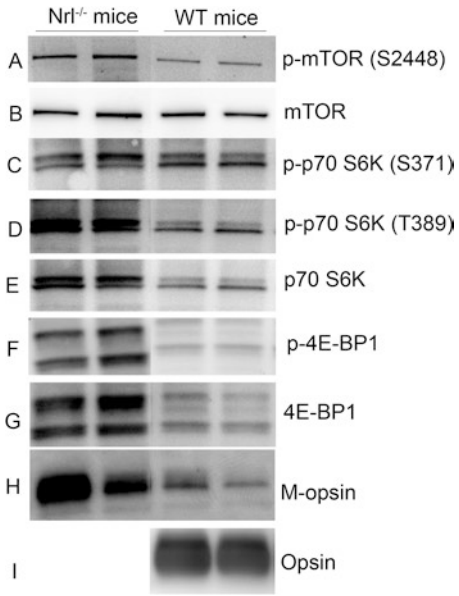


**Fig. 61.1** *Expression of mTOR signaling proteins in wild-type and cone-dominant Nrl knockout mice*. Retinal proteins from rod-dominant wild-type and cone-dominant Nrl knockout mouse retinas (in duplicate) were subjected to immunoblot analysis with mTOR (**b**), phospho-mTOR (S2448) (**a**), phospho-70S6K (S371) (**c**), phospho-70S6K (T389) (**d**), p70S6K (**e**), phospho-4E-BP (**f**), 4E-BP1 (**g**), M-opsin (**h**), and opsin (**i**) antibodies

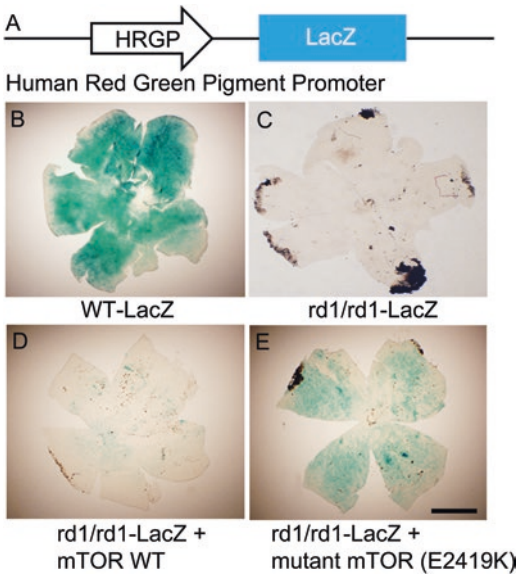


**Fig. 61.2** *Effect of mutant mTOR on cone cell death in an RP mouse model***.** Schematic diagram of HRGP (COP)-LacZ mice (**a**). Wild-type mTOR (**d**) and mutant mTOR E2419K (**e**) were subretinally injected into P5 *rd1/rd1*-LacZ mice under the control of CMV promoter. Two months later, flat mounts were prepared and stained with X-gal to examine cone cell density (**b–e**). Controls for this experiment include wild-type-LacZ mice (**b**) and untreated rd1/rd1-LacZ mice (**c**). Scale bar, 1 mm

### *61.3.2 Mutant mTOR Promotes Cone Survival in rd1 Mice*

We have a mouse model that expresses β-galactosidase (LacZ) under the control of human red and green cone pigment promoter (Fig. 61.2a; Wang et al. 1992) and has expressed an *rd1* mutation in LacZ mice (Fig. 61.2c). We used lipid nanoparticles to deliver wild-type and mutant mTOR to P5 *rd1/rd1*-LacZ mice and examined cone density after 2 months. Flat mounts stained with X-gal (*LacZ* converts colorless X-gal substrate to a blue dye) showed that cone density is well preserved in wild-type LacZ mice (Fig. 61.2b), but not in *rd1/rd1*-LacZ mice (Fig. 61.2c). Cone cell loss could be delayed by subretinal injection of mutant mTOR-E2419K (Fig. 61.2e), but not wild-type mTOR (Fig. 61.2d).

## 61.4 Discussion

The insulin/mTOR pathway is active and promotes cone survival. In degenerative mouse models, this pathway is downregulated. It has been recently reported that conditional ablation of negative regulators of mTOR pathway promotes cone survival in mouse models of retinal degeneration (Venkatesh et al. 2015). Very recently, we reported that activation of Src, which signals in the activation of insulin receptor, promotes cone survival in a mouse model of cone degeneration (Rajala et al. 2016). In the present study, we found that activated mutant of mTOR promotes cone survival in rd1 mice. We used pcDNA3 vector carrying wild-type mTOR and mutant mTOR under the control of cytomegalovirus promoter (CMV), a strong promoter

used to obtain expression of exogenous genes in mammalian and other higher eukaryotic cells. Our results with mutant mTOR construct showed that cone cell density was much weaker in *rd1/rd1* mice than in wild-type mice (Fig. 61.2e vs 61.2b). This finding could be due to the nature of the general promoter without cell specificity. As a proof of principle, we could delay the death of cones with activated mutants of mTOR. In the future, we will target the expression specifically to cone photoreceptor cells and will also study cone function. These findings set the stage for future studies examining the idea that oncogenic proteins may be useful as therapeutic agents to treat retinal degenerations that affect cones.

**Acknowledgments** This study was supported by grants from the National Institutes of Health (EY00871 and NEI Core grant EY021725) and an unrestricted grant from Research to Prevent Blindness, Inc., to the Department of Ophthalmology. The authors thank Dr. Claudio Punzo for providing us with the LacZ mice under the control of human red/green cone opsin promoter, which were generated in Dr. Jeremy Nathan's laboratory at Johns Hopkins School of Medicine. The authors acknowledge Ms. Kathy J. Kyler, Staff Editor, University of Oklahoma Health Sciences Center, for editing this manuscript.

## References

Kim SG, Buel GR, Blenis J (2013) Nutrient regulation of the mTOR complex 1 signaling pathway. Mol Cells 73:4429–4438

Mears AJ, Kondo M, Swain PK et al (2001) Nrl is required for rod photoreceptor development. Nat Genet 29:447–452

Punzo C, Cepko C (2007) Cellular responses to photoreceptor death in the rd1 mouse model of retinal degeneration. Invest Ophthalmol Vis Sci 48:849–857

Punzo C, Kornacker K, Cepko CL (2009) Stimulation of the insulin/mTOR pathway delays cone death in a mouse model of retinitis pigmentosa. Nat Neurosci 12:44–52

Rajala RV, Gardner TW (2016) Burning fat fuels photoreceptors. Nat Med 22:342–343

Rajala RV, McClellan ME, Ash JD et al (2002) In vivo regulation of phosphoinositide 3-kinase in retina through light-induced tyrosine phosphorylation of the insulin receptor beta-subunit. J Biol Chem 277:43319–43326

Rajala A, Anderson RE, Ma JX et al (2007) G-protein-coupled receptor rhodopsin regulates the phosphorylation of retinal insulin receptor. J Biol Chem 282:9865–9873

Rajala A, Wang Y, Rajala RV (2016) Activation of oncogenic tyrosine kinase signaling promotes insulin receptor-mediated cone photoreceptor survival. Oncotarget 7:46924–46942

Reiling JH, Sabatini DM (2006) Stress and mTORture signaling. Oncogene 25:6373–6383

Sabatini DM (2006) mTOR and cancer: insights into a complex relationship. Nat Rev Cancer 6:729–734

Sarbassov DD, Ali SM, Sabatini DM (2005) Growing roles for the mTOR pathway. Curr Opin Cell Biol 17:596–603

Sato T, Nakashima A, Guo L et al (2010) Single amino-acid changes that confer constitutive activation of mTOR are discovered in human cancer. Oncogene 29:2746–2752

Schmelzle T, Hall MN (2000) TOR, a central controller of cell growth. Cell 103:253–262

Urano J, Sato T, Matsuo T et al (2007) Point mutations in TOR confer Rheb-independent growth in fission yeast and nutrient-independent mammalian TOR signaling in mammalian cells. Proc Natl Acad Sci U S A 104:3514–3519

Venkatesh A, Ma S, Le YZ et al (2015) Activated mTORC1 promotes long-term cone survival in retinitis pigmentosa mice. J Clin Invest 125:1446–1458
Wang Y, Macke JP, Merbs SL et al (1992) A locus control region adjacent to the human red and green visual pigment genes. Neuron 9:429–440
Warburg O (1956) On the origin of cancer cells. Science 123:309–314

# Chapter 62
# Maintaining Cone Function in Rod-Cone Dystrophies


**José-Alain Sahel and Thierry Léveillard**

**Abstract** Retinal degenerative diseases are a major cause of untreatable blindness due to a loss of photoreceptors. Recent advances in genetics and gene therapy for inherited retinal dystrophies (IRDs) showed that therapeutic gene transfer holds a great promise for vision restoration in people with currently incurable blinding diseases. Due to the huge genetic heterogeneity of IRDs that represents a major obstacle for gene therapy development, alternative therapeutic approaches are needed. This review focuses on the rescue of cone function as a therapeutic option for maintaining central vision in rod-cone dystrophies. It highlights recent developments in better understanding the mechanisms of action of the trophic factor RdCVF and its potential as a sight-saving therapeutic strategy.

**Keywords** Retinal degeneration · Photoreceptors · Rod-derived cone viability factor · Aerobic glycolysis · Neuroprotective gene therapy · Nucleoredoxin-like-1

## 62.1 Introduction

Retinal degenerative diseases are a major cause of untreatable blindness due to a loss of photoreceptors and their function. For inherited retinal dystrophies (IRDs) caused by specific gene defects, replacing the defective gene with its functional copy represents a promising therapeutic avenue. Recent achievements in gene

J. -A. Sahel (✉)
Sorbonne Universités, UPMC Univ Paris 06, INSERM U968, CNRS UMR 7210, Institut de la Vision, Paris, France

CHNO des Quinze-Vingts, DHU Sight Restore, INSERM-DGOS CIC 1423, Paris, France

Department of Ophthalmology, The University of Pittsburgh School of Medicine, Pittsburgh, PA, USA

T. Léveillard
Sorbonne Universités, UPMC Univ Paris 06, INSERM U968, CNRS UMR 7210, Institut de la Vision, Paris, France



J. D. Ash et al. (eds.), *Retinal Degenerative Diseases*, Advances in Experimental Medicine and Biology 891, https://doi.org/10.1007/978-3-319-75402-4_62

therapy for monogenic recessive diseases strongly support the validity of this approach. Today, the *RPE65* gene replacement is the most notable example of successful gene therapy for retinal degenerative disorders (Acland et al. 2005; Maguire et al. 2008; Hauswirth et al. 2008; Bainbridge et al. 2008; Bennett et al. 2012), and clinical trials of gene therapy for Leber congenital amaurosis (LCA) are currently ongoing in Philadelphia, Iowa, London, Nantes, and Jerusalem. Based on encouraging preclinical results, clinical safety and efficacy proof-of-concept studies were undertaken to treat choroideremia, retinoschisis, Stargardt disease, Usher syndrome, achromatopsia, and Leber hereditary optic neuropathy (LHON). The large number of genes involved in the pathogenesis of IRDs and the dominant toxic gain-of-function mutations, however, are major challenges for gene therapy development, in addition to cost and efficiency concerns. Alternative approaches are therefore needed to treat the currently incurable IRD.

## 62.2 Saving Cone Photoreceptors

*Paul Sieving "50% cone loss compatible with acuity of 20/20… 95% cone loss compatible with a correct orientation and discrimination performance"* Geller and Sieving (1993)

*Alan F. Wright "Keep the cones alive and some 1,5 million people worldwide will see…"* Wright (1997)

### *62.2.1 Cones Need the Rods to Survive*

In retinitis pigmentosa (RP), one of the most common IRDs, mutations selectively affect rod photoreceptors. Intriguingly, secondarily to the death of rods, cones slowly (years to decades) degenerate leading to central vision loss and potentially complete blindness. In all conditions where the rods are destroyed, the cones degenerate secondarily (McCall et al. 1996), and this was established not only in rod-dominated mammalian retina but also in the retina with an equal proportion of rods and cones (Choi et al. 2011). This cascade of retinal degenerative events points on the crucial importance of saving cones for saving human vision and opens horizons for cone-directed therapeutic strategies.

### *62.2.2 Rod-Derived Cone Viability Factor (RdCVF) Rescues Cone Photoreceptors*

Our group (with Saddek Mohand-Said and Thierry Léveillard) was first to hypothesize that rods produce a factor that helps the cone cells to survive, and that this factor may preserve vision in human RP. In experimental models of RP, we provided strong evidence for cone protection by selective transplantation of rods

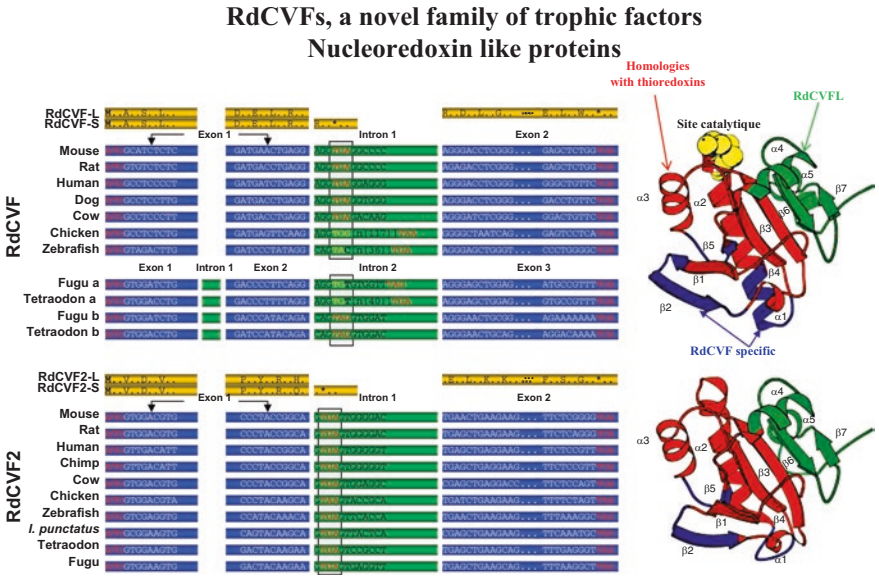


**Fig. 62.1** RdCVFs: a novel family of trophic factors (Modified from Chalmel et al. 2007)

(Mohand-Said et al. 2000) and also showed that cone viability depends on the presence of viable rod photoreceptors (Mohand-Said et al. 1998, 2001). Using cone-enriched primary cultures from chicken embryos and screening an expression library from mouse neural retinas corresponding to 210,000 individual clones, we identified a protein that increased the number of cone cells in culture and rescued cones in the *rd1* mouse retina both in vitro and in vivo (Léveillard et al. 2004). We named this trophic factor rod-derived cone viability factor (RdCVF) (Léveillard et al. 2004) and identified it as a truncated thioredoxin-like protein encoded by the *Nxnl1* gene specifically expressed by photoreceptors (Fig. 62.1) (Léveillard et al. 2004; Reichman et al. 2010). This discovery provided a biochemical basis for paracrine interaction between rods and cones suggested by our previous works (Mohand-Said et al. 1998). We focused on the mechanisms of action of RdCVF and showed that the protective effect of RdCVF on cones is independent of the causative gene, as demonstrated in *rd1* mouse (a model of autosomal recessive RP) (Leveillard et al. 2004) and P23H rat (a model of autosomal dominant RP). We further showed that injection of RdCVF in animal models of RP prevents the shortening of cone outer segments which precedes the cone loss (Yang et al. 2009). Functional studies revealed the exciting property of RdCVF not only to maintain the morphology and viability of cones but also to prevent the loss of function of cone photoreceptors in RP models, inducing orders of magnitude higher electroretinography (ERG) responses (Yang et al. 2009).

The *Nxnl1* gene also encodes by alternative splicing a long form of RdCVF, RdCVFL (Fig. 62.1), a protein with thioredoxin enzymatic activity that interacts with TAU (Wang et al. 2007; Fridlich et al. 2009). The known role of thioredoxins

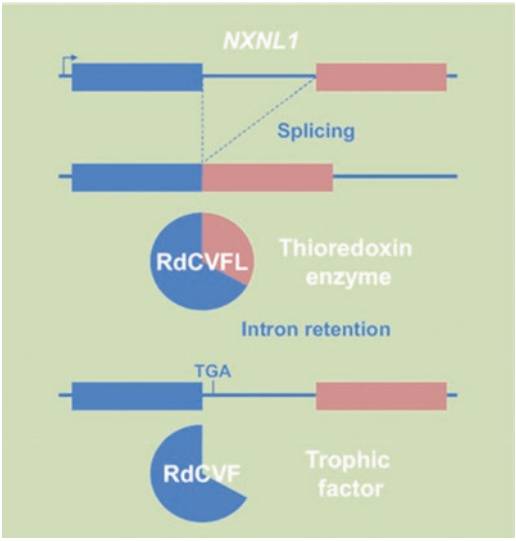


**Fig. 62.2** Genomic organization of the bifunctional gene *NXNL1* (From Léveillard and Sahel 2016)

in the defense mechanism against oxidative damage led us to examine the retinal phenotype of the *Nxnl1*$^{-/-}$ mice exposed to photooxidative stress. We have shown that in the *Nxnl1*$^{-/-}$ mice, both cones and rods degenerate with age and that rods are more susceptible to photooxidative damage due to the absence of RdCVFL (Cronin et al. 2010; Elachouri et al. 2015). Our next research revealed that cones express only one of the two *Nxnl1* gene products, the thioredoxin RdCVFL (Mei et al. 2016), while rods produce the thioredoxin RdCVFL and the trophic factor RdCVF by alternative splicing (Fig. 62.2). Silencing the expression of RdCVFL in cone-enriched culture reduces cell viability, suggesting that RdCVFL is a cell-autonomous mechanism of protection (Mei et al. 2016). Using AAV2/8 vectors that target photoreceptors cells, we demonstrated that RdCVFL is able to protect rod photoreceptors of the *Nxnl1*$^{-/-}$ mouse against light damage (Elachouri et al. 2015). RdCVFL also reduces the oxidation of polyunsaturated fatty acids induced by photoreceptor degeneration in the *rd10* mouse (Byrne et al. 2015). Our results show that the *Nxnl1* gene, through the thioredoxin RdCVFL, is part of an endogenous defense mechanism against photooxidative stress that is likely of great importance for human vision (Elachouri et al. 2015). We have thus elucidated that the thioredoxin RdCVFL is normally expressed by both cones and rods in mouse retina, while the trophic factor RdCVF is specifically expressed by rods (Mei et al. 2016). Our findings highlight not only the duality of the *Nxnl1* gene, but also its biological role to protect cone photoreceptors by two distinct mechanisms.

Our genomic investigations further uncovered a second trophic factor belonging to the RdCVF family, RdCVF2 (encoded by the *Nxnl2* gene) (Chalmel et al. 2007). Similarly to RdCVF, the RdCVF2 short isoform exhibits cone rescue activity that is independent of its putative thiol-oxidoreductase activity. Interestingly, the RdCVF2L protein is able to reduce TAU phosphorylation, as does RdCVFL, but is significantly

less effective than RdCVFL in protecting rods from light damage (Elachouri et al. 2015). This finding suggests that preventing TAU phosphorylation is not sufficient to prevent rod loss and that other yet unidentified target(s) of the thioredoxin RdCVFL remain to be discovered.

Our recent investigations provided evidence that RdCVFL is involved in the defense mechanism against light-induced oxidative injury on rod and cone photoreceptors, while RdCVF protects cones. The relative absence of protection from light damage by RdCVF2L provides important insight into the absence of redundancy between the two genes.

### *62.2.3 RdCVF Promotes Cone Survival by Stimulating Aerobic Glycolysis*

In mouse models of rod-cone degeneration, it was proposed that glucose uptake by cones and/or glucose intracellular concentration in cones may be compromised (Punzo et al. 2009). Over the years, we accumulated a large body of evidence about the cone-saving properties of RdCVF. How these effects occurred, however, was not completely understood until very recently, when we discovered that the mechanism by which RdCVF promotes cone survival is facilitating the flow of glucose into the cell (Ait-Ali et al. 2015). Specifically, we showed that RdCVF binds to Basigin-1 (BSG1), which in turn binds to the glucose transporter GLUT1 creating the complex RdCVF/BSG1/GLUT1 that is formed at the cone surface. This key complex improves (enhances, facilitates) the glucose entry into the cone photoreceptors (Fig. 62.3). Glucose is metabolized by cones via aerobic glycolysis to produce metabolites necessary for the daily renewal of 10% of the cone outer segments. The importance of glucose and nutrients in the survival of photoreceptors is due to the fact that they are among the highest metabolically active and energetically demanding cells in the body. Cone survival relies on the ability of RdCVF to stimulate aerobic glycolysis (Ait-Ali et al. 2015; Cepko and Punzo 2015).

## 62.3 Translating Cone Rescue to the Clinic

Cones underlie all visual functions in lighted environment: this is why cone rescue is a clinically relevant target (Léveillard and Sahel 2010). Preventing the secondary loss of cones by administration of RdCVF is medically rational, since most of the patients with retinal degenerative disease that consult an ophthalmologist have already lost most of the rods, while visual acuity is only reduced when 50% of the cones become nonfunctional (Geller and Sieving 1993). Accordingly, supporting the survival of cones by RdCVF clearly becomes an important goal of translational retinal research.

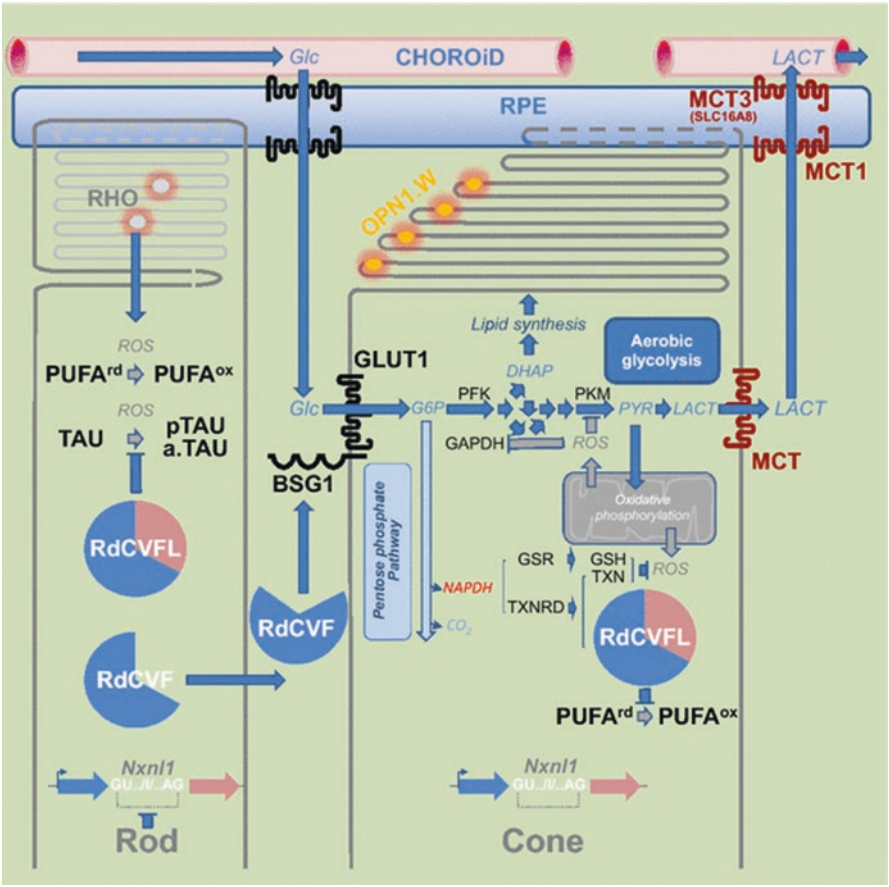


**Fig. 62.3** Metabolic and redox signaling of the *NXNL1* gene products (From Léveillard and Sahel 2016)

### *62.3.1 RdCVF Delivery Using an Adeno-Associated Viral Vector: Phase IB-IIA in Preparation*

As previously emphasized, the alternative splicing of *Nxnl1* results in two protein isoforms: the truncated form RdCVF which is secreted by rods and promotes cone survival and the full-length isoform RdCVFL which is involved in oxidative signaling and protection against hyperoxia. Our recent investigations explored the effects of these different isoforms in murine models of rod-cone dystrophy and demonstrated that the increased expression of RdCVF via systemic and intravitreal injections led to structural and functional rescue of cone photoreceptors in both *rd10* and P23H models, but had little effect on rods (Byrne et al. 2015). RdCVFL on its

own did not significantly rescue cones, although coexpression of RdCVF and RdCVFL increased the observed rescue effect in *rd10* mice. In contrast, the expression of RdCVFL early in the course of the disease prolonged rod function, increased levels of rhodopsin, and decreased the by-products of cellular oxidative stress. These results provide key evidence that RdCVF and RdCVFL protect photoreceptors through separate but complementary mechanisms and show proof of concept for a widely applicable viral vector-mediated gene therapy that may prolong vision in patients suffering from rod-cone dystrophies in a mutation-independent way. A therapy aimed at preventing secondary cone degeneration should thus be pursued using both RdCVF and RdCVFL (Léveillard and Sahel 2016). With the long-standing support of the Foundation Fighting Blindness, a neuroprotective gene therapy aiming to provide sustained release of the vision-saving RdCVF protein to the retina is currently under development. Expressed through an AAV vector, the RdCVF mutation-independent treatment has potential to become a widely applicable gene therapeutic option for treatment of various retinal degenerative diseases (Dalkara et al. 2015).

### *62.3.2 Therapeutic Strategy for Each Patient*

The best suited therapeutic strategy for vision preservation and restoration will largely depend on the careful evaluation of the status of the remaining cells in each patient. The power of most advanced in vivo noninvasive high-resolution imaging technologies is currently used for this purpose, as visualizing retinal morphology in details is of crucial importance not only to diagnose early stages of retinal degeneration and determine the progression rate of the disease but also to choose the most appropriate therapeutic option and monitor therapeutic effects. The adaptive optics infrared reflectance imaging takes a particularly important role in this evaluation, as it allows visualization at cellular level of microstructures such as photoreceptor outer segments, capillaries or vascular wall, and nerve fiber bundles. The researchers from Institut de la Vision and Institut Langevin are currently developing state-of-the-art imaging technologies for gaining a better understanding of retinal diseases and developing sight-saving therapies. These include holographic laser Doppler ophthalmoscopy, which uses infrared light to obtain detailed real-time 3-D images of blood flow through retinal vessels, as well as two-photon imaging to investigate the highly intricate circuitry of the retina. Major enhancements will be made to optical coherence tomography (OCT), an approach that employs near-infrared light to capture images of retinal structure. All these technologies are expected to provide new insights into pathological processes leading to visual impairment, to identify and assign eligible patients to future clinical trials, and to optimize neuroprotective and regenerative therapies in retinal dystrophies.

### *62.3.3 Measuring Outcomes in Patients*

IRDs comprise a large number of genetically and phenotypically highly heterogeneous disorders due to mutations in more than 250 different causative genes (RetNet: https://sph.uth.edu/retnet/sum-dis.htm, accessed November 16, 2016). This huge heterogeneity requires special consideration when selecting patients for clinical trials and choosing outcome measures. Ideally, the outcome measures should be noninvasive, safe, and easy and quick to perform, both for patients and staff (Thompson et al. 2015). Visual acuity is a classical outcome measure used in treatment trials for retinal diseases, but only a change of ≥15 letter score (equivalent to ≥3 lines on a standardized visual acuity chart) is considered significant (Beck et al. 2007). Highly standardized and powerful methods for characterizing patients (e.g., proteomics, metabolomics, genomics, genotype-phenotype correlations, real-time noninvasive high-resolution imaging techniques), as well as patient-reported outcomes (e.g., questionnaires) and performance-based tests, should address the challenging needs of clinical trials for IRDs. Objective behavioral measurements need to be implemented into the battery of outcome measures, including movement patterns, kinematics and kinetics, forces produced by movements, gaze behavior (head + eye orientation), saccade amplitude, eye-head coordination, etc.

## 62.4 Concluding Remarks

In advanced stages of IRD when cone photoreceptor integrity is affected to the point that they do not express anymore the cell surface of RdCVF, the administration of RdCVF will be without benefit. In these cases, optogenetics can make possible the conversion of different retinal cells into "artificial photoreceptors," offering perspectives for vision restoration in a mutation-independent manner, for a wide range of IRDs (Lagali et al. 2008; Zhang et al. 2009; Busskamp et al. 2010; Cronin et al. 2014; Mace et al. 2015). Ophthalmology is a good example of precision medicine. In this context, patient-specific clinical decisions based on new diagnostic and monitoring approaches have crucial importance. Developing living labs for testing of innovative treatments and devices and for evaluation and education of patients in user-centered ecosystems is mandatory. We are convinced that close collaboration between academia, industry, policy makers, and patient associations may significantly contribute to the development of neuroprotective mutation-independent therapy aimed at saving sight by preventing secondary cone degeneration.

**Financial Support** LABEX LIFESENSES [ANR-10-LABX-65], Foundation Fighting Blindness.

## References

Acland GM, Aguirre GD, Bennett J, Aleman TS, Cideciyan AV, Bennicelli J, Dejneka NS, Pearce-Kelling SE, Maguire AM, Palczewski K, Hauswirth WW, Jacobson SG (2005) Long-term restoration of rod and cone vision by single dose rAAV-mediated gene transfer to the retina in a canine model of childhood blindness. Mol Ther 12:1072–1082

Ait-Ali N, Fridlich R, Millet-Puel G, Clerin E, Delalande F, Jaillard C, Blond F, Perrocheau L, Reichman S, Byrne LC, Olivier-Bandini A, Bellalou J, Moyse E, Bouillaud F, Nicol X, Dalkara D, van Dorsselaer A, Sahel JA, Leveillard T (2015) Rod-derived cone viability factor promotes cone survival by stimulating aerobic glycolysis. Cell 161:817–832

Bainbridge JW, Smith AJ, Barker SS, Robbie S, Henderson R, Balaggan K, Viswanathan A, Holder GE, Stockman A, Tyler N, Petersen-Jones S, Bhattacharya SS, Thrasher AJ, Fitzke FW, Carter BJ, Rubin GS, Moore AT, Ali RR (2008) Effect of gene therapy on visual function in Leber's congenital amaurosis. N Engl J Med 358:2231–2239

Beck RW, Maguire MG, Bressler NM, Glassman AR, Lindblad AS, FERRIS FL (2007) Visual acuity as an outcome measure in clinical trials of retinal diseases. Ophthalmology 114:1804–1809

BENNETT J, ASHTARI M, WELLMAN J, Marshall KA, Cyckowski LL, Chung DC, Mccague S, Pierce EA, Chen Y, Bennicelli JL, Zhu X, Ying GS, Sun J, Wright JF, Auricchio A, Simonelli F, Shindler KS, Mingozzi F, High KA, Maguire AM (2012) AAV2 gene therapy readministration in three adults with congenital blindness. Sci Transl Med 4:120ra115

Busskamp V, Duebel J, Balya D, Fradot M, Viney TJ, Siegert S, Groner AC, Cabuy E, Forster V, Seeliger M, Biel M, Humphries P, Paques M, Mohand-Said S, Trono D, Deisseroth K, Sahel JA, Picaud S, Roska B (2010) Genetic reactivation of cone photoreceptors restores visual responses in retinitis pigmentosa. Science 329:413–417

Byrne LC, Dalkara D, Luna G, Fisher SK, Clerin E, Sahel JA, Léveillard T, Flannery JG (2015) Viral-mediated RdCVF and RdCVFL expression protects cone and rod photoreceptors in retinal degeneration. J Clin Invest 125:105–116

Cepko C, Punzo C (2015) Cell metabolism: sugar for sight. Nature 522:428–429

Chalmel F, Léveillard T, Jaillard C, Lardenois A, Berdugo N, Morel E, Koehl P, Lambrou G, Holmgren A, Sahel JA, Poch O (2007) Rod-derived Cone Viability Factor-2 is a novel bifunctional-thioredoxin-like protein with therapeutic potential. BMC Mol Biol 8:74

Choi RY, Engbretson GA, Solessio EC, Jones GA, Coughlin A, Aleksic I, Zuber ME (2011) Cone degeneration following rod ablation in a reversible model of retinal degeneration. Invest Ophthalmol Vis Sci 52:364–373

Cronin T, Raffelsberger W, Lee-Rivera I, Jaillard C, Niepon ML, Kinzel B, Clerin E, Petrosian A, Picaud S, Poch O, Sahel JA, Leveillard T (2010) The disruption of the rod-derived cone viability gene leads to photoreceptor dysfunction and susceptibility to oxidative stress. Cell Death Differ 17:1199–1210

Cronin T, Vandenberghe LH, Hantz P, Juttner J, Reimann A, Kacso AE, Huckfeldt RM, Busskamp V, Kohler H, Lagali PS, Roska B, Bennett J (2014) Efficient transduction and optogenetic stimulation of retinal bipolar cells by a synthetic adeno-associated virus capsid and promoter. EMBO Mol Med 6:1175–1190

Dalkara D, Duebel J, Sahel JA (2015) Gene therapy for the eye focus on mutation-independent approaches. Curr Opin Neurol 28:51–60

Elachouri G, Lee-Rivera I, Clerin E, Argentini M, Fridlich R, Blond F, Ferracane V, Yang Y, Raffelsberger W, Wan J, Bennett J, Sahel JA, Zack DJ, Leveillard T (2015) Thioredoxin rod-derived cone viability factor protects against photooxidative retinal damage. Free Radic Biol Med 81:22–29

Fridlich R, Delalande F, Jaillard C, Lu J, Poidevin L, Cronin T, Perrocheau L, Millet-Puel G, Niepon ML, Poch O, Holmgren A, van Dorsselaer A, Sahel JA, Leveillard T (2009) The thioredoxin-like protein rod-derived cone viability factor (RdCVFL) interacts with TAU and inhibits its phosphorylation in the retina. Mol Cell Proteomics 8:1206–1218

Geller AM, Sieving PA (1993) Assessment of foveal cone photoreceptors in Stargardt's macular dystrophy using a small dot detection task. Vis Res 33:1509–1524

Hauswirth WW, Aleman TS, Kaushal S, Cideciyan AV, Schwartz SB, Wang L, Conlon TJ, Boye SL, Flotte TR, Byrne BJ, Jacobson SG (2008) Treatment of leber congenital amaurosis due to RPE65 mutations by ocular subretinal injection of adeno-associated virus gene vector: short-term results of a phase I trial. Hum Gene Ther 19:979–990

Lagali PS, Balya D, Awatramani GB, Munch TA, Kim DS, Busskamp V, Cepko CL, Roska B (2008) Light-activated channels targeted to ON bipolar cells restore visual function in retinal degeneration. Nat Neurosci 11:667–675

Léveillard T, Sahel JA (2010) Rod-derived cone viability factor for treating blinding diseases: from clinic to redox signaling. Sci Transl Med 2:26ps16

Léveillard T, Sahel JA (2016) Metabolic and redox signaling in the retina. Cell Mol Life Sci 74:3649–3665

Léveillard T, Mohand-Said S, Lorentz O, Hicks D, Fintz AC, Clerin E, Simonutti M, Forster V, Cavusoglu N, Chalmel F, Dolle P, Poch O, Lambrou G, Sahel JA (2004) Identification and characterization of rod-derived cone viability factor. Nat Genet 36:755–759

Mace E, Caplette R, Marre O, Sengupta A, Chaffiol A, Barbe P, Desrosiers M, Bamberg E, Sahel JA, Picaud S, Duebel J, Dalkara D (2015) Targeting channelrhodopsin-2 to ON-bipolar cells with vitreally administered AAV restores ON and OFF visual responses in blind mice. Mol Ther 23:7–16

Maguire AM, Simonelli F, Pierce EA, Pugh EN Jr, Mingozzi F, Bennicelli J, Banfi S, Marshall KA, Testa F, Surace EM, Rossi S, Lyubarsky A, Arruda VR, Konkle B, Stone E, Sun J, Jacobs J, Dell'osso L, Hertle R, Ma JX, Redmond TM, Zhu X, Hauck B, Zelenaia O, Shindler KS, Maguire MG, Wright JF, Volpe NJ, Mcdonnell JW, Auricchio A, High KA, Bennett J (2008) Safety and efficacy of gene transfer for Leber's congenital amaurosis. N Engl J Med 358:2240–2248

Mccall MA, Gregg RG, Merriman K, Goto Y, Peachey NS, Stanford LR (1996) Morphological and physiological consequences of the selective elimination of rod photoreceptors in transgenic mice. Exp Eye Res 63:35–50

Mei X, Chaffiol A, Kole C, Yang Y, Millet-Puel G, Clerin E, Ait-Ali N, Bennett J, Dalkara D, Sahel JA, Duebel J, Léveillard T (2016) The thioredoxin encoded by the rod-derived cone viability factor gene protects cone photoreceptors against oxidative stress. Antioxid Redox Signal 24:909–923

Mohand-Said S, Deudon-Combe A, Hicks D, Simonutti M, Forster V, Fintz AC, Léveillard T, Dreyfus H, Sahel JA (1998) Normal retina releases a diffusible factor stimulating cone survival in the retinal degeneration mouse. Proc Natl Acad Sci U S A 95:8357–8362

Mohand-Said S, Hicks D, Dreyfus H, Sahel JA (2000) Selective transplantation of rods delays cone loss in a retinitis pigmentosa model. Arch Ophthalmol 118:807–811

Mohand-Said S, Hicks D, Léveillard T, Picaud S, Porto F, Sahel JA (2001) Rod-cone interactions: developmental and clinical significance. Prog Retin Eye Res 20:451–467

Punzo C, Kornacker K, Cepko CL (2009) Stimulation of the insulin/mTOR pathway delays cone death in a mouse model of retinitis pigmentosa. Nat Neurosci 12:44–52

Reichman S, Kalathur RK, Lambard S, Ait-Ali N, Yang Y, Lardenois A, Ripp R, Poch O, Zack DJ, Sahel JA, Léveillard T (2010) The homeobox gene CHX10/VSX2 regulates RdCVF promoter activity in the inner retina. Hum Mol Genet 19:250–261

Thompson DA, Ali RR, Banin E, Branham KE, Flannery JG, Gamm DM, Hauswirth WW, Heckenlively JR, Iannaccone A, Jayasundera KT, Khan NW, Molday RS, Pennesi ME, Reh TA, Weleber RG, Zacks DN, Monaciano C (2015) Advancing therapeutic strategies for inherited retinal degeneration: recommendations from the Monaciano Symposium. Invest Ophthalmol Vis Sci 56:918–931

Wang XW, Liou YC, Ho B, Ding JL (2007) An evolutionarily conserved 16-kDa thioredoxin-related protein is an antioxidant which regulates the NF-kappaB signaling pathway. Free Radic Biol Med 42:247–259

Wright AF (1997) A searchlight through the fog. Nat Genet 17:132–134
Yang Y, Mohand-Said S, Danan A, Simonutti M, Fontaine V, Clerin E, Picaud S, Leveillard T, Sahel JA (2009) Functional cone rescue by RdCVF protein in a dominant model of retinitis pigmentosa. Mol Ther 17:787–795
Zhang Y, Ivanova E, Bi A, Pan ZH (2009) Ectopic expression of multiple microbial rhodopsins restores ON and OFF light responses in retinas with photoreceptor degeneration. J Neurosci 29:9186–9196

# Chapter 63
# PKG-Dependent Cell Death in 661W Cone Photoreceptor-like Cell Cultures (Experimental Study)


**Stine Mencl, Dragana Trifunović, Eberhart Zrenner, and François Paquet-Durand**

**Abstract** In humans cone photoreceptors are responsible for high-resolution colour vision. A variety of retinal diseases can compromise cone viability, and, at present, no satisfactory treatment options are available. Here, we present data towards establishing a reliable, high-throughput assay system that will facilitate the search for cone neuroprotective compounds using the murine-photoreceptor cell line 661 W. To further characterize 661 W cells, a retinal marker study was performed, followed by the induction of cell death using paradigms over-activating cGMP-dependent protein kinase G (PKG). We found that 661 W cells may be used to mimic specific aspects of cone degeneration and may thus be valuable for future compound screening studies.

**Keywords** Neurodegeneration · cGMP · CNG channel · *cpfl1* · *rd1* · Achromatopsia

S. Mencl
University Hospital Essen, Department of Neurology, Essen, Germany

Department für Augenheilkunde, Forschungsinstitut für Augenheilkunde, Eberhard Karls Universität Tübingen, Tübingen, Germany

D. Trifunović · F. Paquet-Durand (✉)
Department für Augenheilkunde, Forschungsinstitut für Augenheilkunde, Eberhard Karls Universität Tübingen, Tübingen, Germany
e-mail: francois.paquet-durand@klinikum.uni-tuebingen.de

E. Zrenner
Department für Augenheilkunde, Forschungsinstitut für Augenheilkunde, Eberhard Karls Universität Tübingen, Tübingen, Germany

Centre for Integrative Neuroscience (CIN), Eberhard Karls Universität Tübingen, Tübingen, Germany



J. D. Ash et al. (eds.), *Retinal Degenerative Diseases*, Advances in Experimental Medicine and Biology 891, https://doi.org/10.1007/978-3-319-75402-4_63

## 63.1 Introduction

Human vision is strongly depending on the function of cone photoreceptors. Neurodegenerative diseases affecting cones occur in many eye diseases, including in age-related macular degeneration, diabetic retinopathy, retinitis pigmentosa, and achromatopsia. At present no satisfactory treatment options are available for these diseases. To identify neuroprotective compounds that could potentially preserve cone viability, a reliable, high-throughput test system is needed (Ekstrom et al. 2014).

The cone-photoreceptor-function-loss-1 (*cpfl1*) mouse is an animal model for cone degeneration carrying a mutation in the cone-specific phosphodiesterase 6 (*Pde6*) (Trifunovic et al. 2010). This causes PDE6 enzyme dysfunction and a subsequent rise of intracellular cGMP (Trifunovic et al. 2010). cGMP in turn may act on cyclic nucleotide-gated ion channels (CNGCs) raising intracellular $Ca^{2+}$ levels (Kulkarni et al. 2016) and on cGMP-dependent protein kinase G (PKG) (Paquet-Durand et al. 2009). Here, we show that murine cone-like 661 W cells (Al-Ubaidi et al. 1992) can be used to emulate certain aspects of *cpfl1* cone degeneration and may thus be useful for the development of a high-throughput screening system for cone protective compounds.

## 63.2 Materials and Methods

### *63.2.1 Cell Culture and Cell Viability Testing*

Murine cone-like 661 W cells were maintained in DMEM and kept at 37 °C in a humidified atmosphere and 5% of $CO_2$. Cells were seeded into 24-well plates, 4000 cells/well for short treatment and 2000 cells/well for long treatment. To stop treatment, cells were rinsed in phosphate-buffered saline (PBS) and then stained for 45 min using LIVE/DEAD® Viability/Cytotoxicity Kit (Thermo Fisher Scientific).

### *63.2.2 Immunohistochemistry*

Cells were grown on inserted poly-L-lysine-covered glass plates. Cells were fixed with 4% PFA and stained with primary antibodies (Table 63.1) overnight at 4 °C. DAPI was used as nuclear counterstain.

**Table 63.1** Antibodies used for immunofluorescence

| Antigen | Host | Source/Cat. number | Dilution |
|---|---|---|---|
| Calbindin | Mouse | Swant, 300 | 1:500 |
| $Ca^{2+}$–/calmodulin-dependent kinase 1 (CAMK1) | Rabbit | Acris, AP13883PU-N | 1:100 |
| Calretinin | Mouse | Chemicon, MAB 1568 | 1:300 |
| cGMP | Sheep | Gift from Prof. Jan de Vente | 1:500 |
| Glutamine synthetase | Mouse | Chemicon, MAB 302 | 1:1000 |
| Glycogen phosphorylase (GlyPhos) | Guinea pig | Gift from Prof. B. Pfeiffer-Guglielmi | 1:500 |
| JH 455 (blue opsin) | Rabbit | Gift from Prof. P. Humphries | 1:1000 |
| Neuron-specific enolase (NSE) | Rabbit | Polyscience, 16,625 | 1:3000 |
| Opsin red/green | Rabbit | Millipore/Chemicon, AB 5405 | 1:200 |
| Parvalbumin | Mouse | Sigma, P 3088 | 1:300 |
| PDE6B | Rabbit | ABR, PA1–722 | 1:400 |
| PDE6H | Rabbit | Gift from Prof. P. Ruth | 1:1000 |
| Rhodopsin | Mouse | Chemicon, MAB 5316 | 1:400 |

### *63.2.3 Microscopy, Cell Counting, and Statistical Analysis*

Light and fluorescence microscopy was performed with an Axio Imager Z1 ApoTome Microscope using Zeiss AxioVision 4.7 software. Pictures of LIVE/DEAD® Viability/Cytotoxicity assay were obtained with an Axiovert 35 M Microscope.

For image processing, the Adobe Creative Suite CS5 Standard was used. Live and dead cells were counted manually using ImageJ software. The percentage of dead cells was calculated, normalized to DMSO control, and analysed for significant differences using an unpaired, two-tailed Student's *t*-test.

## 63.3 Results

### *63.3.1 Expression of Retinal Cell-Type-Specific Markers in 661 W Cells*

Previous studies found that 661 W cells were cone-like and expressed blue and red/green cone opsins, as well as cone transducin and arrestin, but not rhodopsin or rod arrestin (Tan et al. 2004). To confirm and further assess the nature of these cells, we tested a variety of retinal cell markers using immunofluorescence.

While 661 W cells did not express rhodopsin, they showed abundant expression of rod and cone PDE6 (Fig. 63.1a–d and e–h), as well as S- and M-opsin (cf. Table 63.2). Furthermore, the cone-specific markers, neuron-specific enolase (NSE), and glycogen phosphorylase (GlyPhos) (Nihira et al. 1995) were strongly expressed

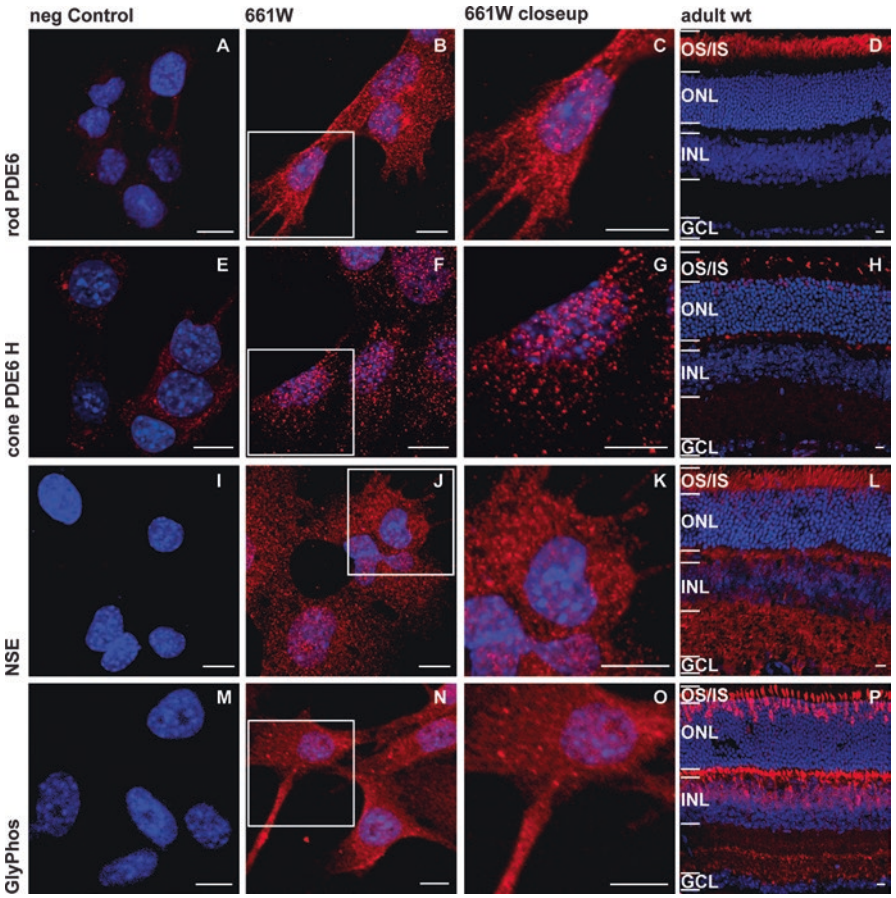


**Fig. 63.1** Retinal cell marker expression in 661 W cells. Marker staining (red) as indicated on the left of each row; DAPI (blue) was used as nuclear counterstain. Columns as indicated in top row; left most column is negative (neg.) control; right most column shows a corresponding staining on wild-type retina, for comparison. (**a**–**d**) Rod PDE6B expression. (**e**–**h**) Cone PDE6H expression. (**i**–**l**) NSE expression. (**m**–**p**) GlyPhos expression. Scale bars = 10 μm. Abbreviations: GCL ganglion cell layer, INL inner nuclear layer, ONL outer nuclear layer, OS/IS outer and inner segments

(Fig. 63.1i–l and m–p). Also, connexin-36, a gap junction protein involved in rod and cone photoreceptor coupling, was expressed in 661 W cells, as were cGMP-dependent PKG-1 and PKG-2 (cf. Table 63.2).

Calbindin, a marker for horizontal cells, amacrine cells, and certain ganglion cell types, was not expressed in 661 W cells (Table 63.2). However, $Ca^{2+}$–/calmodulin-dependent kinase I (CaMK1), a marker for bipolar and amacrine cells in mouse retina, was expressed in the cytoplasm of 661 W cells (Table 63.2).

In summary, the rod-specific phosphodiesterase, CaMK1, PKG1, and PKG2 were expressed in this cell line, as well as six cone-specific proteins, while rhodopsin

**Table 63.2** Expression of retinal cell markers in 661 W cells

| Protein/enzyme | Rod marker | Cone marker | Other markers |
|---|---|---|---|
| Rhodopsin | Negative | | |
| Rod PDE6B | Positive | | |
| Cone PDE6H | | Positive | |
| Neuron-specific enolase | | Positive | |
| Glycogen phosphorylase | | Positive | |
| S-opsin | | Positive | |
| M-opsin | | Positive | |
| Connexin-36 | | Positive | |
| PKG-1 | | | Positive |
| PKG-2 | | | Positive |
| Calbindin | | | Negative |
| $Ca^{2+}$−/calmodulin-dependent kinase 1 | | | Positive |

and calbindin were not expressed (Table 63.2). Thus, the 661 W cell line appeared cone-like and suitable for studies into cone-degeneration mechanisms.

### *63.3.2 Induction of Cell Death in 661 W Cells Using a Selective PKG Activator*

In *cpfl1* cones PDE6 is nonfunctional leading to an accumulation of cGMP (Trifunovic et al. 2010). As described earlier for the *rd1* mouse, this leads to an over-activation of cGMP-dependent PKG (Sahaboglu et al. 2013), likely combined with a permanent opening of CNGC (Paquet-Durand et al. 2011), and eventually cell death.

To emulate a *cpfl1*-like situation in 661 W cells, we blocked PDE6 activity with the highly selective inhibitor, zaprinast (Zhang et al. 2005). Remarkably, 24 h treatment with 500 µm zaprinast did not produce any significant differences between treated (5.4% ± 1.1 SEM) and control group (6.1% ± 1.0, $p = 0.656$) (Fig. 63.2a). In view of the confirmed expression of rod and cone PDE6 in 661 W cells (Fig.63.2a–d and e–h), this was surprising. However, 661 W cells may not be producing sufficient amounts of cGMP so as to activate PKG- and/or CNGC-dependent cell death. In addition, 661 W cells do not express the CNGA3 subunit of the CNGCs (Fitzgerald et al. 2008) rendering CNGCs nonfunctional.

As an alternative to PDE6 inhibition, we treated 661 W cells with a selective PKG activator, the cGMP analogue 8-pCPT-PET-cGMP (Fig. 63.2b). A 24 h treatment with 50 µM PKG activator resulted in a significantly higher percentage of dead cells (6.5% ± 0.3) when compared to control (2.3% ± 0.8, $p < 0.001$), confirming that 661 W cells are vulnerable to PKG over-activation, similar to what was seen in *cpfl1* cones (Trifunovic et al. 2010).

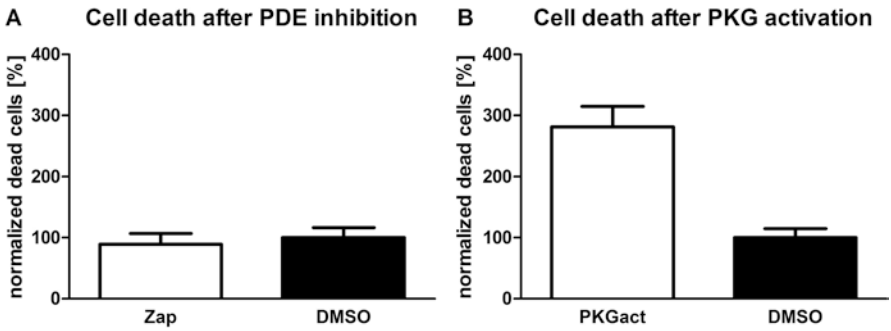


**Fig. 63.2** Induction of cpfl1-like cell death in 661 W cells. (**a**) PDE inhibition with zaprinast (zap) did not increase 661 W cell death. (**b**) After PKG activation with 8-pCPT-PET-cGMP, cell death was significantly increased. Error bars represent SEM

## 63.4 Discussion

The 661 W cell line was obtained from an immortalized murine retinoblastoma (Al-Ubaidi et al. 1992). These cells display the spindle-like morphology of neuronal cells and express several cone photoreceptor-specific genes and proteins (Tan et al. 2004). Our retinal marker study found six cone-specific proteins expressed in 661 W cells. We thus confirmed previous studies and concluded that these cells are more cone- than rod-like and do resemble photoreceptors more than any other retinal cell type.

We wanted to use 661 W cells as model system for cone degeneration. To induce cell death that would correspond to *cpfl1* mouse cone degeneration (Trifunovic et al. 2010, 2016), we first used the PDE6 inhibitor zaprinast. In organotypic retinal explant cultures, 100 μM zaprinast treatment was sufficient to cause selective photoreceptor cell death (Sahaboglu et al. 2013). While this approach did not cause significant 661 W cell death, the direct activation of PKG with a cGMP analogue did result in strong cell death induction. This finding confirmed the functional expression of PKG1 and PKG2 in 661 W cells, in line with previous studies on *rd1* rod and *cpfl1* cone degeneration (Paquet-Durand et al. 2009; Trifunovic et al. 2010).

Taken together, 661 W cell cultures can be used to emulate PKG-dependent cell death and may thus be used as to establish a rapid and high-throughput screening system for cone protective compounds. After identification of a 661 W protective substance, effects may be further validated in a more complex in vitro system, such as organotypic retinal explant cultures, and subsequently in an in vivo animal model, such as the *cpfl1* mouse.

**Acknowledgments and Funding** We thank Bernd Wissinger and Peggy Reuter for helpful discussions and Sandra Bernhard-Kurz and Norman Rieger for skilful technical assistance. This work was supported by grants from the Tistou and Charlotte Kerstan Foundation, the European Union (DRUGSFORD; HEALTH-F2-2012-304963), and Deutsche Forschungsgemeinschaft (PA1751/1-1).

## References

Al-Ubaidi MR, Hollyfield JG, Overbeek PA, Baehr W (1992) Photoreceptor degeneration induced by the expression of simian virus 40 large tumor antigen in the retina of transgenic mice. Proc Natl Acad Sci U S A 89:1194–1198

Ekstrom PA, Ueffing M, Zrenner E, Paquet-Durand F (2014) Novel *in situ* activity assays for the quantitative molecular analysis of neurodegenerative processes in the retina. Curr Med Chem 21:3478–3493

Fitzgerald JB, Malykhina AP, Al-Ubaidi MR, Ding XQ (2008) Functional expression of cone cyclic nucleotide-gated channel in cone photoreceptor-derived 661W cells. Adv Exp Med Biol 613:327–334

Kulkarni M, Trifunovic D, Schubert T, Euler T, Paquet-Durand F (2016) Calcium dynamics change in degenerating cone photoreceptors. Hum Mol Genet 25:3729–3740

Nihira M, Anderson K, Gorin FA, Burns MS (1995) Primate rod and cone photoreceptors may differ in glucose accessibility. Invest Ophthalmol Vis Sci 36:1259–1270

Paquet-Durand F, Hauck SM, van Veen T, Ueffing M, Ekstrom P (2009) PKG activity causes photoreceptor cell death in two retinitis pigmentosa models. J Neurochem 108:796–810

Paquet-Durand F, Beck S, Michalakis S et al (2011) A key role for cyclic nucleotide gated (CNG) channels in cGMP-related retinitis pigmentosa. Hum Mol Genet 20:941–947

Sahaboglu A, Paquet-Durand O, Dietter J et al (2013) Retinitis pigmentosa: rapid neurodegeneration is governed by slow cell death mechanisms. Cell Death Dis 4:e488

Tan E, Ding XQ, Saadi A et al (2004) Expression of cone-photoreceptor-specific antigens in a cell line derived from retinal tumors in transgenic mice. Invest Ophthalmol Vis Sci 45:764–768

Trifunovic D, Dengler K, Michalakis S et al (2010) cGMP-dependent cone photoreceptor degeneration in the cpfl1 mouse retina. J Comp Neurol 518:3604–3617

Trifunovic D, Arango-Gonzalez B, Comitato A et al (2016) HDAC inhibition in the cpfl1 mouse protects degenerating cone photoreceptors in vivo. Hum Mol Genet 25:4462–4472

Zhang X, Feng Q, Cote RH (2005) Efficacy and selectivity of phosphodiesterase-targeted drugs in inhibiting photoreceptor phosphodiesterase (PDE6) in retinal photoreceptors. Invest Ophthalmol Vis Sci 46:3060–3066

# Part VIII
# Retinal Cell Biology

# Chapter 64
# More Than Meets the Eye: Current Understanding of RPGR Function


**Hemant Khanna**

**Abstract** This article summarizes the recent advances in our understanding of a major retinal disease gene RPGR (retinitis pigmentosa GTPase regulator), mutations in which are associated with majority of X-linked forms of retinal degenerations. A great deal of work has been done to uncover the ciliary localization of RPGR and its interacting proteins in the retina. However, the molecular mechanisms of action of RPGR in the photoreceptors are still unclear. Recent studies have begun to shed light on the intracellular pathways in which RPGR is likely involved. The deregulation of such pathways may underlie the pathogenesis of severe retinal degeneration associated with RPGR. With the recent advances in the gene augmentation therapy for RPGR-associated disease, there is a lot of excitement in the field. Patients with *RPGR* mutations, however, present with clinically heterogeneous manifestations. It is therefore imperative to examine the function of RPGR in detail, so that we can design patient-oriented therapeutic strategies for this disease.

**Keywords** RPGR · Cilia · Photoreceptor · Ciliopathies · RCC1 · GTPase · GEF · Retinal degeneration · X-linked retinitis pigmentosa · Retinitis pigmentosa · INPP5E · PDE6δ · Glutamylation · Prenylation

## 64.1 Introduction

Retinal degenerative diseases are a group of clinically and genetically heterogeneous group of blindness disorders. Retinitis pigmentosa (RP) is one of the most severe forms of retinal degeneration, which affects 1 in 3000–3500 individuals (Fishman 1978; Haim 2002). RP is characterized by progressive loss of rod and

H. Khanna (✉)
Department of Ophthalmology and Neurobiology, UMASS Medical School, Worcester, MA, USA
e-mail: hemant.khanna@umassmed.edu



J. D. Ash et al. (eds.), *Retinal Degenerative Diseases*, Advances in Experimental Medicine and Biology 891, https://doi.org/10.1007/978-3-319-75402-4_64

cone photoreceptors (PRs), resulting in diminished to nonrecordable electroretinography responses and blindness (Heckenlively et al. 1988). RP is also observed in syndromic disorders, including Bardet-Biedl syndrome, Senior-Loken syndrome, and Usher syndrome (Otto et al. 2005; Daiger et al. 2007).

Mutations in more than 60 genes are associated with the non-syndromic forms of RP (http://www.sph.uth.tmc.edu/RetNet/) (Daiger 1996). Among these, mutations in the *RPGR* (retinitis pigmentosa GTPase regulator) gene, located on the X chromosome, are one of the most common causes of RP. *RPGR* males usually show signs of visual dysfunction starting as early as 9–10 years of age (Breuer et al. 2002; Branham et al. 2012; Churchill et al. 2013). On the other hand, majority of RPGR-carrier females exhibit mild to moderately reduced visual function. Cases of severe visual impairment in carrier females comparable to that of affected males have also been reported (Souied et al. 1997; Mears et al. 2000; Rozet et al. 2002; Wu et al. 2010; Branham et al. 2012).

Extensive studies done both in patients and animal models of *RPGR* mutations have revealed insights into the natural history of the disease (Hong et al. 2000; Zhang et al. 2002; Rao et al. 2015, 2016b, c), which have paved way to designing therapeutic strategies. Recent gene augmentation therapy studies have generated a great deal of excitement by showing a delay in PR degeneration in canine and mouse models of *RPGR* (Beltran et al. 2012; Deng et al. 2015; Pawlyk et al. 2015; Wu et al. 2015). However, the *RPGR* gene exhibits immense heterogeneity in clinical presentation of the phenotype and in the expression of its mRNA and protein products. We still do not completely understand the role of the major RPGR isoforms and the effect of disease-causing mutations on these isoforms. Such knowledge is crucial for understanding the molecular mechanisms of phenotypic variability observed in *RPGR* patients. Recent studies on RPGR function have identified a unifying theme of its involvement in regulating ciliary trafficking in PRs. Moreover, RPGR cooperates with other ciliary disease proteins, thus indicating a functional overlap between RPGR and other diseases of the cilia. In this article, I will present this unifying theme and propose models of isoform-specific role of RPGR in PRs.

## 64.2 Cilia, PRs, and Disease

Cilia are evolutionarily conserved extensions of the plasma membrane. These extensions are formed by the nucleation of a microtubule cytoskeleton at the mother centriole (also called basal body) in a nondividing cell. Cilia act as antennae to relay external signals to the cell interior. They regulate several indispensable functions, such as photoreception, breaking the left-right symmetry during embryonic development, and olfaction. The ciliary membrane retains a unique protein and membrane signature, and it is this signature that is believed to impart the ability to detect specific signals (Singla and Reiter 2006; Eggenschwiler and Anderson 2007). For example, PRs develop a primary cilium in the form of a light-sensing outer segment (Fig. 64.1). Also see Anand and Khanna (2002) and Khanna (2015). The outer segment is loaded with the proteins involved in the

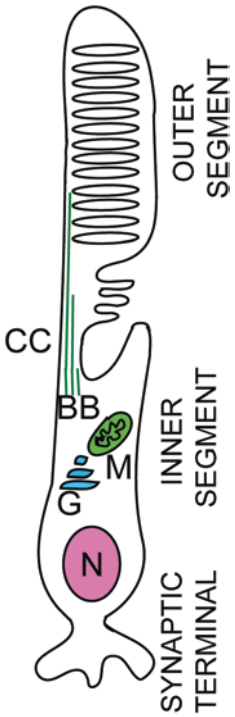


**Fig. 64.1** Schematic representation of a rod photoreceptor cell. The outer segment is loaded with membranous discs that are arranged in a coinstack-like fashion. The inner segment houses the Golgi apparatus (G), mitochondria (M), and the rest of the machinery involved in protein synthesis and trafficking to the outer segment. The trafficking takes place via the bridge-like connecting cilium (CC). N nucleus

phototransduction cascade (such as rhodopsin, cone opsin, transducin, and arrestin), fatty acids, and phospholipids (specific phosphoinositides). This unique composition imparts fluidity to the outer segment membrane and allows efficient capture and processing of light signals (Besharse et al. 2003; Eggenschwiler and Anderson 2007; Boesze-Battaglia et al. 2008; Khanna 2015; Albert et al. 2016).

The PR sensory cilium is nucleated from the basal body at the apical surface of the inner segment. As the microtubules extend, they form a doublet microtubule structure called the connecting cilium (CC) (Fig. 64.1). The CC is analogous to the transition zone of a prototypic cilium and extends into the OS. The CC acts as a conduit for unidirectional or bidirectional transport of cargo moieties between the inner and the outer segments. The CC also acts as a "gatekeeper" to regulate the entry or exit of the cargo, which aids in the maintenance of its unique composition (Besharse et al. 2003; Khanna 2015). The PR outer segments lack the ability to synthesize the resident proteins and thus, rely on their synthesis and transport from the inner segment across the CC. As such, even slight perturbations in the structure or function of the CC result in PR dysfunction and degeneration (Deretic et al. 1995; Hong et al. 2000; Pazour et al. 2002; Li et al. 2013; Pearring et al. 2013; Rao et al. 2015).

Ciliary dysfunction leads to severe diseases, collectively termed ciliopathies. Ciliopathies are genetic disorders that range from earlier-onset developmental anomalies (Meckel-Gruber syndrome and Joubert syndrome) to relatively later-onset diseases (Bardet-Biedl syndrome, Senior-Loken syndrome, and Usher syndrome). These syndromes share blindness due to retinal degeneration as a common clinical manifestation (Badano et al. 2006; Hildebrandt et al. 2011). However, retinal dystrophies are more commonly presented in a non-syndromic manner. About a third of genetic retinal dystrophies that affect the structure and function of the PR cilium lead to RP (Estrada-Cuzcano et al. 2012). Cilia-dependent RP is one of the most severe clinically and genetically heterogeneous forms of retinal dystrophies, and *RPGR* mutations are frequent causes of RP due to ciliary dysfunction (Churchill et al. 2013).

## 64.3 RPGR and Disease

Human genetic and mass spectrometry-based studies have identified several RP-associated genes that localize to the CC (Gherman et al. 2006; Arnaiz et al. 2009). Among these, RPGR is a major ciliary disease protein. *RPGR* mutations account for >80% of X-linked RP (XLRP) cases and 15–20% of simplex (isolated) RP males (Meindl et al. 1996; Roepman et al. 1996; Churchill et al. 2013). Expression analysis of *RPGR* identified two major isoforms: the constitutive (or default) isoform $RPGR^{const}$, encoded by exons 1–19, and the $RPGR^{ORF15}$ isoform, which retains part of intron 15 as the terminal exon (exons 1–15 + part of intron 15) (Vervoort et al. 2000; He et al. 2008; Churchill et al. 2013) (Fig. 64.2). Both isoforms share a common N-terminal domain (exons 1–15) but differ in their C-termini: exon 19 of $RPGR^{const}$ encodes a putative prenylation domain, while the terminal exon (called ORF15) of $RPGR^{ORF15}$ is a mutational hotspot (accounting for ~60% of *RPGR* patients) (Vervoort et al. 2000; Churchill et al. 2013). Within the common N-terminal region, exons 1–11 encode a domain homologous to regulator of chromosome condensation 1 (RCC1); thus, this region is named RCC1-like domain (RLD) (Meindl et al. 1996; Roepman et al. 1996).

Mutation analysis of *RPGR*-XLRP patients revealed that mutations in exon ORF15 (thus affecting the $RPGR^{ORF15}$ isoform) are associated with clinically hetero-

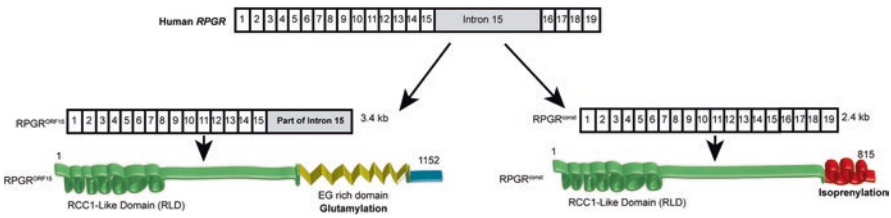


**Fig. 64.2** Schematic representation of the major human RPGR isoforms. The numbers in boxes indicate exons. The location of the protein domains and their posttranslational modifications (in bold) are also indicated

geneous disease, ranging from RP to cone-rod degeneration and macular degeneration (Vervoort et al. 2000; Ayyagari et al. 2002; Breuer et al. 2002; Demirci et al. 2002; Sharon et al. 2003; Ebenezer et al. 2005; Walia et al. 2008). Moreover, it was also postulated that mutations toward the 3′ end of exon ORF15 tend to associate with cone-rod degeneration, although RP patients carrying 3'-ORF15 mutations have also been reported (Vervoort et al. 2000; Ayyagari et al. 2002; Breuer et al. 2002; Demirci et al. 2002; Sharon et al. 2003; Ebenezer et al. 2005; Walia et al. 2008; Zahid et al. 2013; Bassuk et al. 2014). This was puzzling because the *RPGR*$^{ORF15}$ isoform expression can be detected in both rods and cones. A recent study showed that discrepancies in the genotype-phenotype correlation of *RPGR*$^{ORF15}$ patients might in part arise from a spatially restricted effect of the exon ORF15 mutations on the retina (Charng et al. 2016). Although both rod and cone photoreceptors may be affected by the ORF15 mutations, wide spatial distribution of the affected photoreceptors was observed, and the degree of effect of the ORF15 mutations on rods versus cones was variable yet bilaterally consistent in both patients and mouse models. Another major observation was the presentation of macular degeneration in all patients examined in this study. Importantly, no correlation with the position of the mutation in exon ORF15 was detected in these patients.

It is possible that modifier effect underlies the variable presentation of exon ORF15 mutations. Previous studies have identified potential RPGR-interacting proteins that can act as modifiers of retinal diseases in ciliopathies: *RPGRIP1L* (RPGR-interacting protein 1-like) (Khanna et al. 2009) and *CEP290* (centrosomal protein of 290 kDa) (Chang et al. 2006; Rao et al. 2016d). In fact, mouse genetic studies showed that *Cep290* alters the severity of retinal degeneration in the *Rpgr*$^{ko}$ mice (Rao et al. 2016d). Interestingly, analysis of *RPGRIP1L* in *RPGR* patients revealed two variants that are associated with the severity of the disease (Fahim et al. 2011). However, given the considerable phenotypic heterogeneity in *RPGR*-XLRP, it would be important to perform large-scale analyses for modifier genes that can alter the phenotypic presentation of *RPGR* mutations (Appelbaum et al. 2016).

Further validation of a differential effect of the loss of RPGR on rods and cones was obtained using RNAseq analysis of the eyes from the *Rpgr*$^{ko}$ mice in the rod-enriched or cone-only mouse backgrounds. Deregulation of actin cytoskeletal dynamics was one of the major altered pathways in the rod-dominant background. Interestingly, the *Rpgr*$^{ko}$ photoreceptors revealed overexpression of Rhotekin 2 (RTKN2), which modulates actin polymerization. Additional analysis revealed a twofold increase in the polymerized actin levels as compared to globular actin. Furthermore, RTKN2 is an effector of RhoA GTPase, which is also involved in actin polymerization. Effectors of small GTPases bind to its GTP-bound active state. Consistently, increased levels of RhoA-GTP were associated with RTKN2 in the *Rpgr*$^{ko}$ retina as compared to the wild-type counterpart (Rao et al. 2016c).

Loss of *Rpgr* in the all-cone retina of *Nrl*$^{-/-}$ mice (*Rpgr*$^{ko}$-double knockout; *Rpgr*-DKO) revealed unexpected effect on the retina. The *Rpgr*-DKO mice exhibited supranormal cone response by electroretinography (ERG) and substantially retained retinal morphology. Moreover, transcriptomic analysis revealed predominant alterations in the levels of RPE-specific genes involved in visual cycle.

Furthermore, reduced docosahexaenoic acid levels were observed in the double mutant retinas. Combinatorial effect of alterations in the levels of visual cycle gene expression and fatty acid content may underlie the supranormal cone response in the *Rpgr*-DKO mice (Rao et al. 2016c).

## 64.4 RPGR Function

RPGR as a GTPase Regulator: RCC1, to which the RLD of RPGR exhibits homology, is a guanine exchange factor (GEF) of small GTPases (Renault et al. 2001). GEFs catalyze the conversion of inactive GDP-bound GTPases to active GTP-bound forms (Deretic 2013; Barr 2010 #962; Rao and Khanna 2015). Using different N-terminal RPGR regions, it was found that RPGR preferentially interacts with the GDP-bound form of the small GTPase RAB8A (Murga-Zamalloa et al. 2010c). RAB8A plays crucial roles in rhodopsin trafficking in primary cilia (Deretic et al. 1995; Moritz et al. 2001; Wang and Deretic 2014). In addition, activated RAB8A is critical for the generation and maintenance of cilia in cultured cells (Nachury et al. 2007). Given RPGR-RAB8A interaction and the homology of RPGR to RCC1, the next logical step was to test whether or not RPGR can act as a GEF for RAB8A. To this end, using an in vitro GEF assay, it was found that the N-terminal region of RPGR encompassing the RLD, but not RLD alone, could catalyze the conversion of RAB8A-GDP to RAB8A-GTP (Murga-Zamalloa et al. 2010c). Moreover, shRNA-mediated knockdown of RPGR in hTERT-RPE1 cells resulted in the reduced retention of RAB8A at the cilia and shortening of the cilia length. Although the physiological relevance of RAB8A in mouse photoreceptor protein trafficking and of the GEF activity of RPGR toward RAB8A or another GTPase remains to be established, there is clear evidence for a role of RPGR in facilitating RAB8A localization at the cilia. This is corroborated by the interaction of RPGR with CEP290 and PCM1 (pericentriolar material 1), which regulate the ciliary localization of RAB8A (Kim et al. 2008).

Remarkable studies on the crystallization of the RLD of RPGR (residues 1–392) revealed the presence of RCC1-like seven-bladed β-propeller structure (Watzlich et al. 2013). However, significant differences between the structures of the GEF domain of RCC1 and RPGR-RLD were also observed. The RPGR-RLD revealed an unstructured loop at the homologous position of a β-hairpin extension that is involved in the GEF activity of RCC1. Such difference could suggest that RPGR-RLD does not possess active GEF activity. This assumption is not entirely true. Firstly, the GEF activity of RPGR is exhibited by the full-length $RPGR^{const}$ or residues 1–635 ($RPGR^{1–635}$, encoded by exons 1–15), indicating that the residues outside of the RLD are also involved in its activity. Secondly, the solved structure was of residues 1–392, and such domain might assume a different conformation as compared to the full-length protein or $RPGR^{1–635}$. Although crystal structure

analysis provides valuable and critical insights into the structure-function relationships in proteins and assists in understanding the effect of disease mutations, the results of such analyses should be interpreted in the physiological context.

Consistent with the *RPGR* knockdown results in cultured RPE cells, *rpgr*-morpholino (MO)-treated zebra fish embryos or *Rpgr*$^{ko}$ mouse PRs and fibroblasts did not exhibit cilia formation defects but formed shorter cilia (Ghosh et al. 2010; Rao et al. 2016b) (and HK, unpublished observations). Moreover, both models revealed normal retinal and PR development. Although the *Rpgr*$^{ko}$ mice undergo PR degeneration starting around 6–7 months of age (Hong et al. 2000; Rao et al. 2016d), the *rpgr*-MO-treated zebra fish embryos did not exhibit any detectable effect on PR health within the time span of the experiment (5 days post fertilization). This is likely because morpholinos usually remain effective until 5–6 days post fertilization; hence, only developmental defects can be readily detected in such experiments. The subtle ciliary defects due to the loss of RPGR are also consistent with the role of cilia in disease. Loss of cilia results in systemic ciliary defects, leading to severe ciliopathies and, in some cases, embryonic lethality. Although extraocular phenotypes, including sensorineural hearing loss, respiratory tract infections, and respiratory ciliary defects, result in primary cilia dyskinesia (Koenekoop et al. 2003; Zito et al. 2003; Iannaccone et al. 2004; Bukowy-Bieryllo et al. 2013), no systemic ciliary abnormalities in *RPGR* patients and animal models have been reported. Notably, RPGR has been localized to mouse sperm flagella (Khanna et al. 2005), and overexpression of RPGR resulted in male infertility in mice (Brunner et al. 2008). Nonetheless, clinical cases with such manifestations have not been reported. Overall, the loss of RPGR moderately affects cilia function but spares cilia formation, and RPGR's role as a GEF for small GTPases may play a secondary yet significant role in the trafficking of the cargo destined to PR outer segments.

### *64.4.1 RPGR-Containing Protein Complexes*

The N-terminal region of RPGR also mediates majority of its interactions with other proteins. This domain interacts directly with RPGRIP1 (Boylan and Wright 2000; Roepman et al. 2000; Zhao et al. 2003), RPGRIP1L (Khanna et al. 2009), and structural maintenance of chromosomes 1 and 3 (SMC1 and SMC3) (Khanna et al. 2005). Moreover, RPGR exists as distinct multiprotein complexes with other ciliary proteins, including nephrocystin-1 (NPHP1), NPHP2, NPHP4, NPHP5, and CEP290/NPHP6, microtubule-based motor proteins, and intraflagellar transport protein (IFT88) in mammalian retina (Khanna et al. 2005; Otto et al. 2005; Chang et al. 2006; Murga-Zamalloa et al. 2010a, b; Anand and Khanna 2012; Rao et al. 2016d). The C-terminal domain of RPGR$^{ORF15}$ was also found to associate with whirlin (Wright et al. 2012), another ciliary protein mutated in Usher syndrome

(characterized by congenital deafness and RP) (Ebermann et al. 2007), although the physiological relevance of this interaction remains to be established.

All RPGR-associated proteins identified to date are mutated in ciliary diseases that include PR degeneration as a common manifestation. These findings indicate that RPGR plays a wider role in regulating the function of cilia, likely by facilitating the assembly of ciliary protein complexes at the PR connecting cilium.

### *64.4.2 RPGR as a "Gatekeeper"*

The localization of RPGR at the connecting cilium (presumed "gate" to the outer segments) of the PRs and its involvement in modulating cargo trafficking begged the question: does the loss of RPGR affect the composition of the photoreceptor outer segments? To answer this, proteomic analysis of the isolated PR outer segment (or PR sensory cilium) of the *Rpgr*$^{ko}$ mice was performed and compared to the wild-type proteome (Rao et al. 2015). Furthermore, two different stages prior to the onset of any detectable functional or structural deficit were selected. The analysis revealed that RPGR loss does not affect the abundance of key structural and phototransduction proteins in the outer segments. However, major alterations in the levels of proteasomal components, small GTPases involved in vesicular trafficking, and high-molecular-weight soluble proteins in the outer segments were detected in the *Rpgr*$^{ko}$ outer segments. The small GTPases whose levels were most affected in the *Rpgr*$^{ko}$ sensory cilium were IQGAPs (IQ-domain containing GTPase-activating proteins), which are involved, among other pathways, in actin cytoskeletal dynamics. Although the molecular mechanisms underlying these observations need to be further investigated, it is becoming increasingly clear that loss of RPGR results in subtle yet significant defects that accumulate the insult over time in the PRs, leading to their dysfunction and degeneration.

## 64.5 RPGR Isoforms

We are now beginning to understand the pathways in which RPGR may function. However, the precise role of its distinct isoforms is still unclear. Since the cloning of the *RPGR* gene in 1996 (Meindl et al. 1996; Roepman et al. 1996), a vast amount of evidence has been uncovered showing the complex patterns of its alternative splicing. Although there are more than 20 mRNA isoforms associated with *RPGR*, relatively fewer protein isoforms are detected in the retina (Kirschner et al. 1999; He et al. 2008). After further investigations into the expression of the two major isoforms, *RPGR*$^{const}$ and *RPGR*$^{ORF15}$, it was postulated that *RPGR*$^{ORF15}$ shows a retina-restricted expression. This led to the hypothesis that the retina-restricted clinical manifestation due to *RPGR* mutations is because of the differential expression pattern of *RPGR*$^{ORF15}$. However, subsequent studies have shown that the expression of

RPGR$^{ORF15}$ RNA and protein can be detected in the vertebrate kidneys, brain, as well as fibroblasts (Ghosh et al. 2010) (HK, unpublished observations). Thus, further investigations into the function of RPGR isoforms and their tissue-specific roles are needed.

Although the expression of both *RPGR$^{const}$* and *RPGR$^{ORF15}$* isoforms has been examined in detail, the differences in their function and their involvement in regulating photoreceptor health are not completely understood. All known *RPGR* mutations have been identified in exons 1–15 or in exon ORF15. No mutations in exons 16–19 (specific to *RPGR$^{const}$*) have been identified. These observations suggest that mutations in *RPGR* exons 16–19 are critical for the survival of the organism. An alternate hypothesis is that mutations in these exons are indispensable for RPGR function. However, evolutionary conservation and continued expression of the RPGR$^{const}$ isoform from early developmental stages to adults (Hong et al. 2000; Hong et al. 2003; He et al. 2008; Rao et al. 2016b, c, d), argue against such hypothesis. The reported *Rpgr* mutant mice (Hong et al. 2000; Huang et al. 2012) affect both isoforms, and the naturally occurring mouse and canine models carry mutations in exon ORF15 (Zhang et al. 2002). Thus, the specific effect of the loss of *RPGR$^{const}$* could not be delineated in vivo. Nonetheless, biochemical analyses of the RPGR isoforms revealed interesting clues to the role of RPGR in photoreceptors. The next section discusses such studies.

### *64.5.1 RPGR$^{CONST}$ Isoform (1–815 Amino Acids)*

The C-terminal four amino acids of RPGR$^{const}$ (812CTIL815) resemble the CaaX motif, where C is cysteine, A is any aliphatic amino acid, and X is usually leucine (L), methionine (M), or phenylalanine (F). This motif is involved in the prenylation of the protein, which is a posttranslational modification that allows membrane association and protein trafficking (Glomset and Farnsworth 1994).

The first evidence for the prenylation of mouse RPGR$^{const}$ was obtained in 1998 when Anand Swaroop and colleagues used metabolic labeling in COS cells. They went on to show that CTIL motif is involved in the Golgi localization of mouse RPGR$^{const}$ in COS cells (Yan et al. 1998). Recent studies have independently validated that the $^{812}$CTIL$^{815}$ motif is indeed a site for isoprenylation. In addition, the CTIL motif is involved in the ciliary localization of RPGR$^{const}$ (Lee and Seo 2015; Rao et al. 2016b). Furthermore, protein-protein interaction analyses using mass spectrometry revealed that the RPGR-CTIL motif recruits prenyl-binding protein PDE6δ (delta subunit of phosphodiesterase 6) (Rao et al. 2016b), which shuttles prenylated cargo and assists in its release from the membrane at the target sites (Christiansen et al. 2011; Baehr 2014). Binding to PDE6δ ensures ciliary localization of RPGR$^{const}$ (Lee and Seo 2015; Rao et al. 2016b). Previous studies using purified proteins reported that PDE6δ binds to the N-terminus of RPGR (Watzlich et al. 2013). However, later studies using the cell culture platform led to the proposal that both N- and C-termini of RPGR could bind PDE6δ. This phenomenon was further

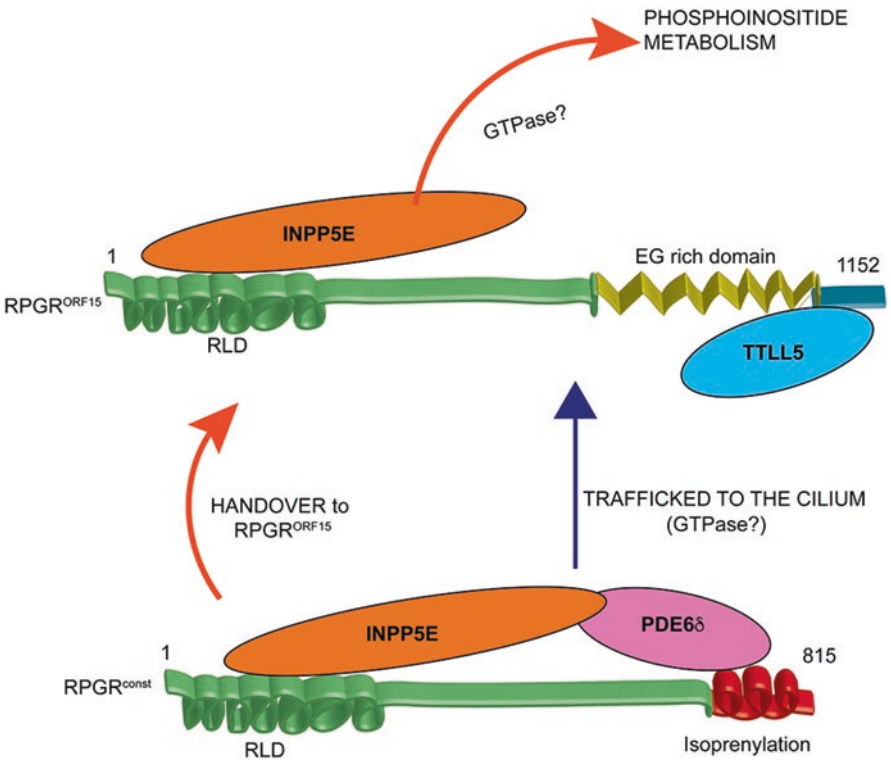


**Fig. 64.3** Schematic representation of the working model of RPGR-INPP5E interaction and the involvement of the major RPGR isoforms. The prenylated RPGR$^{const}$-INPP5E-PDE6D complex is trafficked to the cilium by an as-yet-unknown GTPase. At the cilium, the INPP5E cargo is handed over to the glutamylated RPGR$^{ORF15}$ isoform (by binding top TTLL5). The mechanism of this handover is still being investigated. The INPP5E cargo is then unloaded at the outer segment, where it modulates phosphoinositide metabolism

clarified when it was found that the N-terminus of RPGR interacts with a PDE6δ-interacting protein INPP5E (inositol polyphosphatase 5E) (Rao et al. 2016b). Taken together, although both N- and C-termini of RPGR$^{const}$ can bind to PDE6δ in vitro, the N-terminal site is unavailable to bind due to the binding of INPP5E in physiological conditions. A previous study showed that the knockdown of PDE6δ partly alters the ciliary localization of INPP5E (Humbert et al. 2012). Given RPGR-INPP5E-PDE6δ interaction, it is possible that INPP5E is potentially a cargo for the RPGR-PDE6δ complex and that both RPGR and PDE6δ assist in the ciliary trafficking of INPP5E in cells and PRs. As the N-terminus of RPGR$^{ORF15}$ can also bind INPP5E, it is possible that RPGR$^{const}$ hand over INPP5E to RPGR$^{ORF15}$ for delivery to the outer segment (Fig. 64.3).

What is the physiological relevance of RPGR-INPP5E interaction? Phosphoinositides are a class of membrane phospholipids that participate in diverse biological processes. These are generated from phosphatidylinositol (PtdIns) by

reversible phosphorylation of the inositol headgroup at positions 3, 4, and 5 and interconversion to different phospholipid species, which act as second messengers to mediate cellular responses (Di Paolo and De Camilli 2006). The bulk of PtdIns are represented by three lipids: PtdIns(4)P (PI4P), PtdIns(4,5)$P_2$ (PI45P2), and PtdIns(3,4,5)$P_3$ (PI345P3). The interconversions among these lipids and their localization are spatially regulated by PtdIns kinases and phosphatases (Vicinanza et al. 2008). For example, PI45P2 is found in the plasma membrane and is preferentially dephosphorylated by the 5-phosphatase INPP5E (inositol polyphosphatase 5E) or other phosphatases to PI4P as the membrane carrier translocates to the next compartment (Di Paolo and De Camilli 2006; Conduit et al. 2012; George et al. 2016). INPP5E can also act on PI345P3 to form PI34P2, which in turn regulates membrane protein content (Chavez et al. 2015; Garcia-Gonzalo et al. 2015). The deregulation of phosphoinositide metabolism is associated with ciliary dysfunction, as demonstrated by the association of *INPP5E* with ciliopathies such as Joubert syndrome and polycystic kidney disease (Bielas et al. 2009; Jacoby et al. 2009; Haim 2002). Moreover, loss of INPP5E modulates the lipid phosphoinositide levels of the ciliary membrane, which leads to ciliary dysfunction. (Conduit et al. 2012; Chavez et al. 2015; Garcia-Gonzalo et al. 2015). RPGR is involved in the ciliary trafficking of INPP5E in PRs, and that INPP5E levels are diminished in PR cilia in the absence of both isoforms of RPGR (Rao et al. 2016b). As INPP5E regulates phosphoinositide metabolism and is involved in facilitating ciliary function in PRs (Rajala et al. 2014; He et al. 2016), RPGR may assist in modulating the phosphoinositide content of the PRs.

### *64.5.2 RPGR$^{ORF15}$ Isoform (1–1152 Amino Acids)*

Although the *RPGR$^{ORF15}$* isoform contains less number of exons as compared to the *RPGR$^{const}$*, exon ORF15 is longer than the combined length of exons 16–19. This exon also has an unusual composition of purine-rich repeats, which encompass ~1.5 kb and encode for a protein domain of ~560 amino acids (rich in glutamic acids and glycines, Glu-Gly domain, EG domain). This domain is followed by a short stretch of basic amino acids, also called RPGR$^{C2}$ domain (1071–1152 amino acids) (Vervoort et al. 2000). Exon ORF15 of RPGR is a mutational hotspot. Majority of disease-causing mutations in this exon are predicted frameshift or nonsense changes (Vervoort et al. 2000). As discussed above, ORF15 mutations exhibit immense phenotypic variability. Studies using two canine models of *RPGR$^{ORF15}$* mutations postulated that the mutations in exon ORF15 that increase the acidity of the EG domain alter its solubility and are likely associated with a relatively severe phenotype (Zhang et al. 2002). Further studies are needed to validate this attractive hypothesis.

Due to the highly acidic nature of RPGR$^{ORF15}$, it has been very difficult to express recombinant RPGR$^{ORF15}$ for protein biochemistry experiments. Nonetheless, it was noted that the Glu-Gly domain of RPGR exhibits sequences like those of the poly-

glutamate regions of α-tubulin. Further investigations showed that RPGR$^{ORF15}$ is recognized by GT335, an antibody against the polyglutamated regions of α-tubulin (Rao et al. 2016a; Sun et al. 2016). Moreover, it was found that most of the GT335-associated staining of the PR connecting cilium was the result of GT335's reactivity to RPGR; the GT335-specific staining of the cilium was diminished in the *Rpgr*$^{ko}$ photoreceptors. Notably, human disease mutations in exon ORF15, which alter the polyglutamate content of the Glu-Gly domain exhibited, reduced to no recognition by GT335.

Although this study provided strong evidence that RPGR$^{ORF15}$ is glutamylated at the C-terminus, the mechanism by which RPGR$^{ORF15}$ is glutamylated was not clear. The scientific community did not have to wait for long for this answer. Around the same time, Antonina Roll-Mecak, Tiansen Li, and colleagues reported that RPGR$^{ORF15}$ glutamylation is regulated by tubulin-tyrosine ligase-like 5 (TTLL5) enzyme (Sun et al. 2016), which is mutated in human retinal degenerative diseases (Sergouniotis et al. 2014; Bedoni et al. 2016). Using human disease mutation analyses, they showed that TTLL5 specifically glutamylates RPGR$^{ORF15}$ and that the loss of TTLL5 mimics the loss of *Rpgr* in the mouse retina.

## 64.6 Concluding Remarks

Photoreceptors possess a unique sensory cilium in the form of light-sensing outer segments. The periodic shedding of the outer segment discs and renewal of the membranes and protein components demand stringent yet massive trafficking of the cargo via the connecting cilium. This involvement underscores the importance of the ciliary components that regulate the function of the connecting cilium (Young 1967, 1968; Besharse et al. 1977, 1985, 2003). Although we have significant understanding of the cilia assembly program, little is known about the maintenance of the cilium. Majority of the PR-associated diseases are due to the degeneration of PRs, in which the initial development of the PRs, the connecting cilium, and the outer segment is not affected. Subtle insults build up with age and lead to the dysfunction and degeneration of the PRs.

RPGR provides a unique opportunity to understand the degenerative processes of the PR sensory cilium. Evaluation of RPGR's association with other ciliary proteins and its involvement in regulating the trafficking of INPP5E to the outer segments will provide new information on the pathways that are deregulated during disease. Given that phosphoinositide metabolism is linked to actin cytoskeletal dynamics and autophagy in the PRs (Di Paolo and De Camilli 2006; George et al. 2016; He et al. 2016) and that the loss of RPGR alters the actin network in the retina, future investigations into these pathways will provide novel clues to the mechanisms of regulation of PR ciliary function and development of therapeutic intermediates. For developing early-stage therapeutic interventions, we still need to understand the molecular underpinnings of the disease and examine the mecha-

nisms underlying variable progression and severity of the disease in patients harboring *RPGR* mutations. Thus, we require a clearer understanding of the regulation of $RPGR^{const}$ and $RPGR^{ORF15}$ expression and function in the rod and cone PRs.

**Acknowledgments** The work in my laboratory is supported by grants from the National Institutes of Health (EY022372) and Foundation Fighting Blindness.

## References

Albert A, Alexander D, Boesze-Battaglia K (2016) Cholesterol in the rod outer segment: a complex role in a "simple" system. Chem Phys Lipids 199:94–105

Anand M, Khanna H (2012) Ciliary Transition Zone (TZ) proteins RPGR and CEP290: role in photoreceptor cilia and degenerative diseases. Expert Opin Ther Targets 16:541–551

Appelbaum T, Becker D, Santana E, Aguirre GD (2016) Molecular studies of phenotype variation in canine RPGR-XLPRA1. Mol Vis 22:319–331

Arnaiz O, Malinowska A, Klotz C, Sperling L, Dadlez M, Koll F, Cohen J (2009) Cildb: a knowledgebase for centrosomes and cilia. Database (Oxford) 2009:bap022

Ayyagari R, Demirci FY, Liu J, Bingham EL, Stringham H, Kakuk LE, Boehnke M, Gorin MB, Richards JE, Sieving PA (2002) X-linked recessive atrophic macular degeneration from RPGR mutation. Genomics 80:166–171

Badano JL, Mitsuma N, Beales PL, Katsanis N (2006) The ciliopathies: an emerging class of human genetic disorders. Annu Rev Genomics Hum Genet 7:125–148

Baehr W (2014) Membrane protein transport in photoreceptors: the function of PDEdelta: the Proctor lecture. Invest Ophthalmol Vis Sci 55:8653–8666

Barr F, Lambright DG (2010) Rab GEFs and GAPs. Curr Opin Cell Biol 22(4):461–470

Bassuk AG, Sujirakul T, Tsang SH, Mahajan VB (2014) A novel RPGR mutation masquerading as Stargardt disease. Br J Ophthalmol 98:709–711

Bedoni N et al (2016) Mutations in the polyglutamylase gene TTLL5, expressed in photoreceptor cells and spermatozoa, are associated with cone-rod degeneration and reduced male fertility. Hum Mol Genet 25(20):4546–4555

Beltran WA, Cideciyan AV, Lewin AS, Iwabe S, Khanna H, Sumaroka A, Chiodo VA, Fajardo DS, Roman AJ, Deng WT, Swider M, Aleman TS, Boye SL, Genini S, Swaroop A, Hauswirth WW, Jacobson SG, Aguirre GD (2012) Gene therapy rescues photoreceptor blindness in dogs and paves the way for treating human X-linked retinitis pigmentosa. Proc Natl Acad Sci U S A 109:2132–2137

Besharse JC, Hollyfield JG, Rayborn ME (1977) Photoreceptor outer segments: accelerated membrane renewal in rods after exposure to light. Science 196:536–538

Besharse JC, Forestner DM, Defoe DM (1985) Membrane assembly in retinal photoreceptors. III. Distinct membrane domains of the connecting cilium of developing rods. J Neurosci 5:1035–1048

Besharse JC, Baker SA, Luby-Phelps K, Pazour GJ (2003) Photoreceptor intersegmental transport and retinal degeneration: a conserved pathway common to motile and sensory cilia. Adv Exp Med Biol 533:157–164

Bielas SL et al (2009) Mutations in INPP5E, encoding inositol polyphosphate-5-phosphatase E, link phosphatidyl inositol signaling to the ciliopathies. Nat Genet 41:1032–1036

Boesze-Battaglia K, Damek-Poprawa M, Mitchell DC, Greeley L, Brush RS, Anderson RE, Richards MJ, Fliesler SJ (2008) Alteration of retinal rod outer segment membrane fluidity in a rat model of Smith-Lemli-Opitz syndrome. J Lipid Res 49:1488–1499

Boylan JP, Wright AF (2000) Identification of a novel protein interacting with RPGR. Hum Mol Genet 9:2085–2093

Branham K et al (2012) Mutations in RPGR and RP2 account for 15% of males with simplex retinal degenerative disease. Invest Ophthalmol Vis Sci 53:8232–8237

Breuer DK et al (2002) A comprehensive mutation analysis of RP2 and RPGR in a North American cohort of families with X-linked retinitis pigmentosa. Am J Hum Genet 70:1545–1554

Brunner S, Colman D, Travis AJ, Luhmann UF, Shi W, Feil S, Imsand C, Nelson J, Grimm C, Rulicke T, Fundele R, Neidhardt J, Berger W (2008) Overexpression of RPGR leads to male infertility in mice due to defects in flagellar assembly. Biol Reprod 79:608–617

Bukowy-Bieryllo Z, Zietkiewicz E, Loges NT, Wittmer M, Geremek M, Olbrich H, Fliegauf M, Voelkel K, Rutkiewicz E, Rutland J, Morgan L, Pogorzelski A, Martin J, Haan E, Berger W, Omran H, Witt M (2013) RPGR mutations might cause reduced orientation of respiratory cilia. Pediatr Pulmonol 48:352–363

Chang B, Khanna H, Hawes N, Jimeno D, He S, Lillo C, Parapuram SK, Cheng H, Scott A, Hurd RE, Sayer JA, Otto EA, Attanasio M, O'Toole JF, Jin G, Shou C, Hildebrandt F, Williams DS, Heckenlively JR, Swaroop A (2006) In-frame deletion in a novel centrosomal/ciliary protein CEP290/NPHP6 perturbs its interaction with RPGR and results in early-onset retinal degeneration in the rd16 mouse. Hum Mol Genet 15:1847–1857

Charng J, Cideciyan AV, Jacobson SG, Sumaroka A, Schwartz SB, Swider M, Roman AJ, Sheplock R, Anand M, Peden MC, Khanna H, Heon E, Wright AF, Swaroop A (2016) Variegated yet non-random rod and cone photoreceptor disease patterns in RPGR-ORF15-associated retinal degeneration. Hum Mol Genet 25(24):5444–5459

Chavez M, Ena S, Van Sande J, de Kerchove d'Exaerde A, Schurmans S, Schiffmann SN (2015) Modulation of ciliary phosphoinositide content regulates trafficking and sonic hedgehog signaling output. Dev Cell 34:338–350

Christiansen JR, Kolandaivelu S, Bergo MO, Ramamurthy V (2011) RAS-converting enzyme 1-mediated endoproteolysis is required for trafficking of rod phosphodiesterase 6 to photoreceptor outer segments. Proc Natl Acad Sci U S A 108:8862–8866

Churchill JD, Bowne SJ, Sullivan LS, Lewis RA, Wheaton DK, Birch DG, Branham KE, Heckenlively JR, Daiger SP (2013) Mutations in the X-linked retinitis pigmentosa genes RPGR and RP2 found in 8.5% of families with a provisional diagnosis of autosomal dominant retinitis pigmentosa. Invest Ophthalmol Vis Sci 54:1411–1416

Conduit SE, Dyson JM, Mitchell CA (2012) Inositol polyphosphate 5-phosphatases; new players in the regulation of cilia and ciliopathies. FEBS Lett 586:2846–2857

Daiger SP (1996) RetNet. The Retinal Information Network. https://sph.uth.edu/retnet/ The University of Texas Health Science Center at Houston

Daiger SP, Bowne SJ, Sullivan LS (2007) Perspective on genes and mutations causing retinitis pigmentosa. Arch Ophthalmol 125:151–158

Demirci FY, Rigatti BW, Wen G, Radak AL, Mah TS, Baic CL, Traboulsi EI, Alitalo T, Ramser J, Gorin MB (2002) X-linked cone-rod dystrophy (locus COD1): identification of mutations in RPGR exon ORF15. Am J Hum Genet 70:1049–1053

Deng WT, Dyka FM, Dinculescu A, Li J, Zhu P, Chiodo VA, Boye SL, Conlon TJ, Erger K, Cossette T, Hauswirth WW (2015) Stability and safety of an AAV vector for treating RPGR-ORF15 X-linked retinitis pigmentosa. Hum Gene Ther 26:593–602

Deretic D (2013) Crosstalk of Arf and Rab GTPases en route to cilia. Small GTPases 4:70–77

Deretic D, Huber LA, Ransom N, Mancini M, Simons K, Papermaster DS (1995) Rab8 in retinal photoreceptors may participate in rhodopsin transport and in rod outer segment disk morphogenesis. J Cell Sci 108(Pt 1):215–224

Di Paolo G, De Camilli P (2006) Phosphoinositides in cell regulation and membrane dynamics. Nature 443:651–657

Ebenezer ND, Michaelides M, Jenkins SA, Audo I, Webster AR, Cheetham ME, Stockman A, Maher ER, Ainsworth JR, Yates JR, Bradshaw K, Holder GE, Moore AT, Hardcastle AJ (2005) Identification of novel RPGR ORF15 mutations in X-linked progressive cone-rod dystrophy (XLCORD) families. Invest Ophthalmol Vis Sci 46:1891–1898

Ebermann I, Scholl HP, Charbel Issa P, Becirovic E, Lamprecht J, Jurklies B, Millan JM, Aller E, Mitter D, Bolz H (2007) A novel gene for Usher syndrome type 2: mutations in the long isoform of whirlin are associated with retinitis pigmentosa and sensorineural hearing loss. Hum Genet 121:203–211

Eggenschwiler JT, Anderson KV (2007) Cilia and developmental signaling. Annu Rev Cell Dev Biol 23:345–373

Estrada-Cuzcano A, Roepman R, Cremers FP, den Hollander AI, Mans DA (2012) Non-syndromic retinal ciliopathies: translating gene discovery into therapy. Hum Mol Genet 21:R111–R124

Fahim AT, Bowne SJ, Sullivan LS, Webb KD, Williams JT, Wheaton DK, Birch DG, Daiger SP (2011) Allelic heterogeneity and genetic modifier loci contribute to clinical variation in males with X-linked retinitis pigmentosa due to RPGR mutations. PLoS One 6:e23021

Fishman GA (1978) Retinitis pigmentosa. genetic percentages. Arch Ophthalmol 96:822–826

Garcia-Gonzalo FR, Phua SC, Roberson EC, Garcia G 3rd, Abedin M, Schurmans S, Inoue T, Reiter JF (2015) Phosphoinositides regulate ciliary protein trafficking to modulate hedgehog signaling. Dev Cell 34:400–409

George AA, Hayden S, Stanton GR, Brockerhoff SE (2016) Arf6 and the 5'phosphatase of synaptojanin 1 regulate autophagy in cone photoreceptors. BioEssays 38(Suppl 1):S119–S135

Gherman A, Davis EE, Katsanis N (2006) The ciliary proteome database: an integrated community resource for the genetic and functional dissection of cilia. Nat Genet 38:961–962

Ghosh AK, Murga-Zamalloa CA, Chan L, Hitchcock PF, Swaroop A, Khanna H (2010) Human retinopathy-associated ciliary protein retinitis pigmentosa GTPase regulator mediates cilia-dependent vertebrate development. Hum Mol Genet 19:90–98

Glomset JA, Farnsworth CC (1994) Role of protein modification reactions in programming interactions between ras-related GTPases and cell membranes. Annu Rev Cell Biol 10:181–205

Haim M (2002) Epidemiology of retinitis pigmentosa in Denmark. Acta Ophthalmologica Scand Suppl 223:1–34

He S, Parapuram SK, Hurd TW, Behnam B, Margolis B, Swaroop A, Khanna H (2008) Retinitis Pigmentosa GTPase Regulator (RPGR) protein isoforms in mammalian retina: insights into X-linked retinitis pigmentosa and associated ciliopathies. Vis Res 48:366–376

He F, Agosto MA, Anastassov IA, Tse DY, Wu SM, Wensel TG (2016) Phosphatidylinositol-3-phosphate is light-regulated and essential for survival in retinal rods. Sci Rep 6:26978

Heckenlively JR, Yoser SL, Friedman LH, Oversier JJ (1988) Clinical findings and common symptoms in retinitis pigmentosa. Am J Ophthalmol 105:504–511

Hildebrandt F, Benzing T, Katsanis N (2011) Ciliopathies. N Engl J Med 364:1533–1543

Hong DH, Pawlyk BS, Shang J, Sandberg MA, Berson EL, Li T (2000) A retinitis pigmentosa GTPase regulator (RPGR)-deficient mouse model for X-linked retinitis pigmentosa (RP3). Proc Natl Acad Sci U S A 97:3649–3654

Hong DH, Pawlyk B, Sokolov M, Strissel KJ, Yang J, Tulloch B, Wright AF, Arshavsky VY, Li T (2003) RPGR isoforms in photoreceptor connecting cilia and the transitional zone of motile cilia. Invest Ophthalmol Vis Sci 44:2413–2421

Huang WC, Wright AF, Roman AJ, Cideciyan AV, Manson FD, Gewaily DY, Schwartz SB, Sadigh S, Limberis MP, Bell P, Wilson JM, Swaroop A, Jacobson SG (2012) RPGR-associated retinal degeneration in human X-linked RP and a murine model. Invest Ophthalmol Vis Sci 53:5594–5608

Humbert MC, Weihbrecht K, Searby CC, Li Y, Pope RM, Sheffield VC, Seo S (2012) ARL13B, PDE6D, and CEP164 form a functional network for INPP5E ciliary targeting. Proc Natl Acad Sci U S A 109:19691–19696

Iannaccone A, Wang X, Jablonski MM, Kuo SF, Baldi A, Cosgrove D, Morton CC, Swaroop A (2004) Increasing evidence for syndromic phenotypes associated with RPGR mutations. Am J Ophthalmol 137:785–786; author reply 786

Jacoby M, Cox JJ, Gayral S, Hampshire DJ, Ayub M, Blockmans M, Pernot E, Kisseleva MV, Compere P, Schiffmann SN, Gergely F, Riley JH, Perez-Morga D, Woods CG, Schurmans S (2009) INPP5E mutations cause primary cilium signaling defects, ciliary instability and ciliopathies in human and mouse. Nat Genet 41:1027–1031

Khanna H (2015) Photoreceptor sensory cilium: traversing the ciliary gate. Cell 4:674–686
Khanna H, Hurd TW, Lillo C, Shu X, Parapuram SK, He S, Akimoto M, Wright AF, Margolis B, Williams DS, Swaroop A (2005) RPGR-ORF15, which is mutated in retinitis pigmentosa, associates with SMC1, SMC3, and microtubule transport proteins. J Biol Chem 280:33580–33587
Khanna H et al (2009) A common allele in RPGRIP1L is a modifier of retinal degeneration in ciliopathies. Nat Genet 41:739–745
Kim J, Krishnaswami SR, Gleeson JG (2008) CEP290 interacts with the centriolar satellite component PCM-1 and is required for Rab8 localization to the primary cilium. Hum Mol Genet 17:3796–3805
Kirschner R, Rosenberg T, Schultz-Heienbrok R, Lenzner S, Feil S, Roepman R, Cremers FP, Ropers HH, Berger W (1999) RPGR transcription studies in mouse and human tissues reveal a retina-specific isoform that is disrupted in a patient with X-linked retinitis pigmentosa. Hum Mol Genet 8:1571–1578
Koenekoop RK, Loyer M, Hand CK, Al Mahdi H, Dembinska O, Beneish R, Racine J, Rouleau GA (2003) Novel RPGR mutations with distinct retinitis pigmentosa phenotypes in French-Canadian families. Am J Ophthalmol 136:678–687
Lee JJ, Seo S (2015) PDE6D binds to the C-terminus of RPGR in a prenylation-dependent manner. EMBO Rep 16(12):1581–1582
Li L, Khan N, Hurd T, Ghosh AK, Cheng C, Molday R, Heckenlively JR, Swaroop A, Khanna H (2013) Ablation of the X-linked retinitis pigmentosa 2 (Rp2) gene in mice results in opsin mislocalization and photoreceptor degeneration. Invest Ophthalmol Vis Sci 54:4503–4511
Mears AJ, Hiriyanna S, Vervoort R, Yashar B, Gieser L, Fahrner S, Daiger SP, Heckenlively JR, Sieving PA, Wright AF, Swaroop A (2000) Remapping of the RP15 locus for X-linked cone-rod degeneration to Xp11.4-p21.1, and identification of a de novo insertion in the RPGR exon ORF15. Am J Hum Genet 67:1000–1003
Meindl A, Dry K, Herrmann K, Manson F, Ciccodicola A, Edgar A, Carvalho MR, Achatz H, Hellebrand H, Lennon A, Migliaccio C, Porter K, Zrenner E, Bird A, Jay M, Lorenz B, Wittwer B, D'Urso M, Meitinger T, Wright A (1996) A gene (RPGR) with homology to the RCC1 guanine nucleotide exchange factor is mutated in X-linked retinitis pigmentosa (RP3). Nat Genet 13:35–42
Moritz OL, Tam BM, Hurd LL, Peranen J, Deretic D, Papermaster DS (2001) Mutant rab8 impairs docking and fusion of rhodopsin-bearing post-Golgi membranes and causes cell death of transgenic Xenopus rods. Mol Biol Cell 12:2341–2351
Murga-Zamalloa C, Swaroop A, Khanna H (2010a) Multiprotein complexes of retinitis Pigmentosa GTPase Regulator (RPGR), a ciliary protein mutated in X-Linked Retinitis Pigmentosa (XLRP). Adv Exp Med Biol 664:105–114
Murga-Zamalloa CA, Desai NJ, Hildebrandt F, Khanna H (2010b) Interaction of ciliary disease protein retinitis pigmentosa GTPase regulator with nephronophthisis-associated proteins in mammalian retinas. Mol Vis 16:1373–1381
Murga-Zamalloa CA, Atkins SJ, Peranen J, Swaroop A, Khanna H (2010c) Interaction of retinitis pigmentosa GTPase regulator (RPGR) with RAB8A GTPase: implications for cilia dysfunction and photoreceptor degeneration. Hum Mol Genet 19:3591–3598
Nachury MV, Loktev AV, Zhang Q, Westlake CJ, Peranen J, Merdes A, Slusarski DC, Scheller RH, Bazan JF, Sheffield VC, Jackson PK (2007) A core complex of BBS proteins cooperates with the GTPase Rab8 to promote ciliary membrane biogenesis. Cell 129:1201–1213
Otto EA et al (2005) Nephrocystin-5, a ciliary IQ domain protein, is mutated in Senior-Loken syndrome and interacts with RPGR and calmodulin. Nat Genet 37:282–288
Pawlyk BS, Bulgakov OV, Sun X, Adamian M, Shu X, Smith AJ, Berson EL, Ali RR, Khani S, Wright AF, Sandberg MA, Li T (2015) Photoreceptor rescue by an abbreviated human RPGR gene in a murine model of X-linked retinitis pigmentosa. Gene Ther 23(2):196
Pazour GJ, Baker SA, Deane JA, Cole DG, Dickert BL, Rosenbaum JL, Witman GB, Besharse JC (2002) The intraflagellar transport protein, IFT88, is essential for vertebrate photoreceptor assembly and maintenance. J Cell Biol 157:103–113

Pearring JN, Salinas RY, Baker SA, Arshavsky VY (2013) Protein sorting, targeting and trafficking in photoreceptor cells. Prog Retin Eye Res 36:24–51

Rajala RV, Rajala A, Morris AJ, Anderson RE (2014) Phosphoinositides: minor lipids make a major impact on photoreceptor cell functions. Sci Rep 4:5463

Rao KN, Khanna H (2015) Role of small GTPases in polarized vesicle transport to primary cilium. Res Rep Biol 6:17–24

Rao KN, Li L, Anand M, Khanna H (2015) Ablation of retinal ciliopathy protein RPGR results in altered photoreceptor ciliary composition. Sci Rep 5:11137

Rao KN, Anand M, Khanna H (2016a) The carboxyl terminal mutational hotspot of the ciliary disease protein RPGRORF15 (retinitis pigmentosa GTPase regulator) is glutamylated in vivo. Biol Open 5:424–428

Rao KN, Zhang W, Li L, Anand M, Khanna H (2016b) Prenylated retinal ciliopathy protein RPGR interacts with PDE6delta and regulates ciliary localization of Joubert syndrome-associated protein INPP5E. Hum Mol Genet 25(20):4533–4545

Rao KN, Li L, Zhang W, Brush RS, Rajala RV, Khanna H (2016c) Loss of human disease protein retinitis pigmentosa GTPase regulator (RPGR) differentially affects rod or cone-enriched retina. Hum Mol Genet 25:1345–1356

Rao KN, Zhang W, Li L, Ronquillo C, Baehr W, Khanna H (2016d) Ciliopathy-associated protein CEP290 modifies the severity of retinal degeneration due to loss of RPGR. Hum Mol Genet 25:2005–2012

Renault L, Kuhlmann J, Henkel A, Wittinghofer A (2001) Structural basis for guanine nucleotide exchange on Ran by the Regulator of Chromosome Condensation (RCC1). Cell 105:245–255

Roepman R, van Duijnhoven G, Rosenberg T, Pinckers AJ, Bleeker-Wagemakers LM, Bergen AA, Post J, Beck A, Reinhardt R, Ropers HH, Cremers FP, Berger W (1996) Positional cloning of the gene for X-linked retinitis pigmentosa 3: homology with the guanine-nucleotide-exchange factor RCC1. Hum Mol Genet 5:1035–1041

Roepman R, Bernoud-Hubac N, Schick DE, Maugeri A, Berger W, Ropers HH, Cremers FP, Ferreira PA (2000) The retinitis pigmentosa GTPase regulator (RPGR) interacts with novel transport-like proteins in the outer segments of rod photoreceptors. Hum Mol Genet 9:2095–2105

Rozet JM, Perrault I, Gigarel N, Souied E, Ghazi I, Gerber S, Dufier JL, Munnich A, Kaplan J (2002) Dominant X linked retinitis pigmentosa is frequently accounted for by truncating mutations in exon ORF15 of the RPGR gene. J Med Genet 39:284–285

Sergouniotis PI, Chakarova C, Murphy C, Becker M, Lenassi E, Arno G, Lek M, MacArthur DG, Consortium UC-E, Bhattacharya SS, Moore AT, Holder GE, Robson AG, Wolfrum U, Webster AR, Plagnol V (2014) Biallelic variants in TTLL5, encoding a tubulin glutamylase, cause retinal dystrophy. Am J Hum Genet 94:760–769

Sharon D, Sandberg MA, Rabe VW, Stillberger M, Dryja TP, Berson EL (2003) RP2 and RPGR mutations and clinical correlations in patients with X-linked retinitis pigmentosa. Am J Hum Genet 73:1131–1146

Singla V, Reiter JF (2006) The primary cilium as the cell's antenna: signaling at a sensory organelle. Science 313:629–633

Souied E, Segues B, Ghazi I, Rozet JM, Chatelin S, Gerber S, Perrault I, Michel-Awad A, Briard ML, Plessis G, Dufier JL, Munnich A, Kaplan J (1997) Severe manifestations in carrier females in X linked retinitis pigmentosa. J Med Genet 34:793–797

Sun X, Park JH, Gumerson J, Wu Z, Swaroop A, Qian H, Roll-Mecak A, Li T (2016) Loss of RPGR glutamylation underlies the pathogenic mechanism of retinal dystrophy caused by TTLL5 mutations. Proc Natl Acad Sci U S A 113:E2925–E2934

Vervoort R, Lennon A, Bird AC, Tulloch B, Axton R, Miano MG, Meindl A, Meitinger T, Ciccodicola A, Wright AF (2000) Mutational hot spot within a new RPGR exon in X-linked retinitis pigmentosa. Nat Genet 25:462–466

Vicinanza M, D'Angelo G, Di Campli A, De Matteis MA (2008) Function and dysfunction of the PI system in membrane trafficking. EMBO J 27:2457–2470

Walia S, Fishman GA, Swaroop A, Branham KE, Lindeman M, Othman M, Weleber RG (2008) Discordant phenotypes in fraternal twins having an identical mutation in exon ORF15 of the RPGR gene. Arch Ophthalmol 126:379–384

Wang J, Deretic D (2014) Molecular complexes that direct rhodopsin transport to primary cilia. Prog Retin Eye Res 38:1–19

Watzlich D, Vetter I, Gotthardt K, Miertzschke M, Chen YX, Wittinghofer A, Ismail S (2013) The interplay between RPGR, PDEdelta and Arl2/3 regulate the ciliary targeting of farnesylated cargo. EMBO Rep 14:465–472

Wright RN, Hong DH, Perkins B (2012) RpgrORF15 connects to the usher protein network through direct interactions with multiple whirlin isoforms. Invest Ophthalmol Vis Sci 53:1519–1529

Wu DM, Khanna H, Atmaca-Sonmez P, Sieving PA, Branham K, Othman M, Swaroop A, Daiger SP, Heckenlively JR (2010) Long-term follow-up of a family with dominant X-linked retinitis pigmentosa. Eye (Lond) 24:764–774

Wu Z, Hiriyanna S, Qian H, Mookherjee S, Campos MM, Gao C, Fariss R, Sieving PA, Li T, Colosi P, Swaroop A (2015) A long-term efficacy study of gene replacement therapy for RPGR-associated retinal degeneration. Hum Mol Genet 24:3956–3970

Yan D, Swain PK, Breuer D, Tucker RM, Wu W, Fujita R, Rehemtulla A, Burke D, Swaroop A (1998) Biochemical characterization and subcellular localization of the mouse retinitis pigmentosa GTPase regulator (mRpgr). J Biol Chem 273:19656–19663

Young RW (1967) The renewal of photoreceptor cell outer segments. J Cell Biol 33:61–72

Young RW (1968) Passage of newly formed protein through the connecting cilium of retina rods in the frog. J Ultrastruct Res 23:462–473

Zahid S, Khan N, Branham K, Othman M, Karoukis AJ, Sharma N, Moncrief A, Mahmood MN, Sieving PA, Swaroop A, Heckenlively JR, Jayasundera T (2013) Phenotypic conservation in patients with X-linked retinitis pigmentosa caused by RPGR mutations. JAMA Ophthalmol 131:1016–1025

Zhang Q, Acland GM, Wu WX, Johnson JL, Pearce-Kelling S, Tulloch B, Vervoort R, Wright AF, Aguirre GD (2002) Different RPGR exon ORF15 mutations in Canids provide insights into photoreceptor cell degeneration. Hum Mol Genet 11:993–1003

Zhao Y, Hong DH, Pawlyk B, Yue G, Adamian M, Grynberg M, Godzik A, Li T (2003) The retinitis pigmentosa GTPase regulator (RPGR)- interacting protein: subserving RPGR function and participating in disk morphogenesis. Proc Natl Acad Sci U S A 100:3965–3970

Zito I, Downes SM, Patel RJ, Cheetham ME, Ebenezer ND, Jenkins SA, Bhattacharya SS, Webster AR, Holder GE, Bird AC, Bamiou DE, Hardcastle AJ (2003) RPGR mutation associated with retinitis pigmentosa, impaired hearing, and sinorespiratory infections. J Med Genet 40:609–615

# Chapter 65
# Polarized Exosome Release from the Retinal Pigmented Epithelium

**Mikael Klingeborn, W. Daniel Stamer, and Catherine Bowes Rickman**

**Abstract** The retinal pigmented epithelium (RPE) forms the outer blood-retinal barrier and provides nutrients and recycling of visual pigment to the photoreceptors, among many other functions. The RPE is also a key site of pathophysiological changes in age-related macular degeneration, making it an important focus of study in both visual health and disease. Exosomes are nanometer-sized vesicles that are released by cells in a controlled fashion and mediate a range of extra- and intercellular activities. Some key exosome actions include cell-cell communication, immune modulation, extracellular matrix turnover, stem cell division/differentiation, neovascularization, and cellular waste removal. While much is known about their role in cancer and cardiovascular disease, exosome function in the many specialized tissues of the eye is just beginning to undergo rigorous study. Here we review current knowledge of the functions and roles of exosomes and other small extracellular vesicles released from the RPE. In particular, we discuss the potential role and importance of polarized exosome release from the RPE.

**Keywords** Retinal pigmented epithelium · RPE · Polarized · Exosome · Extracellular vesicle · Age-related macular degeneration · AMD · Biomarker

M. Klingeborn (✉)
Department of Ophthalmology, Duke University, Durham, NC, USA
e-mail: mikael.klingeborn@duke.edu

W. D. Stamer
Department of Ophthalmology, Duke University, Durham, NC, USA

Department of Biomedical Engineering, Duke University, Durham, NC, USA

C. Bowes Rickman
Department of Ophthalmology, Duke University, Durham, NC, USA

Department of Cell Biology, Duke University, Durham, NC, USA



J. D. Ash et al. (eds.), *Retinal Degenerative Diseases*, Advances in Experimental Medicine and Biology 891, https://doi.org/10.1007/978-3-319-75402-4_65

## 65.1 Introduction

Exosomes are formed inside a specialized endosome called a multivesicular endosome (MVE) and are released into the extracellular milieu upon MVE fusion with the plasma membrane (Lo Cicero et al. 2015). For a more detailed description of exosome biogenesis and an overview of the diversity of different cargoes (e.g., lipids, proteins, DNA, RNA) found in exosomes, we refer you to the excellent recent review by Colombo and colleagues (Colombo et al. 2014). It has become increasingly clear that exosomes have specialized functions and play a key role in intercellular signaling and cellular waste management (van der Pol et al. 2012). Exosomes and other extracellular vesicles (EVs) released from the retinal pigmented epithelium (RPE) are likely involved in similar pathways. However, presently very little is known about these vesicles released from RPE. Exosomes make up the smallest-sized subset (ø ≈ 30–150 nm) of EVs (ø ≈ 30–1000 nm). Their biogenesis and extracellular release are distinct from other EVs such as larger microvesicles (ø ≈ 150–500 nm) that bud directly from the plasma membrane (Raposo and Stoorvogel 2013), blebs (ø ≈ 400–800 nm) (Marin-Castano et al. 2005), and apoptotic bodies (ø ≈ 800–5000 nm) (Hristov et al. 2004).

The cancer field, in particular, has taken the lead investigating exosomes and other EVs for novel approaches to therapy, new mechanistic understanding of tumorigenesis, tumor signaling, novel biomarkers, and modulation of metastasis (Dhondt et al. 2016; Lopatina et al. 2016; Srivastava et al. 2016). For example, modulation of extracellular matrix (ECM) by matrix metalloproteinases (MMPs), annexins, and proteoglycans on exosomes has been shown to increase metastasis (Hakulinen et al. 2008; Sakwe et al. 2011; Stepp et al. 2015; You et al. 2015). This ECM-modulating exosomal activity may also play an important role in eye diseases where pathological ECM remodeling of Bruch's membrane is an integral part of the disease mechanism, such as in age-related macular degeneration (AMD) (see Bowes Rickman et al. 2013).

## 65.2 Potential Role of Exosomes in Drusen and Sub-RPE Deposit Formation

Bruch's membrane (BrM) is a pentalaminar basement membrane complex abutting the basal side of the RPE and includes its basolateral cell membrane. It separates the RPE cell monolayer from a capillary bed of the systemic blood circulation (choriocapillaris) and thus plays a crucial role in mediating influx of oxygen, electrolytes, nutrients, and cytokines destined for the RPE and photoreceptors and efflux of waste products and signaling molecules (Curcio and Johnson 2013). The pathogenesis of early AMD is characterized by thickening of BrM due to lipid and protein buildup that leads to formation of sub-RPE deposits that occur as discrete accumulations, called drusen, which can be hard or soft, or as continuous accumulations of basal linear deposits. The lipid buildup is thought to primarily interfere with the

fluid efflux from the RPE across BrM, thereby inflicting stress on the RPE (Curcio and Johnson 2013). Cells under stress are known to increase the release of membranous vesicles including exosomes (King et al. 2012), and this has also been suggested to be the case in RPE cells (Atienzar-Aroca et al. 2016). Thus, it is possible that this process is in part responsible for the deposits in the sub-RPE region.

Interestingly, several proteins found in drusen and sub-RPE deposits, such as annexins, CD63, enolase, and ATP synthase, are known features of exosomes and other EVs (Hageman and Mullins 1999; Hageman et al. 1999; Mullins et al. 2000; Olver and Vidal 2007; Wang et al. 2009a, b, 2010), supporting an exosomal origin for some drusen components. Furthermore, a recent study revealed an interesting role for apolipoprotein E (ApoE) and exosomes in regulating pigment granule formation and processing in pigmented cells (van Niel et al. 2015). Perturbation of this pathway in RPE cells may be relevant for AMD since ApoE is one of the major components found in drusen and sub-RPE deposits (Anderson et al. 2001).

A recent ex vivo study in porcine eyecups studied apical exosome release from the RPE and showed that it could be modulated by L-dopa stimulation (Locke et al. 2014). This drug-mediated modulation of exosome release supports the potential for therapeutic intervention in targeting the release of exosomes and other small EVs from the RPE. Furthermore, this study established that RPE-derived exosome release occurs in the eye and is not a cell culture artifact. However, the ex vivo and in situ models of exosome release from the RPE are not amenable to study basolaterally secreted exosomes. Thus, in the next section, we will discuss RPE cell culture models which can be used to study basolateral exosome release.

## 65.3 The Importance of Polarized Exosome Release from the RPE

Exosomes released from RPE cells under normal conditions are likely involved in cell-cell communication (on both the apical and basal sides) and lipid homeostasis. Studies have shown that exosomes released by stressed RPE exhibit changes in signaling phosphoproteins (Biasutto et al. 2013) and are coated with complement components (Wang et al. 2009a, b), including C5b-9 (Pilzer et al. 2005), suggesting exosomes play a role in modulating complement activation in the immediate extracellular milieu of the RPE cells. Although these studies support a role for RPE-derived exosomes in the AMD disease process, they were limited by several factors: the lack of *bona fide* RPE cell cultures (e.g. the use of ARPE-19 which is an RPE-*like* cell line, lacking many important hallmarks of RPE cells (Beebe 2013; Rizzolo 2014)), superficial exosome characterization, and most important, they did not use polarized RPE cultures grown on cell culture permeable supports (i.e. Transwell, ThinCert, Millicell, etc.). Culture of primary RPE cells on permeable supports is essential to study basolaterally released exosomes, which could be involved in basal deposit formation and intercellular and systemic signaling. A comprehensive characterization of EVs released basolaterally from RPE cells under normal and

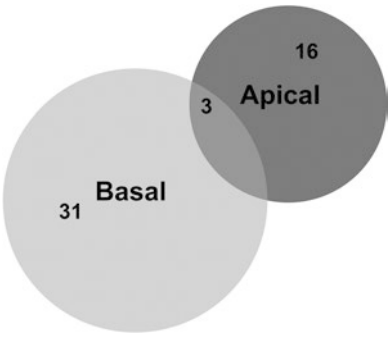


**Fig. 65.1** A Venn diagram showing that exosomal proteins highly co-enriched (within twofold order of magnitude) with the exosome-specific marker Syntenin-1 differ markedly between apically and basolaterally released exosomes in a polarized RPE cell culture model. Note that in these highly stringent exosome-specific proteome datasets, only three proteins (Syntenin-1, CD81, and ST13) are released in exosomes from both sides, emphasizing the exceptional directionality in EV release from polarized RPE monolayers (Klingeborn et al. 2016)

pathophysiological conditions is critical to elucidating the potential role of exosomes in the AMD disease process. Ongoing studies in our laboratory are aimed at addressing this current gap in the field by clarifying changes in the biology of EVs released both apically and basolaterally under conditions of RPE stress relevant to AMD pathophysiology. We performed a mass spectrometry-based proteomic analysis of apically and basolaterally RPE-derived EVs by quantitatively profiling hundreds of proteins in EV preparations of increasing purity. This approach, termed *protein correlation profiling* (PCP) (Andersen et al. 2003; Skiba et al. 2013), permits the analysis of any sub- or extracellular components/complexes that can be enriched by fractionation but not purified to homogeneity. PCP provides a powerful approach both to identify *bona fide* resident proteins and to exclude contaminating proteins from a proteomic dataset. To our surprise, we found that the vast majority of RPE-derived exosomal proteins differed between the apical and basolateral side (Klingeborn et al. 2016; see Fig. 65.1). We used co-enrichment with the exosome-specific marker Syntenin-1 as a benchmark for comparisons. In fact, only three proteins (Syntenin-1, CD81, and ST13) are found in both apical and basolateral proteomes; two of these, Syntenin-1 and CD81, are known exosome markers. Additional support for the importance of studying the polarized exosome release from RPE cells comes from a study showing that human RPE cells release the chaperone protein αB-crystallin in exosomes from their apical side but not on the basal side (Sreekumar et al. 2010).

These results emphasize the importance of studying exosomes released from both sides of polarized cell types since an apical-only approach risks missing important basolaterally released exosomal proteins. Perhaps even more troubling is the risk of mistakenly using findings in the apical RPE exosome proteome to guide research into basolateral-specific biological processes such as lipoprotein particle flux, waste disposal, and nutrient transport, all of which may play a role in sub-RPE deposit and drusen formation under pathological conditions (Curcio and Johnson

2013). The next step will be to study potential changes in the exosome protein cargo derived from RPE cells under conditions of stress relevant to the AMD disease process, such as photooxidative stress and dysregulation of lipid metabolism, to mention a few. Identified proteomic changes may result in novel targets for therapy.

## 65.4 Conclusions and Future Considerations

The source/process of protein and lipid deposition in the sub-RPE region in BrM and subsequent pathognomonic drusen formation in AMD remain unclear. Progress toward understanding deposit formation, accumulation, and biophysical properties of protein plus lipid aggregates should provide novel targets for therapeutic intervention. Using exosomes as biomarkers, therapeutic vehicles, or to modulate their function, release and uptake; holds the potential to lead to treatments for patients with AMD and other diseases of the outer retina.

## References

Andersen JS, Wilkinson CJ, Mayor T et al (2003) Proteomic characterization of the human centrosome by protein correlation profiling. Nature 426:570–574

Anderson DH, Ozaki S, Nealon M et al (2001) Local cellular sources of apolipoprotein E in the human retina and retinal pigmented epithelium: implications for the process of drusen formation. Am J Ophthalmol 131:767–781

Atienzar-Aroca S, Flores-Bellver M, Serrano-Heras G et al (2016) Oxidative stress in retinal pigment epithelium cells increases exosome secretion and promotes angiogenesis in endothelial cells. J Cell Mol Med 20(8):1457–1466

Beebe DC (2013) The use of cell lines to "model" ocular tissues: cautionary tales. Investigative ophthalmology & visual science. 54(8):5720

Biasutto L, Chiechi A, Couch R et al (2013) Retinal pigment epithelium (RPE) exosomes contain signaling phosphoproteins affected by oxidative stress. Exp Cell Res 319:2113–2123

Bowes Rickman C, Farsiu S, Toth CA et al (2013) Dry age-related macular degeneration: mechanisms, therapeutic targets, and imaging. Invest Ophthalmol Vis Sci 54:ORSF68–ORSF80

Colombo M, Raposo G, Thery C (2014) Biogenesis, secretion, and intercellular interactions of exosomes and other extracellular vesicles. Annu Rev Cell Dev Biol 30:255–289

Curcio CA, Johnson M (2013) Structure, function, and pathology of Bruch's membrane. In: Ryan SJ (ed) Retina, 5th edn. Elsevier: Philadelphia, 465–81

Dhondt B, Rousseau Q, De Wever O et al (2016) Function of extracellular vesicle-associated miRNAs in metastasis. Cell Tissue Res 365(3):621–641

Hageman GS, Mullins RF (1999) Molecular composition of drusen as related to substructural phenotype. Mol Vis 5:28

Hageman GS, Mullins RF, Russell SR et al (1999) Vitronectin is a constituent of ocular drusen and the vitronectin gene is expressed in human retinal pigmented epithelial cells. FASEB J 13:477–484

Hakulinen J, Sankkila L, Sugiyama N et al (2008) Secretion of active membrane type 1 matrix metalloproteinase (MMP-14) into extracellular space in microvesicular exosomes. J Cell Biochem 105:1211–1218

Hristov M, Erl W, Linder S et al (2004) Apoptotic bodies from endothelial cells enhance the number and initiate the differentiation of human endothelial progenitor cells in vitro. Blood 104:2761–2766

King HW, Michael MZ, Gleadle JM (2012) Hypoxic enhancement of exosome release by breast cancer cells. BMC Cancer 12:421

Klingeborn M, Dismuke WM, Skiba NP et al (2017) Directional Exosome Proteomes Reflect Polarity-Specific Functions in Retinal Pigmented Epithelium Monolayers. Sci Rep. 7(1):4901

Lo Cicero A, Stahl PD, Raposo G (2015) Extracellular vesicles shuffling intercellular messages: for good or for bad. Curr Opin Cell Biol 35:69–77

Locke CJ, Congrove NR, Dismuke WM et al (2014) Controlled exosome release from the retinal pigment epithelium in situ. Exp Eye Res 129:1–4

Lopatina T, Gai C, Deregibus MC et al (2016) Cross talk between cancer and mesenchymal stem cells through extracellular vesicles carrying nucleic acids. Front Oncol 6:125

Marin-Castano ME, Csaky KG, Cousins SW (2005) Nonlethal oxidant injury to human retinal pigment epithelium cells causes cell membrane blebbing but decreased MMP-2 activity. Invest Ophthalmol Vis Sci 46:3331–3340

Mullins RF, Russell SR, Anderson DH et al (2000) Drusen associated with aging and age-related macular degeneration contain proteins common to extracellular deposits associated with atherosclerosis, elastosis, amyloidosis, and dense deposit disease. FASEB J 14:835–846

Olver C, Vidal M (2007) Proteomic analysis of secreted exosomes. Subcell Biochem 43:99–131

Pilzer D, Gasser O, Moskovich O et al (2005) Emission of membrane vesicles: roles in complement resistance, immunity and cancer. Springer Semin Immunopathol 27:375–387

Raposo G, Stoorvogel W (2013) Extracellular vesicles: exosomes, microvesicles, and friends. J Cell Biol 200:373–383

Rizzolo LJ (2014) Barrier properties of cultured retinal pigment epithelium. Exp Eye Res 126:16–26

Sakwe AM, Koumangoye R, Guillory B et al (2011) Annexin A6 contributes to the invasiveness of breast carcinoma cells by influencing the organization and localization of functional focal adhesions. Exp Cell Res 317:823–837

Skiba NP, Spencer WJ, Salinas RY et al (2013) Proteomic identification of unique photoreceptor disc components reveals the presence of PRCD, a protein linked to retinal degeneration. J Proteome Res 12:3010–3018

Sreekumar PG, Kannan R, Kitamura M et al (2010) alphaB crystallin is apically secreted within exosomes by polarized human retinal pigment epithelium and provides neuroprotection to adjacent cells. PLoS One 5:e12578

Srivastava A, Babu A, Filant J et al (2016) Exploitation of exosomes as nanocarriers for gene-, chemo-, and immune-therapy of cancer. J Biomed Nanotechnol 12:1159–1173

Stepp MA, Pal-Ghosh S, Tadvalkar G et al (2015) Syndecan-1 and its expanding list of contacts. Adv Wound Care (New Rochelle) 4:235–249

van der Pol E, Boing AN, Harrison P et al (2012) Classification, functions, and clinical relevance of extracellular vesicles. Pharmacol Rev 64:676–705

van Niel G, Bergam P, Di Cicco A et al (2015) Apolipoprotein E regulates amyloid formation within endosomes of pigment cells. Cell Rep 13:43–51

Wang AL, Lukas TJ, Yuan M et al (2009a) Autophagy and exosomes in the aged retinal pigment epithelium: possible relevance to drusen formation and age-related macular degeneration. PLoS One 4:e4160

Wang AL, Lukas TJ, Yuan M et al (2009b) Autophagy, exosomes and drusen formation in age-related macular degeneration. Autophagy 5:563–564

Wang L, Clark ME, Crossman DK et al (2010) Abundant lipid and protein components of drusen. PLoS One 5:e10329

You Y, Shan Y, Chen J et al (2015) Matrix metalloproteinase 13-containing exosomes promote nasopharyngeal carcinoma metastasis. Cancer Sci 106:1669–1677

# Chapter 66
# The Impact of Adherens and Tight Junctions on Physiological Function and Pathological Changes in the Retina


**Yang Kong, Jürgen K. Naggert, and Patsy M. Nishina**

**Abstract** The formation of solid tissues is not a simple aggregation of individual cells but rather an ordered assembly of cells connected by junctions. These junctions provide a diffusion barrier as well as mechanical support and a conduit for signalling changes in the environment to the cells. Cell junctions are functionally categorized as occluding (e.g. tight junctions, TJs), anchoring (e.g. adherens junctions, AJs) and communicating junctions (e.g. gap junctions). Each type of the cell junction is formed by protein complexes with extracellular domains and/or intracellular domains, which bind partners that provide scaffolding and signalling components. Cell junctions are ubiquitously expressed in multiple tissues and organs, including the retina. In the retina, their biological impact is not limited to regulating tissue growth and development. Disruption of the complexes mediates both congenital and postnatal pathogenesis. In this review, we will focus on cell junctions, specifically AJs and TJs in the external limiting membrane, in order to articulate their influence on pathophysiology of the retina.

**Keywords** Cell junction · Adherens junction · Tight junction · ELM · Retinal disorders · Therapeutic applications

Y. Kong
The Jackson Laboratory, Bar Harbor, ME, USA

The Graduate School of Biomedical Science and Engineering, University of Maine, Orono, ME, USA

J. K. Naggert · P. M. Nishina (✉)
The Jackson Laboratory, Bar Harbor, ME, USA
e-mail: patsy.nishina@jax.org



J. D. Ash et al. (eds.), *Retinal Degenerative Diseases*, Advances in Experimental Medicine and Biology 891, https://doi.org/10.1007/978-3-319-75402-4_66

## 66.1 Introduction

The growth and development of solid tissues and organs, as well as execution of their biological functions, rely on the precise coordination among individual cells. This coordination is mediated by contact and communication between cells and the microenvironment. Cell junctions, consisting of multiple protein complexes, govern the cell-cell contact, the communication and the interplay between cells and extracellular matrix. Specifically, cell junctions are extensively involved in a number of biological processes among cells within tissues, ranging from proliferation and migration, establishing polarity, and orchestration of solid tissue formation to diffusion of substances as well as signal transduction.

Cell junctions are functionally categorized as occluding (e.g. tight junctions, TJs), anchoring (e.g. adherens junctions, AJs) and communicating junctions (e.g. gap junctions) (Alberts et al. 2002). AJs, situated basally below TJs, provide a physical bridge between cells and stabilize them for forming tissues. TJs are predominantly located at the most apical domain between epithelial cells, which seal the paracellular space to form a selective barrier for diffusion of fluids and solutes (Niessen 2007). Gap junctions are a crucial channel for coupling the transduction of electrical and chemical signals between cells (Pereda 2014). All three types of cell junctions are known to be involved not only in tissue morphogenesis but also associated with multiple pathological changes, such as inflammation, autoimmune disturbances and cancer (Berx and van Roy 2009; El-Amraoui and Petit 2010). A classic example is the role of cell junction remodelling and subsequent loss of cell polarity in cells undergoing epithelial-mesenchymal transition, implicated in tissue development and oncogenesis (Lamouille et al. 2014).

This review will primarily focus on the contributions of AJs and TJs to retinal growth and development as well as the pathogenesis of retinopathies.

## 66.2 AJs and TJs in the Retina

TJs consist of two major structural units: the transmembrane and the intracellular scaffolding components. The transmembrane component contains claudin, occludin and junctional adhesion molecules, which span across the plasma membrane and link two adjacent cells via extracellular adhesion domains. Intracellular scaffolding components, the tight junction proteins, TJP1, TJP-2 and TJP-3, are required to tether additional transmembrane proteins (Anderson and Van Itallie 2009; Furuse 2010). Although AJs may vary in morphologic appearance across tissues, they usually contain two major categories of protein complexes, cadherin-catenin complexes and nectin-afadin complexes, which provide a physical intercellular association by connecting the cytoskeleton and cytoplasmic actin filaments of two neighbouring cells (Meng and Takeichi 2009). Both AJs and TJs are dynamically regulated (Green et al. 2010).

AJs and TJs are implicated in tissue morphogenesis as they both mediate intracellular signal transduction cascades necessary for normal development (Gumbiner

1996). For example, besides being a component of AJs, β-catenin is well known as a core component in the Wnt/β-catenin signalling pathway. Release of β-catenin from the AJs activates Wnt target genes (Brembeck et al. 2006; Heuberger and Birchmeier 2010). The crosstalk of TJ components with multiple signalling pathways has been extensively documented too (Matter and Balda 2003). TJP1, for instance, is capable of regulating tissue development and cell junction dynamics by its intracellular translocation (Gottardi et al. 1996; Sourisseau et al. 2006).

Furthermore, it has been reported that AJs play a profound role in regulating retinal growth and development in drosophila, from initiation of retinal development from neuroepithelium to determination of basal-apical polarity of retinal cells, controlling shape of photoreceptors, etc. (Tepass and Harris 2007). In terms of the function of TJs in the retina, previous studies showed that TJP1, acting as an intracellular signalling molecule, is critical to maintaining homeostasis of retinal pigment epithelial (RPE) cells and retinal morphology (Georgiadis et al. 2010). More importantly, disruptions of both AJs and TJs have been linked to various retinopathies. For instance, aberrant expression of AJ and TJ proteins was found to be associated with autosomal dominant retinitis pigmentosa in adult mice lacking rhodopsin (Campbell et al. 2006). Additionally, altered expressions of AJ- and TJ-associated molecules may undermine the retinal barriers, such as blood-retina barrier, disruption of which facilitates initiation and progression of diabetic retinopathy (Davidson et al. 2000; Forster 2008).

## 66.3 Cell Junctions and External Limiting Membrane (ELM) in Healthy and Sick Retinas

Conventionally, AJs and TJs are regarded as a "fence" that separates the basal and apical portions of the cell. Apart from the RPE, the ELM is a major site in the retina where both AJs and TJs are identifiable. Although the ELM appears as a distinct "membrane" observable by light microscopy or spectral domain optical coherence tomography (SD-OCT), it is actually comprised of continuous zonula adherens (ZA) and occludens junctional complexes between photoreceptor inner segments and the surrounding apical processes of the Müller glial cells or between Müller glial cells (Omri et al. 2010). The ELM functions to maintain retinal structural stability and serves as a permeable barrier to control diffusion of substances. It is reported that impairment of ELM integrity causes subretinal fluid accumulation, which may lead to macula oedema (Omri et al. 2010).

Further evidence that ELM morphology is correlated with certain inherited retinal disorders comes from studies of Stargardt disease, one of the most common forms of macular degeneration in juvenile patients. Stargardt disease is characterized by progressive vision loss due to death of photoreceptor cells. Clinical investigation revealed a thickened ELM as a notable SD-OCT feature in young patients (Burke et al. 2013; Lee et al. 2014).

Crumbs protein, another ELM-associated molecule, was initially identified as a determinant of cell polarity in drosophila (Tepass et al. 1990). Its role in regulating ZA junctions in the neuroretina has been established (Izaddoost et al. 2002). Molecular studies of patients with vision impairment identified mutations in the *Crumbs homologue 1* (*CRB1*) gene in human populations. *CRB1* variants cause autosomal recessive retinitis pigmentosa and Leber congenital amaurosis (Richard et al. 2006), a heterogeneous group of diseases characterized by severe loss of photoreceptor cells and retinal dystrophies. The mouse model, $Crb1^{rd8/rd8}$, which lacks functional CRB1, recapitulates clinical manifestations observed in human patients. Careful characterization of homozygous $Crb1^{rd8}$ mice revealed a loss of ELM integrity, which leads to displacement of photoreceptors and aberrant retinal morphology as focal adhesive support is lost (Mehalow et al. 2003).

Another noteworthy study showed that a defective ELM is also a major contributor to retinal dysplasia (rosette-like structure) in neural retinal leucine zipper (*Nrl*) knockout mice (Stuck et al. 2012). Interestingly, compared to CRB1, which acts as a cell junction-associated molecule, NRL is a critical transcription factor, governing the development of photoreceptors and determining their cell fate. Understanding how NRL and other proteins, which cause ELM fragmentation, affect phenotypic presentation and progression of retinal disorders will be important in defining pathologic mechanisms which can then in turn serve as therapeutic targets.

## 66.4 Manipulation of AJs and TJs on ELM for Clinical Applications

Given the great impact of AJs and TJs on retinal growth and development as well as the correlation of pathological changes at junctions with a variety of retinal disorders, a growing number of researchers have begun to explore clinical implications of AJ and TJ defects and approaches for therapeutic and diagnostic purposes. For instance, some clinical investigations suggest that ELM integrity is directly associated with visual function. Based on the SD-OCT observations, ELM integrity is considered a useful indicator for evaluating the efficacy of surgical procedures (Landa et al. 2012) and serves as a prognostic indicator to assess restoration of visual function post-treatment in a spectrum of retinal diseases, such as diabetic macular oedema, age-related macular degeneration, etc. (Shin et al. 2012; Chhablani et al. 2013).

From the therapeutic perspective, with the advent of cell-based therapies, stem cell-derived cell transplantation appears to provide a promising avenue for curing retinal degenerative diseases. However, a major issue for this type of treatment is the in situ integration of the grafts into recipients, that is, how to guarantee viability of the transplanted cells and optimize their functionality in hosts. For photoreceptor transplantation in the retina, it was found that disrupting ELM integrity either by pharmacological intervention or by genetic modification enhanced the integration of transplanted photoreceptor cells (West et al. 2008; Pearson et al. 2010), suggest-

ing that loss of ELM barrier promotes graft incorporation into recipient retinas. However, engraftment success depended strongly on the disease phenotype, and ELM integrity after transplantation was associated with better engraftment (Barber et al. 2013).

Taken together, it is evident that cell junctions, especially those located on the ELM, are a key element in influencing the course of both inherited and acquired retinal diseases. Modulating biological functions of cell adhesion molecules may have a potential value for clinical applications.

## 66.5 Conclusions and Future Directions

Cell junctions such as AJs and TJs play an indispensable role in growth and development of tissue and organs, including the retina. Disruption of junctional components may drive pathological changes, or alternatively, junctional components may respond to disease phenotypes, which amplify the pathogenesis of the diseases. Currently, the ELM provides the clearest example where abnormalities in cell junctions can be associated with or cause retinal diseases. Probing molecular features of cell junctions in the retina becomes both biologically and clinically informative as evidenced by the findings that ELM abnormalities by SD-OCT in retinal diseases can be used as diagnostic and prognostic indicators. In this regard, more investigations are needed to delineate the regulatory pathways that affect the formation and maturation of cell junctions in the retina and to unveil interacting molecules that act on cell junctions to influence retinal homeostasis and functions. Regulation of such cell adhesion molecules may provide an alternative approach to treating retinal disorders in which disruption of cell junctions contributes to disease. However, determining whether modification of morphological anomalies in the retina by controlling aberrant cell junctions will be accompanied by improvement of retinal functionality also requires additional investigations. Regardless, research on biological features and function of cell junctions in the retina and their pathology will expand our knowledge about these important structures in the retina, knowledge that is critical for rational design of therapeutic interventions.

**Acknowledgments** Our research on the external limiting membrane is funded by the National Eye Institute (R01 EY11996, R01 EY027305, R01 EY028561) and the National Cancer Institute Institutional Grant (P30 CA034196).

## References

Alberts B, Johnson A, Lewis J et al (2002) Cell junctions. In: Molecular biology of the cell, 4th edn. Garland Science, New York

Anderson JM, Van Itallie CM (2009) Physiology and function of the tight junction. Cold Spring Harb Perspect Biol 1:a002584

Barber AC, Hippert C, Duran Y et al (2013) Repair of the degenerate retina by photoreceptor transplantation. Proc Natl Acad Sci U S A 110:354–359
Berx G, van Roy F (2009) Involvement of members of the cadherin superfamily in cancer. Cold Spring Harb Perspect Biol 1:a003129
Brembeck FH, Rosario M, Birchmeier W (2006) Balancing cell adhesion and Wnt signaling, the key role of beta-catenin. Curr Opin Genet Dev 16:51–59
Burke TR, Yzer S, Zernant J et al (2013) Abnormality in the external limiting membrane in early Stargardt disease. Ophthalmic Genet 34:75–77
Campbell M, Humphries M, Kennan A et al (2006) Aberrant retinal tight junction and adherens junction protein expression in an animal model of autosomal dominant Retinitis pigmentosa: the Rho(−/−) mouse. Exp Eye Res 83:484–492
Chhablani J, Kim JS, Freeman WR et al (2013) Predictors of visual outcome in eyes with choroidal neovascularization secondary to age related macular degeneration treated with intravitreal bevacizumab monotherapy. Int J Ophthalmol 6:62–66
Davidson MK, Russ PK, Glick GG et al (2000) Reduced expression of the adherens junction protein cadherin-5 in a diabetic retina. Am J Ophthalmol 129:267–269
El-Amraoui A, Petit C (2010) Cadherins as targets for genetic diseases. Cold Spring Harb Perspect Biol 2:a003095
Forster C (2008) Tight junctions and the modulation of barrier function in disease. Histochem Cell Biol 130:55–70
Furuse M (2010) Molecular basis of the core structure of tight junctions. Cold Spring Harb Perspect Biol 2:a002907
Georgiadis A, Tschernutter M, Bainbridge JW et al (2010) The tight junction associated signalling proteins ZO-1 and ZONAB regulate retinal pigment epithelium homeostasis in mice. PLoS One 5:e15730
Gottardi CJ, Arpin M, Fanning AS et al (1996) The junction-associated protein, zonula occludens-1, localizes to the nucleus before the maturation and during the remodeling of cell-cell contacts. Proc Natl Acad Sci U S A 93:10779–10784
Green KJ, Getsios S, Troyanovsky S et al (2010) Intercellular junction assembly, dynamics, and homeostasis. Cold Spring Harb Perspect Biol 2:a000125
Gumbiner BM (1996) Cell adhesion: the molecular basis of tissue architecture and morphogenesis. Cell 84:345–357
Heuberger J, Birchmeier W (2010) Interplay of cadherin-mediated cell adhesion and canonical Wnt signaling. Cold Spring Harb Perspect Biol 2:a002915
Izaddoost S, Nam SC, Bhat MA et al (2002) Drosophila Crumbs is a positional cue in photoreceptor adherens junctions and rhabdomeres. Nature 416:178–183
Lamouille S, Xu J, Derynck R (2014) Molecular mechanisms of epithelial-mesenchymal transition. Nat Rev Mol Cell Biol 15:178–196
Landa G, Gentile RC, Garcia PM et al (2012) External limiting membrane and visual outcome in macular hole repair: spectral domain OCT analysis. Eye (Lond) 26:61–69
Lee W, Noupuu K, Oll M et al (2014) The external limiting membrane in early-onset Stargardt disease. Invest Ophthalmol Vis Sci 55:6139–6149
Matter K, Balda MS (2003) Signalling to and from tight junctions. Nat Rev Mol Cell Biol 4:225–236
Mehalow AK, Kameya S, Smith RS et al (2003) CRB1 is essential for external limiting membrane integrity and photoreceptor morphogenesis in the mammalian retina. Hum Mol Genet 12:2179–2189
Meng W, Takeichi M (2009) Adherens junction: molecular architecture and regulation. Cold Spring Harb Perspect Biol 1:a002899
Niessen CM (2007) Tight junctions/adherens junctions: basic structure and function. J Invest Dermatol 127:2525–2532
Omri S, Omri B, Savoldelli M et al (2010) The outer limiting membrane (OLM) revisited: clinical implications. Clin Ophthalmol 4:183–195

Pearson RA, Barber AC, West EL et al (2010) Targeted disruption of outer limiting membrane junctional proteins (Crb1 and ZO-1) increases integration of transplanted photoreceptor precursors into the adult wild-type and degenerating retina. Cell Transplant 19:487–503

Pereda AE (2014) Electrical synapses and their functional interactions with chemical synapses. Nat Rev Neurosci 15:250–263

Richard M, Roepman R, Aartsen WM et al (2006) Towards understanding CRUMBS function in retinal dystrophies. Hum Mol Genet 15 Spec No 2:R235–243

Shin HJ, Lee SH, Chung H et al (2012) Association between photoreceptor integrity and visual outcome in diabetic macular edema. Graefes Arch Clin Exp Ophthalmol 250:61–70

Sourisseau T, Georgiadis A, Tsapara A et al (2006) Regulation of PCNA and cyclin D1 expression and epithelial morphogenesis by the ZO-1-regulated transcription factor ZONAB/DbpA. Mol Cell Biol 26:2387–2398

Stuck MW, Conley SM, Naash MI (2012) Defects in the outer limiting membrane are associated with rosette development in the Nrl−/− retina. PLoS One 7:e32484

Tepass U, Harris KP (2007) Adherens junctions in Drosophila retinal morphogenesis. Trends Cell Biol 17:26–35

Tepass U, Theres C, Knust E (1990) Crumbs encodes an EGF-like protein expressed on apical membranes of Drosophila epithelial cells and required for organization of epithelia. Cell 61:787–799

West EL, Pearson RA, Tschernutter M et al (2008) Pharmacological disruption of the outer limiting membrane leads to increased retinal integration of transplanted photoreceptor precursors. Exp Eye Res 86:601–611

# Chapter 67
# TRPV4 Does Not Regulate the Distal Retinal Light Response


**Oleg Yarishkin, Tam T. T. Phuong, Monika Lakk, and David Križaj**

**Abstract** The transient receptor potential vanilloid isoform 4 (TRPV4) functions as polymodal transducer of swelling, heat, stretch, and lipid metabolites, is widely expressed across sensory tissues, and has been implicated in pressure sensing in vertebrate retinas. Although TRPV4 knockout mice exhibit a variety of mechanosensory, nociceptive, and thermo- and osmoregulatory phenotypes, it is not known whether the transmission of light-induced signals in the eye is affected by the loss of TRPV4. We utilized field potentials, a measure of rod and cone signaling, to determine whether TRPV4 impacts on the generation and/or transmission of the photoreceptor light response and neurotransmission. Luminance intensity-response relationships were acquired in anesthetized wild-type and TRPV4$^{-/-}$ mice and evaluated for peak amplitude and implicit time under scotopic and photopic conditions. We found that the morphology of the outer retina is unaffected by the ablation of the *Trpv4* gene. Calcium imaging of dissociated Müller glia showed that selective TRPV4 stimulation induces oscillatory calcium signals in adjacent rods. However, no differences in scotopic or photopic light-evoked signaling in the distal retina were observed in TRPV4-/- eyes, suggesting that TRPV4 signaling in healthy Müller cells does not modulate the transmission of light-evoked signals at rod and cone synapses.

**Keywords** TRPV4 · Müller glia · Photoreceptor

O. Yarishkin · T. T. T. Phuong · M. Lakk
Department of Ophthalmology & Visual Sciences, Moran Eye Institute, Salt Lake City, UT, USA

D. Križaj (✉)
Department of Ophthalmology & Visual Sciences, Moran Eye Institute, Salt Lake City, UT, USA

Department of Bioengineering, University of Utah, Salt Lake City, UT, USA

Department of Neurobiology & Anatomy, University of Utah, Salt Lake City, UT, USA
e-mail: david.krizaj@hsc.utah.edu



J. D. Ash et al. (eds.), *Retinal Degenerative Diseases*, Advances in Experimental Medicine and Biology 891, https://doi.org/10.1007/978-3-319-75402-4_67

## 67.1 Introduction

TRPV4 is a polymodal channel widely expressed across the vertebrate bone, cartilage, muscle, skin and internal organs (lung, bladder, heart, kidney, oviduct), and the brain where it functions as a dominant neuronal and glial volume sensor (White et al. 2016). Its prominent expression across auditory, nociceptive, thermosensitive, mechanosensitive, and visual pathways (White et al. 2016; Redmon et al. 2017) is suggestive of important functional roles in sensory signaling. The strong expression levels of TRPV4 mRNA/protein in the cornea (Mergler et al. 2012), ciliary body (Jo et al. 2016), trabecular meshwork (Ryskamp et al. 2016), lens (Shahidullah et al. 2012), and retina (Ryskamp et al. 2011) predict that this polymodal nonselective cation channel contributes to the regulation of aqueous fluid transport, accommodation, ocular pressure sensing, endocannabinoid signaling, and/or volume regulation in the eye (Krizaj et al. 2014; Krizaj 2016); however whether and what roles TRPV4 plays in visual signaling is unknown. Here, we show that TRPV4 activation in Müller cells, radial glia that play a key role in retinal volume regulation and transretinal propagation of calcium waves (Jo et al. 2015; Phuong et al. 2016), induces a calcium response in adjacent photoreceptors. Moreover, we tested the hypothesis that TRPV4 activation modulates the light response in the outer retina by recording field potentials in wild-type and TRPV4$^{-/-}$ mice under scotopic and photopic conditions.

## 67.2 Materials and Methods

### *67.2.1 Animals*

C57BL/6 J and TRPV4$^{-/-}$ mice were maintained in the university animal vivarium on a 12 h:12 h light-dark cycle and fed lab chow and water ad libitum. Animal handling and anesthetic procedures were approved by the University Institutional Animal Care committees and conform to National Institutes of Health guidelines. Intraocular pressure was elevated through injection of polystyrene microbeads, as described (Ryskamp et al. 2016).

### *67.2.2 Histology*

Immunohistochemical experiments were conducted as described (Renteria et al. 2005; Jo et al. 2015). The primary antibodies were LS-C94498 anti-TRPV4 (Lifespan Biosciences) which showed appropriate immunoblot molecular weight and did not label TRPV4$^{-/-}$ sections (Ryskamp et al. 2011, 2016; Jo et al. 2015, 2016) and glial fibrillary acidic protein (GFAP) (Sigma), a well established marker of retinal gliosis.

### *67.2.3 Electroretinographic Analysis*

Full-field ERGs were recorded as described (Duncan et al. 2006; Barabas et al. 2013). Briefly, 2–3-month-old C57BL/6 and TRPV4$^{-/-}$ mice were dark-adapted and anesthetized with ketamine/xylazine (90 mg/10 mg per kg body weight). The animals were placed on a heating pad, and a golden ERG electrode was placed on the cornea surface. Stimuli were in order of increasing luminance from 0.00025 to 79 cd.s/m$^2$ (scotopic) and from 2.5 to 79 cd.s/m$^2$ (photopic), and 2–12 traces were averaged. The photoflash unit was calibrated to deliver 2.5 cd.s/m$^2$ at 0 dB.

### *67.2.4 Calcium Imaging*

Calcium imaging followed the protocols described in Ryskamp et al. (2011; 2016).

## 67.3 Results

### *67.3.1 TRPV4 Is Localized to RGCs and Müller Glia*

To better visualize the radial Müller processes, we double-labeled retinal sections from hypertensive eyes in which IOP was elevated with microbead injections, for TRPV4 and the gliotic marker GFAP. Expression of the TRPV4 channel was prominent in retinal ganglion cell layer (RGCs; somata in Fig. 67.1a marked by arrows) and Müller perikarya in the inner nuclear layer (INL). TRPV4 was also expressed in the transverse processes of Müller cells within the IPL and ONL (marked by yellow arrowheads in Fig. 67.1a, b). Its expression in the ONL and OPL suggests a potential role in the modulation of photoreceptor function.

### *67.3.2 TRPV4 Activation of Müller Cells Elevates $[Ca^{2+}]_i$ in Adjacent Rod Photoreceptors*

Stimulation of dissociated Müller glia with the selective TRPV4 agonist GSK1016790A triggered $Ca^{2+}$ waves together with large sustained $[Ca^{2+}]_i$ elevations across the endfoot, cell body and the apical process (Fig. 67.2; also Ryskamp et al. 2014). Occasionally, a rod soma was located close to the glial processes, and we observed that passage of the glial $Ca^{2+}$ wave often correlated with $[Ca^{2+}]_i$ elevations within the photoreceptor (Fig. 67.2c, arrowhead). TRPV4-dependent calcium signals were never observed in rods that were apart from Müller cells. They were

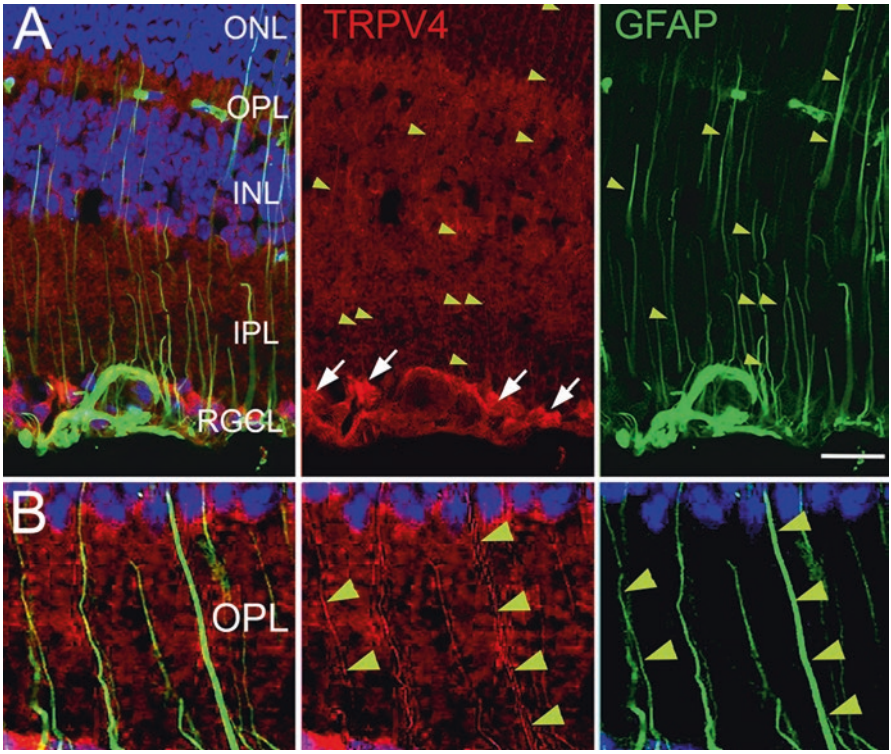


**Fig. 67.1** (**A**) TRPV4 in the hypertensive retina colocalizes with the gliotic marker GFAP. The TRPV4 antibody labels RGC somata (white arrows) and radial processes of Müller cells (yellow arrowheads). Scale bar = 20 um. (**B**) A higher-resolution image from another section

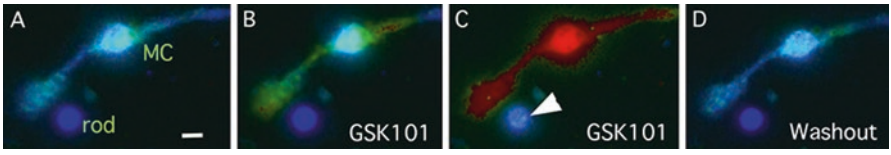


**Fig. 67.2** TRPV4-mediated calcium signals in Müller cell induced by the selective agonist GSK1016790A (GSK101) correlate with oscillatory increase in $[Ca^{2+}]_i$ in the nearby rod soma (white arrowhead). (**A**) Dissociated Müller cell (MC) and rod photoreceptor in control saline show low $[Ca^{2+}]_i$ levels. (**B**) GSK101 induces calcium wave propagation across Müller processes. (**C**) The $[Ca^{2+}]_i$ increase in the endfoot process correlates with transient oscillatory $[Ca^{2+}]_i$ elevations in the rod perikaryon (arrow). (**D**) Washout

typically transient and oscillatory, and disappeared upon agonist washout. We thus hypothesized that TRPV4-induced $Ca^{2+}$ signals drive the release of a neuroactive substance from Müller processes (e.g., Seminario-Vidal et al. 2011), which led us to test whether the channel plays a modulatory role in light-induced signaling.

### 67.3.3 Ablation of TRPV4 Has No Effect on the Amplitude and Kinetics of the Distal Light Response

Transmission of rod- and cone-mediated signals across the outer retina was evaluated with electroretinograms (ERGs) which represent the summed activity of photoreceptors and downstream bipolar cells (Masu et al. 1995; Barabas et al. 2013). We found that neither the kinetics nor sensitivity of ERG signals was altered in mice lacking TRPV4. Representative ERG traces of the scotopic light response are illustrated in Fig. 67.3a, and the cumulative average intensity-response data for a-wave and b-wave response components is shown in Fig. 67.1b, c. No obvious alterations in the amplitude and time course of a-wave, b-wave, and oscillatory potential components could be discerned in TRPV4 KO eyes. Photopic responses were induced by single flashes that followed 30 min light (30 cd s $m^{-2}$) adaptation. Signals consisted of a low-amplitude a-wave (at 15 dB; generated from the small number of mouse cones) that was followed by the fast, cone-driven photopic b-wave with time-to-peak latencies and peak amplitudes that were indistinguishable between control and TRPV4$^{-/-}$ animals. These results demonstrate that TRPV4 channels do not modulate the light response in the outer retina, neither directly through the hypothesized Müller glial "light response" (Rillich et al. 2009) nor indirectly via putative gliotransmitters, released by light from apical Müller cell processes.

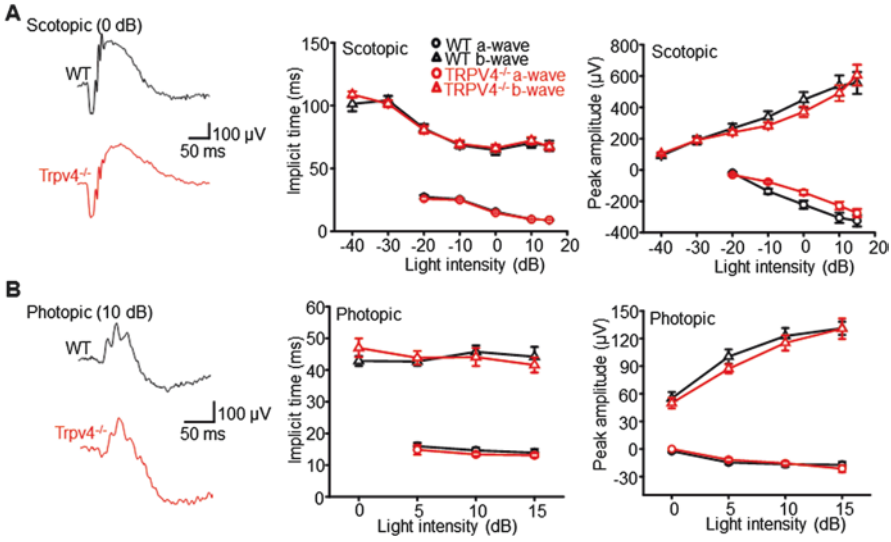


**Fig. 67.3** Ablation of TRPV4 has no effect on the onset kinetics, waveform, and amplitude of (**a**) scotopic and (**b**) photopic a- and b-waves. Wild-type (WT) traces are shown in black; TRPV4$^{-/-}$ traces are shown in red

## 67.4 Discussion

Although the phenotype of TRPV4$^{-/-}$ mice is mild compared to human mutations which may result in debilitating dysplasias and sensorimotor neuropathies (Nilius and Voets 2013), TRPV4$^{-/-}$ animals do show defective osmoregulation (White et al. 2016; Redmon et al. 2017), compromised mechanical and thermal hyperalgesia (Alessandri-Haber et al. 2004), nociception (Chen et al. 2007), visceral sensing (Brierley et al. 2008), and auditory transduction (Tabuchi et al. 2005). Here, we report that analysis of outer retinal light responses does not show any obvious visual signaling phenotypes in mouse retinas that lack TRPV4 channels. While this result might be anticipated given previous immunocytochemical localization of the channel to proximal retinal cell types that include RGCs and Müller glia (Ryskamp et al. 2015), photoreceptors could be influenced by TRPV4-induced $Ca^{2+}$-dependent gliotransmitter release from radial glial processes: (i) Müller cells were reported to sustain both vesicular and nonvesicular release of gliotransmitters ATP and glutamate (Slezak et al. 2012; Newman 2015); (ii) TRPV4 activation drives ATP release in other cell types (Seminario-Vidal et al. 2011); and (iii) preliminary evidence shown in Fig. 67.2 suggests that pharmacological activation of TRPV4 elicits small oscillatory $[Ca^{2+}]_i$ responses in adjacent, non-TRPV4-expressing photoreceptor cells. Nonetheless, the absence of observable ERG phenotype in TRPV4$^{-/-}$ eyes argues against a role for Müller glial TRPV4 channels in modulation of scotopic and photopic light responses in the healthy outer retina. The sensitivity, amplitude, and kinetics profiles of light-evoked ERG signals in TRPV4$^{-/-}$ eyes were indistinguishable from wild-type responses. We conclude that photoreceptor responses are not influenced by TRPV4-mediated gliotransmitter release under conditions that prevail in healthy retinas. However, recent reports suggest that TRPV4 activation in Müller glia could play more significant roles under pathological circumstances associated with retinal detachment, photoreceptor degeneration, ischemia, and increased intraocular pressure (Ryskamp et al. 2014; Taylor et al. 2016). Moreover, TRPV4 is likely to play important functions in pressure, stretch, temperature, and volume sensing in the inner retina, including modulation of the blood-retina barrier permeability, responsiveness of RGC dendrites to intraocular pressure, and force-dependent remodeling of the optic nerve head in diseases such as diabetic retinopathy, ischemia, and glaucoma (Ryskamp et al. 2011; Jo et al. 2015; Phuong et al. 2017; Krizaj 2016).

**Acknowledgments** This study was supported by the NIH (R01EY022076, R01EY027920, P30EY014800), the University of Utah Neuroscience Initiative, Glaucoma Research Foundation, the Willard Eccles Foundation, Glaucoma Research Foundation, the Diabetes and Metabolism Research Center at the University of Utah and unrestricted support from Research to Prevent Blindness to the Moran Eye Institute at the University of Utah.

## References

Alessandri-Haber N, Dina OA, Yeh JJ et al (2004) Transient receptor potential vanilloid 4 is essential in chemotherapy-induced neuropathic pain in the rat. J Neurosci 24:4444–4452

Barabas P, Liu A, Xing W et al (2013) Role of ELOVL4 and very long-chain polyunsaturated fatty acids in mouse models of Stargardt type 3 retinal degeneration. Proc Natl Acad Sci U S A 110:5181–5186

Brierley SM, Page AJ, Hughes PA et al (2008) Selective role for TRPV4 ion channels in visceral sensory pathways. Gastroenterology 134(7):2059–2069

Chen X, Alessandri-Haber N, Levine JD (2007) Marked attenuation of inflammatory mediator-induced C-fiber sensitization for mechanical and hypotonic stimuli in TRPV4$^{-/-}$ mice. Mol Pain 3:31

Duncan JL, Yang H, Doan T et al (2006) Scotopic visual signaling in the mouse retina is modulated by high-affinity plasma membrane calcium extrusion. J Neurosci 26:7201–7211

Jo AO, Ryskamp DA, Phuong TT, Verkman A, Yarishkin O, MacAulay N, Križaj D (2015) Synergistic signaling of TRPV4 and AQP4 channels is required for cell volume and calcium homeostasis regulation in retinal Müller glia. J Neurosci 35(39):13525–13537

Jo AO, Lakk M, Frye AM et al (2016) Differential volume regulation and calcium signaling in two ciliary body cell types is subserved by TRPV4 channels. Proc Natl Acad Sci U S A 113(14):3885–3890

Krizaj D (2016) Polymodal sensory integration in retinal ganglion cells. Adv Exp Med 854:693–698

Krizaj D, Ryskamp DA, Tian N et al (2014) From mechanosensitivity to inflammatory responses: new players in the pathology of glaucoma. Curr Eye Res 39:105–119

Masu M, Iwakabe H, Tagawa Y et al (1995) Specific deficit of the ON response in visual transmission by targeted disruption of the mGluR6 gene. Cell 80(5):757–765

Mergler S, Garreis F, Sahlmüller M et al (2012) Calcium regulation by thermo- and osmosensing transient receptor potential vanilloid channels (TRPVs) in human conjunctival epithelial cells. Histochem Cell Biol. 137:743–761

Newman EA (2015) Glial cell regulation of neuronal activity and blood flow in the retina by release of gliotransmitters. Philos Trans R Soc Lond Ser B Biol Sci 370:1672

Nilius B, Voets T (2013) The puzzle of TRPV4 channelopathies. EMBO Rep. 14:152-163

Phuong TT, Yarishkin O, Križaj D (2016) Subcellular propagation of calcium waves in Müller glia does not require autocrine/paracrine purinergic signaling. Channels 10:421–427

Phuong TTT, Redmon S, Yarishkin O et al (2017) The permeability of human retinal microvascular endothelial cells is modulated by TRPV4-dependent modulation of cytoskeletal and cell-cell adhesion proteins. *Journal of Physiology* 595: 6869–6885

Redmon SN, Shibasaki, Krizaj D (2017) Transient receptor potential cation channel subfamily V member 4. Encyclopedia of Signaling Molecules, 2nd Edition. Sangdun Choi, Ed.

Rentería RC, Strehler EE, Copenhagen DR et al. (2005) Ontogeny of plasma membrane Ca2+ ATPase isoforms in the neural retina of the postnatal rat. Vis Neurosci. 22:263–274

Rillich K, Gentsch J, Reichenbach A et al (2009) Light stimulation evokes two different calcium responses in Müller glial cells of the guinea pig retina. Eur J Neurosci 29:1165–1176

Ryskamp DA, Witkovsky P, Barabas P et al (2011) The polymodal ion channel transient receptor potential vanilloid 4 modulates calcium flux, spiking rate, and apoptosis of mouse retinal ganglion cells. J Neurosci 31:7089–7101

Ryskamp DA, Jo AO, Frye AM et al (2014) Swelling and eicosanoid metabolites differentially gate TRPV4 channels in retinal neurons and glia. J Neurosci 34:15689–15700

Ryskamp DA, Iuso A, Krizaj D (2015) TRPV4 channels link volume regulation, calcium homeostasis and inflammatory signaling in the retina. Channels 9:70–72

Ryskamp DA, Frye AM, Phuong TT et al (2016) TRPV4 regulates calcium homeostasis, cytoskeletal remodeling, conventional outflow and intraocular pressure in the mammalian eye. Sci Rep 6:30583

Seminario-Vidal L, Okada SF, Sesma JI et al (2011) Rho signaling regulates pannexin 1-mediated ATP release from airway epithelia. J Biol Chem 286:26277–26286

Slezak M, Grosche A, Niemiec A et al (2012) Relevance of exocytotic glutamate release from retinal glia. Neuron 74:504–516

Shahidullah M, Mandal A, Delamere NA (2012) TRPV4 in porcine lens epithelium regulates hemichannel-mediated ATP release and Na-K-ATPase activity. Am J Physiol Cell Physiol. 302:C1751–C1761

Tabuchi K, Suzuki M, Minzuno A et al (2005) Hearing impairment in TRPV4 knockout mice. Neurosci Lett 382:304–308

Taylor L, Arnér K, Ghosh F (2016) Specific inhibition of TRPV4 enhances retinal ganglion cell survival in adult porcine retinal explants. Exp Eye Res 154:10–21

White JP, Cibelli M, Urban L et al (2016) TRPV4: molecular conductor of a diverse orchestra. Physiol Rev 96:911–973

# Chapter 68
# Role of Sirtuins in Retinal Function Under Basal Conditions


**Jonathan B. Lin, Shunsuke Kubota, Raul Mostoslavsky, and Rajendra S. Apte**

**Abstract** Sirtuins are $NAD^+$-dependent enzymes that govern cellular homeostasis by regulating the acylation status of their diverse target proteins. We recently demonstrated that both rod and cone photoreceptors rely on NAMPT-mediated $NAD^+$ biosynthesis to meet their energetic requirements. Moreover, we found that this $NAD^+$-dependent retinal homeostasis relies, in part, on maintenance of optimal activity of the mitochondrial sirtuins and of SIRT3 in particular. Nonetheless, it is unknown whether other sirtuin family members also play important roles in retinal homeostasis. Our results suggest that SIRT1, SIRT2, SIRT4, and SIRT6 are dispensable for retinal survival at baseline, as individual deletion of each of these sirtuins does not cause retinal degeneration by fundus biomicroscopy or retinal dysfunction by ERG. These findings have significant implications and inform future

Jonathan B. Lin and Shunsuke Kubota contributed equally to this work.

J. B. Lin
Department of Ophthalmology & Visual Sciences, Washington University School of Medicine, St. Louis, MO, USA

Neuroscience Graduate Program, Division of Biology and Biomedical Sciences, Washington University School of Medicine, St. Louis, MO, USA

S. Kubota
Department of Ophthalmology & Visual Sciences, Washington University School of Medicine, St. Louis, MO, USA

R. Mostoslavsky
Massachusetts General Hospital Cancer Center, Harvard Medical School, Boston, MA, USA

R. S. Apte (✉)
Department of Ophthalmology & Visual Sciences, Washington University School of Medicine, St. Louis, MO, USA

Department of Developmental Biology, Washington University School of Medicine, St. Louis, MO, USA

Department of Medicine, Washington University School of Medicine, St. Louis, MO, USA
e-mail: apte@vision.wustl.edu



J. D. Ash et al. (eds.), *Retinal Degenerative Diseases*, Advances in Experimental Medicine and Biology 891, https://doi.org/10.1007/978-3-319-75402-4_68

studies investigating the mechanisms underlying the central role of $NAD^+$ biosynthesis in retinal survival and function.

**Keywords** Sirtuins · $NAD^+$ · Retinal degeneration · Neurodegeneration · Photoreceptors · Retina

## 68.1 Introduction

Sirtuins are $NAD^+$-dependent enzymes that are critically important for maintaining cellular homeostasis, especially under conditions of metabolic and nutritional stress. Mechanistically, sirtuins regulate cellular homeostasis by modifying the acylation status of their diverse target proteins. Since sirtuins require $NAD^+$ as a cosubstrate, their function is exquisitely dependent on $NAD^+$ availability (Imai et al. 2000; Verdin 2015). The sirtuin family includes numerous members, which localize to unique subcellular compartments: SIRT1 and SIRT2 are present in the nucleus and the cytoplasm (North and Verdin 2007; Tanno et al. 2007); SIRT6 is exclusively nuclear (Liszt et al. 2005); and SIRT3, SIRT4, and SIRT5 are present in the mitochondria (Schwer et al. 2002; Michishita et al. 2005). We recently demonstrated that NAMPT-mediated $NAD^+$ biosynthesis is essential for photoreceptor survival and vision and that SIRT3 and SIRT5 play important roles in retinal homeostasis (Lin et al. 2016). However, whether the other mitochondrial sirtuin SIRT4 and the nuclear/cytoplasmic sirtuins, SIRT1, SIRT2, and SIRT6, play important roles in retinal function under baseline conditions has not been adequately explored. Therefore, we examined the effect of deleting these individual sirtuins on retinal survival and function.

## 68.2 Materials and Methods

### *68.2.1 Animals*

All animal experiments were approved by the Animal Studies Committee and performed in accordance with the Washington University School of Medicine Animal Care and Use guidelines. We purchased floxed SIRT1 mice ($Sirt1^{F/F}$), $Sirt2^{-/-}$ mice, and $Sirt4^{-/-}$ mice, along with strain-matched controls, from Jackson Laboratory (Bar Harbor, ME). We received floxed SIRT6 mice ($Sirt6^{F/F}$) from Dr. Raul Mostoslavsky (Sebastian et al. 2012), rhodopsin-iCre75 transgenic mice from Dr. Ching-Kang Jason Chen (Li et al. 2005), and human red/green pigment-Cre (HRGP-Cre) transgenic mice from Dr. Yun Le (Le et al. 2004). We tested all mice by fundus biomicroscopy and electroretinography at roughly 2–3 months of

age. Whenever possible, we compared mice to littermate controls. We confirmed that all mice were negative for the *rd8* mutation of the *Crb1* gene (Mattapallil et al. 2012) by PCR.

### *68.2.2 Assessment of Retinal Structure and Function*

To assess retinal structure, we performed fundus biomicroscopy with the Micron III™ animal fundus camera (Phoenix Research Laboratories, Pleasanton, CA), as described previously (Lin et al. 2016). We examined multiple mice per genotype and present representative images. To assess retinal function, we performed electroretinography (ERG) with the UTAS-E3000 Visual Electrodiagnostic System running EM for Windows (LKC Technologies, Gaithersburg, MD), as described previously (Lin et al. 2016), testing at least three mice per genotype. For statistical analysis of the ERG data, we used GraphPad Prism version 5.0f (La Jolla, CA) to perform a mixed two-way ANOVA (within-subjects factor, flash intensity; between-subjects factor, genotype). We defined statistical significance as a p value $<0.05$.

## 68.3 Results

### *68.3.1 Deletion of* Sirt1, Sirt2, Sirt4, *or* Sirt6 *Does Not Cause Retinal Degeneration*

To determine whether deletion of individual sirtuins causes retinal degeneration, we assessed the fundus appearance of mice lacking various individual sirtuins, including rod photoreceptor-specific SIRT1 conditional knockout (*Sirt1*$^{-\text{rod}/-\text{rod}}$), cone photoreceptor-specific SIRT1 conditional knockout (*Sirt1*$^{-\text{cone}/-\text{cone}}$), SIRT2 germline knockout (*Sirt2*$^{-/-}$), SIRT4 germline knockout (*Sirt4*$^{-/-}$), rod photoreceptor-specific SIRT6 conditional knockout (*Sirt6*$^{-\text{rod}/-\text{rod}}$), and cone photoreceptor-specific SIRT6 conditional knockout (*Sirt6*$^{-\text{cone}/-\text{cone}}$) mice. We tested photoreceptor-specific conditional knockouts for SIRT1 and SIRT6 because SIRT1 germline knockouts on our desired inbred background die shortly after birth (McBurney et al. 2003) and SIRT6 germline knockouts have a severe neurodegenerative phenotype, dying around 4 weeks of age (Mostoslavsky et al. 2006). At 2–3 months of age, none of the mice we tested had any evidence of retinal degeneration from their fundus appearances (Fig. 68.1a–d). These findings suggest that SIRT1, SIRT2, SIRT4, and SIRT6 are dispensable for retinal survival at baseline.

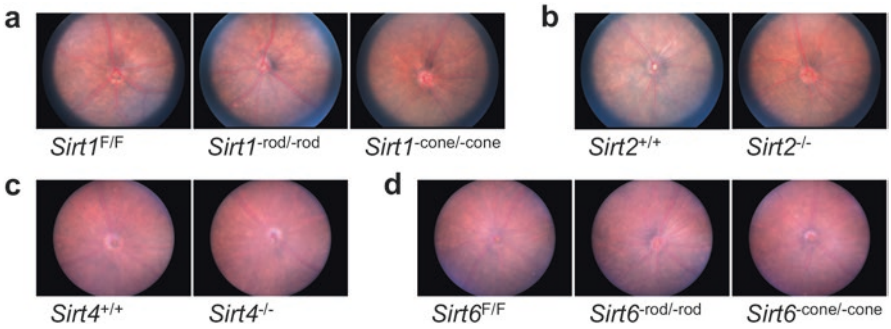


**Fig. 68.1** *Sirt1*$^{-rod/-rod}$ (**a**), *Sirt1*$^{-cone/-cone}$ (**a**), *Sirt2*$^{-/-}$ (**b**), *Sirt4*$^{-/-}$ (**c**), *Sirt6*$^{-rod/-rod}$ (**d**), and *Sirt6*$^{-cone/-cone}$ (**d**) mice all have normal-appearing fundi on retinal imaging at 2–3 months of age

### *68.3.2 Deletion of* Sirt1, Sirt2, Sirt4, *or* Sirt6 *Does Not Cause Retinal Dysfunction*

To determine whether deletion of individual sirtuins causes baseline retinal dysfunction, we also tested these mice with ERG. Consistent with the normal retinal appearances on fundus biomicroscopy, *Sirt1*$^{-rod/-rod}$, *Sirt1*$^{-cone/-cone}$, *Sirt2*$^{-/-}$, *Sirt4*$^{-/-}$, *Sirt6*$^{-rod/-rod}$, and *Sirt6*$^{-cone/-cone}$ mice all had normal retinal function at baseline at 2–3 months of age (Fig. 68.2a–d). Once again, these findings suggest that these sirtuins are not essential for retinal function under basal conditions.

## 68.4 Discussion

Sirtuins have been reported to play important functions in various mouse models of retinal disease (Shindler et al. 2007; Jaliffa et al. 2009; Chen et al. 2013; Zuo et al. 2013; Zeng and Yang 2015). However, we found that individual deletion of *Sirt1*, *Sirt2*, *Sirt4*, or *Sirt6* did not cause retinal degeneration as assessed by fundus biomicroscopy nor did it cause retinal dysfunction by ERG. These findings suggest that these sirtuins are individually dispensable under basal conditions. These findings are important, as we previously demonstrated that NAMPT-mediated $NAD^+$ biosynthesis is essential for retinal function and that SIRT3/SIRT5 may play important roles in $NAD^+$-dependent retinal homeostasis under conditions of stress (Lin et al. 2016). These results expand on our previous findings and clarify the role of various sirtuin family members in retinal survival and function.

Further studies are necessary to determine whether these sirtuins become essential under conditions of stress, such as in light-induced degeneration or in other models of retinal dysfunction or retinal disease, since sirtuin-deficient mice tend not to show severe phenotypes until challenged by metabolic perturbations such as

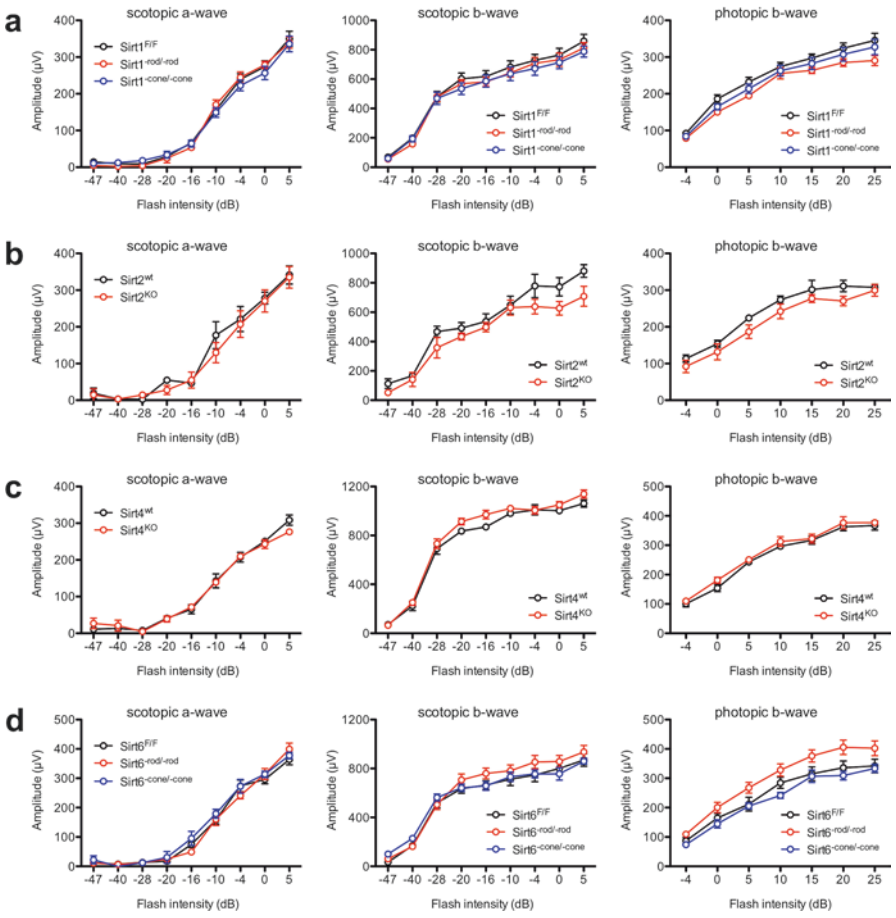


**Fig. 68.2** *Sirt1*$^{-\text{rod}/-\text{rod}}$ (**a**), *Sirt1*$^{-\text{cone}/-\text{cone}}$ (**a**), *Sirt2*$^{-/-}$ (**b**), *Sirt4*$^{-/-}$ (**c**), *Sirt6*$^{-\text{rod}/-\text{rod}}$ (**d**), and *Sirt6*$^{-\text{cone}/-\text{cone}}$ (**d**) mice all have normal scotopic and photopic retinal function by ERG at 2–3 months of age (N.S. by two-way mixed ANOVA). Graphs depict mean ± S.E.M (**a**–**d**)

fasting (Hirschey et al. 2011). Moreover, our experiments in rod- and cone-specific conditional knockouts do not rule out the possibility that SIRT1 and SIRT6 play important roles in non-photoreceptor retinal cells. Indeed, SIRT6 germline knockout mice exhibit retinal dysfunction on ERG by 3 weeks of age, which has been hypothesized to be related to an important role for SIRT6 in inner retinal cells, such as bipolar cells, Müller cells, or perhaps both (Silberman et al. 2014). Cumulatively, our results suggest that SIRT1, SIRT2, SIRT4, and SIRT6 are individually dispensable for retinal survival and function under basal conditions, although further studies are necessary to explore how they interact with one another and whether they become essential under disease conditions.

**Acknowledgments** This work was supported by NIH Grants R01 EY019287 (R.S.A.) and P30 EY02687 (Vision Core Grant); the C.M. and M.A. Reeves Foundation (R.S.A.); Research to Prevent Blindness (R.S.A.); the Hope Center (R.S.A.); the Lacy Foundation (S.K.); the Schulak Family Gift Fund for Retinal Research (R.S.A.); the Jeffrey Fort Innovation Fund (R.S.A.); and the Robert Machemer Foundation (S.K.). Additional funding comes from an unrestricted grant to the Department of Ophthalmology and Visual Sciences of Washington University School of Medicine from Research to Prevent Blindness. J.B.L. was supported by the Washington University in St. Louis Medical Scientist Training Program (NIH Grant T32 GM007200), the Washington University in St. Louis Institute of Clinical and Translational Sciences (NIH Grants UL1 TR000448, TL1 TR000449), the Washington University Diabetic Cardiovascular Disease Center, the American Federation for Aging Research, and the VitreoRetinal Surgery Foundation.

## References

Chen J, Michan S, Juan AM et al (2013) Neuronal sirtuin1 mediates retinal vascular regeneration in oxygen-induced ischemic retinopathy. Angiogenesis 16:985–992

Hirschey MD, Shimazu T, Jing E et al (2011) SIRT3 deficiency and mitochondrial protein hyperacetylation accelerate the development of the metabolic syndrome. Mol Cell 44:177–190

Imai S, Armstrong CM, Kaeberlein M et al (2000) Transcriptional silencing and longevity protein Sir2 is an NAD-dependent histone deacetylase. Nature 403:795–800

Jaliffa C, Ameqrane I, Dansault A et al (2009) Sirt1 involvement in rd10 mouse retinal degeneration. Invest Ophthalmol Vis Sci 50:3562–3572

Le YZ, Ash JD, Al-Ubaidi MR et al (2004) Targeted expression of Cre recombinase to cone photoreceptors in transgenic mice. Mol Vis 10:1011–1018

Li S, Chen D, Sauve Y et al (2005) Rhodopsin-iCre transgenic mouse line for Cre-mediated rod-specific gene targeting. Genesis 41:73–80

Lin JB, Kubota S, Ban N et al (2016) NAMPT-Mediated NAD(+) biosynthesis is essential for vision in mice. Cell Rep 17:69–85

Liszt G, Ford E, Kurtev M et al (2005) Mouse Sir2 homolog SIRT6 is a nuclear ADP-ribosyltransferase. J Biol Chem 280:21313–21320

Mattapallil MJ, Wawrousek EF, Chan CC et al (2012) The Rd8 mutation of the Crb1 gene is present in vendor lines of C57BL/6N mice and embryonic stem cells, and confounds ocular induced mutant phenotypes. Invest Ophthalmol Vis Sci 53:2921–2927

McBurney MW, Yang X, Jardine K et al (2003) The mammalian SIR2alpha protein has a role in embryogenesis and gametogenesis. Mol Cell Biol 23:38–54

Michishita E, Park JY, Burneskis JM et al (2005) Evolutionarily conserved and nonconserved cellular localizations and functions of human SIRT proteins. Mol Biol Cell 16:4623–4635

Mostoslavsky R, Chua KF, Lombard DB et al (2006) Genomic instability and aging-like phenotype in the absence of mammalian SIRT6. Cell 124:315–329

North BJ, Verdin E (2007) Interphase nucleo-cytoplasmic shuttling and localization of SIRT2 during mitosis. PLoS One 2:e784

Schwer B, North BJ, Frye RA et al (2002) The human silent information regulator (Sir)2 homologue hSIRT3 is a mitochondrial nicotinamide adenine dinucleotide-dependent deacetylase. J Cell Biol 158:647–657

Sebastian C, Zwaans BM, Silberman DM et al (2012) The histone deacetylase SIRT6 is a tumor suppressor that controls cancer metabolism. Cell 151:1185–1199

Shindler KS, Ventura E, Rex TS et al (2007) SIRT1 activation confers neuroprotection in experimental optic neuritis. Invest Ophthalmol Vis Sci 48:3602–3609

Silberman DM, Ross K, Sande PH et al (2014) SIRT6 is required for normal retinal function. PLoS One 9:e98831

Tanno M, Sakamoto J, Miura T et al (2007) Nucleocytoplasmic shuttling of the NAD+−dependent histone deacetylase SIRT1. J Biol Chem 282:6823–6832
Verdin E (2015) NAD(+) in aging, metabolism, and neurodegeneration. Science (New York, NY) 350:1208–1213
Zeng Y, Yang K (2015) Sirtuin 1 participates in the process of age-related retinal degeneration. Biochem Biophys Res Commun 468:167–172
Zuo L, Khan RS, Lee V et al (2013) SIRT1 promotes RGC survival and delays loss of function following optic nerve crush. Invest Ophthalmol Vis Sci 54:5097–5102

# Chapter 69
# The Retinol-Binding Protein Receptor 2 (Rbpr2) Is Required for Photoreceptor Survival and Visual Function in the Zebrafish


**Glenn P. Lobo, Gayle Pauer, Joshua H. Lipschutz, and Stephanie A. Hagstrom**

**Abstract** Vitamin A/retinol (ROL) and its metabolites (retinoids) play critical roles in eye development and photoreception. Short-term dietary vitamin A deficiency (VAD) manifests clinically as night blindness, while prolonged VAD is known to cause retinal pigment epithelium (RPE) and photoreceptor degeneration. Therefore, sustained uptake of dietary vitamin A, for ocular retinoid production, is essential for photoreceptor health and visual function. The mechanisms influencing the uptake, storage, and supply of dietary vitamin A, for ocular retinoid production, however, are not fully understood. We investigated, in zebrafish, the physiological role of the retinol-binding protein receptor 2 (Rbpr2), for the uptake of dietary ROL, which is necessary for vision. NIH3T3 cells expressing zebrafish Rbpr2 showed plasma membrane localization patterns and were capable of ROL uptake from its bound form. Using whole-mount in situ hybridization, Rbpr2 was found to be expressed exclusively in the liver, intestine, and pancreas, of staged zebrafish larvae. At 5.5 days post fertilization, TALEN-generated *rbpr2* mutants (*rbpr2*$^{-/-}$) had smaller eyes and shorter OS lengths and showed loss of PNA (cones) and rhodopsin (rods) by immunofluorescence staining. Finally, tests for visual function using optokinetic

G. P. Lobo (✉)
Division of Nephrology, Medical University of South Carolina, Charleston, SC, USA

Department of Ophthalmology, Medical University of South Carolina, Charleston, SC, USA
e-mail: lobo@musc.edu

G. Pauer
Department of Ophthalmic Research, Cole Eye Institute, Cleveland Clinic, Cleveland, OH, USA

J. H. Lipschutz
Division of Nephrology, Medical University of South Carolina, Charleston, SC, USA

S. A. Hagstrom
Department of Ophthalmic Research, Cole Eye Institute, Cleveland Clinic, Cleveland, OH, USA

Department of Ophthalmology, Cleveland Clinic Lerner College of Medicine of Case Western Reserve University, Cleveland, OH, USA



J. D. Ash et al. (eds.), *Retinal Degenerative Diseases*, Advances in Experimental Medicine and Biology 891, https://doi.org/10.1007/978-3-319-75402-4_69

response (OKR) showed no consistent OKR in *rbpr2*$^{-/-}$ larval zebrafish. Our analysis, therefore, suggests that Rbpr2 is capable of ROL uptake and loss of this membrane receptor in zebrafish results in photoreceptor defects that adversely affect visual function.

**Keywords** Vitamin A · Retinol · Rbpr2 · Photoreceptor · Vision

## Abbreviations

| | |
|---|---|
| (11-*cis*-RAL) | 11-*cis*-retinaldehyde |
| PRL | Photoreceptor cell layer |
| RBP4 | Retinol-binding protein 4 |
| Rbpr2 | Retinol-binding protein receptor 2 |
| ROL | All-*trans* retinol |
| RPE | Retinal pigmented epithelium |
| SR-B1 | Scavenger receptor class B type 1 |
| STRA6 | Stimulated by retinoic acid 6 |
| VAD | Vitamin A deficiency |

## 69.1 Introduction

For more than 60 years, dietary vitamin A deficiency (VAD) has been known to cause night blindness and retinal degeneration (Dowling and Wald 1958, 1960). Prolonged VAD can cause a significant interruption in the sequence of reactions needed for vision, including damage to the overall health of the photoreceptors and the quality of color vision and dark adaptation (Perusek and Maeda 2013). Therefore, mechanisms influencing the uptake, storage, and supply of dietary vitamin A for chromophore production play a significant and direct role in visual function (Ross et al. 2001; During and Harrison 2007; Harrison 2012; Lobo et al. 2012a; Kelly and von Lintig 2015). Vertebrates are unable to synthesize vitamin A de novo and must obtain vitamin A from the diet, either as preformed vitamin A (retinol/ROL) or as a provitamin A carotenoid, such as β-carotene (During and Harrison 2007; Harrison 2012; von Lintig 2010). While the scavenger receptor class B type 1 (SR-B1) facilitates dietary carotenoid absorption in the intestine, it is not involved in dietary ROL absorption; therefore the molecular mechanisms regulating uptake of dietary ROL remain unknown (Dew and Ong 1994, 1997; Lobo et al. 2012a; Lobo et al. 2013; Alapatt et al. 2013; Kiefer et al. 2002). This project focuses on elucidating the physiological role of the proposed ROL receptor, *rbpr2* in zebrafish, in support of vision. We hypothesized that the Rbpr2 receptor facilitates ROL uptake and that loss of

*rbpr2* would result in reduced ocular retinoid concentrations, consequently, affecting photoreceptor health and vision.

## 69.2 Materials and Methods

### *69.2.1 Cloning of the Zebrafish Rbpr2 cDNA*

Total RNA from zebrafish larvae was reverse transcribed using the SuperScript One-Step RT-PCR system (Invitrogen), and full-length Rbpr2 cDNA was amplified using forward primer (5′-ATGTTTCTGCTCTCATTAGTGCAGCGGCGA-3′) with reverse primer (5′-TCA GATGTCTAGCGGTGCTGGTTCTGTCTCAGC-3′) using the Expand High Fidelity PCR system (Roche). The Rbpr2 cDNA was cloned in frame into the pCDNA3.1 V5/His TOPO vector (Invitrogen) to obtain full-length Rbpr2-V5-tagged plasmid (pRbpr2-V5).

### *69.2.2 Cell Lines, Cell Culture, and Plasmid Transfections*

For Rbpr2 subcellular localization, NIH3T3 cells were seeded at 40–50% confluence and transfected with ~ 3 μg of purified pRbpr2-V5 plasmid DNA using X-tremeGENE HP transfection reagent (Roche) essentially as previously outlined (Lobo et al. 2016). Post 72 h, cells were subjected to indirect immunofluorescence analysis, by exposure to the anti-V5 primary antibody (which detects the V5-tagged Rbpr2 protein) followed by the anti-rabbit conjugated Alexa 488 secondary antibody (Invitrogen), as previously outlined (Lobo et al. 2012b).

### *69.2.3 Expression and Purification of Human Holo-RBP4*

Human RBP4 cDNA cloned into the pET3a bacterial expression vector was used to express RBP4 in *E.Coli.* RBP4 was refolded in the presence of molar excess of all-*trans* retinol and finally eluted on a DE3 ion exchange column. Collected protein fractions (holo-hRBP4) were examined by UV-visible spectroscopy, and holo-hRBP4 expression was confirmed by SDS-PAGE using an anti-Rbp4 antibody. Fractions containing at least 90% holo-hRBP were pooled together and concentrated in a Centricon centrifugal filter device (cutoff 10,000 kDa) (Millipore) to 5 mg/ml.

### *69.2.4 RBP4 Binding and Retinol Uptake Studies*

NIH3T3 cells expressing Rbpr2 were cultured in six-well cell culture plates with serum-free medium (SFM) containing holo-hRBP4 (2 μM). After 16 h of incubation in SFM media, cells were washed twice with 1X PBS, pH 7.4, harvested, and resuspended in 200 μL of 1X PBS, pH 7.4. Retinoids were then extracted with 1 volume of methanol and 1 volume of acetone followed by 2 volumes of hexane and subjected to HPLC analysis, as described previously (Golczak et al. 2010).

### *69.2.5 Zebrafish Experiments*

Whole-mount in situ hybridization in staged zebrafish larvae was performed according to published protocols and as previously described (Lobo et al. 2012b). *Danio rerio* Rbpr2 cDNA (ZGC, 162946) was cloned into the vector pCRII-TOPO (Invitrogen), and antisense RNA probes were synthesized using T7 polymerase following protocols as outlined by the manufacturer (Roche). The measurements of OKR were made with the oculomotor analysis system (VisioTracker; TSE Systems) using 5.5 dpf larvae as previously described (Daniele et al. 2016).

## 69.3 Results

### *69.3.1 Zebrafish Rbpr2-Mediated Uptake from Holo-RBP4*

The intestinal uptake of dietary lipids, including vitamin A (retinol/ROL), was hypothesized to be facilitated by plasma membrane receptors (Dew and Ong 1994, 1997; Harrison 2012). Therefore, to determine localization patterns of zebrafish Rbpr2, we transfected the full-length zebrafish pRbpr2-V5 plasmid, in parental NIH3T3 cells. Expression of Rbpr2 was confirmed by immunoblotting and immunohistochemistry (Fig. 69.1a, b). Cells were fixed and stained, and, using indirect immunofluorescence and confocal imaging, we observed Rbpr2 to be localized primarily to the plasma membrane (Fig. 69.1b). In order to determine whether Rbpr2 shares the retinol/ROL transport function of Stra6, we studied uptake of ROL-bound RBP4 (holo-RBP4) in NIH3T3/Rbpr2-expressing cells. Cells expressing Rbpr2 exhibited increased ROL uptake in comparison with cells transfected with the empty vector control, values were comparable with those reported by others in similar experiments (Fig. 69.1c) (Isken et al. 2008; Alapatt et al. 2013; Li et al. 2007). Thus plasma membrane localization patterns of zebrafish Rbpr2, and the ability to bind and transport ROL, like that of human STRA6 and mouse Rbpr2, suggest a potential role for this receptor in the uptake of dietary retinol.

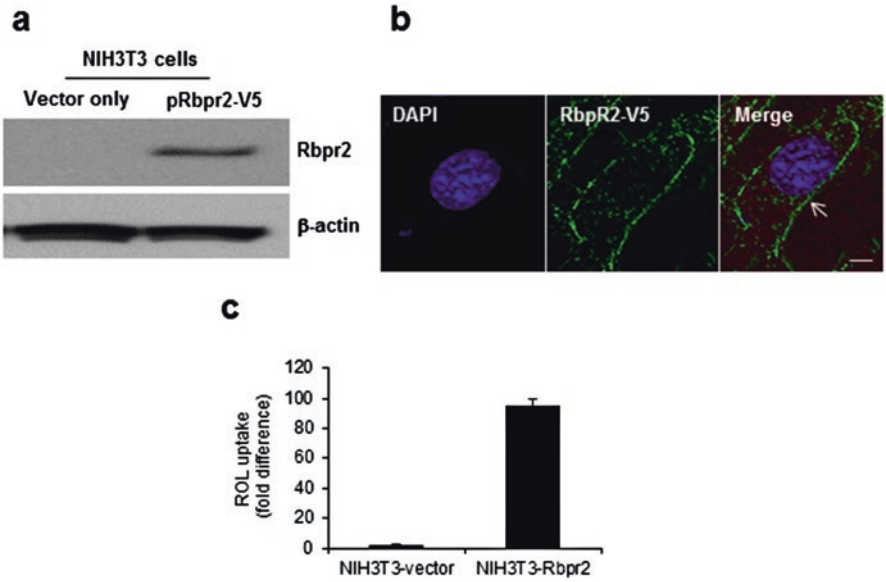


**Fig. 69.1** Zebrafish Rbpr2 localizes to the plasma membrane and is capable of retinol uptake. (**a**–**b**) Expression of V5-tagged Rbpr2 (pRbpr2-V5) in NIH3T3 cells was confirmed by western blotting and immunofluorescence. Zebrafish Rbpr2 showed predominant plasma membrane localization patterns (arrow). (**c**) Retinol/ROL uptake assays followed by HPLC analysis showed Rbpr2-expressing NIH3T3 cells were capable of ROL uptake, compared to vector-only transfected NIH3T3 cells

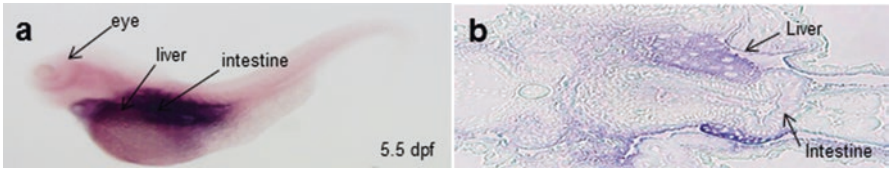


**Fig. 69.2** Rbpr2 is expressed in tissues mediating retinol uptake and storage. (**a**) Whole-mount in situ hybridization (WISH) at 5.5 dpf using antisense Rbpr2 probe and (**b**) sagittal cross sections of 5.5 dpf Rbpr2-WISH stained larvae showed specific intestinal, liver, and pancreas expression patterns

### *69.3.2 Rbpr2 Is Expressed in Tissues Responsible for ROL Uptake and Storage*

We next used zebrafish to analyze Rbpr2 function in vivo. We tested *rbpr2* mRNA expression patterns with antisense RNA probes using whole-mount in situ hybridization (WISH). Starting from 1-day post fertilization (dpf), Rbpr2 expression was evident in the intestine, liver, and pancreas and was maintained in these organs to 5.5 dpf (Fig. 69.2a). Interestingly, unlike zebrafish Stra6, Rbpr2 was not expressed

in the larval eye (Isken et al. 2008) (Fig. 69.2a). To determine specific subcellular distribution patterns of Rbpr2, we embedded 5.5 dpf WISH stained larvae in JB-4 plastic resin and performed sagittal cross sections. Our analysis confirmed that Rbpr2 was expressed primarily within the intestinal enterocytes, liver hepatocytes, and pancreas (Fig. 69.2b). Because these tissues mediate uptake, storage, and distribution of retinol, our findings suggest that Rbpr2 could play a physiologically relevant role in whole-body ROL homeostasis (Alapatt et al. 2013; Sun 2012; Harrison 2012).

### *69.3.3 Rbpr2 Mutants Show Photoreceptor Degeneration and Loss of Visual Function*

We then used a TALEN approach to perform a Rbpr2 loss-of-function study. In retinal cross sections, *rbpr2*$^{-/-}$ larvae showed slightly smaller eyes, retinal lamination layer disruption, and thinner RPE layer, as compared to wild-type sibling controls (Fig. 69.3a, b). Immunostaining for cones (PNA-568) and rods (Rho-488) at 5.5 dpf showed shorter OS lengths and loss of cone and rod staining in *rbpr2*$^{-/-}$ larvae, when compared to wild-type siblings (Fig. 69.3c–f). For larval zebrafish, the OKR has been used to measure parameters ranging from saccade frequency to more sophisticated measures, such as optokinetic gain, in the evaluation of visual function (Daniele et al. 2016). The contrast-response function was measured for 5.5 dpf wild-type control and *rbpr2*$^{-/-}$ larvae. For wild-type larvae, OKR increased linearly with the log of contrast, while no consistent OKR was detected in *rbpr2*$^{-/-}$ larvae, which resulted in a flat contrast-response function (Fig. 69.3g). Thus loss of cone and rod photoreceptors in *rbpr2*$^{-/-}$ zebrafish larvae resulted in significantly *rbpr2*$^{-/-}$ impaired visual function (Fig. 69.3g).

## 69.4 Discussion

Continuous uptake, storage, and supply of dietary vitamin A/retinol (ROL) are critical for generating optimal levels of ocular retinoids, for eye development and RPE health and in sustaining photoreception. Absorption of dietary ROL by the small intestine is a necessary first step in the metabolism of vitamin A. Previous studies had suggested that intestinal absorption and liver storage of retinol might be receptor mediated. We therefore investigated, in zebrafish, the physiological role of the retinol-binding protein receptor 2 (*rbpr*2), in the uptake of dietary ROL, which is required for vision. Membrane-localized Rbpr2 was capable of ROL uptake from its bound form, indicating that this receptor could act as a ROL transporter. Expression of Rbpr2 in staged zebrafish larvae showed predominant liver and intestinal patterns, the very tissues implicated in the storage and absorption of ROL. Mutant

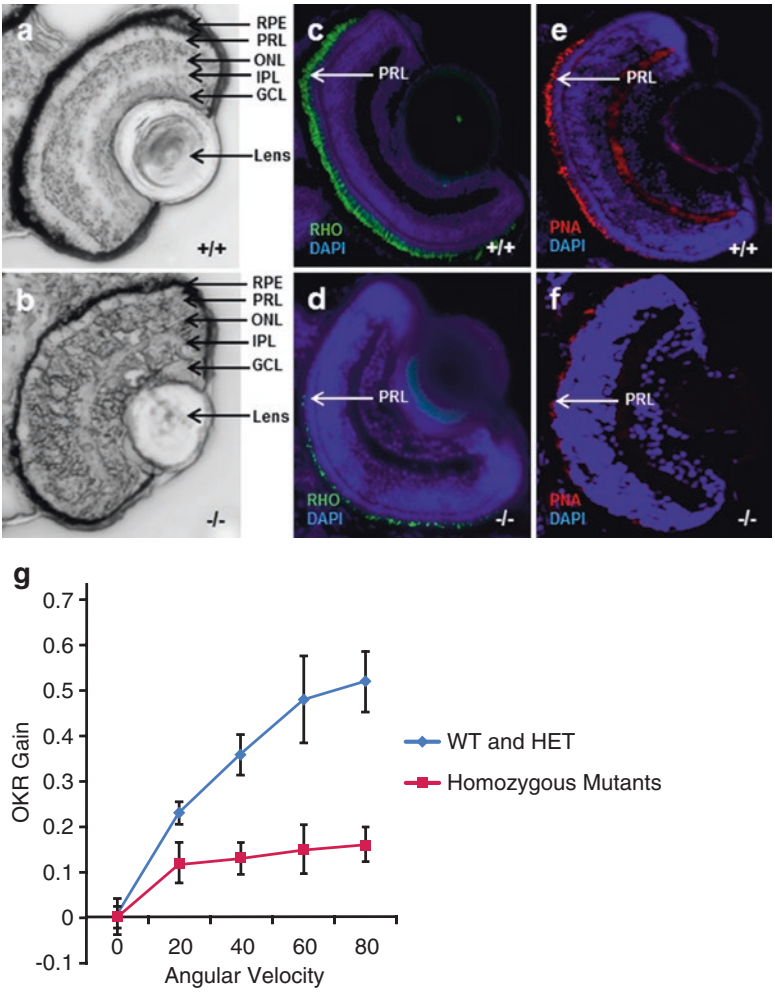


**Fig. 69.3** *rbpr2* mutants show photoreceptor defects and loss of visual function. Compared to wild-type larvae controls, (**a**) retinal sections of *rbpr2* mutant larvae (**b**) showed thinner RPE cell layer and disruption of retinal lamination layers. *rbpr2* mutants (**d**, **f**) showed shorter OS lengths, loss of PNA (cone), and rhodopsin (rod) staining, as compared to wild-type siblings (**c**, **e**). (**g**) Contrast-response function measured from smooth-pursuit eye movements showed significantly lower OKR gain in *rbpr2* mutants as compared to wild-type and heterozygote larvae at 5.5 dpf

*rbpr2*$^{-/-}$ zebrafish larvae showed significant eye phenotypes and loss of visual function by OKR. The loss of visual function correlated with the observed cone and rod photoreceptor degeneration, likely due to low ocular retinoid levels. Therefore, based on our in vitro and in vivo analysis, Rbpr2 likely functions as a transporter for dietary ROL, and loss of this receptor significantly impacts photoreceptor health and visual function, in a zebrafish vertebrate model.

**Acknowledgments** This study was supported by NIH grant EY025034-02 (GPL) and, in part, by a Knights Templar Eye Foundation Career-Starter Grant (GPL) and a Knights Templar Eye Foundation Career-Renewal Grant (GPL), NIH grant DK074038 (JHL), and a VA Merit award 2I01BX000820 (JHL).

## References

Alapatt P, Guo F, Komanetsky SM et al (2013) Liver retinol transporter and receptor for serum retinol-binding protein (RBP4). J Biol Chem 288:1250–1265

Daniele LL, Emran F, Lobo GP et al (2016) Mutation of wrb, a component of the guided entry of tail-anchored protein pathway, disrupts photoreceptor synapse structure and function. Invest Ophthalmol Vis Sci 57:2942–2954

Dew SE, Ong DE (1994) Specificity of the retinol transporter of the rat small intestine brush border. Biochemistry 33:12340–12345

Dew SE, Ong DE (1997) Absorption of retinol from the retinol:retinol-binding protein complex by small intestinal gut sheets from the rat. Arch Biochem Biophys 338:233–236

Dowling JE, Wald G (1958) Vitamin A deficiency and Night Blindness. Proc Natl Acad Sci U S A 44:648–661

Dowling JE, Wald G (1960) The biological function of Vitamin A acid. Proc Natl Acad Sci U S A 46:587–608

During A, Harrison EH (2007) Mechanisms of provitamin A (carotenoid) and vitamin A (retinol) transport into and out of intestinal Caco-2 cells. J Lipid Res 48:2283–2294

Golczak M, Bereta B, Maeda A et al (2010) Molecular Biology and Analytical Chemistry Methods Used to Probe the Retinoid Cycle. Retinoids-Methods Mol Biol 65:229–245

Harrison EH (2012) Mechanisms involved in the intestinal absorption of dietary vitamin A and provitamin A carotenoids. Biochim Biophys Acta 1821:70–77

Isken A, Golczak M, Oberhauser V et al (2008) RBP4 disrupts vitamin A uptake homeostasis in a STRA6-deficient animal model for Matthew-Wood syndrome. Cell Metab 7:258–268

Kelly M, von Lintig J (2015) STRA6: role in cellular retinol uptake and efflux. Hepatobiliary Surg Nutr 4:229–242

Kiefer C, Sumser E, Wernet MF et al (2002) A class B scavenger receptor mediates the cellular uptake of carotenoids in Drosophila. Proc Natl Acad Sci U S A 99:10581–10586

Li Z, Korzh V, Gong Z et al (2007) Localized rbp4 expression in the yolk syncytial layer plays a role in yolk cell extension and early liver development. BMC Dev Biol 7:117–125

Lobo GP, Amengual J, Palczewski G et al (2012a) Mammalian carotenoid-oxygenases: key players for carotenoid function and homeostasis. Biochim Biophys Acta 1821:78–87

Lobo GP, Isken A, Hoff S et al (2012b) BCDO2 acts as a carotenoid scavenger and gatekeeper for the mitochondrial apoptotic pathway. Development 139:2966–2977

Lobo GP, Amengual J, Baus D et al (2013) Genetics and diet regulate vitamin A production via the homeobox transcription factor ISX. J Biol Chem 288:9017–9027

Lobo GP, Au A, Kiser PD, Hagstrom SA (2016) Involvement of endoplasmic reticulum stress in TULP1 induced retinal degeneration. PLoS One 11:e0151806

Perusek L, Maeda T (2013) Vitamin A derivatives as treatment options for retinal degenerative diseases. Forum Nutr 5:2646–2666

Ross AC, Zolfaghari R, Weisz J (2001) Recent advances in the biotransformation, transport, and metabolism of retinoids. Curr Opin Gastroenterol 17:184–192

Sun H (2012) Membrane receptors and transporters involved in the function and transport of vitamin A and its derivatives. Biochim Biophys Acta 1821:99–112

Von Lintig J (2010) Colors with functions: elucidating the biochemical and molecular basis of carotenoid metabolism. Annu Rev Nutr 30:35–56

# Chapter 70
# Opposite Roles of MerTK Ligands Gas6 and Protein S During Retinal Phagocytosis


**Emeline F. Nandrot**

**Abstract** MerTK is required for photoreceptor outer segment (POS) phagocytosis by retinal pigment epithelial (RPE) cells, a diurnal function essential for vision maintenance. In vivo, MerTK is stimulated at the time of the phagocytic peak through an intracellular signaling pathway. However, MerTK ligands Gas6 and Protein S are expressed in both RPE cells and photoreceptors, and at least one of them required for phagocytosis to occur. Still, their exact role in the retina was not clear until recently. This review combines results from different studies to shed the light on a tissue-specific regulation of MerTK function by its ligands. Indeed, with opposite effects on RPE phagocytosis and changes in their expression levels around the time of POS uptake, Gas6 and Protein S may contribute to the tight control of the acute phagocytic peak in the retina.

**Keywords** Retinal pigment epithelium · Phagocytosis · Photoreceptor outer segments · MerTK · Ligands · Gas6 · Protein S · Circadian rhythm

## 70.1 Introduction

MerTK is the internalization receptor necessary for phagocytosis of apoptotic cells by macrophages (Scott et al. 2001), as well as of photoreceptor outer segments (POS) by RPE cells (D'Cruz et al. 2000; Nandrot et al. 2000; Feng et al. 2003). In the retina, this task allows the elimination of aged POS tips on a daily basis following a circadian rhythm peaking 2 h after light onset (Young and Bok 1969; LaVail 1976). Phagocytosis is crucial to alleviate the oxidative stress linked to constant light exposure of photoreceptors and to allow the renewal of POS membranes (Strauss 2005). When deregulated or absent, retinal pathologies ensue with an either early or late onset – such as rod-cone dystrophies with early macular involvement

E. F. Nandrot (✉)
Sorbonne Université, INSERM, CNRS, Institut de la Vision,
17 rue Moreau, Paris F-75012, France
e-mail: emeline.nandrot@inserm.fr



J. D. Ash et al. (eds.), *Retinal Degenerative Diseases*, Advances in Experimental Medicine and Biology 891, https://doi.org/10.1007/978-3-319-75402-4_70

(atypical retinitis pigmentosa) or age-related macular degeneration (AMD) – in animal models and patients (Dowling and Sidman 1962; Gal et al. 2000; Tschernutter et al. 2006; Nandrot et al. 2004).

Until recently, the role of MerTK ligands in the retina was not clear because MerTK is directly activated in vivo at the time of the phagocytic peak via an intracellular signaling pathway initiated by the alphavbeta5 integrin–Mfg-E8 receptor–ligand couple (Nandrot et al. 2004; Nandrot et al. 2007). In addition, single-knockout models for each ligand do not develop any phenotype (Hall et al. 2005; Prasad et al. 2006; Burstyn-Cohen et al. 2012), while RCS rats lacking MerTK are affected by a severe retinal degeneration rendering them blind by the age of 3 months (Dowling and Sidman 1962). The interest in studying MerTK ligands during POS phagocytosis was sparked again when a study showed that double-knockout mice present a degenerative phenotype similar to RCS rats (Burstyn-Cohen et al. 2012).

## 70.2 Presentation of MerTK and Related Ligands Gas6 and Protein S

### *70.2.1 The TAM Receptor Family and Apoptotic Cell Recognition*

MerTK belongs to the TAM – Tyro3, Axl, and MerTK – family of tyrosine kinase receptors (Hafizi and Dahlbäck 2006a). TAM receptors are composed of an extracellular domain – two immunoglobulin-like domains and two type III fibronectin repeats –, a transmembrane domain and a cytoplasmic domain mainly comprising the tyrosine kinase domain. TAMs are not necessary during development but carry a role in general tissue homeostasis through the elimination of various kinds of apoptotic cells (AC) and the control of innate immune system responses (Lemke 2013). However, in the retina only MerTK and Tyro3 are expressed in RPE microvilli, and absence of Tyro3 does not lead to any retinal degeneration (Prasad et al. 2006).

Specific recognition of ACs and POS extremities requires exposure of phosphatidylserines (PtdSer) on their surface (Fadok et al. 1992; Ruggiero et al. 2012). PtdSer are normally found on the inner leaflet of the plasma membrane but flip to the outer leaflet when cells become apoptotic for immediate recognition and clearance by macrophages. In the retina, only the outmost tip of POS to be tethered and engulfed by RPE cells exposes PtdSer in a timely fashion (Ruggiero et al. 2012). PtdSer are recognized either directly by receptors on the phagocyte surface such as CD36 (Ryeom et al. 1996) or indirectly via bridge molecules such as Mfg-E8 and Gas6/Protein S (Hanayama et al. 2002; Nandrot et al. 2007; Nakano et al. 1997; Anderson et al. 2003; Hall et al. 2002).

### 70.2.2 Gas6 and Protein S: Two Shared Ligands with Similar Structures

Two cognate ligands have been described for TAM receptors, Gas6 and Protein S (Stitt et al. 1995; Varnum et al. 1995). These vitamin K-dependent ligands share a similar molecular structure: a Gla domain (PtdSer binding), four EGF-like domains, and a sex-hormone-binding globulin domain (receptor binding) (Hafizi and Dahlbäck 2006b). However, they can be used in distinct functions. Protein S has a prominent role in the anticoagulation cascade and has been shown to be implicated in atherosclerosis and angiogenesis though its participation in phagocytosis (Walker 1980; Liao et al. 2009; Burstyn-Cohen et al. 2009). The Gas6–Axl complex has also been linked to angiogenesis inhibition (Gallicchio et al. 2005) and is in general associated with cell survival and/or proliferation (Melaragno et al. 2004; Stenhoff et al. 2004), as well as cell migration and adhesion (McCloskey et al. 1997).

Importantly, Gas6 and Protein S are implicated in AC clearance by macrophages (Nakano et al. 1997; Anderson et al. 2003). First linked to PtdSer, Protein S molecules bind to TAM receptors and mediate their activation by inducing receptor dimerization and autophosphorylation (Uehara and Shacter 2008). Gas6 has the capability to bind PtdSer and stimulates receptor activation (Nakano et al. 1997; Hall et al. 2002), but its precise role in apoptotic cell clearance is not clear. Gas6 absence does not lead to any phenotype in mice, thus Protein S is sufficient to elicit phagocytosis (Prasad et al. 2006; Lew et al. 2014).

### 70.2.3 What About the Retina?

Since the identification of MerTK in RCS rats, studies have been testing the implication of Gas6 and Protein S in POS elimination. In vitro, both have been shown to stimulate POS phagocytosis by primary RPE cells and retinal explants, with a prominent role for Protein S (Hall et al. 2001, 2002, 2005; Prasad et al. 2006). Surprisingly, Gas6 and Protein S are both expressed by the retina and RPE cells (Hall et al. 2001; Prasad et al. 2006). This raises the following question: do both RPE and photoreceptors contribute to POS phagocytosis?

As well, in absence of a phenotype in single-knockout mice, their in vivo contribution was debated, until the creation of a mouse model inactivated for both Gas6 and Protein S that develops a blindness similarly to MerTK-deficient rats or mice (Burstyn-Cohen et al. 2012). This phenotype made it clear that at least one of these ligands is required in the retina, potentially because of their role in MerTK dimerization itself necessary for further intracellular receptor activation (Uehara and Shacter 2008; Lew et al. 2014). However, no other participation in the phagocytic process had been investigated.

## 70.3 Role of MerTK Ligands During Retinal Phagocytosis

### *70.3.1 Opposite Roles During in Vitro Phagocytosis*

We recently investigated the effect of increasing doses of Gas6 and Protein S, either alone or in combination, on POS phagocytosis by RPE-J cells in comparison with J774 macrophages (Law et al. 2015). As expected, both ligands stimulated macrophages at all doses with an additive effect at some doses when combined. Surprisingly, increasing doses of Gas6 appear to inhibit RPE-J cell phagocytosis, while Protein S has a dose-dependent stimulatory effect, and they compensate each other when combined (Fig. 70.1). This suggests that, in the retina, changes in Gas6 and Protein S amounts could contribute to the regulation of MerTK activity.

### *70.3.2 In Vivo Variation of Expression Levels Along the Light/Dark Cycle*

In order to assess respective levels of each ligand, we analyzed their mRNA expression profiles along the light/dark cycle by qPCR on isolated retina and RPE/choroid (RPE/Ch) (Parinot et al. under revision). Overall *Gas6* was more expressed than *Pros1* (Protein S), and more present in the retina than RPE/Ch as previously suggested (Hall et al. 2005). *Gas6* expression in RPE/Ch decreased just before the phagocytic peak and increased just after (Fig. 70.2), while in the retina it was quite stable with a slight increase just before the peak (data not shown). *Pros1* expression followed a bimodal rhythm: it increased markedly just before and at phagocytic

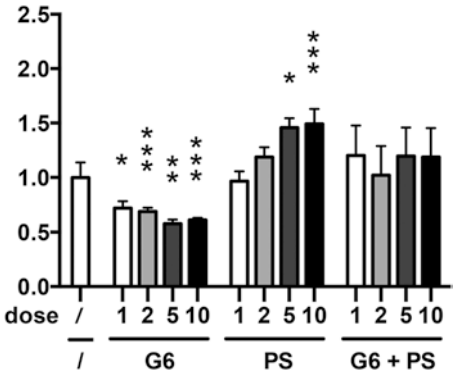


**Fig. 70.1** Antagonistic role of MerTK ligands Gas6 and Protein S on POS phagocytosis by RPE-J cells. POS internalization (FITC/DAPI ratio) was quantified after cells were challenged for 3 h with FITC-POS alone (/) or with the addition of various doses of Gas6 (G6) and/or Protein S (PS) as indicated (μg/mL). *$P < 0.05$, **$P < 0.01$, ***$P < 0.001$ (Modified from © Law et al. 2015. Originally published in *The Journal of Biological Chemistry*, https://doi.org/10.1074/jbc.M114.628297)

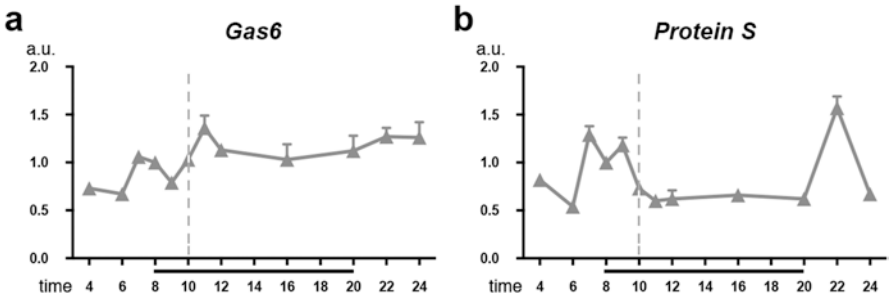


**Fig. 70.2** Different cyclic expression of MerTK ligands *Gas6* and *Pros1* mRNAs. mRNA expression profiles for *Gas6* (**a**) and *Pros1* (**b**) in the RPE/choroid of wild-type animals at different times of the day as indicated were assessed by qPCR. The black bar under each graph represents the time points during which lights are on in the animal facility, and the dotted vertical line indicates phagocytic peak time. All quantifications are expressed in arbitrary units (a.u.) as mean ± SD, $N = 3–6$ independent samples. The reference set as 1 for comparison is the quantification at 8:00 AM (light onset) for each gene (From Parinot et al. under revision)

peak time in RPE/Ch (Fig. 70.2) and retina, respectively, and a second peak occurs at light offset (retina) and right after (RPE/Ch). This suggests that higher amounts of stimulatory Protein S may be available in the interphotoreceptor matrix (IPM) in time for POS phagocytosis while inhibitory Gas6 levels decrease.

## 70.4 Perspectives

Activity of MerTK can be regulated by many ways mostly through intracellular activation via alphavbeta5 integrin signaling (Nandrot et al. 2004) and by the cleavage of its extracellular domain both in vitro and in vivo (Law et al. 2015). This cleavage is augmented by Gas6 and diminished by Protein S, which could explain their respective inhibitory and stimulatory roles on RPE phagocytosis. Thus, bioavailable levels of each ligand in the IPM at different times of the light/dark cycle might help control the height and the duration of MerTK activation, hence contributing on a daily basis to the tight control of the sharp peak of POS phagocytosis. In addition, these results suggest a potential competition for ligand binding on MerTK.

## References

Anderson HA, Maylock CA, Williams JA et al (2003) Serum-derived protein S binds to phosphatidylserine and stimulates the phagocytosis of apoptotic cells. Nat Immunol 4(1):87–91

Burstyn-Cohen T, Heeb MJ, Lemke G (2009) Lack of protein S in mice causes embryonic lethal coagulopathy and vascular dysgenesis. J Clin Invest 119(10):2942–2953

Burstyn-Cohen T, Lew ED, Través PG et al (2012) Genetic dissection of TAM receptor-ligand interaction in retinal pigment epithelial cell phagocytosis. Neuron 76:1123–1132
D'Cruz PM, Yasumura D, Weir J et al (2000) Mutation of the receptor tyrosine kinase gene Mertk in the retinal dystrophic RCS rat. Hum Mol Genet 9:645–651
Dowling JE, Sidman RL (1962) Inherited retinal dystrophy in the rat. J Cell Biol 14:73–109
Fadok VA, Voelker DR, Campbell PA et al (1992) Exposure of phosphatidylserine on the surface of apoptotic lymphocytes triggers specific recognition and removal by macrophages. J Immunol 148(7):2207–2216
Feng W, Yasumura D, Matthes MT et al (2003) Mertk triggers uptake of photoreceptor outer segments during phagocytosis by cultured retinal pigment epithelial cells. J Biol Chem 277:17016–17022
Gal A, Li Y, Thompson DA et al (2000) Mutations in MERTK, the human orthologue of the RCS rat retinal dystrophy gene, cause retinitis pigmentosa. Nat Genet 26:270–271
Gallicchio M, Mitola S, Valdembri D et al (2005) Inhibition of vascular endothelial growth factor receptor 2-mediated endothelial cell activation by Axl tyrosine kinase receptor. Blood 105(5):1970–1976
Hafizi S, Dahlbäck B (2006a) Signalling and functional diversity within the Axl subfamily of receptor tyrosine kinases. Cytokine Growth Factor Rev 17(4):295–304
Hafizi S, Dahlbäck B (2006b) Gas6 and protein S. Vitamin K-dependent ligands for the Axl receptor tyrosine kinase subfamily. FEBS J 273(23):5231–5244
Hall MO, Prieto AL, Obin MS et al (2001) Outer segment phagocytosis by cultured retinal pigment epithelial cells requires Gas6. Exp Eye Res 73(4):509–520
Hall MO, Obin MS, Prieto AL et al (2002) Gas6 binding to photoreceptor outer segments requires gamma-carboxyglutamic acid (Gla) and Ca(2+) and is required for OS phagocytosis by RPE cells in vitro. Exp Eye Res 75(4):391–400
Hall MO, Obin MS, Heeb MJ et al (2005) Both protein S and Gas6 stimulate outer segment phagocytosis by cultured rat retinal pigment epithelial cells. Exp Eye Res 81:581–591
Hanayama R, Tanaka M, Miwa K et al (2002) Identification of a factor that links apoptotic cells to phagocytes. Nature 417(6885):182–187
LaVail MM (1976) Rod outer segment disk shedding in rat retina: relationship to cyclic lighting. Science 194:1071–1074
Lemke G (2013) Biology of the TAM receptors. Cold Spring Harb Perspect Biol 5(11):a009076
Law AL, Parinot C, Chatagnon J et al (2015) Cleavage of Mer tyrosine kinase (MerTK) from the cell surface contributes to the regulation of retinal phagocytosis. J Biol Chem 290(8):4941–4952
Lew ED, Oh J, Burrola PG et al (2014) Differential TAM receptor-ligand-phospholipid interactions delimit differential TAM bioactivities. elife 3:e03385
Liao D, Wang X, Li M et al (2009) Human protein S inhibits the uptake of AcLDL and expression of SR-A through Mer receptor tyrosine kinase in human macrophages. Blood 113(1):165–174
McCloskey P, Fridell YW, Attar E et al (1997) GAS6 mediates adhesion of cells expressing the receptor tyrosine kinase Axl. J Biol Chem 272:23285–23291
Melaragno MG, Cavet ME, Yan C et al (2004) Gas6 inhibits apoptosis in vascular smooth muscle: role of Axl kinase and Akt. J Mol Cell Cardiol 37:881–887
Nakano T, Ishimoto Y, Kishino J et al (1997) Cell adhesion to phosphatidylserine mediated by a product of growth arrest-specific gene 6. J Biol Chem 272(47):29411–29414
Nandrot E, Dufour EM, Provost AC et al (2000) Homozygous deletion in the coding sequence of the c-mer gene in RCS rats unravels general mechanisms of physiological cell adhesion and apoptosis. Neurobiol Dis 7:586–599
Nandrot EF, Kim Y, Brodie SE et al (2004) Loss of synchronized retinal phagocytosis and age-related blindness in mice lacking alphavbeta5 integrin. J Exp Med 200:1539–1545
Nandrot EF, Anand M, Almeida D et al (2007) Essential role for MFG-E8 as ligand for alphavbeta5 integrin in diurnal retinal phagocytosis. Proc Natl Acad Sci U S A 104:12005–12010
Parinot C, Chatagnon J, Roux S et al (in revision) Gas6 and Protein S ligands cooperate to regulate MerTK rhythmic activity required for circadian retinal phagocytosis

Prasad D, Rothlin CV, Burrola P et al (2006) TAM receptor function in the retinal pigment epithelium. Mol Cell Neurosci 33(1):96–108

Ruggiero L, Connor MP, Chen J et al (2012) Diurnal, localized exposure of phosphatidylserine by rod outer segment tips in wild-type but not Itgb5−/− or Mfge8−/− mouse retina. Proc Natl Acad Sci U S A 109(21):8145–8148

Ryeom SW, Silverstein RL, Scotto A et al (1996) Binding of anionic phospholipids to retinal pigment epithelium may be mediated by the scavenger receptor CD36. J Biol Chem 271(34):20536–20539

Scott RS, McMahon EJ, Pop SM et al (2001) Phagocytosis and clearance of apoptotic cells is mediated by MER. Nature 411:207–211

Stenhoff J, Dahlback B, Hafizi S (2004) Vitamin K-dependent Gas6 activates ERK kinase and stimulates growth of cardiac fibroblasts. Biochem Biophys Res Commun 319:871–878

Stitt TN, Conn G, Goret M et al (1995) The anticoagulation factor protein S and its relative, Gas6, are ligands for the Tyro 3/Axl family of receptor tyrosine kinases. Cell 80(4):661–670

Strauss O (2005) The retinal pigment epithelium in visual function. Physiol Rev 85(3):845–881

Tschernutter M, Jenkins SA, Waseem NH et al (2006) Clinical characterisation of a family with retinal dystrophy caused by mutation in the Mertk gene. Br J Ophthalmol 90:718–723

Uehara H, Shacter E (2008) Auto-oxidation and oligomerization of protein S on the apoptotic cell surface is required for Mer tyrosine kinase-mediated phagocytosis of apoptotic cells. J Immunol 180(4):2522–2530

Varnum BC, Young C, Elliott G et al. (1995) Axl receptor tyrosine kinase stimulated by the vitamin K-dependent protein encoded by growth-arrest-specific gene 6. Nature 373(6515):623–626

Walker FJ (1980) Regulation of activated protein C by a new protein. A possible function for bovine Protein S. J Biol Chem 255(12):5521–5524

Young RW, Bok D (1969) Participation of the retinal pigment epithelium in the rod outer segment renewal process. J Cell Biol 42:392–403

# Chapter 71
# Redundant and Nonredundant Functions of Akt Isoforms in the Retina


**Raju V. S. Rajala and Ammaji Rajala**

**Abstract** Serine/threonine kinase Akt is a downstream effector of the phosphoinositide 3-kinase pathway that is involved in many processes, including providing neuroprotection to stressed photoreceptor cells. Akt exists in three isoforms designated as Akt1, Akt2, and Akt3. All of these isoforms are expressed in the retina. We previously reported that Akt2 knockout mice were susceptible to light stress-induced photoreceptor degeneration, whereas Akt1 deletion had no effect on the retina. We hypothesized that the phenotype of Akt2 knockout mice may be due to the inactivation of specific substrate(s) in the retina. Yeast two-hybrid screening of a bovine retinal cDNA library with Akt2 identified a multidomain protein, POSH (plenty of SH3s), that acts as a scaffold for the JNK pathway of neuronal death. Our results suggest a stable interaction between Akt2 and POSH. Previous studies show that overexpression of POSH leads to cell death. The cell death that we observed in Akt2 knockout mice could be due to the absence of inactivation of POSH-mediated JNK signaling in the retina.

**Keywords** Akt isoforms · Akt2 · Light stress · Scaffold protein · POSH · JNK signaling · Yeast two-hybrid assay · Retinal degeneration

R. V. S. Rajala (✉)
Department of Ophthalmology, University of Oklahoma Health Sciences Center, Oklahoma City, OK, USA

Department of Physiology, University of Oklahoma Health Sciences Center, Oklahoma City, OK, USA

Department of Cell Biology, University of Oklahoma Health Sciences Center, Oklahoma City, OK, USA

Dean McGee Eye Institute, Oklahoma City, OK, USA
e-mail: raju-rajala@ouhsc.edu

A. Rajala
Department of Ophthalmology, University of Oklahoma Health Sciences Center, Oklahoma City, OK, USA

Dean McGee Eye Institute, Oklahoma City, OK, USA



J. D. Ash et al. (eds.), *Retinal Degenerative Diseases*, Advances in Experimental Medicine and Biology 891, https://doi.org/10.1007/978-3-319-75402-4_71

## 71.1 Introduction

Blindness and visual impairment are characteristic features of retinal degeneration, and apoptosis is the most common pathological phenotype. Survival factors suppress apoptosis in a transcription-independent manner by activating the serine/threonine kinase Akt, which then phosphorylates and inactivates components of the apoptotic machinery. Akt, the downstream effector of phosphoinositide 3-kinase (PI3K) and its activation, has been shown to promote cell survival. Akt exists in three isoforms designated as Akt1, Akt2, and Akt3. These isoforms share more than 80% amino acid sequence homology but respond differently to growth factor stimulation. Studies from our laboratory and others have shown the expression of all three isoforms in the retina and in photoreceptor cells (Li et al. 2008; Reiter et al. 2003). However, we demonstrated that Akt2 knockout mice exhibited a greater sensitivity to light stress-induced photoreceptor degeneration, whereas Akt1deletion had no effect on the retina (Li et al. 2007). The retinal degeneration phenotype of Akt2 was not rescued by the functional Akt1 and Akt3 in the retina, suggesting a nonredundant role of Akt2 in the retina. These observations led to the hypothesis that unique substrates of Akt2 in the retina may not be regulated by Akt1 and Akt3 or the phenotype of Akt2 knockout mice may be due to the inactivation of specific substrate(s). In the present study, we identified a specific Akt2-specific substrate in the retina.

## 71.2 Materials and Methods

### *71.2.1 Plasmids and Vectors*

The bovine retinal cDNA library was kindly provided by Dr. Wolfgang Behr, University of Utah, Salt Lake City. The pLexA-ΔPH-Akt1, pLexA-ΔPH-Akt2, and pLexA-lamin were kindly provided by Dr. Anne Vojtek, University of Michigan, Ann Arbor. The mammalian expression constructs of hemagglutinin (HA)-tagged Akt1, Akt2, and Akt3 were kindly provided by Dr. Morris Birnbaum, University of Pennsylvania, Philadelphia.

### *71.2.2 Yeast Two-Hybrid Screen of the Bovine Retinal cDNA Library*

The yeast two-hybrid screen was performed in the L40 yeast strain using pLexA-ΔPH-Akt2 against a bovine retinal cDNA library ($3.6 \times 10^6$) cloned in frame fusion with the *GAL4* activation domain in the pGAD10. After transformation by the lithium acetate procedure (Rajala et al. 2004; Rajala and Chan 2005), yeast were plated on a tryptophan-leucine-histidine-deficient medium plus 5 mM aminotriazole.

Colonies growing in the absence of histidine were subsequently tested for β-galactosidase activity (Rajala et al. 2004). The plasmids of the library producing yeast colonies of a $His^+/LacZ^+$ phenotypes were isolated, and the cDNA inserts of these positive plasmids were sequenced.

### *71.2.3 Cell Lines and Culture Conditions*

HEK 293 T cells were maintained in DMEM medium containing 10% (v/v) FBS at 37°C. Approximately $2.5 \times 10^5$ cells were seeded in each 60 mm culture dish 12–18 h prior to transfection. Calcium phosphate-mediated DNA transfection was performed using each of the Akt1, Akt2, and Akt3 plasmids. Cells were harvested for experiments ~48 h post-transfection.

### *71.2.4 GST Pull-Down Assay*

The cDNA encoding POSH encompassing the amino acids 447–550 was cloned into a pGEX bacterial expression vector, which contains a protein tag of glutathione S-transferase (GST). The pGEX-POSH construct or GST control vector was transformed into BL21 (DE3) cells, and the GST-POSH or GST was purified as described (Rajala et al. 2004). Pull-down experiments were carried out as described (Rajala et al. 2004), using 5 μg of GST-POSH fusion or GST protein that had been adsorbed onto a GST-Sepharose 4B matrix. HEK-293 T cells expressing Akt1, Akt2, and Akt3 lysates were incubated with GST/GST-POSH proteins at 4 °C for 1.5 h, with continuous stirring. The Sepharose beads were washed three times in 500 μl HNTG buffer [20 mM HEPES (pH 7.5), 150 mM NaCl, 0.1% Triton X-100, and 10% glycerol] and centrifuged at 5000 rpm for 30–60 s at 4 °C. Bound proteins were eluted by boiling in 2X SDS sample buffer 5 min before 10% SDS-PAGE. After SDS-PAGE, the gels were subjected to immunoblot analysis with anti-HA and anti-GST antibodies.

## 71.3 Results

### *71.3.1 Identification of POSH as a Substrate of Akt2*

The bovine retinal cDNA library was screened against Akt2 and identified POSH as one of the interacting proteins. We isolated HIS3 and LacZ-positive clones, and the majority of the clones represent the protein POSH. The multidomain protein POSH acts as a scaffold for the JNK pathway of neuronal death (Xu et al. 2003).

### *71.3.2 POSH Interacts Specifically with Akt2*

Yeast transformations were performed by the lithium acetate method, as described elsewhere (Rajala and Chan 2005). Briefly, 0.5 μg of each plasmid of pLexA-ΔPH-Akt1, pLexA-ΔPH-Akt2, or pLexA-lamin and VP16-POSH (amino acids 447–550) was used to simultaneously transform the L40 yeast strain that harbors both His and LacZ reporters under the control of LexA-binding sites. Transformants were plated on media lacking tryptophan and leucine, or tryptophan, leucine, and histidine plus 5 mM aminotriazole. Growth on media lacking tryptophan and leucine secured the presence of both plasmids independently of protein-protein interactions and further eliminated the possibility of false negatives. Selection on media lacking tryptophan, leucine, and histidine plus 5 mM aminotriazole was used to detect potential interactions. Cells surviving on these plates were further screened for the LacZ phenotype by filter assay (Rajala et al. 2004). Lifted colonies were scored for LacZ phenotypes by detection of a blue color in the presence of 5-bromo-4-chloro-3-indolyl β-D-galactosidase after incubation at room temperature for 4 h. Our results showed specific interaction between Akt2 and POSH (Fig. 71.1). In this assay, we did not observe any interaction between Akt1 and POSH or laminin and POSH.

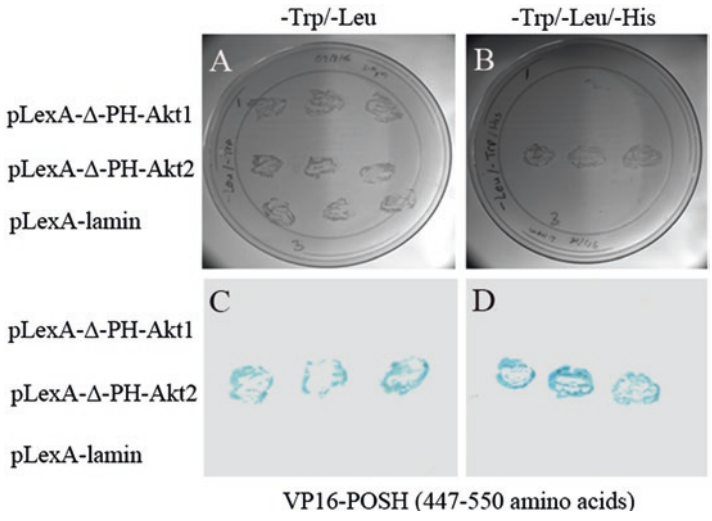


**Fig. 71.1** *Interactions of Akt2 with POSH in the yeast two-hybrid assay.* Yeast plasmid of pLexA-ΔPH-Akt1, pLexA-ΔPH-Akt2, or pLexA-lamin and VP16-POSH was used to simultaneously transform the L40 yeast strain that harbors both His and LacZ reporters under the control of LexA-binding sites. Transformants were plated on media lacking tryptophan and leucine (**a**), or tryptophan, leucine, and histidine plus 5 mM aminotriazole (**b**). Cells surviving on these plates were further screened for the LacZ phenotype by filter assay (**c**, **d**). Lifted colonies were scored for LacZ phenotypes by detection of a blue color in the presence of 5-bromo-4-chloro-3-indolyl β-D-galactosidase after incubation at room temperature for 2–4 h

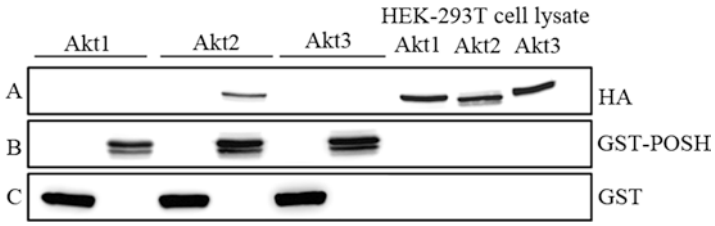


**Fig. 71.2** *GST pull-down experiments.* Individual HA-tagged Akt isoforms were expressed in HEK-293 T mammalian cells. Expressed proteins were incubated with GST or GST-POSH, and then GST pull-down assays were carried out. The bound proteins were washed and subjected to immunoblot analysis with anti-HA (**a**) and anti-GST (**b**, **c**) antibodies

We further examined the specific interaction between Akt2 and POSH in vitro using GST pull-down assays. The results clearly suggest a stable interaction between Akt2 and POSH. We observed no interaction of POSH with Akt1 or Akt3 (Fig. 71.2).

### *71.3.3 Localization of Mixed-Lineage Protein Kinase 3 (MLK3) in the Retina*

Immunolocalization studies suggest that MLK3 is predominantly localized to rod inner segments, ganglion cell layers, and outer and inner plexiform layers of the retina (Fig. 71.3a). The results indicate the expression of MLK3 in the retina.

## 71.4 Discussion

Our earlier studies showed that Akt2 has nonredundant functions in the retina. We hypothesize that this may be mediated through specific downstream target of Akt2. In the present study, we identified POSH as an Akt2 substrate. The interaction between POSH and Akt2 has also been observed outside the retina (Figueroa et al. 2003; Xu et al. 2003). POSH is an adapter protein with no catalytic function. Previous studies have demonstrated that POSH is involved in the JNK signaling pathway (Xu et al. 2003). Overexpression of POSH in cells has been shown to induce cell death (Lyons et al. 2007). A complex containing POSH, mixed-lineage protein kinase 3 (MLK3), and JNK was reported to trigger cell death. Activated Akt2 has been shown to phosphorylate MLK3, which results in the dissociation of MLK3 from the POSH and JNK complex and results in cell survival. The same signaling pathway might be occurring in the retina, as Akt2 knockout mice have increased susceptibility to light-induced photoreceptor degeneration. We found the expression of MLK3 (Fig. 71.3) and POSH (data not shown) in the retina. Further

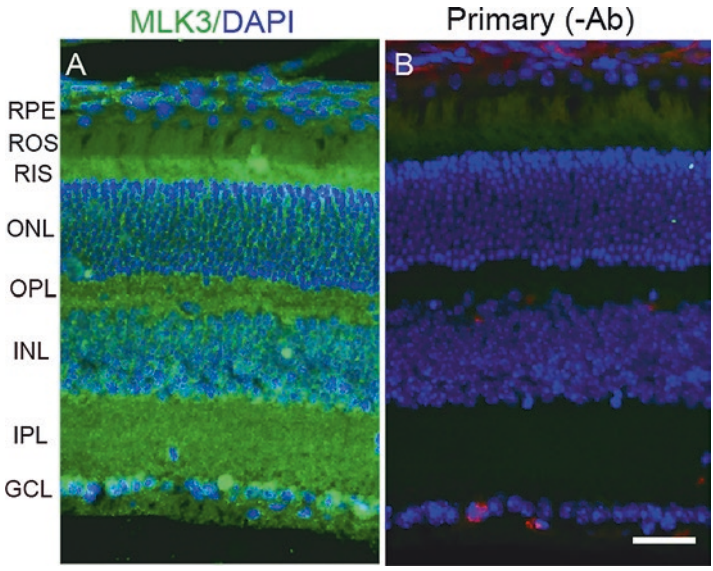


**Fig. 71.3** *Immunofluorescence analysis of MLK3 in the retina*. Prefer-fixed sections of mouse retinas were stained for MLK3 (**a**) and DAPI (**a**, **b**), and the immunofluorescence was analyzed by epifluorescence. Panel **B** represents the omission of MLK3 antibody. RPE retinal pigment epithelium, ROS rod outer segments, RIS rod inner segments, ONL outer nuclear layer, OPL outer plexiform layer, INL inner nuclear layer, IPL inner plexiform layer, GCL ganglion cell layer. Scale bar 50 μm

studies are required to examine the regulation of POSH by Akt2 and to understand the functional roles of JNK, MLK3, and POSH in the retina.

**Acknowledgments** This study was supported by grants from the National Institutes of Health (EY00871, and NEI Core grant EY021725) and an unrestricted grant from Research to Prevent Blindness, Inc. to the Department of Ophthalmology. The technical help of Dr. Ashok K. Dilly is appreciated. The authors acknowledge Ms. Kathy J. Kyler, staff editor, University of Oklahoma Health Sciences Center, for editing this manuscript.

## References

Figueroa C, Tarras S, Taylor J et al (2003) Akt2 negatively regulates assembly of the POSH-MLK-JNK signaling complex. J Biol Chem 278:47922–47927

Li G, Anderson RE, Tomita H et al (2007) Nonredundant role of Akt2 for neuroprotection of rod photoreceptor cells from light-induced cell death. J Neurosci 27:203–211

Li G, Rajala A, Wiechmann AF et al (2008) Activation and membrane binding of retinal protein kinase Balpha/Akt1 is regulated through light-dependent generation of phosphoinositides. J Neurochem 107:1382–1397

Lyons TR, Thorburn J, Ryan PW et al (2007) Regulation of the Pro-apoptotic scaffolding protein POSH by Akt. J Biol Chem 282:21987–21997

Rajala RV, Chan MD (2005) Identification of a NPXY motif in growth factor receptor-bound Protein 14 (Grb14) and its interaction with the Phosphotyrosine-Binding (PTB) domain of IRS-1. Biochemistry 44:7929–7935

Rajala RV, McClellan ME, Chan MD et al (2004) Interaction of the retinal insulin receptor beta-subunit with the P85 subunit of Phosphoinositide 3-Kinase. Biochemistry 43:5637–5650

Reiter CE, Sandirasegarane L, Wolpert EB et al (2003) Characterization of insulin signaling in rat retina in vivo and ex vivo. Am J Physiol Endocrinol Metab 285:E763–E774

Xu Z, Kukekov NV, Greene LA (2003) POSH acts as a scaffold for a multiprotein complex that mediates JNK activation in apoptosis. EMBO J 22:252–261

# Chapter 72
# Photoreceptor Outer Segment Isolation from a Single Canine Retina for RPE Phagocytosis Assay

**Raghavi Sudharsan, Michael H. Elliott, Natalia Dolgova, Gustavo D. Aguirre, and William A. Beltran**

**Abstract** Protocols for photoreceptor outer segment (POS) isolation that can be used in phagocytosis assays of retinal pigment epithelium (RPE) cells have routinely used a large number of cow or pig eyes. However, when working with large animal models (e.g., dog, cats, transgenic pigs) of inherited retinal degenerative diseases, access to retinal tissues may be limited. An optimized protocol is presented in this paper to isolate sufficient POS from a single canine retina for use in RPE phagocytosis assays.

**Keywords** Inherited retinal degeneration · Photoreceptor outer segment isolation · Retinal pigment epithelium · Phagocytosis · Canine

## 72.1 Introduction

The RPE has a number of important functions in the retina including transport of nutrients, secretion of neurotrophic factors, recycling of 11-cis retinal in the visual cycle, and phagocytosis and degradation of outer segment discs shed from the photoreceptors (Strauss 2005). Since RPE cells interact closely with the photoreceptors, mutations that affect RPE cells compromise photoreceptor function and vice versa.

R. Sudharsan · N. Dolgova · G. D. Aguirre · W. A. Beltran (✉)
Division of Experimental Retinal Therapies, Department of Clinical Sciences and Advanced Medicine, School of Veterinary Medicine, University of Pennsylvania, Philadelphia, PA, USA
e-mail: wbeltran@vet.upenn.edu

M. H. Elliott
Department of Ophthalmology, University of Oklahoma Health Science Centre, Oklahoma City, OK, USA



J. D. Ash et al. (eds.), *Retinal Degenerative Diseases*, Advances in Experimental Medicine and Biology 891, https://doi.org/10.1007/978-3-319-75402-4_72

In recent years, there has been increased interest in characterizing RPE function and assessing RPE health in large animal models of diseases that either directly affect the RPE, such as in the RPE65 form of Leber congenital amaurosis (LCA) (Gu et al. 1997; Marlhens et al. 1997; Aguirre et al. 1998), bestrophinopathies (Guziewicz et al. 2007; Xiao et al. 2010), or in diseases with mutations that affect primarily the photoreceptors with a secondary impact on RPE health and viability.

Phagocytosis of POS by either RPE primary cultures or cell lines is often used as a measure of RPE function in vitro. Current published protocols utilize a large number of rodent, cattle, or pig eyes to isolate the necessary amounts of POS for phagocytosis assays. Such protocols frequently require >20 cattle or pig eyes (Martin et al. 2005; Mao and Finnemann 2013) and are not optimal for use with large animal models of inherited retinal diseases for which retinal tissue resources are usually limited. In this paper, we present an optimized protocol for isolation of POS from a single retina of an adult dog. In addition, we present a simple protocol for primary canine RPE cell culture and show that these can be combined for use in RPE phagocytosis assays.

## 72.2 Isolation of POS from a Single Canine Retina

This protocol has been modified from the POS preparation protocol presented in Martin et al. (2005) and scaled down for preparation of POS from a single neuroretina of a large animal such as that of a dog.

### *72.2.1 Materials Required for POS Isolation*

1. Phosphate-buffered saline (PBS) (Thermo Scientific, catalog no. 28372)—500 ml.
2. Sucrose solutions prepared in PBS: 47%, 37%, 32%, and 10%—up to 10 ml per retina.
3. 2 ml tissue grinder (Wheaton, catalog no. 358003).
4. Beckman polyallomer tubes (9/16 × 31/2 in., catalog no. 331372).
5. Beckman Coulter Optima L-90 K Ultracentrifuge.
6. Beckman SW 41 TI swinging-bucket rotor.
7. Disposable transfer pipettes (7.5 ml capacity) (Samco Scientific Corporation, catalog no. 225).
8. 5 and 10 ml disposable serological pipettes (Fisherbrand).
9. Neubauer hemocytometer.

Chill all solutions to 4 °C. Rotor should be pre-cooled to 4 °C.

### *72.2.2 Protocol for POS Isolation*

1. Place a single, fresh or frozen (stored at −80 °C) canine neuroretina in a tissue grinder. Place the grinding chamber on ice. Add 1 ml of cold 47% sucrose-PBS solution. Use eight passes of the pestle to completely homogenize the tissue.
2. Transfer homogenized retinal extract to a Beckman polyallomer tube (9/16 × 31/2 in.) using a disposable transfer pipette.
3. Add 1.5 ml of cold 47% sucrose-PBS solution and mix well using the transfer pipette.
4. Carefully layer 6 ml of cold 37% sucrose-PBS solution on top. Slowly release the solution along the wall of the tube using a 10 ml serological pipette.
5. Next, layer 1.5 ml of cold 32% sucrose-PBS solution on top of the 37% sucrose-PBS solution layer.
6. Transfer the tube to a pre-cooled SW 41 TI rotor, taking care not to disturb the sucrose layers. Balance the rotor carefully.
7. Centrifuge in a Beckman Ultracentrifuge at 25,000 rpm for 90 min at 4 °C.
8. After centrifugation, POS layer will be formed at the junction of the 37% and 32% sucrose-PBS layer. Carefully remove the 32% sucrose-PBS solution using a disposable transfer pipette.
9. Use a new disposable transfer pipette to aspirate the isolated POS and transfer to a new Beckman polyallomer tube. Add 10 ml of 10% sucrose-PBS solution. Mix gently by pipetting.
10. Balance the rotor carefully and spin at 25,000 rpm in the ultracentrifuge for 20 min at 4 °C.
11. Remove the supernatant and resuspend the POS pellet in 0.5 ml of 10% sucrose-PBS solution.
12. POS yield can be calculated by counting the number of POS using a Neubauer hemocytometer.
13. Store POS at −80 °C.

**Note** For experiments where unbleached POS are required, or when working with light-sensitive mutant retinas, collection and all steps in the POS isolation protocol must be carried out under dim-red illumination.

Using this protocol, yield from a single canine retina ranged from 10,000 to 50,000 full-length POS and between 10 and 25 million full-length and fragmented POS ($n = 4$) (Fig. 72.1).

## 72.3 Primary RPE Cell Culture

The protocol for primary RPE cell culture was modified slightly from Stramm et al. (1983, 1990).

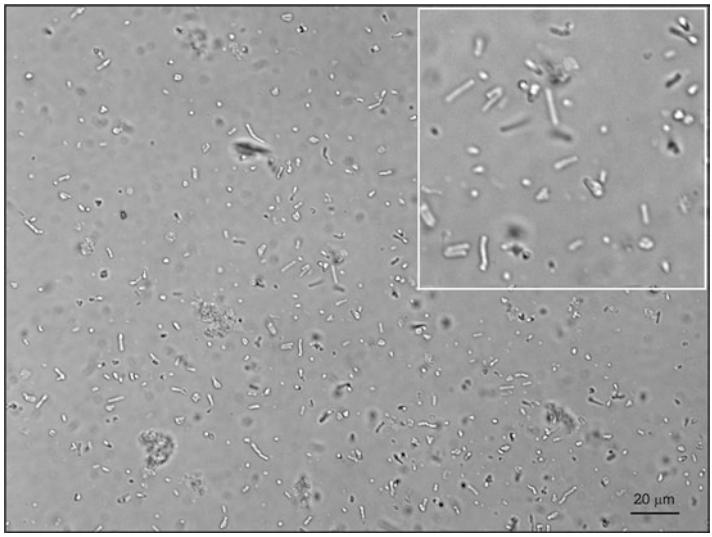


**Fig. 72.1** *POS isolated from a single canine retina*. POS were isolated from single canine retinas ($n = 4$). Image was acquired using a Zeiss Axioplan microscope

### *72.3.1 Materials Required for Primary RPE Cell Culture*

All reagents, media, instruments, and containers used for cell culture should be appropriately sterilized.

1. Transportation media: $CO_2$-independent medium (Gibco, catalog no. 18045-088) containing 2% penicillin/streptomycin (Lonza, catalog no. 17-602E).
2. 0.25% Trypsin-EDTA (Gibco, catalog no. 25200–056).
3. *Growth medium*: 20% FBS (Sigma, catalog no. F2442), 1% penicillin/streptomycin, 1% L-glutamine (Lonza, catalog no. 17-605E), 1% sodium pyruvate (Gibco, catalog no. 11360–070), 1% Eagle's minimum essential medium (MEM), nonessential amino acids (Sigma, catalog no. M7145), DMEM/F-12(1:1) medium (Gibco, catalog no. 11320-033).
4. Dulbecco's phosphate-buffered saline without $Ca^{+2}$ and $Mg^{+2}$ (DPBS) (Mediatech, catalog no. MT21-031-CV).
5. Transwell tissue culture plate (Corning Costar, catalog no. 3470).
6. 70% ethanol.
7. 50 ml specimen container.
8. Dissection tools: surgical prep blade, Noyes micro-scissors, microdissection tweezers, gauze.
9. Custom-made aluminum supports (see Fig. 72.2).
10. Sterile 15 ml disposable centrifuge tubes (Falcon, catalog no. 352196).


**Fig. 72.2** *Eyecup holders*. Custom-made aluminum supports of different diameters (indicated on the sides) to fit eyes of various sizes. The supports are sterilized by autoclaving before use

### *72.3.2 Protocol for RPE Cell Culture*

1. Enucleate eye from a dog immediately following euthanasia and store in transportation medium in a specimen container for 8–10 h at 4 °C.
2. All following steps should be performed in the cell culture hood. Dip the eye in 70% ethanol for a couple of minutes, and then rinse twice with DPBS containing 2% penicillin/streptomycin.
3. Dissect eyes by cutting the sclera 3–5 mm away from the limbus. Make a nick using a surgical prep blade and cut using micro-scissors and a microdissecting tweezer.
4. Separate the anterior segment/lens and gently remove the vitreous completely by slowly dragging the posterior cup over a dry sterile gauze.
5. Place the posterior cup on a sterile aluminum support. Fill the eyecup with DPBS and gently remove the detached retina.
6. Rinse the RPE layer thoroughly with DPBS.
7. Fill the eyecup with 0.25% trypsin-EDTA and incubate at 37 °C in a 5% $CO_2$ tissue culture incubator for 30 mins.
8. Collect detached RPE cells in trypsin-EDTA using a 1 ml pipette, transfer to a sterile 15 ml tube, and store at 37 °C in a 5% $CO_2$ tissue culture incubator.
9. Refill the eyecup with trypsin-EDTA. Repeat incubation and collection four to five times.
10. Pellet cells by centrifugation (1000 rpm, 5 min) and resuspend in the growth medium.
11. Seed RPE cells on Transwell tissue culture plates at a density of $10^5$ cells/$cm^2$.
12. Incubate cells at 37 °C in a 5% $CO_2$ tissue culture incubator for 2–3 weeks to form a confluent monolayer. Change medium 2–3 times a week during this period.

## 72.4 RPE Phagocytosis Assay

POS isolated from a single canine retina and RPE cells obtained from canine eyes can be used for RPE phagocytosis assay. In typical experiments, POS isolated from a single canine retina were used for feeding confluent RPE cells grown on six out of eight wells of an eight-chambered glass slide. Results from RPE phagocytosis assay are shown in Figs. 72.3 and 72.4.

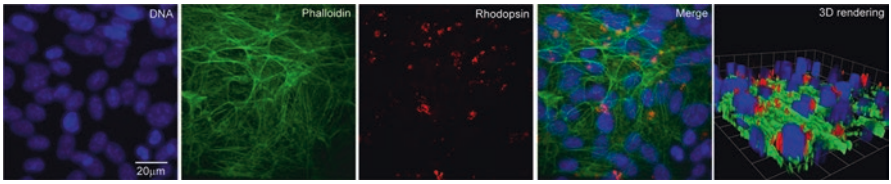


**Fig. 72.3** *Phagocytosis of canine POS by ARPE-19 cells*. Confluent polarized ARPE-19 cells were stained with DAPI nuclear stain, Alexa Fluor 488 phalloidin, and anti-rhodopsin antibody after POS phagocytosis. Images were acquired using a Leica DMI 4000 inverted microscope equipped with a Yokogawa spinning disk confocal head and a Hamamatsu EMCCD 510 camera. Over 50 fields each containing ~50 cells were counted to evaluate the percentage of cells showing ROS phagocytosis. 65 ± 5% of the ARPE-19 cells were found to phagocytize ROS

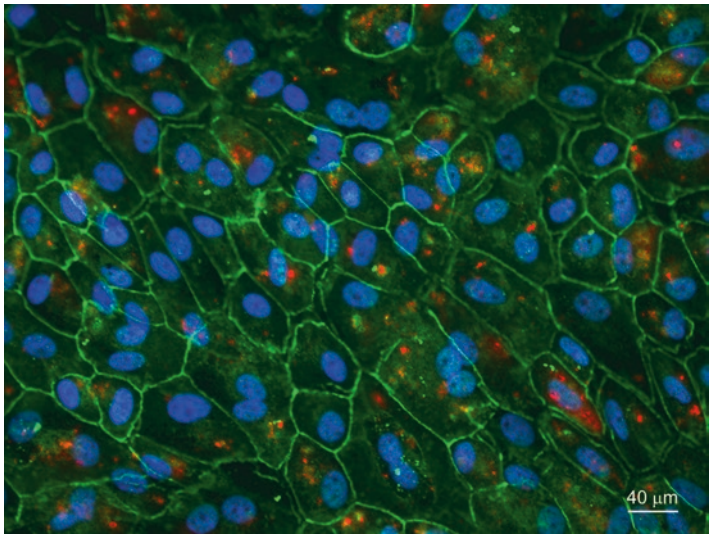


**Fig. 72.4** *Phagocytosis of canine POS by primary canine RPE cells*. Confluent polarized canine primary RPE cells were stained with anti-rhodopsin and anti-ZO-1 antibody after POS phagocytosis. Images were acquired using a Zeiss Axioplan epifluorescence microscope

### 72.4.1 Materials Required for RPE Phagocytosis Assay

1. Primary RPE monolayer or ARPE-19 cells (ATCC, catalog no. CRL-2302) grown on 8-chambered glass slide (Lab-Tek, catalog no. 155411) in growth medium.
2. *Polarization medium*: Dulbecco's MEM (DMEM) (Mediatech, catalog no. MT10-013-CV) with 1% FBS.
3. POS.
4. Neubauer hemocytometer.

### 72.4.2 Materials Required for Antibody Staining After Phagocytosis

1. Phosphate-buffered saline (PBS) (Thermo Scientific, catalog no. 28372).
2. Fixative: 4% paraformaldehyde prepared in PBS.
3. Permeabilization: 0.2% Triton X-100 (Fisher Scientific, catalog no. BP151-100) in PBS.
4. Blocking buffer: 5% BSA and 4.5% fish gelatin (Sigma, catalog no. G7765-250ML) in PBS.
5. Dilution buffer for Alexa Fluor 488 phalloidin: 1% BSA in PBS.
6. Antibodies:
   (a) Mouse anti-rhodopsin antibody (Millipore, catalog no. MAB5356).
   (b) Rabbit anti-ZO-1 antibody (Invitrogen, catalog no. 402200).
   (c) Alexa labeled anti-mouse and anti-rabbit secondary antibodies (Invitrogen).
7. Alexa Fluor 488 phalloidin (Molecular probes, catalog no. A12379).
8. DAPI (4′,6-Diamidino-2-Phenylindole, Dihydrochloride) (ThermoFisher Scientific, catalog no. D1306).

### 72.4.3 Protocol for RPE Phagocytosis Assay

1. Day 1: Seed primary RPE cells or ARPE-19 cells in *growth medium* on 8-chambered glass slides for next-day confluence. Incubate at 37 °C in 5% $CO_2$ tissue culture incubator for 24 h.
2. Day 2: Change cell *growth medium* to *polarization medium*. Incubate overnight at 37 °C in the 5% $CO_2$ tissue culture incubator.
3. Day 3: Thaw POS; calculate POS density using a hemocytometer. Centrifuge to pellet POS, and then resuspend in polarization medium.
4. Overlay POS suspension on the RPE cells in each chamber at an approximate density of 10 POS per cell.

5. Incubate in the cell culture incubator for 5 h.
6. Remove medium and wash cells three times with DPBS.
7. Fix cells with 4% paraformaldehyde at room temperature for 20 min. Wash three times with DPBS. Store at 4 °C or proceed with antibody and phalloidin-alexa-488 labeling.

### *72.4.4 Labeling POS with Anti-rhodopsin Antibody and Counterlabeling with ZO-1 Antibody or Alexa Fluor 488 phalloidin*

1. Permeabilize cells in the 8-chambered glass slide with 0.2% Triton X-100 in PBS for 5 min. Wash three times with PBS.
2. Incubate cells in blocking buffer for 30 min at room temperature.
3. Incubate with anti-rhodopsin antibody alone or along with anti-ZO-1 antibody diluted in blocking buffer (mouse-anti-rhodopsin 1:400, rabbit-anti-ZO-1 antibody 1:100) for 1 h at 37 °C.
4. Wash three times with PBS.
5. Incubate with appropriate alexa-labeled secondary antibodies diluted 1:400 in blocking buffer for 1 h at room temperature.
6. Wash three times with PBS.
7. If performing phalloidin staining, incubate with Alexa Fluor 488 phalloidin diluted 1:50 in 1% BSA-PBS for 30 min at room temperature.
8. Wash three times with PBS.
9. Counterstain nuclei with DAPI stain. Wash once with PBS.
10. Detach media chamber from the slide. Apply appropriate mounting medium and coverslip and image using widefield epifluorescence or confocal microscopy.

**Acknowledgments** The authors are grateful to the staff of RDSF facility for animal husbandry, Ms. Lydia Melnyk, for research coordination. This work is supported by NEI/NIH grants R24EY022012, R24EY023937, EY06855, EY017549, P30EY-001583, P30-EY021725, the Foundation Fighting Blindness, Hope for Vision, an unrestricted grant from Research to Prevent Blindness, and Van Sloun Fund for Canine Genetic Research.

## References

Aguirre GD, Baldwin V, Pearce-Kelling S et al (1998) Congenital stationary night blindness in the dog: common mutation in the RPE65 gene indicates founder effect. Mol Vis 4:23

Gu SM, Thompson DA, Srikumari CR et al (1997) Mutations in RPE65 cause autosomal recessive childhood-onset severe retinal dystrophy. Nat Genet 17:194–197

Guziewicz KE, Zangerl B, Lindauer SJ et al (2007) Bestrophin gene mutations cause canine multifocal retinopathy: a novel animal model for best disease. Invest Ophthalmol Vis Sci 48:1959–1967

Mao Y, Finnemann SC (2013) Analysis of photoreceptor outer segment phagocytosis by RPE cells in culture. Methods Mol Biol 935:285–295

Marlhens F, Bareil C, Griffoin JM et al (1997) Mutations in RPE65 cause Leber's congenital amaurosis. Nat Genet 17:139–141

Martin RE, Elliott MH, Brush RS et al (2005) Detailed characterization of the lipid composition of detergent-resistant membranes from photoreceptor rod outer segment membranes. Invest Ophthalmol Vis Sci 46:1147–1154

Strauss O (2005) The retinal pigment epithelium in visual function. Physiol Rev 85:845–881

Stramm LE, Haskins ME, McGovern MM, Aguirre GD (1983) Tissue culture of cat retinal pigment epithelium. Exp Eye Res 36:91–101

Stramm LE, Wolfe JH, Schuchman EH et al (1990) Beta-glucoronidase mediated pathway essential for retinal pigment epithelial degradtion of glycosaminoglycans. Disease expression and in vito disease correction using retroviral mediated cDNA transfer. Exp Eye Res 50:521–532

Xiao Q, Hartzell HC, Yu K (2010) Bestrophins and retinopathies. Pflugers Arch 460:559–569

# Chapter 73
# Preservation of Photoreceptor Nanostructure for Electron Tomography Using Transcardiac Perfusion Followed by High-Pressure Freezing and Freeze-Substitution


**Stefanie Volland and David S. Williams**

**Abstract** The phototransductive membrane disks of a vertebrate photoreceptor outer segment (OS) are highly susceptible to perturbations during preservation for electron microscopy. To optimize their preservation for nanostructural studies, such as with electron tomography (ET), we developed a protocol, using a combination of chemical and physical fixation approaches, including transcardiac perfusion, high-pressure freezing, and freeze-substitution.

**Keywords** Photoreceptor · Electron tomography · High-pressure freezing · Freeze-substitution · Disk membrane morphogenesis

## 73.1 Introduction

Phototransduction takes place in stacked membrane disks contained within the OS of the vertebrate photoreceptor. These disks are turned over by the shedding of older disks at the OS tip and the formation of new disks at the base of the OS (Young 1967). Because disk morphogenesis involves complex membrane-shaping

S. Volland (✉)
Department of Ophthalmology, Stein Eye Institute, UCLA School of Medicine, Los Angeles, CA, USA
e-mail: svolland@ucla.edu

D. S. Williams (✉)
Department of Ophthalmology, Stein Eye Institute, UCLA School of Medicine, Los Angeles, CA, USA

Department of Neurobiology, UCLA School of Medicine, Los Angeles, CA, USA

Molecular Biology Institute, UCLA School of Medicine, Los Angeles, CA, USA

Brain Research Institute, UCLA School of Medicine, Los Angeles, CA, USA
e-mail: dswilliams@ucla.edu



J. D. Ash et al. (eds.), *Retinal Degenerative Diseases*, Advances in Experimental Medicine and Biology 891, https://doi.org/10.1007/978-3-319-75402-4_73

mechanisms, it is necessary to first define the membrane organization at the base of the OS. To achieve this goal, we studied the disk membrane nanostructure by using ET (Volland et al. 2015). For these studies tissue preservation is paramount, but also challenging. The disk membranes, especially the nascent disk membranes, seem to be particularly susceptible to anoxia and mechanical damage, which readily leads to artifacts during tissue preparation.

Chemical fixation methods, such as those involving transcardiac perfusion, allow quick and effective delivery of fixative to target organs in situ and can help stabilize delicate tissue, prior to dissection (Sosinsky et al. 2008). On the other hand, high-pressure freezing (HPF) and other physical fixation approaches (e.g., slam freezing) are preferable to chemical fixation as they allow fixation within milliseconds, rather than seconds to minutes for chemical fixation. But they pose their own set of limitations (Studer et al. 2001). Only small tissue samples of about 300 μm in thickness can be frozen without ice crystal damage (McDonald and Auer 2006), which means that tissues like the retina need to be exposed by ocular enucleation and dissection prior to HPF. Previous reports have shown that a combination of chemical and physical fixation methods can yield superior results when sensitive tissues are being processed (Murk et al. 2003; Sosinsky et al. 2008). Here, we provide a detailed description of a combination protocol that was optimized for the preservation of photoreceptor disk membranes. This protocol was used to study the nanostructure of these membranes by ET.

## 73.2 Transcardiac Perfusion

Wild-type mice of the strain C57BL/6J were treated in accordance with the appropriate institutional guidelines. Animals were kept under a 12 h light/12 h dark cycle and used at an age of 4–8 weeks. The mice were deeply anesthetized before an abdominal incision and thoracotomy were performed to expose the heart. A G20 needle, attached to a catheter, was inserted into the left ventricle, and the right atrium was cut open. Chilled (4 °C) 0.1 M phosphate buffered saline was then passed through the catheter, using gravity to drive the perfusion. After 1 min, the perfusate was switched to chilled (4 °C) Karnovsky fixative (2% paraformaldehyde and 2.5% glutaraldehyde in 0.1 M phosphate buffer). Each mouse was then perfused with ~20 ml fixative before the eyes were enucleated and dissected quickly. Small pieces of retinal tissue (~1 mm × 1 mm) were kept in fixative solution on ice until they were frozen under high pressure within 1 h of initial fixation.

## 73.3 High-Pressure Freezing and Freeze-substitution

Each piece of retinal tissue was placed in a Leica flat specimen carrier (diameter, 1.5 mm; depth, 200 μm), with additional 0.1 M phosphate buffer, and transferred to a freezer holder where the specimen chamber was sealed with a diamond screw.

The holder was attached to a handle and placed in an EMPACT2 high-pressure freezer (Leica Microsystems, Wetzlar, Germany). The tissue was then frozen within milliseconds under high pressure of >2000 bar, allowing samples of up to 300 μm in thickness to be frozen without the perturbation of cellular ultrastructure from ice crystal formation. After freezing, samples were collected and transferred in liquid nitrogen to an EM AFS2 automatic freeze-substitution unit (Leica Microsystems, Wetzlar, Germany). The specimen carriers containing the tissue were quickly placed in 1.5 ml Eppendorf tubes filled with 1% osmium tetroxide and 0.1% uranyl acetate in acetone at −90 °C, within the freeze-substitution unit. Over the course of 88 h, the temperature was gradually raised from −90 °C to room temperature (20 °C) while the fixative slowly replaced the water in the samples. After freeze-substitution, samples were washed 3× for 5 min in acetone and propylene oxide consecutively, before they were infiltrated with 1:2 and 2:1 parts Araldite 502 resin (Electron Microscopy Sciences, Hatfield, USA) to propylene oxide, respectively, for 30 min each. Finally, samples were transferred to pure Araldite 502 resin for another 30 min and then placed in flat molds and polymerized at 60 °C for 48 h. Sections, 300 nm thick, were collected on formvar-coated, copper, slot grids and stained for contrast with 10% uranyl acetate in methanol and 0.4% lead citrate in 0.4% sodium hydroxide for 10 min each. Gold fiducials (Ted Pella, Redding, USA) of 15 and 20 nm diameters were then placed on opposite sides (top and bottom) of the slot grids. At this stage grids can be carbon coated to stabilize the sections in the electron beam during image acquisition, but we usually didn't find this to be necessary.

## 73.4 Electron Tomography and Data Processing

ET is an extension of conventional transmission electron microscopy, with the difference that the sections are thicker and imaged at higher acceleration voltages. We performed ET on mouse retinal sections, using an FEI Tecnai TF20, operated at 200 kV, and FEI's "batch tomography" software (Hillsboro, USA). A series of images were recorded as the section was tilted from −70° to +70°, with 2° increments at the lower tilt angles (range ± 40°) and 1° increments above +40° and below - 40°. The images were collected with a 16-megapixel CCD camera (TVIPS) at magnifications between 14,500× and 19,000× and with an under-focus of approximately −1 to 3 μm. To obtain dual-tilt data sets, the grids were rotated by 90° on the x-y axis after the acquisition of a first tilt series, and a second tilt axis was recorded, centered on the same point.

We used "eTomo" in the IMOD software package (Boulder, USA) to generate tomographic reconstructions of the acquired double-tilt series through fiducial-based alignment (Fig. 73.1a, b). A median filter of n4 was used to improve the reconstruction appearance if deemed necessary (Fig. 73.1a). After tomogram reconstruction, segmentation and subsequent image processing were conducted using "3dmod" (IMOD, Boulder, USA). Every 3–10 z-slices of the tomographic

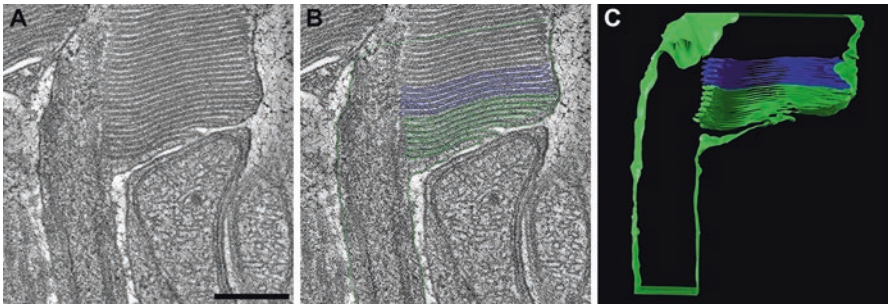


**Fig. 73.1** Photoreceptor morphology after the combined fixation approach, using transcardiac perfusion and HPF (modified from Volland et al. 2015). (**a**) Z-slice from a tomographic reconstruction of the basal area of a mouse rod OS (median filter n4). (**b**) Z-slice from the same tomogram (no filter), with 3-D renderings, tracing the connecting cilium, nascent disks and the OS plasma membrane in light green, and mature disks in dark blue. (**c**) Overview of a 3-D model of the rod OS basal area, based on the tomogram shown in (**a**) and (**b**). Scale bar 300 μm

reconstruction were traced manually to create a 3-D model of the membrane disks at the photoreceptor OS base (Fig. 73.1c). The photoreceptors OS plasma membrane and membranes continuous with it were modeled in light green, in contrast to mature disks, modeled in dark blue (Fig. 73.1b, c). Videos of 3-D models were generated using Chimera (UCSF, San Francisco, USA), while videos of tomogram reconstructions were generated using 3dmod (IMOD, Boulder, USA) and Fiji (NIH), an open-source processing package (e.g., Suppl. Movies in Volland et al. 2015).

## 73.5 Conclusions

ET is a powerful tool to visualize the 3-D ultrastructure of cells and, in particular, allows insight into complex membrane organization (McDonald and Auer 2006). In order to obtain optimal images from mouse photoreceptors, we used a combination of chemical and physical fixation approaches, including transcardiac perfusion, high-pressure freezing, and freeze-substitution. These samples were well suited for ET and enabled us to study the formation of nascent disks using 3-D visualization. Overall, we were able to show that a combination of different fixation methods allows for better preservation than either method can on its own.

**Acknowledgments** This study was supported by NIH grants R01EY24667, R01EY13408, and P30EY00331. We thank Ivo Atanasov for technical assistance and acknowledge the use of instruments at the Electron Imaging Center for Nanomachines, supported by UCLA and NIH grant S10RR23057.

## References

McDonald KL, Auer M (2006) High-pressure freezing, cellular tomography, and structural cell biology. BioTechniques 4:137–143. 139, 141

Murk JL, Posthuma G, Koster AJ et al (2003) Influence of aldehyde fixationon on the morphology of endosomes and lysosomes: quantitative analysis and electron tomohgraphy. J Microsc 212:81–90

Sosinsky GE, Crum J, Jones YJ et al (2008) The combination of chemical fixation procedures with high pressure freezing and freeze substitution preserves highly labile tissue ultrastructure for electron tomography applications. J Struct Biol 161:359–371

Studer D, Graber W, Al-Amoudi A, Eggli P (2001) A new approach for cryofixation by high-pressure freezing. J Microsc 203:285–294

Volland S, Louise CH, Kong C et al (2015) Three-dimensional organization of nascent rod outer segment disk membranes. PNAS 112:14870–14875

Young RW (1967) The renewal of photoreceptor cell outer segments. J Cell Biol 33:61–72

# Chapter 74
# Microtubule-Associated Protein 1 Light Chain 3 (LC3) Isoforms in RPE and Retina


**Anuradha Dhingra, Desiree Alexander, Juan Reyes-Reveles, Rachel Sharp, and Kathleen Boesze-Battaglia**

**Abstract** Microtubule-associated protein 1 light chain 3 (MAP1LC3), a human homologue of yeast Atg8, is an essential component of autophagy. LC3 plays a critical role in hybrid degradation pathways in which some but not all components of autophagy are coupled with phagocytosis in a process known as LC3-associated phagocytosis (LAP). LC3 exists as three highly homologous isoforms in human (LC3A, LC3B, and LC3C) with two of these (LC3A and LC3B) in mouse. LC3B predominated in both fetal and adult human retinal pigment epithelium (RPE) relative to LC3A and LC3C, while in mouse RPE and neural retina, LC3A and LC3B were expressed at approximately equivalent levels. In situ hybridization studies localized LC3A and LC3B transcripts in the retina and RPE. LC3B protein was detected in C57Bl6/J RPE and retinal lysates and was absent in the *LC3BKO* mouse.

**Keywords** LC3 isoforms · Phagocytosis · Retinal pigment epithelium

## 74.1 Introduction

Autophagy proteins are strongly expressed in the retina and in the RPE, with accumulation of proteins and damaged organelles a common characteristic of the aging RPE as well as of age-related macular degeneration (Mitter et al. 2012; Rodriguez-Muela et al. 2013; Boya et al. 2016; Kauppinen et al. 2016; Szatmari-Toth et al. 2016). In addition to macroautophagy, the catabolic cell survival mechanism, normal vision is also dependent on a hybrid autophagy-phagocytosis degradative pathway termed LC3-associated phagocytosis (LAP) (Kim et al. 2013; Frost et al. 2015; Martinez et al. 2015). LAP plays a critical role in visual pigment regeneration (Kim et al. 2013) as well as the complete degradation of phagosomes (Frost et al. 2015). LAP and autophagy both rely on the lipidation of LC3 to LC3II which enables its

A. Dhingra · D. Alexander · J. Reyes-Reveles · R. Sharp · K. Boesze-Battaglia (✉)
Department of Biochemistry, SDM, University of Pennsylvania, Philadelphia, PA, USA
e-mail: battagli@upenn.edu



J. D. Ash et al. (eds.), *Retinal Degenerative Diseases*, Advances in Experimental Medicine and Biology 891, https://doi.org/10.1007/978-3-319-75402-4_74

membrane association to either double-membrane autophagosomes or single membrane phagosome. The three isoforms of human MAP1LC3, LC3A, LC3B, and LC3C, differ in their posttranslational modifications (He et al. 2003), with mouse orthologs corresponding to LC3A and LC3B. These isoforms share a high degree of sequence similarity and have a conserved C terminal glycine site for PE conjugation (Schaaf et al. 2016). Herein, we have characterized LC3 isoforms in human and mouse RPE.

## 74.2 Materials and Methods

### *74.2.1 Animals*

C57Bl6/J (WT) mice and the *LC3BKO* mouse line (strain name: B6;129P2-Map1Lc3b$^{tm1Mrab}$/J; stock # 009336) (Cann et al. 2008) were purchased from Jackson Laboratory (Bar Harbor, ME). *GFP-LC3* mice expressing a cDNA encoding EGFP fused at its C-terminus to rat LC3B under control of the CAG promoter as described (Mizushima et al. 2004) were obtained from RIKEN BioResource Center (RBRC00806; GFP-LC3#53). Mice were backcrossed to C57BL/6 J for 22 generations at RIKEN (personal communication). Maintenance of mouse colonies and all experiments involving animals were performed as described previously (Frost et al. 2015).

### *74.2.2 Antibodies*

Primary antibodies used were mouse anti-actin (A2228; Sigma-Aldrich, St. Louis, MO); rabbit anti-LC3 (ab48394), anti-LC3A (ab62720), and anti-GFP (ab290) from Abcam; rabbit and mouse anti-LC3B (2775S and D11, respectively) from Cell Signaling Technology; and rabbit anti-LC3C (18726–1-AP) from Proteintech.

### *74.2.3 Immunoblotting and Immunostaining*

ARPE19 and hfRPE and hRPE (human fetal and adult RPE cells, respectively) were maintained as described (Frost et al. 2015). Immunostaining and immunoblotting were performed as described (Frost et al. 2015). For westerns, primary antibody concentrations were anti-LC3B (1:1500), anti-LC3A (1:1000), anti-LC3C (1:1,1000), anti-β-actin (1:5000), or anti-GFP (1:1000).

### *74.2.4 In Situ Hybridization*

RNA in situ hybridization was performed using RNAscope Fluorescent Multiplex reagent kit as per the manufacturer's instructions (Advanced Cell Diagnostics). Probes included LC3A and LC3B (18ZZ Mm-Map1lc3a targeting 38-1006 of NM_025735.3 and 20ZZ Mm-Map1lc3b targeting 43-1081 of NM_026160.4).

### *74.2.5 RT-PCR*

Quantitative real-time RT-PCR was performed using total RNA from mouse retina and RPE as described previously (Nikonov et al. 2013). The mouse PCR primers used were based on sequences available from Harvard PrimerBank. The following human PCR primers were used:

LC3A (NM_032514):

CGTCCTGGACAAGACCAAGT (forward), CTCGTCTTTCTCCTGCTCGT (reverse).

LC3B (NM_022818.4):

AGCAGCATCCAACCAAAATC (forward), CTGTGTCCGTTCACCAACAG (reverse).

LC3C (NM_001004343.2):

CGGAAGCCTTTTACTTGCTG (forward), GTCTGTCCTCAAGGCTGCTC (reverse).

## 74.3 Results

### *74.3.1 LC3B Is the Predominant Splice Variant in Human RPE*

The relative expression levels of the three LC3 isoforms were determined in hfRPE and ARPE19 cells by qRT-PCR with primers specific for each isoform. In both cell types, LC3B is expressed at significantly higher levels than LC3A, and LC3C was undetectable (Fig. 74.1a). The protein expression of LC3 isoforms was confirmed by immunoblotting; however due to a high degree of sequence homology across the isoforms, many of the commercially available antibodies show cross-reactivity as described (Klionsky et al. 2016). Figure 74.1b shows protein sequence alignments of the three isoforms, with invariant residues in red and similar residues in yellow boxes; regions corresponding to antibody epitopes are indicated (Fig. 74.1b). When

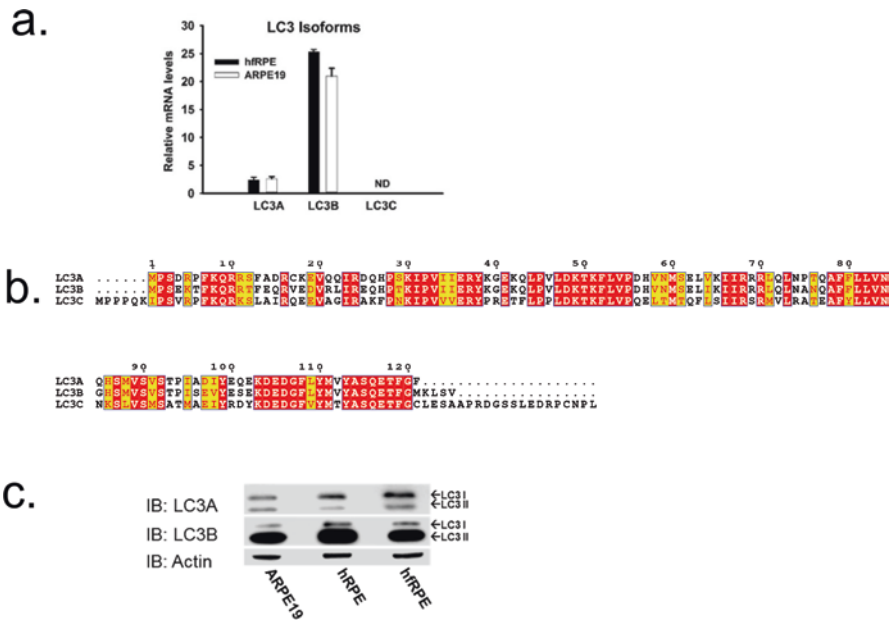


**Fig. 74.1** *LC3A and LC3B mRNA and protein expression in human RPE.* (**a**) LC3A, LC3B, and LC3C transcript levels by qRT-PCR in human RPE cells. Results are mean (±SD) of three individual experiments. ND: not detectable. (**b**) Amino acid alignment (using T-coffee algorithms interfaced with ESPRIPT for visual representation) of the three LC3 isoforms with identical residues highlighted in red and similar residues highlighted in yellow. Locations of epitopes for anti-LC3A and anti-LC3C are indicated by green rectangles; both anti-LC3B antibodies used were raised against synthetic peptides corresponding to an N-terminal region of LC3B; and lipidation sites are indicated by green arrow. (**c**) Western blot showing LC3A and LC3B proteins in ARPE19, hRPE, and hfRPE cells.

anti-LC3A or anti-LC3B antibody (D11) was used for immunoblotting, ARPE19, hRPE, and hfRPE cell lysates gave the expected size bands corresponding to unlipidated and lipidated forms of LC3A and LC3B (Fig. 74.1c); anti-LC3C did not show any specific band (data not shown).

### *74.3.2 LC3A and LC3B Transcripts Are Expressed in the Mouse Retina and RPE*

In mouse RPE and retina, the transcript levels of the two isoforms LC3A and LC3B were comparable in both WT retina and WT RPE (Fig. 74.2a). As expected, LC3B transcript was absent in the *LC3BKO* mouse; moreover, there was no significant upregulation of LC3A. In situ hybridization indicated LC3A (green) and B (red) transcripts are both present in the RPE and retina (Fig. 74.2b, left). As expected, the levels of LC3B were higher in the GFP-LC3$^{tg/tg}$, and only LC3A was detectable in the *LC3BKO* (Fig. 74.2b).

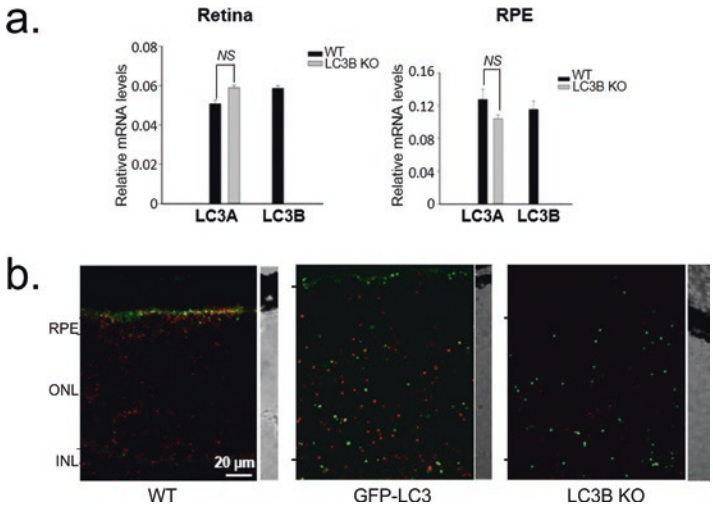


**Fig. 74.2** *Expression of LC3A and LC3B transcripts in the mouse retina and RPE.* (**a**) LC3A and B transcript levels examined by qRT-PCR on mouse retina (left) and RPE (right) for WT and *LC3BKO* as indicated. Results are mean (±SD) of three individual experiments. NS, nonsignificant. (**b**) Confocal micrographs from RNA scope in situ hybridization for LC3A (green) and LC3B (red) in *WT*, GFP-LC3, and *LC3BKO* mouse retinal sections (left) and transmitted light image for orientation (right). ONL, outer nuclear layer; INL, inner nuclear layer

### *74.3.3 Absence of LC3B Does Not Result in Compensatory Upregulation of LC3A Protein*

LC3 isoform protein expression was confirmed in the WT, GFP-LC3$^{tg/tg}$, GFP-LC3$^{tg/wt}$, and *LC3BKO* by immunoblot. Given that the LC3 isoforms have significant homology (Fig. 74.3a), using different genotypes allowed us to further define specificity of the anti-LC3A and anti-LC3B antibodies. When probed with the anti-LC3B antibody (D11), LC3 doublets were detected in all genotypes except for *LC3BKO* (Fig. 74.3b); GFP-LC3$^{tg/tg}$ and GFP-LC3$^{tg/wt}$ also showed higher bands (corresponding to GFP-LC3 fusion protein with both D11 and anti-GFP antibodies). The LC3 doublet was observed in both *LC3BKO* and WT retina with the anti-LC3A antibody. The expression levels in the WT and *LC3BKO* RPE are comparable, suggesting no compensatory upregulation of LC3A in the *LC3BKO*.

Expression of LC3B in the mouse RPE was further evaluated by immunostaining of WT and *LC3BKO* retinal sections. Because the D11 antibody is not optimal for immunostaining applications, we used another LC3B antibody (anti-rabbit LC3 from Cell Signaling). Numerous LC3-positive structures are observed in WT RPE (Fig. 74.3c), with almost negligible levels in the LC3BKO. Interestingly, there appears to be more rhodopsin-positive puncta in the LC3B KO RPE, suggesting phagosomal accumulation. Mice used in immunostaining experiments were

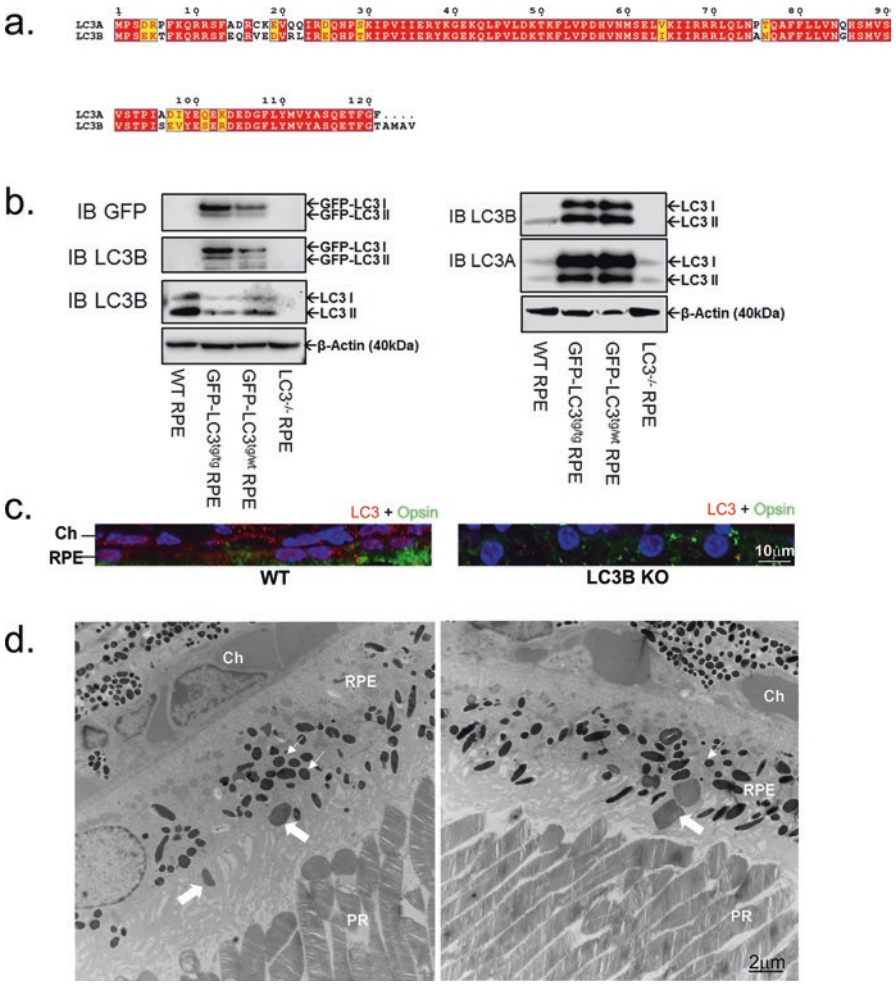


**Fig. 74.3** *Expression of LC3A and LC3B in the mouse RPE*. (**a**) Amino acid alignment of mouse LC3 isoforms. (**b**) Representative immunoblots showing expression of LC3B (with antibodies D11, left, and ab48394, right) and LC3A proteins in RPE from different genotypes. (**c**) Confocal micrographs of WT and *LC3BKO* mouse RPE immunostained for LC3B and opsin. (**d**) Electron micrographs obtained as described (Frost et al. 2015) from *LC3KO* retina 7 h after light onset, showing outer segment uptake (thick arrows) and phagosome accumulation (thin arrow)

sacrificed at 6 h after light onset, past the burst of phagocytosis in WT. Delayed phagosome uptake or maturation was also inferred from EM analysis. Figure 74.3d shows the uptake of outer segments and accumulation of the phagosomes in EM images from *LC3BKO* retina isolated at 2 pm. The RPE phagocytic machinery and retinal phenotype in the *LC3BKO* mouse are currently under investigation.

## 74.4 Discussion

Given the critical role of LAP in RPE function and retinal homeostasis (Frost et al. 2015; Kim et al. 2013), it is important to establish the expression profile of the LC3 isoforms. The studies herein show that LC3B transcripts represent the predominant isoform in mouse RPE and retina; LC3B protein is the most abundant LC3 isoform in human and mouse RPE; and in the absence of LC3B, there is no compensatory increase in the levels of LC3A. However, compensatory increases in the level of other LC3-like proteins (GABARAPs) cannot be ruled out. Our results also point to altered phagocytic processing in the absence of LC3B. Our current studies are focused on understanding the role played by LC3B in RPE and to further characterize the structural/functional defects in the absence of this protein.

**Acknowledgments** Studies were supported by NIH grants EY010420 and EY026525 (KBB). The authors thank the PDM-live cell imaging core and the UPENN EM core for analyses.

## References

Boya P, Esteban-Martinez L, Serrano-Puebla A et al (2016) Autophagy in the eye: development, degeneration, and aging. Prog Retin Eye Res 55:206–245

Cann GM, Guignabert C, Ying L et al (2008) Developmental expression of LC3alpha and beta: absence of fibronectin or autophagy phenotype in LC3beta knockout mice. Dev Dyn 237:187–195

Frost LS, Lopes VS, Bragin A et al (2015) The contribution of melanoregulin to microtubule-associated protein 1 light chain 3 (LC3) associated phagocytosis in retinal pigment epithelium. Mol Neurobiol 52:1135–1151

He H, Dang Y, Dai F et al (2003) Post-translational modifications of three members of the human MAP1LC3 family and detection of a novel type of modification for MAP1LC3B. J Biol Chem 278:29278–29287

Kauppinen A, Paterno JJ, Blasiak J et al (2016) Inflammation and its role in age-related macular degeneration. Cell Mol Life Sci 73:1765–1786

Kim JY, Zhao H, Martinez J et al (2013) Noncanonical autophagy promotes the visual cycle. Cell 154:365–376

Klionsky DJ, Abdelmohsen K, Abe A et al (2016) Guidelines for the use and interpretation of assays for monitoring autophagy (3rd edition). Autophagy 12:1–222

Martinez J, Malireddi RK, Lu Q et al (2015) Molecular characterization of LC3-associated phagocytosis reveals distinct roles for Rubicon, NOX2 and autophagy proteins. Nat Cell Biol 17:893–906

Mitter SK, Rao HV, Qi X et al (2012) Autophagy in the retina: a potential role in age-related macular degeneration. Adv Exp Med Biol 723:83–90

Mizushima N, Yamamoto A, Matsui M et al (2004) In vivo analysis of autophagy in response to nutrient starvation using transgenic mice expressing a fluorescent autophagosome marker. Mol Biol Cell 15:1101–1111

Nikonov SS, Lyubarsky A, Fina ME et al (2013) Cones respond to light in the absence of transducin beta subunit. J Neurosci 33:5182–5194

Rodriguez-Muela N, Koga H, Garcia-Ledo L et al (2013) Balance between autophagic pathways preserves retinal homeostasis. Aging Cell 12:478–488

Schaaf MB, Keulers TG, Vooijs MA et al (2016) LC3/GABARAP family proteins: autophagy-(un) related functions. FASEB J 30:3961–3978

Szatmari-Toth M, Kristof E, Vereb Z et al (2016) Clearance of autophagy-associated dying retinal pigment epithelial cells – a possible source for inflammation in age-related macular degeneration. Cell Death Dis 7:e2367

# Part IX
# Stem Cells

# Chapter 75
# The iPSc-Derived Retinal Tissue as a Tool to Study Growth Factor Production in the Eye

**Maryam Alavi and Petr Baranov**

**Abstract** Traumatic, inherited, and age-related degenerative diseases of the retina, such as retinal detachment, glaucoma, retinitis pigmentosa, and age-related macular degeneration, are characterized by the irreversible loss of retinal neurons. Several growth factors, including glial cell-derived neurotrophic factor and pigment epithelium-derived factor, have been shown to rescue retinal neurons in animal models of retinal disease. Here we describe a scalable and robust system to study the growth factor induction in the retina: retinal organoids derived from the induced pluripotent stem cells. We have demonstrated that they secrete GDNF and PEDF at the levels tenfold above detection limit for ELISA. We also have shown that growth factor production in this system may be upregulated by specific trigger, demonstrating the feasibility of this approach for drug discovery.

**Keywords** Retina · Growth factors · Neuroprotection · Glial cell line-derived neurotrophic factors · Pigment epithelium-derived neurotrophic factor · Induced pluripotent stem cells

## 75.1 Introduction

Retinal degenerative disorders, such as retinitis pigmentosa and age-related macular degeneration, are characterized by the progressive and irreversible loss of light-sensitive cells – photoreceptors. A number of large molecules, such as growth factors (GF) and cytokines, have been used to rescue neurons from death and delay or even prevent vision deterioration in a variety of animal models. However, the clinical translation of these treatments is complicated by the challenges associated with GF delivery and bioavailability. Small molecules, on other hand, can be easily administered into the eye and have better tissue distribution profiles. The critical

M. Alavi · P. Baranov (✉)
The Schepens Eye Research Institute, Massachusetts Eye and Ear, an affiliate of Harvard Medical School, Boston, MA, USA
e-mail: petr_baranov@meei.harvard.edu



J. D. Ash et al. (eds.), *Retinal Degenerative Diseases*, Advances in Experimental Medicine and Biology 891, https://doi.org/10.1007/978-3-319-75402-4_75

question is how to identify a potent compound among millions of chemicals available. For the classic "direct neuroprotection" approach, the major readout for drug screening is cell survival in culture – the ability of the compound to prevent cell death, caused by specific stress (Fuller et al. 2014). While this strategy has already identified potent antioxidants and neuroprotectants, the selection of the small molecule for further development is limited by the cell system and stress factors used for the screening.

Alternative approach, namely, "indirect neuroprotection" (or endogenous neuroprotection), suggests that the small molecules are used to induce the production of endogenous growth factors in the retina. With this method the selection of the small molecules is based on their capacity to induce growth factor expression in the retina. One of the requirements for the successful implementation of our strategy is the availability of cell-based assays to investigate the upregulation of neuroprotective factors. This system has to be representative of retinal tissue and therefore contain multiple cell types, including neurons and glia. It has been demonstrated that retinal eyecups – tissue-like structures, containing major retinal cell types – can be obtained using three-dimensional differentiation protocol (Eiraku and Sasai 2012). Here we show that these eyecups can be used to study growth factor expression and induction. To demonstrate the feasibility of this approach, we have profiled the time-course ciliary neurotrophic factor (CNTF) and glial cell line-derived neurotrophic factor (GDNF) expression during the retinal differentiation. We also have studied the GDNF induction by bFGF in these cultures.

## 75.2 Materials and Methods

### *75.2.1 The Differentiation of Retinal Tissue from Induced Pluripotent Stem Cells*

Retinal tissue was differentiated according to protocols developed by Sasai (Eiraku and Sasai 2012) and modified by Arsenjevic (Decembrini et al. 2014). Briefly, mouse-induced pluripotent stem cells (Ng et al. 2011) were plated into low-adhesion polypropylene 96-well plates (10,000 cells per well 50 microliters of optic vesicle medium). On the second day, 50 microliters of 2% Matrigel solution was added to induce neuroepithelium formation. On day 9, optic vesicle medium was replaced with optic cup medium (supplemented with 1% knockout serum, N2, and B27), and aggregates were transferred to 40% oxygen environment (Fig. 75.1).

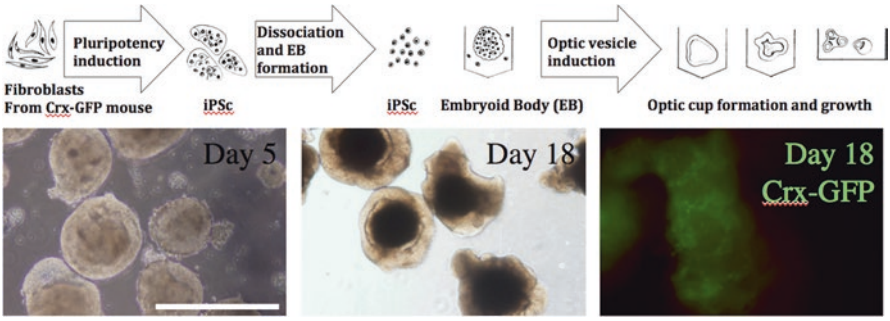


**Fig. 75.1** An outline of eyecup differentiation from mouse-induced pluripotent stem cells. iPSc are derived from fibroblasts, isolated from Crx-GFP mouse. The iPSc are dissociated and re-plated into low-adhesion plate (96 wells) to form embryoid bodies, which are forced into forebrain and retina formation by adding 1% Matrigel. Eyecups are transferred into T75 flasks and cultured in media, supplemented with N2 and B27. This highly efficient protocol allows us to establish cultures, containing >80% of photoreceptors. The EB and eyecups at day 18 of differentiation are shown above. Scale bar 500 um

### *75.2.2 Characterization of iPSc-Derived Eyecups by Flow Cytometry*

For flow cytometry analysis, cell aggregates were collected at day 26 of differentiation and then dissociated with papain. Cells were fixed with 4% PFA, incubated with primary antibodies overnight at +4 °C (all at 1:200 dilution), followed by washing and staining with isotype-specific PE-conjugated secondary antibodies for 1 h at room temperature (1:400 dilution).

### *75.2.3 Growth Factor Assessment in iPSc-Derived Eyecups*

To assess growth factor production, the supernatant was collected at several stages of differentiation (days 0, 5, 11, 16, 20, 25, 30, and 35). The growth factor content (PEDF, GDNF) was analyzed using ELISA (R&D Systems) according to the manufacturer's instructions. To increase the sensitivity of the assay, samples were incubated with capture antibodies at +37 °C. For the GDNF induction, eyecups at day 26 of differentiation were treated with recombinant bFGF (dose range up to 1 microgram per ml) for 24 h and GDNF production was assessed by ELISA.

## 75.3 Results

### *75.3.1 The Differentiation of Retinal Tissue from Induced Pluripotent Stem Cells and Characterization of iPSc-Derived Eyecups by Flow Cytometry*

This differentiation protocol led to retinal development in more than 80% of the aggregates (as determined by using Crx-Gfp transgenic mouse iPSc line). The flow cytometry analysis showed the presence of multiple retinal cell types, with the percentage similar to the native retina (Fig. 75.2): the majority of cells in three-dimensional culture were photoreceptors (up to 80%).

### *75.3.2 Growth Factor Assessment in iPSc-Derived Eyecups*

PEDF concentration increased from 80 pg/ml to 160 pg/ml in the supernatant of the developing eyecups from day 0 to day 35. GDNF content in the supernatant increased from non-detectable levels to 8 pg/ml. This level was sufficient to study the upregulation of GF in culture. When treated with the bFGF, GDNF was upregulated in a dose-dependent manner from 25 pg/ml to 50 pg/ml (Fig. 75.3).

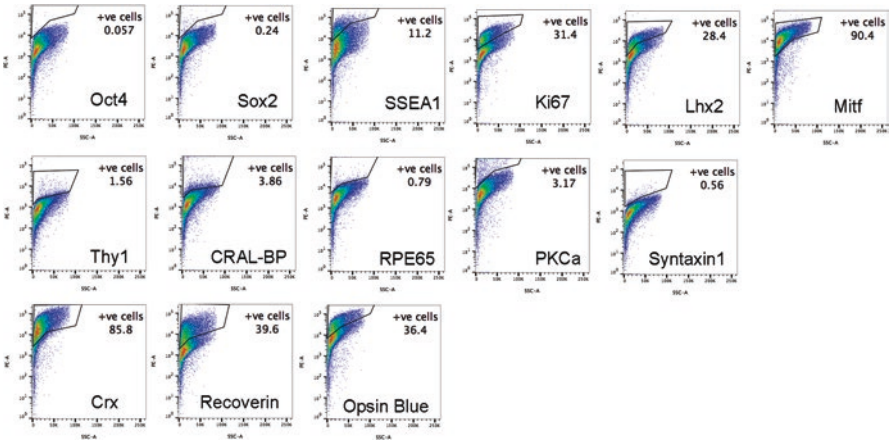


**Fig. 75.2** Cell content in differentiating retinal tissue. At day 26 of differentiation, the iPSc-derived eyecups contain most of the retinal cell types as detected by flow cytometry: ganglion cells (Thy1), Muller glia (CRAL-BP), retinal pigment epithelium clusters (RPE 65), bipolar cells (PKCa), amacrine cells (Syntaxin1), rod (Recoverin, Crx), and cone (Opsin Blue, Crx) photoreceptors. We did not detect significant number of pluripotent cells (Sox2, Oct4); however some of the cells continued to proliferate (Ki67)

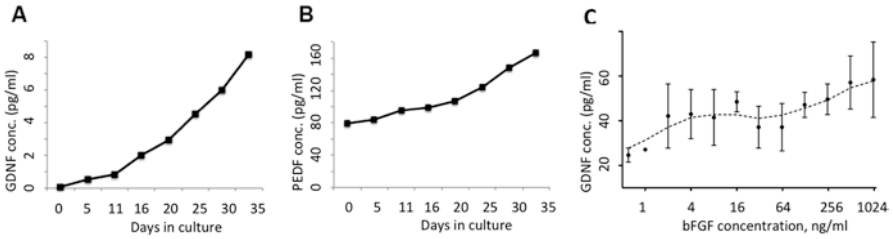


**Fig. 75.3** The timecourse profile of growth factor production in the iPSc-derived eyecups. The production of PEDF and GDNF increased with time (**a**, **b**). The RT-PCR confirmed the ELISA findings. The treatment of these eyecups with high concentrations of bFGF at day 26 of differentiation (**c**) led to the upregulation of GDNF production at 2 ng/ml of bFGF and above (p=0.04, t-test)

## 75.4 Discussion

Treatment of animal models of retinal degeneration with different cytokines or growth factors can delay or prevent retinal neuron loss; at least six classes of growth factors show promise in various animal models of retinal degeneration and photoreceptor loss: ciliary neurotrophic factor (Wen et al. 2012), nerve growth factor (Sun et al. 2007), brain-derived neurotrophic factor (Caffé et al. 2001), basic fibroblast growth factor (LaVail et al. 1992), pigment-epithelium-derived growth factor (LaVail et al. 1992), and glial cell-derived neurotrophic factor (Dalkara et al. 2011). In this study we have developed a system to study GF induction to implement an indirect neuroprotection strategy. In indirect neuroprotection, small molecule triggers are used to induce the expression of endogenous growth factors (GF) by host retinal cells. This approach has been explored for GDNF (Saavedra et al. 2008) and leukemia-inhibitory factor (Vela et al. 2016) in the central nervous system with neurons and astrocytes. Due to the variability of the potential molecular targets for such induction, the effects vary between the cell types, and thus retinal-specific assay, inclusive of multiple cell types, is needed. While isolating primary tissue is an option, it significantly limits the throughput capacity of the screen.

The recent establishment of a protocol for differentiation of three-dimensional retinal cells from mouse and human pluripotent stem cell allows cost-efficient and reproducible generation of bona fide retinal tissue. Here we have demonstrated that these eyecups can be cost-effectively differentiated at high numbers; they contain several cell types (retinal ganglion cells, rod and cone photoreceptors, amacrine and bipolar cells, Muller glia). Our ELISA studies have demonstrated that growth factors of interest (PEDF, GDNF) are produced at the levels exceeding detection limit.

We also have shown that GF production increases with time in culture from day 1 to day 35. The lack of plateau and continuous increase in GF production may be related to the ongoing cell proliferation. In our attempt to demonstrate the utility of that system for GF induction, we have treated mechanically dissociated eyecups with known GDNF inducer – bFGF. The resulting dose-response curve (GDNF concentration measured by ELISA vs. bFGF concentration in culture) confirmed the specificity of the induction.

In summary, our findings demonstrate that iPSc-derived eyecups are an effective tool to study growth factor induction in the retina. This system may be used to identify novel neuroprotective small molecules as well as to study the mechanisms of GF production and secretion in the retina.

**Acknowledgments** The authors thank Tomas Minelli for helping with cell culture. This work was supported by the Alice J. Adler Fellowship of the Schepens Eye Research Institute/Eleanor and Miles Shore 50th Anniversary Fellowships for Scholars in Medicine, Bright Focus Foundation, and Department of Ophthalmology. The flow cytometry core facility is supported by the National Eye Institute core grant P30EY003790.

## References

Caffé AR et al (2001) A combination of CNTF and BDNF rescues rd photoreceptors but changes rod differentiation in the presence of RPE in retinal explants. Invest Ophthalmol Vis Sci 42(1):275–282

Dalkara D et al (2011) AAV mediated GDNF secretion from retinal glia slows down retinal degeneration in a rat model of retinitis pigmentosa. Mol Ther 19(9):1602–1608

Decembrini S et al (2014) Derivation of traceable and transplantable photoreceptors from mouse embryonic stem cells. Stem Cell Rep 2(6):853–865

Eiraku M, Sasai Y (2012) Mouse embryonic stem cell culture for generation of three-dimensional retinal and cortical tissues. Nat Protoc 7(1):69–79

Fuller JA et al (2014) A high content screening approach to identify molecules neuroprotective for photoreceptor cells. In: Retinal degenerative diseases. Advances in experimental medicine and biology. Springer, New York, pp 773–781

LaVail MM et al (1992) Multiple growth factors, cytokines, and neurotrophins rescue photoreceptors from the damaging effects of constant light. Proc Natl Acad Sci U S A 89(23):11249–11253

Ng L et al (2011) Two transcription factors can direct three photoreceptor outcomes from rod precursor cells in mouse retinal development. J Neurosci Off J Soc Neurosci 31(31):11118–11125

Saavedra A, Baltazar G, Duarte EP (2008) Driving GDNF expression: the green and the red traffic lights. Prog Neurobiol 86(3):186–215

Sun X et al (2007) Effects of nerve growth factor for retinal cell survival in experimental retinal detachment. Curr Eye Res 32(9):765–772

Vela L et al (2016) Discovery of enhancers of the secretion of leukemia inhibitory factor for the treatment of multiple sclerosis. J Biomol Screen 21(5):437–445

Wen R et al (2012) CNTF and retina. Prog Retin Eye Res 31(2):136–151

# Chapter 76
# Stem Cell-Based RPE Therapy for Retinal Diseases: Engineering 3D Tissues Amenable for Regenerative Medicine


**Karim Ben M'Barek, Walter Habeler, and Christelle Monville**

**Abstract** Recent clinical trials based on human pluripotent stem cell-derived retinal pigment epithelium cells (hPSC-RPE cells) were clearly a success regarding safety outcomes. However the delivery strategy of a cell suspension, while being a smart implementation of a cell therapy, might not be sufficient to achieve the best results. More complex reconstructed tissue formulations are required, both to improve functionality and to target pathological conditions with altered Bruch's membrane like age-related macular degeneration (AMD). Herein, we describe the various options regarding the stem cell source choices and the different strategies elaborated in the recent years to develop engineered RPE sheets amenable for regenerative therapies.

**Keywords** Human pluripotent stem cell · Human-induced pluripotent stem cell · Human embryonic stem cell · Stem cell · Tissue engineering · Retinal pigment epithelium · Age-related Macular degeneration · Retinitis pigmentosa · Cell therapy · Regenerative medicine

K. Ben M'Barek · W. Habeler
INSERM UMR861, I-Stem, AFM, Corbeil-Essonnes, France

UEVE UMR861, I-Stem, AFM, Corbeil-Essonnes, France

CECS-I-Stem, AFM, Corbeil-Essonnes, France

C. Monville (✉)
INSERM UMR861, I-Stem, AFM, Corbeil-Essonnes, France

UEVE UMR861, I-Stem, AFM, Corbeil-Essonnes, France
e-mail: cmonville@istem.fr



J. D. Ash et al. (eds.), *Retinal Degenerative Diseases*, Advances in Experimental Medicine and Biology 891, https://doi.org/10.1007/978-3-319-75402-4_76

## 76.1 Introduction

The retinal pigment epithelium (RPE) has a pivotal role in maintaining photoreceptor survival, integrity, and functionality (Strauss 2005; da Cruz et al. 2007; Ben M'Barek et al. 2015). RPE cells organize as monolayered epithelium in tight contact with the outer segment of photoreceptors (Strauss 2005). Dysfunctions or degeneration of RPE cells is associated with AMD and retinitis pigmentosa (RP). These diseases that might ultimately lead to blindness are estimated to affect about 30 millions of people worldwide (Gehrs et al. 2006). In addition, AMD disease burden will dramatically increase with a projection of 288 millions of people to be affected by 2040, due to prolonged life expectancies (Wong et al. 2014).

RP is a heterogeneous group of rare diseases caused by diverse genetic mutations (https://sph.uth.edu/retnet/disease.htm). Some of these mutations affect specifically RPE functions like the mutations in *MERTK*, *RPE65*, *CRALBP*, *BEST1*, or *LRAT* genes (Sparrow et al. 2010). *MERTK*, *RPE65*, *CRALBP*, and *LRAT* mutations correspond to about 5% of autosomal recessive RP (Hartong et al. 2006), and a prevalence of 1.5 case in 100,000 births for *BEST1* gene mutations was estimated (Bitner et al. 2012). At the opposite, AMD is a complex pathology caused by the combination of genetic and environmental factors (Ambati et al. 2003). Two forms of AMD are typically described: a dry form (atrophic) that account for 90% of all cases and a wet form (neovascular). RPE degeneration and damages of the Bruch's membrane associated with the formation of protein and lipid deposits, called drusen, are characteristics of the dry form. Wet AMD involves choroidal neovascularization with potential hemorrhages that are susceptible to damage the macula (Ambati et al. 2003).

Treatment options for AMD and RP are extremely limited (Gehrs et al. 2006). Only wet AMD benefits from the recent advance of anti-angiogenic treatments (anti-VEGF therapy). In light of this unmet medical need, regenerative medicine appears as an attractive therapeutic alternative to cure patients.

## 76.2 Stem Cell-Based RPE Production

Replacement of dead/dysfunctional RPE cells by new ones is a strategy that was first proposed in early 1980s (Gouras et al. 1985). Initially, RPE sources consisted of autologous RPE from the periphery, allogeneic RPE from cadavers, or fetal RPE (Binder et al. 2007; Radtke et al. 2008). These sources have a lot of limitations in terms of supply chain, donor to donor variability, and scale-up (limited cell amplification). With the emergence of hPSCs, efforts are now directed to stem cells sources (Thomson et al. 1998; Takahashi et al. 2007).

### *76.2.1 Sources*

Three main sources for stem cell therapy are preferred regarding the following criteria: ability to differentiate into RPE cells, ease of culturing, and suitability for a clinical application.

The first one is the recently described human adult RPE stem cells (RPESCs) (Salero et al. 2012). About 2–3% of human RPE cells, harvested from human eye cadavers, could self-renew in vitro, a prominent characteristic of stem cells. Besides their capacity to differentiate into other lineages, they are able to generate new RPE cells that keep their epithelial morphology after transplantation (Stanzel et al. 2014). This source remains an option that will be tested in clinical trials but amplification and isolation remain difficult.

The second stem cell source is based on human embryonic stem cells (hESCs), which were first derived in 1998 (Thomson et al. 1998). These cells retain pluripotency, meaning that they can be differentiated in any cell type of the adult body (including RPE cells) if the required signaling cues are provided. In addition, they can be amplified for a virtually unlimited number of passages, allowing the possibility of industrialized manufacturing processes.

Human-induced pluripotent stem cells (hiPSCs) represent the third stem cell source (Takahashi et al. 2007). While not being completely identical, hiPSCs share the same pluripotency and self-renewal potentials than hESCs (Wu et al. 2016). hiPSCs differentiated into RPE cells are functional in vivo and restore visual functions of rodents with dystrophic retinas (Kamao et al. 2014) to a similar level than hESC-RPE (Riera et al. 2016).

### *76.2.2 Protocols for the Generation of RPE from hPSCs*

hPSCs (hESC and hiPSC) are able to spontaneously differentiate into RPE cells in adherent cultures after FGF2 withdrawal (Klimanskaya et al. 2004; Lustremant et al. 2013; Leach and Clegg 2015). Protocol improvements were undertaken to reduce the culture duration or to improve the yield. Purity of RPE cells can be achieved by manual selection or using growth factors/small molecules (Bharti et al. 2011; Leach and Clegg 2015). These hPSC-RPE cells display characteristics similar to primary fetal RPE cells. In addition, hPSC-RPE cells could also be obtained concomitantly with the formation of self-forming neural retinas in vitro (Meyer et al. 2011; Reichman et al. 2014).

### *76.2.3 Manufacturing Strategy*

From an industrial perspective, clinical hPSCs should be manufactured in a good manufacturing practice (GMP) and compliant establishment and preserved as frozen cell banks (either a unique master cell bank (MCB) or a MCB and derived working cell banks). This MCB has to be characterized based on regulatory standards that include safety analysis (virology, fungi, mycoplasma, bacteria, and endotoxins), purity, potency (embryonic body formation and alkaline phosphatase activity), and stability. From this MCB of hPSCs, a bank of hPSCs-RPE is derived and banked according to GMP principles. Cryovials of this qualified hPSC-RPE bank could be sent straight to the surgical rooms in order to be thawed and transplanted as a cell suspension without prior additional culture in vitro (Schwartz et al. 2012, 2015). This formulation represents the most practical implementation for the handling and delivery to the surgical site with a simplified logistic. A formulation as a reconstructed epithelial sheet might require an additional culture period of hPSC-RPE cells from the bank in order to organize them as an epithelium. The graft should then be transferred in a closed and sterile packaging to the surgical room. The stability of the graft is therefore limited in time, and scheduling should be carefully prepared to have the graft ready for the day of the surgery. To overcome this limitation, freezing steps might be necessary.

## 76.3 Cell Delivery Strategy: Cell Suspension Versus Reconstructed Tissue

The formulation remains a crucial aspect depending on the nature of the pathology in particular when the Bruch's membrane is altered. First approaches were based on cell suspension, but the field has moved to a more elaborated tissue formulation. The idea is that safety and clinical outcomes might be better as RPE functions depend also on their polarized epithelial organization (Stanzel et al. 2014; Hsiung et al. 2015; Nazari et al. 2015). In addition, the survival of the transplanted cells was improved when transplanted as a cell sheet (Diniz et al. 2013). This paradigm was recently demonstrated to improve the functionality of the graft in vivo in animal models (Ben M'Barek et al. 2017).

## 76.4 Types of Support for Tissue Reconstruction

The delivery of an already formed epithelium requires the use of a supportive matrix allowing the sheet to be safely removed from the culture plate to be then loaded on the transplantation device. In addition, this support might replace damaged Bruch's

membrane in patients. Thus specific qualities are required to support hPSC-RPE functions and survival: thickness, mechanical properties (flexibility, ease of handling), permeability, and eventually biodegradation (nontoxic by-products) (Hynes and Lavik 2010; Kador and Goldberg 2012; Nazari et al. 2015).

### *76.4.1 Synthetic Polymers*

Synthetic polymers have the main advantage of being structurally and chemically precisely defined, with consistency, homogeneous properties, and a high potential for industrial processing (Diniz et al. 2013; Stanzel et al. 2014; Ilmarinen et al. 2015). Among others, ultrathin parylene substrates have proven their safety and efficacy (Hu et al. 2012; Diniz et al. 2013; Pennington and Clegg 2016). They will be tested in phase I/II clinical trial for dry AMD in the USA (clinical trial reference: NCT02590692). Poly-lactic-co-glycolic acid or PLGA is also an attractive substrate that is biodegradable (Song and Bharti 2016). hPSC-RPE can be cultured on such substrate and form an epithelium that can be transplanted (Bharti et al. 2014; Song and Bharti 2016). This combination will also be tested in a USA-based clinical trial (Song and Bharti 2016). Finally, a porous polyester scaffold is currently tested in the UK (NCT01691261) (Ramsden et al. 2013).

### *76.4.2 Biological Materials*

Various biological scaffolds have been proposed like Descemet's membranes (Thumann et al. 1997) or human amniotic membranes (hAMs) (Kiilgaard et al. 2012). hAMs, obtained from cesarean sections of normal births (Capeans et al. 2003), are well-tolerated in the subretinal space (Kiilgaard et al. 2012). Our group, in collaboration with the Institut de la Vision and St Louis Hospital (France), is developing the use of this scaffold for a phase I/II clinical trial targeting RP caused by a RPE dysfunction.

### *76.4.3 No Support*

A Japanese group developed a strategy without additional scaffold (Kamao et al. 2014). RPE are allowed to form an epithelium on a collagen coating. Then the collagen coating is digested to liberate the sheet. So far, one patient has been transplanted using this strategy (Mandai et al. 2017).

## 76.5 Conclusion

First clinical trials have demonstrated the safety of hESC-RPE implantation and have paved the way for optimized systems. Future clinical trials with engineered tissue based on the various scaffolds described herein will give clues about the formulations that provide the best results to patients.

**Acknowledgments** I-Stem is supported by the AFM-Téléthon. This work was supported by grants from the Fondation pour la Recherche Medicale (Bio-engineering program - DBS20140930777), the LABEX REVIVE (ANR-10-LABX-73), NeurATRIS (Investissements d'Avenir - ANR-11-INBS-0011), INGESTEM: the National Infrastructure Engineering for Pluripotent and differentiated Stem cells (Investissements d'Avenir - ANR-11-INBS-000).

## References

Ambati J, Ambati BK, Yoo SH et al (2003) Age-related macular degeneration: etiology, pathogenesis, and therapeutic strategies. Surv Ophthalmol 48:257–293

Ben M'Barek K, Regent F, Monville C (2015) Use of human pluripotent stem cells to study and treat retinopathies. World J Stem cells 7:596–604

Bharti K, Miller SS, Arnheiter H (2011) The new paradigm: retinal pigment epithelium cells generated from embryonic or induced pluripotent stem cells. Pigment Cell Melanoma Res 24:21–34

Bharti K, Rao M, Hull SC et al (2014) Developing cellular therapies for retinal degenerative diseases. Invest Ophthalmol Vis Sci 55:1191–1202

Binder S, Stanzel BV, Krebs I et al (2007) Transplantation of the RPE in AMD. Prog Retin Eye Res 26:516–554

Bitner H, Schatz P, Mizrahi-Meissonnier L et al (2012) Frequency, genotype, and clinical spectrum of best vitelliform macular dystrophy: data from a national center in Denmark. Am J Ophthalmol 154(403–412):e404

Ben M'Barek K, Habeler W, Plancheron A et al (2017) Human ESC-derived retinal epithelial cell sheets potentiate rescue of photoreceptor cell loss in rats with retinal degeneration. Sci Transl Med. 9(421)

Capeans C, Pineiro A, Pardo M et al (2003) Amniotic membrane as support for human retinal pigment epithelium (RPE) cell growth. Acta Ophthalmol Scand 81:271–277

da Cruz L, Chen FK, Ahmado A et al (2007) RPE transplantation and its role in retinal disease. Prog Retin Eye Res 26:598–635

Diniz B, Thomas P, Thomas B et al (2013) Subretinal implantation of retinal pigment epithelial cells derived from human embryonic stem cells: improved survival when implanted as a monolayer. Invest Ophthalmol Vis Sci 54:5087–5096

Gehrs KM, Anderson DH, Johnson LV et al (2006) Age-related macular degeneration--emerging pathogenetic and therapeutic concepts. Ann Med 38:450–471

Gouras P, Flood MT, Kjedbye H et al (1985) Transplantation of cultured human retinal epithelium to Bruch's membrane of the owl monkey's eye. Curr Eye Res 4:253–265

Hartong DT, Berson EL, Dryja TP (2006) Retinitis pigmentosa. Lancet 368:1795–1809

Hsiung J, Zhu D, Hinton DR (2015) Polarized human embryonic stem cell-derived retinal pigment epithelial cell monolayers have higher resistance to oxidative stress-induced cell death than nonpolarized cultures. Stem Cells Transl Med 4:10–20

Hu Y, Liu L, Lu B et al (2012) A novel approach for subretinal implantation of ultrathin substrates containing stem cell-derived retinal pigment epithelium monolayer. Ophthalmic Res 48:186–191

Hynes SR, Lavik EB (2010) A tissue-engineered approach towards retinal repair: scaffolds for cell transplantation to the subretinal space. Graefes Arch Clin Exp Ophthalmol Albrecht Von Graefes Arch Klin Exp Ophthalmol 248:763–778

Ilmarinen T, Hiidenmaa H, Koobi P et al (2015) Ultrathin polyimide membrane as cell carrier for subretinal transplantation of human embryonic stem cell derived retinal pigment epithelium. PLoS One 10:e0143669

Kador KE, Goldberg JL (2012) Scaffolds and stem cells: delivery of cell transplants for retinal degenerations. Expert Rev Ophthalmol 7:459–470

Kamao H, Mandai M, Okamoto S et al (2014) Characterization of human induced pluripotent stem cell-derived retinal pigment epithelium cell sheets aiming for clinical application. Stem Cell Rep 2:205–218

Kiilgaard JF, Scherfig E, Prause JU et al (2012) Transplantation of amniotic membrane to the subretinal space in pigs. Stem Cells Int 2012:716968

Klimanskaya I, Hipp J, Rezai KA et al (2004) Derivation and comparative assessment of retinal pigment epithelium from human embryonic stem cells using transcriptomics. Cloning Stem Cells 6:217–245

Leach LL, Clegg DO (2015) Concise review: making stem cells retinal: methods for deriving retinal pigment epithelium and implications for patients with ocular disease. Stem Cells 33:2363–2373

Lustremant C, Habeler W, Plancheron A et al (2013) Human induced pluripotent stem cells as a tool to model a form of Leber congenital amaurosis. Cell Reprogram 15:233–246

Meyer JS, Howden SE, Wallace KA et al (2011) Optic vesicle-like structures derived from human pluripotent stem cells facilitate a customized approach to retinal disease treatment. Stem Cells 29:1206–1218

Mandai M, Watanabe A, Kurimoto Y et al (2017) Autologous Induced Stem-Cell-Derived Retinal Cells for Macular Degeneration. N Engl J Med. 376:1038–1046

Nazari H, Zhang L, Zhu D et al (2015) Stem cell based therapies for age-related macular degeneration: the promises and the challenges. Prog Retin Eye Res 48:1–39

Pennington BO, Clegg DO (2016) Pluripotent stem cell-based therapies in combination with substrate for the treatment of age-related macular degeneration. J Ocul Pharmacol Ther Off J Assoc Ocul Pharmacol Ther 32:261–271

Radtke ND, Aramant RB, Petry HM et al (2008) Vision improvement in retinal degeneration patients by implantation of retina together with retinal pigment epithelium. Am J Ophthalmol 146:172–182

Ramsden CM, Powner MB, Carr AJ et al (2013) Stem cells in retinal regeneration: past, present and future. Development 140:2576–2585

Reichman S, Terray A, Slembrouck A et al (2014) From confluent human iPS cells to self-forming neural retina and retinal pigmented epithelium. Proc Natl Acad Sci U S A 111:8518–8523

Riera M, Fontrodona L, Albert S et al (2016) Comparative study of human embryonic stem cells (hESC) and human induced pluripotent stem cells (hiPSC) as a treatment for retinal dystrophies. Mol Ther Methods Clin Dev 3:16010

Salero E, Blenkinsop TA, Corneo B et al (2012) Adult human RPE can be activated into a multipotent stem cell that produces mesenchymal derivatives. Cell Stem Cell 10:88–95

Schwartz SD, Hubschman JP, Heilwell G et al (2012) Embryonic stem cell trials for macular degeneration: a preliminary report. Lancet 379:713–720

Schwartz SD, Regillo CD, Lam BL et al (2015) Human embryonic stem cell-derived retinal pigment epithelium in patients with age-related macular degeneration and Stargardt's macular dystrophy: follow-up of two open-label phase 1/2 studies. Lancet 385:509–516

Song MJ, Bharti K (2016) Looking into the future: using induced pluripotent stem cells to build two and three dimensional ocular tissue for cell therapy and disease modeling. Brain Res 1638:2–14

Sparrow JR, Hicks D, Hamel CP (2010) The retinal pigment epithelium in health and disease. Curr Mol Med 10:802–823

Stanzel BV, Liu Z, Somboonthanakij S et al (2014) Human RPE stem cells grown into polarized RPE monolayers on a polyester matrix are maintained after grafting into rabbit subretinal space. Stem Cell Rep 2:64–77

Strauss O (2005) The retinal pigment epithelium in visual function. Physiol Rev 85:845–881

Takahashi K, Tanabe K, Ohnuki M et al (2007) Induction of pluripotent stem cells from adult human fibroblasts by defined factors. Cell 131:861–872

Thomson JA, Itskovitz-Eldor J, Shapiro SS et al (1998) Embryonic stem cell lines derived from human blastocysts. Science 282:1145–1147

Thumann G, Schraermeyer U, Bartz-Schmidt KU et al (1997) Descemet's membrane as membranous support in RPE/IPE transplantation. Curr Eye Res 16:1236–1238

Wong WL, Su X, Li X et al (2014) Global prevalence of age-related macular degeneration and disease burden projection for 2020 and 2040: a systematic review and meta-analysis. Lancet Glob Health 2:e106–e116

Wu J, Ocampo A, Izpisua Belmonte JC (2016) Cellular metabolism and induced pluripotency. Cell 166:1371–1385

# Chapter 77
# Validation of iPS Cell-Derived RPE Tissue in Animal Models


**Vladimir Khristov, Arvydas Maminishkis, Juan Amaral, Aaron Rising, Kapil Bharti, and Sheldon Miller**

**Abstract** Previous work suggests that replacing diseased Retinal Pigment Epithelium (RPE) with a healthy autologous RPE sheet can provide vision rescue for AMD patients. We differentiated iPSCs into RPE using a directed differentiation protocol. RPE cells at the immature RPE stage were purified and seeded onto either electrospun poly(lactic-co-glycolic acid) (PLGA) scaffolds or non-biodegradable polyester cell culture inserts and compared the two tissues. In vitro, PLGA and polyester substrates produced functionally similar results. Following in vitro evaluation, we tested RPE tissue in animal models for safety and function. Safety studies were conducted in RNU rats using an injection composed of intact cells and homogenized scaffolds. To assess function and develop surgical procedures, the tissues were implanted into an acute RPE injury model pig eye and evaluated using optical coherence tomography (OCT), multifocal ERG (mfERG), and histology. Subretinal injection studies in rats demonstrated safety of the implant. Biodegradability and biocompatibility data from a pig model demonstrated that PLGA scaffold is safe, with the added benefit of being resorbed by the body over time, leaving no foreign material in the eye. We confirmed that biodegradable substrates provide suitable support for RPE maturation and transplantation.

**Keywords** RPE · AMD · Animal Models · Transplantation · Autologous · iPSC · Biodegradable

V. Khristov (✉) · A. Maminishkis · A. Rising · S. Miller
Section on Epithelial and Retinal Physiology and Disease,
National Eye Institute, Bethesda, MD, USA
e-mail: vladimir.khristov@gmail.com

J. Amaral
Laboratory of Retinal Cell and Molecular Biology, National Eye Institute,
Bethesda, MD, USA

K. Bharti
Unit on Ocular Stem Cell and Translational Research, National Eye Institute,
Bethesda, MD, USA



J. D. Ash et al. (eds.), *Retinal Degenerative Diseases*, Advances in Experimental Medicine and Biology 891, https://doi.org/10.1007/978-3-319-75402-4_77

## 77.1 Introduction

Age-related macular degeneration (AMD) is a leading cause of vision loss in the United States among the elderly. The disease is thought to originate from a malfunctioning retinal pigment epithelium (RPE) a monolayer of cells that performs multiple roles required for survival and proper functionality of the photoreceptors, including fluid level regulation, visual pigment recycling, nutrient replenishment, and phagocytosis of photoreceptor outer segments (Tang et al. 2013; Edelman and Miller 1991; Mazzoni et al. 2014). RPE dysfunctions therefore lead to photoreceptor cell death (Longbottom et al. 2009). One potential personalized cell-based therapy for AMD consists of replacing the diseased RPE layer with RPE derived from induced pluripotent stem cells (iPSCs). iPS cells were differentiated into RPE using a directed differentiation protocol that generates RPE in three phases: neuroectoderm/RPE progenitors, committed RPE, and immature RPE (Buchholz et al. 2013). RPE cells at the immature stage were purified and seeded onto either electrospun poly(lactic-co-glycolic acid) (PLGA) scaffolds or on non-biodegradable polyester cell culture inserts. The RPE tissues were evaluated in vitro during the maturation stage for morphology, function, and biodegradability. Next, toxicity and tumorigenicity studies were conducted in RNU rats using a combination of intact cells and homogenized scaffolds. To assess therapeutic benefit, the tissues were implanted into an acute RPE injury model pig eye and evaluated using optical coherence tomography (OCT), multifocal ERG (mfERG), and histology. Our data suggests that the scaffold-RPE construct is safe and efficacious and can be reliably implanted into the subretinal space in a manner analogous to human surgery.

## 77.2 Materials and Methods

### *77.2.1 Manufacturing RPE Implants*

iPS cells are differentiated into RPE using a directed differentiation protocol that generates RPE in three phases: neuroectoderm/RPE progenitors, committed RPE, and immature RPE. RPE cells at the immature RPE stage are purified and seeded onto either electrospun poly(lactic-co-glycolic acid) (PLGA) scaffolds or non-biodegradable polyester cell culture inserts and maintained in RPE-specific media for 5 weeks prior to implantation.

### *77.2.2 Validation of Implants In Vitro*

To assess overall morphology, implants were fixed in 2.5% glutaraldehyde/2.5% formaldehyde fixative for 24 h, postfixed with osmium tetroxide, and critical point dried before being imaged via scanning electron microscopy. To assess intracellular

structures, tissue was double-fixed in PBS-buffered glutaraldehyde (2.5%) and osmium tetroxide (0.5%), dehydrated, and embedded into Spurr's epoxy resin. Ultrathin sections (90 nm) were double-stained with uranyl acetate and lead citrate and viewed in a JEOL JEM 1010 transmission electron microscope (TEM). Implants were also assayed via intracellular microelectrode recordings (Üssing chamber) that measured transepithelial potential (TEP) and total epithelial resistance (Rt). The responses to the perfusion of apical 1 mM $K^+$, ATP were recorded.

## *77.2.3 Subretinal Studies in Rats*

### 77.2.3.1 Implantation Surgery

Rowett nude (RNU) Crl:NIH-FOXn1$^{mu}$ immunocompromised rats were used to study toxicity and tumorigenicity of implanted constructs. The implantation procedure was done under direct visualization of a surgical microscope. An initial sclerotomy was performed posterior to the limbus. Human-equivalent doses of dissociated RPE cells mixed with the corresponding amount of homogenized scaffold material were delivered as a 5 μL injection to the rat subretinal space through a 33 Ga curved tip Hamilton syringe. As a positive control for tumorigenicity, rats received $1 \times 10^5$ subretinal dose of iPSC cells.

### 77.2.3.2 Assessment

Animal eyes were injected with 4% paraformaldehyde until turgid, immersion fixed in 4% paraformaldehyde for 18–24 h, and processed to paraffin block. Sections containing cells in the subretinal space were immunolabeled for the detection of PMEL17.

## *77.2.4 Subretinal Studies in Pigs*

### 77.2.4.1 Implantation Surgery

The pig model was used to develop our transplantation tool and test the safety and efficacy of RPE patches derived from AMD patients' iPS cells. A standard 25 gauge pars plana vitrectomy was followed by induction of a posterior vitreous detachment. The retina at the site of implantation was separated from the native RPE by creating a subretinal fluid bleb. A retinotomy was performed to allow the delivery of the $4 \times 2$ mm implant to the subretinal space. The implant was delivered to the subretinal space through a flattened cannula, with the delivery controlled by the viscous fluid injection (VFI) mode of the vitrectomy machine. Intraoperative optical coherence tomography (OCT) was used to assess implant placement in the subretinal space and to guide retina flattening using fluid-air exchange.

#### 77.2.4.2 Postsurgical Evaluation

We utilized OCT to perform morphological assessments of the retina prior to and after all surgical manipulations of the eye. These longitudinal measurements help to monitor for regeneration of the photoreceptor nuclear layer and the photoreceptor outer segments in addition to evaluating the degradation of the PLGA patch. We also compared healthy, lasered, and implant-overlying retinal regions through multifocal electroretinograms (mfERG).

## 77.3 Results

### *77.3.1 In Vitro RPE Tissue Assessment*

Following maturation of RPE cells on either biodegradable PLGA scaffolds or non-biodegradable polyester membranes, iPSC-derived RPE cells showed classical RPE morphology. Figure 77.1a, b shows SEM and TEM images of iPSC-derived RPE on polyester membranes. Figure 77.1d, e shows analogous iPSC-derived RPE on a biodegradable PLGA scaffold. Both substrates demonstrated ability to support the formation and maintenance of a structurally mature RPE monolayer at the 5-week time point. This included abundant apical processes, apically localized melanosomes, basally localized nuclei, tight junctions, and basal infoldings.

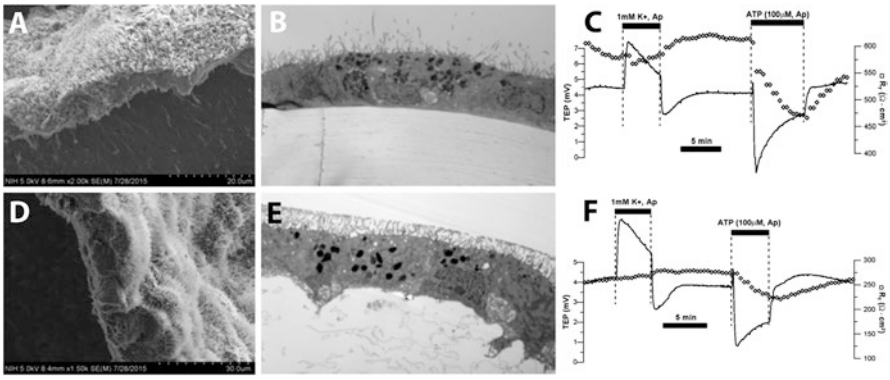


**Fig. 77.1** In vitro assessment of iPSC-derived RPE on polyester and PLGA membranes. iPSC-derived RPE grown on polyester membranes were imaged using SEM (**a**) and TEM (**b**). iPSC-derived RPE grown on PLGA scaffolds were imaged using SEM (**d**) and TEM (**e**). Implants were assayed via intracellular microelectrode recordings (Üssing chamber) that measured transepithelial potential (TEP) and total epithelial resistance (Rt). The responses to the perfusion of apical 1 mM $K^+$, ATP were recorded for iPSC-derived RPE on polyester (**c**) and PLGA (**f**) scaffolds

To assess cell function, electrophysiology recordings were performed on iPSC-derived RPE cells grown on polyester and biodegradable PLGA scaffold as shown in Fig. 77.1c, f, respectively. iPSC-RPE cells in both conditions demonstrated a transepithelial potential of >1 mV, a transepithelial resistance of >200 $\Omega.cm^2$, a depolarization in response to perfusion of 1 mM $K^+$, and a hyperpolarization in response to perfusion of 100 μM ATP.

### *77.3.2 Toxicity and Tumorigenicity in RNU Rats*

Figure 77.2a shows a representative section of the rat subretinal space and the presence of implanted RPE cells. iPSC-RPE cells were generally well-tolerated as assessed by ophthalmic examination and had no effects on general health of the rats. Histologically, eyes receiving iPSC-derived RPE had PMEL17-stained pigmented cells free within the subretinal space in H & E stained sections with variable degrees of localization the native RPE cell layer (Fig. 77.2b, c). While rats receiving subretinal injections of pure iPS cells developed teratomas, none of the animals receiving iPSC-derived RPE cells had tumors.

### *77.3.3 Safety and Efficacy in Pigs*

Studies in pigs established a reliable and reproducible approach for delivering the 4 × 2 mm implant to the subretinal space through the trans-vitreal approach. Figure 77.3a shows both the fundus and intraoperative OCT view of implant delivery to the subretinal space of a pig.

Figure 77.3b, c shows that both a non-biodegradable polyester membrane and a biodegradable PLGA scaffold are well-tolerated in the subretinal space 4 weeks after surgery. OCT evaluations were used to reveal details about retina structure, as well as scaffold integration and degradation over time. In contrast to an empty scaffold (not shown), retinal structures overlying a scaffold carrying RPE cells were generally well preserved. OCT was also used to confirm the gradual degradation of the PLGA scaffold in the subretinal space in the weeks following implantation.

Multifocal electroretinograms (mfERG) were used to monitor retina health and were correlated to the structural findings observed via OCT. The retina overlying a scaffold without cells showed an initial decrease in electrical response, followed by stable low-level activity.

When scaffolds carrying an RPE monolayer were implanted, improved indicators of retina health were observed. Biodegradable scaffolds carrying a monolayer of RPE cells resulted in gradual recovery of the retina function toward healthy levels as assessed by mfERG. In contrast, non-biodegradable scaffolds carrying RPE cells did not show a trend toward recovery (Fig. 77.3d).

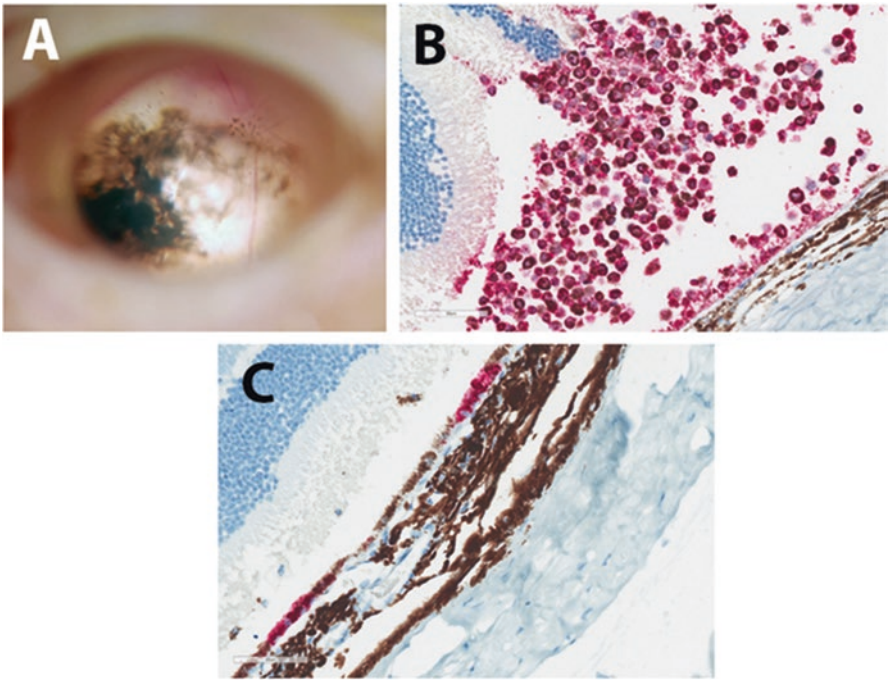


**Fig. 77.2** In vivo assessment of iPSC-derived RPE delivered as subretinal injection in RNU rats. A 5 μL dose of iPSC-derived RPE cells was delivered subretinally in immunocompromised RNU rats (**a**). Four weeks later, PMEL17 (pink) staining shows the presence of RPE cells in the subretinal space either clumped (**b**) or alongside native RPE (**c**)

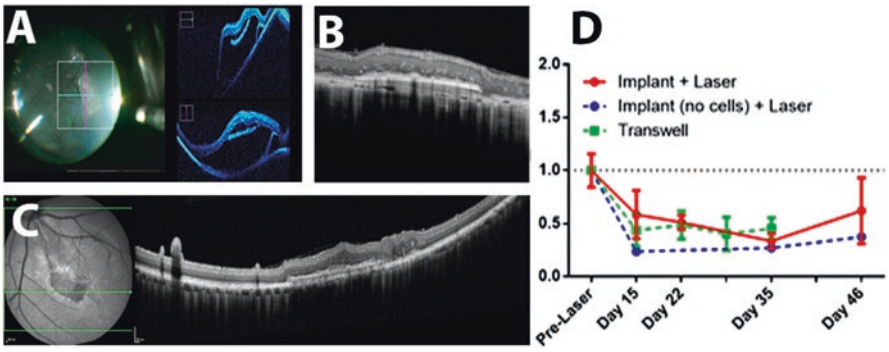


**Fig. 77.3** In vivo assessment of implantability and function of iPSC-derived RPE delivered as a monolayer implant to the subretinal space. A 4 × 2 mm implant is seen via intraoperative OCT in the subretinal space prior to flattening of the retina (**a**). Four weeks postimplantation, a polyester implant carrying RPE cells is observed in the subretinal space (**b**). Four weeks postimplantation, a PLGA implant carrying RPE cells is observed in the subretinal space (**c**). Multifocal electroretinograms were used to assess retina function over heathy, laser-ablated, and implanted RPE cells (**d**)

## 77.4 Discussion

It is important to ensure that iPSC-RPE function closely matches that of native tissue in advance in developing a cell therapy. Functionally, iPSC-RPE cells grown resemble native RPE (Maminishkis et al. 2006). This was determined by measuring the cell properties using several informative assays. A transepithelial potential of >1 mV demonstrates polarization of the monolayer. Additionally, a transepithelial resistance of >200 $\Omega.cm^2$ is telling of an intact layer of cells with established tight junctions. The cells depolarize in response of perfusion to 1 mM $K^+$ which is representative of a dark-to-light transition in the eye. The cells hyperpolarize in response to 100 μM ATP, a multichannel response to the light-peak substrate (Peterson et al. 1997). In vitro assays demonstrated that the iPSC-RPE monolayer on a biodegradable scaffold behaves functionally similar to native RPE.

Any time iPSC-derived tissue is considered for therapy, there is concern for the possibility of tumor formation. This concern is mitigated by tight control of the cell differentiation and purification processes, yielding highly differentiated, pure cell populations. It was no surprise that subretinal injections of iPSC-derived RPE cells in immunocompromised rats resulted in no tumor formation. Additionally, the human cells remained viable in the rat subretinal space due to an immune system lacking lymphocytes. No adverse dose-related ophthalmic findings were observed in the study. In contrast, when injected with at least $1 \times 10^5$ iPSC cells, teratomas developed in the rat subretinal space after several weeks. This pilot study demonstrates that iPSC-derived RPE should not pose a threat through the formation of teratomas, and remain viable provided there is no immune rejection. Further extensive studies are needed to fully evaluate the tumorigenic potential of the iPSC-derived RPE cells.

Subretinal implantation of RPE cells as a monolayer is the preferred delivery method because of better control of implant position in the subretinal space. Additionally, the implant is not altered after in vitro validation, leading to a high degree of confidence that the implanted cells will perform in a predictable manner. We chose the pig model to test RPE patch transplantation and efficacy because of similarities in anatomy to the human eye (Middleton 2010). This implies that surgical tools and procedures used to deliver the RPE implant can be directly transferred to human surgeries. Likewise, methods of evaluating retina health such as OCT and mfERG can be used in human patients. Here, we have developed such a model and demonstrate that we can assess structure and function of the retina for extended periods after implantation.

Our results in pig studies demonstrate the possibility of reliable surgical delivery of a $4 \times 2$ mm implant to the pig subretinal space as well as the ability to follow the overlying retina in terms of both structure (OCT) and function (mfERG). When RPE cells on a biodegradable scaffold are delivered to the subretinal space, the retina shows a trend toward recovery to healthy levels in contrast to the retina overlying an empty scaffold. This indicates that the RPE cells are capable of providing a therapeutic rescue effect after native RPE are damaged by a laser. It must be stated that in order to allow for testing of human cells in a pig model, the pigs are heavily immunosuppressed.

In conclusion, we confirmed that biodegradable substrates provide suitable support for RPE transplantation to counteract degenerative eye disease outcomes. We found that in vitro RPE cells behave similarly on biodegradable and non-biodegradable substrates, forming a tissue which is similar to native RPE in its structural and functional properties. Studies in rats confirmed the safety of the implanted material. Biodegradability and biocompatibility results from a pig model demonstrated that PLGA scaffold is safe with the added benefit of being resorbed by the body over time, leaving no foreign material in the eye. These studies establish animal testing models for validation of subretinal RPE implants and will be used to demonstrate the suitability of our implant for a Phase I clinical trial.

**Acknowledgments** We would like to thank Dr. Mones Abu-Asab of the NEI histology core for TEM image contributions. We would also like to thank the unwavering commitment of the animal care teams at NEI that made this research possible.

## References

Buchholz DE, Pennington BO, Croze RH, Hinman CR, Coffey PJ, Clegg DO (2013) Rapid and efficient directed differentiation of human pluripotent stem cells into retinal pigmented epithelium. Stem Cells Transl Med 2:384–393

Edelman JL, Miller SS (1991) Epinephrine stimulates fluid absorption across bovine retinal pigment epithelium. Invest Ophthalmol Vis Sci 32:3033–3040

Longbottom R, Fruttiger M, Douglas RH, Martinez-Barbera JP, Greenwood J, Moss SE (2009) Genetic ablation of retinal pigment epithelial cells reveals the adaptive response of the epithelium and impact on photoreceptors. Proc Natl Acad Sci U S A 106:18728–18733

Maminishkis A, Chen S, Jalickee S, Banzon T, Shi G, Wang FE, Ehalt T, Hammer JA, Miller SS (2006) Confluent monolayers of cultured human fetal retinal pigment epithelium exhibit morphology and physiology of native tissue. Invest Ophthalmol Vis Sci 47:3612–3624

Mazzoni F, Safa H, Finnemann SC (2014) Understanding photoreceptor outer segment phagocytosis: use and utility of RPE cells in culture. Exp Eye Res 126:51–60

Middleton S (2010) Porcine ophthalmology. Vet Clin North Am Food Anim Pract 26:557–572

Peterson WM, Meggyesy C, Yu K, Miller SS (1997) Extracellular ATP activates calcium signaling, ion, and fluid transport in retinal pigment epithelium. J Neurosci 17:2324–2337

Tang PH, Kono M, Koutalos Y, Ablonczy Z, Crouch RK (2013) New insights into retinoid metabolism and cycling within the retina. Prog Retin Eye Res 32:48–63

# Chapter 78
# Cell Transplantation for Retinal Degeneration: Transition from Rodent to Nonhuman Primate Models

**Trevor J. McGill, David J. Wilson, Jonathan Stoddard, Lauren M. Renner, and Martha Neuringer**

**Abstract** Transplantation of potentially therapeutic cells into the subretinal space is a promising prospective therapy for the treatment of retinal degenerative diseases including age-related macular degeneration (AMD). In rodent models with photoreceptor degeneration, subretinal transplantation of cell suspensions has repeatedly been demonstrated to rescue behaviorally measured vision, maintain electrophysiological responses from the retina and the brain, and slow the degeneration of rod and cone photoreceptors for extended periods. These studies have led to the initiation of a number of FDA-approved clinical trials for application of cell-based therapy for AMD and other retinal degenerative diseases. However, translation from rodent models directly into human clinical trials skips an important intermediary preclinical step that is needed to address critical issues for intraocular cell transplantation. These include determination of the most appropriate and least problematic surgical approach, the application of treatment in an eye with similar size and structure including the presence of a macula, and a thorough understanding of the immunological considerations regarding graft survival and the consequences of grafted cell rejection. This chapter will review these and related issues and will document current efforts to address these concerns.

T. J. McGill (✉) · M. Neuringer
Department of Ophthalmology, Casey Eye Institute, Oregon Health & Science University, Portland, OR, USA

Division of Neuroscience, Oregon National Primate Research Center, Oregon Health & Science University, Portland, OR, USA
e-mail: mcgilltr@ohsu.edu

D. J. Wilson
Department of Ophthalmology, Casey Eye Institute, Oregon Health & Science University, Portland, OR, USA

J. Stoddard · L. M. Renner
Division of Neuroscience, Oregon National Primate Research Center, Oregon Health & Science University, Portland, OR, USA



J. D. Ash et al. (eds.), *Retinal Degenerative Diseases*, Advances in Experimental Medicine and Biology 891, https://doi.org/10.1007/978-3-319-75402-4_78

**Keywords** Cell transplantation · Nonhuman primate · Retinal pigment epithelial cells · Immune rejection · Surgery

## 78.1 Introduction

Age-related macular degeneration (AMD) is the leading cause of blindness in the developed world, affecting over 10 million individuals in the United States alone (Friedman et al. 2004). Evaluations of therapeutic cell types have utilized rodent models with RPE dysfunction and subsequent photoreceptor degeneration to test safety and efficacy prior to translation into clinical application. Transplantation of suspensions of potentially therapeutic human cells (including retinal pigment epithelial (RPE) cells) into the subretinal space of the Royal College of Surgeons (RCS) rat has repeatedly been demonstrated to limit photoreceptor death, reduce the secondary inner retinal changes that subsequently occur, minimize secondary vascular abnormalities, minimize the deterioration of electrophysiological responses recorded from the retina and in the brain, and limit the loss of at least two forms of vision, reflexive optokinetic tracking thresholds and perceptual visual acuity (McGill et al. 2004, 2007a, b, 2017; Lu et al. 2010; McGill et al. 2012; Cuenca et al. 2013; Lund et al. 2001; Wang et al. 2005; Sauve et al. 2006; Gamm et al. 2007; Lund et al. 2007). In nearly all these studies, the cells were delivered to the subretinal space through a transchoroidal surgical approach into peripheral retina – an area with a relatively constant distribution of rods and cones, unlike the human macula/fovea. In addition, survival of the transplanted human cells has generally been aided through the use of immunosuppressive medication, particularly because of the xenogeneic nature of the transplants. While these studies have provided positive proof of principle for cell therapy, multiple aspects of translating this therapy into human eyes have yet to be thoroughly evaluated in models with comparable eye size and immune systems to those of humans. Thus, we will discuss the current status of efforts made to address these critical issues.

## 78.2 Surgical Considerations and Approaches

Treatment of AMD or other retinal degenerations using cell-based therapy requires delivery of cells into the subretinal space through a cannula. The surgical approach to delivering these cells could be a substantial factor in the success of the procedure and the type of complications that might occur. Currently, the typical surgical method for delivery of cells into the subretinal space in clinical trials is via a transretinal approach through the vitreous (Schwartz et al. 2012; Kamao et al. 2014). To minimize damage to the retina, surgeons often elect to use the smallest cannula possible; however, passage of cells through too small a cannula leads to cell death and poor cell recovery (Wilson et al. 2017), so that the actual number of live, intact cells

delivered to the subretinal space may be less than intended. Additionally, this surgical approach, together with the use of a cannula large enough to accommodate the safe passages of cells, results in a retinotomy large enough to allow leakage of cells from the injection site (Kundu et al. 2014). This leakage of cells into the vitreous reduces the number of therapeutic cells in the subretinal space and could potentially lead to membrane formation on the surface of the retina, which may increase the possibility of retinal detachment and proliferative vitreoretinopathy.

Recently, we developed in nonhuman primates a novel method for the delivery of therapeutic cell suspensions into the subretinal space (Wilson et al. 2017). Briefly, a subretinal bleb first was created by injection of balanced salt solution with a small gauge (41 g) cannula. Therapeutic cells were then injected into the previously created bleb via a transscleral approach using a larger (30 g) cannula to allow safe passage of the cells. This approach minimizes the invasiveness of the procedure by (1) eliminating the need for vitrectomy and (2) minimizing the size of retinotomy and therefore reducing cell escape into the subretinal space, while at the same time the use of a larger cannula allows maximal delivery of healthy living cells.

While the above approaches may work for delivery of cells in suspension, they will not work for the delivery of RPE cells on a scaffold. Delivery of a scaffold requires a larger retinal incision and a relatively large device to hold the scaffold while maintaining its orientation, both of which can increase risks of surgical complication (Bharti et al. 2014; Kamao et al. 2014; Shirai et al. 2016; Sugita et al. 2016a). Ultimately, the appropriate surgical approach will depend upon the cell type and the format of the therapeutic cells being delivered, and the consequences of these approaches in human patients are yet to be determined.

## 78.3 Immunological Consequences in Large-Eyed Models

Due to the increase in clinical trials evaluating the safety of cell-based therapy, there has been increased focus placed on the immunological consequences of subretinal cell transplantation (Ingulli 2010; Xian and Huang 2015). One recent study evaluated the survival of allogeneic induced pluripotent stem cell (iPSC)-derived RPE cells following transplantation into the subretinal space of nonimmune suppressed, immune competent pigs (Sohn et al. 2015). In five of six eyes, allogeneic RPE cells survived in the subretinal space for up to ~3 weeks of age, although indicators of immune system reaction were observed. This study did not extend survival past 3 weeks, which limits the interpretation of how allogeneic cells may survive long-term. However, the study did describe a clear immunological response, which suggests that the subretinal space is not completely immune privileged. This would be expected to be particularly true after surgical manipulation and in diseases such as AMD where immune-mediated processes are elevated in the retina (Edwards et al. 2005; Haines et al. 2005).

Other studies have explored long-term survival of allogeneic RPE cells transplanted into the nonhuman primate eye (Kamao et al. 2014). While no histological evidence was provided to support the in vivo data, the investigators concluded that allogeneic RPE

cells were rejected. Follow-up studies by the same group included histological analysis that supports their previous conclusions (Sugita et al. 2016a). However, the histological analysis was conducted at 8 weeks after transplantation; since this is 5 weeks after previous reports in pigs had observed a clear immunological response, 8 weeks' posttransplantation may be too late to visualize an active immune response in the retina.

We have performed a series of subretinal transplantation experiments using GFP-labeled, allogeneic embryonic stem cell-derived RPE delivered into the subretinal space of one or both eyes of non-immunosuppressed, immune competent nonhuman primates. In some cases, cells were delivered into the contralateral eye 4 weeks later. In vivo ophthalmic imaging revealed successful delivery of the cells in all eyes. However, GFP fluorescence of the transplanted cells faded to nonvisible levels by ~3 weeks posttransplantation in the initially injected eye and by ~2 weeks posttransplantation in the second eye. Histological and immunohistochemical analysis revealed an infiltration of mononuclear cells (T-cell, Cd4 positive; B-cell, Cd20 positive) into the choroid and subretinal space that resulted in ablation of grafted cells, disruption of host RPE and choroid in the immediate vicinity of the graft, and the formation of a subretinal scar in the location of the immunological response (Fig. 78.1). Microglial cell activation (Iba1 positive) was evident in all cell-transplanted eyes. Collectively, these results suggest that delivery of allogeneic RPE cells into the subretinal space will result in a swift immunological ablation of the graft within a few weeks of implantation, further prompting the use of immune system modulating drugs or the development of autologous or otherwise immunological matched cell types (Sugita et al. 2016b).

## 78.4 Discussion

Cell transplantation is a promising prospective therapy for retinal degenerative diseases including AMD. While clinical trials are currently underway to test the safety of this therapeutic approach, a number of important issues remain unresolved regarding how best to apply this treatment and ensure its success. Studies are especially needed in large-eyed models with high translational value to application in human patients. Delivery methods and minimization of damage to an already diseased retina continue to be a primary concern in applying this therapy, and no single surgical approach is going to be appropriate for all applications. We and others are developing novel surgical techniques to maximize effectiveness of cell-based therapy while minimizing potential complications, and these approaches are likely to continue to evolve with continued interest in translating cell therapy into clinic. The current literature suggests that transplantation of allogeneic RPE cells into the subretinal space without immune suppressive medications induces an immune response that compromises survival of the cells, and this response is primed by injection in the first eye such that the response is more rapid in the subsequently injected eye of the same animal. These findings have important implications for clinical application of cell-based therapy, underscoring the need for evaluation of autologous cell

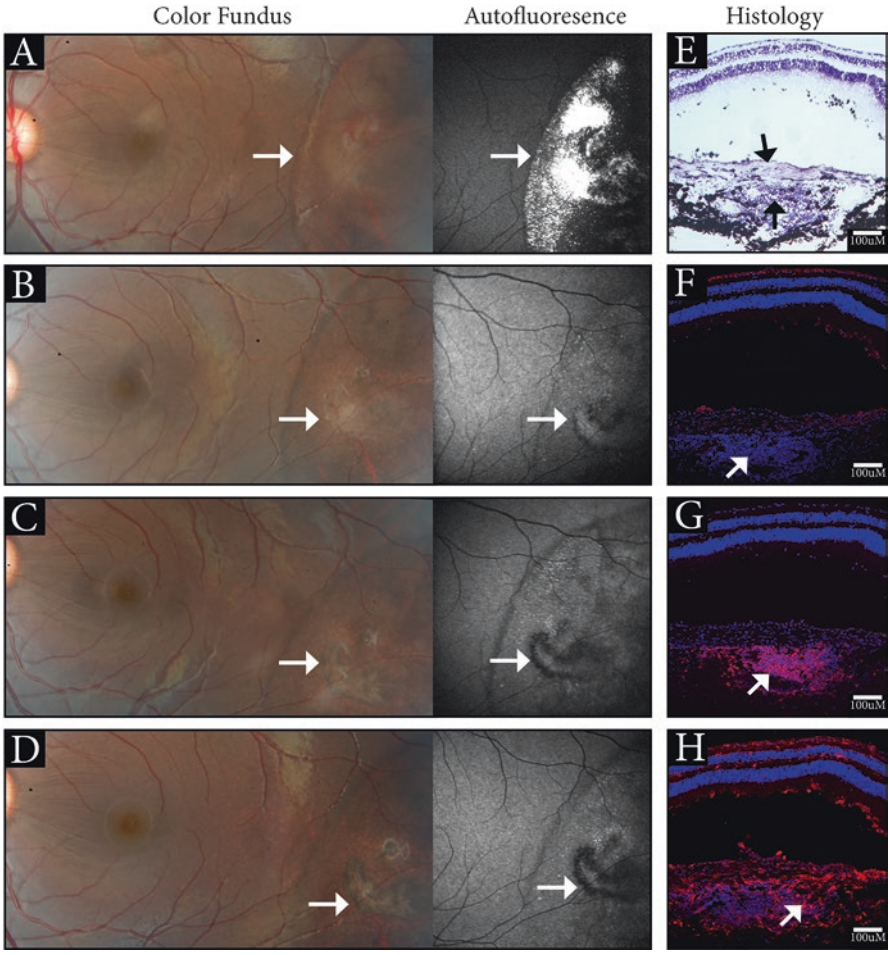


**Fig. 78.1** Rejection of embryonic stem cell-derived RPE cells transplanted into nonhuman primates. Color fundus photos and fundus autofluorescence images (**a**–**d**) illustrate changes in pigment and a loss of GFP fluorescence through time (**a**, 3 days; **b**, 2 weeks; **c**, 4 weeks; **d**, 6 weeks). Histological analysis of graft rejection was performed at ~6 weeks posttransplantation (panels **e**–**h**). Panel (**e**) illustrates a fibrotic scar formation in the subretinal space and mononuclear cells in the choroid (black arrows). Panel (**f**) illustrates a few remaining cd-3-positive (red) T-cells (white arrow; T-cell infiltration occurs from 3 days through 3 weeks post transplantation, not shown). Panel (**g**) illustrates the large number of cd-20-positive B-cells (red) in the choroid (red; white arrow). Panel (**h**) shows activated Iba-1 microglial cells (red) in the area of the rejection (white arrow)

sources, adequate T- and B-cell immune suppression, or novel approaches for circumventing immune rejection. Significant work remains to be done, and a number of important questions need to be answered before cell transplantation for retinal degenerative disease can become the standard of care.

**Acknowledgments** The authors thank Shoukhrat Mitalipov for providing rhesus monkey stem cell lines; Andreas Lauer, Steven Bailey, and Tim Stout for participation in retinal surgeries; and Emily Johnson, Robert Bonnah, Kasie Paul, and the staff of the Department of Comparative Medicine at the ONPRC for their valuable technical assistance and support. The project was supported by grant R01EY21214 (MN) and core grants P30 EY010572 (Casey Eye Institute) and P51OD011092 (ONPRC) from the National Institutes of Health (Bethesda, MD), an unrestricted grant to the Casey Eye Institute from Research to Prevent Blindness, a Sybil B. Harrington Special Scholar Award from Research to Prevent Blindness (TJM), and a grant from the Foundation Fighting Blindness (MN).

**Funding sources** The Wold Macular Degeneration Lab, and the Campbell Stem Cell Lab.

## References

Bharti K, Rao M, Hull SC et al (2014) Developing cellular therapies for retinal degenerative diseases. Invest Ophthalmol Vis Sci 55:1191–1202

Cuenca N, Fernandez-Sanchez L, McGill TJ et al (2013) Phagocytosis of photoreceptor outer segments by transplanted human neural stem cells as a neuroprotective mechanism in retinal degeneration. Invest Ophthalmol Vis Sci 54:6745–6756

Edwards AO, Ritter R, Abel KJ et al (2005) Complement factor H polymorphism and age-related macular degeneration. Science (New York, NY) 308:421–424

Friedman DS, O'Colmain BJ, Munoz B et al (2004) Prevalence of age-related macular degeneration in the United States. Arch Ophthalmol 122:564–572

Gamm DM, Wang S, Lu B et al (2007) Protection of visual functions by human neural progenitors in a rat model of retinal disease. PLoS One 2:e338

Haines JL, Hauser MA, Schmidt S et al (2005) Complement factor H variant increases the risk of age-related macular degeneration. Science (New York, NY) 308:419–421

Ingulli E (2010) Mechanism of cellular rejection in transplantation. Pediatr Nephrol 25:61–74

Kamao H, Mandai M, Okamoto S et al (2014) Characterization of human induced pluripotent stem cell-derived retinal pigment epithelium cell sheets aiming for clinical application. Stem Cell Rep 2:205–218

Kundu J, Michaelson A, Baranov P et al (2014) Approaches to cell delivery: substrates and scaffolds for cell therapy. Dev Ophthalmol 53:143–154

Lu B, Wang S, Girman S et al (2010) Human adult bone marrow-derived somatic cells rescue vision in a rodent model of retinal degeneration. Exp Eye Res 91:449–455

Lund RD, Adamson P, Sauve Y et al (2001) Subretinal transplantation of genetically modified human cell lines attenuates loss of visual function in dystrophic rats. Proc Natl Acad Sci U S A 98:9942–9947

Lund RD, Wang S, Lu B et al (2007) Cells isolated from umbilical cord tissue rescue photoreceptors and visual functions in a rodent model of retinal disease. Stem Cells 25:602–611

McGill TJ, Lund RD, Douglas RM et al (2004) Preservation of vision following cell-based therapies in a model of retinal degenerative disease. Vis Res 44:2559–2566

McGill TJ, Lund RD, Douglas RM et al (2007a) Syngeneic Schwann cell transplantation preserves vision in RCS rat without immunosuppression. Invest Ophthalmol Vis Sci 48:1906–1912

McGill TJ, Prusky GT, Douglas RM et al (2007b) Intraocular CNTF reduces vision in normal rats in a dose-dependent manner. Invest Ophthalmol Vis Sci 48:5756–5766

McGill TJ, Cottam B, Lu B et al (2012) Transplantation of human central nervous system stem cells - neuroprotection in retinal degeneration. Eur J Neurosci 35:468–477

McGill TJ, Bohana-Kashtan O, Stoddard JW, Andrews MD, Pandit N, Rosenberg-Belmaker LR, Wiser O, Matzrafi L, Banin E, Reubinoff B, Netzer N, Irving C (2017) Long-Term Efficacy of GMP Grade Xeno-Free hESC-Derived RPE Cells Following Transplantation. Transl Vis Sci Technol 6(3):17

Sauve Y, Pinilla I, Lund RD (2006) Partial preservation of rod and cone ERG function following subretinal injection of ARPE-19 cells in RCS rats. Vis Res 46:1459–1472

Schwartz SD, Hubschman JP, Heilwell G et al (2012) Embryonic stem cell trials for macular degeneration: a preliminary report. Lancet 379:713–720

Shirai H, Mandai M, Matsushita K et al (2016) Transplantation of human embryonic stem cell-derived retinal tissue in two primate models of retinal degeneration. Proc Natl Acad Sci U S A 113:E81–E90

Sohn EH, Jiao C, Kaalberg E et al (2015) Allogenic iPSC-derived RPE cell transplants induce immune response in pigs: a pilot study. Sci Rep 5:11791

Sugita S, Iwasaki Y, Makabe K et al (2016a) Lack of T cell response to iPSC-derived retinal pigment epithelial cells from HLA homozygous donors. Stem Cell Rep 7:619–634

Sugita S, Iwasaki Y, Makabe K et al (2016b) Successful transplantation of retinal pigment epithelial cells from MHC homozygote iPSCs in MHC-matched models. Stem Cell Rep 7:635–648

Wang S, Lu B, Lund RD (2005) Morphological changes in the Royal College of Surgeons rat retina during photoreceptor degeneration and after cell-based therapy. J Comp Neurol 491:400–417

Wilson DJ, Neuringer M, Stoddard J, Renner LM, Bailey S, Lauer A, McGill TJ (2017) Subretinal cell-based therapy: An analysis of surgical variables to increase cell survival. Retina 37(11):2162–2166.

Xian B, Huang B (2015) The immune response of stem cells in subretinal transplantation. Stem Cell Res Ther 6:161

# Chapter 79
# Talaumidin Promotes Neurite Outgrowth of Staurosporine-Differentiated RGC-5 Cells Through PI3K/Akt-Dependent Pathways

**Yoshiki Koriyama, Ayako Furukawa, Kayo Sugitani, Miwa Kubo, Kenichi Harada, and Yoshiyasu Fukuyama**

**Abstract** Talaumidin, a tetrahydrofuran neolignan isolated from the root of *Aristolochia arcuata*, was an interesting small molecule with neurotrophic activity in the cultured neuron. Talaumidin can promote neurite outgrowth from neurons. However, the mechanism by which talaumidin exerts its neurotrophic actions on retinal neurons has not been elucidated to date. In this study, we describe that talaumidin has neurotrophic properties such as neurite outgrowth in neuroretinal cell line, RGC-5. Talaumidin promotes staurosporine-induced neurite outgrowth in RGC-5 cells. The neurite outgrowth effect of talaumidin was inhibited by phosphatidylinositol 3-kinase (PI3K) inhibitor, LY294002, but not by Erk inhibitor, PD98059. These data suggest that talaumidin promotes neurite outgrowth through PI3K/Akt pathway and that the potential of talaumidin serves as a promising lead compound for the treatment of retinal degenerative disorders.

**Keywords** Retinal ganglion cell · Axon outgrowth · Erk · Akt · Talaumidin · Glaucoma · Survival

Y. Koriyama (✉) · A. Furukawa
Graduate School and Faculty of Pharmaceutical Sciences, Suzuka University of Medical Science, Suzuka, Japan
e-mail: koriyama@suzuka-u.ac.jp

K. Sugitani
Division of Health Sciences, Graduate School of Medicine, Kanazawa University, Kanazawa, Japan

M. Kubo · K. Harada · Y. Fukuyama
Faculty of Pharmaceutical Sciences, Tokushima Bunri University, Tokushima, Japan



J. D. Ash et al. (eds.), *Retinal Degenerative Diseases*, Advances in Experimental Medicine and Biology 891, https://doi.org/10.1007/978-3-319-75402-4_79

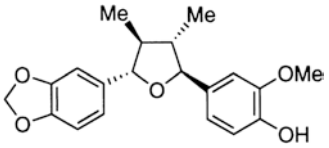


**Fig. 79.1** The chemical structure of talaumidin

## 79.1 Introduction

Talaumidin is a 2,5-biaryl-3,4-dimethyltetrahydrofuran lignan (Fig. 79.1) initially isolated from the bark of *Talauma hodgsonii* Hook. f. and Thoms (Luis et al. 1998). We identified it as an intriguing neurotrophic compound from the root of *Aristolochia arcuata* Masters (Aristolochiaceae), which is used as a stimulant sudorific and diuretic in Brazil. We have reported its biological characters of neurotrophic effects in the cultured rat cortical neurons (Zhai et al. 2004, 2005). However, the mechanism of talaumidin-induced neurite outgrowth is unknown. Furthermore, there are no reports on neurotrophic effects of talaumidin in retinal neurons. In this paper, we report the neurite outgrowth effect of talaumidin in staurosporine-differentiated RGC-5 cells.

## 79.2 Materials and Methods

### *79.2.1 Chemicals*

Talaumidin was synthesized as previously described (Fukuyama et al. 2008). The purity of the compound was determined by nuclear magnetic resonance (NMR).

### *79.2.2 Cell Culture*

RGC-5 cells were produced by Dr. N. Agarwal of the University of North Texas Health Science Center and were received from a line maintained by Dr. H. Hara, at Gifu Pharmaceutical University. RGC-5 cells were cultured in low-glucose Dulbecco's-modified Eagle's medium (DMEM) containing 10% of fetal bovine serum (FBS). The cells were passaged by trypsinization every 3–4 days. RGC-5 cells were cultured overnight prior to use. After washing with DMEM, cells were cultured in medium containing 1% FBS and 400 nM staurosporine to prevent overproliferation and to promote differentiation (Zhai et al. 2005). RGC-5 cells were originally reported to derive from rat retinal ganglion cells showing expression of RGC's marker proteins (Aoun et al. 2003). Recently, VanBergen et al. (2009) reported the re-characterization of RGC-5 cells. Cells were identified to be of mouse origin, and they do not have retinal ganglion cell's properties by themselves.

However, staurosporine-differentiated RGC-5 can be used for neurite outgrowth assay (Koriyama et al. 2011, 2013).

### *79.2.3 Neurite Outgrowth Assay*

Neurite outgrowth of RGC-5 cells was observed by phase-contrast microscopy and assessed by NeuronJ imaging software (http://imagej.net/NeuronJ). To quantify neurite outgrowth, 20 random images were obtained per plate, and cell-bearing processes two-fold longer than the cell body were considered as positive (Koriyama et al. 2011). Over 100 cells were quantified and each data point corresponded to the average of 5 independent dishes. The average neurite length from three independent experiments was expressed as the mean ± SEM.

## 79.3 Results

### *79.3.1 Talaumidin-Induced Neurite Outgrowth from Differentiated RGC-5 Cells*

At 1–10 μM, talaumidin dose-dependently increased neurite outgrowth in differentiated RGC-5 cells (Fig. 79.2). Over 30 μM talaumidin did not show the neurite outgrowth effect because of its toxicity (data not shown).

### *79.3.2 PI3K-Mediated Neurite Outgrowth by Talaumidin*

Firstly, we investigated whether talaumidin promotes neurite outgrowth in differentiated RGC-5 cells. At 10 μM, talaumidin significantly enhanced neurite outgrowth from differentiated RGC-5 cells within 24 h (Fig. 79.3b) compared with no treated control cells (Fig. 79.3a). An extracellular signal-regulated kinase (Erk) inhibitor,

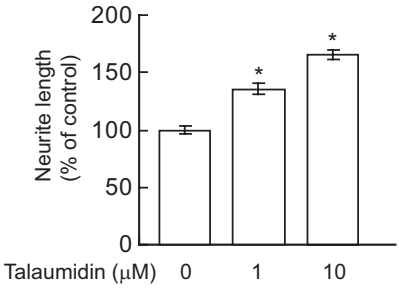


**Fig. 79.2** Talaumidin-induced neurite outgrowth in staurosporine-differentiated RGC-5 cells. Quantification of neurite outgrowth in RGC-5 cells ($n = 100$)

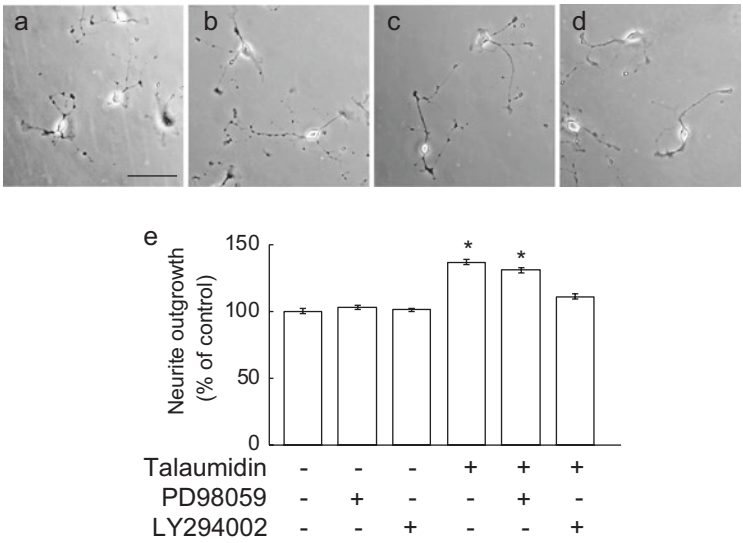


**Fig. 79.3** Morphology of cultured RGC-5 cells differentiated by staurosporine (400 nM). RGC-5 cells in the presence of DMSO as vehicle control (**a**). Scale = 100 μm. RGC-5 cells in the presence of 10 μM talaumidin (**b**). 10 μM talaumidin and 20 μM PD98059, an Erk inhibitor (**c**). 10 μM talaumidin and 20 μM LY294002, PI3K inhibitor (**d**). Quantification of neurite outgrowth (**e**). $^*P < 0.01$ vs vehicle control ($n = 100$)

PD98059, did not change talaumidin-induced neurite outgrowth (Fig. 79.3c). However, a PI3K inhibitor LY29002 significantly suppressed talaumidin-induced neurite outgrowth (Fig. 79.3d). Quantification of neurite outgrowth from RGC-5 cells is shown in Fig. 79.3e.

## 79.4 Discussion

It is reported that RGC-5 cells were identified to be of mouse origin and their expression of RGC characteristics was questioned (VanBergen et al. 2009). They reported that RGC-5 cells, cultured in succinyl concanavalin A, no longer express RGC markers. However, when differentiated by staurosporine, RGC-5 cells express the RGCs markers, Thy1 and the NMDA receptor (Frassetto et al. 2006; Hironaka et al. 2011). In addition, the neuritogenic action in staurosporine-differentiated RGC-5 is parallel with the results of axon outgrowth assay in both retinal explant culture and optic nerve regeneration (Koriyama et al. 2011, 2013). Thus, we analyzed neuritogenic actions using staurosporine-differentiation RGC-5 in this study.

We previously reported the neuroprotective effects of talaumidin using two in vitro models of neurodegenerative diseases. Talaumidin showed protection against Aβ 25–35-induced hippocampal neuronal death. $MPP^+$, a mitochondria complex I inhibitor inducing Parkinson's syndromes in vivo, is known to induce

apoptosis in neurons and thus can be used to make an in vitro model of Parkinson's disease. Talaumidin also showed protection against $MPP^+$-induced hippocampal neuronal death (Zhai et al. 2005). In recent years, talaumidin shows significant neurite outgrowth promotion and neuroprotection in primary cultured rat cortical neurons and in NGF-differentiated PC12 cells (Harada et al. 2015). However, the details of the intracellular mechanisms by which talaumidin exerts neurotrophic actions have not yet been established. Tyrosine phosphorylation of growth factor receptors on ligand binding and the subsequent phosphorylation of the Erk members of the MAPK family have been reported to be essential for mediating cell differentiation. In addition, recent reports suggest that phosphatidylinositol 3-kinase (PI3K) functions in the survival and/or neurite outgrowth pathway (Park et al. 2008; Koriyama et al. 2014). In this study, phosphatidylinositol 3-kinase (PI3K) inhibitor significantly suppressed talaumidin-induced neurite outgrowth in differentiated RGC-5 cells. Our study suggests that PI3K-Akt pathway is the downstream signaling in talaumidin-mediated neurite outgrowth action in differentiated RGC-5 cells. In the future, neurite outgrowth action of talaumidin may be shown to have neuroregenerative activity for the treatment of retinal degeneration disorders.

## References

Aoun P, Simpkins JW, Agarwal N (2003) Role of PPAR-gamma ligands in neuroprotection against glutamate-induced cytotoxicity in retinal ganglion cells. Invest Ophthalmol Vis Sci 44:2999–3004

Frassetto LJ, Schlieve CR, Lieven CJ et al (2006) Kinase-dependent differentiation of a retinal ganglion cell precursor. Invest Ophthalmol Vis Sci 47:427–438

Fukuyama Y, Harada K, Esumi T et al (2008) Synthesis of (−)-talaumidin, a neurotrophic 2, 5-biaryl-3, 4-dimethyltetrahydrofuran lignan, and its stereoisomers. Heterocycles 76:551–567

Harada K, Kubo M, Horiuchi H et al (2015) Systematic asymmetric synthesis of all diastereomers of (−)-talaumidin and their neurotrophic activity. J Org Chem 80:7076–7088

Hironaka K, Inokuchi Y, Fujisawa T et al (2011) Edaravone-loaded liposomes for retinal protection against oxidative stress-induced retinal damage. Eur J Pharm Biopharm 79:119–125

Koriyama Y, Takagi Y, Chiba K et al (2011) Neuritogenic activity of a genipin derivative in retinal ganglion cells is mediated by retinoic acid receptor β expression through nitric oxide/S--nitrosylation signaling. J Neurochem 119:1232–1242

Koriyama Y, Takagi Y, Chiba K et al (2013) Requirement of retinoic acid receptor β for genipin derivative-induced optic nerve regeneration in adult rat retina. PLoS One 8(8):e71252

Koriyama Y, Kamiya M, Arai K et al (2014) Nipradilol promotes axon regeneration through S-nitrosylation of PTEN in retinal ganglion cells. Adv Exp Med Biol 801:751–757

Luis M, Kijjoa A, Silva AMS, Mondranodra IO et al (1998) 2, 5–Diaryl-3,4-dimethytetrahydrofuran Lignans from Talauma hodgsonii. Phytochemistry 48:1079–1081

Park KK, Liu K, Hu Y et al (2008) Promoting axon regeneration in the adult CNS by modulation of the PTEN/mTOR pathway. Science 322:963–966

VanBergen NJ, Wood JP, Chidlow G et al (2009) Recharacterization of the RGC-5 retinal ganglion cell line. Invest Ophthalmol Vis Sci 50:4267–4272

Zhai H, Nakatsukasa M, Mitsumoto Y et al (2004) Neurotrophic effects of talaumidin, a neolignan from Aristolochia arcuata, in primary cultured rat cortical neurons. Planta Med 70:598–602

Zhai H, Inoue T, Moriyama M, Esumi T et al (2005) Neuroprotective effects of 2,5-diaryl-3,4-dimethyltetrahydrofuran neolignans. Biol Pharm Bull 28:289–293

# Index


**A**
*Abca4* mouse model, 396
Achromatopsia, 329, 500
Activating transcription factor 4 (ATF4), 423
Activating transcription factor 6 (ATF6), 422
Adaptive optics (AO), 136–139
Adaptive optics scanning light ophthalmoscopy (AOSLO), 155
Adeno-associated viral (AAV) vectors, 62, 84, 118, 138, 467
  electroretinographic analysis, 63
  immunostaining, 63
  production and delivery, 62
Adenosine monophosphate-activated protein kinase (AMPK), 14
Adherens junctions (AJs)
  ELM, 548–549
  role, 547
  tissue morphogenesis, 546
  and TJs, 547
Advanced glycated end products (AGEs), 187
Aerobic glycolysis, 503
Affymetrix™ GeneChip, 283
Age-related eye disease study (AREDS), 398
Age-related macular degeneration (AMD), 178, 185, 188, 353, 422, 432, 457, 474, 540, 578, 634, 642
  AD, 250
  autoimmune diseases, 249–250
  cardiovascular diseases, 249
  cell-based therapy, 643
  choroidal neovascularization, 30
  cleavage fragments, 46
  complement system, 46
  complement-modulating drugs, 32
  complement-modulating therapies, 30
  fibulin 5, 276
  genetic and molecular studies, 248
  genetic associations, 22–23
  genetic loci, 248
  inflammation, 20, 21
  inflammatory process, 30
  mitochondria, 13
  mitochondrial dysfunction, 14
  multifactorial disease, 46
  oxidative stress, 12
  pathogenesis, 12
  pathology, 279
  prevalence, 20
  PRR, 20, 21
  risk factor, 248, 250
  RPE dysfunction, 12, 642
  therapy, 634
  TLRs, 21, 22, 24, 25
  treatment, 14, 15, 30, 642
  VEGEF, 20
*Aipl1*-deficient mice, 383
AIR inflammatory index, 196
Akt isoforms, 587, 588
  apoptosis, 586
  blindness and visual impairment, 586
  bovine retinal cDNA library, 586–587
  cell lines and culture conditions, 587
  GST pull-down assay, 587, 589
  JNK signaling pathway, 589
  MLK3, 589
  plasmids and vectors, 586
  POSH
    His and LacZ, 588
    identification, 587




J. D. Ash et al. (eds.), *Retinal Degenerative Diseases*, Advances in Experimental Medicine and Biology 891, https://doi.org/10.1007/978-3-319-75402-4

Akt isoforms (*cont.*)
lithium acetate method, 588
protein-protein interactions, 588
retinal degeneration phenotype, 586
serine/threonine kinase, 586
Akt2 knockout mice, 586
Alternative splicing, 393
Alzheimer's disease (AD), 250, 351, 469
AMD disease process, 542, 543
Amoeboid morphology, 186
Amyloid precursor protein (APP), 340
Amyotrophic lateral sclerosis, 469
Analysis of variance (ANOVA), 161
Anaphylatoxin
in choroid, 48–49
RPE signaling, 47, 48
Animal experiments, 389
Animal models, 158
Anti-carboxyethyl pyrrole (CEP), 188
Anti-inflammatory biological agents, 189
Anti-inflammatory therapies, 189
Antioxidant response element (ARE), 4
Anti-retinal antibodies, 195–198
Anti-rhodopsin antibody, 600
Antisense oligonucleotide (AONs), 269
AAV, 84
AON sequences, 85
cell culture, 85
*CHM*, 84
pre-mRNA splicing, 86
SON, 87
transfection, 85
Anti-VEGF drugs, 475–476
AOSLO-derived measurements, 155
Apoptosis, 77
Apoptotic cells (AC), 578
Arf-like protein 3 (ARL3), 318–320
ARL13b, 319, 320, 323
ARL3-GTP, 320
ARPE-19 cells, 458
*Arr1*$^{-/-B}$ retina, 286
Artificial photoreceptors, 70, 506
ARVO Resolution on Treatment of Animals in Research, 168
Aryl-hydrocarbon receptor interacting protein-like 1 (AIPL1), 290
Association for Research in Vision and Ophthalmology (ARVO), 110, 277, 361
Astroglial cells, 205
ATP-binding cassette transporter (ABCA4), 396
Autofluorescence scanning laser ophthalmoscopy (AF-SLO)
AFF count and OS signal slope, 172
bipolar cell mutants, 172
B-scan, 169
CNTL *vs*. STZ, 169
distal OS, 170
genetic and pharmacological manipulation, 173
glucose levels, 169
in vivo ocular imaging, 169
inflammatory monocytes, 169, 172
integration, 171
linear regression curve, 171
mouse models, 168
*Nyx*$^{nob}$ mice, 170
photoreceptor degeneration and RPE changes, 168
retina morphology, 168
Autofluorescent foci, 170
Autoimmune diseases, 249–250
Autoimmune retinopathy (AIR)
anti-retinal antibodies, 197–198, 200
autoimmune diseases, 200
CCR7, 201
cytokine responses, 198–199
diagnosis, 194
electroretinogram amplitudes, 195
gene expression abnormalities, 199–200
immunologic assays, 196
immunosuppression, 201
interferon-γ and IL-10, 198
multiple sclerosis and type 1 diabetes, 200
NK cells, 200
pathophysiology, 200
patients and blood samples, 195–196
peripheral blood cell profiles, 198
rheumatoid arthritis, 201
scotomata, 194
TGFβ, 201
Autophagy proteins, 609
Autosomal dominant (AD), 230
Autosomal dominant retinitis pigmentosa (adRP), 320
genes and mutations, 238, 239
Glu847Lys missense mutation, 241
Glu847Lys mutation, 240
provisional diagnosis, 243
x-linked inheritance, 240
Autosomal recessive (AR), 230
Autosomal recessive bestrophinopathy (ARB), 310
Axiovert 35M microscope, 513
Axon outgrowth, 652
Axoneme, 323

**B**
Balanced salt solution (BSS), 62
Bardet-Biedl syndrome, 522, 524
Basal deposits, 30–33
Basigin-1 (BSG1), 503
Batten disease, 92, 94–95
B-cell lymphoma 2 (*BCL-2*), 466
BCL-2-associated agonist of cell death (BAD), 466
Best vitelliform macular dystrophy (BVMD), 310
*BEST1* gene, 310
Bestrophinopathies, 310, 313
Biogenesis, 37–38
Bisretinoid
  cyclic light, 397
  photodegradation, 396
  RPE, 395
Bisretinoid levels, 398
Bisretinoid photooxidation, 396
Blind retina, 78–79
Blindness disorders, 521
Blood-brain barrier (BBB), 188
Blood-retina barrier (BRB), 467, 474
Blue-light irradiance (BLI), 54–57
Bmal1, 347, 348
BMI1
  phosphorylation status, 362
  phosphorylation status, 363
  PI3K, 362
  polycomb ring finger, 361
  posttranslational modification, 360
  *Rd1*, 360
Bone marrow transplant model, 187
Bovine serum albumin (BSA), 449
Brain-derived neurotrophic factor (BDNF)
  clinical development, 467–469
  inner and outer plexiform layers and ONL, 466
  NGF, 466
  photoreceptor protection, 467
  retinal degenerations, 468, 469
  TrkB signalling, 466
Brain-derived neurotropic factor (BDNF), 78
Bruch's membrane (BrM), 540, 626

**C**
C/EBP homologous protein (CHOP), 423
C1q and tumor necrosis factor-related superfamily (C1q/TNF)
  AAV2 quad YF capsid, 63
  AAV-expressed mutant, 64
  epitope-tagged wild-type, 64
  ERG analysis, 65
  frizzled-related protein, 62
  glucose and lipid metabolism, 61
  membrane-bound and secreted protein, 65
  S163R, 64
  S163R basal deposits, 63
  S163R mutant, 62
  S163R mutation, 62
  wild-type and S163R mutant, 65
C1QTNF4, 223, 226
Calbindin, 514
Calcium indicators, 136, 141
Calpain, 298, 300, 301
Canine, 594, 595, 598
Canine bestrophinopathy (cBest)
  animals and ethics statement, 310
  apical microvilli, 312, 313
  *BEST1*-associated maculopathies, 312
  cytoskeletal organization, 314
  epithelial functional capacity, 313
  histological and IHC assessments, 310–311
  IPM, 314
  macular-selective subretinal lesions, 314
  RPE apical domain, retinal detachment, 312, 313
  RPE-photoreceptor interface, 311–312
Canine gene analysis
  candidate genes, 259
  genes and mutations, 258
  GWAS, 259, 260
  linkage analysis, 259
  NGS, 260, 261
Canine multifocal retinopathy (CMR), 310
Cardiovascular diseases, 249
Cargo displacement factor (CDF), 320
Caspase-1, 188
Cell death, 77–78
Cell death mechanisms, 206
Cell junctions, 546
Cell transplantation, 644
Cell viability, 347
CellTiter-Glo® Luminescent Cell Viability Assay, 459
Cellular immunity, 200, 201
Cellular stress, 422–423
Central nervous system (CNS), 92, 211
Centrosomal protein of 290 kDa (CEP290), 525
Cerium, 119
cGMP, 291–293
  AIPL-/- retinas, 292
  AIPL1-/- mice
    metabolic proteins, 291
    phosphorylation, 292, 293
  animals, 290
  in photoreceptors, 290

cGMP (*cont.*)
mutations, 290
phosphoproteomics, 291
proteomics, 291
Channelrhodopsin 2 (ChR2), 69, 70, 78
Chemical fixation methods, 604
Choroidal endothelial cells (CECs), 48
Choroidal neovascularisation (CNV) model, 40, 178
Choroideremia, 84, 230, 235, 500
Chromosomal locus, 258
Chronic inflammatory process, 185
Cigarette smoke extract (CSE), 424–425
Cilia, 522
Ciliary neurotrophic factor (CNTF), 78, 442
Ciliogenesis/intraflagellar transport, 322
Ciliopathies, 524
Circadian rhythm, 54, 59, 577
and ocular health, 346, 347
retinal circadian clock, 346
SCN, 346
c-Jun N-terminal kinase (JNK)
activation, 352
inhibitors, 353
molecular mechanisms, 352
NFL/RGC, 353
pathologic progression, 355
photoreceptor, 354
retina, 352
retinal layer cells, 352
RPE cells, 353, 354
signaling, 354
CK30PEG nanoparticles, 114, 120
CK30PEG particles, 111, 113
CK30-PEG polymer nanoparticle, 119
Client-owned animals, 262
Cln3
ERGs, 404
experiments with animals, 404
15 Hz ERG, 408
photopic flicker, 405–408
Scotopic Flicker ERG, 405
Clock genes, 346, 347, 349
Complement-modulating drugs, 32
Conditional knockout (CKO), 210, 474
Cone density
AOSLO, 155
cone mosaic, 155
ICC, 153
OCT, 152
Voronoi cells, 152
Cone dystrophy, 282, 285
Cone mosaic, 153
Cone photoreceptor function loss-1 (cpfl1), 330
Cone photoreceptors, 126, 494–495
cone opsin bleaching, 492
eukaryotic cells, 496
functional complexes, 492
Grb14 phosphorylation, 492
IR, 492
mTOR, 492
Nrl knockout mouse retinas, 494–495
rd1 mice, cone survival, 495
RP mouse model, 495
mutations, 492
oncogenic proteins, 496
pcDNA3 vector, 495
plasmids and vectors, 493
protein tyrosine or serine/threonine kinases, 492
retinal degeneration, 495
RP mouse models, 492
subretinal injections, 493
X-gal staining, 494
Cone-rod dystrophy, 257, 261
Cones, 347
Confocal laser scanning microscopy, 310–311
Connecting cilium (CC), 523
Connexins (Cx), 423, 424
cpfl1, 368–372
Critical flicker frequency (CFF), 146
dark-adapted conditions, 148
flicker sweep ERG, 148
light-adapted conditions, 148
photopic, 146–148
scotopic, 146–148
sweep flicker, 147
Crumbs protein, 548
Cryosections, 369
Cryo-substitution, 604–605
C-terminal HSP90 peptide, 382
Cyclic nucleotide-gated (CNG), 328
Cyclic nucleotide-gated ion channels (CNGCs), 512
Cyclin-dependent kinases (CDKs), 360
Cysteine mutant transgene, 128
Cysteines (C), 4
Cytomegalovirus promoter (CMV), 495

**D**

Damage-associated molecular patterns (DAMPs), 21
Damaging retinal degeneration (RD) variants, 222–225
Dark-adapted conditions, 148
Dead/dysfunctional RPE cells, 626

Deep retinal vascular anomalous complexes, 178
Delta subunit of phosphodiesterase 6 (PDE6δ), 529
Depolarizing bipolar cells (DBC), 408
Diabetic macular edema (DME), 474
Diabetic retinopathy (DR), 120, 185, 187, 347, 430–431, 474
Differential splicing, 414–415
Direct neuroprotection, 620
DJ-1
  multifunctional protein, 3
  oxidative stress, 4
  RPE, 5, 6
  translocation, 7
Docosahexaenoic acid (DHA), 441, 487
Down's syndrome, 340
Drusen, 30, 32
Dulbecco's-modified Eagle's medium (DMEM), 650
Dynamin-related protein 1 (Drp1), 13

**E**
Early endosome
  macromolecules, 336
  maturation, 336, 337
  morphology, 336, 337
  neurological disorders, 336
Early endosome autoantigen 1 (EEA1), 338
Electron tomography, 605–606
Electrooculogram (EOG), 310
Electrophysiology, 377
Electroretinogram (ERG)), 145, 232, 329, 376, 557
  15 Hz, 408
  4 to 25 Hz, 405
  photopic flash, 404
  photopic flicker, 405–408
  Scotopic Flicker, 405
  tropicamide eye drops, 404
Electroretinographic analysis, 63
Electroretinography (ERG), 15, 103, 277–279, 501, 525, 563
Embryonic development, 322
Embryonic ectoderm development (EED), 363
Embryonic stem cell-derived RPE cells, 645
EMPACT2 high-pressure freezer, 605
Endoplasmic reticulum protein 29 (ERp29)
  cell survival, 425
  cellular stress, 422–423
  Cx, 423, 424
  homeostasis, 425
  membrane proteins, 422
  neurodegeneration, 424–425
  neuroprotection, 424–425
  PDI-like proteins, 422
  thioredoxin-like domains, 422
Endosome maturation, 336–340
Endosome morphology, 336, 337, 340, 341
Endothelin receptor A (EdnrA), 483
Enhancer of zeste 2 (EZH2), 363
Enlarged endosome, 339, 340
Epidermal growth factor receptor (EGFR), 483
Epidermal growth factors (EGF), 276
Epifluorescence, 310
Epigenetic, 363, 364
Epithelial-mesenchymal transition (EMT), 425
ER-associated degradation (ERAD), 321
ExomeSuite, 222
Exon 3, 414–415, 417
Exon expression
  genome-wide heat maps, 419
  genome-wide map, 418
  heat map analyses, 417–419
  linkage analysis, 416, 417
  measurement, 414–416
  rhodopsin gene, 414
  single gene, 416–417
  transcription and RNA processing, 419
Exosomes, 540
Explant cultures, 388, 390–393
External limiting membrane (ELM), 547–548
Extracellular matrix (ECM), 275, 278
  fibulin 2 or 5, 279
Extracellular signal-regulated kinase (ERK), 351, 652

**F**
F13-L transfection, 391
Factor XIII-A
  activation mechanism, 388
  animal care, 389
  Arg37 and Gly38, 392
  gene expression, 390
  mRNA expression, 389
  optic nerve injury, 391
  protein, 393
  statistical analysis, 390
  types, 391
Fibulin 2
  Arg345Trp mutation, 276
  ECM, 275
  electroretinography, 277–278
  family interface, 276
  histological analysis, 278

Fibulin 2 (*cont.*)
immunohistochemistry, 277
knockout mice, 277
null mice, 276
Fibulin 5, 276, 277, 279
Fish visual system, 388
Fission, 13, 15, 16
Flicker ERG, 404–408, 410
Flow cytometry analysis, 621
Fluorophores damage cells, 396
Foundation fighting blindness, 505
Fusion, 13
FXIII-A, 388

**G**
G protein receptor kinase 1 (GRK1), 319
G protein-coupled receptors (GPCRs), 483
Gamma-glutamyl transferase (GGT), 483
Ganglion cells, 139
Gap junctions, 546
GCaMP6s, 136–139, 141, 142
GDI-displacement factor (GDF), 320
GDNF induction, 621
Gene delivery systems, 118
Gene expression omnibus (GEO), 480
Gene therapy, 102
ERG analysis, 103, 104
immunohistochemistry and morphometry, 103
*Pde6b*, 105
RP mouse model, 102
tamoxifen, 103
Genetic analysis, 233–235
Genetic variants, 266, 268
Genome-Wide Association Studies (GWAS), 259, 260, 262
Germline knockout, 323
Glaucoma, 431–432
Glial cell line-derived neurotrophic factor (GDNF), 620
Glial cell-derived neurotrophic factor (GDNF), 442, 443
Glial fibrillary acidic protein (GFAP), 205
Glial-derived neurotrophic factor, 187
Gliosis, 186, 304, 306
Glucose, 503
Glucose-regulated protein 78 (GRP78), 422
Glutamylation, 532
Glutathione (GSH), 483
Glutathione S-transferase (GST), 587
Glycemic index, 432
Goldfish retinal explants, 390
Gonak™, 111
G-protein-coupled receptors, 47
GraphPad Prism software, 199
Growth factor assessment, 622–623
GTPase-activating protein (GAP), 319
Guanine exchange factor (GEF), 338, 526
Guanylyl cyclase, 327
Guanylyl cyclase-activating proteins (GCAPs), 328
Gut dysbiosis, 430, 432
Gut microbiome, 430–433
Gut-retina axis, 433

**H**
Heat maps, 417–419
Heterogeneity, 305, 306
High-density lipoprotein (HDL) metabolism, 248
High-pressure freezing (HPF), 604–605
Histone deacetylase inhibitor (HDACi), 469
Histone deacetylases (HDAC)
animals, 368
photoreceptor degeneration, 368
*rd10* cultures, 370
TSA, 369, 370
Holographic laser Doppler ophthalmoscopy, 505
Human cancer genome database, 492
Human Gene Mutation Database (HGMD), 381
Human red/green pigment-Cre (HRGP-Cre), 562
Human retinal pigment epithelium (hRPE), 450–454
apoptosis, 454
cell morphology and function, 448
cell nucleus, 453, 454
cell proliferation
FBS, 450–451
VPA, 451–452
VPA and SB, 452–453
cellular environment, 455
cellular proliferation assays, 449
establishment and maintenance, cell cultures, 448
immunoprecipitation assay, 449
nuclear staining, 450
p38 protein
SB, 454
VPA, 452–454
RPE cell proliferation and metaplasia, 448
SB203580, MAPK inhibitor, 454
statistical analysis, 450
vitreoretinal proliferative/neoplastic eye diseases, 455
VPA, 448, 454
Human vision, 512
Humphrey field analyzer (HFA), 441

Hypoxia
factors, 179
HIF1 heterodimers, 179
neovascular AMD and RAP pathology, 179–180
VEGF, 179
Hypoxia-inducible factor 1 (HIF1), 179

**I**
IFN regulatory factor 3 (IRF3), 21
ImageJ software, 513
Immune tolerance, 200, 201
Immunoblot analysis, 378
Immunoblots (IB), 485
Immunoblotting, 610
Immunofluorescence, 377, 513
Immunohistochemistry (IHC), 277, 278, 299, 486, 512–513
Immunostaining, 63, 369, 610
Immunosuppressive therapy, 200
IMOD software package, 605
Implantation surgery, 635
Indirect neuroprotection, 620
Induced pluripotent stem cells (iPSCs), 634
Inflammation, 20, 21, 38–41
Inflammatory cytokines, 285
Ingenuity pathway analysis (IPA), 284
Inherited retinal degeneration, 110
Inherited retinal dystrophies (IRDs), 266, 267, 500
adeno-associated viral vector, 504–505
cone photoreceptors, 500–503
RdCVF (*see* Rod-derived cone viability factor (RdCVF))
rod photoreceptors, 500
measures, patients, 506
monogenic recessive diseases, 500
pathogenesis, 500
retinal degeneration, 499
*RPE65* gene replacement, 500
therapeutic strategy, patient, 505
Inherited retinopathies (IR), 76
Inner limiting membrane (ILM), 159
Inner nuclear layer (INL), 555
Inositol polyphosphatase 5E (INPP5E), 530, 531
Inositol-requiring enzyme 1 (IRE1), 422
Insoluble interphotoreceptor matrix (IPM), 311
Institutional Animal Care and Use Committee (IACUC), 102, 110, 146, 159, 168, 290, 310
Institutional Review Boards (IRB), 221, 231
Insulin receptor (IR), 492
Interdigitation zone (IDZ), 159
Interferon gamma (IFNγ), 196
Interleukin 10 (IL-10), 196
Intermediate filaments (IFs), 304
Interphotoreceptor matrix (IPM), 486, 581
Intracerebroventricular (ICV), 93
Intraclass correlation coefficient (ICC), 153
Intraocular lenses (IOLs)
BLI, 55
cutoff values, 58
MSI, 56
silicone/soft acrylic material, 54
spectral transmittance, 55
transmittance information, 56
ultraviolet radiation, 54
Intronic mutation, 84, 85
Inverted terminal repeats (ITRs), 76
Ionotropic glutamate receptors, 483
iPSC-RPE cells, 637
IQ-domain containing GTPase-activating proteins (IQGAPs), 528

**J**
J haplotype, 14
Joubert syndrome, 318, 320, 524, 531
jREGECO1a, 140
jRGECO1a, 136, 138, 139, 141
Juvenile form (JNCL), 404
Juvenile macular dystrophies, 310

**K**
Knockout (KO), 205
Knockout mice, 277, 347

**L**
Lactate, 376, 378
Late-onset retinal degeneration (L-ORD), 62
Lateral geniculate nucleus (LGN), 352
Late-stage treatment, 104–105
LC3 doublet, 613
LC3 isoform protein expression, 613
LC3A and LC3B transcripts, 612–613
LC3B antibody, 613
LCA4-causing mutations, 381
Leber congenital amaurosis (LCA), 126, 500
AIPL1 FKBP domain, 384
AIPL1 localization, 384
AIRDR, 268
characterized, 381
clinical findings, 266
disease-causing variants, 267
global efforts, 268

Leber congenital amaurosis (LCA) (*cont.*)
HPS90 and HSP70, 382
HSP90 and HSP70, 383
IRD populations, 266
novel disease-causing genes, 267
PDE6 protein, 383
personalised therapeutic strategies, 266
pharmacologic and pharmacogenetic therapies, 268–269
phototransduction signaling proteins, 384
precision medicine, 266
proteasomal degradation, 383
protein farnesylation, 384
RetGC1, 383
rod PDE6 holoenzyme, 383
syndromic forms, 266
Leber hereditary optic neuropathy (LHON), 500
Leber's congenital amaurosis (LCA), 76–77
Leukemia inhibitory factor (LIF)
biological processes, 481
cell differentiation, 481
endothelin signaling, 483
expression intensity, 481, 482
expression pattern, 481
gene expression, 480
GGT, 483
glial cells, 483
microarrays, 480
Pearson correlation coefficient, 480
photoreceptors, 480
protein-coding region, 483
stress, 479
transmembrane receptor activity, 483
Tukey's biweight function, 480
3'UTR, 480, 481
Light and fluorescence microscopy, 513
Light exposure (LE), 467
Light-adapted conditions, 148
Likelihood ratio statistic (LRS), 417
Linkage analysis, 231, 233
Linkage disequilibrium (LD), 259
Lipid peroxidation, 486
Lipidated Cargo, 319
Lipid-based nanoparticles, 120–121
Lipid-protamine-DNA (LPD) complexes, 120
Lipofectamine 2000, 487
Lipofuscin, 395, 397
LIVE/DEAD® Viability/Cytotoxicity assay, 513
Logarithm of the odds (LOD), 417
Longitudinal reflectance profiles (LRP), 169
Luciferase Assays, 111
Luciferase gene, 111
Luciferase reporter assay, 112
Lutein, 441
Lymphoblast cell lines, 85

**M**
M1186, 231
M1186-III-3, 233
Macrophage, 205–206
Macula, 312
Maleimide-azobenzene-glutamate (MAG), 79
Mammalian target of rapamycin (mTOR), 292, 492
Mannose-6-phosphate pathway, 92
Mann-Whitney test, 170
Mapping
human populations, 259
linkage analysis, 259
MLHDs, 262
NGS approach, 261
positional cloning strategies, 259
Matrix metalloproteinases, 396
MCT1
astrocytes, 376
axonopathy, 378
cloning, 376
electrophysiology, 377
haploinsufficiency, 379
heteromeric transporter, 376
immunofluorescence, 377
metabolically active tissues, 376
mice, 376
plexiform layers, 377
visual electrophysiology, 377
Meckel-Gruber syndrome, 524
Melatonin suppression index (MSI), 55–58
Membrane-associated proteins, 318
MerTK
alphavbeta5 integrin signaling, 581
cyclic expression, 581
Gas6 and protein S, 579, 580
in vitro phagocytosis, 580
in vivo variation, light/dark cycle, 580–581
intracellular signaling pathway, 578
ligands, 578
POS, 577
retina, 579
TAM receptor family and apoptotic cell recognition, 578
Metabolism
cellular energy, 292
and deactivation, 294
mitochondrial energy, 294
nucleotide binding, 291
proteins, 292
retinal degeneration, 291
RNA, 290
Metal-based nanoparticles, 118, 119
Microbiota
AMD, 432

diabetic retinopathy, 430–431
diet association, 433
glaucoma, 431–432
gut, 430
gut-retina axis, 433
health and disease, 430
human eye diseases, 430
ocular immunity, 430
uveitis, 430
Microglia, 186
and infiltrating macrophages, 210
Microglial cell activation, 644
Microglial morphology, 210, 211, 213
Miniature longhaired dachshunds (MLHDs), 262
miR-125b, 39, 40
miR-146, 38, 40
miR-155, 38–40
miR-9, 38, 40
miRNAs
AMD, 37–38
as biomarkers, 40–41
biogenesis, 37–38
therapeutic targets, 38–40
Mitochondrial DNA
AMD, 13
treatment, 14, 15
Mitochondrial fission factor (MFF), 13, 15
Mitogen-activated protein (MAP), 351
Mitogen-activated protein kinase (MAPK), 466
Mitophagy, 13, 15
Mixed-lineage protein kinase 3 (MLK3), 589, 590
Modifiers, 261, 262
Morpholinos (MO), 527
Morphometric analysis, 348
Mouse double minute 2 (MDM2), 466
Mouse mutants, 330
Müller cells (MCs), *see* Leukemia inhibitory factor (LIF)
Müller glia, 78, 186, 474–475
characteristics, 304, 305
glial scars, 304
heterogeneity, 305, 306
OS, 306
retinal structure, 304
structural architecture, 303
Multifocal electroretinograms (mfERG), 637
Multigenic form
gene mutation, 261
genes/loci, 258
GWAS, 262
Multivesicular endosome (MVE), 540
Mutation-independent gene therapies
cell death, 77–78
neurotrophic factor signaling, 78
retina, 76–77

**N**
Nanoceria particles, 119
NanoString technologies, 199
NanoString™ analysis, 200
NanoString™ technology, 196
National Institutes of Health guidelines, 554
Neovascularisation, 39, 41, 178
Neurite Outgrowth Assay, 651
Neurodegeneration, 13, 424–425
Neurodegenerative diseases, 512
Neuroinflammation, 206
AMD, 188
DR, 187
RP, 186–187
Neuronal ceroid lipofuscinoses (NCLs)
CLN3 disease, 94, 95
CNS, 92
feature, 94
genes encode, 92
ICV injections, 94
progressing animal models, 94
scAAV2/9 vectors, 95
Tpp1, 93
Neuronal ceroid lipofuscinosis (NCL), 404
NeuronJ imaging software, 651
Neuroprotection, 78, 424–425, 466, 467
Neuroprotective gene therapy, 505
Neuroprotective mutation-independent therapy, 506
Neuroretina, 14
Neurotrophins, 474
Neutrophic factor, 442, 443
Next-generation sequencing (NGS), 238, 260, 261, 268
haplotype analysis, 239
linkage mapping, 239
retinal targeted-capture, 239
Niemann-Pick type C (NPC), 340
NLRP3 inflammasome, 188
N-methyl-N-nitrosourea (MNU), 298–300
Nonhuman primate, 643, 645
Noninvasive imaging, 168
Nonneoplastic AIR, 194
Non-viral gene therapy vectors
CK30PEG particles, 110
retinal degeneration, 110
RPE, 112
Non-viral nanoparticles, 118
Novel variants, 226
*NXNL1* gene
genomic organization, 502
metabolic and redox signaling, 504
*Nyx*$^{nob}$ mice, 168

**O**
Ocular diseases, 118
Ocular gene therapy, 95–96
Oculotoxicity, 152
Oncogene, 492, 496
Ophthalmology, 506
Opsins, 69
Optic atrophy 1 (Opa1), 13
Optic nerve crush (ONC), 352, 442
Optic nerve head (ONH), 162
Optic neuropathy, 352
Optical coherence tomography (OCT), 152, 505, 634
Optogenetics
  AAV-based vectors, 71
  alga/bacteria, 69
  blind retina, 78–79
  degenerative state, 70
  disadvantage, 71
  healthy retina, 70
  human retinal explants, 70
  light sensitivity, 71
  optical control, 69
  optogenetic strategies, 70
  photoreceptor-based strategies, 70
  synaptic connection, 70
  therapeutic strategy, 71
Optokinetic response (OKR), 572, 574, 575
Oral microbiome, 431–432
ORF15, 524
ORF15 region, 231
OS protein trafficking, 323
Oscillation, 347
Outer nuclear layer (ONL), 159, 298, 360, 369, 466
Outer plexiform layer (OPL), 159
Outer segments (OS), 169, 173, 318
Oxidative stress, 458, 462
  AMD, 12
  DJ-1, 4
Oxidised plasma membrane (oxPAPC), 24

**P**
Parkinson disease, 351, 477
Pathogen-associated molecular patterns (PAMPs), 21
Pattern recognition receptors (PRR), 20, 21
PDE6 enzyme dysfunction, 512
PDE6 inhibition, 515
*pde6c*$^{rw76a}$, 328, 329
*pde6c*$^{w59}$, 328, 329
PDEδ, 318
Pearson correlation, 480
PEDF concentration, 622
Pedigree characterization, 232–233
Pericentriolar material 1 (PCM1), 526
Peripheral blood mononuclear cells (PBMC), 196, 198
Personalised therapies, 266
Phagocytic activity, 112
Phagocytosis, 593, 594, 598, 599
Phagocytosis assays, 594
Phalloidin-Alexa-488, 600
Pharmacotherapy, 440
Phenylephrine hydrochloride, 159
Phosphatase and tensin homolog (PTEN), 466
Phosphate-buffered saline (PBS), 512, 594
Phosphatidylinositol (PtdIns), 530
Phosphatidylserines (PtdSer), 578
Phosphodiesterase 6b (PDE6b), 102
Phosphodiesterase of the sixth family (PDE6), 382
Phosphodiesterase type 6 (PDE6)
  cGMP, 328
  *pde6b* mutations, 330–331
  *pde6c* mutations, 330
  *pde6c*rw76a, cGMP accumulation, 329
  *pde6c*rw76a, slow cone degeneration, 328–329
  subunits, 328
Phosphoinositide 3-kinase (PI3K), 466, 586
Phosphoinositides, 530
Phospholipase Cγ1 (PLCɣ1), 466
Phosphoproteomics, 291
Phosphorylation, 292, 293, 360–362
Phosphotidylinositol-3-phosphate (PtdIns-3-P), 337
Photobleaching processes, 398
Photopic flicker, 405–408
Photoreceptor, 112–113, 152
Photoreceptor cell death, 298
Photoreceptor cells, 353, 354
Photoreceptor degeneration, 102, 104, 328–331
  AMD, 204
  cGMP, 327, 331
  light-induced retinal, 204
  macrophages, 204, 205
  neovascular form, 204
  PDE6 (*see* Phosphodiesterase type 6 (PDE6))
  phototransduction cascade, 327
  phototransduction pathway, 328
  retinal disorders, 204
  RPE, 205
Photoreceptor morphology, 606
Photoreceptor OS reflectivity, 171

Photoreceptor outer segment (POS), 24, 577
materials, 594
protocol, 595
Photoreceptor transplantation, 548
Photoreceptors (PRs), 347–349, 522, 523
Photoreduction, 486
Phototransduction, 352, 603
Phototransduction signaling proteins, 384
Pigment epithelium-derived factor (PEDF), *see* Retinal pigment epithelium (RPE)
PIKFyve, 339
PKRD168, 231–232, 234
PKRD320, 223, 224
PKR-like ER kinase (PERK), 422
Pleiotropy, 249, 251
Polycomb repressive complex 1 (PRC1), 363
Polycystic kidney disease, 531
Polymer nanoparticle application, 120
Polymer-based nanoparticles, 118–120
Polymorphisms, 22
Polyproline-rich domain (PRD), 382
Polyunsaturated fatty acids, 486
Postnatal development, 322
Posttranslational modifications
biological processes, 363
BMI1, 360
H2A and H3K27, 364
Posttranslational modifications (PTMs), 6
Posttranslational prenylation and acylation, 319
Potassium voltage-gated channels, 483
Prenylated proteins, 384
Prenylation, 384, 524, 529
Primary antibodies, 610
Primary RPE cell culture
materials, 596–597
protocol, 597
Proliferator-activated receptor gamma coactivator 1 (PGC-1), 15
Protein carbonylation
animal experiments, 299
retinal sections, 299
Protein correlation profiling (PCP), 542
Protein disulfide isomerase (PDI), 422
Protein trafficking, 424, 425
Protein-protein interaction, 529
Proteomics, 291–293
PTEN-induced putative kinase 1 (PINK1), 13
pVMD_Luc vectors, 112

**Q**
QIAamp DNA blood mini kit (QIAGEN), 221
Quantitative real-time PCR, 389

**R**
Rapid degeneration, 330
RCC1-like domain (RLD), 524
Rd1
degeneration, 360
Reactive oxygen species (ROS), 12, 24
Receptor for AGEs (RAGEs), 187
Receptor-interacting protein (RIP), 206
Recombinant inbred (RI), 414
Recoverin, 198–199
Regeneration-associated genes (RAGs), 388
Region of interest (ROI), 152, 169
Regulator of chromosome condensation 1 (RCC1), 524
Retbindin (Rtbdn)
flavin binding and transport, 486
IHC, 486
IPM, 486
light damage, 487–488
lipid peroxidation, 486
lipid peroxidation and energy production, 489
materials and methods, 487
membrane transporter, 488
metabolites, 486
murine retina, 486
neural retina, 486
photoreceptor cells, 488
photoreduction, 486
protein levels, 486
RBP, 486, 488
riboflavin photosensitization, 488
silico analysis, 485
Reticuloplasmin, 422
Retina, 76–77
structural characteristics, 158
Retina disease, 322
Retinal angiomatous proliferation (RAP), 179
choriocapillaris and cone degeneration, 181
human macular region, 181
hypoxia (*see* Hypoxia)
neovascular AMD, 178
retinal and choroidal vasculatures, 178
*Rho/VEGF* and *Vldlr-/-* mice, 180–181
Retinal cell markers, 515
Retinal cell viability, 347, 348
Retinal clock, 346
Retinal degeneration (RD), 290, 292, 352, 353, 355, 360, 362
control analysis, 225, 226
dystrophy, 220
ethics, 221
exclusion analysis, 221
linkage analysis, 222

Retinal degeneration (RD) (*cont.*)
mutations, 220
subjects and clinical examination, 221
Retinal degenerative diseases, 102, 185, 521
Retinal degenerative disorders, 619
Retinal diseases, 268
Retinal dystrophies (RD), 230, 360, 524
Retinal function, 404, 408
Retinal ganglion cell, 650
Retinal ganglion cell layer (RGCs), 555
Retinal ganglion cells (RGCs), 352, 388
Retinal gene therapy, 106
Retinal imaging
AAV, 138
animal preparation, 138
excitation spectra, 136
GCaMP family, 136
jRGECO1a, 136
mouse, 138
Retinal morphometry, 348
Retinal nerve fiber layer (RNFL), 164
Retinal pigment epithelial (RPE), 353, 354, 439
Retinal pigment epithelium (RPE), 5, 6, 20, 159, 205, 247, 310, 340, 422, 460–462, 577–579, 626, 634
AMD model, 458
antioxidant effects, 458
ARPE-19 cells
NaIO3 and H2O2, 460–461
NaIO3-induced cytotoxicity, 461–462
PEDF concentration curve, 462
cell culture, 458
cell monolayer, 540
cell toxicity assay, 459
cell viability assay, 459
ECM-modulating exosomal activity, 540
ex vivo study, 541
exosomal proteins, 542
exosomes, 540
interphotoreceptor matrix, 458, 462
light-sensitive photoreceptors, 457
materials, 458
MVE, 540
necrosis, 462
neuronal cell death, 462
oxidative damage, 458
pathway, 541
polarized exosome, 541–543
recombinant PEDF, 459
statistical analysis, 459
structural/functional injury, 457
toxicity and viability, 458
vertebrate retina, 457
Retinal progenitor cells (RPC), 469
Retinal proteomics, 291
Retinal remodelling, 304
Retinal structure and function, 105
Retinal thickness (RT)
animal models, 158
OCT imaging, 158
ONH, 164
reproducibility, 158
Retinal tissue, 620
drug screening, 620
flow cytometry analysis, 622
GDNF, 620
GF production, 623
growth factor production, 621
oxygen environment, 620
Retinal-choroidal anastomosis, 178
Retinaldehyde, 395
Retinitis pigmentosa (RP), 76, 185–187, 194, 195, 286, 297, 300, 331, 354, 492
animal models, 439
Arg677X mutation, 242
clinical characterization, 238–239
clinical diagnosis, 240
DHA, 441
family ascertainment, 238–239
growth factor, 442, 443
lutein, 441
neutrophic factor, 442, 443
prevalence, 238
segregating haplotypes, 241
valproic acid, 442
vitamin A, 440
Retinitis pigmentosa GTPase regulator (RPGR), 526–532
cilia, 522
ciliopathies, 524, 525
cilium, 532
cone-rod and macular degeneration, 525
function
extraocular phenotypes, 527
gatekeeper, 528
GEFs, 526
protein complexes, 527–528
RAB8A, 526
RLD, 526
*Rpgr*$^{ko}$ mice, 527
*rpgr*-MO-treated zebra fish embryos, 527
gene augmentation therapy, 522
human genetic and mass spectrometry-based studies, 524
isoforms, 522, 524
*RPGR*$^{const}$, 528–531
*RPGR*$^{ORF15}$, 528, 529, 531–532
light-sensing outer segments, 532

ORF15 mutations, 525
phosphoinositide metabolism, 532
PRs, 522, 523
retinal degeneration, 521
*Rpgr*-DKO mice, 525, 526
*Rpgr*$^{ko}$ mice, 525
RTKN2, 525
visual impairment, 522
X chromosome, 522
Retinitis pigmentosa protein 2 (RP2), 319–322
Retinol-binding protein receptor 2 (Rbpr2)
cDNA, 571
cell lines, cell culture and plasmid transfections, 571
holo-RBP4, 571–573
ocular retinoids, 574
photoreceptor degeneration and loss of visual function, 574
RBP4 binding and retinol uptake, 572
ROL uptake and storage, 573–574
vision, 570, 574
visual function, 575
zebrafish, 572, 573
Retinopathy of prematurity (ROP), 474
Retinoschisis, 500
REV-ERB/ROR response element (RRE), 346
RGC-5 cells, 650
Rhodopsin, 321
Rhodopsin kinase (RK), 112
Rhotekin 2 (RTKN2), 525
Riboflavin-binding protein (RBP), 485
Rod degeneration, 368, 370
Rod-derived cone viability factor (RdCVF)
AAV2/8 vectors, 502
aerobic glycolysis, 503
cone-enriched primary cultures, 501
*Nxnl1* gene, 501
P23H rat, 501
photooxidative stress, 502
polyunsaturated fatty acids, 502
*rd1* mouse, 501
TAU phosphorylation, 503
trophic factors, 501
Rowett nude (RNU), 635
Royal College of Surgeons (RCS), 642
*Rp2h-/-* photoreceptors, 322
RPE cell culture, 594
RPE implants, 634
RPE microvilli, 311, 312
RPE Phagocytosis Assay, 594, 598–600
materials, 599
protocol, 599–600
Rpe65-knockout mice, 121
RPE-photoreceptor interface, 310
RPGR, 231, 233
RPGR-INPP5E interaction, 530
RPGR-interacting protein 1-like (*RPGRIP1L*), 525

**S**
Sall1
immunohistochemical analysis, 211
microglia and infiltrating macrophages, 210
microglial morphology, 211–212
monocyte-derived macrophage, 210
mouse strains, 210
postnatal stage, 212–213
tamoxifen, 210
SB203580, MAPK inhibitor, 452, 454
Scaffold protein, 587
Scavenger receptor class B type 1 (SR-B1), 570
Segregating mutations, 242–243
Semidominant inheritance, 240–242
Senior-Loken syndrome, 522, 524
Sense oligonucleotide (SON), 87
Serum-free medium (SFM), 572
Short tandem repeat (STR), 221
Single canine retina, 596
Single nucleotide variants (SNV), 235
Sirtuins
animals, 562–563
cellular homeostasis, 562
metabolic perturbations, 564
$NAD^+$-dependent retinal homeostasis, 564
NAMPT-mediated $NAD^+$ biosynthesis, 562
retinal degeneration, 563–564
retinal disease, 564
retinal dysfunction, 564
retinal structure and function, 563
subcellular compartments, 562
Slow degeneration, 329, 330
Sodium iodate (NaIO3), 458
Solubilization factors, 318
Soper's analysis of variance calculator, 161
Spectral transmittance, 54–57
Spectral-domain optical coherence tomography (SDOCT), *see* Autofluorescence confocal scanning laser ophthalmoscopy (AF-SLO)
Spectral-domain optical coherence tomography (SD-OCT), 15
Spinal cord injury (SCI), 424
Splice modulation, 87
Splice modulation therapy, 84
Standard error of the mean (SEM), 450
Stargardt disease, 500, 547
Streptozotocin (STZ), 168

Subretinal cell transplantation, 643
Subretinal injection technique, 469
Subretinal studies, Pigs
  morphological assessments, 636
  transplantation tool, 635
Superior colliculus (SC), 352
Superoxide dismutase (SOD), 119
Suprachiasmatic nuclei (SCN), 54, 346
Syntenin-1, 542

**T**
Talaumidin, 650
  chemical structure, 650
  mechanism, 650
  PI3K inhibitor, 652
  PI3K-mediated neurite outgrowth, 651–652
  RGC-5 cells, 650, 652
Tamoxifen, 103, 210
Teratogenicity, 152
Tetratricopeptide repeat (TPR) domain, 382
TGF-beta receptor 1 (TGFβ R1), 199
TH signaling suppression, 130
Therapeutic target, 355
Thioredoxins, 501
Thyroid hormone (TH), 126
Tick-over process, 30–31
  basal deposit formation, 31–32
  C3b deposition, 31
  complement-regulating proteins, 30
  convertase-independent proteolysis, 30
Tight junction protein (TJP)-1, 546
Tight junctions (TJs)
  AJs, 546
  components, 546
Tissue morphogenesis, 546
TLR2
  and TLR4, 22
  heterodimerises, 22
  ligand, 24
  ligand concentrations, 22
Toll-like receptor 4 (TLR4), 431
Toll-like receptors (TLRs), 21, 22
Tomogram reconstruction, 605
Transcardiac perfusion, 604
Transchoroidal surgical approach, 642
Transcriptional factor, 213
Transglutaminase, 388
Trans-Golgi network, 337
Transient receptor potential isoform 4 (TRPV4), 555–558
  animal handling and anesthetic procedures, 554
  dysplasias and sensorimotor neuropathies, 558
  electroretinographic analysis, 555
  functions, 558
  GFAP, 556
  histology, 554
  immunocytochemical localization, 558
  mRNA/protein, 554
  Müller cells
    [Ca2+]i elevations, 555–556
    amplitude and kinetics, distal light response, 557–558
    RGCs, 555
  radial glial processes, 558
  scotopic and photopic conditions, 554
  sensory signaling, 554
  visual signaling, 554
Transmembrane component, 546
Transmembrane proteins, 323
Transmitted light microscopy, 310
Trichostatin A (TSA)
  cpfl1 cones, 369–370
  *cpfl1* mice, 368
  HDAC inhibition, 368
Trifluoroacetate (TFA), 111
TRIF-related adaptor molecule (TRAM), 21
Triggering receptor expressed on myeloid cells 1 (TREM1), 285
Tripeptidyl peptidase 1 (TPP1), 93
Tropicamide, 159
Tsang laboratory, 102
Tubulin-tyrosine ligase-like 5 (TTLL5), 532
Tumor necrosis factor (TNF), 353
Tumor necrosis factor alpha (TNFα), 196
Type 2 iodothyronine deiodinase (DIO2), 126
Type 3 iodothyronine deiodinase
  *DIO3*-WT and *DIO3*-Cys, 128
  pCDM8 vector, 127
  qRT-PCR, 127
  *Rpe65-/-* mouse line, 127
  subretinal injection, 127
  TH signaling, 126
  TUNEL assays, 128
Type 3 neovascularization, 178

**U**
UNC119, 318
Unfolded protein response (UPR), 321, 354, 422
User-centered ecosystems, 506
Usher syndrome, 500, 522, 524, 527
Uveitis, 430

**V**
Valproic acid (VPA), *see* Human retinal pigment epithelium (hRPE)
Vascular endothelial growth factor (VEGF), 178, 353
  data and working hypothesis, 475
  hypoxia, 476–477
  MG, 474–475
  retinal integrity, 475–476
Vertebrate photoreceptor, 603
Vertebrates, 570
Viability/Cytotoxicity Kit, 512
Viral vectors, 189
Visual arrestin 1
  Affymetrix™ GeneChip, 283
  animals, 283
  *Arr1*$^{-/-B}$ mice, 284
  cone photoreceptors, 282
  gene expression profiles, 282
  phototransduction, 282
Visual cycle, 396
Vitamin A, 440
Vitamin A deficiency (VAD), 570
Vitamin E, 398
Vitamin E-supplemented diet, 398
Vitelliform lesion formation, 310
Vorinostat (SAHA), 368, 370
Voronoi cells, 152

**W**
Western blotting, 361, 377
Whole-exome sequencing
  bioinformatic analysis, 226
  linkage analysis, 220
  PKRD320, 223
  variant calling, 221–222
Whole-exome sequencing (WES), 231, 232
Whole-mount in situ hybridization (WISH), 573
Wnt/β-catenin signalling pathway, 547
WT photoreceptors, 320–321

**X**
X-box binding protein 1 (XBP1) pathways, 423
X-linked chorioretinal dystrophy, 84
X-linked inhibitor of apoptosis protein (XIAP), 77
X-linked RD (XLRD), 230
X-linked retinitis pigmentosa, 240
X-linked RP (XLRP), 524

**Y**
Yeast two-hybrid assay, 586–588
Yellow-tinted intraocular lense, 54, 55, 57, 59

**Z**
Zebrafish (*Danio rerio*), 328–329, 331, 332, 389–391
  cone density, 152
  repeatability, 152
  reproducibility, 152
ZNF408, 223, 226
Zonula adherens (ZA), 547